

The background of the cover is a microscopic view of a blood smear. A large magnifying glass is positioned in the center, focusing on several white blood cells with prominent nuclei and granules. The cells are stained in shades of purple, blue, and red. The magnifying glass has a silver rim and a black handle.

haematologica

Journal of The Ferrata Storti Foundation

ISSN 0390-6078

Volume 105

FEBRUARY

2020 - 02

www.haematologica.org

haematologica

Looking for a definitive source
of information in hematology?

Haematologica is an Open Access
journal: all articles are completely
free of charge

Haematologica
is listed on *PubMed, PubMedCentral,*
DOAJ, Scopus and many other
online directories

5000 / amount of articles read daily

4300 / amount of PDFs downloaded daily

2.20 / gigabytes transferred daily

WWW.HAEMATOLOGICA.ORG

Editor-in-Chief

Luca Malcovati (Pavia)

Deputy Editor

Carlo Balduini (Pavia)

Managing Director

Antonio Majocchi (Pavia)

Associate Editors

Hélène Cavé (Paris), Steve Lane (Brisbane), PierMannuccio Mannucci (Milan), Simon Mendez-Ferrer (Cambridge), Pavan Reddy (Ann Arbor), Francesco Rodeghiero (Vicenza), Andreas Rosenwald (Wuerzburg), Monika Engelhardt (Freiburg), Davide Rossi (Bellinzona), Jacob Rowe (Haifa, Jerusalem), Wyndham Wilson (Bethesda), Swee Lay Thein (Bethesda), Pieter Sonneveld (Rotterdam)

Assistant Editors

Anne Freckleton (English Editor), Cristiana Pascutto (Statistical Consultant), Rachel Stenner (English Editor), Kate O'Donohoe (English Editor), Ziggy Kennell (English Editor)

Editorial Board

Jeremy Abramson (Boston); Paolo Arosio (Brescia); Raphael Bejar (San Diego); Erik Berntorp (Malmö); Dominique Bonnet (London); Jean-Pierre Bourquin (Zurich); Suzanne Cannegieter (Leiden); Francisco Cervantes (Barcelona); Nicholas Chiorazzi (Manhasset); Oliver Cornely (Köln); Michel Delforge (Leuven); Ruud Delwel (Rotterdam); Meletios A. Dimopoulos (Athens); Inderjeet Dokal (London); Hervé Dombret (Paris); Peter Dreger (Hamburg); Martin Dreyling (München); Kieron Dunleavy (Bethesda); Dimitar Efremov (Rome); Sabine Eichinger (Vienna); Jean Feuillard (Limoges); Carlo Gambacorti-Passerini (Monza); Guillermo Garcia Manero (Houston); Christian Geisler (Copenhagen); Piero Giordano (Leiden); Christian Gisselbrecht (Paris); Andreas Greinacher (Greifswald); Hildegard Greinix (Vienna); Paolo Gresele (Perugia); Thomas M. Habermann (Rochester); Claudia Haferlach (München); Oliver Hantschel (Lausanne); Christine Harrison (Southampton); Brian Huntly (Cambridge); Ulrich Jaeger (Vienna); Elaine Jaffe (Bethesda); Arnon Kater (Amsterdam); Gregory Kato (Pittsburg); Christoph Klein (Munich); Steven Knapper (Cardiff); Seiji Kojima (Nagoya); John Koreth (Boston); Robert Kralovics (Vienna); Ralf Küppers (Essen); Ola Landgren (New York); Peter Lenting (Le Kremlin-Bicetre); Per Ljungman (Stockholm); Francesco Lo Coco (Rome); Henk M. Lokhorst (Utrecht); John Mascarenhas (New York); Maria-Victoria Mateos (Salamanca); Giampaolo Merlini (Pavia); Anna Rita Migliaccio (New York); Mohamad Mohty (Nantes); Martina Muckenthaler (Heidelberg); Ann Mullally (Boston); Stephen Mulligan (Sydney); German Ott (Stuttgart); Jakob Passweg (Basel); Melanie Percy (Ireland); Rob Pieters (Utrecht); Stefano Pileri (Milan); Miguel Piris (Madrid); Andreas Reiter (Mannheim); Jose-Maria Ribera (Barcelona); Stefano Rivella (New York); Francesco Rodeghiero (Vicenza); Richard Rosenquist (Uppsala); Simon Rule (Plymouth); Claudia Scholl (Heidelberg); Martin Schrappe (Kiel); Radek C. Skoda (Basel); Gérard Socié (Paris); Kostas Stamatopoulos (Thessaloniki); David P. Steensma (Rochester); Martin H. Steinberg (Boston); Ali Taher (Beirut); Evangelos Terpos (Athens); Takanori Teshima (Sapporo); Pieter Van Vlierberghe (Gent); Alessandro M. Vannucchi (Firenze); George Vassiliou (Cambridge); Edo Vellenga (Groningen); Umberto Vitolo (Torino); Guenter Weiss (Innsbruck).

Editorial Office

Simona Giri (Production & Marketing Manager), Lorella Ripari (Peer Review Manager), Paola Cariati (Senior Graphic Designer), Igor Ebuli Poletti (Senior Graphic Designer), Marta Fossati (Peer Review), Diana Serena Ravera (Peer Review)

Affiliated Scientific Societies

SIE (Italian Society of Hematology, www.siematologia.it)

SIES (Italian Society of Experimental Hematology, www.siesonline.it)

Information for readers, authors and subscribers

Haematologica (print edition, pISSN 0390-6078, eISSN 1592-8721) publishes peer-reviewed papers on all areas of experimental and clinical hematology. The journal is owned by a non-profit organization, the Ferrata Storti Foundation, and serves the scientific community following the recommendations of the World Association of Medical Editors (www.wame.org) and the International Committee of Medical Journal Editors (www.icmje.org).

Haematologica publishes editorials, research articles, review articles, guideline articles and letters. Manuscripts should be prepared according to our guidelines (www.haematologica.org/information-for-authors), and the Uniform Requirements for Manuscripts Submitted to Biomedical Journals, prepared by the International Committee of Medical Journal Editors (www.icmje.org).

Manuscripts should be submitted online at <http://www.haematologica.org/>.

Conflict of interests. According to the International Committee of Medical Journal Editors (<http://www.icmje.org/#conflicts>), "Public trust in the peer review process and the credibility of published articles depend in part on how well conflict of interest is handled during writing, peer review, and editorial decision making". The ad hoc journal's policy is reported in detail online (www.haematologica.org/content/policies).

Transfer of Copyright and Permission to Reproduce Parts of Published Papers. Authors will grant copyright of their articles to the Ferrata Storti Foundation. No formal permission will be required to reproduce parts (tables or illustrations) of published papers, provided the source is quoted appropriately and reproduction has no commercial intent. Reproductions with commercial intent will require written permission and payment of royalties.

Detailed information about subscriptions is available online at www.haematologica.org. Haematologica is an open access journal. Access to the online journal is free. Use of the Haematologica App (available on the App Store and on Google Play) is free.

For subscriptions to the printed issue of the journal, please contact: Haematologica Office, via Giuseppe Belli 4, 27100 Pavia, Italy (phone +39.0382.27129, fax +39.0382.394705, E-mail: info@haematologica.org).

Rates of the International edition for the year 2019 are as following:

	<i>Institutional</i>	<i>Personal</i>
<i>Print edition</i>	<i>Euro 700</i>	<i>Euro 170</i>

Advertisements. Contact the Advertising Manager, Haematologica Office, via Giuseppe Belli 4, 27100 Pavia, Italy (phone +39.0382.27129, fax +39.0382.394705, e-mail: marketing@haematologica.org).

Disclaimer. Whilst every effort is made by the publishers and the editorial board to see that no inaccurate or misleading data, opinion or statement appears in this journal, they wish to make it clear that the data and opinions appearing in the articles or advertisements herein are the responsibility of the contributor or advisor concerned. Accordingly, the publisher, the editorial board and their respective employees, officers and agents accept no liability whatsoever for the consequences of any inaccurate or misleading data, opinion or statement. Whilst all due care is taken to ensure that drug doses and other quantities are presented accurately, readers are advised that new methods and techniques involving drug usage, and described within this journal, should only be followed in conjunction with the drug manufacturer's own published literature.

Direttore responsabile: Prof. Carlo Balduini; Autorizzazione del Tribunale di Pavia n. 63 del 5 marzo 1955.
Printing: Press Up, zona Via Cassia Km 36, 300 Zona Ind.le Settevene - 01036 Nepi (VT)



Table of Contents

Volume 105, Issue 2: February 2020

About the cover

- 245** 100-YEAR-OLD HAEMATOLOGICA IMAGES: ACUTE PROMYELOCYTIC LEUKEMIA
Carlo L. Balduini

Editorials

- 246** Of mice, genes and aging.
James DeGregori
- 249** Hypo, Hyper, or Combo: new paradigm for treatment of acute myeloid leukemia in older people
Gunnar Juliusson et al.
Rui-Gang Xu and Robert A. S. Ariens
- 252** Is unrelated donor or haploidentical hematopoietic transplantation preferred for patients with acute myeloid leukemia in remission?
Richard Champlin
- 255** *BIRC3* mutations in chronic lymphocytic leukemia – uncommon and unfavorable
Eugen Tausch and Stephan Stilgenbauer
- 257** Insights into the composition of stroke thrombi: heterogeneity and distinct clot areas impact treatment

Centenary Review Article

- 260** Iron metabolism and iron disorders revisited in the hepcidin era
Clara Camaschella et al.

Review Articles

- 273** Innate immune cells, major protagonists of sickle cell disease pathophysiology
Slimane Allali et al.
- 284** Fibrin(ogen) in human disease: both friend and foe
Rui Vilar et al.

Guideline Articles

- 297** Management of adults and children undergoing chimeric antigen receptor T-cell therapy: best practice recommendations of the European Society for Blood and Marrow Transplantation (EBMT) and the Joint Accreditation Committee of ISCT and EBMT (JACIE)
Ibrahim Yakoub-Agha et al.

Articles

Hematopoiesis

- 317** The lifespan quantitative trait locus gene *Securin* controls hematopoietic progenitor cell function
Andreas Brown et al.
- 325** Interferon regulatory factor 2 binding protein 2b regulates neutrophil *versus* macrophage fate during zebrafish definitive myelopoiesis
Luxiang Wang et al.

Red Cell Biology & its Disorders

- 338** Density, heterogeneity and deformability of red cells as markers of clinical severity in hereditary spherocytosis
Rick Huisjes et al.

Macrophage Biology & its Disorders

- 348** Clinicopathological features, treatment approaches, and outcomes in Rosai-Dorfman disease
Gaurav Goyal et al.

The origin of a name that reflects Europe's cultural roots.

Ancient Greek

αἷμα [haima] = blood
αἵματος [haimatos] = of blood
λόγος [logos] = reasoning

Scientific Latin

haematologicus (adjective) = related to blood

Scientific Latin

haematologica (adjective, plural and neuter,
used as a noun) = hematological subjects

Modern English

The oldest hematology journal,
publishing the newest research results.
2018 JCR impact factor = 7.570

Myelodysplastic Syndromes

- 358** Genome analysis of myelodysplastic syndromes among atomic bomb survivors in Nagasaki
Masataka Taguchi et al.

Myeloproliferative Neoplasms

- 366** Molecular quantification of tissue disease burden is a new biomarker and independent predictor of survival in mastocytosis
Georg Greiner et al.

Myeloid Neoplasms

- 375** Loss of RAF kinase inhibitor protein is involved in myelomonocytic differentiation and aggravates *RAS*-driven myeloid leukemogenesis
Veronica Caraffini et al.

Chronic Myeloid Leukemia

- 387** Validation of a *Drosophila* model of wild-type and T315I mutated BCR-ABL1 in chronic myeloid leukemia: an effective platform for treatment screening
Amani Al Outa et al.

Acute Myeloid Leukemia

- 398** Comparisons of commonly used front-line regimens on survival outcomes in patients aged 70 years and older with acute myeloid leukemia
Chetasi Talati et al.
- 407** Alternative donor transplantation for acute myeloid leukemia in patients aged ≥ 50 years: young HLA-matched unrelated or haploidentical donor?
Miguel-Angel Perales et al.
- 414** Allogeneic stem cell transplantation using HLA-matched donors for acute myeloid leukemia with deletion 5q or monosomy 5: a study from the Acute Leukemia Working Party of the EBMT
Xavier Poiré et al.

Non-Hodgkin Lymphoma

- 424** *MYD88* mutations identify a molecular subgroup of diffuse large B-cell lymphoma with an unfavorable prognosis
Joost S. Vermaat et al.
- 435** High activation of STAT5A drives peripheral T-cell lymphoma and leukemia
Barbara Maurer et al.

Chronic Lymphocytic Leukemia

- 448** Biological and clinical implications of *BIRC3* mutations in chronic lymphocytic leukemia
Fary Diop et al.

Plasma Cell Disorders

- 457** Sialyltransferase inhibition leads to inhibition of tumor cell interactions with E-selectin, VCAM1, and MADCAM1, and improves survival in a human multiple myeloma mouse model
Alessandro Naroni et al.
- 468** Daratumumab-based regimens are highly effective and well tolerated in relapsed or refractory multiple myeloma regardless of patient age: subgroup analysis of the phase 3 CASTOR and POLLUX studies
Maria-Victoria Mateos et al.

Complications in Hematology

- 478** Ibrutinib induces multiple functional defects in the neutrophil response against *Aspergillus fumigatus*
Damien Blez et al.

Hemostasis

- 490** Increased incidence of cancer in the follow-up of obstetric antiphospholipid syndrome within the NOH-APS cohort
Jean-Christophe Gris et al.

REGISTER NOW
AND SUBMIT YOUR ABSTRACT

The science of **today** is the
innovation of **tomorrow**



You are invited to attend the 28th Congress of the International Society on Thrombosis and Haemostasis (ISTH). Held in Milan, Italy, from July 11 - 15, 2020, the ISTH 2020 Congress will be the premier meeting in thrombosis, hemostasis and vascular biology and will be attended by thousands of the world's experts.

**REGISTRATION AND ABSTRACT
SUBMISSION ARE NOW OPEN. SUBMIT
YOUR ABSTRACT BY FEBRUARY 4 AT
ISTH2020.ORG**

#ISTH2020

Plan to attend ISTH 2020 to exchange the latest science, discuss the newest clinical applications and present the recent advances to improve patient outcomes around the world.



Coagulation & its Disorders

- 498** Structural analysis of ischemic stroke thrombi: histological indications for therapy resistance
Senna Staessens et al.
- 508** Variable readthrough responsiveness of nonsense mutations in hemophilia A
Luis Martorell et al.

Stem Cell Transplantation

- 519** Validation of Minnesota acute graft-versus-host disease Risk Score
Margaret L. MacMillan et al.

Letters to the Editor

Letters are available online only at www.haematologica.org/content/105/2.toc

- e43** CD117^{hi} expression identifies a human fetal hematopoietic stem cell population with high proliferation and self-renewal potential
Loïc Maillard, et al.
<http://www.haematologica.org/content/105/2/e43>
- e48** Sequential cellular niches control the generation of enucleated erythrocytes from human pluripotent stem cells
Jun Shen, et al.
<http://www.haematologica.org/content/105/2/e48>
- e52** Characterization of the phenotype of human eosinophils and their progenitors in the bone marrow of healthy individuals
Marwan Hassani et al.
<http://www.haematologica.org/content/105/2/e52>
- e57** Complement C3 inhibition by compstatin Cp40 prevents intra- and extravascular hemolysis of red blood cells
Inge Baas et al.
<http://www.haematologica.org/content/105/2/e57>
- e61** Targetable driver mutations in multicentric reticulohistiocytosis
Norihiro Murakami et al.
<http://www.haematologica.org/content/105/2/e61>
- e65** Platelet activation and multidrug resistance protein-4 expression in children and adolescents with different subtypes of primary thrombocytopenia
Fiorina Giona et al.
<http://www.haematologica.org/content/105/2/e65>
- e68** Rac1/2 activation promotes FGFR1 driven leukemogenesis in stem cell leukemia/lymphoma syndrome
Tianxiang Hu et al.
<http://www.haematologica.org/content/105/2/e68>
- e72** Variable global distribution of cell-of-origin from the ROBUST phase III study in diffuse large B-cell lymphoma
Grzegorz S. Nowakowski et al.
<http://www.haematologica.org/content/105/2/e72>
- e76** Differential effects of BTK inhibitors ibrutinib and zanubrutinib on NK-cell effector function in patients with mantle cell lymphoma
Thijs W.H. Flinsenberg et al.
<http://www.haematologica.org/content/105/2/e76>
- e80** Preclinical evidence for an effective therapeutic activity of FL118, a novel survivin inhibitor, in patients with relapsed/refractory multiple myeloma
Lisa C. Holthof et al.
<http://www.haematologica.org/content/105/2/e80>

Case Reports

Case Reports are available online only at www.haematologica.org/content/105/2.toc

- e84** Bone marrow findings in Erdheim-Chester disease: increased prevalence of chronic myeloid neoplasms
Gaurav Goyal et al.
<http://www.haematologica.org/content/105/2/e84>

ANNOUNCING THE AWARDEE 2019

Dr. Ilaria Pagani

Leukaemia Research Group, Cancer Program, SAHMRI, Adelaide, Australia



for her two year project on
'Use of machine learning to integrate clinical data and biomarkers to optimise prediction of TFR'

"It is an honour and a pleasure to be the first John Goldman Research Prize Awardee. Receiving funding support from the European School of Haematology (ESH) is a privilege. It represents a critical step in my career towards becoming an independent investigator and provides the opportunity to build new collaborations.

My project aims to identify bioassays that can be integrated with clinical data in a machine learning system to develop a personalized predictive model for treatment free remission (TFR). I expect it will bring novel insights into the biology of TFR, opening new horizons toward the discovery of targeted therapies and improving TFR patient outcome."

APPLY FOR THE JOHN GOLDMAN AWARD 2020

Submitted projects must:

- aim to develop a method, algorithm or test to reliably identify patients able to benefit from treatment discontinuation, thereby significantly improving the probability of TFR success,
- demonstrate potential to improve healthcare standards for Chronic Myeloid Leukaemia (CML) patients or for patients suffering from other haematological malignancies.

The recipient of this annual award will receive a total of 80 000€ to finance or co-finance a research project on **Treatment Free Remission (TFR)**.

DEADLINE FOR SUBMISSION: MARCH 1, 2020

For further information: Didi.jasmin@univ-paris-diderot.fr
European School of Haematology (ESH)
Saint-Louis Research Institute, Saint-Louis Hospital, Paris 75010, France
www.esh.org

100-YEAR-OLD HAEMATOLOGICA IMAGES: ACUTE PROMYELOCYTIC LEUKEMIA

Carlo L. Balduini

Ferrata-Storti Foundation, Pavia, Italy

E-mail: CARLO L. BALDUINI, - carlo.balduini@unipv.it

doi:10.3324/haematol.2020.247056

Although the association of an exaggerated hemorrhagic syndrome with certain leukemias was described by French authors in 1949,¹ the identification of acute promyelocytic leukemia is unanimously attributed to the Norwegian hematologist LK Hillestad, who, in 1957, described three patients with a special type of acute myeloid leukemia characterized by 'a very rapid fatal course of only a few weeks' duration, a white blood cell picture dominated by promyelocytes, and a severe bleeding tendency due to fibrinolysis and thrombocytopenia.² He proposed giving this disease the name that is still used today.

The cover of this issue was taken from a picture (Figure 1) illustrating an article written in German, the dominant language in the scientific world at the beginning of the last century, and published in *Haematologica* in 1923.³ In this paper, entitled 'Über einen Fall akuter Promyelozytenleukämie' (On a case of acute promyelocytic leukemia), the Swiss hematologist Albert Alder described the case of a young woman who developed acute leukemia characterized by the abnormal proliferation of promyelocytes. The most relevant clinical features were an extremely serious hemorrhagic diathesis and the aggressiveness of the disease that led to death within eight weeks. Based on today's knowledge, the cytological characteristics of the leukemic cells shown in the figure suggest that the patient was affected by a microgranular variant of acute promyelocytic leukemia. This paper, therefore, indicates that the identification of acute promyelocytic leukemia occurred far earlier than commonly thought and has to be attributed to Alder, whose name has been so far known for the description of the Alder anomaly and Alder-Reilly granules in the cytoplasm of leukocytes in some forms of mucopolysaccharidosis.⁴

This ancient *Haematologica* paper is also remarkable for the drug given to the patient: arsenic. This treatment may seem surprising, since arsenic was only recognized in the 1990s as highly effective in the treatment of acute promyelocytic leukemia.⁵ Indeed, arsenic is a very ancient drug and the first information about its use dates back more than 2000 years.⁶ With regards to its antileukemic effect, it was described for the first time in 1878 in one patient with 'leucocythemia' admitted to the Boston City Hospital.⁷ Since then, arsenic was administered as a primary antileukemic agent for a long time until its replacement by radiation therapy and subsequently by modern chemotherapy. The treatment administered by Adler to his young patient was therefore probably the most commonly used substance at that time for subjects with leukemia.

References

1. Croizat P, Favre-Gilly J. Les aspects du syndrome hémorragique des leucémies. *Sang*. 1949;20(7):417-421.
2. Hillestad LK. Acute promyelocytic leukemia. *Acta Medical Scandinava*. 1957;159(3):189-194.
3. Alder A. Über einen Fall akuter Promyelozytenleukämie. *Haematologica*. 1923;4:423-427.
4. Alder A. Über konstitutionell bedingte Granulationsveränderungen der Leukocyten. *Dtsch Arch Klin Med*. 1939;183:372-378.
5. Zhang P, Wang SY, Hu XH. Arsenic trioxide treated 72 cases of acute promyelocytic leukemia. *Chin J Hematol*. 1996;17(2):58-62.
6. Klaassen CD. Heavy metals and heavy-metal antagonists. In: Hardman JG, Gilman AG, Limbird LE, eds. *Goodman & Gilman's The Pharmacological Basis of Therapeutics*. New York: McGraw-Hill, 1996:1649-1672.
7. Cutler EG, Bradford EH. Action of iron, cod-liver oil, and arsenic on the globular richness of the blood. *Am J Med Sci*. 1878;75:74-84.

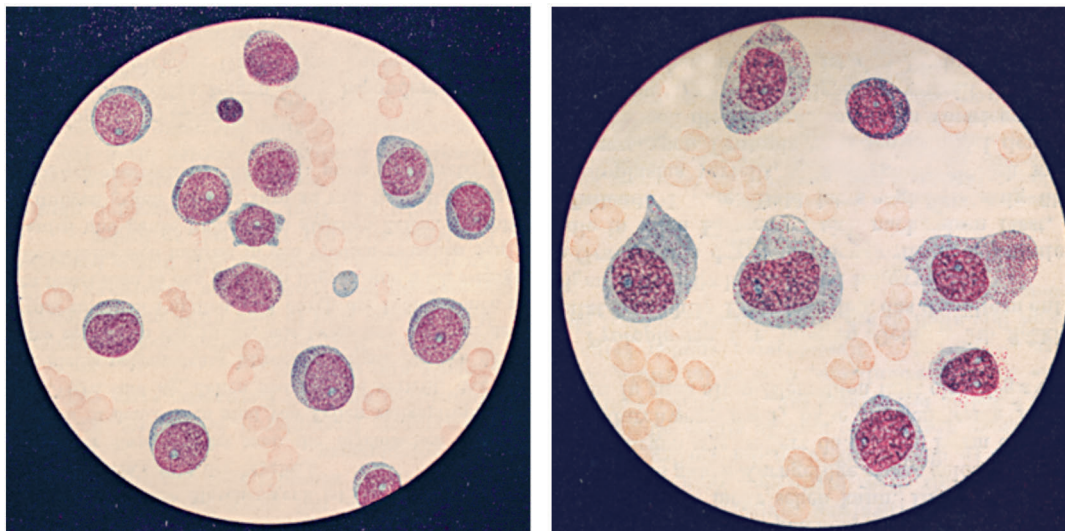


Figure 1. 'Leukemic blood with many promyelocytes and hemistioblasts (Ferrata cells)'. From the paper 'Über einen Fall akuter Promyelozytenleukämie' published by Alder in *Haematologica* in 1923.

Of mice, genes and aging.

James DeGregori

Department of Biochemistry and Molecular Genetics, University of Colorado Anschutz Medical Campus, Aurora, CO, USA

E-mail: JAMES DEGREGORI - james.degregori@cuanschutz.edu

doi:10.3324/haematol.2019.238683

Why do we get old? How much of aging is genetic? And in what genes? There is clearly a genetic basis of aging, as demonstrated from yeast to worms to humans.¹ As one example, different mouse strains have different potential lifespans. Much effort has been invested in understanding the genetic underpinnings of lifespan differences between the long-lived C57Bl/6 strain and the short-lived DBA/2 strain, with 50% mortality in captivity by 914 and 687 days, respectively.² Quantitative trait loci mapping in C57Bl/6 X DBA/2 (BXD) recombinant inbred strains identified a locus on chromosome 11 that is linked to lifespan, narrowing the trait conferring region to 18.6 Mb.³ These previous studies have also shown that the fraction of mouse hematopoietic stem and progenitor cells (HSPC) that lose function in response to hydroxyurea (HU) treatment is inversely correlated with lifespan across BXD strains, including for the chromosome 11 locus. In this issue of *Haematologica*, Brown *et al.* explored the genetic differences within this locus that contribute to both HU sensitivity and longevity.⁴

The authors show that a relatively small region on chromosome 11 is tightly linked to HU sensitivity of HSPC, as BXD recombinant strains that possessed this region displayed the high or low sensitivity of the DBA/2 or C57Bl/6 HSPC, respectively, even when almost all other genes were from the other strain. Previous work had demonstrated that this region suffices to confer the short or long lifespan of the donor strain.³ Notably, the authors demonstrated that HU sensitivity and longevity differences mediated by this locus did NOT coincide, surprisingly, with differences in cell cycling, telomere length, HSPC number, DNA damage responses, senescence or viability. Thus, simple explanations for HSPC sensitivity to HU, which could also account for earlier stem cell exhaustion and aging, such as increased cycling, impaired DNA damage responses or precocious senescence, do not appear to account for strain differences.

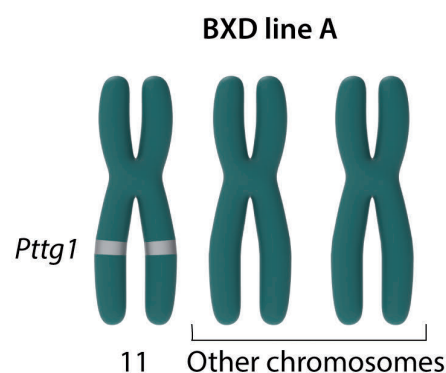
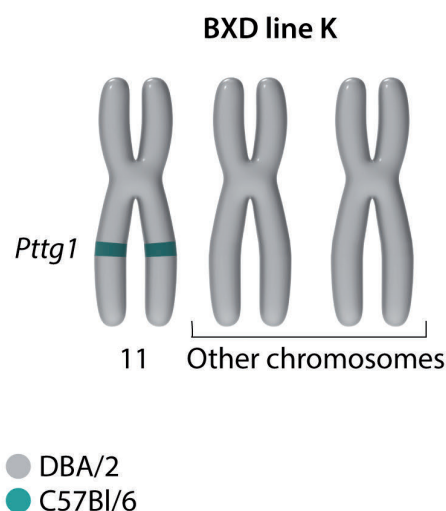
Their subsequent analyses revealed that this locus confers differential expression of the pituitary tumor-transforming gene-1 (*Pttg1*)/*Securin* gene, with substantially higher expression conferred by the DBA/2 locus. Interestingly, the yeast homolog of *Pttg1* is *Pds1p*, shown to regulate the intra-S-phase checkpoint and responses to HU in yeast,⁵ which is consistent with PTTG1 regulation of HU sensitivity. Also, intriguingly, PTTG1 is an inhibitor of separase, the cysteine protease that opens cohesin rings during the metaphase to anaphase transition, suggesting a role for PTTG1 in the cell cycle. Still, while PTTG1 overexpression has been shown to lower progression through S phase and increase senescence and DNA damage in human fibroblasts,⁶ Brown *et al.* demonstrate that these phenotypes are not observed to differ for HSPC from the congenic strains.⁴ Notably, genetic varia-

tion in *Pttg1* (together with other mitotic checkpoint genes) is associated with chromosomal aberrations in healthy humans.⁷ Given that inherited defects in genome stability often result in premature aging,⁸ PTTG1 level-dependent impacts on chromosomal segregation during mitosis could influence longevity.

They further demonstrate that the DBA/2 locus displays an apparent duplication that results in a longer promoter for the *Pttg1* gene, and this longer promoter confers greater transcriptional activity in reporter assays. Much of evolutionary change is associated with alterations of gene expression (without necessarily changing the activity of the encoded protein), involving mutations in cis-regulatory elements.⁹ The evolution of lifespan may similarly involve changes in gene expression, rather than the activity of the gene products. Finally, they showed that ectopic PTTG1 expression in C57Bl/6 HSPC to levels approximating those in DBA/2 cells was sufficient to increase their susceptibility to HU, and downregulation of PTTG1 in HSPC with the DBA/2 locus resulted in a trend towards reduced sensitivity to HU. While more research is needed, variation in the *Pttg1* gene is a strong candidate as a regulator of aging.

Previous studies have shown that CpG DNA methylation profiles across tissues for selected genes can be used as an aging clock, able to predict chronological age as well as “biological age” (a measure of physiological aging, and thus the risk of aging-associated diseases and death for older ages).¹⁰ These clocks have been extensively validated in humans, and epigenetic deviation from the age-average profile for one’s chronological age has been shown to predict various hallmarks of physiological aging including immunosenescence, diseases from cancer to heart disease to Alzheimer’s disease, frailty, and, grimly, time to death. Your clock-predicted biological age is determined by factors such as smoking status, diet, body mass index, exercise, and sleep. For C57Bl/6 mice, CpG sites within three genes have been shown to serve as markers of chronological aging,¹¹ with accelerated changes in methylation in DBA/2 mice coinciding with their reduced longevity. Here, the authors show similar accelerated aging in the congenic mice with the DBA/2 chromosome 11 locus in the C57Bl/6 background. Thus, the DBA/2 version of this locus is sufficient to promote epigenetic aging. While hypothetical, this could be more than an association - given roles for PTTG1 in chromosome cohesin, a known regulator of higher-order chromatin organization and gene expression profiles¹² important for stem cell and differentiation programs, differential expression of PTTG1 could lead to changes in these programs and thus the tissue maintenance which is critical for staying young.

Let’s consider our original question - why do we get old? - at an even higher level. Natural selection only acts



Traits

- HU resistant HSPC
- Longer lifespan
- Lower PTTG1

Traits

- HU sensitive HSPC
- Shorter lifespan
- Higher PTTG1

Figure 1. A small region on chromosome 11 determines hematopoietic stem and progenitor cells (HSPC) traits and lifespan. A simplified schema showing the K and A line BXD congenic mice that demonstrate that HSPC sensitivity to hydroxyurea (HU), lifespan and the expression levels of PTTG1 all map to a 18.6 Mb region on chromosome 11. Chromosomal regions of C57Bl/6 origin are shown in dark gray, and regions from DBA/2 are shown in blue. See Figure 1D of Brown *et al.*⁴ for a more accurate depiction of the congenic regions, as there are small contributions from the other strain on other regions of chromosome 11, with the 18.6 Mb region encompassing the shared overlap between the K and A congenic lines.

to promote longevity to the extent that it benefits the passage of genetic material to subsequent generations.¹³ Different animals have evolved different strategies for somatic maintenance that maximize reproductive success, and the extension of youth through additional investment in tissue maintenance would be disfavored if the costs (often manifested through reduced investment in reproduction) outweigh benefits. As concisely noted by George Williams,¹⁴ “natural selection may be said to be biased in favor of youth over old age whenever a conflict of interests arises.” For a small vulnerable animal like a field mouse that faces high extrinsic hazards (such as predation), natural selection has favored a “fast” life history – a breed early, breed often strategy with little investment in longevity. For larger animals like humans, elephants and whales, or for animals like tortoises, moles, bats and birds that have evolved other strategies to greatly reduce extrinsic hazards, natural selection has favored a “slow” life history, with greater and/or prolonged tissue maintenance leading to longer potential lifespans. While we understand how natural selection has shaped the pathways that control longevity, we know less about what these pathways actually are. Studies from model organisms have clearly demonstrated that modulation of the insulin-like growth factor-1 (IGF-1) pathway, which positively regulates the mTOR pathway and negatively regulates autophagy, can significantly impact longevity.^{1,15} Decreases in IGF-1 and mTOR, or increases in autophagy,

have been shown to prolong lifespans in organisms ranging from yeast to mammals. Additional studies have shown how inflammation can contribute to aging-associated phenotypes, and polymorphisms in genes controlling the IGF-1 pathway and inflammation are enriched in human centenarians,¹⁶ but the extent to which these polymorphisms and their impact on inflammation are contributing to differences in longevity has not been established.

While genetic screens in model organisms have revealed key pathways that regulate lifespan, the mechanisms employed by natural selection in the evolution of lifespans largely remain a mystery. Although one could argue that the selective breeding to generate different mouse strains over the last couple of centuries may not qualify as “natural” selection, the studies of Brown *et al.* reveal at least one potential (and novel) mediator of lifespan control. Key questions remain: Do variations in PTTG1 expression or activity contribute to lifespan differences across species, and perhaps within a species (including variability in the human population)? Would modulation of PTTG1 expression or activity promote the extension of healthspan or lifespan? How do activities known to modulate lifespan, such as dietary restriction and exercise, influence PTTG1 activity? Are there links between known aging pathways such as *via* IGF-1 and PTTG1? Good science generates good questions, leading to new insights (and sometimes even solutions). As a sen-

ior colleague once told me after I had told him that I worked on aging – “Hurry up”.

References

1. Kenyon CJ. The genetics of ageing. *Nature*. 2010;464(7288):504-512.
2. Yuan R, Peters LL, Paigen B. Mice as a mammalian model for research on the genetics of aging. *ILAR J*. 2011;52(1):4-15.
3. de Haan G, Bystrykh LV, Weersing E, et al. A genetic and genomic analysis identifies a cluster of genes associated with hematopoietic cell turnover. *Blood*. 2002;100(6):2056-2062.
4. Brown A, Schuetz D, Han Y, et al. The lifespan quantitative trait locus gene *Securin* controls hematopoietic progenitor cell function. *Haematologica*. 2019;105(2):317-324.
5. Schollaert KL, Poisson JM, Searle JS, Schwanekamp JA, Tomlinson CR, Sanchez Y. A role for *Saccharomyces cerevisiae* Chk1p in the response to replication blocks. *Mol Biol Cell*. 2004;15(9):4051-4063.
6. Hsu YH, Liao LJ, Yu CH, et al. Overexpression of the pituitary tumor transforming gene induces p53-dependent senescence through activating DNA damage response pathway in normal human fibroblasts. *J Biol Chem*. 2010;285(29):22630-22638.
7. Forsti A, Frank C, Smolkova B, et al. Genetic variation in the major mitotic checkpoint genes associated with chromosomal aberrations in healthy humans. *Cancer Lett*. 2016;380(2):442-446.
8. Zhang L, Vijg J. Somatic Mutagenesis in Mammals and Its Implications for Human Disease and Aging. *Annu Rev Genet*. 2018;52:397-419.
9. Prud'homme B, Gompel N, Carroll SB. Emerging principles of regulatory evolution. *Proc Natl Acad Sci U S A*. 2007;104(suppl 1):8605-8612.
10. Horvath S, Raj K. DNA methylation-based biomarkers and the epigenetic clock theory of ageing. *Nat Rev Genet*. 2018;19(6):371-384.
11. Han Y, Eipel M, Franzen J, et al. Epigenetic age-predictor for mice based on three CpG sites. *Elife*. 2018;7.
12. Ball AR Jr, Chen Y-Y, Yokomori K. Mechanisms of cohesin-mediated gene regulation and lessons learned from cohesinopathies. *Biochim Biophys Acta*. 2014;1839(3):191-202.
13. Kirkwood TB. Understanding the odd science of aging. *Cell*. 2005;120(4):437-447.
14. Williams GC. Pleiotropy, Natural Selection, and the Evolution of Senescence. *Evolution*. 1957;11:398-411.
15. van Heemst D. Insulin, IGF-1 and longevity. *Aging Dis*. 2010;1(2):147-157.
16. Franceschi C, Olivieri F, Marchegiani F, et al. Genes involved in immune response/inflammation, IGF1/insulin pathway and response to oxidative stress play a major role in the genetics of human longevity: the lesson of centenarians. *Mech Ageing Dev*. 2005;126(2):351-361.

Hypo, Hyper, or Combo: new paradigm for treatment of acute myeloid leukemia in older people

Gunnar Juliusson,¹ Martin Höglund² and Sören Lehmann^{2,3}

¹Department of Hematology, Skåne University Hospital, Lund, and Department of Hematology, Stem Cell Center, Department of Laboratory Medicine, Lund University, Lund; ²Department of Medical Sciences, Uppsala University, Uppsala and ³Department of Medicine, Karolinska Institute, Stockholm, Sweden

E-mail: GUNNAR JULIUSSON - gunnar.juliusson@med.lu.se

doi:10.3324/haematol.2019.238857

Acute myeloid leukemia (AML)¹ is a serious disease. Using the combination of cytarabine and daunorubicin developed during the 1970s,² with or without subsequent allogeneic stem cell transplantation (alloSCT),³ we now cure more than half of all patients with *de novo* AML up to the age of 60 years.⁴ But the outcome of older patients, that constitute the vast majority, remains dismal. The median age of AML is over 70 years,⁵ and the 3-year overall survival (OS) of patients aged 70-84 years is still less than 20% with intensive chemotherapy, and much worse in AML arising after myelodysplastic syndrome (MDS) or myeloproliferative neoplasia (MPN),^{5,7} or with palliative treatment only.⁵ However, new treatment options are finally emerging.¹

In this issue of *Haematologica*, Talati *et al.* present a large (n=980), retrospective, single-center study on AML patients aged 70 years and older diagnosed between 1995 and 2016.⁸ Intensive combination chemotherapy was given to 37%, hypomethylating agents (HMA) to 26%, and other low-intensity or palliative treatment to 37%. It is well established that specific AML therapy provides better outcome than palliation only.^{5,9} However, in this study, better survival rates were observed with HMA treatment than with intensive therapy (median 14.4 months vs. 10.8 months; *P*=0.004).

The currently approved HMA, 5-azacitidine (Aza) and decitabine (Dec, 5-aza-2'-deoxycytidine) are analogs of the natural pyrimidine cytidine. Dec incorporates into DNA while Aza mainly incorporates into RNA, and to a lesser extent into DNA (Figure 1). DNA incorporation causes hypomethylation by irreversible inhibition of DNA methyl transferases (DNMT) and upregulation of tumor suppressor genes, but it also leads to induction of DNA damage response.¹⁰ The cytotoxic effects are more evident at higher doses while hypomethylation seems to dominate at lower drug concentrations.¹¹ Incorporation

into RNA leads to inhibition of transfer RNA methylation, ultimately resulting in impaired messenger RNA transcription and protein synthesis.^{10,12} In addition, HMA have been shown to affect the immune system in various ways, such as upregulation of tumor antigens and induction of viral defense systems through upregulation of endogenous retroviruses.^{10,13} Intriguingly, it is still unclear what mechanisms are mostly responsible for the clinical effects of HMA in AML.

Aza and Dec were both synthesized in 1964, and biological activity was shown in mice. Clinical trials started in the 1970s.¹⁴ Initially, the maximal tolerated doses of Dec (1.5-2.5 g/m²/course) were tested with clinical activity but resulted in prolonged cytopenia.¹⁵ Subsequently de-escalated doses to the currently recommended 100-150 mg/m²/course of Dec or 525 mg/m²/course of Aza became used for treatment of MDS, for which the US Food and Drug Administration (FDA) in 2004 approved Aza and in 2006 approved Dec. At the time of these studies, the diagnosis entity MDS included patients with bone marrow blasts up to 30%. When MDS with 20-30% blasts were later reclassified as AML,¹⁶ HMA was approved also for AML with low blast counts.¹⁷ Studies in AML with >30% blasts then started,¹⁸ leading to approval in 2015 of Aza for all patients with AML not eligible for intensive treatment.

The present study by Talati *et al.*⁸ confirms the activity of HMA in older patients and is the first to show improved survival with HMA in AML patients aged 70 years and older as compared to intensive treatment, in contrast to other studies¹⁹⁻²² (Table 1 and Figure 1). However, this discrepancy might be of limited importance, for two reasons. Firstly, in clinical practice, we should try to find the optimal therapy for each individual patient, rather than 'one treatment fits all'. Secondly, rapidly emerging therapeutic options may well replace

Table 1. Survival of older acute myeloid leukemia patients with hypomethylating or intensive treatment.

	Study type	Age (years)		Number		Median OS (months)		1-year OS (%)	
		Range	Median	HMA	Intensive	HMA	Intensive	HMA	Intensive
Talati 2019 ⁸	Single	≥70	75	231	305	14.4	10.8	55	43
Dombret 2015 ¹⁸	RCT	≥65	71	43	44	13.3	12.2	56	51
Quintas-Cardama 2012 ¹⁹	Single	≥65	74	557	114	6.5	6.7	31	34
Pleyer 2017 ²⁰	Registry	≥65	77	193	NA	11.8	NA	51	NA
Kantarjian 2012 ²⁷	RCT	≥65	73	242	NA	7.7	NA	27	NA
Sw AML Reg 2012-2018	Registry	≥70	75	276	532	8.5	11.1	36	46

OS: overall survival; HMA: hypomethylating agents; NA: not assessed; Single: single-center study; RCT: multicenter randomized clinical study; Sw AML Reg: Swedish AML Registry, including patients diagnosed from 2012, with survival data updated in September 2019.

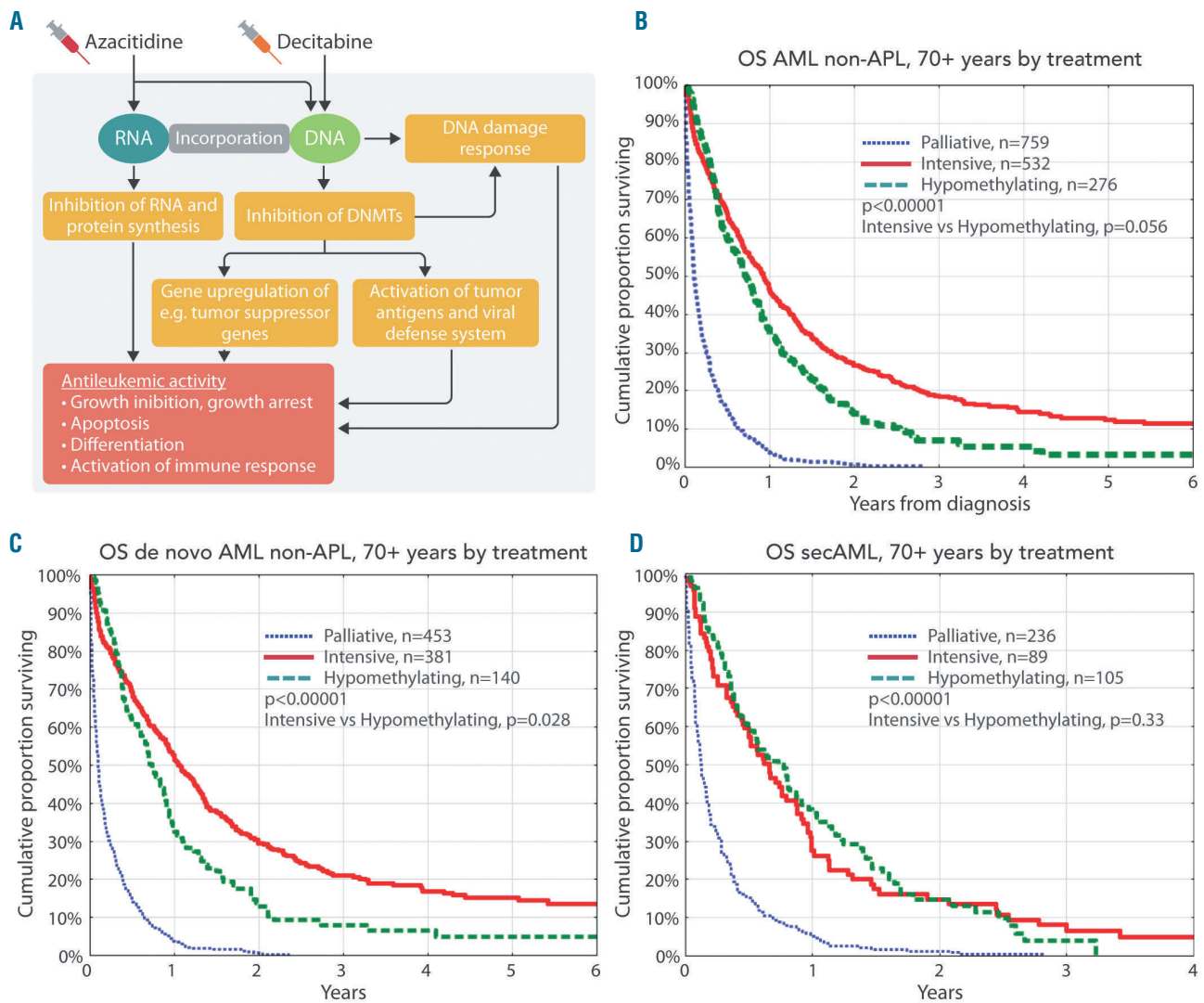


Figure 1. Mechanisms of action of hypomethylating agents, and overall survival of Swedish patients 70 years and older by treatment. (A) Mechanism of action for treatment with hypomethylating agents (HMA). DNA methyl transferases (DNMT). (B) Overall survival (OS) according to therapy. Acute promyelocytic leukemia is excluded (non-APL). All patients 70 years and older. HMA versus intensive treatment; $P=0.056$. (C) *de novo* acute myeloid leukemia (AML). HMA versus intensive treatment; $P=0.028$. (D) AML secondary to previous myelodysplastic syndromes (MDS), myeloproliferative neoplasia (MPN) or chemo-radiotherapy (secAML). HMA versus intensive treatment; $P=0.33$.

monotherapy in the near future.

Intensive AML treatment is toxic and requires massive supportive care and long-term hospitalization. Older patients with comorbidity may not tolerate this, even though half of the selected older patients achieve complete remission from intensive treatment,⁵ and mostly so within one month. Response to HMA is less frequent and often takes much longer to achieve, but is usually well manageable in the outpatient department. The role of intensive consolidation and maintenance has still not been determined, and HMA may serve as maintenance also after intensive chemotherapy.²³ Importantly, subsets of AML respond well to intensive treatment, whereas patients with secondary AML and/or complex or MDS-like genetics do poorly with chemotherapy^{5,7} (Figure 1), and such patients are better off with HMA. Responding patients may be eligible for alloSCT as a curative

approach, whether response was achieved from intensive treatment or from HMA.

Clinical and academic studies always introduce patient selection, and the interpretation of retrospective non-randomized trials should include consideration of potential differences in the actual management of different patient subsets. This problem can be overcome in part by assessing patients' characteristics, prognostic factors and propensity score matching. The Talati *et al.* study includes a large number of patients diagnosed since 1995, i.e. some of them were treated as part of the early development of HMA.⁸ However, results were similar when comparing outcome for patients diagnosed before and after 2005. What is striking is that half the Moffitt Cancer Center patients had prior MDS (some also had prior HMA treatment), as compared to 18% in the AML-001 study,¹⁸ 25% in the Austrian registry study,²⁰ 12% in the Danish popu-

lation-based study including all ages,⁶ and 28% of patients aged ≥ 70 years given AML-specific treatment according to the Swedish AML Registry.^{4,5} Still, the Talati *et al.* study had the best reported median survival with HMA and is the only study so far to show better survival with HMA than with intensive treatment (Table 1).⁸

The therapeutic options for AML in older people are now rapidly expanding, including oral targeted drugs with low toxicity, such as kinase inhibitors with activity in AML with *FLT3*-mutations, oral inhibitors of *IDH*-mutations, and many more.¹ These drugs have been shown to be active as monotherapy, and some are already approved by the FDA. However, both theory and practice indicate synergistic effects of combining drugs with different modes of action. Clinical studies are, therefore, rapidly moving towards regimens with HMA used as backbone therapy, comparing monotherapy with add-on of further drugs, of which there are several. Expectations are high from the combination of HMA with the BCL2-inhibitor venetoclax, that has resulted in very high complete remission (CR) rates (67% CR + CR with incomplete blood count recovery) and a median overall survival of 17.5 months when used as primary treatment of older AML patients (median 74 years),²⁴ although real-world response rates were somewhat lower.²⁵ (The outcome of the phase III study with Aza + venetoclax/placebo may be presented in 2020.) Furthermore, an oral analog of Aza (CC-486) has recently been reported to be effective to maintain remission from AML.²⁶ We thus expect numerous studies evaluating HMA-based new combinations, and all-oral limited-toxicity treatments are within sight.

In summary, traditional combination chemotherapy with or without the addition of targeted therapies is likely to keep its role for years to come for many patients without severe comorbidity up to the age of around 75 years. However, patients with secondary AML and/or high-risk genetics should now already be offered less toxic HMA-based therapies, preferably as part of one of the many ongoing clinical trials, in order to expand our clinical armamentarium as quickly as possible.

References

- Döhner H, Estey E, Grimwade D, et al. Diagnosis and management of AML in adults: 2017 ELN recommendations from an international expert panel. *Blood*. 2017;129(4):424-447.
- Yates JW, Wallace HJ Jr, Ellison RR, Holland JF. Cytosine arabinoside (NSC-63878) and daunorubicin (nsc-83142) therapy in nonlymphocytic leukemia. *Cancer Chemother Rep*. 1973;57(4):485-488.
- Cornelissen JJ, Gratwohl A, Schlenk RF, et al. The European LeukemiaNet AML Working Party consensus statement on allogeneic HSCT for patients with AML in remission: an integrated-risk adapted approach. *Nat Rev Clin Oncol*. 2012;9(10):579-590.
- Juliusson G, Hagberg O, Lazarevic VL, et al. Improved survival of men 50-75 years old with acute myeloid leukemia over a 20-year period. *Blood*. 2019;134(18):1558-1561.
- Juliusson G, Antunovic P, Derolf A, et al. Age and acute myeloid leukemia: real world data on decision to treat and outcomes from the Swedish Acute Leukemia Registry. *Blood*. 2009;113(18):4179-4187.
- Granfeldt Östgård LS, Medeiros BC, Sengelöv H, et al. Epidemiology and clinical significance of secondary and therapy-related acute myeloid leukemia: a national population-based cohort study. *J Clin Oncol*. 2015;33(31):3641-3649.
- Hulegårdh E, Nilsson C, Lazarevic V, et al. Characterization and prognostic features of secondary acute myeloid leukemia in a population-based setting: a report from the Swedish Acute Leukemia Registry. *Am J Hematol*. 2015;90(3):208-214.
- Talati C, Dhulipala VC, Extermann M, et al. Comparisons of commonly used frontline regimens on survival outcomes in patients age 70 years and older with acute myeloid leukemia. *Haematologica*. 2020;105(2):398-406.
- Oran B, Weisdorf DJ. Survival for older patients with acute myeloid leukemia: a population-based study. *Haematologica*. 2012;97(12):1916-1924.
- Diesch J, Zwick A, Garz AK, Palau A, Buschbeck M, Götze KS. A clinical-molecular update on azanucleoside-based therapy for the treatment of hematologic cancers. *Clin Epigenetics*. 2016;8:71.
- Saiki JH, Bodey GP, Hewlett JS, et al. Effect of schedule on activity and toxicity of 5-azacytidine in acute leukemia: a SWOG study. *Cancer*. 1981;47(7):1739-1742.
- Bohl SR, Bullinger L, Rücker FG. Epigenetic therapy: azacytidine and decitabine in acute myeloid leukemia. *Expert Rev Hematol*. 2018;11(5):361-371.
- Chiappinelli KB, Strissel PL, Desrichard A, et al. Inhibiting DNA Methylation Causes an Interferon Response in Cancer via dsRNA Including Endogenous Retroviruses. *Cell*. 2015;162(5):974-986.
- Von Hoff DD, Slavik M, Muggia FM. 5-azacytidine. A new anticancer drug with effectiveness in acute myelogenous leukemia. *Ann Intern Med*. 1976;85(2):237-245.
- Jabbour E, Issa JP, Garcia-Manero G, Kantarjian H. Evolution of Decitabine. Development Accomplishments, Ongoing Investigations, and Future Strategies. *Cancer*. 2008;112(11):2341-2351.
- Vardiman JW, Harris NL, Brunning RD. The World Health Organization (WHO) classification of the myeloid neoplasms. *Blood*. 2002;100(7):2292-2302.
- Fenaux P, Mufti GJ, Hellström-Lindberg E, et al. Azacytidine prolongs overall survival compared with conventional care regimens in elderly patients with low bone marrow blast count acute myeloid leukemia. *J Clin Oncol*. 2010;28(4):562-569.
- Dombret H, Seymour JF, Butrym A, et al. International phase 3 study of azacytidine vs conventional care regimens in older patients with newly diagnosed AML with $>30\%$ blasts. *Blood*. 2015;126(3):291-299.
- Quintas-Cardama A, Ravandi F, Liu-Dumlao T, et al. Epigenetic therapy is associated with similar survival compared with intensive chemotherapy in older patients with newly diagnosed acute myeloid leukemia. *Blood*. 2012;120(24):4840-4845.
- Pleyer L, Döhner H, Dombret H, et al. Azacitidine for front-line therapy of patients with AML: reproducible efficacy established by direct comparison of international phase 3 trial data with registry data from the Austrian Azacytidine Registry of the AGMT study group. *Int J Mol Sci*. 2017;18(2):E415.
- Schuh AC, Döhner H, Pleyer L, Seymour JF, Fenaux P, Dombret H. Azacitidine in adult patients with acute myeloid leukemia. *Crit Rev Oncol Hematol*. 2017;116:159-177.
- Österros A, Eriksson A, Antunovic P, et al. Real-world data on treatment patterns and outcomes of hypomethylating therapy in newly diagnosed acute myeloid leukemia >60 years. *Br J Haematol*. 2020; doi: 10.1111/bjh.16410.
- Huls G, Chitu DA, Havelange V, et al. Azacitidine maintenance after intensive chemotherapy improves DFS in older AML patients. *Blood*. 2019;133(13):1457-1464.
- DiNardo CD, Pratz K, Pullarkat V, et al. Venetoclax combined with decitabine or azacytidine in treatment-naïve, elderly patients with acute myeloid leukemia. *Blood*. 2019;133(1):7-17.
- Winters AC, Gutman JA, Purev E, et al. Real-world experience of venetoclax with azacitidine for untreated patients with acute myeloid leukemia. *Blood Adv*. 2019;3(20):2911-2919.
- Wei AH, Döhner H, Pocock C, et al. The QUAZAR AML-001 Maintenance Trial: Results of a Phase III International, Randomized, Double-Blind, Placebo-Controlled Study of CC-486 (Oral Formulation of Azacitidine) in Patients with Acute Myeloid Leukemia (AML) in First Remission. *Blood*. 2019;134:Supplement_2: LBA-3.
- Kantarjian HM, Thomas XG, Dmoszynska A, et al. Multicenter, randomized, open-label, phase III trial of decitabine versus patient choice, with physician advice, of either supportive care or low-dose cytarabine for the treatment of older patients with newly diagnosed acute myeloid leukemia. *J Clin Oncol*. 2012;30(21):2670-2677.

Is unrelated donor or haploidentical hematopoietic transplantation preferred for patients with acute myeloid leukemia in remission?

Richard Champlin

University of Texas, MD Anderson Cancer Center, Houston, TX, USA

E-mail: RICHARD CHAMPLIN - rchampli@mdanderson.org

doi:10.3324/haematol.2019.239624

In this issue, Perales *et al.*¹ address a controversy in hematopoietic stem cell transplantation: should an HLA-matched unrelated donor or haploidentical transplant be performed for patients who lack a matched sibling?

The preferred donor for allogeneic hematopoietic transplantation is an HLA-matched sibling. For several decades, an unrelated donor transplant has been considered the next option if an HLA-matched donor can be identified; survival after matched related and matched unrelated donor transplants has been similar in most studies.^{2,3} A large worldwide network of unrelated donor registries has been established. Patients are most likely to have an HLA-matched donor among individuals with their same racial and ethnic origin. Matches can be found for about 60% of Caucasians, but only 30% for other ethnicities, primarily due to the racial composition of the existing donor registries.⁴ Some patients have a common HLA haplotype and have hundreds of matched donors, but at least half have rare or unique haplotypes and a matched unrelated donor cannot be found. Transplant outcomes have been best with younger unrelated donors, and males under the age of 40 are generally considered the preferred donors.^{5,6}

The effective development of haploidentical hematopoietic stem cell transplantation (haploHSCT) has been a major therapeutic advance.⁷ The use of post-transplant cyclophosphamide, tacrolimus and mycophenolate mofetil has reduced the rates of acute and chronic graft-versus-host disease (GvHD) with haploHSCT to below the levels reported with matched unrelated donor transplants, and with similar overall survival (OS).⁸ Haploidentical transplantation using this approach is now an established treatment option and is provided by transplant centers around the world.

The success of haploHSCT has led many to consider use of a haploidentical donor, even if a matched unrelated donor is potentially available.⁹ The study reported by Perales *et al.*¹ is a retrospective analysis conducted by the Center for Blood and Marrow Transplantation Research which compares the results of transplants from a young HLA-matched unrelated donor with haploidentical transplants from a sibling or child, in patients with acute myeloid leukemia (AML) in first or second complete remission. They analyzed 822 patients aged 50-75 years; 192 patients received haploidentical transplants and 631 patients had grafts from matched unrelated donors aged 18-40 years. Patients' and disease characteristics of the two groups were similar except unrelated donor recipients were more likely to have poor risk cytogenetics and to receive a myeloablative conditioning regimens. Post-transplant cyclophosphamide based GvHD prophylaxis was used in all patients receiving haploHSCT but none of the unrelated donor transplants. Five-year OS was 32% and

42% after haploHSCT and unrelated donor transplant, respectively ($P=0.04$). Multivariable analysis showed improved survival and a lower risk of leukemia relapse after matched unrelated donor transplantation, with a similar risk of non-relapse mortality with either approach. They concluded that matched unrelated donor transplantation with donors younger than 40 years is preferred.

Large registry analyses have reported similar outcomes of haploidentical transplants with those from matched unrelated donors,⁸ but comparison of haploHSCT and unrelated donor transplants is complicated. Different preparative and GvHD prophylaxis regimens are generally used. Haploidentical transplants are more likely to be rejected than HLA-matched transplants, and most centers have used reduced intensity regimens in older adult patients, but intensified the preparative regimen to include low-dose total body irradiation (TBI) or thiotepa to prevent rejection.

The study by Perales *et al.*¹ has several limitations due to imbalances in the treatment groups. The primary advantage for the unrelated donor group was a reduced rate of leukemia relapse. Myeloablative conditioning produces a lower rate of leukemia relapse than reduced intensity conditioning (RIC) in HLA-matched^{10,11} as well as haploidentical recipients with AML.¹² The unrelated donor group predominantly received myeloablative conditioning, while the haploHSCT group mainly received a reduced intensity regimen with the cyclophosphamide fludarabine low-dose TBI regimen¹³ which is associated with a higher relapse rate than has been reported with other, more intensive, RIC regimens.¹⁴ Other retrospective studies have not reported higher relapse rates with haploHSCT compared to unrelated transplants.^{15,16} Use of a more intensive conditioning in the haploHSCT group may have potentially reduced relapse, but may also have increased non-relapse mortality.

The haploHSCT group had a lower rate of acute and chronic GvHD compared to the unrelated donor group. This is undoubtedly due to the use of post-transplant cyclophosphamide, tacrolimus and mycophenolate mofetil GvHD prophylaxis in the haploHSCT patients; this regimen is now being used for unrelated donor transplants as well, with improvement in control of GvHD.¹⁷⁻²⁰ A formal comparison of post-transplant cyclophosphamide, tacrolimus and mycophenolate mofetil with tacrolimus methotrexate GvHD prophylaxis for unrelated donor transplants is in progress by the Blood and Marrow Transplant Clinical Trials Network.

Advantages and disadvantages of haploidentical hematopoietic stem cell transplantation versus unrelated donor transplantation

Haploidentical donors are identified by the initial family HLA typing so haploHSCT can be performed immedi-

Table 1. Consideration for haploidentical versus unrelated donor transplants.

Haploidentical transplants
• Most (but not all) patients have a haploidentical donor
• Transplants can be performed immediately after family typing
• Transplant center controls the donor and all aspects of the transplant co-ordinates
• Preparative regimens are generally intensified with TBI or thiotepa to prevent rejection
• There is a low rate of severe acute GvHD and chronic GvHD with post transplant cyclophosphamide based GvHD prophylaxis
• Donor specific anti HLA antibodies may produce graft failure; must exclude patients with high titers
• Hemorrhagic cystitis and cardiac toxicity of cyclophosphamide may occur
• There is a longer time to hematologic recovery
HLA matched unrelated donor transplants
• HLA match can be identified for many patients, chance of success depends on race/ethnicity
• Established treatment modality; long track record
• Generally uses same preparative regimen and GvHD prophylaxis as matched related transplants
• Requires time for search process, coordination of the transplant with donor registries; patients may deteriorate during this time; may need to accommodate delays for intercurrent patient or donor problems
• One can often avoid donor specific anti HLA antibodies

GvHD: graft-versus-host disease; TBI: total body irradiation.

ately, without a need to wait for an unrelated donor search. The process for performing the unrelated donor search to identify the donor and deliver the transplant typically takes 2-4 months, although donor registries are working to develop procedures that would shorten this process. This study involved AML patients in first or second remission, which can generally accommodate the time needed to organize an unrelated donor transplant. In more urgent clinical situations, like advanced acute leukemia, precarious patients may progress, clinically deteriorate, or acquire serious infections during the unrelated donor search and never receive a transplant. Often, the patient may develop medical complications that require the unrelated donor transplant to be rescheduled, which can be logistically challenging at short notice. If a prompt transplant is required and a matched unrelated donor is not immediately identified and available, it is appropriate to go forward with a haploHSCT.

Haploidentical transplants with post-transplant cyclophosphamide do have some special toxicities to consider. Hemorrhagic cystitis is a common complication and can be severe.²¹ Cyclophosphamide can produce cardiac toxicity, particularly in those with pre-existing cardiac disease. The patient must have adequate renal function to safely tolerate post-transplant cyclophosphamide. Post-transplant cyclophosphamide does delay time to engraftment and hematologic recovery. Use of peripheral blood stem cells for haploidentical transplants accelerates hematopoietic recovery, but with an increased risk of GvHD.²²

There are patients who lack an acceptable haploidentical donor, and an unrelated donor or cord blood is their only transplant option. These are typically older adults without healthy siblings or children. Cousins or other second-degree relatives who share a haplotype can be utilized for haploHSCT for these patients.

There are some advantages with unrelated donor transplants. It is a well established treatment modality with

over 30 years of experience. A general principle of transplantation is that better matching is associated with intrinsically less alloreactivity and better transplant outcomes. One problem with haploidentical transplants is graft failure due to donor specific anti-HLA antibodies (DSA), particularly if positive by the C1q assay.^{23,24} Diffuse sensitization can be induced by blood transfusions, with high titer anti-HLA antibodies against a broad range of HLA antigens, primarily in parous female recipients. It is often impossible to identify a haploidentical donor without DSA for these individuals, and patients with high levels of DSA are appropriately excluded from trials of haploHSCT. Engraftment is not affected by anti-HLA antibodies that are not donor specific. Often, an HLA-matched or one antigen mismatched unrelated donor can be identified, avoiding donor specific antibodies, in broadly sensitized patients. Note, unrelated donor transplants matched for HLA A, B, C, DR and DQ are generally mismatched at DP, and anti-DP antibodies may be present which may lead to graft failure.²⁵

In conclusion, the study by Perales *et al.*¹ reports that matched unrelated donor transplants with donors younger than 40 years of age is preferred to haploHSCT for patients with AML in complete remission, with improved survival and lower risk of relapse. That may be true for this relatively stable patient population using the preparative and GvHD prophylaxis regimens employed, but this conclusion may not hold for other patient populations where a prompt time to transplant is critical, or with alternative pre- and post-transplant treatment regimens. The ideal study would compare optimized versions of both haploidentical and unrelated donor transplants, and use "intention-to-treat" analysis including all patients for whom a transplant is intended from the time of initial HLA typing. The study by Perales *et al.*¹ should give pause for thought, however, for those considering jumping to haploidentical transplants as a preferred approach in general.

References

- Perales MA, Tomlinson B, Zhang MJ, et al. Alternative donor transplantation for acute myeloid leukemia in patients aged ≥ 50 years: young HLA-matched unrelated or haploidentical Donor? *Haematologica*. 2019;105(2):407-413.
- Weisdorf DJ, Anasetti C, Antin JH, et al. Allogeneic bone marrow transplantation for chronic myelogenous leukemia: comparative analysis of unrelated versus matched sibling donor transplantation. *Blood*. 2002;99(6):1971-1977.
- Gupta V, Tallman MS, He W, et al. Comparable survival after HLA-well-matched unrelated or matched sibling donor transplantation for acute myeloid leukemia in first remission with unfavorable cytogenetics at diagnosis. *Blood*. 2010;116(11):1839-1848.
- Gragert L, Eapen M, Williams E, et al. HLA match likelihoods for hematopoietic stem-cell grafts in the U.S. registry. *N Engl J Med*. 2014;371(4):339-348.
- Kollman C, Spellman SR, Zhang MJ, et al. The effect of donor characteristics on survival after unrelated donor transplantation for hematologic malignancy. *Blood*. 2016;127(2):260-267.
- Shaw BE, Logan BR, Spellman SR, et al. Development of an Unrelated Donor Selection Score Predictive of Survival after HCT: Donor Age Matters Most. *Biol Blood Marrow Transplant*. 2018;24(5):1049-1056.
- Luznik L, O'Donnell PV, Symons HJ, et al. HLA-haploidentical bone marrow transplantation for hematologic malignancies using non-myeloablative conditioning and high-dose, posttransplantation cyclophosphamide. *Biol Blood Marrow Transplant*. 2008;14(6):641-650.
- Ciurea SO, Zhang MJ, Bacigalupo AA, et al. Haploidentical transplant with posttransplant cyclophosphamide vs matched unrelated donor transplant for acute myeloid leukemia. *Blood*. 2015;126(8):1033-1040.
- Ciurea SO, Bittencourt MCB, Milton DR, et al. Is a matched unrelated donor search needed for all allogeneic transplant candidates? *Blood Adv*. 2018;2(17):2254-2261.
- Eapen M, Brazauskas R, Hemmer M, et al. Hematopoietic cell transplant for acute myeloid leukemia and myelodysplastic syndrome: conditioning regimen intensity. *Blood Adv*. 2018;2(16):2095-2103.
- Scott BL, Pasquini MC, Logan BR, et al. Myeloablative Versus Reduced-Intensity Hematopoietic Cell Transplantation for Acute Myeloid Leukemia and Myelodysplastic Syndromes. *J Clin Oncol*. 2017;35(11):1154-1161.
- Solomon SR, St Martin A, Shah NN, et al. Myeloablative vs reduced intensity T-cell-replete haploidentical transplantation for hematologic malignancy. *Blood Adv*. 2019;3(19):2836-2844.
- Kasamon YL, Bolanos-Meade J, Prince GT, et al. Outcomes of Nonmyeloablative HLA-Haploidentical Blood or Marrow Transplantation With High-Dose Post-Transplantation Cyclophosphamide in Older Adults. *J Clin Oncol*. 2015;33(28):3152-3161.
- Ciurea SO, Shah MV, Saliba RM, et al. Haploidentical Transplantation for Older Patients with Acute Myeloid Leukemia and Myelodysplastic Syndrome. *Biol Blood Marrow Transplant*. 2018;24(6):1232-1236.
- Bashey ZA, Zhang X, Brown S, et al. Comparison of outcomes following transplantation with T-replete HLA-haploidentical donors using post-transplant cyclophosphamide to matched related and unrelated donors for patients with AML and MDS aged 60 years or older. *Bone Marrow Transplant*. 2018;53(6):756-763.
- Nagler A, Ruggeri A. Haploidentical stem cell transplantation (HaploSCT) for patients with acute leukemia-an update on behalf of the ALWP of the EBMT. *Bone Marrow Transplant*. 2019;54(Suppl 2):713-718.
- Mielcarek M, Furlong T, O'Donnell PV, et al. Posttransplantation cyclophosphamide for prevention of graft-versus-host disease after HLA-matched mobilized blood cell transplantation. *Blood*. 2016;127(11):1502-1508.
- El Fakih R, Hashmi SK, Ciurea SO, Luznik L, Gale RP, Aljurf M. Post-transplant cyclophosphamide use in matched HLA donors: a review of literature and future application. *Bone Marrow Transplant*. 2019 May 14. [Epub ahead of print]
- Mehta RS, Saliba RM, Chen J, et al. Post-transplantation cyclophosphamide versus conventional graft-versus-host disease prophylaxis in mismatched unrelated donor haematopoietic cell transplantation. *Br J Haematol*. 2016;173(3):444-455.
- Rashidi A, Hamadani M, Zhang MJ, et al. Outcomes of haploidentical vs matched sibling transplantation for acute myeloid leukemia in first complete remission. *Blood Adv*. 2019;3(12):1826-1836.
- Copelan OR, Sanikommu SR, Trivedi JS, et al. Higher Incidence of Hemorrhagic Cystitis Following Haploidentical Related Donor Transplantation Compared with Matched Related Donor Transplantation. *Biol Blood Marrow Transplant*. 2019;25(4):785-790.
- Bashey A, Zhang MJ, McCurdy SR, et al. Mobilized Peripheral Blood Stem Cells Versus Unstimulated Bone Marrow As a Graft Source for T-Cell-Replete Haploidentical Donor Transplantation Using Post-Transplant Cyclophosphamide. *J Clin Oncol*. 2017;35(26):3002-3009.
- Ciurea SO, Thall PF, Milton DR, et al. Complement-Binding Donor-Specific Anti-HLA Antibodies and Risk of Primary Graft Failure in Hematopoietic Stem Cell Transplantation. *Biol Blood Marrow Transplant*. 2015;21(8):1392-1398.
- Ciurea SO, de Lima M, Cano P, et al. High risk of graft failure in patients with anti-HLA antibodies undergoing haploidentical stem-cell transplantation. *Transplantation*. 2009;88(8):1019-1024.
- Spellman S, Bray R, Rosen-Bronson S, et al. The detection of donor-directed, HLA-specific alloantibodies in recipients of unrelated hematopoietic cell transplantation is predictive of graft failure. *Blood*. 2010;115(13):2704-2708.

BIRC3 mutations in chronic lymphocytic leukemia – uncommon and unfavorable

Eugen Tausch and Stephan Stilgenbauer

Department of Internal Medicine III, Ulm University, Ulm, Germany

E-mail: STEPHAN STILGENBAUER - stephan.stilgenbauer@uniklinik-ulm.de

doi:10.3324/haematol.2019.238691

Chronic lymphocytic leukemia (CLL) is characterized by recurrent genomic aberrations as well as gene mutations, and *BIRC3* (Baculoviral IAP Repeat Containing 3, also called *IAP2*) can be affected by both. *BIRC3* is located on chromosome 11 in proximity to *ATM* and 11q deletions include the *BIRC3* locus in approximately 80% of cases.¹ In addition, *BIRC3* can be affected by mutations, mainly nonsense and frameshift variants, with an incidence of 3-5% in untreated patients, making such mutations rare in comparison to *TP53*, *NOTCH1*, *SF3B1* or *ATM* defects.¹⁻⁵ However, as the frequency in fludarabine-refractory cohorts is higher, *BIRC3* abnormalities were discussed to define a high-risk group of CLL patients. Indeed *BIRC3* did turn out to have an adverse prognostic impact in some chemotherapy-treated CLL cohorts.^{1,6} Furthermore, *BIRC3* abnormalities are associat-

ed with worse outcome in other lymphomas, acute lymphoblastic leukemia and solid tumors, including brain tumors in which *BIRC3* is reported to induce malignant transformation of low-grade gliomas to glioblastomas.⁶⁻⁸

While some studies have provided evidence of a clinical impact of mutated *BIRC3* and others have not, the functional implications of *BIRC3* deletion or mutation are partially unexplored. *BIRC3* induces proteasomal degradation of MAP3K14, which is the major driver of non-canonical nuclear factor kappaB (NFκB) activation. Therefore, disrupted *BIRC3* could result in a ligand-independent activation of the constitutive NFκB pathway, inducing cell proliferation and survival.^{7,8} At this point Diop and colleagues began their functional characterization of *BIRC3* mutations in CLL as described in this issue of *Haematologica*.⁹ First they confirmed the importance of

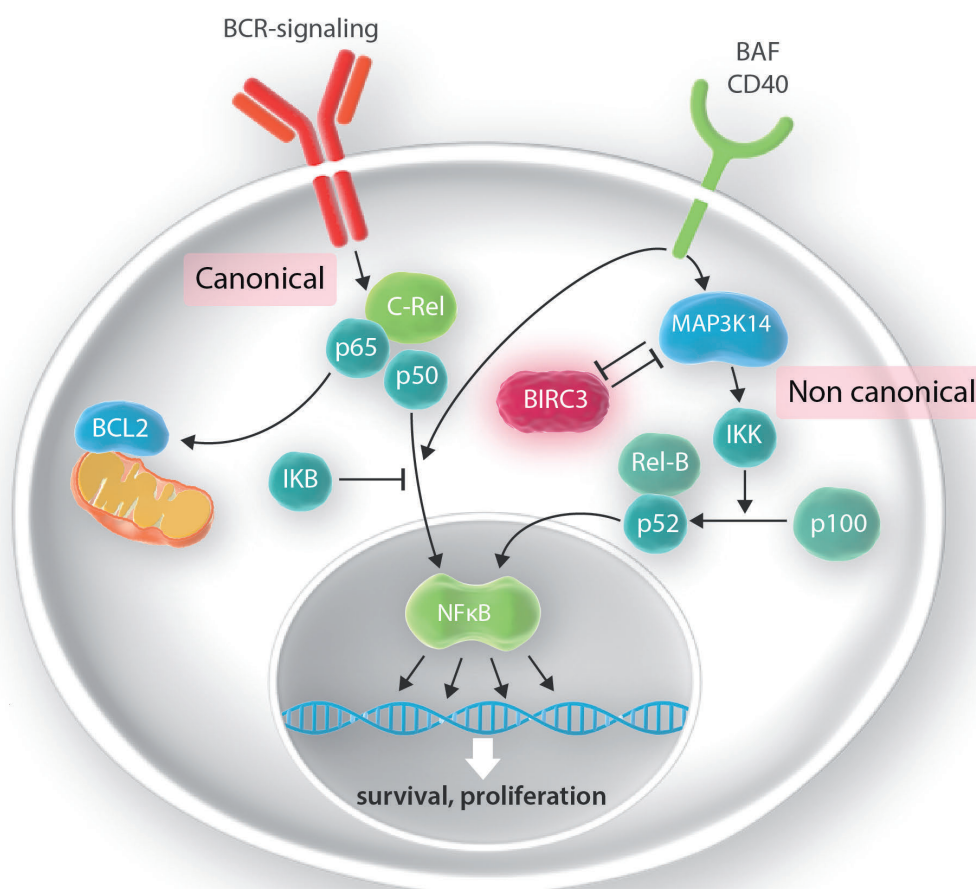


Figure 1. The canonical and non-canonical nuclear factor kappaB pathways. In the canonical nuclear factor kappaB (NFκB) pathway, activation of the B-cell receptor (BCR) results in a shift of the transcription factors c-Rel, p65 and p50 to the nucleus if not sequestered by IκB. In the non-canonical pathway, activation of MAP3K14 results in proteolytic cleavage of p100 to p52, which as a heterodimer with Rel-B serves as a transcription regulator. *BIRC3*, which is part of the negative regulatory complex, induces proteasomal degradation of MAP3K14, the major driver of activation of the non-canonical NFκB pathway.

the BIRC3-Map3K14 interaction for activation of the non-canonical NF κ B pathway. Silencing Map3K14 by short hairpin RNA decreased the levels of NF κ B, which was followed by reduced viability of BIRC3-mutated cells. MAP3K14 could, therefore, be a potential drug target to overcome mutant BIRC3-induced cell proliferation. Next Diop and colleagues evaluated the vulnerability of BIRC3-mutated cell lines and primary CLL cells to fludarabine. Viability assays under fludarabine treatment confirmed that BIRC3-mutated samples had a higher viability than BIRC3 wildtype ones, although still lower than that of TP53-mutated samples after 48 h. Therefore, refractoriness to fludarabine, which has been consistently assigned to TP53 defects in previous clinical and biological studies, is also found to a lesser extent in BIRC3-mutated cells. This translates into a significantly shorter progression-free survival of patients with BIRC3-mutated CLL receiving therapy with fludarabine, cyclophosphamide and rituximab (FCR), as found by the authors in a cohort of 287 previously untreated CLL patients.

This effect on outcome may be different with more modern treatment regimens. Although Diop and colleagues provide some evidence that NF κ B in BIRC3-mutated patients remains active with ibrutinib therapy, there are more downstream targets of Bruton tyrosine kinase (BTK), including MEK/ERK and MAPK, which should remain inhibited by ibrutinib.¹⁰ In general, *in vitro* cultures are less informative regarding the efficacy of BTK inhibitors for which the microenvironment plays a crucial role. In contrast to ibrutinib, treatment with venetoclax resulted in a similarly low viability of BIRC3-mutated and wildtype primary CLL cells.⁹ This appears rational, as BCL2 is not involved in the non-canonical pathway affected by BIRC3. However, there is also some evidence that BCL2 levels are higher in BIRC3-mutated cases, indicating a greater sensitivity to venetoclax.¹¹ Although only limited data on the impact of BIRC3 mutations are available from clinical trials with ibrutinib and venetoclax, an adverse outcome has not been observed, in contrast to del17p/mutated TP53.^{12,13}

Despite the comprehensive work by Diop and colleagues some questions remain in addition to the unclear impact on outcome with novel compounds. This includes the difference between monoallelic and biallelic defects (i.e., mutations and deletions), which considered together should result in a much higher number of affected

patients. Furthermore the role of non-truncating missense variants and mutations outside the C-terminal RING-domain found predominantly in solid tumors, but also in lymphomas and CLL, remains unclear. Therefore, further studies, in particular in cohorts of patients from prospective trials evaluating biologically targeted agents, are warranted before BIRC3 assessment can be put forward as a routine test in general clinical practice.

References

1. Rose-Zerilli MJ, Forster J, Parker H, et al. ATM mutation rather than BIRC3 deletion and/or mutation predicts reduced survival in 11q-deleted chronic lymphocytic leukemia: data from the UK LRF CLL4 trial. *Haematologica*. 2014;99(4):736-742.
2. Rossi D, Brusca A, Spina V, et al. Mutations of the SF3B1 splicing factor in chronic lymphocytic leukemia: association with progression and fludarabine-refractoriness. *Blood*. 2011;118(26):6904-6908.
3. Landau DA, Tausch E, Taylor-Weiner AN, et al. Mutations driving CLL and their evolution in progression and relapse. *Nature*. 2015;526(7574):525-530.
4. Nadeu F, Delgado J, Royo C, et al. Clinical impact of clonal and subclonal TP53, SF3B1, BIRC3, NOTCH1, and ATM mutations in chronic lymphocytic leukemia. *Blood*. 2016;127(17):2122-2130.
5. Baliakas P, Hadzidimitriou A, Sutton L-A, et al. Recurrent mutations refine prognosis in chronic lymphocytic leukemia. *Leukemia*. 2015;29(2):329-336.
6. Rossi D, Fangazio M, Rasi S, et al. Disruption of BIRC3 associates with fludarabine chemorefractoriness in TP53 wild-type chronic lymphocytic leukemia. *Blood*. 2012;119(12):2854-2862.
7. Zarnegar BJ, Wang Y, Mahoney DJ, et al. Noncanonical NF-kappaB activation requires coordinated assembly of a regulatory complex of the adaptors cIAP1, cIAP2, TRAF2 and TRAF3 and the kinase NIK. *Nat Immunol*. 2008;9(12):1371-1378.
8. Rickert RC, Jellusova J, Miletic AV. Signaling by the tumor necrosis factor receptor superfamily in B-cell biology and disease. *Immunol Rev*. 2011;244(1):115-133.
9. Diop F, Moia R, Favini C, et al. Biological and clinical implications of BIRC3 mutations in chronic lymphocytic leukemia. *Haematologica*. 2020;105(2):448-456.
10. Cheng S, Ma J, Guo A, et al. BTK inhibition targets *in vivo* CLL proliferation through its effects on B-cell receptor signaling activity. *Leukemia*. 2014;28(3):649-657.
11. Asslaber D, Wacht N, Leisch M, et al. BIRC3 expression predicts CLL progression and defines treatment sensitivity via enhanced NF- κ B nuclear translocation. *Clin Cancer Res*. 2019;25(6):1901-1912.
12. Tausch E, Bahlo J, Robrecht S, et al. Genetic markers and outcome in the CLL14 trial of the GCLLSG comparing front line obinutuzumab plus chlorambucil or venetoclax in patients with comorbidity. *Hematol Oncol*. 2019;37(S2):84-86.
13. Brown JR, Hillmen P, O'Brien S, et al. Extended follow-up and impact of high-risk prognostic factors from the phase 3 RESONATE study in patients with previously treated CLL/SLL. *Leukemia*. 2018;32(1):83-91.

Insights into the composition of stroke thrombi: heterogeneity and distinct clot areas impact treatment

Rui-Gang Xu and Robert A. S. Ariëns

Discovery and Translational Science Department, Leeds Institute of Cardiovascular and Metabolic Medicine, University of Leeds, Leeds, UK

E-mail: ROBERT A. S. ARIËNS - r.a.s.ariens@leeds.ac.uk

doi:10.3324/haematol.2019.238816

The structure of blood clots has recently become a hot topic in the scientific and medical literature. A search on PubMed for 'clot structure' results in >1,000 publications in the last 25 years, with >400 in the last five years alone. The reason for this surge in studies of the structure of blood clots is that dense clot structures that are resistant to fibrinolysis have been associated with both arterial and venous thrombosis (reviewed by Undas and Ariëns¹), and lead to poor outcome in prospective studies of arterial² and venous³ thrombotic disease. Furthermore, mechanisms from cellular contributions from platelets, red blood cells (RBC)⁴ and white blood cells (neutrophils producing extracellular traps or NET⁵) to clot structure are increasingly being understood. However, many previous studies have focused on individual clot components and their roles in clot structure and function, largely using either *in vitro* or *in vivo* methodology. Holistic approaches to study clot structure in thrombi obtained from patients with thrombosis have until now been few and far between, and are increasingly needed to place studies of individual clot structures into clinical context.

In the current edition of *Haematologica*, *Staessens et al.*⁶ studied the internal organization of 177 thrombi collected from endovascularly treated ischemic stroke patients. The objective of this study was to gain further understanding of the composition of stroke thrombi by histologically analyzing the internal organization of their structural components, including fibrin, RBC, von Willebrand factor (vWF), platelets, leukocytes and DNA. Using bright field and fluorescence microscopy, the authors observed that stroke thrombi are very heterogeneous in nature in two ways. First, they differ distinctly from each other in size, shape, and color. Second, within each thrombus there is considerable heterogeneity, with different areas or segments of the thrombus demonstrating different structural components. Based on the major structural components that are dominant in the thrombi, they were classified into two distinct types: RBC- and platelet-rich areas of the thrombus (Figure 1). Platelet-rich areas are composed of dense fibrin structures, platelets, vWF, leukocytes and extracellular DNA, whereas composition of RBC-rich areas is less complex, with packed RBC and a thin fibrin meshwork filling the gaps in between the packed RBC as the main structural components. *Staessens et al.*⁶ further quantified the relative contribution of each type of thrombus area. It appears that the contribution of both types varies significantly across all thrombi analyzed. For most thrombi, both regions are dispersed throughout, although some thrombi have more clearly defined boundaries, with RBC-rich regions surrounded by platelet-rich regions. The findings obtained in this

study provide interesting insight into the composition and internal organization of stroke thrombi and could be helpful in furthering our understanding of thrombolysis resistance and developing new therapies for acute ischemic stroke. Furthermore, knowledge of the structural composition of thrombi may be important for the relative success of mechanical thrombectomy.

This study makes important and valuable contributions to the previous efforts in the identification of thrombi composition, many of which were based on scanning electron microscopy.⁷⁻¹² There are a number of significant strengths of the current study. First, compared to previous studies,^{10,11} this is the first study to image thrombi obtained from patients with stroke with such detail, including visualization of multiple structural components of thrombi: fibrin, vWF, DNA and blood cells at the same time. Second, the use of immunofluorescence in this study overcomes limitations of conventional staining and generated stunning images, which allow for accurate localization of specific components and provide important structural insight of stroke thrombi both at cellular and molecular levels. In particular, compared with previous studies using conventional staining,^{7,12-14} more detailed organization and structural features of platelet, vWF and fibrin meshes in thrombi were demonstrated. Interestingly, the polyhedral morphology of RBC inside thrombi is also defined in these images, reminiscent of the tightly packed polyhedrocytes previously observed in thrombi formed *in vivo* and *in vitro*.^{15,16} Furthermore, the observation that extracellular DNA and leukocytes were located primarily in the platelet-rich areas, and close to the interface of these areas with others, emphasizes their potential crucial role in the rt-PA resistance observed in patients.

While this study makes big strides forward in our understanding of thrombus structure and function, some limitations remain. The first is that only microscopic methods were used to study the histological composition of thrombi, while there are no data on mechanical or functional properties of the thrombi. Previous studies on mechanical properties have shown that fibrin-rich clots have a higher friction than RBC-rich clots,¹⁷ and the increased percentage of RBC in the clot affects fibrin network heterogeneity and clot stiffness,¹⁸ indicating that differences in thrombi composition may be strongly linked to the mechanical properties of these clots. The mechanical properties of thrombi may in turn impact on the degree of embolization on one hand, and the success rate of thrombus retrieval by endovascular thrombectomy on the other. A comprehensive study of the mechanical properties of thrombi in patients is needed to further our understanding of the possible correlations between

thrombus composition and their mechanical properties, which would be advantageous in guiding the development of new generations of stent retrievers, as well as the selection of optimal thrombectomy therapy for patients. Another limitation of current studies regards the handling and storage of thrombus samples from patients. The thrombi obtained from thrombectomy are likely to undergo structural changes during or after the retrieval process. It is usually not possible to tell if the whole clot has been retrieved, or only fragments of it, and which parts represent the 'head' of the clot or the 'tail'. Furthermore, the internal organization and composition are probably modified by chemical fixation, air exposure or physical manipulation. A standard thrombus processing method needs to be developed to standardize those influences on thrombi during and after the retrieval process.^{19,20} In addition, the thrombi analyzed in this study only represent those that were successfully retrieved by thrombectomy, and were obtained from patients who received either prior rt-PA treatment or not. Future histological studies focusing on thrombi that are resistant to thrombectomy and rt-PA treatment would open a new window for advancing the treatment of acute ischemic stroke using intravascular approaches.

Intriguing new questions are also raised by the current study. For example, the role of polyhedrocytes observed in the thrombus remains poorly characterized. Polyhedrocytes are formed in contracted blood clots and thrombi due to the compression by activated contractile platelets pulling on fibrin. Remarkably, polyhedrocytes were first described in German by Gottlob *et al.* In 1970,²¹ Cynes *et al.* further characterized polyhedral erythrocytes, and described their occurrence in clots made *in vitro* and in thrombi obtained by thrombectomy from patients with myocardial infarction.^{15,16,22} The occurrence of polyhedrocytes in coronary thrombi was independently confirmed by Zalewski *et al.*²³ These studies suggest that polyhedrocytes play important roles in thrombi, by forming a near impermeable seal that impairs diffusion of fibrinolytic enzymes into thrombi, leading to reduced thrombolysis. However, despite the multiple observations and efforts made by previous studies, detailed mechanisms of polyhedrocyte formation in contracted thrombi and their clinical and pathological implications are still underappreciated. Furthermore, thrombus contraction, usually associated with the presence of polyhedrocytes, is another interesting topic. It has been reported that patients with VTE and PE have significantly reduced

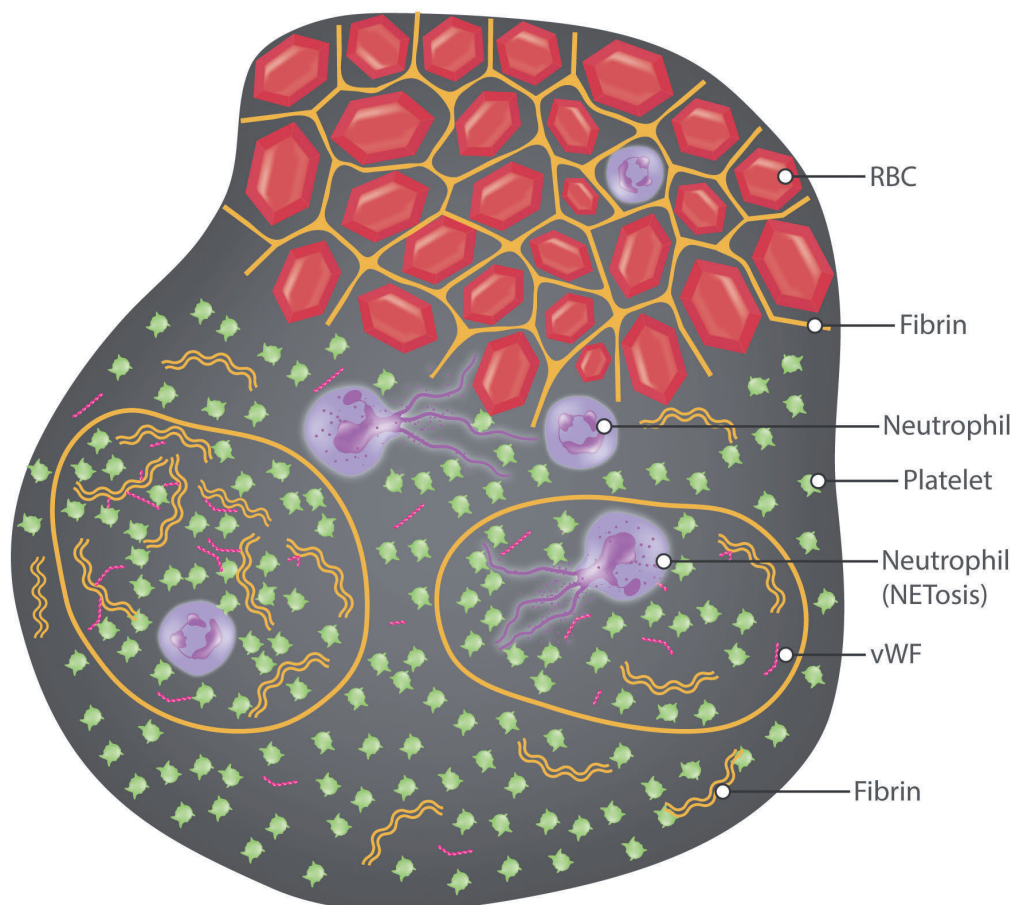


Figure 1. Schematic representation of the composition and organization of ischemic stroke thrombi as reported by Staessens *et al.*⁶ (Top) Red blood cell (RBC) rich area. This area mainly consists of packed RBC (polyhedrocytes) surrounded by thin fibrin fibers, which fill (or 'cement') the space between cells. Leukocytes (neutrophils) are also observed in these areas, but are less abundant. (Bottom) Platelet-rich area. Multiple structural components are found in this area, including platelets, thick fibrin bundles, von Willebrand factor (vWF), leukocytes (neutrophils) and extracellular DNA (due to NETosis).

clot contraction compared to healthy donors,²⁴ suggesting important associations between changes in the ability of blood clots to contract and the incidence of thromboembolism. These observations indicate polyhedrocytes as potential clinical markers of thromboembolism or targets for therapeutic intervention.

How the structure of the stroke thrombi in the report by *Staessens et al.*⁶ compares to other arterial or venous thrombi is another intriguing point. While arterial and venous thrombosis may be closely associated,^{25,26} they are triggered by different initiating mechanisms which may result in differences in the internal structure and composition of the thrombi.²⁷ Arterial thrombi occur under high shear stress, leading to platelet-rich clots that form around ruptured atherosclerotic plaques and the damaged endothelium. In contrast, venous thrombi occur under low shear stress and mostly on an intact, although likely inflamed, endothelium. Compared to arterial thrombi, venous thrombi are thought to favor the formation of clots that are fibrin-rich, encapsulating a large number of RBC in addition to activated platelets. However, despite these differences in initiating mechanisms, recent studies on structural characteristics of arterial thrombi challenge the concept that arterial thrombi are platelet-rich and venous thrombi are RBC-fibrin rich, since the arterial thrombi also contained large amounts of fibrin and RBC in addition to platelets.^{16,23} The current study by *Staessens et al.*⁶ also shows significant areas that are RBC- and fibrin-rich in arterial stroke thrombi. Therefore, differences in the composition of arterial and venous thrombi are likely subtler and may not be as distinct with regards to relative fibrin, platelet and RBC contents as previously thought. Is the clot organization observed in this work for stroke thrombi also applicable to thrombi obtained from other types of thrombosis? More in-depth studies using thrombi obtained from other arterial or venous sources would help answer this very question.

The insightful imaging of thrombi from patients with stroke presented in this paper from our Belgian colleagues clearly contributes to our understanding of the cellular and molecular make-up of thrombi. It also sets an elegant example for future analysis of thrombi from other vascular beds. Once more data are generated regarding the structural heterogeneity of thrombosis in both the venous and arterial circulation, we will be able to associate these findings with *in vitro* blood clot structure from systemic samples, providing tantalizing opportunities for new diagnostic tools. In addition, once the functional consequences of different thrombi structures on the behavior of these thrombi, their stability and future outcome is better documented, we should be able to improve interventional and medical treatment of thrombosis, and explore theranostics or other improved personalized approaches based on the nature of the thrombus that needs to be removed.

References

- Undas A, Ariens RA. Fibrin clot structure and function: a role in the pathophysiology of arterial and venous thromboembolic diseases. *Arterioscler Thromb Vasc Biol.* 2011;31(12):e88-e99.
- Sumaya W, Wallentin L, James SK, et al. Fibrin clot properties inde-

- pendently predict adverse clinical outcome following acute coronary syndrome: a PLATO substudy. *Eur Heart J.* 2018;39(13):1078-1085.
- Siudut J, Świat M, Undas A. Altered fibrin clot properties in patients with cerebral venous sinus thrombosis: association with the risk of recurrence. *Stroke.* 2015;46(9):2665-2668.
 - Weisel J, Litvinov R. Red blood cells: the forgotten player in hemostasis and thrombosis. *J Thromb Haemost.* 2019;17(2):271-282.
 - Martinod K, Wagner DD. Thrombosis: tangled up in NETs. *Blood.* 2014;123(18):2768-2776.
 - Staessens S, Denorme F, François O, et al. Structural analysis of ischemic stroke thrombi: histological indications for therapy resistance. *Haematologica.* 2019;105(2):498-507.
 - Silvain J, Collet JP, Nagaswami C, et al. Composition of coronary thrombus in acute myocardial infarction. *J Am Coll Cardiol.* 2011;57(12):1359-1367.
 - Sadowski M, Ząbczyk M, Undas A. Coronary thrombus composition: links with inflammation, platelet and endothelial markers. *Atherosclerosis.* 2014;237(2):555-561.
 - Ramaola I, Padró T, Peña E, et al. Changes in thrombus composition and profilin-1 release in acute myocardial infarction. *Eur Heart J.* 2014;36(16):965-975.
 - Marder VJ, Chute DJ, Starkman S, et al. Analysis of thrombi retrieved from cerebral arteries of patients with acute ischemic stroke. *Stroke.* 2006;37(8):2086-2093.
 - Simons N, Mitchell P, Dowling R, Gonzales M, Yan B. Thrombus composition in acute ischemic stroke: a histopathological study of thrombus extracted by endovascular retrieval. *J Neuroradiol.* 2015;42(2):86-92.
 - Fitzgerald S, Mereuta OM, Doyle KM, et al. Correlation of imaging and histopathology of thrombi in acute ischemic stroke with etiology and outcome. *J Neurosurg Sci.* 2019;63(3):292-300.
 - Hoshiba Y, Hatakeyama K, Tanabe T, Asada Y, Goto S. Co-localization of von Willebrand factor with platelet thrombi, tissue factor and platelets with fibrin, and consistent presence of inflammatory cells in coronary thrombi obtained by an aspiration device from patients with acute myocardial infarction. *J Thromb Haemost.* 2006;4(1):114-120.
 - Shin JW, Jeong HS, Kwon HJ, Song KS, Kim J. High red blood cell composition in clots is associated with successful recanalization during intra-arterial thrombectomy. *PLoS One.* 2018;13(5):e0197492.
 - Tutwiler V, Mukhitov AR, Peshkova AD, et al. Shape changes of erythrocytes during blood clot contraction and the structure of polyhedrocytes. *Sci Rep.* 2018;8(1):17907.
 - Cines DB, Lebedeva T, Nagaswami C, et al. Clot contraction: compression of erythrocytes into tightly packed polyhedra and redistribution of platelets and fibrin. *Blood.* 2014;123(10):1596-1603.
 - Gunning GM, McArdle K, Mirza M, Duffy S, Gilvarry M, Brouwer PA. Clot friction variation with fibrin content; implications for resistance to thrombectomy. *J Neurointerv Surg.* 2018;10(1):34-38.
 - Gersh KC, Nagaswami C, Weisel JW. Fibrin network structure and clot mechanical properties are altered by incorporation of erythrocytes. *Thromb Haemost.* 2009;102(6):1169-1175.
 - De Meyer SF, Andersson T, Baxter B, et al. Analyses of thrombi in acute ischemic stroke: a consensus statement on current knowledge and future directions. *Int J Stroke.* 2017;12(6):606-614.
 - Staessens S, Fitzgerald S, Andersson T, et al. Histological stroke clot analysis after thrombectomy: Technical aspects and recommendations. *Int J Stroke.* 2019;1747493019884527.
 - Gottlob R, Pötting U, Schattenmann G. [Morphologische Untersuchungen zur Frage der Retraction, der sekundären Quellung und der Lysierbarkeit von Thromben]. *Langenbeck's Archives of Surgery.* 1970;327:1209-1210.
 - Ariens RA. A new red cell shape helps the clot. *Blood.* 2014;123(10):1442-1443.
 - Zalewski J, Bogaert J, Sadowski M, et al. Plasma fibrin clot phenotype independently affects intracoronary thrombus ultrastructure in patients with acute myocardial infarction. *Thromb Haemost.* 2015;113(6):1258-1269.
 - Peshkova AD, Malyasyov DV, Bredikhin RA, et al. Reduced contraction of blood clots in venous thromboembolism is a potential thrombogenic and embologenic mechanism. *TH Open.* 2018;2(1):e104-e115.
 - Franchini M, Mannucci PM. Association between venous and arterial thrombosis: clinical implications. *Eur J Intern Med.* 2012;23(4):333-337.
 - Franchini M, Mannucci PM. Venous and arterial thrombosis: different sides of the same coin? *Eur J Intern Med.* 2008;19(7):476-481.
 - Koupenova M, Kehrel BE, Corkrey HA, Freedman JE. Thrombosis and platelets: an update. *Eur Heart J.* 2016;38(11):785-791.



Iron metabolism and iron disorders revisited in the hepcidin era

Clara Camaschella,¹ Antonella Nai^{1,2} and Laura Silvestri^{1,2}¹Regulation of Iron Metabolism Unit, Division of Genetics and Cell Biology, San Raffaele Scientific Institute, Milan and ²Vita Salute San Raffaele University, Milan, Italy**Haematologica** 2020
Volume 105(2):260-272**ABSTRACT**

Iron is biologically essential, but also potentially toxic; as such it is tightly controlled at cell and systemic levels to prevent both deficiency and overload. Iron regulatory proteins post-transcriptionally control genes encoding proteins that modulate iron uptake, recycling and storage and are themselves regulated by iron. The master regulator of systemic iron homeostasis is the liver peptide hepcidin, which controls serum iron through degradation of ferroportin in iron-absorptive enterocytes and iron-recycling macrophages. This review emphasizes the most recent findings in iron biology, deregulation of the hepcidin-ferroportin axis in iron disorders and how research results have an impact on clinical disorders. Insufficient hepcidin production is central to iron overload while hepcidin excess leads to iron restriction. Mutations of hemochromatosis genes result in iron excess by downregulating the liver BMP-SMAD signaling pathway or by causing hepcidin-resistance. In iron-loading anemias, such as β -thalassemia, enhanced albeit ineffective erythropoiesis releases erythroferrone, which sequesters BMP receptor ligands, thereby inhibiting hepcidin. In iron-refractory, iron-deficiency anemia mutations of the hepcidin inhibitor TMPRSS6 upregulate the BMP-SMAD pathway. Interleukin-6 in acute and chronic inflammation increases hepcidin levels, causing iron-restricted erythropoiesis and anemia of inflammation in the presence of iron-replete macrophages. Our improved understanding of iron homeostasis and its regulation is having an impact on the established schedules of oral iron treatment and the choice of oral *versus* intravenous iron in the management of iron deficiency. Moreover it is leading to the development of targeted therapies for iron overload and inflammation, mainly centered on the manipulation of the hepcidin-ferroportin axis.

Correspondence:CLARA CAMASCHELLA
camaschella.clara@hsr.it

Received: November 4, 2019.

Accepted: December 18, 2019.

Pre-published: January 16, 2020.

doi:10.3324/haematol.2019.232124

Check the online version for the most updated information on this article, online supplements, and information on authorship & disclosures: www.haematologica.org/content/105/2/260

©2020 Ferrata Storti Foundation

Material published in *Haematologica* is covered by copyright. All rights are reserved to the Ferrata Storti Foundation. Use of published material is allowed under the following terms and conditions:

<https://creativecommons.org/licenses/by-nc/4.0/legalcode>.

Copies of published material are allowed for personal or internal use. Sharing published material for non-commercial purposes is subject to the following conditions:

<https://creativecommons.org/licenses/by-nc/4.0/legalcode>,

sect. 3. Reproducing and sharing published material for commercial purposes is not allowed without permission in writing from the publisher.

**Introduction**

Research advances in understanding the biological functions and homeostasis of iron have clarified its role in physiology and disease. Iron, essential for hemoglobin synthesis, is indispensable to all cells for the production of heme and iron-sulfur (Fe/S) clusters, which are components of proteins/enzymes involved in vital biological processes such as respiration, nucleic acid replication and repair, metabolic reactions and host defense. While essential for life, excess iron is toxic. The ability to accept/release electrons explains the propensity of iron to damage cell components and is the reason why body iron must be tightly regulated. The two-faced nature of iron is also evident in its disorders, which span from iron excess to iron deficiency and maldistribution, when some tissues are iron-loaded and others are iron-deficient.

In the new millennium studies of genetic and acquired iron disorders and the development of their corresponding murine models have identified novel iron genes, proteins and pathways and unveiled the central role of the hepcidin-ferroportin axis in systemic iron homeostasis. This review summarizes recent advances in the understanding of iron trafficking, utilization and regulation, emphasizing the implications for iron disorders of hematologic interest; for further insights readers are directed to specific reviews.¹⁻³

Iron trafficking

Iron trafficking is an example of circular economy. Only 1-2 mg iron are absorbed daily in the gut, compensating for an equal loss; most iron (20-25 mg/daily) is recycled by macrophages upon phagocytosis of erythrocytes. The site of regulated non-heme iron uptake is the duodenum: non-heme iron is imported from the lumen by the apical divalent metal transporter 1 (DMT1) after reduction from ferric to ferrous iron by duodenal cytochrome B reductase (DCYTB). Absorption of heme exceeds that of non-heme iron, though the mechanisms remain obscure. In enterocytes non-utilized iron is stored in ferritin - and lost with mucosal shedding - or exported to plasma by basolateral membrane ferroportin according to the body's needs (Figure 1).

The role of transferrin and its receptors

The plasma iron pool is only 3-4 mg and must turn over several times daily to meet the high (20-25 mg) demand of erythropoiesis and other tissues. The iron carrier transferrin is central to iron trafficking. Binding to its ubiquitous receptor TFR1, transferrin delivers iron to cells through the well-known endosomal cycle.¹ This function is crucial not only for erythropoiesis, but also for muscle⁴ and for B- and T-lymphocytes, as highlighted by a *TFR1* homozygous mutation that causes combined immunodeficiency with only mild anemia.⁵ TFR1 is also essential in the gut to maintain epithelial homeostasis independently of its function of an iron importer;⁶ in hepatocytes TFR1 is dispensable for basal iron uptake, but essential in iron loading to finely tune the hepcidin increase.⁷

Transferrin is emerging as a key regulator of iron homeostasis through binding to its second receptor TFR2, which has a lower binding affinity than TFR1⁸ and whose expression is restricted to hepatocytes and erythroblasts. When plasma iron concentration is high, diferric transferrin binds TFR2 inducing upregulation of hepcidin in hepatocytes and a reduction of erythropoietin responsiveness in erythroid cells⁹ where TFR2 binds erythropoietin receptors.¹⁰ The reverse occurs in iron deficiency. The dual function of transferrin as an iron cargo and regulator seems to be dependent on the unequal ability of iron binding of the N and C terminal lobes and operates through the differential interaction of monoferric transferrin with the two receptors.¹¹

Iron recycling

Macrophages phagocytize senescent and damaged erythrocytes, recover iron from heme through heme oxygenase (HMOX) 1 and may utilize, conserve or recycle the metal. The relevance of their role is strengthened by the severity of conditions in which recycling is altered. *HMOX1* mutations in children cause a rare, severe disorder¹² and reduced recycling in inflammation causes anemia. Macrophage ferroportin is crucial for iron balance. Its expression is upregulated by heme and downregulated by inflammatory cytokines contributing to iron sequestration and its translation is repressed by iron. The protein is ultimately controlled at the post-translational level by hepcidin.¹³

Cell iron import

Intracellular iron is used for multiple functions; if not utilized it is stored in ferritin, or exported by ferroportin, in order to maintain the labile iron pool within narrow limits

to avoid toxicity. Although all cells may import, export or store iron, some have specific functions:¹ e.g., erythroblasts are specialized in iron uptake, macrophages and enterocytes in iron export, and hepatocytes in iron storage. Within cells most iron is transferred to mitochondria for heme and Fe/S cluster production. Heme is indispensable for hemoglobin, cytochromes and enzyme activity. Biogenesis of Fe/S clusters is a process conserved from yeast to humans: this prosthetic group is essential to proteins involved in genome maintenance, energy conversion, iron regulation and protein translation.^{14,15} In erythroblasts >80% iron is directed to mitochondria through a "kiss and run" mechanism between endosomes and mitochondria.¹⁶ Mitoferrin 1 and 2 are iron transporters of the inner mitochondrial membrane, the former being essential for zebrafish and murine erythropoiesis.¹⁷

Ferritin may store up to 4,500 iron atoms in a shell-like structure formed by 24 chains, comprising both heavy (H) chains, with ferroxidase activity, and light (L) chains.¹⁸ Ferritin storage of iron provides protection from oxidative damage, and also saves an essential element for future needs. H-ferritin deletion is incompatible with life and its conditional deletion in the gut deregulates the fine mechanism of iron absorption causing iron overload.¹⁹ L-ferritin heterozygous mutations are rare and limited to the 5' iron regulatory element (IRE) - leading to escape from iron regulatory protein (IRP) control and constitutive high ferritin synthesis in hyperferritinemia-cataract syndrome.²⁰ Rare dominant mutations lead to elongated proteins and neuroferritinopathies, a type of neurodegeneration caused by abnormal ferritin aggregates in the basal ganglia and other areas of the brain²¹ (Table 1).

In the clinical setting serum ferritin is a marker of iron deficiency when its level is low, and of iron overload/inflammation when its level is increased, reflecting macrophage ferritin content. However, both the origin and the function of serum ferritin remain largely unexplored. One hypothesis is that the secreted ferritin²² may be re-uptaken by cells as an alternative mechanism of iron recycling, e.g., when iron release from macrophages is limited in inflammation.

The cytosolic chaperon Poly (rC) binding protein 1 (PCBP1) delivers iron to ferritin,²³ and *Pcbp1* null mice have microcytic anemia.²⁴ Ferritin turnover occurs through "ferritinophagy", an autophagic process orchestrated by nuclear receptor co-activator (NCOA)4, a cargo molecule that directs ferritin to lysosomal degradation, to recover iron when needed.^{25,26} PCBP1 also delivers iron to prolyl-hydroxylase (PHD2) the enzyme that induces degradation of hypoxia inducible factors (HIF), one of the several links between iron and the hypoxia pathways.²⁷

Iron export

The ubiquitous iron exporter ferroportin cooperates with the oxidases ceruloplasmin or hephaestin, to release ferric iron to transferrin. Enterocytes, macrophages, hepatocytes and trophoblasts express high ferroportin levels for their specific functions in iron homeostasis. Blocking iron export may be dangerous in some cells. For example, conditional ferroportin deletion in murine cardiomyocytes leads to local iron overload and cardiac failure;²⁸ furthermore, specific deletion of ferroportin in erythroblasts and erythrocytes leads to hemolytic anemia, due to the toxicity of iron derived from hemoglobin oxidation in an environment (red blood cells) with limited antioxidant capacity.^{29,30}

Erythroblasts may also export heme through feline leukemia virus C receptor (FLVCR).^{31,32} The latter two export mechanisms seem counterintuitive in cells that need iron/heme for the production of hemoglobin, but are likely biological safeguard mechanisms that protect erythroid cells from iron/heme excess.

Iron homeostasis

Maintaining iron balance requires tight regulation at cellular, systemic and tissue levels.

Cell iron homeostasis

The IRP-IRE system

This system is based on the post-transcriptional control of iron genes mediated by the interaction of IRP with IRE of their mRNA untranslated regions. In iron-deficiency states, IRP1 and 2 increase iron uptake by stabilizing *TFR1* mRNA and blocking iron storage and export by suppressing ferritin and ferroportin translation. In iron-replete cells, Fe/S clusters convert IRP1 into cytosolic aconitase, while IRP2 undergoes iron-dependent proteasomal degradation. The IRP1/aconitase interconversion on the one hand links iron to tricarboxylic acid and cell metabolism, and on the

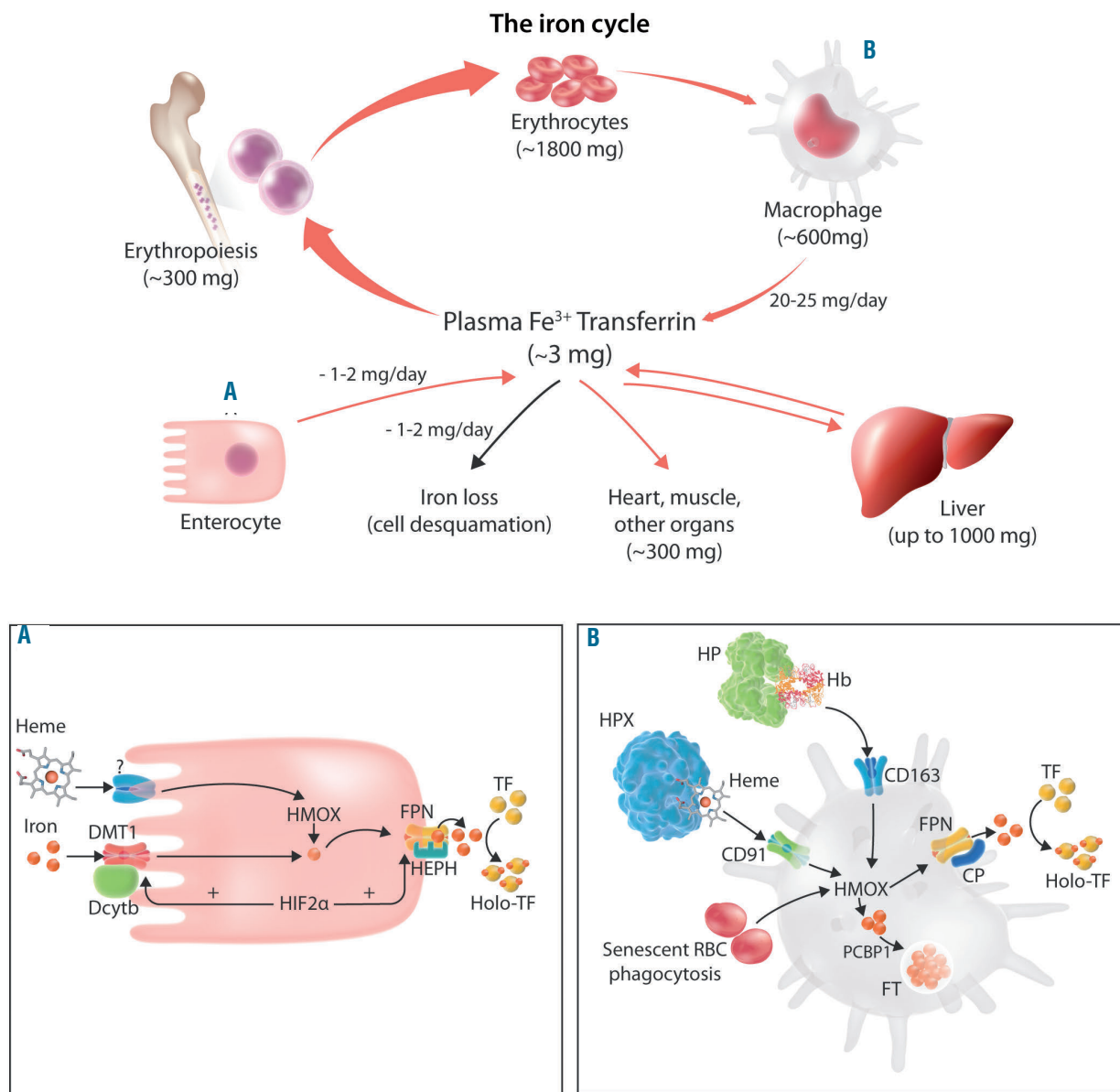


Figure 1. The iron cycle. Iron (Fe) circulates bound to transferrin to be released to all organs/tissues through transferrin receptor 1. Most iron (20-25 mg) recycled by macrophages, which phagocytize senescent red blood cells (RBC), is supplied to the bone marrow for RBC production. The daily uptake of dietary iron by duodenal enterocytes is 1-2 mg; the same amount is lost through cell desquamation and blood loss. Excess iron is stored in the liver and macrophages as a reserve. Arrows indicate directions. Numbers (in mg) are a mean estimate. (A) Focus on intestinal iron absorption. The metal transporter DMT1 takes up ferrous iron, reduced by Dcytb, on the luminal side of the enterocyte. Iron not used inside the cell is either stored in ferritin (FT) or exported to circulating transferrin (TF) by ferroportin (FPN), after ferrous iron is oxidized to ferric iron by hephaestin (HEPH).² Hypoxia inducible factor (HIF)-2α, stabilized by local hypoxia, stimulates the expression of the apical (DMT1) and basolateral (FPN) transporters.⁶³ Heme, after entering the cell through an unknown mechanism, is converted to iron by heme oxygenase. (B) Focus on the iron recycling process. Macrophages recover iron from phagocytized RBC after heme is degraded by heme oxygenase. They also recover heme from hemoglobin (Hb)-haptoglobin (HP) or heme-hemopexin (HPX) complexes.² Iron not used inside the cells is either stored in FT or exported to the circulation by FPN with the cooperation of ceruloplasmin (CP). The latter is the preferential route in normal conditions.

other hand highlights that, through Fe/S clusters, iron controls its own availability. IRP2 binds IRE at normal tissue oxygen, IRP1 acts in hypoxic tissues, such as the duodenum and kidneys.

Murine models of total and tissue-specific IRP inactiva-

tion are providing further insights into the local function of these proteins. Deletion of both *Irps* in mice is incompatible with life; loss of *Irp2* results in mild anemia, erythropoietic protoporphyria and adult-onset neurodegeneration in mice³³ and in patients,³⁴ likely because of function-

Table 1. Genetic and acquired iron disorders.

	Inheritance	Gene	Phenotype
Genetic iron overload without anemia			
HH type 1	AR	<i>HFE</i>	Inappropriate low hepcidin Adult-onset iron overload
HH type 2	AR	<i>HJV</i> <i>HAMP</i>	Low hepcidin Juvenile iron overload
HH type 3	AR	<i>TFR2</i>	Low hepcidin Early-onset iron overload
HH type 4 gain-of-function FPN mutations	AD	<i>SCLA0A1</i>	Hepcidin resistance Severe iron overload
Ferroportin disease loss-of-function FPN mutations	AD	<i>SCLA0A1</i>	Macrophage iron overload
Iron-loading genetic anemias			
Thalassemia syndromes			
α-thalassemia	AR	<i>HBA</i>	Microcytic anemia
β-thalassemia	AR	<i>HBB</i>	+ iron overload
Congenital sideroblastic anemia (non-syndromic)*	X-linked	<i>ALAS2</i>	Microcytic anemia
	AR	<i>SLC25A38</i>	Ringed sideroblasts
		<i>GLRX5</i> <i>HSPA9</i>	Iron overload
Congenital sideroblastic anemia (syndromic)*			
SA and ataxia	X-linked	<i>ABCB7</i>	SA and ataxia
SIFD	AR	<i>TRNT1</i>	SA, immunodeficiency and developmental delay
Congenital dyserythropoietic anemia			
Type 1	AR	<i>CDAN1</i> <i>C15orf41</i>	Anemia, splenomegaly, jaundice, erythroblasts multinuclearity, iron overload
Type 2, HEMPAS	AR	<i>SEC23B</i>	
Type 3	AR	<i>KIF23</i>	
Hypotransferrinemia	AR	<i>TF</i>	Microcytic anemia, iron overload
<i>DMT1</i> mutations	AR	<i>SLC11A1</i>	Microcytic anemia, iron overload
Genetic iron deficiency			
IRIDA	AR	<i>TMPRSS6</i>	Iron-deficiency anemia Refractoriness to oral iron
Genetic regional iron-FT accumulation			
Hyperferritinemia-cataract syndrome	AD	<i>FTL</i> promoter (<i>IRE</i>)	High serum ferritin in the absence of iron overload Congenital cataract due to FT deposition in the lens
Ferritinopathy	AD	<i>FTL</i>	Brain iron accumulation
	AR	<i>FRDA</i>	Neurodegeneration + cardiac iron overload
Acquired iron overload			
Chronic blood transfusions			Iron overload requiring chelation therapy
Acquired iron-loading anemias			
RS MDS	Clonal disorder with somatic mutations	<i>SF3B1</i>	Macrocytic anemia. Ringed sideroblasts. Iron overload
Acquired absolute iron deficiency			
Iron deficiency			Low body iron ± microcytic anemia
Acquired functional iron deficiency			
Anemia of inflammation			Low serum iron. Normocytic anemia Macrophage iron accumulation

HH: hereditary hemochromatosis; AR: autosomal recessive; AD: autosomal dominant; FPN: ferroportin; SA: sideroblastic anemia; *only forms of hematologic interest are shown. SIFD: congenital sideroblastic anemia, B-cell immunodeficiency, periodic fevers, and developmental delay; HEMPAS: hereditary erythroblastic multinuclearity with positive acidified serum lysis test; DMT1: divalent metal transporter 1; IRIDA: iron-refractory, iron-deficiency anemia; FT: ferritin; RS MDS: ringed sideroblast myelodysplastic syndrome.

al iron deficiency. Adult *Irf1*-knockout mice have a normal phenotype in basal conditions. Intestinal epithelium *Irf1* and 2 deletion in adult mice leads to impaired iron absorption and local iron retention because of ferritin-mediated mucosal block.⁵⁵

To escape IRP control, both enterocytes and erythroid cells also have a ferroportin isoform that, lacking the 5' IRE, ensures iron export in iron deficiency while remaining sensitive to degradation by hepcidin.³⁶

Ferritinophagy

In iron deficiency, cells may recover iron through ferritinophagy, a process mediated by the multifunctional protein NCOA4.^{25,26} First described as a transcriptional co-activator of androgen nuclear receptor, this protein is iron-regulated at the post-translational level. In iron-replete cells NCOA4 is bound by the E3 ubiquitin ligase HERC2 and degraded by the proteasome.³⁷ In iron-deficient cells NCOA4 binds ferritin inducing its degradation. NCOA4 also controls DNA duplication origins and its loss *in vitro* predisposes cells to replication stress and senescence,³⁸ coupling cell duplication and iron availability. *Ncoa4*-knockout mice accumulate ferritin in the liver and spleen, have reduced iron recycling and demonstrate increased susceptibility to iron-deficiency anemia.³⁹ The high *NCOA4* expression in erythroblasts²⁴ suggested a role for ferritinophagy in hemoglobinization *in vitro*,²⁴ in zebrafish embryos³⁷ and in mice.⁴⁰ However, the major relevance of the process is in iron-storing macrophages (Nai A. *et al.*, unpublished data) contributing to systemic homeostasis.

Systemic iron homeostasis: the hepcidin-ferroportin axis

The identification of hepcidin was a breakthrough in understanding how the liver is the central regulator of iron homeostasis and how its deregulation leads to iron disorders. The 25 amino acid mature hepcidin peptide controls iron export to the plasma by inducing lysosomal degradation of the iron exporter ferroportin in enterocytes, macrophages and hepatocytes;¹⁵ moreover, hepcidin also occludes the central cavity that exports iron in ferroportin.⁴¹

Hepcidin transcription is upregulated in hepatocytes by circulating and tissue iron, through a crosstalk with liver sinusoidal endothelial cells, which produce the ligands (BMP6 and 2) that activate the hepatocyte BMP-SMAD pathway. *BMP6* expression is regulated by iron,⁴² possibly in the context of an antioxidant response, controlled by NRF2.⁴³ *BMP2* is less iron sensitive and is highly expressed in basal conditions.^{44,45}

Inflammatory cytokines such as interleukin (IL)-6 upregulate hepcidin expression by activating the IL-6R-JAK2-STAT3 pathway. High hepcidin levels induce iron retention in macrophages, high serum ferritin levels and iron-restricted erythropoiesis, all features of anemia of inflammation. For full hepcidin activation the IL-6 pathway requires functional BMP-SMAD signaling.⁴⁶

Hepcidin expression is inhibited by iron deficiency, expansion of erythropoiesis, anemia/hypoxia, testosterone and possibly other factors.^{1,47} The most powerful inhibitor is the liver transmembrane serine protease matrilysin 2, encoded by *TMPRSS6*,⁴⁸ which cleaves the BMP co-receptor hemojuvelin,⁴⁹ thereby attenuating BMP-SMAD signaling and hepcidin transcription. The relevance of *TMPRSS6* is highlighted by iron-refractory, iron-deficiency anemia (IRIDA), which results from

TMPRSS6 mutations in patients⁵⁰ and inactivation in mice.⁴⁸ Deregulated, persistently high hepcidin blocks iron entry into the plasma and leads to iron deficiency. Another local inhibitor, the immunophilin FKBP12, binds the BMP receptor ALK2, suppressing the pathway activation.⁵¹

Erythroferrone (ERFE) is released by erythroid precursors stimulated by erythropoietin to suppress hepcidin expression and favor iron acquisition for hemoglobin synthesis.⁵² In hypoxia hepcidin is also suppressed *in vitro* by soluble hemojuvelin, released by furin,⁵³ an effect unclear *in vivo*, and by platelet-derived growth factor-BB in volunteers exposed to hypoxia.⁵⁴ Proposed models of hepcidin regulation in different conditions are depicted in Figure 2A-D.

Macrophages produce hepcidin in inflammation, potentiating the systemic effect on iron sequestration.⁵⁵

Local effects of hepcidin

As an antimicrobial peptide hepcidin is induced in the skin of patients with necrotizing fasciitis caused by group A streptococcal infections. Mice without hepcidin in keratinocytes fail to block the spread of infection because of a reduction of the neutrophils recruiting chemokine CXCL1.⁵⁶

Cardiomyocytes produce hepcidin with local effect on ferroportin. Conditional cardiomyocyte hepcidin deletion in mice does not affect systemic iron homeostasis but leads to excess iron export, severe contractile dysfunction and heart failure.⁵⁷

Emerging evidence links iron with lipid and glucose metabolism. Genome-wide association studies found overlapping associations for iron and lipid traits.⁵⁸ Adipocytes produce hepcidin in severe obesity⁵⁹ and hepcidin and gluconeogenesis are concomitantly upregulated in conditions of insulin-resistance.⁶⁰ Finally *Tmprss6*-knockout mice with high hepcidin levels are protected from obesity induced by a high-fat diet.⁶¹

Crosstalk between iron, oxygen and erythropoiesis

The hepcidin-ferroportin axis intersects other biological systems, such as IRP, hypoxia responsive pathways and erythropoietin signaling.

Iron absorption revisited

Iron absorption is a physiological example of crosstalk between IRP-hypoxia and the hepcidin-ferroportin axis. In the hypoxic duodenal environment, IRP1 controls translation of hypoxia-inducible factor 2 α (HIF-2 α) which, stabilized by prolyl hydroxylase, upregulates the expression of apical (DMT1) and basolateral (ferroportin) enterocyte iron transporters.⁶² In iron deficiency, absorption is enhanced by hepcidin downregulation, which, favoring export, depletes enterocytes of iron, further stabilizing HIF-2 α ⁶³ (Figure 1). In iron overload, high hepcidin increases enterocyte iron and impairs luminal uptake. In addition, the rapid cell turnover with shedding of ferritin-loaded enterocytes further limits iron absorption. In this way the interaction between local (hypoxia, IRP) and systemic (hepcidin) mechanisms optimizes iron balance.

Crosstalk between iron and erythropoiesis

Iron and erythropoiesis are interconnected at multiple levels and are reciprocally regulated. First, iron tunes renal production of erythropoietin, the growth factor essential for proliferation and differentiation of erythroid cells. The

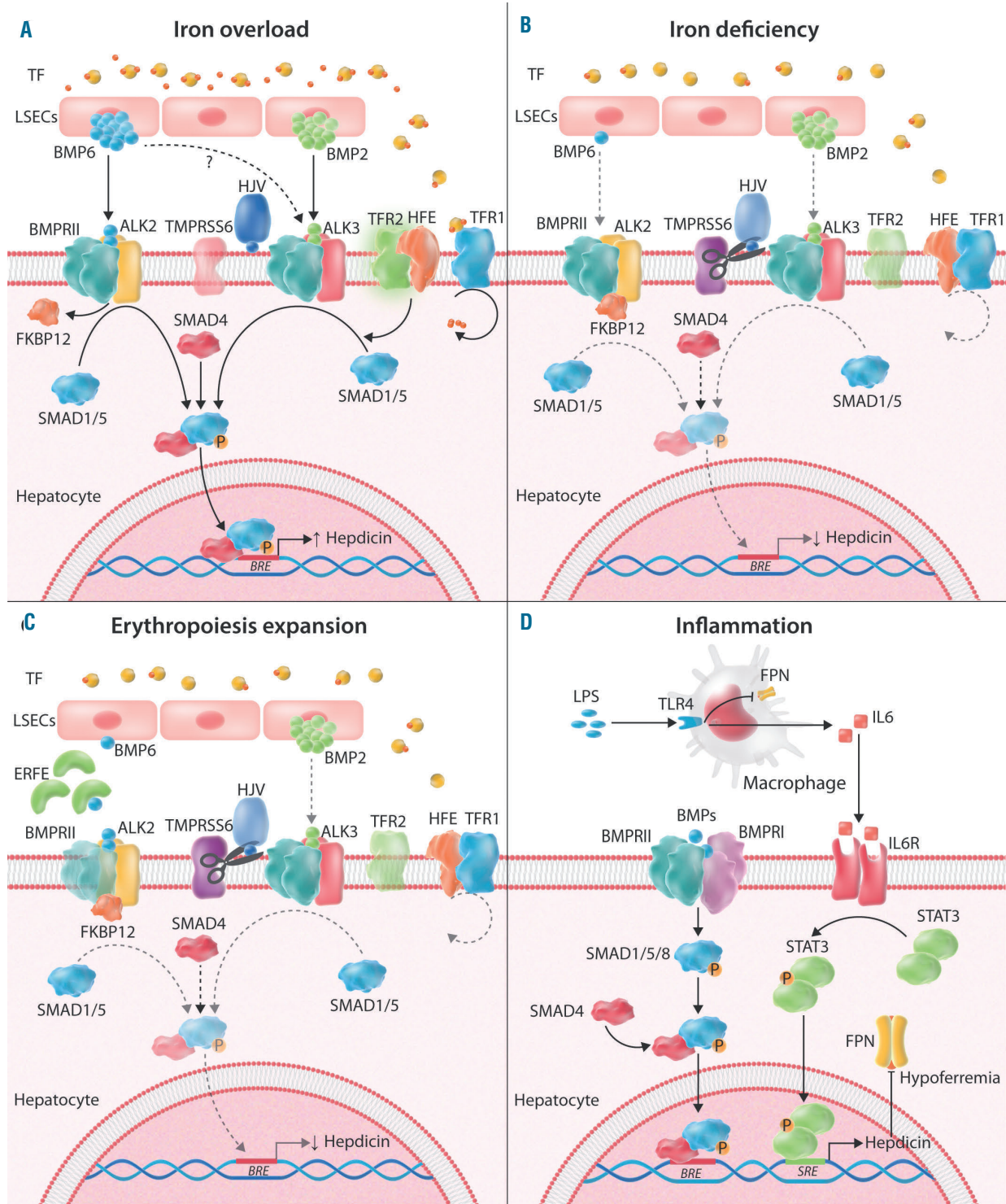


Figure 2. The regulation of hepcidin expression (adapted from Silvestri et al.¹⁴⁷). Schematic representation of a model of hepcidin regulation by two branches of the bone morphogenetic protein (BMP)-SMAD pathway, based on BMP knockout models,^{44,45,148} in (A) iron overload, (B) iron deficiency, (C) erythropoiesis expansion and (D) inflammation. According to a recent study BMP2 and BMP6 work collaboratively *in vivo*, possibly as a heterodimer.¹⁵³ (A) BMP2 produced by liver endothelial cells (LSEC) binds BMP receptor type II, which phosphorylates the BMP receptors type I (ALK3) to activate SMAD1/5/8. The latter associated with SMAD4 translocate to the nucleus to bind BMP responsive elements (BRE) in the hepcidin promoter. In iron overload increased diferric transferrin displaces HFE from transferrin receptor (TFR) 1 to enable iron uptake and stabilizes surface TFR2 potentiating ALK3 signaling. Hemojuvelin (HJV) acts as a BMP co-receptor, while the function of the other hemochromatosis HFE and TFR2 proteins in the pathway activation is still unclear. Iron increases the production of BMP6 by LSEC, thereby activating ALK2 and likely also ALK3 (indicated by a dotted arrow) in the pathway. (B) In iron deficiency TMPRSS6, stabilized on the cell surface,¹⁴⁹ cleaves HJV⁴⁹ and inactivates the BMP2-ALK3 branch of the pathway. TFR2 is destabilized by the lack of diferric transferrin and HFE binds TFR1.¹⁵⁰ The BMP6 pathway is inactive in the absence of the ligand and also because ALK2 is inactivated by FKBP12 binding.⁵¹ Together with epigenetic regulation,¹⁵¹ this suppresses hepcidin expression. (C) Erythropoiesis enhanced by erythropoietin consumes a large amount of iron: low serum iron (and diferric transferrin) suppresses the BMP2-ALK3 pathway,¹⁵² while BMP6 and other BMP are sequestered by erythroferrone (ERFE) released by erythroid cells.^{72,154} The result is hepcidin inhibition. (D) Schematic representation of hepcidin regulation by inflammatory cytokines and of the pathogenesis of anemia of inflammation. Stimulated by inflammation [here indicated by lipopolysaccharide (LPS) through toll-like receptor 4 (TLR4)], macrophages produce interleukin-6 (IL6), which stimulates Janus kinase 2–signal transducer and activator of transcription 3 (JAK2-STAT3) signaling to upregulate hepcidin in association with the BMP-SMAD pathway.

synthesis of erythropoietin is mediated by HIF-2 α . In iron deficiency, IRP1 binding to HIF-2 α 5'IRE represses the latter's translation and decreases erythropoietin production, to limit erythropoiesis and iron consumption. When the mechanism fails, as in *Irf1*-knockout mice, a transient polycythemia occurs in the relatively iron-deficient young animals, which reverts in adult mice with iron sufficiency.^{64,65} In this context prolyl hydroxylase, the enzyme that induces degradation of HIF-2 α , is iron-dependent and is thus inactive in iron deficiency.

Second, in *in vitro* studies, iron deprivation induced a block of early erythroid progenitors, by inactivating mitochondrial aconitase;⁶⁶ this block could be overcome by isocitrate supplementation.⁶⁷ Finally the erythroid response to iron restriction is optimized by the iron sensor TFR2, a partner of erythropoietin receptor.¹⁰ Loss of bone marrow TFR2 in mice increases the sensitivity of erythroblasts to erythropoietin, which causes erythrocytosis, especially in iron deficiency.⁶⁸ Liver TFR2 upregulates hepcidin and *TFR2* mutations cause hemochromatosis.⁶⁹ As a sensor of iron-bound transferrin, erythroid TFR2 regulates erythropoiesis, while liver TFR2, controlling hepcidin, modulates iron acquisition according to erythropoietic needs. The recently demonstrated *TFR2* expression in osteoclasts and osteoblasts⁷⁰ places this iron sensor at the crossroads of red cell production, iron homeostasis and bone turnover.

While iron regulates erythropoiesis, the reverse is also true. The old hypothesis that the erythropoietic drive controls iron absorption through an erythroid regulator⁷¹ was confirmed by the discovery of ERFE, the best example of tissue-mediated regulation of hepcidin. ERFE is a member of the tumor-necrosis factor (TNF)- α family, produced by several tissues, but increased in response to erythropoietin only in erythroid precursors. ERFE sequesters BMP receptor ligands, especially BMP6,⁷² inhibiting BMP-SMAD signaling and hepcidin. However, ERFE fails to suppress hepcidin when the BMP pathway is overactive.⁷³ *Erfe*-knockout mice are not anemic, indicating that ERFE has a modest effect on hepcidin repression in steady state. However, ERFE contributes to iron loading in mice with β -thalassemia.⁷⁴

Iron disorders

The improved understanding of iron physiology has profoundly changed the modern approach to iron disorders, known historically for centuries as iron deficiency (chlorosis) in young females and hemochromatosis (bronze diabetes) in middle-age males. We now suspect hemochromatosis based on iron parameters and confirm the diagnosis by genetic testing well before the development of iron overload and organ damage. We are aware that anemia is a complication of iron deficiency, though not the only one, since other tissues/organs may be iron-depleted before anemia develops, as occurs in chronic heart failure.⁷⁵

Hepcidin is tightly controlled to maintain body iron balance. Loss of this control leads to opposite genetic or acquired disorders (Table 1).

Genetic disorders

Hereditary hemochromatosis

The pathophysiology and diagnosis of hemochromatosis were profoundly influenced by the cloning of the *HFE*

gene⁷⁶ and the definition of the genetic heterogeneity of the disease (Table 1). Overall hemochromatosis is due to “insufficient hepcidin production” or exceptionally to “hepcidin resistance”.⁷⁷ Mutations in genes of the hepcidin-ferroportin axis disrupt iron homeostasis, leading to increased iron absorption, high transferrin saturation and increased toxicity from non-transferrin bound iron (NTBI) species.⁷⁸ The commonest form of hemochromatosis in Caucasians is due to homozygous *HFE*(C282Y) mutations. Genetic tests allow early diagnosis so that individuals with the affected genotypes show high biochemical penetrance (increased transferrin saturation \pm increased serum ferritin) but low clinical expression. Loss-of-function mutations of *HJV*, *TFR2* and *HAMP* (encoding hepcidin) lead to more severe diseases, collectively called “non-*HFE* hemochromatosis”. In all the recessive forms hepcidin is inappropriately low in comparison with iron excess and the onset and severity of iron overload correlate with the hormone deficiency.⁷⁹ The implementation of next-generation sequencing in familial and isolated cases of iron overload⁸⁰ has enabled the identification of mutations in more than one gene and provided examples of digenic inheritance. Both genetic and acquired modifiers contribute to the penetrance of *HFE*-hemochromatosis, interfering with hepcidin expression: e.g., alcohol aggravates the iron burden, whereas blood donations attenuates it.⁷⁷

Ferroportin mutations are inherited in a dominant manner (Table 1). The different effects of these mutations account for the controversy in disease nomenclature. Loss-of-function mutations impair iron export, are associated with iron accumulation in K upffer cells and require no or reduced phlebotomy therapy, representing the true “ferroportin disease”.⁸¹ Gain-of-function mutations lead to hepcidin resistance and the release of too much iron, as occurs in hemochromatosis.

The clinical severity of hemochromatosis is related to NTBI, a toxic iron species bound to low molecular weight molecules, easily taken up by hepatocytes and pancreatic cells via ZIP14 transporter⁸² and by cardiomyocytes through other transporters.⁸³ While iron uptake by transferrin receptor is tightly regulated, the uptake of NTBI is not and persists in iron overload. NTBI leads to the generation of reactive oxygen species and cell damage, causing liver fibrosis (which may progress to cirrhosis and hepatocellular carcinoma), chronic heart failure, diabetes, hypopituitarism and other complications of iron loading.^{77,79}

Iron-refractory iron-deficiency anemia

This form of iron deficiency anemia (IRIDA) was recognized after the discovery of hepcidin as being due to mutations of its inhibitor *TMPRSS6*.⁵⁰ High hepcidin levels lead to a phenotype opposite to that of hemochromatosis, reminiscent of anemia of inflammation.⁸⁴ The anemia is refractory to oral iron and may require intravenous therapy, especially when iron demand is high.⁸⁵ *TMPRSS6* genetic variants modulate iron and hematologic traits in several genome-wide association studies,⁵⁸ alter hepcidin levels in normal subjects⁸⁶ and might confer susceptibility/resistance to iron deficiency, as observed in blood donors.⁸⁷

Other rare recessive disorders of the transferrin receptor pathway – such as hypotransferrinemia and *DMT1* mutations – lead to “atypical microcytic anemia” with

increased transferrin saturation and iron stores, because of decreased iron utilization by blunted erythropoiesis.⁸⁵

Congenital sideroblastic anemia

Ringed sideroblasts are erythroblasts with iron-loaded mitochondria that, clustering around the nucleus, confer the appearance of a ring at Perls iron staining. Hereditary sideroblastic anemias are usually due to heme deficiency: X-linked sideroblastic anemia is caused by mutations in *ALAS2*, the first, rate-limiting enzyme of heme biosynthesis, while recessive forms are associated with mutations of mitochondria glycine importer solute carrier family 25 member 38.⁸⁸ Rare severe cases result from mutations of Fe/S cluster proteins, such as *GLRX5*⁸⁹ or *HSPA9*,⁹⁰ which decrease Fe/S groups and the activity of ferrochelatase, the last enzyme of the heme pathway. Another cause of low heme in *GLRX5* deficiency is the overactive IRP1 that, not being converted to aconitase because of the Fe/S cluster deficit, blocks *ALAS2* translation, thereby preventing heme formation. These disorders reveal the tight connection of heme-Fe/S metabolism. Among syndromic forms, the X-linked *ABC7* deficiency reduces export of Fe/S clusters to the cytosol,⁹¹ while others are associated with immunodeficiency⁹² strengthening the need of Fe/S clusters in other cell types (Table 1). Those due to mitochondrial protein mutations⁹¹ are not discussed here.

Acquired iron disorders

Iron deficiency

Iron deficiency, both isolated and associated with anemia, represents one of the five major causes of disability burden worldwide, especially in women.⁹³ For discussions of the etiology, clinical presentation and treatment of iron deficiency with or without anemia readers are directed to specific reviews.⁹⁴⁻⁹⁶ In absolute iron deficiency low total body and serum iron fully suppress hepcidin, a mechanism of adaptation to increase iron absorption. In functional iron deficiency (e.g., in inflammation) total body iron is not decreased, but iron is sequestered in stores by the high hepcidin levels.^{84,97} This distinction strongly influences the route of iron administration required to treat iron deficiency, as discussed below.

Anemia of inflammation

Proinflammatory cytokines such as IL-6 and IL-1 β , produced in chronic infections, autoimmunity, cancer, renal failure and other chronic disorders activate hepcidin expression leading to iron-restricted erythropoiesis and anemia of inflammation, once named anemia of chronic diseases.^{84,97,98} By withholding iron in macrophages, extracellular Gram-negative microorganisms are deprived of this essential nutrient.^{99,100} This is an innate defense mechanism known as 'nutritional immunity'.¹⁰¹ A recent interpretation is that hypoferrremia prevents the generation of NTBI that potentiates the pathogenicity of Gram-negative bacteria.¹⁰² Anemia, usually moderate and normocytic, is multifactorial, because of concomitant insufficient erythropoietin production and impaired early erythroid commitment.⁹⁸ Microcytosis occurs in longstanding severe inflammation such as in Castleman disease, a lymphoproliferative disorder in which high IL-6 production strongly enhances hepcidin synthesis¹⁰³ or in patients with ectopic hepcidin expression by liver adenomas.¹⁰⁴ Anemia reverts after anti-IL6 receptor treatment in Castleman disease or after surgical removal of the tumor

in the case of adenoma.

Anemia of inflammation regresses with control of the disease. In selected cases intravenous iron or erythropoiesis-stimulating agents are used. Since treatment is often unsatisfactory, manipulation of the hepcidin pathway (blocking either its production or function) is proposed as a novel therapeutic opportunity.⁹⁷

Iron-loading anemias

Low hepcidin levels explain the iron overload that develops in the absence of blood transfusions in "iron-loading anemias", i.e., anemias with ineffective erythropoiesis (Table 1). ERF, released by erythropoietin-stimulated erythroblasts, inhibits hepcidin, despite iron overload. In non-transfusion-dependent β -thalassemia patients, serum ERF levels are high,¹⁰⁵ to ensure iron acquisition for the expanded erythropoiesis.¹⁰⁶ However, since the erythropoiesis is inefficient, excess iron interferes with erythroblast maturation aggravating anemia in a vicious cycle.¹⁰⁷ In patients with transfusion-dependent thalassemia, hepcidin increases following transfusions which partially suppress erythropoiesis.

ERF contributes to the iron loading of some clonal myelodysplastic syndromes. Patients with the ringed sideroblasts subtype of myelodysplastic syndrome (once called refractory anemia with ringed sideroblasts) carry a somatic mutation in the spliceosome gene *SF3B1*.¹⁰⁸ Among other abnormally spliced products, an elongated variant of ERF is more efficient than the wildtype hormone in hepcidin repression.¹⁰⁹

Diagnostic implications

Notwithstanding spectacular advances in our understanding of iron metabolism and homeostasis our diagnostic approach to iron disorders still relies mainly on three historical tests: serum iron, transferrin (or total iron binding capacity) and ferritin. Transferrin saturation (Tsat), i.e. the ratio of serum iron/total iron binding capacity and serum ferritin coupled with genetic testing and non-invasive magnetic resonance imaging measurements of liver iron content, define the nature and severity of iron loading in both hemochromatosis⁷⁷ and thalassemia.¹¹⁰ Other useful markers are the level of serum soluble transferrin receptor (sTfR), related to the expansion of erythropoiesis or iron deficiency, the sTfR/log ferritin ratio for the diagnosis of iron deficiency in inflammation⁹⁸ and the Tsat/log hepcidin ratio to suspect IRIDA.¹¹¹

Enzyme-linked immunosorbent assay kits can measure serum hepcidin levels. However, this does not provide any information additional to serum ferritin, since the two variables are tightly related.^{112,113} Some researchers propose determining hepcidin levels in order to choose the better therapeutic route of administration of iron supplementation (oral vs. intravenous),¹¹⁴ as well as its correct timing¹¹⁵ and schedule.¹¹⁶ However, besides being subject to circadian oscillations, hepcidin levels change rapidly in response to activating and inhibitory signals, making their measurement useful in only a limited number of conditions.⁴⁷ A kit to measure human serum ERF concentration is available for research purposes. Whether the elongated ERF identified in individuals with *SF3B1* mutations will become a biomarker of ringed sideroblast myelodysplastic syndrome¹⁰⁹ remains to be tested.

Therapeutic implications

Hepcidin levels favor response (when low) or resistance (when high) to oral iron administration, explaining part of iron refractoriness.¹¹⁷ The dynamics of the increase in hepcidin levels after oral iron therapy have suggested that alternate-day administration of iron salts is an alternative to daily refracted doses, with the former being a protocol that increases both efficacy and tolerability, at least in women with iron deficiency without or with mild anemia.^{116,118,119} The availability of more tolerated, iron-stable and efficacious preparations has increased the use of intravenous iron, especially of the high-dose single-injection compounds.¹²⁰ However, when used to correct iron deficiency in inflammation, intravenous iron may lead to macrophage iron accumulation whose long-term effects are unknown.

Manipulation of the hepcidin-ferroportin axis is the most logical experimental approach to iron disorders. The rationale is to use hepcidin agonists for iron overload disorders caused by inappropriate/low hepcidin and hepcidin antagonists to release sequestered iron in IRIDA and in anemia of inflammation (Table 2).

Increasing hepcidin levels /decreasing ferroportin activity

In preclinical studies, increasing hepcidin levels prevented iron overload or redistributed iron to sites of safe stor-

age. Potentially useful in hemochromatosis, whose treatment is still based on phlebotomy,⁷⁷ hepcidin agonists are of interest in disorders with ineffective erythropoiesis, such as β -thalassemia.¹⁰⁷ Agonists include hepcidin analogues, minihepcidins, inhibitors of hepcidin repressors such as anti-TMPRSS6 molecules or compounds that block ferroportin activity. By inducing iron restriction hepcidin agonists ameliorated anemia and iron overload in preclinical studies of thalassemia models,^{106,121} a few hepcidin agonists are currently being investigated in phase I-II clinical trials (Table 2). Hepcidin mimics could also be useful to induce iron restriction in polycythemia.¹²² According to recent findings hepcidin might have a role as an antimicrobial peptide in the treatment of Gram-negative sepsis¹⁰² and streptococcal necrotizing fasciitis.⁵⁶

Other approaches

In non-transfusion-dependent β -thalassemia (*Hbb^{th1/h1}* and *Hbb^{th3/4}*) mice transferrin infusions improve the phenotype, increasing hepcidin and hemoglobin levels, improving erythrocyte survival and limiting splenomegaly,^{123,124} effects similar to those observed when *Tfr1* expression is decreased.¹²⁵ Selective inactivation of bone marrow *Tfr2* improves anemia in a non-transfusion-dependent *Hbb^{th3/4}* model, enhancing the sensitivity of erythroid cells to erythropoietin.¹²⁶

Short interfering RNA against *DMT1*, administered in

Table 2. Targeted therapeutic approaches for disorders with low and high hepcidin.

Compounds	Mechanism	Effect
IA. TO INCREASE HEPCIDIN OR REDUCE FERROPORTIN ACTIVITY¹²²		
Hepcidin analogues and minihepcidin ¹²¹	Replacement therapy	
BMPs	Activating the hepcidin signaling pathway	Increased hepcidin
Anti-TMPRSS6 (ASO, siRNA) ¹³⁷	Counteracting hepcidin inhibition	Reduced iron overload
FPN inhibitor VIT-2763 ¹⁵⁵	Blocking the hepcidin receptor	Increased Hb in ineffective erythropoiesis
IB. OTHER APPROACHES		
Transferrin injections ¹²³	Decreasing transferrin receptor 1	Reduction of iron uptake
Protoporphyrin IX ¹³⁸	Inhibiting heme oxygenase 1	Reduction of iron recycling
IIA. TO DECREASE HEPCIDIN OR INCREASE FERROPORTIN ACTIVITY⁹⁷		
Anti cytokines (IL-6, IL-6R) ¹⁰³		
Anti-BMP6 MoAb ¹³⁹		
BMP receptor inhibitors ¹⁴⁰	Reducing the hepcidin signaling pathway	Reduced hepcidin
Anti-hemojuvelin MoAb ¹⁴¹		Reduced macrophage iron sequestration
Heparins ¹⁴²		Correction of hypoferremia
Anti-hepcidin MoAb ¹⁴³		(Partial) correction of anemia
Anti-hepcidin Spiegelmer ¹⁴⁴	Hepcidin binders	
Anti-hepcidin anticalin ¹⁴⁵		
Anti-ferroportin MoAb ¹³⁹	Interfering with hepcidin-ferroportin interaction	
GDP ¹⁴⁶	Blocking iron export and decreasing Stat3 activation	
IIB. OTHER APPROACHES		
Prolylhydroxylase inhibitors ¹³⁴	Increasing EPO	Correction of EPO defect
	Increasing iron absorption	Correction of hypoferremia

I. Compounds potentially useful in hereditary hemochromatosis and β -thalassemia; II. Compounds potentially useful in anemia of inflammation. Compounds tested in clinical trials are indicated in bold. BMP: bone morphogenetic protein; ASO: antisense specific oligonucleotides; siRNA: short interfering RNA; FPN: ferroportin; VIT 2763: small molecule oral ferroportin inhibitor; Hb: hemoglobin; IL: interleukin; MoAb: monoclonal antibodies; GDP: guanosine 5'-diphosphate encapsulated in lipid vesicle; EPO: erythropoietin.

nanoparticles to target intestinal absorption,¹²⁷ established a proof of principle of reducing dietary iron uptake. Another approach might be to block intestinal HIF-2 α by specific antagonists.

Clinical trials are showing that correcting ineffective erythropoiesis by activin ligand traps¹²⁸ not only improves anemia but, in the long-term, also iron loading in both non-transfusion-dependent and transfusion-dependent thalassemia¹²⁹ and ringed sideroblast myelodysplastic syndrome.¹³⁰ Some thiazolidinones have been shown to stimulate hepcidin activity in preclinical studies.¹³¹ The use of proton pump inhibitors reduced the need for phlebotomy in patients with hemochromatosis.¹³²

Decreasing hepcidin levels/increasing ferroportin function

In preclinical models of anemia of inflammation, hepcidin antagonists decreased hepcidin expression, an effect verified in clinical trials for some compounds.¹³³ Another option is to interfere with the hepcidin-ferroportin interaction (Table 2). However, targeting the hepcidin-ferroportin axis may not fully correct this multifactorial anemia characterized by low erythropoietin and a blunted erythropoietic response.^{97,98} Another approach is based on manipulation of the hypoxia-responsive pathway.⁶⁵ Prolyl hydroxylase inhibitors or HIF stabilizers, now tested in chronic kidney disease, by increasing HIF-2 α might target two abnormal processes enhancing both erythropoietin synthesis and iron absorption.¹³⁴

Unresolved issues

Notwithstanding significant advances many questions about iron metabolism and homeostasis remain un-

answered. The mechanisms of intestinal heme absorption are mysterious, as are the roles of secreted ferritin and soluble transferrin receptor. We have just started exploring the autonomous regulation of iron in the heart and vascular wall; the role of iron (deficiency or excess) as a cofactor of metabolic disorders, chronic liver disease, heart failure, pulmonary hypertension and neurodegeneration still requires elucidation. We need to be able to diagnose isolated tissue iron deficiency better and to increase the limited number of iron status markers.

In hematology we need to clarify the relationship between iron and platelet production considering that iron deficiency directs the common erythroid-megakaryocyte precursor towards the platelet lineage.¹³⁵ More information is required on the role of iron in B-lymphocyte development and function, in B-cell malignancies, such as multiple myeloma,¹³⁶ and in response to infectious diseases. We have to explore better how iron/TFR2 intersects the erythropoietin signaling pathway and bone metabolism.

We need novel protocols of iron supplementation and clear indications regarding high-dose intravenous iron to optimize iron therapy. Targeted approaches, now in clinical trials, have the potential to change traditional treatment – such as the time-honored phlebotomy-based regimen – for disorders such as hemochromatosis. Repurposing commercially available compounds, developed for other conditions, to iron/erythroid disorders is another option. All these approaches will, it is hoped, enable a more personalized treatment of iron disorders in the near future.

Acknowledgments

This work was supported in part by an ASH Global Research Award 2017 to AN.

References

- Hentze MW, Muckenthaler MU, Galy B, Camaschella C. Two to tango: regulation of Mammalian iron metabolism. *Cell*. 2010;142(1):24-38.
- Muckenthaler MU, Rivella S, Hentze MW, Galy B. A red carpet for iron metabolism. *Cell*. 2017;168(3):344-361.
- Wang CY, Babitt JL. Liver iron sensing and body iron homeostasis. *Blood*. 2019;133(1):18-29.
- Barrientos T, Laothamatas I, Koves TR, et al. Metabolic catastrophe in mice lacking transferrin receptor in muscle. *EBioMedicine*. 2015;2(11):1705-1717.
- Jabara HH, Boyden SE, Chou J, et al. A missense mutation in TFR1, encoding transferrin receptor 1, causes combined immunodeficiency. *Nat Genet*. 2016;48(1):74-78.
- Chen AC, Donovan A, Ned-Sykes R, Andrews NC. Noncanonical role of transferrin receptor 1 is essential for intestinal homeostasis. *Proc Natl Acad Sci U S A*. 2015;112(37):11714-11719.
- Fillebeen C, Charlebois E, Wagner J, et al. Transferrin receptor 1 controls systemic iron homeostasis by fine-tuning hepcidin expression to hepatocellular iron load. *Blood*. 2019;133(4):344-355.
- Kawabata H, Yang R, Hiramata T, et al. Molecular cloning of transferrin receptor 2. A new member of the transferrin receptor-like family. *J Biol Chem*. 1999;274(30):20826-20832.
- Camaschella C, Pagani A, Nai A, Silvestri L. The mutual control of iron and erythropoiesis. *Int J Lab Hematol*. 2016;38 (Suppl 1):20-26.
- Forejtnikova H, Vieillevoje M, Zermati Y, et al. Transferrin receptor 2 is a component of the erythropoietin receptor complex and is required for efficient erythropoiesis. *Blood*. 2010;116(24):5357-5367.
- Parrow NL, Li Y, Feola M, et al. Lobe specificity of iron-binding to transferrin modulates murine erythropoiesis and iron homeostasis. *Blood*. 2019;134(17):1373-1384.
- Yachie A, Niida Y, Wada T, et al. Oxidative stress causes enhanced endothelial cell injury in human heme oxygenase-1 deficiency. *J Clin Invest*. 1999;103(1):129-135.
- Nemeth E, Tuttle MS, Powelson J, et al. Hepcidin regulates cellular iron efflux by binding to ferroportin and inducing its internalization. *Science*. 2004;306(5704):2090-2093.
- Lill R, Broderick JB, Dean DR. Special issue on iron-sulfur proteins: Structure, function, biogenesis and diseases. *Biochim Biophys Acta*. 2015;1853(6):1251-1252.
- Braymer JJ, Lill R. Iron-sulfur cluster biogenesis and trafficking in mitochondria. *J Biol Chem*. 2017;292(31):12754-12763.
- Hamdi A, Roshan TM, Kahawita TM, Mason AB, Sheftel AD, Ponka P. Erythroid cell mitochondria receive endosomal iron by a "kiss-and-run" mechanism. *Biochim Biophys Acta*. 2016;1863(12):2859-2867.
- Shaw GC, Cope JJ, Li L, et al. Mitoferrin is essential for erythroid iron assimilation. *Nature*. 2006;440(7080):96-100.
- Arosio P, Carmona E, Gozzelino R, Maccarinelli F, Poli M. The importance of eukaryotic ferritins in iron handling and cytoprotection. *Biochem J*. 2015;472(1):1-15.
- Vanoaica L, Darshan D, Richman L, Schumann K, Kuhn LC. Intestinal ferritin H is required for an accurate control of iron absorption. *Cell Metab*. 2010;12(3):273-282.
- Castiglioni E, Soriani N, Girelli D, et al. High resolution melting for the identification of mutations in the iron responsive element of the ferritin light chain gene. *Clin Chem Lab Med*. 2010;48(10):1415-1418.
- Luscietti S, Santambrogio P, Langlois d'Estaintot B, et al. Mutant ferritin L-chains that cause neurodegeneration act in a dominant-negative manner to reduce ferritin iron incorporation. *J Biol Chem*. 2010;285(16):11948-11957.
- Truman-Rosentsvit M, Berenbaum D, Spektor L, et al. Ferritin is secreted via 2 distinct nonclassical vesicular pathways. *Blood*. 2018;131(3):342-352.
- Leidgens S, Bullough KZ, Shi H, et al. Each member of the poly-r(C)-binding protein 1

- (PCBP) family exhibits iron chaperone activity toward ferritin. *J Biol Chem.* 2013;288(24):17791-17802.
24. Ryu MS, Zhang D, Protchenko O, Shakoury-Elizeh M, Philpott CC. PCBP1 and NCOA4 regulate erythroid iron storage and heme biosynthesis. *J Clin Invest.* 2017;127(5):1786-1797.
 25. Mancias JD, Wang X, Gygi SP, Harper JW, Kimmelman AC. Quantitative proteomics identifies NCOA4 as the cargo receptor mediating ferritinophagy. *Nature.* 2014;509(7498):105-109.
 26. Dowdle WE, Nyfeler B, Nagel J, et al. Selective VPS34 inhibitor blocks autophagy and uncovers a role for NCOA4 in ferritin degradation and iron homeostasis in vivo. *Nat Cell Biol.* 2014;16(11):1069-1079.
 27. Nandal A, Ruiz JC, Subramanian P, et al. Activation of the HIF prolyl hydroxylase by the iron chaperones PCBP1 and PCBP2. *Cell Metab.* 2011;14(5):647-657.
 28. Lakhali-Littleton S, Wolna M, Carr CA, et al. Cardiac ferroportin regulates cellular iron homeostasis and is important for cardiac function. *Proc Natl Acad Sci U S A.* 2015;112(10):3164-3169.
 29. Zhang DL, Ghosh MC, Ollivierre H, Li Y, Rouault TA. Ferroportin deficiency in erythroid cells causes serum iron deficiency and promotes hemolysis due to oxidative stress. *Blood.* 2018;132(19):2078-2087.
 30. Zhang DL, Wu J, Shah BN, et al. Erythrocytic ferroportin reduces intracellular iron accumulation, hemolysis, and malaria risk. *Science.* 2018;359(6383):1520-1523.
 31. Keel SB, Doty RT, Yang Z, et al. A heme export protein is required for red blood cell differentiation and iron homeostasis. *Science.* 2008;319(5864):825-828.
 32. Chiabrando D, Marro S, Mercurio S, et al. The mitochondrial heme exporter FLVCR1b mediates erythroid differentiation. *J Clin Invest.* 2012;122(12):4569-4579.
 33. Zhang DL, Ghosh MC, Rouault TA. The physiological functions of iron regulatory proteins in iron homeostasis - an update. *Front Pharmacol.* 2014;5:124.
 34. Costain G, Ghosh MC, Maio N, et al. Absence of iron-responsive element-binding protein 2 causes a novel neurodegenerative syndrome. *Brain.* 2019;142(5):1195-1202.
 35. Galy B, Ferring-Appel D, Becker C, et al. Iron regulatory proteins control a mucosal block to intestinal iron absorption. *Cell Rep.* 2013;3(3):844-857.
 36. Zhang DL, Hughes RM, Ollivierre-Wilson H, Ghosh MC, Rouault TA. A ferroportin transcript that lacks an iron-responsive element enables duodenal and erythroid precursor cells to evade translational repression. *Cell Metab.* 2009;9(5):461-473.
 37. Mancias JD, Pontano Vaites L, Nissim S, et al. Ferritinophagy via NCOA4 is required for erythropoiesis and is regulated by iron dependent HERC2-mediated proteolysis. *Elife.* 2015;4.
 38. Bellelli R, Castellone MD, Guida T, et al. NCOA4 transcriptional coactivator inhibits activation of DNA replication origins. *Mol Cell.* 2014;55(1):123-137.
 39. Bellelli R, Federico G, Matte A, et al. NCOA4 deficiency impairs systemic iron homeostasis. *Cell Rep.* 2016;14(3):411-421.
 40. Gao X, Lee HY, Li W, et al. Thyroid hormone receptor beta and NCOA4 regulate terminal erythrocyte differentiation. *Proc Natl Acad Sci U S A.* 2017;114(38):10107-10112.
 41. Aschemeyer S, Qiao B, Stefanova D, et al. Structure-function analysis of ferroportin defines the binding site and an alternative mechanism of action of hepcidin. *Blood.* 2018;131(8):899-910.
 42. Kautz L, Meynard D, Monnier A, et al. Iron regulates phosphorylation of Smad1/5/8 and gene expression of Bmp6, Smad7, Id1, and Atoh8 in the mouse liver. *Blood.* 2008;112(4):1503-1509.
 43. Lim PJ, Duarte TL, Arezes J, et al. Nrf2 controls iron homeostasis in haemochromatosis and thalassaemia via Bmp6 and hepcidin. *Nat Metab.* 2019;1(5):519-531.
 44. Koch PS, Olsavszky V, Ulbrich F, et al. Angiocrine Bmp2 signaling in murine liver controls normal iron homeostasis. *Blood.* 2017;129(4):415-419.
 45. Canali S, Wang CY, Zumbrennen-Bullough KB, Bayer A, Babitt JL. Bone morphogenetic protein 2 controls iron homeostasis in mice independent of Bmp6. *Am J Hematol.* 2017;92(11):1204-1213.
 46. Theurl I, Schroll A, Sonnweber T, et al. Pharmacologic inhibition of hepcidin expression reverses anemia of chronic inflammation in rats. *Blood.* 2011;118(18):4977-4984.
 47. Girelli D, Nemeth E, Swinkels DW. Hepcidin in the diagnosis of iron disorders. *Blood.* 2016;127(23):2809-2813.
 48. Du X, She E, Gelbart T, et al. The serine protease TMPRSS6 is required to sense iron deficiency. *Science.* 2008;320(5879):1088-1092.
 49. Silvestri L, Pagani A, Nai A, De Domenico I, Kaplan J, Camaschella C. The serine protease matriptase-2 (TMPRSS6) inhibits hepcidin activation by cleaving membrane hemojuvelin. *Cell Metab.* 2008;8(6):502-511.
 50. Finberg KE, Heeney MM, Campagna DR, et al. Mutations in TMPRSS6 cause iron-refractory iron deficiency anemia (IRIDA). *Nat Genet.* 2008;40(5):569-571.
 51. Colucci S, Pagani A, Pettinato M, et al. The immunophilin FKBP12 inhibits hepcidin expression by binding the BMP type I receptor ALK2 in hepatocytes. *Blood.* 2017;130(19):2111-2120.
 52. Kautz L, Jung G, Valore EV, Rivella S, Nemeth E, Ganz T. Identification of erythroferrone as an erythroid regulator of iron metabolism. *Nat Genet.* 2014;46(7):678-684.
 53. Silvestri L, Pagani A, Camaschella C. Furin-mediated release of soluble hemojuvelin: a new link between hypoxia and iron homeostasis. *Blood.* 2008;111(2):924-931.
 54. Sonnweber T, Nachbaur D, Schroll A, et al. Hypoxia induced downregulation of hepcidin is mediated by platelet derived growth factor BB. *Gut.* 2014;63(12):1951-1959.
 55. Theurl I, Theurl M, Seifert M, et al. Autocrine formation of hepcidin induces iron retention in human monocytes. *Blood.* 2008;111(4):2392-2399.
 56. Malerba M, Louis S, Cuvellier S, et al. Epidermal hepcidin is required for neutrophil response to bacterial infection. *J Clin Invest.* 2019 Dec 3. [Epub ahead of print]
 57. Lakhali-Littleton S, Wolna M, Chung YJ, et al. An essential cell-autonomous role for hepcidin in cardiac iron homeostasis. *Elife.* 2016;5.
 58. Benyamin B, Esko T, Ried JS, et al. Novel loci affecting iron homeostasis and their effects in individuals at risk for hemochromatosis. *Nat Commun.* 2014;5:4926.
 59. Bekri S, Gual P, Anty R, et al. Increased adipose tissue expression of hepcidin in severe obesity is independent from diabetes and NASH. *Gastroenterology.* 2006;131(3):788-796.
 60. Vecchi C, Montosi G, Garuti C, et al. Gluconeogenic signals regulate iron homeostasis via hepcidin in mice. *Gastroenterology.* 2014;146(4):1060-1069.
 61. Folgueras AR, Freitas-Rodriguez S, Ramsay AJ, et al. Matriptase-2 deficiency protects from obesity by modulating iron homeostasis. *Nat Commun.* 2018;9(1):1350.
 62. Mastrogiannaki M, Matak P, Peyssonnaud C. The gut in iron homeostasis: role of HIF-2 under normal and pathological conditions. *Blood.* 2013;122(6):885-892.
 63. Schwartz AJ, Das NK, Ramakrishnan SK, et al. Hepatic hepcidin/intestinal HIF-2alpha axis maintains iron absorption during iron deficiency and overload. *J Clin Invest.* 2019;129(1):336-348.
 64. Ghosh MC, Zhang DL, Jeong SY, et al. Deletion of iron regulatory protein 1 causes polycythemia and pulmonary hypertension in mice through translational derepression of HIF-2alpha. *Cell Metab.* 2013;17(2):271-281.
 65. Anderson SA, Nizzi CP, Chang YI, et al. The IRP1-HIF-2alpha axis coordinates iron and oxygen sensing with erythropoiesis and iron absorption. *Cell Metab.* 2013;17(2):282-290.
 66. Bullock GC, Delehanty LL, Talbot AL, et al. Iron control of erythroid development by a novel aconitase-associated regulatory pathway. *Blood.* 2010;116(1):97-108.
 67. Richardson CL, Delehanty LL, Bullock GC, et al. Isocitrate ameliorates anemia by suppressing the erythroid iron restriction response. *J Clin Invest.* 2013;123(8):3614-3623.
 68. Nai A, Lidonni MR, Rausa M, et al. The second transferrin receptor regulates red blood cell production in mice. *Blood.* 2015;125(7):1170-1179.
 69. Camaschella C, Roetto A, Cali A, et al. The gene TFR2 is mutated in a new type of haemochromatosis mapping to 7q22. *Nat Genet.* 2000;25(1):14-15.
 70. Rauner M, Baschant U, Roetto A, et al. Transferrin receptor 2 controls bone mass and pathological bone formation via BMP and Wnt signaling. *Nat Metab.* 2019;1(1):111-124.
 71. Finch CA. Erythropoiesis, erythropoietin, and iron. *Blood.* 1982;60(6):1241-1246.
 72. Arezes J, Foy N, McHugh K, et al. Erythroferrone inhibits the induction of hepcidin by BMP6. *Blood.* 2018;132(14):1473-1477.
 73. Nai A, Rubio A, Campanella A, et al. Limiting hepatic Bmp-Smad signaling by matriptase-2 is required for erythropoietin-mediated hepcidin suppression in mice. *Blood.* 2016;127(19):2327-2336.
 74. Kautz L, Jung G, Du X, et al. Erythroferrone contributes to hepcidin suppression and iron overload in a mouse model of beta-thalassemia. *Blood.* 2015;126(17):2031-2037.
 75. Anker SD, Comin Colet J, Filippatos G, et al. Investigators F-HT. Ferric carboxymaltose in patients with heart failure and iron deficiency. *N Engl J Med.* 2009;361(25):2436-2448.
 76. Feder JN, Gnirke A, Thomas W, et al. A novel MHC class I-like gene is mutated in patients with hereditary haemochromatosis. *Nat Genet.* 1996;13(4):399-408.
 77. Brissot P, Pietrangelo A, Adams PC, de Graaff B, McLaren CE, Loreal O. Haemochromatosis. *Nat Rev Dis Primers.* 2018;4:18016.
 78. Le Lan C, Loreal O, Cohen T, et al. Redox active plasma iron in C282Y/C282Y hemochromatosis. *Blood.* 2005;105(11):4527-4531.
 79. Sandhu K, Flintoff K, Chatfield MD, et al. Phenotypic analysis of hemochromatosis

- subtypes reveals variations in severity of iron overload and clinical disease. *Blood*. 2018;132(1):101-110.
80. McDonald J, Wooderchak-Donahue W, VanSant Webb C, Whitehead K, Stevenson DA, Bayrak-Toydemir P. Hereditary hemorrhagic telangiectasia: genetics and molecular diagnostics in a new era. *Front Genet*. 2015;6:1.
 81. Pietrangelo A. Ferroportin disease: pathogenesis, diagnosis and treatment. *Haematologica*. 2017;102(12):1972-1984.
 82. Jenkitkasemwong S, Wang CY, Coffey R, et al. SLC39A14 is required for the development of hepatocellular iron overload in murine models of hereditary hemochromatosis. *Cell Metab*. 2015;22(1):138-150.
 83. Oudit GY, Sun H, Trivieri MG, et al. L-type Ca²⁺ channels provide a major pathway for iron entry into cardiomyocytes in iron-overload cardiomyopathy. *Nat Med*. 2003;9(9):1187-1194.
 84. Weiss G, Ganz T, Goodnough LT. Anemia of inflammation. *Blood*. 2019;133(1):40-50.
 85. Camaschella C. How I manage patients with atypical microcytic anaemia. *Br J Haematol*. 2013;160(1):12-24.
 86. Nai A, Pagani A, Silvestri L, et al. TMPRSS6 rs855791 modulates hepcidin transcription in vitro and serum hepcidin levels in normal individuals. *Blood*. 2011;118(16):4459-4462.
 87. Kiss JE, Vassallo RR. How do we manage iron deficiency after blood donation? *Br J Haematol*. 2018;181(5):590-603.
 88. Guernsey DL, Jiang H, Campagna DR, et al. Mutations in mitochondrial carrier family gene SLC25A38 cause nonsyndromic autosomal recessive congenital sideroblastic anemia. *Nat Genet*. 2009;41(6):651-653.
 89. Camaschella C, Campanella A, De Falco L, et al. The human counterpart of zebrafish shiraz shows sideroblastic-like microcytic anemia and iron overload. *Blood*. 2007;110(4):1353-1358.
 90. Schmitz-Abe K, Ciesielski SJ, Schmidt PJ, et al. Congenital sideroblastic anemia due to mutations in the mitochondrial HSP70 homologue HSPA9. *Blood*. 2015;126(25):2734-2738.
 91. Ducamp S, Fleming MD. The molecular genetics of sideroblastic anemia. *Blood*. 2019;133(1):59-69.
 92. Chakraborty PK, Schmitz-Abe K, Kennedy EK, et al. Mutations in TRNT1 cause congenital sideroblastic anemia with immunodeficiency, fevers, and developmental delay (SIFD). *Blood*. 2014;124(18):2867-2871.
 93. Disease GBD, Injury I, Prevalence C. Global, regional, and national incidence, prevalence, and years lived with disability for 328 diseases and injuries for 195 countries, 1990-2016: a systematic analysis for the Global Burden of Disease Study 2016. *Lancet*. 2017;390(10100):1211-1259.
 94. Camaschella C. Iron-deficiency anemia. *N Engl J Med*. 2015;372(19):1832-1843.
 95. Lopez A, Cacoub P, Macdougall IC, Peyrin-Biroulet L. Iron deficiency anaemia. *Lancet*. 2016;387(10021):907-916.
 96. Camaschella C. Iron deficiency. *Blood*. 2019;133(1):30-39.
 97. Ganz T. Anemia of inflammation. *N Engl J Med*. 2019;381(12):1148-1157.
 98. Weiss G, Goodnough LT. Anemia of chronic disease. *N Engl J Med*. 2005;352(10):1011-1023.
 99. Drakesmith H, Prentice AM. Hepcidin and the iron-infection axis. *Science*. 2012;338(6108):768-772.
 100. Nairz M, Dichtl S, Schroll A, et al. Iron and innate antimicrobial immunity-Depriving the pathogen, defending the host. *J Trace Elem Med Biol*. 2018;48:118-133.
 101. Hood MI, Skaar EP. Nutritional immunity: transition metals at the pathogen-host interface. *Nat Rev Microbiol*. 2012;10(8):525-537.
 102. Stefanova D, Raychev A, Arezes J, et al. Endogenous hepcidin and its agonist mediate resistance to selected infections by clearing non-transferrin-bound iron. *Blood*. 2017;130(3):245-257.
 103. Song SN, Tomosugi N, Kawabata H, Ishikawa T, Nishikawa T, Yoshizaki K. Down-regulation of hepcidin resulting from long-term treatment with an anti-IL-6 receptor antibody (tocilizumab) improves anemia of inflammation in multicentric Castleman disease. *Blood*. 2010;116(18):3627-3634.
 104. Weinstein DA, Roy CN, Fleming MD, Loda MF, Wolfsdorf JI, Andrews NC. Inappropriate expression of hepcidin is associated with iron refractory anemia: implications for the anemia of chronic disease. *Blood*. 2002;100(10):3776-3781.
 105. Ganz T, Jung G, Naeim A, et al. Immunoassay for human serum erythropoietin. *Blood*. 2017;130(10):1243-1246.
 106. Rivella S. Iron metabolism under conditions of ineffective erythropoiesis in beta-thalassemia. *Blood*. 2019;133(1):51-58.
 107. Camaschella C, Nai A. Ineffective erythropoiesis and regulation of iron status in iron loading anaemias. *Br J Haematol*. 2016;172(4):512-523.
 108. Papaemmanuil E, Cazzola M, Boultonwood J, et al. Chronic Myeloid Disorders Working Group of the International Cancer Genome C. Somatic SF3B1 mutation in myelodysplasia with ring sideroblasts. *N Engl J Med*. 2011;365(15):1384-1395.
 109. Bondu S, Alary AS, Lefevre C, et al. A variant erythropoietin disrupts iron homeostasis in SF3B1-mutated myelodysplastic syndrome. *Sci Transl Med*. 2019;11(500).
 110. Taher AT, Weatherall DJ, Cappellini MD. Thalassemia. *Lancet*. 2018;391(10116):155-167.
 111. Heeney MM, Guo D, De Falco L, et al. Normalizing hepcidin predicts TMPRSS6 mutation status in patients with chronic iron deficiency. *Blood*. 2018;132(4):448-452.
 112. Traglia M, Girelli D, Biino G, et al. Association of HFE and TMPRSS6 genetic variants with iron and erythrocyte parameters is only in part dependent on serum hepcidin concentrations. *J Med Genet*. 2011;48(9):629-634.
 113. Galesloot TE, Vermeulen SH, Geurts-Moespot AJ, et al. Serum hepcidin: reference ranges and biochemical correlates in the general population. *Blood*. 2011;117(25):e218-225.
 114. Bregman DB, Morris D, Koch TA, He A, Goodnough LT. Hepcidin levels predict non-responsiveness to oral iron therapy in patients with iron deficiency anemia. *Am J Hematol*. 2013;88(2):97-101.
 115. Prentice AM, Doherty CF, Abrams SA, et al. Hepcidin is the major predictor of erythrocyte iron incorporation in anemic African children. *Blood*. 2012;119(8):1922-1928.
 116. Stoffel NU, Zeder C, Brittenham GM, Moretti D, Zimmermann MB. Iron absorption from supplements is greater with alternate day than with consecutive day dosing in iron-deficient anemic women. *Haematologica*. 2019 Aug 14. [Epub ahead of print]
 117. Hershko C, Camaschella C. How I treat unexplained refractory iron deficiency anemia. *Blood*. 2014;123(3):326-333.
 118. Moretti D, Goede JS, Zeder C, et al. Oral iron supplements increase hepcidin and decrease iron absorption from daily or twice-daily doses in iron-depleted young women. *Blood*. 2015;126(17):1981-1929.
 119. Stoffel NU, Cercamondi CI, Brittenham G, et al. Iron absorption from oral iron supplements given on consecutive versus alternate days and as single morning doses versus twice-daily split dosing in iron-depleted women: two open-label, randomised controlled trials. *Lancet Haematol*. 2017;4(11):e524-e533.
 120. Auerbach M, Deloughery T. Single-dose intravenous iron for iron deficiency: a new paradigm. *Hematology Am Soc Hematol Educ Program*. 2016 ;2016(1):57-66.
 121. Casu C, Chessa R, Liu A, et al. Minihepcidins improve ineffective erythropoiesis and splenomegaly in a new mouse model of adult beta-thalassemia major. *Haematologica*. 2019 Oct 3. [Epub ahead of print]
 122. Casu C, Nemeth E, Rivella S. Hepcidin agonists as therapeutic tools. *Blood*. 2018;131(16):1790-1794.
 123. Li H, Rybicki AC, Suzuka SM, et al. Transferrin therapy ameliorates disease in beta-thalassemic mice. *Nat Med*. 2010;16(2):177-182.
 124. Gelderman MP, Baek JH, Yalamanoglu A, P et al. Reversal of hemochromatosis by apo-transferrin in non-transfused and transfused Hbbth3/+ (heterozygous B1/B2 globin gene deletion) mice. *Haematologica*. 2015;100(5):611-622.
 125. Li H, Choesang T, Bao W, et al. Decreasing TfR1 expression reverses anemia and hepcidin suppression in β -thalassemic mice. *Blood*. 2017;129(11):1514-1526.
 126. Artuso I, Lidonnici MR, Altamura S, et al. Transferrin receptor 2 is a potential novel therapeutic target for β -thalassemia: evidence from a murine model. *Blood*. 2018;132(21):2286-2297.
 127. Wang X, Zhang M, Flores SRL, et al. Oral gavage of ginger nanoparticle-derived lipid vectors carrying Dmt1 siRNA blunts iron loading in murine hereditary hemochromatosis. *Mol Ther*. 2019;27(3):493-506.
 128. Dussiot M, Maciel TT, Fricot A, et al. An activin receptor IIA ligand trap corrects ineffective erythropoiesis in β -thalassemia. *Nat Med*. 2014;20(4):398-407.
 129. Piga A, Perrotta S, Gamberini MR, et al. Luspatercept improves hemoglobin levels and blood transfusion requirements in a study of patients with β -thalassemia. *Blood*. 2019;133(12):1279-1289.
 130. Platzbecker U, Germing U, Gotze KS, et al. Luspatercept for the treatment of anaemia in patients with lower-risk myelodysplastic syndromes (PACE-MDS): a multicentre, open-label phase 2 dose-finding study with long-term extension study. *Lancet Oncol*. 2017;18(10):1338-1347.
 131. Liu J, Liu W, Liu Y, et al. New thiazolidinones reduce iron overload in mouse models of hereditary hemochromatosis and β -thalassemia. *Haematologica*. 2019;104(9):1768-1781.
 132. Vanclooster A, van Deursen C, Jaspers R, Cassiman D, Koek G. Proton pump inhibitors decrease phlebotomy need in HFE hemochromatosis: double-blind randomized placebo-controlled trial. *Gastroenterology*. 2017;153(3):678-680.e2.
 133. Crielgaard BJ, Lammers T, Rivella S. Targeting iron metabolism in drug discovery and delivery. *Nat Rev Drug Discov*. 2017;16(6):400-423.
 134. Chen N, Hao C, Peng X, et al. Roxadustat

- for anemia in patients with kidney disease not receiving dialysis. *N Engl J Med.* 2019;381(11):1001-1010.
135. Xavier-Ferruccio J, Scanlon V, Li X *et al.* Low iron promotes megakaryocytic commitment of megakaryocytic-erythroid progenitors in humans and mice. *Blood.* 2019;134(18):1547-1557.
 136. Bordini J, Galvan S, Ponzoni M, *et al.* Induction of iron excess restricts malignant plasma cells expansion and potentiates bortezomib effect in models of multiple myeloma. *Leukemia.* 2017;31(4):967-970.
 137. Guo S, Casu C, Gardenghi S, *et al.* Reducing TMPRSS6 ameliorates hemochromatosis and β -thalassemia in mice. *J Clin Invest.* 2013;123(4):1531-1541.
 138. Garcia-Santos D, Hamdi A, Saxova Z, *et al.* Inhibition of heme oxygenase ameliorates anemia and reduces iron overload in a β -thalassemia mouse model. *Blood.* 2018;131(2):236-246.
 139. Sheetz M, Barrington P, Callies S, *et al.* Targeting the hepcidin-ferroportin pathway in anaemia of chronic kidney disease. *Br J Clin Pharmacol.* 2019;85(5):935-948.
 140. Asshoff M, Petzer V, Warr MR, *et al.* Momelotinib inhibits ACVR1/ALK2, decreases hepcidin production, and ameliorates anemia of chronic disease in rodents. *Blood.* 2017;129(13):1823-1830.
 141. Kovac S, Boser P, Cui Y, *et al.* Anti-hemojuvelin antibody corrects anemia caused by inappropriately high hepcidin levels. *Haematologica.* 2016;101(5):e173-176.
 142. Poli M, Asperti M, Naggi A, *et al.* Glycol-split nonanticoagulant heparins are inhibitors of hepcidin expression in vitro and in vivo. *Blood.* 2014;123(10):1564-1573.
 143. Vadhan-Raj S, Abonour R, Goldman JW, *et al.* A first-in-human phase 1 study of a hepcidin monoclonal antibody, LY2787106, in cancer-associated anemia. *J Hematol Oncol.* 2017;10(1):73.
 144. Boyce M, Warrington S, Cortezi B, *et al.* Safety, pharmacokinetics and pharmacodynamics of the anti-hepcidin Spiegelmer lexaptepid pegol in healthy subjects. *Br J Pharmacol.* 2016;173(10):1580-1588.
 145. Hohlbaum AM, Gille H, Trentmann S, *et al.* Sustained plasma hepcidin suppression and iron elevation by anticalin-derived hepcidin antagonist in cynomolgus monkey. *Br J Pharmacol.* 2018;175(7):1054-1065.
 146. Angmo S, Tripathi N, Abbat S, *et al.* Identification of guanosine 5'-diphosphate as potential iron mobilizer: preventing the hepcidin-ferroportin interaction and modulating the interleukin-6/Stat-3 pathway. *Sci Rep.* 2017;7:40097.
 147. Silvestri L, Nai A, Dulja A, Pagani A. Hepcidin and the BMP-SMAD pathway: an unexpected liaison. *Vitam Horm.* 2019;110: 71-99.
 148. Latour C, Besson-Fournier C, Meynard D, *et al.* Differing impact of the deletion of hemochromatosis-associated molecules HFE and transferrin receptor-2 on the iron phenotype of mice lacking bone morphogenetic protein 6 or hemojuvelin. *Hepatology.* 2016;63(1):126-137.
 149. Zhao N, Nizzi CP, Anderson SA, *et al.* Low intracellular iron increases the stability of matriptase-2. *J Biol Chem.* 2015;290(7):4432-4446.
 150. Schmidt PJ, Toran PT, Giannetti AM, Bjorkman PJ, Andrews NC. The transferrin receptor modulates Hfe-dependent regulation of hepcidin expression. *Cell Metab.* 2008;7(3):205-214.
 151. Pasricha SR, Lim PJ, Duarte TL, *et al.* Hepcidin is regulated by promoter-associated histone acetylation and HDAC3. *Nat Commun.* 2017;8(1):403.
 152. Artuso I, Pettinato M, Nai A, *et al.* Transient decrease of serum iron after acute erythropoietin treatment contributes to hepcidin inhibition by ERFE in mice. *Haematologica.* 2019;104(3):e87-e90.
 153. Xiao X, Dev S, Canali S, *et al.* Endothelial Bmp2 knockout exacerbates hemochromatosis in Hfe knockout mice but not Bmp6 knockout mice. *Hepatology.* 2019 Nov 28. [Epub ahead of print]
 154. Wang CY, Xu Y, Traeger L, *et al.* Erythroferrone lowers hepcidin by sequestering BMP2/6 heterodimer from binding to the BMP type I receptor ALK3. *Blood.* 2019 Dec 4. [Epub ahead of print]
 155. Manolova V, Nyffenegger N, Flace A, *et al.* Oral ferroportin inhibitor ameliorates ineffective erythropoiesis in a model of β -thalassemia. *J Clin Invest.* 2019;130(1):491-506

Innate immune cells, major protagonists of sickle cell disease pathophysiology

Slimane Allali,^{1,2,3} Thiago Trovati Maciel,^{2,3} Olivier Hermine^{2,3,4} and Mariane de Montalembert^{1,3}

¹Department of General Pediatrics and Pediatric Infectious Diseases, Reference Center for Sickle Cell Disease, Necker Hospital for Sick Children, Assistance Publique – Hôpitaux de Paris (AP-HP), Paris Descartes University, Paris; ²Laboratory of Cellular and Molecular Mechanisms of Hematological Disorders and Therapeutical Implications, Paris Descartes – Sorbonne Paris Cite University, Imagine Institute, Inserm U1163, Paris; ³Laboratory of Excellence GR-Ex, Paris and ⁴Department of Hematology, Necker Hospital for Sick Children, AP-HP, Paris Descartes University, Paris, France



Haematologica 2020
Volume 105(2):273-283

ABSTRACT

Sickle cell disease (SCD), considered the most common monogenic disease worldwide, is a severe hemoglobin disorder. Although the genetic and molecular bases have long been characterized, the pathophysiology remains incompletely elucidated and therapeutic options are limited. It has been increasingly suggested that innate immune cells, including monocytes, neutrophils, invariant natural killer T cells, platelets and mast cells, have a role in promoting inflammation, adhesion and pain in SCD. Here we provide a thorough review of the involvement of these novel, major protagonists in SCD pathophysiology, highlighting recent evidence for innovative therapeutic perspectives.

Introduction

Sickle cell disease (SCD) is a life-threatening genetic hemoglobin disorder, characterized by chronic hemolytic anemia, recurrent painful vaso-occlusive events and progressive multiple organ damage.¹ It is a global health issue, affecting millions of people worldwide, and its incidence is expected to increase to 400,000 neonates born per year by 2050.² The genetic and molecular bases are fully characterized: SCD originates from a single nucleotide mutation of the β -globin gene, leading to polymerization of the abnormal deoxygenated hemoglobin S (HbS), which results in obstruction of small vessels by sickle-shaped red blood cells (RBC). However, in the last two decades, the pathophysiology has been found to be much more complex than originally thought, involving many factors other than RBC. Innate immune cells include circulating cells, such as monocytes, dendritic cells, neutrophils, eosinophils, basophils, natural killer (NK) cells, invariant natural killer T (iNKT) cells and platelets, along with tissue-resident macrophages and mast cells.

Here we review the evidence for a contribution of innate immune cells to the pathophysiology of SCD.

Monocytes

Monocytes have long been considered important in SCD pathophysiology. Monocytosis is common in SCD and is positively correlated with markers of hemolysis and negatively with hemoglobin level.³ The absolute monocyte count is lower in SCD children being treated with hydroxyurea than in those not receiving such treatment, which may reflect another positive effect of hydroxyurea in SCD.⁴ *In vitro*, the interaction of RBC from SCD patients with cultured human umbilical vein endothelial cells was responsible for enhanced cellular oxidant stress, resulting in a two-fold increase in transendothelial migration of human peripheral blood monocytes.⁵ More importantly, monocytes from SCD patients display an activated profile, with increased expression of CD11b on their surface and increased production of interleukin (IL)-1 β and tumor necrosis factor (TNF)- α as compared with healthy control monocytes.^{6,8} Upregulation of CD1 molecules on monocytes has been described, reflecting the activated status of these cells.⁹ Mononuclear cells

Correspondence:

SLIMANE ALLALI
slimane.allali@aphp.fr

MARIANE DE MONTALEMBERT
mariane.demontal@nck.aphp.fr

Received: June 18, 2019.

Accepted: September 26, 2019.

Pre-published: January 9, 2020.

doi:10.3324/haematol.2019.229989

Check the online version for the most updated information on this article, online supplements, and information on authorship & disclosures: www.haematologica.org/content/105/2/273

©2020 Ferrata Storti Foundation

Material published in *Haematologica* is covered by copyright. All rights are reserved to the Ferrata Storti Foundation. Use of published material is allowed under the following terms and conditions:

<https://creativecommons.org/licenses/by-nc/4.0/legalcode>.
Copies of published material are allowed for personal or internal use. Sharing published material for non-commercial purposes is subject to the following conditions:
<https://creativecommons.org/licenses/by-nc/4.0/legalcode>, sect. 3. Reproducing and sharing published material for commercial purposes is not allowed without permission in writing from the publisher.



from SCD patients also show increased production of superoxide anions, which may be explained by the upregulation of NADPH oxidase components in SCD monocytes.^{10,11} Another sign of SCD monocyte activation is increased numbers of circulating tissue factor-positive monocytes, which contribute to the coagulation abnormalities observed in SCD patients.¹² Tissue factor expression on monocytes from SCD children was found to be positively correlated with pain rate, C-reactive protein level and reticulocyte percentage and negatively with hemoglobin concentration, suggesting a role for hemolysis and inflammation in SCD monocyte activation.¹³

In turn, as compared with normal monocytes, activated monocytes from SCD patients can activate endothelial cells via the nuclear factor (NF)- κ B pathway, resulting in enhanced expression of E-selectin, intracellular adhesion molecule 1 (ICAM-1) and vascular cell adhesion molecule 1 (VCAM-1).⁶ Endothelial activation is mediated by IL-1 β and TNF- α , produced by SCD monocytes, as demonstrated by its abrogation with antibodies targeting these two pro-inflammatory cytokines.⁶ Recently, a prominent role for the monocyte-TNF- α -endothelial activation axis was reported in transgenic sickle mice, with more global benefits from the TNF- α blockers etanercept and infliximab than from the IL-1 β blocker anakinra.¹⁴

Regarding the suspected mechanisms of monocyte activation, a role for hypoxemia was first suggested by a negative correlation between nocturnal oxygen saturation and CD11b expression in monocytes from children with SCD.⁹ The amount of circulating platelet-monocyte aggregates has been reported to be increased in SCD patients as compared with that in healthy controls, suggesting a possible activation of monocytes by platelets, which are known to be activated in SCD.⁷ In whole blood from SCD patients, the formation of platelet-monocyte aggregates is mediated by a P-selectin/P-selectin glycoprotein ligand 1 (PSGL-1) interaction, which may activate monocytes.¹⁵ Other interesting results came from the demonstration that placental growth factor (PlGF) released by RBC can activate monocytes from SCD patients, resulting in increased production of several pro-inflammatory cytokines and chemokines, including IL-1 β , TNF- α , monocyte chemoattractant protein 1 (MCP-1), macrophage inflammatory protein-1 β (MIP-1 β), IL-8 and vascular endothelial growth factor (VEGF), via the activation of Flt-1 and the PI3K/AKT and ERK-1/2 pathways.^{16,17} Placental growth factor plasma levels are higher in SCD patients than in healthy controls and positively correlated with anemia, pulmonary hypertension and the incidence of vaso-occlusive crises (VOC).^{17,18} Monocyte activation may also be mediated by interactions with sickle RBC since epinephrine-activated sickle RBC can promote monocyte adhesion to human umbilical vein endothelial cells.¹⁹ As demonstrated *in vitro* and in whole blood from SCD patients, plasma fibronectin creates a bridge between two integrin α 4 β 1 molecules on monocytes and on SS reticulocytes, mediating the formation of monocyte-reticulocyte aggregates.¹⁵ The interaction between α 4 β 1 on monocytes and Lutheran/basal cell adhesion molecule (Lu/BCAM) on RBC may contribute to the formation of monocyte-RBC aggregates.²⁰ A role for heme, released by intravascular hemolysis, in inducing monocyte activation could be suspected, but contrary to lipopolysaccharide, heme was recently found to be insufficient to induce IL-6 production by monocytes from SCD patients, although it

may potentiate the effects of lipopolysaccharide.²¹

New insights into the role of monocytes in SCD pathophysiology have recently been provided by the description of a patrolling monocyte subset expressing a very high level of heme oxygenase-1 (HO-1^{hi}) in SCD patients.²² Patrolling monocytes are CD14^{low}CD16⁺ monocytes able to scavenge cellular debris derived from the damaged vascular endothelium. *In vitro*, HO-1^{hi} expression was induced in patrolling monocytes on co-culture with heme-treated endothelial cells, and HO-1^{hi} cells had higher levels of endothelial cell-derived material than HO-1^{low} cells, which suggests that patrolling monocytes take up debris from heme-exposed endothelial cells, resulting in HO-1^{hi} expression.²² Importantly, mice lacking patrolling monocytes displayed more vascular stasis in the presence of sickle RBC than did control mice and this effect was attenuated by the transfer of patrolling monocytes, which supports a role for these cells in preventing VOC. Among patients on chronic transfusion exchange therapy, those with recent VOC or a history of recurrent VOC showed the lowest number of HO-1^{hi} patrolling monocytes.²² Hence, SCD patrolling monocytes may play an important role in scavenging cellular debris derived from heme-exposed endothelial cells, thus reducing the risk of VOC. Patrolling monocytes can also take up endothelial-adherent sickle RBC, especially during VOC, and HO-1 upregulation increases the survival of the patrolling monocytes by counteracting the cytotoxic effects of RBC-engulfed material.²³ Further investigations are required to determine whether patrolling monocytes in SCD can remove other blood cells attached to the endothelium, such as neutrophils.

The main findings on the involvement of monocytes in SCD pathophysiology are summarized in Figure 1.

Dendritic cells

Alloimmunization is a major complication of RBC transfusion both in adults and children with SCD, but its pathogenesis remains poorly understood.²⁴ A role for dendritic cells in the mechanisms underlying alloimmunization was recently demonstrated in heme-exposed monocyte-derived dendritic cells from alloimmunized SCD patients as compared with non-alloimmunized patients and healthy controls.²⁵ *In vitro*, heme downregulated maturation of monocyte-derived dendritic cells from non-alloimmunized patients and healthy controls, which resulted in inhibited priming of pro-inflammatory CD4⁺ type 1 T cells by the dendritic cells. By contrast, in alloimmunized patients, heme did not affect the maturation of dendritic cells or their ability to prime Th1 cells. Hence, the defective anti-inflammatory response to heme in alloimmunized patients may result in alterations in T-cell profile with an increase in pro-inflammatory (Th1) and a decrease in anti-inflammatory (Treg) T-cell subsets. Further investigations are required as they may open new therapeutic perspectives to prevent this potentially life-threatening complication.

It has also been suggested that dendritic cells may play a role in the pathogenesis of SCD-related orthopedic complications, such as osteonecrosis, osteoporosis and osteopenia, with there being an overexpression of bone morphogenetic protein (BMP)-6 in monocyte-derived dendritic cells from SCD patients with orthopedic complications as compared with SCD patients without orthopedic complications and healthy controls.²⁶ However, further

investigations are required to confirm the role of dendritic cells and the BMP/SMAD signaling pathway in SCD bone complications.

Neutrophils

Neutrophils have long been suspected to be involved in the pathophysiology of SCD. The absolute neutrophil count is higher in SCD patients in steady-state than in ethnicity-matched healthy controls and is positively correlated with SCD severity.²⁷ A high leukocyte count is also a risk factor for early death, acute chest syndrome (ACS), hemorrhagic stroke and sickle nephropathy.²⁸⁻³¹ Conversely, decreased neutrophil count may have positive effects, as suggested by a report of an alleviated SCD phenotype in a patient with associated congenital neutropenia who experienced the first episodes of VOC after the introduction of granulocyte colony-stimulating factor (G-CSF) to treat neutropenia.³² Thus, G-CSF and granulocyte-macrophage colony-stimulating factor (GM-CSF) should be strictly avoided in SCD patients because myeloid growth factors are responsible for VOC and ACS.^{33,34} Hydroxyurea may have clinical benefit for SCD patients even in the absence of elevated fetal hemoglobin (HbF) level, but a decrease in neutrophil count is always observed in such cases, and hydroxyurea seems most effective in patients with the greatest reduction in neutrophils.³⁵

In addition to these quantitative aspects, several studies have highlighted the activated state of neutrophils from

SCD patients, with increased adhesive properties at baseline and even more during VOC.^{36,37} Clinical manifestations of SCD have been found to be associated with the expression of adhesion molecules on leukocytes.³⁸ Hydroxyurea may also benefit SCD patients by suppressing neutrophil activation and correcting the dysregulated expression of adhesion markers on these cells.^{39,40} An important step in understanding the role of neutrophils in SCD pathophysiology was the intravital microscopy demonstration in SCD mice of increased neutrophil adhesion to the endothelium but also to sickle RBC in postcapillary venules.⁴¹ In this model, mice deficient in endothelial P-selectin and E-selectin displayed defective leukocyte recruitment to the vessel wall and were protected against vaso-occlusion. E-selectin was found to induce a secondary wave of activating signals, resulting in the clustering of activated macrophage-1 antigen (Mac-1) on the leading edge of adherent neutrophils, thereby allowing for the capture of sickle RBC and platelets. Here again, inactivation of E-selectin or Mac-1 prevented neutrophil-RBC and neutrophil-platelet interactions, thereby improving blood flow in the microcirculation and mouse survival.⁴² These findings suggest that interactions between activated endothelium, activated neutrophils, captured sickle RBC and platelets can contribute to decreased blood flow, further accentuating RBC sickling, neutrophil recruitment and tissue ischemia.⁴³ In blood samples from SCD patients, studied in microfluidic flow chambers, neutrophils rolling on E-selectin under shear stress were found

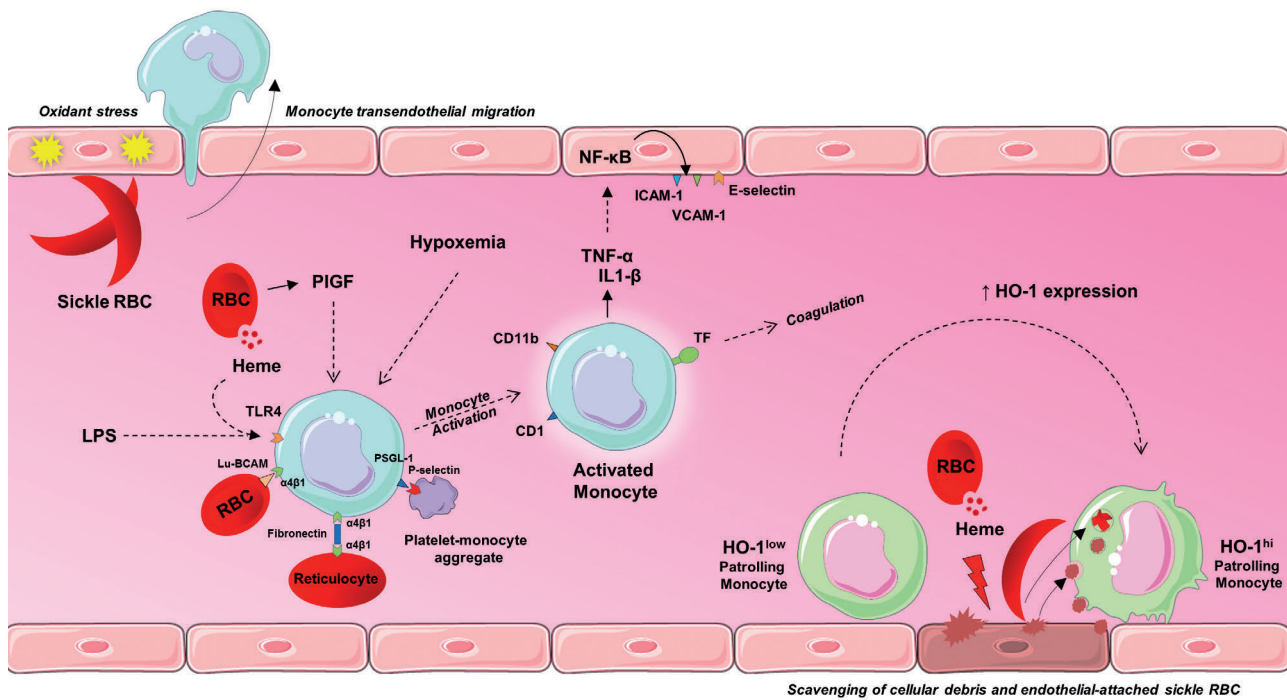


Figure 1. Monocytes in sickle cell disease. Interaction of sickle red blood cells (RBC) with endothelial cells enhances cellular oxidant stress, resulting in increased transendothelial migration of blood monocytes. Suspected mechanisms of monocyte activation in sickle cell disease (SCD) involve hypoxemia, platelet-monocyte aggregates mediated by P-selectin/P-selectin glycoprotein ligand 1 interaction, RBC/reticulocyte-monocyte interactions, placental growth factor released from RBC and co-stimulation of toll-like receptor 4 by heme and lipopolysaccharide. SCD activated monocytes display increased expression of CD1, CD11b and tissue factor on their surfaces, as well as increased production of interleukin-1 β and tumor necrosis factor- α . In turn, activated monocytes activate endothelial cells through the nuclear factor- κ B pathway, resulting in enhanced expression of intercellular adhesion molecule 1, vascular cell adhesion molecule 1 and E-selectin. Patrolling monocytes uptake cellular debris derived from heme-exposed endothelial cells, thus leading to high expression of heme oxygenase-1. Patrolling monocytes also scavenge endothelium-adherent sickle RBC. HO-1: heme oxygenase-1; ICAM-1: intercellular adhesion molecule 1; IL-1- β : interleukin 1 beta; LPS: lipopolysaccharide; Lu/BCAM: Lutheran/basal cell adhesion molecule; NF- κ B: nuclear factor kappa B; PIGF: placental growth factor; PSGL-1: P-selectin glycoprotein ligand 1; TF: tissue factor; TLR4: toll-like receptor 4; TNF- α : tumor necrosis factor alpha; VCAM-1: vascular cell adhesion molecule 1.

to promote a catch-bond formation between endothelial cell E-selectin and neutrophil L-selectin via tetrasaccharide sialyl Lewis^x (sLe^x) expressed on L-selectin.⁴⁴ This interaction triggers the activation of high-affinity β_2 -integrins, which leads to the formation of shear-resistant bonds with ICAM-1 on inflamed endothelium. Rivipansel, a synthetic pan-selectin antagonist previously shown to improve blood flow and survival in SCD mice, effectively blocks E-selectin recognition of sLe^x on L-selectin, thereby inhibiting neutrophil adhesion.^{44,45} In a prospective multicenter, randomized, placebo-controlled, double-blind, phase II trial of 76 SCD patients, those in the rivipansel arm showed a non-significant trend toward reduced time to resolution of VOC, and a significant 83% reduction in mean cumulative intravenous opioid analgesic use.⁴⁶ These results have supported an ongoing phase III trial of rivipansel for SCD VOC (#NCT02187003). However, the most encouraging results were obtained with another selectin antagonist specifically targeting P-selectin. In a randomized, placebo-controlled, double-blind, phase II trial of 198 SCD patients, treatment with crizanlizumab, a humanized monoclonal antibody directed against P-selectin, significantly reduced the median rate of VOC per year by 45%.⁴⁷ A phase III trial with crizanlizumab is currently in progress (#NCT03814746) and this drug was recently approved by the US Food and Drug Administration. Among other potential therapeutic agents targeting neutrophils, sevuparin, a novel drug candidate derived from heparin, was found to inhibit adhesion of RBC and leukocytes from SCD patients to human umbilical vein endothelial cells and prevented vaso-occlusion in sickle mice via a multimodal mechanism of action, including P- and L-selectin binding.^{48,49} Therefore, a phase II clinical trial of sevuparin for preventing VOC in SCD patients is ongoing (#NCT02515838). Intravenous immunoglobulin could also inhibit RBC–neutrophil interactions and neutrophil adhesion to endothelium in sickle mice by inhibiting Mac-1, and no adverse effects were observed in a phase I clinical trial of intravenous immunoglobulin in SCD patients.⁵⁰ A phase II trial is currently ongoing (#NCT01757418).

An important point is that activated platelets as well as endothelial cells express P-selectin, which binds to PSGL-1 on neutrophils, thereby enhancing the formation of platelet–neutrophil aggregates.⁵¹ In SCD mice, such platelet–neutrophil aggregates have been observed in pulmonary arteriole microemboli, with resolution after selective platelet P-selectin inhibition, which suggests the potential therapeutic interest of targeting P-selectin to prevent ACS.⁵² In the crizanlizumab phase II trial, the ACS rate did not differ between the active-treatment group and the placebo group, but this finding may be explained by the rarity of ACS in this trial, and further studies are needed to determine whether P-selectin blockade prevents ACS in SCD patients.⁴⁷ The platelet–neutrophil association is also mediated by interactions between glycoprotein Ib α (GPIb α) on platelets and Mac-1 on neutrophils, which is positively regulated by the serine/threonine kinase isoform AKT2 in neutrophils during vascular inflammation.⁵³ Here again, specific inhibition of AKT or GPIb α was recently found to attenuate *in vitro* neutrophil–platelet aggregation in SCD patients' blood, thereby opening new therapeutic perspectives for the prevention and treatment of VOC.^{54,55}

Besides selectin-dependent interactions, adhesion of neutrophils to activated endothelium is modulated by different mediators, such as endothelin-1, with elevated plas-

ma levels in SCD patients. In SCD mice, endothelin-1 appears to upregulate TNF- α -induced Mac-1 expression on neutrophils. Blocking endothelin receptors, especially the endothelin B receptor, on neutrophils strongly attenuates their recruitment, as demonstrated by intravital microscopy of SCD mice and microfluidic microscopy of SCD human blood.⁵⁶

Another major point is that SCD patients, like SCD mice, display very high proportions of aged neutrophils, which have been positively correlated with endothelial adhesion, Mac-1 expression and the formation of neutrophil extracellular traps (NET).⁵⁷ Neutrophil aging appears to be mediated by microbiota via TLR/Myd88 signaling, and depletion of gut microbiota with antibiotics in SCD mice led to a significant reduction in the number of aged neutrophils, along with improved blood flow and increased survival. A reduced number of aged neutrophils has been reported in SCD patients receiving penicillin, which suggests an additional positive impact of prophylactic antibiotic treatment, mediated by microbiota depletion and reduction in the number of aged neutrophils.⁵⁷ Moreover, bone marrow from SCD mice showed an accumulation of aged neutrophils, possibly impairing osteoblast function; thus, by reducing the number of aged neutrophils, microbiota depletion may improve osteoblast function and bone loss in SCD.⁵⁸

In both SCD mice and patients, elevated plasma heme levels during VOC were found to promote the formation of NET, which are decondensed chromatin with granular enzymes released by activated neutrophils.⁵⁹ In SCD mice, the presence of NET in the lungs contributes to acute lung injury and is associated with hypothermia and death, which can be prevented by clearing NET with DNase I or by scavenging heme with hemopexin.⁵⁹ Together with heme being able to trigger ACS in SCD mice, these results suggest that NET induced by heme may be involved in the pathogenesis of ACS.⁶⁰ Heme may also contribute to a susceptibility to infections in SCD patients by inducing HO-1 expression during neutrophilic differentiation, thereby impairing the ability of neutrophils to mount a bactericidal oxidative burst. Indeed, a novel neutrophil progenitor subset expressing high levels of HO-1 was recently identified in the bone marrow of SCD children but not healthy controls.⁶¹

The main findings on the involvement of neutrophils in SCD pathophysiology are summarized in Figure 2.

Eosinophils

Independently of parasitic infections, eosinophils are more numerous in steady-state SCD patients than in healthy controls and display an activated phenotype.^{62,63} An increase in absolute eosinophil count appears to result from an increased level of GM-CSF in SCD.⁶⁴ *In vitro*, adhesion of circulating eosinophils to fibronectin was found to be enhanced in SCD patients and mediated by $\alpha 4\beta 1$ (VLA-4), lymphocyte function-associated antigen 1 (LFA-1) and Mac-1 integrins.⁶² Subsequently, eosinophils from SCD patients were found to demonstrate greater spontaneous migration and release higher levels of peroxidase, eosinophil-derived neurotoxin and reactive oxygen species (ROS) than eosinophils from healthy controls.⁶³ Hydroxyurea treatment seems to reduce absolute eosinophil count and eosinophil adhesion and degranulation, which suggests an additional beneficial effect of hydroxyurea in SCD.⁶³

Basophils

Few studies have focused on basophils in SCD. In a cohort of 54 SCD patients and 27 healthy controls, basophil count and degranulation, assessed by flow cytometry with the Basotest, were similar in patients and controls.⁶⁵ Further studies are required to determine whether activated basophils could contribute to SCD pathophysiology.

Natural killer cells

The absolute number of NK cells has been reported to be increased in SCD patients not receiving disease-modifying therapy (hydroxyurea or chronic transfusions) as compared to the numbers in healthy controls and patients on hydroxyurea.^{4,66} Further enhancement during VOC has also been reported.⁶⁷ More importantly, the cytotoxicity of NK cells from SCD patients not on disease-modifying therapy, unlike that of patients receiving hydroxyurea or exchange transfusions, seems significantly increased compared with the cytotoxicity of NK cells from controls.⁶⁶ Because NK cells are capable of graft rejection, this observation of NK cell number and function normalization with hydroxyurea may explain why SCD patients receiving hydroxyurea before bone-marrow transplantation seem to have a reduced risk of graft rejection.⁶⁸ This finding raises the question of whether it would be beneficial to combine hydroxyurea with chronic transfusion in the pretransplant

period, especially with non-myeloablative or HLA-mismatched transplants.

As for iNKT cells, a potential role for NK cells in SCD pulmonary inflammation was described in SCD mice. The mRNA level of adenosine A_{2A} receptor (A_{2A}R) was increased six-fold in pulmonary NK cells from SCD mice as compared with the level in control mice, and activating A_{2A}R on NK cells decreased the number of these cells and improved baseline pulmonary function.⁶⁹

Invariant natural killer T cells

iNKT cells are known to contribute to hepatic and renal ischemia-reperfusion injury in mice.⁷⁰ Their role has, therefore, been investigated in SCD, which is characterized by repeated microvascular ischemia-reperfusion injury. Lung, liver and spleen iNKT cells were found to be more numerous, more activated and more responsive to hypoxia-reoxygenation in SCD mice than in control mice.⁷¹ Similarly, SCD patients have shown enhanced levels of circulating iNKT cells, together with increased levels of activation markers and increased interferon (IFN)- γ production, especially during VOC.⁷¹ Treating SCD mice with anti-CD1d antibody to inhibit iNKT-cell activation ameliorated pulmonary dysfunction and decreased pulmonary levels of IFN- γ and CXCR3, which suggests an important role of this pathway in SCD pulmonary inflammation.⁷¹ In

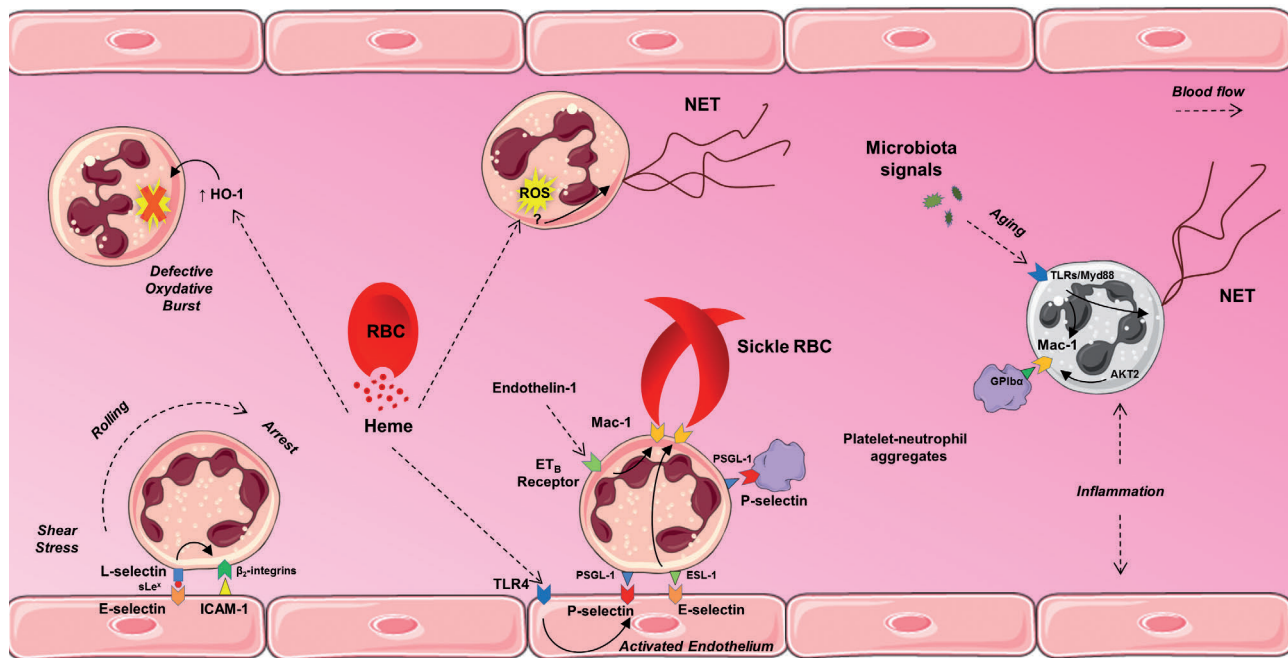


Figure 2. Neutrophils in sickle cell disease. Neutrophils rolling on E-selectin under shear stress promote catch-bond formation between E-selectin and L-selectin via sLe^x expressed on L-selectin. This interaction triggers activation of high-affinity β_2 -integrins, which leads to shear-resistant bonds with intercellular adhesion molecule 1. Neutrophil adhesion also occurs through interactions between P-selectin glycoprotein ligand 1 (PSGL-1) and endothelial P-selectin, which is upregulated in response to toll-like receptor 4 activation by heme released from red blood cells (RBC). E-selectin induces a secondary wave of activating signals, which leads to the clustering of activated macrophage-1 antigen (Mac-1) on the leading edge of adherent neutrophils, allowing for the capture of sickle RBC. Endothelin-1 promotes Mac-1 expression through the endothelin B receptors on neutrophils. Activated platelets express P-selectin, which binds PSGL-1, thereby enhancing the formation of platelet-neutrophil aggregates. The platelet-neutrophil association is also mediated by interactions between glycoprotein Iba and Mac-1, which is positively regulated by AKT2 in neutrophils during vascular inflammation. Neutrophil aging is promoted by the microbiota via TLR/Myd88 signaling and is positively correlated with Mac-1 expression and neutrophil extracellular trap (NET) formation. Heme also promotes NET formation, possibly via generation of reactive oxygen species in neutrophils, and induces expression of heme oxygenase-1 during neutrophilic differentiation, thereby impairing the bactericidal oxidative burst. ESL-1: E-selectin ligand-1; ET: endothelin; GP: glycoprotein; HO-1: heme oxygenase-1; ICAM-1: intercellular adhesion molecule 1; ROS: reactive oxygen species; TLR: toll-like receptor.

the same line of evidence, crossing SCD mice with lymphocyte-deficient mice resulted in decreased pulmonary dysfunction, whereas the adoptive transfer of iNKT cells reconstituted injury.

In SCD mice, pulmonary iNKT-cell activation was associated with a nine-fold increase in $A_{2A}R$ mRNA level as compared with the level in control mice. Treating SCD mice with an $A_{2A}R$ agonist improved pulmonary inflammation and prevented further hypoxia-reoxygenation-induced lung injury by inhibiting iNKT-cell activation.⁶⁹ In SCD patients, $A_{2A}R$ was induced during VOC in CD4⁺ but not CD4⁻ iNKT cells.⁷² This induction may serve to inhibit iNKT-cell activation over time in a counter-regulatory mechanism, thereby limiting the extent of the inflammatory immune response. $A_{2A}R$ transcription seems to be induced by NF- κ B activation because the use of NF- κ B inhibitors in cultured human iNKT cells blocked the induction of $A_{2A}R$ mRNA and protein.⁷² Furthermore, iNKT cells from SCD patients showed concomitant high expression of $A_{2A}R$ and CD39, the ecto-ATPase that converts ATP and ADP to AMP, thereby resulting in increased adenosine production, which limits iNKT-cell activation.⁷³ In a phase I trial of the $A_{2A}R$ agonist regadenoson in 27 adult SCD patients, iNKT-cell activation, measured by phospho-NF- κ B, IFN- γ and $A_{2A}R$ expression, was increased in patients as compared with controls and during VOC as compared with steady-state.⁷⁴ A 24-hour infusion of regadenoson during VOC decreased the activation of

iNKT cells by 50%, to levels similar to those in steady-state patients and in controls, without any reported toxicity. However, in a phase II, randomized, placebo-controlled trial of 92 SCD patients, a 48-hour infusion of regadenoson at the same dose during VOC did not significantly decrease iNKT-cell activation or the severity of the crises.⁷⁵

Another approach based on iNKT-specific depletion with the humanized IgG1 κ monoclonal antibody NKTT120 is currently under investigation, and it has already been shown that a single intravenous bolus produces rapid, specific and sustained iNKT-cell depletion, thereby allowing for a regimen of infusion every 3 months.⁷⁶ Because iNKT cells play important roles in immunity, there are legitimate concerns about a possible increase in susceptibility to infections, but no adverse effect was reported in a first multicenter, single-ascending-dose trial designed to determine the pharmacokinetics, pharmacodynamics and safety in SCD patients in steady-state. The next step should be a randomized, double-blind, placebo-controlled trial to assess the efficacy of NKTT120 in preventing VOC occurrence.

Platelets

Platelets are essential in hemostasis and thrombosis, but they are also important mediators of vascular inflammation. Platelets were found to be activated in SCD patients in steady-state and even more so during VOC.^{8,77} Platelet

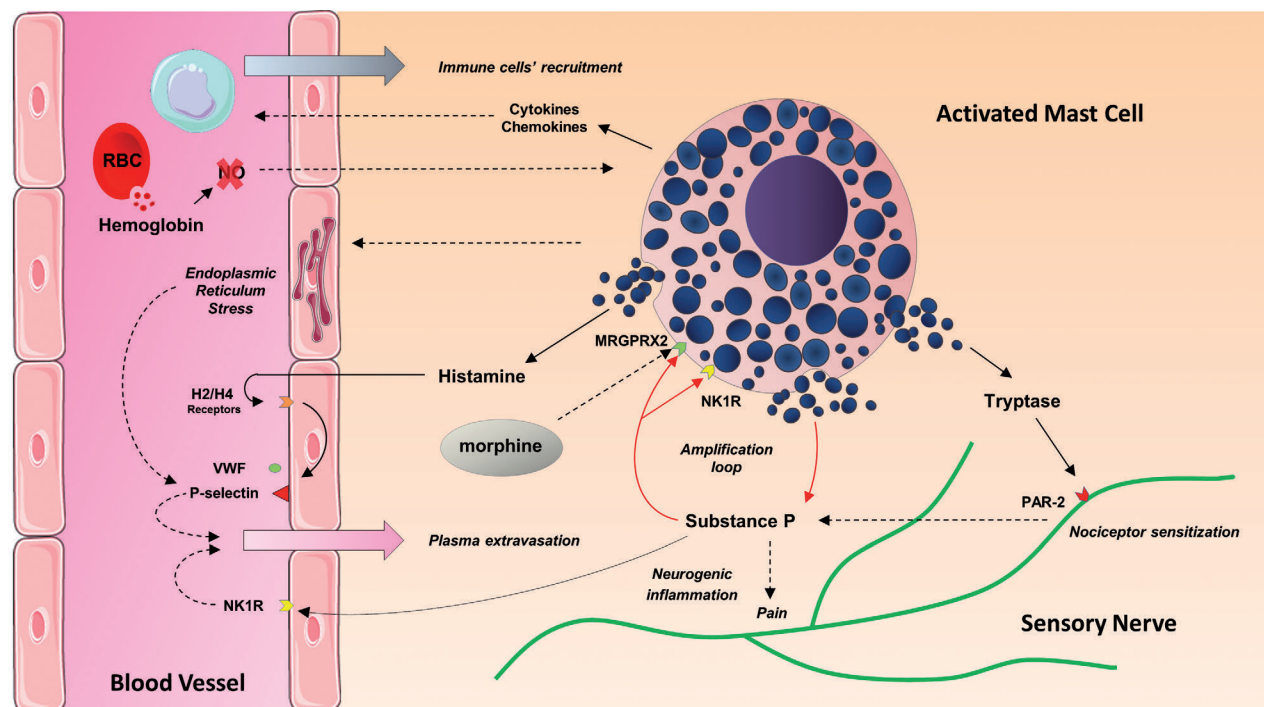


Figure 3. Mast cells in sickle cell disease. Histamine released from mast cells (MC) stimulates endothelial H_2 and H_4 receptors, thereby inducing the release of von Willebrand factor and expression of P-selectin. Tryptase released from MC activates protease-activated receptor 2 on peripheral nerve endings, thus contributing to nociceptor sensitization and stimulating the release of substance P (SP). SP released from MC and from sensory nerve endings increases plasma extravasation via neurokinin 1 receptor (NK1R) and promotes neurogenic inflammation. SP also acts on MC via NK1R and MAS-related G-protein-coupled receptor X2 (MRGPRX2), thus inducing more SP release in an amplification loop of MC activation. MRGPRX2 stimulation by SP induces the release of several cytokines and chemokines, which promotes immune cell recruitment. MC degranulation in response to morphine is also mediated by MRGPRX2. Hemolysis in sickle cell disease (SCD) may contribute to MC activation because it is responsible for nitric oxide depletion, which is known to activate MC. MC activation appears to contribute to endothelial dysfunction in SCD, via endoplasmic reticulum stress-mediated P-selectin expression and increased endothelial permeability. NO: nitric oxide; PAR-2: protease-activated receptor 2; RBC: red blood cell; VWF: von Willebrand factor.

Table 1. The main potential therapeutic agents targeting innate immune cells in sickle cell disease.

Therapeutic agent	Targeted innate immune cells	Mechanism of action	Study ID #	Phase
Hydroxyurea	Neutrophils, eosinophils, monocytes, NK cells, platelets	Multimodal mechanism including myelosuppression	FDA-approved	III
Crizanlizumab (SEG101)	Neutrophils, platelets	P-selectin inhibitor (monoclonal antibody)	NCT03814746 FDA-approved	III
Rivipansel (GMI-1070)	Neutrophils, platelets	Pan-selectin inhibitor	NCT02187003	III
Sevuparin	Neutrophils, platelets	Multimodal mechanism including P- and L-selectin inhibition	NCT02515838	II
IVIg	Neutrophils	Inhibits neutrophil adhesion and RBC-neutrophil interactions	NCT01757418	II
NKTT120	iNKT cells	iNKT cell depletion (monoclonal antibody)	NCT01783691	I
Ticagrelor	Platelets	ADP receptor antagonist	NCT03615924	III

ID #: identification number; NK cells: natural killer cells; FDA: US Food and Drug Administration; IVIG: intravenous immunoglobulin; RBC: red blood cell; iNKT cells: invariant natural killer T cells; ADP: adenosine diphosphate.

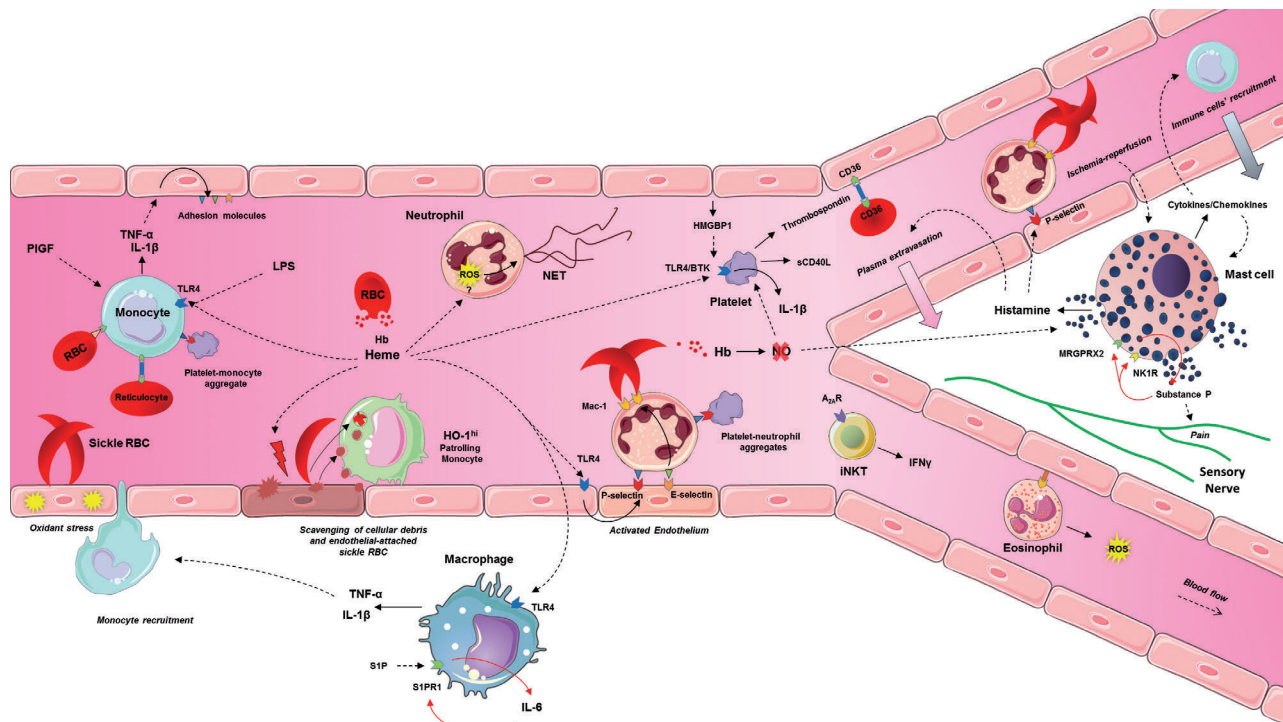


Figure 4. Main roles of innate immune cells in sickle cell disease. Innate immune cells promote inflammation, adhesion and pain in sickle cell disease (SCD). Monocytes may be activated by several mechanisms, including interactions with red blood cells (RBC), reticulocytes and platelets, as well as toll-like receptor 4 (TLR4) stimulation by heme and lipopolysaccharide. Activated monocytes produce pro-inflammatory cytokines, such as interleukin (IL)-1 β and tumor necrosis factor- α , which activate endothelial cells, resulting in enhanced expression of adhesion molecules. The interaction of sickle RBC with endothelial cells induces cellular oxidant stress, which leads to transendothelial migration of blood monocytes. Patrolling monocytes scavenge endothelium-adherent sickle RBC and take up cellular debris derived from heme-exposed endothelial cells, thereby leading to high expression of heme oxygenase-1. Macrophages may be activated by heme, released from RBC in SCD, resulting in increased production of pro-inflammatory cytokines, especially IL-1 β , through activation of the NLRP3 inflammasome. Elevated plasma levels of sphingosine-1-phosphate (S1P) induce IL-6 expression via S1P receptor 1 (S1PR1), and IL-6 in turn promotes S1PR1 expression by macrophages, leading to a vicious cycle of chronic inflammation. Neutrophil adhesion involves endothelial P-selectin, which is upregulated in response to TLR4 activation by heme in SCD. Heme may also promote neutrophil extracellular trap formation via the generation of reactive oxygen species (ROS) in neutrophils. Endothelial E-selectin induces the clustering of macrophage-1 antigen (Mac-1) on the leading edge of adherent neutrophils, allowing for the capture of sickle RBC. P-selectin is also expressed by platelets, which promotes the formation of platelet-neutrophil aggregates. The platelet NLRP3 inflammasome is activated in SCD, via HMGB1/TLR4 and Bruton tyrosine kinase, leading to enhanced production of pro-inflammatory cytokines, including IL-1 β . Increased platelet activation may also result from depletion of nitric oxide (NO), secondary to the release of free hemoglobin from RBC. Activated platelets release soluble CD40L and thrombospondin, which binds CD36 on both endothelial cells and RBC, thereby promoting RBC adhesion to microvascular endothelium. Mast cell activation in SCD may be mediated by ischemia-reperfusion, hemolysis with NO depletion, and chronic inflammation. Substance P released from mast cells promotes neurogenic inflammation and pain, but it also activates mast cells themselves via neurokinin 1 receptor and MAS-related G-protein-coupled receptor X2, thereby inducing a vicious cycle of substance P release as well as the release of pro-inflammatory cytokines and chemokines, which promotes immune cell recruitment. Histamine released from mast cells also induces plasma extravasation and endothelial P-selectin expression. Invariant natural killer T-cell activation in SCD is associated with increased interferon- γ production and A_{2a} receptor expression. Adhesion of circulating eosinophils to fibronectin in SCD is mediated by several integrins, including Mac-1, and activated eosinophils are responsible for enhanced ROS production. A_{2a}R: adenosine A_{2a} receptor; BTK: Bruton tyrosine kinase; Hb: hemoglobin; HO-1: heme oxygenase-1; IFN: interferon; iNKT cell: invariant natural killer T cell; LPS: lipopolysaccharide; MRGPRX2: MAS-related G-protein-coupled receptor X2; NET: neutrophil extracellular traps; NK1R: neurokinin 1 receptor; PIGF: placental growth factor; TLR: toll-like receptor 4; TNF- α : tumor necrosis factor alpha.

activation was positively correlated with pulmonary arterial hypertension, and activated platelets might contribute to this severe complication of SCD by promoting *in situ* thrombosis and releasing vasoactive molecules or mitogenic mediators.⁷⁷ Recently, elevated plasma levels of soluble CD40L and thrombospondin-1, two platelet-derived molecules, were reported in SCD patients with a history of ACS, which suggests a role for activated platelets in the pathogenesis of this syndrome.⁷⁸ In support of this hypothesis, antiplatelet agents such as the ADP receptor antagonist clopidogrel significantly improved lung injury in SCD mice.⁵¹ As described above, activated platelets can form aggregates with several cells, including RBC, monocytes and neutrophils, and platelet–neutrophil aggregates may contribute to pulmonary arteriole microemboli in SCD mice.⁵² By releasing thrombospondin, which binds CD36 on both endothelial cells and RBC, platelets also promote sickle RBC adhesion to microvascular endothelium, resulting in vaso-occlusion.⁷⁹ These findings have supported clinical trials of two antiplatelet agents in SCD patients, namely the ADP receptor antagonists prasugrel and ticagrelor. However, a phase III trial of prasugrel in SCD children did not find a significant reduction of VOC rate, and ticagrelor did not affect diary-reported pain in a phase IIb trial of young adults with SCD.^{80,81} A ticagrelor phase III trial on VOC rate in children with SCD is currently ongoing (#NCT03615924).

Increased platelet activation in SCD may result from decreased nitric oxide bioavailability and endothelial dysfunction with an abnormal prothrombotic microvasculature.⁷⁷ However, new insights into mechanisms of platelet activation in SCD were provided by the recent demonstration that the platelet NLRP3 inflammasome is activated in SCD patients in steady-state, and even more during VOC, via HMGB1/TLR4 and Bruton tyrosine kinase (BTK).⁸² The NLRP3 inflammasome mediates platelet activation/aggregation and thrombus formation via recognition of various pathogen-associated molecular patterns (PAMP) and damage-associated molecular patterns (DAMP) from injured tissues, such as HMGB1, whose level was found to be higher in plasma from SCD patients than in plasma from healthy controls.⁸² The platelet NLRP3 inflammasome is involved in IL-1 β signaling and platelets from SCD patients were found to produce increased amounts of pro-inflammatory cytokines, including IL-1 β .⁸⁵ *In vitro*, pharmacological or antibody-mediated inhibition of HMGB1/TLR4 and BTK decreased the ability of SCD patients' plasma to induce caspase-1 activation in platelets from healthy controls. Similarly, in sickle mice, inhibition of NLRP3 or BTK reduced caspase-1 activity and platelet aggregation.⁸² These findings may open therapeutic perspectives in SCD, especially for the BTK inhibitor ibrutinib, which is approved by the US Food and Drug Administration to treat B-cell malignancies.

Macrophages

A polarization of liver macrophages into a M1 pro-inflammatory phenotype was recently described in SCD mice, with higher expression of TNF- α and IL-6 by these cells than by liver macrophages from control mice.⁸⁴ This could contribute to the pathogenesis of SCD liver damage because pro-inflammatory activation of liver macrophages is known to induce monocyte recruitment, with enhanced cytokine production leading to hepatocyte apoptosis and fibrosis. Additionally, administration

of hemopexin to SCD mice attenuated the pro-inflammatory status of liver macrophages, which strongly suggests a role for heme in inducing the SCD macrophage phenotypic switch toward an M1 phenotype.⁸⁴ Macrophages may also be a major source of IL-1 β in SCD because heme induces IL-1 β processing through NLRP3 inflammasome activation in macrophages.⁸⁵

Infiltration of macrophages has been described in kidneys of SCD mice, with macrophage stimulating protein 1 (MSP1) accumulation in glomerular capillaries.⁸⁶ MSP1 activates RON kinase on glomerular endothelial cells, leading to the phosphorylation of ERK and AKT and resulting in increased von Willebrand factor expression, cell motility and glomeruli permeability. Treating SCD mice with a RON inhibitor (BMS-777607) attenuated glomerular endothelial injury, which suggests that this molecule could be used to prevent renal disease in SCD patients.⁸⁶

Another interesting finding concerns sphingosine-1-phosphate (S1P), a biolipid contributing to chronic inflammation, whose plasma levels are elevated in SCD patients and mice. In SCD mice, S1P induces IL-6 expression in macrophages via S1P receptor 1 (S1PR1) and IL-6 in turn promotes S1PR1 expression in macrophages of several organs, which leads to a vicious cycle promoting chronic inflammation and tissue damage.⁸⁷ Treating SCD mice with a S1PR1 antagonist (FTY720) reduced systemic inflammation and improved tissue damage in the spleen, liver, kidneys and lungs, which suggests that this drug, approved by the US Food and Drug Administration to treat multiple sclerosis as an immunosuppressant, may benefit SCD patients.⁸⁷

Mast cells

Growing evidence is suggesting a role for mast cells in the pathophysiology of SCD. The chronic pain in this disease shares many characteristics with that encountered in mastocytosis, and the clinical signs of mast cell activation syndrome have been described in SCD patients.⁸⁸ Increased plasma levels of several mast cell mediators, including histamine and substance P, have been reported in steady-state with further enhancement during VOC.^{89,90} The plasma tryptase level is also slightly increased during VOC as compared with the level in steady-state but without reaching pathological values, which suggests mast-cell activation rather than increased numbers of mast cells.⁸⁹ In SCD patients, plasma histamine level was found to be negatively correlated with HbF level, a well-known protective factor in SCD, and positively with absolute neutrophil count, absolute platelet count and C-reactive protein level, which suggests a role for inflammation in the mechanisms leading to mast-cell activation.⁸⁹ Histamine may contribute to SCD pathogenesis, because stimulation of endothelial histamine H₂ and H₄ receptors induced the release of von Willebrand factor and P-selectin expression by endothelial cells, thus promoting adhesion of sickle RBC.⁹¹ Furthermore, the plasma level of substance P was found to be negatively correlated with hemoglobin concentration and positively with the levels of markers of hemolysis.⁹⁰ These findings may reflect SCD hemolysis being responsible for depletion of nitric oxide, which is known to induce mast-cell activation.⁹²

Substance P, a neuropeptide released from mast cells and from sensory nerve endings, acts as a primary pain neurotransmitter and a neuromodulator. Via neurokinin 1 receptor (NK1R), substance P contributes to neurogenic inflammation by increasing venular permeability and plas-

ma extravasation, but it also acts on the mast cells themselves, promoting a vicious cycle of mast-cell activation and substance P release.⁹³ Furthermore, tryptase released from mast cells activates protease-activated receptor 2 (PAR-2) on peripheral nerve endings, thus contributing to nociceptor sensitization and stimulating the release of substance P, which in turn activates mast cells.⁹⁴ Substance P and tryptase levels were higher in the skin of SCD mice than in that of control mice and both proteins colocalized with activated mast cells.^{93,95} Inhibition of mast cells, with the mast-cell stabilizer cromolyn or the *c-kit*/tyrosine kinase inhibitor imatinib, decreased substance P and tryptase levels as well as systemic inflammation, neurogenic inflammation, reflected by Evans blue leakage, and hyperalgesia. Importantly, these results were confirmed in transgenic SCD mice lacking mast cells.⁹³ In the same line of evidence, in an SCD patient with chronic myeloid leukemia, imatinib treatment completely resolved repeated VOC, and discontinuation of the treatment coincided with VOC recurrence.⁹⁶ However, this may be explained, at least in part, by a decrease in leukocyte and neutrophil counts during imatinib treatment, and further studies are needed. A clinical trial of imatinib or another *c-kit*/tyrosine kinase inhibitor in SCD patients may be considered.

Treating SCD mice with a high-affinity opioid nociception receptor agonist, AT-200, known to inhibit the release of substance P from sensory nerve endings, inhibited mast-cell activation/degranulation as well as neurogenic inflammation, with a greater antinociceptive effect than that of morphine.⁹⁷ In SCD mice, morphine was found to stimulate the release of substance P from mast cells, thereby promoting neurogenic inflammation and hyperalgesia mediated by mast-cell activation.⁹³ In SCD patients, morphine is considered a reference analgesic for VOC but it may actually have deleterious effects by inducing the release of mast-cell mediators, including substance P and histamine.⁸⁹ Importantly, human mast-cell degranulation in response to morphine was recently found to be mediated by MAS-related G-protein-coupled receptor X2 (MRGPRX2), which is also a major receptor for substance P, mediating innate immune cell recruitment, neurogenic inflammation, and pain.^{98,99}

Mast-cell activation may have an additional role in promoting blood-brain barrier dysfunction in SCD. *In vitro*, activated mast cells from SCD mice induced endoplasmic reticulum stress in brain endothelial cells, with increased P-selectin expression and increased endothelial permeability.¹⁰⁰ Hence, mast-cell activation may contribute to endothelial dysfunction in SCD via endoplasmic reticulum stress-mediated P-selectin expression.

The main findings on the involvement of mast cells in SCD pathophysiology are summarized in Figure 3.

The main potential therapeutic agents targeting innate immune cells in SCD are described in Table 1.

Conclusion

Findings from our review suggest that innate immune cells do indeed play important roles in SCD in promoting inflammation, adhesion and pain, the hallmarks of the disease (Figure 4).

Among suspected mechanisms underlying innate immune cell activation, free hemoglobin and heme released by hemolysis may play a crucial role by activating TLR4 or generating ROS that can activate the inflammatory.⁸⁵ Nitric oxide depletion by free hemoglobin may also contribute, especially to platelet and mast-cell activation. Innate immune cells usually possess a large repertoire of receptors, including cytokine and chemokine receptors, which enables them to respond to various inflammatory signals. Hence, their activation in SCD is likely promoted by chronic and acute inflammation. SCD patients have increased susceptibility to infections, and PAMP, such as bacterial lipopolysaccharides or endotoxins, could also contribute, as could DAMP originating from injured tissues following ischemia/reperfusion.

Once activated, innate immune cells release a wide range of cytokines and chemokines, thus promoting a vicious cycle of immune cell recruitment and activation. Pro-inflammatory cytokines produced mainly by monocytes and macrophages, but also by platelets and other innate immune cells, can activate the endothelium together with heme, resulting in increased expression of adhesion molecules. Neutrophils are crucial factors in endothelial adhesion but monocytes and platelets also contribute to decreased blood flow and vaso-occlusion via the formation of RBC–monocyte, platelet–monocyte and platelet–neutrophil aggregates. However, activated innate immune cells are not just deleterious protagonists in SCD, as illustrated by patrolling monocytes, which scavenge endothelial debris and adherent sickle RBC.

Innate immune cells may play a specific role in SCD. For example, mast cells promote neurogenic inflammation via substance P release. However, the main complications of SCD, such as VOC, ACS and stroke, likely result from interlinked actions of innate immune cells. Further investigations are required to better understand the involvement of these novel, important protagonists in SCD pathophysiology, their respective roles in acute and chronic complications, as well as the mechanisms underlying their activation, in order to develop innovative treatments targeting innate immune cells in SCD.

References

1. Ware RE, de Montalembert M, Tshilolo L, Abboud MR. Sickle cell disease. *Lancet*. 2017;390(10091):311-323.
2. Piel FB, Steinberg MH, Rees DC. Sickle cell disease. *N Engl J Med*. 2017;376(16):1561-1573.
3. Wongtong N, Jones S, Deng Y, Cai J, Ataga KI. Monocytosis is associated with hemolysis in sickle cell disease. *Hematology*. 2015;20(10):593-597.
4. Nickel RS, Osunkwo I, Garrett A, et al. Immune parameter analysis of children with sickle cell disease on hydroxycarbamide or chronic transfusion therapy. *Br J Haematol*. 2015;169(4):574-583.
5. Sultana C, Shen Y, Rattan V, Johnson C, Kalra VK. Interaction of sickle erythrocytes with endothelial cells in the presence of endothelial cell conditioned medium induces oxidant stress leading to transendothelial migration of monocytes. *Blood*. 1998;92(10):3924-3935.
6. Belcher JD, Marker PH, Weber JP, Heibel RP, Vercellotti GM. Activated monocytes in sickle cell disease: potential role in the activation of vascular endothelium and vaso-occlusion. *Blood*. 2000;96(7):2451-2459.
7. Wun T, Cordoba M, Rangaswami A, Cheung AW, Paglieroni T. Activated monocytes and platelet-monocyte aggregates in

- patients with sickle cell disease. *Clin Lab Haematol.* 2002;24(2):81-88.
8. Inwald DP, Kirkham FJ, Peters MJ, et al. Platelet and leucocyte activation in childhood sickle cell disease: association with nocturnal hypoxaemia. *Br J Haematol.* 2000;111(2):474-481.
 9. Sloma I, Zilber MT, Charron D, Girot R, Tamouza R, Gelin C. Upregulation and atypical expression of the CD1 molecules on monocytes in sickle cell disease. *Hum Immunol.* 2004;65(11):1370-1376.
 10. Dias-Da-Motta F, Arruda VR, Muscara MN, et al. The release of nitric oxide and superoxide anion by neutrophils and mononuclear cells from patients with sickle cell anaemia. *Br J Haematol.* 1996;93(2):333-340.
 11. Marcal LE, Dias-da-Motta PM, Rehder J, et al. Up-regulation of NADPH oxidase components and increased production of interferon-gamma by leukocytes from sickle cell disease patients. *Am J Hematol.* 2008;83(1): 41-45.
 12. Setty BN, Key NS, Rao AK, et al. Tissue factor-positive monocytes in children with sickle cell disease: correlation with biomarkers of haemolysis. *Br J Haematol.* 2012;157(3):370-380.
 13. Ragab SM, Soliman MA. Tissue factor-positive monocytes expression in children with sickle cell disease: clinical implication and relation to inflammatory and coagulation markers. *Blood Coagul Fibrinolysis.* 2016;27(8):862-869.
 14. Solovey A, Somani A, Belcher JD, et al. A monocyte-TNF-endothelial activation axis in sickle transgenic mice: therapeutic benefit from TNF blockade. *Am J Hematol.* 2017;92(11):1119-1130.
 15. Brittain JE, Knoll CM, Ataga KI, Orringer EP, Parise IV. Fibronectin bridges monocytes and reticulocytes via integrin alpha4beta1. *Br J Haematol.* 2008;141(6):872-881.
 16. Selvaraj SK, Giri RK, Perelman N, Johnson C, Malik P, Kalra VK. Mechanism of monocyte activation and expression of proinflammatory cytochemokines by placenta growth factor. *Blood.* 2003;102(4):1515-1524.
 17. Perelman N, Selvaraj SK, Batra S, et al. Placenta growth factor activates monocytes and correlates with sickle cell disease severity. *Blood.* 2003;102(4):1506-1514.
 18. Sundaram N, Tailor A, Mendelsohn L, et al. High levels of placenta growth factor in sickle cell disease promote pulmonary hypertension. *Blood.* 2010;116(1):109-112.
 19. Zennadi R, Chien A, Xu K, Batchvarova M, Telen MJ. Sickle red cells induce adhesion of lymphocytes and monocytes to endothelium. *Blood.* 2008;112(8):3474-3483.
 20. Chaar V, Picot J, Renaud O, et al. Aggregation of mononuclear and red blood cells through an alpha4beta1-Lu/basal cell adhesion molecule interaction in sickle cell disease. *Haematologica.* 2010;95(11):1841-1848.
 21. Dagur PK, McCoy JP, Nichols J, et al. Haem augments and iron chelation decreases toll-like receptor 4 mediated inflammation in monocytes from sickle cell patients. *Br J Haematol.* 2018;181(4):552-554.
 22. Liu Y, Jing F, Yi W, et al. HO-1(hi) patrolling monocytes protect against vaso-occlusion in sickle cell disease. *Blood.* 2018;131(14):1600-1610.
 23. Liu Y, Zhong H, Bao W, et al. Patrolling monocytes scavenge endothelial adherent sickle RBC: a novel mechanism of inhibition of vaso-occlusion in SCD. *Blood.* 2019;134(7):579-590.
 24. Yazdanbakhsh K, Ware RE, Noizat-Pirenne F. Red blood cell alloimmunization in sickle cell disease: pathophysiology, risk factors, and transfusion management. *Blood.* 2012;120(3):528-537.
 25. Godefroy E, Liu Y, Shi P, et al. Altered heme-mediated modulation of dendritic cell function in sickle cell alloimmunization. *Haematologica.* 2016;101(9):1028-1038.
 26. Abhishek K, Kumar R, Arif E, Patra PK, Choudhary SB, Sohail M. Induced expression of bone morphogenetic protein-6 and Smads signaling in human monocytes derived dendritic cells during sickle-cell pathology with orthopedic complications. *Biochem Biophys Res Commun.* 2010;396(4):950-955.
 27. Anyaegbu CC, Okpala IE, Akren'Ova YA, Salimonu LS. Peripheral blood neutrophil count and candidal activity correlate with the clinical severity of sickle cell anaemia (SCA). *Eur J Haematol.* 1998;60(4): 267-268.
 28. Platt OS, Brambilla DJ, Rosse WF, et al. Mortality in sickle cell disease. Life expectancy and risk factors for early death. *N Engl J Med.* 1994;330(23):1639-1644.
 29. Castro O, Brambilla DJ, Thorington B, et al. The acute chest syndrome in sickle cell disease: incidence and risk factors. The Cooperative Study of Sickle Cell Disease. *Blood.* 1994;84(2):643-649.
 30. Ohene-Frempong K, Weiner SJ, Sleeper LA, et al. Cerebrovascular accidents in sickle cell disease: rates and risk factors. *Blood.* 1998;91(1):288-294.
 31. Wigfall DR, Ware RE, Burchinal MR, Kinney TR, Foreman JW. Prevalence and clinical correlates of glomerulopathy in children with sickle cell disease. *J Pediatr.* 2000;136(6):749-753.
 32. Wali Y, Beshlawi I, Fawaz N, et al. Coexistence of sickle cell disease and severe congenital neutropenia: first impressions can be deceiving. *Eur J Haematol.* 2012;89(3): 245-249.
 33. Adler BK, Salzman DE, Carabasi MH, Vaughan WP, Reddy VV, Prchal JT. Fatal sickle cell crisis after granulocyte colony-stimulating factor administration. *Blood.* 2001;97(10):3313-3314.
 34. Pieters RC, Rojer RA, Saleh AW, Saleh AE, Duits AJ. Molgramostim to treat SS-sickle cell leg ulcers. *Lancet.* 1995;345(8948):528.
 35. Charache S. Mechanism of action of hydroxyurea in the management of sickle cell anemia in adults. *Semin Hematol.* 1997;34(3 Suppl 3):15-21.
 36. Fadlon E, Vordermeier S, Pearson TC, et al. Blood polymorphonuclear leukocytes from the majority of sickle cell patients in the crisis phase of the disease show enhanced adhesion to vascular endothelium and increased expression of CD64. *Blood.* 1998;91(1):266-274.
 37. Lum AF, Wun T, Staunton D, Simon SI. Inflammatory potential of neutrophils detected in sickle cell disease. *Am J Hematol.* 2004;76(2):126-133.
 38. Okpala I, Daniel Y, Haynes R, Odoemene D, Goldman J. Relationship between the clinical manifestations of sickle cell disease and the expression of adhesion molecules on white blood cells. *Eur J Haematol.* 2002;69(3):135-144.
 39. Benkerrou M, Delarche C, Brahimi L, et al. Hydroxyurea corrects the dysregulated L-selectin expression and increased H(2)O(2) production of polymorphonuclear neutrophils from patients with sickle cell anemia. *Blood.* 2002;99(7):2297-2303.
 40. Almeida CB, Scheiermann C, Jang JE, et al. Hydroxyurea and a cGMP-amplifying agent have immediate benefits on acute vaso-occlusive events in sickle cell disease mice. *Blood.* 2012;120(14):2879-2888.
 41. Turhan A, Weiss LA, Mohandas N, Collier BS, Frenette PS. Primary role for adherent leukocytes in sickle cell vascular occlusion: a new paradigm. *Proc Natl Acad Sci U S A.* 2002;99(5):3047-3051.
 42. Hidalgo A, Chang J, Jang JE, Peired AJ, Chiang EY, Frenette PS. Heterotypic interactions enabled by polarized neutrophil microdomains mediate thromboinflammatory injury. *Nat Med.* 2009;15(4):384-391.
 43. Zhang D, Xu C, Manwani D, Frenette PS. Neutrophils, platelets, and inflammatory pathways at the nexus of sickle cell disease pathophysiology. *Blood.* 2016;127(7):801-809.
 44. Morikis VA, Chase S, Wun T, Chaikof EL, Magnani JL, Simon SI. Selectin catch-bonds mechanotransduce integrin activation and neutrophil arrest on inflamed endothelium under shear flow. *Blood.* 2017;130(19):2101-2110.
 45. Chang J, Patton JT, Sarkar A, Ernst B, Magnani JL, Frenette PS. GMI-1070, a novel pan-selectin antagonist, reverses acute vascular occlusions in sickle cell mice. *Blood.* 2010;116(10):1779-1786.
 46. Telen MJ, Wun T, McCavit TL, et al. Randomized phase 2 study of GMI-1070 in SCD: reduction in time to resolution of vaso-occlusive events and decreased opioid use. *Blood.* 2015;125(17):2656-2664.
 47. Ataga KI, Kutlar A, Kanter J, et al. Crizanlizumab for the prevention of pain crises in sickle cell disease. *N Engl J Med.* 2017;376(5):429-439.
 48. Telen MJ, Batchvarova M, Shan S, et al. Sevuparin binds to multiple adhesive ligands and reduces sickle red blood cell-induced vaso-occlusion. *Br J Haematol.* 2016;175(5): 935-948.
 49. White J, Lindgren M, Liu K, Gao X, Jendeberg L, Hines P. Sevuparin blocks sickle blood cell adhesion and sickle-leucocyte rolling on immobilized L-selectin in a dose dependent manner. *Br J Haematol.* 2019;184(5):873-876.
 50. Manwani D, Chen G, Carullo V, et al. Single-dose intravenous gammaglobulin can stabilize neutrophil Mac-1 activation in sickle cell pain crisis. *Am J Hematol.* 2015; 90(5):381-385.
 51. Polanowska-Grabowska R, Wallace K, Field JJ, et al. P-selectin-mediated platelet-neutrophil aggregate formation activates neutrophils in mouse and human sickle cell disease. *Arterioscler Thromb Vasc Biol.* 2010;30(12):2392-2399.
 52. Bennewitz MF, Jimenez MA, Vats R, et al. Lung vaso-occlusion in sickle cell disease mediated by arteriolar neutrophil-platelet microemboli. *JCI Insight.* 2017;2(1):e89761.
 53. Li J, Kim K, Hahm E, et al. Neutrophil AKT2 regulates heterotypic cell-cell interactions during vascular inflammation. *J Clin Invest.* 2014;124(4):1483-1496.
 54. Kim K, Li J, Barazia A, et al. ARQ 092, an orally-available, selective AKT inhibitor, attenuates neutrophil-platelet interactions in sickle cell disease. *Haematologica.* 2017;102(2):246-259.
 55. Jimenez MA, Novelli E, Shaw GD, Sundt P. Glycoprotein Ibalpha inhibitor (CCP-224) prevents neutrophil-platelet aggregation in Sickle Cell Disease. *Blood Adv.* 2017;1(20): 1712-1716.
 56. Koehl B, Nivoit P, El Nemer W, et al. The endothelin B receptor plays a crucial role in the adhesion of neutrophils to the endothelium in sickle cell disease. *Haematologica.* 2017;102(7):1161-1172.
 57. Zhang D, Chen G, Manwani D, et al. Neutrophil ageing is regulated by the micro-

- biome. *Nature*. 2015;525(7570):528-532.
58. Rana K, Pantoja K, Xiao L. Bone marrow neutrophil aging in sickle cell disease mice is associated with impaired osteoblast functions. *Biochem Biophys Res*. 2018;16:110-114.
 59. Chen G, Zhang D, Fuchs TA, Manwani D, Wagner DD, Frenette PS. Heme-induced neutrophil extracellular traps contribute to the pathogenesis of sickle cell disease. *Blood*. 2014;123(24):3818-3827.
 60. Ghosh S, Adisa OA, Chappa P, et al. Extracellular hemin crisis triggers acute chest syndrome in sickle mice. *J Clin Invest*. 2013;123(11):4809-4820.
 61. Evans C, Orf K, Horvath E, et al. Impairment of neutrophil oxidative burst in children with sickle cell disease is associated with heme oxygenase-1. *Haematologica*. 2015;100(12):1508-1516.
 62. Canalli AA, Conran N, Fattori A, Saad ST, Costa FF. Increased adhesive properties of eosinophils in sickle cell disease. *Exp Hematol*. 2004;32(8):728-734.
 63. Pallis FR, Conran N, Fertrin KY, Olalla Saad ST, Costa FF, Franco-Penteado CF. Hydroxycarbamide reduces eosinophil adhesion and degranulation in sickle cell anaemia patients. *Br J Haematol*. 2014;164(2):286-295.
 64. Conran N, Saad ST, Costa FF, Ikuta T. Leukocyte numbers correlate with plasma levels of granulocyte-macrophage colony-stimulating factor in sickle cell disease. *Ann Hematol*. 2007;86(4):255-261.
 65. Qari MH, Zaki WA. Flow cytometric assessment of leukocyte function in sickle cell anemia. *Hemoglobin*. 2011;35(4):367-381.
 66. Abraham AA, Lang H, Meier ER, et al. Characterization of natural killer cells expressing markers associated with maturity and cytotoxicity in children and young adults with sickle cell disease. *Pediatr Blood Cancer*. 2019;66(5):e27601.
 67. Al Najjar S, Adam S, Ahmed N, Qari M. Markers of endothelial dysfunction and leukocyte activation in Saudi and non-Saudi haplotypes of sickle cell disease. *Ann Hematol*. 2017;96(1):141-146.
 68. Dedeken L, Le PQ, Azzi N, et al. Haematopoietic stem cell transplantation for severe sickle cell disease in childhood: a single centre experience of 50 patients. *Br J Haematol*. 2014;165(3):402-408.
 69. Wallace KL, Linden J. Adenosine A2A receptors induced on iNKT and NK cells reduce pulmonary inflammation and injury in mice with sickle cell disease. *Blood*. 2010;116(23):5010-5020.
 70. Lappas CM, Day YJ, Marshall MA, Engelhard VH, Linden J. Adenosine A2A receptor activation reduces hepatic ischemia reperfusion injury by inhibiting CD1d-dependent NKT cell activation. *J Exp Med*. 2006;203(12):2639-2648.
 71. Wallace KL, Marshall MA, Ramos SI, et al. NKT cells mediate pulmonary inflammation and dysfunction in murine sickle cell disease through production of IFN-gamma and CXCR3 chemokines. *Blood*. 2009;114(3):667-676.
 72. Lin G, Field JJ, Yu JC, et al. NF-kappaB is activated in CD4+ iNKT cells by sickle cell disease and mediates rapid induction of adenosine A2A receptors. *PLoS One*. 2013;8(10):e74664.
 73. Yu JC, Lin G, Field JJ, Linden J. Induction of anti-inflammatory purinergic signaling in activated human iNKT cells. *JCI Insight*. 2018;3(17).
 74. Field JJ, Lin G, Okam MM, et al. Sickle cell vaso-occlusion causes activation of iNKT cells that is decreased by the adenosine A2A receptor agonist regadenoson. *Blood*. 2013;121(17):3329-3334.
 75. Field JJ, Majerus E, Gordeuk VR, et al. Randomized phase 2 trial of regadenoson for treatment of acute vaso-occlusive crises in sickle cell disease. *Blood Adv*. 2017;1(20):1645-1649.
 76. Field JJ, Majerus E, Ataga KI, et al. NNKTT120, an anti-iNKT cell monoclonal antibody, produces rapid and sustained iNKT cell depletion in adults with sickle cell disease. *PLoS One*. 2017;12(2):e0171067.
 77. Villagra J, Shiva S, Hunter LA, Machado RF, Gladwin MT, Kato GJ. Platelet activation in patients with sickle disease, hemolysis-associated pulmonary hypertension, and nitric oxide scavenging by cell-free hemoglobin. *Blood*. 2007;110(6):2166-2172.
 78. Garrido VT, Sonzogni L, Mtatiro SN, Costa FF, Conran N, Thein SL. Association of plasma CD40L with acute chest syndrome in sickle cell anemia. *Cytokine*. 2017;97:104-107.
 79. Brittain HA, Eckman JR, Swerlick RA, Howard RJ, Wick TM. Thrombospondin from activated platelets promotes sickle erythrocyte adherence to human microvascular endothelium under physiologic flow: a potential role for platelet activation in sickle cell vaso-occlusion. *Blood*. 1993;81(8):2137-2143.
 80. Heeney MM, Hoppe CC, Abboud MR, et al. A multinational trial of prasugrel for sickle cell vaso-occlusive events. *N Engl J Med*. 2016;374(7):625-635.
 81. Kanter J, Abboud MR, Kaya B, et al. Ticagrelor does not impact patient-reported pain in young adults with sickle cell disease: a multicentre, randomised phase IIb study. *Br J Haematol*. 2019;184(2):269-278.
 82. Vogel S, Arora T, Wang X, et al. The platelet NLRP3 inflammasome is upregulated in sickle cell disease via HMGB1/TLR4 and Bruton tyrosine kinase. *Blood Adv*. 2018;2(20):2672-2680.
 83. Davila J, Manwani D, Vasovic L, et al. A novel inflammatory role for platelets in sickle cell disease. *Platelets*. 2015;26(8):726-729.
 84. Vinchi F, Costa da Silva M, Ingoglia G, et al. Hemopexin therapy reverts heme-induced proinflammatory phenotypic switching of macrophages in a mouse model of sickle cell disease. *Blood*. 2016;127(4):473-486.
 85. Dutra FF, Alves LS, Rodrigues D, et al. Hemolysis-induced lethality involves inflammasome activation by heme. *Proc Natl Acad Sci U S A*. 2014;111(39):E4110-4118.
 86. Khaibullina A, Adjei EA, Afangbedji N, et al. RON kinase inhibition reduces renal endothelial injury in sickle cell disease mice. *Haematologica*. 2018;103(5):787-798.
 87. Zhao S, Adebisi MG, Zhang Y, et al. Sphingosine-1-phosphate receptor 1 mediates elevated IL-6 signaling to promote chronic inflammation and multitissue damage in sickle cell disease. *FASEB J*. 2018;32(5):2855-2865.
 88. Afrin LB. Mast cell activation syndrome as a significant comorbidity in sickle cell disease. *Am J Med Sci*. 2014;348(6):460-464.
 89. Allali S, Lionnet F, Mattioni S, et al. Plasma histamine elevation in a large cohort of sickle cell disease patients. *Br J Haematol*. 2019;186(1):125-129.
 90. Brandow AM, Wanderssee NJ, Dasgupta M, et al. Substance P is increased in patients with sickle cell disease and associated with haemolysis and hydroxycarbamide use. *Br J Haematol*. 2016;175(2):237-245.
 91. Wagner MC, Eckman JR, Wick TM. Histamine increases sickle erythrocyte adherence to endothelium. *Br J Haematol*. 2006;132(4):512-522.
 92. Brooks AC, Whelan CJ, Purcell WM. Reactive oxygen species generation and histamine release by activated mast cells: modulation by nitric oxide synthase inhibition. *Br J Pharmacol*. 1999;128(3):585-590.
 93. Vincent L, Vang D, Nguyen J, et al. Mast cell activation contributes to sickle cell pathobiology and pain in mice. *Blood*. 2013;122(11):1853-1862.
 94. Amadesi S, Nie J, Vergnolle N, et al. Protease-activated receptor 2 sensitizes the capsaicin receptor transient receptor potential vanilloid receptor 1 to induce hyperalgesia. *J Neurosci*. 2004;24(18):4300-4312.
 95. Kohli DR, Li Y, Khasabov SG, et al. Pain-related behaviors and neurochemical alterations in mice expressing sickle hemoglobin: modulation by cannabinoids. *Blood*. 2010;116(3):456-465.
 96. Stankovic Stojanovic K, Thiolier B, Garandeau E, Lecomte I, Bachmeyer C, Lionnet F. Chronic myeloid leukaemia and sickle cell disease: could imatinib prevent vaso-occlusive crisis? *Br J Haematol*. 2011;155(2):271-272.
 97. Vang D, Paul JA, Nguyen J, et al. Small-molecule nociceptin receptor agonist ameliorates mast cell activation and pain in sickle mice. *Haematologica*. 2015;100(12):1517-1525.
 98. Navines-Ferrer A, Serrano-Candelas E, Lafuente A, Munoz-Cano R, Martin M, Gastaminza G. MRGPRX2-mediated mast cell response to drugs used in perioperative procedures and anaesthesia. *Sci Rep*. 2018;8(1):11628.
 99. Green DP, Limjunyawong N, Gour N, Pundir P, Dong X. A mast-cell-specific receptor mediates neurogenic inflammation and pain. *Neuron*. 2019;101(3):412-420.
 100. Tran H, Mittal A, Sagi V, et al. Mast cells induce blood brain barrier damage in SCD by causing endoplasmic reticulum stress in the endothelium. *Front Cell Neurosci*. 2019;13:56.



Fibrin(ogen) in human disease: both friend and foe

Rui Vilar,¹ Richard J. Fish,¹ Alessandro Casini² and Marguerite Neerman-Arbez^{1,3}

¹Department of Genetic Medicine and Development, University of Geneva Faculty of Medicine, ²Division of Angiology and Hemostasis, University Hospitals and University of Geneva Faculty of Medicine and ³iGE3, Institute of Genetics and Genomics in Geneva, Geneva, Switzerland

Haematologica 2020
Volume 105(2):284-296

ABSTRACT

Fibrinogen is an abundant protein synthesized in the liver, present in human blood plasma at concentrations ranging from 1.5-4 g/L in healthy individuals with a normal half-life of 3-5 days. With fibrin, produced by thrombin-mediated cleavage, fibrinogen plays important roles in many physiological processes. Indeed, the formation of a stable blood clot, containing polymerized and cross-linked fibrin, is crucial to prevent blood loss and drive wound healing upon vascular injury. A balance between clotting, notably the conversion of fibrinogen to fibrin, and fibrinolysis, the proteolytic degradation of the fibrin mesh, is essential. Disruption of this equilibrium can cause disease in distinct manners. While some pathological conditions are the consequence of altered levels of fibrinogen, others are related to structural properties of the molecule. The source of fibrinogen expression and the localization of fibrin(ogen) protein also have clinical implications. Low levels of fibrinogen expression have been detected in extra-hepatic tissues, including carcinomas, potentially contributing to disease. Fibrin(ogen) deposits at aberrant sites including the central nervous system or kidney, can also be pathological. In this review, we discuss disorders in which fibrinogen and fibrin are implicated, highlighting mechanisms that may contribute to disease.

Correspondence:

MARGUERITE NEERMAN-ARBEZ
marguerite.neerman-arbez@unige.ch

Received: September 19, 2019.

Accepted: November 21, 2019.

Pre-published: January 16, 2020.

doi:10.3324/haematol.2019.236901

Check the online version for the most updated information on this article, online supplements, and information on authorship & disclosures: www.haematologica.org/content/105/2/284

©2020 Ferrata Storti Foundation

Material published in Haematologica is covered by copyright. All rights are reserved to the Ferrata Storti Foundation. Use of published material is allowed under the following terms and conditions:

<https://creativecommons.org/licenses/by-nc/4.0/legalcode>.

Copies of published material are allowed for personal or internal use. Sharing published material for non-commercial purposes is subject to the following conditions:

<https://creativecommons.org/licenses/by-nc/4.0/legalcode>,

sect. 3. Reproducing and sharing published material for commercial purposes is not allowed without permission in writing from the publisher.



Introduction

Fibrinogen biosynthesis takes place in hepatocytes, starting with expression of three genes, *FGA*, *FGB* and *FGG*, clustered in a 50 kb region of human chromosome 4. The genes encode fibrinogen $\text{A}\alpha$, $\text{B}\beta$ and γ chains, respectively. Both *FGA* and *FGG* are transcribed to produce two transcripts. The major transcript encoding $\text{A}\alpha$ is transcribed from five exons, but a minor transcript, resulting from splicing of a sixth exon, encodes the $\text{A}\alpha\text{E}$ chain which is present in 1-3% of circulating fibrinogen molecules. For *FGG*, a major γ chain mRNA is transcribed from ten exons while in the minor γ' chain intron 9 is retained, substituting the four amino acids encoded by exon 10 with 20 γ' COOH-terminal residues. γ/γ' and γ'/γ' represent approximately 8 to 15% of a healthy person's total fibrinogen.^{1,2}

The fibrinogen genes are co-regulated both for basal expression and when upregulated upon an inflammation-driven acute phase response.³ The latter leads to a prompt increase in plasma fibrinogen after bleeding or clotting events, or to support wound healing.³ Each fibrinogen gene is thought to be regulated by a proximal promoter and local enhancer elements. These appear to act together with tissue-restricted transcription factors, regulatory chromatin marks and a looped architecture to co-regulate expression of the three-gene cluster.^{4,5} CpG DNA methylation of the fibrinogen regulatory regions,⁶ and microRNA^{7,8} can also contribute to cell- and state-specific fibrinogen expression.

Fibrinogen mRNA are translated into nascent polypeptides with signal peptides that are cleaved in the lumen of the endoplasmic reticulum. Here the chains assemble, with the assistance of chaperones, first as $\text{A}\alpha\text{-}\gamma$ or $\text{B}\beta\text{-}\gamma$ dimers and then as trimeric molecules, by addition of the missing chain. NH_2 -terminal disulfide bridges connect two trimers producing hexameric molecules. These transit to the Golgi apparatus, where the final $\text{B}\beta$ and γ chain *N*-glycosylation steps take place.⁹ While

properly assembled fibrinogen is secreted as a 340 kDa glycoprotein, misfolded proteins are retained intracellularly and degraded by quality control mechanisms.¹⁰

During human development, hemostatic proteins, including fibrinogen, are present in plasma around the time of the termination of hepatic histogenesis and spleen vascularization (~10-11 weeks of gestation), reaching levels at term similar to those in the adult.¹¹ Fetal fibrinogen has qualitative differences, notably delayed fibrin formation, which persist for approximately 1 year after birth. Neonatal clots are less dense than those of an adult and have a different three-dimensional structure.¹² However, this does not have a significant impact on coagulation parameters such as bleeding time.

Circulating fibrinogen promotes hemostasis as the soluble fibrin precursor, but also by bridging activated platelets, and enabling a correct disposition of erythrocytes, macrophages and fibroblasts around a wound.¹³ The development and control of these processes is important to stop bleeding, enhance wound healing and promote tissue regeneration. In addition, fibrin(ogen) is implicated in preventing microbial invasion and proliferation upon trauma,¹⁴ enhancing host defenses through the assembly of matrices that entrap invaders and recruit and activate host immune cells.¹⁵

The association of fibrin(ogen) with disease results from different mechanisms. These include triggering signaling pathways within given physiological contexts, and alterations in the normal range of fibrinogen levels or in its structure. The latter can contribute to altered fibrin clot properties which can impair thrombin and plasminogen binding. In this review, we focus on the involvement of fibrin(ogen) in the development of a range of human disorders, describing its role in different pathological mechanisms.

Bleeding disorders

Bleeding or hemorrhage is the escape of blood from the closed cardiovascular system due to damaged blood vessels.¹⁶ The natural control of bleeding is known as hemostasis.¹⁷ Many defects in hemostatic proteins, including fibrinogen, can cause pathological hemorrhage.

Quantitative and qualitative variations in fibrinogen plasma levels can be inherited or acquired. Inherited disorders are divided into type I and II.¹⁸ Type I, comprising afibrinogenemia and hypofibrinogenemia, affect the concentration of plasma fibrinogen (<1.5 g/L). Type II, including dysfibrinogenemia and hypodysfibrinogenemia, affect the quality of circulating fibrinogen, the latter also affecting plasma levels.¹⁹

Afibrinogenemia, which has an estimated prevalence of one to two cases per 10⁶ people,²⁰ is an inherited disease characterized by the absence of circulating fibrinogen due to homozygous or compound heterozygous mutations in one of the fibrinogen genes. These may affect mRNA production, splicing or stability, protein production or stability, or hexamer assembly, storage, or secretion.²¹ An initial case of afibrinogenemia in a 9-year old boy was described in 1920,²² but the first causative mutation was identified many years later.^{23,24} Since then, dozens of other causative mutations have been reported for afibrinogenemia. The majority of these are null mutations, i.e., large deletions, frameshift, early-truncating nonsense, or splice-site muta-

tions. Missense mutations are mostly grouped in the conserved COOH-terminal globular domains of the B β and γ chains which has given insights into structural determinants of fibrinogen hexamer assembly and secretion.¹⁰

Bleeding is the main symptom of afibrinogenemia, often occurring in the neonatal period at the umbilical cord. The natural course of afibrinogenemia is usually characterized by spontaneous and severe bleeding, involving all tissues, such as the skin, the oral cavity, the genitourinary tract, the gastrointestinal tract and the central nervous system (CNS). Intracranial hemorrhage is potentially fatal.²⁵ In addition, bone cysts, prolonged wound healing and spontaneous spleen rupture are typically observed through the life of afibrinogenemic patients.¹⁹ Hemarthroses are also frequent but less invalidating than in patients with hemophilia. Women are particularly at risk of bleeding during the child-bearing period. Even in women with no known fibrinogen disorder, in a prospective study aimed at determining hemostatic markers predictive of the severity of postpartum hemorrhage, only fibrinogen concentration was independently associated after multivariate analysis.²⁶ In particular, a fibrinogen concentration lower than 2 g/L was found to have positive predictive value for bleeding events.

Paradoxically, afibrinogenemic patients are at risk of thrombosis, a finding replicated in fibrinogen-deficient mice, since primary hemostasis enables thrombus formation, but clots lacking fibrin are unstable and tend to embolize.²⁷ The reasons for increased thrombotic risk are not entirely understood, but could be related to the absence of thrombin sequestration by the fibrin clot, leading to excessive platelet activation.²⁸

Fibrinogen infusions are efficient to treat acute bleeding and prevent bleeding in the case of surgery. Plasma-derived fibrinogen concentrate is the treatment of choice, providing the safest and most efficient profile among the sources of fibrinogen. Modalities of long-term fibrinogen supplementation (on-demand *versus* prophylactic), as well as the optimal trough fibrinogen level to target, are still unresolved issues. Some concerns have been raised regarding a potential link between fibrinogen infusion and the occurrence of thrombotic events, although available clinical and biological data are controversial.²⁹

While the role of fibrinogen in hereditary bleeding disorders is well-documented,^{30,31} similar afibrinogenemia phenotypes have been reported in mice and zebrafish models. The *Fga* knock-out mouse (*Fga*^{-/-})³² shows spontaneous bleeding, loss of platelet aggregation and clotting function and reduced survival. Serious injuries, overcome by wildtype mice, were lethal for the *Fga*^{-/-} animals. Females could not maintain gestation and fatal uterine bleeding was observed. Many of the latter effects were corrected by a transgene for the A α chain, or the A α E isoform, in *Fga*^{-/-} mice.³³ Fibrinogen-deficient zebrafish have an adult bleeding phenotype with cephalic and ventral hemorrhaging and reduced survival compared with that of control fish.³⁴ In addition, venous thrombosis could not be induced by laser in embryonic zebrafish, clearly demonstrating a hemostatic deficiency.³⁵

Congenital hypofibrinogenemia is much more frequent than afibrinogenemia and is often caused by heterozygous fibrinogen gene mutations. Recently, a systematic analysis of exome/genome data from about 140,000 individuals belonging to the genome Aggregation Database showed that the worldwide prevalence of recessive fibrinogen dis-

orders varies from 1 in 10⁶ persons in East Asians to 24.5 in 10⁶ persons in non-Finnish Europeans.³⁶ Subjects with moderate or mild hypofibrinogenemia are usually asymptomatic since their fibrinogen levels are sufficient to prevent bleeding and pregnancy failure.³⁷ However, in the presence of another hemostatic abnormality or trauma, they may also bleed and suffer pregnancy loss or postpartum hemorrhage. In some cases, due to mutations in *FGG*, the mutant fibrinogen forms aggregates in the endoplasmic reticulum of hepatocytes and can cause liver disease.¹⁹

Qualitative fibrinogen disorders are commonly associated with heterozygous missense mutations in one of the fibrinogen genes and are more frequent than severe quantitative disorders. Although the exact prevalence is not established, it is estimated to be 1 in 100 to 1,000 individuals (0.1-1.0%).³⁶ Two mutation “hotspots” account for over 70% of the detected dysfibrinogenemia mutations. They are at the Arg35 codon in exon 2 of *FGA*, encoding a critical residue in the thrombin cleavage site of the A α chain, and the Arg301 codon in exon 8 of *FGG*, encoding part of the γ chain “hole A” fibrin polymerization site.²⁰ Other causative missense mutations are mainly located in the COOH-terminus of the A α chain which, unlike the B β and γ chains, does not contain a large, highly conserved globular domain. Thus, missense mutations in this region do not have a severe impact on hexamer assembly and secretion but can produce a dysfunctional fibrinogen molecule present in the patient’s circulation. Of note, almost all dysfibrinogenemic variants affect fibrin polymerization, which results in a variable tendency for bleeding. An updated list of dysfibrinogenemia variants and related phenotypes is available in a recent review³⁸ and an open-access online database (<http://site.geht.org/base-fibrinogene/>).

Patients with dysfibrinogenemia are frequently asymptomatic but can suffer from bleeding and/or thromboembolic complications.³⁹ Women are particularly at risk of adverse clinical outcomes, including miscarriages or postpartum thromboses.¹⁹ Symptoms are heterogeneous with a poor segregation of the clinical phenotype even among carrier relatives of the same causative mutation. Using integrative hemostatic models, taking into account the molecular anomaly, fibrin clot properties and family history, may improve assessment of a patient’s phenotype.

Acquired fibrinogen diseases are far more common than inherited ones. Acquired hypofibrinogenemia may result from different causes including disseminated intravascular coagulation, in which activation and consumption of coagulation factors depletes their plasma availability. Fibrin degradation products seen in disseminated intravascular coagulation further impair normal fibrinogen function.⁴⁰ Low fibrinogen levels due to disseminated intravascular coagulation are commonly observed in patients with acute promyelocytic leukemia.⁴¹ Patients with liver disease can also have low plasma fibrinogen due to impaired production. Hemodilution, massive hemorrhage or medication affecting liver protein biosynthesis can also contribute to hypofibrinogenemia.⁴² Acquired dysfibrinogenemia results from a health condition e.g., liver disease affecting post-translational modifications of fibrinogen, notably sialylation. Autoantibodies interfering with the physiological functions of fibrinogen have also been reported.⁴² As reviewed previously,⁴³ several studies have investigated the use of fibrinogen replacement in acquired coagulopathies. Although it is an important treatment option for acquired coagulopathic bleeding, more studies in different

clinical settings are necessary to optimize the dosage. In addition, hyperfibrinolysis contributes to the bleeding manifestations in these acquired coagulopathies, highlighting the importance of a subtle balance between fibrin formation and fibrin degradation.⁴⁴ Lysine analogues (e.g. tranexamic acid) have proven their efficacy in selected clinical situations, such as major trauma (CRASH-2 trial⁴⁵) and postpartum hemorrhage (WOMAN trial⁴⁶).

Cardiovascular disease

Thrombosis occurs in the major cardiovascular diseases (CVD): ischemic heart disease, stroke, and venous thromboembolism.⁴⁷ Arterial thrombosis is associated with the formation and rupture of an atherosclerotic plaque leading to accumulation of platelets, whereas venous thrombosis is linked to endothelial dysfunction and blood stasis which trigger the aggregation of fibrin and red blood cells.⁴⁸

The involvement of elevated fibrinogen as a risk factor for CVD remains controversial. Early prospective studies found a clear relationship between plasma fibrinogen and CVD event risk⁴⁹⁻⁵¹ and the most comprehensive analysis to date confirmed this.⁵² Data from 154,211 subjects with no known history of coronary heart disease or stroke, from 31 prospective studies, revealed associations between fibrinogen level, major ischemic cardiovascular events and nonvascular mortality. The hazard ratio for coronary heart disease and stroke was 1.8 per g/L increase in plasma fibrinogen. Similar conclusions were drawn from a study on the presence and severity of new-onset coronary atherosclerosis in the Han Chinese population.⁵³ In 2,288 subjects referred for coronary angiography, plasma fibrinogen was positively associated with the presence and severity of coronary atherosclerosis, after adjustment for cardiovascular risk factors.

Biases in these evaluations may exist due to unmeasured confounding factors and causality between plasma fibrinogen and CVD events cannot be demonstrated. The elevated fibrinogen levels measured may result from an inflammatory state caused by the underlying pathology, and therefore be a consequence of the illness itself. Nevertheless, further evidence reinforces the hypothesis that the fibrinogen level may directly influence CVD events or progression. Intravenous infusion of human fibrinogen into mice, giving a 1.7-fold increase in plasma fibrinogen, led to resistance to thrombolysis, increased thrombus fibrin content, quicker fibrin formation, greater fibrin network density and increased clot strength and stability.⁵⁴

The appeal of fibrinogen as a causal factor for CVD comes from its roles in both thrombosis and inflammation.^{52,53} Higher levels of fibrinogen can promote CVD events through different pathways (Figure 1A), which, even if they result from a pre-existing inflammatory condition, may further contribute to a poorer clinical state. Fibrinogen may favor atherogenesis when converted to fibrin and its atherogenic degradation products, or trigger lipid deposition and local inflammation resulting in the formation, destabilization, and rupture of atherosclerotic plaques. Promotion of thrombogenesis is another possible mechanism. Fibrin(ogen) acts as a scaffold for blood clots, enhancing platelet aggregation and fibrin formation, making thrombi more resistant to lysis.⁵⁵ Furthermore,

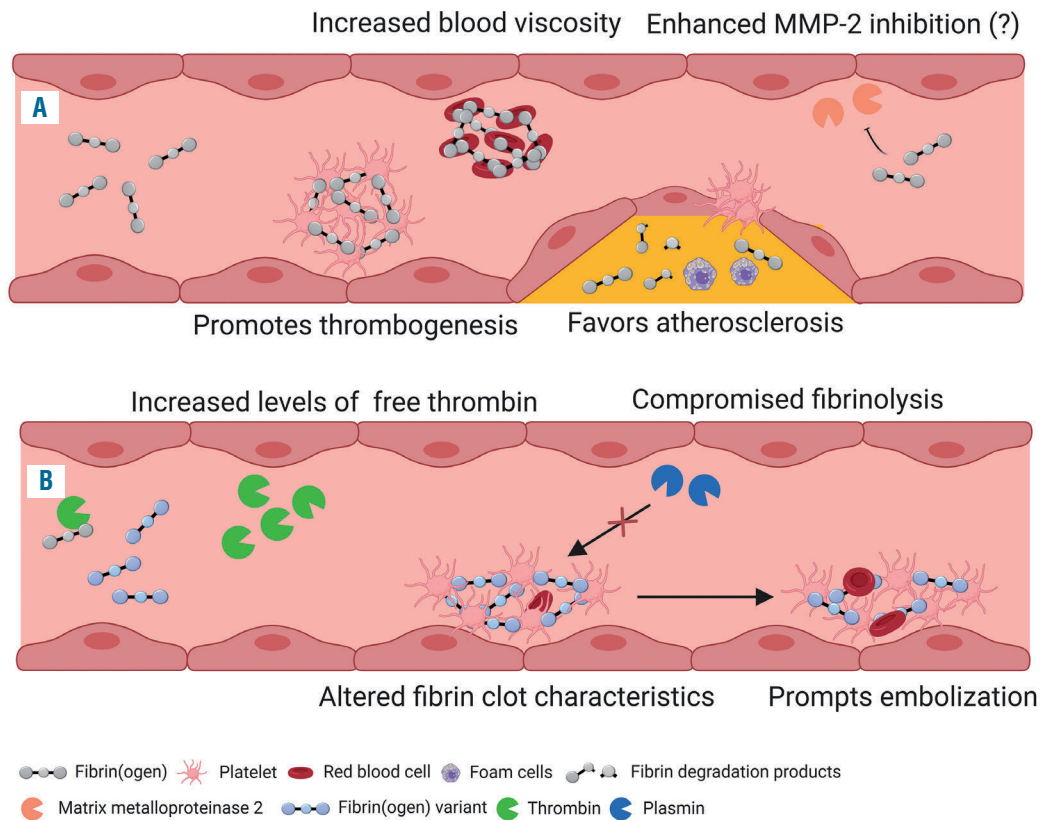


Figure 1. Possible mechanisms linking fibrinogen with cardiovascular diseases. (A) Potential contributions of high levels of plasma fibrinogen to cardiovascular diseases. (B) Effects of structural variations in fibrinogen. This figure was prepared using BioRender.com. MMP-2: matrix metalloprotease 2.

fibrin(ogen) can interact with red blood cells, mediating erythrocyte sedimentation and blood viscosity, while also permitting red blood cells to attach to thrombi. Besides contributing to thrombus size, structure, and stability, red blood cells can alter fibrin network organization, suppress plasmin generation and reduce clot permeability, possibly delaying fibrinolysis and prolonging clot resolution, which may contribute to CVD.⁴⁶ Fibrinogen is also a selective matrix metalloproteinase 2 (MMP-2) inhibitor. High plasma fibrinogen levels could lead to MMP-2 insufficiency in humans. As this enzyme is vital for healthy organ development and repair, excessive MMP-2 inhibition could result in arthritic and cardiac disorders similar to those seen in patients with MMP-2 gene deficiency.⁵⁶

There is, therefore, a potential clinical interest in fibrinogen-lowering drugs for the prevention and/or treatment of CVD. However, some studies have not found a link between high plasma fibrinogen levels and disease. While several single nucleotide polymorphisms have been associated with elevated fibrinogen, the analysis of 24 independent genome-wide significant single nucleotide polymorphisms in 28 European ancestry cohorts, including 91,323 individuals, did not support a causal relationship between plasma fibrinogen and CVD events.⁵⁷ A more recent Mendelian randomization study using genetic variants to uncover evidence for a causal relationship between fibrinogen as a modifiable risk factor, and CVD events as an outcome, came to similar conclusions.⁵⁸ After accounting for horizontal pleiotropy, the effect of fibrinogen on CVD is likely to be small and so resolving any causal effect

will require further analysis using larger sample sizes.

Structural variability in fibrinogen can be linked to CVD. Increased plasma fibrinogen γ' concentration is associated with the risk of myocardial infarction and other thrombotic states.⁵⁹ Epidemiological data suggest decreased levels of γ' may be associated with venous thrombosis, due to the capacity of γ' to counteract a common risk factor for venous thrombosis i.e. plasma activated protein C resistance.⁶⁰ However, increased levels of fibrinogen γ' are associated with arterial thrombosis. This has been attributed to the capacity of the γ' chain to modulate the fibrin clot architecture toward a more thrombotic fibrin network.⁶¹ Whether γ' is causal in this disease or a consequence of increased inflammation is not clear, and further studies are necessary to evaluate the hemostatic properties of fibrinogen γ' depending on the disease type. Nevertheless, haplotype data are concordant: a haplotype which shows decreased fibrinogen γ' levels was associated with an increased risk of venous but not arterial thrombosis in different studies.^{62,63} By contrast, a haplotype linked to increased γ' was associated with arterial thrombosis, although contradictory results have been reported.^{64,65}

Fibrinogen variants found in congenital dysfibrinogenemia can contribute to CVD in different ways (Figure 1B). These include elevated levels of free thrombin resulting from impaired binding to fibrinogen, or altered strength, structure and stability of the fibrin clot, prompting embolization or compromised fibrinolysis.⁵⁸ In particular, patients carrying dysfibrinogenemic mutations which sig-

nificantly increase thrombosis risk (*Online Supplementary Table S1*) can have a family history of CVD, and experience thrombotic events at a young age.³⁷ Interestingly, four out of seven mutations result in an amino acid change to cysteine, which may bind to albumin, resulting in structurally abnormal clots.⁶⁶ Polymorphisms in the fibrinogen genes⁶⁷ have also been linked to CVD: for example, A α p.Thr331Ala, which alters factor XIII-mediated cross-linking, results in fibrin clots prone to undergo embolization.⁶⁸ Post-translational modifications of fibrinogen (e.g., oxidation, phosphorylation, glycosylation and sialylation), might also have a role in CVD by affecting clot architecture, the rate and form of fibrin networks or the interaction with platelets and fibrinolysis.⁶⁷ In accordance with this, dysfibrinogenemic variants that result in the over-sialylation of fibrinogen, aberrant fibrin polymerization or hypofibrinolysis were identified with relatively high prevalence in patients with chronic thromboembolic pulmonary hypertension.⁶⁹ Fibrinolytic resistance and high proportions of monosialyated B β chains were linked to angiogenesis and growth of fibroblasts and endothelial cells, resulting in chronic inflammation and remodeling of pulmonary cells.⁷⁰

Other known cardiovascular risk factors, including body mass index, smoking, and diabetes mellitus, can also affect the fibrin network and CVD risk.⁷¹

Cancer

Coagulation factors have been linked with malignancy for over a 100 years and high plasma fibrinogen levels, in particular, have been associated with cancer development and progression. Fibrinogen can be produced by some non-hepatocyte-derived cancer cells and present in the surroundings of tumors, such as in breast cancer.⁷²

A meta-analysis examining the prognostic effect of circulating fibrinogen in solid tumors showed a positive correlation between pretreatment fibrinogen levels and poorer survival (hazard ratio=1.51).⁷³ Conflicting results came from studies on hematologic cancers,⁷⁴⁻⁷⁶ but overall patients with elevated baseline plasma fibrinogen levels had a significantly poorer clinical outcome.

Fibrinogen-deficient mice (*Fga*^{-/-}) were protected against hematogenous pulmonary metastasis, but not tumor growth after intravenous injection of lung carcinoma and melanoma cell lines. Hirudin, a thrombin inhibitor, further reduced the metastatic potential of circulating cancer cells in *Fga*^{-/-} mice, while plasmin depletion had no effect.⁷⁷ In a colon cancer model, the thrombin-fibrinogen axis was shown to mediate primary tumor development, as it was diminished in *Fga*^{-/-} mice.⁷⁸

The aforementioned associations between fibrinogen and cancer do, however, still require investigation as they do not prove causality. Several hypotheses can be made for the molecular mechanisms implicating fibrinogen in the initiation and development of neoplasms (Figure 2). First, fibrinogen binds growth factors, including vascular endothelial growth factor and fibroblast growth factor.¹³ Thus, extracellular matrix-residing fibrinogen may serve as a reservoir, controlling growth factor bioavailability and accessibility, and influencing cancer cell proliferation, inhibition of apoptosis, angiogenesis and metastases.⁷² For example, fibrinogen produced by epithelial cancer cells promotes lung and prostate cancer cell growth through an

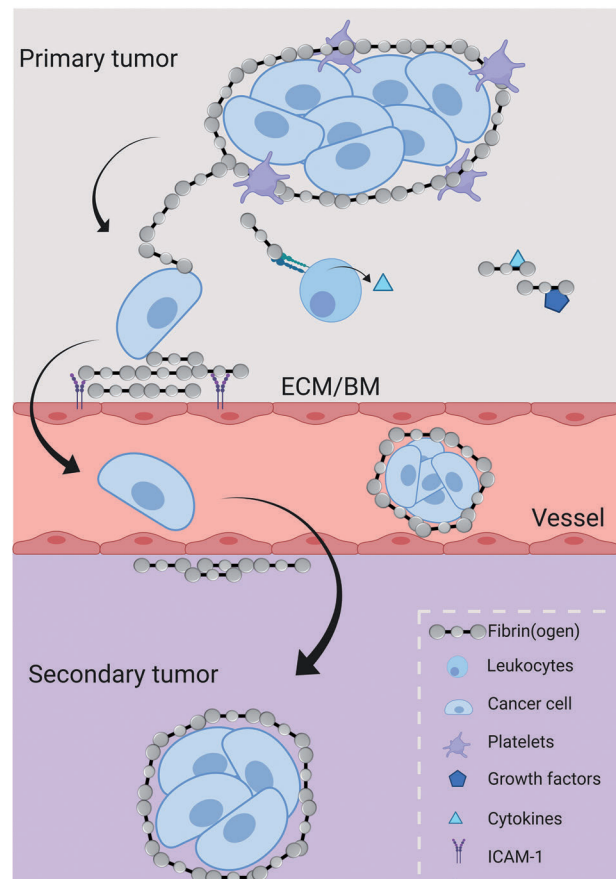


Figure 2. Schematic diagram of pro-tumorigenic mechanisms involving fibrin(ogen). Fibrin(ogen) binds and surrounds cancer cells, forming a structure that protects tumors from immune cells, in a process that may be enhanced by attracted platelets. By interacting with endothelial cells via intercellular adhesion molecule-1, among other receptors, fibrin(ogen) contributes to the extravasation, cell migration and establishment of secondary tumors, while the link with leukocytes via $\alpha_M\beta_2$ results in the production of pro-inflammatory cytokines (e.g., interleukin-1 β) rendering an inflammatory microenvironment that potentially favors tumor progression. The presence of fibrin(ogen) surrounding the tumor, in addition to its protective role, may generate thrombotic events which could prompt a worse clinical outcome. Finally, fibrinogen's ability to bind different growth factors further contributes to tumor maintenance. This figure was adapted from Simpson-Haidaris *et al.*⁷² and prepared using BioRender.com. BM: basement membrane; ECM: extracellular matrix; ICAM-1: intercellular adhesion molecule 1.

interaction with fibroblast growth factor 2.⁷⁹ Second, fibrinogen binds to several cell types. Fibrinogen-mediated cellular bridging may provide traction for cancer cell adhesion, shape changes, motility, and invasive potential.⁷² An example is fibrin(ogen) binding to endothelial intercellular adhesion molecule-1, facilitating the lodging of circulating tumor cells.⁸⁰ Finally, the fibrinogen interaction with platelets via β_3 -integrins facilitates the protection of tumor cells from natural killer-cell cytotoxicity, permitting escape from host immune surveillance.⁸¹ Furthermore, interaction with integrin receptor $\alpha_M\beta_2$ has been suggested to modulate the inflammatory response by inducing leukocyte adhesion to endothelial cells and production of pro-inflammatory cytokines in peripheral blood mononuclear cells.⁸² Thus, fibrinogen influences an inflammatory tumor microenvironment to favor tumor progression.

These studies suggest that modulating fibrinogen levels in cancer patients may have therapeutic potential. Lowering plasma fibrinogen, either via drug therapy or

lifestyle changes, may help to prolong survival in cancer patients. Likewise, other approaches targeting fibrinogen-dependent interactions (e.g., inhibitors of fibrinogen- $\alpha_M\beta_2$ interactions) may also prove useful in cancer treatment and/or prevention.⁷³

Neurological disorders

The biological complexity of several neurological diseases involving the CNS, such as Alzheimer disease and multiple sclerosis, is not yet fully understood. However, the need to study CNS cells within their environmental context is clear.

The brain vasculature consists of dynamic metabolic structures that work as a continuum from artery to arteriole to capillary to venule to vein.^{83,84} The blood-brain barrier (BBB) is essential to separate blood from extracellular fluid in the CNS. The BBB is formed by endothelial cells that maintain critical interactions with other cells, together with a basement membrane that affords an anchor for many signaling processes at the vasculature.⁸⁴ By providing a dynamic physical and metabolic barrier between the CNS and systemic circulation, the BBB ensures constant protection of the neural microenvironment from the influx of potentially harmful substances including plasma proteins, immune cells, pathogens and drugs, while maintaining the efflux of toxins and waste products.^{83,84} Disruption of the BBB is an early event that occurs in many neurological disorders, such as Alzheimer disease, in which, along with microglial activation and neuronal cell death, the neuropathological hallmarks include extracellular deposition of amyloid- β (A β) in senile plaques and blood vessel walls, and the intracellular accumulation of neurofibrillary tangles containing phosphorylated tau proteins.⁸⁵ Brain micro-hemorrhages are frequently observed in patients with Alzheimer disease, and BBB disruption correlates with disease progression.⁸⁶ In animal models of Alzheimer disease, BBB leakage precedes other neuropathological alterations in the brain,⁸⁷ suggesting that damage to the barrier is implicated in the initiation and progression of the disease.⁸⁵ BBB disruption is also one of the earliest representative events in the pathology of multiple sclerosis.⁸⁸ Indeed, BBB disturbance is linked to the inflammation and white matter injury that define this neuroinflammatory disorder.^{83,85} Fibrinogen may extravasate into the CNS upon such events. Once in the brain, fibrin(ogen) can induce signaling networks via binding sites for multiple receptors and proteins, acting as a mediator of neurodegeneration and an activator of innate immunity.⁸⁵

Fibrin deposits are found in early multiple sclerosis lesions and areas of demyelination in close association with inflammation and damaged axons.⁸⁹ In Alzheimer disease, fibrin deposits accumulate within CNS blood vessels in conjunction with cerebral amyloid angiopathy.⁹⁰ In the perivascular brain parenchyma, fibrin co-localizes with A β plaques,⁹¹ macrophages,⁹² areas of pericyte loss⁹³ and dystrophic neurites.⁹⁴

Fibrin formation exposes the cryptic epitope $\gamma 377$ –395, which binds with high affinity to the $\alpha_M\beta_2$ integrin on microglia and infiltrating macrophages, activating multiple signal transduction pathways to promote inflammatory responses. This is associated with antigen presentation, release of reactive oxygen species⁹⁵ and secretion of the

leukocyte-recruiting chemokines CCL2, and CXCL10.⁹⁶ In multiple sclerosis this may lead to T-cell recruitment and local differentiation of myelin antigen-specific T helper 1 cells to promote autoimmunity and demyelination.⁹⁶ In animal models of Alzheimer disease, fibrin(ogen) was shown to accumulate in areas of dendritic spine elimination, even independently and distal to A β peptides that aggregate to form neurotoxic and stable oligomers, with ensuing cognitive impairment.⁹⁷ The fibrinogen-mediated elimination depends on microglial $\alpha_M\beta_2$ receptor activation and generation of reactive oxygen species. However, the fibrin-A β interaction has an additive effect on poor outcome. A β can activate contact pathway coagulation to drive fibrin formation,⁹⁸ protect fibrin from degradation⁹⁹ and allow a constant inflammatory signal.

Fibrin(ogen) contributes to neurological disease by inhibiting remyelination after vascular damage.⁸⁵ Fibrinogen can activate bone morphogenetic protein (BMP) receptor activin A receptor type I and downstream BMP-specific SMAD proteins in oligodendrocyte progenitor cells, independently of BMP ligands.¹⁰⁰ This prevents oligodendrocyte progenitor cells from differentiating into myelinating oligodendrocytes and promotes an astrocyte-like cell fate. Fibrin-M1-like activation of microglia¹⁰¹ and macrophages⁹⁶ can also be toxic to oligodendrocyte progenitor cells and further impair remyelination.⁸⁵ Another possible mechanism is through fibrin-induced phosphorylation of extracellular signal-regulated kinases and production of nerve growth factor receptor in Schwann cells, maintaining them in a proliferating, non-myelinating state.¹⁰²

Neurite outgrowth inhibition¹⁰³ and glial scar formation¹⁰⁴ may also be triggered by fibrinogen, leading to cerebrovascular pathologies. Fibrinogen inhibits neurite outgrowth by binding the $\alpha_3\beta_3$ integrin and trans-activating epidermal growth factor receptor in neurons.¹⁰³ Inhibition of axonal regeneration occurs indirectly by prompting astrocytosis and stimulating the production of inhibitory proteoglycans that form the glial scar. Fibrinogen can carry a latent transforming growth factor- β that is activated when it encounters primary astrocytes, stimulating the production of neurocan, a strong inhibitor of neurite outgrowth.¹⁰⁴

Consistent with these observations, reducing fibrinogen levels with anrod,¹⁰⁵ manipulating the conversion of fibrinogen into insoluble fibrin with hirudin¹⁰¹ and interfering with fibrinolysis by tissue plasminogen activator¹⁰⁶ all attenuated injuries and promoted regeneration and functional recovery. Similar results were also obtained after treatment with $\gamma 377$ –395 peptide¹⁰⁷ or a monoclonal antibody against the same epitope,¹⁰⁸ revealing an essential role for fibrin in peripheral nerve damage and repair.

In summary, fibrin(ogen) can induce degenerative changes in the CNS through different mechanisms that initiate or potentiate neurodegenerative processes after vascular disruption (Figure 3A). While many studies have found that fibrin(ogen) promotes neuroinflammation through binding to the $\alpha_M\beta_2$ integrin on macrophages and microglia, pericyte-deficient mice lack a significant neuroinflammatory response until late in the disease. These mice suffer from early BBB breakdown and accumulation of white matter fibrin(ogen) that is associated with diminished blood flow and hypoxia. However, following white-matter injury, no changes were detected in astrocyte, microglia or macrophage responses or pro- and anti-

inflammatory cell profiles and/or numbers of astrocytes and microglia in the resting state. This suggests that fibrin(ogen)-driven neurodegeneration can also be inflammation-independent (Figure 3B).¹⁰⁵

Association studies have correlated elevated plasma fibrinogen levels with cognitive decline, independently of inflammatory markers.^{109,110} Proteomic studies detected higher fibrinogen levels on platelets from subjects with secondary progressive multiple sclerosis.¹¹¹ This highlights dysfunctional coagulation as a common thread among diverse neurovascular abnormalities. Fibrin(ogen) may,

however, be beneficial in acute CNS injuries by delaying regeneration until the extracellular environment is conducive to repair.¹⁰⁰

Pharmacological agents targeting fibrinogen or fibrinogen interactions with CNS cells or other players may have potential as therapeutics for neurological diseases. Such drugs could include agents that enhance fibrin(ogen) degradation, protect the BBB to limit fibrin(ogen) entry into the CNS, or selectively inhibit the interactions of fibrinogen and fibrin with their CNS receptors, $\alpha_M\beta_2$ or $A\beta$, while preserving the beneficial functions of fibrinogen.⁸⁵

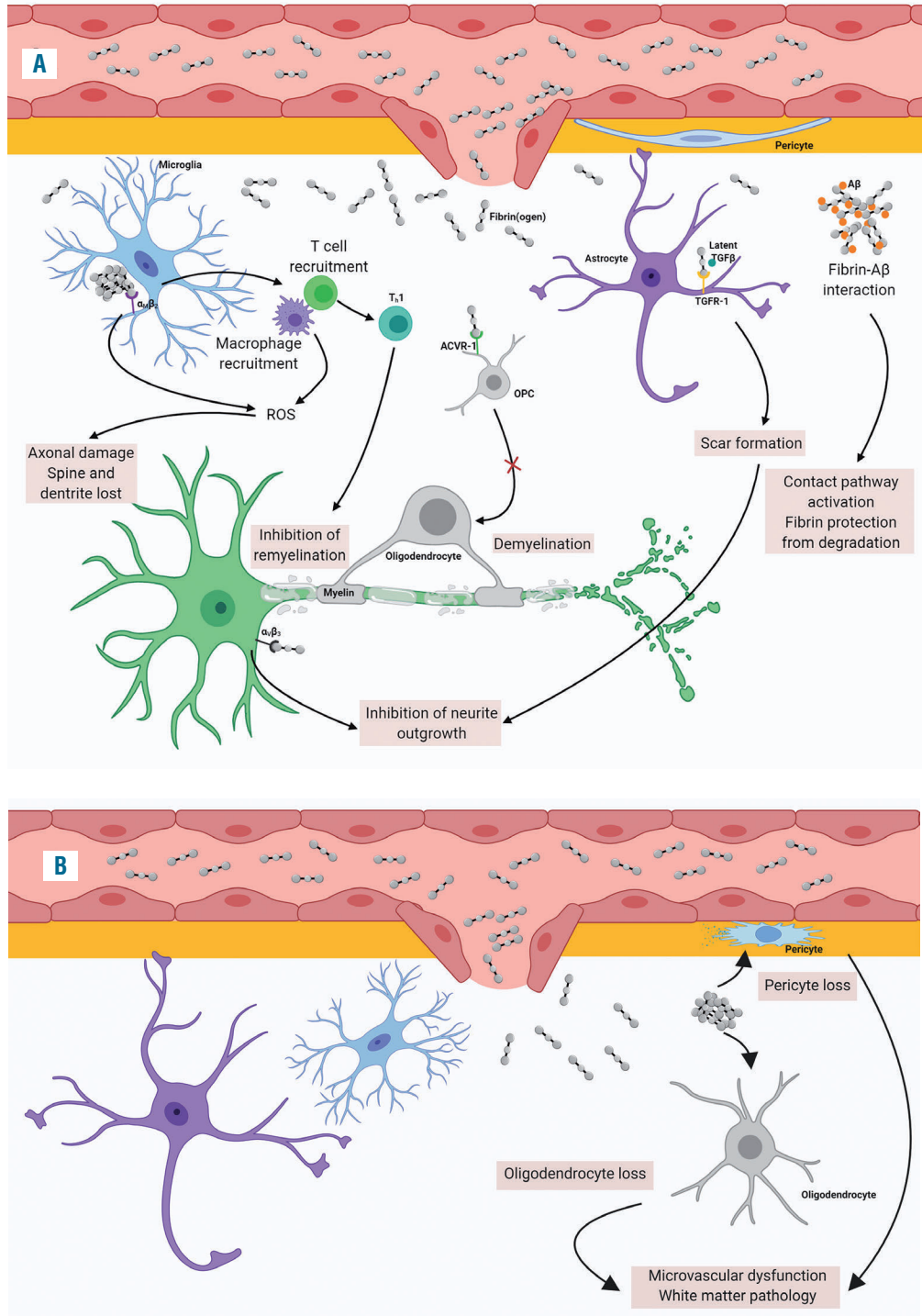


Figure 3. Schematic representation of the mechanisms linking fibrin(ogen), neurological diseases and cognitive impairment upon blood-brain barrier break-age. (A) The main components of the pathways that ultimately lead to neuroinflammation and neurodegeneration are described in this panel, including the interaction with $A\beta$ peptides observed in Alzheimer disease. (B) An alternative mechanism that does not implicate inflammation. Increased fibrin(ogen) accumulation results in pericyte and oligodendrocyte loss, without affecting astrocytes or microglia. This will lead to microvascular dysfunction and white matter pathology. This figure has been adapted from Petersen *et al.*⁸⁵ and Merlini *et al.*⁹⁷ and created with BioRender.com. ACVR1: activin A receptor type 1; $A\beta$: amyloid- β ; OPC: oligodendrocyte progenitor cell; ROS: reactive oxygen species; TGF β 1: transforming growth factor- β receptor type 1; T_H1: T helper 1 cells.

Microbial infections and allergic reactions

Fibrin(ogen) is implicated in defense against pathogen invasion,¹¹² for example in peritonitis. Recent findings from experiments *in vitro* and *in vivo* show that at the air-liquid interface formed following a skin wound fibrin can accumulate perpendicularly to generate a protective biofilm.¹⁴ These structures, which are an end product of clotting and fibrin formation, prevent blood cell loss from the wound but also block the entry and early proliferation of bacteria at the injury site. However, in other settings fibrin(ogen) enhances bacterial virulence¹⁵ or contributes to the development and perpetuation of allergic reactions.¹¹³

Certain bacteria express virulence factors that appropriate fibrin(ogen) to facilitate their entry into the host, limiting the antimicrobial role of fibrinogen and protecting the organisms from pharmacological treatments. Virulence factors can also enhance bacterial proliferation and dissemination.¹¹²

The anti- or pro-invasion effects of fibrin(ogen) reflect the activity of bacterial virulence factors (Table 1) which have adapted to unique host microenvironments. For example, different murine models of *Staphylococcus aureus* endocarditis require distinct factors for valve colonization. Microbial adhesion and colonization in mice with mechanically damaged valves involve fibrin(ogen), whereas in a model of cardiac valve inflammation, fibrin(ogen) depletion with anrod did not impair bacterial colonization. Bacterial volume increased in anrod-treated mice compared to that in controls.¹¹⁴ Further comprehension of the roles of coagulation factors on bacterial virulence may lead to therapeutic strategies for the treatment of infectious diseases, particularly given the increasing demand to find a solution to antibiotic resistance.¹¹⁵

In fungal infections, proteases contribute to inflammation through interactions with the kinin system as well as the coagulation and fibrinolytic cascades.¹¹⁶ In this context, the fibrin(ogen) interaction with $\alpha_M\beta_2$ is implicated, as it

may further react with toll-like receptor 4 (TLR4) in immune cells, resulting in a highly efficient signaling complex that regulates the development of antifungal reactions, but also allergic airway disease.¹¹³ Fungal proteinases cleave fibrinogen into cleavage products (FCP) which, together with $\alpha_M\beta_2$ and TLR4, were found to be essential for fungal elimination by T and B lymphocytes, dendritic cells and macrophages. The fibrinogen hexamer can also inhibit fungal growth, perhaps due to low affinity fibrinogen-target receptor interactions. However, the putative $\alpha_M\beta_2$ /TLR4/FCP complex also triggered innate fungistatic immunity, modest allergic airway hyper-responsiveness and neutrophilia.¹¹⁵ Interestingly, this $\alpha_M\beta_2$ /TLR4/FCP association has been described in unrelated settings, including endotoxemia and malaria.^{117,118} Thus, FCP that play a role in infection-mediated inflammatory responses have a pivotal role in the clinical outcome of patients with fungi-induced autoimmunity.¹¹³

Finally, fibrin(ogen) also seems to be implicated in bacteria-driven hypersensitivity reactions. Pharmacological or genetic depletion of fibrinogen in mice improved the animals' survival when they were challenged with high concentrations of lipopolysaccharide, and impeded the development of a variety of inflammatory conditions.¹⁵ In humans, afibrinogenemic patients have reduced responses in a delayed-type hypersensitivity reaction induced by exposure to bacterial antigens.¹¹⁹

Obesity and diabetes

Nutrient excess leads to imbalances in cellular and molecular mediators of immunity and inflammation.¹²⁰ These may drive metabolic dysfunction while triggering a hypercoagulable state, with elevated circulating levels of fibrinogen being among key coagulation components.¹²¹ Initial risk, severe morbidity and mortality outcomes for vessel-occlusive disorders correlate positively with the

Table 1. Factors associated with fibrinogen-induced virulence.^{15,112}

Factor	Virulence mechanisms
Clumping factor A	<ul style="list-style-type: none"> • Mediates the binding of bacteria to fibrin(ogen) immobilized on a surface • Forms an abscess that prevents or inhibits platelet aggregation, complement activation and opsonophagocytosis
Fibronectin binding proteins A and B	<ul style="list-style-type: none"> • Contribute to biofilm formation • Bind plasminogen to facilitate staphylokinase activity (see below)
Bone sialoprotein-binding protein	<ul style="list-style-type: none"> • Prevents thrombin-mediated cleavage of fibrinogen
Extracellular fibrinogen-binding protein	<ul style="list-style-type: none"> • Formation of a protective shield of fibrin(ogen) that prevents phagocytosis and innate immune cell recognition • Sequestration of fibrinogen preventing its interaction with neutrophils
Endocarditis- and biofilm-associated pilus-A	<ul style="list-style-type: none"> • Mediation of bacterial attachment to host fibrinogen, which permits building biofilms that <ul style="list-style-type: none"> ◦ shield bacteria from immune cell recognition, antibiotics, and urine flow (if applicable) ◦ contribute to nutrient acquisition
Coagulase and von Willebrand factor-binding protein	<ul style="list-style-type: none"> • Coagulase mediates formation of a fibrin(ogen)-containing inner pseudocapsule that envelopes bacterial microcolonies • vWbp contributes to an extended outer dense protective layer • Both induce thrombin activation to form a fibrin(ogen) protective shield around the bacteria against phagocytosis and innate immune cell recognition
Staphylokinase	<ul style="list-style-type: none"> • Contributes to the activation of plasminogen, which readily degrades fibrin to prevent microbial entrapment or permit bacterial detachment and dispersion throughout the host • Neutralizes the bactericidal effects of α-defensins secreted from polymorphonuclear cells

degree of obesity.^{121,122} Thus, obesity represents a major risk factor for other pathologies, including thromboembolic events, CVD, diabetes, cancer and fatty liver disease.^{120,121}

Fibrinogen may be involved in the pathology of obesity. Levels of fibrinogen are higher in obese patients with type 2 diabetes than in obese subjects without type 2 diabetes.¹²³ In addition, plasma fibrinogen levels correlate with fasting insulin levels and disease state advancement in noninsulin-dependent diabetics,¹²⁴ and while insulin infusion decreases fibrinogen biosynthesis in normal subjects,¹²⁵ insulin resistance/deficiency may contribute to hyperfibrinogenemia.¹²⁶ Furthermore, fibrinogen from diabetic patients generates denser, fibrinolysis-resistant clots, while insulin treatment leads to changes in fibrinogen and a more permeable clot.¹²⁷ These alterations have been attributed to the glycation of fibrinogen and its effect on fibrin clots, potentially contributing to the risk of thrombosis.

Mice fed with a high-fat diet developed fibrin(ogen) deposits in white adipose tissue and liver which co-localized with macrophage accumulation.¹²⁸ In contrast to *Fib γ ^{Δ5}* mice and mice without factor XIII A, *Fib γ ^{390-396A}* animals were protected from increased body weight with a high-fat diet, specifically at the fat mass level. These animals, with fibrin(ogen)- γ residues 390 to 396 replaced with alanine and therefore lacking an $\alpha_M\beta_2$ -binding motif on fibrin(ogen),¹²⁹ showed less systemic and local inflammation, demonstrated by lower levels of pro-inflammatory molecules, adipose tissue macrophages and smaller white adipose tissue adipocytes¹²⁸ when compared to those of wild-type animals. In addition, the fibrinogen γ 390-396A variant led to lower liver weight, steatosis, serum alanine aminotransferase and hepatic inflammatory markers, and conferred some degree of protection against the develop-

ment of induced fatty liver disease. Glucose clearance and insulin sensitivity were improved, revealing improved glucose metabolism.

Thus fibrin(ogen)-driven inflammation, via leukocyte interactions in adipose tissue and liver, worsens obesity and increases its downstream harmful effects. Targeting thrombin or fibrin(ogen) may improve the morbidity of obesity-linked pathologies.

Amyloidosis

Amyloidosis is a group of disorders originating from mutations that cause conformational changes, typically involving β -sheet structures, in soluble proteins. These then aggregate as extracellular amyloid fibril deposits in various organs. In systemic forms, amyloidosis can progressively induce organ dysfunction, and be fatal.¹³⁰

Fibrinogen-driven renal hereditary amyloidosis is a rare group of disorders with autosomal-dominant inheritance caused by heterozygosity for mutations in the α C-domain, which result in improper folding and amyloid formation followed by accumulation and deposition in the kidneys.⁶⁶ Other elements present in the deposits can further contribute to fibrin(ogen) amyloid formation, namely amyloidosis-enhancing factor¹³¹ and serum amyloid A.¹³² The latter binds to purified fibrinogen and induces amyloid formation and spontaneous dense, matted fibrin(ogen) deposits, independently of thrombin. However, its involvement in renal amyloidosis has not yet been demonstrated.

Fibrinogen-derived amyloid deposits disrupt kidney structure and impair kidney function, effects that become more severe over time, with accumulation of the amyloid. Amyloidosis is associated with hypertension, nephrotic

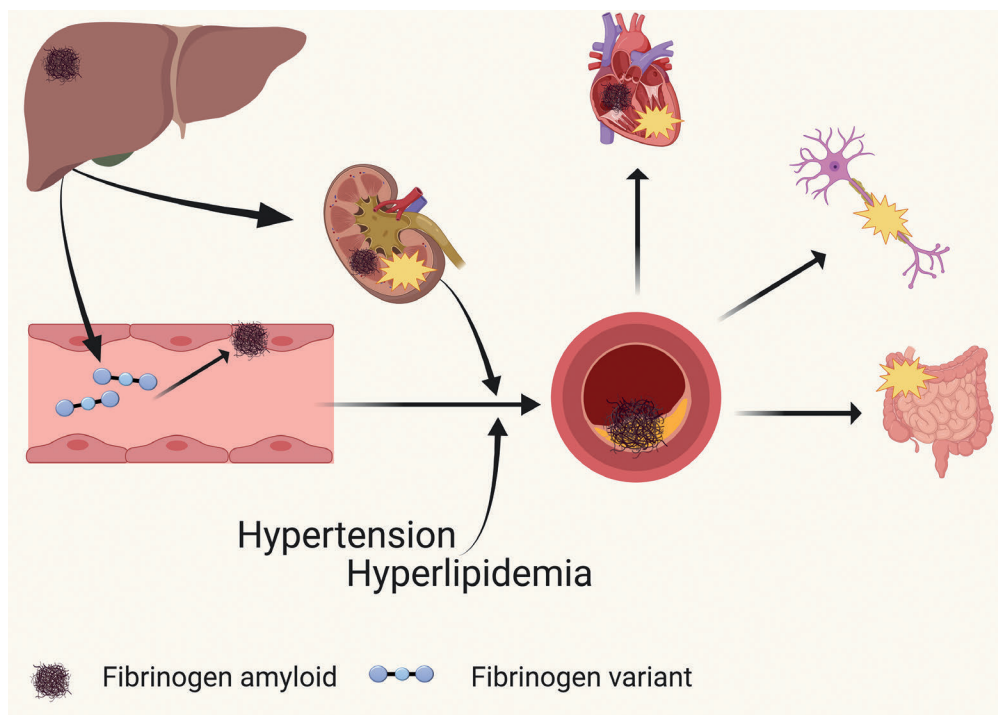


Figure 4. Pathogenesis of fibrinogen amyloidosis and its visceral, vascular, cardiac and neurological implications. Fibrinogen variants are produced in the liver where they may rarely cause hepatic amyloidosis. In addition to the kidney, where deposits prompt renal failure, fibrinogen has different targets. It may also accumulate in vascular and cardiac walls, resulting in impaired endothelial function. This, together with nephrotic syndrome, hyperlipidemia and hypertension, facilitates atheroma formation and eventually results in coronary atherosclerosis. Fibrinogen may be the basis of neuropathic features as well as the symptoms of gut dysmotility in patients with fibrinogen amyloidosis. This image was adapted from Picken MM¹³⁵ and created with BioRender.com.

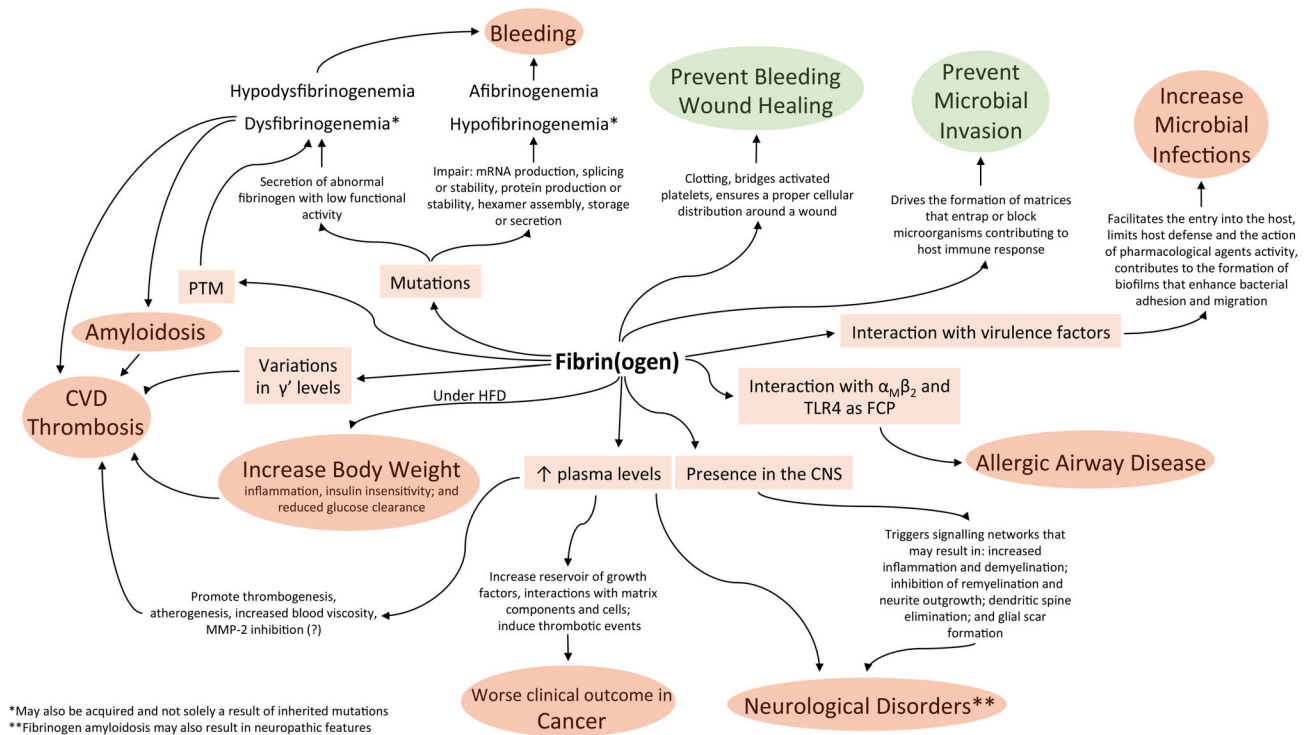


Figure 5. Scheme summarizing the mechanisms of fibrin(ogen) as a friend (in green) and foe (in red) in human disease. Square boxes represent abnormalities that prompt fibrinogen involvement in illness settings. CNS: central nervous system; CVD: cardiovascular diseases; FCP: fibrinogen cleavage products; HFD: high-fat diet; MMP-2: matrix metalloproteinase 2; PTM: post-translational modifications; TLR4: toll-like receptor 4.

syndrome, and renal failure.⁶⁶ Several renal amyloidogenic mutations in fibrinogen have been described (*Online Supplementary Table S2*). Patients with these mutations do not have a bleeding disorder and, when measured, the clotting times of patients with these variants are normal, except those with p.Thr544LeufsTer24 who had a prolonged thrombin time and low fibrinogen level.¹³³

While the kidney is the predominant organ for fibrinogen-amyloid deposition, the pathology of hereditary fibrinogen amyloidosis is not restricted to involvement of this organ. Fibrinogen amyloidosis patients show a high incidence of cardiovascular atheromatous disease with a family history of coronary/vascular disease.¹³⁴ Fibrinogen deposits are found in vascular walls and atheromatous plaques, associating fibrinogen variant amyloidosis and atherosclerosis. While nephrotic syndrome with hyperlipidemia and hypertension may facilitate atheroma formation, the cardiovascular findings are unlikely to be caused by renal failure alone. Thus, hereditary fibrinogen amyloidosis is a complex systemic amyloid disease that is associated with cardiac amyloid deposition, angiopathy and atheromatosis^{134,135} (Figure 4).

There are currently no treatments available to resolve amyloid deposits. Disease management consists of interrupting amyloidogenic protein supply with supportive care to failing organs, and transplantation. Hepato-renal transplantation appears to prevent disease progression and allows reversal of some organ dysfunction.^{134,135}

Conclusions

As the thrombin substrate for generating fibrin, fibrinogen has a critical role in controlling bleeding upon vascular injury, as well as being a major determinant in wound healing, tissue regeneration and mediation of inflammatory responses that help the immune system fight invading pathogens. However, several layers of evidence point to fibrin(ogen) as a contributor in pathological settings (Figure 5). These contributions may result from altered plasma concentration, modified structural properties, or from the impact of polymorphisms on clot permeability, stiffness and resistance to lysis. The presence of fibrin(ogen) in particular locations is a determinant in the development of disease. Here we have discussed human disorders in which the role of fibrin(ogen) is supported by clinical data and animal models. Fibrin(ogen) is also a likely protagonist in fibrotic and arthritic diseases. Continued research will allow a better understanding of these complex disease settings and the impact of fibrin(ogen). Whether the presence, quality or abundance of fibrin(ogen) has a causal role, or is a consequence of the underlying pathology, should be a focal point. Such research will help to evaluate the usefulness of targeting fibrin(ogen) in a variety of human disease settings.

References

- Mosesson MW, Siebenlist KR, Meh DA. The structure and biological features of fibrinogen and fibrin. *Ann N Y Acad Sci*. 2001;936:11-30.
- Standeven KF, Ariens RA, Grant PJ. The molecular physiology and pathology of fibrin structure/function. *Blood Rev*. 2005;19(5):275-288.
- Fish RJ, Neerman-Arbez M. Fibrinogen gene regulation. *Thromb Haemost*. 2012;108(3):419-426.
- Espitia Jaimes C, Fish RJ, Neerman-Arbez M. Local chromatin interactions contribute to expression of the fibrinogen gene cluster. *J Thromb Haemost*. 2013;16(10):2070-2082.
- Fort A, Fish RJ, Attanasio C, et al. A liver enhancer in the fibrinogen gene cluster. *Blood*. 2011;117(1):276-282.
- Vorjohann S, Pitetti J-L, Nef S, et al. DNA methylation profiling of the fibrinogen gene landscape in human cells and during mouse and zebrafish development. *PLoS One*. 2013;8(8):e73089.
- Fort A, Borel C, Migliavacca E, et al. Regulation of fibrinogen production by microRNAs. *Blood*. 2010;116(14):2608-2615.
- Lukowski SW, Fish RJ, Martin-Levilain J, et al. Integrated analysis of mRNA and miRNA expression in response to interleukin-6 in hepatocytes. *Genomics*. 2015;106(2):107-115.
- Redman CM, Xia H. Fibrinogen biosynthesis. *Ann N Y Acad Sci*. 2001;936(1):480-495.
- Vu D, Di Sanza C, Caille D, et al. Quality control of fibrinogen secretion in the molecular pathogenesis of congenital afibrinogenemia. *Hum Mol Genet*. 2005;14(21):3271-3280.
- Bleyer WA, Hakami N, Shepard TH. The development of hemostasis in the human fetus and newborn infant. *J Pediatr*. 1971;79(5):838-853.
- Brown AC, Hannan RT, Timmins LH, et al. Fibrin network changes in neonates after cardiopulmonary bypass. *Anesthesiology*. 2016;124(5):1021-1031.
- Weisel JW, Litvinov RI. Fibrin formation, structure and properties. *Subcell Biochem*. 2017;82:405-456.
- Macrae FL, Duval C, Papareddy P, et al. A fibrin biofilm covers blood clots and protects from microbial invasion. *J Clin Invest*. 2013;123(8):3356-3368.
- Ko Y-P, Flick MJ. Fibrinogen Is at the interface of host defense and pathogen virulence in staphylococcus aureus infection. *Semin Thromb Hemost*. 2016;42(4):408-421.
- Furie B, Furie BC. Mechanisms of thrombus formation. *N Engl J Med*. 2008;359(9):938-949.
- Smith SA, Travers RJ, Morrissey JH. How it all starts: initiation of the clotting cascade. *Crit Rev Biochem Mol Biol*. 2015;50(4):326-336.
- Neerman-Arbez M, de Moerloose P. Hereditary fibrinogen abnormalities. In: Kaushansky K, Lichtman MA, Prchal JT, Levi MM, Press OW, Burns LJ, et al., eds. *Williams Hematology*, 9e. New York, NY: McGraw-Hill Education, 2015.
- de Moerloose P, Casini A, Neerman-Arbez M. Congenital fibrinogen disorders: an update. *Semin Thromb Hemost*. 2013;39(6):585-595.
- Casini A, Blondon M, Tintillier V, et al. Mutational epidemiology of congenital fibrinogen disorders. *Thromb Haemost*. 2018;118(11):1867-1874.
- Vu D, Neerman-Arbez M. Molecular mechanisms accounting for fibrinogen deficiency: from large deletions to intracellular retention of misfolded proteins. *J Thromb Haemost*. 2007;5 (Suppl 1):125-131.
- Rabe F, Salomon E. Ueber-faserstoffmangel im Blute bei einem Falle von Hämophilie. *Ann Intern Med*. 1920;95:2-14.
- Neerman-Arbez M, Antonarakis SE, Honsberger A, et al. The 11 kb FGA deletion responsible for congenital afibrinogenemia is mediated by a short direct repeat in the fibrinogen gene cluster. *Eur J Hum Genet*. 1999;7(8):897-902.
- Neerman-Arbez M, Honsberger A, Antonarakis SE, et al. Deletion of the fibrinogen [correction of fibrogen] alpha-chain gene (FGA) causes congenital afibrinogenemia. *J Clin Invest*. 1999;103(2):215-218.
- Lak, Keihani, Elahi, et al. Bleeding and thrombosis in 55 patients with inherited afibrinogenemia. *Br J Haematol*. 1999;107(1):204-206.
- Charbit B, Mandelbrot L, Samain E, et al. The decrease of fibrinogen is an early predictor of the severity of postpartum hemorrhage. *J Thromb Haemost*. 2007;5(2):266-273.
- Ni H, Denis CV, Subbarao S, et al. Persistence of platelet thrombus formation in arterioles of mice lacking both von Willebrand factor and fibrinogen. *J Clin Invest*. 2000;106(3):385-392.
- Mosesson MW. Antithrombin I. Inhibition of thrombin generation in plasma by fibrin formation. *Thromb Haemost*. 2003;89(1):9-12.
- Korte W, Poon M-C, Iorio A, et al. Thrombosis in inherited fibrinogen disorders. *Transfus Med Hemother*. 2017;44(2):70-76.
- Litvinov RI, Weisel JW. What is the biological and clinical relevance of fibrin? *Semin Thromb Hemost*. 2016;42(4):333-343.
- Menegatti M, Peyvandi F. Treatment of rare factor deficiencies other than hemophilia. *Blood*. 2019;133(5):415-424.
- Suh TT, Holmback K, Jensen NJ, et al. Resolution of spontaneous bleeding events but failure of pregnancy in fibrinogen-deficient mice. *Genes Dev*. 1995;9(16):2020-2033.
- Degen JL, Drew AF, Palumbo JS, et al. Genetic manipulation of fibrinogen and fibrinolysis in mice. *Ann N Y Acad Sci*. 2001;936:276-290.
- Fish RJ, Di Sanza C, Neerman-Arbez M. Targeted mutation of zebrafish fga models human congenital afibrinogenemia. *Blood*. 2014;123(14):2278-2281.
- Hu Z, Lavik KI, Liu Y, et al. Loss of fibrinogen in zebrafish results in an asymptomatic embryonic hemostatic defect and synthetic lethality with thrombocytopenia. *J Thromb Haemost*. 2019;17(4):607-617.
- Paraboschi EM, Duga S, Asselta R. Fibrinogen as a pleiotropic protein causing human diseases: the mutational burden of α , β , and γ chains. *Int J Mol Sci*. 2017;18(12):2711.
- Casini A, Undas A, Palla R, et al. Diagnosis and classification of congenital fibrinogen disorders: communication from the SSC of the ISTH. *J Thromb Haemost*. 2018;16(9):1887-1890.
- Casini A, Neerman-Arbez M, Ariens RA, et al. Dysfibrinogenemia: from molecular anomalies to clinical manifestations and management. *J Thromb Haemost*. 2015;13(6): 909-919.
- Casini A, Blondon M, Lebreton A, et al. Natural history of patients with congenital dysfibrinogenemia. *Blood*. 2015;125(3):553-561.
- Iba T, Levy JH, Warkentin TE, et al. Diagnosis and management of sepsis-induced coagulopathy and disseminated intravascular coagulation. *J Thromb Haemost*. 2019;17(11):1989-1994.
- Chang H, Kuo MC, Shih LY, et al. Clinical bleeding events and laboratory coagulation profiles in acute promyelocytic leukemia. *Eur J Haematol*. 2012;88(4):321-328.
- Besser MW, MacDonald SG. Acquired hypofibrinogenemia: current perspectives. *J Blood Med*. 2016;7:217-225.
- Levy JH, Goodnough LT. How I use fibrinogen replacement therapy in acquired bleeding. *Blood*. 2015;125(9):1387-1393.
- Kolev K, Longstaff C. Bleeding related to disturbed fibrinolysis. *Br J Haematol*. 2016;175(1):12-23.
- CRASH-2 Trial Collaborators, Shakur H, Roberts I, et al. Effects of tranexamic acid on death, vascular occlusive events, and blood transfusion in trauma patients with significant haemorrhage (CRASH-2): a randomised, placebo-controlled trial. *Lancet*. 2010;376(9734):23-32.
- WOMAN Trial Collaborators. Effect of early tranexamic acid administration on mortality, hysterectomy, and other morbidities in women with post-partum haemorrhage (WOMAN): an international, randomised, double-blind, placebo-controlled trial. *Lancet*. 2017;389(10084):2105-2116.
- Raskob GE, Angchaisuksiri P, Blanco AN, et al. Thrombosis: a major contributor to global disease burden. *Arterioscler Thromb Vasc Biol*. 2014;34(11):2363-2371.
- Byrnes JR, Wolberg AS. Red blood cells in thrombosis. *Blood*. 2017;130(16):1795-1799.
- Kannel WB, Wolf PA, Castelli WP, et al. Fibrinogen and risk of cardiovascular disease: the Framingham Study. *JAMA*. 1987;258(9):1183-1186.
- Meade TW, Chakrabarti R, Haines AP, et al. Haemostatic function and cardiovascular death: early results of a prospective study. *Lancet*. 1980;315(8177):1050-1054.
- Wilhelmsen L, Svärdsudd K, Korsan-Bengtson K, et al. Fibrinogen as a risk factor for stroke and myocardial infarction. *N Engl J Med*. 1984;311(8):501-505.
- Danesh J, Lewington S, Thompson SG, et al. Plasma fibrinogen level and the risk of major cardiovascular diseases and nonvascular mortality: an individual participant meta-analysis. *JAMA*. 2005;294(14):1799-1809.
- Zhang Y, Zhu C-G, Guo Y-L, et al. Higher fibrinogen level is independently linked with the presence and severity of new-onset coronary atherosclerosis among Han Chinese population. *PLoS One*. 2014;9(11): e113460.
- Machlus KR, Cardenas JC, Church FC, et al. Causal relationship between hyperfibrinogenemia, thrombosis, and resistance to thrombolysis in mice. *Blood*. 2011;117(18):4953-4963.
- Lowe GDO. Fibrinogen assays for cardiovascular risk assessment. *Clin Chem*. 2010;56(5):693-695.
- Sarker H, Hardy E, Haimour A, et al. Identification of fibrinogen as a natural inhibitor of MMP-2. *Sci Rep*. 2019;9(1):4340.
- Sabater-Lleal M, Huang J, Chasman D, et al. Multiethnic meta-analysis of genome-wide association studies in >100 000 subjects identifies 23 fibrinogen-associated loci but

- no strong evidence of a causal association between circulating fibrinogen and cardiovascular disease. *Circulation*. 2013;128(12):1310-1324.
58. Ward-Caviness CK, de Vries PS, Wiggins KL, et al. Mendelian randomization evaluation of causal effects of fibrinogen on incident coronary heart disease. *PLoS One*. 2019;14(5):e0216222.
 59. Lovely RS, Falls LA, Al-Mondhry HA, et al. Association of gammaA/gamma' fibrinogen levels and coronary artery disease. *Thromb Haemost*. 2002;88(1):26-31.
 60. Omarova F, Uitte de Willige S, Simioni P, et al. Fibrinogen γ' increases the sensitivity to activated protein C in normal and factor V Leiden plasma. *Blood*. 2014;124(9):1531-1538.
 61. Macrae FL, Domingues MM, Casini A, et al. The (patho)physiology of fibrinogen γ' . *Semin Thromb Hemost*. 2016;42(4):344-355.
 62. Nowak-Gottl U, Weiler H, Hernandez I, et al. Fibrinogen alpha and gamma genes and factor VLeiden in children with thromboembolism: results from 2 family-based association studies. *Blood*. 2009;114(9):1947-1953.
 63. Uitte de Willige S, de Visser MC, Houwing-Duistermaat JJ, et al. Genetic variation in the fibrinogen gamma gene increases the risk for deep venous thrombosis by reducing plasma fibrinogen gamma' levels. *Blood*. 2005;106(13):4176-4183.
 64. Cheung EY, Uitte de Willige S, Vos HL, et al. Fibrinogen gamma' in ischemic stroke: a case-control study. *Stroke*. 2008;39(3):1033-1035.
 65. Uitte de Willige S, Doggen CJ, MC DEV, et al. Haplotypes of the fibrinogen gamma gene do not affect the risk of myocardial infarction. *J Thromb Haemost*. 2006;4(2):474-476.
 66. Soria J, Mirshahi S, Mirshahi SQ, et al. Fibrinogen α C domain: its importance in physiopathology. *Res Pract Thromb Haemost*. 2019;3(2):173-183.
 67. de Maat MP, Verschuur M. Fibrinogen heterogeneity: inherited and noninherited. *Curr Opin Hematol*. 2005;12(5):377-383.
 68. Carter AM, Catto AJ, Kohler HP, et al. alpha-fibrinogen Thr312Ala polymorphism and venous thromboembolism. *Blood*. 2000;96(3):1177-1179.
 69. Morris TA, Marsh JJ, Chiles PG, et al. High prevalence of dysfibrinogenemia among patients with chronic thromboembolic pulmonary hypertension. *Blood*. 2009;114(9):1929-1936.
 70. Planquette B, Sanchez O, Marsh JJ, et al. Fibrinogen and the prediction of residual obstruction manifested after pulmonary embolism treatment. *Eur Respir J*. 2018;52(5):1801467.
 71. Stec JJ, Silbershatz H, Tofler GH, et al. Association of fibrinogen with cardiovascular risk factors and cardiovascular disease in the Framingham Offspring Population. *Circulation*. 2000;102(14):1634-1638.
 72. Simpson-Haidaris PJ, Rybarczyk B. Tumors and fibrinogen. *Ann N Y Acad Sci*. 2001;936(1):406-425.
 73. Perisanidis C, Psyrri A, Cohen EE, et al. Prognostic role of pretreatment plasma fibrinogen in patients with solid tumors: a systematic review and meta-analysis. *Cancer Treat Rev*. 2015;41(10):960-970.
 74. Wada H, Mori Y, Okabayashi K, et al. High plasma fibrinogen level is associated with poor clinical outcome in DIC patients. *Am J Hematol*. 2003;72(1):1-7.
 75. Dai K, Zhang Q, Li Y, et al. Plasma fibrinogen levels correlate with prognosis and treatment outcome in patients with non-M3 acute myeloid leukemia. *Leuk Lymphoma*. 2019;60(6):1503-1511.
 76. Elmoamy S, Afif A. Can biomarkers of coagulation, platelet activation, and inflammation predict mortality in patients with hematological malignancies? *Hematology*. 2018;23(2):89-95.
 77. Palumbo JS, Kombrinck KW, Drew AF, et al. Fibrinogen is an important determinant of the metastatic potential of circulating tumor cells. *Blood*. 2000;96(10):3302-3309.
 78. Adams GN, Rosenfeldt L, Frederick M, et al. Colon cancer growth and dissemination relies upon thrombin, stromal PAR-1, and fibrinogen. *Cancer Res*. 2015;75(19):4235-4243.
 79. Sahni A, Simpson-Haidaris PJ, Sahni SK, et al. Fibrinogen synthesized by cancer cells augments the proliferative effect of fibroblast growth factor-2 (FGF-2). *J Thromb Haemost*. 2008;6(1):176-183.
 80. Roche Y, Pasquier D, Rambeaud JJ, et al. Fibrinogen mediates bladder cancer cell migration in an ICAM-1-dependent pathway. *Thromb Haemost*. 2003;89(6):1089-1097.
 81. Zheng S, Shen J, Jiao Y, et al. Platelets and fibrinogen facilitate each other in protecting tumor cells from natural killer cytotoxicity. *Cancer Sci*. 2009;100(5):859-865.
 82. Jennewein C, Tran N, Paulus P, et al. Novel aspects of fibrin(ogen) fragments during inflammation. *Mol Med*. 2011;17(5-6):568-573.
 83. Sweeney MD, Kisler K, Montagne A, et al. The role of brain vasculature in neurodegenerative disorders. *Nat Neurosci*. 2018;21(10):1318-1331.
 84. Daneman R, Prat A. The blood-brain barrier. *Cold Spring Harb Perspect Biol*. 2015;7(1):a020412.
 85. Petersen MA, Ryu JK, Akassoglou K. Fibrinogen in neurological diseases: mechanisms, imaging and therapeutics. *Nat Rev Neurosci*. 2018;19(5):283-301.
 86. Bowman GL, Kaye JA, Moore M, et al. Blood-brain barrier impairment in Alzheimer disease: stability and functional significance. *Neurology*. 2007;68(21):1809-1814.
 87. Ujiie M, Dickstein DL, Carlow DA, et al. Blood-brain barrier permeability precedes senile plaque formation in an Alzheimer disease model. *Microcirculation*. 2003;10(6):463-470.
 88. Reich DS, Lucchinetti CF, Calabresi PA. Multiple sclerosis. *N Engl J Med*. 2018;378(2):169-180.
 89. Marik C, Felts PA, Bauer J, et al. Lesion genesis in a subset of patients with multiple sclerosis: a role for innate immunity? *Brain*. 2007;130(Pt 11):2800-2815.
 90. Hultman K, Strickland S, Norris EH. The APOE ϵ 4/ ϵ 4 genotype potentiates vascular fibrin(ogen) deposition in amyloid-laden vessels in the brains of Alzheimer's disease patients. *J Cereb Blood Flow Metab*. 2013;33(8):1251-1258.
 91. Ryu JK, McLamon JG. A leaky blood-brain barrier, fibrinogen infiltration and microglial reactivity in inflamed Alzheimer's disease brain. *J Cell Mol Med*. 2009;13(9a):2911-2925.
 92. Fiala M, Liu QN, Sayre J, et al. Cyclooxygenase-2-positive macrophages infiltrate the Alzheimer's disease brain and damage the blood-brain barrier. *Eur J Clin Invest*. 2002;32(5):360-371.
 93. Miners JS, Schulz I, Love S. Differing associations between A β accumulation, hypoperfusion, blood-brain barrier dysfunction and loss of PDGFRB pericyte marker in the pre-cuneus and parietal white matter in Alzheimer's disease. *J Cereb Blood Flow Metab*. 2018;38(1):103-115.
 94. Cortes-Canteli M, Mattei L, Richards AT, et al. Fibrin deposited in the Alzheimer's disease brain promotes neuronal degeneration. *Neurobiol Aging*. 2015;36(2):608-617.
 95. Davalos D, Akassoglou K. Fibrinogen as a key regulator of inflammation in disease. *Semin Immunopathol*. 2012;34(1):43-62.
 96. Ryu JK, Petersen MA, Murray SG, et al. Blood coagulation protein fibrinogen promotes autoimmunity and demyelination via chemokine release and antigen presentation. *Nat Commun*. 2015;6:8164.
 97. Merlini M, Rafalski VA, Rios Coronado PE, et al. Fibrinogen induces microglia-mediated spine elimination and cognitive impairment in an Alzheimer's disease model. *Neuron*. 2019;101(6):1099-1108.
 98. Zamolodchikov D, Renne T, Strickland S. The Alzheimer's disease peptide β -amyloid promotes thrombin generation through activation of coagulation factor XII. *J Thromb Haemost*. 2016;14(5):995-1007.
 99. Zamolodchikov D, Strickland S. A β delays fibrin clot lysis by altering fibrin structure and attenuating plasminogen binding to fibrin. *Blood*. 2012;119(14):3342-3351.
 100. Petersen MA, Ryu JK, Chang KJ, et al. Fibrinogen activates BMP signaling in oligodendrocyte progenitor cells and inhibits remyelination after vascular damage. *Neuron*. 2017;96(5):1003-1012.
 101. Davalos D, Kyu Ryu J, Merlini M, et al. Fibrinogen-induced perivascular microglial clustering is required for the development of axonal damage in neuroinflammation. *Nat Commun*. 2012;3:1227.
 102. Akassoglou K, Yu WM, Akpınar P, et al. Fibrin inhibits peripheral nerve remyelination by regulating Schwann cell differentiation. *Neuron*. 2002;33(6):861-875.
 103. Schachtrup C, Lu P, Jones LL, et al. Fibrinogen inhibits neurite outgrowth via beta 3 integrin-mediated phosphorylation of the EGF receptor. *Proc Natl Acad Sci U S A*. 2007;104(28):11814-11819.
 104. Schachtrup C, Ryu JK, Helmrick MJ, et al. Fibrinogen triggers astrocyte scar formation by promoting the availability of active TGF-beta after vascular damage. *J Neurosci*. 2010;30(17):5843-5854.
 105. Montagne A, Nikolakopoulou AM, Zhao Z, et al. Pericyte degeneration causes white matter dysfunction in the mouse central nervous system. *Nat Med*. 2018;24(3):326-337.
 106. Zou T, Ling C, Xiao Y, et al. Exogenous tissue plasminogen activator enhances peripheral nerve regeneration and functional recovery after injury in mice. *J Neuropathol Exp Neurol*. 2006;65(1):78-86.
 107. Ugarova TP, Lishko VK, Podolnikova NP, et al. Sequence γ 377-395(P2), but not γ 190-202(P1), is the binding site for the α MI-domain of integrin α M β 2 in the γ C-domain of fibrinogen. *Biochemistry*. 2003;42(31):9365-9373.
 108. Ryu JK, Rafalski VA, Meyer-Franke A, et al. Fibrin-targeting immunotherapy protects against neuroinflammation and neurodegeneration. *Nat Immunol*. 2018;19(11):1212-1223.
 109. van Oijen M, Witteman JC, Hofman A, et al. Fibrinogen is associated with an increased risk of Alzheimer disease and vascular dementia. *Stroke*. 2005;36(12):2637-2641.

110. Pedersen A, Stanne TM, Redfors P, et al. Fibrinogen concentrations predict long-term cognitive outcome in young ischemic stroke patients. *Res Pract Thromb Haemost.* 2018;2(2):339-346.
111. Bijak M, Olejnik A, Rokita B, et al. Increased level of fibrinogen chains in the proteome of blood platelets in secondary progressive multiple sclerosis patients. *J Cell Mol Med.* 2019;23(5):3476-3482.
112. Negron O, Flick MJ. Does fibrinogen serve the host or the microbe in *Staphylococcus aureus* infection? *Curr Opin Hematol.* 2019;26(5):343-348.
113. Landers CT, Tung HY, Knight JM, et al. Selective fibrinogen cleavage by diverse proteinases initiates innate allergic and antifungal immunity through CD11b. *J Biol Chem.* 2019;294(22):8834-8847.
114. Liesenborghs L, Meyers S, Lox M, et al. *Staphylococcus aureus* endocarditis: distinct mechanisms of bacterial adhesion to damaged and inflamed heart valves. *Eur Heart J.* 2019;40(39):3248-3259.
115. Watve MG, Tickoo R, Jog MM, et al. How many antibiotics are produced by the genus *Streptomyces*? *Arch Microbiol.* 2001;176(5):386-390.
116. Yike I. Fungal proteases and their pathophysiological effects. *Mycopathologia.* 2011;171(5):299-323.
117. Barrera V, Skorokhod OA, Baci D, et al. Host fibrinogen stably bound to hemozoin rapidly activates monocytes via TLR-4 and CD11b/CD18-integrin: a new paradigm of hemozoin action. *Blood.* 2011;117(21):5674-5682.
118. Ling GS, Bennett J, Woollard KJ, et al. Integrin CD11b positively regulates TLR4-induced signalling pathways in dendritic cells but not in macrophages. *Nat Commun.* 2014;5:3039.
119. Colvin RB, Mosesson MW, Dvorak HF. Delayed-type hypersensitivity skin reactions in congenital afibrinogenemia lack fibrin deposition and induration. *J Clin Invest.* 1979;63(6):1302-1306.
120. Lumeng CN, Saltiel AR. Inflammatory links between obesity and metabolic disease. *J Clin Invest.* 2011;121(6):2111-2117.
121. Morange PE, Alessi MC. Thrombosis in central obesity and metabolic syndrome: mechanisms and epidemiology. *Thromb Haemost.* 2013;110(4):669-680.
122. Stalls CM, Triplett MA, Viera AJ, et al. The association between body mass index and coronary artery disease severity: a comparison of black and white patients. *Am Heart J.* 2014;167(4):514-520.
123. Avellone G, di Garbo V, Cordova R, et al. Effects of heparin treatment on hemostatic abnormalities in obese non-insulin-dependent diabetic patients. *Metabolism.* 1997;46(8):930-934.
124. Handley DA, Hughes TE. Pharmacological approaches and strategies for therapeutic modulation of fibrinogen. *Thromb Res.* 1997;87(1):1-36.
125. De Feo P, Volpi E, Lucidi P, et al. Physiological increments in plasma insulin concentrations have selective and different effects on synthesis of hepatic proteins in normal humans. *Diabetes.* 1993;42(7):995-1002.
126. De Feo P, Gaisano MG, Haymond MW. Differential effects of insulin deficiency on albumin and fibrinogen synthesis in humans. *J Clin Invest.* 1991;88(3):833-840.
127. Undas A, Ariens RA. Fibrin clot structure and function: a role in the pathophysiology of arterial and venous thromboembolic diseases. *Arterioscler Thromb Vasc Biol.* 2011;31(12):e88-e99.
128. Kopec AK, Abrahams SR, Thornton S, et al. Thrombin promotes diet-induced obesity through fibrin-driven inflammation. *J Clin Invest.* 2017;127(8):3152-3166.
129. Flick MJ, Du X, Witte DP, et al. Leukocyte engagement of fibrin(ogen) via the integrin receptor alphaMbeta2/Mac-1 is critical for host inflammatory response in vivo. *J Clin Invest.* 2004;113(11):1596-1606.
130. Glenner GG. Amyloid deposits and amyloidosis. The beta-fibrilloses (first of two parts). *N Engl J Med.* 1980;302(23):1283-1292.
131. Hol PR, Snel FW, Niewold TA, et al. Amyloid-enhancing factor (AEF) in the pathogenesis of AA-amyloidosis in the hamster. *Virchows Arch B Cell Pathol Incl Mol Pathol.* 1986;52(3):273-281.
132. Page MJ, Thomson GJA, Nunes JM, et al. Serum amyloid A binds to fibrin(ogen), promoting fibrin amyloid formation. *Sci Rep.* 2019;9(1):3102.
133. Uemichi T, Liepnieks JJ, Yamada T, et al. A frame shift mutation in the fibrinogen A alpha chain gene in a kindred with renal amyloidosis. *Blood.* 1996;87(10):4197-4203.
134. Stangou AJ, Banner NR, Hendry BM, et al. Hereditary fibrinogen A alpha-chain amyloidosis: phenotypic characterization of a systemic disease and the role of liver transplantation. *Blood.* 2010;115(15):2998-3007.
135. Picken MM. Fibrinogen amyloidosis: the clot thickens! *Blood.* 2010;115(15):2985-2986.



Management of adults and children undergoing chimeric antigen receptor T-cell therapy: best practice recommendations of the European Society for Blood and Marrow Transplantation (EBMT) and the Joint Accreditation Committee of ISCT and EBMT (JACIE)

Ibrahim Yakoub-Agha,¹ Christian Chabannon,² Peter Bader,³ Grzegorz W. Basak,⁴ Halvard Bonig,⁵ Fabio Ciceri,⁶ Selim Corbacioglu,⁷ Rafael F. Duarte,⁸ Hermann Einsele,⁹ Michael Hudecek,⁹ Marie José Kersten,¹⁰ Ulrike Köhl,¹¹ Jürgen Kuball,¹² Stephan Mielke,¹³ Mohamad Mohty,¹⁴ John Murray,¹⁵ Arnon Nagler,¹⁶ Stephen Robinson,¹⁷ Riccardo Saccardi,¹⁸ Fermin Sanchez-Guijo,¹⁹ John A. Snowden,²⁰ Micha Srour,²¹ Jan Styczynski,²² Alvaro Urbano-Ispizua,²³ Patrick J. Hayden²⁴ and Nicolaus Kröger²⁵

¹CHU de Lille, LIRIC, INSERM U995, Université de Lille, Lille, France; ²Institut Paoli-Calmettes & Module Biothérapies, INSERM CBT-1409, Centre d'Investigations Cliniques de Marseille, Marseille, France; ³Clinic for Children and Adolescents, University Children's Hospital, Frankfurt, Germany; ⁴Department of Hematology, Oncology and Internal Medicine, Medical University of Warsaw, Warsaw, Poland; ⁵Institute for Transfusion Medicine and Immunohematology of Goethe University and German Red Cross Blood Service, Frankfurt, Germany; ⁶Università Vita-Salute San Raffaele, IRCCS Ospedale San Raffaele, Milan, Italy; ⁷Department of Pediatric Hematology, Oncology and Stem Cell Transplantation, University Hospital of Regensburg, Regensburg, Germany; ⁸Hospital Universitario Puerta de Hierro Majadahonda, Madrid, Spain; ⁹Medizinische Klinik und Poliklinik II, Universitätsklinikum Würzburg, Würzburg, Germany; ¹⁰Department of Hematology, Amsterdam UMC, University of Amsterdam, Cancer Center Amsterdam and LYMMCARE, Amsterdam, the Netherlands; ¹¹Fraunhofer Institute for Cellular Therapeutics and Immunology (IZI) and Institute of Clinical Immunology, University of Leipzig, Leipzig as well as Institute for Cellular Therapeutics, Hannover Medical School, Hannover, Germany; ¹²Department of Hematology and Laboratory of Translational Immunology, University Medical Center Utrecht, Utrecht, the Netherlands; ¹³Department of Laboratory Medicine/Department of Cell Therapy and Allogeneic Stem Cell Transplantation (CAST), Karolinska Institutet and University Hospital, Stockholm, Sweden; ¹⁴Hôpital Saint-Antoine, AP-HP, Sorbonne Université, INSERM UMRS 938, Paris, France; ¹⁵Christie Hospital NHS Trust, Manchester, UK; ¹⁶The Chaim Sheba Medical Center, Tel-Hashomer, Affiliated with the Sackler School of Medicine, Tel-Aviv University, Tel-Aviv, Israel; ¹⁷University Hospitals Bristol NHS Foundation Trust, Bristol, UK; ¹⁸Hematology Department, Careggi University Hospital, Florence, Italy; ¹⁹IBSAL-Hospital Universitario de Salamanca, CIC, Universidad de Salamanca, Salamanca, Spain; ²⁰Department of Haematology, Sheffield Teaching Hospitals NHS Foundation Trust, Sheffield, UK; ²¹Service des Maladies du Sang, CHU de Lille, Lille, France; ²²Department of Pediatric Hematology and Oncology, Collegium Medicum, Nicolaus Copernicus University Torun, Bydgoszcz, Poland; ²³Department of Hematology, ICMHO, Hospital Clínic de Barcelona, Barcelona, Spain; ²⁴Department of Hematology, Trinity College Dublin, St. James's Hospital, Dublin, Ireland and ²⁵Department of Stem Cell Transplantation, University Medical Center Hamburg, Hamburg, Germany

ABSTRACT

Chimeric antigen receptor (CAR) T cells are a novel class of anti-cancer therapy in which autologous or allogeneic T cells are engineered to express a CAR targeting a membrane antigen. In Europe, tisagenlecleucel (Kymriah™) is approved for the treatment of refractory/relapsed acute lymphoblastic leukemia in children and young adults as well as relapsed/refractory diffuse large B-cell lymphoma, while axicabtagene ciloleucel (Yescarta™) is approved for the treatment of relapsed/refractory high-grade B-cell lymphoma and primary mediastinal B-cell lymphoma. Both agents are genetically engineered autologous T cells targeting CD19. These practical recommendations, prepared under the auspices of the European Society of Blood and Marrow Transplantation, relate to patient

Haematologica 2018
Volume 105(2):297-316

Correspondence:

PATRICK J. HAYDEN
phayden@stjames.ie

Received: June 16, 2019.

Accepted: November 19, 2019.

Pre-published: November 21, 2019.

doi:10.3324/haematol.2019.229781

Check the online version for the most updated information on this article, online supplements, and information on authorship & disclosures: www.haematologica.org/content/105/2/297

©2020 Ferrata Storti Foundation

Material published in Haematologica is covered by copyright. All rights are reserved to the Ferrata Storti Foundation. Use of published material is allowed under the following terms and conditions:

<https://creativecommons.org/licenses/by-nc/4.0/legalcode>.

Copies of published material are allowed for personal or internal use. Sharing published material for non-commercial purposes is subject to the following conditions:

<https://creativecommons.org/licenses/by-nc/4.0/legalcode>,

sect. 3. Reproducing and sharing published material for commercial purposes is not allowed without permission in writing from the publisher.



care and supply chain management under the following headings: patient eligibility, screening laboratory tests and imaging and work-up prior to leukapheresis, how to perform leukapheresis, bridging therapy, lymphodepleting conditioning, product receipt and thawing, infusion of CAR T cells, short-term complications including cytokine release syndrome and immune effector cell-associated neurotoxicity syndrome, antibiotic prophylaxis, medium-term complications including cytopenias and B-cell aplasia, nursing and psychological support for patients, long-term follow-up, post-authorization safety surveillance, and regulatory issues. These recommendations are not prescriptive and are intended as guidance in the use of this novel therapeutic class.

Introduction

The first experimental attempts to engineer T cells to express chimeric antigen receptors (CAR) were performed 30 years ago.^{1,2} The ultimate goal was to produce functional, high-affinity, CAR T cells in which the T-cell receptor is re-directed towards a tumor antigen of choice.³ Following refinements in the signaling properties of a CAR within the context of a T cell, development progressed rapidly from the laboratory to clinical trials and CAR T cells targeting CD19 now represent a novel and promising therapy for patients with refractory/relapsed B-cell malignancies including acute lymphoblastic leukemia (ALL) and diffuse large B-cell lymphoma (DLBCL).³⁻⁷ CAR T cells are also being assessed as treatment for other hematologic diseases such as multiple myeloma and acute myeloid leukemia as well as for solid tumors.^{5,8-10}

Tisagenlecleucel (Kymriah™, previously CTL019, Novartis, Basel, Switzerland) consists of autologous CAR T cells genetically modified *ex vivo* using a lentiviral vector encoding an anti-CD19 CAR that includes a domain of the 4-1BB co-stimulatory molecule. It is indicated for the treatment of children and young adults up to the age of 25 years with relapsed/refractory B-ALL and was approved by the Food and Drug Administration (FDA) on 30th August, 2017. It was subsequently FDA-approved on May 1st, 2018 for the treatment of adult patients with relapsed or refractory large B-cell lymphoma after two or more lines of systemic therapy, including DLBCL not otherwise specified, high-grade B-cell lymphoma and DLBCL arising from follicular lymphoma. The European Medicines Agency (EMA) approved similar indications on August 22nd, 2018.

Axicabtagene ciloleucel, (Yescarta™, previously KTE-C19, Gilead, USA) is an autologous CAR T-cell product which has been genetically modified *ex vivo* using a retroviral vector encoding an antibody fragment targeting CD19 and an intracellular domain including the CD28 co-stimulatory molecule. It was FDA-approved on October 18th, 2017 for the treatment of adult patients with relapsed or refractory large B-cell lymphoma after two or more lines of systemic therapy, including DLBCL not otherwise specified, primary mediastinal large B-cell lymphoma, high grade B-cell lymphoma, and DLBCL arising from follicular lymphoma. The EMA approved its use in relapsed or refractory DLBCL and primary mediastinal large B-cell lymphoma after two or more lines of systemic therapy, on August 23rd, 2018.

While CAR T cells are rationally designed, targeted therapies, they nevertheless frequently induce life-threatening toxicities that can be mitigated by planning and proper hospital organization. Comprehensive training should be provided to all categories of personnel includ-

ing scientists, nurses and physicians, and close collaboration with a range of other specialists, especially intensive care unit staff and the neurology/neuroimaging services, is required.^{11,12}

As CAR T cells represent a novel class of therapy and as both of the currently available products have only been evaluated in phase II studies to date, close post-marketing surveillance is mandatory. The EMA has endorsed the use of the European Blood and Marrow Transplantation (EBMT) registry for the collection of 15-year follow-up data on treated patients in order to ensure that evaluation of the efficacy and safety of commercially available CAR T cells continues on an ongoing basis. The Center for International Blood and Marrow Transplant Research (CIBMTR) fulfills a similar function in the United States of America (USA). The newly updated EBMT Registry Cellular Therapy form is designed to capture the efficacy and side-effects of modern cellular therapies and to provide the required post-marketing surveillance through Post-Authorization Safety Surveillance (PASS) and other studies. The main objective for professionals in the field is to evaluate how these innovative treatments compare with the alternative therapeutic options and current standards-of-care. Phase III studies are underway.¹³

The clinical use of CAR T cells is early in its evolution and it is, as yet, unclear whether CAR T-cell therapy constitutes a definitive treatment or whether disease cure will require further immunologically based consolidation such as allogeneic stem cell transplantation, especially for ALL. In trials on the use of CAR T-cell therapy in DLBCL, long-term disease control is observed in up to 50% of patients. As some of these patients may be cured, allogeneic transplantation as consolidation may not be necessary.¹⁴⁻¹⁶ This issue can only be resolved with longer follow-up.

Research areas include dual antigen targeting to counter one of the most common resistance mechanisms, which is loss of the targeted antigen, the inclusion of safety switches such as suicide genes in order to mitigate side-effects when they occur, 'off the shelf' allogeneic CAR T products, the refinement of co-stimulatory domains to enhance persistence and avoid immune escape, and the use of non-viral vectors and semi-automated on-site production to simplify the manufacturing process.

Although this field will inevitably change over the coming years, these first EBMT guidelines on CAR T cells are intended to provide practical, clinically relevant recommendations for hematologists and other cancer specialists and their teams involved in the administration of CAR T-cell therapies, especially the commercially available products. These guidelines may also be a useful resource for other stakeholders such as pharmacists or health service administrators involved in the planning and delivery of

CAR T-cell therapies, given the complexity of their production and administration and their high cost.

Methodology

The Practice Harmonization and Guidelines subcommittee of the Chronic Malignancies Working Party of the EBMT proposed the project in December 2018. The EBMT Board accepted the proposal and worked with experts in the field to produce practical clinical recommendations on the management of adults and children undergoing autologous CAR T-cell therapy. A survey was sent to centers active in this field to solicit feedback on current approaches to the topics covered in these guidelines.¹⁷ Their responses (41 of 50 centers) along with a literature review and assessment of both the licensing study protocols and the summaries of product characteristics (SPC) of the commercially available CAR T-cell products inform these recommendations. Finally, three teleconferences were held in preparation for a 2-day workshop that took place in Lille on 4th-5th April, 2019.

These recommendations are intended to reflect current best practice in this novel and rapidly moving field and to support clinicians and other healthcare professionals in delivering consistent, high-quality care. They principally apply to the CAR T-cell therapies that are currently commercially available for the treatment of hematologic malignancies. Given the absence of randomized trial evidence in this field, a decision was made not to grade these recommendations. They therefore represent the consensus view of the authors.

When patients are receiving CAR T-cell therapies in clinical trials, physicians should follow the relevant trial protocols. The management of disease relapse following CAR T-cell therapy is outside the scope of these recommendations.

Patient eligibility for chimeric antigen receptor T-cell therapy

The decision to treat a patient with CAR T cells therapy should be made collectively at a multidisciplinary team meeting in a designated center for CAR T-cell therapy. The patients' medical history and physical condition are important factors in determining their suitability for treatment.

Trial eligibility criteria and EBMT recommendations are shown in Table 1.

Screening laboratory tests and imaging

Table 2 summarizes a recommended minimum set of tests that should be performed at screening in order to assess organ function and patient eligibility.

Work-up prior to apheresis

The current set of rules that apply to human tissue and cell procurement in the European Union derives from the Tissue and Cell Directives published in 2004 (2004/23/EC) and 2006 (2006/17/EC; 2006/86/EC). The European Union Commission recently convened a stakeholder meeting to examine whether revision of the Tissue and Cell

Directives was required. Although a number of arguments, including manufacturing of Advanced Therapy Medicinal Products, were brought forward in favor of revising the directives, no formal decision has yet been made.

The current rules are solely based on the donor-recipient relationship, whether autologous or allogeneic, and do not address the intended use of the collected material. As a consequence, the same requirements apply both to the collection of mononuclear cells for stem cell transplantation and when procuring the starting material for the manufacture of Advanced Therapy Medicinal Products, unless the Marketing Authorization Holder stipulates specific additional requirements.

Cross-border shipment of the collected cell product requires compliance with national regulations both in the country of origin and in the country of destination. Obtaining authorization to export human autologous-derived elements will require knowledge of the patient's viral serology.

Table 3 presents a checklist that should be verified before starting the leukapheresis procedure.

How to perform leukapheresis

Scheduling of leukapheresis must be coordinated with the pharmaceutical company as lack of manufacturing capacity is currently one of the bottlenecks in the availability of CAR T-cell therapies.²⁰ Confirmation of an agreed manufacturing slot is therefore mandatory prior to deciding on a date for apheresis. With technical advances and more patients likely to become candidates for these treatments in the coming years, limitations in the capacity of collection centers are likely to become a challenge.

Any of the commercially available leukapheresis devices are, in principle, suitable for apheresis. While companies may suggest preferences for devices or systems, local experience, local permits and the regulatory approval status of individual devices and systems should guide the selection of technology. Technically, unmobilized leukapheresis is most similar to apheresis for off-line extracorporeal photopheresis or for the collection of allogeneic mononuclear cells intended for post-transplant immunotherapy (donor lymphocyte infusions); no specific apheresis protocols have so far been proposed by cell processor manufacturers or by the CAR T-cell manufacturers. Proof of proper validation and maintenance of equipment and established training processes for personnel operating or supervising the use of cell processors are key elements required by the Marketing Authorization Holders in order to qualify and onboard sites that are authorized to collect cells for CAR T-cell manufacturing. Prior accreditation in compliance with the 7th edition of the Foundation for the Accreditation of Cellular Therapy (FACT) - Joint Accreditation Committee of the International Society for Cell Therapy and EBMT (JACIE) Standards for Hematopoietic Cellular Therapies or the FACT Standards for Immune Effector Cells confirms the presence of a pre-existing Quality Management System, although additional requirements are often identified, including those from pharmaceutical providers and health service commissioners.²¹

Further information on the technical aspects of apheresis is provided in the *Online Supplement*.

Table 1. Eligibility criteria for the selection of patients for clinical trials.

Characteristics	ELIANA (ALL Kymriah™)	JULIET (DLBCL Kymriah™)	ZUMA-1 (High-grade B-cell NHL Yescarta™)	EBMT recommendations	Comment
Age limit (NHL)	N/A	≥18 years SPC - No data are available on children < 18 years of age	≥18 years SPC - No data are available on children < 18 years of age	No upper age limit	Decision should be based on physical condition rather than age
Age limit (ALL)	'Age 3 years at the time of screening to age 21 years at the time of initial diagnosis' SPC- up to 25 years of age	N/A	N/A	Follow SPC	Ability to collect sufficient cells by apheresis can be a limiting factor in infants and small children
ECOG PS Performance Status	Karnofsky (age ≥16 years) or Lansky (age <16 years) PS ≥50 at screening	ECOG PS of either 0 or 1 at screening	ECOG PS of 0 or 1	>2 not recommended Note, however, that real-world data with Yescarta™ included patients with ECOG PS >2 ¹⁸	Prognosis may be less poor if the decline in PS is due to active disease
History of malignancy	No prior malignancy, except carcinoma <i>in situ</i> of the skin or cervix treated with curative intent and with no evidence of active disease	No previous or concurrent malignancy except adequately treated BCC or SCC, <i>in situ</i> cancer of the breast or cervix treated and without recurrence for 3 years, primary malignancy resected and in remission for more than 5 years	No history of malignancy other than nonmelanoma skin cancer or carcinoma <i>in situ</i> (e.g. cervix, bladder, breast) or follicular lymphoma unless disease free for at least 3 years	Absence of history of malignancy other than carcinoma <i>in situ</i> (e.g. cervix, bladder, breast) unless disease- free and off therapy for at least 3 years	
Prior allo-HCT	Not excluded; however, excluded if grade II-IV acute or extensive chronic GvHD	Excluded	Excluded	Not a contraindication	Active GvHD is listed as a reason to delay treatment in the Kymriah™ and Yescarta™ SPC
Prior anti-CD19/anti-CD3 BiTE antibodies or any other CD19 therapy	Excluded Not a contraindication as per SPC	Excluded	Excluded if prior CD19 targeted therapy	Not a contraindication	
Previous CAR T-cell therapy	Not applicable in trials Not in SPC	Not applicable in trials Not in SPC	Excluded	Not a contraindication	Further CAR T-cell therapy outside of clinical trials is to be avoided
History of autoimmune disease	Not an exclusion criterion	Not an exclusion criterion	Not an exclusion criterion	Not recommended in active autoimmune disease resulting in end-organ injury or requiring systemic immunosuppression or systemic disease-modifying agents within the last 2 years	Individualized risk-benefit assessment required
Current systemic immunosuppressive treatment	Any GvHD therapy must be stopped more than 4 weeks prior to enrollment to confirm that GvHD recurrence is not observed	Any immunosuppressive medication must be stopped more than 4 weeks prior to enrollment	Any immunosuppressive medication must be stopped more than 4 weeks prior to enrollment	Contraindication	Intermittent topical, inhaled or intranasal corticosteroids are allowed
Existing or suspected fungal, bacterial, viral, or other infection	Active or latent HBV or HCV (test within 8 weeks of screening) or any uncontrolled infection at screening	Uncontrolled active or latent HBV or active HCV; Uncontrolled acute life- threatening bacterial, viral or fungal infection (e.g. blood cultures positive <72 h prior to screening)	Known history of HIV, HBV (HepBs Ag positive) or HCV (anti-HCV); Clinically significant active infection, or currently receiving IV antibiotics or within 7 days of enrollment	Relative contra-indication; individualized risk-benefit assessment required	Active infection should be controlled and on treatment prior to leukapheresis

continued on the next page

continued from the previous page

History of CNS disease	CNS involvement by malignancy defined as CNS-3 as per NCCN guidelines excluded; however, those with history of effectively treated CNS disease were eligible	Active CNS involvement by malignancy excluded	Subjects with detectable CSF malignant cells, or brain metastases, or with history of CSF malignant cells or brain metastases excluded	Relative contra indication; individualized risk-benefit assessment required ¹⁹	Caution required as higher risk of neurological toxicity
------------------------	--	---	--	---	--

ALL: acute lymphoblastic leukemia; DLBCL: diffuse large B-cell lymphoma; NHL: non-Hodgkin lymphoma; EBMT: European Society for Blood and Marrow Transplantation; N/A: not available; SPC: summary of product characteristics; ECOG: Eastern Cooperative Oncology Group; PS: performance status; BCC: basal cell carcinoma; SCC: squamous cell carcinoma; allo-HCT: allogeneic hematopoietic cell transplantation; GvHD: graft-versus-host disease; BiTE: bispecific monoclonal antibodies; CAR: chimeric antigen receptor; HBV: hepatitis B virus; HCV: hepatitis C virus; HIV: human immunodeficiency virus; CNS: central nervous system; NCCN: National Comprehensive Cancer Network.

Table 2. The minimum required tests.

Test methods	Trials and/or SPC	EBMT recommendations	Comment
Disease confirmation		Histology only for NHL Immunophenotyping for ALL	
Hematology			
Hematology	ANC >1.0x10 ⁹ /L in NHL trials	ANC >1.0x10 ⁹ /L	Evidence of adequate bone marrow reserve
Chemistry			
Bilirubin	<26-34 µmol/L	<34 µmol/L; higher limit acceptable (<43 µmol/L) with Gilbert syndrome	No trial data regarding patients outside of these parameters
AST/ALT	<5xULN	<5x ULN	Attempt to identify causes e.g. active infections
Creatinine clearance	Age- and gender-dependent cut-offs for ELIANA trial, > 60 mL/min/1.73m ² (JULIET)	> 30 mL/min	Caution is required in patients with CrCl of <60 mL/min
Virology			
Hepatitis B*	Active or latent hepatitis B (test within 8 weeks of screening) (ELIANA, JULIET)	Mandatory in some countries. To be done within 30 days of leukapheresis and results must be available at the time of collection and shipment	As per national guidelines Serology/molecular testing
Hepatitis C*	Active hepatitis C (test within 8 weeks of screening) (ELIANA, JULIET)	Mandatory in some countries. To be done within 30 days of leukapheresis and results must be available at the time of collection and shipment	As per national guidelines Serology/molecular testing
HIV*	HIV positive test within 8 weeks of screening - ineligible for CAR T trials	Mandatory in some countries. To be done within 30 days of leukapheresis and results must be available at the time of collection and shipment	Kymriah™ is using a lentiviral vector whereas Yescarta™ uses a retroviral vector
Other work-up			
Cardiac function	Hemodynamically stable and LVEF >45% confirmed by echocardiogram or MUGA scan; Patients with cardiac involvement by NHL were excluded from some trials	LVEF >40%; assess for pericardial effusion by echocardiography; ECG	Work-up of effusions required to identify causes
CNS imaging	ZUMA-1 trial required an MRI of the brain to confirm there was no evidence of lymphoma	MRI not required except in those with a history of CNS disease or current neurological symptoms of concern	A baseline MRI can be helpful, should severe neurological toxicities arise
Lumbar puncture	Patients with active CNS disease were excluded from trials	Lumbar puncture not required except in those with a history of CNS disease or current neurological symptoms of concern	
Fertility	Females of childbearing potential must have a negative serum or urine pregnancy test within 48 h of infusion (ELIANA)	Females of childbearing potential must have a negative serum or urine pregnancy test	Test must be repeated and confirmed negative within 8 days of the CAR T-cell infusion

SPC: summary of product characteristics; EBMT: European Society for Blood and Marrow Transplantation; NHL: non-Hodgkin lymphoma; ALL: acute lymphoblastic leukemia; ANC: absolute neutrophil count; AST: aspartate aminotransferase; ALT: alanine aminotransferase; ULN: upper limit of normal; CrCl: creatinine clearance; HIV: human immunodeficiency virus; CAR: chimeric antigen receptor; LVEF: left ventricular ejection fraction; MUGA: multiple-gated acquisition; MRI: magnetic resonance imaging; CNS: central nervous system. *Leukapheresis material for Kymriah™ manufacturing will not be accepted from patients with a positive test for active hepatitis B virus, hepatitis C virus or HIV (SPC)

Only one of the commercial CAR T-cell manufacturers – Novartis – currently requires cryopreservation of the mononuclear cells on site. It is stipulated that the white blood cell count should be adjusted to 1.0 (0.5-2.0) $\times 10^9/\text{mL}$, that an approved (approved by the company and local regulators) cryoprotectant be added slowly and that the cells be frozen in controlled-rate freezers prior to storage in vapor phase liquid nitrogen. To produce Kymriah™, Novartis will accept cells that have been harvested within the preceding 18 months and cryopreserved with appropriate quality management surveillance. Whether autologous blood mononuclear cells intended for CAR T-cell manufacturing should be prospectively collected and cryopreserved in selected patients at high risk of relapse is already under debate. The other commercial manufacturers will collect fresh apheresis product packed in their own specified shipping containers. Until shipping, these apheresis products are stored refrigerated (2-8°C).

Manufacturers' requirements for quality control are currently very limited and may be exceeded by local requirements. There may also be differences between FDA and

EMA requirements.²² Accredited and validated testing methods must be used. In addition to testing for infectious disease markers in peripheral blood samples on the day of collection, reasonable quality control should include sterility testing as well as some hemocytometric parameters (white blood cell count, hematocrit, CD3⁺, and viable CD45⁺ counts). Sampling of the collected cell product must follow the manufacturer's requirements so as not to compromise downstream processing steps, while also complying with local manufacturing authorizations.

Depending on the disease burden, it may be possible to arrange for leukapheresis before starting salvage chemotherapy to treat disease relapse. There is evidence that cumulative chemotherapy exposure adversely affects the quality of circulating T cells. Although apheresis can be performed in patients with absolute lymphocyte counts as low as $0.1 \times 10^9/\text{L}$, the likelihood of reaching the target number of autologous lymphocytes and successfully manufacturing the drug product is higher in individuals with absolute lymphocyte counts exceeding $0.5 \times 10^9/\text{L}$. In addition, the choice of salvage therapy (chemotherapy,

Table 3. Checklist prior to apheresis.

Prior to apheresis	Trials/SPC	EBMT recommendations	Comment
ECOG PS score	Not specified	ECOG PS score ≤ 2	At discretion of apheresis practitioner
Days after last chemotherapy		Allow for recovery from cytotoxic chemotherapy	Need for marrow recovery from prior chemotherapy
Days off corticosteroids	Three (Kymriah™) to 7 (Yescarta™) days off or on no more than prednisolone 5 mg equivalent	Ideally, 7 days to minimize effect on lymphocyte collection	A shorter period of as few as 3 days was considered acceptable by Kansagra <i>et al.</i> ¹² Physiological replacement doses of hydrocortisone permitted
Mandatory blood tests			
Hepatitis B, hepatitis C, HIV, syphilis, and HTLV	Mandatory for all trials	Mandatory in some countries. To be done within 30 days of leukapheresis and results must be available at the time of collection and shipment	Only serological testing is required; nucleic acid testing is not necessary if all serological testing is negative
Blood tests to ascertain suitability for apheresis			
C-reactive protein		Recommended to assess for ongoing infection	In patients with active infection, eligibility for apheresis will need to be decided on a case-by-case basis
Standard electrolytes and renal function		Required	Apheresis may predispose to electrolyte imbalance and limited fluid tolerance
Blood values required for optimal apheresis performance			
Hemoglobin		Hemoglobin >80 g/L Hematocrit >0.24	To establish a good interface during collection
Absolute neutrophil count		> $1.0 \times 10^9/\text{L}$	Consistent with recovery from prior chemotherapy
Absolute lymphocyte count		> $0.2 \times 10^9/\text{L}$ *	Higher count required in small children. Of note, $0.2 \times 10^9/\text{L}$ CD3 ⁺ count is the minimum threshold
Platelet count		> $30 \times 10^9/\text{L}$	Transfuse as required
Full blood count		To be repeated at the end of apheresis procedure	Apheresis can remove more than 30% of circulating platelets

SPC: summary of product characteristics; EBMT: European Society for Blood and Marrow Transplantation; ECOG PS: Eastern Cooperative Oncology Group Performance Status; HIV: human immunodeficiency virus; HTLV: human T-lymphotropic virus. *This threshold specifically applies to count recovery following corticosteroid therapy where an absolute lymphocyte count >0.2 is a surrogate marker of corticosteroid washout.

serotherapy and radiotherapy) may adversely affect subsequent attempts at leukapheresis and washout periods need to be considered.

Table 4 provides recommendations on washout periods following various salvage treatments before starting leukapheresis. In addition, it should be noted that prior use of blinatumomab is not a contraindication to anti-CD19 CAR T-cell therapy.²³

Bridging therapy

Bridging therapy refers to the administration of anti-cancer drugs including chemotherapy to maintain disease control during the period between lymphocyte collection and the final administration of the CAR T-cell product.¹⁶ This time window may be longer than anticipated for logistical reasons, sometimes but not always related to manufacturing, and will be specifically monitored through EBMT Registry collection of 'real world' data.

The goal of bridging therapy is to prevent clinically significant disease progression leading to impaired organ function or any other complications that might prevent the patient proceeding with lymphodepletion and receiving the CAR T cells. It is also hoped that treatment of rapidly proliferating disease will establish a balanced *in vivo* target-effector ratio to allow for effective CAR T-cell adoptive immunotherapy. In brief, the aim is not so much to achieve disease remission as to establish adequate disease control prior to the CAR T-cell infusion.

The optimal bridging therapy for any individual will depend on disease- and patient-specific factors. However, clinicians should bear in mind that patients receiving chemotherapeutic agents, either alone or in combination, will subsequently receive lymphodepleting therapy and will be at risk of specific CAR T-cell-related complications such as cytokine release syndrome (CRS), encephalopathy and tumor lysis syndrome. Bridging therapy should therefore ideally not induce major complications, such as infections, bleeding or any organ dysfunction that might interfere with the planned lymphodepleting therapy and CAR T-cell infusion. Bridging therapy can be omitted in the presence of stable, low burden disease if the turn-around

time for the CAR T cells is expected to be short. Importantly, certain agents, especially immunotherapeutic drugs with a longer half-life, may interfere with the expansion or persistence of the infused CAR T cells and should be avoided. Examples include alemtuzumab, daratumumab, checkpoint inhibitors and brentuximab vedotin.

When choosing bridging therapy for lymphoma patients, factors to be considered include the prior response to chemotherapy and chemo-immunotherapy, the overall tumor burden and the distribution and sites of tumor involvement. Options include parenteral agents such as rituximab, gemcitabine, oxaliplatin, bendamustine or pixantrone; oral chemotherapy regimens e.g. variants of prednisolone, etoposide, procarbazine, and cyclophosphamide (PEP-C), or oral cyclophosphamide 100 mg once daily; novel targeted therapies such as lenalidomide or ibrutinib; high-dose corticosteroids e.g. dexamethasone 40 mg for 4 days or high-dose methylprednisolone, repeated as needed; or radiotherapy to symptomatic or large masses.^{24,25}

In ALL, the risk of CRS has been found to correlate with the leukemic blast burden at the time of the CAR T-cell infusion. Bridging chemotherapy is therefore especially important in ALL and the chosen agents are typically drawn from known B-ALL chemotherapy regimens although doses are often reduced to lower the risk of infectious complications and organ dysfunction.^{5,26} Novel and targeted agents, for example, tyrosine kinase inhibitors and monoclonal antibodies, may also be used although it is important to consider whether the agent is capable of inducing a rapid response and whether the therapy might interact with subsequent lymphodepleting and CAR T-cell therapy. Whatever treatment is chosen, bridging therapy should only be given after leukapheresis so that the quality of the CAR T-cell product is not affected. The patient can be monitored after leukapheresis and during and following bridging chemotherapy either at the treating center or at the referring center provided that there are clear lines of communication between the centers regarding the choice of any treatments and the management of any complications. Frequent monitoring, including laboratory testing and imaging, is mandatory in

Table 4. Wash-out period before leukapheresis (adapted from Kansagra *et al.*¹²).

Type of therapy	SPC	EBMT recommendations	Comments
Allo-HCT	No guidance	Patients should be off immunosuppression and GvHD-free	A minimum of 1 month is recommended
Donor lymphocyte infusion	No guidance	4 weeks	6 to 8 weeks may be safer to rule out any GvHD
High-dose chemotherapy	No guidance	3-4 weeks depending on the intensity of the chemotherapy	Recovery from cytopenias is required
CNS-directed therapy	No guidance	1 week	
Short-acting cytotoxic/anti-proliferative drugs	No guidance	3 days	Recovery from cytopenias is required
Systemic corticosteroids	No guidance	Ideally, 7 days to minimise any effect on lymphocyte collection	A shorter period of as few as 3 days was considered acceptable by Kansagra <i>et al.</i> ¹² Regardless of timing, an ALC > 0.2 x 10 ⁹ /L is preferable given the likely effect of recent corticosteroids on lymphocyte quality

SPC: summary of product characteristics; EBMT: European Society for Blood and Marrow Transplantation; Allo-HCT: allogeneic hematopoietic cell transplantation; GvHD: graft-versus-host disease; CNS: central nervous system; ALC: absolute lymphocyte count.

order to prevent or rapidly treat complications that might arise while awaiting the arrival of the CAR T-cell product.

Lymphodepleting conditioning

The use of lymphodepleting (LD) conditioning prior to the CAR T-cell infusion creates a 'favorable' environment for CAR T-cell expansion and survival *in vivo*, probably by eliminating regulatory T cells.²⁷ In addition, it can lead to the upregulation of tumor immunogenicity and improve disease control.²⁸ Furthermore, there are data demonstrating that LD conditioning works to promote homeostatic proliferation of adoptively transferred T cells via increases in the pro-survival/proliferation cytokines, interleukin (IL)-7 and IL-15, and in conjunction with a lack of competition with wildtype T cells.²⁹⁻³¹

Many drugs have been used for LD conditioning including cyclophosphamide, fludarabine, pentostatin and bendamustine as well as total body irradiation.³² In a clinical trial involving 30 patients with B-ALL at the Fred Hutchinson Cancer Research Center, fludarabine and cyclophosphamide was associated with superior CAR T-cell persistence and better disease-free survival when compared to single-agent cyclophosphamide or cyclophosphamide in combination with etoposide.^{33,34} Fludarabine-cyclophosphamide is the most widely used LD conditioning regimen.^{35,36}

LD conditioning is usually administered on a 3-to-5 day schedule prior to the infusion of the CAR T cells. If the center does not have established policies and infrastructure to allow for safe outpatient-based administration, hospitalization is recommended during this period to ensure close monitoring and optimal hydration.

Items to consider before starting LD conditioning are shown in Table 5A.

Laboratory tests to review before starting LD conditioning are shown in Table 5B.

If there is a long delay (in general, more than 3 weeks) between completing LD conditioning and the subsequent CAR T-cell infusion, and the white blood cell count is $>1.0 \times 10^9/L$, then consideration should be given to re-treating the patient with LD chemotherapy prior to administration of the CAR T cells.

Product receipt and thawing

The currently licensed CAR T-cell products are delivered frozen and must be maintained at very low temperatures during shipping, receipt and temporary storage until they are thawed immediately prior to use. Hospitals have adopted different approaches to product receipt, taking into account local organizational and regulatory issues. The unit receiving the CAR T-cell products will need to have suitable storage containers and facilities for genetically manipulated material; depending on national legislation, a storage site may need regulatory approval as gene therapy medicinal products are also genetically modified organisms.²¹ As the manufacturing companies use differently sized cryostorage cassettes, custom-made cryo racks, at least one for each company, must be obtained. A storage site with secured access and an adequate number of trained staff licensed to work with biohazards and liquid nitrogen are required, both at the hospital pharmacy and at the cell processing facility.

The designated receiving laboratory will receive advance notice from the manufacturer and the product will be delivered in a sealed liquid nitrogen dewar (vacuum flask). Upon receipt, the seals of the dewar are inspected for breaches; seals are broken, if applicable; the temperature log is read out; and the product is inspected for bag integrity and identity according to the label; the bag in its cassette is subsequently transferred to a liquid nitrogen storage container until it is brought to the bedside. The company-specific product receipt documentation must be completed; personnel authorized to handle products are provided with specific and detailed training from the relevant manufacturer. When the ward is ready to receive the product, the cassette is transferred to a laboratory dewar and this is transported to the ward.

In some countries, the use of water baths, carefully calibrated to 35-37°C, remains acceptable; use of an automated thawing device is preferable. Representative examples of such devices are the Sahara™ (Sarstedt) and Plasmatherm™ (Barkey) devices. While the thawing of CAR T cells is, in principle, the same as for cryopreserved hematopoietic progenitor cells collected by apheresis, the much smaller volumes of CAR T-cell products only require very short thawing times. We recommend that thawing times be established locally with similarly-sized mock products, ideally with mononuclear cell suspensions in protein-saline-dimethylsulfoxide freezing buffer and testing of post-thaw viability, but at a minimum, with protein-saline-dimethylsulfoxide buffer without cells and observation of the time until the buffer assumes the slushy consistency of a ready-to-spike cryo product. If thawing is conducted in a water bath, the spike ports that protrude out of the water must be carefully massaged to ensure that they thaw in synchrony with the rest of the product. The spike ports of the thawed product are uncapped, disinfected and aseptically spiked with the transfusion set, the air trap is filled completely with the cell suspension (no falling drops, as this shears cells) and air is evacuated from the infusion line. The individual responsible for the thawing and preparation of the infusion varies between countries and health care systems. We propose that the decision as to who is responsible should be primarily based on competence, meaning that those individuals who normally thaw autologous transplants are likely best qualified. On this basis, pharmacy, processing facility and clinical transplant staff are all acceptable candidates and bedside thawing is preferable.

Infusion of chimeric antigen receptor T cells

Before starting to thaw the CAR T-cell product, the patient should be assessed. Some factors to consider are shown in Table 6. A transfusion set is required for the administration of the cells. In general, a typical transfusion filter set with 50-200 µm pore size is used; this is, in fact, mandatory in some countries. Importantly, fluid infusion sets are not suitable because of the sub-micrometer bacterial filters. Transfusion sets with leukocyte-depletion filters are also unacceptable. It should be noted that the manufacturers recommend the use of non-filtered tubing sets although our recommendations, and some local regulatory requirements, deviate from this approach.

Pre-medication to prevent adverse reactions is reasonable with the important exception of corticosteroids

Table 5A. Checklist before starting the conditioning.

	SPCs	EBMT recommendations	Comments
CAR T-cell product	The availability of the CAR T-cell product must be confirmed prior to starting the LD conditioning	LD conditioning should only be administered following receipt of product on site	Exceptional situations may necessitate the administration of LD conditioning following confirmation of successful production but prior to arrival
Clinical conditions		Active infections must be excluded or under control before starting LD conditioning	Patient has to be able to tolerate LD conditioning
WBC	LD conditioning should be administered before the Kymriah™ infusion unless the WBC count within 1 week of the infusion is $\leq 1.0 \times 10^9/L$	Administer LD conditioning to all patients regardless of WBC or ALC	Some investigators have suggested that patients with low ALC ($< 0.1 \times 10^9/L$) may not require LD as these patients are already “lymphodepleted”

SPC: summary of product characteristics; EBMT: European Society for Blood and Marrow Transplantation; CAR: chimeric antigen receptor; LD: lymphodepletion; WBC: white blood cell count; ALC: absolute lymphocyte count.

Table 5B. Checklist of laboratory tests prior to conditioning.

Test methods	Trials and SPC	EBMT recommendations	Comment
Chemistry			
C-reactive protein and/or fibrinogen level		Required to rule out ongoing infection	LD is contraindicated in patients with active infection. Active infection must be excluded or under control before starting LD
Bilirubin	$< 26\text{--}34 \mu\text{mol/L}$	$< 34 \mu\text{mol/L}$; higher limit acceptable ($> 43 \mu\text{mol/L}$) with Gilbert syndrome	No trial data regarding patients outside of these parameters
AST/ALT	$< 5 \times \text{ULN}$	$< 5 \times \text{ULN}$	Attempt to identify causes e.g. active infections
Creatinine clearance		$> 30 \text{ mL/min}$	Modify drugs doses according to creatinine clearance
Other work-up			
Cardiac function		Repeat cardiac investigations only if clinically indicated (e.g. cardiotoxic bridging chemotherapy)	LVEF $> 40\%$; assess for pericardial effusion by echocardiography; ECG

SPC: summary of product characteristics; EBMT: European Society for Blood and Marrow Transplantation; AST: aspartate aminotransferase; ALT: alanine aminotransferase; LD: lymphodepletion; ULN: upper limit of normal; LVEF: left ventricular ejection fraction; ECG: electrocardiogram.

which may damage the CAR T-cell product; typically, paracetamol derivatives and antihistamines, such as chlorpheniramine or diphenhydramine, are used. Individual guidelines are provided by the manufacturers.

The product is aseptically connected to the port of a central venous catheter. The line to be used for the CAR T-cell infusion must be clearly designated; as with blood and stem cell products, no concurrent medication may be given during the CAR T-cell infusion. Infusion should begin as rapidly after spiking as possible, but no later than 30 min thereafter. The small volumes and cell numbers allow for rapid (less than 30 min) drip infusion of the cell suspension. The infusion bag and set should be disposed of as a biohazard and genetically modified organism waste in compliance with institutional policies and country-specific regulations. Transfusion of the low-volume CAR T-cell product is typically uneventful.

Short-term complications and management: infusion to day +28

The rapid *in vivo* proliferation of CAR T cells may be associated with potentially life-threatening toxicities such

as CRS and neurotoxicity, which generally occur within 14 and 28 days of the CAR T-cell infusion, respectively.^{11,36-38} LD conditioning may also contribute to the cytopenias.

Hospitalization

Some centers have established policies and infrastructure that allow for the safe administration of CAR T cells on an outpatient, ambulatory care basis. However, for ambulatory care to work, clear protocols, staffing and training need to be in place so that patients are able to access a coordinator on a 24/7 basis. Centers must also be able to provide both immediate review and the emergency admission of patients under the care of experienced staff. As such arrangements are not currently available in most European centers, we recommend that patients are admitted to hospital during the early post-infusion period unless high-level ambulatory care and rapid re-admission pathways are already well established, as in centers already providing ambulatory hematopoietic cell transplantation (HCT). Table 7 summarizes our recommendations relating to the first 28 days following the CAR T-cell infusion. These are in line with a number of clinical trial protocols and the recommendations of scientific societies.^{21,39}

Tumor lysis syndrome

CAR T-cell therapy can result in the rapid destruction of tumor cells and therapy-associated adverse events including tumor lysis syndrome.⁴⁰⁻⁴² Standard hospital protocols should apply. Tumor lysis in certain locations (gut, biliary tree, lungs, genitourinary tract) may lead to perforation

and the release of commensal organisms resulting in peritonitis.⁴³

Infections

Active infections should be fully treated and under control prior to the administration of LD conditioning and the

Table 6. Checklist and pre-medication before chimeric antigen receptor T-cell infusion.

	SPC	EBMT recommendations	Comment
Active infection	Reasons to delay treatment: active uncontrolled infection (Kymriah™ and Yescarta™)	Contraindication	CAR T-cell infusion should be delayed until the infection has been successfully treated or controlled
Cardiac arrhythmia not controlled with medical management	Reasons to delay treatment: unresolved SAR (esp. pulmonary reactions, cardiac reactions or hypotension) from preceding chemotherapies (Kymriah™ and Yescarta™)	Cardiologist opinion is required	Specific individualized risk-benefit assessment required
Hypotension requiring vasopressor support	See above	Contraindication	CAR T-cell infusion should be delayed until the hypotension has been fully treated
New-onset or worsening of another non-hematologic organ dysfunction ≥ grade 3		Work-up is needed to identify the cause	Specific individualized risk-benefit assessment required
Significant worsening of the clinical condition since start of LD	Reasons to delay treatment: significant clinical worsening of leukemia burden or lymphoma following LD chemotherapy (Kymriah™)	Work-up is needed to identify the cause	Specific individualized risk-benefit assessment required
Pre-medication	‘It is recommended that patients be pre-medicated with paracetamol and diphenhydramine or another H1 antihistamine within approximately 30 to 60 minutes prior to Kymriah™ infusion’ ‘Paracetamol given orally and diphenhydramine or chlorpheniramine intravenous or oral (or equivalent) approximately 1 hour before Yescarta™ infusion is recommended’	As per SPC	
Concomitant medication	Corticosteroids should NOT be used prior to or around the time of the infusion except in case of a life-threatening emergency	As per SPC	

SPC: summary of product characteristics; EBMT: European Society for Blood and Marrow Transplantation; CAR: chimeric antigen receptor; SAR: severe adverse reaction; LD: lymphodepletion.

Table 7. Recommendations regarding the first month after chimeric antigen receptor T-cell infusion.

Period	SPC and protocols	EBMT recommendations	Comments
Day 0 to day +14 post-infusion	Some protocols require 5-14 days hospitalization after the infusion	Ideally, 14 days hospitalization	Shorter hospitalization periods as well as outpatient follow-up are possible in centers that can provide 24/7 contact with immediate availability of specialist inpatient care. Patients must be located within 30 min of the center
From hospital discharge to day +28 post-infusion	Some protocols require that patients be located within 30 to 60 min of the center	Patients must be located within 60 min of the treating unit or a well-equipped center* The continuous presence of a caregiver who is educated to recognize the signs and symptoms of CRS and ICANS is required	CRS and, in particular, ICANS can occur after the patient has left the hospital. In addition, life-threatening complications may occur during this period e.g. septic shock in neutropenic patients

SPC: summary of product characteristics; CRS: cytokine release syndrome; ICANS: immune effector cell-associated neurotoxicity syndrome. * Centers competent to manage such complications.

infusion of CAR T-cell products, especially given the likely cytokine-driven exacerbation of inflammatory processes. The presence of fever should prompt blood and urine cultures, a chest radiograph, and, depending on symptoms, respiratory viral screening, cytomegalovirus and Epstein-Barr virus nucleic acid testing, computed tomography imaging, lumbar puncture, and/or brain magnetic resonance imaging. Empiric antimicrobial therapy based on symptoms and institutional protocols should not be delayed based on the presumption of CRS and clinicians should consider the prior duration of neutropenia.⁴⁵

To reduce the time from recognition of suspected sepsis to treatment with antimicrobial medications, institutions may consider the use of patient group directives or conditional orders. These orders allow nursing staff to respond rapidly to signs and symptoms of infection, an example being the automatic administration of specific intravenous antibiotics following the detection of a fever.

Cytokine release syndrome

CRS is a form of systemic inflammatory response following the infusion of CAR T cells. However, CRS has also been described following the administration of various monoclonal antibodies including bi-specific antibodies and anti-lymphocyte globulin and as a complication of haploidentical transplantation.^{44,48} CRS is the most common complication after CAR T-cell therapy. Depending on the type of CAR T-cell therapy, the disease characteristics and the grading system which has been used, the reported incidence has ranged from 30-100% and for CRS grade 3 or 4 from 10-30%.⁴⁹

The activation of CAR T cells is the triggering event of CRS. This leads to the release of effector cytokines such as interferon- γ , tumor necrosis factor- α and IL-2. These molecules are, in turn, capable of activating the monocyte/macrophage system and inducing the production of a broad spectrum of pro-inflammatory cytokines (including IL-1, IL-6, IL-10, interferon γ and monocyte chemoattractant protein-1) leading to a raised level of C-reactive protein and sometimes hyperferritinemia. In pre-clinical models (humanized immunodeficient mice), it has been shown that human monocytes are the main source of IL-1 and IL-6 during CRS. The syndrome can be prevented by monocyte depletion or by blocking the IL-6 receptor with tocilizumab. Tocilizumab does not, however, protect mice against late lethal neurotoxicity characterized by meningeal inflammation. In contrast, an anti-IL-1 receptor antagonist (anakinra) appeared to prevent CRS and neurotoxicity in animal models.^{36,50,51}

Severe CRS shares clinical features with macrophage activation syndrome, including fever, hyperferritinemia and multi-organ dysfunction. CRS usually occurs between 1 and 14 days after the CAR T-cell infusion and can last from 1 to 10 days.^{11,52} Its severity is variable and is evaluated according to a novel grading scale recently proposed by an American Society for Transplantation and Cellular Therapy (ASTCT) consensus panel.³⁸ Rare but fatal cases with neurological involvement have been reported in the literature.¹¹ Risk factors for CRS include tumor burden, the presence of active infection at the time of the infusion, the dose of infused CAR T cells, the type of CAR T-cell construct and the choice of LD regimen.^{37,53-55}

The treatment for severe cases, in addition to symptomatic measures, consists of the administration of tocilizumab (a monoclonal antibody against IL-6 receptor)

and, sometimes, corticosteroids. Tocilizumab should be administered no more than four times during one episode of CRS. Siltuximab (monoclonal antibody against IL-6) can be used as a second-line treatment (Figure 1).

An algorithm outlining the management of CRS is shown in Figure 1.

Neurological toxicity

The neurological toxicity seen in CAR T-cell recipients, previously called CAR-related encephalopathy syndrome (CRES), has recently been termed immune effector cell-associated neurotoxicity syndrome (ICANS).³⁸ This is the second most common adverse event following CAR T-cell infusion and its incidence has been reported at rates varying from 12% to 55%. In a recent study of 100 patients, the median time-to-onset of the first neurological symptoms was 6 days (range, 1-34 days) after the CAR T-cell infusion.⁵⁷ The duration of symptoms is generally between 2 and 9 days although late complications may occur.^{11,38,57} In general, it develops either at the same time as or following resolution of CRS. Deterioration in handwriting has been shown to be an early predictor of central neurotoxicity. Therefore, daily writing tests over the first months following the CAR T-cell infusion can be used as a simple tool to detect incipient ICANS.

The spectrum of symptoms and signs is non-specific, ranging from confusion, headaches, tremors, hallucinations and abnormal movements to seizures, papilloedema and coma. Any neurological symptom occurring after the CAR T-cell infusion must therefore be considered as CAR T-related until proven otherwise. However, the ASTCT consensus panel recommended excluding non-specific symptoms such as headache, tremor, myoclonus, asterixis, and hallucinations as they are usually managed symptomatically and do not generally trigger specific interventions.

Severe cases have been reported, occasionally leading to death, due to multifocal hemorrhage, cerebral edema and laminar cortical necrosis. The severity is correlated with the increase in specific biomarkers such as C-reactive protein, ferritin and IL-6.^{11,58-60} Close monitoring of patients using validated nursing tools is necessary to identify early manifestations of neurotoxicity. This requires serial cognitive testing.

Rapid access to neurological expertise is needed. Cross-sectional imaging (computed tomography, magnetic resonance imaging), electroencephalography, and cerebrospinal fluid examination may all be required in the management of these complex patients. Anti-epileptic prophylaxis with agents such as levetiracetam is not routinely recommended except in patients with a history of seizures or central nervous system disease.

Pre-existing neurological comorbidities may be a risk factor for the development of ICANS. Disease-associated factors include ALL, tumor burden, history of meningeal involvement and prior central nervous system-directed therapies.^{11,58-60} The intensity of ICANS has been correlated with the depth of lymphopenia and the homeostatic expansion of CAR T cells. Moreover, the severity of ICANS has also been found to be associated with the severity and early onset of CRS as measured by the extent of fever within 36 h of the infusion, hemodynamic instability, tachypnea and hypoalbuminemia reflecting loss of vascular integrity and capillary leakage.

The CARTOX scoring system was updated by the

ASTCT consensus panel and has been replaced by the Immune Effector Cell-Associated Encephalopathy (ICE) score shown in Table 8.³⁸ A different assessment tool for screening delirium in children, adapted from Traube *et al.*, is shown in Table 9.⁶¹

Laboratory monitoring of cytokine release syndrome and neurotoxicity

In addition to routine daily hematology and chemistry laboratory tests, C-reactive protein and ferritin levels are of use in the monitoring of patients developing CRS and neurotoxicity. Although assaying IL-6 or other cytokine levels is theoretically interesting, cytokine testing is not routinely performed in most centers at present.

Atypical lymphocytes that can mimic blasts are not uncommon at the peak of CAR T-cell expansion and can be found in the peripheral blood, bone marrow, and even the cerebrospinal fluid of patients treated with these therapies. Flow cytometry can be used to exclude relapse. Repeating microbiological testing and imaging to rule out infection is recommended in febrile patients.

Antibiotic prophylaxis

The combined effect of prior treatments (immunochemotherapy and/or autologous or allogeneic HCT, bridging chemotherapy administered after leukapheresis and LD conditioning) all increase the risk of opportunistic infections in patients receiving CAR T-cell therapy. Approximately one-third of patients have prolonged neutropenia (beyond day +30) and up to 20% of patients have neutropenia lasting more than 90 days. B-cell depletion and hypogammaglobulinemia are additional risk factors for infections.^{15,16,63,64}

After CRS and ICANS, infections are one of the most common side effects of CAR T-cell therapy. Most infections are seen within the first 30 days and are bacterial, and to a lesser extent, respiratory viral infections. Invasive fungal infections are rare and are mostly observed in ALL patients who have undergone prior allogeneic stem cell transplantation.⁶⁵

CAR T-cell recipients, like patients undergoing allogeneic HCT, are at increased risk of a range of infections at the

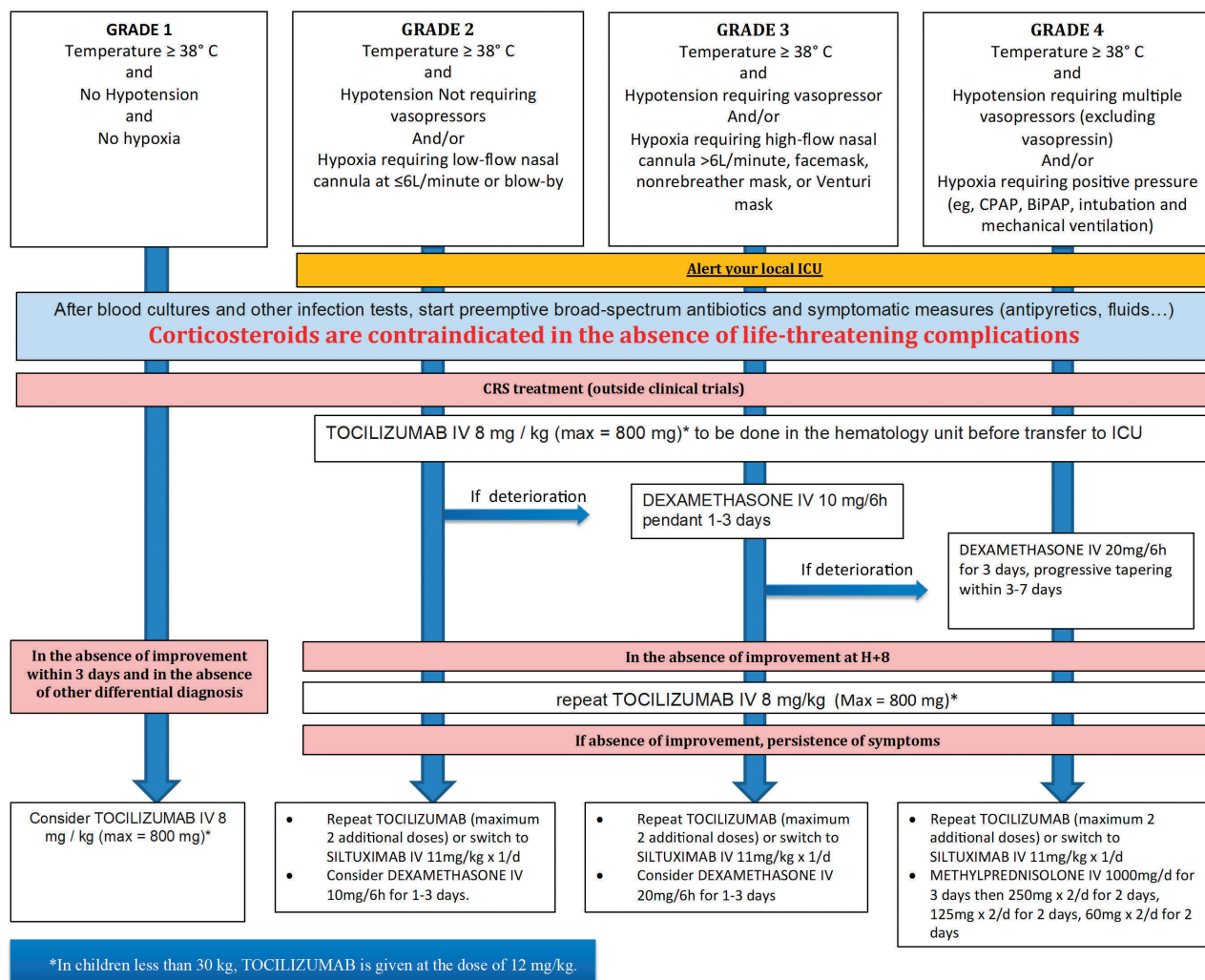


Figure 1. Management of cytokine release syndrome. Adapted from Yakoub-Agha *et al.*⁵⁶ CPAP: continuous positive airway pressure; BiPAP: biphasic positive airway pressure; ICU: intensive care unit; CRS: cytokine release syndrome.

different stages of their treatment course and appropriate antimicrobial prophylaxis is required. In general, centers performing allogeneic HCT will be familiar with the care of such patients and there is, as yet, no evidence that there

are infectious issues specific to CAR T-cell therapy. Table 10 summarizes recommendations for prophylaxis against the most common infections.

There is no evidence to suggest that cytomegalovirus,

Table 8. Immune Effector Cell-Associated Encephalopathy (ICE) score to neurological toxicity assess. Adapted from Lee *et al.*³⁸

Test	Points
Orientation: orientation to year, month, city, hospital	4
Naming: ability to name three objects (e.g. table, television, pillow)	3
Following commands: ability to follow simple commands (e.g. "smile" or "open your mouth")	1
Writing: ability to write a standard sentence (e.g. "Happy to have my family around")	1
Attention: ability to count backwards from 100 by 10	1

Table 9. Cornell Assessment of Pediatric Delirium (CAPD) to assess encephalopathy in children <12 years. Adapted from Traube *et al.*⁶¹

	always	often	sometimes	rarely	never
Eye contact with caregiver	0	1	2	3	4
Purposeful actions	0	1	2	3	4
Aware of their surroundings	0	1	2	3	4
Being restless	4	3	2	1	0
Being inconsolable	4	3	2	1	0
Being underactive	4	3	2	1	0
Slow response to interactions	4	3	2	1	0
Communicating needs and wants	4	3	2	1	0

Table 10. Anti-infective prophylaxis after chimeric antigen receptor T-cell therapy.

	Trials	EBMT recommendation	Comment
Neutropenia	G-CSF should be used according to published guidelines	G-CSF to shorten duration of neutropenia from 14 days post-infusion can be considered	Avoid if patient has CRS or ICANS There are theoretical concerns regarding macrophage activation
Antibacterial prophylaxis	Not recommended	Not recommended*	Can be considered in case of prolonged neutropenia and should be based on local guidelines e.g. with levofloxacin or ciprofloxacin
Anti-viral prophylaxis	Subjects should receive prophylaxis for infection with herpes virus, according to NCCN guidelines or standard institutional practice	Valaciclovir 500 mg bid or aciclovir 800 mg bd	Start from LD conditioning until 1 year post-CAR T-cell infusion and/or until CD4 ⁺ count >0.2x10 ⁹ /L
Anti-pneumocystis prophylaxis	Subjects should receive prophylaxis for infection with <i>Pneumocystis pneumonia</i> , according to NCCN guidelines or standard institutional practice	Co-trimoxazole 480 mg once daily or 960 mg three times each week To start from LD conditioning until 1 year post-CAR T-cell infusion and/or until CD4 ⁺ count >0.2x10 ⁹ /L	Can be started later depending on center guidelines. In case of co-trimoxazole allergy, pentamidine inhalation (300 mg once every month), dapsone 100 mg daily or atovaquone 1500 mg once daily are other agents to consider
Systemic anti-fungal prophylaxis	Subjects should receive prophylaxis for fungal infections according to NCCN guidelines or standard institutional practice	Not recommended routinely; however, consider in patients with prolonged neutropenia and on corticosteroids	In patients with prior allo-HCT, prior invasive aspergillosis and those receiving corticosteroids, posaconazole prophylaxis should be considered
IV immunoglobulins	Gammaglobulin will be administered for hypogammaglobulinaemia according to institutional guidelines. At a minimum, trough IgG levels should be kept above 400 mg/dL, especially in the setting of infection	Routine in children, consider in adults who have had infections with encapsulated organisms	Clinical evidence does not support routine use in adults following allo-HCT

EBMT: European Society for Blood and Marrow Transplantation; G-CSF: granulocyte colony stimulating factor; CRS: cytokine release syndrome; ICANS: immune effector cell-associated neurotoxicity syndrome; NCCN: National Comprehensive Cancer Network; LD: lymphodepleting conditioning; IV: intravenous; IgG: immunoglobulin G; allo-HCT: allogeneic hematopoietic cell transplantation. *In patients with neutropenic fever, empiric treatment with broad spectrum antibiotics is strongly recommended.

Epstein-Barr virus or adenoviruses are significant clinical problems after CAR T-cell therapy. Little is known regarding the risk of hepatitis B and C virus reactivation as patients with these infections were specifically excluded from the trials. It is not possible to provide recommendations regarding the use of CAR T-cell therapy in patients with human immunodeficiency virus infection as seropositive individuals were also excluded. The pharmaceutical companies may, however, manufacture a drug product for a patient positive for hepatitis B, hepatitis C or human immunodeficiency virus if the viral load is below the level of detection following treatment. For patients with a history of hepatitis B infection, prophylaxis with tenofovir is recommended.⁶⁶

Medium-term complications and management: day +28 to day +100

Potential toxicities during this period include delayed tumor lysis syndrome, delayed hemophagocytic lymphohistiocytosis/macrophage activation syndrome and CRS, B-cell aplasia, hypogammaglobulinemia, graft-versus-host disease (GvHD), and infections. Neutropenia, thrombocytopenia and anemia are common but generally resolve slowly over several months. Growth factor support may be indicated in the early stages.

Table 11 summarizes tests to be performed during this period and their recommended frequency.

Delayed macrophage activation syndrome and cytokine release syndrome

In the experience of CAR T-cell therapy for ALL, CRS typically occurred between 1 and 14 days after the CAR T-cell infusion, whereas in patients with chronic lymphocytic leukemia, CRS usually occurred later, between 14 and 21 days after the infusion.⁴² Regardless of the timing, delayed macrophage activation syndrome and CRS are managed using standard approaches.

B-cell aplasia and hypogammaglobulinemia

B-cell aplasia is an almost universal on-target, off-tumor toxicity and results in hypogammaglobulinemia. It occurs in all responding patients and can persist for several years. This absence of CD19-positive cells correlated with functional persistence of CTL019 cells below the limits of

detection of flow cytometry, whereas CTL019 remained detectable by means of quantitative polymerase chain reaction analysis.⁴² B-cell aplasia can therefore serve as a marker for monitoring CD19-specific CAR T-cell activity over time.^{42,67}

Persistent B-cell lymphopenia is associated with sinopulmonary infections, notably with encapsulated bacteria; consideration can be given to vaccination although there is no evidence and immunoglobulin levels should be monitored.⁴⁵ It has therefore been standard practice in pediatric centers to administer empiric immunoglobulin replacement following the administration of CAR T cells. Children with B-cell aplasia should receive immunoglobulin replacement to maintain IgG levels according to institutional guidelines for IgG substitution (i.e. $\geq 500\text{mg/dL}$).⁴² In some cases, this may be a long-term requirement.

There is no consensus regarding systematic supplementation in adults who have been shown to have long-lived CD19-negative plasma cells that continue to confer humoral immunity in patients who were successfully treated with CAR T cells targeting CD19. Nevertheless, intravenous immunoglobulin replacement is recommended in patients with hypogammaglobulinemia and recurrent infections with encapsulated bacteria. Patients may transition to home-administered subcutaneous immunoglobulins after 6 months.

Graft-versus-host disease

Donor-derived CAR T cells may rarely trigger GvHD if harvested from, and then returned to, patients who have undergone allogeneic HCT. Current evidence suggests that the risk of inducing GvHD with the use of donor-derived CAR T cells is low.⁶⁸⁻⁷⁰ However, vigilance is required as this complication is potentially severe and life-threatening. If suspected, GvHD should be diagnosed and managed using standard protocols, balancing the potential benefit of introducing systemic immunosuppression against its effect on anti-tumor CAR T-cell function.

Infections

Beyond 30 days, viral infections predominate including respiratory viral infections, cytomegalovirus viremia and pneumonia. Later infections may reflect prolonged immunoglobulin deficiency (up to 46% at day 90) as well as lymphopenia.⁷¹ Severe co-infections with CRS include respiratory virus infections (some nosocomial),

Table 11. Monitoring of patients during medium-term follow-up.

Test	Purpose	Frequency	Comment
FBC, biochemistry panel, LDH, fibrinogen, CRP	Standard follow-up	At every visit and as clinically indicated	
CMV, EBV, adenovirus	Viral reactivation	As clinically indicated	
Quantitative immunoglobulins or serum protein electrophoresis	Immune reconstitution	Monthly	Consider IV immunoglobulins
Peripheral blood immunophenotyping – CD3/4/8/16/56/19*	Immune recovery	Once monthly for first 3 months, three monthly thereafter in first year	Guide to anti-infective prophylaxis
CAR T-cell monitoring where kits are available for routine monitoring of anti-CD19 CAR T cells	CAR T-cell persistence	Peripheral blood flow cytometry or transgene by molecular methods as clinically indicated	Not recommended by CAR T-cell manufacturers

FBC: full blood count; LDH: lactate dehydrogenase; CRP: C-reactive protein; CMV: cytomegalovirus; EBV: Epstein-Barr virus; IV: intravenous; CAR: chimeric antigen receptor.

cytomegalovirus, human herpes virus-6 or Epstein-Barr viremia, *Clostridium difficile* colitis, cholangitis, and viral encephalitis.^{67,72-74}

Nursing and psychological support of patients

CAR T cells are generally being administered in a small number of regional specialist centers to which patients are referred from general hospitals. Patients who are treated with CAR T cells may therefore experience high levels of anxiety due to their new environment as well as their prognosis. Many will be socially isolated and at a significant distance from their established support networks. The role of the clinical nurse specialist is vital to the success of the procedure as well as providing essential bedside support. Referral to local counselling/psychology services should be offered to these patients when appropriate.

Patients who are being treated on an outpatient basis and their caregivers should receive comprehensive education on the symptoms of CRS and neurotoxicity and patients should attend the treating hospital without delay in the event that they begin to feel unwell. On discharge, they should be instructed to remain within 1 hour’s travel of the treating hospital for at least 4 weeks following the infusion, during which time a caregiver should always be present. If the patient lives further away, then alternative accommodation, such as a local hotel or apartment, will be required. Independently of whether the patient is living at home or lodging in a local apartment, ambulatory care arrangements for rapid re-admission should be well established.

All patients must be informed of the potential risks and the precautions that they need to take, as described in the relevant product patient information leaflet. They may also receive further written information, according to local practice, in the form of a patient information booklet or leaflet. This should include information and education on the symptoms of CRS and serious neurological adverse reactions, the need to report any symptoms immediately to their treating physician and the need to remain in close proximity to the center in which the CAR T cells were administered for at least 4 weeks following the infusion.

Patients must be advised to keep their Patient Advice Card with them at all times and to show it to any health-care professional they encounter, especially if they are admitted to another hospital. Patients are advised not to drive for 8 weeks after the infusion and only after resolution of any neurological symptoms. This is due to the risk of delayed neurological toxicity. It is also preferable to have a responsible adult such as a parent, spouse or other caregiver available during the first 3 months following the infusion. A reliable, consistent and well-informed caregiver is essential.

Long-term follow-up from day +100 onwards – ‘late effects’

Little is known about the long-term effects of CAR T-cell therapy. Only a small cohort of patients has been followed for more than 2 years. The main identified complications are prolonged cytopenias and hypogammaglobu-

Table 12. Recommended minimum frequency of attendance at centers for monitoring for late effects after chimeric antigen receptor T-cell therapy.

Post CAR-T	Stable patients	Complications	Disease monitoring	Comment
Day +100 to 1 year	Three-monthly	As clinically indicated	Frequency of visits required is disease-specific and monitoring could be performed by CAR T-cell center or referring clinician	Patients who proceed to subsequent allo-HCT, cytotoxic therapy and/or immune effector cell therapy should be followed as per Majhail <i>et al.</i> 2012 ²⁵
One year to 15 years	Annually			

CAR: chimeric antigen receptor; allo-HCT: allogeneic hematopoietic cell transplantation

Table 13. Recommended tests to be performed at long-term follow-up clinics.

Test	Purpose	Frequency	Comment
Full blood count, biochemistry panel	Standard follow-up	At every visit	
Viral infection (PB PCR, NPA)	Viral reactivation	As clinically indicated	
Quantitative immunoglobulins ± serum protein electrophoresis	Immune reconstitution	At every visit	
Peripheral blood immunophenotyping – CD3/4/8/16*56/19*	Immune reconstitution	Every second visit	No longer required following normalization
CAR T-cell monitoring where kits are available for routine monitoring of anti-CD19 CAR T*	CAR T-cell persistence	Every visit. However, no longer required when absent for two consecutive tests	Testing for CAR T-cell persistence is not standard. Checking for B-cell depletion as a surrogate marker is an option
Endocrine function and other standard late effects testing appropriate to age	Standard follow-up	As clinically indicated	

PB: peripheral blood; PCR: polymerase chain reaction; NPA: naso-pharyngeal aspirate; CAR: chimeric antigen receptor. *Equivalent test methods for other immune effector cells as they become available

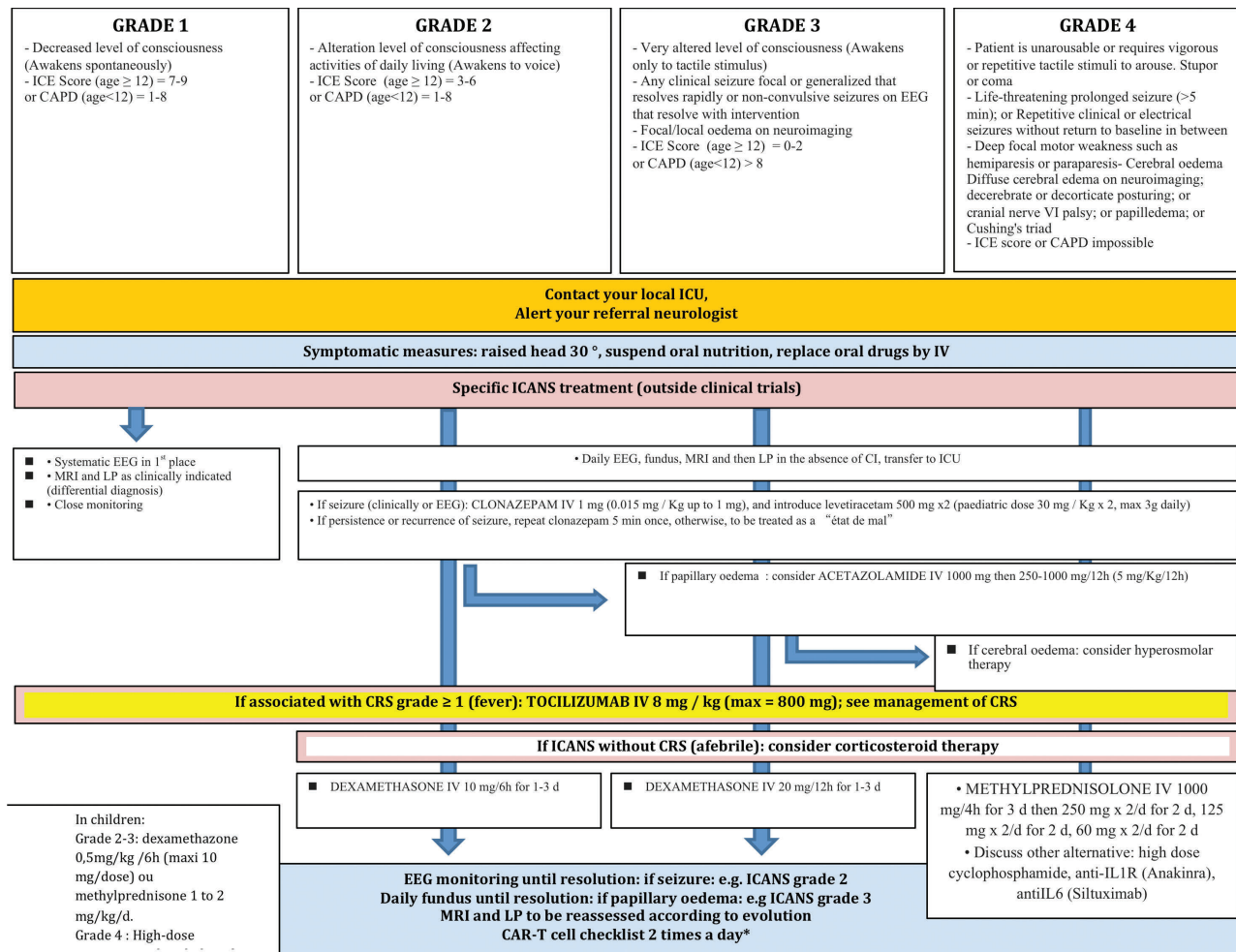


Figure 2. Management of chimeric antigen receptor T-cell-related neurological toxicity. Adapted from Cornillon *et al.*⁶² ICE. Immune effector cell-associated encephalopathy; CAPD: Cornell Assessment of Pediatric Delirium; EEG: electroencephalography; ICU: intensive care unit; IV: intravenous; ICANS: effector cell-associated neurotoxicity syndrome; MRI: magnetic resonance imaging; LP: lumbar puncture; CRS: cytokine release syndrome; IL1R: interleukin-1 receptor; IL-6: interleukin 6.

linemia. There are also more theoretical concerns about the risk of secondary malignancies and both neurological and autoimmune diseases.

It should be recognized that all patients will have been treated previously with multiple anti-cancer therapies, some having also undergone allogeneic HCT. Some patients may receive CAR T-cell treatment at overseas centers and may then return to a CAR T-cell therapy or HCT center. There is a duty-of-care on all CAR T-cell-administering centers to arrange for appropriate local follow-up. In cases of geographical transition, formal communication, including discharge correspondence and other clinical material such as imaging files, should be provided to new healthcare providers.

Protocols and policies (standard operating procedures) for long-term follow-up will need to be put in place. These should cover shared care and out-reach arrangements and should be based on service level agreements between CAR T-cell centers and referring centers.

Multidisciplinary teams dealing with CAR T-cell therapies should arrange for long-term follow-up of treated patients in order to capture disease status and the late effects of CAR T-cell and prior treatments. The multidisciplinary team should include a physician with responsibility

for CAR T-cell administration, disease-specific specialists, long-term follow-up nursing staff, data managers and clinical trial staff.

Long-term follow-up clinics may be incorporated into local arrangements for generic allogeneic HCT 'late effects' clinics with other allogeneic HCT patients, although dedicated clinics for the late effects of CAR T-cell therapy can be developed if a critical mass of survivors is reached.

The clinic should systematically monitor for the following outcomes: (i) disease status – remission, minimal residual disease, relapse, management of relapse, death, (ii) further treatments administered after CAR T-cell therapy, including allogeneic HCT and other immune effector cell therapy/Advanced Therapy Medicinal Products; (iii) late effects – for stable patients in ongoing remission, 3-monthly monitoring for the first year, annually thereafter or as clinically appropriate; (iv) infections, (v) immunological status – cell markers, immunoglobulins, including CAR T-cell persistence; (vi) new cancers, including secondary myeloid diseases; (vii) new autoimmunity and autoimmune diseases; (viii) endocrine, reproductive and bone health (including growth and development in children and young adult patients); (ix) neurological status (including recovery from ICANS); (x) psychological status

and quality of life; (xi) cardiovascular status, including echocardiographic assessments and risk factors for cardiovascular disease, such as 'metabolic syndrome'; (xii) respiratory status; and (xiii) gastrointestinal and hepatic status.

The role of vaccination following CAR T-cell therapy remains unclear. Until further evidence is available, no specific recommendation can be made. This is, in particular, a problem with small children who might not yet have completed their basic immunization schedule and who therefore need close follow-up.

In view of long-term B-cell depletion, the advisability of vaccination and adherence to the standard recommended national schedules needs to be evaluated for each individual based on the history of infections and laboratory assessments of cellular and humoral immunity.⁷⁵ If vaccines are given, specific antibody responses should be assessed.

Post-authorization safety surveillance

As tisagenlecleucel (KymriahTM) and axicabtageneclisoleucel (YescartaTM) are the first agents in a novel class of therapies based on the genetic modification of autologous T cells using viral vectors, the EMA and the FDA have made marketing approval conditional on 15-year post-authorization safety surveillance (PASS). At an EMA-sponsored stakeholder workshop on how to best capture the long-term side effects of different CAR T-cell products over the next 15 years, it was felt that the reporting of CAR T-cell safety and efficacy in one European registry would avoid the creation of data silos and would allow for the risks and benefits of the different agents to be transparently compared on a common platform. Such a registry would also set an excellent example as to how public registries can not only improve patient care but also help to support affordable health care.⁷⁶ In March 2019, the EBMT received a qualification opinion from the EMA which found the cellular therapy module of the EBMT registry to be fit-for-purpose for the regulatory overseeing of pharmaco-epidemiological studies concerning CAR T-cell therapy.⁷⁷

A modified version of the MED-A cell therapy form will be used for CAR T cells and other academic- or industry-manufactured cell therapies. The data submission time points are day 0, day +100, 6 months, and annually thereafter. This module has already proven to be effective in capturing basic data sets on academic and commercial CAR T-cell infusions, although the EMA has requested additional safeguards during data capture for regulatory purposes. However, the current minimal data set requested by the EMA for commercial products does not require detailed product information such as CD4 and CD8 ratios or transduction efficiencies, as companies consider these to be sensitive proprietary information. Agreed access to a more detailed data set regarding products being evaluated in clinical trials might benefit all those working in the CAR T-cell research field.

In the USA, the FDA has implemented product-specific Risk Evaluation and Mitigation Strategy (REMS) programs. In parallel, the National Cancer Institute-funded Moonshot Initiative program called Cellular Immunotherapy Data Resource, awarded to the CIBMTR in October 2018, will allow for the collection of real-world data. In recent years, the EBMT has worked with the

CIBMTR to develop common data collection policies so the prospect of robust global datasets on the efficacy and safety of CAR T-cell therapies is on the horizon.

It is expected that patients receiving CAR T-cell therapies in both investigator-led and pharma-sponsored trials might also have their follow-up data collected in the EBMT registry. In order to address concerns that pharmaceutical companies may have about the confidentiality of commercially sensitive clinical data, trial data reported to the EBMT registry can be embargoed until investigating centers decide to make such data accessible to the public. Early data collection might also create a virtuous circle whereby knowledge of increased activity might help those lobbying for an improved infrastructure for CAR T-cell therapies across Europe in terms of funding opportunities, regulatory frameworks, and, ultimately, commercial drug approval. EMA approval for the use of the EBMT registry also places certain responsibilities on the EBMT. As a formal data controller, the EBMT will need to guarantee a fair and transparent mode of data sharing in order to improve the assessment of the many different agents and ultimately to improve our knowledge on how best to use CAR T-cell therapies.

JACIE and regulatory issues

FACT-JACIE standards were initially developed for the accreditation of HCT programs.^{78,79} The current 7th edition of the standards also covers immune effector cells (IEC) to accommodate the rapidly evolving field of cellular therapy, mainly, although not exclusively, genetically modified cells, such as CAR T cells. FACT-JACIE standards do not cover the manufacturing of CAR T cells but do include the supply chain and handover of responsibilities when the product is provided by a third party. Specific clauses in the standards detail the following requirements, among others: the need for the appropriate recognition of side effects related to the infusion of IEC, a policy for the rapid escalation of care in critically ill patients, the availability of specific drugs for CRS and other complications and a labeling system to guarantee both the identification and traceability of the product from the collection to the manufacturer and back to the clinical unit. In all involved areas, there is the need for evidence of adequate staffing and training, satisfactory levels of competency, validated procedures and efficient communication. Documentation is available at www.jacie.org.

During the introductory phase of developing CAR T cells, some centers received 'focused' site visits for IEC. However, now that the 7th edition of the standards is well established, inspection of IEC standards should be routinely incorporated within standard JACIE site visits, particularly as there is much dependency on the wider accreditation requirements of the HCT program i.e., clinical, apheresis, pharmacy and processing laboratory service, along with quality management system requirements. In fact, in the current 7th edition, only 2% and 6% of items are specifically related to either IEC or HCT, respectively, and 92% of the items are common to all forms of cellular therapy.

In addition to JACIE, the complexity of the clinical management of patients receiving CAR T-cell therapy has led to competent authorities and other regulatory bodies in some European countries requiring the administration of CAR T cells and other IEC within the context of an

accredited allogeneic HCT program, where established facilities, staffing and expertise can support most aspects of the CAR T-cell pathway. Regardless, the logistical impact of IEC administration within a HCT program has to be carefully planned; an implementation plan aimed at meeting all accreditation and other regulatory requirements, while engaging all professionals, services and infrastructure, is essential. Before starting, an assessment of the number of eligible patients and likely resource requirements will usually have to be reviewed by the competent authorities and other regulators, as well as by funding bodies. As mandated by the EMA, the pharmaceutical manufacturers also have their own requirements and routinely inspect facilities before a CAR T-cell program is commenced.

The EBMT and JACIE expect that most CAR T-cell activity in Europe will be delivered by experienced allogeneic HCT centers and, ultimately, as the accreditation cycles of centers roll through to the 7th edition of the standards, the IEC standards will be covered at routine allogeneic HCT re-accreditation inspections. For the minority of centers that undertake CAR T-cell therapy outside of an accredited allogeneic HCT program, there are a number of options. Given that CAR T-cell therapy is presently used predominantly in B-cell non-Hodgkin lymphoma, there is the possibility of achieving the IEC standards as part of the accreditation covering autologous HCT, given that referral for autologous HCT is common in lymphoma practice. The same considerations could also apply to myeloma specialists working outside of allogeneic HCT programs, as IEC accreditation standards could be aligned to autologous HCT activity or referral routes routinely established in every myeloma service.

In the event of CAR T-cell or related therapies becoming more broadly applicable to non-hematologic cancers and

therefore potentially outside mainstream transplant practice, there are a number of possible routes. First, there may be referral to an accredited HCT program, where shared care arrangements can be easily accommodated within the quality management systems and service level agreements. This is a model that already applies to occasional HCT in solid tumors, such as germ cell tumors, where patients are referred back at a mutually agreed, often early, stage after transplantation for ongoing care by the referring medical or clinical oncologists.

An alternative strategy would be to undertake independent IEC accreditation specifically for CAR T-cell and other IEC therapies. This would have to be an individual decision, based on the number of patients undergoing therapy in a given center, as to whether the establishment of a functional quality system and other generic measures were justified just for CAR T-cell or other IEC therapy. The EBMT and JACIE are currently evaluating the demand and feasibility of this approach, which has been adopted by FACT.

Currently, the general recommendation from the EBMT and JACIE is that CAR T cells and other IEC are best delivered within the framework of an accredited HCT program, whether allogeneic or autologous, with shared care policies and service level agreements incorporated into the quality systems of the HCT program. Importantly, JACIE also provides a robust method to ensure that programs meet the quality and other requirements for mandatory long-term data submission to the EBMT registry, as well as potential benchmarking of survival outcomes.

Acknowledgments

The authors would like to thank all respondents to the international survey on the management of patients receiving CAR T-cell therapy.

References

- Kuwana Y, Asakura Y, Utsunomiya N, et al. Expression of chimeric receptor composed of immunoglobulin-derived V regions and T-cell receptor-derived C regions. *Biochem Biophys Res Commun.* 1987;149(3):960-968.
- Gross G, Waks T, Eshhar Z. Expression of immunoglobulin-T-cell receptor chimeric molecules as functional receptors with antibody-type specificity. *Proc Natl Acad Sci U S A.* 1989;86(24):10024-10028.
- Quesnel B. CAR T-cells: a John von Neumann legacy. *Curr Res Transl Med.* 2018;66(2):35-36.
- Sadelain M, Brentjens R, Riviere I. The basic principles of chimeric antigen receptor design. *Cancer Discov.* 2013;3(4):388-398.
- Gauthier J, Yakoub-Agha I. Chimeric antigen-receptor T-cell therapy for hematological malignancies and solid tumors: clinical data to date, current limitations and perspectives. *Curr Res Transl Med.* 2017; 65(3):93-102.
- Ghobadi A. Chimeric antigen receptor T cell therapy for non-Hodgkin lymphoma. *Curr Res Transl Med.* 2018;66(2):43-49.
- Grupp S. Beginning the CAR T cell therapy revolution in the US and EU. *Curr Res Transl Med.* 2018;66(2):62-64.
- Feldmann A, Arndt C, Bergmann R, et al. Retargeting of T lymphocytes to PSCA- or PSMA positive prostate cancer cells using the novel modular chimeric antigen receptor platform technology "UniCAR". *Oncotarget.* 2017;8(19):31368-31385.
- Atanackovic D, Radhakrishnan SV, Bhardwaj N, Luetkens T. Chimeric antigen receptor (CAR) therapy for multiple myeloma. *Br J Haematol.* 2016;172(5):685-698.
- Radhakrishnan SV, Bhardwaj N, Luetkens T, Atanackovic D. Novel anti-myeloma immunotherapies targeting the SLAM family of receptors. *Oncoimmunology.* 2017;6(5):e1308618.
- Gauthier J, Turtle CJ. Insights into cytokine release syndrome and neurotoxicity after CD19-specific CAR-T cell therapy. *Curr Res Transl Med.* 2018;66(2):50-52.
- Kansagra AJ, Frey NV, Bar M, et al. Clinical utilization of chimeric antigen receptor T cells in B cell acute lymphoblastic leukemia: an expert opinion from the European Society for Blood and Marrow Transplantation and the American Society for Blood and Marrow Transplantation. *Biol Blood Marrow Transplant.* 2019;25(3):e76-e85.
- Chabannon C, Kuball J, Bondanza A, et al. Hematopoietic stem cell transplantation in its 60s: a platform for cellular therapies. *Sci Transl Med.* 2018;10(436).
- Kochenderfer JN, Somerville RPT, Lu T, et al. Long-duration complete remissions of diffuse large B cell lymphoma after anti-CD19 chimeric antigen receptor T cell therapy. *Mol Ther.* 2017;25(10):2245-2253.
- Locke FL, Ghobadi A, Jacobson CA, et al. Long-term safety and activity of axicabtagene ciloleucel in refractory large B-cell lymphoma (ZUMA-1): a single-arm, multicentre, phase 1-2 trial. *Lancet Oncol.* 2019;20(1):31-42.
- Schuster SJ, Bishop MR, Tam CS, et al. Tisagenlecleucel in adult relapsed or refractory diffuse large B-cell lymphoma. *N Engl J Med.* 2019;380(1):45-56.
- Hayden PJ, Sirait T, Koster L, Snowden JA, Yakoub-Agha I. An international survey on the management of patients receiving CAR T-cell therapy for hematological malignancies on behalf of the Chronic Malignancies Working Party of EBMT. *Curr Res Transl Med.* 2019;67(3):79-88.
- Thieblemont C, Legouil S, Di Blasi R, et al. Real-world results on CD19 CAR T-cell for 60 french patients with relapsed/refractory diffuse large B-cell lymphoma included in a temporary authorization for use (ATU) program. *EHA Library.* 2019:S1600.
- Frigault MJ, Dietrich J, Martinez-Lage M, et al. Tisagenlecleucel CAR-T cell therapy in secondary CNS lymphoma. *Blood.*

- 2019;134(11):860-866.
20. Couzin-Frankel J. Supply of promising T cell therapy is strained. *Science*. 2017; 356(6343):1112-1113.
 21. Yakoub-Agha I, Ferrand C, Chalandon Y, et al. [Prerequisite for hematopoietic cellular therapy programs to set up chimeric antigen receptor T-cell therapy (CAR T-cells): Guidelines from the Francophone Society of Bone Marrow Transplantation and Cellular Therapy (SFGM-TC)]. *Bull Cancer*. 2017;104(12S):S43-S58.
 22. Kohl U, Arsenieva S, Holzinger A, Abken H. CAR T cells in trials: recent achievements and challenges that remain in the production of modified T cells for clinical applications. *Hum Gene Ther*. 2018;29(5): 559-568.
 23. Park JH, Riviere I, Gonen M, et al. Long-term follow-up of CD19 CAR therapy in acute lymphoblastic leukemia. *N Engl J Med*. 2018;378(5):449-459.
 24. Mounier N, El Gnaoui T, Tilly H, et al. Rituximab plus gemcitabine and oxaliplatin in patients with refractory/relapsed diffuse large B-cell lymphoma who are not candidates for high-dose therapy. A phase II Lymphoma Study Association trial. *Haematologica*. 2013;98(11):1726-1731.
 25. Sim AJ, Jain MD, Figura NB, et al. Radiation therapy as a bridging strategy for CAR T cell therapy with axicabtagene ciloleucel in diffuse large B-cell lymphoma. *Int J Radiat Oncol Biol Phys*. 2019 Jun 5. [Epub ahead of print]
 26. Maude SL. Tisagenlecleucel in pediatric patients with acute lymphoblastic leukemia. *Clin Adv Hematol Oncol*. 2018;16(10):664-666.
 27. Suryadevara CM, Desai R, Farber SH, et al. Preventing Lck activation in CAR T cells confers treg resistance but requires 4-1BB signaling for them to persist and treat solid tumors in nonlymphodepleted hosts. *Clin Cancer Res*. 2018;25(1):358-368.
 28. Hirayama AV, Gauthier J, Hay KA, et al. The response to lymphodepletion impacts PFS in patients with aggressive non-Hodgkin lymphoma treated with CD19 CAR T cells. *Blood*. 2019;133(17):1876-1887.
 29. Gattinoni L, Finkelstein SE, Klebanoff CA, et al. Removal of homeostatic cytokine sinks by lymphodepletion enhances the efficacy of adoptively transferred tumor-specific CD8+ T cells. *J Exp Med*. 2005;202(7):907-912.
 30. Thiant S, Yakoub-Agha I, Magro L, et al. Plasma levels of IL-7 and IL-15 in the first month after myeloablative BMT are predictive biomarkers of both acute GVHD and relapse. *Bone Marrow Transplant*. 2010;45(10):1546-1552.
 31. Thiant S, Labalette M, Trauet J, et al. Plasma levels of IL-7 and IL-15 after reduced intensity conditioned allo-SCT and relationship to acute GVHD. *Bone Marrow Transplant*. 2011;46(10):1374-1381.
 32. Shank BR, Do B, Sevin A, et al. Chimeric antigen receptor T cells in hematologic malignancies. *Pharmacotherapy*. 2017;37(3):334-345.
 33. Turtle CJ, Hanafi L-AA, Berger C, et al. Immunotherapy of non-Hodgkin's lymphoma with a defined ratio of CD8+ and CD4+ CD19-specific chimeric antigen receptor-modified T cells. *Sci Transl Med*. 2016;8(355):355ra116.
 34. Hay KA, Gauthier J, Hirayama AV, et al. Factors associated with durable EFS in adult B-cell ALL patients achieving MRD-negative CR after CD19 CAR T-cell therapy. *Blood*. 2019;133(15):1652-1663.
 35. Turtle CJ, Hay KA, Hanafi L-A, et al. Durable molecular remissions in chronic lymphocytic leukemia treated with CD19-specific chimeric antigen receptor-modified T cells after failure of ibrutinib. *J Clin Oncol*. 2017;35(26):3010-3020.
 36. Neelapu SS, Tummala S, Kebriaei P, et al. Chimeric antigen receptor T-cell therapy - assessment and management of toxicities. *Nat Rev Clin Oncol*. 2018;15(1):47-62.
 37. Maude SL, Shpall EJ, Grupp SA. Chimeric antigen receptor T-cell therapy for ALL. *Hematology Am Soc Hematol Educ Program*. 2014;2014(1):559-564.
 38. Lee DW, Santomasso BD, Locke FL, et al. ASTCT consensus grading for cytokine release syndrome and neurologic toxicity associated with immune effector cells. *Biol Blood Marrow Transplant*. 2019;25(4):625-638.
 39. Yakoub-Agha I. Clinical units to set up chimeric antigen receptor T-cell therapy (CAR T-cells): Based on the recommendations of the Francophone Society of Bone Marrow Transplantation and Cellular Therapy (SFGM-TC). *Curr Res Transl Med*. 2018;66(2):57-58.
 40. Porter DL, Levine BL, Kalos M, Bagg A, June CH. Chimeric antigen receptor-modified T cells in chronic lymphoid leukemia. *N Engl J Med*. 2011;365(8):725-733.
 41. Kochenderfer JN, Dudley ME, Carpenter RO, et al. Donor-derived CD19-targeted T cells cause regression of malignancy persisting after allogeneic hematopoietic stem cell transplantation. *Blood*. 2013;122(25): 4129-4139.
 42. Maude SL, Frey N, Shaw PA, et al. Chimeric antigen receptor T cells for sustained remissions in leukemia. *N Engl J Med*. 2014;371(16):1507-1517.
 43. Fishman JA, Hogan JJ, Maus MV. Inflammatory and infectious syndromes associated with cancer immunotherapies. *Clin Infect Dis*. 2019;69(6):909-920.
 44. Topp MS, Gockebueg N, Stein AS. Correction to *Lancet Oncol* 2015; 16: 60, 61. Safety and activity of blinatumomab for adult patients with relapsed or refractory B-precursor acute lymphoblastic leukaemia: a multi-centre, single-arm, phase 2 study. *Lancet Oncol*. 2015;16(4):e158.
 45. Abboud R, Keller J, Slade M, et al. Severe cytokine-release syndrome after T cell-replete peripheral blood haploidentical donor transplantation is associated with poor survival and anti-IL-6 therapy is safe and well tolerated. *Biol Blood Marrow Transplant*. 2016;22(10):1851-1860.
 46. Teachey DT, Grupp SA. Cytokine release syndrome after haploidentical stem cell transplantation. *Biol Blood Marrow Transplant*. 2016;22(10):1736-1737.
 47. Ureshino H, Ando T, Kizuka H, et al. Tocilizumab for severe cytokine-release syndrome after haploidentical donor transplantation in a patient with refractory Epstein-Barr virus-positive diffuse large B-cell lymphoma. *Hematol Oncol*. 2017;36(1):324-327.
 48. Raj RV, Hamadani M, Szabo A, et al. Peripheral blood grafts for T cell-replete haploidentical transplantation increase the incidence and severity of cytokine release syndrome. *Biol Blood Marrow Transplant*. 2018;24(8):1664-1670.
 49. Frey N, Porter D. Cytokine release syndrome with chimeric antigen receptor T cell therapy. *Biol Blood Marrow Transplant*. 2019;25(4):e123-e127.
 50. Giavridis T, van der Stegen SJC, Eyquem J, et al. CAR T cell-induced cytokine release syndrome is mediated by macrophages and abated by IL-1 blockade. *Nat Med*. 2018;24(6):731-738.
 51. Norelli M, Camisa B, Barbiera G, et al. Monocyte-derived IL-1 and IL-6 are differentially required for cytokine-release syndrome and neurotoxicity due to CAR T cells. *Nat Med*. 2018;24(6):739-748.
 52. Maude SL, Frey N, Shaw PA, et al. Chimeric antigen receptor T cells for sustained remissions in leukemia. *N Engl J Med*. 2014;371(16):1507-1517.
 53. Turtle CJ, Sommermeyer D, Berger C, et al. Therapy of B cell malignancies with CD19-specific chimeric antigen receptor-modified T cells of defined subset composition. *Blood*. 2014;124(21):384.
 54. Lee DW, Kochenderfer JN, Stetler-Stevenson M, et al. T cells expressing CD19 chimeric antigen receptors for acute lymphoblastic leukaemia in children and young adults: a phase 1 dose-escalation trial. *Lancet*. 2015;385(9967):517-528.
 55. Frey N. Cytokine release syndrome: who is at risk and how to treat. *Best Pract Res Clin Haematol*. 2017;30(4):336-340.
 56. Yakoub-Agha I, Moreau AS, Ahmad I, et al. [Management of cytokine release syndrome in adult and pediatric patients undergoing CAR-T cell therapy for hematological malignancies: recommendation of the French Society of Bone Marrow and Cellular Therapy (SFGM-TC)]. *Bull Cancer*. 2019;106(1S):S102-S109.
 57. Rubin DB, Danish HH, Ali AB, et al. Neurological toxicities associated with chimeric antigen receptor T-cell therapy. *Brain*. 2019;142(5):1334-1348.
 58. Hay KA, Turtle CJ. Chimeric antigen receptor (CAR) T cells: lessons learned from targeting of CD19 in B-cell malignancies. *Drugs*. 2017;77(3):237-245.
 59. Neelapu SS, Tummala S, Kebriaei P, et al. Chimeric antigen receptor T-cell therapy - assessment and management of toxicities. *Nat Rev Clin Oncol*. 2018;15(1):47-62.
 60. Mahadeo KM, Khazal SJ, Abdel-Azim H, et al. Management guidelines for paediatric patients receiving chimeric antigen receptor T cell therapy. *Nat Rev Clin Oncol*. 2018;16(1):45-63.
 61. Traube C, Silver G, Kearney J, et al. Cornell Assessment of Pediatric Delirium: a valid, rapid, observational tool for screening delirium in the PICU*. *Crit Care Med*. 2013;42(3):656-663.
 62. Cornillon J, Hadhoum N, Roth-Guepin G, et al. [Management of CAR-T cell-related encephalopathy syndrome in adult and pediatric patients: recommendations of the French Society of Bone Marrow Transplantation and Cellular Therapy (SFGM-TC)]. *Bull Cancer*. 2019 Jun 12. [Epub ahead of print]
 63. Maude SL, Teachey DT, Porter DL, Grupp SA. CD19-targeted chimeric antigen receptor T-cell therapy for acute lymphoblastic leukemia. *Blood*. 2015;125(26):4017-4023.
 64. Neelapu SS, Locke FL, Bartlett NL, et al. Axicabtagene ciloleucel CAR T-cell therapy in refractory large B-cell lymphoma. *N Engl J Med*. 2017;377(26):2531-2544.
 65. Hill JA, Li D, Hay KA, et al. Infectious complications of CD19-targeted chimeric antigen receptor-modified T-cell immunotherapy. *Blood*. 2017;131(1):121-130.
 66. Strati P, Nastoupil LJ, Fayad LE, Samaniego F, Adkins S, Neelapu SS. Safety of CAR T-cell therapy in patients with B-cell lymphoma and chronic hepatitis B or C virus infection. *Blood*. 2019;133(26):2800-2802.

67. Maude SL, Laetsch TW, Buechner J, et al. Tisagenlecleucel in children and young adults with B-cell lymphoblastic leukemia. *N Engl J Med.* 2018;378(5):439-448.
68. Dai H, Zhang W, Li X, et al. Tolerance and efficacy of autologous or donor-derived T cells expressing CD19 chimeric antigen receptors in adult B-ALL with extramedullary leukemia. *Oncoimmunology.* 2015;4(11):e1027469.
69. Kebriaei P, Singh H, Huls MH, et al. Phase I trials using Sleeping Beauty to generate CD19-specific CAR T cells. *J Clin Invest.* 2016;126(9):3363-3376.
70. Anwer F, Shaukat AA, Zahid U, et al. Donor origin CAR T cells: graft versus malignancy effect without GVHD, a systematic review. *Immunotherapy.* 2017;9(2):123-130.
71. Hill JA, Li D, Hay KA, et al. Infectious complications of CD19-targeted chimeric antigen receptor-modified T-cell immunotherapy. *Blood.* 2018;131(1):121-130.
72. Kochenderfer JN, Dudley ME, Feldman SA, et al. B-cell depletion and remissions of malignancy along with cytokine-associated toxicity in a clinical trial of anti-CD19 chimeric-antigen-receptor-transduced T cells. *Blood.* 2012;119(12):2709-2720.
73. Lee DW, Gardner R, Porter DL, et al. Current concepts in the diagnosis and management of cytokine release syndrome. *Blood.* 2014;124(2):188-195.
74. Brudno JN, Kochenderfer JN. Toxicities of chimeric antigen receptor T cells: recognition and management. *Blood.* 2016;127(26):3321-3330.
75. Majhail NS, Rizzo JD, Lee SJ, et al. Recommended screening and preventive practices for long-term survivors after hematopoietic cell transplantation. *Biol Blood Marrow Transplant.* 2012;18(3):348-371.
76. European Medicines Agency. CAR T cell therapy registries workshop. 2019 [cited; Available from: https://www.ema.europa.eu/en/documents/report/report-car-t-cell-therapy-registries-workshop_en.pdf
77. European Medicines Agency. Qualification opinion on cellular therapy module of the European Society for Blood & Marrow Transplantation (EBMT) Registry. 2019 February 28, 2019 [cited; Available from: <https://www.ebmt.org/ebmt/news/ebmt-receives-regulatory-qualification-european-medicine-agency-ema-use-its-patient>
78. Snowden JA, McGrath E, Duarte RF, et al. JACIE accreditation for blood and marrow transplantation: past, present and future directions of an international model for healthcare quality improvement. *Bone Marrow Transplant.* 2017;52(10):1367-1371.
79. Saccardi R, McGrath E, Snowden AJ. JACIE accreditation of HSCT programs. *The EBMT Handbook.* 2019:35-40.

The lifespan quantitative trait locus gene *Securin* controls hematopoietic progenitor cell function



Andreas Brown,¹ Desiree Schuetz,¹ Yang Han,² Deidre Daria,³
Kalpana J. Nattamai,³ Karina Eiwen,¹ Vadim Sakk,¹ Johannes Pospiech,¹
Thomas Saller,¹ Gary van Zant,⁴ Wolfgang Wagner² and Hartmut Geiger^{1,3}

¹Institute of Molecular Medicine and Stem Cell Aging, Ulm University, Ulm, Germany; ²Helmholtz-Institute for Biomedical Engineering, Stem Cell Biology and Cellular Engineering, RWTH Aachen University Medical School, Aachen, Germany; ³Division of Experimental Hematology and Cancer Biology, Cincinnati Children's Hospital Medical Center and University of Cincinnati, Cincinnati, OH, USA and ⁴University of Kentucky College of Medicine, UK Medical Center, Lexington, KY, USA

Haematologica 2020
Volume 105(2):317-324

ABSTRACT

The percentage of murine hematopoietic stem and progenitor cells, which present with a loss of function upon treatment with the genotoxic agent hydroxyurea, is inversely correlated to the mean lifespan of inbred mice, including the long-lived C57BL/6 and short-lived DBA/2 strains. Quantitative trait locus mapping in BXD recombinant inbred strains identified a region spanning 12.5 cM on the proximal part of chromosome 11 linked to both the percentage of dysfunctional hematopoietic stem and progenitor cells as well as regulation of lifespan. By generating and analyzing reciprocal congenic mice for this locus, we demonstrate that this region indeed determines the sensitivity of hematopoietic stem and progenitor cells to hydroxyurea. These cells do not present, as previously anticipated, with differences in cell cycle distribution; neither do they present with changes in the frequency of cells undergoing apoptosis, senescence, replication stalling and re-initiation activity, excluding the possibility that variations in proliferation, replication or viability underlie the distinct response of these cells from the congenic and parental strains. An epigenetic aging clock in blood cells was accelerated in C57BL/6 mice congenic for the DBA/2 version of the locus. We verified pituitary tumor-transforming gene-1 (*Pttg1*)/*Securin* as the quantitative trait gene regulating the differential response of hematopoietic stem and progenitor cells to hydroxyurea treatment and which might therefore be linked to the regulation of lifespan.

Introduction

We previously reported a correlation between the frequency of hematopoietic stem and progenitor cells (HSPC) from a set of inbred mouse strains with impaired progenitor cell function upon treatment with hydroxyurea (HU) and the mean lifespan of these mice. The set of inbred strains also included C57BL/6 (B6) (low frequency of HSPC dysfunctional in response to HU, long lifespan) and DBA/2 (D2) (high frequency of HSPC dysfunctional in response to HU, short lifespan). In these experiments, the *in vitro* cobblestone area forming cell (CAFC) assay was used to determine the number of functional HSPC before and after treatment with HU. Given that HU kills proliferating cells *via* the induction of DNA strand breaks that arise from stalled replication forks after depletion of the nucleotide pool, this finding was interpreted as a significantly higher percentage of HSPC from D2 *versus* B6 in S-phase, and subsequently that elevated levels of HSPC proliferation could be negatively linked to lifespan.¹⁻³ Using BXD recombinant inbred (RI) mice, which are genetic chimeras based on B6 and D2, subsequently a quantitative trait locus (QTL) was mapped to chromosome 11 linked to the frequency of HSPC susceptible to HU. Interestingly, the same locus showed also a linkage to the mean lifespan within the BXD RI set of mice, transforming the reported phenotypic correlation into a genetic connection, implying a common underlying gene and thus mechanism for

Correspondence:

HARTMUT GEIGER
hartmut.geiger@cchmc.org

Received: November 25, 2018.

Accepted: May 9, 2019.

Pre-published: May 9, 2019.

doi:10.3324/haematol.2018.213009

Check the online version for the most updated information on this article, online supplements, and information on authorship & disclosures: www.haematologica.org/content/105/2/317

©2020 Ferrata Storti Foundation

Material published in *Haematologica* is covered by copyright. All rights are reserved to the Ferrata Storti Foundation. Use of published material is allowed under the following terms and conditions:

<https://creativecommons.org/licenses/by-nc/4.0/legalcode>. Copies of published material are allowed for personal or internal use. Sharing published material for non-commercial purposes is subject to the following conditions: <https://creativecommons.org/licenses/by-nc/4.0/legalcode>, sect. 3. Reproducing and sharing published material for commercial purposes is not allowed without permission in writing from the publisher.



the regulation of both phenotypes. To verify the linkage, and identify the underlying quantitative trait gene, we generated B6 as well as D2 mice that are reciprocally congenic for this locus on chromosome 11.

Methods

Mice

Laboratory C57BL/6J (B6), DBA/2J (D2) and BXD inbred mice were obtained from Janvier Labs (France). All mice were fed acidified water and food *ad libitum*, and housed under pathogen-free conditions at the University of Kentucky, Division of Laboratory Animal Resource, the animal facility at CCHMC. Mouse experiments were performed in compliance with the German Law for Welfare of Laboratory Animals and were approved by the Regierungspräsidium Tübingen or approved by the IACUCs of the University of Kentucky and CCHMC.

Quantitative trait locus mapping

Linkage analysis and determination of the likelihood ratio statistic values for suggestive linkage were performed as described by using WebQTL (<http://www.genenetwork.org/webqtl/main.py?FormID=submitSingleTrait>), identifying the restrictive chromosome 11 locus, among others, correlating to mean life span and HU sensitivity.^{3,6}

Generation of congenic mice

Congenic animals were generated in five generations by a marker-assisted backcrossing strategy as described^{3,5,7-9} (Figure 1C). The particular DBA/2J genomic region was derived from BXD31, one of the BXD recombinant inbred strains used in the quantitative trait locus (QTL) mapping and which phenotypically best demonstrated the decline in HSC in old age and the HU sensitivity.³

Preparation of hematopoietic tissue and cells

For the isolation of total bone marrow (BM), tibiae, femur and hips of mice were isolated and flushed using a syringe and a G21 needle. Mononuclear (low density bone marrow, LDBM) cells were isolated by Histopaque low-density centrifugation (#10831, Sigma). Lineage depletion was performed using the mouse lineage cell depletion Kit (#130-090-858, Miltenyi Biotec) according to their protocol.

Cobblestone area forming cell assay

Cobblestone area forming cell (CAFC) assay was performed as described.¹ Briefly, 1,000 FBMD-1 cells, a stromal cell line, were seeded in each well of 96-well plates. Plates were incubated at 33°C in 5% CO₂, and used seven days later for CAFC assay. BM cells were either treated with 200 µg/mL HU or its solvent (PBS) and seeded onto the pre-established stromal layers in six dilutions, serially in 3-fold increments from 333 to up to 81,000 cells/well (12 wells per dilution). At this time, the medium was switched from 5% horse serum and 10% fetal bovine serum to 20% horse serum. Alternatively, mice were treated with HU *in vivo* as indicated following bone marrow isolation and seeding. After seven days, all wells were evaluated for the presence or absence of cobblestone areas and the frequency of the appearance of a colony calculated using L-Cal software (STEMCELL Technologies).

Analysis of the epigenetic aging signature

Analysis of DNA methylation levels was analyzed at three age-associated CG dinucleotides (CpG) as described previously.¹⁰ Briefly, genomic DNA was isolated from blood samples, bisulfite converted, and DNA methylation was analyzed within the three

genes (*Prima1*, *Hsf4*, *Kcns1*) by pyrosequencing. The DNA methylation results at these sites can be integrated into a multivariable model for epigenetic age predictions in B6 mice, which clearly correlate with the chronological age.¹⁰

Statistical analysis

All statistical analyses were performed using Student's *t*-test or two-way Anova, when appropriate with GraphPad Prism 6 software. For Figure 4C, linear and non-linear regression was calculated. The number of biological repeats (n) is indicated in the figure legends. Error bars are Standard Error of Mean (SEM).

Results

Hematopoietic stem and progenitor cells from BXD RI strains show highly divergent reactions when exposed to HU as judged by their ability to form cobblestones on stromal feeder layers in the CAFC assay after seven days of culture (CAFC day 7 assay).⁹ Re-analyzing the initial phenotypic data based on the most recent marker map (New Genotypes 2017 dataset) provided for BXD RI strains, we verified the initially identified locus on chromosome 11 (35-75 Mb) linked (with a suggestive threshold of 10.53/10.88) to both HU susceptibility of HSPC as well as mean lifespan of the analyzed mice (Figure 1A and B and *Online Supplementary Tables S1A* and *B*, and *S3*). We used a marker assisted speed congenic approach to obtain a reciprocal set of mice congenic for the chromosome 11 locus (Figure 1C). These novel mouse lines were named line A (D2 onto B6) and K (B6 onto D2). We performed whole genome SNP mapping of our congenic mouse strains to identify the length of the congenic intervals transferred as well as the overlap between the reciprocal strains. Ultimately, the common region transferred in line A and line K spans an 18.6 Mb (8.3 cM) region on chromosome 11 from rs26900200, 37,929,686 bp to rs3088940, 56,516,067 bp with no other transferred intervals stemming from the donor strains that are identical between the two congenic strains. The SNP analysis further revealed a small set of additional congenic regions in both line A and K animals, though not covering identical regions (Figure 1D, *Online Supplementary Table S2* and *Online Supplementary Figure S1*). This interval contains about 130 protein coding genes (*Online Supplementary Table S3*).

Next, based on the CAFC assay, we tested whether the genotype of the locus conferred in the congenic strains correlated with the magnitude of our phenotype of HSPC susceptible to HU. HU treatment efficiently suppresses BrdU incorporation and thus active S-Phase in freshly isolated Lin-cKit⁺ (LK) cells from all strains (*Online Supplementary Figure S2A*). Indeed, HSPC isolated from B6 or line K (B6 onto D2) mice presented with a lower frequency of dysfunctional HSPC in response to short-term *in vivo* as well as to *ex vivo* treatment with HU, while inversely, D2 and line A (D2 onto B6) HSPC were more sensitive to HU (Figure 2A and *Online Supplementary Figure S2B*). These data confirm that the interval on chromosome 11 shared among the congenic strains confers this phenotype and might thus contain a gene regulating the response of HSPC to HU.

Since HU inhibits dNTP synthesis,¹¹ and a lack of dNTP causes replication fork stalling and thus DNA damage and apoptosis,¹² it is believed that the frequency of cells susceptible to HU treatment is an indirect measurement for

the frequency of cells in the S-phase of the cell division cycle. It has been thus concluded that the underlying mechanism of the distinct susceptibility of HSPC from the inbred strains is due to distinct S-phase frequencies. BM cells with the Lin-cKit⁺ surface marker combination (hematopoietic progenitor cells, LK cells) are highly enriched for CAFC day 7 cells (*Online Supplementary Figure S2C*). However, analysis of the frequency of LK cells from the inbred and the congenic strains in different stages of the cell division cycle by *in vivo* BrdU incorporation and flow cytometry, as well as that of hematopoietic stem cells (HSC) and less primitive progenitors (LSK), revealed almost identical patterns and especially almost identical frequencies of cells in S-phase among all the strains tested (Figure 2B). HU susceptibility in HSPC does therefore not correlate with the frequency of HSPC in S-phase, which

excludes differences in cycling frequencies as the underlying mechanism for the phenotype observed, as well as in general HU susceptibility as surrogate for the frequency of cells in S-phase. Consistent with that finding was the fact that HSPC from all groups had similar telomere lengths. Short telomeres can be seen as a surrogate marker for high levels of proliferation (*Online Supplementary Figure S2D*). In addition, the frequency of LK and LSK was very similar in all strains, while D2-derived mice displayed a general higher HSC frequency, as already reported,¹ which is, however, not mirrored in B6/line A mice and thus locus-independent. That finding excludes a difference in the number of these cells as a factor contributing to the phenotype (Figure 2C). Furthermore, the frequencies of HSPC undergoing apoptosis upon *ex vivo* HU treatment and under steady state conditions *in vivo* were at a low level

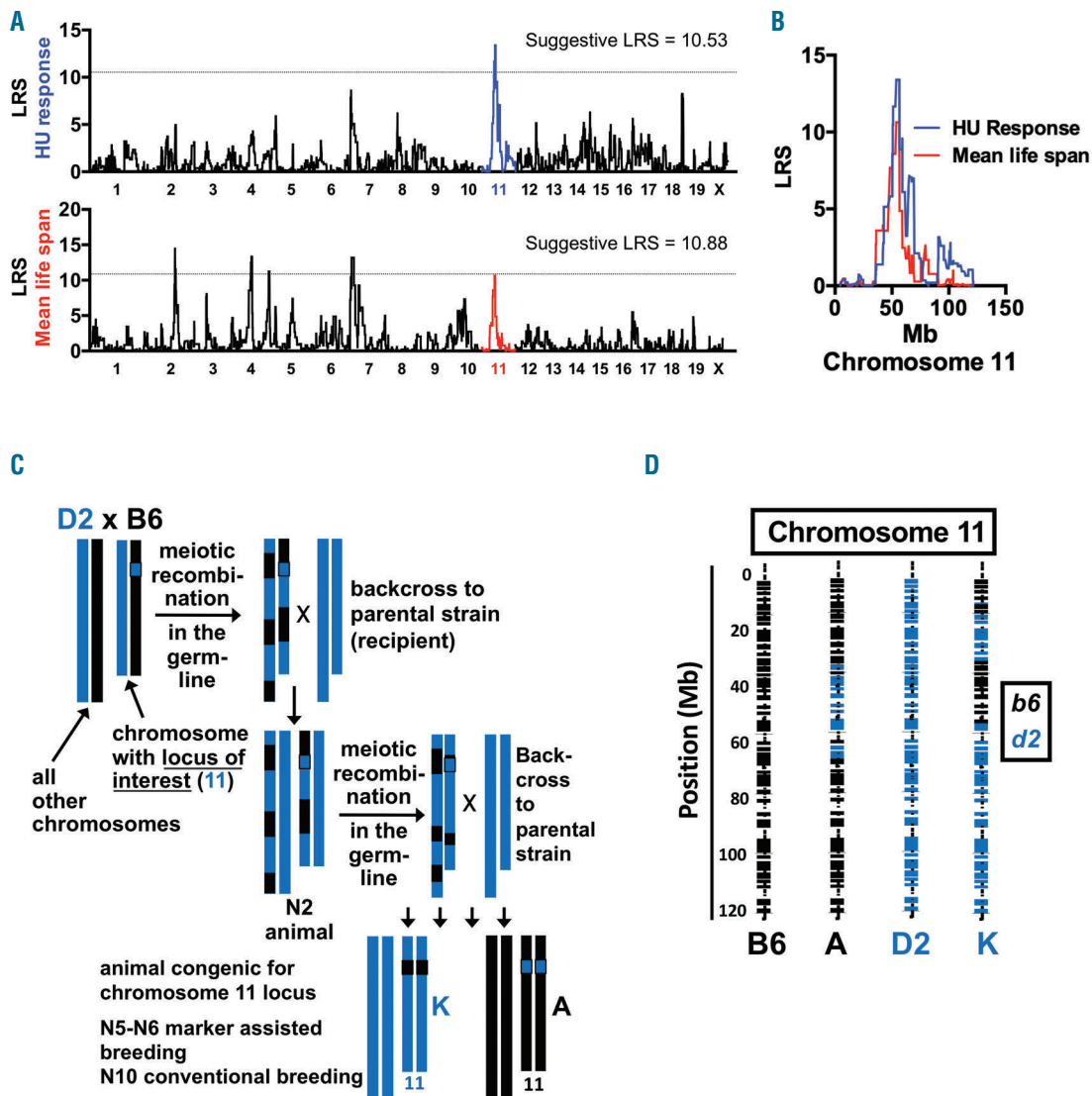


Figure 1. Quantitative trait locus (QTL) analysis of hydroxyurea (HU) responses and mean life spans of BXD mice and generation of mice congenic for the corresponding chromosome 11 locus. (A) WebQTL analysis of HU sensitivity rates and mean life spans of hematopoietic stem and progenitor cells (HSPC) isolated from various BXD and parental strains, identifying a proximal part of chromosome 11, among others, involved in this phenotype. Values are in Likelihood Ratio Statistics (LRS). (B) QTL analysis of mean life spans and HU responses of the various BXD strains for chromosome 11. (C) Schematic illustration showing the generation of the congenic mouse strains line A and K. Briefly, after crossing B6 with D2 mice, F1 littermates were backcrossed with the corresponding parental strains (B6/D2). Offspring were backcrossed in four rounds with parental strains reciprocal for the corresponding chromosome 11 specific SNP *D11Mit20* to finally obtain B6 or D2 mice congenic for the proximal locus on chromosome 11 of D2 or B6, respectively. (D) SNP analysis of chromosome 11 from strains B6, D2, A and K.

among these groups, even when regarding S-phase specific apoptosis rates as well senescence in response to HU as indicated by the level of the senescence marker p16 in HSPC (Figure 2D and *Online Supplementary Figure S2E and F*). In addition, whereas HU treatment almost completely blocks BrdU incorporation, LK cells from all strains preserve their ability to re-enter active S-phase in a locus-independent manner 3 and even 16 hours (h) after HU is removed, excluding the possibility that enhanced levels of senescence, apoptosis or difference in re-initiation of replication after stalling are causative for the HU sensitivity phenotype (Figure 2E and *Online Supplementary Figure S2G*). Similarly, LK cells from all strains showed comparable frequencies of γ H2AX foci per cells upon HU treatment and 3 h post HU removal, which also excludes a role of variation in stalling of replication and the subsequent

DNA damage for our phenotype (Figure 2F). In aggregation, these data exclude a likely contribution of differences in cell cycle and replication parameters as well as differential senescence or apoptosis to the highly unequal HU susceptibilities of HSPC in the inbred and congenic strains, while the underlying mechanism still remains to be identified.

A D2-allele at the genetic microsatellite marker *D11Mit174* (Chr.11:42,593,949-42,594,095, which is within the area with the highest level of linkage) correlated in the BXD RI set, as anticipated, with higher HU-susceptibility rates of HSPC and a lower mean life span (Figure 3A). The gene *Pttg1* (*Securin*), which has been reported to inhibit mitotic division,^{13,14} is located in very close proximity (+ 800 kb) to *D11Mit174*.¹⁵ In addition, the yeast homolog of *Securin*, *Pds1p*, was reported to be critically

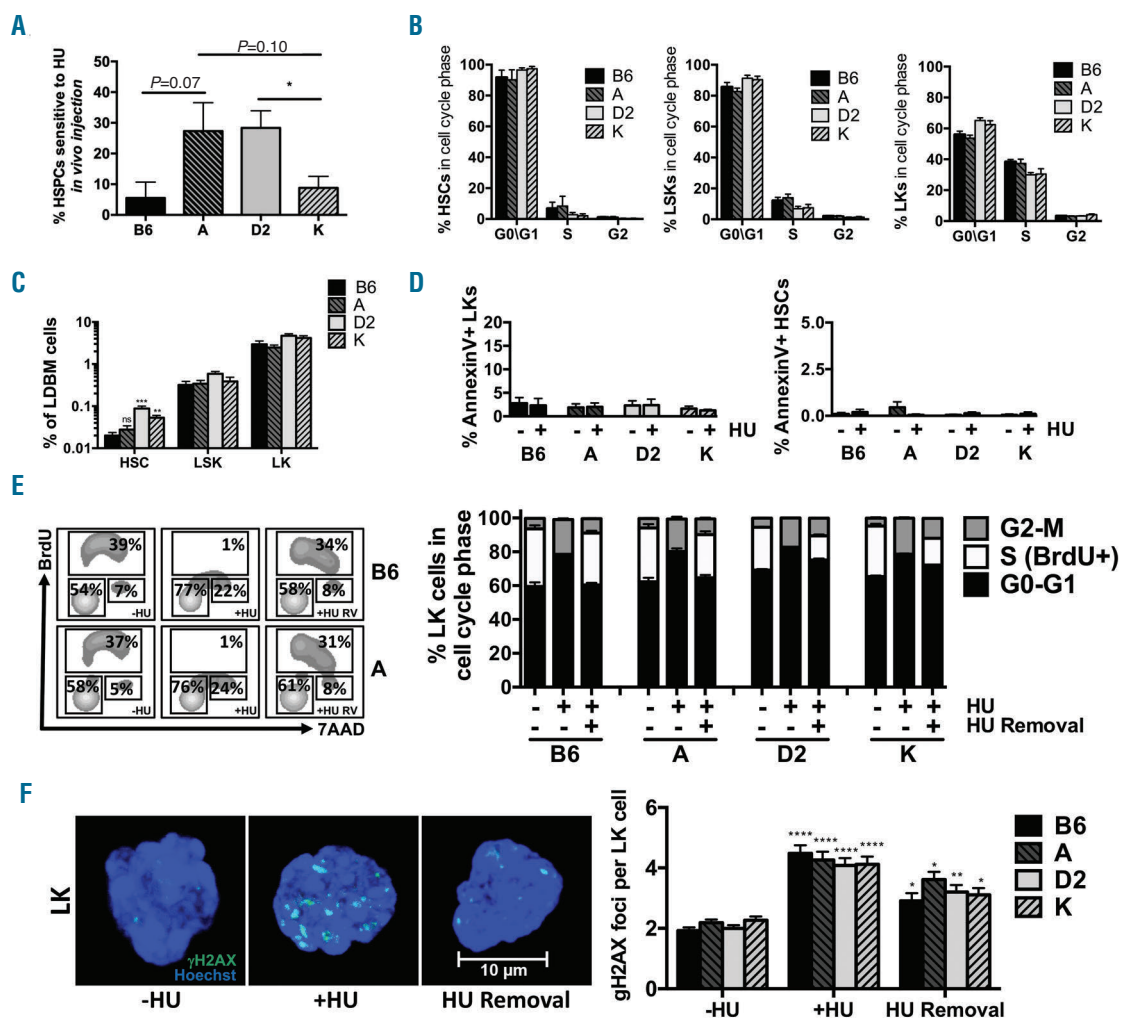


Figure 2. The chromosome 11 locus controls sensitivity of hematopoietic stem and progenitor cells (HSPC) to hydroxyurea (HU) exposure but not HSPC frequency, cell cycle activity, apoptosis and replication fork stalling. (A) Mice from all four groups were injected with 10 mg HU/kg body weight or its solvent (PBS) for 1 hour (h) following isolation of bone marrow (BM) cells and processing for the cobblestone area-forming cell (CAFC) assay. Shown is the fraction of HSPC sensitive to HU. $n=5-12$. (B) Cell cycle distributions of HSPC (left), Lin-Sca1⁺cKit⁺ cells (LSK) (middle) and Lin⁺cKit⁺ cells (LK) (right) of bromodeoxyuridine (BrdU)-treated mice. $n=4$. (C) Relative low density bone marrow cells (LDBM) frequencies per tibia and femur of Lin⁺cKit⁺ cells (LK), Lin-Sca1⁺cKit⁺ cells (LSK) and hematopoietic stem cells (HSC) of the four mouse strains. $n=4$. (D) (Left) LDBM cells from the four strains were treated with HU or its solvent (PBS) for 1 h. Thereafter, LK cells (left) and HSC (right) were analyzed in terms of apoptosis (AnnexinV). $n=4$. (E) LDBM cells were either treated with a control (-HU), HU for 1 h or accordingly following HU removal (RV) by washing twice with medium and an additional resting period of 3 h (+HU RV). Thirty minutes prior to staining, all samples were co-cultured with BrdU. (Left) Representative BrdU/7AAD FACS plots of LK cells from the indicated strains. (Right) Quantification of LK cell cycle distribution. $n=3$. (F) LK cells from all four mouse strains were either treated with a control, HU for 1 h or accordingly following HU RV and an additional resting period of 3 h (+HU RV). Thereafter, cells were harvested and stained against γ H2AX. (Left) Representative confocal images. (Right) Quantification of the number of γ H2AX foci per cell. $n=3$. Significances are related to the corresponding -HU controls. * $P<0.05$; ** $P<0.01$; *** $P<0.001$; **** $P<0.0001$.

involved in the regulation of the intra-S-checkpoint and regulation of the response of yeast to treatment with HU.¹⁶ Previously, a 3-11-fold overexpression of *Pttg1* in various D2 tissues compared to B6 was demonstrated.¹⁷⁻¹⁹ This renders *Pttg1* a prime candidate quantitative trait gene in the interval on chromosome 11. To investigate whether the *Pttg1* mediates the HU response, we analyzed its expression in our experimental mouse strains. We observed a 3-5-fold increase in gene and protein expression in D2 or line A derived HSPC compared to the corresponding cells from B6 or line K mice (Figure 3B and C). A D2-allele of the locus thus confers elevated expression of Pttg1. Analyzing *Pttg1*-associated promoter and exon regions in silico revealed a 7 bp insertion downstream of the transcription start (NCBI Reference Sequence: NC_000077.6) in the D2 genome, potentially positively affecting binding of transcription factors (TF) (Online Supplementary Figure S3A). Since the occurrence of these D2- and A/J-specific 7 bp was previously reported to result in reduced *Pttg1* expression in contrast to what we find in

D2 animals,²⁰ we further determined the promoter structure of *Pttg1* in more detail by polymerase chain reaction (PCR) of genomic DNA. Surprisingly, the *Pttg1* promoter region was present in two differently sized versions (the two fragments differ in size by approx. 700 bp) in D2 and line A mice (Figure 3D). DNA sequencing revealed that the short version in D2 (D2_1) was identical to the B6 *Pttg1* promoter, while the longer version (D2_2) was unique to D2 and included the already described 7 bp insertion in addition to an additional 675 bp region between the transcription and the ORF start, which is not completely annotated in common genome databases at the present time in contrast to the 7 bp insertion (Online Supplementary Figure S3B and C). This could imply a likely gene duplication of *Pttg1* within the congenic locus. We next tested whether the distinct types of promoter regions are causative for the dissimilar *Pttg1* expression patterns. By applying a dual-specific luciferase assay, we observed an almost 3-fold increase in activity of the D2_2-specific promoter compared to the B6 and the shorter D2_1 variants, suggesting

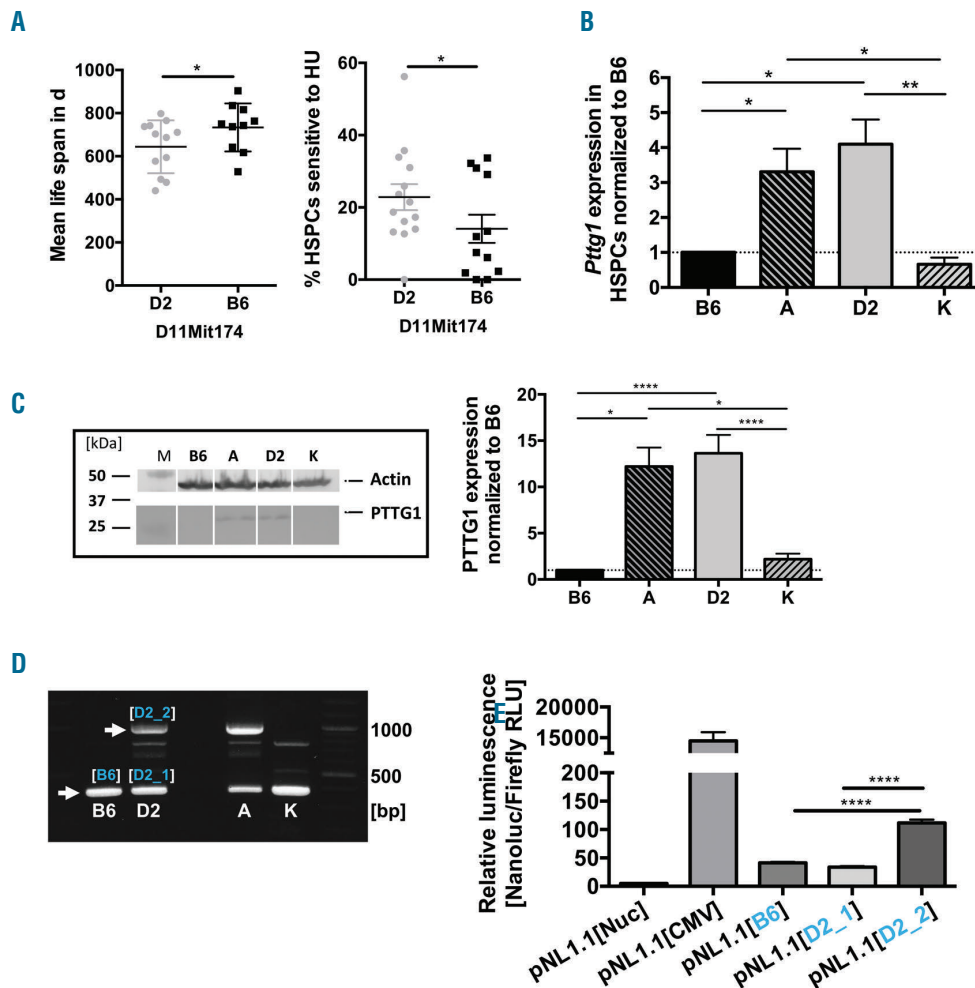
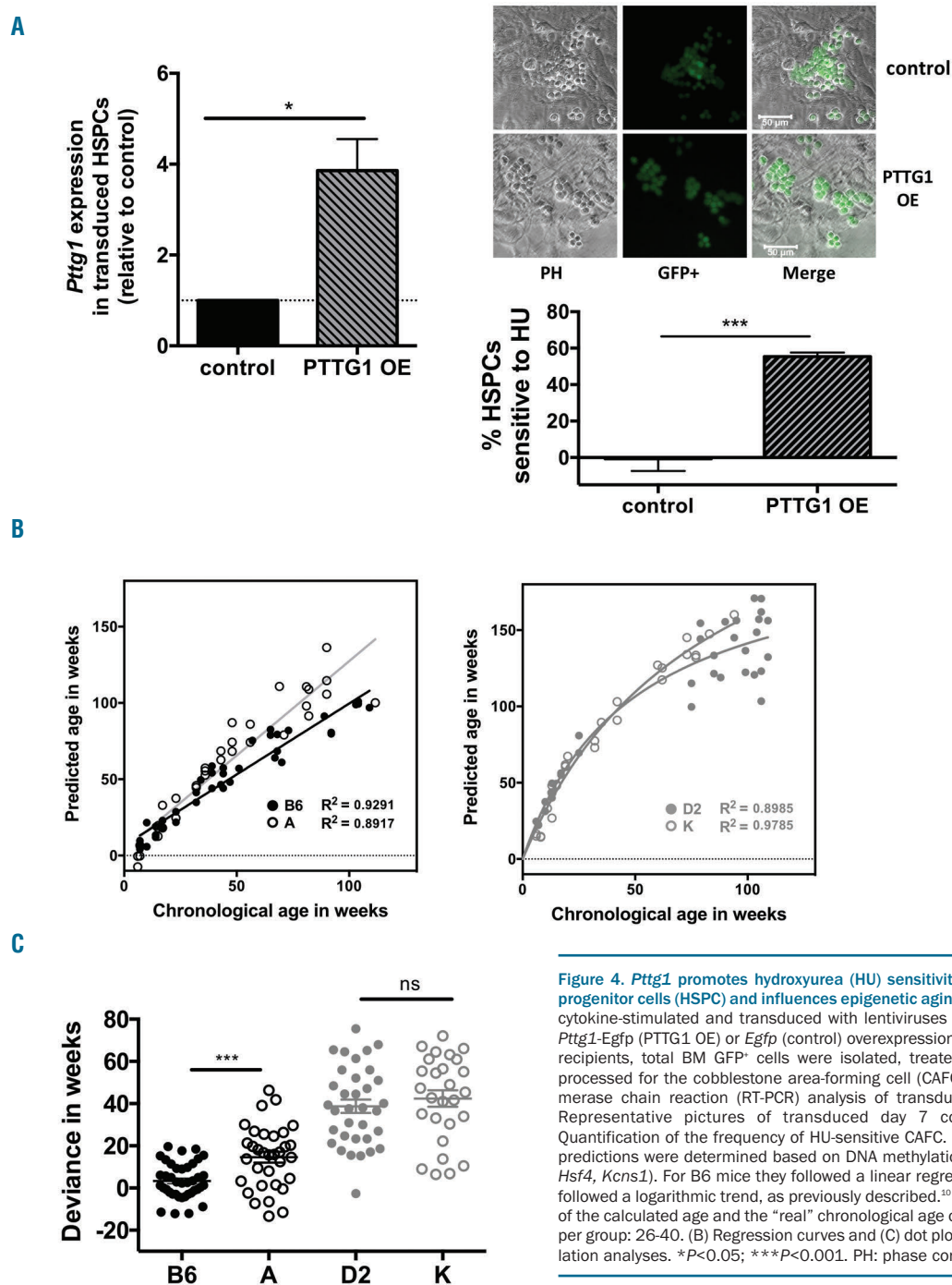


Figure 3. Chromosome 11 associated *Pttg1* has an altered promoter sequence in D2/A mice leading to enhanced expression. (A) Mean life span (left) or hydroxyurea (HU) sensitivity rates of hematopoietic stem and progenitor cells (HSPC) (right) of BXD mouse strains relative to the occurrence of the SNP *D11Mit174*. (B) *Pttg1* gene expression in HSPC from the indicated mouse strains. n=3. (C) PTTG1 protein expression in HSPC from the four mouse strains. (Left) Representative western blot images. (Right) Quantification. n=3. (D) Polymerase chain reaction analysis of genomic DNA from lines B6, D2, A and K using the primers 5'NheI-B6/D2_PTTG1_pr1 and 3'EcoRV-B6/D2_PTTG1_pr2. Major bands corresponding to the different promoters are indicated with arrows. (E) Dual-specific luciferase assay for the indicated promoter constructs, including a negative (pNL1.1[Nuc]) and a positive (pNL1.1[CMV]) control. The corresponding constructs to Figure 3D are highlighted in blue. n=3 (3 rounds with triplicates). *P<0.05; **P<0.01; ****P<0.0001.

that not the 7 bp insertion but the additional 675 bp region drive elevated levels of *Pttg1* expression in D2 or A cells (Figure 3E). We also identified several exon-specific SNP causing amino acid substitutions in *Pttg1*. Using 3D *in silico* models that predict the protein structure of PTTG1, no obvious difference in the structure was observed between the B6 and D2 variants besides a slight increase in 310 helices, a common secondary structure, which renders an additional contribution of the coding SNP of *Pttg1* to the phenotype less likely (Online Supplementary Figure S4A).

To test whether *Pttg1* is indeed the QTL gene within the described locus, and thus whether the increased HU-sensitivity of HSPC is caused by elevated *Pttg1* levels, we over-

expressed a *Pttg1*-Egfp fusion gene by lentiviral transduction in B6 HSPC. The level of expression of the transgene was within the range of the difference in gene expression between B6 and D2 HSPC and thus in a physiological range (Figure 4A, left panel). Transduced BM cells were transplanted into B6 recipients for their *in vivo* expansion. We sorted GFP⁺ BM cells five weeks post transplantation to analyze the susceptibility of HSPC to HU with the CAFC assay. BM cells of the transplanted mice were presented with similar rates of transduction (GFP⁺ cells), excluding a potential bias of certain subpopulations upon transduction (Online Supplementary Figure S4B and C). Elevated expression of *Pttg1* in B6 HSPC resulted in a significant increase



in their susceptibility to HU treatment (Figure 4A, right panel). Similarly, upon downregulation of *Pttg1* in progenitor cells from line A and D2 mice, we observed a trend towards reduced HU sensitivity (Online Supplementary Figure S4D). These data confirm a causative role for distinct levels of expression of *Pttg1* for the susceptibility of HSPC to short-term HU treatment, and thus strongly imply that *Pttg1* is the QTL gene within the QTL locus.

Ultimately, the question remains whether the locus also accounts for a variation in life span. Previously, the methylation status of CpG sites within the genes *Prima1*, *Hsf4*, *Kcns1* was shown to qualify as a reliable predictor of chronological age of B6 mice.¹⁰ This same study also revealed enhanced epigenetic aging of the D2 strain in accordance with its general reduced mean life span, supporting the possibility that the panel might also serve as a marker for the biological age in mice. Applying this B6-trained marker panel to our (congenic) experimental strains, we observed that epigenetic age predictions correlated with chronological age in B6 ($R^2=0.93$) and line A mice ($R^2=0.89$). Notably, epigenetic aging was clearly accelerated in line A mice compared to B6 (Figure 4B and C). We have previously demonstrated that in D2 mice the same epigenetic age predictor significantly accelerated epigenetic age predictions that rather follow a logarithmic regression,¹⁰ which, however, line K did not deviate from (Figure 4B and C). More in depth analyses for line K would warrant the development of an improved age predictor that is adjusted to more control samples of D2, as the initial marker panel was trained on B6. However, the data are consistent with a possible role of the QTL in affecting lifespan at least of line A mice, which will need to be tested in longevity studies of larger cohorts of animals.

Discussion

Forward genetic approaches in BXD RI strains have been shown to allow for the identification of QTL linked to lifespan and changes in various tissues and cells upon aging.^{22,23} We previously reported the likely linkage of a locus on the distal part of murine chromosome 11 to two phenotypes, regulation of lifespan as well the susceptibility of HSPC to short-term treatment with HU. While this finding implies a common mechanism of regulation for the two phenotypes, speculations on the mechanistic connection between these two phenotypes remains difficult without the identification of the gene within the locus regulating at least one of the phenotypes. Here, by generating and analyzing reciprocal strains congenic for the interval on chromosome 11 (B6 onto D2 and D2 onto B6), we verify the initial linkage analysis by demonstrating that this locus indeed controls the susceptibility of HSPC to HU. Other loci than the chromosome 11 locus may at least in part also contribute to the HU response phenotype, as line A and K mice are also congenic for other loci in addition to the locus on chromosome 11 (Online Supplementary Figure S4). The proximal locus on chromosome 11, which spans about 18.6 Mb, is, however, the only region which is identical between both congenic mouse strains, making a substantial contribution of other loci less likely (Online Supplementary Table S2). Unexpectedly, elevated sensitivity of HSPC to HU is not linked to altered cell cycle activity and thus elevated numbers of HSPC in S-phase, nor to apoptosis, senescence or

enhanced replication fork stalling as might be anticipated by previously reported outcomes to HU exposure. The precise mechanism that confers elevated susceptibility thus still remains to be further investigated. Our data strongly support *Pttg1/Securin* to be the QTL gene in that interval, as elevated levels of its expression conferred by the D2 allele result in increased HU susceptibility of HSPC. Recently, *Pttg1* overexpression was reported to restrict BrdU incorporation and cause enhanced levels of senescence and DNA damage in proliferating human fibroblasts,²⁴ a feature which is not mirrored in HSPC according to our data. Thus, these mechanistic differences illustrate the unique properties of HSPC with respect to cell cycle regulation and DNA damage response, as also demonstrated recently.²⁵⁻²⁷ The initial linkage data also imply a role for *Pttg1* in regulating lifespan. The primary role of *Pttg1* is an inhibition of Separase. This cysteine protease opens cohesin rings to allow for transition from metaphase to anaphase.²⁸ *Pttg1* is thus seen primarily as a target of the anaphase promoting complex (APC/C) to initiate chromosome segregation, although other additional roles have been described in the literature, such as a central role in pituitary tumor formation when overexpressed.²⁹ Interestingly, the APC/C is directly involved in regulating lifespan in yeast and results in dysregulation of rDNA biology,³⁰ while likely dominant negative mutations in cohesin genes have been recently identified as novel contributors to the initiation of acute myeloid leukemia through modulation of chromatin accessibility in HSPC and subsequent inhibition of differentiation by recruiting “stemness” transcription factors to the daughter cells upon division. Extended presence of cohesin, in the case of elevated levels of *Pttg1*, might thus contribute to loss of HSPC potential, which would be consistent with our phenotype (Online Supplementary Figure S4B). Hence, the two phenotypes might be mechanistically connected via alterations in the epigenetic landscape rather than changes in chromatid cohesion itself. This interpretation is supported by the finding that age-associated DNA methylation changes are acquired at a different pace in congenic mouse strains. It is thus possible that HU treatment interferes with epigenetic parameters regulated by *Pttg1/Securin*.

Acknowledgments

We thank the FACS core at Ulm University, especially Ali Gawanbacht-Ramhormose and Sarah Warth for cell sorting and the Central Animal Facility of Ulm University as well as the Comprehensive Mouse and Cancer Core at CCHMC for help with mouse experiments. We are grateful to José Cancelas for providing FBMD-1 stromal feeder cells. We thank Karin Müller from the Internal Medicine III Department for assistance with the GloMax 96 luminometer, Sebastian Iben from the Dermatology Department for helpful advice regarding the promoter studies and all lab members for fruitful discussions.

Funding

Work in the laboratory of HG is supported by the Deutsche Forschungsgemeinschaft SFB 1074, the RTG 1789, and FOR 2674. AB was supported by a Bausteinprogramm of the Medical Faculty of Ulm University. WW was supported by the Else Kröner-Fresenius-Stiftung (2014_A193); by the Interdisciplinary Center for Clinical Research within the faculty of Medicine at the RWTH Aachen University (O3-3); by the Deutsche Forschungsgemeinschaft (WA 1706/8-1 and WA1706/11 1).

References

- De Haan G, Nijhof W, Van Zant G. Mouse strain-dependent changes in frequency and proliferation of hematopoietic stem cells during aging: correlation between lifespan and cycling activity. *Blood*. 1997; 89(5):1543-1550.
- Lopes M, Cotta-Ramusino C, Pellicoli A, et al. The DNA replication checkpoint response stabilizes stalled replication forks. *Nature*. 2001;412(6846):557-561.
- De Haan G, Bystrykh LV, Weersing E, et al. A genetic and genomic analysis identifies a cluster of genes associated with hematopoietic cell turnover. *Blood*. 2002;100(6):2056-2062.
- Geiger H, Rennebeck G, Van Zant G. Regulation of hematopoietic stem cell aging in vivo by a distinct genetic element. *Proc Natl Acad Sci USA*. 2005; 102(14):5102-5107.
- Geiger H, True JM, De haan G, Van Zant G. Age- and stage-specific regulation patterns in the hematopoietic stem cell hierarchy. *Blood*. 2001;98(10):2966-2972.
- Manly KF, Cudmore RH, Meer JM. Map Manager QTX, cross-platform software for genetic mapping. *Mamm Genome*. 2001; 12(12):930-932.
- Van Zant G, Holland BP, Eldridge PW, Chen JJ. Genotype-restricted growth and aging patterns in hematopoietic stem cell populations of allophenic mice. *J Exp Med*. 1990; 171(5):1547-1565.
- Wakeland E, Morel L, Achey K, Yui M, Longmate J. Speed congenics: a classic technique in the fast lane (relatively speaking). *Immunol Today*. 1997;18(10):472-477.
- De Haan G, Van Zant G. Dynamic changes in mouse hematopoietic stem cell numbers during aging. *Blood*. 1999;93(10):3294-3301.
- Han Y, Eipel M, Franzen J, et al. Epigenetic age-predictor for mice based on three CpG sites. *Elife*. 2018;7.
- Young CW, Schochetman G, Karnofsky DA. Hydroxyurea-induced inhibition of deoxyribonucleotide synthesis: studies in intact cells. *Cancer Res*. 1967;27(3):526-534.
- Koç A, Wheeler LJ, Mathews CK, Merrill GF. Hydroxyurea arrests DNA replication by a mechanism that preserves basal dNTP pools. *J Biol Chem*. 2004;279(1):223-230.
- Funabiki H, Kumada K, Yanagida M. Fission yeast Cut1 and Cut2 are essential for sister chromatid separation, concentrate along the metaphase spindle and form large complexes. *EMBO J*. 1996;15(23):6617-6628.
- Funabiki H, Yamano H, Kumada K, Nagao K, Hunt T, Yanagida M. Cut2 proteolysis required for sister-chromatid separation in fission yeast. *Nature*. 1996;381(6581):438-441.
- Hood HM, Metten P, Crabbe JC, Buck KJ. Fine mapping of a sedative-hypnotic drug withdrawal locus on mouse chromosome 11. *Genes Brain Behav*. 2006;5(1):1-10.
- Schollaert KL, Poisson JM, Searle JS, Schwanekamp JA, Tomlinson CR, Sanchez Y. A role for *Saccharomyces cerevisiae* Chk1p in the response to replication blocks. *Mol Biol Cell*. 2004;15(9):4051-4063.
- Bottomly D, Walter NA, Hunter JE, et al. Evaluating gene expression in C57BL/6J and DBA/2J mouse striatum using RNA-Seq and microarrays. *PLoS One*. 2011; 6(3):e17820.
- Geisert EE, Lu L, Freeman-anderson NE, et al. Gene expression in the mouse eye: an online resource for genetics using 103 strains of mice. *Mol Vis*. 2009;15:1730-1763.
- Freeman NE, Templeton JP, Orr WE, Lu L, Williams RW, Geisert EE. Genetic networks in the mouse retina: growth associated protein 43 and phosphatase tensin homolog network. *Mol Vis*. 2011;17:1355-1372.
- Keeley PW, Zhou C, Lu L, Williams RW, Melmed S, Reese BE. Pituitary tumor-transforming gene 1 regulates the patterning of retinal mosaics. *Proc Natl Acad Sci USA*. 2014;111(25):9295-9300.
- Vadnais C, Davoudi S, Afshin M, et al. CUX1 transcription factor is required for optimal ATM/ATR-mediated responses to DNA damage. *Nucleic Acids Res*. 2012; 40(10):4483-4495.
- Lang DH, Gerhard GS, Griffith JW, et al. Quantitative trait loci (QTL) analysis of longevity in C57BL/6J by DBA/2J (BXD) recombinant inbred mice. *Aging Clin Exp Res*. 2010;22(1):8-19.
- Henckaerts E, Langer JC, Snoeck HW. Quantitative genetic variation in the hematopoietic stem cell and progenitor cell compartment and in lifespan are closely linked at multiple loci in BXD recombinant inbred mice. *Blood*. 2004;104(2):374-379.
- Hsu YH, Liao LJ, Yu CH, et al. Overexpression of the pituitary tumor transforming gene induces p53-dependent senescence through activating DNA damage response pathway in normal human fibroblasts. *J Biol Chem*. 2010; 285(29):22630-22638.
- Moehrl BM, Nattamai K, Brown A, et al. Stem Cell-Specific Mechanisms Ensure Genomic Fidelity within HSCs and upon Aging of HSCs. *Cell Rep*. 2015;13(11):2412-2424.
- Brown A, Pospiech J, Eiwien K, et al. The Spindle Assembly Checkpoint Is Required for Hematopoietic Progenitor Cell Engraftment. *Stem Cell Reports*. 2017; 9(5):1359-1368.
- Brown A, Geiger H. Chromosome integrity checkpoints in stem and progenitor cells: transitions upon differentiation, pathogenesis, and aging. *Cell Mol Life Sci*. 2018;75(20):3771-3779.
- Luo S, Tong L. Structural biology of the separase-securin complex with crucial roles in chromosome segregation. *Curr Opin Struct Biol*. 2018;49:114-122.
- Sapochnik M, Nieto LE, Fuertes M, Arzt E. Molecular Mechanisms Underlying Pituitary Pathogenesis. *Biochem Genet*. 2016;54(2):107-119.
- Sun D, Luo M, Jeong M, et al. Epigenomic profiling of young and aged HSCs reveals concerted changes during aging that reinforce self-renewal. *Cell Stem Cell*. 2014; 14(5):673-688.

Interferon regulatory factor 2 binding protein 2b regulates neutrophil versus macrophage fate during zebrafish definitive myelopoiesis

Luxiang Wang,^{1*} Shuo Gao,^{1*} Haihong Wang,^{1*} Chang Xue,^{1*} Xiaohui Liu,¹ Hao Yuan,¹ Zixuan Wang,¹ Saijuan Chen,¹ Zhu Chen,¹ Hugues de Thé,^{1,2} Yiyue Zhang,³ Wenqing Zhang,³ Jun Zhu^{1,2} and Jun Zhou¹

¹CNRS-LIA Hematology and Cancer, Sino-French Research Center for Life Sciences and Genomics, State Key Laboratory of Medical Genomics, Rui-Jin Hospital, Shanghai Jiao Tong University School of Medicine, Shanghai, China; ²Université de Paris 7/INSERM/CNRS UMR 944/7212, Equipe Labellisée No. 11 Ligue Nationale Contre le Cancer, Hôpital St. Louis, Paris, France and ³Division of Cell, Developmental and Integrative Biology, School of Medicine, South China University of Technology, Guangzhou, China

*LW, SG, HW and CX contributed equally to this work.



Haematologica 2020
Volume 105(2):325-337

ABSTRACT

A proper choice of neutrophil-macrophage progenitor cell fate is essential for the generation of adequate myeloid subpopulations during embryonic development and in adulthood. The network governing neutrophil-macrophage progenitor cell fate has several key determinants, such as myeloid master regulators CCAAT enhancer binding protein alpha (C/EBP α) and spleen focus forming virus proviral integration oncogene (PU.1). Nevertheless, more regulators remain to be identified and characterized. To ensure balanced commitment of neutrophil-macrophage progenitors toward each lineage, the interplay among these determinants is not only synergistic, but also antagonistic. Depletion of interferon regulatory factor 2 binding protein 2b (Irf2bp2b), a well-known negative transcription regulator, results in a bias in neutrophil-macrophage progenitor cell fate in favor of macrophages at the expense of neutrophils during the stage of definitive myelopoiesis in zebrafish embryos. Mechanistic studies indicate that Irf2bp2b acts as a downstream target of C/EBP α , repressing PU.1 expression, and that SUMOylation confers the repressive function of Irf2bp2b. Thus, Irf2bp2b is a novel determinant in the choice of fate of neutrophil-macrophage progenitor cells.

Introduction

Hematopoiesis is the process by which uncommitted hematopoietic stem cells proliferate and differentiate into all mature blood cell types.¹ The stepwise development of multipotent hematopoietic stem cells undergoes sequential lineage potential limitations toward oligopotent and unipotent progenitor cells, eventually restricting their output.² The molecular network governing every stage of hematopoiesis involves an interplay between multiple lineage-specific transcription factors/cofactors and epigenetic modifiers.³ Any tiny disturbance of these factors could bias the lineage-restricted cell fate toward an alternate fate.⁴

Neutrophil-macrophage progenitors (NMP) generate neutrophil-macrophage lineage cells, mainly neutrophils, monocytes, and macrophages. The gene regulatory network governing NMP cell fate is composed of primary determinants, CCAAT enhancer binding protein alpha (C/EBP α) and spleen focus forming virus proviral integration oncogene (PU.1), along with secondary determinants Gfi and Egr/Nab.^{5,6} Neutrophil cell fate specification requires C/EBP α , whereas macrophage cell fate specification depends on PU.1.^{7,8} The relative levels of C/EBP α and PU.1 determine the choice of NMP cell fate. A low C/EBP α :PU.1 ratio shifts the balance toward macrophage differentiation, whereas a high ratio directs granulocyte differentiation.⁶ To keep myeloid lineage fidelity, the interplay among

Correspondence:

JUN ZHOU
zj10802@rjh.com.cn

JUN ZHU
zhuj1966@yahoo.com or
jun.zhu@paris7.jussieu.fr

WENQING ZHANG
mczhangwq@scut.edu.cn

Received: January 25, 2019.

Accepted: May 20, 2019.

Pre-published: May 23, 2019.

doi:10.3324/haematol.2019.217596

Check the online version for the most updated information on this article, online supplements, and information on authorship & disclosures: www.haematologica.org/content/105/3/325

©2020 Ferrata Storti Foundation

Material published in *Haematologica* is covered by copyright. All rights are reserved to the Ferrata Storti Foundation. Use of published material is allowed under the following terms and conditions:

<https://creativecommons.org/licenses/by-nc/4.0/legalcode>. Copies of published material are allowed for personal or internal use. Sharing published material for non-commercial purposes is subject to the following conditions: <https://creativecommons.org/licenses/by-nc/4.0/legalcode>, sect. 3. Reproducing and sharing published material for commercial purposes is not allowed without permission in writing from the publisher.



the determinants is important not only in initiating the differentiation toward one lineage, but also in inhibiting that of the other lineage. Gfi1 and Egr/Nab, the downstream transcription factors of C/EBP α and PU.1, function as mutually antagonistic repressors to inhibit lineage-specific genes in mice.^{5,9} It has also been reported that the suppression of *irf8*, a downstream gene of Pu.1, leads to a depletion of macrophages and an expansion of neutrophils during zebrafish primitive myelopoiesis.¹⁰ *Irf8* knockout mice even develop a chronic myeloid leukemia-like disease.^{11,12} Mechanistically, interferon regulatory factor 8 (IRF8) impedes the ability of C/EBP α to stimulate neutrophil differentiation by preventing its binding to chromatin.¹² In addition to the transcription factors involved in the C/EBP α and PU.1 network, Runx1 was shown to repress *pu.1* in a Pu.1-Runx1 negative feedback loop and determine macrophage *versus* neutrophil fate.¹³

Interferon regulatory factor 2 binding protein (IRF2BP2) is a member of the IRF2BP family that was initially identified as an interferon regulatory factor 2 (IRF2)-dependent corepressor in inhibiting the expression of interferon-responsive genes.¹⁴ The IRF2BP family is highly conserved during evolution, and is structurally characterized by an N-terminal zinc finger motif which mediates homo- or hetero-dimerization/multimerization between different IRF2BP2 family members, and a C-terminal ring finger motif that interacts with its partners.¹⁵ IRF2BP2 is described as a corepressor in most published works.^{14,16,17} The significance of IRF2BP2 in hematopoiesis was first revealed by genetic studies in *Irf2bp2*-deficient mice. IRF2BP2, with its binding partner ETO2, and the NCOR1/SMRT corepressor complex, participates in erythroid differentiation.¹⁶ As a ubiquitously distributed nuclear protein, IRF2BP2 plays multiple roles in various types of hematopoietic cells. For example, IRF2BP2 exerts a repressive effect on target genes of nuclear factor of activated T cells (NFAT), which is another partner of IRF2BP2.¹⁷ IRF2BP2 has also been shown to restrain naïve CD4 T-cell activation by inhibiting proliferation and CD25 expression.¹⁸ Moreover, *Irf2bp2*-deficient macrophages were inflammatory in mice.¹⁹ In recent years, four patients with acute promyelocytic leukemia carrying a novel fusion IRF2BP2-RAR α have been reported. Nevertheless, the potential role of IRF2BP2 in leukemogenesis is still unclear.^{20,23}

In this study, we provide *in vivo* evidence demonstrating that a deficiency of *irf2bp2b* triggers biased NMP cell fate choice, favoring macrophage development during zebrafish definitive myelopoiesis, which adds *Irf2bp2b* to the repertoire of factors regulating NMP cell fate decision. Mechanistic studies indicate that *Irf2bp2b*, which is under the control of C/ebp α , inhibits *pu.1* expression. We further reveal that SUMOylation is indispensable for the transcriptional repression of *Irf2bp2b*.

Methods

Maintenance and generation of mutant zebrafish

Zebrafish were raised, bred, and staged according to standard protocols.²⁴ For the generation of crisp9-mediated *irf2bp2b* knockout zebrafish, guide RNA targeting exon 1 of *irf2bp2b* was designed using an online tool, ZiFiT Targeter software.

Plasmid construction

The zebrafish *irf2bp2b* gene and its serial mutants were cloned into PCS2+ vector. The upstream sequences of zebrafish *pu.1* and *irf2bp2b* genes were cloned into PGL3 promoter vector (Promega).

Whole-mount *in situ* hybridization

Digoxigenin-labeled RNA probes were transcribed with T7, T3 or SP6 polymerase (Ambion, Life Technologies, USA). Whole-mount *in situ* hybridization (WISH) was performed as described previously.²⁵

Semi-quantitative reverse transcriptase polymerase chain reaction

The RNA preparation, cDNA synthesis, and quantitative reverse transcriptase polymerase chain reaction (RT-qPCR) were performed as described in the *Online Supplementary Methods*.

Retroviral transduction

The IRF2BP2 cDNA was inserted into a pMSCV-neo vector. For retroviral transduction, plat-E cells were transiently transfected with retroviral vectors. 32Dcl3 cells were transduced by spinoculation (1,300 g at 30°C for 90 min) in a retroviral supernatant supplemented with cytokines and 4 μ g/mL polybrene (Sigma). Transduced cells were selected by G418 treatment (800 mg/mL, Sigma).

Statistical analysis

The statistical significance of a difference between two means was evaluated by the unpaired Student *t*-test. For multiple comparisons, one-way analysis of variance was performed, followed by a least significant difference post-hoc test for multiple comparisons. Differences were considered statistically significant at $P < 0.05$.

Ethics

The animal protocol described above was reviewed and approved by the Animal Ethical and Welfare Committee, Rui-Jin Hospital, Shanghai Jiao Tong University School of Medicine (Shanghai, China).

Results

Deficiency of zebrafish *irf2bp2b* causes a reduction of the neutrophil population and a simultaneous expansion of the macrophage population during definitive myelopoiesis

The IRF2BP gene family includes three members, IRF2BP1, IRF2BP2 and IRF2BP3, which are highly conserved throughout evolution.¹⁵ All the family members bear a nearly identical N-terminal C4-type zinc finger motif and a C-terminal C3HC4-type ring finger motif, whereas the intermediate domain between the zinc finger and the ring finger motifs shows relatively low similarity at the protein level.¹⁵ There are two paralog genes of *irf2bp2* named *irf2bp2a* and *irf2bp2b* in zebrafish, whereas a unique IRF2BP2 gene exists in the human genome, which generates two isoforms also named IRF2BP2a and IRF2BP2b due to alternative splicing. Human IRF2BP2a has a 16 amino acid-long additional sequence in its intermediate domain compared with IRF2BP2b. This additional sequence in human IRF2BP2a is not conserved in zebrafish *Irf2bp2a/2b* (*Online Supplementary Figure S1*). Phylogenetic analysis showed that the two paralogs and human IRF2BP2 arose from a common ancestor, suggesting that

functional divergence occurred early in vertebrate evolution.²⁶

The zebrafish is an excellent model organism for the study of hematopoiesis.²⁷ Like mammalian hematopoiesis, zebrafish hematopoiesis also consists of primitive and definitive waves which emerge sequentially in distinct anatomical sites.

Human *IRF2BP2* mRNA is distributed in dozens of tissues, with the most prominent expression being found in bone marrow (<https://www.ncbi.nlm.nih.gov/gene/359948>). Zebrafish *irf2bp2b* is also ubiquitously expressed in developing embryos. *irf2bp2b* transcript was detected in the green fluorescent protein (GFP)-positive cells enriched from Tg(*gata1:eGFP*), Tg(*pu.1:eGFP*), Tg(*mpx:eGFP*), and Tg(*mpeg1.1:eGFP*) embryos (Online Supplementary Figure S2). To evaluate the effects of *irf2bp2b* on hematopoietic differentiation and lineage commitment, a mutant line was generated using the CRISPR/Cas9 system targeting the first exon of the *irf2bp2b* gene and introducing a 26 nt deletion which results in a truncated protein by frameshifting

(Figure 1A, B). Moreover, the mutant *irf2bp2b* gene was cloned into an HA-tagged expressing vector and transfected into HEK293T cells. As expected, a short protein was detected by western blot analysis. Meanwhile, immunofluorescence analysis showed that this Irf2bp2b mutant protein lost its nuclear localization due to loss of the nuclear localization signal²⁸ (Figure 1C, D).

A series of hematopoietic-related markers was detected by WISH analysis during the stage of primitive hematopoiesis in *irf2bp2b*-deficient embryos. The primitive macrophages and neutrophils derived from the rostral blood island, as well as the erythrocytes and neutrophils originating from the intermediate cell mass remained unchanged (Online Supplementary Figure S3A-L, W).

Definitive pluripotent hematopoietic stem cells arise from the ventral wall of the dorsal aorta, the zebrafish equivalent of the aorta/gonad/mesonephros of mammals, then migrate through the caudal hematopoietic tissue to the thymus and kidney marrow. WISH analyses revealed that the expression of the hematopoietic stem/progenitor

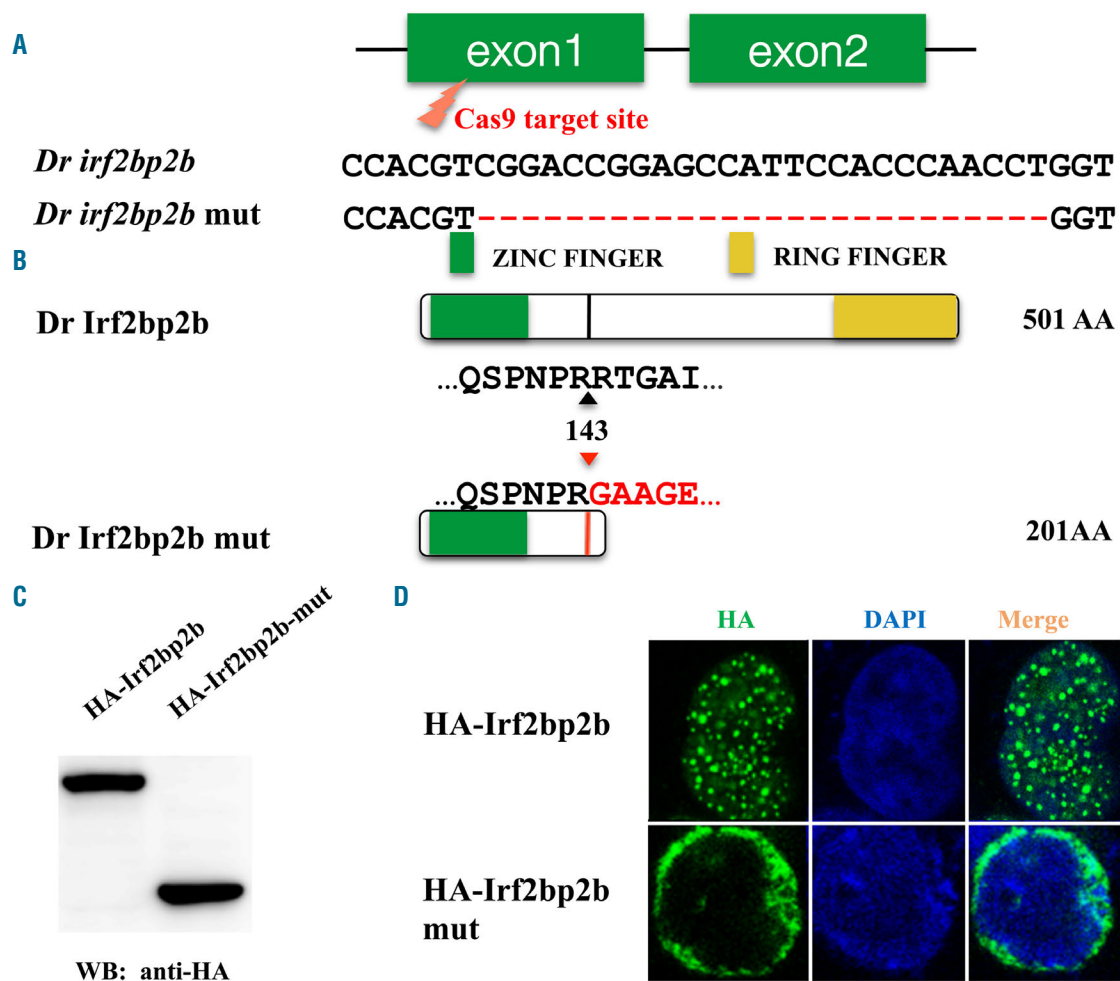


Figure 1. The establishment of a zebrafish *irf2bp2b* knockout line. (A) Schematic representation of the Cas9 target site in the first exon of zebrafish *irf2bp2b*. The deleted nucleotides in the mutant gene are marked by hyphens. (B) Schematic representation of wildtype (501 amino acids) and mutant Irf2bp2b proteins (201 amino acids). The site where the frameshift was introduced is marked by triangles. (C) Western blot analysis of HA-tagged wildtype and mutant Irf2bp2b proteins. (D) Immunofluorescence analysis of wildtype (top panel) and mutant Irf2bp2b (bottom panel) proteins, demonstrating that the truncated protein lost its nuclear localization. AA: amino acids; mut: mutated; WB: western blot; HA: human influenza hemagglutinin; DAPI: 4',6-diamidino-2-phenylindole.

cell-related markers *runx1* and *c-myb* was relatively unchanged in *irf2bp2b*-deficient embryos (Online Supplementary Figure S3M-R, X). The erythroid marker *hb α 1* (Online Supplementary Figure S3S-T), and the lymphoid marker *rag1* (Online Supplementary Figure S3U-V) were also unaffected.

As for myelopoiesis, a significant decrease in multiple neutrophil markers, including *c/ebp1* (a marker of neutrophil progenitors)²⁹ and *mpx/lyz* (a marker of mature neutrophils),³⁰ and a simultaneous increase of monocyte and macrophage markers such as *csf1r* (a monocyte/macrophage marker)³⁰ and *mfap4/mpeg1.1* (an early embryonic macrophage marker)^{31,32} were observed from 36 hours post fertilization (hpf) to 5 days post fertilization (dpf) in *irf2bp2b*-deficient mutants compared to controls (Figure 2A-I). The decreased neutrophil population was further confirmed by Sudan black staining³³ at 3 dpf in the ventral wall of the dorsal aorta (Figure 2J-J', M), as well as in *irf2bp2b*^{-/-}//Tg(*mpx:eGFP*) embryos at 5 dpf in caudal hematopoietic tissue (Figure 2K-K', M). Similarly, an expanded macrophage population was found in *irf2bp2b*^{-/-}//Tg(*mpeg1.1:eGFP*) embryos at 5 dpf (Figure 2L-L', M). Flow cytometry analysis was performed to quantify the numbers of neutrophils and macrophages, and the results showed a 34.9% reduction of eGFP-positive cells in *irf2bp2b*^{-/-}//Tg(*mpx:eGFP*) embryos and a 21.4% increase in *irf2bp2b*^{-/-}//Tg(*mpeg1.1:eGFP*) embryos (Figure 2N-P). The *irf2bp2b*^{-/-} zebrafish were not only viable but also fertile, which made the myelopoiesis study possible in adults. Morphological staining of the 3-month old adult zebrafish kidney marrow further confirmed the expanded macrophages and reduced neutrophils (Figure 3A-C). Meanwhile, FACS analyses were also done with whole kidney marrow from Tg(*mpx:eGFP*) and *irf2bp2b*^{-/-}//Tg(*mpx:eGFP*) lines in 3-month old adults. The myeloid cell populations were analyzed, and many fewer neutrophils were found in *irf2bp2b*^{-/-}//Tg(*mpx:eGFP*) zebrafish than in controls (29.7% *mpx*⁺ vs. 84.0% *mpx*⁺) (Figure 3D, E).

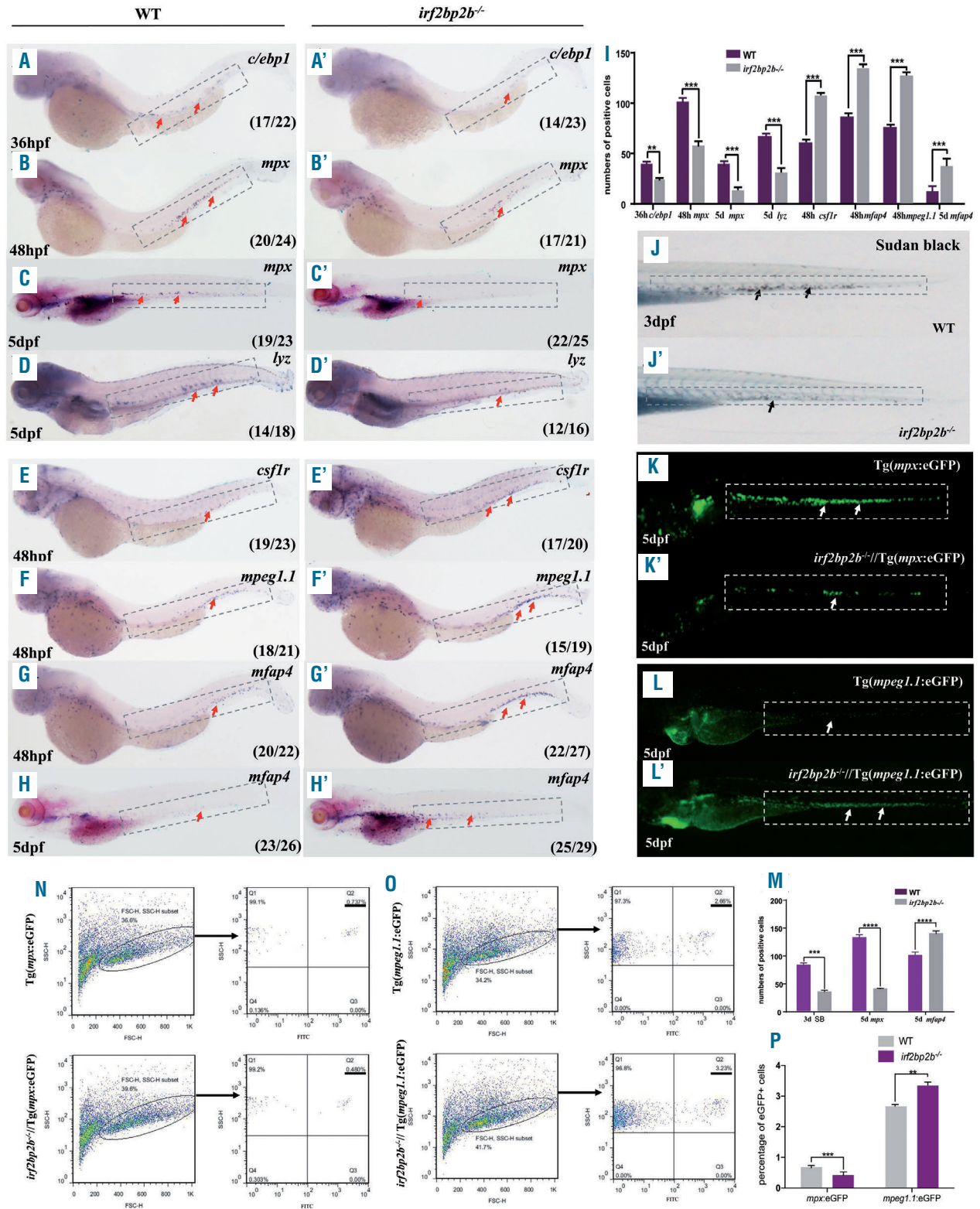
An opposite phenotype emerged when *irf2bp2b* mRNA was injected into one-cell stage wildtype embryos (Figure 3F-H). It is worth noting that the overall numbers of cells positive for the pan-myeloid marker *l-plastin*³⁰ (which is a marker of both neutrophils and macrophages), were comparable among *irf2bp2b*-deficient mutants, *irf2bp2b*-overexpressing embryos and wildtype embryos (Figure 3I-L). In addition, embryos injected with a specific *irf2bp2b* morpholino (MO) exactly phenocopied the aberrant myelopoiesis that occurs in *irf2bp2b* knockout embryos (Online Supplementary Figure S4A-D, I).

All of the abnormalities in *irf2bp2b*-deficient and morphant embryos could be effectively rescued with the wildtype zebrafish *irf2bp2b* mRNA, confirming the specificity of the phenotype (Online Supplementary Figure S4E-F, I). It should be noted that zebrafish *irf2bp2a* mRNA did not rescue the defects of myelopoiesis, indicating that the two paralogs might have distinct roles (*data not shown*). Accordingly, loss of *irf2bp2a* resulted in a quite different phenotype in zebrafish myelopoiesis, which could not be rescued by *irf2bp2b* mRNA, either (experiments ongoing). Moreover, human *IRF2BP2b* mRNA, but not *IRF2BP2a* mRNA, could rescue the biased myelopoiesis in zebrafish *irf2bp2b*-deficient mutants, suggesting that human *IRF2BP2b* is the functional ortholog of zebrafish *irf2bp2b* in this process (Online Supplementary Figure S4G-H, I and *data not shown*).

Ir2bp2b regulates neutrophil-macrophage progenitor fate by repressing *pu.1* expression

The imbalanced proportion of neutrophil and macrophage populations in *irf2bp2b*-defective mutants can result from either abnormalities in apoptosis or proliferation rate. To distinguish between these possibilities, terminal deoxynucleotidyl transferase dUTP nick end labeling (TUNEL) and antiphosphohistone H3 (pH3) antibody staining assays were performed to assess the apoptosis and proliferation status of neutrophils and macrophages, respectively. Neither TUNEL nor pH3 assays revealed discernable differences in the percentages of double-positive stained cells (TUNEL⁺GFP⁺, pH3⁺GFP⁺) in *irf2bp2b*^{-/-}//Tg(*mpx:eGFP*) and *irf2bp2b*^{-/-}//Tg(*mpeg1:eGFP*) embryos compared to the percentage in controls, indicating that there is no change in the status of either apoptosis or proliferation of each lineage in *irf2bp2b*-deficient embryos (Online Supplementary Figure S5). Moreover, the fact that *l-plastin*-positive cell numbers remained unchanged in both *irf2bp2b*-overexpressing and -deficient embryos suggest that *irf2bp2b* might participate in regulating neutrophil *versus* macrophage commitment.

The relative levels of the master regulators PU.1 and C/EBP α are critical in macrophage *versus* neutrophil cell fate specification.⁶ To ensure balanced commitment of NMP, the endogenous levels of PU.1 and C/EBP α must be appropriately tuned to a proper range. Overexpression of PU.1 can bias myeloid output to macrophages, whereas overexpression of C/EBP α has an opposite effect. Thus either *pu.1* upregulation or *c/ebp α* downregulation within NMP could be the cause of biased myelopoiesis toward macrophages in *irf2bp2b* mutants. We tried to examine the expression levels of *pu.1* and *c/ebp α* by WISH analysis. No obvious difference was observed between the wildtype and *irf2bp2b*^{-/-} embryos. However, considering that *Pu.1* is expressed in multiple hematopoietic cell lineages, such as hematopoietic stem cells, common lymphoid progenitors, and common myeloid progenitors,³⁴ and *C/ebp α* is also widely expressed in hematopoietic stem cells and myeloid cells,³⁵ changes in their levels of expression within NMP might be difficult to show. Due to the lack of a lineage cell detection cocktail for the zebrafish hematopoietic system, we were unable to isolate the NMP subpopulation by flow cytometry to compare the endogenous expression levels of *pu.1* and *c/ebp α* . RT-qPCR was performed to detect the expression of *c/ebp α* and *pu.1* in wildtype and *irf2bp2b*-deficient whole embryos, and no obvious changes were observed (Online Supplementary Figure S6), suggesting that changes occurring in NMP might be masked. To resolve this problem, we used a murine myeloid progenitor cell line 32Dcl3 retrovirally transduced with human *IRF2BP2b*. RT-qPCR analyses revealed that the transcript level of *Pu.1* was downregulated, whereas that of *C/ebp α* was unaffected (Figure 4A). Meanwhile, expression of multiple monocyte differentiation-related genes such as *Mcsfr*, *Mmp1*, *Thr2*, and *Irf8* was reduced, whereas expression of neutrophil differentiation-related genes, including *Gcsfr*, *Ltf*, *Prtn3*, and *Elane*, was induced (Figure 4A). These observations imply that an alteration of *pu.1* expression, rather than that of *c/ebp α* , might account for the shift in the balance of neutrophil and macrophage populations in *irf2bp2b*-deficient zebrafish embryos. Since *IRF2BP2* is a negative transcription regulator, we wondered whether *pu.1* is a direct target of *Ir2bp2b*, which could be upregulated in *irf2bp2b*-deficient NMP. To test



this hypothesis, we divided the 8.5 kb zebrafish *pu.1* promoter into four fragments, which were inserted separately into a luciferase reporter vector.¹⁵ The luciferase expression in all of these four constructs was inhibited when co-transfected with *irf2bp2b* in HEK293T cells. The most prominent repression was found within the fragment nearest to the transcription start site (-1.7 kb) (Figure 4B). Next, a series of *in vivo* experiments was performed. The 8.5 kb *pu.1* promoter was cloned into a mCherry reporter vector (*pu.1*:mCherry, Tol2 backbone), which was co-injected with Tol2 transposase mRNA into wildtype

zebrafish embryos with or without *irf2bp2b* mRNA. Overexpression of *irf2bp2b* led to significantly reduced expression of mCherry (Figure 4C-D). Moreover, *pu.1* MO was injected into *irf2bp2b*^{-/-} embryos, and effective rescue of aberrant myelopoiesis was obtained (Figure 4E-J, O). These observations suggest that the level of *pu.1* expression might be elevated in NMP in *irf2bp2b* mutants. To further demonstrate that Irf2bp2b regulates zebrafish NMP cell fate choice through repression of *pu.1*, we took advantage of a zebrafish *pu.1*^{G242D} mutant line, in which the level of *pu.1* transcripts is normal but its protein stability is dra-

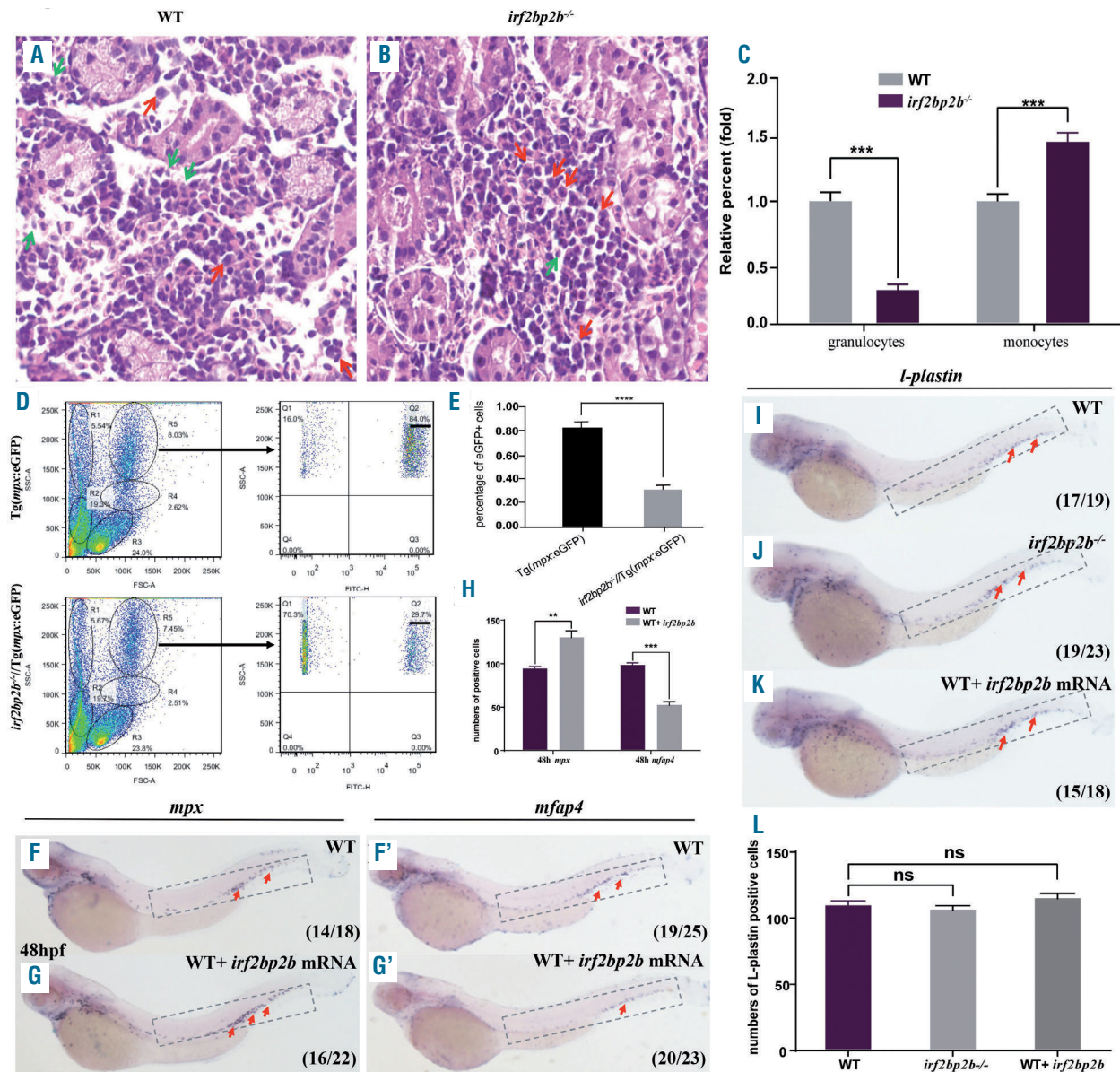


Figure 3. Biased myelopoiesis in *irf2bp2b*-deficient adult zebrafish. (A, B) Hematoxylin & eosin staining for morphological analysis of the kidney marrow collected from 3-month old adult wildtype (1 male and 1 female) and *irf2bp2b*^{-/-} (2 males and 1 female) zebrafish. One representative image of each group is shown. Green and red arrows indicate typical neutrophils and macrophages, respectively. (C) Statistical results for A, B. Error bars represent the mean \pm standard deviation (SD) of at least 15 images. *** $P < 0.001$ (Student *t* test). (D) FACS analysis of whole kidney marrows from Tg(*mpx*:eGFP) and *irf2bp2b*^{-/-}/Tg(*mpx*:eGFP) lines in 3-month old adults. The myeloid cells in the R5 gate were analyzed with fluorescence. (E) Statistical results for D. Error bars represent the mean \pm SD of three replicates. **** $P < 0.0001$ (Student *t* test). (F-G') Whole-mount *in situ* hybridization (WISH) using *mpx* and *mfap4* to monitor neutrophil and macrophage development in embryos injected with wildtype or *irf2bp2b* mRNA. (I-K) WISH analyses of the pan-myeloid marker *l-plastin* in embryos injected with wildtype, *irf2bp2b*^{-/-}, and *irf2bp2b* mRNA embryos. (H, L) Statistical results for F-G', I-K. Error bars represent the mean \pm SD of at least 15-30 embryos. ns: not statistically significant; ** $P < 0.01$; *** $P < 0.001$ (Student *t* test).

matically decreased.¹⁵ In *pu.1*^{G242D/G242D} homozygous embryos, biased myelopoiesis toward neutrophils occurred, as expected. It should be noted that no obvious rescue effect was observed in the *irf2bp2b*^{-/-}*pu.1*^{G242D/G242D} double-mutant embryos compared to *pu.1*^{G242D/G242D} embryos, indicating that *pu.1* is indeed downstream of Irf2bp2b in determining NMP cell fate (Figure 4K-O).

Irf2bp2b represses *pu.1* gene transcription by binding directly to its promoter

IRF2BP2 has frequently been described as a co-repressor.^{14,16,17} We therefore set out to investigate how

Irf2bp2b represses *pu.1* expression. The C-terminal C3HC4-type ring finger motif of IRF2BP2 is responsible for mediating its binding with interacting partners.^{14,16,17} The N-terminal C4-type zinc finger motif was believed to enable homo- and hetero-dimerization/multimerization between different IRF2BP2 family members.¹⁵ However, C4 zinc fingers are typically found in DNA-binding domains of transcription factors including GATA1-6 as well as nuclear receptors RAR and RXR.^{36,37} The possibility that IRF2BP2 functions as a transcription repressor by directly binding DNA should not, therefore, be excluded.

To characterize how Irf2bp2b represses transcription in

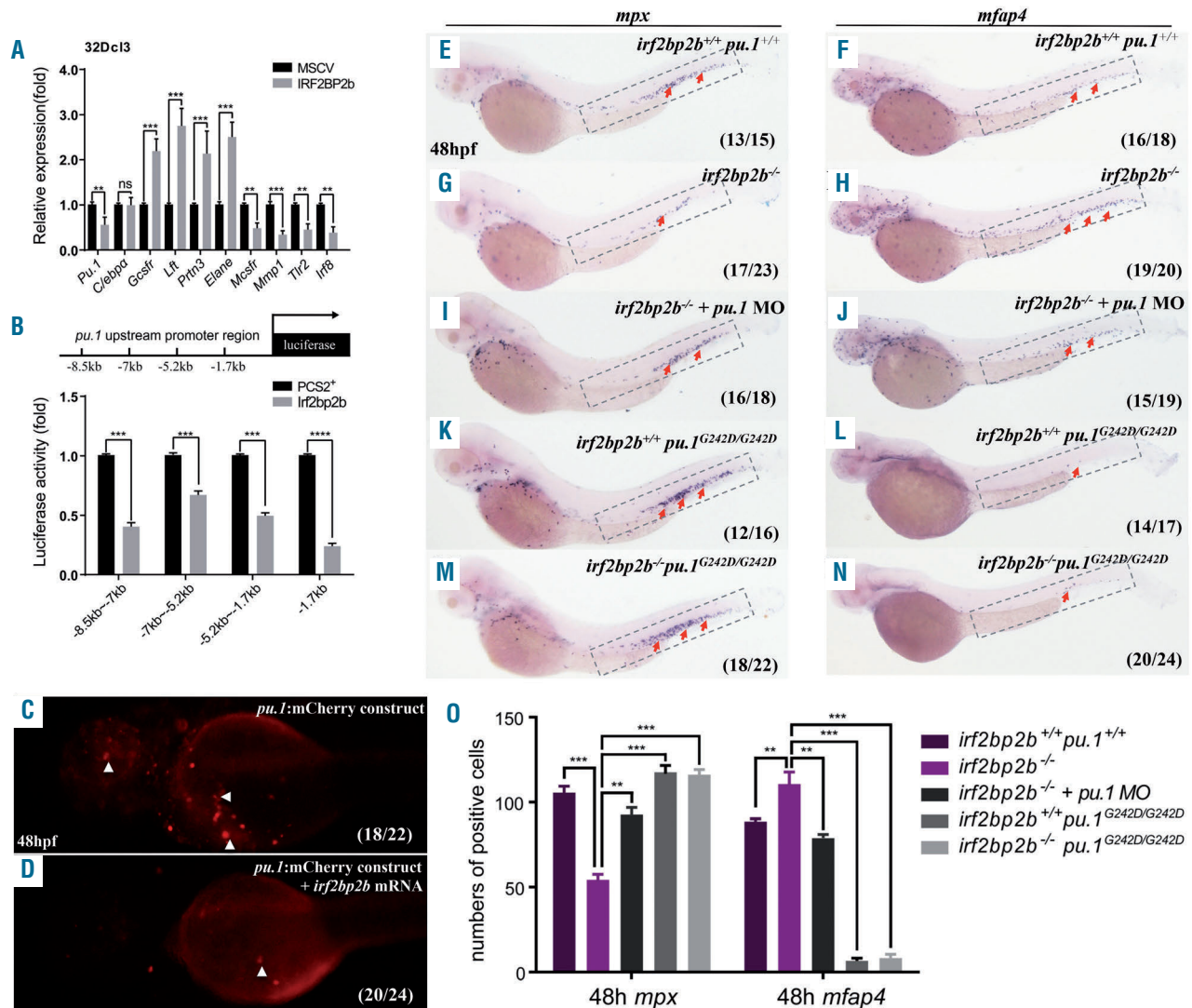


Figure 4. Irf2bp2b dictates neutrophil-macrophage progenitor cell fate through inhibition of *pu.1* expression. (A) Quantitative reverse transcriptase polymerase chain reaction analysis of neutrophil and macrophage development-related genes in 32Dcl3 cells constitutively expressing human IRF2BP2b. Error bars represent the mean \pm standard deviation (SD) of at least three replicates. ns: not statistically significant; ** P <0.01; *** P <0.001 (Student *t* test). (B) Schematic diagram of the -8.5kb zebrafish *pu.1* promoter dual luciferase report vector (top panel). Dual luciferase vectors each with a fragment of the zebrafish *pu.1* promoter, as indicated, were co-transfected into HEK293T cells with an *irf2bp2b*-expressing vector or empty vector pCS2⁺. Luciferase activity with *irf2bp2b* expression was detected and normalized to empty vector pCS2⁺ which was set to 1.0 (bottom panel). Error bars represent the mean \pm SD of at least three replicates. *** P <0.001; **** P <0.0001 (Student *t* test). (C, D) Representative fluorescent images of transient mCherry expression at 48 hours post-fertilization (hpf) of wildtype (WT) and *irf2bp2b*-overexpressing embryos injected with a -8.5 kb *pu.1*:mCherry construct. (E-N) Whole-mount *in situ* hybridization (WISH) assay of *mpx* and *mfap4* in WT embryos, (E, F), *irf2bp2b*^{-/-} mutant embryos (G, H), *irf2bp2b*^{-/-} mutant embryos injected with *pu.1* morpholino (I, J), *pu.1*^{G242D/G242D} mutants (K, L), and *irf2bp2b*^{-/-}*pu.1*^{G242D/G242D} double-mutant embryos (M, N). (O) Statistic result for E-N. Error bars represent the mean \pm standard error of mean of 15-30 embryos. ** P <0.01; *** P <0.001 (analysis of variance followed by the least significant difference *post-hoc* test for multiple comparisons).

the choice of NMP cell fate, a series of point mutations in critical cysteines were introduced into the ring finger motif (C420/423A, named RM hereafter) and the zinc finger motif (C14/17A, named ZM hereafter) of Irf2bp2b, as previously reported¹⁵ (Figure 5A). For the Irf2bp2b RM mutant, interaction with its partners was abolished, while the polymerization and putative DNA-binding capacities of the ZM mutant were both abrogated. A tetramerization motif from human P53 (amino acids 324-355) was fused in-frame with the Irf2bp2b ZM mutant (tet-ZM), restoring the polymerization capacity of this mutant (Figure 5A). Immunofluorescence analysis (anti-HA antibody) of HEK293T cells transfected with the Irf2bp2b mutants described above demonstrated that these mutations did not affect nuclear localization as expected (*Online Supplementary Figure S7*).²⁸

The results from *in vivo* rescue assays revealed that only the RM mutant displayed a significant rescue effect similar to wildtype *irf2bp2b*, while the ZM and tet-ZM mutants did not (Figure 5B-L). These data indicate that direct DNA binding would be indispensable for the ability of Irf2bp2b to repress *pu.1* gene expression in NMP cell fate choice.

Correspondingly, the luciferase activity assays showed that only wildtype Irf2bp2b and RM mutant, but not ZM and tet-ZM mutants, exhibited strong repressive effects on luciferase expression with a -1.7 kb zebrafish *pu.1* promoter (Figure 6A). This fragment was further narrowed down to a short 132 bp region (A region) (Figure 6B). To validate that the A region is an Irf2bp2b binding site, *in*

vivo chromatin immunoprecipitation polymerase chain reaction (CHIP-PCR) was performed in zebrafish embryos expressing GFP or Irf2bp2b-GFP using an anti-GFP antibody. In this assay, the *pu.1* promoter A region was specifically co-immunoprecipitated with Irf2bp2b-GFP (Figure 6C).

Since positively charged amino acids are important to fit into the negatively charged phosphate backbone of DNA, several arginines (R10/11/36/55/59) within the C4 zinc finger motif were mutated. Luciferase assays showed that only the Irf2bp2b^{R55/59L} double-mutant completely lost the ability to repress luciferase expression from the *pu.1* promoter (Figure 6D). Notably, CHIP-PCR analysis has shown that the Irf2bp2b^{R55/59L} mutant could not co-immunoprecipitate the *pu.1* promoter A region (Figure 6C). As anticipated, this mutant lost the rescue effect in *irf2bp2b*^{-/-} embryos (Figure 6E-J, K). These results indicate that Irf2bp2b represses *pu.1* gene expression by directly binding to its promoter and R55/R59 are two critical amino acids for Irf2bp2b DNA binding.

Taken together, these findings suggest that Irf2bp2b most likely functions as a transcription repressor, rather than a co-repressor, in NMP fate choice during zebrafish myelopoiesis.

The repressive property of Irf2bp2b is dependent on SUMOylation

IRF2BP2 is a co-repressor molecule for its interacting transcription factors.^{14,17} In the current study, we demon-

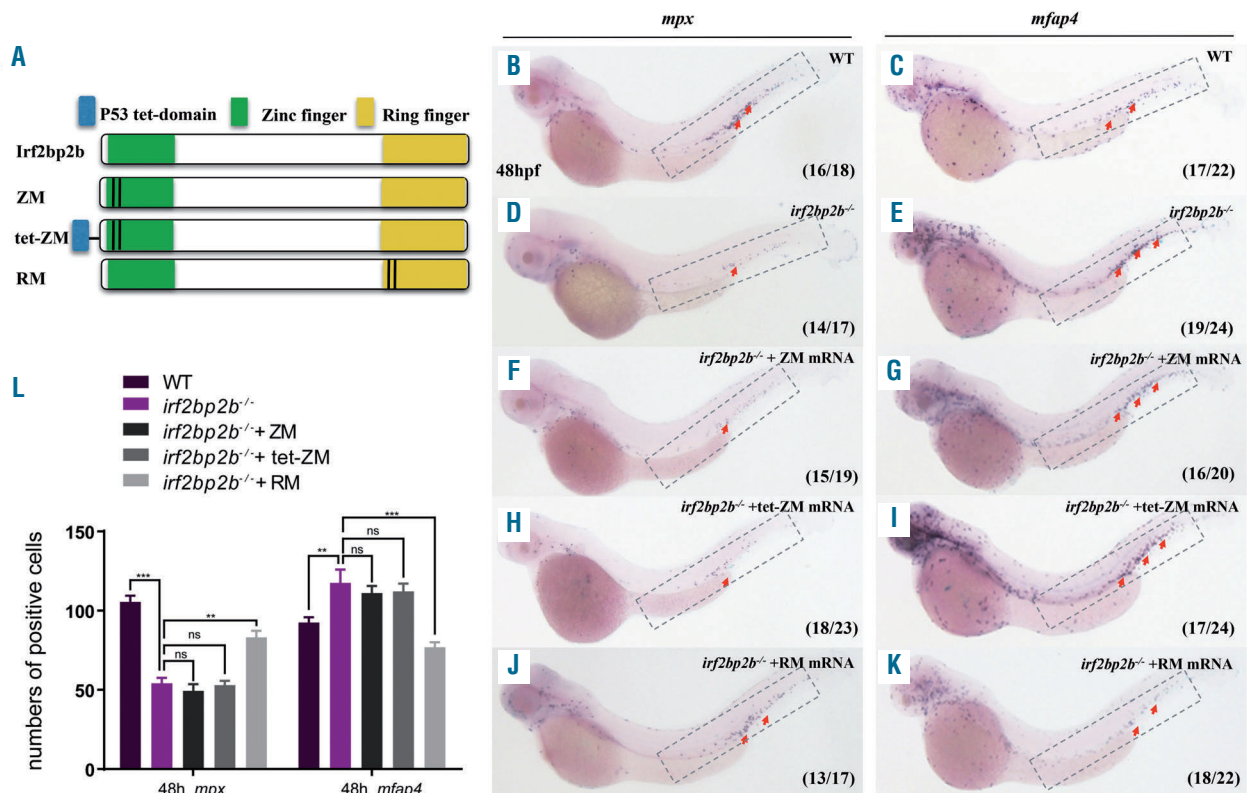


Figure 5. DNA-binding is indispensable for Irf2bp2b in regulating neutrophil-macrophage progenitor cell fate. (A-L) *Irf2bp2b* mRNA rescue assays in *irf2bp2b*^{-/-} embryos. (A) Structure of variant forms of Irf2bp2b, including wildtype (WT), and ZM, tet-ZM, and RM mutants. (B-L) *Mpx* and *mfap4* probes were used in whole-mount *in situ* hybridization (WISH) to examine the rescue effect of injecting *irf2bp2b* ZM (F, G), tet-ZM (H, I), and RM mutant mRNA (J, K). (L) Error bars represent the mean \pm standard error of mean of 15-30 embryos. ns: not statistically significant; ** $P < 0.01$; *** $P < 0.001$ (analysis of variance followed by the least significant difference post-hoc test for multiple comparisons).

strated that zebrafish Irf2bp2b inhibits *pu.1* expression. Thus, we investigated the reason underlying the repressive property of IRF2BP2.

Post-translational modification of proteins plays a pivotal role in regulating their function. SUMOylation is an important type of post-translational modification which involves a cascade of dedicated enzymes that facilitate the covalent modification of specific lysine residues on target proteins with monomers or polymers of SUMO (small ubiquitin-like modifier).³⁸ The SUMOylation of substrate proteins is frequently linked with transcriptional repression.³⁹ In fact, multiple adducts (the smallest one was about 10 kD larger than the unmodified protein, which was nearly the size of one SUMO molecule) of Irf2bp2b were detected by western blot (Figure 7A). The SUMO-targeted lysine usually lies in the canonical motif Ψ Kxe.⁴⁰ A SUMO consensus motif VKKE (lysine 496) located at the C-terminus of Irf2bp2b was predicted by bioinformat-

ics (Online Supplementary Figure S1). The putative lysine was mutated to arginine (Irf2bp2b^{K496R}) to abolish covalent binding with the SUMO molecule. The modified bands of the Irf2bp2b^{K496R} mutant protein disappeared as expected (Figure 7A, B). In addition, an Irf2bp2b^{E496A} mutant was constructed to destroy the conservation of the SUMO consensus motif which still allowed the accessibility of lysine 496 to other modifiers. The modified bands disappeared as Irf2bp2b^{K496R} mutant did (Figure 7C), indicating that Irf2bp2b is a SUMOylated substrate.

In HEK293T cells, GFP-SUMO was co-transfected with HA-tagged wildtype Irf2bp2b or Irf2bp2b^{K496R} mutant. Immunoprecipitation assays showed that GFP-SUMO coprecipitated with HA-tagged wildtype Irf2bp2b, but not with the Irf2bp2b^{K496R} mutant (Figure 7D). This further indicated that Irf2bp2b is indeed SUMOylated in cells.

Luciferase reporter assays with zebrafish *pu.1* promoter were then conducted to assess the repressive capacity of

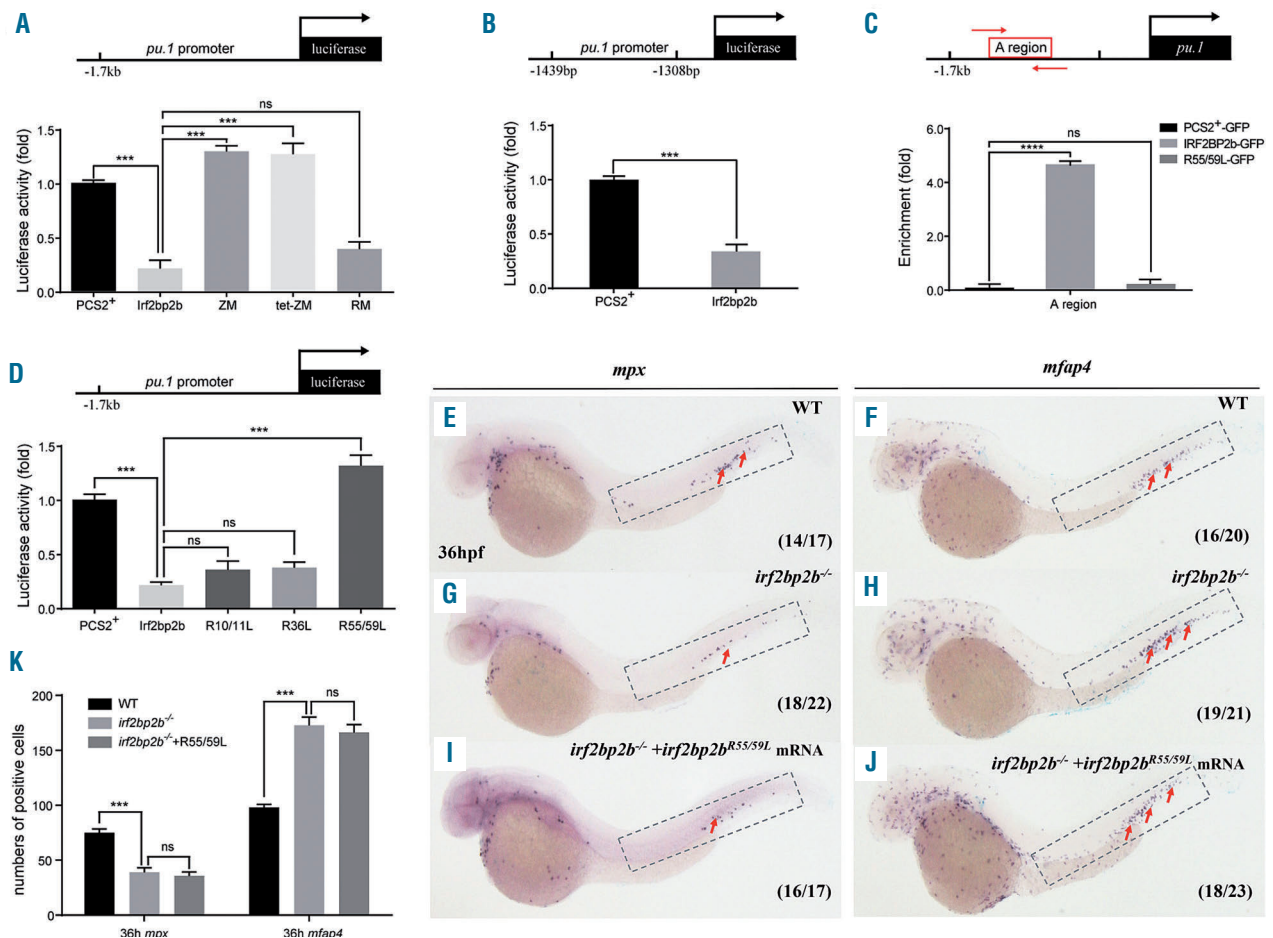


Figure 6. DNA-binding property is indispensable for Irf2bp2b in regulating neutrophil-macrophage progenitor cell fate (continued). (A) Ability of Irf2bp2b mutants to repress the zebrafish *pu.1* promoter (-1.7kb). Error bars represent the mean \pm standard error of mean (SEM) of at least three replicates. *** P <0.001 [analysis of variance (ANOVA) followed by the least significant difference (LSD) *post-hoc* test for multiple comparisons]. (B) Irf2bp2b represses luciferase expression from the *pu.1* promoter 132bp A region (from -1308 bp to -1439 bp). Error bars represent the mean \pm standard deviation (SD) of at least three replicates. *** P <0.001 (Student *t* test). (C) Chromatin immunoprecipitation polymerase chain reaction analysis of *pu.1* promoter A region in zebrafish embryos expressing green fluorescent protein (GFP), Irf2bp2b-GFP or Irf2bp2b^{R55/59L}-GFP using an anti-GFP antibody. The position of the primers used to amplify the *pu.1* promoter A region are indicated with red arrows. Error bars represent the mean \pm SEM of at least three replicates. *** P <0.0001 (ANOVA followed by the LSD *post-hoc* test for multiple comparisons). (D) Luciferase repression assays of Irf2bp2b mutants on zebrafish *pu.1* promoter (-1.7 kb). Error bars represent the mean \pm SEM of at least three replicates. *** P <0.001 (ANOVA followed by the LSD *post-hoc* test for multiple comparisons). (E-J) Irf2bp2b^{R55/59L} mRNA rescue assays in Irf2bp2b^{-/-} mutant embryos. *Mpx* and *mfap4* probes were used in whole-mount *in situ* hybridization to examine rescue effects associated with injection of Irf2bp2b^{R55/59L} mutant mRNA. (K) Error bars represent the mean \pm SEM of at least three replicates. *** P <0.001 (ANOVA followed by the LSD *post-hoc* test for multiple comparisons).

Irf2bp2b upon its SUMOylation. The results showed that the Irf2bp2b-SUMO fusion, which mimics fully SUMOylated Irf2bp2b, displayed even stronger repression than the wildtype Irf2bp2b, whereas the Irf2bp2b^{K496R} mutant lost the ability to repress transcription (Figure 7B, E). Consistently, Irf2bp2b-SUMO and Irf2bp2b^{K496R} mutants had completely different rescue effects in *irf2bp2b*-deficient mutants (Figure 7F-N).

Overall, these data support the concept that Irf2bp2b is a SUMOylated protein in cells and that SUMOylation is indispensable for its property of repressing transcription.

Irf2bp2b mediates the antagonistic effect of C/ebpα on *pu.1* in neutrophil-macrophage progenitor cell fate

To ensure balanced commitment of NMP toward each lineage, the mutual antagonistic interplay of the master regulators PU.1 and C/EBPα is very important.^{5,41} Since Irf2bp2b represses *pu.1* expression in zebrafish NMP cell

fate choice, we questioned whether *irf2bp2b* is a C/ebpα target.

Two putative C/ebpα binding sites located at -37 bp (CS1) and -1595 bp (CS2) upstream of the transcription start site were predicted in the zebrafish *irf2bp2b* promoter by bioinformatics analysis. A luciferase reporter vector was constructed with the zebrafish *irf2bp2b* -2.2kb promoter and co-transfected with either a *c/ebpα*-expressing vector or an empty vector. Luciferase expression was significantly enhanced by C/ebpα (Figure 8A). A similar enhancement of expression was also obtained when an mCherry-expressing vector carrying the same *irf2bp2b* promoter (*irf2bp2b*:mCherry, in a Tol2 backbone) was co-injected with *c/ebpα* and Tol2 transposase mRNA into zebrafish embryos (Figure 8B, C). This enhancement was completely abolished when the predicted C/ebpα binding sites were deleted in the *irf2bp2b* promoter (Figure 8D).

Finally, *c/ebpα* mRNA was injected into *irf2bp2b*^{-/-} knock-

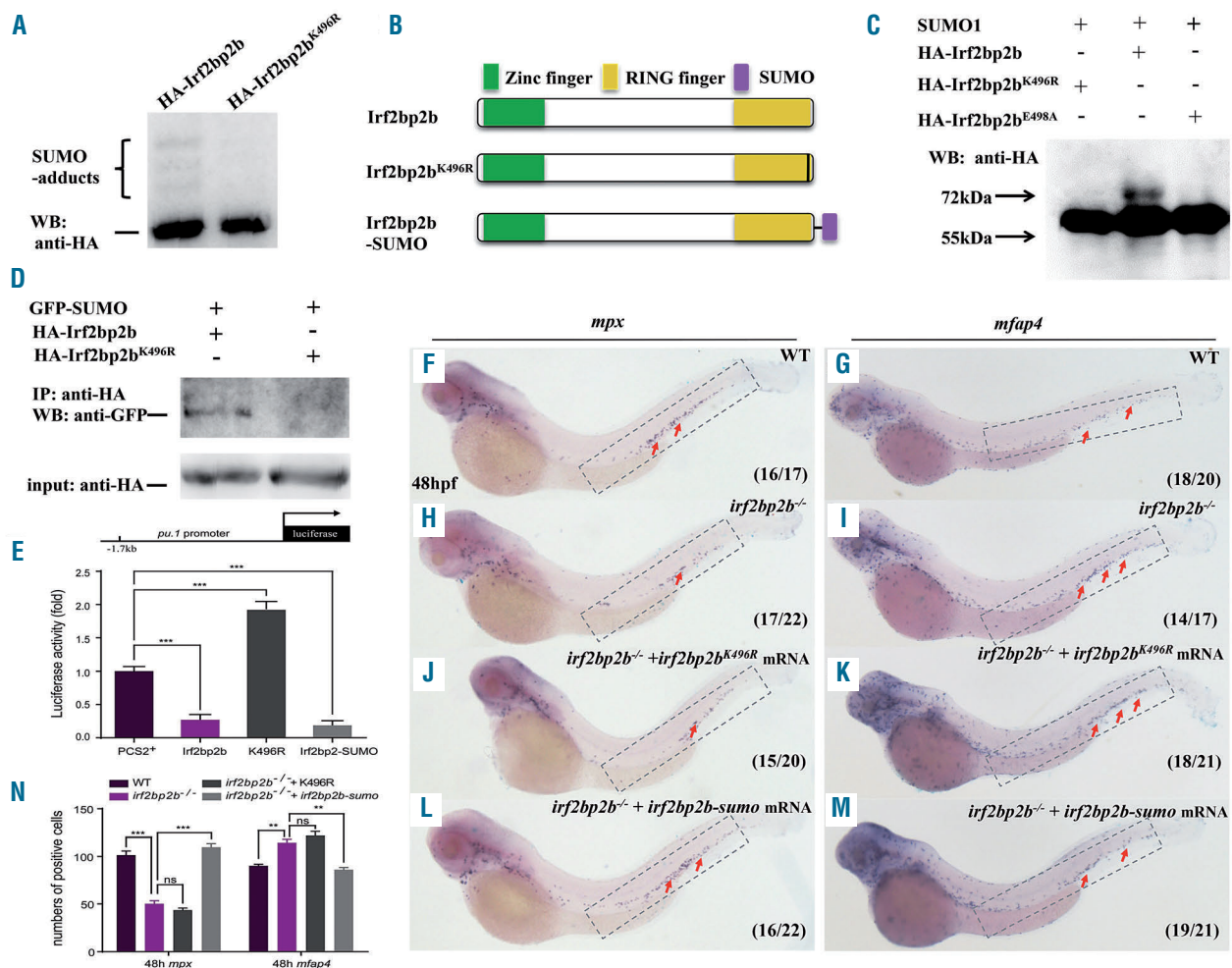


Figure 7. SUMOylation is indispensable for transcription repression of Irf2bp2b. (A) Western blot analysis (anti-HA) of HA-tagged wildtype (WT) and Irf2bp2b^{K496R} mutant proteins expressed in HEK293T cells. (B) The structure of variant forms of Irf2bp2b, including WT, Irf2bp2b^{K496R}, and Irf2bp2b-SUMO mutants. (C) Western blot analysis (anti-HA) of HA-tagged WT, Irf2bp2b^{K496R} and Irf2bp2b^{E498A} mutant proteins expressed in HEK293T cells. (D) HA-tagged WT or Irf2bp2b^{K496R} mutant protein was immunoprecipitated with an anti-HA antibody from HEK293T cells co-expressing GFP-SUMO, and SUMOylated Irf2bp2b protein was detected by western blot with an anti-GFP antibody. (E) Repression of luciferase expression from the zebrafish *pu.1* promoter (-1.7kb) by Irf2bp2b mutants. Error bars represent the mean \pm standard error of mean (SEM) of at least three replicates. *** $P < 0.001$ [analysis of variance (ANOVA) followed by the least significant difference (LSD) *post-hoc* test for multiple comparisons]. (F-M) *Irf2bp2b*-SUMO and *irf2bp2b*^{K496R} rescue assays in *irf2bp2b*^{-/-} mutant embryos. *Mpx* and *mfap4* probes were used in whole-mount *in situ* hybridization to examine rescue effects of injections of *irf2bp2b*^{K496R} mutant (J, K) or *irf2bp2b*-sumo (L, M) mRNA. (N) Error bars represent the mean \pm SEM of 15-30 embryos. ns: not statistically significant; ** $P < 0.01$; *** $P < 0.001$ (ANOVA followed by the LSD *post-hoc* test for multiple comparisons).

out and wildtype embryos. The overexpression of *c/ebpα* mRNA induced biased myelopoiesis toward neutrophils in control embryos (Figure 8E, F, I, J, M), but had no effect on myelopoiesis in *irf2bp2b*^{-/-} embryos (Figure 8G, H, K-M).

Meanwhile, to elucidate whether *gfi1* could also be a secondary determinant of *C/ebpα*, *gfi1* mRNA was injected into wildtype embryos. Although *gfi1* overexpression did give rise to a remarkable expansion of the neutrophil population, the macrophage population was unaffected (*data not shown*). Moreover, this overexpression did not have any rescue effect in *irf2bp2b*-deficient embryos (Online Supplementary Figure S8E, F, I).

In summary, these data indicate that *Irf2bp2b* plays a pivotal role in mediating the antagonistic function of *C/ebpα* on *pu.1* transcription regulation, which fine tunes the level of *pu.1* expression in NMP and determines the

choice of NMP cell fate in order to maintain a normal neutrophil and macrophage population ratio (Figure 8N).

Discussion

Although multiple regulators involved in hematopoietic lineage restriction have been characterized, the molecular details of NMP differentiation are still under debate. The relationship between the master regulators PU.1 and *C/EBPα* in myelopoiesis is complicated, being not only synergistic, but also antagonistic.⁴¹ On the one hand, *C/EBPα* can stimulate *PU.1* expression by directly binding to its promoter.^{42,43} On the other hand, *C/EBPα* can interact directly with PU.1 and block its function, or inhibit *PU.1* indirectly through activation of the transcription repressor *GFI1*,^{44,45} which in turn inhibits PU.1 activity through a

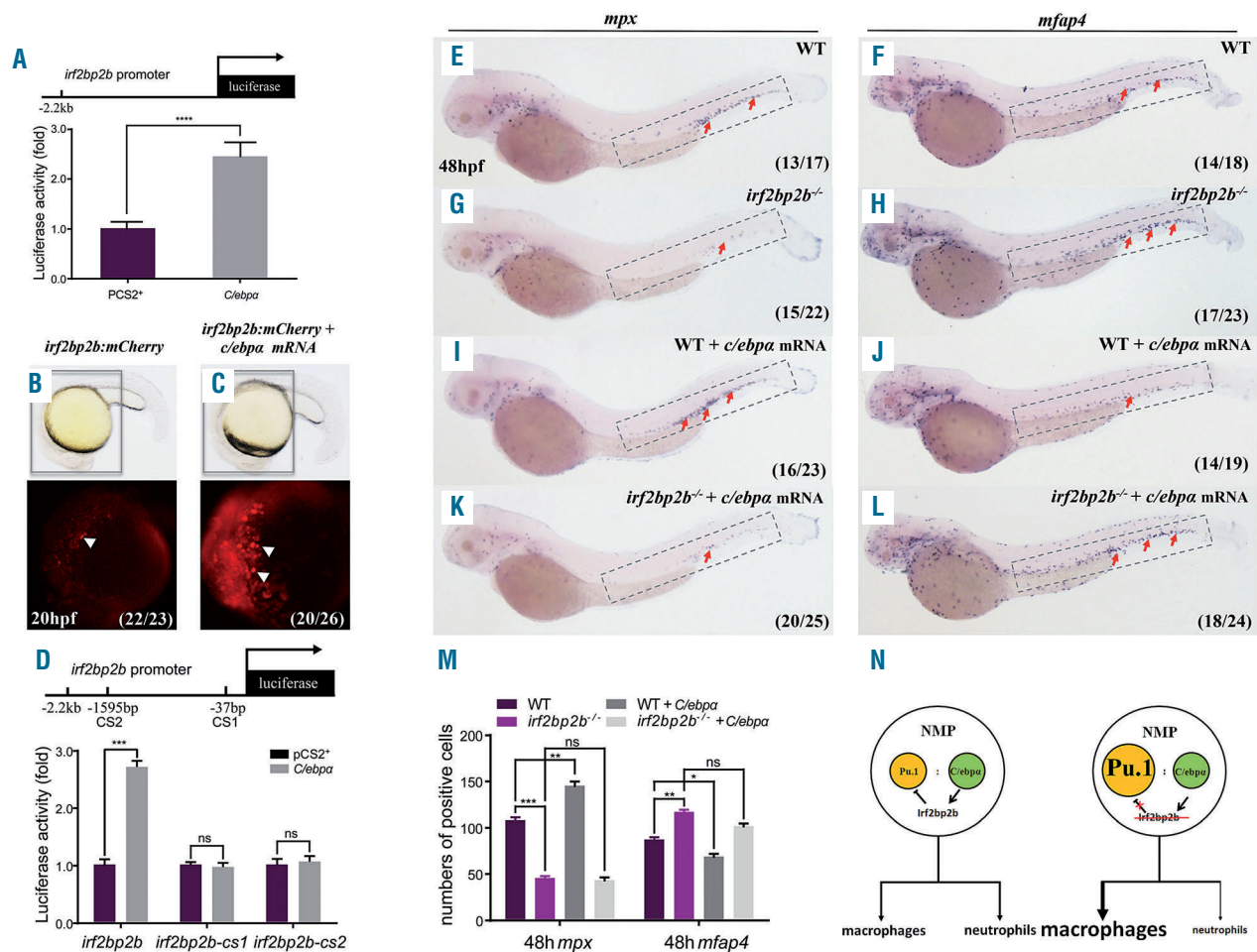


Figure 8. *Irf2bp2b* mediates the antagonistic effect of *C/ebpα* on *pu.1*. (A) Schematic diagram of the zebrafish *irf2bp2b* promoter (-2.2 kb) (top panel). *C/ebpα* activation on the *irf2bp2b* promoter was measured by a luciferase activity assay (bottom panel). Error bars represent the mean \pm standard deviation (SD) of at least three replicates. **** $P < 0.0001$ (Student t test). (B, C) Representative fluorescent images of transient mCherry expression at 20 hours post-fertilization (hpf) of wild-type (WT) and *c/ebpα*-overexpressing embryos injected with an *irf2bp2b*:mCherry construct (top panel). Corresponding bright field images (bottom panel). (D) Schematic diagram of the zebrafish *irf2bp2b* promoter (-2.2 kb), in which two putative *C/ebpα* binding sites are predicted (CS1, CS2) (top panel). Luciferase activity assays of *C/ebpα* activation on the *irf2bp2b* CS1 and CS2 mutant promoters (bottom panel). Data shown are the mean \pm SD of at least three independent experiments. Error bars represent the mean \pm SD of at least three replicates. *** $P < 0.001$ (Student t test). (E-L) *C/ebpα* mRNA overexpression in WT and *irf2bp2b*^{-/-} mutant embryos. *Mpx* and *mfap4* probes were used in whole-mount *in situ* hybridization analysis to investigate any rescue effect. (M) Statistical results for E-L. Error bars represent the mean \pm standard error of mean of 15-30 embryos. ns: not statistically significant; * $P < 0.1$; ** $P < 0.01$; *** $P < 0.001$ (analysis of variance followed by the least significant difference *post-hoc* test for multiple comparisons). (N) Schematic depiction of the regulation of neutrophil and macrophage fate in WT (left panel) and *irf2bp2b*^{-/-} (right panel) zebrafish.

protein-protein interaction.⁴⁶ In the present study, we determined that in the balance between granulocyte and macrophage commitment, zebrafish *irf2bp2b* acts as a direct target of C/ebp α to repress *pu.1* expression. Our data also suggest that during the stage of definitive myelopoiesis in zebrafish, it is the C/ebp α -Irf2bp2b-Pu.1 axis, not the C/ebp α -Gfi1-Pu.1 one, that regulates NMP cell fate. Thus zebrafish Irf2bp2b acts as a novel player in NMP cell fate decision and adds a new layer of complexity to this fine-tuning process.

It should be noted that the primitive macrophages and neutrophils developed normally in *irf2bp2b*-deficient embryos (Online Supplementary Figure S3C, D, G, H, K, L). Previously it was reported that a Pu.1-Runx1 negative feedback loop determines the macrophage *versus* neutrophil fate of cells originating in the rostral blood island.¹³ Runx1 was shown to inhibit the *pu.1* promoter directly in the study; however, injection of *runx1* mRNA into our *irf2bp2b*-deficient embryos could not rescue the aberrant myelopoiesis (Online Supplementary Figure S8G, I). To further elucidate whether *irf2bp2b* regulates primitive myeloid differentiation, we first determined whether *irf2bp2b* is present in primitive *versus* definitive progenitor cells (Online Supplementary Figure S9A). We then injected *irf2bp2b* mRNA into one-cell stage wildtype embryos. The biased myelopoiesis could only be observed in the ventral wall of the dorsal aorta at 48 hpf (Figure 3F-H). By contrast, *c/ebp1*, *lyz*, and *mfap4* were all normally expressed in the rostral blood island at 22 hpf (Online Supplementary Figure S9B-H). Based on these observations, we believe that even though *irf2bp2b* is expressed in both primitive and definitive myeloid progenitor cells, distinct regulatory mechanisms are implicated in cell fate determination of NMP derived from the ventral wall of the dorsal aorta/caudal hematopoietic tissue and the rostral blood island.

The DNA-binding properties of IRF2BP2 have never been studied. Although C4-type zinc fingers are found in Irf2bp2, GATA, RAR α , and RXR, there are still some differences. While a single C-X2-C-X17-C-X2-C type zinc finger exists in Irf2bp2, two consecutive ones are contained in GATA. RAR α and RXR have two C-X2-C-X13-C-X2-C type zinc fingers. GATA binds specifically to a consensus sequence.⁴⁷ Physiologically the RAR-RXR heterodimer binds to responsive elements that consist of two

AGGTCA core motifs.⁴⁸ To determine the binding site of Irf2bp2b within the *pu.1* promoter, we first investigated whether it was similar to that of GATA or RAR/RXR. Two putative GATA binding sites (GS1, GS2) were predicted within the 132 bp A region, whereas no RAR/RXR binding sites could be found. However, both GATA site deletion constructs could still be inhibited by Irf2bp2b (Online Supplementary Figure S10). Therefore, Irf2bp2b presumably has its own binding site.

The majority of APL patients bear a PML-RAR α fusion gene. However, in APL variants RAR α is fused with genes other than PML. Recently, four APL cases with a novel fusion, IRF2BP2-RAR α , were identified.²⁰⁻²³ All X-RAR α fusion-related APL are characterized by blockage at the promyelocyte stage and inhibition of a large set of differentiation-related genes targeted by co-repressors recruited onto the RAR α moiety.⁴⁹ It should be noted that the zinc finger motif of IRF2BP2 was intact in all four patients carrying the IRF2BP2-RAR α oncoprotein,²⁰⁻²³ thus two potential DNA-binding domains from each moiety are retained simultaneously in the fusion. Such a phenomenon is very rare in a chimeric fusion protein composed of two transcription factors. This raises a few questions about IRF2BP2-RAR α -related APL. Since dimerization is one of the prerequisites for all X-RAR α fusions,⁵⁰ does the IRF2BP2 moiety serve merely as an interface for dimerization of IRF2BP2-RAR α , or does IRF2BP2 make other contributions, such as DNA binding, to the pathogenesis of APL? Does IRF2BP2-RAR α arise at the NMP level? If it is expressed in NMP, could IRF2BP2-RAR α trigger the biased choice of NMP cell fate favoring granulopoiesis? Further studies are needed to answer these questions.

Acknowledgments

The authors are grateful to Y Chen and J Jin (both from Shanghai Jiao Tong University School of Medicine, Shanghai, China) for technical support. We thank Dr. X Jiao, Dr. Maria Mateyak, and Dr. Sunny Sharma (all from the Department of Cell Biology and Neuroscience, Rutgers University, Piscataway, NJ, USA) for their critical reading of this manuscript.

Funding

This work was supported by research funding from the National Natural Science Foundation of China (31871471).

References

- Evans T. Developmental biology of hematopoiesis. *Hematol Oncol Clin North Am.* 1997;11(6):1115-1147.
- Carrelha J, Meng Y, Kettyle LM, et al. Hierarchically related lineage-restricted fates of multipotent haematopoietic stem cells. *Nature.* 2018;554(7690):106-111.
- Gottgens B. Regulatory network control of blood stem cells. *Blood.* 2015;125(17):2614-2620.
- Yuan H, Zhou J, Deng M, et al. Sumoylation of CCAAT/enhancer-binding protein alpha promotes the biased primitive hematopoiesis of zebrafish. *Blood.* 2011;117(26):7014-7020.
- Laslo P, Spooner CJ, Warmflash A, et al. Multilineage transcriptional priming and determination of alternate hematopoietic cell fates. *Cell.* 2006;126(4):755-766.
- Dahl R, Walsh JC, Lancki D, et al. Regulation of macrophage and neutrophil cell fates by the PU.1:C/EBPalpha ratio and granulocyte colony-stimulating factor. *Nat Immunol.* 2003;4(10):1029-1036.
- Zhang DE, Zhang P, Wang ND, Hetherington CJ, Darlington GJ, Tenen DG. Absence of granulocyte colony-stimulating factor signaling and neutrophil development in CCAAT enhancer binding protein alpha-deficient mice. *Proc Natl Acad Sci U S A.* 1997;94(2):569-574.
- Scott EW, Simon MC, Anastasi J, Singh H. Requirement of transcription factor PU.1 in the development of multiple hematopoietic lineages. *Science.* 1994;265(5178):1573-1577.
- Hock H, Hamblen MJ, Rooke HM, et al. Intrinsic requirement for zinc finger transcription factor Gfi-1 in neutrophil differentiation. *Immunity.* 2003;18(1):109-120.
- Li L, Jin H, Xu J, Shi Y, Wen Z. Irf8 regulates macrophage versus neutrophil fate during zebrafish primitive myelopoiesis. *Blood.* 2011;117(4):1359-1369.
- Tamura T, Kurotaki D, Koizumi S. Regulation of myelopoiesis by the transcription factor IRF8. *Int J Hematol.* 2015;101(4):342-351.
- Kurotaki D, Yamamoto M, Nishiyama A, et al. IRF8 inhibits C/EBP α activity to restrain mononuclear phagocyte progenitors from differentiating into neutrophils. *Nat Commun.* 2014;5:4978.
- Jin H, Li L, Xu J, et al. Runx1 regulates embryonic myeloid fate choice in zebrafish through a negative feedback loop inhibiting Pu.1 expression. *Blood.* 2012;119(22):5239-5249.

14. Childs KS, Goodbourn S. Identification of novel co-repressor molecules for interferon regulatory factor-2. *Nucleic Acids Res.* 2003;31(12):3016-3026.
15. Yeung KT, Das S, Zhang J, et al. A novel transcription complex that selectively modulates apoptosis of breast cancer cells through regulation of FASTKD2. *Mol Cell Biol.* 2011;31(11):2287-2298.
16. Stadhouders R, Cico A, Stephen T, et al. Control of developmentally primed erythroid genes by combinatorial co-repressor actions. *Nat Commun.* 2015;6:8893.
17. Cameiro FR, Ramalho-Oliveira R, Mognol GP, Viola JP. Interferon regulatory factor 2 binding protein 2 is a new NFAT1 partner and represses its transcriptional activity. *Mol Cell Biol.* 2011;31(14):2889-2901.
18. Secca C, Faget DV, Hanschke SC, et al. IRF2BP2 transcriptional repressor restrains naive CD4 T cell activation and clonal expansion induced by TCR triggering. *J Leukoc Biol.* 2016;100(5):1081-1091.
19. Chen HH, Keyhanian K, Zhou X, et al. IRF2BP2 reduces macrophage inflammation and susceptibility to atherosclerosis. *Circ Res.* 2015;117(8):671-683.
20. Yin CC, Jain N, Mehrotra M, et al. Identification of a novel fusion gene, IRF2BP2-RARA, in acute promyelocytic leukemia. *J Natl Compr Canc Netw.* 2015;13(1):19-22.
21. Shimomura Y, Mitsui H, Yamashita Y, et al. New variant of acute promyelocytic leukemia with IRF2BP2-RARA fusion. *Cancer Sci.* 2016;107(8):1165-1168.
22. Jovanovic JV, Chillon MC, Vincent-Fabert C, et al. The cryptic IRF2BP2-RARA fusion transforms hematopoietic stem/progenitor cells and induces retinoid-sensitive acute promyelocytic leukemia. *Leukemia.* 2017;31(3):747-751.
23. Mazharuddin S, Chattopadhyay A, Levy MY, Redner RL. IRF2BP2-RARA t(1;17)(q42.3;q21.2) APL blasts differentiate in response to all-trans retinoic acid. *Leuk Lymphoma.* 2018;59(9):2246-2249.
24. Kimmel CB, Ballard WW, Kimmel SR, Ullmann B, Schilling TF. Stages of embryonic development of the zebrafish. *Dev Dyn.* 1995;203(3):253-310.
25. Thisse C, Thisse B. High-resolution in situ hybridization to whole-mount zebrafish embryos. *Nat Protoc.* 2008;3(1):59-69.
26. Teng AC, Kuraitis D, Deeke SA, et al. IRF2BP2 is a skeletal and cardiac muscle-enriched ischemia-inducible activator of VEGFA expression. *FASEB J.* 2010;24(12):4825-4834.
27. Gore AV, Pillay LM, Venero Galanternik M, Weinstein BM. The zebrafish: a fantastic model for hematopoietic development and disease. *Wiley Interdiscip Rev Dev Biol.* 2018;7(3):e312.
28. Teng AC, Al-Montashiri NA, Cheng BL, et al. Identification of a phosphorylation-dependent nuclear localization motif in interferon regulatory factor 2 binding protein 2. *PLoS One.* 2011;6(8):e24100.
29. Lektrom-Himes J, Xanthopoulos KG. CCAAT/enhancer binding protein epsilon is critical for effective neutrophil-mediated response to inflammatory challenge. *Blood.* 1999;93(9):3096-3105.
30. Meijer AH, van der Sar AM, Cunha C, et al. Identification and real-time imaging of a myc-expressing neutrophil population involved in inflammation and mycobacterial granuloma formation in zebrafish. *Dev Comp Immunol.* 2008;32(1):36-49.
31. Zakrzewska A, Cui C, Stockhammer OW, Benard EL, Spaink HP, Meijer AH. Macrophage-specific gene functions in Spi1-directed innate immunity. *Blood.* 2010;116(3):e1-11.
32. Spilsbury K, O'Mara MA, Wu WM, Rowe PB, Symonds G, Takayama Y. Isolation of a novel macrophage-specific gene by differential cDNA analysis. *Blood.* 1995;85(6):1620-1629.
33. Le Guyader D, Redd MJ, Colucci-Guyon E, et al. Origins and unconventional behavior of neutrophils in developing zebrafish. *Blood.* 2008;111(1):132-141.
34. Nutt SL, Metcalf D, D'Amico A, Polli M, Wu L. Dynamic regulation of PU.1 expression in multipotent hematopoietic progenitors. *J Exp Med.* 2005;201(2):221-231.
35. Avellino R, Delwel R. Expression and regulation of C/EBP α in normal myelopoiesis and in malignant transformation. *Blood.* 2017;129(15):2083-2091.
36. Vonderfecht TR, Schroyer DC, Schenck BL, McDonough VM, Pikaart MJ. Substitution of DNA-contacting amino acids with functional variants in the Gata-1 zinc finger: a structurally and phylogenetically guided mutagenesis. *Biochem Biophys Res Commun.* 2008;369(4):1052-1056.
37. Urnov FD. A feel for the template: zinc finger protein transcription factors and chromatin. *Biochem Cell Biol.* 2002;80(3):321-333.
38. Han ZJ, Feng YH, Gu BH, Li YM, Chen H. The post-translational modification, SUMOylation, and cancer. *Int J Oncol.* 2018;52(4):1081-1094.
39. Garcia-Dominguez M, Reyes JC. SUMO association with repressor complexes, emerging routes for transcriptional control. *Biochim Biophys Acta.* 2009;1789(6-8):451-459.
40. Rodriguez MS, Dargemont C, Hay RT. SUMO-1 conjugation in vivo requires both a consensus modification motif and nuclear targeting. *J Biol Chem.* 2001;276(16):12654-12659.
41. Weston BR, Li L, Tyson JJ. Mathematical analysis of cytokine-induced differentiation of granulocyte-monocyte progenitor cells. *Front Immunol.* 2018;9:2048.
42. Kummalue T, Friedman AD. Cross-talk between regulators of myeloid development: C/EBP α binds and activates the promoter of the PU.1 gene. *J Leukoc Biol.* 2003;74(3):464-470.
43. Yeamans C, Wang D, Paz-Priel I, Torbett BE, Tenen DG, Friedman AD. C/EBP α binds and activates the PU.1 distal enhancer to induce monocyte lineage commitment. *Blood.* 2007;110(9):3136-3142.
44. Lidonnici MR, Audia A, Soliera AR, et al. Expression of the transcriptional repressor Gfi-1 is regulated by C/EBP α and is involved in its proliferation and colony formation-inhibitory effects in p210BCR/ABL-expressing cells. *Cancer Res.* 2010;70(20):7949-7959.
45. Reddy VA, Iwama A, Iotzova G, et al. Granulocyte inducer C/EBP α inactivates the myeloid master regulator PU.1: possible role in lineage commitment decisions. *Blood.* 2002;100(2):483-490.
46. Dahl R, Iyer SR, Owens KS, Cuylear DD, Simon MC. The transcriptional repressor GFI-1 antagonizes PU.1 activity through protein-protein interaction. *J Biol Chem.* 2007;282(9):6473-6483.
47. Trainor CD, Omichinski JG, Vandergon TL, Gronenborn AM, Clore GM, Felsenfeld G. A palindromic regulatory site within vertebrate GATA-1 promoters requires both zinc fingers of the GATA-1 DNA-binding domain for high-affinity interaction. *Mol Cell Biol.* 1996;16(5):2238-2247.
48. de The H, Vivanco-Ruiz MM, Tiollais P, Stunnenberg H, Dejean A. Identification of a retinoic acid responsive element in the retinoic acid receptor beta gene. *Nature.* 1990;343(6254):177-180.
49. de The H, Pandolfi PP, Chen Z. Acute promyelocytic leukemia: a paradigm for oncoprotein-targeted cure. *Cancer Cell.* 2017;32(5):552-560.
50. Zhou J, Peres L, Honore N, Nasr R, Zhu J, de The H. Dimerization-induced corepressor binding and relaxed DNA-binding specificity are critical for PML/RARA-induced immortalization. *Proc Natl Acad Sci U S A.* 2006;103(24):9238-9243.



Ferrata Storti Foundation

Density, heterogeneity and deformability of red cells as markers of clinical severity in hereditary spherocytosis

Rick Huisjes,¹ Asya Makhro,² Esther Llaudet-Planas,³ Laura Hertz,⁴ Polina Petkova-Kirova,⁴ Liesbeth P. Verhagen,¹ Silvia Pignatelli,¹ Minke A.E. Rab,¹ Raymond M. Schifflers,¹ Elena Seiler,² Wouter W. van Solinge,¹ Joan-LLuis Vives Corrons,³ Lars Kaestner,^{4,5} Maria Mañú-Pereira,⁶ Anna Bogdanov² and Richard van Wijk¹

Haematologica 2020
Volume 105(2):338-347

¹Department of Clinical Chemistry and Hematology, University Medical Center Utrecht, Utrecht University, Utrecht, the Netherlands; ²Red Blood Cell Research Group, Institute of Veterinary Physiology, Vetsuisse Faculty and the Zurich Center for Integrative Human Physiology (ZIHP), University of Zurich, Zurich, Switzerland; ³Red Blood Cell Defects and Hematopoietic Disorders Unit, Josep Carreras Leukemia Research Institute, Badalona, Barcelona, Spain; ⁴Theoretical Medicine and Biosciences, Medical Faculty, Saarland University, Homburg/Saar, Germany; ⁵Experimental Physics, Saarland University, Saarbruecken, Germany and ⁶Rare Anemia Research Unit, Vall d'Hebron Research Institution, University Hospital Vall d'Hebron, Barcelona, Spain

ABSTRACT

Hereditary spherocytosis (HS) originates from defective anchoring of the cytoskeletal network to the transmembrane protein complexes of the red blood cell (RBC). Red cells in HS are characterized by membrane instability and reduced deformability and there is marked heterogeneity in disease severity among patients. To unravel this variability in disease severity, we analyzed blood samples from 21 HS patients with defects in ankyrin, band 3, α -spectrin or β -spectrin using red cell indices, eosin-5-maleimide binding, microscopy, the osmotic fragility test, Percoll density gradients, vesiculation and ektacytometry to assess cell membrane stability, cellular density and deformability. Reticulocyte counts, CD71 abundance, band 4.1 a:b ratio, and glycated hemoglobin were used as markers of RBC turnover. We observed that patients with moderate/severe spherocytosis have short-living erythrocytes of low density and abnormally high intercellular heterogeneity. These cells show a prominent decrease in membrane stability and deformability and, as a consequence, are quickly removed from the circulation by the spleen. In contrast, in mild spherocytosis less pronounced reduction in deformability results in prolonged RBC lifespan and, hence, cells are subject to progressive loss of membrane. RBC from patients with mild spherocytosis thus become denser before they are taken up by the spleen. Based on our findings, we conclude that RBC membrane loss, cellular heterogeneity and density are strong markers of clinical severity in spherocytosis.

Correspondence:

RICHARD VAN WIJK
r.vanWijk@umcutrecht.nl

Received: April 3, 2018.

Accepted: May 28, 2019.

Pre-published: May 30, 2019.

doi:10.3324/haematol.2018.188151

Check the online version for the most updated information on this article, online supplements, and information on authorship & disclosures: www.haematologica.org/content/105/2/338

©2020 Ferrata Storti Foundation

Material published in *Haematologica* is covered by copyright. All rights are reserved to the Ferrata Storti Foundation. Use of published material is allowed under the following terms and conditions:

<https://creativecommons.org/licenses/by-nc/4.0/legalcode>.

Copies of published material are allowed for personal or internal use. Sharing published material for non-commercial purposes is subject to the following conditions:

<https://creativecommons.org/licenses/by-nc/4.0/legalcode>,

sect. 3. Reproducing and sharing published material for commercial purposes is not allowed without permission in writing from the publisher.



Introduction

Hereditary spherocytosis (HS) is the most common form of chronic hereditary hemolytic anemia in the Caucasian population, with an estimated prevalence of 1:2000 – 1:5000.¹⁻³ HS usually originates from mutations in *ANK1* (ankyrin), *SLC4A1* (band 3), *SPTA1* (α -spectrin), *SPTB* (β -spectrin) or *EPB42* (protein 4.2).¹ Anemia in HS may require transfusion(s) and in severe cases splenectomy. A characteristic feature of HS is red blood cell (RBC) membrane instability, which leads to membrane loss and formation of dense cells with reduced RBC deformability.⁴⁻⁶ Increased RBC density is an important feature of HS⁷ and is reflected, for example, by increased mean corpuscular hemoglobin concentration (MCHC).^{8,9}

HS is a very heterogeneous RBC disorder, resulting from a wide range of molecular defects and characterized by a high degree of heterogeneity in RBC properties and disease severity.⁸⁻¹² In fact, considerable differences in disease severity are reported even between HS patients with identical mutations. It therefore seems rea-

sonable to assume that the heterogeneity in disease severity is not only a reflection of particular genotypes but is also affected by other factors that control RBC properties.

Healthy RBC become increasingly dense during their lifespan,^{13,14} but this process is accelerated in HS.¹ Shedding of essentially hemoglobin-free vesicles results in an increase in MCHC and a corresponding increase in RBC density and intracellular viscosity.^{13,15} Electrogenic potassium leakage also contributes to RBC dehydration in HS patients and is not compensated by an accumulation of Na⁺.^{16,17} As a result, the intracellular K⁺ concentration in the RBC of HS patients is approximately 13 mmol/L lower than that in the cells of healthy subjects,¹⁶ which results in net ion and water loss. Compensatory activation of Na,K-ATPase in the RBC of patients is insufficient to prevent the loss of K⁺ and dissipation of K⁺/Na⁺ gradients. The function of other electroneutral ion transporters (KCC, NKCC, Na/Li exchanger) in RBC of HS patients was reported to be indistinguishable from that of cells of healthy controls.^{16,18}

In this study, we investigated a unique and genetically well-diagnosed group of HS patients in whom we performed an in-depth analysis of RBC properties, such as membrane instability, cellular density, cellular heterogeneity, vesiculation, turnover and lifespan. The data obtained were then correlated to clinical manifestations of HS in both non-splenectomized and splenectomized patients, in order to identify markers of disease severity. Our results indicate that clinical severity in HS cannot be solely attributed to the protein harboring the mutation, but rather to the stability of the whole cytoskeletal network. RBC density, heterogeneity and deformability were identified as potential markers of severity. We found that the presence of dense RBC is strongly associated with milder manifestations of HS. We hypothesize that unstable RBC from patients with clinically more severe disease are removed from the circulation before they acquire the features of senescence.

Methods

Subjects

Patients previously diagnosed with HS were enrolled in the CoMMiTMenT-study (<http://www.rare-anaemia.eu/>). This study was approved by the Medical Ethical Research Board of the University Medical Center Utrecht, the Netherlands, under reference code 15/426M and by the Ethical Committee of Clinical Investigations of Hospital Clinic, Spain, (IDIBAPS) under reference code 2013/8436.

Hemocytometry analysis

Hemocytometry parameters were analyzed on an Abbott Sapphire cell analyzer (Abbott Diagnostics Division, Santa Clara, CA, USA) and ADVIA 2120 (Hematology System, Siemens Healthcare Diagnostics, Forchheim, Germany).

Capillary-based measurements of mean corpuscular volume and mean corpuscular hemoglobin concentration

Triplicate heparinized blood samples were put in capillaries and centrifuged for 5 min at 12,000 rpm (Hematocrit 20, Hettich Zentrifugen). Mean corpuscular volume (MCV) was calculated using the formula $MCV = \text{hematocrit}/\text{RBC number}$. MCHC was calculated using the formula $MCHC = \text{hemoglobin}/\text{hematocrit}$.

Separation on a Percoll density gradient and determination of intracellular potassium levels

Intact blood samples were layered over a 90% isotonic Percoll solution containing plasma-like components as described elsewhere.¹⁹ Briefly, Percoll density gradient and RBC separation were performed during centrifugation at 50,000 *g* for 15 min. (Sorvall RC 5C plus, rotor SM-24). Intracellular potassium was measured using an Instrumentation Laboratory IL943 Flame Photometer, as described by Jokinen *et al.*²⁰

Osmotic gradient ektacytometry, the osmotic fragility test and eosin-5-maleimide binding

Osmotic gradient ektacytometry measurements of RBC from healthy controls and HS patients were obtained using the Osmoscan module on a Lorrca MaxSis (Mechatronics, The Zwaag, the Netherlands) as described elsewhere.^{5,21} The osmotic fragility test was carried out as previously described by Parpart *et al.*²² and eosin-5-maleimide (EMA) binding was determined according to previously published protocols.^{12,23}

Red blood cell production, heterogeneity, vesiculation and turnover rate markers

RBC were stained with anti-CD71 and isotype controls and were subsequently measured using a BD FACS Gallios.²⁴ Measuring glycosylated hemoglobin (HbA1c) is an established way to acquire information about RBC clearance and RBC age in research on hemolytic anemias.^{15,25} HbA1c levels were measured using a Menarini/ARKRAY HA-8180V. The band 4.1a:b ratio was detected in RBC membrane lysates after protein separation by inverse sodium dodecylsulfate polyacrylamide gel electrophoresis (SDS-PAGE) (15-7.5%) and visualization of protein bands using Coomassie blue staining. RBC projected area and its heterogeneity were evaluated by microscopy as described elsewhere.^{26,27} RBC vesicles were identified in plasma preserved with citrate-phosphate-dextrose-adenine¹⁹ by staining them with mouse anti-human CD235a-APC and measured using a Beckman Coulter CytoFLEX flow cytometer (*Online Supplementary Figure S1*).

Statistical analysis and phenotype correlations

One-way analysis of variance with *post-hoc* correction (Tukey test) was used to compare sample means and the Fisher exact test was applied to determine whether clinical severity was proportionally distributed along the different genotypes. In non-splenectomized patients, clinical severity was assessed based on: (i) hemoglobin concentration and (ii) reticulocyte count, as previously defined by Bolton-Maggs *et al.*¹¹ (i.e., mild and moderate/severe). To prevent any confounding by splenectomized patients, phenotype correlations were only carried out for unsplenectomized HS patients.

Results

Baseline characteristics and red cell features of patients with hereditary spherocytosis

Twenty-one patients with HS were included in this study and categorized according to clinical severity (Table 1).¹¹ HS was confirmed by targeted next-generation sequencing of the seven genes most commonly mutated in HS²⁸. Splenectomy or a moderate/severe expression of disease was statistically overrepresented in patients with mutations in *ANK1* and *SPTB* ($P < 0.05$). Therefore, the phenotypic expression of HS due to *ANK1* and *SPTB* mutations appears to be more severe than that of HS due to *SLC4A1* and/or *SPTA1* defects. Decreased EMA stain-

ing, reflecting band 3 protein loss, was seen in all patients. Patients with *SPTA1* mutations tended to have greater EMA staining (Figure 1A), although the number of patients was too low to draw firm conclusions. The maximal deformability of RBC, reflected by a decrease in maximal elongation index (EI_{max}) as determined by the Osmoscan, was decreased in all HS patients compared to that in healthy controls. This decrease was more pronounced in patients with *ANK1* and *SPTB* mutations than in patients with mutations in *SPTA* or *SCL4A1* (Figure 1B). On the other hand, cells from patients with *SLC4A1* mutations tended to be more dehydrated as their O_{hyper} values (hypertonic osmolarity at 50% of EI_{max}) were lower than those in both control blood samples and patients with *SPTA1* mutations (Figure 1C). The latter patients also showed the least pronounced loss of surface area-to-volume ratio, reflected by a normal O_{min} (hypotonic osmolarity where EI is minimal) (Figure 1D) on the Osmoscan and normal results in the osmotic fragility test

(50% lysis point) (Figure 1E). Membrane stability was compromised in all other HS patients.

As expected, RBC turnover was increased in all patients: reticulocyte counts were high (Table 1) and the band 4.1a:b ratio, a marker of aging, was lower in all patients than in healthy controls (Table 1).

The heterogeneity of the RBC, reflected by the red blood cell distribution width (RDW), was greater in patients with HS than in healthy controls (Figure 1F) as was the MCHC (Figure 1G). Intracellular K^+ content was reduced in all patients but tended to be higher in HS patients with *SPTA1* mutations (Figure 1H).

An increase in heterogeneity in cell projected areas (mean projected area distribution width, MPA DW) (Figure 2A) and a decrease in absolute mean values in projected area (MPA) (Figure 2B) were seen in all HS patients compared to those in controls. Patients with *SLC4A1* and *SPTA1* mutations had cellular projected areas more similar to those of the healthy control group (Figure 2A, B).

Table 1. Hemocytometry, chemistry parameters, cell-age markers and genotypes of patients with mild or moderate/severe hereditary spherocytosis (HS) and splenectomized HS patients included in this study.

N.	Sex	Age (years)	Genotype	Hb (g/dL)	RBC (10^{12} /L)	Hct (%)	MCV (fL)	Ret (%)	MCHC (g/L)	RDW (%CV)	EMA (%)	O _{min} (mOsmo/l/L)	EI _{max} (A.U.)	O _{hyper} (mOsmo/l/L)	OFT (g/L NaCl)	Band 4.1/4.2 ratio (A.U.)	CD71 (%)
Mild HS¹¹																	
1	♂	75	<i>ANK1</i> c.344T>C p.Leu115Pro	136	4.1	n.a.	n.a.	7.2	n.a.	16.2	85	162	0.555	457	7.0	0.70	0.8
2	♂	46	<i>SLC4A1</i> c.1030C>T p.Arg344*	153	4.7	n.a.	n.a.	3.2	n.a.	15.2	71	163	0.563	417	6.6	0.87	1.4
3	♂	40	<i>SLC4A1</i> c.1421C>A p.Ala474Asp	140	4.9	n.a.	n.a.	4.0	n.a.	12.3	93	162	0.557	427	5.7	0.99	1.2
4	♀	55	<i>SLC4A1</i> c.2057+1G>A (splicing)	136	4.0	36.5	91.1	7.8	372	14.0	73	158	0.554	405	6.4	0.82	2.7
5	♀	18	<i>SLC4A1</i> c.2057+1G>A (splicing)	131	3.7	35.7	96.9	9.4	367	13.1	77	166	0.569	410	6.1	0.84	1.4
6	♂	58	<i>SLC4A1</i> c.2348T>A p.Ile783Asn	132	4.1	36.5	88.4	8.9	363	15.7	68	169	0.548	429	6.8	n.a.	3.5
7	♂	40	<i>SPTA1</i> c.678G>A p.Glu227fs + α^{LELY}	127	4.1	35.9	87.8	5.8	355	15.0	94	175	0.600	453	5.6	0.84	0.9
8	♂	54	<i>SPTA1</i> c.[4339-99C>T; c.4347G>T] p.[(?; Lys1449Asn)]; c.4339-99C>T p.(?)	121	3.5	34.7	98.3	3.9	348	15.3	94	160	0.566	458	5.7	n.a.	0.9
Moderate/severe HS¹¹																	
9	♂	4	<i>ANK1</i> c.341C>T p.Pro114Leu	116	3.8	30.0	80.1	9.1	386	14.5	72	162	0.509	398	6.6	0.72	2.2
10	♀	3	<i>ANK1</i> c.1943delC p.Ala648fs	117	4.02	36.3	90.4	11.9	321	21.1	59	164	0.503	424	6.6	n.a.	0.2
11	♂	5	<i>ANK1</i> c.2394_2397delCAGT p.Ser799fs	120	4.1	32.2	78.6	18.4	372	25.4	67	185	0.472	462	7.8	n.a.	7.3
12	♀	26	<i>ANK1</i> c.2559-2A>G (splicing)	102	3.3	29.4	89.5	18.3	346	24.1	84	170	0.537	446	6.4	0.60	5.3
13	♂	1	<i>SPTB</i> c.154delC p.Arg52fs	86	3.38	30.2	89.5	11.9	284	24.7	66	168	0.532	456	5.7	n.a.	4.8
14	♂	3	<i>SPTB</i> c.2470C>T p.Gln824*	78	2.9	23.7	81.9	10.6	328	23.8	71	180	0.534	475	6.7	n.a.	2.9
15	♂	4	<i>SPTB</i> c.5937+1G>A p.(?)	84	3.09	27.7	89.7	16.7	303	23.4	74	173	0.541	459	7.0	n.a.	5.5
16	♀	42	<i>SPTA1</i> c.2755G>T p.Glu919* + α^{LELY}	113	3.5	31.7	91.8	8.2	355	16.0	89	178	0.567	471	5.9	n.a.	2.1
Splenectomized HS¹¹																	
17	♂	31	<i>ANK1</i> c.341C>T p.Pro114Leu	152	4.9	84.7	41.9	8.4	362	11.8	76	179	0.533	437	7.4	1.08	0.1
18	♀	46	<i>ANK1</i> c.344T>C p.Leu115Pro	143	4.6	n.a.	n.a.	2.8	n.a.	12.4	74	158	0.590	423	7.4	1.18	0.2
19	♀	84	<i>SLC4A1</i> c.2057+1G>A (splicing)	160	4.8	121.8	45.1	12.6	354	11.0	67	164	0.565	417	7.1	1.07	0.2
20	♂	71	<i>SPTB</i> c.2136_2137delinsTT	164	4.84	100.9	48.8	2.2	337	13.2	77	173	0.509	445	7.3	0.99	0.3
21	♂	40	<i>SPTB</i> c.3449G>A p.Trp1150*	163	4.94	92.0	45.5	12.2	359	11.9	73	183	0.512	440	7.8	1.22	0.3

Clinical severity in non-splenectomized HS patients was assigned according to Bolton-Maggs *et al.*¹¹ on the basis of (i) hemoglobin concentration and (ii) reticulocyte count. Mild HS was defined as hemoglobin levels between 110–150 g/L, moderate HS as hemoglobin levels between 80–120 g/L and severe HS as hemoglobin levels lower than 80 g/L. HS patients with hemoglobin levels between 110 and 120 g/L were categorized as having mild or moderate disease on the basis of their reticulocyte levels (i.e., lower or higher than 6% reticulocytes). Novel mutations are displayed in bold font and the pathogenicity of novel missense variants was predicted with SIFT, PolyPhen-2, and MutationTaster (results not shown). Notation of α^{LELY} represents *SPTA1* c.[5572C>G; 6531-12C>T] p.[(Leu1858Val);(?)]. N: number; Hb: hemoglobin; RBC: red blood cells; Hct: hematocrit; MCV: mean corpuscular volume; Ret: reticulocytes; MCHC: mean corpuscular hemoglobin concentration; RDW: red cell distribution width; EMA: eosin-5'-maleimide; %CV: percent coefficient of variation; HS: hereditary spherocytosis; n.a.: not available.

Patients with HS presented with greater heterogeneity in cell density compared with healthy subjects, showing more subfractions of the M fraction and a broader distribution width of the M fraction (Figure 2C-E). These changes were more pronounced in patients with mutations in *ANK1* and *SPTA1*. Furthermore, the M fraction of patients with *SLC4A1* mutations was lower than that of healthy controls or other HS patients (Figure 2F, *Online Supplementary Figure S2*).

In summary, specific changes were observed in parameters associated with membrane stability, stiffness and deformability, as well as RBC heterogeneity in our cohort of HS patients.

Red blood cell markers of severity of hereditary spherocytosis

As described in Table 1, the severity of HS in non-splenectomized patients was determined based on the

decrease in hemoglobin concentration and increase in reticulocyte count.¹¹ In our patients hemoglobin concentration correlated positively with MCHC (Figure 3A). Inverse correlations were observed between hemoglobin and RDW (Figure 3B), and between hemoglobin and reticulocyte count (Figure 3C). Furthermore, inverse correlations were observed between hemoglobin and parameters defining RBC hydration status such as intracellular K^+ and O_{hyper} (Figure 3D, E).

Decreases in RBC lifespan were assessed by a reduction in changes in HbA1c in non-splenectomized patients with severe HS, whereas in patients with mild disease manifestations or in splenectomized patients HbA1c levels were within the normal range (Figure 4A).

Patients with moderate/severe HS had less deformable RBC, reflected by lower EI_{max} values, than patients with mild HS or splenectomized patients (Figure 4B). The RBC of patients with mild HS also tended to be more

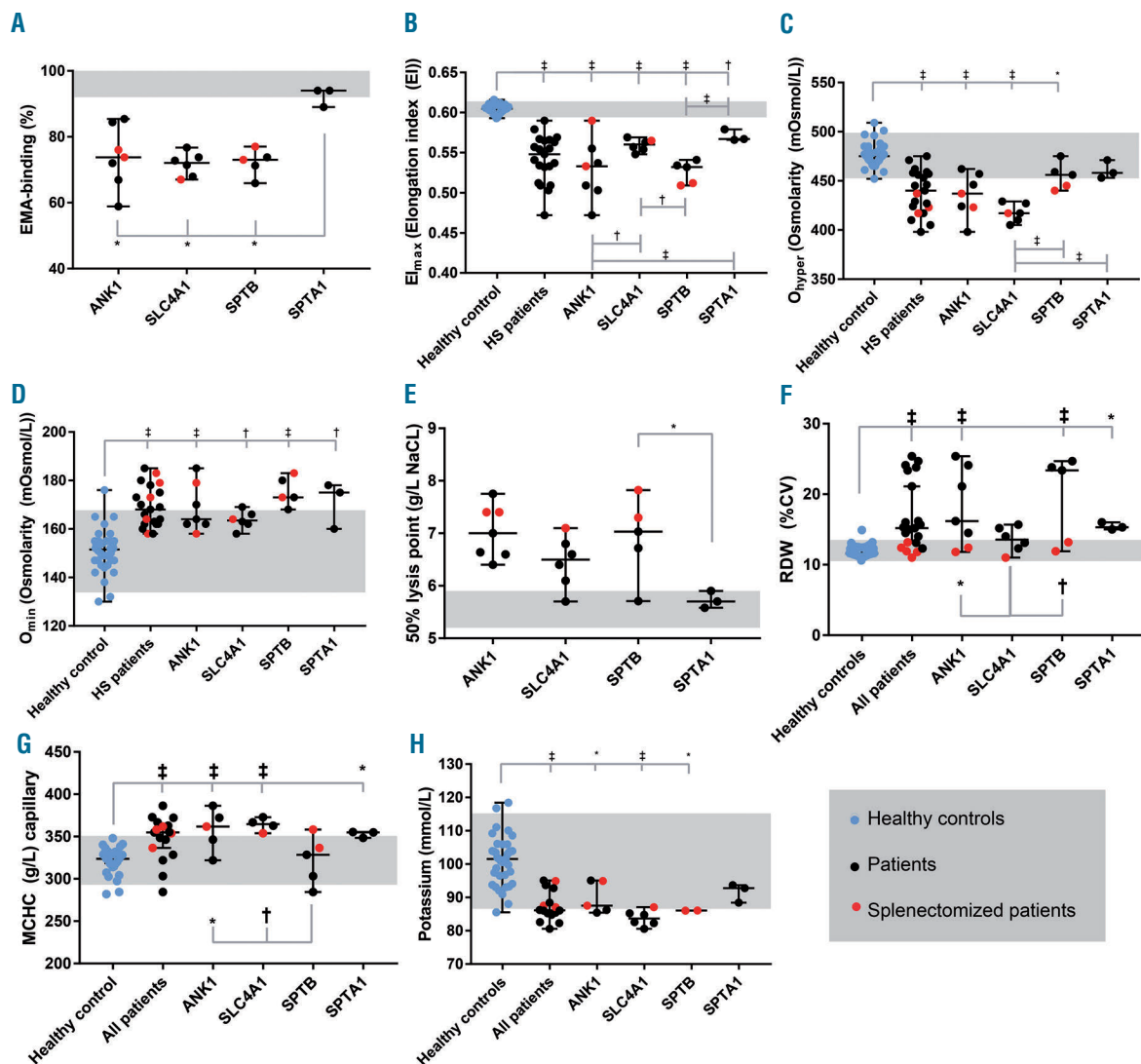


Figure 1. Basic characteristics (median \pm range) of healthy controls and patients with hereditary spherocytosis. Patients with hereditary spherocytosis (HS) were grouped as a whole and according to their affected genes [*ANK1* (ankyrin), *SLC4A1* (band 3), *SPTB* (β -spectrin) and *SPTA1* (α -spectrin)]. Blue circles represent healthy controls, black circles represent unsplenectomized HS patients and red circles represent splenectomized HS patients. The gray range indicates the reference range for healthy controls. (A) Eosin-5'-maleimide (EMA)-binding (%), (B) maximum deformability (EI_{max}), (C) hydration state of the red blood cells reflected by O_{hyper} , (D) osmotic fragility measured by osmotic gradient ektacytometry and reflected by O_{min} , (E) 50% lysis point in the osmotic fragility test, (F) red blood cell distribution width (RDW) (percent coefficient of variation, %CV), (G) mean corpuscular hemoglobin concentration (MCHC) by capillary measurements (g/L) (%CV), (H) intracellular potassium (mmol/L). Significant differences are depicted with horizontal bars, and significance levels are noted: * $P \leq 0.05$, † $P \leq 0.01$ or ‡ $P \leq 0.001$.

dehydrated, based on the O_{hyper} measurements (Figure 4C). In line with this, patients with mild HS showed higher MCHC values than moderately/severely affected patients (Figure 4D) and had a higher density of the M fraction, based on this latter's position within the Percoll gradient (Figure 4E, *Online Supplementary Figure S2*).

Based on reduced MPA, membrane loss was more pronounced in patients with moderate/severe HS (Figure 4F). In line with this, the number of RBC vesicles detected in the plasma of patients with moderate/severe HS was higher than that in patients with mild HS (Figure 4G). However, no difference in EMA staining was observed between patients with mild or moderate/severe HS (Figure 4C). Intercellular heterogeneity (RDW and MPA DW) was increased in patients with moderate/severe HS compared to those with mild HS and healthy controls (Figure 4I, J).

In summary, the RBC of patients with more severe expression of the disease had a reduced lifespan and less stable membrane. Their cells were smaller and more heterogeneous in size and density. Strikingly, patients with mild HS had denser RBC with higher MCHC (Figure 4D, E).

Effect of splenectomy on red blood cell markers of disease severity

Performed in patients with moderate/severe HS,

splenectomy results in an increase in hemoglobin levels and erythrocyte counts (*data not shown*). In our cohort splenectomy was also associated with a decrease in RDW (Figure 5A) and normalization of RBC morphology (*Online Supplementary Figures S3 and S4*). The survival of RBC from splenectomized HS patients, as assessed by HbA1c content or band 4.1a:b ratio, was found to be increased (Figure 5B, C).

Several parameters remained unaffected by splenectomy. Splenectomy did not alter MCHC (Figure D) or intracellular K^+ levels (Figure 5E) and did not correct band 3 loss (Figure 5F). It also did not affect deformability (no effect on El_{max} or O_{hyper}) (Figure 5G, H). However, the cells did survive for a longer time in the circulation despite an increase in osmotic fragility (Figure 5I).

Discussion

This comprehensive study in a well-characterized cohort of patients offers insight into the variable phenotypic manifestations of HS, possible causes of clinical heterogeneity and severity, and the impact of splenectomy. We show here that strong markers of moderate/severe expression of HS are: (i) lower RBC density, reflected by differences in MCHC and fractionation of RBC on the Percoll density gradient; (ii) reduced RBC deformability

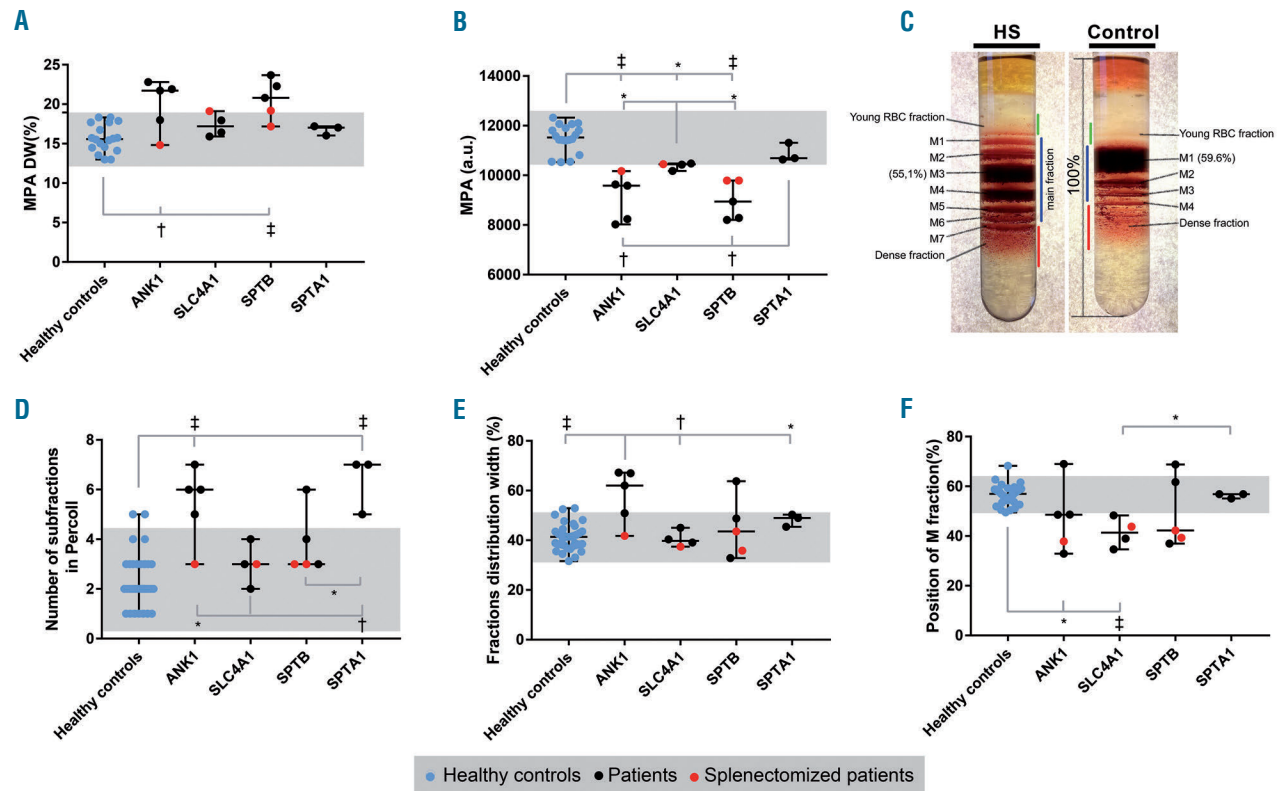


Figure 2. Red blood cell heterogeneity in hereditary spherocytosis. Red blood cell (RBC) heterogeneity was measured in healthy controls and patients with hereditary spherocytosis (HS) by microscopy (A, B) and Percoll density gradients (C-F). HS patients were grouped according to their affected genes [*ANK1* (ankyrin), *SLC4A1* (band 3), *SPTB* (β -spectrin) and *SPTA1* (α -spectrin)]. (A) Mean projected area distribution width (MPA DW). (B) Mean projected area (MPA). (C) An example of a blood sample from a patient with HS and a healthy control. On the samples the young RBC fraction, the main RBC fraction (M fraction) and dense RBC fractions are designated with green, blue and red lines, respectively. The M fraction is subdivided into subfractions (M1, M2, etc.). The position of the M fraction is calculated from the position of the most intense (*n* arbitrary units, a.u.) subfraction relative to the total length of the Percoll column. The HS patient has seven RBC subfractions, and the position of the most intense subfraction (i.e. subfraction M3) is lower than in the control subject (i.e. subfraction M1). (D) The number of subfractions in the RBC density gradient. (E) Fraction distribution width (%). (F) Position of the M fraction (%). Significant differences are noted: * $P \leq 0.05$, † $P \leq 0.01$ or ‡ $P \leq 0.001$.

and increased membrane loss, as determined by RBC vesicle numbers and a decrease in MPA; and (iii) heterogeneity in the RBC population reflected by differences in RDW and fractionation of RBC using a Percoll gradient.

We conclude that patients with moderate/severe HS have short-lived RBC of lower density and abnormally high intercellular heterogeneity, whereas patients with mild HS have a less pronounced reduction in RBC deformability resulting in the cells living longer and being subject to progressive loss of membrane. RBC from patients with mild HS thus become denser before they are taken up by the spleen.

Genotype to phenotype correlations in hereditary spherocytosis

While previous studies were limited to protein analysis by SDS-PAGE,¹² we used next-generation sequencing to establish the cause of HS. This enabled us to define the primary genetic defect unequivocally, in contrast to other conventional techniques such as SDS-PAGE, which may lead to confounding results as it may be influenced by secondary protein defects in HS. Regardless of the underlying mutation, all patients shared common features such as increases in reticulocyte counts and MCHC, dehydration and increases of RBC density and heterogeneity and an overall reduction in deformability of the RBC due to destabilization of cytoskeletal structures.^{1,29} We also observed that red cell size, intracellular K^+ content and reticulocyte counts did not differ between patients with *SLC4A1*, *ANK1*, *SPTB* and *SPTA1* mutations (Figures 1H and 2B, Table 1). Within one group of patients with the same mutated protein we noted marked differences in severity and clinical manifestations of the disease, with the *ANK1* group showing the greatest diversity. We also

noted that patients with *SPTA1* mutations had a less severe phenotype (based on hemoglobin level, reticulocyte count, RDW, intracellular K^+ , and EMA staining) compared to the other patients. This is in contrast with the more severe phenotype of patients with *SPTA1* mutations reported in other studies.³⁰ Similarly, our patients with *SPTB* mutations presented with normal MCHC values, whereas in other studies MCHC was shown to be elevated in patients carrying *SPTB* mutations.³¹ Given the relatively small numbers of patients within each group we cannot draw firm conclusions on links between genotype and phenotypic expression.

Red blood cell density as a marker of clinical severity

Decreased hemoglobin, hematocrit and RBC counts associated with increased markers of hemolysis and erythropoietic activity were previously reported as markers of HS severity.⁹ Among the molecular mechanisms defining severity of HS, a major role was assigned to RBC membrane instability and loss of membrane proteins²⁸ (MCHC, EMA test, SDS-PAGE), along with decreased deformability as measured by osmotic gradient ektacytometry.⁵ In our cohort, increased disease severity was associated with membrane instability and extensive membrane and band 3 protein loss over a shorter time (Figure 4B, G-I). RBC turnover in patients with severe HS was reflected by a decrease in HbA1c levels, which were higher than those in patients with mild HS (Figure 4A). The RBC in patients with moderate/severe HS had lower MCHC than those of patients with mild HS (Figures 3A and 4D). The average M fraction density of RBC from patients with moderate/severe HS did not differ from that of cells of healthy controls, whereas the cells from patients with mild HS showed an increase in density (Figure 4E)

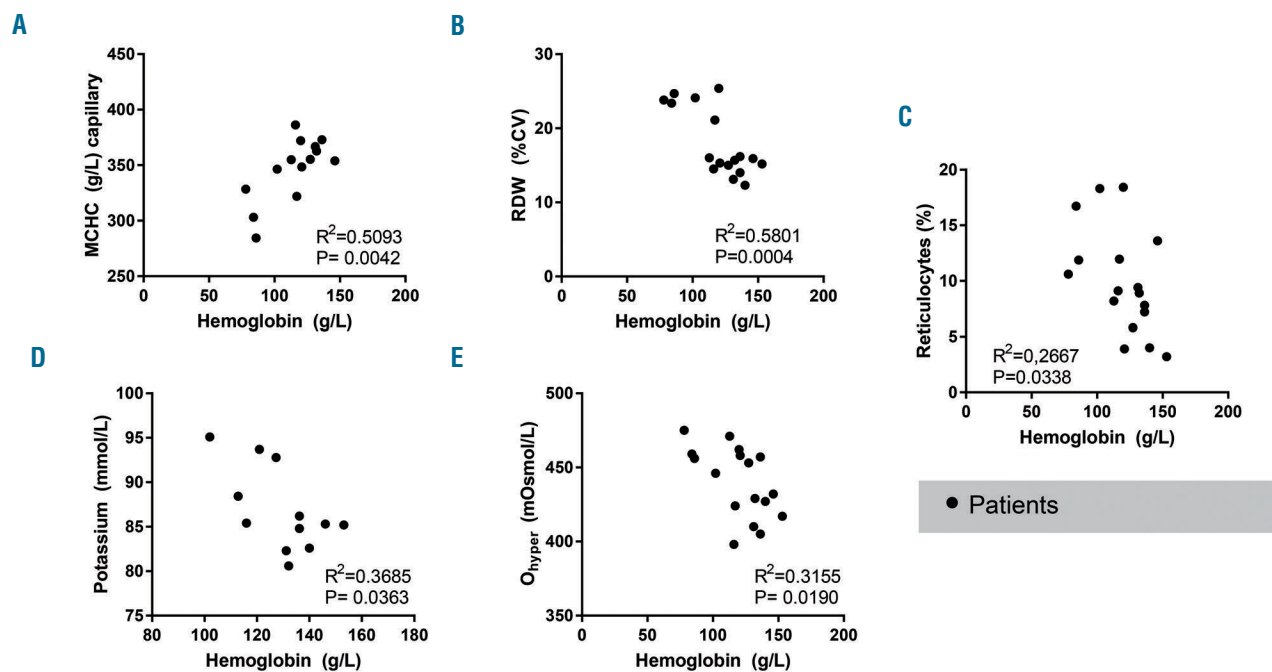
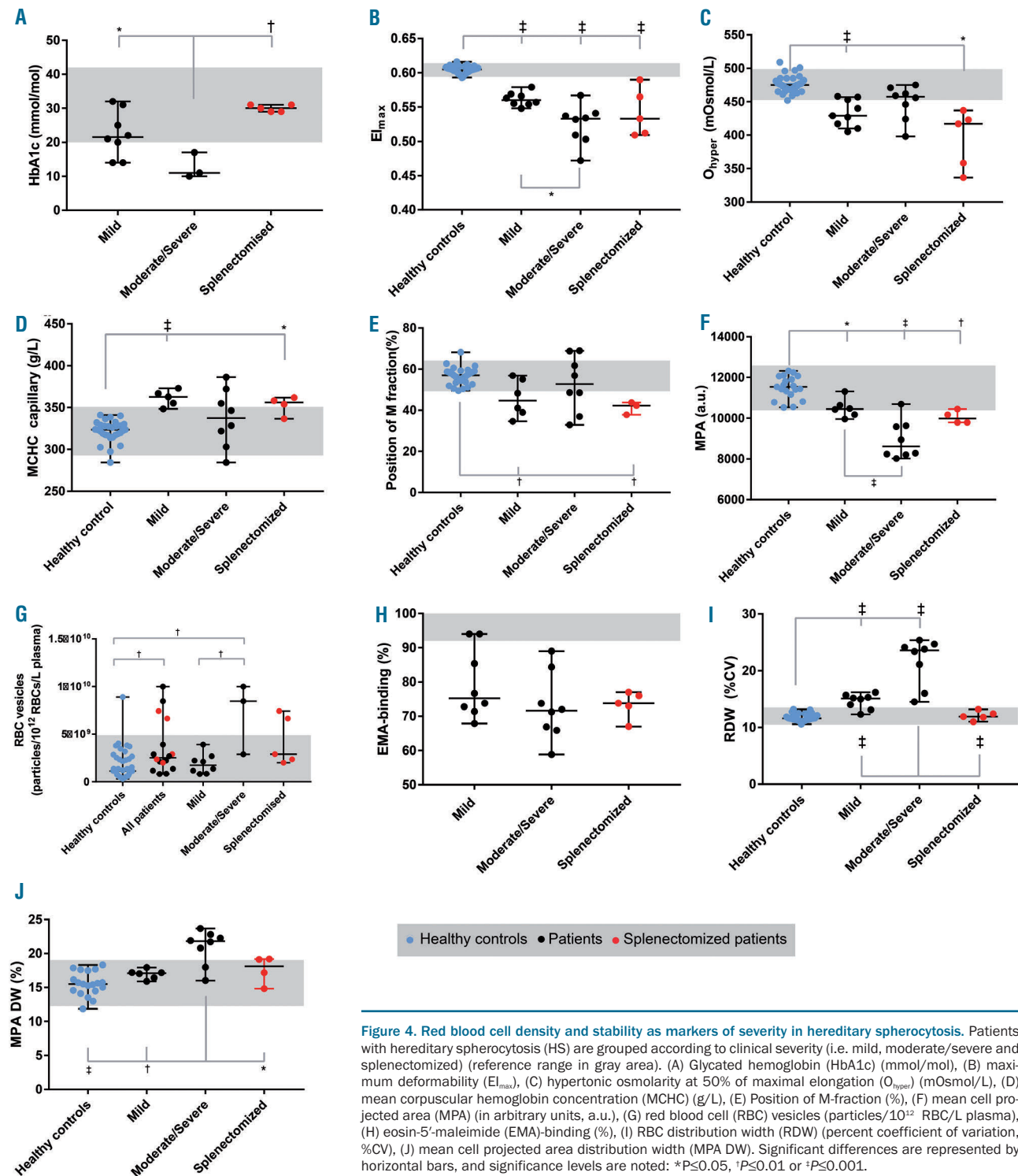


Figure 3. Red blood cell parameters and their relationship to clinical severity in unsplenectomized hereditary spherocytosis patients. (A) Mean corpuscular hemoglobin concentration (MCHC) (g/L), (B) red blood cell distribution width (RDW) (percent coefficient of variation, %CV), (C) reticulocytes (%), (D) intracellular potassium (mmol/L), (E) hypertonic osmolality at 50% of maximal elongation (O_{hyper}) (mOsmol/L).

and lower deformability as they “aged”, spending more time in the circulation getting more “senescent” than the highly unstable cells of patients with severe HS. Thus, RBC lifespan and decrease in EI_{max} appeared to be reliable markers of disease severity (Figure 4B), regardless of the genotype.

Delayed clearance of RBC in patients with mild HS allows a more gradual loss of the cell membrane (Figure 4G, *Online Supplementary Figure S3*), which results in bet-

ter conservation of RBC deformability (Figure 4B) and the ability to form dense cells (Figure 4C-E, *Online Supplementary Figure S2*). Direct measurements of membrane shedding by monitoring plasma-borne vesicles is challenging due to their fast sequestration and clearance.³²⁻³⁴ However, higher levels of circulating RBC vesicles were detected in plasma from patients with moderate/severe HS (Figure 4G). This finding is in line with an increase in other markers of membrane loss, such as



changes in gross morphology toward a spherocytic form (*Online Supplementary Figure S3*), as well as a higher number of microcytes, as determined by quantitative digital microscopy (*Online Supplementary Figure S4*).

Red blood cell heterogeneity and deformability as a marker of clinical severity

Another parameter we found to reflect disease severity in HS is RBC heterogeneity. Increases in RDW, RDW/hemoglobin and MCHC/RDW ratios were suggested to be markers of the clinical severity of HS.³⁵ We also found in our study that RDW correlates with HS severity

(Figure 3B). However, since absolute RDW values are known to vary between laboratories and depend on the age and physical activity of the subjects,⁴ we also used microscopy, confirming that patients with severe HS did indeed have a broader range of RBC shapes and MPA DW (Figure 4J, *Online Supplementary Figure S3*).

Word of caution regarding automated detection of hematocrit and mean corpuscular hemoglobin concentration in patients with hereditary spherocytosis

MCHC was previously suggested to be prognostic for the severity of HS in non-splenectomized patients.^{9,11} We

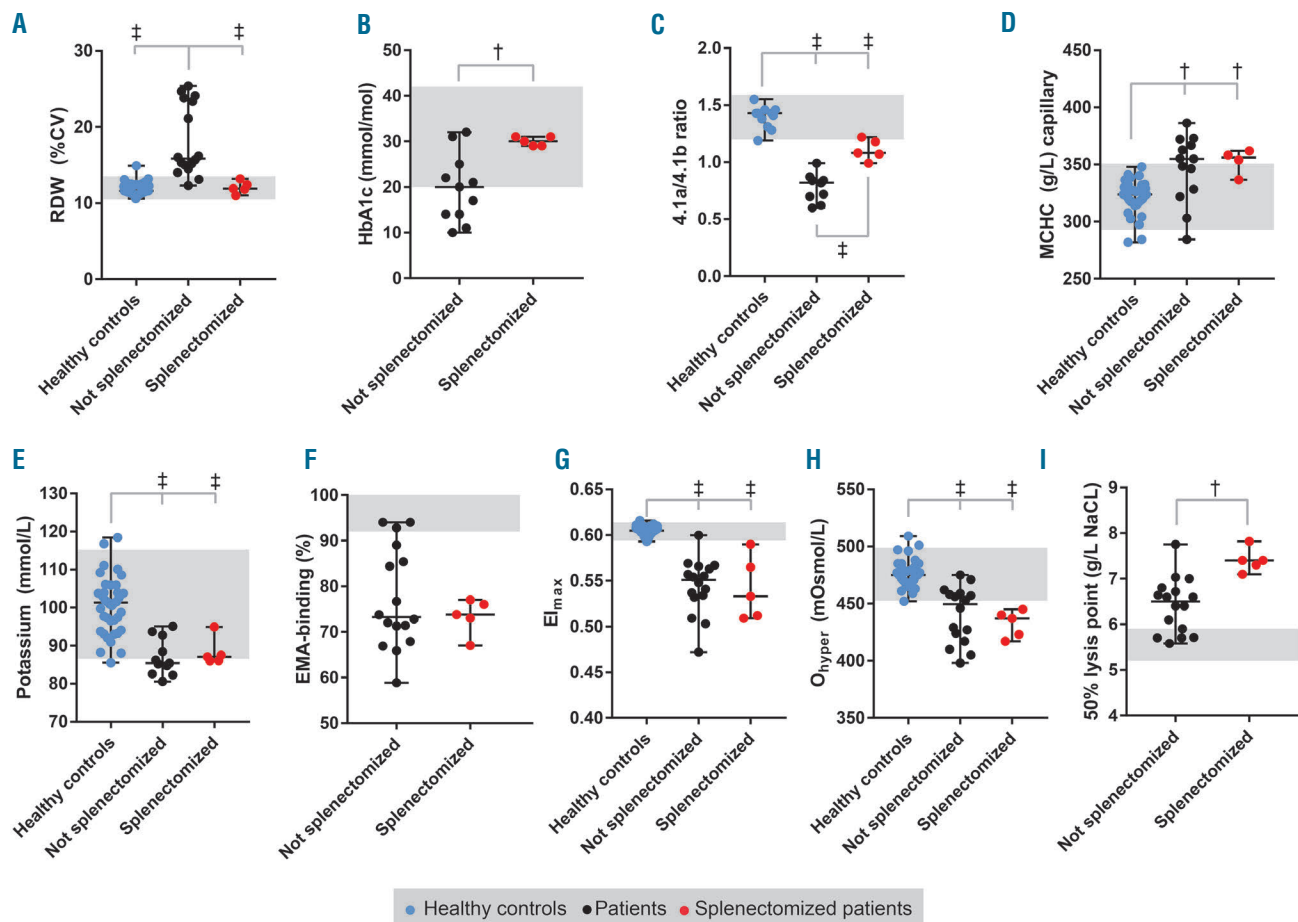


Figure 5. Role of splenectomy on red blood cell parameters in hereditary spherocytosis. Blue circles represent healthy controls, black circles represent (unsplenectomized) hereditary spherocytosis (HS) patients and red circles represent splenectomized HS patients. HS patients are grouped according to clinical severity (i.e. mild, moderate/severe and splenectomized). (A) Red cell distribution width (RDW (percent coefficient of variation, %CV)), (B) glycated hemoglobin (HbA1c) (mmol/mol), (C) band 4.1a/4.1b ratio, (D) mean corpuscular hemoglobin concentration (MCHC) (g/L), (E) intracellular potassium (mmol/L), (F) eosin-5'-maleimide (EMA)-binding hemoglobin (%), (G) maximum deformability ($E_{I_{max}}$), (H) hydration state of the red blood cells reflected by hypertonic osmolarity at 50% of maximal elongation (O_{hyper}) (mOsm/L), (I) 50% lysis point in the osmotic fragility test (g/L NaCl). Significant differences are noted: * $P \leq 0.05$, † $P \leq 0.01$ or ‡ $P \leq 0.001$.

Table 2. Summary of parameters that characterize disease severity in hereditary spherocytosis.

Disease Severity	MCHC	Density (Percoll, O_{hyper})	RDW	Reticulocytes	Deformability ($E_{I_{max}}$)	Membrane loss (vesiculation)
Mild	↑↑	↑↑	=	↑	↓	↑
Moderate/severe	↑	↑	↑↑	↑↑	↓↓	↑↑
Splenectomized	↑↑	=	=	↑	=	=

The ↑ symbol indicates increased compared to healthy controls, ↓ indicates decreased compared to healthy controls and = indicates the same as in healthy controls. MCHC: mean corpuscular hemoglobin concentration; RDW: red cell distribution width; $E_{I_{max}}$: maximal elongation index,

used a capillary-based method with determination of the hematocrit to measure MCHC. In line with previous observations,³⁶⁻³⁸ we found that automated measurements of MCHC of pathological RBC are imprecise for HS patients (see *Online Supplementary Figure S5*). Inaccuracy of automated MCHC detection of dehydrated RBC has been discussed for over 30 years.³⁶ It results from a substantial overestimation of MCV, both values being reliant on hematocrit detection or calculation methods.^{39,40} As mentioned previously, others have shown that increased hemoglobin concentrations correlate with milder disease severity scores in HS.^{9,11} We show that MCHC, calculated based on the capillary hematocrit, correlated with blood hemoglobin content (Figures 1G, 3A, and 4D).

Conclusions

This study reveals the factors defining RBC longevity and erythropoietic activity in patients with HS. These factors include membrane stability, which in turn depends on the localization of mutations affecting vertical or horizontal interactions within the membrane cytoskeleton and on the presence of splenic filtering capacity. Mild HS is asso-

ciated with prolonged survival of RBC in the circulation, allowing greater loss of membrane, which results in smaller and denser RBC. Shorter-lived, unstable RBC from patients with severe HS phenotype are more heterogeneous and less dense, as reflected by lower MCHC.

Parameters that specifically mark clinical severity in HS are summarized in Table 2 and are RBC density (MCHC, Percoll, O_{hyper}), RBC deformability (EI_{max}), and RBC heterogeneity (RDW). These parameters may be used to monitor the success of supportive therapy and assist in the development of new personalized treatment regimens.

Funding

Funding for the research leading to these results was received from the European Seventh Framework Program under grant agreement number 602121 (CoMMiTMeT) and from the European Union's Horizon 2020 Research and Innovation Programme under grant agreement number 675115 — RELEVANCE — H2020-MSCA-ITN-2015/H2020-MSCA-ITN-2015. This work was generated within the European Reference Network on Rare Hematological Diseases (ERN-EuroBloodNet) – FPA No. 739541

References

- Perrotta S, Gallagher PG, Mohandas N. Hereditary spherocytosis. *Lancet*. 2008;372(9647):1411-1426.
- Morton NE, Mackinney a a, Kosower N, Schilling RF, Gray MP. Genetics of spherocytosis. *Am J Hum Genet*. 1962;170-184.
- Gallagher PG. Hereditary elliptocytosis: spectrin and protein 4.1R. *Semin Hematol*. 2004;41(2):142-164.
- Da Costa L, Mohandas N, Sorette M, Grange MJ, Tchernia G, Cynober T. Temporal differences in membrane loss lead to distinct reticulocyte features in hereditary spherocytosis and in immune hemolytic anemia. *Blood*. 2001;98(10):2894-2899.
- Lazarova E, Gulbis B, Oirschot B van, van Wijk R. Next-generation osmotic gradient ektacytometry for the diagnosis of hereditary spherocytosis: interlaboratory method validation and experience. *Clin Chem Lab Med*. 2017;55(3):394-402.
- Huisjes R, Bogdanova A, van Solinge WW, Schiffelers RM, Kaestner L, van Wijk R. Squeezing for life – properties of red blood cell deformability. *Front Physiol*. 2018;9:656.
- Michaels LA, Cohen AR, Zhao H, Raphael RI, Manno CS. Screening for hereditary spherocytosis by use of automated erythrocyte indexes. *J Pediatr*. 1997;130(6):957-960.
- Cynober T, Mohandas N, Tchernia G. Red cell abnormalities in hereditary spherocytosis: Relevance to diagnosis and understanding of the variable expression of clinical severity. *J Lab Clin Med*. 1996;128(3):259-269.
- Rocha S, Costa E, Rocha-Pereira P, et al. Complementary markers for the clinical severity classification of hereditary spherocytosis in splenectomized patients. *Blood Cells Mol Dis*. 2011;46(2):166-170.
- Eber SW, Armbrust R, Schröter W. Variable clinical severity of hereditary spherocytosis: relation to erythrocytic spectrin concentration, osmotic fragility, and autohemolysis. *J Pediatr*. 1990;117(3):409-416.
- Bolton-Maggs PHB, Langer JC, Iolascon A, Tittensor P, King M-J, General Haematology Task Force of the British Committee for Standards in Haematology. Guidelines for the diagnosis and management of hereditary spherocytosis - 2011 update. *Br J Haematol*. 2012;156(1):37-49.
- King MJ, Behrens J, Rogers C, Flynn C, Greenwood D, Chambers K. Rapid flow cytometric test for the diagnosis of membrane cytoskeleton-associated haemolytic anaemia. *Br J Haematol*. 2000;111(3):924-933.
- Bosch FH, Werre JM, Schipper L, et al. Determinants of red blood cell deformability in relation to cell age. *Eur J Haematol*. 1994;52(1):35-41.
- Waugh RE, Narla M, Jackson CW, Mueller TJ, Suzuki T, Dale GL. Rheologic properties of senescent erythrocytes: loss of surface area and volume with red blood cell age. *Blood*. 1992;79(5):1351-1358.
- Bosman GJCGM. Survival of red blood cells after transfusion: processes and consequences. *Front Physiol*. 2013;4:376.
- Vives Corrons JL, Besson I. Red cell membrane Na⁺ transport systems in hereditary spherocytosis: relevance to understanding the increased Na⁺ permeability. *Ann Hematol*. 2001;80(9):535-539.
- Gallagher PG. Disorders of erythrocyte hydration. *Blood*. 2017;130(25):2699-2708.
- De Franceschi L, Olivieri O, Miraglia del Giudice E, et al. Membrane cation and anion transport activities in erythrocytes of hereditary spherocytosis: effects of different membrane protein defects. *Am J Hematol*. 1997;55(3):121-128.
- Makhro A, Huisjes R, Verhagen LP, et al. Red cell properties after different modes of blood transportation. *Front Physiol*. 2016;7:288.
- Jokinen CH, Swaim WR, Nuttall FC. A case of hereditary xerocytosis diagnosed as a result of suspected hypoglycemia and observed low glycohemoglobin. *J Lab Clin Med*. 2004;144(1):27-30.
- Da Costa L, Suner L, Galimand J, et al. Diagnostic tool for red blood cell membrane disorders: assessment of a new generation ektacytometer. *Blood Cells Mol Dis*. 2016;56(1):9-22.
- Parpart AK, Lorenz PB, Parpart ER, Gregg JR, Chase AM. The osmotic resistance (fragility) of human red cells. *J Clin Invest*. 1947;26(4):636-640.
- King M-J, Telfer P, MacKinnon H, et al. Using the eosin-5-maleimide binding test in the differential diagnosis of hereditary spherocytosis and hereditary pyropoikilocytosis. *Cytometry B Clin Cytom*. 2008;74(4):244-250.
- Ghosh S, Chakraborty I, Chakraborty M, Mukhopadhyay A, Mishra R, Sarkar D. Evaluating the morphology of erythrocyte population: an approach based on atomic force microscopy and flow cytometry. *Biochim Biophys Acta*. 2016;1858(4):671-681.
- Lutz HU, Bogdanova A. Mechanisms tagging senescent red blood cells for clearance in healthy humans. *Front Physiol*. 2013;4:387.
- Makhro A, Kaestner L, Bogdanova A. NMDA receptor activity in circulating red blood cells: methods of detection. *Methods Mol Biol*. 2017;1677:265-282.
- Huisjes R, van Solinge WW, Levin MD, van Wijk R, Riedl JA. Digital microscopy as a screening tool for the diagnosis of hereditary hemolytic anemia. *Int J Lab Hematol*. 2018;40(2):159-168.
- van Vuren A, van der Zwaag B, Huisjes R et al. The Complexity of Genotype-Phenotype Correlations in Hereditary Spherocytosis: A Cohort of 95 Patients. *Hemasphere*. 2019 Aug 7;3(4):e276.
- Narla J, Mohandas N. Red cell membrane disorders. *Int J Lab Hematol*. 2017;39 Suppl 1:47-52.
- Chonat S, Risinger M, Dagaonkar N, et al. The spectrum of alpha-spectrin associated hereditary spherocytosis. *Blood*. 2015;126(23):941.
- Maciag M, Płochocka D, Adamowicz-

- Salach A, Burzyńska B. Novel beta-spectrin mutations in hereditary spherocytosis associated with decreased levels of mRNA. *Br J Haematol.* 2009;146(3):326-332.
32. Willekens FLA, Werre JM, Groenen-Döpp YAM, Roerdinkholder-Stoelwinder B, de Pauw B, Bosman GJCGM. Erythrocyte vesiculation: a self-protective mechanism? *Br J Haematol.* 2008;141 (4):549-556.
33. Ciana A, Achilli C, Gaur A, Minetti G. Membrane remodelling and vesicle formation during ageing of human red blood Cells. *Cell Physiol Biochem.* 2017;42(3):1127-1138.
34. Willekens FLA, Werre JM, Kruijt JK, et al. Liver Kupffer cells rapidly remove red blood cell-derived vesicles from the circulation by scavenger receptors. *Blood.* 2005;105(5): 2141-2145.
35. Salvagno GL, Sanchis-Gomar F, Picanza A, Lippi G. Red blood cell distribution width: a simple parameter with multiple clinical applications. *Crit Rev Clin Lab Sci.* 2015; 52(2):86-105.
36. Mohandas N, Clark MR, Kissinger S, Bayer C, Shohet SB. Inaccuracies associated with the automated measurement of mean cell hemoglobin concentration in dehydrated cells. *Blood.* 1980;56(1):125-128.
37. Berda-Haddad Y, Faure C, Boubaya M, et al. Increased mean corpuscular haemoglobin concentration: artefact or pathological condition? *Int J Lab Hematol.* 2017;39(1):32-41.
38. Zandecki M, Genevieve F, Gerard J, Godon A. Spurious counts and spurious results on haematology analysers: a review. Part II: white blood cells, red blood cells, haemoglobin, red cell indices and reticulocytes. *Clin Lab Haematol.* 2007;29(1):21-41.
39. Kokholm G. Simultaneous measurements of blood pH, pCO₂, pO₂ and concentrations of hemoglobin and its derivatives-a multicenter study. *Scand J Clin Lab Invest.* 1990;50 (sup203):75-86.
40. O'Connor G, Molloy AM, Daly L, Scott JM. Deriving a useful packed cell volume estimate from haemoglobin analysis. *J Clin Pathol.* 1994;47(1):78-79.



Clinicopathological features, treatment approaches, and outcomes in Rosai-Dorfman disease

Gaurav Goyal,¹ Aishwarya Ravindran,² Jason R. Young,³ Mithun V. Shah,¹ N. Nora Bennani,¹ Mrinal M. Patnaik,¹ Grzegorz S. Nowakowski,¹ Gita Thanarajasingam,¹ Thomas M. Habermann,¹ Robert Vassallo,⁴ Taimur Sher,⁵ Sameer A. Parikh,¹ Karen L. Rech² and Ronald S. Go¹ on behalf of the Mayo Clinic Histiocytosis Working Group

¹Division of Hematology, Mayo Clinic, Rochester, MN; ²Department of Laboratory Medicine and Pathology, Mayo Clinic, Rochester, MN; ³Department of Radiology, Mayo Clinic, Rochester, MN; ⁴Division of Pulmonary Medicine, Mayo Clinic, Rochester, MN; ⁵Division of Hematology, Mayo Clinic, Jacksonville, FL, USA

Haematologica 2020
Volume 105(2):348-357

ABSTRACT

Rosai-Dorfman disease is a rare subtype of non-Langerhans cell histiocytosis. With the last major report published in 1990, there is a paucity of contemporary data on this disease. Our objective was to report the clinicopathological features, treatments and outcomes of patients seen at a tertiary referral center. Sixty-four patients with histopathological diagnosis of Rosai-Dorfman disease were identified from 1994 to 2017 (median age 50 years; range, 2-79). The median duration from symptom onset to diagnosis was seven months (range, 0-128), which was also reflected in the number of biopsies required to establish the diagnosis (median 2; range, 1-6). The most common presentation was subcutaneous masses (40%). Of the 64 patients, 8% had classical (nodal only) and 92% had extra-nodal disease (67% extra-nodal only). The most common organs involved were skin and subcutaneous tissue (52%), followed by lymph nodes (33%). Three patients had an overlap with Erdheim-Chester disease, which had not been described before. Two of these were found to have MAP2K1 mutations. Commonly utilized first line treatments were surgical excision (38%) and systemic corticosteroids (27%). Corticosteroids led to a response in 56% of the cases. Of those treated initially, 15 (30%) patients developed recurrent disease. The most commonly used systemic agent was cladribine (n=6), with 67% overall response rate. Our study demonstrates that Rosai-Dorfman disease has diverse clinical manifestations and outcomes. While this disease has been historically considered a benign entity, a subset of patients endures an aggressive course necessitating the use of systemic therapies.

Correspondence:

RONALD S. GO
go.ronald@mayo.edu

GAURAV GOYAL
goyal.Gaurav@mayo.edu/ggoyal@uabmc.edu

Received: February 14, 2019.

Accepted: April 18, 2019.

Pre-published: April 19, 2019.

doi:10.3324/haematol.2019.219626

Check the online version for the most updated information on this article, online supplements, and information on authorship & disclosures: www.haematologica.org/content/105/2/348

©2020 Ferrata Storti Foundation

Material published in *Haematologica* is covered by copyright. All rights are reserved to the Ferrata Storti Foundation. Use of published material is allowed under the following terms and conditions:

<https://creativecommons.org/licenses/by-nc/4.0/legalcode>.

Copies of published material are allowed for personal or internal use. Sharing published material for non-commercial purposes is subject to the following conditions:

<https://creativecommons.org/licenses/by-nc/4.0/legalcode>,

sect. 3. Reproducing and sharing published material for commercial purposes is not allowed without permission in writing from the publisher.



Introduction

Rosai-Dorfman disease (RDD) is a rare non-Langerhans cell histiocytosis characterized histopathologically by the accumulation of CD68-positive, S100-positive, and CD1a-negative histiocytes with frequent emperipolesis. RDD was first described in 1965 in four African children with lymphadenopathy by Destombes, and was called “adenitis with lipid excess”, owing to the lipid-laden histiocytes in the tissue specimen.¹ In 1969, Rosai and Dorfman reported a separate series of four patients with massive cervical lymphadenopathy with specific histopathological features, and called it “sinus histiocytosis with massive lymphadenopathy”.² Since the original description, further reports, including a summary of 423 cases from an international registry in 1990, described both nodal and extranodal manifestations of the disease.³

In the last decade, the understanding of the biology of related histiocytic disorders such as Erdheim-Chester disease (ECD) and Langerhans cell histiocytosis

(LCH) has been enhanced by the discovery of recurrent BRAF and related mitogen activated protein kinase – extracellular signal-regulated kinase (MAP-ERK) pathway mutations.^{4,6} The identification of these specific mutations in both LCH and ECD further supported their consideration as neoplastic disorders rather than reactive inflammatory conditions. Recently, mutually exclusive *KRAS* and *MAP2K1* mutations were identified in one-third of RDD patients, pointing toward a neoplastic process in this disease as well.⁷ Due to the rarity of RDD, the clinical spectrum and treatment outcomes are not well defined. Hence, we undertook this study to evaluate our institutional experience with RDD patients in a more contemporary setting.

Methods

The medical records of patients with RDD evaluated at a tertiary referral center from January 1, 1994 to December 15, 2017 were identified and reviewed after approval from the Institutional Review Board. Definitive histopathological diagnosis by tissue biopsy review was necessary for inclusion in the study. All biopsies identified at our institution (n=28) were re-reviewed by two pathologists with expertise in histiocytic disorders (K.L.R. and A.R.).⁸⁻¹⁰ Data abstracted from the medical records included: demographic characteristics, symptoms at disease presentation, histopathological features, treatment modalities utilized, and outcomes. In addition, radiologic and genomic findings were captured where available. Next generation sequencing (NGS) using an oncogene panel (FoundationOne® or Tempus®) was performed on five RDD tissue samples and one blood sample (Guardant360®).¹¹⁻¹³ All patients in the study were followed up by a medical record review until death or November 10, 2018, whichever was earlier. For patients that were lost to the follow up, additional information was acquired via a telephone interview and survey forms. To minimize errors and bias, the medical records were independently reviewed by two investigators (GG and AR).

The majority of the patients did not undergo positron emission tomography – computed tomography (PET-CT) scans for baseline evaluation or treatment-response assessment. Hence, we utilized data from the reports of imaging studies available — radiographs, CT scans, and magnetic resonance imaging (MRI) scans. The imaging studies selected to be included in the manuscript were reviewed independently by a radiologist with expertise in histiocytic disorders (JRY).¹⁴ RDD patients were classified into subgroups based on the location, as well as associated conditions.¹⁵ The sites of disease were based on histopathologic or radiographic findings and include those found at the follow-up as well. Based on the location, RDD involving the lymph nodes alone was classified as “classical” and others as “extranodal”. Based on consensus definitions of concomitant disorders, RDD was classified as “neoplasia-associated” RDD, “immune-related” RDD, and “IgG4-related” RDD.⁸

As there is no United States Food and Drug Administration (US-FDA) approved treatment for RDD, the patients were treated with various therapeutic agents/modalities. We assessed treatment response by reviewing the clinical documentation. The response criteria were defined clinically and radiologically as we have previously described in ECD.¹⁶ Because RDD is a relapsing-remitting disease, we assessed the overall response rate (ORR), which incorporated complete as well as partial remissions (complete or partial resolution of symptoms or imaging finding suspected due to RDD). Descriptive statistics were used to summarize the data.

Results

Patient characteristics and presenting features

We included 64 RDD patients in the study. Of these, 8% had classical (nodal only) and 92% had extra-nodal RDD (67% extra-nodal only) (Table 1). Overall, 47 (73%) had multi-site disease and 17 (27%) had solitary or single-site disease. The median age at diagnosis was 50 years (range, 2-79). Five patients were less than 18 years of age (age 2, 2, 11, 14, and 15 years, respectively). In the entire cohort, there was a slight female preponderance (female: male 1.5:1). The median duration from symptom onset to diagnosis was seven months (range, 0-128; mean 18 months). The most common presenting symptom was painful or painless subcutaneous masses (40%; Figure 1A). Symptoms due to lymphadenopathy were reported only in 11% of patients (Figure 1A). C-reactive protein level at diagnosis was available in 21 (33%) of patients, with a median value of 12 mg/L (range <0.3 to 198 mg/L; normal value <8 mg/L).

RDD subtypes

Overall, eight patients had neoplasia-associated RDD. Of these, three patients had RDD (two testicular, one vocal cord) in conjunction with ECD of other organ systems, characterized as mixed or overlap histiocytosis. Three patients had RDD subsequent to the diagnosis of a hematologic malignancy (peripheral T-cell lymphoma not otherwise specified, marginal zone B-cell lymphoma, myelodysplastic syndrome with excess blasts-1), while two patients developed a hematologic malignancy after RDD diagnosis (mantle cell lymphoma, Waldenström's

Table 1. Clinical and baseline features of patients with Rosai-Dorfman disease.

Total patients	64
RDD/ECD overlap (mixed histiocytosis)	3 (5%)
Median age at diagnosis (years)	50 years (range, 2-79)
Female: Male	1.5:1
Classification	
Familial	0
Classical (node-only)	5 (8%)
Extranodal	59 (92%)
Neoplasia-associated	8 (13%)
IgG4-related	3 (5%)
Immune-related	5 (8%)
Race	
White	40 (63%)
Black	9 (14%)
Asian	3 (5%)
Other/unknown	12 (18%)
Median time from symptom to diagnosis (months)	7 (range, 0-128)
Median number of biopsies for diagnosis	2 (range 1-6)
Median duration of follow-up (months)	31 (range 0-249)
Median overall survival since onset of symptoms (months)	140 (range 8-684)
Lost to follow up	15 (23%)
Deaths	4

macroglobulinemia). Immune-related RDD was diagnosed in five patients, with one case each of rheumatoid arthritis, multiple sclerosis, Sjögren's syndrome, systemic lupus erythematosus, and warm autoimmune hemolytic anemia. Serologic evaluation was not indicated in the remaining patients due to a lack of clinical features of concomitant autoimmune disorders. Three patients had high IgG4 level expression in lesional lymphoplasmacytic cells on immunohistochemistry, but only one had elevated serum IgG4 levels. None of these patients had other features consistent with IgG4-related disease.

Organ involvement

Among the entire cohort, 24 (38%) patients underwent a PET-CT scan, while 16 (25%) underwent body imaging with a CT scan or MRI. The most common organ involved on physical examination and imaging was skin and subcutaneous tissue (52%), followed by lymph nodes (33%) (Figures 1B and 2).

1. Skin and subcutaneous tissue

The most common presenting feature was subcutaneous nodules, either solitary or multiple, and presented at different locations on the body (chest, arm, back, and thigh). Six of the 33 (18%) cases in this group presented with primarily cutaneous lesions, either a purple or erythematous rash, or plaque-like lesions (Figure 3). Of the five pediatric cases, one patient had subcutaneous nodules.

2. Lymph nodes

Based on a clinical and radiographic record review, lymph node involvement by RDD was present in 21

(33%) cases, with isolated lymph node disease in three (5%) cases. The size of the lymph nodes ranged from 1-2 cm, with none of the patients demonstrating "massive lymphadenopathy" as described in prior reports (≥ 7 cm).^{2,3} Despite lymphadenopathy, B-symptoms (fever, drenching night sweats, weight loss) were noted only in three (5%) patients. The most common distribution of lymph node involvement was generalized, which occurred in seven (11%) cases. Isolated axillary and cervical lymphadenopathy was seen in five (8%) cases each. All of these cases presented as multiple lymph nodes (Figure 4). Thoracic lymphadenopathy was seen in the remaining four (6%) patients, and presented as mediastinal or para-tracheal lymphadenopathy. Of the five pediatric cases, three had lymph node involvement (one each of cervical, generalized, and retrocrural lymph nodes).

3. Bone

RDD of the bones was present in 16 (25%) patients, and varied in location from metaphyseal heads of the femur and humerus to the ribs, pelvis and vertebrae. The lesions were mostly lytic in appearance and centered in the medullary space, although sclerotic lesions were seen occasionally as well. Soft tissue lesions with bone involvement were seen in four (6%) patients, with two in thoracic/lumbar spine, and one each in the mandible and acetabulum of the hip. Among the five pediatric patients, two had bone RDD involving the skull and humerus, respectively. Bone pain was not reported among patients with long-bone involvement, but common among patients with spine or pelvic bone disease.

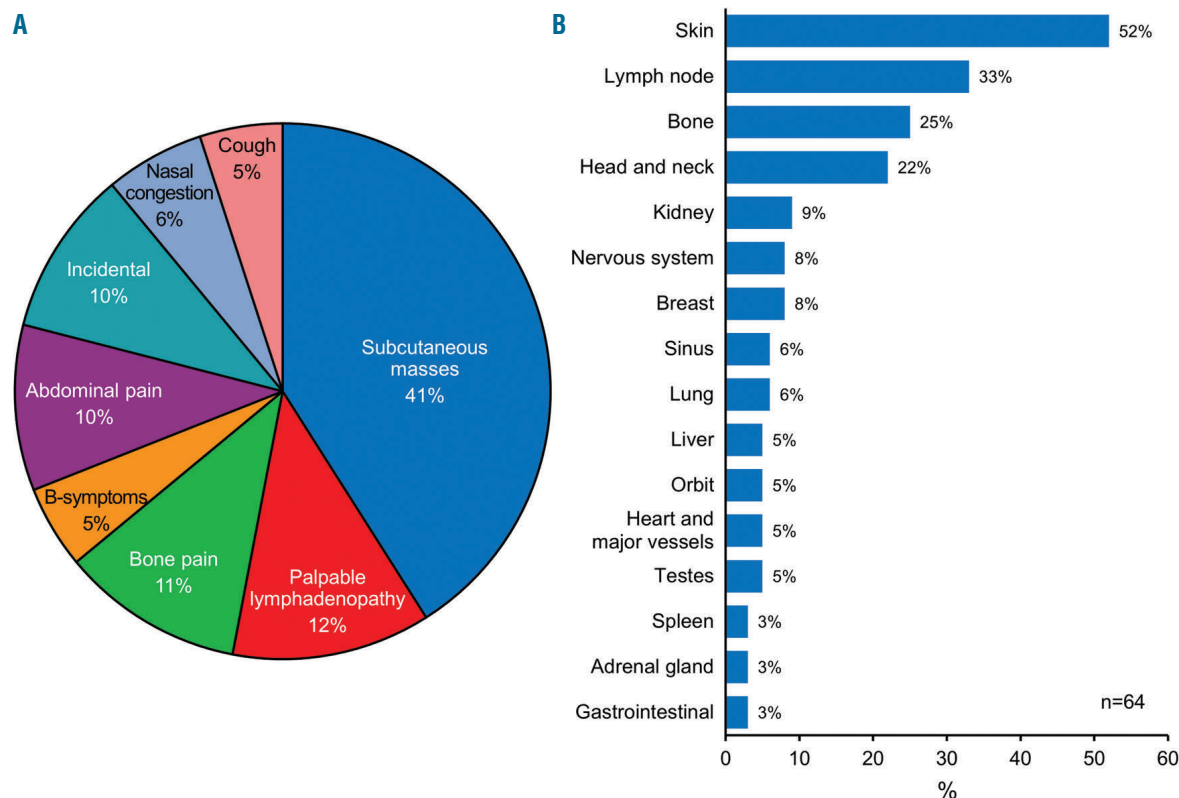


Figure 1. Clinical manifestations and organ involvement among patients with Rosai-Dorfman disease A) Presenting features and B) Organ involvement

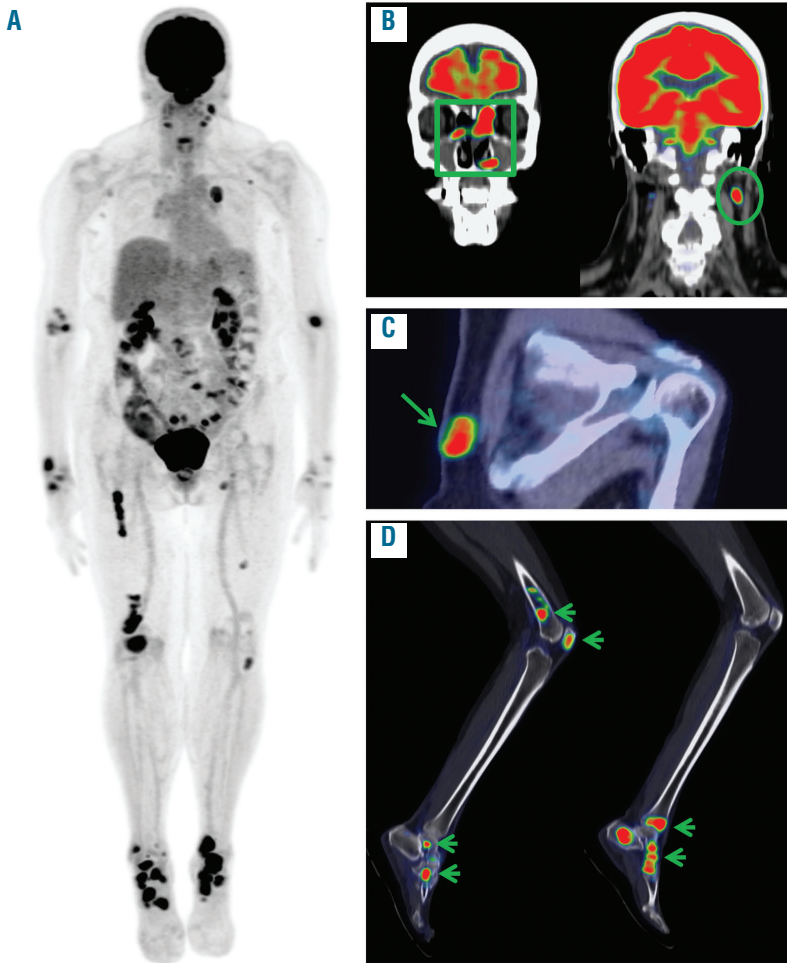


Figure 2. Common imaging findings of Rosai-Dorfman disease on fluorodeoxyglucose (FDG) PET/CT. (A) Maximum intensity projection depicting several FDG avid subcutaneous, lymph node and osseous lesions. (B) Coronal fusion images demonstrate FDG avid paranasal sinus (square) and lymph node (circle) disease. (C) Axial fusion image shows an FDG avid subcutaneous soft tissue lesion. (D) Sagittal fusion images of the bilateral lower extremities demonstrate several FDG avid osseous lesions.

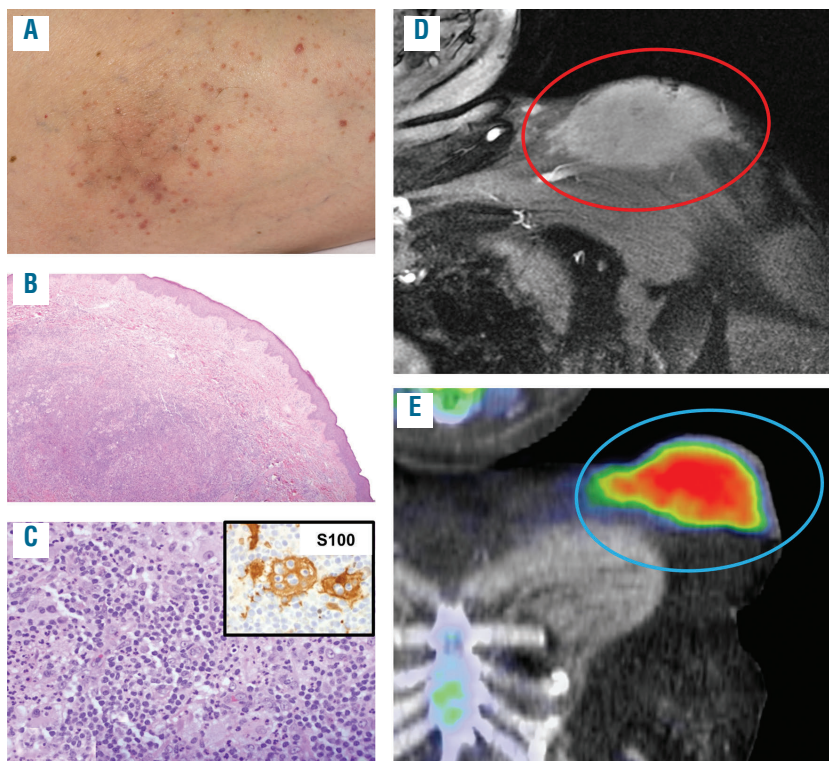


Figure 3. Cutaneous Rosai-Dorfman Disease (RDD). (A) Petechial rash and subcutaneous nodule. (B) Nodular lymphohistiocytic infiltrates in the dermis form a dome shaped lesion. (C) Within a background of small lymphocytes and neutrophils, RDD histiocytes show round nuclei, open chromatin, central nucleoli, and abundant pale cytoplasm containing engulfed lymphocytes (emperipolesis). These cells are S100+ by immunohistochemistry (inset). (D) Enhanced coronal MRI of the left shoulder depicting a large homogeneously enhancing subcutaneous mass (oval). (E) Fused FDG PET/CT of the same patient demonstrating hypermetabolism of this mass (oval).

4. Head and neck (including orbit)

Head and neck RDD lesions were noted in seven (11%) patients. Orbital involvement occurred in three (5%) cases, one of which was a pediatric patient. One of these also had ciliary body and scleral involvement. Other RDD sites in the head and neck region included the trachea (n=2), nose (n=1), and vocal cord (n=1).

5. Glandular tissue

RDD involving the glands was seen in nine cases, most common being breast tissue (n=5), with abnormalities on mammogram or MRI (Figure 5). Two patients each had involvement of lacrimal and parotid salivary gland without any evidence of dry eyes or mouth.

6. Kidneys, adrenals, abdomen and retroperitoneum

RDD of the kidneys was seen in six patients, most commonly as solitary parenchymal mass or nodule, and less commonly as perinephric coating, without the classic "hairy kidney" appearance as seen with ECD.¹⁷ None of these patients had renal failure from RDD of the kidneys. Two of these patients had adrenal nodules. Other abdominal sites included mesentery and peritoneum in one patient each.

7. Nervous system

Central nervous system (CNS) involvement manifested as dural- or parenchymal-based lesions in four cases. Parenchymal lesions were observed on MRI imaging in

three patients, manifesting as frontal or temporal solitary masses. One of these patients had pachymeningeal disease along with cerebral subcortical white matter infiltrative lesions. Additionally, one patient had optic nerve involvement causing visual disturbance.

8. Cardiovascular and respiratory system

Cardiovascular involvement was uncommon, noted as a right atrial mass encasing the coronary artery in one patient and aortic infiltration in two patients (Figure 5). Pulmonary RDD was seen in four patients and presented as a parenchymal nodule, interstitial pneumonitis, or solitary pleura-based lesion.

9. Bone marrow, liver, and spleen

Biopsy proven bone marrow involvement was seen in one patient while three others had an increased bone marrow signal on PET-CT. Liver involvement occurred in three cases and two had spleen lesions (Figure 5).

10. Other sites

RDD involving the testes was noted in three cases, two of which had ECD of other tissue sites (Figure 5). RDD of the maxillary and ethmoid sinuses was noted on CT scan of the head in four cases, with sinus-related symptoms in three patients. Two patients had paravertebral soft tissue nodules, one of whom presented with compression of the spinal cord from mass effect. Colon- and rectal-based polypoid lesions were found in two patients.

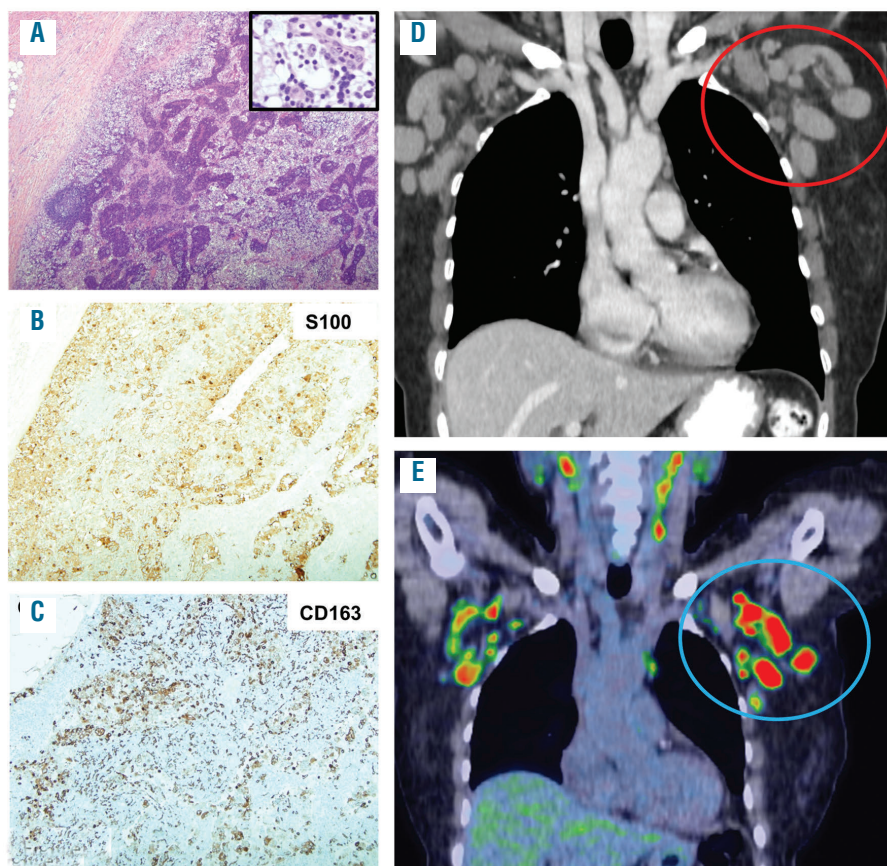


Figure 4. Rosai-Dorfman disease RDD in lymph node. (A) The RDD infiltrate expands the sinuses of the lymph node. Characteristic RDD histiocytes show abundant cytoplasm with emperipolesis (inset). (B) The RDD histiocytes are highlighted by immunohistochemistry for S100, and (C) CD163. (D) Enhanced coronal thoracic CT depicting bilateral axillary lymphadenopathy (circle). (E) Fused FDG PET/CT of the same patient demonstrating hypermetabolism of bilateral cervical and axillary lymph nodes (circle).

Histopathologic and molecular features

The median number of biopsies required to establish a diagnosis was two (range, 1-6). Eleven (18%) patients underwent ≥ 3 tissue biopsies. Classic histopathologic features of RDD were enlarged histiocytes demonstrating emperipolesis, expressing CD163 and S100, but not CD1a by immunohistochemistry (Figure 3). However, the pathognomonic RDD histiocytes were infrequently found within the infiltrates in some extranodal lesions, and often were obscured by the inflammatory background or fibrosis. The inflammation accompanying RDD infiltrates was characterized by secondary lymphoid follicles and abundant plasma cells. Due to these features, the histopathology was most often mistaken as non-specific chronic inflammation, with the diagnosis of RDD only recognized following a repeat tissue biopsy or review at our institution (n=11).

Among the five patients who underwent NGS, one showed a *CDC73* truncation in exon 5, and another had a *KRAS* c.351A>T (*K117N*) mutation. Interestingly, two of the three patients with RDD/ECD overlap showed the presence of a *MEK1* mutation, one on testicular tissue

[*MAP2K1* c.157T>C (*F53L*)] and the other on peripheral blood [*MAP2K1* c.167A>C (*Q56P*)]. No pathogenic mutation was detected in the tissue specimen of the remaining two cases. None of these specimens demonstrated the presence of known oncogenic gene fusions on RNA sequencing. *BRAF-V600E* mutation testing was performed in two cases and both were negative: one by immunohistochemistry and one by cell-free DNA polymerase chain reaction.

Treatments and outcome

1. First line treatments

Treatment and initial follow-up data were available for 57 (89%) patients (Table 2 and Figure 6). Of these, eight (14%) patients were initially observed. All of the patients who were observed and with follow-up data (n=3; 38%) eventually required treatment, with a median time to treatment of 30 months. Overall, the most common first-line therapeutic modality was surgical excision in 24 (38%) patients. The duration of response to surgery was variable (median 12 months, range 2-162), with 33% relapse rate. Of the relapses, five (21%) patients under-

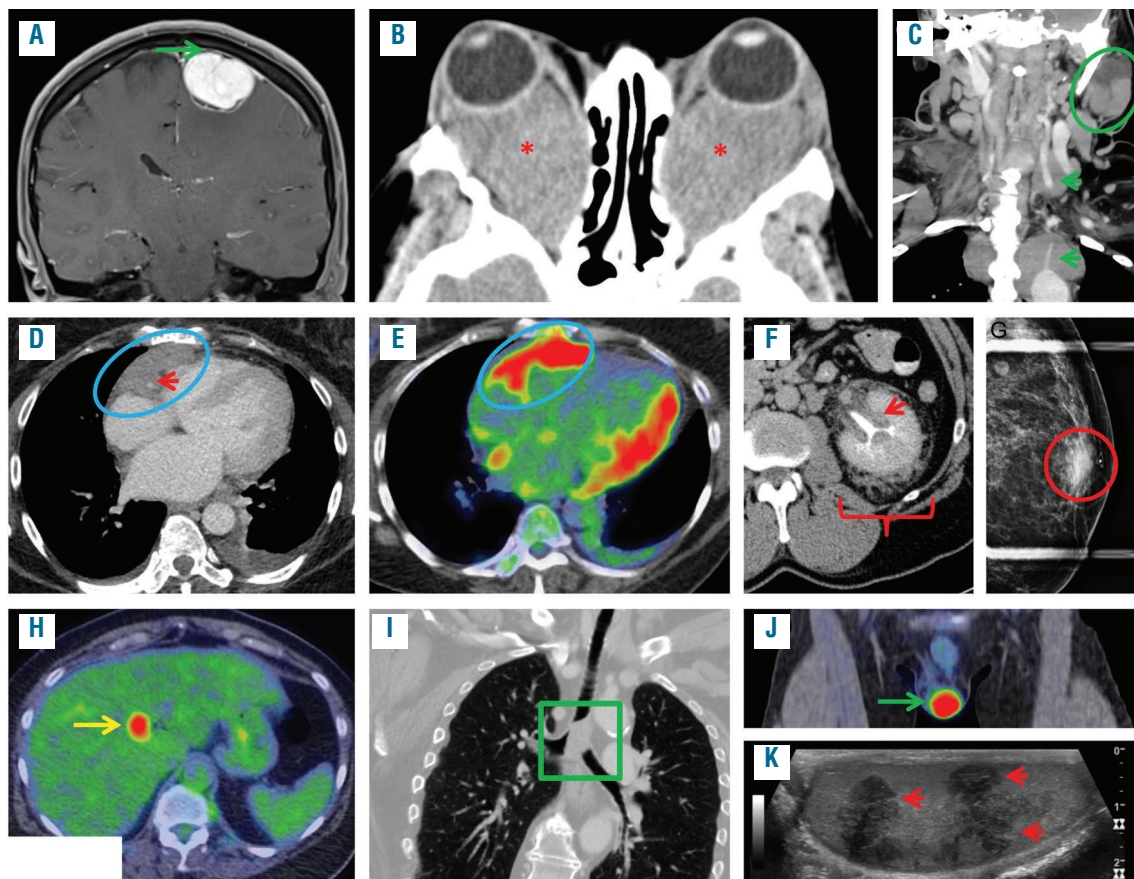


Figure 5. A variety of less common Rosai-Dorfman disease imaging findings. (A) Coronal contrast enhanced head MRI depicting a homogeneously enhancing extra-axial intracranial soft tissue mass. Note the lack of dural tail (arrow) characteristic of the more common and similar appearing meningioma. (B) Enhanced axial orbit CT showing large intraconal soft tissue masses (*) and associated exophthalmos. (C) Enhanced coronal CT of the neck showing a soft tissue lesion involving the left parotid (circle) along with soft tissue lesions encasing arteries of the neck (arrowheads). (D & E) Axial CT and FDG PET/CT images of the thorax demonstrating an FDG avid soft tissue lesion in the right atrioventricular groove (oval), encasing the right coronary artery (arrowhead). (F) Delayed enhanced axial CT of the abdomen depicting perinephric (bracket) and renal hilar (arrow) infiltrative soft tissue. (G) Cranial-caudal compression mammogram elucidating a palpable subareolar mass (circle). (H) Fused axial FDG PET/CT demonstrating a focal FDG avid biopsy proven hepatic lesion. (I) Enhanced reformatted CT of the chest demonstrating a soft tissue lesion in the lower airway, overriding the carina (square). (J & K) Fused coronal FDG PET/CT and testicular ultrasound demonstrating a hypermetabolic (14.2 SUVmax) testicle (arrow) with multiple corresponding hypochoic lesions on ultrasound (arrowheads) in a patient with RDD/ECD overlap.

went subsequent surgery, and three (13%) received systemic therapy. The most common site of RDD in patients who underwent surgery was subcutaneous nodules (13 or 54%), with other single cases of isolated thyroid, bone, breast, lacrimal gland, nasal septum and dura involve-

ment, respectively. Among the five patients who required subsequent surgery, one had a nasal septal mass that recurred, while three had other disease sites (bone, soft tissue, subcutaneous tissue) that required resection subsequently. Additionally, there was one patient with KRAS

Table 2. Treatments and overall response rates (ORR) in patients with Rosai-Dorfman disease.

Treatment	First line	ORR	2 nd /later line	ORR
Surgery	24	24 (100%)	7	6 (100%)
Surgery + RT	1	1 (100%)	1	1 (100%)
Corticosteroids	17	10 (56%)	3	2 (67%)
Rituximab	2	2 (100%)	1	1 (100%)
Observation	8	0		
RT	2	0	4	1 (25%)
Prednisone + 6-MP/azathioprine	2	2 (100%)	1	1 (100%)
CVP	–	–	1	1 (100%)
Cladribine	–	–	6	4 (67%)
Mycophenolate	–	–	1	0
Etoposide + Vinblastine + prednisone	1	0	1	0
Prednisone + MTX/6-MP	–	–	3	2 (100%)
Vinblastine + prednisone + 6-MP + MTX	–	–	1	1 (100%)
Clofarabine + vinblastine + etoposide + prednisone	–	–	1	0
Pegylated-interferon	–	–	1	1 (100%)
Hydroxyurea	–	–	1	0

RT: Radiation therapy; 6-MP: 6-Mercaptopurine; CVP: cyclophosphamide, vincristine, prednisone; MTX: methotrexate

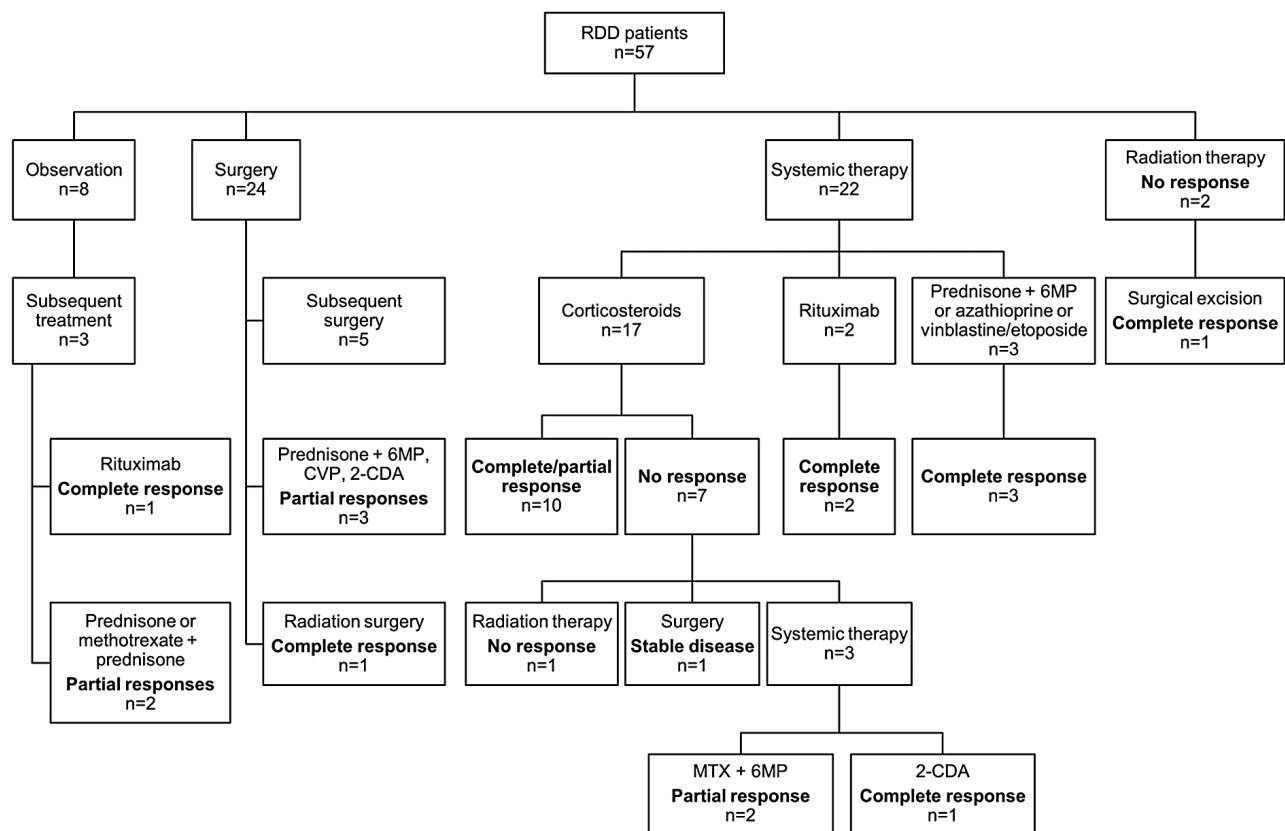


Figure 6. Treatments and outcomes of patients with Rosai-Dorfman disease (RDD) from diagnosis until first response where available. 6MP: 6-mercaptopurine; CVP: cyclophosphamide, vincristine, prednisone; 2-CDA: cladribine; MTX: methotrexate

c.351A>T (K117N) mutation who had a recurrence in the trachea after the resection of subcutaneous nodules. The three cases that required subsequent systemic therapy had multiple subcutaneous lesions and lymph node involvement at presentation.

Corticosteroids were used as the first-line therapy in 17 (27%) patients. Of these, responses were observed in 56% of the cases, with a maximum response duration of 71 months and a relapse rate of 53%. The agent used in most cases was prednisone at doses of 1 mg/kg with prolonged but variably designed taper of 6-12 weeks. Responses were seen both clinically as well as radiologically, although uniform imaging re-assessment was not performed in over 50% cases. Twelve (70%) of the patients who received corticosteroids had lymph node involvement. Of these, seven responded, with a median duration of response of eight months (range, 3-25 months). There were two RDD patients with CNS involvement (dural and cerebellar, respectively) who noted improvement in symptoms after prednisone treatment. One patient had ocular (scleral) involvement and noted improvement in vision with corticosteroid eye drops. Corticosteroids were well-tolerated overall, and no major dose-limiting toxicities were reported. Radiation therapy was utilized in two cases (one subcutaneous and one bone) without any response. Other first-line therapies included combinations of rituximab, azathioprine, or 6-mercaptopurine with prednisone and resulted in universal responses in the four patients treated. The organs involved in these patients were mostly lymph nodes and subcutaneous tissues, and no relapses were noted.

The three patients with overlap RDD/ECD underwent resection of the solitary RDD lesions in the testes (n=2) and vocal cords (n=1). Two of these underwent cladribine chemotherapy that led to an ongoing response at a median follow-up of two years, and one has been observed for 2 years without ECD progression in the perinephric region.

2. Second line and subsequent treatments

Of the 49 patients that were treated initially, 15 (30%) developed recurrent disease after the first course treatment and were treated with other empiric modalities (Table 2, Figure 6). The most common chemotherapeutic agent used was cladribine (5 mg/m²/day for five days every 28 days) for 3-4 cycles, primarily used as second line therapy in six (10%) patients, with a 67% ORR. Of those who responded, no relapses were seen at median follow-up of 16 months (range, 2-26). Prednisone in combination with 6-mercaptopurine, azathioprine, or methotrexate was also successfully used in a few cases with subcutaneous and lymph node involvement. Interestingly, rituximab administered as four once-weekly doses in combination with corticosteroids resulted in a sustained ORR of 100% in the three patients who were treated, two of whom had primary lymph node involvement and third with multiple subcutaneous lesions along with lymphadenopathy. Two of these patients had immune-related RDD (warm autoimmune hemolytic anemia, multiple sclerosis). Other systemic chemotherapies that led to sustained responses utilized vinblastine and cyclophosphamide based regimens (Table 2). Radiation therapy was utilized in four patients (one each subcutaneous, tracheal, orbit, and bone), with a complete radiographic response seen in only one case of tracheal RDD, with an eventual recurrence in the multisystem distribution with an under-

lying *KRAS* mutation.

Less commonly utilized therapies included pegylated interferon alfa (135 mcg subcutaneous weekly in one patient) leading to regression of subcutaneous nodules and stability of the optic nerve lesion, and hydroxyurea (1000 mg oral daily in one patient) which initially resulted in some in the vision from orbital masses, but eventually progressed within three months. One of the patients received CVP (cyclophosphamide, vincristine, prednisone) regimen for RDD involving multiple subcutaneous sites, and achieved a sustained partial response.

The median duration of follow-up after diagnosis for the entire cohort was 31 months (range, 0-249). Of the cohort with complete follow-up information (n=49), four patients had died at the time of last follow-up. Of these, three patients died from other malignancies: concomitant peripheral T-cell lymphoma (n=1), acute myeloid leukemia 1 year subsequent to RDD with concomitant myelodysplastic syndrome (n=1), and metastatic gallbladder carcinoma 12 years subsequent to RDD (n=1). The cause of death for the fourth patient was unknown.

Discussion

In this study, we report a large contemporary series of RDD patients. Over the study period of 23 years, our referral center saw RDD patients at an average rate of three cases per year. However, the recognition of this disease appears to be increasing, with 29 (45%) cases seen within the last 5 years of the study. Contrary to the historically reported RDD cohort with massive lymphadenopathy, we found that the majority of cases presented as subcutaneous lesions.³ Lymphadenopathies were the second most common manifestation. However, they were not massive or limited to cervical lymph nodes alone as described by Foucar *et al.* in the initial landmark series of RDD.³ The reason for this difference in organ involvement is unclear, but may be related to a difference in the study population between the two studies. Compared to the historical cohort reported by Foucar *et al.*, our cohort had more patients who were older (mean age 48 *versus* 20 years), from the United States (97% *versus* 38%), and Caucasians (63% *versus* 43%).³ Moreover, our center is a tertiary referral center; hence it may not include some classic RDD cases that received treatment in the community. It may also be biased towards incidentally found RDD when being extensively evaluated by means of imaging studies for other unrelated disorders. However, the majority of the patients in our cohort were referred to hematology for primary RDD diagnosis and received systemic treatments. Our findings highlight that RDD is syndromic in nature with a wide spectrum of manifestations, and our experience may be more representative of RDD in the United States.

The histopathological diagnosis of RDD can be challenging due to its rarity and non-specific histologic findings, especially in the extranodal forms. In contrast to LCH and ECD, the RDD tissue may harbor very few lesional cells, and often shows a prominent inflammatory background with plasma cells, or lymphoid follicle formation and neutrophilic infiltrates.¹⁵ The difficulty in diagnosing RDD histopathologically is exemplified by the numerous biopsies required to achieve the diagnosis of RDD in our patients. On some occasions, a histopatholog-

ical re-review of previous biopsy slides by our expert pathologists yielded the diagnosis of RDD. This suggests that there is value in having the suspicious biopsy specimens reviewed by centers with expertise in histiocytic disorders, such as those listed by the Histiocytosis Association (<https://www.histio.org>) or Erdheim-Chester disease Global Alliance (<http://erdheim-chester.org>). There is also a need for a systematic study of the spectrum of histopathologic manifestations of RDD, as has been undertaken in ECD.¹⁸

The pathogenesis of RDD is not well understood, and it is unclear whether it should be classified as a neoplastic or benign disorder. Historical studies found the RDD cells to be polyclonal in nature.¹⁹ However, there are recent reports of *MAP-ERK* pathway alterations in about a third of RDD patients, which suggests that at least a subset may be neoplastic in nature.^{5,7,20,21} We recently reported on tissue NGS results of 10 RDD patients that demonstrated oncogenic alterations among four (40%), including the one patient with a RDD/ECD overlap and the one with *KRAS-K117N* included in the report herein.²² Interestingly, in the series, only 1 of 5 RDD cases without any oncogenic mutations required systemic therapy while all patients with molecular alterations (*PTEN* copy loss, *SMARCA4* frameshift loss, *KRAS-K117N*) had progressive disease requiring chemotherapy.²² Furthermore, about a third of the patients in the current series had a disease behaving more like a malignant hematological neoplasm, requiring second line systemic treatments. We also report a novel finding of a RDD/ECD overlap in three patients, two of whom were found to harbor *MAP2K1* mutations. In the past, a RDD/LCH overlap has been described as well.²³ These findings, in conjunction with the accumulating molecular and clinical data, add further evidence to the contention that a subset of RDD may be neoplastic and related to the other histiocytic neoplasms.

There is a paucity of systematic studies analyzing first-line treatments and outcomes in RDD. Historically, it was reported that about 50% of the RDD cases with involvement of lymph nodes or cutaneous disease may experience spontaneous remissions.^{24,25} In our series, about 40% of the patients who were observed subsequently required treatment. This suggests that there is a role for monitoring without therapy in a subset of RDD patients who are asymptomatic and have no internal organ involvement. Surgical resection has been suggested as a curative option for some isolated RDD cases.^{15,26,27} In our series, one-third of the patients who underwent initial surgery required subsequent therapy. Our series also suggests that corticosteroids may be considered as a treatment option for nodal only disease, or to relieve symptoms from CNS/ocular involvement. However, the duration of response may be short-lived. The optimal duration of therapy is unknown and the patients need to be monitored for the adverse effects from steroids.

Although several RDD patients were treated adequately by corticosteroids or surgical resection, about a third in our series had recurrent disease. The most commonly used therapeutic agent was cladribine and resulted in high overall response rates (~70%). This is similar to that reported in previous case reports.^{28,29} Some other empirically used agents that led to sustained clinical responses were prednisone in combination with other immunosuppressive therapies (6-mercaptopurine, azathioprine, and low-dose oral methotrexate) or anti-CD-20 monoclonal

antibody, rituximab, especially in immune-related RDD. These agents have been reported to provide benefit in RDD in the past as well.^{25,30-32} Vinblastine in combination with other immunosuppressive agents led to partial response in the lymphadenopathy, consistent with prior reports of its benefit.^{33,34} Although the second-line regimen were heterogeneous, our study suggests that patients with immune-related RDD may benefit from rituximab or immunosuppressive agents, and others may be treated with cytotoxic agents such as cladribine as used in ECD.

Prior reports suggested the potential role of radiation therapy in refractory disease causing imminent symptoms such as airway obstruction or vision loss.^{25,31,35,36} In our experience, radiation therapy resulted in a response in only one of six patients. This patient had an isolated tracheal lesion. Hence, there might be a potential role for radiation therapy in patients who have a single site of disease.

Our study's major strength is that it is the largest contemporary case series among adult patients with RDD. We show that the most common manifestation of RDD may be dermatologic in nature, and the lymphadenopathy may not be massive as previously thought to be. We also report the unique entity of a "hybrid" RDD/ECD overlap, which has not been previously reported. A major limitation of our study is the lack of uniform imaging and response assessment in all patients. However, the charts were independently reviewed by two investigators to minimize bias. Another limitation is the lack of genetic sequencing data on all the patients, and our focus was primarily on the clinical manifestations, treatments and outcomes. Additionally, one of the challenges in conducting a study of a rare and chronic disease such as RDD is the lack of long-term follow-up data on the patients. Of the patients that had complete follow-up data (n=49), no one died from RDD. In the previous largest reported series, 4 of 238 (~2%) patients with sufficient follow-up died from effects of RDD.³ Although the mortality from RDD appears low, it may cause significant morbidity through end organ damage, and is potentially lethal if left untreated.

Despite the progress made in the understanding of the biology of LCH and ECD, our knowledge regarding the ontogeny and pathogenesis of RDD has lagged behind. Our study provides important information regarding the clinical spectrum and natural history for this entity. Due to the varying outcomes with similar histopathology, RDD may be considered a syndrome rather than a single disease entity. On one end of the spectrum are patients with "benign" single-system unifocal RDD such as a solitary subcutaneous nodule that can be observed or excised, and may lead to sustained remissions. On the other end, however, are the patients who are truly "neoplastic" and may need closer monitoring or systemic therapy. Although both these entities demonstrate similar histopathologic features to be diagnosed as RDD, there may be differences in the molecular/genetic architecture that differentiate benign from neoplastic RDD. Hence, more studies are needed to appropriately correlate phenotypic and molecular characteristics of RDD. Further studies focused at the hematopoietic stem cell compartment are also needed to ascertain the cell of origin of RDD, as that may provide insights into the pathogenesis and therapeutics. As discovery of *MAP-ERK* mutations in other histiocytic neoplasms has enabled successful targeted therapy with MEK-

inhibitors, the ongoing study of cobimetinib in histiocytic disorders (NCT02649972), which includes RDD, will hopefully provide the first FDA approved treatment for this disease.³⁷

Acknowledgments

This study was partly presented at the 2017 American Society of Hematology conference, Atlanta, GA, USA.

References

- Destombes P. [Adenitis with lipid excess, in children or young adults, seen in the Antilles and in Mali. (4 cases)]. *Bull Soc Pathol Exot Filiales*. 1965;58(6):1169-1175.
- Rosai J, Dorfman RF. Sinus histiocytosis with massive lymphadenopathy. A newly recognized benign clinicopathological entity. *Arch Pathol*. 1969;87(1):63-70.
- Foucar E, Rosai J, Dorfman R. Sinus histiocytosis with massive lymphadenopathy (Rosai-Dorfman disease): review of the entity. *Semin Diagn Pathol*. 1990;7(1):19-73.
- Badalian-Very G, Vergilio JA, Degar BA, et al. Recurrent BRAF mutations in Langerhans cell histiocytosis. *Blood*. 2010;116(11):1919-1923.
- Diamond EL, Durham BH, Haroche J, et al. Diverse and targetable kinase alterations drive histiocytic neoplasms. *Cancer Discov*. 2016;6(2):154-165.
- Haroche J, Charlotte F, Arnaud L, et al. High prevalence of BRAF V600E mutations in Erdheim-Chester disease but not in other non-Langerhans cell histiocytoses. *Blood*. 2012;120(13):2700-2703.
- Garces S, Medeiros LJ, Patel KP, et al. Mutually exclusive recurrent KRAS and MAP2K1 mutations in Rosai-Dorfman disease. *Mod Pathol*. 2017;30(10):1367-1377.
- Chan JKC PS, Fletcher CDM, Weiss LM, Grogg KL. Follicular dendritic cell sarcoma. In: Swerdlow SH CE, Harris NL, Jaffe ES, Pileri SA, Stein H, Theile J, ed. WHO Classification of tumours of haematopoietic and lymphoid tissues: IARC; 2017:476-479.
- Chan JKC PS, Delsol G, Fletcher CDM, Weiss LM, Grogg KL. Follicular dendritic cell sarcoma. In: Swerdlow SH CE, Harris NL, Jaffe ES, Pileri SA, Stein H, Theile J, Vardiman JW, ed. WHO Classification of tumours of haematopoietic and lymphoid tissues: IARC; 2008:363-364.
- Ravindran A, Goyal G, Failing JJ, Go RS, Rech KL. Florid dermatopathic lymphadenopathy: A morphological mimic of Langerhans cell histiocytosis. *Clin Case Rep*. 2018;6(8):1637-1638.
- Beaubier N, Tell R, Huether R, et al. Clinical validation of the Tempus xO assay. *Oncotarget*. 2018;9(40):25826-25832.
- Frampton GM, Fichtenholtz A, Otto GA, et al. Development and validation of a clinical cancer genomic profiling test based on massively parallel DNA sequencing. *Nat Biotechnol*. 2013;31(11):1023-1031.
- Lanman RB, Mortimer SA, Zill OA, et al. Analytical and clinical validation of a digital sequencing panel for quantitative, highly accurate evaluation of cell-free circulating tumor DNA. *PLoS One*. 2015; 10(10): e0140712.
- Young JR, Johnson GB, Murphy RC, Go RS, Broski SM. (18)F-FDG PET/CT in Erdheim-Chester disease: imaging findings and potential BRAF mutation biomarker. *J Nucl Med*. 2018;59(5):774-779.
- Abla O, Jacobsen E, Picarsic J, et al. Consensus recommendations for the diagnosis and clinical management of Rosai-Dorfman-Destombes disease. *Blood*. 2018; 131(26):2877-2890.
- Goyal G, Shah MV, Call TG, Litzow MR, Hogan WJ, Go RS. Clinical and radiologic responses to cladribine for the treatment of Erdheim-Chester disease. *JAMA Oncol*. 2017; 3(9):1253-1256.
- Purysko AS, Westphalen AC, Remer EM, Coppa CP, Leao Filho HM, Herts BR. Imaging manifestations of hematologic diseases with renal and perinephric involvement. *Radiographics*. 2016; 36(4): 1038-1054.
- Ozkaya N, Rosenblum MK, Durham BH, et al. The histopathology of Erdheim-Chester disease: a comprehensive review of a molecularly characterized cohort. *Mod Pathol*. 2018;31(4):581-597.
- Paulli M, Bergamaschi G, Tonon L, et al. Evidence for a polyclonal nature of the cell infiltrate in sinus histiocytosis with massive lymphadenopathy (Rosai-Dorfman Disease). *Br J Haematol*. 1995;91(2):415-418.
- Matter MS, Bihl M, Juskevicius D, Tzankov A. Is Rosai-Dorfman disease a reactive process? Detection of a MAP2K1 L115V mutation in a case of Rosai-Dorfman disease. *Virchows Archiv*. 2017;471(4):545-547.
- Shanmugam V, Margolskee E, Kluk M, Giordadze T, Orazi A. Rosai-Dorfman disease harboring an activating KRAS K117N missense mutation. *Head Neck Pathol*. 2016; 10(3):394-399.
- Goyal G, Lau D, Nagle AM, et al. Tumor mutational burden and other predictive immunotherapy markers in histiocytic neoplasms. *Blood*. 2019;133(14):1607-1610.
- Litzner BR, Subtil A, Vidal CI. Combined cutaneous Rosai-Dorfman disease and localized cutaneous Langerhans cell histiocytosis within a single subcutaneous nodule. *Am J Dermatopathol*. 2015;37(12):936-939.
- Lima FB, Barcelos PS, Constancio AP, Nogueira CD, Melo-Filho AA. Rosai-Dorfman disease with spontaneous resolution: case report of a child. *Rev Bras Hematol Hemoter*. 2011;33(4):312-314.
- Pulsoni A, Anghel G, Falucci P, et al. Treatment of sinus histiocytosis with massive lymphadenopathy (Rosai-Dorfman disease): report of a case and literature review. *Am J Hematol*. 2002;69(1):67-71.
- Al-Khateeb TH. Cutaneous Rosai-Dorfman Disease of the face: a comprehensive literature review and case report. *J Oral Maxillofac Surg*. 2016;74(3):528-540.
- Forest F, N'Guyen A T, Fesselet J, et al. Meningeal Rosai-Dorfman disease mimicking meningioma. *Ann Hematol*. 2014;93(6):937-940.
- Aouba A, Terrier B, Vasiliu V, et al. Dramatic clinical efficacy of cladribine in Rosai-Dorfman disease and evolution of the cytokine profile: towards a new therapeutic approach. *Haematologica*. 2006;91(12 Suppl):ECR52.
- Konca C, Ozkurt ZN, Deger M, Aki Z, Yagci M. Extranodal multifocal Rosai-Dorfman disease: response to 2-chlorodeoxyadenosine treatment. *Int J Hematol*. 2009;89(1):58-62.
- Horneff G, Jurgens H, Hort W, Karitzky D, Gobel U. Sinus histiocytosis with massive lymphadenopathy (Rosai-Dorfman disease): response to methotrexate and mercaptopurine. *Med Pediatr Oncol*. 1996;27(3):187-192.
- Maklad AM, Bayoumi Y, Tunio M, Alshakweer W, Dahar MA, Akbar SA. Steroid-resistant extranodal Rosai-Dorfman disease of cheek mass and ptosis treated with radiation therapy. *Case Rep Hematol*. 2013;2013:428297.
- Petschner F, Walker UA, Schmitt-Graff A, Uhl M, Peter HH. ["Catastrophic systemic lupus erythematosus" with Rosai-Dorfman sinus histiocytosis. Successful treatment with anti-CD20/rutuximab]. *Dtsch Med Wochenschr*. 2001;126(37):998-1001.
- Jabali Y, Smrcka V, Pradna J. Rosai-Dorfman disease: successful long-term results by combination chemotherapy with prednisone, 6-mercaptopurine, methotrexate, and vinblastine: a case report. *Int J Surg Pathol*. 2005;13(3):285-289.
- Scheel MM, Rady PL, Tying SK, Pandya AG. Sinus histiocytosis with massive lymphadenopathy: presentation as giant granuloma annulare and detection of human herpesvirus 6. *J Am Acad Dermatol*. 1997;37(4):643-646.
- Toguri D, Louie AV, Rizkalla K, Franklin J, Rodrigues G, Venkatesan V. Radiotherapy for steroid-resistant laryngeal Rosai-Dorfman disease. *Curr Oncol*. 2011;18(3): e158-162.
- Paryani NN, Daugherty LC, O'Connor MI, Jiang L. Extranodal rosai-dorfman disease of the bone treated with surgery and radiotherapy. *Rare Tumors*. 2014;6(4):5531.
- Diamond EL, Durham BH, Ulaner GA, et al. Efficacy of MEK inhibition in patients with histiocytic neoplasms. *Nature*. 2019; 567(7749):521-524.



Ferrata Storti Foundation

Genome analysis of myelodysplastic syndromes among atomic bomb survivors in Nagasaki

Masataka Taguchi,¹ Hiroyuki Mishima,² Yusuke Shiozawa,³ Chisa Hayashida,² Akira Kinoshita,² Yasuhito Nannya,³ Hideki Makishima,³ Makiko Horai,¹ Masatoshi Matsuo,¹ Shinya Sato,¹ Hidehiro Itonaga,¹ Takeharu Kato,¹ Hiroaki Taniguchi,⁴ Daisuke Imanishi,¹ Yoshitaka Imaizumi,¹ Tomoko Hata,¹ Motoi Takenaka,⁵ Yukiyoishi Moriuchi,⁴ Yuichi Shiraishi,⁴ Satoru Miyano,^{6,7} Seishi Ogawa,³ Koh-ichiro Yoshiura² and Yasushi Miyazaki¹

¹Department of Hematology, Atomic Bomb Disease Institute, Nagasaki University Graduate School of Biomedical Sciences, Nagasaki; ²Department of Human Genetics, Atomic Bomb Disease Institute, Nagasaki University Graduate School of Biomedical Sciences, Nagasaki; ³Department of Pathology and Tumor Biology, Graduate School of Medicine, Kyoto University, Kyoto; ⁴Department of Hematology, Sasebo City General Hospital, Sasebo; ⁵Department of Dermatology, Nagasaki University Graduate School of Biomedical Sciences, Nagasaki; ⁶Laboratory of DNA Information Analysis, Human Genome Center, The Institute of Medical Science, The University of Tokyo, Tokyo and ⁷Laboratory of Sequence Analysis, Human Genome Center, The Institute of Medical Science, The University of Tokyo, Tokyo, Japan

Haematologica 2020
Volume 105(2):358-365

Correspondence:

YASUSHI MIYAZAKI
y-miyaza@nagasaki-u.ac.jp

Received: February 12, 2019.

Accepted: May 16, 2019.

Pre-published: May 17, 2019.

doi:10.3324/haematol.2019.219386

Check the online version for the most updated information on this article, online supplements, and information on authorship & disclosures: www.haematologica.org/content/105/2/358

©2020 Ferrata Storti Foundation

Material published in Haematologica is covered by copyright. All rights are reserved to the Ferrata Storti Foundation. Use of published material is allowed under the following terms and conditions:

<https://creativecommons.org/licenses/by-nc/4.0/legalcode>.

Copies of published material are allowed for personal or internal use. Sharing published material for non-commercial purposes is subject to the following conditions:

<https://creativecommons.org/licenses/by-nc/4.0/legalcode>,

sect. 3. Reproducing and sharing published material for commercial purposes is not allowed without permission in writing from the publisher.



ABSTRACT

Ionizing radiation is a risk factor for myeloid neoplasms including myelodysplastic syndromes (MDS), and atomic bomb survivors have been shown to have a significantly higher risk of MDS. Our previous analyses demonstrated that MDS among these survivors had a significantly higher frequency of complex karyotypes and structural alterations of chromosomes 3, 8, and 11. However, there was no difference in the median survival time between MDS among survivors compared with those of *de novo* origin. This suggested that a different pathophysiology may underlie the causative genetic aberrations for those among survivors. In this study, we performed genome analyses of MDS among survivors and found that proximally exposed patients had significantly fewer mutations in genes such as *TET2* along the DNA methylation pathways, and they had a significantly higher rate of 11q deletions. Among the genes located in the deleted portion of chromosome 11, alterations of *ATM* were significantly more frequent in proximally exposed group with mutations identified on the remaining allele in 2 out of 5 cases. *TP53*, which is frequently mutated in therapy-related myeloid neoplasms, was equally affected between proximally and distally exposed patients. These results suggested that the genetic aberration profiles in MDS among atomic bomb survivors differed from those in therapy-related and *de novo* origin. Considering the role of *ATM* in DNA damage response after radiation exposure, further studies are warranted to elucidate how 11q deletion and aberrations of *ATM* contribute to the pathogenesis of MDS after radiation exposure.

Introduction

Myelodysplastic syndromes (MDS) are clonal myeloid disorders characterized by cytopenias related to ineffective hematopoiesis, dysplasia, and progression to acute myeloid leukemia.¹ The pathogenesis of MDS is not yet fully understood; however, recently developed DNA sequencing technologies have clearly demonstrated the important roles of genome alterations. The most frequent mutations observed in *de novo* MDS are in the genes coding splicing factors (e.g. *SF3B1* and *SRSF2*), followed by mutations in the genes for DNA methylation (e.g. *TET2* and *DNMT3A*) and histone modification (e.g. *ASXL1* and *EZH2*).²⁻⁴ Typically, these somatic muta-

tions are sequentially acquired *de novo* with age, and lead to the development of MDS through the aging-related hematopoietic condition called clonal hematopoiesis of indeterminate potential (CHIP).⁵⁻⁸

Chemotherapy and radiotherapy are well-known risk factors for the development of myeloid neoplasms (therapy-related myeloid neoplasms, t-MN) including MDS (t-MDS), and the clinical and genetic features of t-MDS are different from those of *de novo* MDS with some overlap.⁹ For example, response to treatment and survival rates are very poor for t-MDS, and the karyotypes of t-MDS frequently show deletions of the long arms or the whole of chromosomes 5 and 7, often associated with complex karyotypes.¹⁰ The most frequently mutated gene in t-MDS is *TP53* followed by *RUNX1*. However, *TET2* mutations are less frequent in t-MDS than in *de novo* cases. Several reports have demonstrated that chemotherapy/radiotherapy provides an opportunity for the proliferation of pre-existing hematopoietic stem cells carrying mutations in genes such as *TP53* and *RUNX1*, which eventually progresses to overt t-MN.¹¹

Atomic bomb (A-bomb) radiation has also been reported to be a risk factor for developing MDS, with the degree of risk being associated with radiation dose exposure and distance from the hypocenter.¹² Our previous reports showed an increase in chromosomal aberrations and complex karyotypes in MDS among the proximally exposed survivors. However, the median survival time and time to progression to leukemia did not differ between the proximally and distantly exposed groups.¹³ Detailed comparisons of chromosomal aberrations between A-bomb survivors and unexposed patients with MDS demonstrated that structural alterations in chromosomes 3, 8, and 11 were significantly increased in MDS among survivors, while alterations in chromosomes 5 and 7 were equally frequent in both groups.¹⁴

These observations suggest that MDS among A-bomb survivors may have a different pathogenesis compared with *de novo* and t-MDS cases, which may be reflected by their different patterns of genome alterations. To address these issues, we analyzed MDS among A-bomb survivors using next generation sequencing technologies. We found different profiles of driver mutations among proximally exposed patients, as well as frequent deletion of the long arm of chromosome 11 associated with aberrations of ATM.

Methods

We analyzed 32 patients diagnosed as having MDS, and three patients as idiopathic cytopenia of undetermined significance among A-bomb survivors (*Online Supplementary Table S1*), and we divided them into two groups: patients exposed within 2.7 km of the hypocenter were categorized as the proximally exposed (PE) group, and the others as the distally exposed (DE) group according to the approach adopted by the Radiation Effect Research Foundation¹⁵ (*Online Supplementary Methods*). In this study, we compared clinical/genome data between PE and DE groups because these two groups would have lived in similar circumstances (stayed in Nagasaki after A-bomb under similar environmental circumstances including medical access) except for the dose of A-bomb radiation, more than 5mGy (at 2.7 km) or less, which suggested DE as an appropriate control for PE. Based on our previous epidemiological analysis, excess relative risk (ERR) of

MDS among survivors that had been exposed to 5mGy would be 0.02 (ERR, 4.3 / Gy).¹² Several different sequencing methods were applied in this study depending on the amount and the quality of DNA samples (*Online Supplementary Tables S1 and S2*).

First, we performed whole exome sequencing (WES) with matched germline controls for five patients in the PE group, coded as unbiased-WES (U-WES), then WES without matched germline controls (B-WES-T) for three and eight patients in the PE and DE groups, respectively. Limited number of genes (356 genes) were validated for B-WES-T, which were putative drivers of hematologic malignancies^{3,4,16,17} or candidate genes identified through U-WES (*Online Supplementary Table S3*). Targeted capture sequencing (T-S) of 154 genes was performed for another ten and nine patients in the PE and DE groups, respectively, without matched controls. Target genes were selected based on published data^{3,4,16,17} and results of the U-WES cases (*Online Supplementary Table S4*).

We also investigated three cases (U-WES-3, 4, and 7) using whole genome sequencing (WGS) with matched germline controls (*Online Supplementary Methods and Online Supplementary Table S5*).

The DNA copy number alterations (CNA) were analyzed with a SNP array (CytoScan HD Array, Affymetrix, Santa Clara, CA, USA), and CNA in T-S cases were identified in the sequencing data using the CNACS pipeline,¹⁸ because of the insufficient quality and quantity of DNA for SNP array. Although copy number states of whole chromosomes could not be evaluated, frequently affected regions in MDS, such as the long arms of chromosome 5 (5q), 7q, and 20q, were included among the targets. We also targeted the genes affected by 11q deletion to evaluate the whole arm of 11q because this region was of interest in this study. This study was approved by the ethics committee of Nagasaki University.

Further details of the methods used for this study are available in the *Online Supplementary Methods*.

Results

Clinical features of patients in this study

The major clinical characteristics of the 35 patients who took part in this study are listed in Table 1 with further details provided in *Online Supplementary Table S1*. The median exposure distance from the hypocenter was 1.1 km in the PE group and 3.4 km in the DE group ($P < 0.001$). There were no significant differences in the sex, subtype of MDS, age at diagnosis, or age at the time of the bombing between the two groups. The frequencies of abnormal karyotype and complex karyotype were higher in PE but without statistical significance (Table 1). There was no difference in survival time after diagnosis between two groups ($P = 0.652$) (*Online Supplementary Figure S7*).

Somatic mutations, mutational spectrum, and clonal architecture of myelodysplastic syndromes in the proximally exposed group

Among the five patients (U-WES-3, 4, 5, 7, 8) in the PE group who were analyzed using WGS and/or WES, we identified 5-15 somatic missense and nonsense SNV (mean 9.2 per sample), and 0-2 somatic INDEL (insertions or deletions; mean 1 per sample) on coding exons (Figure 1 and *Online Supplementary Table S6*) per patient. The number of somatic SNV identified using WGS of three patients (U-WES-3, 4 and 7) in the PE group was 1,695, 573, and 756, respectively (*Online Supplementary Tables S7-1, -2, and -3*). The most frequent pattern of nucleotide sub-

Table 1. Patients' characteristics.

Characteristics	PE group (n=18)	DE group (n=17)	P
Sex			
Male	9	5	0.31
Female	9	12	
MDS type (WHO, 2008)			
RCUD	2	1	0.79
RCMD	7	10	
RAEB-1	3	1	
RAEB-2	4	2	
MDS/AML	1	1	
ICUS	1	2	
Age at diagnosis (y.o)			
Median	73	74	0.85
(range)	(57-86)	(53-83)	
Exposure distance (km)			
Median	1.1	3.4*	<0.001
(range)	(0.5-2.5)	(2.8-7.5)	
Age at exposure (y.o)			
Median	12	12	0.86
(range)	(2-19)	(3-19)	
Number of chromosomal abnormality (G-banding)			
0 (normal karyotype)	4	7	0.31
1-2	8	8	
3 (complex)	6	2	

*The data of three patients were excluded when calculating the exposure distance in the distally exposed (DE) group because they were not present at the time of the bombing but entered within a 2 km radius from the hypocenter within two weeks after the bombing. PE: proximally exposed; RCUD: refractory cytopenia with uni-lineage dysplasia; RCMD: RC with multi-lineage dysplasia; RAEB: refractory anemia with excess blasts; ICUS: idiopathic cytopenia of undermined significance; MDS: myelodysplastic syndromes; AML: acute myeloid leukemia.

stitution was cytosine-to-thymine (C to T) (Figure 2 and *Online Supplementary Figure S3*). Clonal heterogeneities of MDS in these patients were inferred from the analysis of variant allele frequencies of the identified somatic SNV (*Online Supplementary Figure S4*).

Comparison of mutated genes between the proximally exposed and distally exposed groups

Using the U-WES, B-WES-T, and T-S methods, somatic and oncogenic mutations were identified in 16 out of 18 patients (89%) in PE, and 12 out of 17 patients (71%) in DE groups (Figure 3 and *Online Supplementary Tables S6, S8 and S9*). Among these mutations, in DE group, *TET2* was most frequently affected (5 out of 17 patients, 29%), followed by *SF3B1* (3 out of 17, 18%) and *STAG2* (18%) (Figure 4). However, none of the PE patients had *TET2* or *STAG2* mutations, and the most frequently mutated gene was *SF3B1* (4 out of 18 patients, 22%). There was a statistically significant difference in the frequency of *TET2* mutations between the two groups ($P=0.019$), but not for *STAG2* ($P=0.104$). Mutations in *TP53* were identified at very similar frequencies in the two groups: PE: 2 out of 18 patients (11%); DE: 2 out of 17 (12%) ($P=1.00$). There was also no significant difference in the frequency of *RUNX1* mutations between the two groups (11% and 6% in PE and DE, respectively; $P=1.00$).

Mutated genes were categorized on the basis of their assumed roles in functional pathways (Figure 5 and *Online Supplementary Table S10*). We found that gene mutations

along the DNA methylation pathways were significantly less frequent in the PE group (1 out of 18 patients, 5.6%) than in the DE group (7 out of 17, 41%; $P=0.018$). Genes coding RNA splicing factors were mutated with equal frequency in both groups. Mutations in genes for transcription factors and the chromatin modification pathway were more frequent in PE than in DE without statistical significance (transcription factors, 39% and 24%, respectively, $P=0.47$; chromatin modification pathway, 33% and 12%, respectively, $P=0.23$).

Copy number alterations and affected genes on 11q

Copy number alterations were evaluated by SNP array or T-S as described in the Methods and the *Online Supplementary Methods*, although the T-S data did not cover whole chromosomes. Using these methods, we identified CNA in 11 out of 18 (61%), and 7 out of 17 patients (41%) in the PE and DE groups, respectively (Figure 6A and *Online Supplementary Table S11*). CNA in chromosomes 11 and 20 were more frequent in PE (Figure 6B and *Online Supplementary Figure S5A*). Among the CNA, 11q deletion was identified only in PE with statistically significant difference (33% and 0% in PE and DE, respectively; $P=0.019$). Copy number loss of chromosome 5q and chromosome 7 were identified with almost equal frequency in both groups [chromosome 5q: PE: 4 out of 18 patients (22%); DE: 2 out of 17 (12%), $P=0.66$; chromosome 7: PE: 22%; DE: 5 out of 17 (29%), $P=0.71$] (*Online Supplementary Figure S5B and C*).

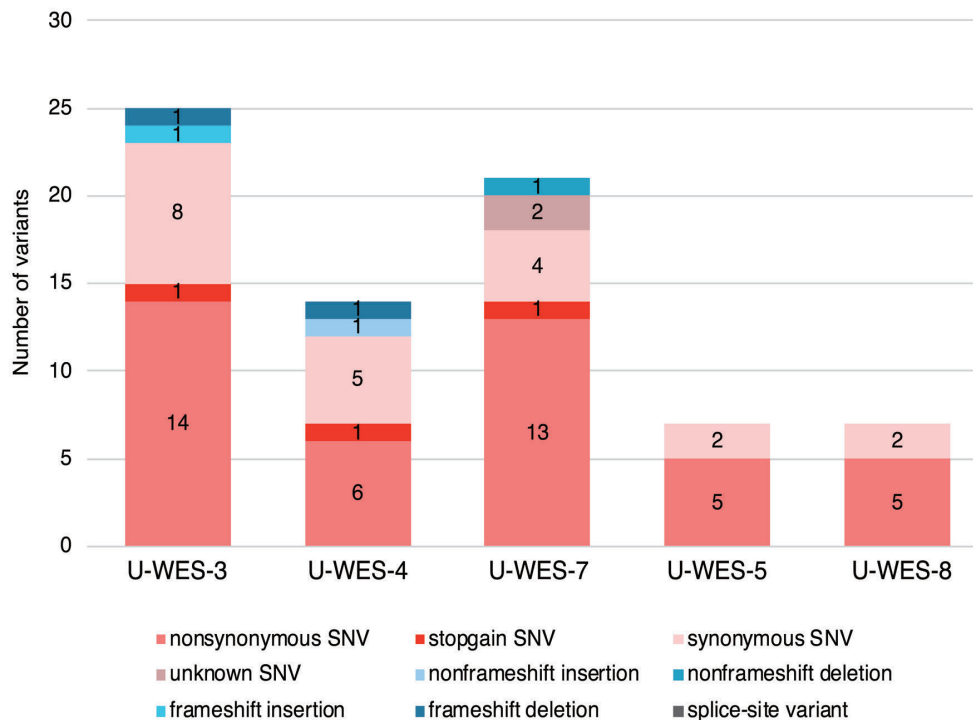


Figure 1. Somatic mutations identified in coding exons of five patients in the proximally exposed group. Each numerical number on the bar charts represents the number of variants of each mutation type identified using whole exome sequencing. No splice site variants were identified among these five patients. U-WES: unbiased-whole exome sequencing.

There are several genes observed to be recurrently affected in MDS and acute myeloid leukemia on 11q, such as *ATM*, *KMT2A*, and *CBL*.^{3,11,16,17} Copy number loss of *ATM*, *KMT2A*, and *CBL* were identified in five, five, and four patients in the PE group, respectively (Table 2), while copy number gain of *KMT2A* and *CBL* were found in one patient in the DE group (*Online Supplementary Figure S6*). We also identified mutations in *ATM* on the remaining allele in two patients (U-WES-3 and -5) in the PE group; thus, both *ATM* alleles were affected in these patients. Alterations of *ATM* were significantly more frequent in PE than in DE patients (28% and 0%, respectively; $P=0.046$).

Discussion

To better understand how A-bomb radiation contributed to the pathogenesis of MDS among survivors, we analyzed DNA samples from these MDS patients using next generation sequencing and SNP arrays for the first time. We found no apparent increase in the number of SNV among MDS patients proximally exposed to A-bomb radiation compared with those reported for patients with *de novo* or secondary MDS/AML.^{5,11} The pattern of nucleotide substitutions was also similar to that observed in *de novo* cases with C-to-T substitution being the most frequent, although this analysis was performed for only three patients in our cohort. We previously reported that the number of chromosomal aberrations was significantly increased in MDS among A-bomb survivors, especially in proximally exposed patients.¹³ This finding led us to predict increased nucleotide alterations in MDS among

patients in the PE group but this was not the case. In spite of the genotoxic effects of ionizing radiation, it did not apparently contribute to increase the mutational burden in MDS. This may be related to the specific nature of A-bomb radiation: one-off, whole-body exposure that was mostly external. This could explain, at least in part, the reason why there was no difference in survival of MDS patients between the PE and DE groups (*Online Supplementary Figure S7*), and between exposed and unexposed *de novo* MDS, or by the distance from the hypocenter, as we previously reported.^{13,14} Considering that our previous study showed cytogenetic risk categories (by revised-International Prognostic Scoring System) significantly divided survival for both MDS among survivors and those unexposed, the same cytogenetic hits seemed to have had a similar influence on their survival.^{13,14}

However, we found significant differences in the profile of mutated genes between proximally and distally exposed patients. *TET2* mutations, which are one of the most frequent alterations in myeloid neoplasms including MDS,^{3,4} were not detected in the PE group but were observed in the DE group, as frequently as reported for *de novo* MDS (approx. 29%). This was related, at least in part, to the significantly less mutations along with DNA methylation pathways in the PE group, as *TET2* is one of the major genes in this pathway. Mutations in *TP53* and genes coding splicing factors, such as *SF3B1*, were comparable to those in *de novo* cases,^{3,4} and were equally frequent in the PE and DE groups. *TP53* is the most frequently mutated gene in t-MN including t-MDS, and it is highly correlated with poor outcome.¹¹ Our previous work

demonstrated no significant difference in survival time between A-bomb survivors with MDS and unexposed MDS patients,^{13,14} which could be partly explained by their similar frequency of *TP53* mutations. Taken together, these findings suggest that the profile of gene mutations in MDS among proximally exposed survivors is different to that of *de novo* MDS patients (reduction or lack of *TET2* mutations in PE cases) and t-MDS patients (fewer *TP53* mutations in PE cases).

A study on mutations of *RUNX1* in MDS among A-bomb survivors (both proximally and distally exposed cases) in Hiroshima noted an increased alteration rate of 46% (6 out of 13 cases) and a missense/frameshift mutation rate of 31% (4 out of 13 cases).¹⁹ In the present study,

however, 3 out of 35 cases (8.6%) had *RUNX1* mutations, which was as frequent as reported for *de novo* MDS (approx. 10%). There is no clear explanation for this difference in the frequency of *RUNX1* mutations but the small number of cases examined in each study (13 cases in the Hiroshima study, and 35 cases in this study) might have played a role. It is also possible that the differences in MDS subtypes influenced the results between two studies, as *RUNX1* mutations are enriched in high-risk MDS.³ In the Hiroshima study, among 13 patients analyzed, there were one patient with refractory anemia with excess blasts (RAEB), eight with RAEB in transformation (RAEB-t), and one AML, sharing 76.9% (10 out of 13) by MDS with increased blasts. Our patient cohort contained

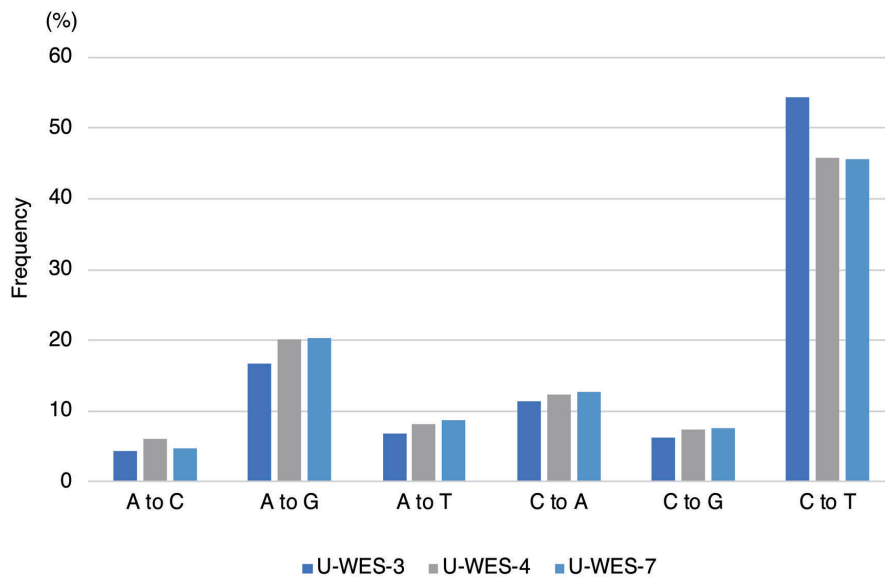


Figure 2. Pattern of nucleotide substitutions in the whole genomes of three patients in the proximally exposed group. The pattern of nucleotide substitution was examined in three patients in the proximally exposed group who were analyzed using whole genome sequencing. Frequencies of each pattern of substitution are represented on the y-axis.

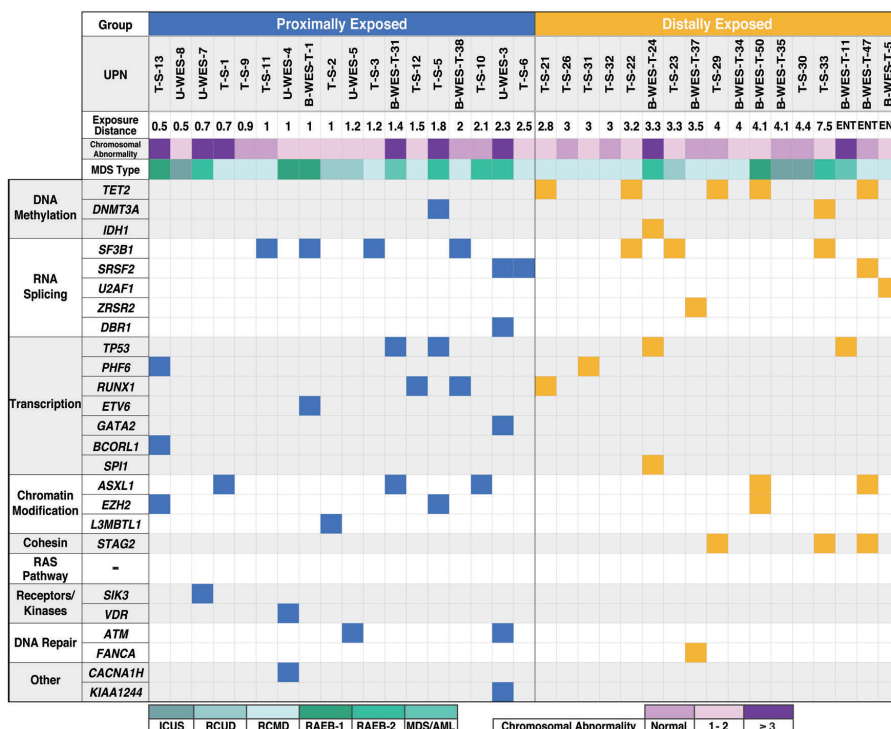


Figure 3. Somatic mutations in myelodysplastic syndromes (MDS) among A-bomb survivors. Each row and column represents a mutated gene and patient, respectively. Identified gene mutations are shown as blue (proximally exposed group) or yellow (distally exposed group) squares. Assumed functional pathways are shown on the far left. UPN: unique patient number; ENT: entered within a 2 km radius from the hypocenter within two weeks after the atomic bombing. RCUD: refractory cytopenia with uni-lineage dysplasia; RCMD: RC with multi-lineage dysplasia; RAEB: refractory anemia with excess blasts; ICUS: idiopathic cytopenia of undetermined significance; AML: acute myeloid leukemia. DE: distally exposed group; PE: proximally exposed group.

12 patients with RAEB or AML, which was 34.3% (12 out of 35) of all participants.

Copy number alterations are frequently found in MDS.^{20,21} In this study, we found a significantly higher frequency of copy number loss for 11q in the PE group than in the DE group ($P=0.019$). Loss of chromosomes 5 or 7, which occurs more frequently in t-MDS (40-50%), and is usually accompanied by a complex karyotype, was observed at an almost equal frequency in the PE and DE groups but less frequently than in t-MDS. Although we did not analyze the entire genes within the commonly deleted region of 11q in the PE group, we detected mutations on the residual *ATM* allele in 2 out of 5 cases (U-WES-3 and U-WES-5) but not in *KMT2A* or *CBL*. The *ATM* mutations, p.D2448V and p.G2891D, were located in the FAT and PI3K domains, respectively. Because of the pathogenic nature of these mutations, U-WES-3 and U-WES-5 appeared to lack expression of functional *ATM* pro-

tein. Deletions or mutations of *ATM* have been reported in *de novo* MDS^{3,4,7,8,22} and it does not seem to be specific to MDS among A-bomb survivors. However, the significantly higher frequency of 11q deletion and the presence of biallelic alterations of *ATM* strongly suggested its importance in the pathogenesis of MDS among survivors.

Since ionizing radiation induces DNA double-strand breaks (DSB),^{23,24} deletions and translocations are frequently observed as a consequence of exposure. Accordingly, our previous study demonstrated that chromosomal translocations were significantly increased in MDS among A-bomb survivors; however, the translocations involving 11q23 where *KMT2A* locates were rare.¹⁴ We observed a significantly higher frequency of 11q aberrations but not translocations among survivors, compared with MDS of unexposed patients.¹⁴ Taken together, these results indicated that aberrations of 11q, especially hemizygous deletion of 11q, could be caused by A-bomb radiation.

Table 2. Copy number alterations and mutations of candidate genes in the frequently affected region on chromosome 11q.

Group	UPN	Candidate genes					
		CNA	ATM Mutation	CNA	KMT2A Mutation	CNA	CBL Mutation
PE	U-WES-3	Loss	D2448V	Loss	–	Loss	–
	U-WES-4	Loss	–	Loss	–	Loss	–
	U-WES-5	Loss	G2891D	Loss	–	Loss	–
	U-WES-7	–	–	Loss	–	–	–
	U-WES-8	Loss	–	–	–	–	–
	T-S-3	Loss	–	Loss	–	Loss	–
DE	B-WES-11	–	–	Gain	–	Gain	–
Frequency of alterations (CNA and mutations) in PE- and DE-group		28 % and 0 % ($P=0.046$)		28 % and 6 % ($P=0.18$)		22 % and 6 % ($P=0.34$)	

Minus sign (–) indicates no copy number alterations (CNA) or mutations. PE: proximally exposed group; DE: distally exposed group.

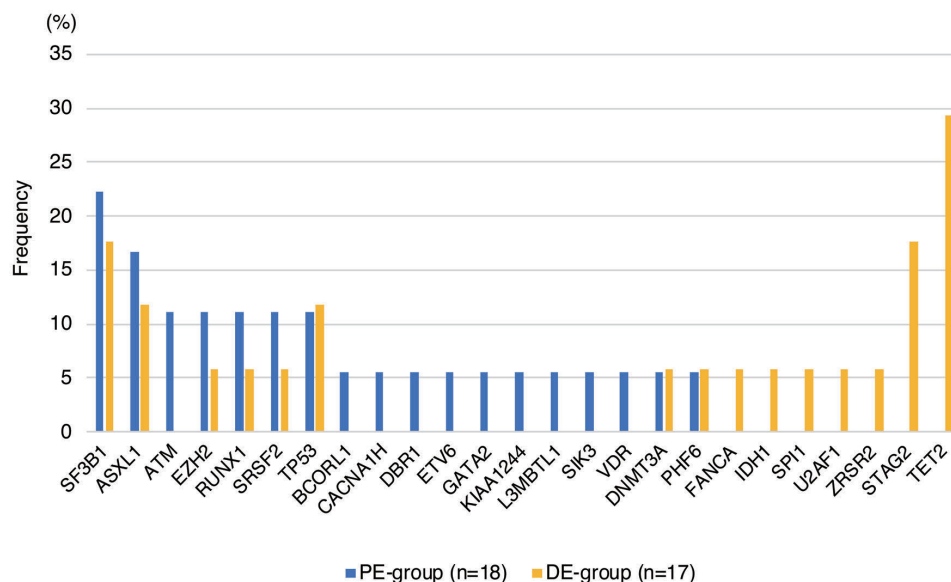


Figure 4. Frequencies of somatic gene mutations in the proximally and distally exposed groups. Frequencies were calculated as the percentage of patients in each group carrying the different mutated genes.

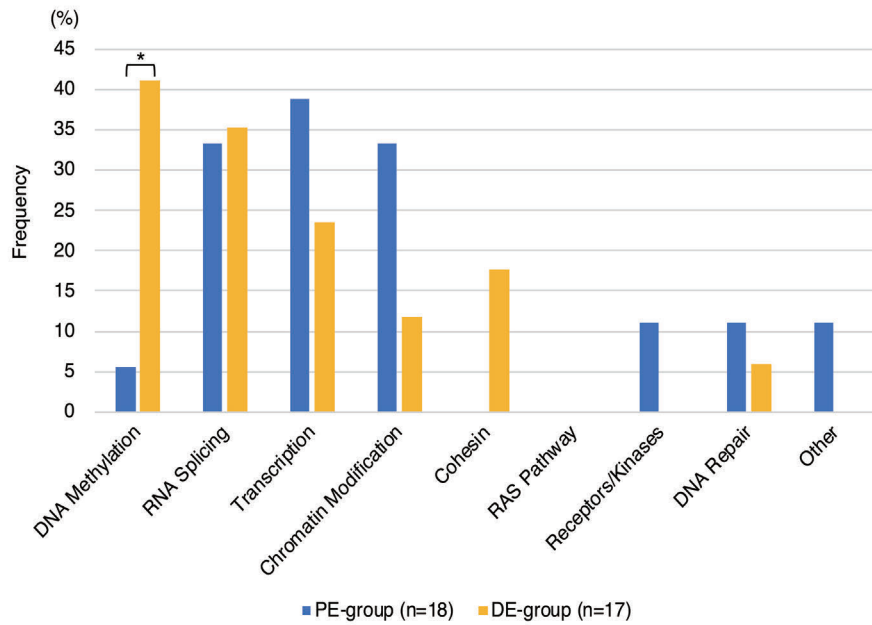


Figure 5. Frequencies of mutated genes categorized by assumed functional pathway. Frequencies were calculated as the percentage of patients in each group carrying mutated genes within the different functional pathways. * $P=0.018$ using Fisher's exact test. DE: distally exposed group; PE: proximally exposed group.

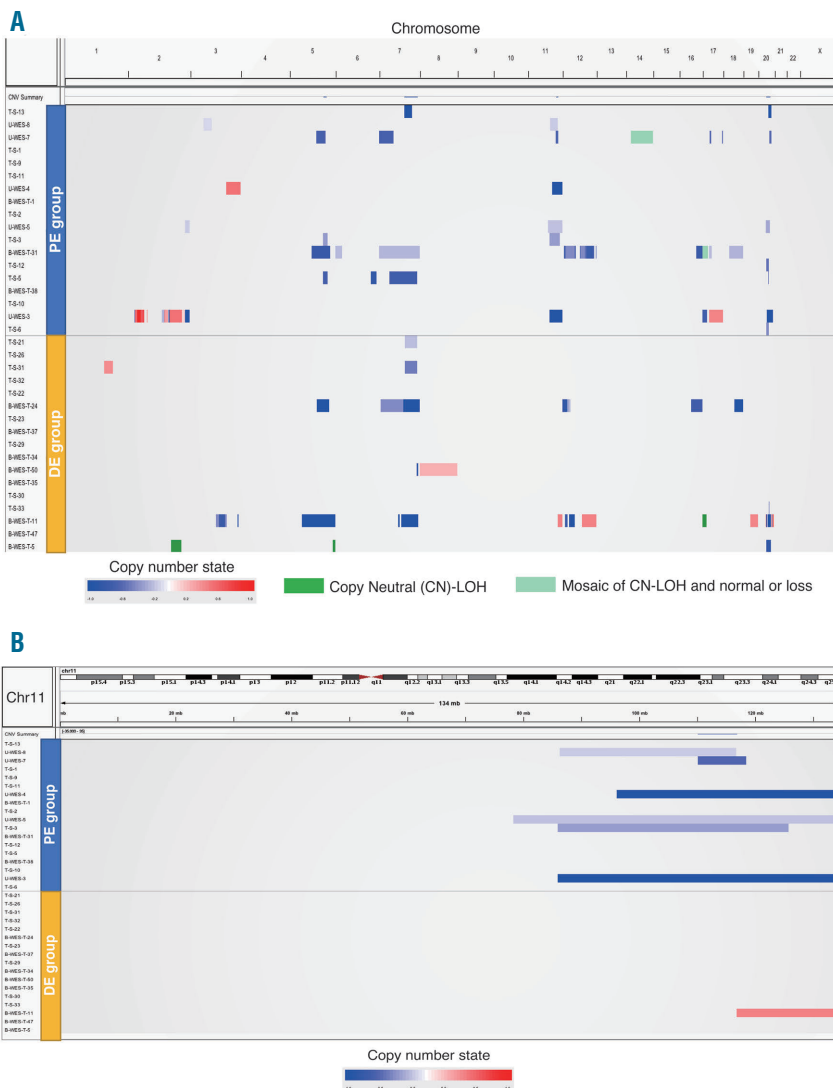


Figure 6. Copy number alterations in myelodysplastic syndromes (MDS) among A-bomb survivors. Each row represents the copy number alterations (CNA) in each patient. The order of patients was in accordance with the exposure distance. (A) CNA on whole chromosomes except for chromosome Y, (B) CNA on chromosome 11. DE: distally exposed group; PE: proximally exposed group.

ATM protein is a key molecule in DNA damage response, in particular, for DSB caused by ionizing radiation,^{25,26,27} and it is possible that the loss of one allele of *ATM* was the initial event for clonal selection towards the development of MDS among A-bomb survivors. It is assumed that immature hematopoietic cells that lost *ATM* following A-bomb radiation either responded poorly or incorrectly to other DNA damage generated at the same time. This might also explain why *TET2* mutations, which are common in *de novo* MDS, and are usually thought to be an initiating mutation for *de novo* MDS, were observed at a low frequency in the PE group in this study. Considering the gain-of-function alterations of *KMT2A* and *CBL* in MDS,^{28,29,30} the defect in *ATM* function generated by 11q deletion that has also been found in *de novo* MDS^{3,22} would have a greater impact on the initiation of MDS among A-bomb survivors. It is necessary to investigate whether alterations in *ATM*, rather than *TET2*, are frequently present in A-bomb survivors who have clonal hematopoiesis of indeterminate potential (CHIP).

In conclusion, we reported a profile of genetic alterations in MDS among survivors exposed to A-bomb radiation, such as fewer mutations in genes along DNA methylation pathways, and frequent 11q deletions and

aberrations in *ATM*. Further investigations are warranted to elucidate the role of these genetic alterations in the pathogenesis of MDS after radiation exposure.

Funding

This work was partly supported by JSPS KAKENHI (Grant Number 26461426) (Y. Miyazaki), MEXT KAKENHI (Grant number 17H04209) (K-IY, Y. Miyazaki), the Program of the Network-type Joint Usage/Research Center for Radiation Disaster Medical Science (MT, MH, K-IY, Y. Miyazaki), the Takeda Science Foundation (K-IY, Y. Miyazaki), Practical Research for Innovative Cancer Control (Grant number 16ck0106073h0003) (SO), the Project for Cancer Research and Therapeutic Evolution (Grant number P-CREATE, 16cm0106501h0001) from Japan AMED (SO), and JSPS KAKENHI (Grant number 15H05909) (SO).

Acknowledgments

We thank Mariko Yozaki, Naoko Ito, Hiroe Urakami, Azumi Yukawa, and Chihiro Yoshikawa for their technical assistance, and Natasha Beeton-Kempen (Edanz Group, www.edanzediting.com/ac) for editing a draft of this manuscript.

For original sequence data, please contact Masataka Taguchi (mtaguchi-ngs@umin.org), and Yasushi Miyazaki (y-miyaza@nagasaki-u.ac.jp).

References

- Adès L, Itzykson R, Fenaux P. Myelodysplastic syndromes. *Lancet*. 2014; 383(9936):2239-2252.
- Yoshida K, Sanada M, Shiraishi Y, et al. Frequent pathway mutations of splicing machinery in myelodysplasia. *Nature*. 2011;478(7367):64-69.
- Haferlach T, Nagata Y, Grossmann V, et al. Landscape of genetic lesions in 944 patients with myelodysplastic syndromes. *Leukemia*. 2014;28(2):241-247.
- Papaemmanuil E, Gerstung M, Malcovati L, et al. Clinical and biological implications of driver mutations in myelodysplastic syndromes. *Blood*. 2013;122(22):3616-3627; quiz 3699.
- Makishima H, Yoshizato T, Yoshida K, et al. Dynamics of clonal evolution in myelodysplastic syndromes. *Nat Genet*. 2017;49(2):204-212.
- Steensma DP, Bejar R, Jaiswal S, et al. Clonal hematopoiesis of indeterminate potential and its distinction from myelodysplastic syndromes. *Blood*. 2015; 126(1):9-16.
- Genovese G, Kähler AK, Handsaker RE, et al. Clonal hematopoiesis and blood-cancer risk inferred from blood DNA sequence. *N Engl J Med*. 2014;371(26):2477-2487.
- Jaiswal S, Fontanillas P, Flannick J, et al. Age-related clonal hematopoiesis associated with adverse outcomes. *N Engl J Med*. 2014;371(26):2488-2498.
- Ganser A, Heuser M. Therapy-related myeloid neoplasms. *Curr Opin Hematol*. 2017;24(2):152-158.
- Smith SM, Le Beau MM, Huo D, et al. Clinical-cytogenetic associations in 306 patients with therapy-related myelodysplasia and myeloid leukemia: the University of Chicago series. *Blood*. 2003;102(1):43-52.
- Wong TN, Ramsingh G, Young AL, et al. Role of TP53 mutations in the origin and evolution of therapy-related acute myeloid leukaemia. *Nature*. 2015;518(7540):552-555.
- Iwanaga M, Hsu W-L, Soda M, et al. Risk of myelodysplastic syndromes in people exposed to ionizing radiation: a retrospective cohort study of Nagasaki atomic bomb survivors. *J Clin Oncol*. 2011;29(4):428-434.
- Matsuo M, Iwanaga M, Kondo H, et al. Clinical features and prognosis of patients with myelodysplastic syndromes who were exposed to atomic bomb radiation in Nagasaki. *Cancer Sci*. 2016;107(10):1484-1491.
- Horai M, Satoh S, Matsuo M, et al. Chromosomal analysis of myelodysplastic syndromes among atomic bomb survivors in Nagasaki. *Br J Haematol*. 2018; 180(3):381-390.
- Young R, Kerr G eds. Reassessment of the Atomic Bomb Radiation Dosimetry for Hiroshima and Nagasaki, Dosimetry System 2002, Report of the Joint US-Japan Working Group. Hiroshima: Radiation Effects Research Foundation. 2005.
- Kihara R, Nagata Y, Kiyoi H, et al. Comprehensive analysis of genetic alterations and their prognostic impacts in adult acute myeloid leukemia patients. *Leukemia*. 2014;28(8):1586-1595.
- Cancer Genome Atlas Research Network, Ley TJ, Miller C, et al. Genomic and epigenomic landscapes of adult de novo acute myeloid leukemia. *N Engl J Med*. 2013; 368(22):2059-2074.
- Yoshizato T, Nannya Y, Atsuta Y, et al. Genetic abnormalities in myelodysplasia and secondary acute myeloid leukemia: impact on outcome of stem cell transplantation. *Blood*. 2017;129(17):2347-2358.
- Harada H, Harada Y, Tanaka H, Kimura A, Inaba T. Implications of somatic mutations in the *AML1* gene in radiation-associated and therapy-related myelodysplastic syndrome/acute myeloid leukemia. *Blood*. 2003;101(2):673-680.
- Tiu RV, Gondek LP, O'Keefe CL, et al. Prognostic impact of SNP array karyotyping in myelodysplastic syndromes and related myeloid malignancies. *Blood*. 2011; 117(17):4552-4560.
- Stevens-Kroef MJ, Olde Weghuis D, Elldrissi-Zaynoun N, et al. Genomic array as compared to karyotyping in myelodysplastic syndromes in a prospective clinical trial. *Genes Chromosom. Cancer*. 2017; 56(7):524-534.
- Wang SA, Abruzzo LV, Hasserjian RP, et al. Myelodysplastic syndromes with deletions of chromosome 11q lack cryptic MLL rearrangement and exhibit characteristic clinicopathologic features. *Leuk Res*. 2011; 35(3):351-357.
- Cannan WJ, Pederson DS. Mechanisms and Consequences of Double-Strand DNA Break Formation in Chromatin. *J Cell Physiol*. 2016;231(1):3-14.
- Price BD, D'Andrea AD. Chromatin remodeling at DNA double-strand breaks. *Cell*. 2013;152(6):1344-1354.
- Banin S, Moyal L, Shieh S, et al. Enhanced phosphorylation of p53 by ATM in response to DNA damage. *Science*. 1998;281(5383):1674-1677.
- Canman CE, Lim DS, Cimprich KA, et al. Activation of the ATM kinase by ionizing radiation and phosphorylation of p53. *Science*. 1998;281(5383):1677-1679.
- Guleria A, Chandna S. ATM kinase: Much more than a DNA damage responsive protein. *DNA Repair*. 2016;39:1-20.
- Dicker F, Haferlach C, Sundermann J, et al. Mutation analysis for RUNX1, MLL-PTD, FLT3-ITD, NPM1 and NRAS in 269 patients with MDS or secondary AML. *Leukemia*. 2010;24(8):1528-1532.
- Dorrance AM, Liu S, Chong A, et al. The Mll partial tandem duplication: differential, tissue-specific activity in the presence or absence of the wild-type allele. *Blood*. 2008;112(6):2508-2511.
- Sanada M, Suzuki T, Shih L-Y, et al. Gain-of-function of mutated C-CBL tumour suppressor in myeloid neoplasms. *Nature*. 2009;460(7257):904-908.



Molecular quantification of tissue disease burden is a new biomarker and independent predictor of survival in mastocytosis

Georg Greiner,^{1,2} Michael Gurbisz,¹ Franz Ratzinger,¹ Nadine Witzeneder,^{1,3} Svenja Verena Class,⁴ Gregor Eisenwort,^{2,3} Ingrid Simonitsch-Klupp,⁴ Harald Esterbauer,^{1,2} Matthias Mayerhofer,⁵ Leonhard Müllauer,⁴ Wolfgang R. Sperr,^{2,3} Peter Valent,^{2,3} and Gregor Hoermann^{1,2,6}

Haematologica 2020
Volume 105(2):366-374

¹Department of Laboratory Medicine, Medical University of Vienna, Vienna; ²Ludwig Boltzmann Institute for Hematology and Oncology, Medical University of Vienna, Vienna; ³Department of Internal Medicine I, Division of Hematology and Hemostaseology, Medical University of Vienna, Vienna; ⁴Department of Pathology, Medical University of Vienna, Vienna; ⁵Ludwig Boltzmann Institute of Osteology, Hanusch Hospital, Vienna and ⁶Central Institute of Medical and Chemical Laboratory Diagnostics, University Hospital Innsbruck, Innsbruck, Austria

ABSTRACT

A high allele burden of the *KIT* D816V mutation in peripheral blood or bone marrow aspirates indicates multi-lineage hematopoietic involvement and has been associated with an aggressive clinical course of systemic mastocytosis. Since mast cells are substantially under-represented in these liquid specimens, their mutation burden likely underestimates the tumor burden of the disease. We used a novel previously validated digital polymerase chain reaction (PCR) method for *KIT* D816V analysis to systematically analyze the mutation burden in formalin-fixed, paraffin-embedded bone marrow tissue sections of 116 mastocytosis patients (91 with indolent and 25 with advanced systemic mastocytosis), and to evaluate for the first time the clinical value of the tissue mutation burden as a novel biomarker. The *KIT* D816V mutation burden in the tissue was significantly higher and correlated better with bone marrow mast cell infiltration ($r=0.68$ vs. 0.48) and serum tryptase levels ($r=0.68$ vs. 0.58) compared to that in liquid specimens. Furthermore, the *KIT* D816V tissue mutation burden was: (i) significantly higher in advanced than in indolent systemic mastocytosis ($P=0.001$); (ii) predicted survival of patients in multivariate analyses independently; and (iii) was significantly reduced after response to cytoreductive therapy. Finally, digital PCR was more sensitive in detecting *KIT* D816V in bone marrow sections of indolent systemic mastocytosis patients than melting curve analysis after peptide nucleic acid-mediated PCR clamping (97% vs. 89% ; $P<0.05$). In summary, digital PCR-based measurement of *KIT* D816V mutation burden in the tissue represents a novel biomarker with independent prognostic significance that can also be employed for monitoring disease progression and treatment response in systemic mastocytosis.

Correspondence:

GREGOR HOERMANN
gregor.hoermann@meduniwien.ac.at

Received: January 29, 2019.

Accepted: April 18, 2019.

Pre-published: April 24, 2019.

doi:10.3324/haematol.2019.217950

Check the online version for the most updated information on this article, online supplements, and information on authorship & disclosures: www.haematologica.org/content/105/2/366

©2020 Ferrata Storti Foundation

Material published in *Haematologica* is covered by copyright. All rights are reserved to the Ferrata Storti Foundation. Use of published material is allowed under the following terms and conditions:

<https://creativecommons.org/licenses/by-nc/4.0/legalcode>.

Copies of published material are allowed for personal or internal use. Sharing published material for non-commercial purposes is subject to the following conditions:

<https://creativecommons.org/licenses/by-nc/4.0/legalcode>,

sect. 3. Reproducing and sharing published material for commercial purposes is not allowed without permission in writing from the publisher.



Introduction

Systemic mastocytosis (SM) is a clonal hematopoietic disorder characterized by abnormal infiltration of mast cells (MC) in various organs, including the bone marrow (BM).¹ The somatic *KIT* D816V mutation leads to growth factor-independent activation of the receptor tyrosine kinase KIT.^{2,3} Detection of the mutation in the BM, peripheral blood (PB), or another extra-cutaneous organ is a minor diagnostic criterion for SM.^{1,4} Although this typical driver mutation is present in a vast majority of all patients with SM, the clinical course in SM is highly variable.⁵ The World Health Organization (WHO) classification divides mastocytosis into cutaneous mastocytosis (CM), indolent SM (ISM), smoldering SM (SSM), aggressive SM (ASM), SM with an associated hematologic neoplasm (SM-AHN), and mast cell leukemia (MCL).^{1,4,6}

These last three entities are collectively referred to as advanced mastocytosis, based on their increased risk of progression and death.^{4,7}

Molecular diagnostics has become increasingly important in SM. Molecular techniques with a high analytical sensitivity, such as allele-specific quantitative polymerase chain reaction (qPCR) or digital PCR (dPCR), are required to reliably detect the *KIT* mutation in liquid specimens (PB or BM aspirate).⁸⁻¹³ Melting curve analysis after peptide nucleic acid (PNA)-mediated PCR clamping (clamp-PCR) is widely used for qualitative detection of the *KIT* mutation in formalin-fixed paraffin-embedded (FFPE) tissue biopsies despite its limited analytical sensitivity that requires micro-dissection of BM MC in a number of cases.^{14,15} We have recently shown that dPCR is suitable as a new sensitive method for *KIT* D816V testing in SM that also reliably quantifies the variant allele frequency (VAF).¹⁶ A high mutant allele burden in liquid specimens was indicative of multi-lineage involvement with *KIT* D816V and was associated with an aggressive clinical course and advanced forms of SM.¹⁶⁻²⁰ However, in the majority of patients, only a small fraction of *KIT* D816V⁺ MC and/or MC precursors, if any, is found in liquid specimens.²¹ Therefore, quantification of *KIT* D816V VAF in liquid specimens typically only evaluates multi-lineage involvement in the non-MC compartment. In line with this observation, only a moderate correlation of *KIT* D816V VAF in liquid specimens with MC infiltration or serum tryptase as surrogate markers for disease burden in SM has been described.^{17,20} In contrast, the percentage of *KIT* D816V⁺ MC is typically much higher in BM tissue biopsies compared to BM aspirates.^{22,23} Therefore, molecular measurements in liquid specimens substantially underestimate the disease burden in SM, in particular in ISM. Moreover, while a reduction of the mutation burden in liquid specimens has been described in response to cytoreductive treatment in patients with advanced SM and multi-lineage involvement,^{18,24} its value as a follow-up parameter in ISM and advanced SM without multi-lineage involvement remains uncertain. Molecular quantification of *KIT* D816V disease burden in the tissue has the potential to overcome these limitations as a biomarker of disease burden in SM.

The quantification of *KIT* D816V VAF has not been assessed systematically in BM tissue sections of SM patients. Here we investigated the clinical value of dPCR-based *KIT* D816V tissue mutation burden quantification as a novel biomarker in SM.

Methods

Patients

We examined 390 samples (211 FFPE BM sections, 106 BM aspirates, 73 PB) from 116 SM patients (58 females, 58 males), diagnosed between April 1988 and February 2016 and included in a

local registry. PB and BM samples at diagnosis and during follow up were obtained after informed consent and the study was approved by the institutional review board (EK:1750/2017). According to WHO criteria,^{1,6} 83 patients were diagnosed with ISM, 8 with SSM, 7 with ASM, 3 with MCL, and 15 with SMAHN. Patients' characteristics are shown in Table 1. During the course of disease, 36 patients (31%) received a cytoreductive treatment with a median of two different regimens (range 1-5) (*Online Supplementary Table S1*). Fifty-seven FFPE BM sections from lymphoma patients undergoing a staging biopsy, and in whom no BM infiltration was detected, were used as control material (*Online Supplementary Table S2*). Quantification of BM infiltration by MC, flow cytometry of MC, and measurement of serum tryptase is described in the *Online Supplementary Methods*.

Molecular analysis of *KIT* D816V

Genomic DNA was extracted from (FFPE) BM sections as well as PB and/or aspirated BM cells as previously described and dPCR for *KIT* D816V was performed with the PrimePCR ddPCR mutation assay for *KIT* wild-type and the *KIT* D816V point mutation (Bio-Rad Laboratories, Munich, Germany) and analyzed on the QX-200 droplet-reader (Bio-Rad Laboratories), as described in detail in the *Online Supplementary Methods*.¹⁶ In addition, qualitative detection of *KIT* codon 816 mutations was performed using melting curve analysis after PNA-mediated PCR clamping as described.¹⁴⁻¹⁶

Statistical analysis

Statistical analysis was performed using R (version 3.4.2, Vienna, Austria)²⁵ and GraphPad Prism (GraphPad Software, La Jolla, CA, USA). Applied tests are described in detail in the *Online Supplementary Methods* and $P < 0.05$ was considered to be significant.

Results

The *KIT* D816V tissue allele burden is a novel biomarker in systemic mastocytosis

The *KIT* D816V tissue allele burden was studied by dPCR in 211 FFPE BM sections from 116 SM patients (Table 1). Median VAF was 1.9%, with a range between 0.027% and 60% indicating a substantial difference in the tissue mutation burden over various orders of magnitude between patients. When we compared the *KIT* D816V VAF in FFPE BM section with that in matched PB or BM aspirates samples, higher tissue allele burden levels were observed (Figure 1A), whereas a strong correlation was found between PB and BM aspirates ($r = 0.99$) (*Online Supplementary Figure S1*). A comparison between the log transformed *KIT* D816V VAF in the tissue and liquid specimens (BM aspirate $n = 96$, PB $n = 12$ in cases for which no BM aspirate was available for molecular analysis) in 108 matched samples from 79 patients, revealed a direct correlation in non-parametric analysis ($r = 0.87$) but a constant and proportional deviation was found in Passing Bablok regression analysis (intercept: 1.72, 95%CI: 1.53-1.91; slope: 0.59, 95%CI: 0.52-0.65) (Figure 1B). In addition, Bland-Altman plot displayed a deviation tendency to higher *KIT* D816V allele burden in FFPE BM sections, particularly in samples with low VAF (Figure 1C). In summary, these findings indicate that the *KIT* D816V VAF in FFPE BM sections was not interchangeable with allele burden measurements in liquid specimens and represents a new biological variable of disease burden in SM patients.

Table 1. Patients' characteristics.

Patients' characteristics	ISM (n=91)	Advanced SM (n=25)	Total cohort (n=116)
Age (median, range)	50 (23–82)	64 (21–91)	53 (21–91)
Sex (female male)	50 41	8 17	58 58
<i>KIT</i> D816V positive *	88/91 (97%)	17/25 (68%) [†]	105/116 (91%)

ISM: indolent systemic mastocytosis; n: number. *As assessed by digital polymerase chain reaction. [†]One additional patient was tested positive for *KIT* D816H.

The *KIT* D816V tissue allele burden correlates with mast cell infiltration and serum tryptase levels

In a next step, we correlated *KIT* D816V VAF with BM MC infiltration and serum tryptase levels as established surrogate parameters of disease burden in *KIT* D816V positive SM patients (n=105). The correlation of mutant allele burden with BM MC infiltration as determined by immunohistochemistry was higher for DNA isolated from BM FFPE sections (r=0.68) (Figure 2A) than from liquid specimens (r=0.48) (Figure 2B). Likewise, a higher correlation with serum tryptase was observed for tissue mutation burden (r=0.68) (Figure 2C) than for liquid mutation burden (r=0.58) (Figure 2D). When we stratified the samples into ISM and advanced SM, a higher correlation of BM MC infiltration with the mutation burden in the tissue (compared to liquid samples) was observed for both subgroups, with a generally higher correlation in ISM patients (*Online Supplementary Figure S2A and B*). In contrast, we found only a modest correlation of the mutation burden with serum tryptase for both specimens in advanced SM, while the correlation with tryptase substantially increased from liquid (r=0.55) to tissue VAF (r=0.70) in ISM (*Online Supplementary Figure S2C and D*). Together, the *KIT* D816V allele burden in FFPE BM sections reflects the burden of neoplastic cells in SM better than established mutant allele burden measurements in PB or BM aspirate.

The *KIT* D816V tissue allele burden is higher in advanced than in indolent systemic mastocytosis

Next, we compared surrogate markers of disease burden

in SM patients between ISM (n=91) and advanced SM (n=25). The median BM MC infiltration was higher in advanced SM (20%) compared to ISM (7%) ($P<0.01$) (Figure 3A). Likewise, a tendency towards higher levels of serum tryptase levels were observed in advanced SM (median 140 ng/mL vs. 37 ng/mL; $P=0.07$) (Figure 3B). Within the *KIT* D816V positive patients, a significantly higher mutant allele burden was observed in advanced SM both in liquid specimens (21.31% vs. 0.34%; $P<0.01$) (Figure 3C) as well as in BM tissue samples (23.40% vs. 1.65%; $P<0.001$) (Figure 3D).

However, the observed difference was bigger in liquid specimens due to the higher *KIT* D816V allele burden in BM tissue (compared to liquid specimens) in our ISM patients. When we analyzed SSM patients within the ISM cohort (n=8), particularly high levels of MC infiltration (median: 35%, range: 20-80%), serum tryptase (median: 234 ng/mL, range: 188-545 ng/mL), liquid mutant allele burden (median: 35.40%, range: 10.60-39.10%) as well as tissue mutant allele burden (median: 10.94%, range: 3.90-36.90%) were found (Figure 3). In summary, our data indicate that tissue mutation burden is a promising novel biomarker of disease burden in SM.

The *KIT* D816V tissue allele burden predicts survival in systemic mastocytosis and reflects response to cytoreductive treatment

To define the prognostic value of tissue mutation burden quantification, we associated *KIT* D816V tissue VAF results with the clinical end points overall survival (OS)

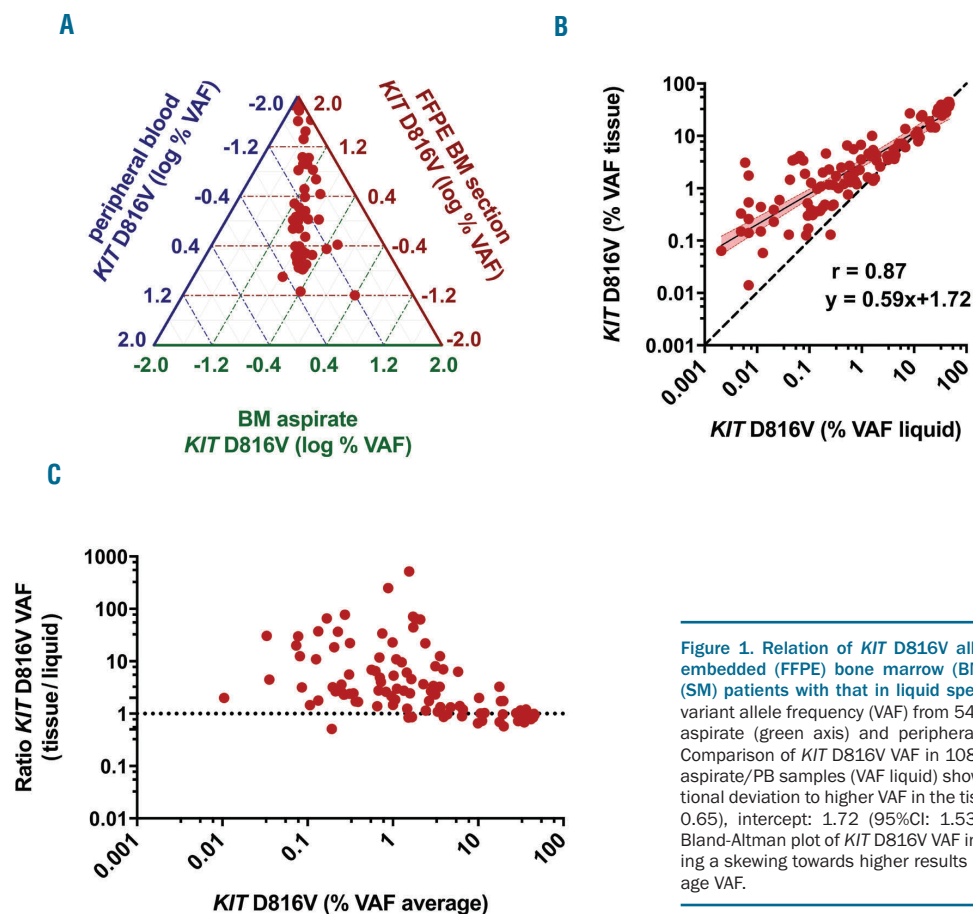


Figure 1. Relation of *KIT* D816V allele burden in formalin-fixed paraffin-embedded (FFPE) bone marrow (BM) sections of systemic mastocytosis (SM) patients with that in liquid specimens. (A) Ternary plot of *KIT* D816V variant allele frequency (VAF) from 54 paired FFPE BM section (red axis), BM aspirate (green axis) and peripheral blood (PB) (blue axis) samples. (B) Comparison of *KIT* D816V VAF in 108 paired FFPE BM (VAF tissue) and BM aspirate/PB samples (VAF liquid) showing a systematic constant and proportional deviation to higher VAF in the tissue ($r=0.87$; slope: 0.59 (95%CI: 0.52-0.65), intercept: 1.72 (95%CI: 1.53-1.91) for log transformed data). (C) Bland-Altman plot of *KIT* D816V VAF in the tissue and liquid specimens showing a skewing towards higher results in the tissue for samples with low average VAF.

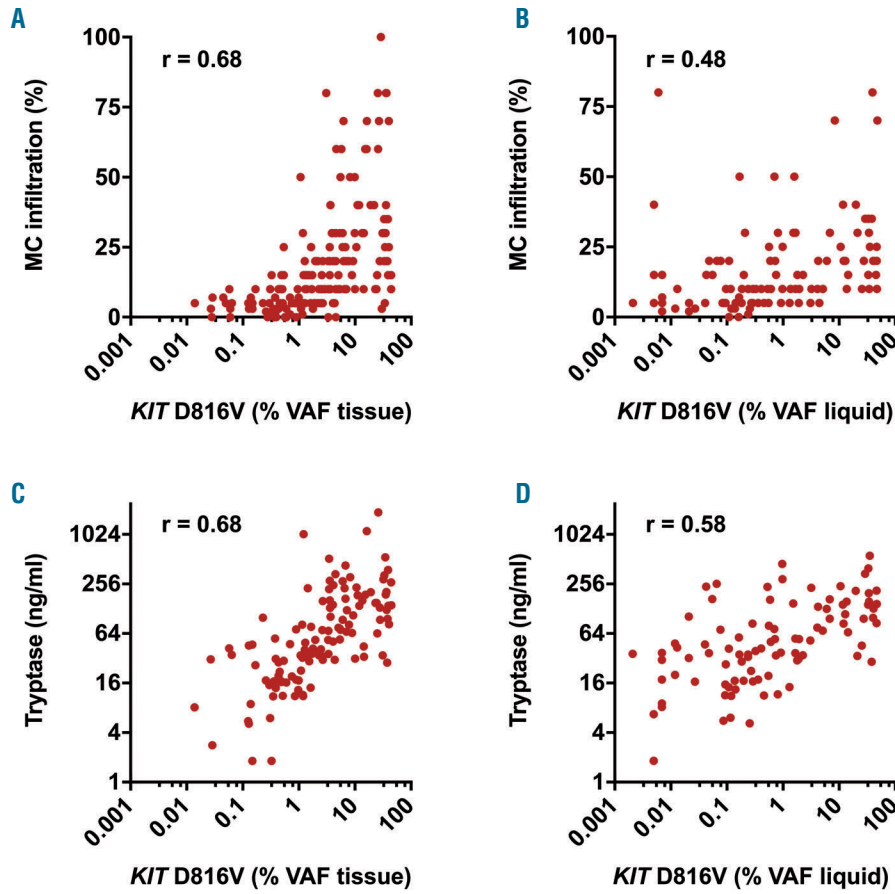


Figure 2. Association of *KIT* D816V allele burden with biomarkers of disease burden in systemic mastocytosis (SM). Correlation of *KIT* D816V mutation burden in 185 formalin-fixed paraffin-embedded (FFPE) bone marrow (BM) sections [variant allele frequency (VAF) tissue: A and C] and 108 BM aspirate/peripheral blood (PB) samples (VAF liquid: B and D) with immunohistologically determined BM mast cell (MC) infiltration (A and B) and serum tryptase (C and D). *r*: Spearman's correlation coefficient.

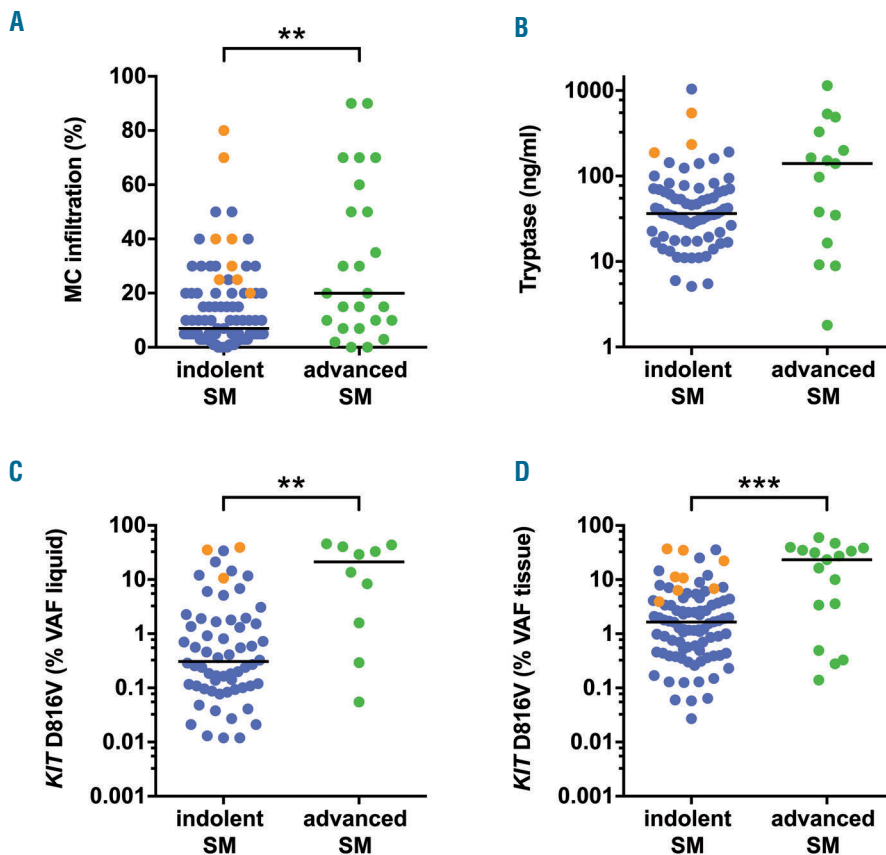


Figure 3. Biomarkers of disease burden in indolent and advanced systemic mastocytosis (SM). Bone marrow (BM) mast cell (MC) infiltration (A), serum tryptase levels (B), and *KIT* D816V mutant allele burden in BM aspirate/peripheral blood samples [variant allele frequency (VAF) liquid: C] and formalin-fixed paraffin-embedded (FFPE) BM sections (VAF tissue; D) were assessed for indolent (ISM) (blue, n=91) and advanced (green, n=25) SM patients. Samples from smoldering SM patients within the ISM cohort are shown in orange. ** $P < 0.01$; *** $P < 0.001$.

Table 2. Parameters for progression-free survival (PFS) in systemic mastocytosis.

Progression-free survival (PFS)	Univariate			Multivariate		
	HR	[95% CI]	P	HR	[95% CI]	P
Molecular quantification of <i>KIT</i> D816V allele burden						
VAF in liquid specimen $\geq 2\%$	5.99	[2.41-14.88]	<0.0001			n.s.
VAF in tissue $\geq 9\%$	15.82	[5.31-47.16]	<0.0001	50.71	[4.23-607.90]	0.002
Clinical characteristics						
Age > 65 years	1.06	[1.04-1.10]	<0.0001			n.s.
Sex	3.25	[1.26-8.38]	0.015			n.s.
B-findings						
MC infiltration in BM biopsy >30%	3.12	[1.32-7.37]	0.010			n.s.
Serum tryptase level >200 $\mu\text{g/L}$	2.43	[0.90-6.58]	n.s.			n.s.
Organomegaly without dysfunction *	3.93	(1.65-9.35)	0.001			n.s.
C-findings						
Hemoglobin <10 g/dL	16.59	[5.43-50.67]	<0.0001			n.s.
Platelets <100x10 ⁹ /L	17.44	[5.93-51.29]	<0.0001	21.26	[2.64-171.30]	0.004
Hepatomegaly with dysfunction [†]	6.97	[1.52-31.93]	0.012			n.s.
Alkaline phosphatase >150 U/L	3.32	[1.36-8.19]	0.008			n.s.
Weight loss	3.41	[1.40-8.27]	0.007			n.s.
Albumin levels <35 g/L	3.38	[0.98-11.57]	n.s.			n.s.

Multivariate analyses regarding the prognostic impact of *KIT* D816V tissue variant allele frequency (VAF) and clinical characteristics (including B- and C-findings) on PFS of 103 patients with SM. HR: hazard ratio; CI: confidence interval; MC: mast cell; BM: bone marrow; n.s.: not significant. *Organomegaly including hepatomegaly, splenomegaly, or lymphadenopathy. [†]Hepatomegaly with ascites and/or portal hypertension.

and progression-free survival (PFS) in *KIT* D816V⁺ SM patients (n=103; no survival data available for 2 patients) in univariate and multivariate analyses including *KIT* D816V VAF in liquid specimens, age, sex, B-findings (BM MC infiltration, serum tryptase, organomegaly), and C-findings (anemia, thrombocytopenia, hypalbuminemia, weight loss, hepatomegaly with liver dysfunction, and increased alkaline phosphatase) as additional variables. In univariate analyses, PFS was adversely influenced by the majority of established risk factors including a high *KIT* D816V tissue allele burden with a hazard ratio (HR) of 15.82 (95%CI: 5.31-47.16) and a high *KIT* D816V liquid allele burden with a HR of 5.99 (95%CI: 2.41-14.88) (Table 2). In multivariate analysis including all molecular and clinical variables, only thrombocytopenia (HR: 21.26, 95%CI: 2.64-171.30; $P=0.004$) and a high *KIT* D816V allele burden in the tissue (HR: 50.71, 95%CI: 4.23-607.90; $P=0.002$) remained independent risk markers for PFS (Table 2). Similar results were obtained for OS with a HR of 12.79 (95%CI: 4.22-38.76) for a high *KIT* D816V tissue allele burden and 4.69 (95%CI: 1.84-11.98) for a high *KIT* D816V liquid allele burden in univariate analysis and a significant independent influence in multivariate analysis only for the tissue mutation burden (HR: 18.12, 95%CI: 1.98-165.57; $P=0.01$) (Online Supplementary Table S3). Using the maximum selected rank statistics method, 9% VAF in the tissue represents an optimal cut-off differentiating between surviving and non-surviving patients. In the group with <9% tissue mutant allele burden (n=79), the median PFS and OS was not reached, whereas in patients with a *KIT* D816V allele burden of $\geq 9\%$ (n=24) the median PFS was 4.1 years (Figure 4A) and the median OS 4.6 years (Figure 4B). The observed differences in survival were highly significant both for OS and PFS (Log-rank test; $P<0.0001$ each).

Moreover, the *KIT* D816V tissue allele burden could be followed in 26 patients over a median observation time of 42 months (range 2-172 months). In patients with stable disease and no cytoreductive therapy, no substantial increase or decrease in the *KIT* D816V allele burden was

Table 3. Sensitivity of molecular techniques to detect the *KIT* D816V in the tissue.

P<0.05	n. (%)	Clamp PCR		Total
		negative	positive	
dPCR	negative	3 (3%)	0 (0%)	3 (3%)
	positive	7 (8%)	81 (89%)	88 (97%)
	total	10 (11%)	81 (89%)	91 (100%)

Results of digital polymerase chain reaction (dPCR) and melting curve analysis after peptide nucleic acid-mediated PCR clamping (clamp PCR) to detect *KIT* D816V in formalin-fixed paraffin-embedded bone marrow sections of indolent systemic mastocytosis patients (n=91).

observed. In contrast, marked changes in *KIT* D816V tissue VAF were found in patients with advanced SM receiving cytoreductive therapy. In particular, six patients who showed a response to cytoreductive treatment (cladribine n=3, midostaurin and cladribine n=3) showed a significant decrease in the *KIT* D816V tissue burden (92% median reduction comparing post- with pre-therapeutic samples; $P<0.01$). Representative examples of two patients are shown in Figure 4C and D. In addition, Figure 4E shows a patient with complete remission after allogeneic stem cell transplantation, in whom low minimal residual disease (MRD) was detected by dPCR at an early time point (day 93) after transplantation. In total, our data show that dPCR-based tissue mutation burden measurement is feasible for monitoring treatment responses and to assess MRD levels in patients with SM.

Digital polymerase chain reaction is a sensitive diagnostic test to detect *KIT* D816V in formalin-fixed paraffin-embedded bone marrow sections

Finally, we assessed the performance of dPCR as a diagnostic test to detect the *KIT* D816V mutation in FFPE BM section compared to melting curve analysis after PNA-mediated PCR clamping on diagnostic BM section from 116 SM patients (Table 1). In the total cohort, 105 patients (91%) were tested positive for *KIT* D816V by dPCR

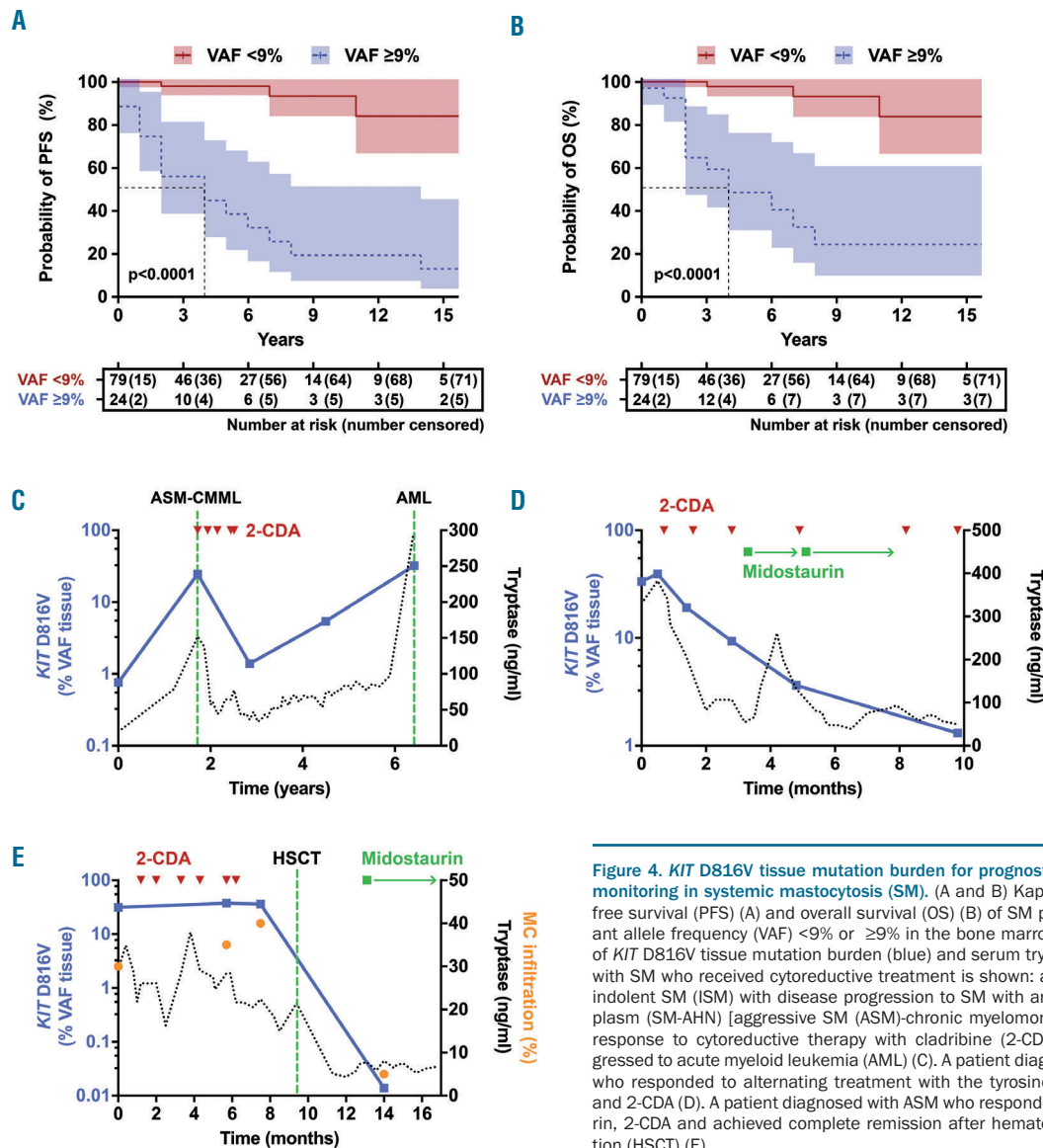


Figure 4. KIT D816V tissue mutation burden for prognostication and therapy response monitoring in systemic mastocytosis (SM). (A and B) Kaplan-Meier plot for progression-free survival (PFS) (A) and overall survival (OS) (B) of SM patients with a KIT D816V variant allele frequency (VAF) <9% or ≥9% in the bone marrow (BM) tissue. (C-E) Follow up of KIT D816V tissue mutation burden (blue) and serum tryptase (black) in three patients with SM who received cytoreductive treatment is shown: a patient initially diagnosed as indolent SM (ISM) with disease progression to SM with an associated hematologic neoplasm (SM-AHN) [aggressive SM (ASM)-chronic myelomonocytic leukemia (CMML)] and response to cytoreductive therapy with cladribine (2-CDA). Later on, the patient progressed to acute myeloid leukemia (AML) (C). A patient diagnosed with mast cell leukemia who responded to alternating treatment with the tyrosine kinase inhibitor midostaurin and 2-CDA (D). A patient diagnosed with ASM who responded to treatment with midostaurin, 2-CDA and achieved complete remission after hematopoietic stem cell transplantation (HSCT) (E).

whereas the mutation was detected in 98 patients (84%) by melting curve analysis. When analyzing SM subgroups, the mutation was detected with equal sensitivity in 17 patients with advanced SM (68%) by both methods. In contrast, 88 ISM patients (97%) were tested positive by dPCR compared to 81 (89%) by clamp PCR (Table 3). The observed difference in sensitivity was statistically significant ($P < 0.05$) in favor of dPCR. To confirm the specificity of the results, we analyzed FFPE BM sections of control subjects ($n=57$). No KIT codon 816 mutation was detected by either method, indicating 100% specificity.

When we further characterized patients that were tested ‘false-negative’ by melting curve analysis after PNA-mediated PCR clamping ($n=7$), a relatively low VAF for KIT D816V was observed (median 0.7%, range 0.027-2.1%). While some of these patients showed a mutant allele burden clearly below the limit of detection established for this method,¹⁵ others were found to have a low amount of total KIT copies (<1000) reflecting impaired quality or quantity of these specimens (Online

Supplementary Figure S3D). However, importantly, constrained validity of the analysis was not recognizable by melting curve analysis after PNA-mediated PCR clamping. In this regard, quantitative dPCR results allow for an additional quality control of the specimen within the same assay. Altogether, dPCR was superior over clamp PCR to detect the KIT D816V mutation in FFPE BM sections of patients with SM.

Discussion

Although it is generally appreciated that the quantification of the total burden of KIT-mutated neoplastic cells in SM is an important prognostic parameter, quantification of the KIT mutant allele burden has so far been limited to liquid specimens (PB or BM aspirate). This is a critical point, as neoplastic MC and their progenitors are not easily aspirable from BM and are very rarely circulating in the PB; they are thus substantially underrepresented in liquid

specimens compared to BM biopsy material. We had previously investigated the analytical validity of dPCR for *KIT* D816V in detail according to laboratory standards before applying the technology here.¹⁶ In the current study, we used dPCR for mutant allele burden measurement in FFPE BM sections of SM patients. To the best of our knowledge, this is the first study that comprehensively assesses the tissue mutation burden as a novel molecular biomarker in SM.

Our results suggest that the *KIT* D816V allele burden in BM tissue was not interchangeable with that in liquid specimens (PB or BM aspirate). In particular, a number of ISM patients showed substantially higher levels in FFPE tissue. In SM patients with multi-lineage involvement, the *KIT* D816V mutation is also present in CD34⁺ hematopoietic stem/precursor cells, eosinophils, basophils, monocytes or neutrophils.²⁶⁻²⁸ These cells are abundant in the liquid specimens and represent the main source of *KIT* D816V in PB of ISM patients with high mutant allele burden.¹⁹ In contrast, a MC infiltration of >10% is commonly found in the BM tissue of ISM patients.^{22,23} The mutation burden in FFPE BM sections, therefore, reflects both the 'infiltration burden' of *KIT* D816V⁺ MC in the tissue and the multi-lineage involvement of the mutation in non-MC. Accordingly, the mutation burden in BM tissue correlated better with the established markers of disease burden in SM (serum tryptase levels and BM MC infiltration) than molecular parameters performed on liquid specimens.

A high MC burden in the BM biopsy (>30% infiltration of cellularity) and high serum total tryptase (>200 ng/mL) also represent B-findings ('burden of disease') for definition of SSM.⁴ Although the clinical course in SSM is often stable for many years, progression to advanced SM can occur. Therefore, SSM represents a rare high-risk subcategory compared to ISM.²⁹ Quantification of *KIT* D816V allele burden in FFPE might be useful as an additional molecular marker of disease burden in SSM since it includes all *KIT* D816V positive cells in the tissue. In our study, a particularly high tissue allele burden was found in SSM patients. However, the numbers of samples tested were too small to allow us to draw a final conclusion as to the value of *KIT* D816V allele burden measurement in FFPE BM sections as an additional criterion of SSM. Multi-center studies with larger patient cohorts are currently being prepared to investigate the definitive value of measurement of tissue mutation burden and its applicability as a B-finding in SSM.

The current definition of advanced SM relies largely on the presence of C-findings ('cytoreduction-requiring') as markers of organopathy in ASM.^{1,4} For these patients, cytoreductive treatment is required.^{4,30} With the development of tyrosine kinase inhibitor (TKI) treatment in SM as a more specific therapeutic option,^{31,32} additional subgroups of patients might benefit from treatment and are the subject of ongoing clinical trials.³³⁻³⁵ Thus, prognostic biomarkers are warranted to define patients at risk that do not meet the current ASM criteria. We and others have shown that multi-lineage involvement of *KIT* D816V indicated by a high mutant allele burden in PB was associated with an aggressive clinical course.¹⁷⁻²⁰ In liquid specimens, we have previously used a 2% VAF cut-off to stratify OS in SM patients.¹⁸ Jara-Acevedo *et al.* used a 6% VAF cut-off in PB to discriminate between MC-restricted *versus* multi-lineage SM.¹⁹ In this study, we used a higher cut-off of 9%

VAF in BM sections to take into account the higher ISM mutational burden in the tissue. Using this cut-off, highly significant differences in both PFS and OS were observed and the tissue mutation burden remained an independent poor risk marker in multivariate analysis when B- and C-findings were considered. This is an important and novel finding as all previous studies assessing the mutation burden in liquid samples (PB and BM aspirate samples) found a significant effect on survival only in univariate but not in multivariate analyses.^{17,18,20,36,37} This difference might be explained by the close association of multi-lineage *KIT* D816V involvement (indicated by a high liquid mutation burden) with advanced SM (indicated by the presence of C-findings). Our observations have a clear clinical impact and strongly argue for inclusion of assessment of the *KIT* D816V mutation burden in prognostic scoring systems for mastocytosis. A potential limitation of our study is that different cytoreductive treatment modalities were applied in this retrospective analysis with a relatively high proportion of interferon- α or cladribine. In fact, more effective treatment regimens may improve OS in the future.³¹ However, the vast majority of patients with a low tissue mutation burden experienced no events despite the lack of any cytoreductive treatment, suggesting mutation burden analysis is important irrespective of treatment.

Therapy response criteria in advanced SM mainly rely on resolution of C-findings as markers of SM-mediated organopathy to define major response.³⁸ In addition, reduction of MC infiltration and/or of serum tryptase levels is used to define complete remission, incomplete remission, and pure clinical response.³⁸ The TKI midostaurin showed high efficacy in advanced SM with 45% major response and marked decreases in BM MC burden and serum tryptase.³¹ Both measurements are valuable surrogate parameters of disease burden in SM, but they do have some limitations.³⁹ While the basal level of total tryptase is well established as being quite a stable parameter in SM, single time-point measurements might be substantially influenced by MC activation or allergic reactions.⁴⁰⁻⁴² On the other hand, quantification of MC burden is a rather robust parameter of disease burden, but relies on experienced hematopathologists.⁴³ In this regard, measurement of *KIT* D816V allele burden might be useful as an additional objective response parameter. Recently, a $\geq 25\%$ reduction in expressed *KIT* D816V allele burden in PB was described as an independent 'on treatment' marker for improved OS in midostaurin-treated patients with advanced SM.²⁴ Based on the results of individual patients before and after cytoreductive treatment, FFPE-based allele burden measurement as a more direct marker of the number of all *KIT* D816V positive cells in the tissue might be an interesting additional follow-up parameter for treatment response. This might be of particular relevance for ISM patients undergoing TKI treatment in the future, since the mutation burden in liquid specimens substantially underestimates the disease burden in ISM. Furthermore, the high sensitivity of the assay makes it applicable for *KIT* D816V-based MRD measurement in patients that achieve complete remission in the histopathological assessment. However, further multi-centric studies are needed to definitively establish the tissue mutation burden as a parameter for therapy response in SM.

A potential limitation of dPCR and any other molecular test detecting specifically *KIT* D816V is that neither rare non-D816V mutations of *KIT* nor somatic mutations in

other genes can be monitored. In particular, mutations of *SRSF2*, *ASXL1* and *RUNX1* are found in aggressive forms of mastocytosis and *TET2* mutations have been described to precede the acquisition of *KIT* D816V in some patients.^{37,44} *KIT* D816V-negative clonal cells in advanced SM might be overlooked by dPCR while sequencing of a gene panel would identify them. Thus, additional next generation sequencing (NGS)-based monitoring of the disease might be warranted, particularly when there is clinical suspicion of disease progression despite a low *KIT* D816V allele burden. Here we show a higher clinical sensitivity of dPCR to detect *KIT* D816V in BM sections of SM patients compared to the clamp PCR that is widely used for tissue analysis. This is partly due to the higher analytical sensitivity of dPCR, which allows low mutant alleles to be detected.¹⁶ The analytical sensitivity of clamp PCR can be increased by analysis of micro-dissected neoplastic MC.¹⁴ Micro-dissection of MC has been used to detect *KIT* D816V in SM patients but requires time-consuming sample processing and is not widely available for routine diagnostics. In this regard, dPCR seems sufficiently sensitive, as it allows the detection of *KIT* D816V without micro-dissection in >95% of all ISM patients. However, micro-dissection of MC is still valuable to detect non-D816V mutations in *KIT* by clamp PCR or sequencing. Thus, both molecular techniques for *KIT* D816V detection are necessary and helpful, but the dPCR technique may have some advantages and should be considered in the future. One advantage of dPCR is the quantification of *KIT* wild-type alleles in the sample as quality control. Samples with borderline quality/quantity of DNA isolated from FFPE material are easily identified. In a number of these samples, clamp PCR could have shown false negative results if no additional (quantitative) quality control measurements for amplifiable DNA had been applied. Beside these assays, a number of other molecular tests, such as qPCR or ultra-sensitive NGS, have been described for quantification of *KIT* D816V in PB or BM aspirate.^{15,17,45}

We have previously shown an excellent correlation of dPCR and qPCR in these liquid specimens with easier inter-laboratory standardization and lack of amplification bias in highly fragmented DNA as potential advantages of dPCR.¹⁶ For diagnostic assessment, the high analytical sensitivity of digital PCR is sufficient to use not only trephines but also BM aspirates.¹⁶ In addition, qPCR and dPCR detect the mutation in the PB of the majority of patients,^{16,46,47} arguing for an early molecular assessment during the diagnostic workup of SM.⁹

In summary, dPCR for *KIT* D816V is a valuable diagnostic test to detect and quantify the mutation in FFPE BM sections of SM patients. The clinical sensitivity to detect the mutation is superior to clamp PCR without micro-dissection of MC. The *KIT* D816V mutant allele burden in FFPE BM sections correlates with BM MC infiltration and serum tryptase levels and represents a novel molecular parameter which differs from the mutant allele burden in PB or BM aspirate. Importantly, dPCR-based measurement of *KIT* D816V mutation burden in the tissue represents a novel biomarker with independent prognostic significance that can also be employed for follow-up analyses in SM. We therefore propose to include the measurement of tissue mutation burden in future studies for prognosis, SSM definition, and monitoring of disease progression and treatment response in SM patients.

Acknowledgments

The authors thank Jana Strasakova (Department of Laboratory Medicine, Medical University of Vienna) for technical support.

Funding

This study was supported by the Austria Science Fund (FWF) project P26079-B13, the SFB projects F4701-B20 and F4704-B20, the Medical-Scientific Fund of the Mayor of Vienna and a research grant of the Austrian Society of Laboratory Medicine and Clinical Chemistry (ÖGLMKC).

References

- Horny H-P, Metcalfe DD, Akin C, et al. Mastocytosis. In: Swerdlow SH, Campo E, Harris NL, Jaffe ES, Pileri SA, Stein H, et al., eds. WHO Classification of Tumours of Haematopoietic and Lymphoid Tissue. Revised 4th ed. Lyon: International Agency for Research on Cancer (IARC), 2017:62-69.
- Nagata H, Worobec AS, Oh CK, et al. Identification of a point mutation in the catalytic domain of the protooncogene c-kit in peripheral blood mononuclear cells of patients who have mastocytosis with an associated hematologic disorder. *Proc Natl Acad Sci U S A*. 1995;92(23):10560-10564.
- Longley BJ, Tyrrell L, Lu SZ, et al. Somatic c-KIT activating mutation in urticaria pigmentosa and aggressive mastocytosis: establishment of clonality in a human mast cell neoplasm. *Nat Genet*. 1996;12(3):312-314.
- Valent P, Akin C, Metcalfe DD. Mastocytosis: 2016 updated WHO classification and novel emerging treatment concepts. *Blood*. 2017;129(11):1420-1427.
- Arock M, Valent P. Pathogenesis, classification and treatment of mastocytosis: state of the art in 2010 and future perspectives. *Expert Rev Hematol*. 2010;3(4):497-516.
- Valent P, Horny HP, Escribano L, et al. Diagnostic criteria and classification of mastocytosis: a consensus proposal. *Leuk Res*. 2001;25(7):603-625.
- Valent P, Akin C, Hartmann K, et al. Advances in the Classification and Treatment of Mastocytosis: Current Status and Outlook toward the Future. *Cancer Res*. 2017;77(6):1261-1270.
- Valent P, Akin C, Escribano L, et al. Standards and standardization in mastocytosis: consensus statements on diagnostics, treatment recommendations and response criteria. *Eur J Clin Invest*. 2007;37(6):435-453.
- Arock M, Sotlar K, Akin C, et al. KIT mutation analysis in mast cell neoplasms: recommendations of the European Competence Network on Mastocytosis. *Leukemia*. 2015;29(6):1223-1232.
- Valent P, Escribano L, Broesby-Olsen S, et al. Proposed diagnostic algorithm for patients with suspected mastocytosis: a proposal of the European Competence Network on Mastocytosis. *Allergy*. 2014;69(10):1267-1274.
- Kristensen T, Vestergaard H, Bindslev-Jensen C, Moller MB, Broesby-Olsen S, Mastocytosis Centre OUH. Sensitive KIT D816V mutation analysis of blood as a diagnostic test in mastocytosis. *Am J Hematol*. 2014;89(5):493-498.
- Kristensen T, Vestergaard H, Bindslev-Jensen C, et al. Prospective evaluation of the diagnostic value of sensitive KIT D816V mutation analysis of blood in adults with suspected systemic mastocytosis. *Allergy*. 2017;72(11):1737-1743.
- Kristensen T, Vestergaard H, Moller MB. Improved detection of the KIT D816V mutation in patients with systemic mastocytosis using a quantitative and highly sensitive real-time qPCR assay. *J Mol Diagn*. 2011;13(2):180-188.
- Sotlar K. c-kit mutational analysis in paraffin material. *Methods Mol Biol*. 2013;999:59-78.
- Sotlar K, Escribano L, Landt O, et al. One-step detection of c-kit point mutations using peptide nucleic acid-mediated polymerase chain reaction clamping and hybridization probes. *Am J Pathol*. 2003;162(3):737-746.
- Greiner G, Gurbisz M, Ratzinger F, et al. Digital PCR: A Sensitive and Precise Method for KIT D816V Quantification in

- Mastocytosis. *Clin Chem.* 2018;64(3):547-555.
17. Erben P, Schwaab J, Metzgeroth G, et al. The KIT D816V expressed allele burden for diagnosis and disease monitoring of systemic mastocytosis. *Ann Hematol.* 2014;93(1):81-88.
 18. Hoermann G, Gleixner KV, Dinu GE, et al. The KIT D816V allele burden predicts survival in patients with mastocytosis and correlates with the WHO type of the disease. *Allergy.* 2014;69(6):810-813.
 19. Jara-Acevedo M, Teodosio C, Sanchez-Munoz L, et al. Detection of the KIT D816V mutation in peripheral blood of systemic mastocytosis: diagnostic implications. *Mod Pathol.* 2015;28(8):1138-1149.
 20. Broesby-Olsen S, Kristensen T, Vestergaard H, et al. KIT D816V mutation burden does not correlate to clinical manifestations of indolent systemic mastocytosis. *J Allergy Clin Immunol.* 2013;132(3):723-728.
 21. Mayado A, Teodosio C, Dasilva-Freire N, et al. Characterization of CD34(+) hematopoietic cells in systemic mastocytosis: Potential role in disease dissemination. *Allergy.* 2018; 73(6):1294-1304.
 22. Horny HP, Parwaresch MR, Lennert K. Bone marrow findings in systemic mastocytosis. *Hum Pathol.* 1985;16(8):808-814.
 23. Krokowski M, Sotlar K, Krauth MT, Fodinger M, Valent P, Horny HP. Delineation of patterns of bone marrow mast cell infiltration in systemic mastocytosis: value of CD25, correlation with subvariants of the disease, and separation from mast cell hyperplasia. *Am J Clin Pathol.* 2005;124(4): 560-568.
 24. Jawhar M, Schwaab J, Naumann N, et al. Response and progression on midostaurin in advanced systemic mastocytosis: KIT D816V and other molecular markers. *Blood.* 2017;130(2):137-145.
 25. Development Core Team, R: A language and environment for statistical computing. R Foundation for Statistical Computing, Vienna, Austria. ISBN 3-900051-07-0. 2005.
 26. Garcia-Montero AC, Jara-Acevedo M, Teodosio C, et al. KIT mutation in mast cells and other bone marrow hematopoietic cell lineages in systemic mast cell disorders: a prospective study of the Spanish Network on Mastocytosis (REMA) in a series of 113 patients. *Blood.* 2006;108(7): 2366-2372.
 27. Kocabas CN, Yavuz AS, Lipsky PE, Metcalfe DD, Akin C. Analysis of the lineage relationship between mast cells and basophils using the c-kit D816V mutation as a biologic signature. *J Allergy Clin Immunol.* 2005;115(6):1155-1161.
 28. Garcia-Montero AC, Jara-Acevedo M, Alvarez-Twose I, et al. KIT D816V-mutated bone marrow mesenchymal stem cells in indolent systemic mastocytosis are associated with disease progression. *Blood.* 2016;127(6):761-768.
 29. Pardanani A, Lim KH, Lasho TL, et al. WHO subvariants of indolent mastocytosis: clinical details and prognostic evaluation in 159 consecutive adults. *Blood.* 2010;115(1):150-151.
 30. Ustun C, Arock M, Kluijn-Nelemans HC, et al. Advanced systemic mastocytosis: from molecular and genetic progress to clinical practice. *Haematologica.* 2016;101(10):1133-1143.
 31. Gotlib J, Kluijn-Nelemans HC, George TI, et al. Efficacy and Safety of Midostaurin in Advanced Systemic Mastocytosis. *N Engl J Med.* 2016;374(26):2530-2541.
 32. Bibi S, Arock M. Tyrosine Kinase Inhibition in Mastocytosis: KIT and Beyond KIT. *Immunol Allergy Clin North Am.* 2018;38(3):527-543.
 33. Lortholary O, Chandresris MO, Bulai Livideanu C, et al. Masitinib for treatment of severely symptomatic indolent systemic mastocytosis: a randomised, placebo-controlled, phase 3 study. *Lancet.* 2017; 389(10069):612-620.
 34. van Anrooij B, Oude Elberink JNG, Span LE, et al. Midostaurin in indolent systemic mastocytosis patients: an open-label phase 2 trial. *J Allergy Clin Immunol.* 2018; 142(3):1006-1008.
 35. DeAngelo DJ, Quiry AT, Radia D, et al. Clinical Activity in a Phase 1 Study of Blu-285, a Potent, Highly-Selective Inhibitor of KIT D816V in Advanced Systemic Mastocytosis (AdvSM). *Blood.* 2017;130 (Suppl 1):2-2.
 36. Jawhar M, Schwaab J, Hausmann D, et al. Splenomegaly, elevated alkaline phosphatase and mutations in the SRSF2/ASXL1/RUNX1 gene panel are strong adverse prognostic markers in patients with systemic mastocytosis. *Leukemia.* 2016;30(12):2342-2350.
 37. Jawhar M, Schwaab J, Schnittger S, et al. Additional mutations in SRSF2, ASXL1 and/or RUNX1 identify a high-risk group of patients with KIT D816V(+) advanced systemic mastocytosis. *Leukemia.* 2016; 30(1):136-143.
 38. Valent P, Akin C, Sperr WR, et al. Aggressive systemic mastocytosis and related mast cell disorders: current treatment options and proposed response criteria. *Leuk Res.* 2003; 27(7):635-641.
 39. Sperr WR, Jordan JH, Fiegl M, et al. Serum tryptase levels in patients with mastocytosis: correlation with mast cell burden and implication for defining the category of disease. *Int Arch Allergy Immunol.* 2002;128 (2):136-141.
 40. Kabashima K, Nakashima C, Nonomura Y, et al. Biomarkers for evaluation of mast cell and basophil activation. *Immunol Rev.* 2018;282(1):114-120.
 41. Theoharides TC, Valent P, Akin C. Mast Cells, Mastocytosis, and Related Disorders. *N Engl J Med.* 2015;373(2):163-172.
 42. Valent P, Sperr WR, Sotlar K, et al. The serum tryptase test: an emerging robust biomarker in clinical hematology. *Expert Rev Hematol.* 2014;7(5):683-690.
 43. Jawhar M, Schwaab J, Horny HP, et al. Impact of centralized evaluation of bone marrow histology in systemic mastocytosis. *Eur J Clin Invest.* 2016;46(5):392-397.
 44. Jawhar M, Schwaab J, Schnittger S, et al. Molecular profiling of myeloid progenitor cells in multi-mutated advanced systemic mastocytosis identifies KIT D816V as a distinct and late event. *Leukemia.* 2015;29(5):1115-1122.
 45. Kristensen T, Broesby-Olsen S, Vestergaard H, Bindslev-Jensen C, Moller MB. Targeted ultradeep next-generation sequencing as a method for KIT D816V mutation analysis in mastocytosis. *Eur J Haematol.* 2016;96(4): 381-388.
 46. Kristensen T, Vestergaard H, Bindslev-Jensen C, et al. Prospective evaluation of the diagnostic value of sensitive KIT D816V mutation analysis of blood in adults with suspected systemic mastocytosis. *Allergy.* 2017;72(11):1737-1743.
 47. Broesby-Olsen S, Oropeza AR, Bindslev-Jensen C, et al. Recognizing mastocytosis in patients with anaphylaxis: value of KIT D816V mutation analysis of peripheral blood. *J Allergy Clin Immunol.* 2015;135(1): 262-264.

Loss of RAF kinase inhibitor protein is involved in myelomonocytic differentiation and aggravates RAS-driven myeloid leukemogenesis

Veronica Caraffini,¹ Olivia Geiger,¹ Angelika Rosenberger,¹ Stefan Hatzl,¹ Bianca Perfler,¹ Johannes L. Berg,¹ Clarice Lim,² Herbert Strobl,² Karl Kashofer,³ Silvia Schauer,³ Christine Beham-Schmid,³ Gerald Hoefler,³ Klaus Geissler,^{4,5} Franz Quehenberger,⁶ Walter Kolch,⁷ Dimitris Athineos,⁸ Karen Blyth,⁸ Albert Wölfel,¹ Heinz Sill¹ and Armin Zebisch^{1,9}

¹Division of Hematology, Medical University of Graz, Graz, Austria; ²Otto Loewi Research Center, Immunology and Pathophysiology, Medical University of Graz, Graz, Austria;

³Diagnostic and Research Institute of Pathology, Medical University of Graz, Graz, Austria; ^{4,5}Medical Department with Hematology, Oncology and Palliative Medicine, Hospital Hietzing, Vienna, Austria; ⁶Sigmund Freud University, Vienna, Austria; ⁹Institute of Medical Informatics, Statistics and Documentation, Medical University of Graz, Graz, Austria; ⁷Systems Biology Ireland and Conway Institute, University College Dublin, Dublin, Ireland; ⁸Cancer Research UK Beatson Institute, Glasgow, UK and ⁹Otto Loewi Research Center for Vascular Biology, Immunology and Inflammation, Division of Pharmacology, Medical University of Graz, Graz, Austria

ABSTRACT

RAS-signaling mutations induce the myelomonocytic differentiation and proliferation of hematopoietic stem and progenitor cells. Moreover, they are important players in the development of myeloid neoplasias. RAF kinase inhibitor protein (RKIP) is a negative regulator of RAS-signaling. As RKIP loss has recently been described in RAS-mutated myelomonocytic acute myeloid leukemia, we now aimed to analyze its role in myelomonocytic differentiation and RAS-driven leukemogenesis. Therefore, we initially analyzed RKIP expression during human and murine hematopoietic differentiation and observed that it is high in hematopoietic stem and progenitor cells and lymphoid cells but decreases in cells belonging to the myeloid lineage. By employing short hairpin RNA knockdown experiments in CD34⁺ umbilical cord blood cells and the undifferentiated acute myeloid leukemia cell line HL-60, we show that RKIP loss is indeed functionally involved in myelomonocytic lineage commitment and drives the myelomonocytic differentiation of hematopoietic stem and progenitor cells. These results could be confirmed *in vivo*, where Rkip deletion induced a myelomonocytic differentiation bias in mice by amplifying the effects of granulocyte macrophage-colony-stimulating factor. We further show that RKIP is of relevance for RAS-driven myelomonocytic leukemogenesis by demonstrating that *Rkip* deletion aggravates the development of a myeloproliferative disease in *Nras*^{G12D}-mutated mice. Mechanistically, we demonstrate that RKIP loss increases the activity of the RAS-MAPK/ERK signaling module. Finally, we prove the clinical relevance of these findings by showing that RKIP loss is a frequent event in chronic myelomonocytic leukemia, and that it co-occurs with RAS-signaling mutations. Taken together, these data establish RKIP as novel player in RAS-driven myeloid leukemogenesis.

Introduction

Activating RAS-signaling mutations comprise sequence variants within the RAS oncogenes themselves, but also can affect upstream activators and regulators of RAS-signaling cascades. Among others, these include *CBL*, *PTPN11*, *NF1* as well as a wide range of receptor tyrosine kinases with relevance for physiological and malignant



Haematologica 2018
Volume 105(2)375-386

Correspondence:

ARMIN ZEBISCH
armin.zebisch@medunigraz.at

Received: October 21, 2018.

Accepted: May 15, 2019.

Pre-published: May 16, 2019.

doi:10.3324/haematol.2018.209650

Check the online version for the most updated information on this article, online supplements, and information on authorship & disclosures: www.haematologica.org/content/105/2/375

©2020 Ferrata Storti Foundation

Material published in *Haematologica* is covered by copyright. All rights are reserved to the Ferrata Storti Foundation. Use of published material is allowed under the following terms and conditions:

<https://creativecommons.org/licenses/by-nc/4.0/legalcode>.

Copies of published material are allowed for personal or internal use. Sharing published material for non-commercial purposes is subject to the following conditions:

<https://creativecommons.org/licenses/by-nc/4.0/legalcode>, sect. 3. Reproducing and sharing published material for commercial purposes is not allowed without permission in writing from the publisher.



hematopoiesis. *RAS*-signaling mutations skew hematopoiesis into the myelomonocytic lineage and ultimately drive the proliferation of these cells.¹ Mechanistically, they constitutively activate downstream signaling cascades, including the *RAS*-mitogen activated protein kinase/extracellular signal-regulated kinase (MAPK/ERK) and Phosphoinositide 3-kinase/AKT pathways.² While this already causes myelomonocytic lineage commitment and increased proliferation of hematopoietic stem and progenitor cells (HSPC) per se,^{1,3,4} it also increases the sensitivity to granulocyte macrophage-colony-stimulating factor (GM-CSF),⁵ which augments these biological effects even further. Importantly, both increased myelomonocytic lineage commitment and proliferation are considered as key steps in the pathogenesis of myelomonocytic leukemias. Indeed, *RAS*-signaling mutations are essential players within the development of these malignancies and cause a myeloproliferative disease (MPD) with hyperproliferation of the monocytic and granulocytic lineages in mice.^{6,9} In agreement with these data, *RAS*-signaling mutations are frequently detected in myeloid neoplasias. More than 10-20% of acute myeloid leukemia (AML) cases exhibit either *NRAS* or *KRAS* mutations, respectively.¹⁰⁻¹² A myeloid neoplasia with particular dependence on aberrant *RAS*-signaling is chronic myelomonocytic leukemia (CMML), an aggressive malignancy characterized by increased myelomonocytic differentiation and proliferation. Indeed, more than 40% of CMML patients exhibit one or more mutations in the *RAS*-signaling genes.^{13,14} Recently, it was shown that the extent of *RAS*-signaling activation in myeloid neoplasias is not only determined by the presence of mutations, but also by the aberrant expression profiles of one or more of its regulators. This can also be of relevance for *RAS*-driven myeloid leukemogenesis, as shown for the *RAS*-signaling inhibitor *SPRY2*, which demonstrates decreased expression levels in *TET2*-mutated patients.¹⁵

RAF kinase inhibitor protein (RKIP) is a negative regulator of various intracellular signaling modules, including the *RAS*-MAPK/ERK and nuclear factor- κ B pathways.^{16,17} A somatic loss of RKIP expression has been described in a variety of solid cancers and a metastasis-suppressor function could be shown *in vitro* and *in vivo*.^{18,19} We have previously shown that a leukemia-specific loss of RKIP occurs in patients with therapy-related AML with a predisposing germline mutation in *CRAF*.²⁰ On a functional level, RKIP drives the oncogenic potential of mutant *CRAF*, thereby contributing to leukemogenesis in these patients. Subsequently, we could show that RKIP loss is of relevance for other subtypes of AML as well.^{12,21,22} It occurs in up to 20% of AML cases and contributes to leukemogenesis by increasing the proliferation of AML cells.^{12,21} In agreement with the data from therapy-related AML (t-AML) patients with *CRAF* germline mutations, RKIP loss is correlated with *RAS*-signaling mutations and increased the leukemogenic potential of mutant *RAS* in a series of *in vitro* assays. Interestingly, we observed that RKIP loss is also correlated with myelomonocytic and monocytic AML phenotypes, which suggests that RKIP might play a role in myelomonocytic differentiation as well.^{12,20,23}

In this study, we aimed to clarify a connection between RKIP and myeloid skewing of hematopoiesis in more detail and demonstrate that RKIP loss contributes to myelomonocytic lineage commitment of HSPC *in vitro* and *in vivo*. We further show relevance of RKIP for *RAS*-driven myelomonocytic leukemogenesis, by demon-

strating that *Rkip* deletion aggravates myelomonocytic MPD development in *Nras*^{G12D}-mutated mice. Mechanistically, we show that RKIP loss potentiates the *RAS*-induced activation of the *RAS*-MAPK/ERK signaling cascade. Finally, we prove the clinical relevance of these findings by showing that RKIP loss is a frequent event in primary CMML patient samples and frequently co-occurs with *RAS*-signaling mutations. These data establish RKIP as a novel player in *RAS*-driven myeloid leukemogenesis.

Methods

Primary patient samples and cell lines

Chronic myelomonocytic leukemia patient samples were collected at the Division of Hematology, Medical University of Graz, Austria, as well as in the Austrian Biodatabase for CMML. All samples were processed and stored as described in detail in the *Online Supplementary Methods*. Healthy CD34⁺ HSPC were collected from umbilical cord blood specimens (EasySep, STEMCELL Technologies) according to the manufacturer's instructions and processed as described before.²⁴ Peripheral blood samples from healthy donors were used to collect CD14⁺ monocytes (MACS, Miltenyi Biotec), B lymphocytes and granulocytes (LymphoprepTM, STEMCELL Technologies and human B Lymphocyte enrichment set, BD biosciences) according to the manufacturer's protocol. 293T, NB4 and HL-60 cell lines were obtained from the German National Resource Center for Biological Material (DSMZ, Braunschweig, Germany). Low passage stocks were frozen and cells were always passaged for less than six months after resuscitation. Additionally, cells were screened by variable number of tandem repeat profiling (VNTR) for authenticity.²¹ Lentiviral transduction of cell lines and primary HSPC were performed as previously described.^{12,21,22}

Mouse experiments

All mouse experiments were performed on a C57BL/6 strain background. Survival analyses were based on groups of at least eleven animals, all other experiments comprised at least three animals. Genotyping was performed using tail tips as previously described.^{19,25} Mice with complete deletion of *Rkip* (*Rkip*^{-/-}) as well as their controls (*Rkip*^{+/+}) were obtained from Professor John Sedivy (Brown University, Providence, RI, USA). *Mx1-Cre* mice were obtained from Dr. Karen Blyth (Cancer Research UK Beatson Institute, Glasgow, UK), *Nras-LSL*^{G12D} (JAX stock #008304; hereafter referred to as *Nras*) from The Jackson Laboratory (Bar Harbor, ME, USA).²⁶ *Mx1-Cre* and *Nras* animals were kept in a heterozygous situation and crossed to *Rkip*^{-/-} and *Rkip*^{+/+} mice to obtain *Mx1-Cre/Nras/Rkip*^{-/-} and *Mx1-Cre/Nras/Rkip*^{+/+} genotypes, respectively. Detailed procedures of mouse analysis are presented in the *Online Supplementary Methods*.

Immunoblot analysis, real time quantitative polymerase chain reaction, next-generation sequencing, flow cytometry and *in vitro* differentiation assays

These assays were extensively described previously^{11,21,22,27-30} and are presented in detail in the *Online Supplementary Methods*.

Database retrieval and statistical analyses

Microarray expression data for RKIP expression in murine hematopoietic cell compartments were downloaded via the Gene Expression Omnibus (<https://www.ncbi.nlm.nih.gov/geo/>), accession numbers GSE27787,³¹ GSE5677,³² GSE27816³³ and GSE20377.³⁴ For the statistical analysis of *in vitro* and *in vivo* experiments, paired and unpaired Student's *t*-tests, respectively, were employed. For

comparisons in primary patient samples, we used the Wilcoxon-Mann-Whitney test for continuous variables and the Fisher's Exact test for dichotomous variables. The effects of RKIP expression on survival were tested by the log-rank test. SPSS version 22.0 (SPSS Inc.) was employed for these calculations. All tests were two-sided and $P < 0.050$ was considered statistically significant.

Study approval

The study was reviewed and approved by the institutional review board (28-481 ex 15/16) and conducted in accordance with the Declaration of Helsinki. Mouse experiments were approved by the Federal Ministry for Science, Research and Economy (GZ: BMWF-66.010/0050-II/3b/2013).

Results

RAF kinase inhibitor protein expression is high in hematopoietic stem and progenitor cells and lymphoid cells but low in cells belonging to the myeloid lineage

Hypothesizing that RKIP loss is a driver for

myelomonocytic lineage commitment, one would assume that cells with myelomonocytic differentiation would demonstrate lower RKIP expression levels. In a first step, we therefore employed an HL-60 *in vitro* differentiation model. HL-60 is an undifferentiated AML cell line and can be forced into the myelomonocytic lineage by addition of 1,25 dihydroxyvitamin D₃.³⁵ Interestingly, we observed that 1,25D₃-induced differentiation in these cells was accompanied by a significant decrease in the amount of RKIP protein ($P = 0.002$) (Figure 1A). We then aimed to delineate RKIP expression in human hematopoiesis by studying CD34⁺ HSPC derived from three umbilical cord blood specimens on the one hand, as well as mature lymphocytes, granulocytes and monocytes from four healthy individuals on the other. Due to the restricted cell numbers available, we studied *RKIP* mRNA by the means of quantitative-polymerase chain reaction (qPCR) in these experiments. However, we have previously shown that decreased expression of RKIP at the protein level is accompanied by its downregulation at the mRNA level as well.^{12,20-22} In accordance with HL-60 data, RKIP was

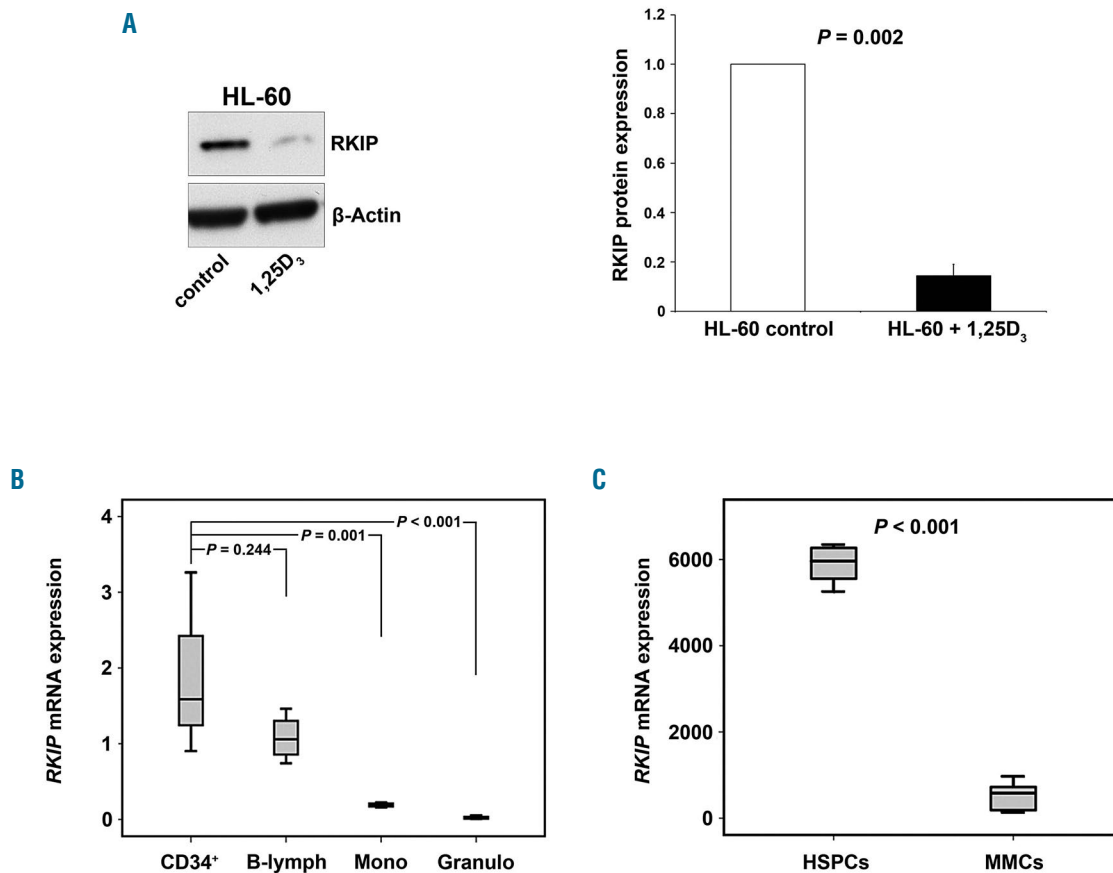


Figure 1. RAF kinase inhibitor protein (RKIP) expression is low in cells belonging to the myeloid lineage. (A) Immature HL-60 acute myeloid leukemia (AML) cells were treated with 100nM 1,25-dihydroxyvitamin D₃ (1,25D₃) for 48 hours to induce myeloid differentiation. Immunoblot analysis demonstrates a decrease in RKIP protein expression in 1,25D₃ treated cells. The graph represents the mean of three independent experiments ±Standard Deviation; expression values are given as x-fold expression of the HL-60 control. Statistical significance was evaluated using Student's t-test. (B) Box plots showing *RKIP* mRNA expression, studied via quantitative polymerase chain reaction in CD34⁺ hematopoietic stem and progenitor cells (HSPC) (CD34⁺, n=3), lymphocytes (B-lymph, n=4), monocytes (Mono, n=4) and granulocytes (Granulo, n=4) from healthy donors. In comparison to HSPC, RKIP mRNA expression is significantly reduced in monocytes and granulocytes, while no significant difference was observed for lymphocytes. Graphs denote the x-fold RKIP expression levels of NB4 cells, which were used as a calibrator and arbitrarily set to a value of 1. *P*-values were calculated using Student's t-test. (C) Box plots showing that the expression of *RKIP* mRNA in differentiated cells belonging to the myeloid lineage (MMC) is also decreased in mice. These data were generated by re-analysis of a previously published murine microarray gene expression profiling dataset.³¹ HSPC included long-term hematopoietic stem cells (lin⁻, Sca⁺, kit⁺, CD34⁺), short-term hematopoietic stem cells (lin⁻, Sca⁺, kit⁺, CD34⁻), LSK (lin⁻, Sca⁺, kit⁺) and hematopoietic progenitor cells (lin⁻). Myelomonocytic cells (MMC) included Gr-1⁺ neutrophils and Mac-1⁺ monocytes/macrophages. Statistical significance was calculated by Student's t-test.

prominently expressed in healthy CD34⁺ HSPC (Figure 1B). RKIP expression levels in lymphocytes were similar to those observed in HSPC ($P=0.244$), while they were significantly reduced in monocytes ($P=0.001$) and granulocytes ($P<0.001$).

Finally, we sought to confirm these findings in a murine

setting. We therefore performed a database retrieval *via* the Gene Expression Omnibus (GEO) database and re-analyzed RKIP mRNA in a previous publication of Konuma *et al.*³¹ (GEO data set GDS3997) who performed microarray analyses in different hematopoietic cell and progenitor compartments in C57BL/6 mice. In agreement

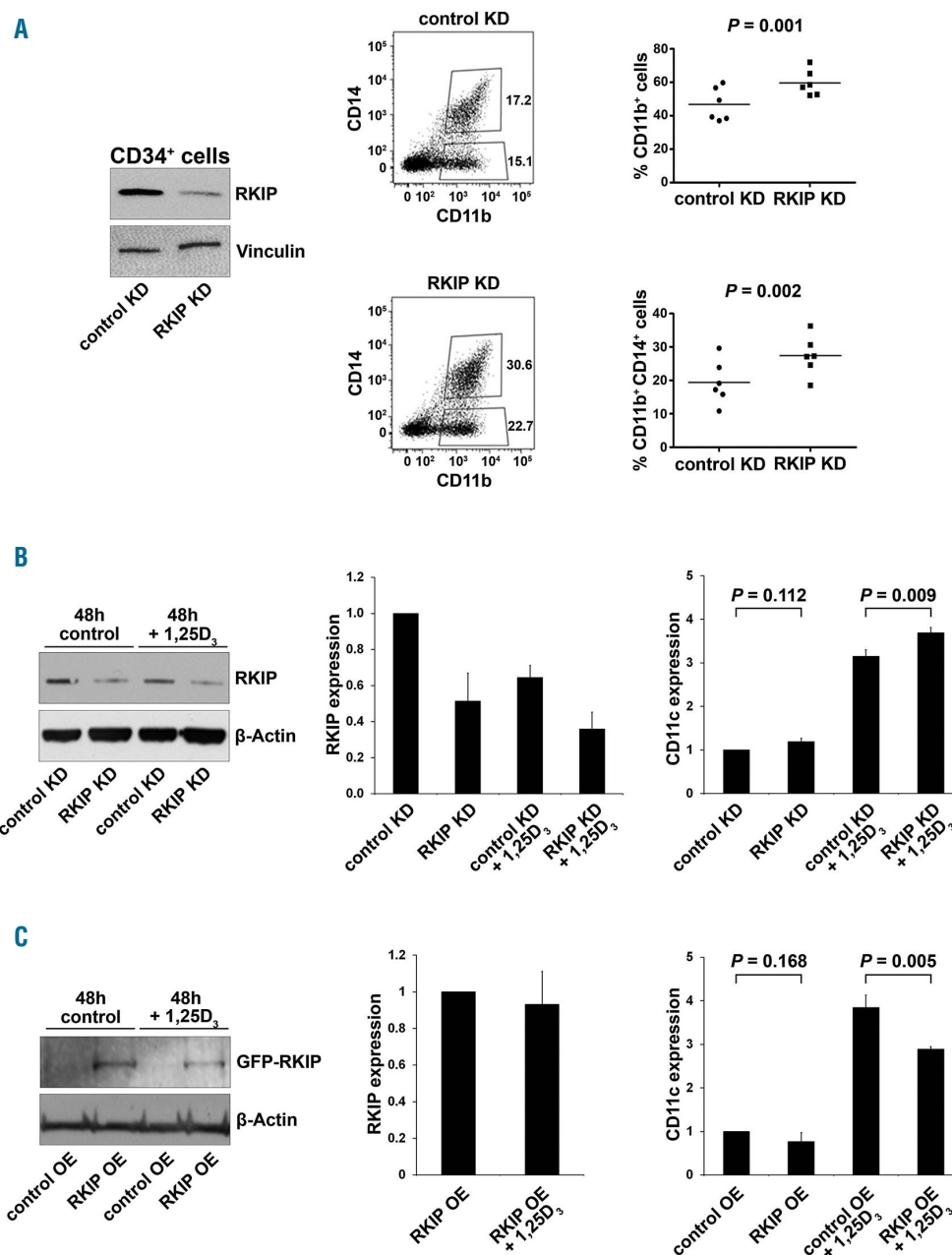


Figure 2. RAF kinase inhibitor protein (RKIP) is functionally involved in myeloid lineage differentiation. (A) RKIP shRNA knockdown (KD) in CD34⁺ human hematopoietic stem and progenitor cells (HSPC) increased the myelomonocytic differentiation induced by a granulocyte-macrophage colony-stimulating factor (GM-CSF)/flt-3 ligand (FL)/stem cell factor (SCF)/tumor necrosis factor- α (TNF α) cytokine mix. (Left) Immunoblot showing the successful knockdown of RKIP. Control KD denotes control transduced cells. Representative flow cytometry plots showing increased expression of the myelomonocytic surface markers CD11b and CD14 in CD34⁺ HSPC with RKIP KD shown in the middle. (Right) Results of all six experiments performed; median is also shown. Statistical significance was calculated by Student's *t*-test. Of note, RKIP KD as a single event without the addition of cytokines was insufficient to induce differentiation (*data not shown*). (B) RKIP KD in HL-60 AML cells increased 1,25D₃-induced myelomonocytic differentiation, as assessed by flow cytometric expression of CD11c. (Left) Immunoblot showing the successful knockdown of RKIP; (right) mean CD11c expression of three independent experiments \pm Standard Deviation (SD); expression values are given as x-fold expression of HL-60 control KD cells, statistical significance was evaluated by Student's *t*-test. (C) RKIP overexpression (RKIP OE) in HL-60 AML cells reduced 1,25D₃ induced myelomonocytic differentiation, as assessed by flow cytometric expression of CD11c. HL-60 cells were transduced with eGFP-C1-6xG-hRKIP (RKIP OE) or empty vector (control OE). (Left) Immunoblot showing successful RKIP overexpression; (right) mean CD11c expression of three independent experiments \pm SD. Expression values are given as x-fold expression of HL-60 control OE cells. Statistical significance was evaluated by Student's *t*-test. Note that HL-60 cells were treated with 10nM 1,25D₃.

with our findings in HL-60 and in healthy human individuals, *RKIP* mRNA levels were high in HSPC and lymphocytes but significantly reduced in more differentiated cells of the myeloid lineage ($P < 0.001$) (Figure 1C). Of note, by focusing on specific HSPC compartments within GDS3997 and three additional datasets,³¹⁻³⁴ we observed that *RKIP* expression remains high until the granulocyte-macrophage-progenitor (GMP) stage and decreases during the terminal stages of myelomonocytic differentiation (Online Supplementary Figure S1).

Knockdown of RAF kinase inhibitor protein amplifies the myelomonocytic differentiation of hematopoietic stem and progenitor cells

Having shown that *RKIP* levels are high in HSPC and reduced in differentiated myeloid cells, we next aimed to investigate whether *RKIP* expression levels are of functional relevance for the myeloid lineage commitment of HSPC. Therefore, we performed lentiviral knockdown of *RKIP* in CD34⁺ human HSPC isolated from umbilical cord blood specimens (Figure 2A). Subsequently, cells were

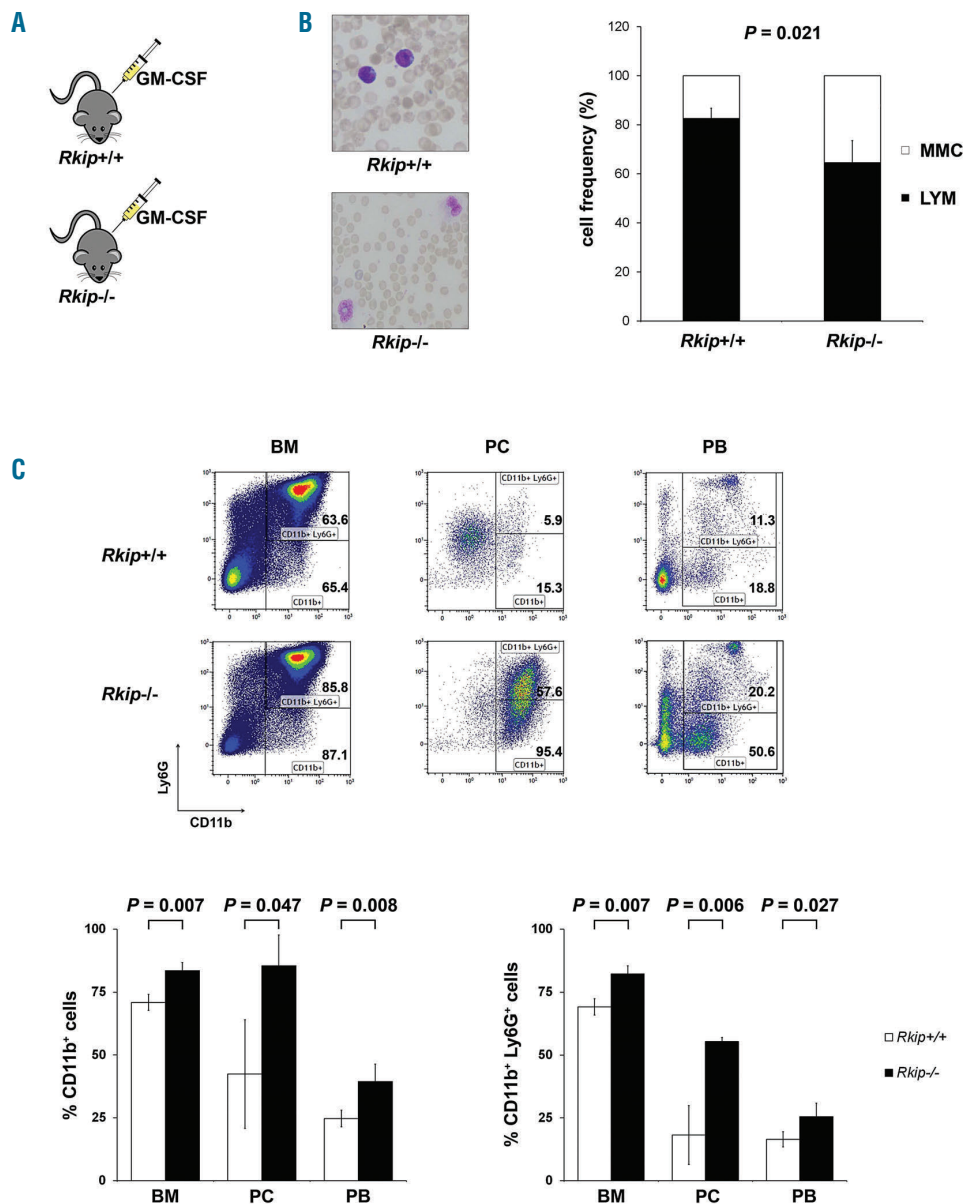


Figure 3. *Rkip* deletion causes increased myeloid lineage commitment in a murine model by increasing the sensitivity to granulocyte-macrophage colony-stimulating factor (GM-CSF). (A) To assess the effects of GM-CSF *in vivo*, four mice with a deletion of *Rkip* (*Rkip*^{-/-}), as well as four control mice (*Rkip*^{+/+}), were injected intraperitoneally with 500ng GM-CSF twice a day for four days and were analyzed on day 5. (B) Cytological analysis of peripheral blood smears from these mice revealed a significant increase in the number of myelomonocytic cells (MMC) in *Rkip*^{-/-} animals. A representative peripheral blood smear picture is shown. Lymphoid cells are shown as LYM. Graphs show the average \pm Standard Deviation (SD). Statistical significance was evaluated by Student's *t*-test. (C) Representative flow cytometric plots of the mice presented in (B) showing an increased percentage of CD11b⁺ and CD11b⁺ Ly6G⁺ cells in the bone marrow (BM), peritoneal cavity (PC), and peripheral blood (PB) of *Rkip*^{-/-} mice. Graphs show the average \pm SD. Statistical significance was evaluated by Student's *t*-test. *RKIP*: RAF kinase inhibitor protein.

treated with a granulocyte-macrophage colony-stimulating factor (GM-CSF)/flt-3 ligand (FL)/stem cell factor (SCF)/tumor necrosis factor- α (TNF α) cytokine mix to induce myelomonocytic differentiation.²⁹ Five days later,

the expression of myelomonocytic surface markers CD11b and CD14 was assessed. In these experiments, myelomonocytic differentiation was significantly increased in HSPC transduced with the RKIP shRNA

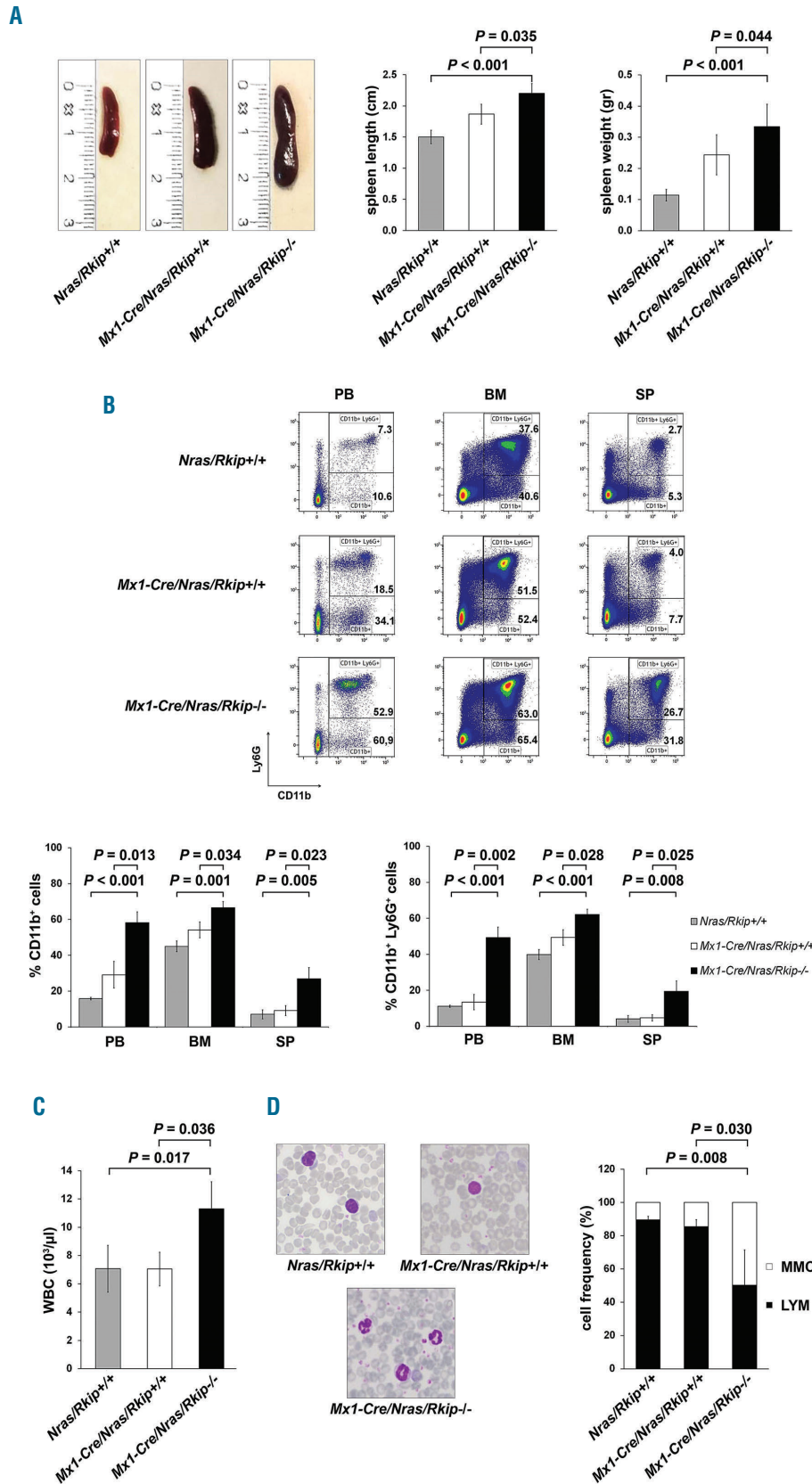


Figure 4. Deletion of *Rkip* aggravates myeloproliferation and myeloproliferative disease (MPD) development in *Nras*-mutated mice. An *Nras* driven mouse model of myeloproliferation (*Mx1-Cre/Nras*) was used to study the effects of *Rkip*^{-/-} on *Ras*-driven myeloproliferation and MPD development. Mice were electively killed at an age of six months after the first plpC injection, *Mx1-Cre/Nras/Rkip*^{-/-} mice (n=3) were compared to control mice (*Mx1-Cre/Nras/Rkip*^{+/+}; n=3) as well as to mice without *Mx1-Cre* (*Nras/Rkip*^{+/+}; n=4). (A) Representative images of spleens from *Nras/Rkip*^{+/+}, *Mx1-Cre/Nras/Rkip*^{+/+} and *Mx1-Cre/Nras/Rkip*^{-/-} mice as well as bar graphs of spleen lengths and weights, showing splenomegaly in animals with *Rkip* deletion. (B) Representative flow cytometric plots showing an increase in the percentage of CD11b⁺ and CD11b⁺ Ly6G⁺ myelomonocytic cells in peripheral blood (PB), bone marrow (BM) and spleen (SP) of *Mx1-Cre/Nras/Rkip*^{-/-} mice when these were compared to *Nras/Rkip*^{+/+} animals as well as when compared to *Mx1-Cre/Nras/Rkip*^{+/+} littermates. (C) Peripheral blood counts demonstrate an increased number of white blood cells (WBC) in *Mx1-Cre/Nras/Rkip*^{-/-} mice. (D) The leukocytosis in *Mx1-Cre/Nras/Rkip*^{-/-} mice is caused by an increased number of myelomonocytic cells (MMC), as shown in the representative PB smear and as shown in the flow cytometric analyses shown above. Graphs show the average \pm Standard Deviation. Statistical significance was calculated by Student's t-test. RKIP: RAF kinase inhibitor protein.

(HSPC RKIP KD) as compared to HSPC control KD ($P=0.001$ for CD11b⁺ cells and $P=0.002$ for CD11b⁺ CD14⁺ cells) (Figure 2A), confirming a role of RKIP loss in myeloid differentiation of HSPC. RKIP KD as a single event without the addition of cytokines was insufficient to induce myelomonocytic differentiation (*data not shown*). Of note, RKIP is a negative regulator of RAS-MAPK/ERK signaling. To evaluate whether RKIP KD indeed enhances RAS-MAPK/ERK signaling in HSPC, we studied the phosphorylation of ERK (pERK) in the conditions mentioned above. Indeed, HSPC with RKIP KD displayed increased pERK levels (Figure 6A), suggesting that the RKIP-induced aggravation of differentiation might be mediated *via* activation of the RAS-MAPK/ERK pathway.

To further corroborate the role of RKIP in myelomonocytic differentiation, we again employed the 1,25D₃-based HL-60 differentiation model and performed additional RKIP modulation by transfection of RKIP siRNA and overexpression constructs, respectively (Online Supplementary Figure S2). Initially, we thereby sought to confirm the role of RKIP on RAS-MAPK/ERK signaling and therefore studied the expression of pERK. In agreement with the results from healthy CD34⁺ HSPC, RKIP KD thereby increased pERK levels, which corroborates the role of RKIP as a regulator of RAS-MAPK/ERK signaling (Figure 6B). To study the role of RKIP on myelomonocytic differentiation, we assessed the CD11c surface expression in these experiments, which was previously established as the most suitable marker for this HL-60-based experimental approach.³⁶ 1,25D₃-treated HL-60 cells harboring RKIP knockdown thereby demonstrated an increased potential to differentiate into the myeloid lineage as assessed by an increase in the expression of CD11c ($P=0.009$) (Figure 2B). The oppo-

site effect was observed after RKIP overexpression ($P=0.005$) (Figure 2C). Finally, we studied the effect of RKIP modulation without additional 1,25D₃ incubation. As seen for healthy HSPC, myelomonocytic differentiation could not be induced in this scenario ($P=0.112$ for RKIP knockdown and $P=0.168$ for RKIP overexpression).

Rkip deletion contributes to the development of a myelomonocytic-lineage-biased hematopoietic system in a murine *in vivo* model

After demonstrating the functional involvement of RKIP loss in myelomonocytic differentiation *in vitro*, we focused on its effects *in vivo*. To do this, we analyzed the hematopoietic system in a murine model with a complete deletion of *Rkip* (*Rkip*^{-/-}) (Online Supplementary Table S1 and Online Supplementary Figures S3 and S4). In agreement with the *in vitro* data, RKIP loss as a single event thereby proved insufficient to increase the amount of myelomonocytic cells. *Rkip* deletion alone further proved insufficient to increase the proliferation of specific HSPC compartments (Online Supplementary Figure S4). As our *in vitro* data already suggested that RKIP acts as a modulator for the sensitivity to extracellular inducers of differentiation, we aimed to challenge the hematopoietic system of *Rkip*^{-/-} mice by the additional intraperitoneal injection of GM-CSF in a next step (Figure 3A). Indeed, *Rkip*^{-/-} mice demonstrated an increased percentage of CD11b⁺ as well as CD11b⁺ Ly6G⁺ myelomonocytic cells in bone marrow, peritoneal cavity cells and peripheral blood in these experiments (Figure 3B and C). As seen in the *in vitro* experiments mentioned above, *Rkip* deletion also enhanced RAS-MAPK/ERK signaling, as evidenced by increased pERK levels in *Rkip*^{-/-} mice (Figure 6C). Taken together, our

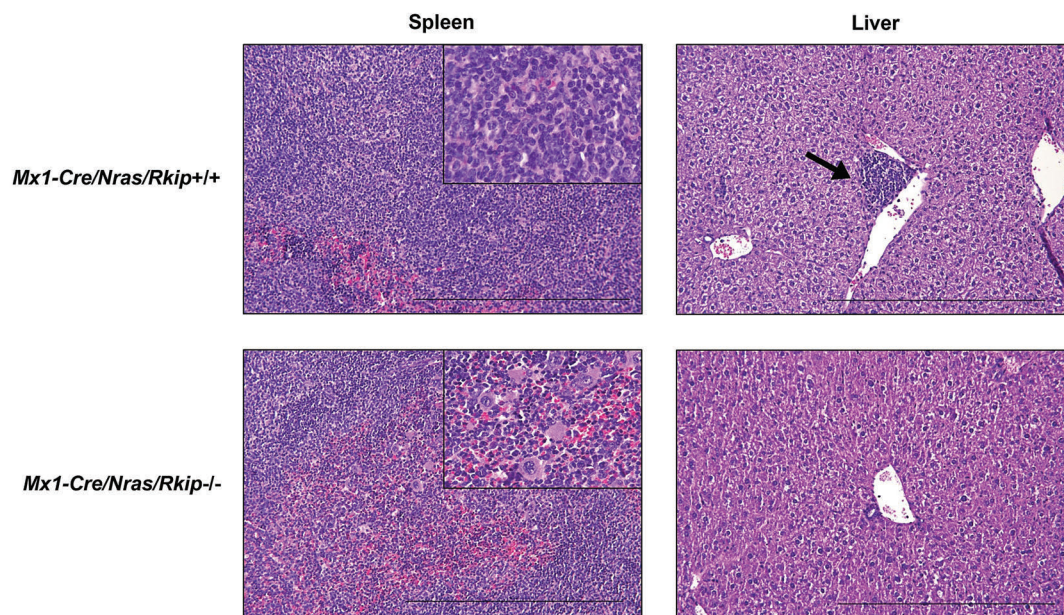


Figure 5. Induction of myeloproliferation in *Nras*-mutated mice with *Rkip* deletion coincides with a mitigation of histiocytic sarcoma development. Representative Hematoxylin & Eosin stained sections of spleen and liver of the mouse genotypes as indicated. Mice were electively killed at an age of six months after the first plpC injection. As in the flow cytometric analyses, animals with *Rkip* deletion demonstrated increased myeloproliferation (spleen, bottom left and insert bottom left showing multiple megakaryocytes) as compared to the *Rkip*^{+/+} mice (spleen top left, and insert top left showing almost exclusively histiocytic sarcoma). The formation of histiocytic sarcomas was mitigated in the *Rkip* deleted genotypes as also clearly seen in the liver sample (bottom right, no infiltrate) compared to the *Rkip*^{+/+} liver showing infiltration by histiocytic sarcoma (top right, arrow). The black bar denotes a distance of 500 μ m. RKIP: RAF kinase inhibitor protein.

data indicate that RKIP loss enhances RAS-MAPK/ERK signaling on the one hand and increases GM-CSF-induced myelomonocytic lineage commitment and differentiation of HSPC on the other. Furthermore, they suggest that RKIP exerts its role in terminal myelomonocytic differentiation by acting as a rheostat that modulates the sensitivity to external stimuli, such as 1,25D₃ and growth factors, respectively.

Rkip deletion aggravates myeloproliferation and the development of a myelomonocytic myeloproliferative disease in Ras-mutated mice

Increased myelomonocytic lineage commitment is a key step in myeloid leukemogenesis. However, *Rkip*^{-/-} mice failed to develop myeloid neoplasias in our study (*data not shown*). As the functional assays delineating the role of RKIP in myelomonocytic differentiation suggested that RKIP rather acts as an amplifier of activated GM-CSF/RAS signaling, we next crossed *Rkip*^{-/-} mice with *Mx1-Cre/Nras*-

mutated animals (*Online Supplementary Figure S5*). The *Mx1-Cre/Nras* was chosen because: (i) RKIP loss and RAS-signaling mutations have previously been shown to co-occur in AML;^{12,20,22} and (ii) RKIP loss has been demonstrated to potentiate the oncogenic effects of RAS-signaling mutations in functional *in vitro* assays.^{12,20} Interestingly, *Mx1-Cre/Nras* mice on a pure C57BL/6 background develop a myeloproliferation that preferentially affects the myelomonocytic lineages. However, previously published data have demonstrated that these mice ultimately succumb to histiocytic sarcomas (HS) and only randomly develop a full blown MPD.⁸ In the current study, we electively analyzed mice at an age of six months after the first pIpC injection and thereby observed that myeloproliferation was aggravated in *Mx1-Cre/Nras/Rkip*^{-/-} mice, who consistently demonstrated splenomegaly, as well as increased myeloid infiltration of bone marrow, spleen and liver as compared to *Nras/Rkip*^{+/+} and to *Mx1-Cre/Nras/Rkip*^{+/+} animals (Figures 4A and B, and 5). In addi-

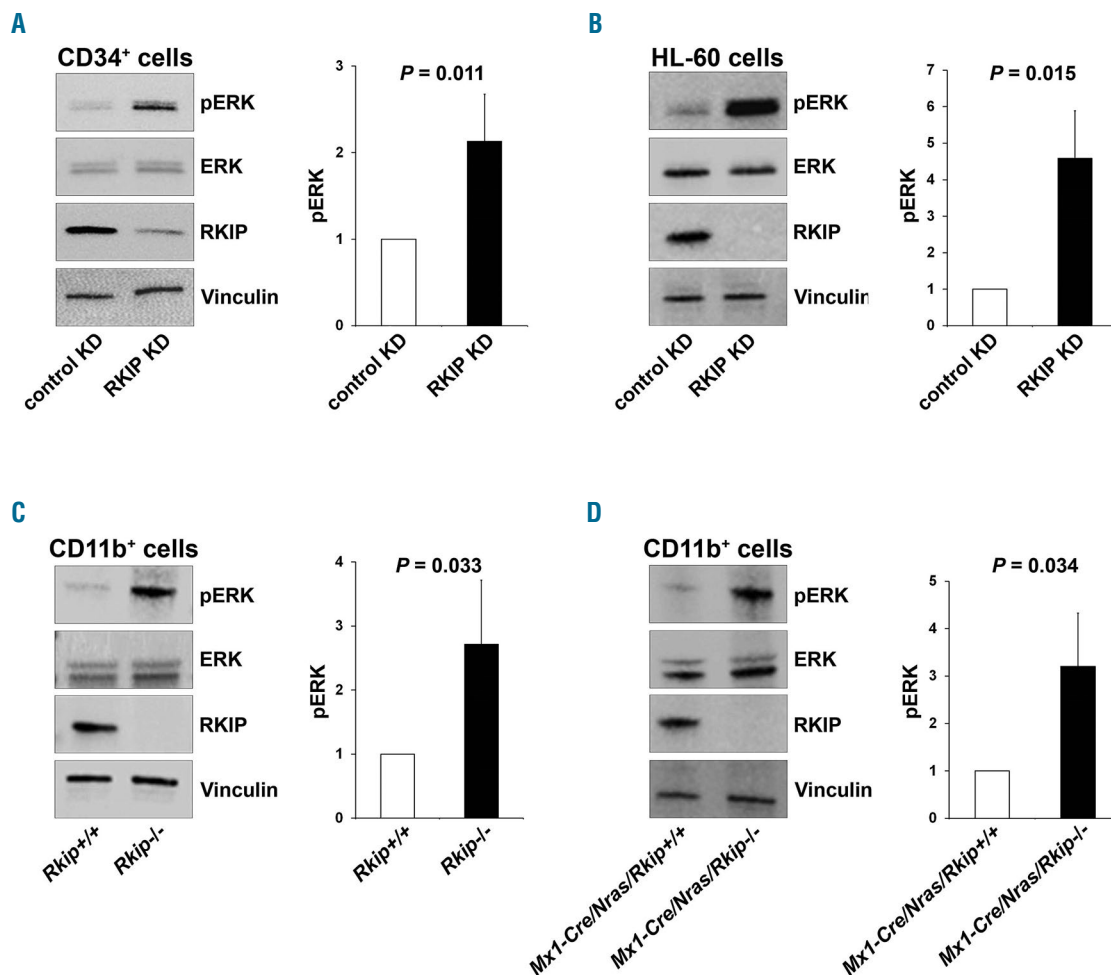


Figure 6. RAF kinase inhibitor protein (RKIP) regulates RAS-MAPK/ERK signaling in the myeloid system. (A) RKIP shRNA knockdown (KD) in CD34⁺ human hematopoietic stem and progenitor cells (HSPC) increased RAS-MAPK/ERK signaling, as measured by the phosphorylation of ERK (pERK). (Left) A representative immunoblot. Graph represents the mean of three independent experiments \pm Standard Deviation (SD); pERK intensity is given as x-fold change to the CD34⁺ control KD. (B) RKIP shRNA KD in HL-60 increased pERK levels as well. (Left) Representative immunoblot. Graph represents the mean of three independent experiments \pm SD; pERK intensity is given as x-fold change to the HL-60 control KD. (C) Rkip deletion enhanced the activity of RAS-MAPK/ERK signaling in CD11b⁺ cells isolated from the bone marrow of mice. (Left) A representative immunoblot. Graph represents the mean of three independent experiments \pm SD; pERK intensity is given as x-fold change to the *Rkip*^{+/+} control genotype. (D) Rkip deletion also increased the activity of RAS-MAPK/ERK signaling in CD11b⁺ cells isolated from *Nras*-mutated mice. A representative immunoblot and the graph is presented as described above, *Mx1-Cre/Nras/Rkip*^{+/+} were used as control group. Mice experiments were performed using n=3 mice for each genotype. Statistical significance was evaluated by Student's *t*-test in all cases.

tion, only the *Mx1-Cre/Nras/Rkip^{-/-}* genotype exhibited a full blown MPD, as evidenced by an accompanying leukocytosis in the peripheral blood (Figure 4C and D, and *Online Supplementary Table S2*).³⁷ We then studied a potential involvement of the RAS-MAPK/ERK pathway in this process. As seen in the experiments described above, Rkip deletion again enhanced the activation of ERK. Importantly, these effects on RAS-MAPK/ERK signaling were visible both in the absence of mitogens and following GM-CSF stimulation (Figure 6D and *Online Supplementary Figure S6*). In agreement with data from Li *et al.*,⁸ HS were detected in all *Nras*-mutated mice studied; however, the phenotype was mitigated in the *Mx1-Cre/Nras/Rkip^{-/-}* animals. Transformation into secondary AML did not occur in any of the mice, as assessed by morphological and flow cytometric evaluation of peripheral blood, bone marrow and spleen (*data not shown*). Interestingly, although MPD development was aggravated in *Mx1-Cre/Nras/Rkip^{-/-}* animals, the median survival was similar between *Mx1-Cre/Nras/Rkip^{-/-}* and *Mx1-Cre/Nras/Rkip^{+/+}* mice ($P=0.339$) (*Online Supplementary Figure S7*). Histopathological examination of moribund *Mx1-Cre/Nras/Rkip^{+/+}* mice thereby revealed that these mice suffered from extensive HS (*Online Supplementary Table S3* and *Online Supplementary Figure S8*). In agreement with the data from 6-month old mice, the *Mx1-Cre/Nras/Rkip^{-/-}* mice had a mitigated HS phenotype but an increased myeloproliferation/MPD occurrence. Future studies, using models without the predisposition to HS, will, therefore, be necessary to unambigu-

ously delineate the effect of Rkip on the survival of *Ras*-driven MPD.

Taken together, these data indicate that RKIP aggravates the effects of mutated *Nras* on RAS-MAPK/ERK signaling on the one hand, as well as on myeloproliferation and MPD development on the other.

RAF kinase inhibitor protein loss is frequently observed in primary chronic myelomonocytic leukemia patient specimens and co-occurs with RAS-signaling mutations

Finally, we aimed to delineate the clinical relevance of these findings and therefore analyzed a cohort of 41 primary CMML patients' specimens for RKIP protein expression by immunoblot (Figure 7A and B; for details of clinical characteristics as well as treatment regimens administered see *Online Supplementary Table S4*). We chose this disease because increased myelomonocytic lineage commitment and pathological RAS-signaling are seminal steps in its pathogenesis. RKIP protein loss was defined as previously reported^{12,22} and could be detected in 12 of 41 (29.3%) of CMML patients' samples. Interestingly, RKIP loss at the protein level also correlated with decreased expression of its mRNA ($P<0.001$) (Figure 7C). This is in agreement with data from AML, where RKIP loss has been shown to be caused by increased expression of miR-23a,^{21,22} and suggests that a similar mechanism might be present in CMML as well. Most interestingly, however, we observed that RKIP loss correlated with a more pronounced myelomonocytic phenotype, as assessed by the

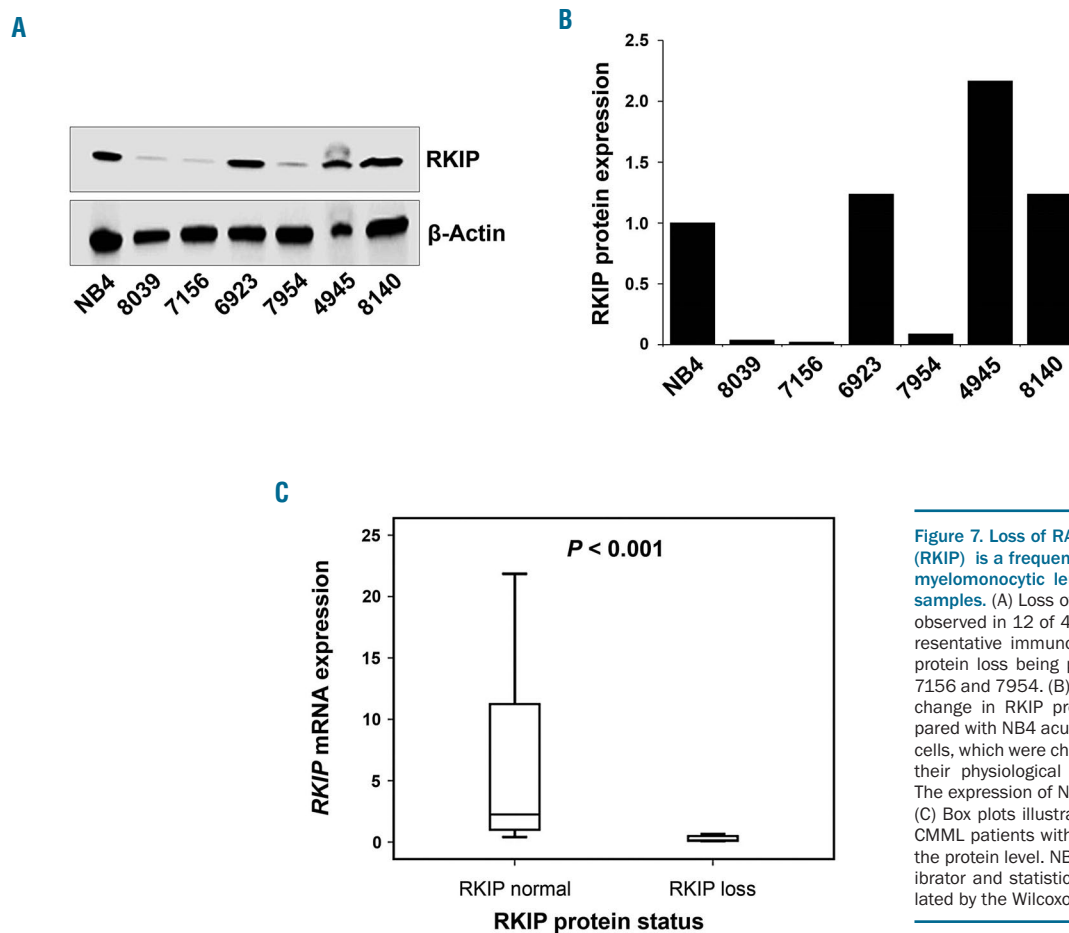


Figure 7. Loss of RAF kinase inhibitor protein (RKIP) is a frequent event in primary chronic myelomonocytic leukemia (CMML) patients' samples. (A) Loss of RKIP at protein level was observed in 12 of 41 (29.3%) of cases. A representative immunoblot is shown, with RKIP protein loss being present in patients 8039, 7156 and 7954. (B) Graphs showing the x-fold change in RKIP protein expression as compared with NB4 acute myeloid leukemia (AML) cells, which were chosen as a calibrator due to their physiological *RKIP* expression levels.¹² The expression of NB4 was arbitrarily set to 1. (C) Box plots illustrating *RKIP* mRNA levels in CMML patients with and without RKIP loss at the protein level. NB4 AML cells served as calibrator and statistical significance was calculated by the Wilcoxon-Mann-Whitney test.

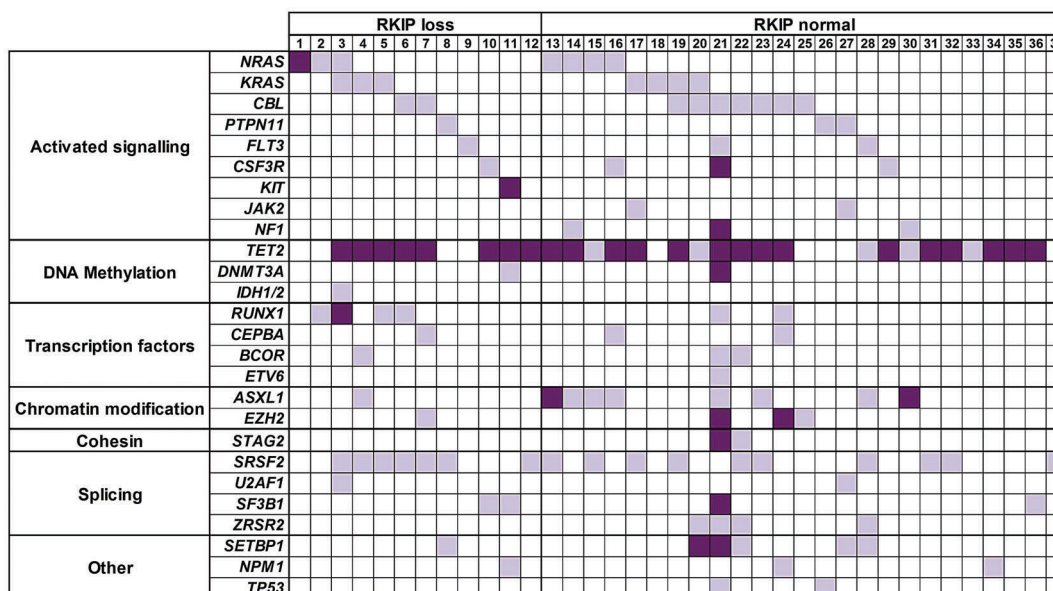


Figure 8. RAS-signaling mutations are frequent in chronic myelomonocytic leukemia (CMML) patients with RAF kinase inhibitor protein (RKIP) loss. Thirty-nine genes with recurrent mutations in myeloid neoplasias were screened for mutations by the means of next-generation sequencing.¹¹ The heatmap shows the distribution and number of mutations observed in each CMML patient (n=37). Every column describes one CMML patient specimen, defined as either “RKIP loss” or “RKIP normal” according to the immunoblot results. Light purple indicates the presence of one mutation; dark purple is used to demonstrate the presence of multiple mutations. Genes without sequence variations in any of the patients are not shown.

percentage of myelomonocytic cells (MMC; monocytes and granulocytes) in the peripheral blood (86% vs. 76%, $P=0.030$) (Online Supplementary Table S4). This is in agreement with our functional data and with previous findings from AML.¹² To investigate the molecular landscape of CMML patients with RKIP loss, we performed next-generation sequencing (NGS) covering 39 genes with recurrent mutations in myeloid neoplasms (Figure 8). In total, these analyses could be performed in 37 of 41 patients. All together, we discovered 186 mutations in 37 of 37 (100%) of the patients. Thirty-three of 37 had more than one mutation with a median of four variants per sample (range 1-32). In agreement with previous studies,³⁸ the most frequently affected genes were *TET2* (75.7%), *SRSF2* (46.0%), *CBL* (24.3%), and *ASXL1* (24.3%). Mutations in *NRAS* and *KRAS* affected 13 of 37 (35.1%) of the patients (Online Supplementary Table S5). This high frequency was even increased, when mutations affecting RAS-signaling were grouped (including *NRAS*, *KRAS*, *CBL*, *PTPN11*, *FLT3*, *CSF3R*, *KIT*, *JAK2*, and *NF1*). Twenty-nine of 37 (78.4%) of CMML patients' specimens showed one or more mutations within these genes. Most interestingly, however, almost all patients with RKIP loss (11 of 12, 91.7%) exhibited one or more mutations in RAS-signaling genes. Together with the previously published data from AML, this indicates that RKIP loss and RAS-signaling mutations co-occur in myeloid neoplasms, which proves the clinical relevance of the functional *in vivo* data mentioned above. Of note, RAS-signaling mutations were also frequent in patients with normal RKIP expression (18 of 25, 72%; comparison to patients with RKIP loss, $P=0.232$), which suggests that RKIP loss is not the only second genetic hit that interacts with RAS-signaling mutations in myeloid leukemogenesis. Indeed, such

interactions have previously been shown for a variety of genetic aberrations, including aberrant expression of members of the dual specificity phosphatase (*DUSP*) and *SPROUTY* (*Spry*) families, as well as for mutations in *ASXL1* and *TET2*.^{15,39-41} Finally, overall survival (OS) was similar between patients with and without RKIP loss ($P=0.913$) (Online Supplementary Figure S9). It must be noted, however, that these analyses are limited by the fact that these patients were managed with different treatment modalities, which ranged from best supportive care to high-dose chemotherapy. Subgroup analyses focusing on uniformly treated patients only could not be carried out due to the small sample size of this cohort.

Discussion

Hematopoietic stem and progenitor cells have the potential to differentiate into both myeloid and lymphoid hematopoietic cells. Although tight control and regulation programs are in place to maintain this system in homeostasis, skewing of hematopoiesis into the myeloid lineage can be achieved by a multitude of genetic aberrations. This includes RAS-signaling mutations,¹ which drive the myelomonocytic lineage commitment by increasing the sensitivity of intracellular signaling cascades to extracellular growth factors, such as GM-CSF.^{5,42} In this study, we hypothesized that a loss of the RAS-signaling inhibitor RKIP plays a role in myelomonocytic differentiation as well. Therefore, we initially analyzed RKIP expression during human and murine hematopoietic differentiation and observed that it is high in HSPC and lymphoid cells but decreases in cells belonging to the myeloid lineage. By modulating RKIP expression in

healthy HSPC and undifferentiated AML cell lines, we could further show that loss of RKIP expression is an important driver of myelomonocytic lineage commitment. This could be corroborated in subsequent *in vivo* studies, where we did show that RKIP loss increases the activation of RAS-MAPK/ERK signaling, and consequently, the GM-CSF-induced myelomonocytic differentiation of HSPC. Of note, we observed that RKIP exerts its role in myelomonocytic lineage commitment of HSPC by acting as an amplifier of GM-CSF signaling rather than inducing the differentiation process on its own. This has previously been shown for other alterations affecting RAS-signaling as well⁴³⁻⁴⁵ and further highlights the importance of physiological and pathological GM-CSF/RAS-signaling regulation in hematopoiesis.

Increased myelomonocytic lineage commitment has also been proposed to be an essential pre-phase of myeloid neoplasms.⁴⁶ Indeed, a role of RKIP in myeloid leukemogenesis has been suggested previously, as its somatic loss of expression was described as a frequent event in AML.^{12,20-22} In line with our functional data presented above, it thereby correlated with myelomonocytic AML phenotypes.¹² In the current study, we further strengthen these data by demonstrating that RKIP loss is indeed of functional relevance for the development of myelomonocytic leukemias. Again, it acted as an amplifier of pathologic RAS-signaling, as it aggravated the activity of the RAS-MAPK/ERK pathway as well as the development of a myelomonocytic MPD in mice that carry a somatically inducible mutation in *Nras* within the hematopoietic system. These data are further strengthened by our analysis of 41 primary CMML patients' specimens, where we observed that RKIP loss occurs in almost 30% of cases on the one hand, and that it co-occurs with RAS-signaling mutations on the other. The data are, therefore, in agreement with previous studies of our group, where we did observe a clinical correlation and a functional synergism between RAS-signaling mutations and RKIP loss in different subtypes of AML.^{12,20,22} They are also in agreement with previous observations, where RAS-driven leukemogenesis could be significantly aggravated by additional inactivation of RAS-MAPK/ERK signaling inhibitors belonging to the dual specificity phosphatase (*DUSP*) and *SPROUTY* (*Spry*) families.^{15,39,41} Together with the previously shown aggravation of RAS-induced myeloid leukemogenesis by mutations in *ASXL1* and *TET2*,^{15,40} respectively, these data indicate that activated RAS-signaling in human leukemias is far more complex than initially believed and cannot be explained by the occurrence of RAS-signaling mutations alone.

Finally, our data might also be of relevance for the future development of targeted treatment approaches in myeloid neoplasias, particularly for those aiming to inhibit specific signal transduction cascades. This is based on our observation that both the signaling and leukemogenic effects of RAS mutations can be influenced by aberrant expression of RAS-signaling regulator proteins. So far, development of these agents has often been hindered by the fact they showed disappointing efficacy in

clinical trials, even though the results from pre-clinical models had been promising. An example for such a history of drug development are MEK-inhibitors, which efficiently attenuate *Ras*-driven MPD in mice, but show disappointing results in clinical trials of myeloid malignancies.⁴⁷ Among others, one reason for this is the fact that the monogenic pre-clinical model does not adequately reflect the situation in myeloid neoplasia patients, who usually exhibit a complex network of co-occurring and interacting genetic aberrations within their neoplastic clone. Therefore, more detailed knowledge of the co-occurrence of mutational and non-mutational aberrations in patients' specimens, as well as the functional consequences thereof, might not only help to extend our knowledge about the pathogenesis of this aggressive malignancy, but also to more specifically select patients that might profit from targeted therapies directed at cellular signaling. One successful example of this approach is the recent observation that sensitivity to MEK inhibitors in *Nras*-mutated mice can be increased by the co-occurrence of *Tet2* deletion and decreased *Spry2* expression levels.¹⁵ With these data, the authors identified a specific subgroup of RAS-mutated patients that will be the best candidates for MEK-directed therapy. The fact that simultaneous occurrence of RAS mutations and RKIP loss potentiated RAS-MAPK/ERK signaling as well, might identify another group of patients with particular sensitivity to this therapeutic approach. Future studies will, therefore, be warranted to specifically test this hypothesis.

In conclusion, we show that the RAS-signaling regulator RKIP plays a central role in myelomonocytic lineage commitment of HSPC. We further show its relevance for myelomonocytic leukemogenesis by demonstrating that *Rkip* deletion enhances RAS-MAPK/ERK signaling and aggravates the development of a myelomonocytic MPD in *Nras*-mutated mice. Finally, we prove the clinical relevance of these findings by showing that RKIP loss is a frequent event in primary CMML patients' samples and frequently co-occurs with RAS-signaling mutations. These data establish RKIP as a novel player in RAS-driven myeloid leukemogenesis.

Acknowledgments

The authors would like to thank Prof. John Sedivy for providing *Rkip*^{-/-} mice.

Funding

This study was supported by research funding from the Austrian Science Fund (grant P26619-B19 to A. Zebisch) and from the Science Foundation Ireland (grant 14/IA/2395 to W. Kolch). Work in the laboratories of A. Zebisch, A. Wölfler, and H. Sill is further supported by Leukämiehilfe Steiermark. PhD candidate V. Caraffini received funding from the Austrian Science Fund (grant P26619-B19 to A. Zebisch) and was trained within the frame of the PhD Program Molecular Medicine of the Medical University of Graz. PhD candidate J.L. Berg received funding from the Medical University of Graz within the PhD Program Molecular Medicine.

This work was supported by Biobank Graz.

References

- Fatrai S, Van Gosliga D, Han L, Daenen SMGJ, Vellenga E, Schuringa JJ. KRASG12V enhances proliferation and initiates myelomonocytic differentiation in human stem/progenitor cells via intrinsic and extrinsic pathways. *J Biol Chem*. 2011;286(8):6061-6070.
- Downward J. Targeting RAS signalling pathways in cancer therapy. *Nat Rev Cancer*. 2003;3(1):11-22.
- Geest CR, Coffey PJ. MAPK signaling pathways in the regulation of hematopoiesis. *J Leukoc Biol*. 2009;86:237-250.
- Zebisch A, Czernilofsky A, Keri G, Smigelskaite J, Sill H, Troppmair J. Signaling Through RAS-RAF-MEK-ERK: from Basics to Bedside. *Curr Med Chem*. 2007;14(5):601-623.
- Van Meter MEM, Díaz-Flores E, Archard JA, et al. K-RasG12D expression induces hyperproliferation and aberrant signaling in primary hematopoietic stem/progenitor cells. *Blood*. 2007;109(9):3945-3952.
- Braun BS, Tuveson DA, Kong N, et al. Somatic activation of oncogenic Kras in hematopoietic cells initiates a rapidly fatal myeloproliferative disorder. *Proc Natl Acad Sci U S A*. 2004;101(2):597-602.
- Chan IT, Kutok JL, Williams IR, et al. Conditional expression of oncogenic K-ras from its endogenous promoter induces a myeloproliferative disease. *J Clin Invest*. 2004;113(4):528-538.
- Li Q, Haigis KM, McDaniel A, et al. Hematopoiesis and leukemogenesis in mice expressing oncogenic NrasG12D from the endogenous locus. *Blood*. 2011;117(6):2022-2032.
- Wang J, Kong G, Liu Y, et al. Nras(G12D/+) promotes leukemogenesis by aberrantly regulating hematopoietic stem cell functions. *Blood*. 2013;121(26):5203-5207.
- Papaemmanuil E, Gerstung M, Bullinger L, et al. Genomic Classification and Prognosis in Acute Myeloid Leukemia. *N Engl J Med*. 2016;374(23):2209-2221.
- Kashofer K, Gornicec M, Lind K, et al. Detection of prognostically relevant mutations and translocations in myeloid sarcoma by next generation sequencing. *Leuk Lymphoma*. 2018;59(2):501-504.
- Zebisch A, Wölfler A, Fried I, et al. Frequent loss of RAF kinase inhibitor protein expression in acute myeloid leukemia. *Leukemia*. 2012;26(8):1842-1849.
- Patnaik MM, Tefferi A. Cytogenetic and molecular abnormalities in chronic myelomonocytic leukemia. *Blood Cancer J*. 2016;6(2):e393.
- Geissler K, Jäger E, Barna A, et al. Chronic myelomonocytic leukemia patients with RAS pathway mutations show high in vitro myeloid colony formation in the absence of exogenous growth factors. *Leukemia*. 2016;30(11):2280-2281.
- Kunimoto H, Meydan C, Nazir A, et al. Cooperative Epigenetic Remodeling by TET2 Loss and NRAS Mutation Drives Myeloid Transformation and MEK Inhibitor Sensitivity. *Cancer Cell*. 2018;33(1):44-59.
- Yeung K, Seitz T, Li S, et al. Suppression of Raf-1 kinase activity and MAP kinase signalling by RKIP. *Nature*. 1999;401(6749):173-177.
- Al-Mulla F, Bitar MS, Taqi Z, Yeung KC. RKIP: Much more than Raf Kinase inhibitor protein. *J Cell Physiol*. 2013;228(8):1688-1702.
- Al-Mulla F, Hagan S, Behbehani AI, et al. Raf kinase inhibitor protein expression in a survival analysis of colorectal cancer patients. *J Clin Oncol*. 2006;24(36):5672-5679.
- Escara-Wilke J, Keller JM, Ignatoski KMW, et al. Raf kinase inhibitor protein (RKIP) deficiency decreases latency of tumorigenesis and increases metastasis in a murine genetic model of prostate cancer. *Prostate*. 2015;75(3):292-302.
- Zebisch A, Haller M, Hiden K, et al. Loss of RAF kinase inhibitor protein is a somatic event in the pathogenesis of therapy-related acute myeloid leukemias with C-RAF germline mutations. *Leukemia*. 2009;23(6):1049-1053.
- Hatzl S, Geiger O, Kuepper MK, et al. Increased expression of miR-23a mediates a loss of expression in the RAF kinase inhibitor protein RKIP. *Cancer Res*. 2016;76(12):3644-3654.
- Caraffini V, Perfler B, Berg JL, et al. Loss of RKIP is a frequent event in myeloid sarcoma and promotes leukemic tissue infiltration. *Blood*. 2018;131(7):826-830.
- Zebisch A, Staber PB, Delavar A, et al. Two Transforming C-RAF Germ-Line Mutations Identified in Patients with Therapy-Related Acute Myeloid Leukemia. *Cancer Res*. 2006;66(7):3401-3408.
- Taschner S, Koesters C, Platzer B, et al. Down-regulation of RXR expression is essential for neutrophil development from granulocyte-monocyte progenitor. *Blood*. 2007;109(3):971-979.
- Wang J, Liu Y, Li Z, et al. Endogenous oncogenic NRAS mutation promotes aberrant GM-CSF signaling in granulocytic/monocytic precursors in a murine model of chronic myelomonocytic leukemia. *Blood*. 2010;116(26):5991-6002.
- Haigis KM, Kendall KR, Wang Y, et al. Differential effects of oncogenic K-Ras and N-Ras on proliferation, differentiation and tumor progression in the colon. *Nat Genet*. 2008;40(5):600-608.
- Lal R, Lind K, Heitzer E, et al. Somatic TP53 mutations characterize preleukemic stem cells in acute myeloid leukemia. *Blood*. 2017;129(18):2587-2591.
- Gaksch L, Kashofer K, Heitzer E, et al. Residual disease detection using targeted parallel sequencing predicts relapse in cytogenetically normal acute myeloid leukemia. *Am J Hematol*. 2018;93(1):23-30.
- Caux C, Massacrier C, Dubois B, et al. Respective involvement of TGF- and IL-4 in the development of Langerhans cells and non-Langerhans dendritic cells from CD34+progenitors. *J Leukoc Biol*. 1999;66(5):781-791.
- Zebisch A, Lal R, Müller M, et al. Acute myeloid leukemia with TP53 germ line mutations. *Blood*. 2016;128(18):2270-2272.
- Konuma T, Nakamura S, Miyagi S, et al. Forced expression of the histone demethylase Fbx10 maintains self-renewing hematopoietic stem cells. *Exp Hematol*. 2011;39(6):697-709.
- Sung L-Y, Gao S, Shen H, et al. Differentiated cells are more efficient than adult stem cells for cloning by somatic cell nuclear transfer. *Nat Genet*. 2006;38(11):1323-1328.
- Moran-Crusio K, Reavie L, Shih A, et al. Tet2 loss leads to increased hematopoietic stem cell self-renewal and myeloid transformation. *Cancer Cell*. 2011;20(1):11-24.
- Wang Y, Krivtsov AV, Sinha AU, et al. The Wnt/ -catenin Pathway Is Required for the Development of Leukemia Stem Cells in AML. *Science*. 2010;327(5973):1650-1653.
- White SL, Belov L, Barber N, Hodgkin PD, Christopherson RI. Immunophenotypic changes induced on human HL60 leukaemia cells by 1,25-dihydroxyvitamin D3 and 12-O-tetradecanoyl phorbol-13-acetate. *Leuk Res*. 2005;29(10):1141-1151.
- Kim K, Seoh JY, Cho SJ. Phenotypic and Functional Analysis of HL-60 Cells Used in Opsonophagocytic-Killing Assay for Streptococcus pneumoniae. *J Korean Med Sci*. 2015;30(2):145-150.
- Kogan SC, Ward JM, Anver MR, et al. Bethesda proposals for classification of nonlymphoid hematopoietic neoplasms in mice. *Blood*. 2002;100(1):238-245.
- Yoshimi A, Balasis ME, Vedder A, et al. Robust patient-derived xenografts of MDS/MPN overlap syndromes capture the unique characteristics of CMML and JMML. *Blood*. 2017;130(4):397-407.
- Zhao Z, Chen CC, Rillaan CD, et al. Cooperative loss of RAS feedback regulation drives myeloid leukemogenesis. *Nat Genet*. 2015;47(5):539-543.
- Abdel-Wahab O, Adli M, Lafave LM, et al. ASXL1 Mutations Promote Myeloid Transformation Through Loss of PRC2-Mediated Gene Repression. *Cancer Cell*. 2012;22(2):180-193.
- Geiger O, Hatzl S, Kashofer K, et al. Deletion of SPRY4 is a frequent event in secondary acute myeloid leukemia. *Ann Hematol*. 2015;94(11):1923-1924.
- Wang X, Studzinski GP. Activation of extracellular signal-regulated kinases (ERKs) defines the first phase of 1,25-dihydroxyvitamin d3-induced differentiation of HL60 cells. *J Cell Biochem*. 2001;80(4):471-482.
- Wang X, Studzinski GP. Kinase Suppressor of RAS (KSR) Amplifies the Differentiation Signal Provided by Low Concentrations 1,25-Dihydroxyvitamin D3. *J Cell Physiol*. 2004;198(3):333-342.
- Wang J, Zhao Y, Kauss MA, Spindel S, Lian H. Akt regulates vitamin D3-induced leukemia cell functional differentiation via Raf/MEK/ERK MAPK signaling. *Eur J Cell Biol*. 2009;88(2):103-115.
- Wang X, Studzinski GP. Oncoprotein Cot1 represses kinase suppressors of Ras1/2 and 1,25-dihydroxyvitamin D3-induced differentiation of human acute myeloid leukemia cells. *J Cell Physiol*. 2011;226(5):1232-1240.
- Mason CC, Khorashad JS, Tantravahi SK, et al. Age-related mutations and chronic myelomonocytic leukemia. *Leukemia*. 2016;30(4):906-913.
- Smith CC, Shah NP. The role of kinase inhibitors in the treatment of patients with acute myeloid leukemia. *Am Soc Clin Oncol Educ Book*. 2013;313-8.

Validation of a *Drosophila* model of wild-type and T315I mutated BCR-ABL1 in chronic myeloid leukemia: an effective platform for treatment screening

Amani Al Outa,¹ Dana Abubaker,² Ali Bazarbachi,^{1,3} Marwan El Sabban,¹ Margret Shirinian² and Rihab Nasr¹

¹Department of Anatomy, Cell Biology and Physiology, Faculty of Medicine, American University of Beirut; ²Department of Experimental Pathology, Immunology and Microbiology, Faculty of Medicine, American University of Beirut and ³Department of Internal Medicine, Faculty of Medicine, American University of Beirut, Beirut, Lebanon



Haematologica 2018
Volume 105(2):387-397

ABSTRACT

Chronic myeloid leukemia (CML) is caused by a balanced chromosomal translocation resulting in the formation of *BCR-ABL1* fusion gene encoding a constitutively active BCR-ABL1 tyrosine kinase, which activates multiple signal transduction pathways leading to malignant transformation. Standard treatment of CML is based on tyrosine kinase inhibitors (TKI); however, some mutations have proven elusive particularly the T315I mutation. *Drosophila melanogaster* is an established *in vivo* model for human diseases including cancer. The targeted expression of chimeric human/fly and full human BCR-ABL1 in *Drosophila* eyes has been shown to result in detrimental effects. In this study, we expressed human BCR-ABL1^{p210} and the resistant BCR-ABL1^{p210/T315I} fusion oncogenes in *Drosophila* eyes. Expression of BCR-ABL1^{p210/T315I} resulted in a severe distortion of the ommatidial architecture of adult eyes with a more prominent rough eye phenotype compared to milder phenotypes in BCR-ABL1^{p210} reflecting a stronger oncogenic potential of the mutant. We then assessed the efficacy of the currently used TKI in BCR-ABL1^{p210} and BCR-ABL1^{p210/T315I} expressing flies. Treatment of BCR-ABL1^{p210} expressing flies with potent kinase inhibitors (dasatinib and ponatinib) resulted in the rescue of ommatidial loss and the restoration of normal development. Taken together, we provide a CML tailored BCR-ABL1^{p210} and BCR-ABL1^{p210/T315I} fly model which can be used to test new compounds with improved therapeutic indices.

Introduction

Chronic myeloid leukemia (CML) is a myeloproliferative neoplasm secondary to a precise cytogenetic abnormality involving a balanced chromosomal translocation between the Abelson murine leukemia (*ABL1*) gene on chromosome 9 and the breakpoint cluster region (*BCR*) on chromosome 22. This creates the (*BCR-ABL1*) fusion gene on chromosome 22 which encodes a constitutively active tyrosine kinase BCR-ABL.¹ Based on the breakpoints in BCR this translocation results in the formation of (p190, p210 and p230) fusion genes.² Overall, 95% of CML patients harbor the p210-kDa fusion protein, BCR-ABL1^{p210}.^{3,4} The BCR-ABL1 fusion oncoprotein increases the replication machinery and enhances cell growth which is mediated by downstream signaling pathways such as RAS, RAF, JUN kinase, MYC and STAT.⁵⁻¹¹

CML treatment was revolutionized with the development of tyrosine kinase inhibitors (TKI) which competitively inhibit the Adenosine triphosphate (ATP) binding site in the BCR-ABL1 kinase domain¹² and hence block the phosphorylation of proteins in the downstream signaling cascade. The first generation TKI (imatinib) showed major therapeutic improvement in the IRIS study (International Randomized Study of Interferon and STI571).¹³ However, imatinib success was

Correspondence:

MARGRET SHIRINIAN
ms241@aub.edu.lb

RIHAB NASR
rn03@aub.edu.lb

Received: February 15, 2019.

Accepted: May 16, 2019.

Pre-published: May 17, 2019.

doi:10.3324/haematol.2019.219394

Check the online version for the most updated information on this article, online supplements, and information on authorship & disclosures: www.haematologica.org/content/105/2/387

©2020 Ferrata Storti Foundation

Material published in *Haematologica* is covered by copyright. All rights are reserved to the Ferrata Storti Foundation. Use of published material is allowed under the following terms and conditions:

<https://creativecommons.org/licenses/by-nc/4.0/legalcode>.

Copies of published material are allowed for personal or internal use. Sharing published material for non-commercial purposes is subject to the following conditions:

<https://creativecommons.org/licenses/by-nc/4.0/legalcode>,

sect. 3. Reproducing and sharing published material for commercial purposes is not allowed without permission in writing from the publisher.



outsuited by the emergence of resistance caused by point mutations in the ABL1 kinase domain which necessitated the development of second-generation TKI.^{14,15} Dasatinib¹⁶⁻¹⁸ and nilotinib¹⁹⁻²¹ revealed faster and deeper molecular responses compared to imatinib in patients with newly diagnosed chronic phase CML. *In vitro*, dasatinib is more potent than imatinib²²⁻²⁴ and inhibits a wider spectrum of kinases including the Src family.²⁵ Nilotinib has a greater affinity than imatinib to the ATP binding site in BCR-ABL1 and its spectrum of kinase inhibition involves platelet-derived growth factor receptor (PDGFR) and c-Kit receptors.²⁶ Although nilotinib and dasatinib tackled the majority of imatinib-resistant mutations, neither of them targeted the T315I mutation (threonine to isoleucine substitution at position 315 in the ABL1 kinase domain) (BCR-ABL1^{T315I}).²³ Ponatinib, a third generation TKI, remains the only clinically available drug that is designed to overcome the T315I gatekeeper mutation.^{27,28} However, post-marketing safety issues with ponatinib involved serious cardiovascular events which led to its temporary suspension and then reintroduction with special patient recommendations.^{29,30}

In addition to the burden of resistance, therapy with TKI is hindered by their inability to eradicate leukemic stem cells and hence relapse often accompanies discontinuation of therapy.³¹ This fact imparts lifelong therapy with TKI despite accompanying side effects which result in ever-expanding costs for remission sustainment. Therefore, it seems evident that despite the breakthrough with TKI, CML remains a pathology that requires vigilant assessment of curative therapeutic interventions.

One simple, multicellular and genetically tractable animal model that has been exploited in recent years for modelling human diseases, including cancer, is *Drosophila melanogaster*.³² A myriad of advantages is held by this 3 mm long fruit fly as an *in vivo* model for dissecting the contribution of cellular mechanisms to human cancers and therapeutic screening. Fogerty *et al.* utilized *Drosophila* to decipher functional analogies between fly ABL1 and human BCR-ABL1 via neural-specific expression of p185 or p210 BCR-ABL1 transgenes. In these transgenes, BCR and the N-terminal sequences are derived from human oncogenes while the C-terminal ABL1 tail is from *Drosophila*. Both transgenes were capable to substitute the fruit fly ABL1 during axon genesis and flies expressing BCR-ABL1 revealed an increase in the phosphorylation of Enabled (Ena), a substrate for *Drosophila* Abl (dAbl). Expression of chimeric BCR-ABL1 in *Drosophila* eyes and CNS resulted in a rough eye phenotype and CNS developmental defects.³³ Furthermore, a recent study showed that the expression of human BCR-ABL1^{p210} in *Drosophila* activates the dAbl pathway and its upstream regulators Ena and Disabled (Dab).³⁴

In this study, we have overexpressed human BCR-ABL1^{p210} and mutated BCR-ABL1^{p210/T315I} in *Drosophila* compound eyes. BCR-ABL1^{p210/T315I} expression induced a significantly more severe rough eye phenotype compared to BCR-ABL1^{p210} pointing towards more aggressive tumorigenic capacities of the gatekeeper mutation. We have further assessed the efficiency of the current TKI used in clinics in modifying the characteristic eye phenotypes of transgenic flies. Dasatinib and ponatinib rescued the eye defects observed upon expression of BCR-ABL1^{p210} making this model a valuable screening platform to pre-clinically evaluate the efficacy of potential novel therapies for CML.

Methods

Fly stocks

Fly stocks were maintained at 25°C on standard agar-based medium. GMR-GAL4 (BDSC 1104) were obtained from Bloomington Stock Center. Treatment was performed at 18°C. Fly work was done following the institutional guide for the care and use of laboratory animals.

Generation of transgenic flies

Transgenic flies, harboring human BCR-ABL1^{p210} and BCR-ABL1^{p210/T315I} were generated using Phi C31 integrase system and were inserted in the 3rd chromosome for GAL4-UAS expression. BCR-ABL1^{p210} and BCR-ABL1^{p210/T315I} were inserted into pUAST-attB *Drosophila* expression vector (Custom DNA cloning). pUAST-attB-myc BCR-ABL1^{p210} and pUAST-attB-myc BCR-ABL1^{p210/T315I} were injected into y1 w67c23; P {CaryP} ABLattP2 (8622 BDSC) embryos to generate transgenic flies (BestGene Inc, Chino Hills, CA).

TKI administration

Imatinib (I-5577), nilotinib (N-8207), dasatinib (D-3307) and ponatinib (P-7022) were obtained from LC laboratories, MA, USA. Stock solutions were dissolved in DMSO and the required amount of TKI was added to instant *Drosophila* medium (Carolina Biological Supply Company). Since DMSO is known to be toxic to *Drosophila*,⁴⁰ 0.03% DMSO was used for low TKI concentrations and 0.3% for high concentrations.

Scoring of eye phenotypes and measurement of eye defect area

A grading score, that was modified from the score previously published,³⁵ was used for scoring and is based on the number of ommatidial fusions, the extent of bristle organization and ommatidial loss (*Online Supplementary Table S1*). For the measurement of the posterior eye defect area, Image J³⁶ was used. Scanning electron microscopy images were coded by one researcher and analysis was blindly performed by another researcher. N=20 flies from each genotype at each temperature were scored and the experiment was done in triplicate. For the measurement of posterior eye defect area an average of n=20-30 flies from each group was quantified and the experiment was done at least twice.

Scanning electron microscopy

Adult flies were fixed in 2% glutaraldehyde and 2% formaldehyde in phosphate buffered saline (PBS) (1x), washed, dehydrated with a series of increasing ethanol concentrations, dried with a critical point dryer (k850, Quorum Technologies), mounted on standard aluminum heads and coated with 20 nm layer of gold. Analysis was performed using Tescan, Mira III LMU, Field Emission Gun (FEG) scanning electron microscopy (SEM) with a secondary electron detector.

Western blot analysis

Fly heads were homogenized in Laemmli buffer and samples were loaded in 8% SDS-PAGE. Anti-ABL1 (SC-23, 1:1000, Santa Cruz Biotechnology, Santa Cruz, CA) and phospho-ABL1 (#2868, 1:500, Cell Signaling Technology) primary antibodies and anti-mouse (SC-2318, 1:5000, Santa Cruz Biotechnology, Santa Cruz, CA) and anti-rabbit (NA934, 1:5000, GE Healthcare) secondary antibodies were used for protein detection. An extract (150 µg) from 20-30 flies was used.

Statistical analysis

The statistical significance of the difference between the average scores of the rough eye phenotype and the average scores of

the posterior eye defect area was evaluated using two-way analysis of variance (ANOVA) followed by the Tukey's multiple comparisons test. One-way ANOVA was used when comparing the averages of the posterior eye defect area for dose response and was followed by Tukey's multiple comparisons test. Associations with $p < 0.05$ were considered significant. Statistical tests were done using GraphPad Prism 6.0 software.

Results

Expression of human BCR-ABL1 in *Drosophila* eyes induces transformation

To assess the transformative potential of human BCR-ABL1^{p210} and BCR-ABL1^{p210/T3151} in *Drosophila*, we expressed the transgenes in the adult eye using the glass-multimer reporter promoter GMR-GAL4 which drives the expression in all differentiating photoreceptor cells posterior to the morphogenetic furrow.³⁷ GMR-GAL4>w¹¹¹⁸ flies were used as a control. The temperature sensitivity of the GAL4-UAS system allowed us to the control BCR-ABL1 expression levels.³⁸ Therefore crosses were performed at 18°C, 25°C, and 29°C allowing for a reciprocal increase in transgene expression upon increased temperatures. Enclosed flies were imaged using light microscopy and SEM and evaluations of phenotypes were performed using a grading score (Online Supplementary Table S1) which graded the severity of the phenotype based on the extent of mechano-sensory bristles alignment, misplacement and duplication as well as the extent of ommatidial facets loss indicating the disruption in cellular proliferation and differentiation collectively defining interrupted normal development.³⁹ BCR-ABL1^{p210} and BCR-ABL1^{p210/T3151} showed a rough eye phenotype with increased severity at a higher temperature compared to control flies. At 18°C BCR-ABL1^{p210} and BCR-ABL1^{p210/T3151} flies exhibited a rough eye phenotype characterized by ommatidial fusions and areas of lost ommatidial facets, particularly at the posterior end of the eye, as well as multiple ectopic mechano-sensory bristles which are duplicated at some instances (Figure 1 B, F, J; Figure 2 B, F, J). At 25°C, a more severe rough eye was observed in both BCR-ABL1^{p210} and BCR-ABL1^{p210/T3151} with loss of the majority of ommatidial facets (Figure 1 D, H, L; Figure 2 D, H, L). At 29°C, the severity increased to involve the loss of the majority of mechano-sensory bristles in addition to the total loss of ommatidial facets in both BCR-ABL1^{p210} and BCR-ABL1^{p210/T3151} expressing flies (Figure 1 N, P, R; Figure 2 N, P, R). The average roughness of BCR-ABL1^{p210} significantly increased from 6.2 at 18°C to 8.2 ($P < 0.0001$) at 25°C and to 9.5 ($P < 0.0001$) at 29°C (Figure 1). As for BCR-ABL1^{p210/T3151}, the average roughness significantly increased from 6.6 at 18°C to 8.9 ($P < 0.0001$) at 25°C and to 10 ($P < 0.0001$) at 29°C (Figure 2). Western blot analysis confirmed the expression and phosphorylation of BCR-ABL1^{p210} and BCR-ABL1^{p210/T3151} in *Drosophila* eyes (Figure 3).

Dasatinib and ponatinib rescue human BCR-ABL1^{p210} mediated defects in *Drosophila*

Since expression of BCR-ABL1 at high temperature induced severe eye defects in adult flies, we opted to use the lowest temperature (18°C) which produced milder phenotypes for TKI screening efficiency allowing the easy visualization of any rescue due to drug activity. Four TKI were tested which included imatinib, nilotinib, dasatinib

and ponatinib. BCR-ABL1^{p210} flies were crossed to GMR-Gal4 flies and progeny were fed on multiple concentrations of the TKI (treated) or on DMSO alone (untreated). Untreated BCR-ABL1^{p210} and BCR-ABL1^{p210/T3151} flies showed the same defects described previously at 18°C focusing particularly on the posterior end of the eye with a characteristic defective area characterized by loss of ommatidial facets (Figures 4-6). The posterior eye defect area in untreated BCR-ABL1^{p210} flies showed an average of 4580 μm^2 and 4044 μm^2 on 0.03% DMSO and 0.3% DMSO respectively (Figures 4-6). On the other hand, untreated BCR-ABL1^{p210/T3151} expressing flies showed a wider area of defect at the posterior end with an average significant increase in the defect area to 11148 μm^2 ($P < 0.0001$) and 8728 μm^2 ($P < 0.0001$) on 0.03% DMSO and 0.3% DMSO respectively as compared to untreated BCR-ABL1^{p210} expressing flies (Figures 4-6).

Feeding 150 μM or 1500 μM imatinib to BCR-ABL1^{p210} expressing flies did not eliminate the posterior eye defect. However, the average posterior eye defect area showed a tendency to decrease with 1500 μM imatinib (3047 μm^2) as compared to that of 150 μM imatinib (4142 μm^2) and untreated flies (4044 μm^2) (Figure 4). Interestingly, the percentage of flies with total rescue (total disappearance of the posterior eye defect) with 150 μM and 1500 μM imatinib was 4% and 21% respectively. Similarly, feeding 28 μM (Online Supplementary Figure S1 E, K) or 280 μM (Online Supplementary Figure S1 F, L) nilotinib to BCR-ABL1^{p210} expressing flies did not eliminate the posterior eye defect. However, the average posterior eye defect area showed a tendency to decrease with 280 μM nilotinib (2480 μm^2) compared to that of 28 μM nilotinib (3871 μm^2) and untreated flies (4044 μm^2) (Online Supplementary Figure S1). The percentage of flies with total rescue with 28 μM and 280 μM nilotinib was 7% and 13% respectively.

Testing the potent TKI (dasatinib and ponatinib) showed more efficient rescue. Feeding 20 μM dasatinib or 280 μM ponatinib to BCR-ABL1^{p210} expressing flies improves the overall eye ommatidial arrangement and more specifically eliminates the characteristic posterior eye defect by restoring its normal ommatidial development (Figure 5 D, H; Figure 6 D, H). The average posterior eye defect area significantly decreased from 4580 μm^2 (in untreated flies) to 0 μm^2 ($P < 0.0001$) with 20 μM dasatinib (Figure 5) and from 4044 μm^2 (in untreated flies) to 267 μm^2 ($P < 0.0001$) with 280 μM ponatinib (Figure 6). The percentage of flies with total rescue was 100% with dasatinib and 86% with ponatinib.

A dose-response analysis for BCR-ABL1^{p210} expressing flies treated with dasatinib showed a significant decrease in the average posterior eye defect area from 4580 μm^2 in untreated flies to 2372 μm^2 ($P < 0.0001$) with 1 μM dasatinib, to 131 μm^2 ($P < 0.0001$) with 10 μM and to 0 μm^2 ($P < 0.0001$) with 20 μM dasatinib. The percentage of flies with total rescue increased from 25% to 92% and to 100% with 1 μM , 10 μM and 20 μM dasatinib respectively (Figure 7). Similarly, ponatinib also showed a dose-response whereby the average posterior eye defect area decreased significantly from 4044 μm^2 in untreated flies to 1684 μm^2 ($P < 0.0001$) with 28 μM and to 267 μm^2 ($P < 0.0001$) with 280 μM ponatinib (Figure 7). The percentage of flies with total rescue increased from 48% to 86% with 28 μM and 280 μM ponatinib respectively.

The BCR-ABL1^{p210/T3151} mutation is known to exhibit

resistance to imatinib, nilotinib and dasatinib in CML patients and this was confirmed in our model whereby the characteristic posterior eye defect did not show ommatidial rescue when feeding BCR-ABL1^{p210/T3151} expressing flies imatinib (Figure 4 Q, W, R, X), dasatinib (Figure 5 L, P) or nilotinib (Online Supplementary Figure S1

Q, W, R, X). However, feeding ponatinib to BCR-ABL1^{p210/T3151} expressing flies did not show the expected rescue of the posterior eye defect (Figure 6 L, P). Western blot analysis confirmed the expression and phosphorylation of BCR-ABL1^{p210} and BCR-ABL1^{p210/T3151} in *Drosophila* eyes from untreated or treated flies (Figures 5-6).

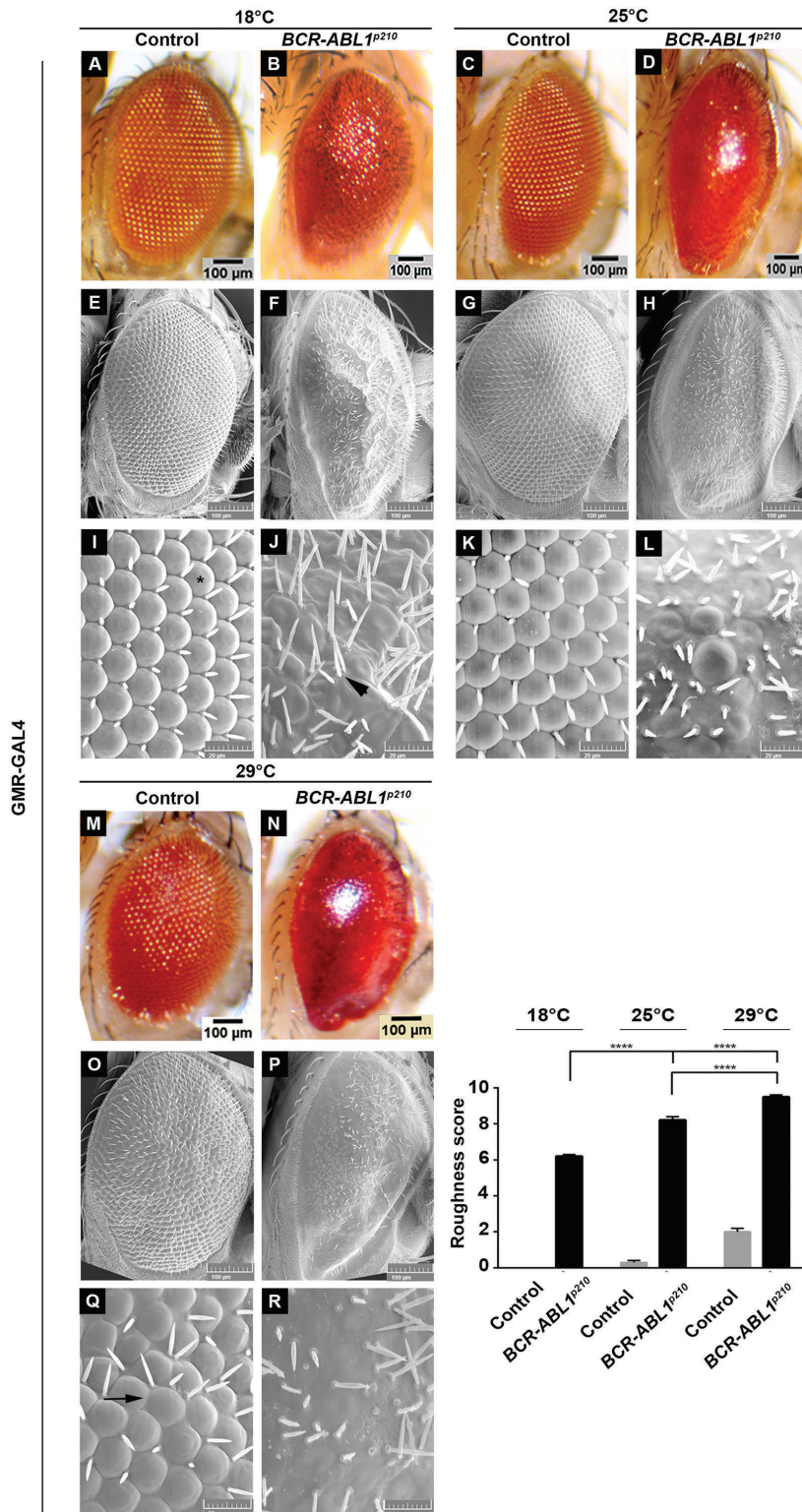


Figure 1. Rough eye phenotype induced by over-expression of human BCR-ABL1^{p210}. Light (A-D, M-N) and scanning electron (E-L, O-R) micrographs of adult *Drosophila* compound eyes expressing BCR-ABL1^{p210} under the control of the eye specific promoter GMR-GAL4. Flies were raised on 18°C (A, B, E, F, I, J) 25°C (C, D, G, H, K, L) or 29°C (M-R). I-L and Q-R are high magnifications of the centremost region of E-H and O-P respectively (1,370x). GMR-GAL4>w¹¹¹⁸ were used as control. Ommatidial facets are depicted in (I) by (*), misplaced mechanosensory bristles in (J) depicted by arrowheads and ommatidial fusions in (Q) are shown by arrow. Posterior is to the left. Lower right panel represents quantification of severity of roughness of the adult fly eye using a grading scale. Genotypes indicated are under the control of eye specific promoter GMR-GAL4. Data represents mean ± SEM. ****, P<0.0001.

Discussion

In this study, we established a transgenic *Drosophila* model expressing human BCR-ABL1 to serve as a credible platform for CML drug screening. Contrary to what has been done previously by Fogerty *et al.* where chimeric human/fly BCR-ABL1 was expressed in *Drosophila*³³ we expressed a full human BCR-ABL1^{p210} protein. In a recent

study, a CML *Drosophila* model expressing the human BCR-ABL1^{p210} was used to study genes and pathways that play a role in CML onset and progression.³⁴

The *Drosophila* eye, with its highly organized reiterative ommatidial structure, constitutes an efficient and relatively easy read out capable of amplifying subtle changes caused by disturbance to normal development. Therefore, we chose this epithelial monolayer as a target tissue for

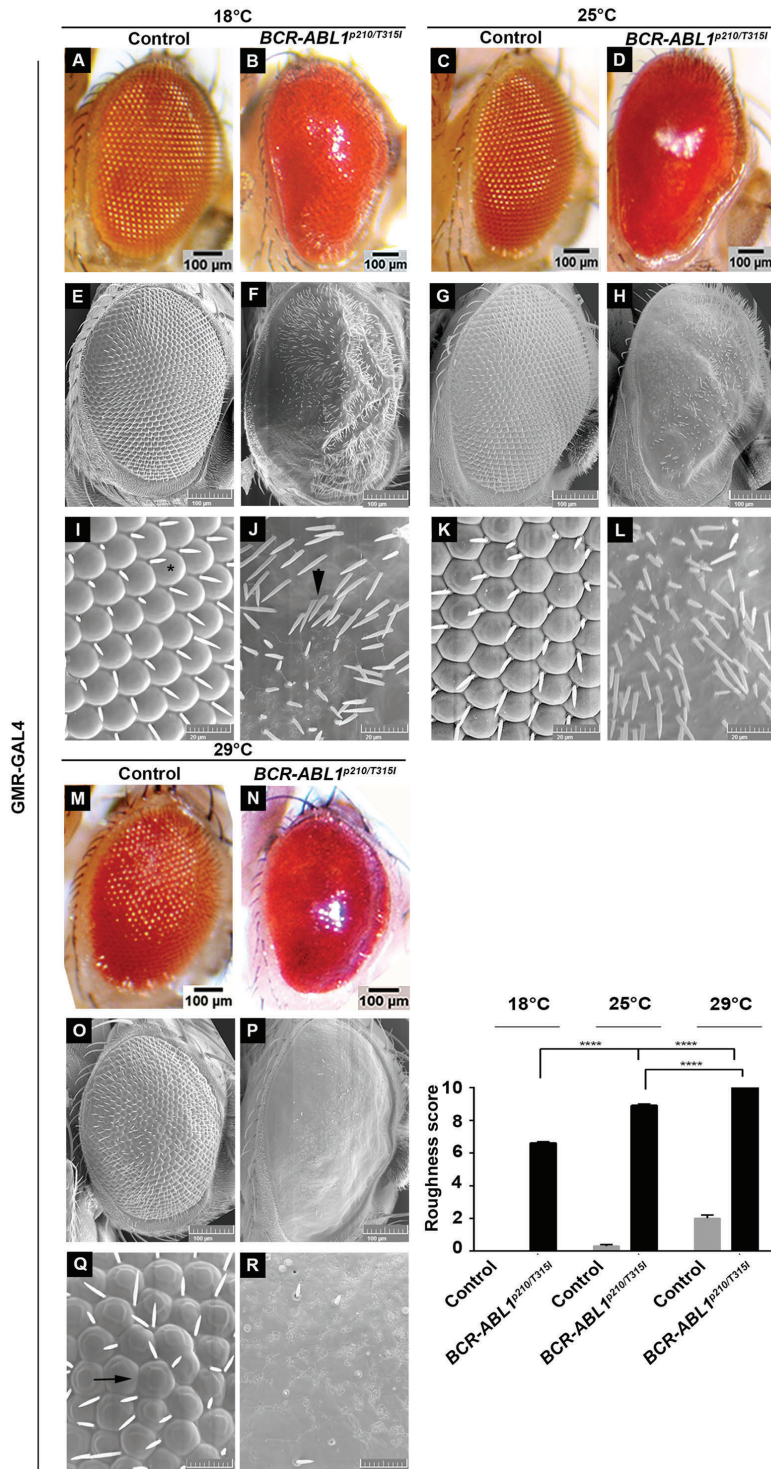


Figure 2. Rough eye phenotype induced by overexpression of human BCR-ABL1^{p210/T315I}. Light (A-D, M-N) and scanning electron (E-L, O-R) micrographs of adult *Drosophila* melanogaster compound eyes expressing BCR-ABL1^{p210/T315I} under the control of the eye specific promoter GMR-GAL4. Flies were raised on 18°C, 25°C or 29°C. I-L and Q-R are high magnifications of the centre region of E-H and O-P respectively (1,370x). GMR-GAL4>w¹¹¹⁸ were used as control. Ommatidial facets are depicted in (I) by (*), misplaced mechanosensory bristles in (J) depicted by arrowheads and ommatidial fusions in (Q) are shown by arrow. Posterior is to the left. Lower right panel represents quantification of severity of roughness of the adult fly eye using a grading scale. Genotypes indicated are under the control of eye specific promoter GMR-GAL4. Data represents mean ± SEM. ****, P<0.0001.

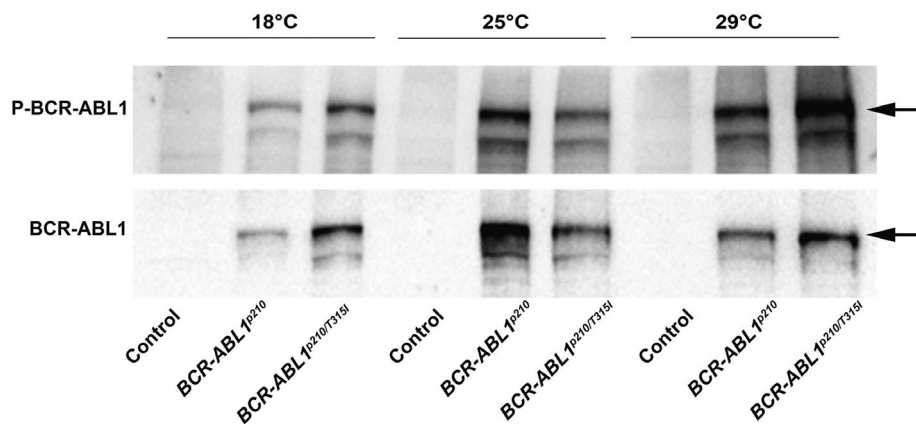


Figure 3. Expression of BCR-ABL1^{p210} and BCR-ABL1^{p210/T315I} in the compound eyes. Representative Western blot of the expression of BCR-ABL1 and phosphorylated levels in transgenic adult fly heads expressing BCR-ABL1^{p210} and BCR-ABL1^{p210/T315I} at different temperatures (18°C, 25°C, and 29°C). Genotypes indicated are under the control of eye specific promoter GMR-GAL4. GMR-GAL4>^{w¹¹¹⁸} were used as control.

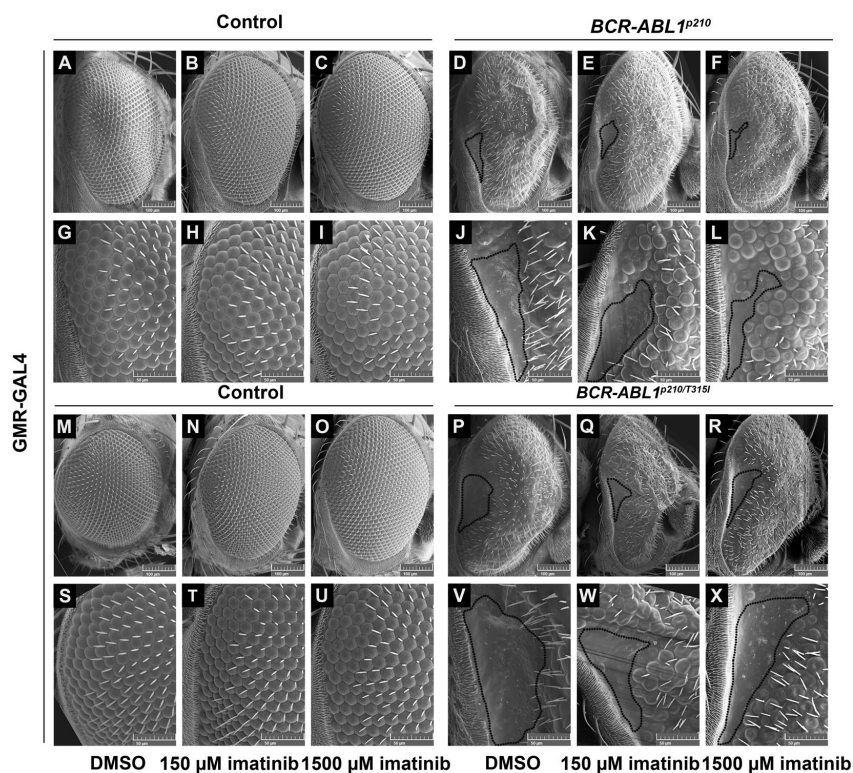
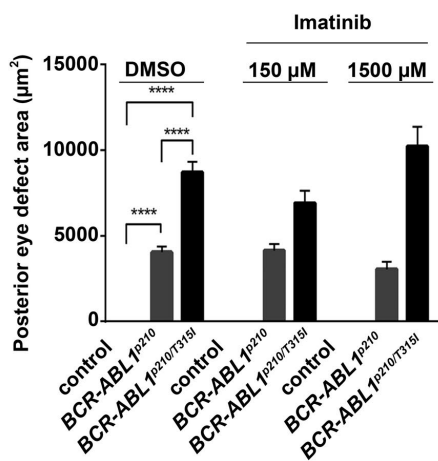


Figure 4. Imatinib shows a tendency to decrease BCR-ABL1^{p210} mediated eye defect. Scanning electron micrographs (A-X) of adult *Drosophila* compound eyes from flies fed on 0.3% DMSO only or imatinib. Posterior is to the left. GMR-GAL4>^{w¹¹¹⁸} were used as control. A-F are high magnification of the posterior end of the eye in G-L and S-X respectively (692 x). Normal development in control flies fed on DMSO or imatinib is observed. BCR-ABL1^{p210} (D, J) and BCR-ABL1^{p210/T315I} (P, V) expressing flies fed on DMSO show characteristic defective area with loss of ommatidial facets. Area is marked with a representative dashed line. Feeding low or high dose imatinib to BCR-ABL1^{p210} (E, K, F, L) and BCR-ABL1^{p210/T315I} (Q, W, R, X) retained the defective area in the posterior end of the eye marked with a dashed line. Compare to D, J and P, V respectively. Lower panel represents measurement of the posterior eye defect area (μm²). Data represents mean ± SEM. ****, P<0.0001.



expressing human BCR-ABL1^{p210} and human BCR-ABL1^{p210/T315I}. Bernardoni *et al.*³⁴ recently showed that expression of human BCR-ABL1^{p210} in *Drosophila* eyes was destructive to the normal eye development and resulted in a “glazy” eye phenotype as demonstrated by light microscopy images. We went further to investigate the effect of increased temperature on transgene expression as well as used SEM analysis in addition to light microscopy to show the subtle details of the eye phenotypes. Moreover, we opted to investigate whether one of the

most elusive BCR-ABL1 mutations (T315I) behaves similarly or differently to the wild type. We found that, with increased temperature, the rough eye phenotype was more prominent in T315I mutant BCR-ABL1 (Figures 1-2). To validate our model for treatment screening, we focused on a specific area in the posterior end of the eye which was evident to be defective in both BCR-ABL1^{p210} and BCR-ABL1^{p210/T315I} expressing flies. BCR-ABL1^{p210/T315I} expressing flies showed a more severe phenotype characterized by a wider defective area of lost ommatidial facets

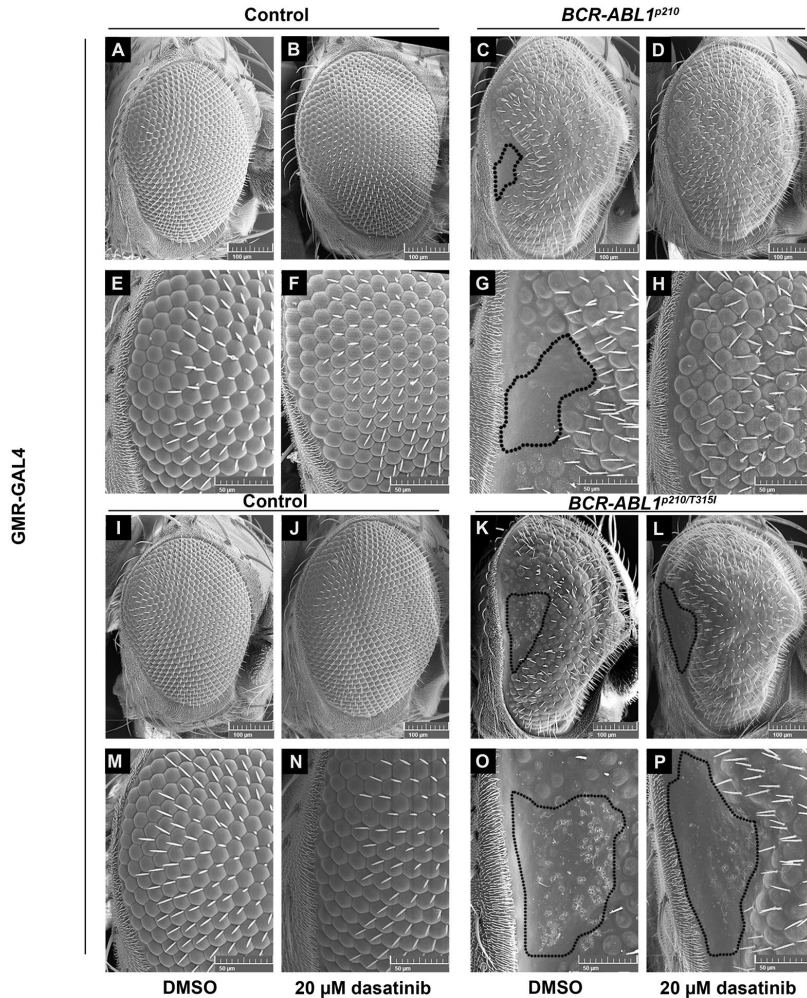
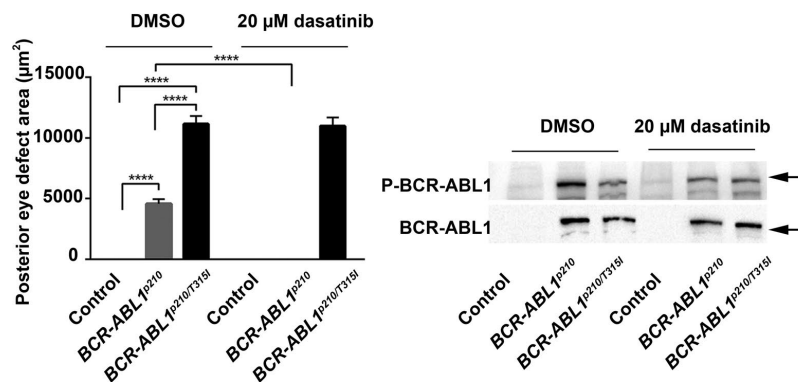


Figure 5. Dasatinib rescues BCR-ABL1^{p210} driven eye defect and shows target specificity *in vivo*. Scanning electron micrographs of adult *Drosophila* compound eyes from flies fed on 0.03% DMSO only or dasatinib. Posterior is to the left. GMR-GAL4>w¹¹¹⁸ were used as control. E-H and M-P are high magnification of the posterior end of the eye in A-D and I-L respectively (692x). Normal development in control flies fed on DMSO (A, E, I, M) or dasatinib is observed. BCR-ABL1^{p210} (C, G) and BCR-ABL1^{p210/T315I} (K, O) expressing flies fed on DMSO show characteristic defective area with loss of ommatidial facets. Area is marked with a representative dashed line. Ommatidial development in this area was restored with BCR-ABL1^{p210} flies fed on 20 μM dasatinib (D, H). Compare to (C, G). BCR-ABL1^{p210/T315I} flies showed no restoration of ommatidial development (L, P). Compare to (K, O). Lower left panel represents measurement of the posterior eye defect area (μm²). Data represents mean ± SEM. ****, P<0.0001. Lower right panel is a representative Western blot of the expression of BCR-ABL1 and phosphorylated levels in transgenic untreated and treated adult fly heads. Genotypes indicated are under the control of eye specific promoter GMR-GAL4.



as compared to flies expressing the wild type variant BCR-ABL1^{p210} indicating that the transformation capacity of T315I is much higher than the wild type BCR-ABL1^{p210}. Similar results were obtained when expressing BCR-ABL1^{p210/T315I} in other tissues where more detrimental effects were seen when compared to BCR-ABL1^{p210}. For example, expression of BCR-ABL1 in the fly imaginal discs resulted in pupal lethality with BCR-ABL1^{p210} expressing flies *versus* embryonic/larval lethality with BCR-ABL1^{p210/T315I} expressing flies (unpublished data).

We further validated the model by assessing the capability of the conventional treatments used in clinics for CML patients of improving the eye defects observed in the adult eyes of BCR-ABL1^{p210} and BCR-ABL1^{p210/T315I} flies. These TKI include imatinib as first generation TKI, nilotinib and dasatinib as second and ponatinib as third generation TKI. Dasatinib and ponatinib resulted in the full rescue of the BCR-ABL1^{p210} eye defect (Figures 5-6) in 100% and 86% of flies respectively. Imatinib and nilotinib (Figure 4; *Online Supplementary Figure S1*) exhibited a lower

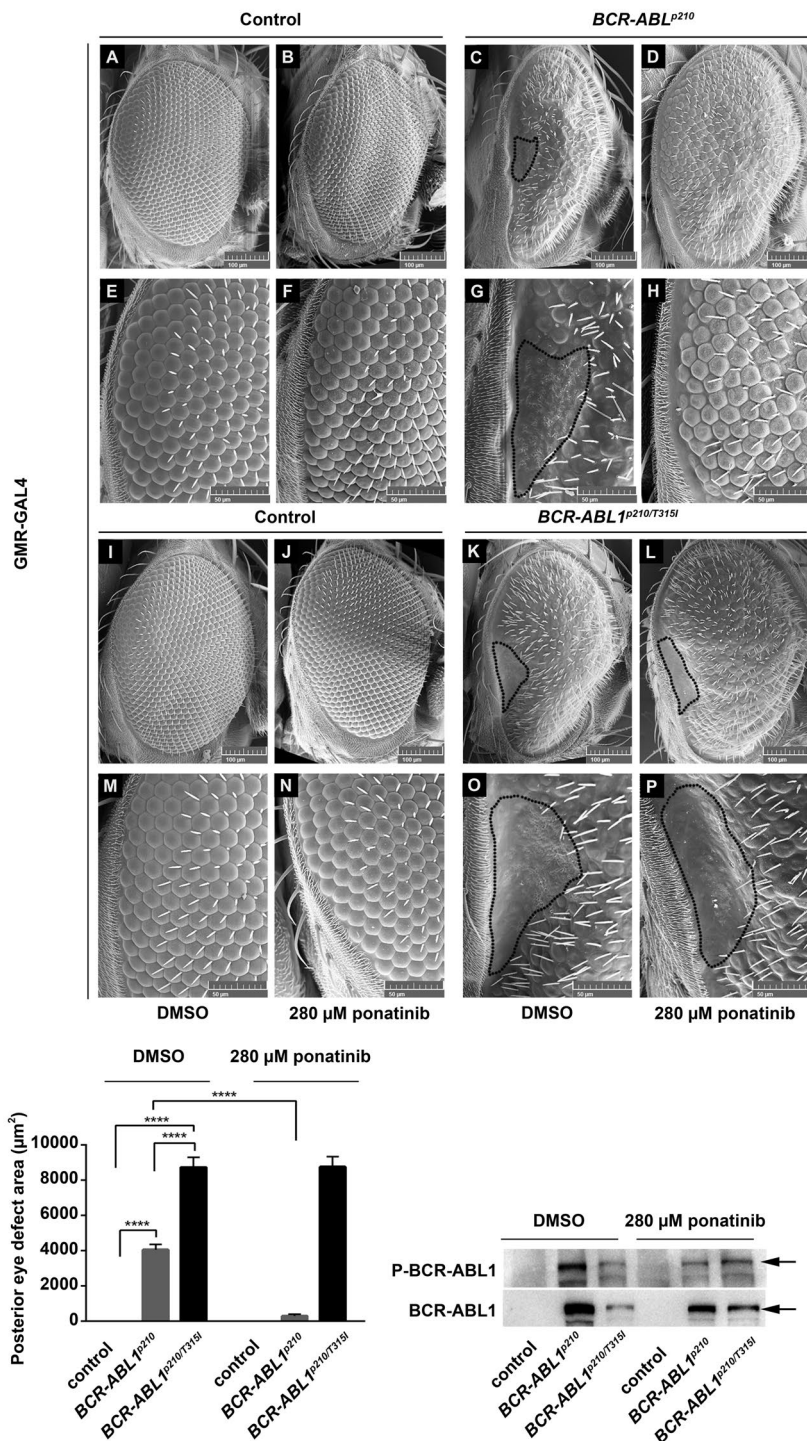


Figure 6. Ponatinib rescues BCR-ABL1^{p210} driven eye defect. Scanning electron micrographs of adult *Drosophila* compound eyes from flies fed on 0.3% DMSO only or ponatinib. Posterior is to the left. GMR-GAL4>w¹¹¹⁸ were used as control. E-H and M-P are high magnification of the posterior end of the eye in A-D and I-L respectively (692x). Normal development in control flies fed on DMSO or ponatinib is observed. BCR-ABL1^{p210} (C, G) and BCR-ABL1^{p210/T315I} (K, O) expressing flies fed on DMSO show characteristic defective area with loss of ommatidial facets. Area is marked with a representative dashed line. Ommatidial development in this area was restored with BCR-ABL1^{p210} flies fed on ponatinib (D, H). Compare to (C, G). BCR-ABL1^{p210/T315I} flies showed no restoration of ommatidial development (L, P). Compare to (K, O). Lower left panel represents measurement of the posterior eye defect area (μm²). Data represents mean ± SEM. *****, *P*<0.0001. Lower right panel is a representative Western blot of the expression of BCR-ABL1 and phosphorylated levels in transgenic untreated and treated adult fly heads. Genotypes indicated are under the control of eye specific promoter GMR-GAL4.

percentage of rescue, 21% and 13% respectively; this might be attributed to the difference in the drug potencies among to of imatinib and other TKI. Compared to imatinib, Dasatinib exhibits a 325-fold higher potency of BCR-ABL1 inhibition *in vitro* whereas nilotinib is only 20-fold more potent.²³ Another possible explanation for the limited rescuing efficacy of imatinib and nilotinib could be the activation of dAbl by BCR-ABL1 expression shown

previously by Bernardoni *et al.*,³⁴ which demonstrated that human BCR-ABL1 expression interferes with the dAbl signaling pathway and increases Ena phosphorylation, a dAbl target. On the other hand, using *Drosophila* wing epithelium as an *in vivo* model, Singh *et al.*⁴¹ demonstrated that activated dAbl exerts a positive feedback loop on *Drosophila* Src members leading to an increase in their activity and hence signal amplification. It is well known

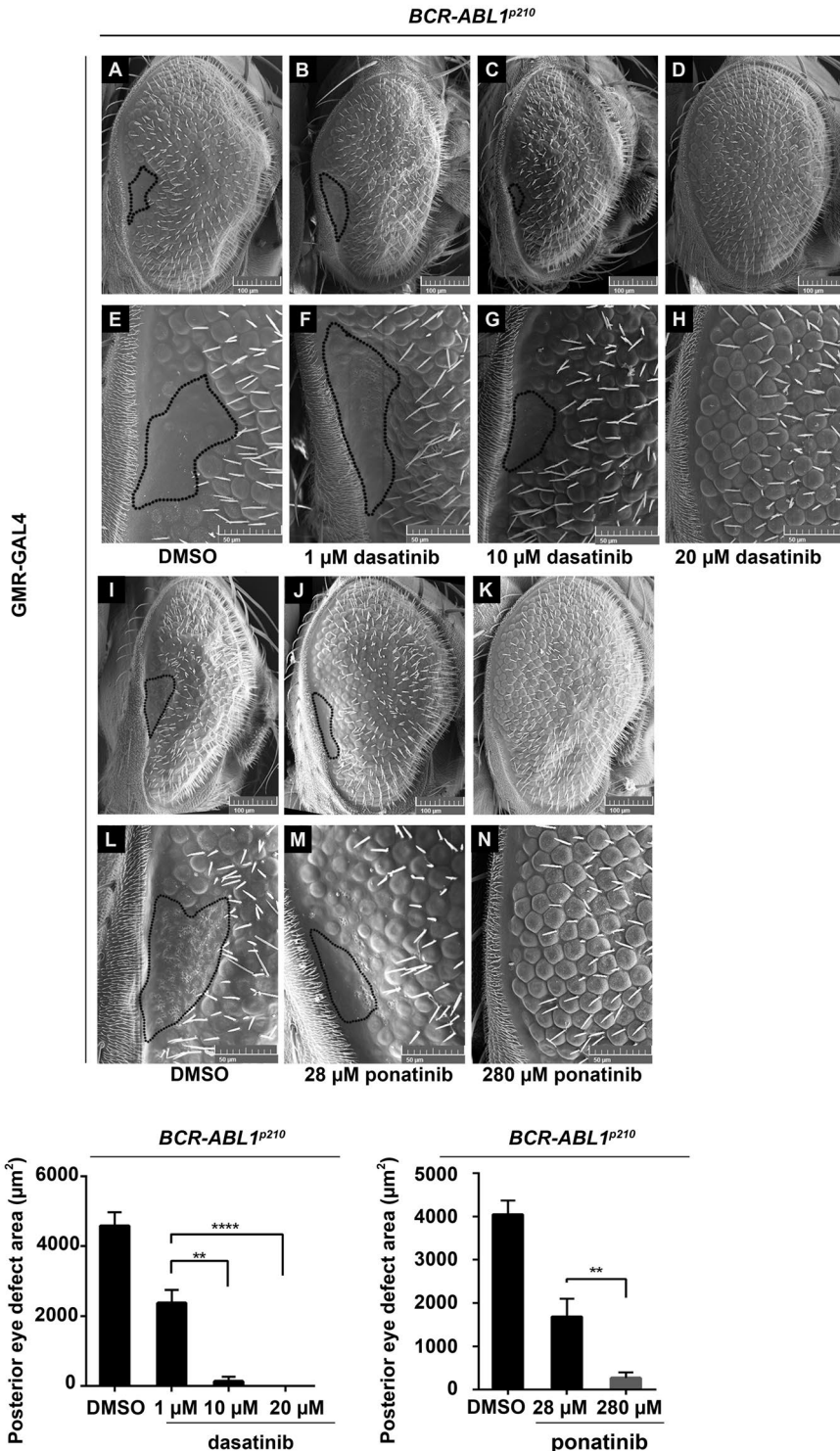


Figure 7. Dasatinib and ponatinib rescue BCR-ABL1^{p210} driven eye defect in a dose dependent manner. Scanning electron micrographs of adult *Drosophila* compound eyes from flies expressing BCR-ABL1^{p210} and fed on 0.03% DMSO (A, E), 1 μM (B, F), 10 μM (C-G) or 20 μM (D, H) dasatinib and flies fed on 0.3% DMSO (I, L), 28 μM ponatinib (J, M) or 280 μM ponatinib (K, N). Posterior is to the left. E-H and L-N are high magnification of the posterior end of the eye in A-D and I-K respectively (692x). Posterior eye defect area is marked with a representative dashed line. Lower panels represent measurement of the posterior eye defect area (μm²). Data represents mean ± SEM. ** $P < 0.01$; **** $P < 0.0001$.

that both dAbl⁴² and *Drosophila* Src⁴³ play important roles in *Drosophila* eye development; therefore it is possible that upon human BCR-ABL1 expression in *Drosophila* eyes, the dAbl signaling pathway is activated which in its turn activates *Drosophila* Src members and amplifies BCR-ABL1 mediated effects. Interestingly, Src is one of the kinases inhibited by dasatinib and ponatinib but not imatinib and nilotinib, therefore, this might possibly explain the more robust rescuing effect seen by dasatinib and ponatinib. Dasatinib demonstrated target specificity *in vivo* whereby BCR-ABL1^{p210/T3151} flies fed on dasatinib showed the expected resistance to treatment. BCR-ABL1^{p210/T3151} resistance to imatinib and nilotinib was also confirmed as there was no rescue of ommatidial development. In contrary to what was expected, ponatinib was not successful in rescuing progeny expressing BCR-ABL1^{p210/T3151}. While this phenomenon is hard to explain we would like to focus on the fact that the eye defect area was significantly larger upon BCR-ABL1^{p210/T3151} expression compared to the area upon BCR-ABL1^{p210} expression. Noting this significant increase in the average posterior eye defect area, we hypothesize that the phenotype was still very severe to allow for any drug reversal. Moreover, noting that the choice of the dose was limited by DMSO toxicity, the ponatinib dose used may not have been high enough to reverse the defect. On the other hand, we tried to test ponatinib to rescue the unpublished lethality phenotype of BCR-ABL1^{p210/T3151} flies; interestingly feeding ponatinib to BCR-ABL1^{p210/T3151} expressing

flies rescued larval lethality and allowed development to the pupal stage which suggests that the drug's response is tissue dependent. Feeding ponatinib or dasatinib to BCR-ABL1^{p210} expressing flies resulted in the rescue of pupal lethality and enclosure of adult flies (*unpublished data*).

We propose an *in vivo* model for BCR-ABL1 driven transformation where we show the efficacy of the current potent treatments in reversing a very subtle phenotype in a specific location in the posterior end of the adult compound eye. This system could be used to assess the efficacy of novel compounds by performing high throughput library testing *in vivo*. We believe that a *Drosophila* CML model to screen for potential compounds is required in this field especially as the currently used TKI do not target CML stem cells and hence are not curative.

Acknowledgements

MS and RN are funded by the National Council for Scientific Research-Lebanon (CNRS-L). AA is the recipient of CNRS-L/AUB Doctoral Scholarship award. We thank KAS Central Research Science Laboratory (CRSL) at the American University of Beirut (AUB) for their technical help in scanning electron microscopy imaging. The expert assistance from the DTS basic research core facilities at AUB is appreciated. We would like to thank Mr. Abdel Rahman Itani and Ms. Shireen Badini for their help in coding and scoring scanning electron microscopy images.

We acknowledge the Bloomington *Drosophila* Stock Center (NIH P40OD018537) for providing fly stocks.

References

- Rowley JD. Letter: A new consistent chromosomal abnormality in chronic myelogenous leukaemia identified by quinacrine fluorescence and Giemsa staining. *Nature*. 1973;243(5405):290-293.
- Jain P, Kantarjian H, Patel KP, et al. Impact of BCR-ABL transcript type on outcome in patients with chronic-phase CML treated with tyrosine kinase inhibitors. *Blood*. 2016;127(10):1269-1275.
- Shepherd P, Suffolk R, Halsey J, Allan N. Analysis of molecular breakpoint and mRNA transcripts in a prospective randomized trial of interferon in chronic myeloid leukaemia: no correlation with clinical features, cytogenetic response, duration of chronic phase, or survival. *Br J Haematol*. 1995;89(3):546-554.
- Groffen J, Stephenson JR, Heisterkamp N, de Klein A, Bartram CR, Grosveld G. Philadelphia chromosomal breakpoints are clustered within a limited region, bcr, on chromosome 22. *Cell*. 1984;36(1):93-99.
- Mandanas RA, Leibowitz DS, Gharehbaghi K, et al. Role of p21 RAS in p210 bcr-abl transformation of murine myeloid cells. *Blood*. 1993;82(6):1838-1847.
- Okuda K, Matulonis U, Salgia R, Kanakura Y, Druker B, Griffin JD. Factor independence of human myeloid leukemia cell lines is associated with increased phosphorylation of the proto-oncogene Raf-1. *Exp Hematol*. 1994;22(11):1111-1117.
- Raitano AB, Halpern JR, Hambuch TM, Sawyers CL. The Bcr-Abl leukemia oncogene activates Jun kinase and requires Jun for transformation. *Proc Natl Acad Sci U S A*. 1995;92(25):11746-11750.
- Sawyers CL, Callahan W, Witte ON. Dominant negative MYC blocks transformation by ABL oncogenes. *Cell*. 1992;70(6):901-910.
- Shuai K, Halpern J, ten Hoeve J, Rao X, Sawyers CL. Constitutive activation of STAT5 by the BCR-ABL oncogene in chronic myelogenous leukemia. *Oncogene*. 1996;13(2):247-254.
- Carlesso N, Frank DA, Griffin JD. Tyrosyl phosphorylation and DNA binding activity of signal transducers and activators of transcription (STAT) proteins in hematopoietic cell lines transformed by Bcr/Abl. *J Exp Med*. 1996;183(3):811-820.
- Ilaria RL, Jr., Van Etten RA. P210 and P190(BCR/ABL) induce the tyrosine phosphorylation and DNA binding activity of multiple specific STAT family members. *J Biol Chem*. 1996;271(49):31704-31710.
- Druker BJ, Talpaz M, Resta DJ, et al. Efficacy and safety of a specific inhibitor of the BCR-ABL tyrosine kinase in chronic myeloid leukemia. *N Engl J Med*. 2001;344(14):1031-1037.
- O'Brien SG, Guilhot F, Larson RA, et al. Imatinib compared with interferon and low-dose cytarabine for newly diagnosed chronic-phase chronic myeloid leukemia. *N Engl J Med*. 2003;348(11):994-1004.
- Jabbour E, Kantarjian HM, Saglio G, et al. Early response with dasatinib or imatinib in chronic myeloid leukemia: 3-year follow-up from a randomized phase 3 trial (DASISION). *Blood*. 2014;123(4):494-500.
- Larson R, Hochhaus A, Hughes T, et al. Nilotinib vs imatinib in patients with newly diagnosed Philadelphia chromosome-positive chronic myeloid leukemia in chronic phase: ENESTnd 3-year follow-up. *Leukemia*. 2012;26(10):2197-2203.
- Lombardo LJ, Lee FY, Chen P, et al. Nilotinib vs imatinib in patients with newly diagnosed Philadelphia chromosome-positive chronic myeloid leukemia in chronic phase: ENESTnd 3-year follow-up. *Leukemia*. 2012;26(10):2197-2203.
- Larson RA, Hochhaus A, Hughes TP, et al. Nilotinib vs imatinib in patients with newly diagnosed Philadelphia chromosome-positive chronic myeloid leukemia in chronic phase: ENESTnd 3-year follow-up. *Leukemia*. 2012;26(10):2197-2203.
- Lombardo LJ, Lee FY, Chen P, et al. Nilotinib vs imatinib in patients with newly diagnosed Philadelphia chromosome-positive chronic myeloid leukemia in chronic phase: ENESTnd 3-year follow-up. *Leukemia*. 2012;26(10):2197-2203.
- Lombardo LJ, Lee FY, Chen P, et al. Nilotinib vs imatinib in patients with newly diagnosed Philadelphia chromosome-positive chronic myeloid leukemia in chronic phase: ENESTnd 3-year follow-up. *Leukemia*. 2012;26(10):2197-2203.

- Discovery of N-(2-chloro-6-methylphenyl)-2-(6-(4-(2-hydroxyethyl)-piperazin-1-yl)-2-methylpyrimidin-4-ylamino)thiazole-5-carboxamide (BMS-354825), a dual Src/Abl kinase inhibitor with potent antitumor activity in preclinical assays. *J Med Chem.* 2004;47(27):6658-6661.
23. O'Hare T, Walters DK, Stoffregen EP, et al. In vitro activity of Bcr-Abl inhibitors AMN107 and BMS-354825 against clinically relevant imatinib-resistant Abl kinase domain mutants. *Cancer Res.* 2005;65(11):4500-4505.
 24. Tokarski JS, Newitt JA, Chang CY, et al. The structure of Dasatinib (BMS-354825) bound to activated ABL kinase domain elucidates its inhibitory activity against imatinib-resistant ABL mutants. *Cancer Res.* 2006;66(11):5790-5797.
 25. Shah NP, Tran C, Lee FY, Chen P, Norris D, Sawyers CL. Overriding imatinib resistance with a novel ABL kinase inhibitor. *Science.* 2004;305(5682):399-401.
 26. Weisberg E, Manley PW, Breitenstein W, et al. Characterization of AMN107, a selective inhibitor of native and mutant Bcr-Abl. *Cancer Cell.* 2005;7(2):129-141.
 27. Cortes JE, Kim D-W, Pinilla-Ibarz J, et al. Long-Term Follow-up of Ponatinib Efficacy and Safety in the Phase 2 PACE Trial. *Blood.* 2014;124(21):3135-3135.
 28. Cortes JE, Kim DW, Pinilla-Ibarz J, et al. A phase 2 trial of ponatinib in Philadelphia chromosome-positive leukemias. *N Engl J Med.* 2013;369(19):1783-1796.
 29. Breccia M, Pregno P, Spallarossa P, et al. Identification, prevention and management of cardiovascular risk in chronic myeloid leukaemia patients candidate to ponatinib: an expert opinion. *Ann Hematol.* 2017;96(4):549-558.
 30. Muller MC, Cervantes F, Hjorth-Hansen H, et al. Ponatinib in chronic myeloid leukemia (CML): Consensus on patient treatment and management from a European expert panel. *Crit Rev Oncol Hematol.* 2017;120:52-59.
 31. Mahon F-X, Réa D, Guilhot J, et al. Discontinuation of imatinib in patients with chronic myeloid leukaemia who have maintained complete molecular remission for at least 2 years: the prospective, multicentre Stop Imatinib (STIM) trial. *Lancet Oncol.* 2010;11(11):1029-1035.
 32. Gonzalez C. *Drosophila melanogaster*: a model and a tool to investigate malignancy and identify new therapeutics. *Nat Rev Cancer.* 2013;13(3):172.
 33. Fogerty FJ, Juang JL, Petersen J, Clark MJ, Hoffmann FM, Mosher DF. Dominant effects of the bcr-abl oncogene on *Drosophila* morphogenesis. *Oncogene.* 1999;18(1):219-232.
 34. Bernardoni R, Giordani G, Signorino E, et al. A new BCR-ABL1 *Drosophila* model as a powerful tool to elucidate pathogenesis and progression of chronic myeloid leukemia. *Haematologica.* 2019;104(4):717-728.
 35. Shirinian M, Kambris Z, Hamadeh L, et al. A Transgenic *Drosophila melanogaster* Model To Study Human T-Lymphotropic Virus Oncoprotein Tax-1-Driven Transformation In Vivo. *J Virol.* 2015;89(15):8092-8095.
 36. Schneider CA, Rasband WS, Eliceiri KW. NIH Image to ImageJ: 25 years of image analysis. *Nat Methods.* 2012;9(7):671-675.
 37. Freeman M. Reiterative use of the EGF receptor triggers differentiation of all cell types in the *Drosophila* eye. *Cell.* 1996;87(4):651-660.
 38. Duffy JB. GAL4 system in *Drosophila*: a fly geneticist's Swiss army knife. *Genesis.* 2002;34(1-2):1-15.
 39. Xin S, Weng L, Xu J, Du W. The role of RBF in developmentally regulated cell proliferation in the eye disc and in Cyclin D/Cdk4 induced cellular growth. *Development.* 2002;129(6):1345-1356.
 40. Cvetković VJ, Mitrović TL, Jovanović B, et al. Toxicity of dimethyl sulfoxide against *Drosophila melanogaster*. *Biol Nyssana.* 2015;6(2):91-95.
 41. Singh J, Aaronson SA, Mlodzik M. *Drosophila* Abelson kinase mediates cell invasion and proliferation through two distinct MAPK pathways. *Oncogene.* 2010;29(28):4033-4045.
 42. Xiong W, Rebay I. Abelson tyrosine kinase is required for *Drosophila* photoreceptor morphogenesis and retinal epithelial patterning. *Dev Dyn.* 2011;240(7):1745-1755.
 43. Takahashi F, Endo S, Kojima T, Saigo K. Regulation of cell-cell contacts in developing *Drosophila* eyes by Dsrc41, a new, close relative of vertebrate c-src. *Genes Dev.* 1996;10(13):1645-1656.



Ferrata Storti Foundation

Comparisons of commonly used front-line regimens on survival outcomes in patients aged 70 years and older with acute myeloid leukemia

Chetasi Talati,¹ Varun C Dhulipala,² Martine Extermann,^{3,4} Najla Al Ali,¹ Jongphil Kim,^{2,5} Rami Komrokji,^{1,6} Kendra Sweet,^{1,6} Andrew Kuykendall,^{1,2} Marina Sehic,¹ Tea Reljic,² Benjamin Djulbegovic,^{1,2} and Jeffrey E. Lancet^{1,6}

¹H. Lee Moffitt Cancer Center and Research Institute, Tampa, FL; ²Maury Regional Cancer Center, Columbia, TN; ³Senior Adult Oncology Program, H. Lee Moffitt Cancer Center and Research Institute, Tampa, FL; ⁴Department of Oncology Sciences, University of South Florida, Tampa, FL; ⁵Department of Biostatistics and Bioinformatics, Moffitt Cancer Center, Tampa, FL and ⁶Malignant Hematology Department, H Lee Moffitt Cancer Center and Research Institute, Tampa, FL, USA

Haematologica 2020
Volume 105(2):398-406

ABSTRACT

In older patients with acute myeloid leukemia, the more frequent presence of biologically inherent therapy-resistant disease and increased comorbidities translate to poor overall survival and therapeutic challenges. Optimal front-line therapies for older patients with acute myeloid leukemia remain controversial. We retrospectively evaluated survival outcomes in 980 elderly (≥ 70 years) acute myeloid leukemia patients from a single institution between 1995 and 2016. Four treatment categories were compared: high-intensity (daunorubicin/cytarabine or equivalent), hypomethylating agent, low-intensity (low-dose cytarabine or similar without hypomethylating agents), and supportive care therapy (including hydroxyurea). At a median follow up of 20.5 months, the median overall survival for the entire cohort was 7.1 months. Multivariate analysis identified secondary acute myeloid leukemia, poor-risk cytogenetics, performance status, front-line therapy, age, white blood cell count, platelet count, and hemoglobin level at diagnosis as having an impact on survival. High-intensity therapy was used in 360 patients (36.7%), hypomethylating agent in 255 (26.0%), low-intensity therapy in 91 (9.3%), and supportive care in 274 (28.0%). Pairwise comparisons between hypomethylating agent therapy and the three other treatment groups demonstrated statistically significant superior median overall survival with hypomethylating agent [14.4 months] vs. high-intensity therapy 10.8 months, hazard ratio 1.35, 95% confidence interval (CI): 1.10-1.65; $P=0.004$], low-intensity therapy (5.9 months, hazard ratio 2.01, 95%CI: 1.53-2.62; $P<0.0001$), and supportive care (2.1 months, hazard ratio 2.94, 95%CI: 2.39-3.61; $P<0.0001$). Our results indicate a significant survival benefit with hypomethylating agents compared to high-intensity, low-intensity, or supportive care. Additionally, high-intensity chemotherapy resulted in superior overall outcomes compared to low-intensity therapy and supportive care. Results from this study highlight the need for novel therapeutic approaches besides utilization of intensive chemotherapy in this specific aged population.

Correspondence:

CHETASI TALATI
chetasi.talati@gmail.com

Received: October 9, 2018.

Accepted: May 7, 2019.

Pre-published: May 9, 2019.

doi:10.3324/haematol.2018.208637

Check the online version for the most updated information on this article, online supplements, and information on authorship & disclosures: www.haematologica.org/content/105/2/398

©2020 Ferrata Storti Foundation

Material published in Haematologica is covered by copyright. All rights are reserved to the Ferrata Storti Foundation. Use of published material is allowed under the following terms and conditions:

<https://creativecommons.org/licenses/by-nc/4.0/legalcode>.

Copies of published material are allowed for personal or internal use. Sharing published material for non-commercial purposes is subject to the following conditions:

<https://creativecommons.org/licenses/by-nc/4.0/legalcode>,

sect. 3. Reproducing and sharing published material for commercial purposes is not allowed without permission in writing from the publisher.



Introduction

The incidence of acute myeloid leukemia (AML) increases with age, with a median age of ≥ 65 years at time of diagnosis.¹⁻³ Between 1975 and 2001, the 5-year survival of younger AML patients has more than doubled, yet the survival of patients over the age of 65 continues to remain dismal. These differences can primarily be attributed to the clinical and functional heterogeneity of disease in elderly patients. Compared with their younger counterparts, older patients have AML

that is more frequently associated with chemotherapeutic resistance, unfavorable cytogenetics, increased frequency of somatic mutations, and preceded by myelodysplastic syndromes, making therapeutic decisions difficult.^{4,5} Many patients have their treatment chosen more on the basis of chronological age rather than the inherent disease biology (i.e. karyotype, molecular heterogeneity, antecedent hematologic disorders, and leukocyte count at diagnosis) and overall fitness of patients.⁶

Like many other malignancies, optimizing medical care of patients with AML is dependent on clinical trials. Unfortunately, older patients, particularly those who are ≥ 70 years of age, are under-represented in randomized controlled trials. The lack of clear clinical data in this subset of patients often leads to uncertainty regarding optimal treatment strategies.

Over the past decade, new treatment strategies have emerged targeting the biological challenges in AML; however, there has been a lack of significant progress in optimizing strategies in the older AML population. Numerous studies have assessed risk stratification of this subgroup of patients with a goal toward building a comprehensive approach; however, a model to help guide treatment has yet to be validated.^{2,7-10} The lack of a validated decision model has led to individualized and variable care of older AML patients. In an attempt to create a comprehensive decision analysis model, we present the results of a very large, single institution retrospective study of 980 patients aged ≥ 70 years. The aim of our study was to compare survival outcomes of older AML patients treated with various induction regimens. Such a study offers the advantage of combining cytogenetics, comorbidities, and functional status information and importantly accounts for therapeutic decisions in older patients with AML.¹¹⁻¹⁴

Methods

Data collection

We retrospectively analyzed patients ≥ 70 years of age who presented to Moffitt Cancer Center between 1995 and 2016 for evaluation of newly diagnosed and previously untreated AML. The study was approved by the University of South Florida institutional review board. Inclusion criteria for the study were age 70 years or older and diagnosis of AML that was untreated prior to patient presentation at our institution. Patients with antecedent hematologic malignancies were included regardless of treatment. Compiled data were supplemented by direct review of medical records as necessary. A dual data entry technique was used to ensure data accuracy and quality. Baseline patient characteristics collected included vital status, age at diagnosis, sex, race/ethnicity, comorbidities for calculation of Charlson comorbidity index (CCI), Eastern Cooperative Oncology Group (ECOG) performance status, and antecedent hematologic disease and its treatment. Collected disease-specific characteristics included baseline cytogenetics, type of AML (*de novo* or secondary AML), complete blood count with peripheral blood blast percentage at time of diagnosis, choice of therapy, responses to treatment including complete remission (CR), complete remission with incomplete count recovery (CRi), relapsed disease, partial remission, and whether allogeneic hematopoietic stem cell transplant was performed. We defined secondary AML as an AML arising from an antecedent hematologic disorder or therapy-related AML.

Treatment groups

Patients were categorized into four different treatment groups: high-intensity therapy [defined as cytarabine and daunorubicin/idarubicin (7+3) or "7+3" equivalent], low-intensity therapy (defined as low-dose cytarabine or similar but not including hypomethylating agents), hypomethylating agent (HMA) therapy, and supportive care (including hydroxyurea). "7+3" equivalent regimens included high-dose cytarabine-based regimens, specifically CLAG+/-M (cladribine, cytarabine, granulocyte colony stimulating factor (G-CSF), with or without Mitoxantrone), MEC (Mitoxantrone, etoposide, cytarabine), and HIDAC (high-dose cytarabine) regimens. A categorical distinction between low-intensity therapy and HMA therapy was made on the basis of recent randomized reports suggesting the modest superiority of HMA *versus* conventional care regimens (including low-dose cytarabine), in addition to practice pattern differences worldwide that utilized either HMA or low-dose cytarabine as standard front-line therapy for older adults with newly diagnosed AML. Patients enrolled in clinical trials were assigned to one of the four treatments groups depending on the intensity of treatment received as part of the clinical trial.^{15,16}

Definition of clinical end points

Response to therapy was defined as those who achieved CR or CRi as per the 2003 International Working Group response criteria for AML.¹⁷ Overall survival was defined as time from date of diagnosis of AML to date of death if known or censored at the time of last follow up. Relapse-free survival was calculated as time from achievement of CR or CRi to date of relapse as defined by International Working Group 2003 criteria.

Statistical analysis

Survival function was estimated by the Kaplan-Meier method and compared across groups using the log-rank test. Cox proportional hazards regression model was used to determine the association between the variables and overall survival. Variables with $P < 0.25$ in the univariate model were included in the initial multivariate analysis. The backward elimination method was used to select the variables for the ultimate multivariate model. Variables with $P > 0.05$ were excluded. Pairwise comparisons of survival between different treatment groups were performed using the stratified log-rank test and propensity score matching to adjust for potential treatment indication bias between groups. Within pairwise comparison groups, the stratified Cox proportional hazards regression model was used to assess correlations between clinical variables and overall survival. Patients who had no information on response were considered as non-responders per the intention-to-treat approach. For treatment-related mortality (TRM) at day 30, patients who were censored before 30 days ($n=5$) were not eligible and were excluded from the analysis. Raw P -values were computed by the χ^2 test, and the Bonferroni method was used to adjust for multiplicity. A two-sided $P < 0.05$ was considered significant. Statistical analysis was performed using SAS version 14.3 (Cary, NC, USA).

Results

In the total cohort of 980 patients, 360 (36.7%) received high-intensity therapy, 255 (26.0%) received HMA therapy, 91 (9.3%) received low-intensity therapy, and 274 (28.0%) received supportive care; their baseline characteristics are represented in Table 1. Median age of patients when first diagnosed with AML was 75.6 years (range, 70-95.7 years). Among patients with antecedent hematologic

Table 1. Demographics and clinicopathological characteristics.

Clinical Parameter	All Patients	Front-line Therapy Group			Supportive Care (n=274)	P
		HMA (n=255)	HI Therapy (n=360)	LI Therapy (n=91)		
Median age (range), years	75.6 (70-95.7)	76.5 (70.1-95.2)	73.9 (70-89.8)	77.9 (70.5-90.4)	77 (70-95.7)	<0.0001
Sex						0.18
Male	650 (66.3%)	162 (63.5%)	247 (68.6%)	67 (73.6%)	174 (63.5%)	
Female	330 (33.7%)	93 (36.5%)	113 (31.4%)	24 (26.4%)	100 (36.5%)	
Race/ethnicity						0.63
Other	75 (7.7%)	22 (8.6%)	28 (7.8%)	4 (4.4%)	21 (7.7%)	
White	905 (92.3%)	233 (91.4%)	332 (92.2%)	87 (95.6%)	253 (92.3%)	
Type of AML						<0.0001
De novo	422 (43.1%)	123 (48.2%)	193 (53.6%)	22 (24.2%)	84 (30.7%)	
Secondary	558 (56.9%)	132 (51.8%)	167 (46.4%)	69 (75.8%)	190 (69.3%)	
Prior hematologic disease**	507 (51.7%)	110 (43.1%)	153 (42.5%)	66 (72.5%)	178 (65%)	<0.0001
HMA for prior hematology malignancy	264 (52.1%)	31 (28.2%)	82 (53.6%)	46 (69.7%)	105 (59%)	<0.0001
ECOG PS						<0.0001
0-1	777 (79.3%)	212 (83.1%)	303 (84.2%)	78 (85.7%)	184 (67.2%)	
2-4	186 (19%)	42 (16.5%)	46 (12.8%)	11 (12.1%)	87 (31.8%)	
Median WBC, ×10 ⁹ /L	3.3 (0.2-230.7)	2.5 (0.2-147.8)	5.3 (0.2-230.7)	3 (0.6-215.3)	3.4 (0.6-215.7)	<0.0001
Median platelet, ×10 ⁹ /L	51 (1-996)	69 (1-743)	50.5 (2-996)	50 (1-274)	39 (4-485)	<0.0001
Median hemoglobin, g/dL	9.4 (4.8-15.2)	9.5 (5-15.2)	9.3 (4.8-14.5)	9.6 (6.9-13.9)	9.3 (4.8-14.7)	0.073
Median PB blasts, %	14 (1-99)	10 (1-93)	21 (1-98)	8 (1-99)	13 (1-96)	<0.0001
Median BM blasts, %	35 (2-98)	30 (4-94)	45.5 (2-98)	33.5 (9-91)	30 (16-94)	<0.0001
Karyotype (n=874)						<0.0001
Adverse	304 (31%)	85 (33.3%)	80 (22.2%)	36 (39.6%)	103 (37.6%)	
Diploid/intermediate	554 (56.5%)	147 (57.6%)	234 (65%)	47 (51.6%)	126 (46%)	
Favorable	16 (1.6%)	3 (1.2%)	11 (3.1%)	0 (0%)	2 (0.7%)	
FLT3-ITD mutation (n=328 tested)	36 (11%)	10 (8.7%)	23 (16.9%)	0 (0%)	3 (5.4%)	0.019
NPM1 mutation (n=320 tested)	39 (12.2%)	10 (8.8%)	23 (18%)	2 (9.1%)	4 (7.1%)	0.080

*P-value was computed by χ^2 test or Kruskal-Wallis test. **Myelodysplastic syndrome accounted for >97% of all prior hematologic malignancies; others included myelofibrosis, polycythemia vera, and essential thrombocytosis. AML: acute myeloid leukemia; BM: bone marrow; ECOG PS: Eastern Cooperative Oncology Group Performance Status; HI: high intensity; HMA: hypomethylating agent; LI: low intensity; PB: peripheral blood; WBC: white blood cell.

disorders (51.7%), myelodysplastic syndrome accounted for 93.9% of the population and over one-third (36.5%) of such patients had received HMA. In the HMA-treated AML cohort (n=255), 31 patients (12.1%) had previously received HMA therapy for an antecedent hematologic disorder. Cytogenetically, 56.5% of the patients had intermediate-risk or normal diploid karyotype whereas 31% had poor-risk karyotype as defined by National Comprehensive Cancer Network.¹⁸

Clinical variables that affected survival

We performed a univariate analysis on the entire cohort to identify clinical variables that may have affected survival. We found that secondary AML, poor-risk cytogenetics, increasing age at diagnosis, CCI score ≥ 3 , ECOG performance status ≥ 2 , increasing white blood cell (WBC) count at diagnosis, lower hemoglobin level at diagnosis, and lower platelets at the time of diagnosis, and choice of front-line therapy negatively affected overall survival (Table 2). However, our multivariate analysis showed that only increasing age [hazard ratio (HR)=1.14, 95% confidence interval (CI): 1.05-1.23; $P=0.002$], increasing WBC (HR 1.19, 95% CI: 1.13-1.25; $P<0.0001$), secondary AML (HR=1.44, 95% CI: 1.23-1.68; $P<0.0001$), poor-risk cytoge-

netics (HR = 1.92, 95% CI: 1.64-2.25; $P<0.0001$), higher ECOG performance status (HR = 1.80, 95% CI: 1.48-2.18; $P<0.0001$), and choice of front-line therapy affected overall survival (Table 3). Interestingly, CCI did not affect overall survival in the multivariate analysis.

Choice of front-line treatment and its effect on survival outcomes

The median overall survival for the entire cohort of 980 patients was 7.1 months, with a median follow up of 20.5 months. Per Kaplan-Meier survival analysis and log-rank test for significance (Figure 1), median overall survival was significantly greater for patients treated with HMA compared with those who received high-intensity therapy (14.4 vs. 10.8 months; HR=1.35, 95% CI: 1.10-1.65; $P=0.004$). Moreover, patients in the HMA treatment group also had better overall survival than patients in the low-intensity therapy (14.4 vs. 5.9 months, HR = 2.01, 95% CI: 1.53-2.62; $P<0.0001$) or supportive care groups (14.4 vs. 2.1 months, HR = 2.94, 95% CI: 2.39-3.61; $P<0.0001$). The estimated survival probability at one year with HMA treatment was significantly greater at 55.4% versus 42.7% with high-intensity therapy, 25.3% with low-intensity therapy, and 14.2% with supportive care ($P<0.0001$).

Table 2. Univariate analyses, with dichotomization of Eastern Cooperative Oncology Group Performance Status (0-1 vs. ≥ 2).

Clinical Parameter	P	Hazard Ratio	95% Confidence Interval	
			Lower	Upper
Sex				
Male	Reference			
Female	0.28	1.08	0.94	1.24
Race/ethnicity				
White	Reference			
Other	0.97	1.00	0.78	1.27
Type of AML				
<i>De novo</i>	Reference			
Secondary	<0.0001	1.56	1.36	1.78
Prior hematologic disease				
No	Reference			
Yes	<0.0001	1.52	1.33	1.74
Karyotype				
Favorable or intermediate	Reference			
Adverse	<0.0001	1.82	1.57	2.11
ECOG PS				
0-1	Reference			
2-4	<0.0001	2.10	1.77	2.48
Clinical trial as front-line therapy				
No	Reference			
Yes	0.97	1.00	0.83	1.20
Front-line therapy				
HMA	Reference			
HI therapy	0.002	1.32	1.11	1.57
LI therapy	<0.0001	1.92	1.50	2.46
Supportive care	<0.0001	3.38	2.80	4.07
CCI				
0-2	Reference			
≥ 3	0.011	1.28	1.06	1.55
Age at diagnosis (per 5-year increase)	<0.0001	1.16	1.09	1.25
BM blast at diagnosis (per 10% increase)	0.42	1.01	0.98	1.05
WBC, per 1 log increase	<0.0001	1.12	1.07	1.17
Platelets, per 1 log increase	<0.0001	0.72	0.68	0.78
Hemoglobin, per 1 log increase	<0.0001	0.88	0.84	0.91

AML: acute myeloid leukemia; BM: bone marrow; CCI: Charlson comorbidity Index; ECOG PS: Eastern Cooperative Oncology Group Performance Status; HI: high intensity; HMA: hypomethylating agent; LI: low intensity; PB: peripheral blood; WBC: white blood cell.

High-intensity therapy resulted in superior median overall survival compared with supportive care (10.8 vs. 2.1 months; $P < 0.0001$) and low-intensity therapy (10.4 vs. 5.9 months; $P = 0.001$), and low-intensity therapy was superior to supportive care (5.9 vs. 2.1 months; $P < 0.0001$).

Because 185 patients (36.5%) had prior hematologic disease and thus received prior HMA, we created a univariate and multivariate model after excluding this subgroup, yielding a cohort of 795 HMA-naïve patients and assessed the impact of front-line treatment modality (Table 3). Variables that emerged as prognostically significant were identical to the variables from the multivariate model for the entire cohort. Within this HMA-naïve group, Kaplan-Meier analysis for overall survival was again noted to be superior in patients treated with HMA versus the other therapy groups, including the high-intensity ($P = 0.008$),

low-intensity ($P < 0.0001$), and supportive care treatment groups ($P < 0.0001$) (*data not shown*).

A pairwise comparison using propensity score matching to minimize the selection bias for front-line treatment was used to create a multivariate model to validate the prognostic impact of the different variables. The multivariate model confirmed our previous findings regarding the effects of HMA versus high-intensity treatment (HR=0.78, 95%CI: 0.63-0.97; $P = 0.027$) and HMA versus low-intensity treatment (HR=0.56, 95%CI: 0.42-0.74; $P < 0.0001$) on mortality. In patients with non-adverse risk karyotype (intermediate-risk and favorable-risk), superiority of HMA treatment was also demonstrated compared to intensive chemotherapy (HR=0.71, 95%CI: 0.55-0.92; $P = 0.008$). Low-intensity treatment was also inferior to high-intensity treatment (HR=1.32, 95%CI: 1.01-1.72; $P = 0.040$) (*data not shown*).

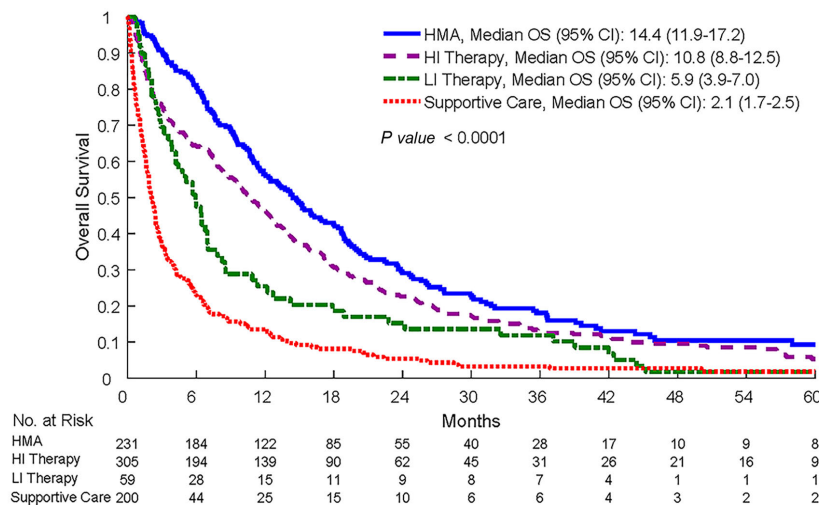


Figure 1. Overall survival (OS) among various front-line therapies for acute myeloid leukemia (AML) in patients ≥ 70 years old. CI: confidence interval; HI: high intensity; HMA: hypomethylating agent; LI: low intensity.

Survival outcomes based on time periods

To account for changes that have occurred over the years in AML treatments and supportive care management, the entire cohort was divided and grouped according to the year of treatment initiation: Group A (treatment before 2005, $n=140$) and Group B (treatment after 2005, $n=840$). A trend towards improved median overall survival (mOS) was noted among the 2 groups but did not reach statistical significance (Group A vs. B, mOS 5.7 months vs. 7.3 months; $P=0.051$). Baseline characteristics of Group B is provided in *Online Supplementary Table S1*. When assessing for the survival outcomes of HMA-naïve patients from Group B, the difference in mOS due to chosen front-line therapy persisted ($P<0.0001$) (*Online Supplementary Figure S1*).

Survival outcomes in patients with previous hypomethylating agent exposure

We also assessed the efficacy of front-line treatments in the small subset of evaluable patients who had previously received HMA for non-AML diagnoses ($n=185$), focusing on identifying whether a benefit was seen in this subgroup *versus* high-intensity treatment. Of these 185 patients, 24 patients (13.0%) received HMA subsequently for AML diagnosis, 55 (29.7%) received high-intensity therapy, 32 (17.3%) received low-intensity therapy, and 74 (40%) received supportive care only. We noted similarly poor median overall survival among the HMA group (7.8 months), the high-intensity therapy group (5.9 months), and the low-intensity group (5.9 months). However, all three treatment groups had better overall survival than the supportive care group (2.9 months) ($P<0.0001$) (*data not shown*). Moreover, multivariate analysis of the group also demonstrated the inferiority of supportive *versus* HMA and high-intensity and low-intensity therapy (Table 3). This improved survival *versus* supportive care suggested that this subgroup may benefit from some other type of therapy rather than supportive care only.

Responses and early mortality rates

The rate of composite CR (CR and CRi) and 30-day TRM (defined as death within 30 days of treatment initiation) were compared among the HMA, high-intensity,

and low-intensity treatment groups (Figure 2). The rate of composite CR was significantly higher in the cohort treated with high-intensity chemotherapy than in the HMA (43.1% vs. 22.7%; adjusted $P<0.001$) and low-intensity therapy groups (43.1% vs. 7.7%; adjusted $P<0.001$). Early TRM was significantly lower with HMA treatment at 1.2%, compared with 7.5% with high-intensity chemotherapy (adjusted $P<0.01$). Among the patients who achieved CR/CRi, we calculated a median relapse-free survival of 10.5 months with HMA *versus* 9.1 months with high-intensity treatment ($P=0.09$) and 4.4 months with low-intensity treatment, which was significantly inferior to both HMA ($P=0.009$) or high-intensity treatment ($P=0.036$). However, it should be noted that the low-intensity subgroup had an extremely small sample size ($n=5$).

Discussion

Treatment of elderly patients with AML is a therapeutic challenge for clinicians as the choice of optimal front-line regimens continues to remain controversial. Here we present the results of the largest single institution report of outcomes amongst AML patients ≥ 70 years old. Using pairwise comparisons with propensity score matching, our results indicated a survival benefit with front-line HMA compared with high-intensity, low-intensity, or supportive care therapies. These results confirm and expand on previous reports that elderly patients with AML can benefit from treatment over supportive care.^{2,10,19,20}

Clinical trials with the HMA azacitidine or decitabine have previously demonstrated their ability to induce remission and prolong survival in elderly AML patients.^{16,19,21-23} After adjusting for potential treatment bias between the treatment groups with propensity score matching, we observed a statistically significant overall survival benefit with HMA *versus* our other treatment groups, with patients treated with HMA having median overall survival of 14.4 months. Our results were comparable to the 12.1 months previously observed by Dombret *et al.*¹⁵

Not unexpectedly, high-intensity chemotherapy was

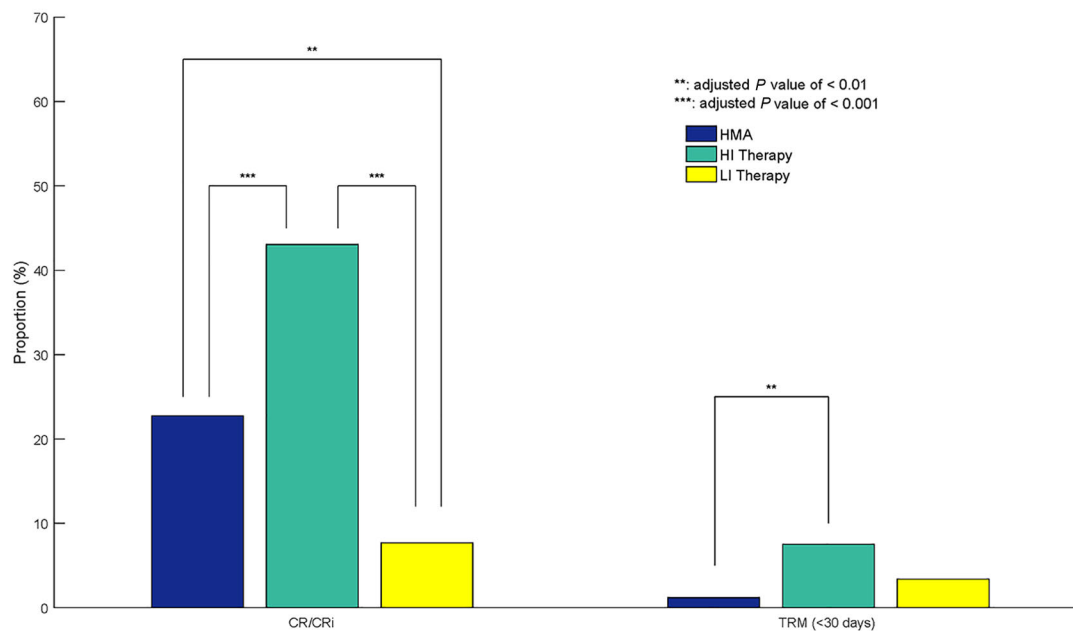


Figure 2. Treatment responses based on various treatment modalities. CR/Cri: complete response or complete response with incomplete count recovery; HI: high intensity; HMA: hypomethylating agent; LI: low intensity; TRM: treatment-related mortality.

also shown to be superior to supportive care with respect to overall survival. Interestingly, among the high-intensity and low-intensity treatment cohorts, overall survival significantly favored high-intensity treatment. Superior outcomes with high-intensity chemotherapy *versus* lower intensity chemotherapy and supportive care have been previously reported in older AML patients.^{1,3,24,25} Together with our results, it is apparent that providing any treatment is superior to no treatment (supportive care) and these data may provide support to select intensive chemotherapy over lower intensity treatment in eligible patients. However, given the heterogeneity of the disease, risk stratification based on biological features of disease, functional status, comorbidity assessment, and cytogenetics rather than age alone should help guide treatment decisions.^{2,6,10,26,27}

Although the superiority of high-intensity treatment over supportive care or low-intensity treatment was evident, high-intensity treatment failed to show survival superiority *versus* HMA in both our univariate and multivariate analyses. We found that high-intensity therapy conferred at least 35% higher risk of mortality than treatment with HMA. To eliminate the selection bias in our retrospective non-randomized study and to be able to accurately estimate the effects of treatment by reducing the bias due to confounding variables (such as baseline CCI among other co-variables), we implemented the propensity score matching method. Even with this method, the overall survival benefit was upheld with HMA treatment compared with high-intensity treatment (*Online Supplementary Table S2*). Our findings contrast somewhat from data previously reported by Quintas-Cardama *et al.* that indicated therapeutic equivalence between HMA and high-intensity therapy, including within the intermediate-risk cytogenetic group.²⁸ However, our data focused on a somewhat older popula-

tion and used propensity score matching to minimize selection bias for front-line treatment options.

The higher rate of TRM that we observed with high-intensity treatment compared with HMA treatment (7.2% *vs.* 1.5%) may be implicated as a potential cause for the overall inferior survival, although it cannot be the sole reason for overall inferiority. Distinct disease biology of AML in older patients (compared with younger patients with AML) is certainly a contributing factor for suboptimal treatment responses. Secondary AML originating from a prior myelodysplastic syndrome is common in the elderly and portends a poor prognosis. In our patient cohort, a significant proportion (56.9%) had secondary AML, primarily stemming from myelodysplastic syndromes. For this subgroup of patients, induction with intensive chemotherapy is frequently utilized, but the duration of response and long-term outcomes continue to remain poor.²⁹

Treatment with a prior HMA has been previously shown to be an independent negative predictive factor for responses and overall survival in patients with secondary AML.³⁰ In our analysis of this high-risk subgroup with prior HMA exposure, treatment with a high-intensity regimen did not produce significantly superior overall outcomes (HR=1.25, 95%CI: 0.68-2.27; $P=0.47$) compared with HMA. Moreover, low-intensity treatment also failed to produce improved outcomes compared with HMA treatment (HR=1.42, 95%CI: 0.76-2.66; $P=0.28$). Interestingly, the supportive care cohort had far inferior outcomes than patients in the HMA group (HR=2.29, 95%CI: 1.30-4.02; $P=0.004$). These results further reinforce the notion that some therapy may be superior to supportive care only, including that a clinical trial should be strongly considered whenever possible for this group.

A small minority (12.1%) of the patients in the HMA cohort had been previously treated with HMA. Typical approaches for such patients at our institution include

Table 3. Multivariate analysis and comparisons of entire cohort versus patients without prior exposure to hypomethylating agent prior to diagnosis of acute myeloid leukemia and versus patients who received hypomethylating agent prior to the diagnosis of acute myeloid leukemia.

Clinical Parameter	All Patients (n=980)				Without Prior Exposure to HMA (n=795)				With Prior Exposure to HMA (n=185)			
	P	Hazard Ratio	95%CI Lower	95%CI Upper	P	Hazard Ratio	95%CI Lower	95%CI Upper	P	Hazard Ratio	95%CI Lower	95%CI Upper
Type of AML												
De novo	Reference				Reference				Excluded			
Secondary	<0.0001	1.44	1.23	1.69	0.001	1.34	1.13	1.59				
Karyotype												
Favorable or intermediate	Reference				Reference				Reference			
Adverse	<0.0001	1.92	1.64	2.25	<0.0001	2.02	1.69	2.41	0.001	1.87	1.29	2.72
ECOG PS												
0-1	Reference				Reference				Excluded			
2-4	<0.0001	1.80	1.48	2.18	<0.0001	1.82	1.47	2.26				
Front-line therapy												
HMA	Reference				Reference				Reference			
HI therapy	0.004	1.35	1.10	1.65	0.024	1.29	1.03	1.61	0.47	1.25	0.68	2.27
LI therapy	<0.0001	2.01	1.53	2.62	<0.0001	2.12	1.54	2.91	0.28	1.42	0.76	2.66
Supportive care	<0.0001	2.94	2.39	3.61	<0.0001	3.02	2.40	3.81	0.004	2.29	1.30	4.02
Age at diagnosis (per 5-year increase)	0.002	1.14	1.05	1.23	0.036	1.10	1.01	1.21	0.001	1.38	1.14	1.67
WBC, per 1 log increase	<0.0001	1.19	1.13	1.25	<0.0001	1.18	1.11	1.25	<0.0001	1.34	1.16	1.54
Platelets, per 1 log increase	<0.0001	0.81	0.75	0.87	<0.0001	0.80	0.73	0.88	0.002	0.80	0.69	0.92
Hemoglobin, per 1 log increase	<0.0001	0.91	0.86	0.95	0.0003	0.91	0.86	0.96	0.035	0.87	0.77	0.99

AML: acute myeloid leukemia; CI: confidence interval; ECOG PS: Eastern Cooperative Oncology Group Performance Status; HI: high intensity; HMA: hypomethylating agent; LI: low intensity; WBC: white blood cell.

clinical trials (if available), intensive chemotherapy, lower-intensity approaches, or best supportive care. If HMA therapy is continued, we may utilize a different dosing schedule (10-day decitabine or 7-day azacitidine if treated with a 5-day schedule) or switch to the alternative HMA agent. Although limited, our data suggest that patients treated previously with HMA do not benefit from any specific standard-of-care approach, indicating the importance of clinical trials for this subpopulation.

Since the Food and Drug Administration approval of CPX-351 for secondary AML (AML with myelodysplasia-related changes and therapy-related AML) that established a new standard of care for this distinct high-risk AML subgroup, the treatment landscape for AML has become increasingly complex.³¹ CPX-351 is considered an intensive chemotherapy and is demonstrated to have similar early TRM as “7+3”. However, CPX-351 has not been compared head-to-head with HMA-based therapies and were not included in our study. But such a comparison is warranted to determine the optimal treatment choice for older AML patients aged ≥ 70 years.

While the results of our study are potentially practice-changing, there are several limitations. Although this is the largest single-institution series of AML patients ≥ 70 years of age, a referral bias affecting baseline disease characteristics is expected. In our cohort, 50% of the patients had prior hematologic malignancy and >90% of these patients had diagnosis of MDS. In addition, treatment outcomes of patients seen at a tertiary care center may not reflect outcomes of the general community, thereby limiting its general applicability. For instance, per the SEER registry studies, only 10-20% of elderly patients are treated with HMA or intensive chemotherapy, compared with

58% of the patients in our cohort.^{11,13} The non-randomized retrospective nature of this study also does not allow for definitive conclusions to be made as there might be some inadvertent, inherent biases introduced that we did not consider, although we attempted to account for such bias *via* utilization of propensity score matching.

Although most patients in our cohort had cytogenetic results, the lack of molecular data in our analysis is another study limitation. Prior studies have shown that with advanced age there is an increase in the incidence of unfavorable cytogenetics, aberrant karyotypes, and molecular abnormalities.³²⁻³⁶ Testing newly diagnosed AML patients irrespective of their age for key molecular markers (including FLT3, NPM1, and KIT) should be universally done given their prognostic and therapeutic implications. Unfortunately, molecular testing and routine testing of all elderly patients with AML have only become a standard practice during the past ten years. The lack of available testing likely explains the lack of available molecular data in our database, which incorporates patients dating back to 1995.

Accurate assessment of baseline performance status and comorbidity measurements in elderly patients with AML can provide useful prognostic information and help guide treatment decisions. Functionality and comorbidity are independent prognostic variables and should be measured independently in elderly patients.³⁷ A retrospective study by Etienne *et al.* reported that patients with a CCI score >1 had significantly lower rates of obtaining a CR than those having CCI scores <1.³⁸ Analyses of the SEER data have also shown that survival of those with CCI of 0-1 improved with therapy, whereas those with CCI >2 experienced early death and had minimal improvements in

overall survival.¹¹ It should be noted that, despite these survival differences, the SEER registries lacked functional and cytogenetic data, thus limiting applicability of these results. In our analysis, 79.3% of patients had an ECOG performance status of 0 or 1, and only 13.4% of patients had a high CCI of ≥ 3 . The fact that most of our patients had good performance status or low CCI could account for the increased tolerability to induction chemotherapy, therefore conferring an additional survival advantage to treatment compared with supportive care or low-intensity treatment. On the other hand, Juliusson *et al.* demonstrated in a leukemia registry that even older patients with poor performance status seemed to benefit from chemotherapy compared with best supportive care.²⁰

Although the need for quality of life (QOL) assessments before and after treatment are well recognized in AML, and may represent an important outcome measure, currently, clinical trials mainly focus on quantitative assessments of life rather than qualitative. Geriatric assessments in combination with conventional clinical and disease-specific factors can accurately predict vulnerability to treatment toxicity; however, such assessment models specific to AML are lacking.³⁹ Oliva *et al.* reported a study on elderly AML patients in which QOL physical functioning was of prognostic relevance; however, these results did not correlate with physician-assessed ECOG performance status.⁴⁰ As shown previously, even hematologic improvements from reduction in transfusions can lead to improved

QOL.^{41,42} Although QOL is an important measure of treatment outcomes, our study did not capture such information, posing a limitation regarding the effects of treatment options on QOL. Therefore, prospective studies regarding whether HMA treatment *versus* intensive chemotherapy can improve QOL are warranted to assess this vital component of AML care.

In conclusion, as shown in our analysis of a large patient cohort, patients over the age of 70 years with AML had a significant survival benefit with HMA or high-intensity therapy compared with supportive care or low-intensity therapy. Moreover, patients who were treated with HMA showed a striking survival advantage over those who received traditional high-intensity therapy. Because of the present lack of a clear decision model to allow for comparing treatments more objectively, elderly patients with AML may receive suboptimal treatment. The results presented here contribute to an ongoing effort to design a comprehensive decision analysis model comparing treatment effectiveness to baseline characteristics in elderly patients with AML.

Funding

This work was supported by National Institutes of Cancer grant 5R01CA168677-02 (PI – Martine Extermann, MD, PhD) and in part by the Biostatistics Core Facility at the Moffitt Cancer Center & Research Institute, a National Cancer Institute-designated Comprehensive Cancer Center (P30CA076292-16).

References

- Baz R, Rodriguez C, Fu AZ, et al. Impact of remission induction chemotherapy on survival in older adults with acute myeloid leukemia. *Cancer*. 2007;110(8):1752-1759.
- Colovic M, Colovic N, Radokjovic M, et al. Induction chemotherapy versus palliative treatment for acute myeloid leukemia in a consecutive cohort of elderly patients. *Ann Hematol*. 2012;91(9):1363-1370.
- Lowenberg B, Ossenkoppele GJ, van Putten W, et al. High-dose daunorubicin in older patients with acute myeloid leukemia. *N Engl J Med*. 2009;361(13):1235-1248.
- Leith CP, Kopecky KJ, Chen IM, et al. Frequency and clinical significance of the expression of the multidrug resistance proteins MDR1/P-glycoprotein, MRP1, and LRP in acute myeloid leukemia: a Southwest Oncology Group Study. *Blood*. 1999;94(3):1086-1099.
- Leith CP, Kopecky KJ, Godwin J, et al. Acute myeloid leukemia in the elderly: assessment of multidrug resistance (MDR1) and cytogenetics distinguishes biologic subgroups with remarkably distinct responses to standard chemotherapy. A Southwest Oncology Group study. *Blood*. 1997;89(9):3323-3329.
- Gupta V, Chun K, Yi QL, et al. Disease biology rather than age is the most important determinant of survival of patients $>$ or = 60 years with acute myeloid leukemia treated with uniform intensive therapy. *Cancer*. 2005;103(10):2082-2090.
- Breccia M, Frustaci AM, Cannella L, et al. Comorbidities and FLT3-ITD abnormalities as independent prognostic indicators of survival in elderly acute myeloid leukaemia patients. *Hematol Oncol*. 2009;27(3):148-153.
- Prebet T, Boissel N, Reutenauer S, et al. Acute myeloid leukemia with translocation (8;21) or inversion (16) in elderly patients treated with conventional chemotherapy: a collaborative study of the French CBF-AML intergroup. *J Clin Oncol*. 2009;27(28):4747-4753.
- Rollig C, Thiede C, Gramatzki M, et al. A novel prognostic model in elderly patients with acute myeloid leukemia: results of 909 patients entered into the prospective AML96 trial. *Blood*. 2010;116(6):971-978.
- Vey N, Coso D, Bardou VJ, et al. The benefit of induction chemotherapy in patients age $>$ or = 75 years. *Cancer*. 2004;101(2):325-331.
- Oran B, Weisdorf DJ. Survival for older patients with acute myeloid leukemia: a population-based study. *Haematologica*. 2012;97(12):1916-1924.
- Thein MS, Ershler WB, Jemal A, Yates JW, Baer MR. Outcome of older patients with acute myeloid leukemia: an analysis of SEER data over 3 decades. *Cancer*. 2013;119(15):2720-2727.
- Medeiros BC, Satram-Hoang S, Hurst D, et al. Big data analysis of treatment patterns and outcomes among elderly acute myeloid leukemia patients in the United States. *Ann Hematol*. 2015;94(7):1127-1138.
- Shah BK, Ghimire KB. Improved survival among older acute myeloid leukemia patients - a population-based study. *Acta Oncol*. 2014;53(7):935-938.
- Dombret H, Seymour JF, Butrym A, et al. International phase 3 study of azacitidine vs conventional care regimens in older patients with newly diagnosed AML with $>30\%$ blasts. *Blood*. 2015;126(3):291-299.
- Kantarjian HM, Thomas XG, Dmoszynska A, et al. Multicenter, randomized, open-label, phase III trial of decitabine versus patient choice, with physician advice, of either supportive care or low-dose cytarabine for the treatment of older patients with newly diagnosed acute myeloid leukemia. *J Clin Oncol*. 2012;30(21):2670-2677.
- Cheson BD. Overview of the revised response criteria for acute myelogenous leukemia. *Clin Adv Hematol Oncol*. 2004;2(5):277-279.
- O'Donnell MR, Tallman MS, Abboud CN, et al. Acute Myeloid Leukemia, Version 3.2017, NCCN Clinical Practice Guidelines in Oncology. *J Natl Compr Canc Netw*. 2017;15(7):926-957.
- Fenaux P, Mufti GJ, Hellstrom-Lindberg E, et al. Azacitidine prolongs overall survival compared with conventional care regimens in elderly patients with low bone marrow blast count acute myeloid leukemia. *J Clin Oncol*. 2010;28(4):562-569.
- Juliusson G, Antunovic P, Derolf A, et al. Age and acute myeloid leukemia: real world data on decision to treat and outcomes from the Swedish Acute Leukemia Registry. *Blood*. 2009;113(18):4179-4187.
- Cashen AF, Schiller GJ, O'Donnell MR, DiPersio JF. Multicenter, phase II study of decitabine for the first-line treatment of older patients with acute myeloid leukemia. *J Clin Oncol*. 2010;28(4):556-561.
- Maurillo L, Venditti A, Spagnoli A, et al. Azacitidine for the treatment of patients with acute myeloid leukemia: report of 82 patients enrolled in an Italian

- Compassionate Program. *Cancer*. 2012; 118(4):1014-1022.
23. Al-Ali HK, Jaekel N, Junghanss C, et al. Azacitidine in patients with acute myeloid leukemia medically unfit for or resistant to chemotherapy: a multicenter phase I/II study. *Leuk Lymphoma*. 2012;53(1):110-117.
 24. Lowenberg B, Zittoun R, Kerkhofs H, et al. On the value of intensive remission-induction chemotherapy in elderly patients of 65+ years with acute myeloid leukemia: a randomized phase III study of the European Organization for Research and Treatment of Cancer Leukemia Group. *J Clin Oncol*. 1989;7(9):1268-1274.
 25. Arellano M, Winton E, Pan L, et al. High-dose cytarabine induction is well tolerated and active in patients with de novo acute myeloid leukemia older than 60 years. *Cancer*. 2012;118(2):428-433.
 26. Walter RB, Othus M, Borthakur G, et al. Prediction of early death after induction therapy for newly diagnosed acute myeloid leukemia with pretreatment risk scores: a novel paradigm for treatment assignment. *J Clin Oncol*. 2011;29(33):4417-4423.
 27. Appelbaum FR, Gundacker H, Head DR, et al. Age and acute myeloid leukemia. *Blood*. 2006;107(9):3481-3485.
 28. Quintas-Cardama A, Ravandi F, Liu-Dumlao T, et al. Epigenetic therapy is associated with similar survival compared with intensive chemotherapy in older patients with newly diagnosed acute myeloid leukemia. *Blood*. 2012;120(24):4840-4845.
 29. Rizzieri DA, O'Brien JA, Broadwater G, et al. Outcomes of patients who undergo aggressive induction therapy for secondary acute myeloid leukemia. *Cancer*. 2009; 115(13):2922-2929.
 30. Bello C, Yu D, Komrokji RS, et al. Outcomes after induction chemotherapy in patients with acute myeloid leukemia arising from myelodysplastic syndrome. *Cancer*. 2011;117(7):1463-1469.
 31. Lancet JE, Uy GL, Cortes JE, et al. CPX-351 (cytarabine and daunorubicin) Liposome for Injection Versus Conventional Cytarabine Plus Daunorubicin in Older Patients With Newly Diagnosed Secondary Acute Myeloid Leukemia. *J Clin Oncol*. 2018;36(26):2684-2692.
 32. Moorman AV, Roman E, Willett EV, et al. Karyotype and age in acute myeloid leukemia. Are they linked? *Cancer Genet Cytogenet*. 2001;126(2):155-161.
 33. Andersson A, Johansson B, Lassen C, et al. Clinical impact of internal tandem duplications and activating point mutations in FLT3 in acute myeloid leukemia in elderly patients. *Eur J Haematol*. 2004;72(5):307-313.
 34. Stirewalt DL, Kopecky KJ, Meshinchi S, et al. FLT3, RAS, and TP53 mutations in elderly patients with acute myeloid leukemia. *Blood*. 2001;97(11):3589-3595.
 35. Schoch C, Kern W, Krawitz P, et al. Dependence of age-specific incidence of acute myeloid leukemia on karyotype. *Blood*. 2001;98(12):3500.
 36. Lindsley RC, Mar BG, Mazzola E, et al. Acute myeloid leukemia ontogeny is defined by distinct somatic mutations. *Blood*. 2015;125(9):1367-1376.
 37. Extermann M, Overcash J, Lyman GH, Parr J, Balducci L. Comorbidity and functional status are independent in older cancer patients. *J Clin Oncol*. 1998;16(4):1582-1587.
 38. Etienne A, Esterni B, Charbonnier A, et al. Comorbidity is an independent predictor of complete remission in elderly patients receiving induction chemotherapy for acute myeloid leukemia. *Cancer*. 2007; 109(7):1376-1383.
 39. Sherman AE, Motyckova G, Fega KR, et al. Geriatric assessment in older patients with acute myeloid leukemia: a retrospective study of associated treatment and outcomes. *Leuk Res*. 2013;37(9):998-1003.
 40. Oliva EN, Nobile F, Alimena G, et al. Quality of life in elderly patients with acute myeloid leukemia: patients may be more accurate than physicians. *Haematologica*. 2011;96(5):696-702.
 41. Oliva EN, D'Angelo A, Martino B, et al. More concern about transfusion requirement when evaluating quality of life in anemic patients. *J Clin Oncol*. 2002; 20(14):3182-3183.
 42. Oliva EN, Finelli C, Santini V, et al. Quality of life and physicians' perception in myelodysplastic syndromes. *Am J Blood Res*. 2012;2(2):136-147.

Alternative donor transplantation for acute myeloid leukemia in patients aged ≥ 50 years: young HLA-matched unrelated or haploidentical donor?

Miguel-Angel Perales,^{1*} Benjamin Tomlinson,^{2*} Mei-Jie Zhang,^{3,4} Andrew St. Martin,³ Amer Beitinjaneh,⁵ John Gibson,⁶ William Hogan,⁷ Natasha Kekre,⁸ Hillard Lazarus,² David Marks,⁹ Joseph McGuirk,¹⁰ Rizwan Romee,¹¹ Melhem Solh,¹² John E. Wagner,¹³ Daniel J. Weisdorf,¹⁴ Marcos de Lima² and Mary Eapen³

*MAP and BT share first authorship

¹Adult Bone Marrow Transplant Services, Department of Medicine, Memorial Sloan-Kettering Cancer Center, and Department of Medicine, Weill Cornell Medical College, New York, NY, USA; ²Seidman Cancer Center, University Hospitals Cleveland Medical Center, Case Western Reserve University, Cleveland, OH, USA; ³Center for International Blood and Marrow Transplant Research, Department of Medicine, Medical College of Wisconsin, Milwaukee, WI, USA; ⁴Division of Biostatistics, Institute for Health and Society, Medical College of Wisconsin, Milwaukee, WI, USA; ⁵UM Sylvester Comprehensive Cancer Center, University of Miami, Miami, FL, USA; ⁶Institute of Haematology, Royal Prince Alfred Hospital, Camperdown, NSW, Australia; ⁷Bone Marrow Transplant Program, Mayo Clinic, Rochester, MN, USA; ⁸Blood and Marrow Transplant Program, The Ottawa Hospital, Ottawa, ON, Canada; ⁹University Hospitals Bristol National Health Service Foundation Trust, Bristol, UK; ¹⁰Division of Hematologic Malignancies and Cellular Therapy, University of Kansas Medical Center, Kansas City, KS, USA; ¹¹Division of Hematologic Malignancies and Transplantation, Dana-Farber Cancer Institute, Harvard Medical School, Boston, MA, USA; ¹²The Blood and Marrow Transplant Program at Northside Hospital, Atlanta, GA, USA; ¹³BMT Program, University of Minnesota Masonic Children's Hospital, Minneapolis, MN, USA and ¹⁴University of Minnesota Medical Center, Minneapolis, MN, USA

ABSTRACT

We sought to study whether survival after haploidentical transplantation is comparable to that after matched unrelated donor transplantation for 822 patients aged 50-75 years with acute myeloid leukemia in first or second complete remission. One hundred and ninety-two patients received grafts from haploidentical donors (sibling 25%; offspring 75%) and 631 patients from matched unrelated donors aged 18-40 years. Patients' and disease characteristics of the two groups were similar except that recipients of matched unrelated donor transplantation were more likely to have poor risk cytogenetics and more likely to receive myeloablative conditioning regimens. Time from documented remission to transplant did not differ by donor type. Five-year overall survival was 32% and 42% after haploidentical and matched unrelated donor transplant, respectively ($P=0.04$). Multivariable analysis showed higher mortality (hazard ratio 1.27, $P=0.04$) and relapse (hazard ratio 1.32, $P=0.04$) after haploidentical transplantation, with similar non-relapse mortality risks. Chronic graft-versus-host disease was higher after matched unrelated donor compared to haploidentical transplantation when bone marrow was the graft (hazard ratio 3.12, $P<0.001$), but when the graft was peripheral blood, there was no difference in the risk of chronic graft-versus-host disease between donor types. These data support the view that matched unrelated donor transplant with donors younger than 40 years is to be preferred.

Introduction

Standard post-remission therapy for eligible patients with high risk or relapsed acute myeloid leukemia (AML), including older patients, is an allogeneic



Haematologica 2018
Volume 105(2):407-413

Correspondence:

MARY EAPEN
meapen@mcw.edu

Received: December 21, 2018.

Accepted: May 16, 2019.

Pre-published: May 17, 2019.

doi:10.3324/haematol.2018.215202

Check the online version for the most updated information on this article, online supplements, and information on authorship & disclosures: www.haematologica.org/content/105/2/407

©2020 Ferrata Storti Foundation

Material published in Haematologica is covered by copyright. All rights are reserved to the Ferrata Storti Foundation. Use of published material is allowed under the following terms and conditions:

<https://creativecommons.org/licenses/by-nc/4.0/legalcode>. Copies of published material are allowed for personal or internal use. Sharing published material for non-commercial purposes is subject to the following conditions: <https://creativecommons.org/licenses/by-nc/4.0/legalcode>, sect. 3. Reproducing and sharing published material for commercial purposes is not allowed without permission in writing from the publisher.



hematopoietic cell transplant from a matched sibling or an alternative donor such as a haploidentical or unrelated donor. The introduction of transplantation of T-cell replete bone marrow or peripheral blood from a haploidentical relative using post-transplant cyclophosphamide for graft-versus-host disease (GvHD) has gained broad acceptance with consistently favorable outcomes.¹⁻⁵ Others have reported comparable outcomes after haploidentical donor compared to unrelated donor transplantation for AML.⁶⁻⁸ Yet in a recent report from the Center for International Blood and Marrow Transplant Research (CIBMTR) and the European Society for Blood and Marrow Transplant (EBMT), non-relapse mortality and overall mortality were higher after transplantation of grafts from haploidentical (offspring) donors compared to HLA-matched siblings for AML and acute lymphoblastic leukemia (ALL) in patients aged 55-76 years.⁹ An earlier study of allogeneic transplantation for older patients with hematologic malignancy concluded HLA-matched sibling donor transplants was associated with lower GvHD and better survival in patients with good performance scores compared to HLA-matched unrelated donor (MUD) who were younger than their recipients.¹⁰ Published reports have recorded better survival after transplantation of bone marrow or peripheral blood grafts from unrelated adult donors aged ≤ 40 years.¹¹ Thus with increasing numbers of transplants being performed for AML in older patients (≥ 50 years), a clinically relevant question is whether to use a haploidentical relative or a young MUD when considering alternative donor transplantation.

Methods

Patients

Data are reported to the CIBMTR from 195 transplant centers in the United States and 90 of these centers contributed data for the current analysis. Patients are followed longitudinally until death or lost to follow up. Eligible patients were aged 50-76 years with AML, transplanted in first or second remission in the United States between 2008 and 2015 and with commonly used conditioning regimens (*Online Supplementary Table S1*). Patients received bone marrow or peripheral blood from a haploidentical donor (sibling or offspring mismatched at ≥ 2 HLA loci) or an 8/8 HLA-matched MUD aged 18-40 years. Unrelated donors aged >40 years were excluded as over 90% of unrelated donors selected for recent transplants in the US are aged 18-40 years old.¹¹ Excluded patients included those transplanted in relapse ($n=248$) and receiving transplant regimens that included anti-thymocyte globulin or alemtuzumab ($n=76$) or CD34 selected peripheral blood ($n=56$) or *ex vivo* T-cell depletion ($n=34$). Patients provided written informed consent for research. The Institutional Review Board of the National Marrow Donor Program approved this study.

End points

The primary end point was overall mortality. Death from any cause was considered an event and surviving patients were censored at last follow up. Relapse was defined as the first detection of one of the following: hematologic, cytogenetic or molecular leukemia recurrence, and non-relapse mortality was defined as death in remission. Treatment failure was defined as relapse or death (inverse of leukemia-free survival). Neutrophil recovery was defined as the first of three consecutive days of an achieved absolute neutrophil count $\geq 0.5 \times 10^9/L$ and platelet recovery was defined as the first date of an achieved platelet count $\geq 20 \times 10^9/L$

after seven consecutive days of no platelet transfusions. Grade II-IV acute GvHD and chronic GvHD were based on reports from each transplant center using standard criteria.^{12,13}

Statistical analysis

Differences in patients', disease and transplant characteristics between the two groups (i.e. donor type) were compared using the χ^2 statistic for categorical variables. The probabilities of overall survival and leukemia-free survival were calculated using the Kaplan-Meier estimator.¹⁴ The probabilities of neutrophil and platelet recovery, acute and chronic GvHD, non-relapse mortality and relapse were calculated using the cumulative incidence estimator to accommodate competing risks.¹⁵ Cox regression models were built to study the effect of donor type (MUD vs. haploidentical) and other factors associated with overall mortality, grade II-IV acute GvHD, chronic GvHD, relapse, non-relapse mortality and treatment failure.¹⁶ Variables tested included: donor age (tested as a continuous variable), recipient age, sex, performance score, hematopoietic cell transplant co-morbidity (HCT-CI) score, cytomegalovirus (CMV) serostatus, disease status, cytogenetic risk, transplant conditioning regimen intensity and transplant period. All variables that attained $P \leq 0.05$ were held in the final multi-variable model with the exception of the variable for donor type that was held in all steps of model building and the final model regardless of level of significance. There was no first order interaction between donor type and other variables including conditioning regimen intensity. Transplant center effect on survival was tested using the frailty approach.¹⁷ All P -values are two-sided. All analyses were made using SAS version 9.4 (Cary, NC, USA).

Results

Patients', disease and transplant characteristics

Characteristics of recipients of haploidentical ($n=192$) and MUD ($n=631$) transplants were similar except that recipients of haploidentical transplants were more likely to have favorable or intermediate risk cytogenetics ($P=0.03$), and to have received reduced intensity conditioning regimen ($P<0.0001$) (Table 1). The predominant reduced intensity conditioning regimen for haploidentical transplantation was low-dose total body irradiation (200 cGy), cyclophosphamide (29 mg/kg) and fludarabine (150 mg/m²). The predominant reduced intensity conditioning regimen for MUD transplantation was busulfan or melphalan with fludarabine. The median ages of recipients of haploidentical and MUD transplantations were 61 and 61 years, respectively. The median time to haploidentical transplantation from diagnosis for patients in CR1 and CR2 were 5 and 20 months, respectively. The corresponding time to MUD transplantation was 5 and 18 months. Bone marrow was the predominant graft for haploidentical transplants and peripheral blood the predominant graft for MUD transplants. All recipients of haploidentical transplantation received a uniform GvHD prophylaxis regimen: post-transplant cyclophosphamide with a calcineurin inhibitor and mycophenolate. Recipients of MUD transplantation received a calcineurin inhibitor containing GvHD prophylaxis; calcineurin inhibitor with methotrexate was the predominant regimen. Haploidentical donors (25% siblings and 75% offspring) were mismatched at ≥ 2 HLA-loci and the median donor age was 37 years (range: 17-69). MUD were allele-level matched at HLA-A, -B, -C and -DRB1 and their median age was 27 years (range 18-40). The median follow up of

Table 1. Patients', disease and transplant characteristics.

Variable	Haploidentical donor	Unrelated donor	P
Number	192	631	
Age, years			0.7
50 – 59	85 (44%)	266 (42%)	
60 – 69	89 (46%)	312 (49%)	
70 – 79	18 (9%)	53 (8%)	
Sex, male/female	104 (54%)/88 (46%)	356 (56%)/275 (44%)	0.6
Performance score			<0.001
90 – 100	114 (59%)	384 (61%)	
≤ 80	67 (35%)	241 (38%)	
Not reported	11 (6%)	6 (<1%)	
HCT- comorbidity index			0.1
0 – 2	108 (56%)	310 (49%)	
≥3	84 (44%)	317 (50%)	
Not reported	–	4 (<1%)	
Cytomegalovirus serostatus			0.7
Negative	63 (33%)	220 (35%)	
Positive	128 (67%)	405 (64%)	
Not reported	1 (<1%)	6 (<1%)	
Disease status			0.03
First complete remission	146 (76%)	524 (83%)	
Second complete remission	46 (24%)	107 (17%)	
Cytogenetic risk			0.03
Favorable	8 (4%)	20 (3%)	
Intermediate	148 (77%)	425 (67%)	
Poor	35 (18%)	176 (28%)	
Not reported	1 (<1%)	10 (2%)	
Conditioning regimen			<0.001
<i>Myeloablative</i>			
Busulfan/cyclophosphamide	25 (13%)	108 (17%)	
Busulfan/fludarabine	3 (1%)	171 (27%)	
TBI + other agents	19 (10%)	–	
<i>Reduced intensity</i>			
Busulfan/fludarabine	–	234 (37%)	
Melphalan/fludarabine	10 (5%)	118 (18%)	
TBI/cyclophosphamide/fludarabine	124 (65%)	–	
TBI + other agents	11 (6%)	–	
Graft type			<0.001
Bone marrow	132 (69%)	96 (15%)	
Peripheral blood	60 (31%)	535 (85%)	
Donor-recipient relationship/HLA-match			
Haploidentical sibling	48 (25%)	–	
Offspring	144 (75%)	–	
HLA match: A, B, C, DRB1	–	631 (100%)	
Donor age, median (range)	37 (16–69)	27 (18–40)	<0.001
Transplant period			0.007
2008 – 2011	46 (24%)	216 (34%)	
2012 – 2015	146 (76%)	415 (66%)	
Median follow up of survivors			
months (range)	42 (12–97)	47 (5–124)	

HCT: hematopoietic cell transplant; TBI: total body irradiation.

recipients of haploidentical and MUD transplantations were 42 months (range 12-97) and 47 months (range 5-124), respectively.

Overall mortality

The risks for overall mortality was higher after transplantation of bone marrow or peripheral blood from haploidentical compared to MUD after adjusting for HCT-CI score and cytogenetic risk (Table 2 and Figure 1A). Overall mortality risks were higher in patients with a HCT-CI score of 3 or higher compared to score 0-2 (HR 1.39, 95%CI: 1.14-1.68; $P=0.001$) and poor risk cytogenetics compared to intermediate/good risk cytogenetics (HR 1.46, 95%CI: 1.18-1.81; $P=0.001$). Donor age was not associated with overall mortality (HR 1.00, 95%CI: 0.98-1.01; $P=0.9$). In a subset analysis limited to patients in CR1, overall mortality risk was also higher after haploidentical compared to MUD transplant (HR 1.31, 95%CI: 1.01-1.70; $P=0.05$). Although transplant conditioning regimen intensity was not associated with mortality risk (HR 0.88, 95%CI: 0.72-1.08; $P=0.2$), we tested for an interaction between donor type and conditioning regimen intensity and found none ($P=0.7$). An effect of transplant center on overall mortality was explored and none was found.

Causes of death differed by donor type ($P=0.01$); recurrent disease was the most common cause of death in both treatment groups although this was higher after haploidentical (59%) compared to MUD (54%) transplants. Only 2% of deaths after haploidentical transplant was attributed to GvHD compared to 14% after MUD transplant. There were no differences in proportion of deaths attributed to graft failure, infection, interstitial pneumonitis or organ failure by donor type.

Hematopoietic recovery

The median times to neutrophil and platelet recovery after haploidentical and MUD transplantation was 17

versus 14 days for neutrophils ($P<0.001$) and 26 *versus* 17 days for platelets ($P<0.001$). The day-28 rates of neutrophil recovery were 89% (95%CI: 84-93) and 98% (95%CI: 97-99) ($P<0.001$) and the day-100 rates of platelet recovery 89% (95%CI: 84-93) and 96% (95%CI: 95-98) ($P=0.004$) after haploidentical and MUD transplantation, respectively. The 1-year cumulative incidence of primary or secondary graft failure after haploidentical and MUD transplantation were 11% (95%CI: 7-16) and 9% (95%CI: 7-11) ($P=0.4$).

Graft-versus-host disease

Compared to MUD transplantation, grade II-IV acute GvHD was significantly lower after haploidentical transplantation (HR 0.53, 95%CI: 0.38-0.75; $P<0.001$). Independent of donor type, grade II-IV acute GvHD was higher in patients with HCT-CI score of 3 or higher (HR 1.34, 95%CI: 1.06-1.69; $P=0.01$) and with myeloablative conditioning regimens (HR 1.42, 95%CI: 1.14-1.79; $P=0.003$). The day-100 incidence of grade II-IV acute GvHD after haploidentical and MUD transplantation was 21% (95%CI: 15-27) and 35% (95%CI: 32-39), respectively ($P<0.001$). Chronic GvHD risk was higher after MUD compared to haploidentical donor transplantation when bone marrow was the graft (HR 3.12, 95%CI: 1.75-5.56; $P<0.001$). The 2-year probability of chronic GvHD following a bone marrow graft from a haploidentical donor was 15% (95%CI: 10-22) compared to 36% (95%CI: 27-46) from a MUD ($P<0.001$). However, when the graft was peripheral blood, there was no difference in risk of chronic GvHD by donor type (HR 1.08, 95%CI: 0.71-1.69; $P=0.7$). The 2-year probabilities of chronic GvHD following a peripheral blood graft from haploidentical and MUD were 46% (95%CI: 31-60) and 55% (50-59), respectively ($P=0.3$). Among patients who developed chronic GvHD, its severity differed by donor type; extensive chronic GvHD was reported in 74% of haploidentical compared to 88% of MUD transplant recipients ($P=0.01$).

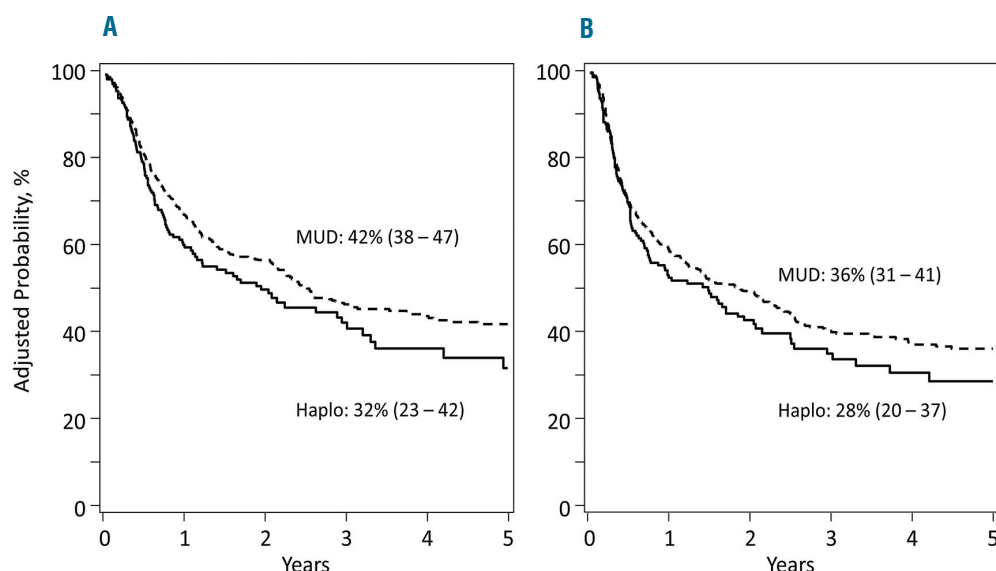


Figure 1. 5-year adjusted probability of overall survival (OS). (A) OS: the 5-year adjusted probability of OS after transplantation of grafts from haploidentical (Haplo) donor (32%, 95%CI: 23-42) and matched unrelated donor (MUD) (42%, 95%CI: 38-47). (B) Leukemia-free survival: the 5-year adjusted probability of disease-free survival after transplantation of grafts from Haplo donor (28%, 95%CI: 20-37) and MUD (36%, 95%CI: 31-41).

Treatment failure

There were no differences in treatment failure by donor type (Table 2 and Figure 1B). Independent of donor type, treatment failure was higher in patients with HCT-CI score of ≥ 3 (HR 1.28, 95%CI: 1.06-1.53; $P=0.009$) and those with poor cytogenetic risk (HR 1.56, 95%CI: 1.27-1.90; $P<0.001$). Donor age was not associated with treatment failure (HR 0.99, 95%CI: 0.98-1.01; $P=0.8$). In a subset analysis limited to transplantation in CR1, there were no differences in treatment failure by donor type (HR 1.22, 95%CI: 0.95-1.56; $P=0.1$).

Non-relapse mortality and relapse

Non-relapse mortality risk did not differ by donor type

(Table 2 and Figure 2A). Independent of donor type, non-relapse mortality was higher for HCT-CI score of >3 (HR 1.40, 95%CI: 1.03-1.90; $P=0.03$). Relapse occurred in 299 patients. Of the 299 patients who relapsed, two ($<1\%$) patients had only molecular relapse, 80 (27%) only cytogenetic relapse, 56 (19%) hematologic relapse, 59 (20%) molecular and hematologic relapse, and 102 (34%) cytogenetic and hematologic relapse. Relapse was higher after transplantation from haploidentical donors compared to MUD (Table 2 and Figure 2B). Independent of donor type, the risk of relapse was higher with poor risk cytogenetics (HR 1.82, 95%CI: 1.43-2.33; $P<0.001$). Donor age was not associated with non-relapse mortality (HR 1.01, 95%CI: 0.98-1.03; $P=0.5$) or relapse (HR 0.99, 95%CI: 0.98-1.01; $P=0.4$).

Table 2. Effect of donor type on transplant outcomes.

Outcome	Number Events/Evaluable	Hazard Ratio (95% confidence interval)	P
Overall mortality			
Unrelated donor	316/631	1.00	
Haploidentical donor	100/192	1.27 (1.01 – 1.60)	0.04
Non-relapse mortality			
Unrelated donor	135/624	1.00	
Haploidentical donor	36/191	1.01 (0.70 – 1.46)	0.9
Relapse			
Unrelated donor	224/624	1.00	
Haploidentical donor	75/191	1.32 (1.01 – 1.72)	0.04
Treatment failure			
Unrelated donor	359/624	1.00	
Haploidentical donor	111/191	1.19 (0.96 – 1.49)	0.1

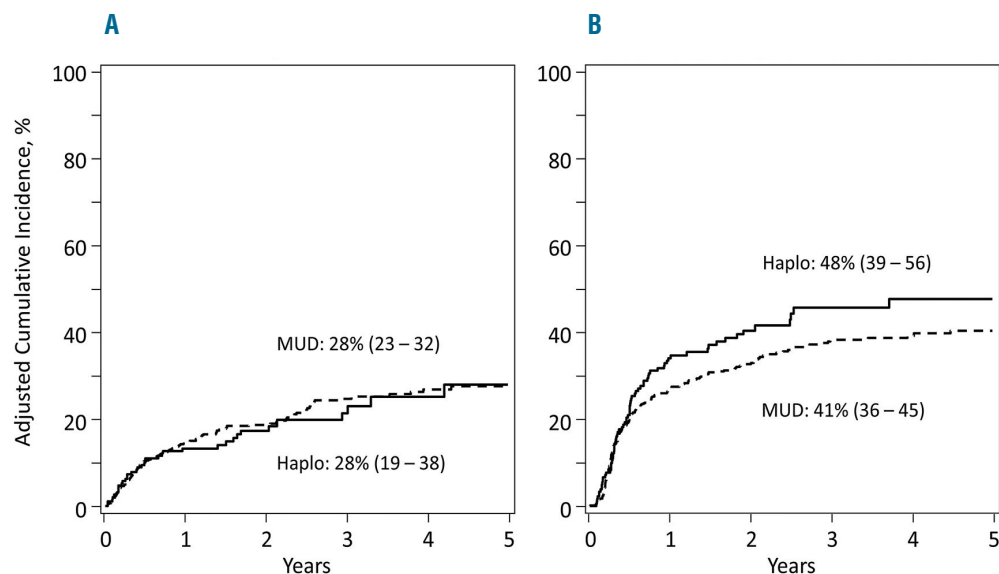


Figure 2. 5-year adjusted cumulative incidences of relapse and non-relapse mortality (NRM). (A) NRM: the 5-year adjusted cumulative incidence of NRM after transplantation of grafts from haploidentical (Haplo) donor (28%, 95%CI: 19-38) and matched unrelated donor (MUD) (28%, 95%CI: 19-38). (B) Relapse: the 5-year adjusted cumulative incidence of relapse after transplantation of grafts from Haplo donor (48%, 95%CI: 39-56) and MUD (41%, 95%CI: 36-45).

Discussion

Acute myeloid leukemia remains one of the main indications for allogeneic stem cell transplantation, and with an aging population, it is expected that both the incidence of AML and the number of transplants in older patients with AML will increase.¹⁸ Furthermore, recent trends also show an increase in haploidentical transplants with use of post-transplant cyclophosphamide for GvHD prophylaxis. Although an earlier CIBMTR report showed no difference in survival after haplo-identical and MUD transplantation, transplant outcomes in patients older than 50 years were not analyzed as a separate cohort.⁵ In the setting of HLA-matched sibling donor transplantation for patients older than 50 years with hematologic malignancy, survival was higher compared to MUD transplants with donors aged <50 years in patients with performance scores of 90 or 100.¹⁰ In those with performance scores 80 or lower, there were no significant differences in survival by donor type.¹⁰ With the increasing use of haplo-identical donors for AML, the current analysis sought to study whether survival after haploidentical donor transplantation would be better compared to transplantation of grafts from a young MUD (donor age 18-40 years). The results showed a survival advantage after MUD transplantation that can be attributed to lower relapse risks. Our findings lend support to our hypothesis that a young MUD should be the donor of choice when available. Furthermore, the data presented here suggest comparable times to transplantation in both treatment groups, confirming timely access to unrelated donors is no longer a barrier.

The prognostic significance of donor age and donor-recipient HLA match in the setting of unrelated donor transplantation has been confirmed in several reports, including a recent report that concluded there was a 5.5% increase in the hazard ratio for overall mortality for every 10-year increment in the age of the donor.^{11,19} The observed excess mortality with increasing donor age was attributed to higher non-relapse mortality and not leukemia recurrence.¹¹ In contrast, the effect of donor age for haplo-identical transplants is mixed. In a relatively young population with hematologic malignancy that predominantly used parental donors, a male donor under 30 years of age was associated with best survival.²⁰ On the other hand, for adults with hematologic malignancy, neither donor-recipient relationship or donor age was associated with transplant outcomes. In the current analysis, the better HLA-matching between the recipient and the unrelated donor may have also improved survival after MUD transplantation. Higher survival was recorded after HLA-matched sibling compared to haploidentical transplant for patients with acute leukemia who were older than 55 years confirming the importance of HLA matching for allogeneic transplantation.⁹

Unlike other reports that compared haploidentical to MUD or HLA-matched sibling transplants, relapse risks after MUD transplants were lower in the current analysis after adjusting for cytogenetic risk, transplant conditioning intensity and graft type.^{6,9} Predictably, relapse was higher in patients with poor risk cytogenetics, in recipients of reduced intensity conditioning regimens, and after transplantation of bone marrow.²¹ The recent Blood and Marrow Transplant Clinical Trials Network trial, BMT CTN 0901, showed higher relapse in patients with AML conditioned with reduced intensity regimens and was

consistent with other reports demonstrating the benefit of myeloablative regimens for AML.²² Furthermore, a recent CIBMTR report on graft type and haploidentical transplants demonstrated lower relapse risks with peripheral blood compared to bone marrow, but without a survival advantage.⁵ Consistent with clinical practice, recipients of haploidentical transplants were more likely to receive bone marrow and reduced intensity conditioning regimen. Therefore, we carefully addressed the effect of conditioning regimen intensity ($P=0.2$) and graft type ($P=0.6$) in the model for survival and found none. Nevertheless, it is plausible that the observed higher relapse risk associated with haploidentical transplantation may, in part, be attributed to the low-dose TBI, cyclophosphamide and fludarabine regimen, the predominant regimen for haploidentical transplants in the current analysis. As shown by others, we found that both acute and chronic GvHD were lower in recipients of haploidentical transplantation.⁵ The decreased risk of chronic GvHD, however, was restricted to the recipients of bone marrow graft. As the use of peripheral blood increases in haploidentical transplants, we will likely observe increased rates of chronic GvHD.⁵ This remains a significant consideration, particularly in the older patient where the morbidity and impact on quality of life associated with chronic GvHD can be significant.²³⁻²⁵

The current analysis has several limitations related to the use of data reported to an observation registry. First, we are unable to study donor choices and it is possible that some transplant centers prioritize the selection of a haploidentical donor. Second, we are unable to properly separate the effect of conditioning regimen and graft type, as these factors are confounded with donor type. Third, while every attempt was made to adjust for the observed difference in survival, there may be several unknown or unmeasured factors we could not consider. Finally, it should be noted that we did not observe a center effect, although fewer centers performed haploidentical transplants.

While the use of haploidentical transplantation with post-transplant cyclophosphamide is increasing rapidly, and several early studies suggest similar outcomes to patients transplanted with matched related or unrelated donors, it remains important to analyze outcomes in specific patient populations and diseases. In the current analysis, with its focus on patients aged 50 years or older with AML in first or second remission, we observed higher mortality after haploidentical compared to MUD transplantation with donors younger than 40 years. We acknowledge donor selection is ideally studied in the setting of a controlled clinical trial. However, the disparate availability of MUD and related haploidentical donors remains a challenge, and attempts to study outcomes of donor choice both retrospectively and prospectively may be necessary.

Funding

The CIBMTR is funded by Public Health Service Grant U24-CA076518 from the National Cancer Institute, the National Heart, Lung and Blood Institute and the National Institute of Allergy and Infectious Diseases; Grant U10HL069294 from National Cancer Institute, the National Heart, Lung and Blood Institute; contract HHS250201200016C with Health Resources and Services Administration; Grants N00014-15-1-0848 and N00014-16-

1-2020 from the Office of Naval Research. The views expressed in this article do not reflect the official policy or position of the National Institute of Health, the Department of the Navy, the Department of Defense, Health Resources and Services Administration or any other agency of the U.S. Government or Corporate Sponsor.

References

- O'Donnell PV, Luznik L, Jones RJ, et al. Nonmyeloablative bone marrow transplantation from partially HLA-mismatched related donors using posttransplantation cyclophosphamide. *Biol Blood Marrow Transplant.* 2002;8(7):377-386.
- Luznik L, O'Donnell PV, Symons HJ, et al. HLA-haploidentical bone marrow transplantation for hematologic malignancies using nonmyeloablative conditioning and high-dose, posttransplantation cyclophosphamide. *Biol Blood Marrow Transplant.* 2008;14(6):641-650.
- Brunstein CG, Fuchs EJ, Carter SL, et al. Alternative donor transplantation after reduced intensity conditioning: results of parallel phase 2 trials using partially HLA-mismatched related bone marrow or unrelated double umbilical cord blood grafts. *Blood.* 2011;118(2):282-288.
- Kasamon YL, Bolanos-Meade J, Prince GT, et al. Outcomes of Nonmyeloablative HLA-Haploidentical Blood or Marrow Transplantation With High-Dose Post-Transplantation Cyclophosphamide in Older Adults. *J Clin Oncol.* 2015;33(28):3152-3161.
- Bashey A, Zhang MJ, McCurdy SR, et al. Mobilized Peripheral Blood Stem Cells Versus Unstimulated Bone Marrow As a Graft Source for T-Cell-Replete Haploidentical Donor Transplantation Using Post-Transplant Cyclophosphamide. *J Clin Oncol.* 2017;35(26):3002-3009.
- Ciurea SO, Zhang MJ, Bacigalupo AA, et al. Haploidentical transplant with posttransplant cyclophosphamide vs matched unrelated donor transplant for acute myeloid leukemia. *Blood.* 2015;126(8):1033-1040.
- Versluis J, Labopin M, Ruggeri A, et al. Alternative donors for allogeneic hematopoietic stem cell transplantation in poor-risk AML in CR1. *Blood Adv.* 2017;1(7):477-485.
- Santoro N, Labopin M, Giannotti F, et al. Unmanipulated haploidentical in comparison with matched unrelated donor stem cell transplantation in patients 60 years and older with acute myeloid leukemia: a comparative study on behalf of the ALWP of the EBMT. *J Hematol Oncol.* 2018;11(1):55.
- Robinson TM, Fuchs EJ, Zhang MJ, et al. Related donor transplants: has posttransplantation cyclophosphamide nullified the detrimental effect of HLA mismatch? *Blood Adv.* 2018;2(11):1180-1186.
- Alousi AM, Le-Rademacher J, Saliba RM, et al. Who is the better donor for older hematopoietic transplant recipients: an older-aged sibling or a young, matched unrelated volunteer? *Blood.* 2013; 121(13):2567-2573.
- Kollman C, Spellman SR, Zhang MJ, et al. The effect of donor characteristics on survival after unrelated donor transplantation for hematologic malignancy. *Blood.* 2016;127(2):260-267.
- Przepiorka D, Weisdorf D, Martin P, et al. 1994 Consensus Conference on Acute GVHD Grading. *Bone Marrow Transplant.* 1995;15(6):825-828.
- Flowers ME, Kansu E, Sullivan KM. Pathophysiology and treatment of graft-versus-host disease. *Hematol Oncol Clin North Am.* 1999;13(5):1091-1112, viii-ix.
- Kaplan EL, Meier P. Nonparametric Estimation from Incomplete Observations. *J Am Stat Assoc.* 1958;53(282):457-481.
- Lin DY. Non-parametric inference for cumulative incidence functions in competing risks studies. *Stat Med.* 1997;16(8):901-910.
- Cox DR. Regression Models and Life-Tables. *J R Stat Soc Series B Stat Methodol.* 1972;34(2):187-220.
- Andersen PK, Klein JP, Zhang MJ. Testing for centre effects in multi-centre survival studies: a Monte Carlo comparison of fixed and random effects tests. *Stat Med.* 1999;18(12):1489-1500.
- Muffy L, Pasquini MC, Martens M, et al. Increasing use of allogeneic hematopoietic cell transplantation in patients aged 70 years and older in the United States. *Blood.* 2017;130(9):1156-1164.
- Pidala J, Lee SJ, Ahn KW, et al. Nonpermissive HLA-DPB1 mismatch increases mortality after myeloablative unrelated allogeneic hematopoietic cell transplantation. *Blood.* 2014;124(16):2596-2606.
- McCurdy SR, Zhang MJ, St Martin A, et al. Effect of donor characteristics on haploidentical transplantation with posttransplantation cyclophosphamide. *Blood Adv.* 2018;2(3):299-307.
- Eapen M, Brazauskas R, Hemmer M, et al. Hematopoietic cell transplant for acute myeloid leukemia and myelodysplastic syndrome: conditioning regimen intensity. *Blood Adv.* 2018;2(16):2095-2103.
- Scott BL, Pasquini MC, Logan BR, et al. Myeloablative Versus Reduced-Intensity Hematopoietic Cell Transplantation for Acute Myeloid Leukemia and Myelodysplastic Syndromes. *J Clin Oncol.* 2017;35(11):1154-1161.
- Sun CL, Francisco L, Baker KS, Weisdorf DJ, Forman SJ, Bhatia S. Adverse psychological outcomes in long-term survivors of hematopoietic cell transplantation: a report from the Bone Marrow Transplant Survivor Study (BMTSS). *Blood.* 2011;118(17):4723-4731.
- Sun CL, Kersey JH, Francisco L, et al. Burden of morbidity in 10+ year survivors of hematopoietic cell transplantation: report from the bone marrow transplantation survivor study. *Biol Blood Marrow Transplant.* 2013;19(7):1073-1080.
- Lee SJ, Logan B, Westervelt P, et al. Comparison of Patient-Reported Outcomes in 5-Year Survivors Who Received Bone Marrow vs Peripheral Blood Unrelated Donor Transplantation: Long-term Follow-up of a Randomized Clinical Trial. *JAMA Oncol.* 2016;2(12): 1583-1589.



Ferrata Storti Foundation

Allogeneic stem cell transplantation using HLA-matched donors for acute myeloid leukemia with deletion 5q or monosomy 5: a study from the Acute Leukemia Working Party of the EBMT

Xavier Poiré,¹ Myriam Labopin,^{2,3,4,5} Emmanuelle Polge,^{2,3,4,5} Edouard Forcade,⁶ Arnold Ganser,⁷ Liisa Volin,⁸ Mauricette Michallet,⁹ Didier Blaise,¹⁰ Ibrahim Yakoub-Agha,¹¹ Johan Maertens,¹² Carlos Richard Espiga,¹³ Jan Cornelissen,¹⁴ Jürgen Finke,¹⁵ Mohamad Mohty,^{2,3,4,5*} Jordi Esteve^{16*} and Arnon Nagler^{2,3,17*}

¹Section of Hematology, Cliniques Universitaires St-Luc, Brussels, Belgium; ²Acute Leukemia Working Party of the EBMT; ³Sorbonne Université, Paris, France; ⁴INSERM UMR 938, Paris, France; ⁵Service d'Hématologie, Hôpital Saint-Antoine, Paris, France; ⁶CHU Bordeaux, Hôpital Haut-Leveque, Pessac, France; ⁷Department of Hematology, Hemostasis, Oncology and Stem Cell Transplantation, Hannover Medical School, Hannover, Germany; ⁸HUCH Comprehensive Cancer Center, Stem Cell Transplantation Unit, Helsinki, Finland; ⁹Service d'Hématologie, Centre Hospitalier Lyon Sud, Lyon, France; ¹⁰Institut Paoli Calmette, Programme de Transplantation Thérapie Cellulaire, Marseille, France; ¹¹CHU de Lille, LIRIC INSERM U995, Université Lille2, Lille, France; ¹²University Hospital Gasthuisberg, Leuven, Belgium; ¹³Servicio de Hematologica-Hemoterapia, Hospital U. Marqués de Valdecilla, Santander, Spain; ¹⁴Department of Hematology, Erasmus MC Cancer Institute, Rotterdam, the Netherlands; ¹⁵Department of Medicine-Hematology-Oncology, University of Freiburg, Freiburg, Germany; ¹⁶Hematology Department, Hospital Clinic, Barcelona, Spain and ¹⁷Chaim Sheba Medical Center, Tel-Hashomer, Israel.

*MM, JE and AN contributed equally to this work.

Haematologica 2020
Volume 105(2):414-423

Correspondence:

XAVIER POIRÉ
xavier.poire@uclouvain.be

Received: January 7, 2019.

Accepted: April 24, 2019.

Pre-published: May 2, 2019.

doi:10.3324/haematol.2019.216168

Check the online version for the most updated information on this article, online supplements, and information on authorship & disclosures: www.haematologica.org/content/105/2/414

©2020 Ferrata Storti Foundation

Material published in Haematologica is covered by copyright. All rights are reserved to the Ferrata Storti Foundation. Use of published material is allowed under the following terms and conditions:

<https://creativecommons.org/licenses/by-nc/4.0/legalcode>.

Copies of published material are allowed for personal or internal use. Sharing published material for non-commercial purposes is subject to the following conditions:

<https://creativecommons.org/licenses/by-nc/4.0/legalcode>,

sect. 3. Reproducing and sharing published material for commercial purposes is not allowed without permission in writing from the publisher.



ABSTRACT

Deletion 5q or monosomy 5 (-5/5q-) in acute myeloid leukemia (AML) is a common high-risk feature that is referred to allogeneic stem cell transplantation. However, -5/5q- is frequently associated with other high-risk cytogenetic aberrations such as complex karyotype, monosomal karyotype, monosomy 7 (-7), or 17p abnormalities (abn(17p)), the significance of which is unknown. In order to address this question, we studied adult patients with AML harboring -5/5q- having their first allogeneic transplantation between 2000 and 2015. Five hundred and one patients with -5/5q- have been analyzed. Three hundred and thirty-eight patients (67%) were in first remission and 142 (28%) had an active disease at time of allogeneic transplantation. The 2-year probabilities of overall survival and leukemia-free survival were 27% and 20%, respectively. The 2-year probability of treatment-related mortality was 20%. We identified four different cytogenetic groups according to additional abnormalities with prognostic impact: -5/5q- without complex karyotype, monosomal karyotype or abn(17p), -5/5q- within a complex karyotype, -5/5q- within a monosomal karyotype and the combination of -5/5q- with abn(17p). In multivariate analysis, factors associated with worse overall survival and leukemia-free survival across the four groups were active disease, age, monosomal karyotype, and abn(17p). The presence of -5/5q- without monosomal karyotype or abn(17p) was associated with a significantly better survival rate while -5/5q- in conjunction with monosomal karyotype or abn(17p) translated into a worse outcome. The patients harboring the combination of -5/5q- with abn(17p) showed very limited benefit from allogeneic transplantation.

Introduction

Allogeneic stem cell transplantation (SCT) is a standard of care in patients with intermediate and high-risk acute myeloid leukemia (AML).^{1,2} High-risk AML is mainly defined by the presence of determined poor-risk cytogenetic abnormalities at diagnosis together with specific mutational events.³⁻⁶ In general, conventional post-remission high-dose chemotherapy is not capable of eradicating the leukemic-initiating stem-cell population of high-risk AML, harboring strong chemoresistance mechanisms,⁷ and only the potent graft-versus-leukemia (GvL) effect mediated by SCT may provide the capability to eradicate this cell population and overcome the poor prognosis of these high-risk AML subtypes, as previously demonstrated.^{2,8-10} Among the heterogeneous group of high-risk AML, prognosis can be further stratified based on specific genetic abnormalities, and the potential benefit of SCT differs among these diverse AML subtypes.¹¹ Monosomy 5 or deletion of the long arm of chromosome 5 (-5/5q) has been part of the definition of high-risk AML for many years.¹² Furthermore, monosomal karyotype (MK) described ten years ago referred to a cytogenetic risk category constantly associated with a very poor outcome.^{13,14} Within this subgroup, patients harboring a single monosomy, including monosomy 5, have a relatively better outcome than patients with two or more monosomies.¹⁵ We recently reported the outcome of SCT in 125 patients with AML and abnormalities of the short arm of chromosome 17 [abn(17p)] transplanted in first remission. The addition of -5/5q- to abn(17p) translated into a very bad outcome with a 2-year leukemia-free survival (LFS) of about 12%.¹⁶ The benefit of SCT in this subgroup appears very limited, which raises the question of the role of SCT in these patients. However, this observation was based on a limited number of patients and it was difficult to draw any conclusions as to whether the dismal outcomes were driven by -5/5q- itself or by the combination of -5/5q- with abn(17p) or TP53 mutations. In addition, the frequent association of -5/5q- with abn(17p) suggests co-operation between TP53 deletion/mutations and loss of putative tumor suppressor genes localized in the commonly deleted 5q region.¹⁷⁻¹⁹ However, -5/5q- is also well-represented in patients with MK and complex karyotype (CK) without abn(17p). The interaction observed between -5/5q- and abn(17p) in our previous dataset raised the question of the impact of other additional adverse cytogenetic abnormalities such as monosomy 7 or deletion 7q (-7/7q-), abn(17p), CK and MK on the outcomes of AML with -5/5q- after SCT, and this formed the rationale for our current retrospective study.

Methods

Patient selection and data collection

This is a retrospective registry-based analysis on behalf of the Acute Leukemia Working Party (ALWP) of the European Society for Blood and Marrow Transplantation (EBMT). The EBMT is a non-profit, scientific society representing more than 600 transplant centers, mainly in Europe, that are required to report all consecutive stem cell transplantations and their follow up once a year. Data are entered, managed and maintained in a central database with internet access; each EBMT center is represented in this database. Audits are routinely performed to determine

the accuracy of the data. Patients or legal guardians provide informed consent authorizing the use of their personal information for research purposes. The study was approved by the ALWP review board.

Eligibility criteria for the study included all patients >18 years with *de novo* or secondary AML transplanted between 1st January 2000 and 31st December 2015 from an HLA-matched sibling or a fully-matched (10/10) unrelated donor. Patients undergoing second transplantation, as well as patients receiving a haplo-identical or cord-blood transplantation, were excluded. We further selected patients harboring -5/5q- and having a full karyotype report within the database in order to study the prognostic effect of additional cytogenetic features. A total of 501 patients from 148 centers met the study inclusion criteria and have been selected for further analysis. Myeloablative conditioning (MAC) and reduced-intensity conditioning (RIC) have been defined elsewhere.²⁰

The following variables were selected and included in the analysis: year of transplantation, age, gender, white blood cell count (WBC) at diagnosis, number of induction courses to achieve complete remission (CR), status at transplantation, time from diagnosis to SCT, type of conditioning regimen, use of total body irradiation (TBI), *in vivo* T-cell depletion (including both anti-thymocyte globulins and alemtuzumab), cytomegalovirus (CMV) status of donor and recipient, donor type, source of stem cells, Karnofsky performance status (KPS) at transplantation, engraftment, presence of acute and chronic graft-versus-host disease (GvHD), and grade of acute GvHD. For the analysis of additional cytogenetic abnormalities, we included in our analysis the presence of abn(17p), -7/7q-, MK and CK classified according to cytogenetic status according to Medical Research Council UK criteria.⁵ MK has been defined according to Breems *et al.*,¹³ and CK was defined by the presence of >3 chromosomal abnormalities.

Statistical analysis and end point definitions

The primary end point was LFS. Secondary end points included relapse incidence (RI), non-relapse mortality (NRM), overall survival (OS), acute and chronic GvHD, and refined GvHD-free/relapse-free survival (GRFS). All outcomes were measured from the time of transplant. LFS was defined as survival without relapse; patients alive without relapse were censored at the time of last contact. OS was based on death from any cause. NRM was defined as death without previous relapse. GRFS was defined as survival without grade 3-4 acute GvHD, extensive chronic GvHD, relapse or death.²¹ Surviving patients were censored at the time of last contact. The probabilities of OS, LFS, and GRFS were calculated by the Kaplan-Meier test, and those of acute and chronic GvHD, NRM, and relapse by the cumulative incidence estimator to accommodate competing risks. For NRM, relapse was the competing risk, and for relapse, the competing risk was NRM. For acute and chronic GvHD, death without the event and relapse were the competing risks.

For all univariate analyses, continuous variables were categorized and the median value was used as a cut-off point. A Cox proportional hazards model was used for multivariate regression including factors associated with LFS in univariate analysis and individual cytogenetic abnormalities. Finally, we defined four groups according to the presence of CK, MK and the presence or not of individual cytogenetic abnormalities significantly associated with the outcome. Patients', disease and transplant-related characteristics for the four groups were compared by using χ^2 statistics for categorical variables and the Kruskal-Wallis test for continuous variables. Factors differing in distribution between the groups or conceptually important were included in the final Cox

model. We performed a first multivariate analysis including the following individual cytogenetics: *abn(11q23)*, *abn(17p)* and *-7/7q-*. Then, MK and CK were added to the same model and thereafter we performed a stepwise selection for the cytogenetics variables (P in/out = 0.10). *Abn 17p*, MK and CK remained in the Cox model for OS. *Abn 17p* and MK also remained in the Cox model for relapse, LFS and GRFS. The final Cox model contained all variables that were selected for at least one end point. Proportional hazards assumptions were checked systematically using the Grambsch-Therneau residual-based test. All interactions between cytogenetics groups and other co-variables were tested. Results were expressed as hazard ratio (HR) with 95% confidence interval (CI). Statistical analyses were performed with SPSS 24.0 (SPSS Inc., Chicago, IL, USA) and R 3.4.1 [R Core Team (2017). R: A language and environment for statistical computing. R Foundation for Statistical Computing, Vienna, Austria. URL: <https://www.R-project.org/>].

Results

Patients' characteristics

Patients' characteristics are summarized in Table 1. Five hundred and one patients met the study inclusion criteria. Median follow up was 57 months [Interquartile Range (IQR): 27-116 months] and median age was 55-years old (range: 18-75 years). The main MAC regimen was the combination of cyclophosphamide with TBI followed by cyclophosphamide and busulfan, or fludarabine and busulfan. The main RIC regimen was the association of fludarabine and busulfan, followed by fludarabine and low-dose TBI, or fludarabine and melphalan. The most frequent GvHD prophylaxis was the association of cyclosporine and methotrexate (44%) followed by cyclosporine and mycophenolate mofetil (29%). Additional cytogenetic abnormalities besides *-5/5q* are illustrated in Figure 1. The vast majority of the patients showed a CK (87%) and/or MK (67%) in combination with *-5/5q-*. Patients also showed frequent association with *abn(17p)* (39%) and *-7/7q-* (37%), although the vast majority of these additional cytogenetic features were observed in the context of a complex or monosomal karyotype. Very few patients presented with *abn(3q26)* ($n=22$) or *abn(11q23)* ($n=42$). Most of those adverse cytogenetic features were not present as a single additional abnormality but rather existed in combination.

Transplantation outcomes: relapse incidence, non-relapse mortality, leukemia-free survival, overall survival and graft-versus-host disease in the entire cohort

The 2-year cumulative incidence of relapse in the overall series was 59.9% (95%CI: 55.3-64.2) (Online Supplementary Figure S1A), and the median time to relapse was four months (IQR 0.2-130). In univariate analysis, a matched sibling donor (MSD), and the presence of additional cytogenetic abnormalities defined as CK, MK and *abn(17p)* were all associated with an increased RI (Table 2). The 2-year probability of NRM was 19.9% (95%CI: 16.4-23.7) (Online Supplementary Table S1B). NRM was strongly associated with donor type and disease status in univariate analysis. None of the additional cytogenetic events impacted NRM (Table 2).

The 2-year probability of LFS in this entire cohort was 20.2% (95% CI: 16.4-23.9) (Online Supplementary Figure

S1C). In univariate analysis, we found that younger age (< 55-year old), being in first complete remission (CR1), better KPS (>80%) and administration of MAC were all significantly associated with better LFS. CK, MK, *abn(17p)* and *-7/7q-* also impacted on LFS (Table 2). The 2-year OS was 27% (95%CI: 22.8-31.2) (Online Supplementary Figure S1D). Similarly to LFS, younger age (< 55-year old), being in CR1, better KPS (>80%) and administration of MAC led to better OS in univariate analysis. Notably, CK, MK, *abn(17p)* and *-7/7q-* impacted prognosis (Table 2).

The cumulative incidence of grade II-IV acute GvHD was 29.3% (95%CI: 25.2-33.4) and the 2-year cumulative incidence of chronic GvHD was 27.3% (95%CI: 23.2-31.5), leading to a 2-year probability of GRFS of 13.1% (95%CI: 10-16.3). In univariate analysis, the use of MUD and not being in remission at SCT were associated with a higher incidence of grade II-IV acute GvHD. In contrast, advanced disease status was associated with a lower risk of chronic GvHD, a fact probably due to the high risk of early relapse among patients not transplanted in remission. A female donor to a male recipient led to higher incidence of chronic GvHD in univariate analysis. The presence of additional cytogenetic abnormalities was not asso-

Table 1. Patients' characteristics from the entire cohort (n=501).

Median follow-up (range)	21 months (2-173)
Median age (range)	55 years (18-75)
Time from diagnosis to SCT (range)	5 months (0.1-24)
Median year of SCT (range)	2010 (2000-2015)
Disease status at SCT, N (%)	
CR1	338 (68%)
CR2/CR3	21 (4%)
Active disease	142 (28%)
Secondary AML, N (%)	104 (21%)
Donor type, N (%)	224/277 (45%/55%)
MSD/MUD	
Patients' gender, N (%)	271/230 (54%/46%)
MF	
Female donor to male recipient, N (%)	92 (19%)
KPS \geq 80%, N (%)	447 (94%)
Patient CMV positive, N (%)	314 (64%)
Donor CMV positive, N (%)	254 (52%)
Conditioning intensity, N (%)	
MAC/RIC	223/278 (45%/55%)
Missing	2
Conditioning regimen, N (%)	
Busulfan-based	225 (45%)
TBI-based	139 (28%)
Fludarabine-Busulfan	143 (29%)
Fludarabine Melphalan	40 (8%)
Stem cell source, N (%)	
BM/PB	82/419 (16%/84%)
<i>In vivo</i> TCD, N (%)	282 (57%)
ATG	246 (49%)
Alemtuzumab	36 (7%)
Missing	7

SCT: allogeneic stem cell transplantation; N: number; CR1: first remission; CR2: second remission; CR3: third remission; AML: acute myeloid leukemia; MSD: matched sibling donor; MUD: matched unrelated donor; M: male; F: female; KPS: Karnofsky's performance status; CMV: cytomegalovirus; MAC: myeloablative conditioning regimen; RIC: reduced-intensity conditioning regimen; BM: bone marrow; PB: peripheral blood; TCD: Tcell depletion; ATG: anti-thymocyte globulin.

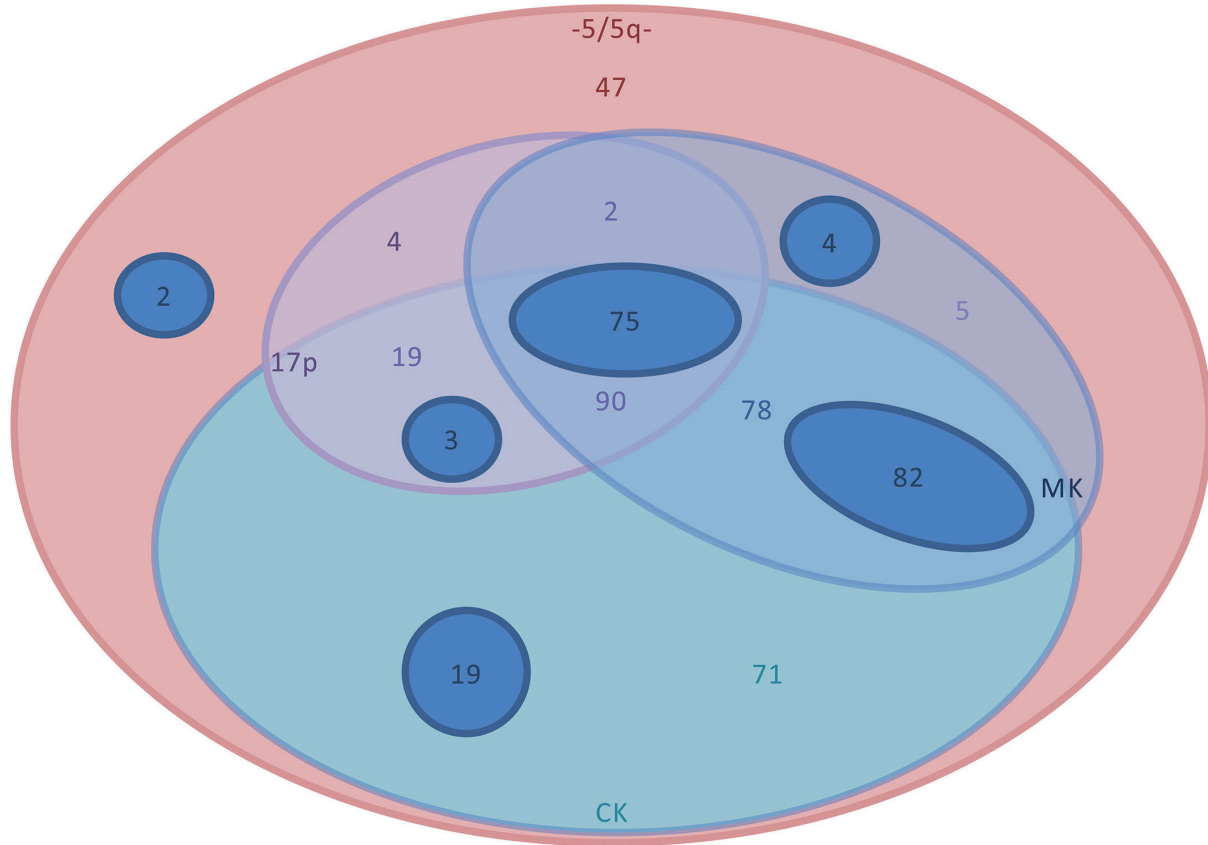


Figure 1. Additional cytogenetic abnormalities. Distribution of additional cytogenetic abnormalities. Only 47 patients harbored -5/5q- without -7/7q-, CK, MK or abn(17p). The vast majority of the patients showed a CK (87%) and/or MK (67%) in combination with -5/5q-. The main groups were the combination of CK, MK and abn(17p), the association of MK and CK and the patients with CK. The dark blue circles illustrate patients with -7/7q- among the different cytogenetic groups.

Table 2. Univariate analysis of additional cytogenetic abnormalities.

	2y (% , 95%CI)	RI	P	NRM	P	LFS	P	OS	P	GRFS	P
	2y (% , 95%CI)			2y (% , 95%CI)		2y (% , 95%CI)		2y (% , 95%CI)		2y (% , 95%CI)	
CK											
Yes	62 (57-67)		0.004	20 (16-24)	0.7	18 (14-21)	0.0007	22 (18-27)	<0.0001	11 (8-14)	0.001
No	44 (31-56)			19 (11-30)		37 (25-49)		56 (44-69)		26 (15-37)	
MK											
Yes	64 (57-69)		0.0004	20 (15-24)	0.56	16 (12-20)	0.0001	22 (17-27)	0.0003	10 (7-14)	0.002
No	51 (43-59)			21 (15-28)		28 (21-36)		38 (30-46)		19 (13-26)	
Abn(17p)											
Yes	66 (58-72)		0.02	22 (16-28)	0.44	13 (8-18)	<0.0001	16 (11-22)	<0.0001	7 (3-10)	0.0002
No	56 (50-62)			19 (15-24)		25 (20-30)		34 (28-39)		17 (13-22)	
-7/7q-											
Yes	62 (54-68)		0.28	22 (16-28)	0.36	17 (11-22)	0.02	20 (14-26)	0.002	10 (6-14)	0.01
No	59 (53-64)			19 (15-24)		22 (17-27)		31 (26-37)		15 (11-19)	
Abn3q26											
Yes	68 (37-87)		0.23	15 (3-35)	0.92	16 (0-35)	0.24	13 (0-29)	0.16	19 (0-38)	0.73
No	60 (55-64)			20 (17-24)		20 (17-24)		28 (23-32)		13 (10-16)	
Abn11q23											
Yes	54 (37-69)		0.42	19 (8-34)	0.95	26 (12-41)	0.21	35 (18-51)	0.18	19 (7-32)	0.04
No	60 (56-65)			20 (16-24)		20 (16-23)		26 (22-30)		13 (9-16)	0.04

CK: complex karyotype; MK: monosomal karyotype; abn(17p): 17p abnormalities; -7/7q-: monosomy 7 or deletion 7q; abn3q26: abnormalities of chromosome 3q26; abn11q2: abnormalities of 11q2; RI: relapse incidence; 2y: 2 years; CI: confidence interval; NRM: non-relapse mortality; LFS: leukemia-free survival; OS: overall survival; GRFS: graft-versus-host disease and relapse-free survival.

ciated with the risk of developing acute or chronic GvHD. The factors associated with GRFS were the same as those described for LFS and OS (see above and Table 2). The main cause of death was disease-related (61%), followed by infections (16%) and GvHD (13%).

The multivariate analysis performed in the entire cohort confirmed the strong impact of disease status at the time of transplantation on RI, NRM, LFS and OS (*Online Supplementary Table S1*). Increasing age was associated with higher NRM, which translated into significantly worse LFS and OS without impacting RI. The use of MUD was associated with higher NRM with no effect on OS. A good performance status at SCT was associated with less relapse and improved LFS and OS. Conditioning intensity did not impact any SCT outcome parameters in multivariate

analysis. While active disease at SCT and MUD were associated with higher incidence of grade II-IV GvHD, no factor was associated with chronic GvHD in multivariate analysis (*Online Supplementary Table S2*). In our stepwise selection of cytogenetic variables (as described in the methods), *-7/7q-* lost any significance on outcomes and we kept only CK, MK and *abn(17p)* in our final multivariate model. There was a significant correlation between *Abn(17p)* and decreased LFS, OS and GRFS.

Outcomes by cytogenetic subgroups

In order to elucidate the impact of additional cytogenetic abnormalities on outcomes of patients with AML and *-5/5q-*, we defined four different subgroups within our entire cohort in a hierarchical manner according to the

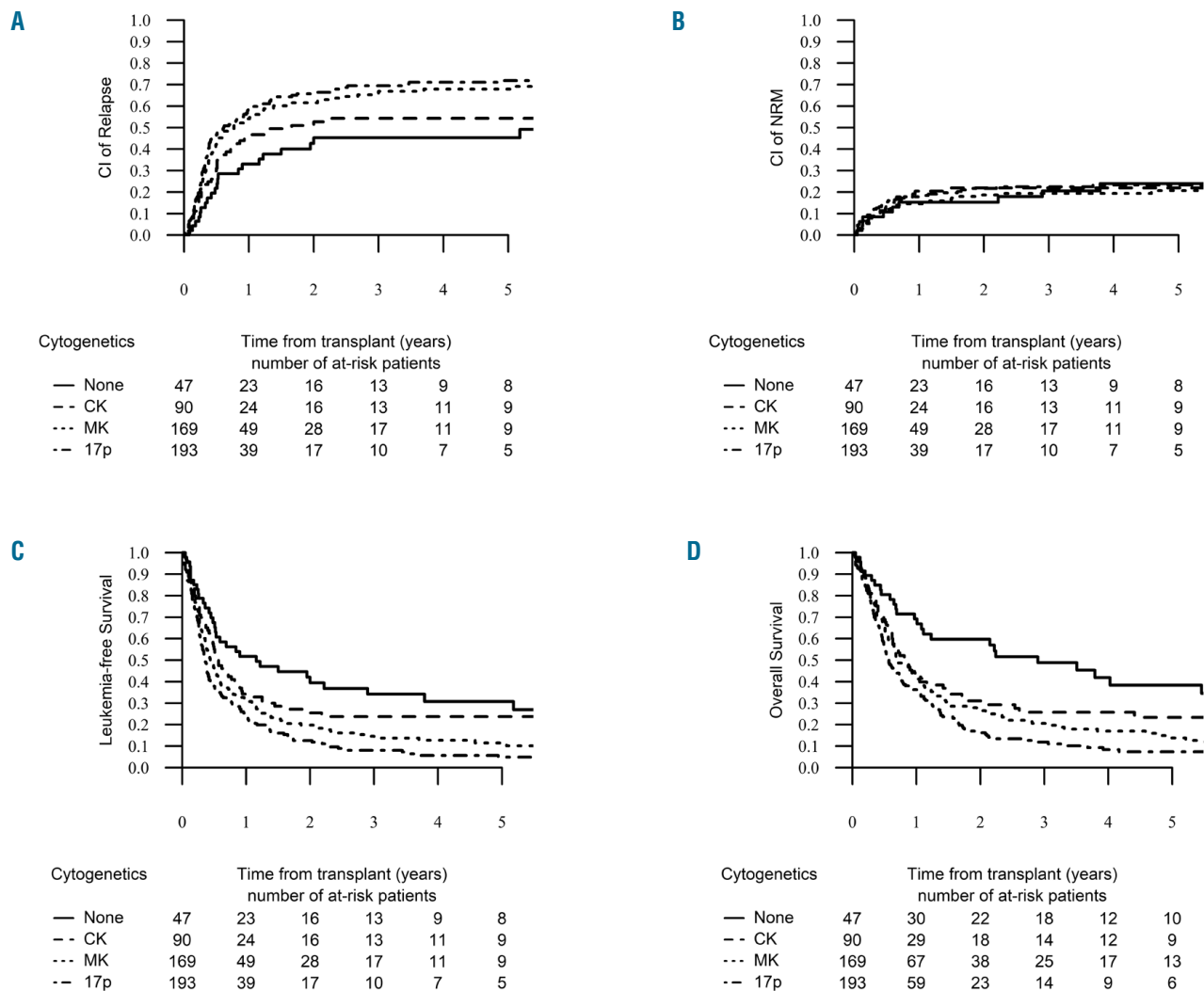


Figure 2. Relapse incidence (RI), non-relapse mortality (NRM), leukemia-free survival (LFS) and overall survival (OS) by cytogenetic groups. The 2-year cumulative incidence of relapse increased significantly from the “none group” up to the “*abn(17p)* group”, reaching 45.3% [95% CI: 29.9-59.5], 52.7% [95% CI: 40.9-63.1], 61.5% [95% CI: 53.5-68.6] and 65.7% [95% CI: 58.1-72.3] in the none, CK, MK and *abn(17p)* groups, respectively ($P=0.006$) (A). The 2-year probability of NRM was similar across the four groups, reaching 19.9% [95% CI: 16.4-23.7] ($P=0.86$) (B). The 2-year probability of LFS was 39.4% [95% CI: 24.8-54] for the “none group”, 25.4% [95% CI: 15.6-35.3] for the “CK group”, 19.8% [95% CI: 13.5-26.1] for the “MK group” and 12.6% [95% CI: 7.5-17.7] for the “*abn(17p)* group” ($P<0.001$) (C). The 2-year probability of OS decreased significantly from the “none group” down to the “*abn(17p)* group”, reaching 59.7% [95% CI: 45.2-74.2], 31% [95% CI: 20.5-41.6], 26.5% [95% CI: 19.4-33.5] and 16.3% [95% CI: 10.5-22] in each group respectively ($P<0.001$) (D).

presence of CK, MK and abn(17p), based on their prognostic impact shown in univariate and multivariate analysis and their capability to distinguish biologically and clinically meaningful cytogenetic categories. Our study contains 154 monosomy 5 and 347 deletion 5q. We decided to

study -5 and 5q- together in order to analyze the impact of MK separately from -5. Indeed, all of our -5 patients except one fulfilled the definition of MK. Thus, the “5q sole group” contained 47 patients with 5q abnormalities but absence of additional -7/7q-, abn(17p), CK or MK. Notably, no case of -5 was included in this group. The “CK group” included 90 patients who fulfilled the definition of CK but without abn(17p) or MK. Only one patient with -5 was included in this group. The “MK group” was comprised of the group of patients with -5/5q- within a MK with the exception of abn(17p), and finally, the “abn(17p) group” encompassed the combination of -5/5q- with abn(17p) regardless of the presence of other cytogenetic features. Due to the lack of significance of -7/7q- in our multivariate analysis, this abnormality was not taken into account in our prognostic classification. Patients’ characteristics were well balanced between those four cytogenetic subgroups (*Online Supplementary Table S3*). The 2-year probability of NRM was similar across the four groups ($P=0.86$), but the 2-year cumulative incidence of relapse increased significantly from the “5q sole” up to the “abn(17p)” group, reaching 45.3% (95%CI: 29.9-59.5), 52.7% (95%CI: 40.9-63.1), 61.5% (95%CI: 53.5-68.6) and 65.7% (95%CI: 58.1-72.3) in the 5q sole, CK, MK and abn(17p) groups, respectively ($P=0.006$) (Figure 2A and B). Median time to relapse was 6.2 months (IQR: 3.5-16.3), for the “5q sole group”, 4.7 months (IQR: 2.3-8) for the “CK group”, 4.5 months (IQR: 2.3-9.1) for the “MK group” and 3.9 months (IQR: 2.2-8.7) for the “abn(17p) group” ($P=0.12$). This different RI across cytogenetic subgroups also determined other important outcomes. Thus, the 2-year probability of LFS was 39.4% (95%CI: 24.8-54) for the “5q sole group”, 25.4% (95%CI: 15.6-35.3) for the “CK group”, 19.8% (95%CI: 13.5-26.1) for the “MK group” and 12.6% (95%CI: 7.5-17.7) for the “abn(17p) group” ($P<0.001$) (Figure 2C). The 2-year probability of OS also decreased significantly from the “5q sole group” down to the “abn(17p) group”, reaching 59.7% (95% CI: 45.2-74.2, 31% [95% CI: 20.5-41.6], 6.5% [95% CI: 19.4-33.5] and 16.3% [95% CI: 10.5-22] in each group, respectively ($P<0.001$) (Figure 2D). The 2-year probability of GRFS followed the same trend, with 26.5% [95% CI: 13-39.9] for the “5q sole group”, 17% [95% CI: 8.5-25.4] for the “CK group”, 14.2% [95% CI: 8.7-19.7] for the “MK group” and only 6.6% [95% CI: 2.8-10.4] for the “abn(17p) group” ($P<0.001$) (*Online Supplementary Figure S2*). In contrast, the cumulative incidence of grade II-IV acute GvHD and the 2-year cumulative incidence of chronic GvHD were not different across the four groups ($P=0.33$ and $P=0.8$, respectively).

In multivariate analysis, taking the “5q sole group” as a reference, the “CK group” did not show any significant difference in RI, NRM, LFS, OS, LFS and GRFS. In contrast, patients in the “MK group” and “abn(17p) group” experienced higher incidence of RI and lower LFS, OS and GRFS compared to the “5q sole group” (Table 3). To minimize the strong impact of disease status on outcome, we decided to run the univariate by cytogenetic subgroups focusing on the 338 patients transplanted in CR1. The “MK group” and “abn(17p) group” had the same negative impact on RI, LFS and OS (Figure 3). As detailed above, the presence of -7/7q- was excluded from the “5q sole group”, but was present in 21% of the “CK group”, 51% of the “MK group”, and 40% of the “abn(17p) group”. Given the high overlap between the -7/7q and the “MK

Table 3. Multivariate analysis using a Cox proportional hazard model by cytogenetic subgroups. Only variables with a $P<0.05$ in univariate analysis.

	P	HR	95% CI
RI			
Age (per 10 year)	0.65	1.03	0.91-1.16
MUD vs. MSD	0.44	0.91	0.71-1.16
Active disease vs. CR	<0.0001	1.73	1.32-2.27
KPS \geq 80%	0.06	0.64	0.40-1.01
RIC vs. MAC	0.11	1.25	0.95-1.63
5q sole (reference)		1	
CK	0.67	1.12	0.66-1.91
MK	0.02	1.74	1.09-2.8
Abn(17p)	0.002	2.11	1.32-3.37
NRM			
Age (per 10 year)	0.0007	1.48	1.18-1.85
MUD vs. MSD	0.001	2.07	1.32-3.25
Active disease vs. CR	0.002	2.00	1.3-3.08
KPS \geq 80%	0.22	0.61	0.27-1.35
RIC vs. MAC	0.23	0.76	0.48-1.19
5q sole (reference)		1	
CK	0.96	1.02	0.46-2.26
MK	0.63	1.19	0.58-2.47
Abn(17p)	0.22	1.55	0.76-3.14
LFS			
Age (per 10 year)	0.03	1.12	1.01-1.25
MUD vs. MSD	0.35	1.11	0.90-1.36
Active disease vs. CR	<0.0001	1.8	1.43-2.27
KPS \geq 80%	0.03	0.64	0.43-0.96
RIC vs. MAC	0.44	1.1	0.87-1.38
5q sole (reference)		1	
CK	0.7	1.09	0.70-1.69
MK	0.03	1.57	1.05-2.33
Abn(17p)	0.001	1.93	1.30-2.84
OS			
Age (per 10 year)	0.006	1.16	1.04-1.3
MUD vs. MSD	0.24	1.14	0.92-1.41
Active disease vs. CR	<0.0001	1.88	1.49-2.38
KPS \geq 80%	0.04	0.66	0.44-0.98
RIC vs. MAC	0.46	1.09	0.86-1.38
5q sole (reference)		1	
CK	0.25	1.31	0.83-2.08
MK	0.006	1.80	1.19-2.72
Abn(17p)	0.0002	2.19	1.45-3.30
GRFS			
Age (per 10 year)	0.08	1.14	1.04-1.26
MUD vs. MSD	0.18	1.15	0.94-1.41
Active disease vs. CR	<0.0001	1.64	1.31-2.04
KPS \geq 80%	0.06	0.68	0.46-1.01
RIC vs. MAC	0.77	1.03	0.82-1.3
5q sole (reference)		1	
CK	0.14	1.37	0.90-2.09
MK	0.008	1.69	1.15-2.48
Abn(17p)	0.0003	2.03	1.39-2.98

HR: hazard ratio; CI: confidence interval; RI: relapse incidence; MUD: matched unrelated donor; MSD: matched sibling donor; CR: complete remission; KPS: Karnofsky's performance status; RIC: reduced-intensity conditioning; MAC: myeloablative conditioning; abn(17p): 17p abnormalities; CK: complex karyotype; MK: monosomal karyotype; NRM: non-relapse mortality; LFS: leukemia-free survival; OS: overall survival; GRFS: graft-versus-host and relapse-free survival.

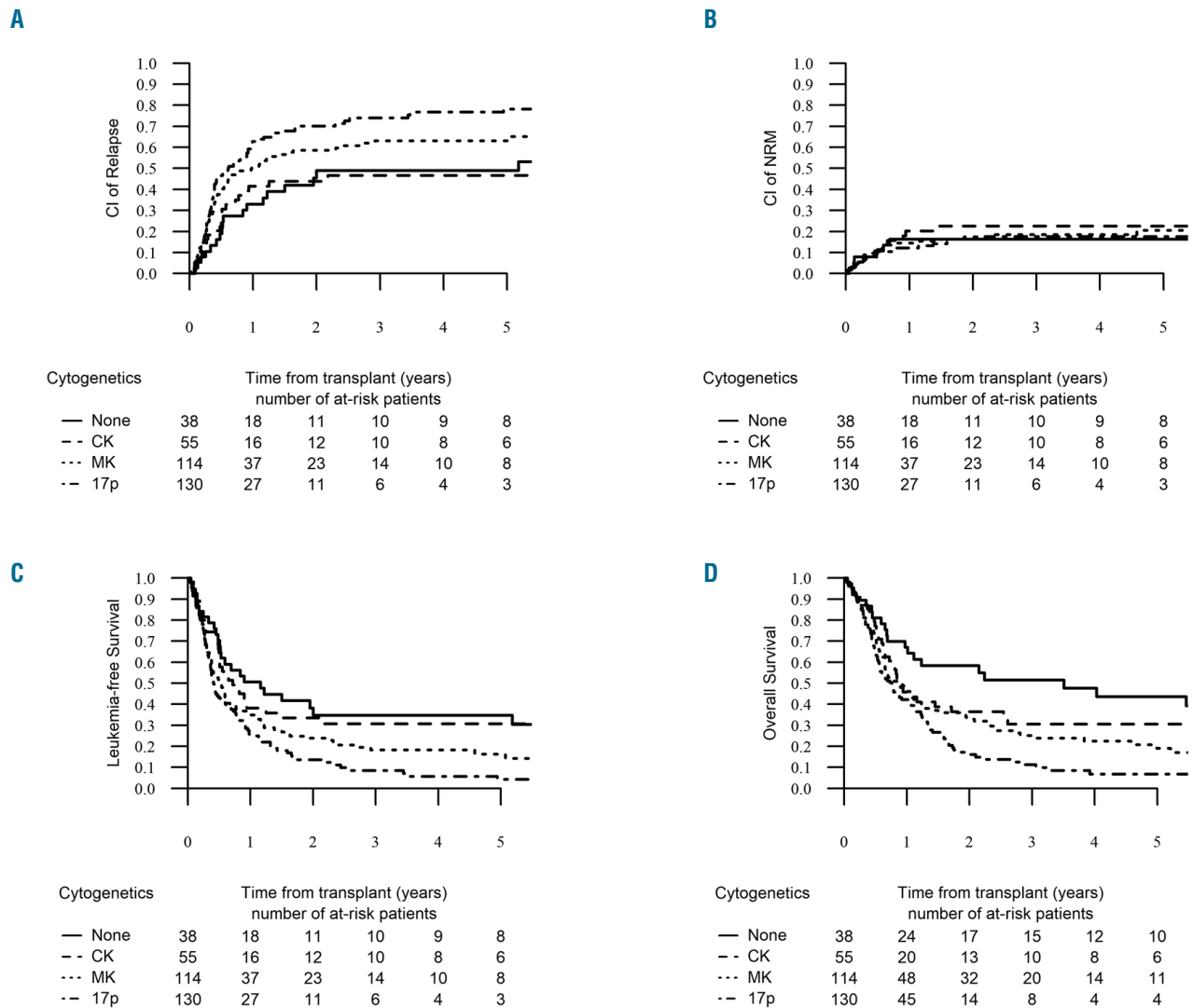


Figure 3. Relapse incidence (RI), non-relapse mortality (NRM), leukemia-free survival (LFS) and overall survival (OS) by cytogenetic groups in patients in first remission. The 2-year cumulative incidence of relapse increased significantly from the “none group” up to the “abn(17p) group”, reaching 48.9% [95% CI: 30.9-64.7], 43.9% [95% CI: 29.6-57.4], 58.7% [95% CI: 48.7-67.4] and 70.1% [95% CI: 60.6-77.8] in the none, CK, MK and abn(17p) groups, respectively ($P=0.006$) (A). The 2-year probability of NRM was similar across the four groups, reaching 19.9% [95% CI: 16.4-23.7] ($P=0.87$) (B). The two-year probability of LFS was 34.7% [95% CI: 18.6-50.9] for the “none group”, 33.5% [95% CI: 19.9-47] for the “CK group”, 23.9% [95% CI: 15.7-32] for the “MK group” and 13.6% [95% CI: 7-20.2] for the “abn(17p) group” ($P<0.001$) (C). The 2-year probability of OS decreased significantly from the “none group” down to the “abn(17p) group”, reaching 58.5% [95% CI: 42.3-74.6], 36.5% [95% CI: 22.6-50.3], 33% [95% CI: 23.9-42] and 16.1% [95% CI: 8.9-23.3] in each group, respectively ($P<0.001$) (D).

group”, we then performed a univariate analysis within the “MK group” comparing the outcome between patients with presence or absence of additional -7/7q- and did not find any significant impact on RI, NRM, LFS, OS and GRFS. We also looked at the impact of MK within the “abn(17p)”; MK lost its negative impact in this very high-risk subgroup, even though the group of abn(17p) patients without MK was rather small ($n=26$) (*data not shown*).

Discussion

-5/5q- is a common finding in AML, consistently associated with poor outcomes after standard chemotherapy with long-term overall survival of about 5%.^{5,22} SCT has

been shown to significantly improve the outcome of high-risk AML subsets, with a probability of disease cure in the range of 40%.^{1,8,9,23} Nonetheless, in our large cohort of 501 AML patients harboring -5/5q- undergoing first SCT, the 2-year probability of OS and LFS was only 27% and 20%, respectively, outcomes which clearly appear inferior to those reported for other high-risk cytogenetic AML,⁸ suggesting an independent deleterious effect of -5/5q- on transplant outcome. Indeed, in the EBMT registry, we found 3,021 patients with adverse cytogenetics according to the MRC classification with the exception of -5/5q-, and we found a 2-year OS and LFS of 43% and 37%, respectively. In contrast, our results resemble those of patients with MK AML.²⁴⁻²⁶ Indeed, most of the patients in our cohort harbored additional adverse cyto-

genetic features, such as MK (67%), which may have been confounded with the true impact of -5/5q-. Moreover, inferior outcomes of this cohort may also be explained by the fact that about 30% of our patients had active disease at the time of SCT, which appears, as expected, to be a strong predictor for worse outcomes in multivariate analysis.⁸ Nevertheless, even when focusing on patients in CR1, the observed outcomes in the current cohort are still in the range of 25% at two years, suggesting that our population represents a higher-risk group. Not surprisingly, younger age and a better performance status were both associated with better OS and LFS in line with previously published data,^{1,27,28} but this observation should be weighed against the underlying selection bias inherent in such a registry-based study. Conditioning intensity lost all impact on outcomes in multivariate analysis. This observation has been confirmed in other studies where the benefit of conditioning intensity was lost in chemorefractory disease, such as MK AML and those involving TP53 deregulation.^{26,29}

The main objective of our study was to evaluate the impact of additional cytogenetic abnormalities in a cohort of AML patients with -5/5q-. The presence of -5/5q- is rarely an isolated event in AML as it is frequently associated with other adverse cytogenetic features, such as CK, MK, -7/7q- or abn(17p).^{5,22,30} The independent impact of -5/5q- was questioned by Breems *et al.* in the first report on MK, in which any single monosomy carried a better outcome than the full definition of MK,^{13,15,31} with no specific effect for -5/5q-. More recently, Middeke *et al.* described 236 high-risk AML patients after SCT, and found that -5/5q- was associated with worse outcomes compared to CK and/or MK AML, and that abn(17p) translated into the worst survival after SCT.³² Those data suggested that the bad prognosis of MK AML after SCT was mainly related to the presence of -5/5q- and/or abn(17p), but these observations have not been completely confirmed by others.^{15,33} In our multivariate Cox model, we found that either the presence of MK or abn(17p) were both significantly associated with worse OS and LFS, while CK and -7/7q- had no impact on any outcome parameter. Most of those additional cytogenetic abnormalities and/or characteristics are typically not present as a single additional event to -5/5q- (Figure 1) making it difficult to weigh the impact of each individual additional event. To avoid the confounding effect of largely overlapping cytogenetic categories, we decided to define four well-delimited groups based on a hierarchical prognostic effect of MK and additional abn(17p) in -5/5q- AML: the “5q sole group”, “CK group”, “MK group”, and “abn(17p) group”. These cytogenetic categorizations allowed us to confirm the strong deleterious prognostic effect of additional MK and abn(17p) in this entity in multivariate analysis. In contrast, we did not observe differences in any outcome parameters between the “5q sole group” and the “CK group” with a relatively better 2-year OS (close to 40% for patients transplanted in CR1). The additional cytogenetic abnormalities found in both of those groups could only be numerical abnormalities and some structural abnormalities. The weaker prognostic impact of numerical abnormalities such as trisomy has already been suggested in other studies.^{13,34} On the contrary, the

presence of -5/5q- within MK is translated into worse LFS and OS, which is in agreement with most published data,^{24,33} but different from the report from Middeke *et al.*³² Finally, we confirmed the deleterious effect on outcomes of the combination of -5/5q- with any abn(17p), which has been suggested from our previous dataset.¹⁶ The impact of abn(17p) clearly appears stronger than MK, as MK did not impact outcomes within the “abn(17p)” group.

Patients with -5/5q- AML in CR1 without MK and/or abn(17p) appear to benefit from allogeneic SCT, with long-term survival achieved in more than 40% of the patients. In contrast, patients harboring the combination of -5/5q- with abn(17p) represent a very poor subgroup due to an intrinsic and well-known chemoresistance and to a potential lack of sensitivity to a GvL effect.¹⁶ If SCT remains the only option for those high-risk patients in CR1, it should be integrated into a post-transplant intervention program including low-dose decitabine,³⁵ prophylactic donor leukocyte infusions,^{36,37} a combination of both or other P53-independent therapeutic agents. Lenalidomide has been shown to have a specific effect on myelodysplastic syndrome (MDS) with isolated 5q- through inhibition of the 5q- clone, leading to 60% hematologic response and 40% cytogenetic response.³⁸⁻⁴⁰ However, responses have been much lower in patients with higher-risk MDS and AML, especially if harboring CK or MK.³⁸ Combinations with standard chemotherapy or hypomethylating agents are associated with objective responses even in patients harboring high-risk features^{38,41} with the exception of TP53 mutated clones.^{42,43} Another option might be to integrate lenalidomide as maintenance therapy after SCT, but previous experiences raised serious concerns about an increased risk of acute GvHD.^{44,45} However, interesting results from the combination of lenalidomide and azacytidine have been recently published.⁴⁶

In conclusion, our study, based on a large cohort of patients with AML and -5/5q- undergoing SCT, showed that this strategy led to long-term survival in about 20% of the patients, which seems inferior to other high-risk AML subsets. One of the largest limitations in this study might be the lack of centralized cytogenetic analysis and the selection of patients with an available full cytogenetic report; an essential requirement for the proposed analysis. Active disease at the time of SCT remains the strongest prognostic factor of worse survival and precautions have to be taken when bridging these patients to SCT. Novel therapeutic pre-transplant strategies must be developed to increase the proportion of patients in remission before SCT. Finally, we found that the benefit from SCT in this cytogenetic entity is highly dependent on the presence of particular additional adverse cytogenetic features. Indeed, patients without MK or abn(17p) benefit the most from SCT, whereas the additional presence of MK and/or abn(17p) leads to a very poor outcome. SCT is therefore questionable in this subgroup of patients with the current standard approach, especially if they are not in CR1 at the time of SCT. Development of pre-transplant and post-transplant pharmacological and immunological interventions to sustain a response in a larger proportion of patients is urgently needed in these patients.

References

1. Cornelissen JJ, van Putten WL, Verdonck LF, et al. Results of a HOVON/SAKK donor versus no-donor analysis of myeloablative HLA-identical sibling stem cell transplantation in first remission acute myeloid leukemia in young and middle-aged adults: benefits for whom? *Blood*. 2007;109(9):3658-3666.
2. Koreth J, Schlenk R, Kopecky KJ, et al. Allogeneic stem cell transplantation for acute myeloid leukemia in first complete remission: systematic review and meta-analysis of prospective clinical trials. *JAMA*. 2009;301(22):2349-2361.
3. Dohner H, Estey EH, Amadori S, et al. Diagnosis and management of acute myeloid leukemia in adults: recommendations from an international expert panel, on behalf of the European LeukemiaNet. *Blood*. 2010;115(3):453-474.
4. Dohner H, Weisdorf DJ, Bloomfield CD. Acute Myeloid Leukemia. *N Engl J Med*. 2015;373(12):1136-1152.
5. Grimwade D, Hills RK, Moorman AV, et al. Refinement of cytogenetic classification in acute myeloid leukemia: determination of prognostic significance of rare recurring chromosomal abnormalities among 5876 younger adult patients treated in the United Kingdom Medical Research Council trials. *Blood*. 2010;116(3):354-365.
6. Grimwade D, Ivey A, Huntly BJ. Molecular landscape of acute myeloid leukemia in younger adults and its clinical relevance. *Blood*. 2016;127(1):29-41.
7. Schoch C, Kern W, Kohlmann A, et al. Acute myeloid leukemia with a complex aberrant karyotype is a distinct biological entity characterized by genomic imbalances and a specific gene expression profile. *Genes Chromosomes Cancer*. 2005;43(3):227-238.
8. Schlenk RF, Dohner K, Mack S, et al. Prospective evaluation of allogeneic hematopoietic stem-cell transplantation from matched related and matched unrelated donors in younger adults with high-risk acute myeloid leukemia: German-Austrian trial AMLHD98A. *J Clin Oncol*. 2010;28(30):4642-4648.
9. Stelljes M, Beelen DW, Braess J, et al. Allogeneic transplantation as post-remission therapy for cytogenetically high-risk acute myeloid leukemia: landmark analysis from a single prospective multicenter trial. *Haematologica*. 2011;96(7):972-979.
10. Versluis J, Hazenberg CL, Passweg JR, et al. Post-remission treatment with allogeneic stem cell transplantation in patients aged 60 years and older with acute myeloid leukaemia: a time-dependent analysis. *Lancet Haematol*. 2015;2(10):e427-e436.
11. Ferrant A, Labopin M, Frasson F, et al. Karyotype in acute myeloblastic leukemia: prognostic significance for bone marrow transplantation in first remission: a European Group for Blood and Marrow Transplantation study. *Acute Leukemia Working Party of the European Group for Blood and Marrow Transplantation (EBMT)*. *Blood*. 1997;90(8):2931-2938.
12. Grimwade D, Walker H, Oliver F, et al. The importance of diagnostic cytogenetics on outcome in AML: analysis of 1,612 patients entered into the MRC AML 10 trial. The Medical Research Council Adult and Children's Leukaemia Working Parties. *Blood*. 1998;92(7):2322-2333.
13. Breems DA, Van Putten WL, De Greef GE, et al. Monosomal karyotype in acute myeloid leukemia: a better indicator of poor prognosis than a complex karyotype. *J Clin Oncol*. 2008;26(29):4791-4797.
14. Haferlach C, Alpermann T, Schnittger S, et al. Prognostic value of monosomal karyotype in comparison to complex aberrant karyotype in acute myeloid leukemia: a study on 824 cases with aberrant karyotype. *Blood*. 2012;119(9):2122-2125.
15. Jang JE, Min YH, Yoon J, et al. Single monosomy as a relatively better survival factor in acute myeloid leukemia patients with monosomal karyotype. *Blood Cancer J*. 2015;5:e358.
16. Poiré X, Labopin M, Maertens J, et al. Allogeneic stem cell transplantation in adult patients with acute myeloid leukaemia and 17p abnormalities in first complete remission: a study from the Acute Leukemia Working Party (ALWP) of the European Society for Blood and Marrow Transplantation (EBMT). *J Hematol Oncol*. 2017;10(1):20.
17. Castro PD, Liang JC, Nagarajan L. Deletions of chromosome 5q13.3 and 17p loci cooperate in myeloid neoplasms. *Blood*. 2000;95(6):2138-2143.
18. Kulasekararaj AG, Smith AE, Mian SA, et al. TP53 mutations in myelodysplastic syndrome are strongly correlated with aberrations of chromosome 5, and correlate with adverse prognosis. *Br J Haematol*. 2013;160(5):660-672.
19. Stoddart A, Fernald AA, Wang J, et al. Haploinsufficiency of del(5q) genes, Egr1 and Apc, cooperate with Tp53 loss to induce acute myeloid leukemia in mice. *Blood*. 2014;123(7):1069-1078.
20. Bacigalupo A, Ballen K, Rizzo D, et al. Defining the intensity of conditioning regimens: working definitions. *Biol Blood Marrow Transplant*. 2009;15(12):1628-1633.
21. Ruggeri A, Labopin M, Ciceri F, et al. Definition of GvHD-free, relapse-free survival for registry-based studies: an ALWP-EBMT analysis on patients with AML in remission. *Bone Marrow Transplant*. 2016;51(4):610-611.
22. Byrd JC, Mrozek K, Dodge RK, et al. Pretreatment cytogenetic abnormalities are predictive of induction success, cumulative incidence of relapse, and overall survival in adult patients with de novo acute myeloid leukemia: results from Cancer and Leukemia Group B (CALGB 8461). *Blood*. 2002;100(13):4325-4336.
23. Slovák ML, Kopecky KJ, Cassileth PA, et al. Karyotypic analysis predicts outcome of preremission and postremission therapy in adult acute myeloid leukemia: a Southwest Oncology Group/Eastern Cooperative Oncology Group Study. *Blood*. 2000;96(13):4075-4083.
24. Brands-Nijenhuis AV, Labopin M, Schouten HC, et al. Monosomal karyotype as an adverse prognostic factor in patients with acute myeloid leukemia treated with allogeneic hematopoietic stem-cell transplantation in first complete remission: a retrospective survey on behalf of the ALWP of the EBMT. *Haematologica*. 2016;101(2):248-255.
25. Cornelissen JJ, Breems D, van Putten WL, et al. Comparative analysis of the value of allogeneic hematopoietic stem-cell transplantation in acute myeloid leukemia with monosomal karyotype versus other cytogenetic risk categories. *J Clin Oncol*. 2012;30(17):2140-2146.
26. Poiré X, Labopin M, Cornelissen JJ, et al. Outcome of conditioning intensity in acute myeloid leukemia with monosomal karyotype in patients over 45 year-old: A study from the acute leukemia working party (ALWP) of the European group of blood and marrow transplantation (EBMT). *Am J Hematol*. 2015;90(8):719-724.
27. Sorror M, Storer B, Sandmaier BM, et al. Hematopoietic cell transplantation-comorbidity index and Karnofsky performance status are independent predictors of morbidity and mortality after allogeneic nonmyeloablative hematopoietic cell transplantation. *Cancer*. 2008;112(9):1992-2001.
28. Sorror ML, Storb RF, Sandmaier BM, et al. Comorbidity-age index: a clinical measure of biologic age before allogeneic hematopoietic cell transplantation. *J Clin Oncol*. 2014;32(29):3249-3256.
29. Lindsley RC, Saber W, Mar BG, et al. Prognostic Mutations in Myelodysplastic Syndrome after Stem-Cell Transplantation. *N Engl J Med*. 2017;376(6):536-547.
30. Strickland SA, Sun Z, Ketterling RP, et al. Independent Prognostic Significance of Monosomy 17 and Impact of Karyotype Complexity in Monosomal Karyotype/Complex Karyotype Acute Myeloid Leukemia: Results from Four ECOG-ACRIN Prospective Therapeutic Trials. *Leuk Res*. 2017;59:55-64.
31. Raza S, TaherNazerHussain F, Patnaik M, et al. Autosomal monosomies among 24,262 consecutive cytogenetic studies: prevalence, chromosomal distribution and clinicopathologic correlates of sole abnormalities. *Am J Hematol*. 2011;86(4):353-356.
32. Middeke JM, Beelen D, Stadler M, et al. Outcome of high-risk acute myeloid leukemia after allogeneic hematopoietic cell transplantation: negative impact of abn(17p) and -5/5q. *Blood*. 2012;120(12):2521-2528.
33. Breems DA, Van Putten WL, Lowenberg B. The impact of abn(17p) and monosomy -5/del(5q) on the prognostic value of the monosomal karyotype in acute myeloid leukemia. *Blood*. 2013;121(15):3056-3057.
34. Chilton L, Hills RK, Harrison CJ, et al. Hyperdiploidy with 49-65 chromosomes represents a heterogeneous cytogenetic subgroup of acute myeloid leukemia with differential outcome. *Leukemia*. 2014;28(2):321-328.
35. Pusic I, Choi J, Fiala MA, et al. Maintenance Therapy with Decitabine after Allogeneic Stem Cell Transplantation for Acute Myelogenous Leukemia and Myelodysplastic Syndrome. *Biol Blood Marrow Transplant*. 2015;21(10):1761-1769.
36. Tsigotis P, Byrne M, Schmid C, et al. Relapse of AML after hematopoietic stem cell transplantation: methods of monitoring and preventive strategies. A review from the ALWP of the EBMT. *Bone Marrow Transplant*. 2016;51(11):1431-1438.
37. Yafour N, Beckerich F, Bulabois CE, et al. How to prevent relapse after allogeneic hematopoietic stem cell transplantation in patients with acute leukemia and myelodysplastic syndrome. *Curr Res Transl Med*. 2017;65(2):65-69.
38. Ades L, Prebet T, Stamatoullas A, et al. Lenalidomide combined with intensive chemotherapy in acute myeloid leukemia and higher-risk myelodysplastic syndrome with 5q deletion. Results of a phase II study by the Groupe Francophone Des Myelodysplasies. *Haematologica*. 2017;102(4):728-735.
39. Chen Y, Kantarjian H, Estrov Z, et al. A phase II study of lenalidomide alone in relapsed/refractory acute myeloid leukemia

- or high-risk myelodysplastic syndromes with chromosome 5 abnormalities. *Clin Lymphoma Myeloma Leuk.* 2012;12(5):341-344.
40. Germing U, Lauseker M, Hildebrandt B, et al. Survival, prognostic factors and rates of leukemic transformation in 381 untreated patients with MDS and del(5q): a multicenter study. *Leukemia.* 2012;26(6):1286-1292.
 41. Sekeres MA, O'Keefe C, List AF, et al. Demonstration of additional benefit in adding lenalidomide to azacitidine in patients with higher-risk myelodysplastic syndromes. *Am J Hematol.* 2011;86(1):102-103.
 42. Jadersten M, Saft L, Smith A, et al. TP53 mutations in low-risk myelodysplastic syndromes with del(5q) predict disease progression. *J Clin Oncol.* 2011;29(15):1971-1979.
 43. Sebaa A, Ades L, Baran-Marzack F, et al. Incidence of 17p deletions and TP53 mutation in myelodysplastic syndrome and acute myeloid leukemia with 5q deletion. *Genes Chromosomes Cancer.* 2012;51(12):1086-1092.
 44. Alsina M, Becker PS, Zhong X, et al. Lenalidomide maintenance for high-risk multiple myeloma after allogeneic hematopoietic cell transplantation. *Biol Blood Marrow Transplant.* 2014;20(8):1183-1189.
 45. Sockel K, Bornhaeuser M, Mischak-Weissinger E, et al. Lenalidomide maintenance after allogeneic HSCT seems to trigger acute graft-versus-host disease in patients with high-risk myelodysplastic syndromes or acute myeloid leukemia and del(5q): results of the LENAMAINT trial. *Haematologica.* 2012;97(9):e34-e35.
 46. Craddock C, Slade D, De Santo C, et al. Combination Lenalidomide and Azacitidine: A Novel Salvage Therapy in Patients Who Relapse After Allogeneic Stem-Cell Transplantation for Acute Myeloid Leukemia. *J Clin Oncol.* 2019;JCO1800889.



Ferrata Storti Foundation

MYD88 mutations identify a molecular subgroup of diffuse large B-cell lymphoma with an unfavorable prognosis

Joost S. Vermaat,^{1,2,3} Sebastiaan F. Somers,³ Liesbeth C. de Wreede,⁴ Willem Kraan,^{2,5} Ruben A.L. de Groen,³ Anne M. R. Schrader,⁶ Emile D. Kerver,⁷ Cornelis G. Scheepstra,⁸ Henriëtte Berenschot,⁹ Wendy Deenik,¹⁰ Jurgen Wegman,^{1,11} Rianne Broers,¹² Jan-Paul D. de Boer,¹³ Marcel Nijland,¹⁴ Tom van Wezel,⁶ Hendrik Veelken,³ Marcel Spaargaren,^{2,5} Arjen H. Cleven,⁶ Marie José Kersten^{1,2} and Steven T. Pals^{2,5}

Haematologica 2020
Volume 105(2):424-434

¹Department of Hematology, Amsterdam University Medical Center, University of Amsterdam; ²Lymphoma and Myeloma Center Amsterdam-LYMMCARE, and Cancer Center Amsterdam (CCA), Amsterdam; ³Department of Hematology, Leiden University Medical Center, Leiden; ⁴Department of Biomedical Data Sciences, Leiden University Medical Center, Leiden; ⁵Department of Pathology, Amsterdam University Medical Center, University of Amsterdam, Amsterdam; ⁶Department of Pathology, Leiden University Medical Center, Leiden; ⁷Department of Internal Medicine & Hematology, Onze Lieve Vrouwe Gasthuis, Amsterdam; ⁸Department of Pathology, Onze Lieve Vrouwe Gasthuis, Amsterdam; ⁹Department of Internal Medicine & Hematology, Albert Schweitzer Hospital, Dordrecht; ¹⁰Department of Internal Medicine & Hematology, Tergooi Hospital, Hilversum; ¹¹Department of Internal Medicine & Hematology, Deventer Hospital, Deventer; ¹²Department of Internal Medicine & Hematology, Waterland Hospital, Purmerend; ¹³Department of Medical Oncology & Hematology, Antoni van Leeuwenhoekziekenhuis, Amsterdam and ¹⁴Department of Hematology, University Medical Center Groningen, Groningen, the Netherlands

Correspondence:

JOOST S. VERMAAT
j.s.p.vermaat@lumc.nl

Received: December 24, 2018.

Accepted: May 22, 2019.

Pre-published: May 23, 2019.

doi:10.3324/haematol.2018.214122

Check the online version for the most updated information on this article, online supplements, and information on authorship & disclosures: www.haematologica.org/content/105/2/424

©2020 Ferrata Storti Foundation

Material published in *Haematologica* is covered by copyright. All rights are reserved to the Ferrata Storti Foundation. Use of published material is allowed under the following terms and conditions:

<https://creativecommons.org/licenses/by-nc/4.0/legalcode>.

Copies of published material are allowed for personal or internal use. Sharing published material for non-commercial purposes is subject to the following conditions:

<https://creativecommons.org/licenses/by-nc/4.0/legalcode>,

sect. 3. Reproducing and sharing published material for commercial purposes is not allowed without permission in writing from the publisher.



ABSTRACT

The 2016 World Health Organization classification defines diffuse large B-cell lymphoma (DLBCL) subtypes based on Epstein-Barr virus (EBV) infection and oncogenic rearrangements of *MYC/BCL2/BCL6* as drivers of lymphomagenesis. A subset of DLBCL, however, is characterized by activating mutations in *MYD88/CD79B*. We investigated whether *MYD88/CD79B* mutations could improve the classification and prognostication of DLBCL. In 250 primary DLBCL, *MYD88/CD79B* mutations were identified by allele-specific polymerase chain reaction or next-generation-sequencing, *MYC/BCL2/BCL6* rearrangements were analyzed by fluorescence *in situ* hybridization, and EBV was studied by EBV-encoded RNA *in situ* hybridization. Associations of molecular features with clinicopathologic characteristics, outcome, and prognosis according to the International Prognostic Index (IPI) were investigated. *MYD88* and *CD79B* mutations were identified in 29.6% and 12.3%, *MYC*, *BCL2*, and *BCL6* rearrangements in 10.6%, 13.6%, and 20.3%, and EBV in 11.7% of DLBCL, respectively. Prominent mutual exclusivity between EBV positivity, rearrangements, and *MYD88/CD79B* mutations established the value of molecular markers for the recognition of biologically distinct DLBCL subtypes. *MYD88*-mutated DLBCL had a significantly inferior 5-year overall survival than wild-type *MYD88* DLBCL (log-rank; $P=0.019$). DLBCL without any of the studied aberrations had superior overall survival compared to cases carrying ≥ 1 aberrancy (log-rank; $P=0.010$). *MYD88* mutations retained their adverse prognostic impact upon adjustment for other genetic and clinical variables by multivariable analysis and improved the prognostic performance of the IPI. This study demonstrates the clinical utility of defining *MYD88*-mutated DLBCL as a distinct molecular subtype with adverse prognosis. Our data call for sequence analysis of *MYD88* in routine diagnostics of DLBCL to optimize classification and prognostication, and to guide the development of improved treatment strategies.

Introduction

Diffuse large B-cell lymphoma (DLBCL) is characterized by substantial heterogeneity in tumor biology and clinical behavior.^{1,2} Currently, rituximab, cyclophosphamide, doxorubicin, vincristine, and prednisone (R-CHOP) is used as a 'one-size-fits-all' treatment. Unfortunately, a considerable percentage of patients will experience chemorefractory disease or relapse, resulting in a 5-year overall survival (OS) of approximately 60%.³ Particularly, patients with chemorefractory disease or an early relapse have a poor prognosis. For optimal counseling, DLBCL patients are categorized in risk groups according to the IPI.⁴ The IPI consists of clinical and biochemical parameters, but does not include tumor biological characteristics or provide any indication for precision medicine.⁵

The recently updated WHO classification of lymphoid neoplasms (2016) recognizes this heterogeneity by including selected drivers of lymphomagenesis for subclassification of DLBCL, *i.e.* the delineation of high-grade B-cell lymphomas (HGBL) with *MYC* and *BCL2* and/or *BCL6* rearrangements, and of Epstein-Barr virus-positive (EBV⁺) DLBCL.⁶ *MYC*, *BCL2*, and *BCL6* rearrangements are found in respectively 4-14%, 20-30%, and ~20% of DLBCL.⁷⁻⁹ HGBL comprise approximately 5-10% of all DLBCL.^{9,11} It is thought that the combination of *MYC*-stimulated cell proliferation and anti-apoptotic effects of *BCL2* in HGBL cause aggressive growth, relative resistance to therapy, and inferior OS.¹² In addition, Asian studies showed a frequency of 1-14% EBV positivity in DLBCL and an association with inferior survival.^{13,14} EBV-associated viral proteins, such as latent membrane proteins (LMP)-1/2 and nuclear antigens, stimulate proliferation of B-cells via activation of nuclear factor-kappa-B (NFκB), regulate immune evasion, and inhibit apoptosis.¹³

In the search for additional oncogenic drivers and to discriminate different molecular DLBCL subtypes, large next-generation-sequencing (NGS) studies have revealed specific mutational profiles that reflect the dysregulation of distinct intracellular pathways, including epigenetic regulation and NF-κB, Toll-like receptor (TLR), and B-cell receptor (BCR) signalling.^{1,2,15,16} Recurrent 'hotspot' mutations in *MYD88* (L265P) and *CD79B* (Y196) belong to the most prevalent sequence alterations in DLBCL. By altering the toll/interleukin-1 receptor domain of MYD88, the L265P increases interaction and consecutive phosphorylation of downstream targets, potentially without external stimuli from the TLR.¹⁷ The connection of MYD88 with BCR signalling within the so-called 'My-T-BCR' supercomplex facilitates activation of the NF-κB pathway via TLR9.² Hotspot mutations, such as Y196, in the CD79B subunit of the BCR lead to increased BCR expression and inhibition of feedback in the BCR signalling pathway by attenuating downstream Lyn kinase. Therefore, *CD79B* mutations are thought to contribute to lymphomagenesis by enhancing chronic active BCR signalling.¹⁸

Both *MYD88* and *CD79B* mutations are more prevalent in the so-called non-germinal center B-cell (GCB)-type DLBCL according to the cell-of-origin (COO) concept, originally developed on the basis of gene expression profiling.^{1,2,19} In addition, the prevalence of these mutations varies greatly among DLBCL originating at different anatomical sites. We recently described a high percentage of *MYD88* L265P and *CD79B* Y196 mutations in intravascular large B-cell lymphomas (44% *MYD88* and 26%

CD79B).²⁰ A high frequency of these mutations has also been found in other extranodal DLBCL, such as primary cutaneous DLBCL, leg type,²¹ orbita/vitreoretinal DLBCL,²²⁻²⁴ primary breast DLBCL,²⁵ and DLBCL presenting at immune-privileged (IP) sites, *i.e.* primary testicular DLBCL (PTL)²⁶ and primary central nervous system B-cell lymphoma (PCNSL).²⁷⁻²⁹ Several studies have shown that *MYD88* mutations are associated with inferior OS in DLBCLs compared to wild-type *MYD88*.^{30,31}

Despite the increasing knowledge of the landscape of genetic drivers in DLBCL, the clinical implications of different oncogenic driver mutations remain unclear,³² and the R-CHOP regimen is used as a uniform treatment. Since patients with chemorefractory disease or relapses after R-CHOP have a poor outcome, the global 5-year OS in DLBCL is approximately 60%.³ While HGBL patients have been recognized as a particularly unfavorable subgroup, prognostication for the remaining DLBCL is based on clinical and biochemical parameters that define the IPI as well as primary extranodal manifestations.^{4,5} In contrast, the prognostic significance and interaction of mutations in *MYD88* and *CD79B* with standard molecular aberrations (as designated by the WHO 2016) have not yet been conclusively elucidated. Therefore, the present study investigated whether the assessment of the mutational status of *MYD88* and *CD79B* would improve the classification and prognostication of DLBCL.

Methods

Patient cohort

This retrospective study investigated a cohort of 250 primary DLBCL. DLBCL patients were diagnosed between 2000-2016 at the Amsterdam University Medical Center (AUMC), the Leiden University Medical Center (LUMC), and their affiliated hospitals. In all cases, diagnosis was centrally revised following the WHO classification 2008. A subset of this cohort was previously published without survival analysis.^{28,29} As our academic hospitals are tertiary referral centers, this cohort is enriched for IP locations. Formalin-fixed and paraffin-embedded (FFPE) tissue samples were obtained during standard diagnostic procedures. The study was performed in accordance with the Dutch Code for Proper Secondary Use of Human Tissue in accordance with the local institutional board requirements and the revised Declaration of Helsinki 2008 and was approved by the medical ethics committees of both the AUMC (W15_213#15.0253) and the LUMC (B16.048). Patients were eligible in case tissue was available and *MYD88* mutational analysis was successful.

Histopathologic and molecular characterization

In the majority, immunohistochemistry was performed for CD20, CD10, BCL6, MUM1, and BCL2. The Hans' algorithm was used for the COO classification.³³ The EBV status was assessed by EBER-ISH. *MYC*, *BCL2*, and *BCL6* rearrangements were analyzed by FISH using break-apart probes. Antibodies and probes are depicted in the *Online Supplementary Table S1*.^{20,29} In the AUMC, DNA was isolated using the QIAamp DNA Micro kit (Qiagen) and mutational status of *MYD88* and *CD79B* was established by allele-specific PCR, followed by mutation-specific primers and confirmed by Sanger sequencing, as described before.^{28,29} In the LUMC, DNA isolation was automatically performed with the TPS robot (Siemens Healthcare Diagnostics), as presented previously.³⁴ The Ampliseq Cancer Hotspot Panel V.2-V.4 (Thermo Fisher Scientific) was used for the detection of variants in *MYD88* (exons

3&5) and CD79B (exons 5&6). The minimum coverage threshold was 100 on-target reads with a minimum variant allele frequency of $\geq 10\%$ of the reads. Variants were analyzed using Geneticist Assistant NGS Interpretative Workbench (v.1.4.15, SoftGenetics, State College). As described, identified variants were classified into five classes based on potential pathogenicity and only class 4 (possibly pathogenic) and class 5 variants (pathogenic) were reported.³⁵

Statistical analysis

The correlation between the clinicopathologic parameters and biological aberrations was examined with the Chi-square test or ANOVA. The Kaplan-Meier method was applied to estimate 5-year OS and progression free survival (PFS). The starting point for time-to-event analysis was the date of the histological diagnosis. An event for OS was defined as death by any cause. An event for PFS was determined as relapse, disease progression, or death by any cause (whatever came first). If patients received palliative treatment and no remission evaluation was performed during the follow-up, an event for progression was defined at three weeks before patients succumbed to their disease. Observational intervals of patients without any event at the time of the last follow up or at 5 years after diagnosis were censored. The median follow up time for the whole cohort was determined by the use of reverse Kaplan-Meier.³⁶ The log-rank test was performed to compare risk groups. The Cox proportional-hazards model was used to estimate hazard ratios (HR) including 95% confidence intervals (95%-CI). Adjusted HR were obtained in a multivariable Cox model. Competing risks analysis was used to estimate the cumulative incidences of relapse/progression, with non-relapse mortality considered as competing risk. Gray's test was performed to compare cumulative incidences, whereas a cause-specific Cox proportional-hazards model was used to estimate the impact of risk factors on them.³⁷ The incremental prognostic value of *MYD88* and/or *CD79B* was assessed by comparing Harrell's cross-validated C statistic for Cox models with and without *MYD88* and/or *CD79B*.³⁸ All statistical analyses were performed using SPSS software (version 23, IBM SPSS statistics) and RStudio (version 1.1442, RStudio, Inc. packages survival, prodlm, dynpred and cmprsk). P-values were two-sided and $P < 0.05$ was considered statistically significant.

Results

Patient characteristics

Table 1 depicts the baseline characteristics of the 250 DLBCL patients (AUMC N=224 patients and LUMC N=26 cases). The median age at diagnosis was 61.4 years (range 18.6-89.6). A total of 38 DLBCL patients were immune-compromised, due to inherited conditions (severe combined immunodeficiency disorder, common variable immunodeficiency disorder), human immunodeficiency virus (HIV) infection, or extended use of therapeutic immunosuppression necessitated by organ transplantation or auto-immune disorders. Based on anatomical locations, 75 patients (30.0%) had strictly nodal DLBCL and in 67 patients (26.8%) the lymphoma presented in IP sites: 33 patients with PTL and 35 patients with PCNSL of whom one patient had testicular and CNS locations synchronously. The remaining 108 patients (43.2%) had extranodal disease in non-IP sites (with or without nodal involvement). With respect to staging, PCNSL was considered as advanced disease equivalent to Ann Arbor Stage IV for assignment of the IPI and subsequent statisti-

Table 1. Patient characteristics at time of diagnosis.

	All patients (N=250)
Gender	
Male	168 (67.2 %)
Female	82 (32.8 %)
Median age in years (range)	61.4 (18.6-89.6)
History of immune deficiency	38 (15.2 %)
HIV	16 (6.4 %)
Organ transplantation with prolonged use of immune suppressive drugs	7 (2.8 %)
SCID/CVID	3 (1.2 %)
Other ^a	13 (5.2 %)
Anatomical lymphoma location	
Nodal	75 (30.0 %)
Extranodal ^b (with or without nodal location)	108 (43.2 %)
Immune-privileged	67 (26.8 %)
CNS location ^c	35 (14.0 %)
Testis location	32 (13.2 %)
Ann Arbor ^d	(N = 248)
I	51 (20.6 %)
II	32 (12.9 %)
III	26 (10.5 %)
IV	139 (56.0 %)
IPI ^e	(N = 241)
0	20 (8.3 %)
1	41 (17.0 %)
2	90 (37.3 %)
3	58 (24.1 %)
4	24 (10.0 %)
5	8 (3.3 %)
First line treatment	
R-CHOP	160 (64.0 %)
CHOP	25 (10.0 %)
Other chemotherapy ^e	5 (2.0 %)
Radiotherapy only	1 (0.4 %)
Surgery only	2 (0.8 %)
None /Palliative	34 (13.6 %)
High-dose methotrexate regimens (HD-MTX) ^f	23 (9.2 %)
Radiotherapy	
With curative intent	
Palliative care only	77 (30.8 %)
	60 (24.0 %)
	17 (6.8 %)
Response to first line treatment	
Complete response	166 (66.4 %)
Partial response	14 (5.6 %)
Stable disease	2 (0.8 %)
Progressive disease	67 (26.8 %)
Too early to call	1 (0.4 %)

HIV: human immunodeficiency virus; SCID: severe combined immunodeficiency disorder; CVID: common variable immunodeficiency disorder; CNS: central nervous system; IPI: international prognostic index; (R-)CHOP: (rituximab), cyclophosphamide, doxorubicin, vincristine, prednisone. ^aOthers include inflammatory bowel disease, Sjögren, sarcoidosis, atopic dermatitis, and/or auto-immune haemolytic anaemia. ^bExtranodal comprised lung, liver, spleen, bone marrow, breast, soft tissue, thyroid, bone, (ad)renal, orbital, stomach, skin, pancreas, bowel, bladder, ovary, and naso-/oropharynx locations. ^cOne patient experienced both CNS and testicular locations. ^dPCNSL were classified as advanced stage (Ann-Arbor stage IV) and subsequently received one risk point for IPI. ^e(R-)C(E)OP: (rituximab), cyclophosphamide, (etoposide), vincristin, prednisone. ^fSpecific regimens include HD-MTX + cytarabine + carmustine, HD-MTX + cytarabine, rituximab + HD-MTX + prednisone (RMP), cyclophosphamide + doxorubicin + teniposide + prednisone + vincristine + bleomycin (CHVMP/BV), HD-MTX + procarbazine + lomustine, HD-MTX + cytarabine + thiopeta + rituximab (MATRIx), HD-MTX + teniposide + carmustin + prednisone (MBVP) (+ rituximab).

cal analyses. With this definition, 83 patients (33.5%) were categorized as having regional disease (Ann Arbor stage I-II) and 165 patients (66.5%) had advanced disease (stage III-IV). Sixty-one patients (25.3%) had an IPI risk score of 0/1, 148 patients (61.4%) an IPI of 2-3, and 32 patients (13.3%) an IPI of 4-5. The IPI of nine patients was

unknown. The majority of (extra)nodal and testicular DLBCL patients were treated with R-CHOP (N=160), CHOP (N=25), or (R)CHOP-like treatments (N=5) with curative intent. Curative treatment regimens incorporating high-dose methotrexate were initiated for 23 patients with PCNSL. Because of older age, poor clinical Eastern

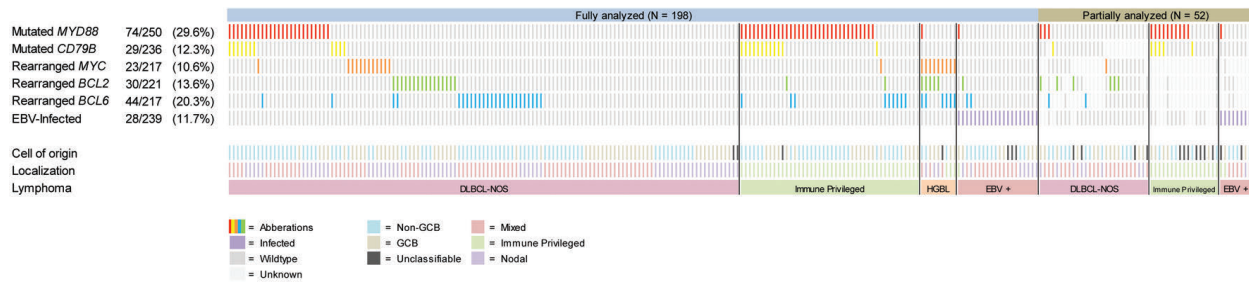


Figure 1. OncoPrint plot of the molecular analysis of 250 cases with diffuse large B-cell lymphoma (DLBCL). EBV: Epstein-Barr virus; GCB: germinal center B-cell; IP: immune-privileged. Of 52 cases, molecular analysis was not complete due to results that were ambiguous to interpret or no FFPE material was left for subsequent analysis.

Table 2. Hans' algorithm and molecular analysis at time of diagnosis.

	All patients (N=250)	Nodal (N=75)	Extranodal with/without nodal (N=108)	Immune-privileged (N=67)	P*
Cell-of-origin, according to Hans' algorithm (N=250)					
GCB	100 (40.0 %)	36 (48.0 %)	38 (58.3 %)	26 (38.8%)	0.228
Non-GCB	130 (52.0 %)	35 (46.7 %)	63 (35.2 %)	32 (47.8 %)	
Unclassifiable	20 (8.0 %)	4 (5.3 %)	7 (6.5 %)	9 (13.4 %)	
MYD88 (N=250)					
Wildtype	176 (70.4 %)	62 (82.7 %)	92 (85.2 %)	22 (32.8 %)	<0.001
Mutated	74 (29.6 %)	13 (17.3 %)	16 (14.8 %)	45 (67.2 %)	
CD79B (N=236)					
Wildtype	207 (87.7 %)	70 (95.9 %)	88 (90.7 %)	49 (74.2 %)	<0.001
Mutated	29 (12.3 %)	3 (4.1 %)	9 (9.3 %)	17 (25.8 %)	
MYC (N=217)					
Wildtype	194 (89.4 %)	59 (85.5 %)	89 (90.8 %)	46 (92.0 %)	0.434
Rearranged	23 (10.6 %)	10 (14.5 %)	9 (9.2 %)	4 (8.0 %)	
BCL2 (N=221)					
Wildtype	191 (86.4 %)	53 (74.6 %)	89 (89.9 %)	49 (96.1 %)	0.001
Rearranged	30 (13.6 %)	18 (25.4 %)	10 (10.1 %)	2 (3.9 %)	
BCL6 (N=217)					
Wildtype	173 (79.7 %)	57 (82.6 %)	78 (79.6 %)	38 (76.0 %)	0.675
Rearranged	44 (20.3 %)	12 (17.4 %)	20 (20.4 %)	12 (24.0 %)	
High grade B-cell lymphoma (N=221)					
Negative	212 (95.9 %)	66 (95.7 %)	98 (97.0 %)	48 (94.1 %)	0.686
Positive	9 (4.1 %)	3 (4.3 %)	3 (3.0 %)	3 (5.9 %)	
EBV status (N=239)					
Negative	211 (88.3 %)	65 (89.0 %)	88 (83.8 %)	58 (95.1 %)	0.091
Positive	28 (11.7 %)	8 (11.0 %)	17 (16.2 %)	3 (4.9 %)	
Genetic aberrations (N=198)					
None	51 (25.8 %)	21 (31.8 %)	27 (32.1 %)	3 (6.3 %)	0.002
One or more	147 (74.2 %)	45 (68.2 %)	57 (67.9 %)	45 (93.8 %)	

EBV: Epstein-Barr virus. *P-value indicating a difference in distribution between the three subgroups as calculated by Pearson's χ^2 test. The number between brackets in the left hand column represents the number of patients from whom this information was available.

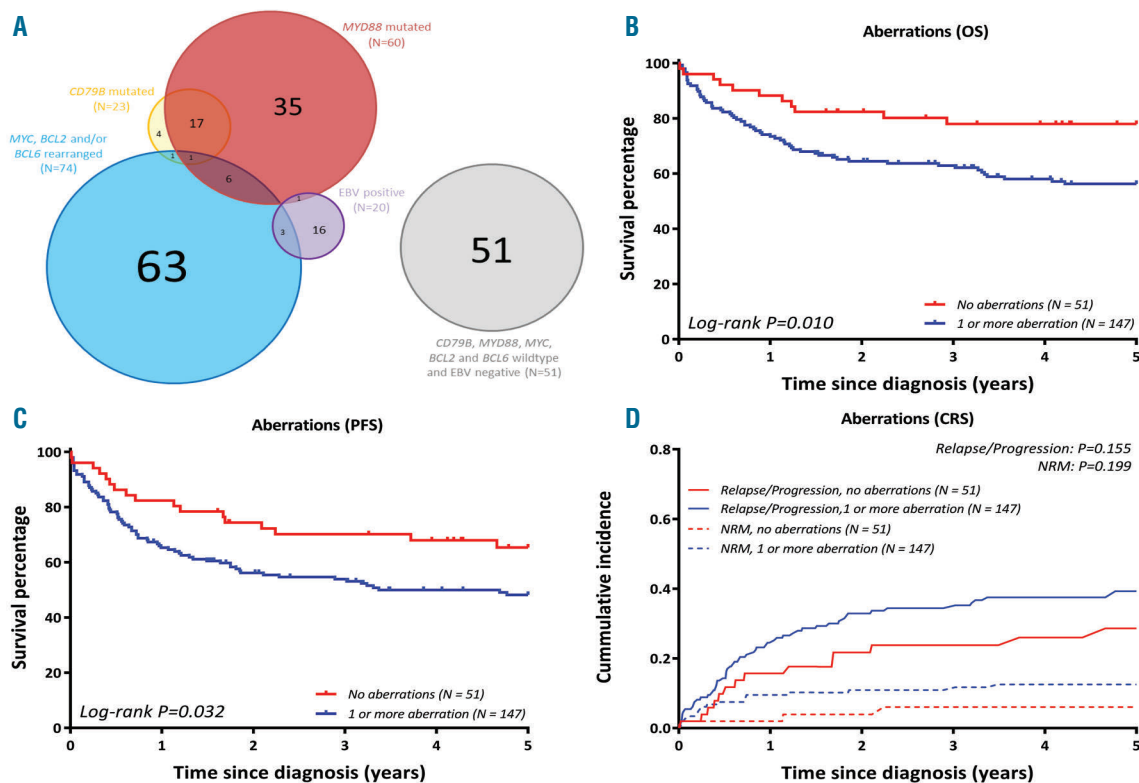


Figure 2. Molecular characterization discriminates distinct DLBCL subgroups with prognostic impact. (A) Venn diagram demonstrating the overlap of aberrations for 198 fully analysed DLBCL. (B) DLBCL without detected aberrations showed a superior overall survival compared to DLBCL with ≥ 1 affected aberrations (for cases with complete aberration analysis), identifying a novel good-risk group. (C) PFS of the novel identified risk group (for cases with complete driver analysis). (D) Cumulative incidences of novel identified risk group (for cases with complete driver analysis). CRS: competing risk; PFS: progression free survival.

Cooperative Oncology Group Performance Status (ECOG-PS), or patients' refusal of treatment, 34 patients received palliative care only, mainly with steroids or (local) radiotherapy. The median follow up time was 6.6 years (range 0.1-15.7).³⁶

Molecular characterization: mutated *MYD88* discriminates a distinct DLBCL subgroup

According to the Hans' algorithm, DLBCL were classified as GCB (N=100, 40.0%), non-GCB (N=130, 52.0%), or unclassifiable (N=20, 8.0%), with no statistical difference between nodal, extranodal, and IP locations ($P=0.228$) (Table 2).³³

In 198 patients (79.2%), molecular analysis for *MYD88* and *CD79B* mutations, *MYC*, *BCL2*, and *BCL6* rearrangements, and EBV infection was complete, whereas in 52 patients, partial data sets were available (Figure 1; Table 2). *MYD88* mutations were identified in 74 cases (29.6%), of whom 67 harbored the hotspot *L265P* mutation. The other *MYD88* variants were *S219C* (N=5) and *S243N* (N=2). In line with a published meta-analysis,³⁰ mutated *MYD88* was significantly correlated with older age (≥ 65 years), anatomical lymphoma location, and non-GCB subtype ($P=0.006$; $P<0.001$; $P=0.042$, respectively). *CD79B* mutations were detected in 29 patients (12.3%), including the hotspot *Y196* mutation (N=28) and the *L188* mutation (N=2, one patient had both mutations). *MYC*, *BCL2*, and *BCL6* were rearranged in 23 (10.6%), 30 (13.6%), and 44 (20.3%) DLBCL, respectively, with a total of nine HGBL patients (4.1%).

As suggested by previous reports and other studies, *MYD88* and *CD79B* mutations were significantly more common in IP-DLBCL (67.2% resp. 25.8%) compared to nodal (17.3% resp. 4.1%) and other extranodal sites (14.8% resp. 9.3%) ($P<0.001$ and $P<0.001$).^{26,29,39} In contrast, *BCL2* rearrangements were more prevalent in nodal and extranodal DLBCL ($P=0.001$), whereas *MYC* and *BCL6* rearrangements were evenly distributed across the anatomical sites. EBV was positive in 28 patients (11.7%) and was not associated with an anatomical location ($P=0.091$).

In the 198 cases with complete molecular analysis, hardly any overlap between the presence of oncogenic rearrangements, EBV positivity, or *MYD88* and/or *CD79B* mutations was observed (Figure 2A), suggesting that they represent distinct DLBCL subgroups with different drivers of lymphomagenesis. *CD79B* mutations co-occurred with *MYD88* mutations in 18 of 23 cases (78.2%). In contrast, *MYD88* mutations co-occurred with any rearrangement in only 7 of 60 patients (11.7%) and with EBV positivity in only one case (1.7%). EBV infection was detected in only 3 of 71 cases (4.2%) with a rearrangement. In 51 patients (25.8%) with full molecular characterization, no aberrancy was detected.

Mutated *MYD88* predicts inferior survival

All outcomes are reported at the 5-year survival. For the entire cohort, the OS was 61.0% (95%-CI 55.1-67.5) and the PFS was 52.6% (95%-CI 46.6-59.3). Cumulative incidences of relapse/progression and non-relapse mortality

Table 3A. Prognostic impact of molecular aberrations and IPI risk factors on overall survival: univariable and multivariable analysis.

	Overall survival							
	Univariable		Multivariable Model 1 (IPI)		Multivariable Model 2 (IPI + molecular aberrations WHO 2016)		Multivariable Model 3 (IPI + molecular aberrations WHO 2016 + MYD88 + CD79B)	
	HR	95%-CI	HR	95%-CI	HR	95%-CI	HR	95%-CI
IPI: >2 Extranodal Yes (<i>vs.</i> No)	1.37	0.91-2.07	1.41	0.90-2.22	1.49	0.94-2.37	1.71	1.07-2.74
IPI: Stage III/IV (<i>vs.</i> I/II)	2.33	1.41-3.85	1.67	0.98-2.84	1.71	0.97-3.00	1.84	1.04-3.25
IPI: ECOG Performance Score >2 (<i>vs.</i> <1)	8.15	5.23-12.7	7.53	4.67-12.15	8.69	5.23-14.45	8.16	4.90-13.59
IPI: Age >60 (<i>vs.</i> <60)	1.54	1.00-2.37	1.35	0.85-2.13	1.38	0.87-2.19	1.33	0.83-2.12
IPI: LDH >Upper limit (<i>vs.</i> Normal)	1.53	1.01-2.31	1.14	0.74-1.77	1.15	0.73-1.81	1.29	0.82-2.05
<i>MYC</i>								
Rearranged (<i>vs.</i> Wildtype)	1.62	0.88-3.00			1.71	0.89-3.27	1.86	0.93-3.69
<i>BCL2</i>								
Rearranged (<i>vs.</i> Wildtype)	0.74	0.37-1.47			0.51	0.24-1.08	0.57	0.26-1.24
<i>BCL6</i>								
Rearranged (<i>vs.</i> Wildtype)	1.21	0.71-2.04			0.94	0.53-1.65	1.00	0.55-1.83
EBV Status								
Positive (<i>vs.</i> Negative)	1.54	0.86-2.78			1.29	0.67-2.47	1.65	0.82-3.30
<i>CD79B</i>								
Mutated (<i>vs.</i> Wildtype)	1.43	0.81-2.53					0.76	0.38-1.49
<i>MYD88</i>								
Mutated (<i>vs.</i> Wildtype)	1.64	1.08-2.48					1.87	1.10-3.20
Cross-validated C-index			0.6		0.69		0.70	

For the multivariable model, unknown was regarded as a separate category for these variables for which some data were missing (not reported).

were 37.2% (95%-CI 31.2-43.3) and 10.1% (95%-CI 6.4-13.9), respectively. Figure 3 shows the survival outcomes presented for the anatomical location, IPI-score, and MYD88 status. The survival outcomes of COO and the other aberrations are outlined in the *Online Supplementary Figure S2* (none of these factors had a significant impact).

The IPI clearly predicted OS (Figure 3): patients with IPI scores of 0/1, 2/3, and 4/5 had an OS of 84.9% (95%-CI 76.3-94.5), 58.0% (95%-CI 50.3-66.8), and 34.4% (95%-CI 21.3-55.5), respectively. IPI also showed a significant difference in cumulative incidences of relapses (Gray's; $P=0.025$) and non-relapse mortality (Gray's; $P=0.006$). In addition to the IPI, DLBCL with IP locations had inferior outcomes (OS 47.1%, 95%-CI 36.5-60.9; PFS 41.0%, 95%-CI 30.7-54.9) compared to nodal (OS 71.2%, 95%-CI 61.4-82.4; PFS 55.7%, 95%-CI 45.3-68.6) and other extranodal sites (OS 62.6%, 95%-CI 53.9-72.7; PFS 58.1%, 95%-CI 49.4-68.2) (log-rank; $P=0.004$ and $P=0.024$). This unfavorable prognosis was particularly associated with the CNS location. Within the IP group, patients with CNS location had a significantly inferior 5-year OS of 29.9% (95%-CI 17.7-50.5) compared to 65.5% (95%-CI 50.9-84.3%) for PTL (log-rank; $P=0.003$).

With respect to the molecular markers, patients without any detected aberrancy demonstrated a good-risk profile with a superior OS (78.0%, 95%-CI 67.2-90.4, *versus* 56.3%, 95%-CI:48.6-65.2; Figure 2B) (log-rank; $P=0.010$) and PFS (65.4%, 95%-CI 53.2-80.3, *versus* 48.2%, 95%-CI 40.6-57.3; Figure 2C) (log-rank; $P=0.031$) compared to patients who had one or more aberration(s). The cumulative incidence of relapse/progression for this good-risk profile was 28.6% (95%-CI 15.8-41.4) compared to 39.3% (95%-CI 31.2-47.4) (Gray's; $P=0.155$). This good risk profile included patients with a lower ECOG-PS, age<60 years, and more GCB subtypes (Chi square; $P=0.012$, $P=0.001$, and $P=0.006$, respectively) compared to patients with one or more aberrations. Patients in the good risk category seem to be susceptible for immune-chemotherapy with enduring responses, however, the molecular background of this subgroup remains unknown. In IP-DLBCL, a total of 93.8% of the patients were classified in the risk group with ≥ 1 aberrations.

MYD88-mutated DLBCLs had a significantly inferior 5-year OS compared to DLBCL with wild-type MYD88 (log-rank; $P=0.019$; HR 1.64, 95%-CI 1.08-2.48) and significantly inferior 5-year PFS (log-rank; $P=0.049$; HR 1.46,

95%-CI 1.00-2.14). Employing competing risk analysis, *MYD88*-mutated DLBCL revealed significantly higher relapse rates (46.6%, 95%-CI 35.1-58.1) than cases with wild-type *MYD88* (33.3%, 95%-CI 26.2-40.4)(Gray's; $P=0.029$; CSH 1.62, 95%-CI 1.06-2.48), while non-relapse mortality showed no significant difference (Gray's; $P=0.832$). Mutated *CD79B* showed higher cumulative incidence for relapse/progression (56.3%, 95%-CI 37.9-74.8) *versus* wild-type *CD79B* (35.1%, 95%-CI 28.5-41.8)(Gray's; $P=0.019$, CSH: 1.82, 95%-CI 1.06-3.14), whereas no significant difference was found for OS (HR 1.43, 95%-CI 0.81-2.53).

Despite relatively high HR, none of the other molecular aberrations was a significantly adverse prognostic factor for OS (Table 3), which can be explained by the lack of power due to the low incidence of these aberrations. For these molecular data, univariate cause-specific hazards for relapse/progression showed similar results. The nine HGBL had an OS of 50.0% (95%-CI 24.1-100) compared to 63.6% (95%-CI 57.3-70.6) (log-rank; $P=0.628$) for non-HGBL.

Prognostic significance of *MYD88* mutations in multivariable analysis

To evaluate the prognostic impact of mutated *MYD88* on survival outcomes in addition to other molecular aberrations and the IPI, the initial multivariable Cox regression model included the standard individual IPI risk factors (Model 1, Table 3A/3B). In the second model, the current WHO 2016 molecular aberrations (EBV and oncogenic rearrangements) were added. In the third model, also *MYD88* and *CD79B* mutations were included. *MYD88* mutations showed prognostic significance for OS (HR 1.87, 95%-CI 1.10-3.20) in addition to ECOG-PS (≥ 2) (HR 8.16, 95%-CI 4.90-13.59) and Ann Arbor stage (III/IV) (HR 1.84, 95%-CI 1.04-3.25). In this third model, oncogenic rearrangements, mutated *CD79B*, elevated LDH, and age (>65 years) did not have a significant impact. The performance of the IPI prognostic model was improved by adding all molecular aberrations and mutated *MYD88* and *CD79B* as risk factors, as indicated by an increase in cross-validated C-index (CVC) from 0.67 to 0.70. *MYD88* did not have a significant impact on the cause-specific survival

Table 3B. Prognostic impact of molecular aberrations and IPI risk factors on relapse/progression: univariable and multivariable analysis.

	Univariable		Cause-specific hazards (CSH) for relapse/progression					
	HR	95%-CI	Multivariable Model 1 IPI	Multivariable Model 2 (IPI + molecular aberrations WHO 2016)	Multivariable Model 3 (IPI + molecular aberrations WHO 2016 + <i>MYD88</i> + <i>CD79B</i>)	HR	95%-CI	
IPI: >2 Extranodal								
Yes (<i>vs.</i> No)	1.57	0.99-2.41	1.55	0.99-2.41	1.63	1.04-2.57	1.81	1.14-2.86
IPI: Stage								
III/IV (<i>vs.</i> I/II)	2.76	1.63-4.68	2.12	1.22-3.67	2.06	1.17-3.63	2.14	1.19-3.82
IPI: ECOG Performance Score								
>2 (<i>vs.</i> <1)	4.48	2.58-7.78	4.48	2.58-7.78	5.09	2.86-9.05	4.60	2.57-8.22
IPI: Age								
>60 (<i>vs.</i> <60)	1.14	0.75-1.74	1.11	0.71-1.72	1.14	0.73-1.79	1.12	0.71-1.77
IPI: LDH								
>Upper limit (<i>vs.</i> Normal)	0.98	0.64-1.50	0.77	0.49-1.21	0.77	0.48-1.22	0.82	0.51-1.31
<i>MYC</i>								
Rearranged (<i>vs.</i> Wildtype)	1.63	0.86-3.09			1.84	0.94-3.49	1.90	0.96-3.77
<i>BCL2</i>								
Rearranged (<i>vs.</i> Wildtype)	1.34	0.75-2.40			1.03	0.56-1.90	1.23	0.66-2.30
<i>BCL6</i>								
Rearranged (<i>vs.</i> Wildtype)	1.01	0.57-1.78			0.89	0.49-1.59	0.91	0.49-1.68
EBV Status								
Positive (<i>vs.</i> Negative)	0.79	0.36-1.71			0.66	0.29-1.49	0.79	0.34-1.86
<i>CD79B</i>								
Mutated (<i>vs.</i> Wildtype)	1.82	1.06-3.13					1.23	0.64-2.36
<i>MYD88</i>								
Mutated (<i>vs.</i> Wildtype)	1.62	1.06-2.48					1.42	0.85-2.37
Cross-validated C-index			0.63		0.63		0.64	

For the multivariable model, unknown was regarded as a separate group (not reported).

(HR 1.42, 95%-CI 0.85-2.37), whilst ECOG-PS, Ann Arbor stage, and extranodal location were prognostic in this model.

Further multivariable analyses were performed to evaluate the prognostic significance of *MYD88* mutational status in comparison to the COO subtype or anatomical lymphoma location. The COO subtype did not improve the performance of models 2 and 3 (results not shown). However, the prognostic impact of model 2 was improved by adding the anatomical lymphoma location (CVC index

= 0.71, model 4, presented in the *Online Supplementary Table S1*) and outperforms model 2 (Table 3A, CVC index = 0.69, including the IPI factors and molecular aberrations of WHO 2016). Model 4 demonstrated a nearly identical prognostic performance when compared to model 3 (CVC index = 0.70, including the IPI factors, molecular aberrations of WHO 2016 and the mutational status of *MYD88* and *CD79B*). When adding the mutational status of *MYD88* and *CD79B* to model 4, the performance of this model 5 was not improved (CVC index 0.71, *Online*

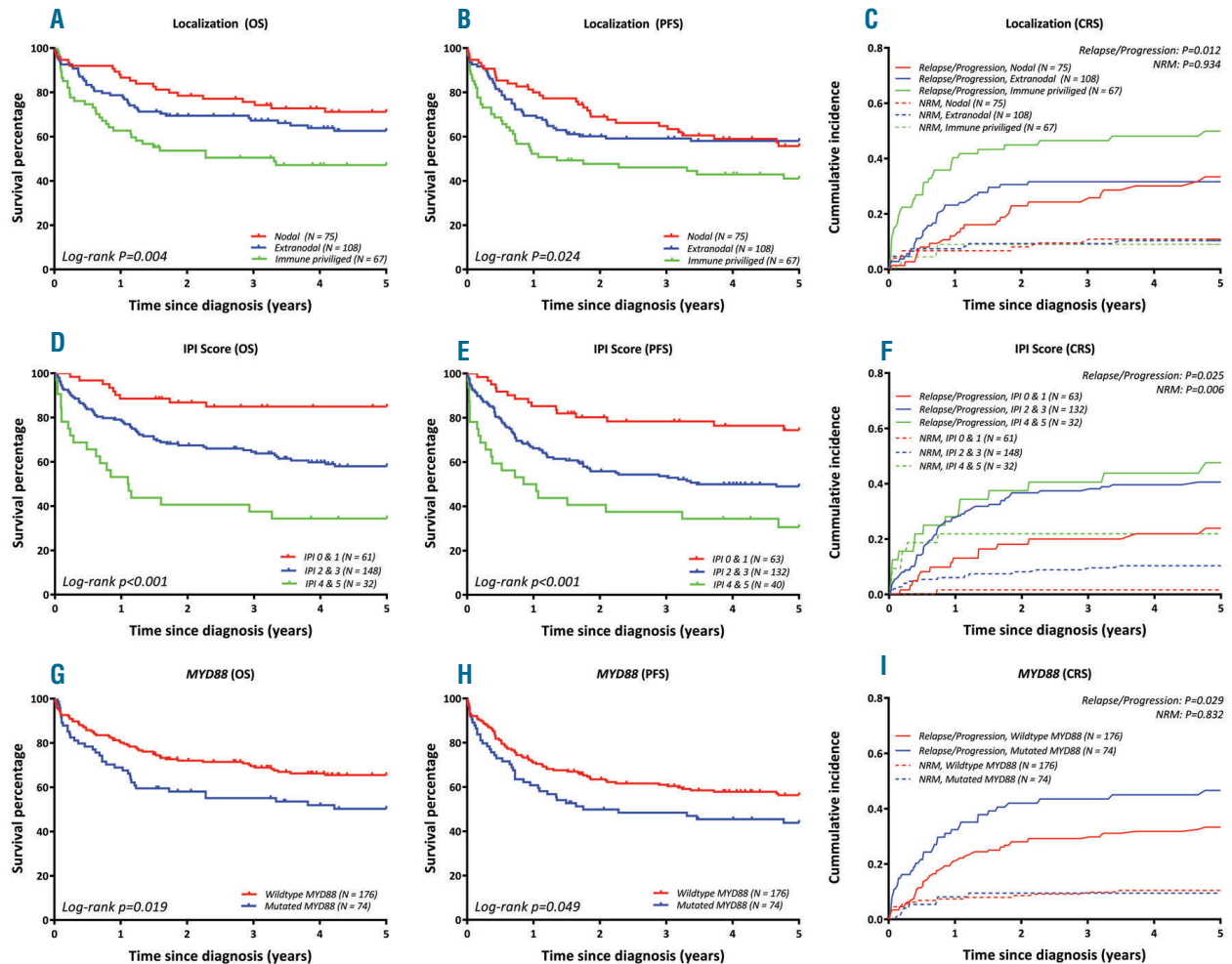


Figure 3. Prognostic significance of anatomical location, IPI Score and *MYD88* in DLBCL. OS, PFS, and cumulative incidence of relapse/progression compared to NRM (1st row: Location, 2nd row: IPI Score, 3rd row: *MYD88*). CRS: competing risk; OS: overall survival; PFS: progression free survival; NRM: non-relapsed mortality.

Table 4. Mutated *MYD88* improved the prognostic performance of the IPI.

	Overall survival		Cause-specific hazard (CSH) for relapse/progression					
	Univariable	Multivariable	Univariable		Multivariable		Multivariable	
	HR	95%-CI	HR	95%-CI	HR	95%-CI	HR	95%-CI
IPI-score								
As continuous variable	1.73	1.45-2.08	1.77	1.47-2.13	1.45	1.21-1.73	1.47	1.22-1.76
<i>MYD88</i>								
Mutated (vs. Wildtype)			1.83	1.19-2.80			1.69	1.09-2.60
Cross-validated C-index		0.57		0.61		0.53		0.57

Supplementary Table S1). As such, the prognostic impact of the *MYD88* mutational status on mortality was not superior to the anatomical lymphoma location.

Next, we explored whether mutated *MYD88* could improve the prognostic performance of the currently used IPI risk model (Table 4). The inclusion of the IPI as a continuous variable (0-5 points) and the *MYD88* status in the multivariable analysis demonstrated an independent and similar impact of mutated *MYD88* (HR 1.83, 95%-CI 1.19-2.80) and IPI (HR 1.77, 95%-CI 1.47-2.13) on OS. Similar effects were observed for cause-specific survival (Table 4). For the models, OS and relapse/progression, an increase in CVC-index was observed from 0.57 to 0.61 and 0.53 to 0.57, respectively. Altogether, these multivariable survival analyses demonstrated the significant prognostic importance of mutated *MYD88*, next to (genetic) aberrations and clinical/biochemical variables, and the improvement of adding mutated *MYD88* to the prognostic performance of the IPI.

To evaluate possible confounding of the impact of mutated *MYD88* and with the outcomes by anatomical lymphoma location, we performed a sensitivity analysis for OS on the cohort stratified by the anatomical lymphoma location, including CNS involvement. For patients with CNS involvement (N=35), *MYD88* had an unadjusted HR of 1.94 (95%-CI 0.77-4.90) in the univariable analysis. For patients without CNS involvement (N=215), *MYD88* did not have a significant impact on OS with an adjusted HR of 1.81 (95%-CI 0.96-3.42), when applying the multivariable analysis as described for model 3 (Table 3B). Although not statistically significant, the adjusted HR for this subgroup was similar to the original HR for the entire cohort.

Discussion

To the best of our knowledge, this is the first study evaluating the clinical significance of mutated *MYD88* and *CD79B* in DLBCL, in addition to the oncogenic drivers that are currently included in the WHO classification 2016 (EBV status and *MYC*, *BCL2*, and *BCL6* rearrangements), the IPI risk factors, and well-defined anatomical locations.

The strength of this study is the large number of patients with good clinical annotation and complete molecular analysis (N=198). In addition, our study shows that the incorporation of the mutational status of *MYD88* into a clinical/biochemical risk score as the IPI is feasible. An increase in the predictive performance of the IPI risk model as is illustrated by an increase in the CVC-index, suggests that this model can be improved by the introduction of molecular aberrations. However, while interpreting the results, we have encountered several limitations. *MYD88*-mutated DLBCL more often had extranodal location, older age (and thus a high IPI), and non-GCB subtype. Therefore, these patients were more frequently subjected to palliative care. Possibly the interaction between treatment and mutated *MYD88* has not been tested as more data is needed. We present an average effect over different treatment modalities. Since the reported frequencies and survival outcomes are similar to previous reports in the literature, our cohort appears to be representative for the target population.^{3,7-9,13} To investigate the prognostic significance of mutated *MYD88* adjusted for the IPI for the entire cohort, we considered PCNSL as advanced dis-

ease stage, although it is not common practice to apply the IPI in PCNSL patients. Additionally, our cohort is enriched for IP locations. Therefore, a sensitivity analysis was performed excluding PCNSL patients, demonstrating that the adjusted HR of *MYD88* for OS was similar to the entire cohort. This indicates that our results are not affected by confounding by CNS localisation. Hence, we believe that our data corroborate the clinical relevance of mutant *MYD88* for the diagnostic classification and prognostication of DLBCL and support implementation of *MYD88* mutational analysis in routine diagnostics. The simplicity and accessibility to examine *MYD88* mutations and associated low costs permit an efficient timely implementation. In addition, *CD79B* mutations were prognostic in the univariate analysis, but when adjusted for other aberrations in the multivariable analysis the prognostic importance disappeared. This finding may be explained by the prominent overlap between *MYD88* and *CD79B* mutations, as 78.2% of mutated *CD79B* had co-occurring *MYD88* mutations.

An important result of our study is the recognition of the prominent mutual exclusivity between the presence of mutations in *MYD88* and/or *CD79B*, *MYC*, *BCL2*, and *BCL6* rearrangements, and EBV infection, indicating that *MYD88* and/or *CD79B*-mutated tumors present a distinct DLBCL subcategory. In accordance with a large meta-analysis and two other studies,^{30,40,41} *MYD88* L265P mutations were preferentially found in specific anatomical sites (e.g. testis and CNS) and were significantly associated with non-GCB subtypes, older age, and poor OS. However, the published literature has studied neither explicitly analysed IP sites, nor evaluated the interaction of *MYD88* mutations with EBV status or oncogenic rearrangements in multivariable analysis. Other NGS studies have recently demonstrated high frequencies of mutated *MYD88* (15-18%) in large cohorts of DLBCL.^{1,2,15,42-44} Besides a certain association of mutated *MYD88* with poor OS (e.g. in non-GCB DLBCL), cluster analysis of multiple genes indicated distinct DLBCL subentities, including mutated *MYD88* as an important classifier for NF- κ B pathway activation. Again, these NGS studies did not take into account specific anatomical sites or investigated the interaction and prognostic significance of mutated *MYD88* in correlation with the EBV status or *MYC*, *BCL2*, and *BCL6* rearrangements.

In this context, our study adds important new knowledge by demonstrating *MYD88* mutations as an adverse prognostic factor for OS and relapse/progression in a multivariate analysis that takes all major known clinical and WHO classification-defined risk factors into account. This insight does not only show that the incorporation of the mutational status of *MYD88* into a clinical/biochemical risk score as the IPI is feasible, but also highlights the importance of assessing *MYD88* at the time of diagnosis for an optimal classification and patient counselling. An increase in the predictive performance of the IPI risk model, as is illustrated by an increase in the CVC-index, formally suggests that this model can be improved by the introduction of molecular aberrations. However, the prognostic impact of the *MYD88* mutational status on the presented multivariable models was not superior to anatomical lymphoma location. Whether the *MYD88* mutational status outperforms the predictive performance of anatomical lymphoma location in the described prognostic models needs further validation in an external cohort. Of note,

no difference was found for non-relapse mortality, indicating that mutated *MYD88* is a lymphoma-specific poor prognostic factor. Routine diagnostic assessment of *MYD88* mutations is likely to gain decisive importance for DLBCL since several approaches may therapeutically target *MYD88*.^{45,46} Several studies have indicated that DLBCL with mutated *MYD88* and/or *CD79B* are more sensitive to Bruton's Tyrosine Kinase (BTK)-inhibitors.⁴⁶⁻⁴⁸ As such, the objective analysis of *MYD88* mutations will not only improve diagnostic classification and prognostication, but might also enable patient selection for precision medicine such as treatment with BTK-inhibitors. However, the predictive significance of mutated *MYD88* with or without *CD79B* mutations needs to be validated in upcoming clinical trials, including precision medicine targeting the BCR and TLR cascades.

Finally, as a corollary of this study, we identified a novel good risk DLBCL group characterized by the absence of detected genetic aberrations. These DLBCL appeared to be highly sensitive to standard immune-chemotherapy as a first-line treatment. Future studies, employing a larger NGS targeted gene panel, may elucidate the genetic drivers in this group. We anticipate that there might be a parallel with the study of Chapuy *et al.*,¹⁵ which identified a good-risk DLBCL group harbouring mainly aberrations in epigenetic pathways.

Studies by Rossi *et al.* and Kurtz *et al.*,^{49,50} have analysed liquid biopsies in DLBCL demonstrating that the mutational load in circulating-free tumor DNA obtained by NGS technologies reliably mirror the mutational profiles of DLBCL tissues, including mutated *MYD88*. Additionally, digital droplet PCR techniques enable the quantification of low amounts of mutated *MYD88* in any

physiological fluid.⁵¹ Further investigation is needed to determine whether the analysis of mutated *MYD88* in liquid biopsies prior to and during therapy will be significantly predictive for the treatment response and to establish its specificity and sensitivity.

Conclusion

The present study demonstrates that the presence of *MYD88* and *CD79B* mutations is almost mutually exclusive with EBV infection and *MYC*, *BCL2*, and *BCL6* rearrangements, indicating distinctive molecular DLBCL subgroups that can be readily appreciated in clinical practice. Mutant *MYD88* showed its prognostic importance for inferior survival outcomes, even next to other genetic and clinical prognosticators and IPI. Additionally, patients lacking all analysed aberrancies represented a novel risk group with superior survival outcomes. Taken together and after validation in an independent cohort, these results provide a rationale for including *MYD88* mutational analysis in the routine diagnostics of DLBCL, to improve classification and prognostication, as well as to guide future treatment strategies.

Acknowledgments

The authors would like to thank the involved research technicians, data managers and physicians for their contributions to this manuscript.

Funding

This study was supported in part by research funding from 'Egbers Stichting AMC Foundation', 'Stichting Fonds Oncologie Holland', and Lymph&Co (JSV, SFS, RAG, AHC, WK, MS, MJK, and STP).

References

- Reddy A, Zhang J, Davis NS, Moffitt AB, Love CL, Waldrop A, et al. Genetic and functional drivers of diffuse large B cell lymphoma. *Cell*. 2017;171(2):481-94 e15.
- Phelan JD, Young RM, Webster DE, Roulland S, Wright GW, Kasbekar M, et al. A multiprotein supercomplex controlling oncogenic signalling in lymphoma. *Nature*. 2018;560(7718):387-391.
- Cunningham D, Hawkes EA, Jack A, Qian W, Smith P, Mouncey P, et al. Rituximab plus cyclophosphamide, doxorubicin, vincristine, and prednisolone in patients with newly diagnosed diffuse large B-cell non-Hodgkin lymphoma: a phase 3 comparison of dose intensification with 14-day versus 21-day cycles. *Lancet (London, England)*. 2013;381(9880):1817-1826.
- A predictive model for aggressive non-Hodgkin's lymphoma. *N Engl J Med*. 1993; 329(14):987-994.
- Wight JC, Chong G, Grigg AP, Hawkes EA. Prognostication of diffuse large B-cell lymphoma in the molecular era: moving beyond the IPI. *Blood Rev*. 2018;32(5):400-415.
- Swerdlow SH, Campo E, Pileri SA, Harris NL, Stein H, Siebert R, et al. The 2016 revision of the World Health Organization classification of lymphoid neoplasms. *Blood*. 2016;127(20):2375-2390.
- Rosenthal A, Younes A. High grade B-cell lymphoma with rearrangements of *MYC* and *BCL2* and/or *BCL6*: Double hit and triple hit lymphomas and double expressing lymphoma. *Blood Rev*. 2013;31(2):37-42.
- Shustik J, Han G, Farinha P, Johnson NA, Ben Neriah S, Connors JM, et al. Correlations between *BCL6* rearrangement and outcome in patients with diffuse large B-cell lymphoma treated with CHOP or R-CHOP. *Haematologica*. 2010;95(1):96-101.
- Schmidt-Hansen M, Berendse S, Marafioti T, McNamara C. Does cell-of-origin or *MYC*, *BCL2* or *BCL6* translocation status provide prognostic information beyond the International Prognostic Index score in patients with diffuse large B-cell lymphoma treated with rituximab and chemotherapy? A systematic review. *Leukemia & lymphoma*. 2017;58(10):2403-2418.
- Akyurek N, Uner A, Benekli M, Barista I. Prognostic significance of *MYC*, *BCL2*, and *BCL6* rearrangements in patients with diffuse large B-cell lymphoma treated with cyclophosphamide, doxorubicin, vincristine, and prednisone plus rituximab. *Cancer*. 2012;118(17):417347-83.
- McPhail ED, Maurer MJ, Macon WR, Feldman AL, Kurtin PJ, Ketterling RP, et al. Inferior survival in high-grade B-cell lymphoma with *MYC* and *BCL2* and/or *BCL6* rearrangements is not associated with *MYC/IG* gene rearrangements. *Haematologica*. 2018;103(11):1899-1907.
- Leskov I, Pallasch CP, Drake A, Iliopoulou BP, Souza A, Shen CH, et al. Rapid generation of human B-cell lymphomas via combined expression of *Myc* and *Bcl2* and their use as a preclinical model for biological therapies. *Oncogene*. 2013;32(8):1066-1072.
- Gao X, Li J, Wang Y, Liu S, Yue B. Clinical characteristics and prognostic significance of EBV positivity in diffuse large B-cell lymphoma: A meta-analysis. *PloS one*. 2018;13(6):e0199398.
- Lu TX, Liang JH, Miao Y, Fan L, Wang L, Qu XY, et al. Epstein-Barr virus positive diffuse large B-cell lymphoma predict poor outcome, regardless of the age. *Scientific reports*. 2015;5:12168.
- Chapuy B, Stewart C, Dunford AJ, Kim J, Kamburov A, Redd RA, et al. Molecular subtypes of diffuse large B cell lymphoma are associated with distinct pathogenic mechanisms and outcomes. *Nature medicine*. 2018;24(5):679-690.
- Schmitz R, Wright GW, Huang DW, Johnson CA, Phelan JD, Wang JQ, et al. Genetics and pathogenesis of diffuse large B-cell lymphoma. *New Engl J Med*. 2018; 378(15):1396-1407.
- Ngo V.N. YRM, Schmitz R., et al. Oncogenically active *MYD88* mutations in human lymphoma. *Nature*. 2011;(3)470:7.
- Davis RE, Ngo VN, Lenz G, Tolar P, Young RM, Romesser PB, et al. Chronic active B-cell-receptor signalling in diffuse large B-cell lymphoma. *Nature*. 2010;463(7277):88-92.
- Alizadeh AA, Eisen MB, Davis RE, Ma C, Lossos IS, Rosenwald A, et al. Distinct

- types of diffuse large B-cell lymphoma identified by gene expression profiling. *Nature*. 2000;403(6769):503-511.
20. Schrader AMR, Jansen PM, Willemze R, Vermeer MH, Cleton-Jansen AM, Somers SF, et al. High prevalence of MYD88 and CD79B mutations in intravascular large B-cell lymphoma. *Blood*. 2018;131(18):2086-2089.
 21. Zhou XA, Louissaint A, Jr., Wenzel A, Yang J, Martinez-Escala ME, Moy AP, et al. Genomic analyses identify recurrent alterations in immune evasion genes in diffuse large B cell lymphoma, leg type. *J Invest Dermatol*. 2018;138(11):2365-2376.
 22. Bonzheim I, Giese S, Deuter C, Susskind D, Zierhut M, Waizel M, et al. High frequency of MYD88 mutations in vitreoretinal B-cell lymphoma: a valuable tool to improve diagnostic yield of vitreous aspirates. *Blood*. 2015;126(1):76-79.
 23. Cani AK, Soliman M, Hovelson DH, Liu CJ, McDaniel AS, Haller MJ, et al. Comprehensive genomic profiling of orbital and ocular adnexal lymphomas identifies frequent alterations in MYD88 and chromatin modifiers: new routes to targeted therapies. *Mod Pathol*. 2016; 29(7):685-697.
 24. Raja H, Salomao DR, Viswanatha DS, Pulido JS. Prevalence of Myd88 L265p mutation in histologically proven, diffuse large B-cell vitreoretinal lymphoma. *Retina*. 2016;36(3):624-628.
 25. Taniguchi K, Takata K, Chuang SS, Miyata-Takata T, Sato Y, Satou A, et al. Frequent MYD88 L265P and CD79B mutations in primary breast diffuse large B-cell lymphoma. *Am J Surg Pathol*. 2016; 40(3):324-334.
 26. Kraan W, van Keimpema M, Horlings HM, Schilder-Tol EJ, Oud ME, Noorduyn LA, et al. High prevalence of oncogenic MYD88 and CD79B mutations in primary testicular diffuse large B-cell lymphoma. *Leukemia*. 2014; 28(3):719-720.
 27. Chapuy B, Roemer MG, Stewart C, Tan Y, Abo RP, Zhang L, et al. Targetable genetic features of primary testicular and primary central nervous system lymphomas. *Blood*. 2016;127(7):869-881.
 28. Kersten MJ, Kraan W, Doorduijn J, Bromberg J, Lam K, Kluin PM, et al. Diffuse large B cell lymphomas relapsing in the CNS lack oncogenic MYD88 and CD79B mutations. *Blood Cancer J*. 2014;12;4:e266.
 29. Kraan W, Horlings HM, van Keimpema M, Schilder-Tol EJ, Oud ME, Scheepstra C, et al. High prevalence of oncogenic MYD88 and CD79B mutations in diffuse large B-cell lymphomas presenting at immune-privileged sites. *Blood Cancer J*. 2013; 3:e139.
 30. Lee JH, Jeong H, Choi JW, Oh H, Kim YS. Clinicopathologic significance of MYD88 L265P mutation in diffuse large B-cell lymphoma: a meta-analysis. *Scientific reports*. 2017;7(1):1785.
 31. Yu S, Luo H, Pan M, Palomino LA, Song X, Wu P, et al. High frequency and prognostic value of MYD88 L265P mutation in diffuse large B-cell lymphoma with R-CHOP treatment. *Oncology Lett*. 2018;15(2):1707-1715.
 32. Vermaat JS, Pals ST, Younes A, Dreyling M, Federico M, Aurer I, et al. Precision medicine in diffuse large B-cell lymphoma: hitting the target. *Haematologica*. 2015; 100(8):989-993.
 33. Hans CP, Weisenburger DD, Greiner TC, Gascoyne RD, Delabie J, Ott G, et al. Confirmation of the molecular classification of diffuse large B-cell lymphoma by immunohistochemistry using a tissue microarray. *Blood*. 2004;103(1):275-282.
 34. van Eijk R, Stevens L, Morreau H, van Wezel T. Assessment of a fully automated high-throughput DNA extraction method from formalin-fixed, paraffin-embedded tissue for KRAS, and BRAF somatic mutation analysis. *Exp Mol Pathol*. 2013; 94(1):121-125.
 35. Sibinga Mulder BG, Mieog JS, Handgraaf HJ, Farina Sarasqueta A, Vasen HF, Potjer TP, et al. Targeted next-generation sequencing of FNA-derived DNA in pancreatic cancer. *J Clin Pathol*. 2017;70(2):174-178.
 36. Schemper M, Smith TL. A note on quantifying follow-up in studies of failure time. *Control Clin Trials*. 1996;17(4):343-346.
 37. Kim HT. Cumulative incidence in competing risks data and competing risks regression analysis. *Clin Cancer Res*. 2007;15;13(2 Pt 1):559-565.
 38. Houwelingen HC PH. *Dynamic Prediction in Clinical Survival Analysis*. Chapman & Hall., 2012.
 39. Zheng M, Perry AM, Bierman P, Loberiza F, Jr., Nasr MR, Szwajcer D, et al. Frequency of MYD88 and CD79B mutations, and MGMT methylation in primary central nervous system diffuse large B-cell lymphoma. *Neuropathology*. 2017;37(6):509-516.
 40. Rovira J, Karube K, Valera A, Colomer D, Enjuanes A, Colomo L, et al. MYD88 L265P mutations, but no other variants, identify a subpopulation of DLBCL patients of activated B-cell origin, extranodal involvement, and poor outcome. *Clin Cancer Res*. 2016;22(11):10.
 41. Dubois S, Viailly PJ, Bohers E, Bertrand P, Ruminy P, Marchand V, et al. Biological and clinical relevance of associated genomic alterations in MYD88 L265P and non-L265P-mutated diffuse large B-cell lymphoma: analysis of 361 cases. *Clin Cancer Res*. 2017;23(9):2232-2244.
 42. Intlekofer AM, Joffe E, Batlevi CL, Hilden P, He J, Seshan VE, et al. Integrated DNA/RNA targeted genomic profiling of diffuse large B-cell lymphoma using a clinical assay. *Blood Cancer J*. 2018;12;8(6):60.
 43. Karube K, Enjuanes A, Dlouhy I, Jares P, Martin-Garcia D, Nadeu F, et al. Integrating genomic alterations in diffuse large B-cell lymphoma identifies new relevant pathways and potential therapeutic targets. *Leukemia*. 2018;32(3):675-684.
 44. Xu PP, Zhong HJ, Huang YH, Gao XD, Zhao X, Shen Y, et al. B-cell function gene mutations in diffuse large B-cell lymphoma: a retrospective cohort study. *EBioMedicine*. 2017;16:106-114.
 45. Yu X, Li W, Deng Q, Li L, Hsi ED, Young KH, et al. MYD88 L265P Mutation in lymphoid malignancies. *Cancer Res*. 2018; 78(10):2457-2462.
 46. de Groen RAL, Schrader AMR, Kersten MJ, Pals ST, Vermaat JSP. MYD88 in the driver's seat of B-cell lymphomagenesis: from molecular mechanisms to clinical implications. *Haematologica*. 2019;104(12):2337-2248.
 47. Grommes C, Pastore A, Palaskas N, Tang SS, Campos C, Schartz D, et al. Ibrutinib unmasks critical role of Bruton tyrosine kinase in primary CNS lymphoma. *Cancer Discov*. 2017;7(9):1018-1029.
 48. Lionakis MS, Dunleavy K, Roschewski M, Widemann BC, Butman JA, Schmitz R, et al. Inhibition of B cell receptor signaling by ibrutinib in primary CNS lymphoma. *Cancer Cell*. 2017;31(6):833-43 e5.
 49. Wilson WH, Young RM, Schmitz R, Yang Y, Pittaluga S, Wright G, et al. Targeting B cell receptor signaling with ibrutinib in diffuse large B cell lymphoma. *Nat Med* 2015; 21(8):922-926.
 50. Kurtz DM, Scherer F, Jin MC, Soo J, Craig AFM, Esfahani MS, et al. Circulating tumor DNA measurements as early outcome predictors in diffuse large B-cell lymphoma. *J Clin Oncol*. 2018; 36(28):2845-2853.
 51. Rossi D, Diop F, Spaccarotella E, Monti S, Zanni M, Rasi S, et al. Diffuse large B-cell lymphoma genotyping on the liquid biopsy. *Blood*. 2017;129(14):1947-1957.
 52. Hiemcke-Jiwa LS, Minnema MC, Radersma-van Loon JH, Jiwa NM, de Boer M, Leguit RJ, et al. The use of droplet digital PCR in liquid biopsies: a highly sensitive technique for MYD88 p.(L265P) detection in cerebrospinal fluid. *Hematol Oncol*. 2018;36(2):429-35.

High activation of STAT5A drives peripheral T-cell lymphoma and leukemia

Barbara Maurer,^{1,2,3} Harini Nivarthi,⁴ Bettina Wingelhofer,^{1,2} Ha Thi Thanh Pham,^{1,2} Michaela Schleder,^{1,5} Tobias Suske,² Reinhard Grausenburger,³ Ana-Iris Schiefer,⁵ Michaela Prchal-Murphy,³ Doris Chen,⁴ Susanne Winkler,¹ Olaf Merkel,⁵ Christoph Kornauth,⁵ Maximilian Hofbauer,¹ Birgit Hochgatterer,¹ Gregor Hoermann,⁶ Andrea Hoelbl-Kovacic,³ Jana Prochazkova,⁴ Cosimo Lobello,⁷ Abbarna A. Kumaraswamy,⁸ Johanna Latzka,⁹ Melitta Kitzwögerer,¹⁰ Andreas Chott,¹¹ Andrea Janikova,¹² Šárka Pospíšilova,^{7,12} Joanna I. Loizou,⁴ Stefan Kubicek,⁴ Peter Valent,¹³ Thomas Kolbe,^{14,15} Florian Grebien,^{1,16} Lukas Kenner,^{1,5,17} Patrick T. Gunning,⁷ Robert Kralovics,⁴ Marco Herling,¹⁸ Mathias Müller,² Thomas Rülcke,¹⁹ Veronika Sexl³ and Richard Moriggl^{1,2,20}

¹Ludwig Boltzmann Institute for Cancer Research, Vienna, Austria; ²Institute of Animal Breeding and Genetics, University of Veterinary Medicine Vienna, Vienna, Austria; ³Institute of Pharmacology and Toxicology, University of Veterinary Medicine Vienna, Vienna, Austria; ⁴CeMM Research Center for Molecular Medicine of the Austrian Academy of Sciences, Vienna, Austria; ⁵Department of Clinical Pathology, Medical University of Vienna, Vienna, Austria; ⁶Department of Laboratory Medicine, Medical University of Vienna, Vienna, Austria; ⁷Central European Institute of Technology (CEITEC), Center of Molecular Medicine, Masaryk University, Brno, Czech Republic; ⁸Department of Chemistry, University of Toronto Mississauga, Mississauga, Ontario, Canada; ⁹Karl Landsteiner Institute of Dermatological Research, St. Poelten, Austria and Department of Dermatology and Venereology, Karl Landsteiner University for Health Sciences, St. Poelten, Austria; ¹⁰Department of Clinical Pathology, Karl Landsteiner University of Health Sciences, St. Poelten, Austria; ¹¹Institute of Pathology and Microbiology, Wilheminspital, Vienna, Austria; ¹²Department of Internal Medicine – Hematology and Oncology, Faculty of Medicine Masaryk University and University Hospital Brno, Brno, Czech Republic; ¹³Department of Internal Medicine I, Division of Hematology and Hemostaseology and Ludwig Boltzmann Cluster Oncology, Medical University of Vienna, Vienna, Austria; ¹⁴Biomodels Austria, University of Veterinary Medicine Vienna, Vienna, Austria; ¹⁵IFA-Tulln, University of Natural Resources and Applied Life Sciences, Tulln, Austria; ¹⁶Institute of Medical Biochemistry, University of Veterinary Medicine Vienna, Vienna, Austria; ¹⁷Unit of Laboratory Animal Pathology, University of Veterinary Medicine Vienna, Vienna, Austria; ¹⁸Department I of Internal Medicine, Center for Integrated Oncology (CIO) Köln-Bonn, Excellence Cluster for Cellular Stress Response and Aging-Associated Diseases (CECAD), Center for Molecular Medicine Cologne (CMMC), University of Cologne, Cologne, Germany; ¹⁹Institute of Laboratory Animal Science, University of Veterinary Medicine Vienna, Vienna, Austria and ²⁰Medical University of Vienna, Vienna, Austria

ABSTRACT

Recurrent gain-of-function mutations in the transcription factors *STAT5A* and much more in *STAT5B* were found in hematopoietic malignancies with the highest proportion in mature T- and natural killer-cell neoplasms (peripheral T-cell lymphoma, PTCL). No targeted therapy exists for these heterogeneous and often aggressive diseases. Given the shortage of models for PTCL, we mimicked graded *STAT5A* or *STAT5B* activity by expressing hyperactive *Stat5a* or *STAT5B* variants at low or high levels in the hematopoietic system of transgenic mice. Only mice with high activity levels developed a lethal disease resembling human PTCL. Neoplasia displayed massive expansion of CD8⁺ T cells and destructive organ infiltration. T cells were cytokine-hypersensitive with activated memory CD8⁺ T-lymphocyte characteristics. Histopathology and mRNA expression profiles revealed close correlation with distinct subtypes of PTCL. Pronounced *STAT5* expression and activity in samples from patients with different subsets underline the relevance of JAK/STAT as a therapeutic target. JAK inhibitors or a selective *STAT5* SH₂ domain inhibitor induced cell death and ruxolitinib blocked T-cell neoplasia *in vivo*. We conclude that enhanced *STAT5A* or *STAT5B* action both drive PTCL development, defining both *STAT5* molecules as targets for therapeutic intervention.



Haematologica 2018
Volume 105(2):435-447

Correspondence:

RICHARD MORIGGL
richard.moriggl@vetmeduni.ac.at

Received: January 18, 2019.

Accepted: May 21, 2019.

Pre-published: May 23, 2019.

doi:10.3324/haematol.2019.216986

Check the online version for the most updated information on this article, online supplements, and information on authorship & disclosures: www.haematologica.org/content/105/2/435

©2020 Ferrata Storti Foundation

Material published in *Haematologica* is covered by copyright. All rights are reserved to the Ferrata Storti Foundation. Use of published material is allowed under the following terms and conditions:

<https://creativecommons.org/licenses/by-nc/4.0/legalcode>. Copies of published material are allowed for personal or internal use. Sharing published material for non-commercial purposes is subject to the following conditions: <https://creativecommons.org/licenses/by-nc/4.0/legalcode>, sect. 3. Reproducing and sharing published material for commercial purposes is not allowed without permission in writing from the publisher.



Introduction

Peripheral (mature) T-cell lymphomas (PTCL) are heterogeneous neoplasms often accompanied by aggressive courses and extranodal organ infiltration. PTCL have variable histology, immunophenotype, and molecular features.^{1,2} The World Health Organization (WHO) classification of lymphoid neoplasms distinguishes more than 30 mature T- and natural killer (NK)-cell neoplasms. The most common subtype is PTCL, not otherwise specified (NOS), which collects together cases not attributable to other, better defined, entities. PTCL, NOS is a highly dynamic category with respect to consensus features, proposed cell of origin, and prognostic subsets based on molecular signatures.³ PTCL, NOS with a follicular T-helper (T_{FH}) cell phenotype relates to angioimmunoblastic T-cell lymphoma (AITL), with which it is co-categorized in a provisional group.⁴ Another distinguishable PTCL, NOS subset is constituted by cases with cytotoxic features. High-throughput methodologies helped in such histogenetic assignments and in the prognostically relevant separation of non-T_{FH} type PTCL, NOS from AITL and anaplastic large cell lymphoma.^{2,3,5-7} Eminent problems, particularly in PTCL, NOS, are the inefficacy of the poly-chemotherapies historically designed for aggressive B-cell lymphomas and the lack of high-fidelity mouse models⁸⁻¹⁰ in which to investigate biological principles and to address preclinical questions.

The molecular landscape of PTCL, NOS reveals that altered T-cell receptor signaling, epigenetic modifiers, and immune evasion mechanisms are common.^{3,5,7,11-17} Activating mutations in the JAK-STAT pathway affecting mostly the interleukin-2 receptor (*IL2R*), *JAK1*, *JAK3*, *STAT3*, and *STAT5B* were found in many mature T- and NK-cell neoplasms.^{18,19} The entities with the highest incidence of *STAT5B* and *STAT3* mutations are anaplastic large cell lymphoma, cutaneous T-cell lymphoma (CTCL; comprising mycosis fungoides and Sézary syndrome), enteropathy-associated T-cell lymphoma, hepatosplenic T-cell lymphoma, NK/T-cell lymphoma, T-cell prolymphocytic leukemia, and the auto-aggressive CD8⁺ T-large granular lymphocyte leukemia.^{15,20-22} Furthermore, mutations in chromatin remodelers, GTPases, DNA repair machinery or co-repressors have been associated with JAK/STAT hyperactivation.¹⁹

STAT5B^{N642H} is the most frequent recurrent gain-of-function mutation in the closely related genes encoding for the transcription factors *STAT5A* and *STAT5B*. It is associated with unfavorable disease progression in patients^{15,23-31} and leads to an aggressive CD8⁺ T-cell neoplasia in mice.³² JAK-STAT signaling is a central cancer pathway driving survival and cell cycle progression, but it also promotes differentiation and senescence as safety pathways. *STAT5A* and *STAT5B* play important roles in immune cells³³ and absence of lymphoid *STAT5* results in loss of CD8⁺, $\gamma\delta$, and regulatory T cells (T_{reg}).³⁴ Differentiation of CD8⁺ T cells is regulated by *STAT5* in a dose-dependent manner³⁵ and enhances effector and memory CD8⁺ T-cell survival and proliferation. High levels of tyrosine phosphorylated *STAT5* (pYSTAT5) are associated with a negative prognosis in many myeloid neoplasms.³⁶

Aggressive CD8⁺ T-cell neoplasia resulted in early death upon *STAT5B*^{N642H} expression.³² Enhanced pYSTAT5 can also be mimicked by the hyperactive *Stat5a*^{S710F} variant (cS5^F).³⁷ We generated and compared graded *STAT5* activ-

ity mouse models within the hematopoietic system. Low activity models displayed only a modest CD8⁺ T-cell expansion, whereas those with high *STAT5* activity developed aggressive CD8⁺ PTCL-like disease reminiscent of human PTCL, NOS with cytotoxic features. Although *STAT5A*- and *STAT5B*-induced changes largely overlap, *STAT5B* hyperactivation was more aggressive than *STAT5A* hyperactivation. Comparative analyses revealed that *STAT5A* and *STAT5B* overexpression is common in human mature T-cell lymphomas. The clinical JAK1/2/3 inhibitors ruxolitinib and tofacitinib³⁸ as well as a selective *STAT5* inhibitor³⁹ specifically reduced viability of PTCL cells. Ruxolitinib blocked PTCL disease *in vivo*. We conclude that *STAT5* activation drives PTCL and that patients with PTCL can benefit from JAK/STAT inhibitors.

Methods

Animals and generation of transgenic mice

Mice were maintained on a C57BL/6N background, housed in a specific-pathogen-free facility under standardized conditions and monitored daily for signs of disease. All animal experiments were carried out according to the animal license protocols (BMWF-66.009/0281-I/3b/2012, BMWFW-68.205/0166-WF/V/3b/2015, BMWFW-68.205/0117-WF/V/3b/2016 and BMWFW-68.205/0103-WF/V/3b/2015) approved by the institutional Ethics Committee and the Austrian Ministry BMWF authorities. All transgenic mice were hemizygous. Non-transgenic littermates served as controls. We used the *vav*-hematopoietic vector *vav-hCD4* (*HS21/45*)⁴⁰ to generate transgenic mice expressing cS5^F in the hematopoietic system at different levels (called cS5A^{lo} [B6N-Tg(Vav-cS5F)564Biat] and cS5A^{hi} [B6N-Tg(Vav-cS5F)565Biat]), as described in the *Online Supplementary Methods*. Details of hSTAT5B and hSTAT5B^{N642H} mice have been published.³² All primers used are listed in *Online Supplementary Table S1*.

Patients' samples

Retrospective immunohistological analysis, approved by the ethics committee of the Medical University of Vienna (1437/2016), was done on formalin-fixed, paraffin-embedded patients' specimens of 35 PTCL, NOS, 14 AITL, 6 mycosis fungoides, and 29 CTCL (from 23 patients) cases and 5 non-diseased lymph nodes, kindly provided by the Medical University of Vienna, Austria, the Karl Landsteiner University of Health Sciences, St. Poelten, Austria, Wilheminspital (Wiener Krankenanstaltenverbund), Vienna, Austria, and the University Hospital Brno, Czech Republic. Samples were included in this study after patients had given informed consent in accordance with the Declaration of Helsinki. Diagnoses of samples were made according to the 2008 WHO criteria by experienced hematopathologists or expert dermatopathologists. Patients with CTCL were diagnosed according to the WHO-EORTC classification for cutaneous lymphomas as follows: mycosis fungoides (stage IA: n=10, stage IB: n=1, stage IIA: n=1, stage IIB: n=6), Sézary syndrome (n=2), and lymphomatoid papulosis (n=3).

Histological analysis of murine and human sections

Formalin-fixed, paraffin-embedded 3 μ m consecutive mouse organ sections were stained with hematoxylin (Merck, Darmstadt, Germany) and eosin G (Carl Roth, Karlsruhe, Germany). Immunohistochemistry was performed using anti-

bodies against CD3, Ki67, pYSTAT5, STAT5A and STAT5B (Online Supplementary Table S4, Online Supplementary Methods). For immunohistochemical analysis of STAT5A and STAT5B expression in human samples, tissue microarrays were built including 14 AITL, 35 PTCL, NOS, 7 CTCL, and 6 mycosis fungoides cases each represented by duplicate or triplicate core biopsies. In addition, paraffin-preserved sections of 29 CTCL samples (from 23 patients) were analyzed. Five non-neoplastic lymph nodes served as controls. Quantification of the staining is described in the Online Supplementary Methods. Images were taken with a Zeiss Imager Z1 microscope (Carl Zeiss, Oberkochen, Germany).

RNA sequencing

mRNA was isolated from CD8⁺ T cells harvested from lymph nodes [wildtype (wt) - 2-3 mice pooled per sample, cS5A^{lo}, cS5A^{hi}, hSTAT5B^{N642H} n=5, hSTAT5B n=4]. RNA sequencing was performed with Illumina HiSeq-2500 (Illumina, San Diego, CA, USA) at the VBCF next-generation sequencing unit (www.vbcf.ac.at). Details of the analysis are provided in the Online Supplementary Methods.

RNA-sequencing data can be found in the GEO database with the accession identities GSE124102 and GSE93847.

Statistical analysis

Data are reported as mean values \pm standard error of mean and were analyzed by GraphPad Prism[®] 5 (San Diego, CA, USA) or RStudio Version 1.0.153 (Boston, MA, USA). *In vitro* data, western blots, quantitative reverse transcriptase polymerase chain reactions (qRT-PCR) and viability assays were repeated at least three times (unless indicated otherwise). The numbers of animals or patients are stated in each figure or figure legend. Applied statistical tests are mentioned in the respective figure legend. *P* values <0.05 were accepted as statistically significant and denoted as follows: **P*<0.05; ***P*<0.01; ****P*<0.001, and *****P*<0.0001.

Results

STAT5A or STAT5B activation leads to a mature CD8⁺ T-cell disease in mice

To test whether hyperactive STAT5 signaling alone is sufficient to drive PTCL, we generated transgenic mice with graded expression of wildtype (wt) *STAT5B* or gain-of-function *Stat5a* or *STAT5B*. We used the well-characterized hyperactive *Stat5a*^{S710E} (cS5^{hi}) variant³⁷ expressed at

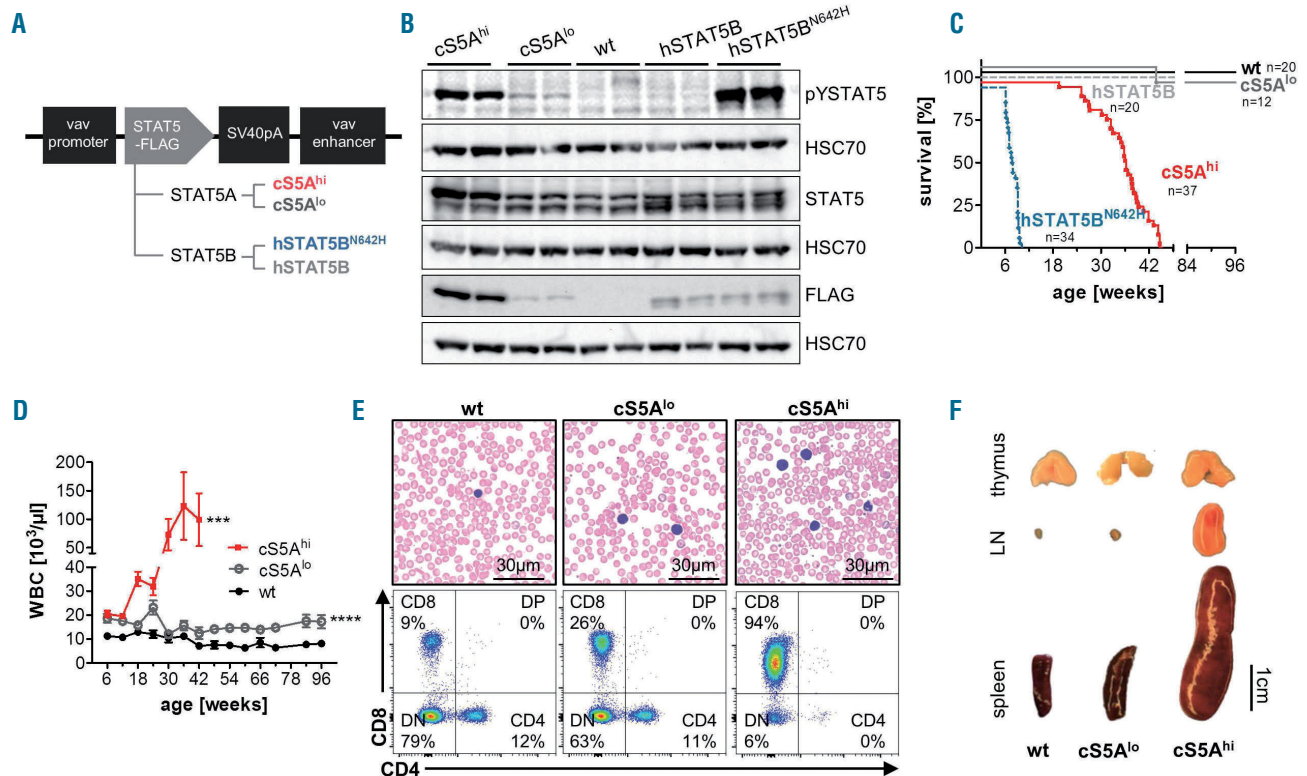


Figure 1. Expression of a gain-of-function *Stat5a* or *STAT5B* variant leads to a polyclonal CD8⁺ T-cell disease. (A) Schematic representation of the FLAG-tagged *STAT5* constructs for generation of transgenic mouse lines expressing hyperactive *Stat5a* (cS5A^{lo} and cS5A^{hi}) or human *STAT5B* (hSTAT5B and hSTAT5B^{N642H}). (B) Immunoblot on lymph node lysates from cS5A^{hi}, cS5A^{lo}, wildtype (wt), hSTAT5B, and hSTAT5B^{N642H} mice (n=2/genotype) using antibodies to FLAG, phosphotyrosine(Y694)-STAT5 (pYSTAT5) and STAT5. HSC70 was used as a loading control. Representative blot of four experiments. (C) Kaplan-Meier disease-free survival plot of wt (n=20), cS5A^{lo} (n=12), cS5A^{hi} (n=37), hSTAT5B (n=20) and hSTAT5B^{N642H} (n=34) mice; *P*≤0.0001 with the log-rank (Mantel-Cox) test. (D) White blood cell (WBC) count measured at 6-week intervals from wt (n≥6), cS5A^{lo} (n≥8) and cS5A^{hi} (n≥10) mice for 66 weeks (cS5A^{hi} until 42 weeks). *****P*<0.0001, wt vs. cS5A^{lo} *P*=0.003. (E) Representative blood smears of 32-week old mice, scale bar 30 μ m, and representative flow cytometry dot plots of CD4 and CD8 cells in peripheral blood of 32-week old wt, cS5A^{lo} and cS5A^{hi} mice. (F) Macroscopic appearance of thymi, lymph nodes (LN), and spleens of representative age-matched wt, cS5A^{lo} and cS5A^{hi} mice.

low or high level, human (h)STAT5B served as a negative control and hSTAT5B^{N642H} served as a positive T-cell neoplastic model.³² All transgenes contain a C-terminal FLAG-tag driven under control of the *vav*-promoter enabling expression from the hematopoietic stem cell stage onwards throughout all blood lineages⁴⁰ (hereafter referred to as cS5A^F, cS5A^{lo}, cS5A^{hi}, hSTAT5B and hSTAT5B^{N642H}) (Figure 1A, *Online Supplementary Figure S1A-D*). We confirmed significantly elevated pYSTAT5 levels in hematopoietic organs of cS5A^{hi} and hSTAT5B^{N642H} mice whereas the cS5A^{lo} animals showed a modest increase in pYSTAT5 (Figure 1B, *Online Supplementary Figure S1E*). Kidney, colon and liver did not display significant transgene expression (*Online Supplementary Figure S1E*). Transgene expression was verified by qRT-PCR in FACS-sorted CD4⁺, CD8⁺, CD19⁺, CD11b⁺ and NK cells of 8-week old cS5A^{lo} and cS5A^{hi} mice, with CD8⁺ T cells showing highest transgene mRNA expression (*Online Supplementary Figure S1F*).

Enhanced STAT5 activation in the hematopoietic system led to development of neoplasia resulting in death between 25 to 45 weeks of age irrespective of gender in cS5A^{hi} mice, which was significantly later than in hSTAT5B^{N642H} mice which develop a lethal disease within 10 weeks.³² cS5A^{lo} were as long-lived as wt mice; hSTAT5B mice were also followed for more than 1 year without showing signs of disease (Figure 1C). The strong lymphoma phenotype of hSTAT5B^{N642H} mice suggests a role of STAT5A as a possible balancer due to STAT5A/B heterodimerization, but only high pYSTAT5 levels drive the disease.

White blood cell counts rose steadily in cS5A^{hi} mice to a level comparable to that in diseased hSTAT5B^{N642H} mice, whereas cS5A^{lo} exerted only a subtle effect, resulting in doubling of the white cell count compared to that in wt mice (Figure 1D, *Online Supplementary Figure S1H*), also seen in the blood smears (Figure 1E). Like hSTAT5B^{N642H} mice, adult cS5A^{hi} massively expanded CD8⁺ T cells and the phenotype in cS5A^{lo} mice was intermediate (Figure 1E, *Online Supplementary Figure S1G, H*). At 32 weeks of age, cS5A^{hi} mice had massively enlarged lymph nodes at all lymphatic sites and severe splenomegaly, but cS5A^{lo} mice did not show any pathological abnormalities. Interestingly, macroscopically, STAT5A transgenic thymi showed no obvious differences from those of age-matched controls (Figure 1F). Our further analysis focused on the comparison of cS5A^{hi} mice and their wt littermates.

Expanded CD8⁺ T cells exert a mature cytotoxic T-lymphocyte phenotype

At the age of 25–45 weeks all cS5A^{hi} mice developed terminal disease. CD8⁺ T cells were dominant in spleen (Figure 2A, *Online Supplementary Figure S2A*), peripheral blood, lymph nodes and bone marrow of cS5A^{hi} mice (*Online Supplementary Figure S2B*). While relative levels of CD4⁺ T, CD19⁺ B and CD11b⁺Gr1^{hi} myeloid cells were decreased (*Online Supplementary Figure S2A-C*), absolute numbers of these cell types were elevated, although to a lesser extent than CD8⁺ T cells (Figure 2A). In contrast, both the relative and absolute numbers of NK cells were decreased (Figure 2A, *Online Supplementary Figure S2A*). Western blot analysis of lymphocyte subpopulations confirmed the highest levels of cS5A^F expression in CD8⁺ T cells (*Online Supplementary Figure S2D*). The cS5A^{lo} mice did not display a phenotype despite increased CD8⁺ T-cell

numbers and pronounced pYSTAT5 levels (*Online Supplementary Figure S2E-I*).

To assess the functionality of the cytotoxic T cells (CTL), we injected the C57BL/6 isogenic CTL-responsive lymphoma cell line E.G7 or the colon carcinoma cell line MC-38 into flanks of 10-week old wt, cS5A^{lo} or cS5A^{hi} mice. In comparison to tumors in wt hosts, tumors in cS5A^{lo} and cS5A^{hi} mice were significantly smaller or absent and infiltrated more by CD8⁺ T cells, indicating that the expanded CD8⁺ T cells retained functionality (Figure 2B, *Online Supplementary Figure S2J*).

Next, we sought to further characterize the disease-causing cells. cS5A^{hi} CD8⁺ T cells retained CD2, CD3 and CD5 expression (Figure 2C, *Online Supplementary Figure S2K*). CD25⁺ and CD44⁺ CD8⁺ T cells were expanded in peripheral blood and hematopoietic organs of cS5A^{hi} animals (Figure 2D, *Online Supplementary Figure S2L, M*), indicative of an activated/memory-like T-cell phenotype.⁴¹ CD8⁺ T cells can be divided into effector (T_{EM}) and central memory (T_{CM}) subsets, either representing a rapid effector cell or exerting lymph node-homing properties with potent proliferative potential.^{42,43} cS5A^{hi} mice displayed elevated levels of CD44⁺CD62L⁺CD8⁺ (T_{CM}) and CD44⁺CD62L⁺CD8⁺ (T_{EM}) T cells (Figure 2E, *Online Supplementary Figure S2N, O*). Gene set enrichment analysis on differentially expressed genes in CD8⁺ T cells of cS5A^{hi} compared to cS5A^{lo} mice also correlated to a memory/effector signature (*Online Supplementary Figure S2P*).⁴⁴ The homing and activation marker CCR7 was also expressed on a subpopulation; CD8⁺CD62L⁺CCR7⁺ cells in particular were more frequent in cS5A^{hi} than in wt cases (*Online Supplementary Figure S2Q, R*). Furthermore, hyperactive STAT5A signaling led to more T_{reg} and $\gamma\delta$ T cells (*Online Supplementary Figure S2S, T*).

Together, these data indicate that hyperactivation of STAT5A in cS5A^{hi} transgenic mice induces mature T-cell neoplasia with an activated cytotoxic CD8⁺ memory phenotype.

STAT5-driven CD8⁺ T cells infiltrate organs

Enlarged lymph nodes, splenomegaly and infiltration of T cells into organs such as the skin, liver, lung and bone marrow are hallmarks in human PTCL. Histological analysis of tissues from cS5A^{hi} mice revealed disrupted lymph nodes and spleen architecture with dense infiltration of CD3⁺ T cells and increased proliferation (Ki67⁺) within lymphomas (Figure 3A, B, *Online Supplementary Figure S3A*). With regards to skin pathology, diseased mice displayed a thickened dermis with diffuse infiltration of CD3⁺ T cells (*Online Supplementary Figure S3B, C*). Moreover, peribronchial and interstitial T-cell infiltrations were detected in lungs of cS5A^{hi} mice (Figure 3C). Hepatic T-cell infiltration in portal tracts and sinusoids as well as diffuse perivascular and interstitial renal infiltrates were prominent (Figure 3D, *Online Supplementary Figure S3D*). Higher numbers of Ki67⁺ cells indicated active proliferation of infiltrating T cells (Figure 3C, D, *Online Supplementary Figure S3B, D*, quantification summarized in *Online Supplementary Figure S3E*).

Transferred cS5A^{hi} CD8⁺ T cells induce peripheral T-cell lymphoma in non-irradiated recipients

To establish the disease-initiating potency of the mature and differentiated cS5A^{hi}-CD8⁺ T cells, we transferred CD8⁺ Ly5.2⁺/CD45.2⁺ T cells from lymph nodes or spleens

of diseased cS5A^{hi} transgenic mice into non-irradiated immunocompetent Ly5.1⁺/CD45.1⁺ recipient mice (Figure 4A). Recipients of cS5A^{hi} CD8⁺ T cells showed an increase in white blood cell count starting from 8 weeks after transplantation due to an expansion of the Ly5.2⁺ cS5A^{hi}-CD8⁺ T cells in contrast to wt-derived CD8⁺ T cells (Figure 4B, *Online Supplementary Figure S4A*). Recipients of cS5A^{hi}-

CD8⁺ T cells had splenomegaly (*Online Supplementary Figure S4B*) and high levels of donor-derived cS5A^{hi}-CD8⁺ T cells in organs (Figure 4C, D, *Online Supplementary Figure S4C, D*). We conclude that cS5A^{hi}-CD8⁺ T cells can expand and rapidly infiltrate multiple organs in wt recipients. This indicates that high pYSTAT5 in CD8⁺ T cells induces a transplantable disease.

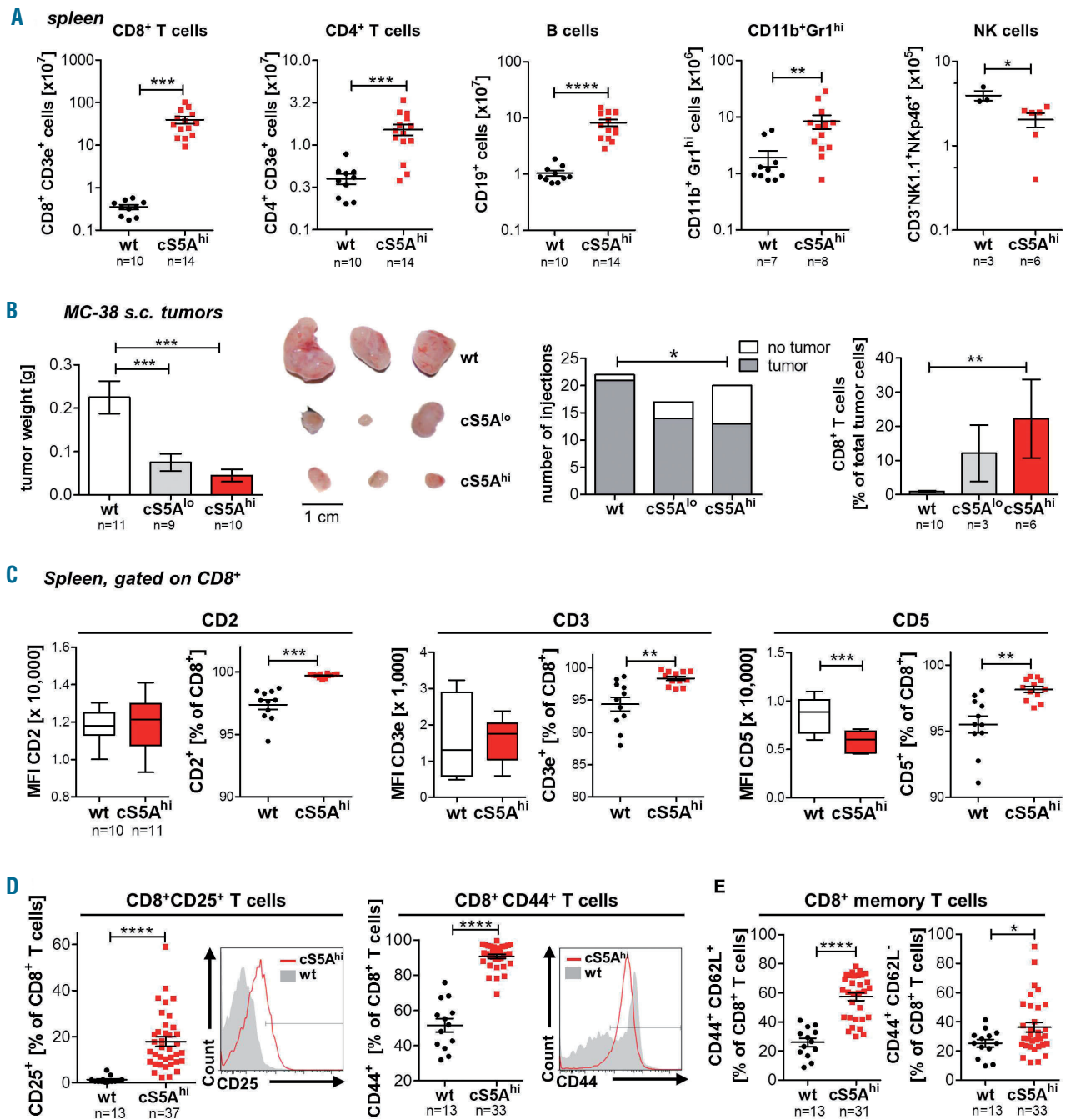


Figure 2. High STAT5A activity promotes CD8⁺ T-cell neoplasia. (A) Flow cytometric analysis of splenocytes of diseased cS5A^{hi} mice and wildtype (wt) littermates showing absolute CD8⁺ T-cell ($P=0.0001$), CD4⁺ T-cell ($P=0.0002$), B-cell ($P\leq 0.0001$, all unpaired t -test with the Welch correction), CD11b⁺Gr1^{hi} ($P=0.0014$) and natural killer (NK)-cell numbers ($P=0.0237$, both unpaired t -test) (B) Left: tumor weight of subcutaneous (s.c.) MC-38 tumors 18 days after injection of 1×10^6 cells in both flanks of 10-week old wt ($n=11$), cS5A^{lo} ($n=9$) and cS5A^{hi} ($n=10$) mice (one-way analysis of variance with the Tukey multiple comparison test). Middle: macroscopic view of isolated MC-38 tumors, scale bar represents 1 cm. Right: tumor incidence per injection of MC-38 cells (logistic regression, $P=0.031$) and percentage of CD8⁺ T-cell tumor infiltrating cells (Kruskal-Wallis test with the Dunn multiple comparison test). (C) Flow cytometric analysis of CD2, CD3 and CD5 expression on CD8⁺ wt ($n=10$) and cS5A^{hi} ($n=11$) splenocytes. Mean fluorescent intensity (MFI) unpaired t -test (CD2 $P=0.85$, CD3 $P=0.91$, CD5 $P=0.0002$), relative expression unpaired t -test with the Welch correction (CD2 $P=0.0001$, CD3 $P=0.0044$, CD5 $P=0.0021$). (D) Flow cytometric characterization of splenic wt ($n=13$) and cS5A^{hi} ($n=31$) CD8⁺ T cells: CD25 (left, $P<0.0001$, unpaired t -test) and CD44 expression (right, $P<0.0001$, unpaired t -test with the Welch correction) with representative histograms and (E) CD44⁺CD62L⁺ (left, $P<0.0001$, unpaired t -test with the Welch correction) and CD44⁺CD62L⁻ expression (right, $P=0.0492$, unpaired t -test).

c55A^{hi}- or hSTAT5B^{N642H}-dependent gene expression profiles are highly correlated to human peripheral T-cell lymphoma

Next, we performed RNA-sequencing and subsequent gene set enrichment analysis with CD8⁺ T cells from 15-week old wt, c55A^{lo} and c55A^{hi} mice to identify c55A^F-

dependent changes in global gene expression patterns. Only very few genes were deregulated in c55A^{lo} CD8⁺ T cells, reflecting mild changes. Comparing up- or down-regulated genes in c55A^{hi} CD8⁺ T cells to wt and c55A^{lo}, there were 182 commonly up- (63.6%) and 101 (26%) commonly down-regulated genes. In addition, 71 (24.8%)

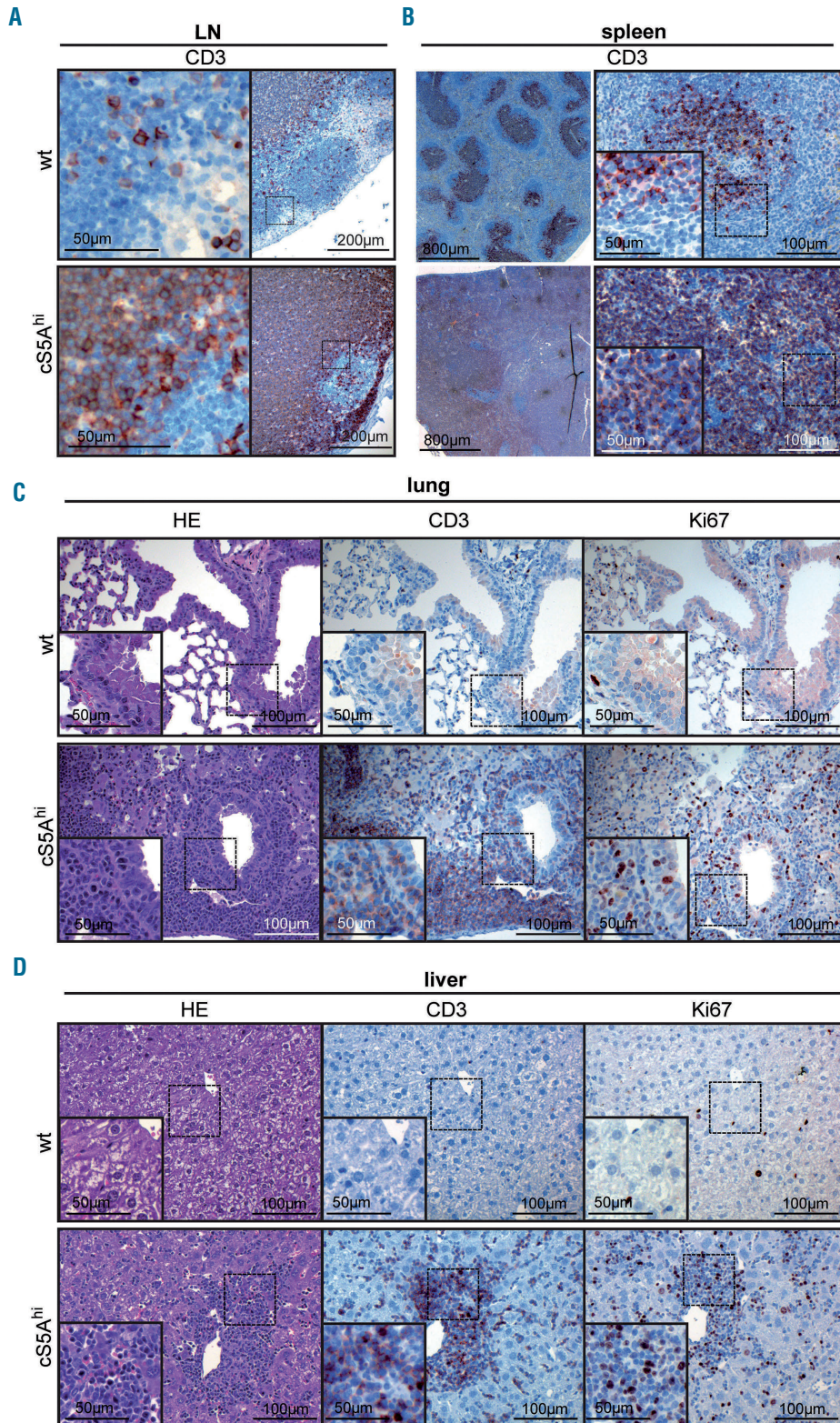


Figure 3. Expanded CD8⁺ T cells infiltrate peripheral organs. (A) CD3 staining of a representative enlarged lymph node (LN) of a diseased c55A^{hi} mouse and age-matched wildtype (wt) mouse LN. (B) CD3 staining on consecutive cuts of representative spleens of wt controls and diseased c55A^{hi} mice. (C, D) Hematoxylin & eosin (HE) (left), CD3 (middle) and Ki67 (right) staining of consecutive sections of lung (C) and liver (D) of diseased c55A^{hi} and age-matched wt mice. (A-D) Scale bars indicate 50, 100, 200, or 800 μ m.

or 30 genes (10.5%) were specifically upregulated in cS5A^{hi} vs. wt or cS5A^{hi} vs. cS5A^{lo} cells, respectively. Most downregulated genes (253 genes, 65.2%) were seen in cS5A^{hi} compared to wt mice, whereas only 11 genes (2.8%) showed lowered expression in cS5A^{hi} compared to cS5A^{lo} animals (Figure 5A, *Online Supplementary Figure S5A*). We confirmed differential expression of well-described STAT5-target genes *Pim1*, *Bcl2*, *Bcl6* and *Cish* by qRT-PCR (*Online Supplementary Figure S5B*). Gene set enrichment analysis on genes significantly up- or down-regulated in wt vs. cS5A^{hi} or cS5A^{lo} vs. cS5A^{hi} mice confirmed the IL-2-STAT5 signaling axis and revealed enrichment of *E2F* and *Myc* targets and G2M checkpoint genes as well as a lowered interferon (IFN) response in STAT5 hyperactive mice (Figure 5B, *Online Supplementary Figure S5C*). This matches the described STAT5-IFN axis in transformation.⁴⁵ *Stat5a* and *Stat5b* share very similar roles in T cells.⁴⁶ However, sequencing efforts attribute an important role to the activating STAT5B^{N642H} variant.^{28,32} To compare the phenotypically largely overlapping, though much more aggressive, disease of hSTAT5B^{N642H} and cS5A^{hi} mice, we contrasted gene expression patterns of wt, cS5A^{lo}, cS5A^{hi}, hSTAT5B and hSTAT5B^{N642H} CD8⁺ T cells (Figure 5C, *Online Supplementary Figure S5D*, RNA-sequencing of hSTAT5B and hSTAT5B^{N642H} as published³²). The hSTAT5B and cS5A^{lo} expression profiles cluster with that of wt T cells (*Online Supplementary Figure S5D*), whereby hyperactive STAT5A and STAT5B signaling share 373 (28.8%) commonly deregulated genes (Figure

5D). Importantly, both CD8⁺ T-cell neoplasia models are enriched for genes reported to be altered in PTCL, NOS with cytotoxic T-cell features⁶⁷ (Figure 5E and *Online Supplementary Table S5*), the closest match being to deregulated cS5A^{hi} genes in the tested T-cell lymphoma gene sets (*Online Supplementary Figure S5E*). Enrichr pathway analysis⁴⁷ of the shared cS5A^{hi} and hSTAT5B^{N642H} gene expression signature revealed an upregulation of cytokine-cytokine receptor interaction and JAK/STAT signaling. The exclusive hSTAT5B^{N642H} genes can be attributed to enhanced cell cycle and division, which may explain its sensitivity to Aurora Kinase inhibition³² (*Online Supplementary Figure S5F*, *Online Supplementary Table S6*).

We conclude that the immunophenotype, pathology and gene signatures of the cS5A^{hi}-induced PTCL-like disease overlap with those of human PTCL, NOS with cytotoxic T-cell features, which is associated with a particularly poor prognosis. hSTAT5B^{N642H} correlates similarly but is more aggressive. This implies that a significant threshold of STAT5 activity is not only required to induce, but is also sufficient to promote PTCL development.

Elevated STAT5 activation in human mature T-cell lymphomas

Subsequently, we investigated STAT5A or STAT5B expression and cellular localization in PTCL entities by specific immunohistochemical STAT5A or STAT5B staining. Quantification of nuclear STAT5 staining intensity revealed that PTCL, NOS cases had higher expression

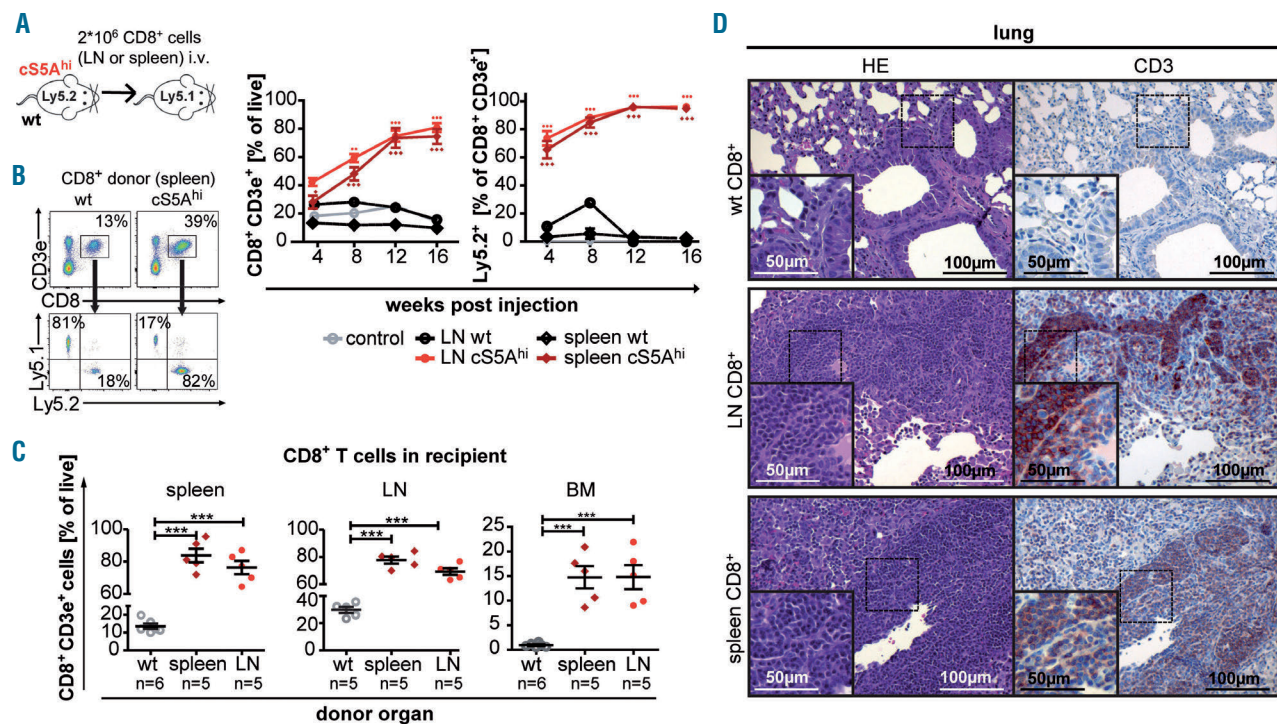


Figure 4. cS5A^{hi} CD8⁺ T-cell transfer recapitulates an aggressive T-cell lymphoma/leukemia phenotype. (A) Scheme of CD8⁺ T-cell transfer. LN: lymph node; wt: wildtype; i.v.: intravenous. (B) Representative flow cytometry dot plots of recipient's peripheral blood 12 weeks after injection showing gating on CD3e⁺ CD8⁺ T cells and further Ly5.1/2 gating (left). CD8⁺ T cells and %Ly5.2⁺ donor-derived CD8⁺ T cells (right) in recipient's peripheral blood measured after injection at 4-week intervals for 16 weeks (n=6/organ source, untreated control n=2, wt LN n=1, P<0.0001). (C) Endpoint analysis: percentage of CD8⁺ T cells in spleen (left), LN (middle) and bone marrow (BM) (right) of control (wt-CD8⁺ recipients), spleen- and LN-derived cS5A^{hi}-CD8⁺ T-cell recipients (P<0.0001). Two-way analysis of variance (ANOVA) with the Bonferroni post test (B) and one-way ANOVA with the Tukey multiple comparison test. (D) Hematoxylin & eosin (HE) and anti-CD3 staining of representative consecutive sections from lungs of wt and cS5A^{hi}-CD8⁺ T-cell recipients. Scale bars indicate 50 or 100 μm.

and activation of STAT5A and STAT5B (score 3 or 4) than non-reactive lymph node samples (score 1 Figure 6A, B), in line with nuclear staining indicative of enhanced STAT5-mediated transcriptional activity. Comparable results were obtained when samples of AITL and various CTCL cases were analyzed (Online Supplementary Figure S6A-C), in line with previous reports.⁴⁸⁻⁵¹ pYSTAT5 staining on PTCL and AITL cases confirmed that nuclear STAT5A/B staining corresponds to elevated pYSTAT5 levels (Online Supplementary Figure S6D). Analysis of STAT5A and STAT5B mRNA expression levels in 18

PTCL, NOS samples compared to non-diseased human lymph nodes (n=4) showed six-fold and two-fold upregulation of STAT5A and STAT5B expression, respectively (Figure 6C, Online Supplementary Figure S6E). Similar results were obtained when we compared seven AITL cases to control tissue (Online Supplementary Figure S6F). Enhanced STAT5A expression was strongly correlated with elevated STAT5B levels (Online Supplementary Figure S6E-F). To increase the numbers of patients and disease entities, tissue microarrays were quantified for STAT5A and STAT5B expression – with highly positive STAT5A

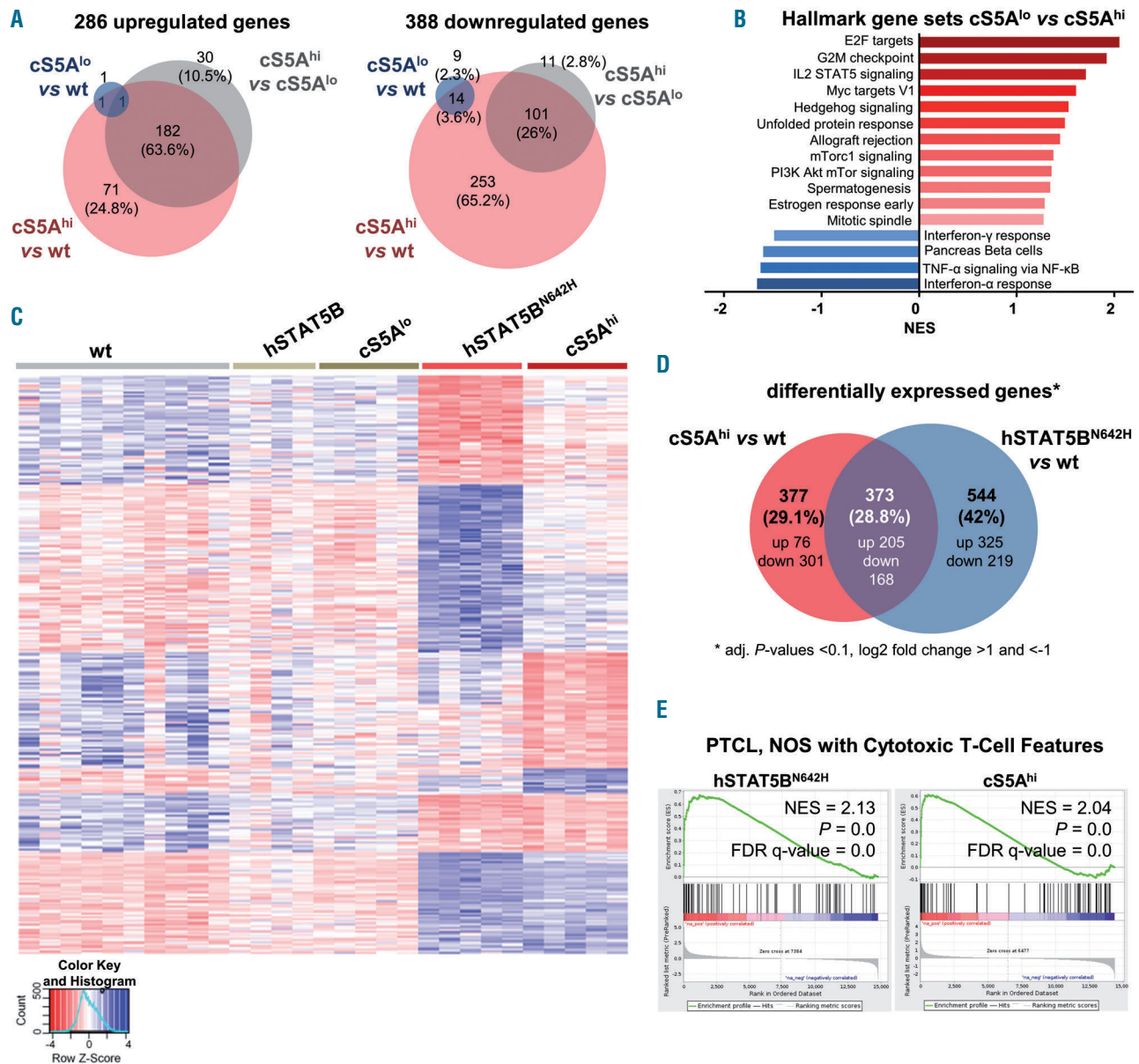


Figure 5. Transcriptional profiling reveals close correlation to human peripheral T-cell lymphoma. (A) CD8⁺ T-cell RNA-sequencing (performed with Illumina HiSeq2500) analysis showing the number of significantly (left) up- and (right) down-regulated genes in wildtype (wt), cS5A^{lo} and cS5A^{hi} CD8⁺ T cells obtained from lymph nodes (n=5/genotype; adjusted *P*-values <0.1, log₂ fold change >1 and <-1). (B) Summary of gene set enrichment analysis (GSEA) of hallmark gene sets enriched in cS5A^{hi} vs. cS5A^{lo} CD8⁺ T cells [false discovery rate (FDR) ≤0.25, adjusted *P*-value ≤0.05]. (C) RNA isolated from CD8⁺ T cells of wt (n=10), hSTAT5B (n=4), hSTAT5B^{N642H}, cS5A^{lo} and cS5A^{hi} (all n=5) mice were subjected to RNA-sequencing. Heatmap of genes deregulated in a comparison of all genotypes to wt controls (n=1,055) clustered for up- and down-regulated genes specific to individual conditions, as well as for genes shared between hSTAT5B^{N642H} and cS5A^{hi}. Scaled, log transformed normalized counts from DESeq2 were used for the analysis. (D) Venn diagram of differentially expressed genes in cS5A^{hi} vs. wt and hSTAT5B^{N642H} vs. wt CD8⁺ T cells (adjusted *P*-values <0.1, log₂ fold change >1 and <-1). (E) GSEA of STAT5B^{N642H} and cS5A^{hi} expression data shows a correlation to peripheral T-cell lymphoma, not otherwise specified (PTCL, NOS) with cytotoxic T-cell features. NES: normalized enrichment score. The gene set was compiled from literature.^{6,7}

and STAT5B nuclear staining intensities across PTCL entities (Figure 6D, *Online Supplementary Figure S6G*).

In brief, patient-derived PTCL samples displayed *STAT5* upregulation and enhanced intensity of STAT5A/B nuclear staining, pointing to an important role of STAT5 in various PTCL subsets. These findings establish elevated expression of STAT5A/B across human PTCL entities, which we finally set out to target pharmacologically.

Proliferation of peripheral T-cell lymphoma cells is highly sensitive to targeted JAK/STAT pathway therapy

Primary cultures of cS5A^{hi} CTL were cytokine-dependent and hypersensitive to IL-2, IL-4 and IL-7. This indicates higher cytokine-induced proliferation of cS5A^{hi} compared to wt cells (Figure 7A, *Online Supplementary*

Figure S7A), also reflected by the longer pYSTAT5 persistence after IL-2 withdrawal (Figure 7B, *Online Supplementary Figure S7B*). Results from our mouse models³² and recent literature^{30,52} indicate that inhibition of STAT5 signaling may represent a therapeutic option in PTCL patients. We investigated the effects of the Food and Drug Administration-approved JAK1/2 inhibitor ruxolitinib and JAK1/2/3 inhibitor tofacitinib³⁸, as cS5A^F depends on upstream cytokine signaling, as well as the STAT5 inhibitor AC-3-19, which was described to inhibit pYSTAT5 activation and downstream target genes.^{39,53} In the presence of IL-2, cS5A^{hi} mice-derived CTL cells were treated with increasing concentrations of these JAK and STAT5 inhibitors, which led to decreased STAT5 activation and cell viability (Figure 7C, *Online Supplementary*

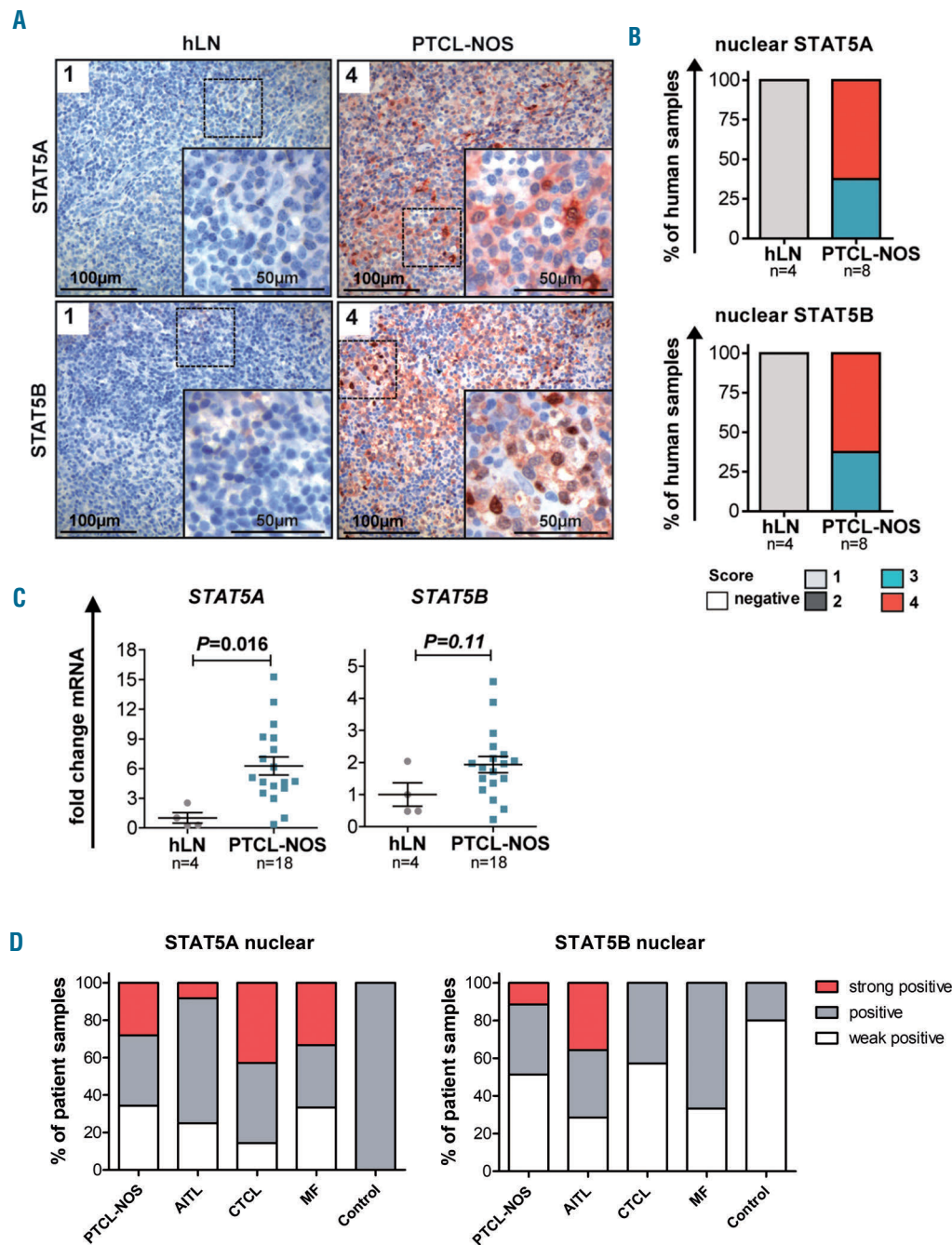


Figure 6. Enhanced STAT5 expression and activity in peripheral T-cell lymphoma, not otherwise specified. (A) STAT5A (top) and STAT5B (bottom) staining of representative non-diseased human lymph nodes (hLN, n=4) and peripheral T-cell lymphoma, not otherwise specified (PTCL, NOS) cases (n=8) with nuclear STAT5A/B staining intensity scoring. Scale bars indicate 100 or 50 μm. (B) Summary of scoring of nuclear STAT5A (top) and STAT5B (bottom) staining intensity ranging from 1 (low) to 4 (high). (C) *STAT5A* (left) and *STAT5B* (middle) mRNA levels of non-diseased hLN (n=4) vs. PTCL, NOS lymphoma tissue (n=18, *STAT5A* P=0.016, *STAT5B* P=0.11, unpaired t-test). Mean *STAT5A* or *STAT5B* expression in hLN was normalized to 1. (D) Statistical summary of nuclear *STAT5A* (left) and *STAT5B* (right) staining intensity, classified as weakly positive, positive and strongly positive, of 35 PTCL, NOS, 14 angioimmunoblastic T-cell lymphoma (AITL), 7 cutaneous T-cell lymphoma (CTCL), 6 mycosis fungoides (MF), and 5 control samples spotted on a tissue microarray.

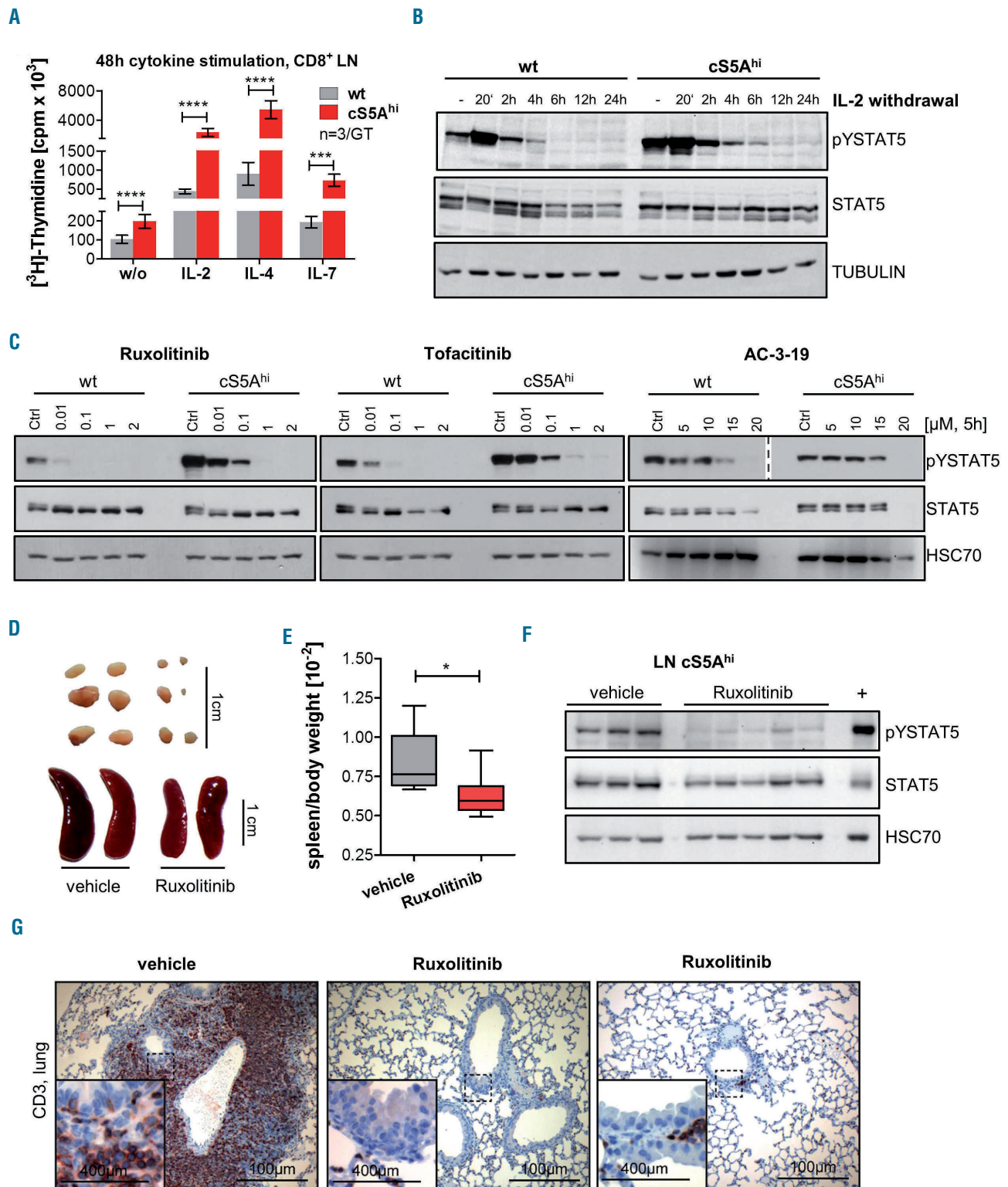


Figure 7. Dependence of cS5A^{hi} on upstream cytokine signaling can be used for targeted pharmacological therapy. (A) [³H]Thymidine incorporation in CD8⁺ T cells isolated from lymph nodes (LN) of 35-week old wildtype (wt) and cS5A^{hi} mice after stimulation with interleukin (IL)-2 (100 U/mL, $P \leq 0.0001$), IL-4 (100 ng/mL, $P \leq 0.0001$), IL-7 (10 ng/mL, $P = 0.0002$) or without (w/o) cytokines ($P \leq 0.0001$, $n = 3$ /genotype in triplicate, all unpaired *t*-test). (B) Immunoblot for pYSTAT5 and STAT5 on IL-2-cultured wt and cS5A^{hi} LN cells sampled at specific time points after IL-2 withdrawal. α -TUBULIN was used as a loading control. Representative blot of three experiments. (C) *In vitro* treatment of wt and cS5A^{hi} LN-derived T cells with increasing concentrations of ruxolitinib (left), tofacitinib (middle) or AC-3-19 (right) for 5 h blotted for pYSTAT5 (AC-3-19 – two different exposures are shown indicated by the dashed line) and STAT5. An equal amount of dimethylsulfoxide was used as a control. HSC70 served as a loading control. Representative blot of three experiments. (D) *In vivo* treatment of cS5A^{hi} mice with 45 mg/kg ruxolitinib ($n = 6$) or vehicle ($n = 6$) for 30 days. Macroscopic appearance of LN (top) and spleen (bottom) and (E) spleen/body weight ratio after 30 days of treatment (Mann Whitney test, $P = 0.026$). (F) Immunoblot (representative blot of two) on LN lysates of vehicle- or ruxolitinib-treated cS5A^{hi} mice for pYSTAT5 and STAT5, HSC70 was used as a loading control and diseased cS5A^{hi} spleen lysate was used as a positive control. (G) CD3 staining of lung sections of vehicle- and ruxolitinib-treated cS5A^{hi} mice, scale bars represent 400 or 100 μ m.

Figure S7C). All three inhibitors reduced the viability of cS5A^{hi}-derived CTL cells already at low concentrations, with the half maximal inhibitory concentration (IC₅₀) being ~4.1 μM for AC-3-19, ~0.005 μM for ruxolitinib and ~0.03 μM for tofacitinib (Online Supplementary Figure S7C). Sensitivity to STAT5 inhibition could be confirmed in human PTCL cell lines. AC-3-19 treatment reduced the viability of Mac2A, FePD, SU-DHL-1, Mac1 and SR786 (IC₅₀ 5-10 μM) (Online Supplementary Figure S7D). When we used ruxolitinib we found that Mac1- and Mac2A cells that harbor a JAK2 translocation were sensitive.⁵⁴ Control cell lines were only affected at significantly higher concentrations (AC-3-19: <20 μM) (Online Supplementary Figure S7D, summary on mutations in human cells in Online Supplementary Table S7). In addition, ruxolitinib blocked neoplastic cell growth in cS5A^{hi} mice, as exemplified by reductions of splenomegaly and lymphadenopathy (Figure 7D-E). The specificity of the treatment was validated by reduced pYSTAT5 in lymph nodes and spleen (Figure 7E, Online Supplementary Figure S7E). Most impressively, the T-cell infiltration in peripheral organs was drastically reduced in treated mice (Figure 7G, Online Supplementary Figure S7F, G). Collectively, these data verify that malignant cS5A^{hi}-CTL and human PTCL cells critically depend on STAT5 signaling.

Discussion

PTCL patients face an unfavorable prognosis as chemotherapy results in a poor 5-year overall survival rate.^{2,55} Targeted treatment options only exist for ALK⁺ anaplastic large cell lymphoma and are urgently needed for the other 30 PTCL entities. The cohort of patients we investigated revealed increased expression and activity of both STAT5A and STAT5B proteins in mature T-cell lymphomas. Using cS5A^{hi} transgenic mice we unambiguously associated STAT5A activity with PTCL phenotype. Importantly, mRNA expression changes of cS5A^{hi} mice closely matched gene expression profiles of human T-cell neoplasia and overlapped with the profile of the more aggressive hSTAT5B^{N642H} mouse model.³² Importantly, clinical JAK1/2/3 inhibitors ruxolitinib and tofacitinib⁵⁶ and selective STAT5 inhibitors³⁹ reduced neoplastic PTCL cell growth.

Previous transgenic models addressing leukemogenesis downstream of STAT5 employed either wt or STAT5 gain-of-function variants in a lymphoid-restricted manner resulting in expansion of mature T cells, lymphoblastic or B-cell lymphoma.⁵⁶⁻⁵⁹ Broad hematopoietic expression resulted in enhanced granulopoiesis.⁶⁰ Here, we engineered expression of the well-characterized hyperactive STAT5A variant cS5^F using the *vav*-promoter starting expression from the hematopoietic stem cell stage.⁴⁰ cS5A^{hi} mice developed effector/memory- CD8⁺ T-cell malignancies featuring pronounced organ infiltration. Transgene expression was observed in all major blood lineages tested, but neoplastic expansion of CD8⁺ T cells was most prominent. This argues for the susceptibility of the T-cell lineage to STAT5 hyperactivation and it emphasizes the role of JAK1/3/STAT3/5 signaling in the outgrowth of T-cell lymphomas. We suggest that CD8⁺ T cells outcompete cS5A^F-mediated effects on other lineages due to faster cell cycle progression, higher survival, cytokine sensitivity and cell fate-specific expression differences. We speculate that

STAT5-mediated effects are more negatively controlled in myeloid over lymphoid cell types and that low pYSTAT5 levels, as mimicked in cS5A^{lo} mice, do not promote neoplasia. Gene-dosage and graded STAT5 activity levels in our study showed a clear positive correlation between STAT5 activation status and CD8⁺ T-cell numbers.^{34,35} Senescence, diminished oligomer formation or differentiation capacity might contribute to the differences between cS5A^{lo} and cS5A^{hi}. Although the level of pYSTAT5 in cS5A^{lo} mice was significant, it was nevertheless lower than in cS5A^{hi} or hSTAT5B^{N642H} mice, and malignant transformation did not occur in the cS5A^{lo} animals. Thus, the real driver of PTCL disease might be the amount of pYSTAT5 resulting in enhanced and prolonged transcriptional activity.

In PTCL several factors account for STAT5 activation – such as mutations in STAT5 or in upstream signaling components (e.g. IL-2R, JAK1, JAK3). Surprisingly, recurrent mutations in epigenetic and chromatin remodeling factors parallel JAK/STAT activation and the epigenetic landscape is also shaped by STAT3/5 and its versatile interaction partners.^{52,61} However, until now a detailed understanding of these factors in PTCL is lacking. Increased pYSTAT5 levels have also been reported upon autocrine PDGFα signaling in PTCL, NOS.⁶² In CTCL, overexpression of oncogenic miR-155,⁴⁹ downregulation of tumor-suppressive miR-22,⁵⁰ enhanced progression by lymphotoxin-α-dependent lymphangiogenesis,⁶³ STAT5-dependent CD80 expression,⁵¹ resistance to vorinostat⁴⁸ and risk of disease progression⁶⁴ were attributed to enhanced STAT5 signaling. The identification of recurrent and mutually exclusive gain-of-function mutations in STAT3 suggests that these proteins share redundant functions in PTCL.^{18,23,28} Thus, dual STAT3/5 inhibition is needed in future therapy, which could be approached by SH₂-domain blockers. Certainly, mutations or translocations in the upstream JAK proteins boost STAT5 signaling,^{25,29,30,65} further emphasizing the potential benefit of JAK and STAT inhibitors.

The cS5A^{hi} model recapitulates clinical features of PTCL with high STAT5 activation. Among the few high-fidelity mouse models for other PTCL subsets,^{9,66-69} the cS5A^{hi} model closely phenocopies pathological hallmarks of cytotoxic CD8⁺ T-cell PTCL. Importantly, cS5A^{hi}-expressing cells are hypersensitive to the Food and Drug Administration-approved JAK1/2 inhibitor ruxolitinib, which is currently being studied in phase II clinical trials for the treatment of relapsed PTCL and adult T-cell leukemia/lymphoma (NCT01431209, NCT02974647, NCT01712659). In line with this, JAK-inhibitor treatment of Sézary syndrome,²⁹ T-cell prolymphocytic leukemia,^{54,70} and adult T-cell leukemia/lymphoma⁷¹ revealed reduced proliferation and immunomodulatory effects on the PTCL tumor microenvironment.³ Moreover, a small molecule inhibitor of STAT5 SH₂ domain-phosphopeptide interactions³⁹ resulted in strongly reduced viability in PTCL lines with high STAT5 activity and its successor compound showed significant effects in acute myeloid leukemia.⁵³ Although these inhibitors are currently considered lead compounds, specific STAT5 inhibitors are also expected to enter clinical trials and combinations with kinase inhibitors could be tested.

In conclusion, our cS5A^{hi} transgenic mouse model indicates that STAT5 is a driver and STAT5 itself or its interaction partners are potential drug targets in PTCL. The STAT5-dependent CD8⁺ PTCL mouse model described

here represents a tool to investigate molecular mechanisms of PTCL development. Our model serves for identification and pre-clinical testing of novel interventional strategies to target STAT5-dependent PTCL. We conclude that both STAT5A and STAT5B are oncogenes in PTCL, and STAT5B is more transforming. Overall, mutation induced-cytokine sensitivity drives PTCL due to enhanced STAT3/STAT5 signaling.

Acknowledgments

Jerry Adams (WEHI, Australia) kindly provided us with the

vav-hCD4 (HS21/45) plasmid and Dagmar Stoiber (LBI-CR, Vienna, Austria) with the E.G7 cell line. We thank Safia Zahma (LBI-CR, Vienna, Austria), Elisabeth Gurnhofer, Sigurd Krieger (both at the Department of Clinical Pathology, Medical University Vienna, Austria), Sabine Fajmann (Institute of Pharmacology and Toxicology, University of Veterinary Medicine, Vienna, Austria), and Boris Kovacic (Institute of Medical Genetics, Medical University of Vienna, Vienna, Austria) for technical support. We thank also our mouse facility team and Jisung Park (Department of Chemistry, University of Toronto Mississauga, Canada) for synthesizing the inhibitor AC-3-19 used in this study.

References

- Foss FM, Zinzani PL, Vose JM, Gascoyne RD, Rosen ST, Tobinai K. Peripheral T-cell lymphoma. *Blood*. 2011;117(25):6756-6767.
- Armitage JO. The aggressive peripheral T-cell lymphomas: 2017. *Am J Hematol*. 2017;92(7):706-715.
- Wang T, Feldman AL, Wada DA, et al. GATA-3 expression identifies a high-risk subset of PTCL, NOS with distinct molecular and clinical features. *Blood*. 2014;123(19):3007-3015.
- Siaghani PJ, Song JY. Updates of peripheral T cell lymphomas based on the 2017 WHO classification. *Curr Hematol Malig Rep*. 2018;13(1):25-36.
- Laginestra MA, Piccaluga PP, Fuligni F, et al. Pathogenetic and diagnostic significance of microRNA deregulation in peripheral T-cell lymphoma not otherwise specified. *Blood Cancer J*. 2014;4(11):259.
- Iqbal J, Wright G, Wang C, et al. Gene expression signatures delineate biological and prognostic subgroups in peripheral T-cell lymphoma. *Blood*. 2014;123(19):2915-2923.
- Iqbal J, Weisenburger DD, Greiner TC, et al. Molecular signatures to improve diagnosis in peripheral T-cell lymphoma and prognostication in angioimmunoblastic T-cell lymphoma. *Blood*. 2010;115(5):1026-1036.
- Heinrich T, Rengstl B, Muik A, et al. Mature T-cell lymphomagenesis induced by retroviral insertional activation of Janus kinase 1. *Mol Ther*. 2013;21(6):1160-1168.
- Warner K, Crispatzu G, Al-Ghaili N, et al. Models for mature T-cell lymphomas—a critical appraisal of experimental systems and their contribution to current T-cell tumorigenic concepts. *Crit Rev Oncol Hematol*. 2013;88(3):680-695.
- Spinner S, Crispatzu G, Yi JH, et al. Re-activation of mitochondrial apoptosis inhibits T-cell lymphoma survival and treatment resistance. *Leukemia*. 2016;30(7):1520-1530.
- Piccaluga P, Tabanelli V, Pileri S. Molecular genetics of peripheral T-cell lymphomas. *Int J Hematol*. 2014;99(3):219-226.
- Wang C, McKeithan TW, Gong Q, et al. IDH2R172 mutations define a unique subgroup of patients with angioimmunoblastic T-cell lymphoma. *Blood*. 2015;126(15):1741-1752.
- Wilcox RA. A three-signal model of T-cell lymphoma pathogenesis. *Am J Hematol*. 2016;91(1):113-122.
- Kataoka K, Nagata Y, Kitanaka A, et al. Integrated molecular analysis of adult T cell leukemia/lymphoma. *Nat Genet*. 2015;47(11):1304-1315.
- Schrader A, Crispatzu G, Oberbeck S, et al. Actionable perturbations of damage responses by TCL1/ATM and epigenetic lesions form the basis of T-PLL. *Nat Commun*. 2018;9(1):697.
- Litvinov IV, Tetzlaff MT, Thibault P, et al. Gene expression analysis in cutaneous T-cell lymphomas (CTCL) highlights disease heterogeneity and potential diagnostic and prognostic indicators. *Oncoimmunology*. 2017;6(5):e1306618-e1306618.
- Warner K, Weit N, Crispatzu G, Admirand J, Jones D, Herling M. T-cell receptor signaling in peripheral T-cell lymphoma – a review of patterns of alterations in a central growth regulatory pathway. *Curr Hematol Malig Rep*. 2013;8(3):163-172.
- Swerdlow SH, Campo E, Pileri SA, et al. The 2016 revision of the World Health Organization classification of lymphoid neoplasms. *Blood*. 2016;127(20):2375-2390.
- Van Arnem JS, Lim MS, Elenitoba-Johnson KSJ. Novel insights into the pathogenesis of T-cell lymphomas. *Blood*. 2018;131(21):2320-2330.
- Lone W, Alkhiniji A, Manikkam Umakanthan J, Iqbal J. Molecular insights into pathogenesis of peripheral T cell lymphoma: a review. *Curr Hematol Malig Rep*. 2018;13(4):318-328.
- Coppe A, Andersson EI, Binatti A, et al. Genomic landscape characterization of large granular lymphocyte leukemia with a systems genetics approach. *Leukemia*. 2017;31(5):1243-1246.
- Koskela HLM, Eldfors S, Ellonen P, et al. Somatic STAT3 mutations in large granular lymphocytic leukemia. *N Engl J Med*. 2012;366(20):1905-1913.
- Rajala HLM, Eldfors S, Kuusanmäki H, et al. Discovery of somatic STAT5b mutations in large granular lymphocytic leukemia. *Blood*. 2013;121(22):4541-4550.
- Bandapalli OR, Schuessele S, Kunz JB, et al. The activating STAT5B N642H mutation is a common abnormality in pediatric T-cell acute lymphoblastic leukemia and confers a higher risk of relapse. *Haematologica*. 2014;99(10):e188-e192.
- Kiel MJ, Velusamy T, Rolland D, et al. Integrated genomic sequencing reveals mutational landscape of T-cell prolymphocytic leukemia. *Blood*. 2014;124(9):1460-1472.
- Kontro M, Kuusanmaki H, Eldfors S, et al. Novel activating STAT5B mutations as putative drivers of T-cell acute lymphoblastic leukemia. *Leukemia*. 2014;28(8):1738-1742.
- Nicolae A, Xi L, Pittaluga S, et al. Frequent STAT5B mutations in $\gamma\delta$ hepatosplenic T-cell lymphomas. *Leukemia*. 2014;28(11):2244-2248.
- Küçük C, Jiang B, Hu X, et al. Activating mutations of STAT5B and STAT3 in lymphomas derived from $\gamma\delta$ -T or NK cells. *Nat Commun*. 2015;6:6025.
- Kiel MJ, Sahasrabudhe AA, Rolland DCM, et al. Genomic analyses reveal recurrent mutations in epigenetic modifiers and the JAK-STAT pathway in Sezary syndrome. *Nat Commun*. 2015;6:8470.
- Dufva O, Kankainen M, Kelkka T, et al. Aggressive natural killer-cell leukemia mutational landscape and drug profiling highlight JAK-STAT signaling as therapeutic target. *Nat Commun*. 2018;9(1):1567.
- Cross NCP, Hoade Y, Tapper WJ, et al. Recurrent activating STAT5B N642H mutation in myeloid neoplasms with eosinophilia. *Leukemia*. 2018;33(2):415-425.
- Pham HTT, Maurer B, Prchal-Murphy M, et al. STAT5B(N642H) is a driver mutation for T cell neoplasia. *J Clin Invest*. 2018;128(1):387-401.
- Heltemes-Harris LM, Farrar MA. The role of STAT5 in lymphocyte development and transformation. *Curr Opin Immunol*. 2012;24(2):146-152.
- Hoelbl A, Kovacic B, Kerenyi MA, et al. Clarifying the role of Stat5 in lymphoid development and Abelson-induced transformation. *Blood*. 2006;107(12):4898-4906.
- Ermakova O, Piszczek L, Luciani L, et al. Sensitized phenotypic screening identifies gene dosage sensitive region on chromosome 11 that predisposes to disease in mice. *EMBO Mol Med*. 2011;3(1):50-66.
- Roberts KG, Li Y, Payne-Turner D, et al. Targetable kinase-activating lesions in Ph-like acute lymphoblastic leukemia. *N Engl J Med*. 2014;371(11):1005-1015.
- Moriggl R, Sexl V, Kenner L, et al. Stat5 tetramer formation is associated with leukemogenesis. *Cancer Cell*. 2005;7(1):87-99.
- Kontzias A, Kotlyar A, Laurence A, Changelian P, O'Shea JJ. Jakinibs: a new class of kinase inhibitors in cancer and autoimmune disease. *Curr Opin Pharmacol*. 2012;12(4):464-470.
- Cumaraswamy AA, Lewis AM, Geletu M, et al. Nanomolar-potency small molecule inhibitor of STAT5 protein. *ACS Med Chem Lett*. 2014;5(11):1202-1206.
- Ogilvy S, Metcalf D, Gibson L, Bath ML, Harris AW, Adams JM. Promoter elements of *vav* drive transgene expression in vivo throughout the hematopoietic compartment. *Blood*. 1999;94(6):1855-1863.
- Berard M, Tough DF. Qualitative differences between naïve and memory T cells. *Immunology*. 2002;106(2):127-138.
- Krishnan L, Gurnani K, Dicaire C, et al. Rapid clonal expansion and prolonged maintenance of memory CD8+ T cells of the effector (CD44highCD62Llow) and central

- (CD44^{high}CD62L^{high}) phenotype by an archaeosome adjuvant independent of TLR2. *J Immunol.* 2007;178(4):2396-2406.
43. Grange M, Buferme M, Verdeil G, Leserman L, Schmitt-Verhulst A, Auphan-Anezin N. Activated STAT5 promotes long-lived cytotoxic CD8⁺ T cells that induce regression of autochthonous melanoma. *Cancer Res.* 2012;72(1):76-87.
 44. Luckey CJ, Bhattacharya D, Goldrath AW, Weissman IL, Benoist C, Mathis D. Memory T and memory B cells share a transcriptional program of self-renewal with long-term hematopoietic stem cells. *Proc Natl Acad Sci U S A.* 2006;103(9):3304-3309.
 45. Kollmann S, Grundschober E, Maurer B, et al. Twins with different personalities: STAT5B – but not STAT5A – has a key role in BCR/ABL-induced leukemia. *Leukemia.* 2019 Jan 24. [Epub ahead of print]
 46. Villarino A, Laurence A, Robinson GW, et al. Signal transducer and activator of transcription 5 (STAT5) paralog dose governs T cell effector and regulatory functions. *eLife.* 2016;5.
 47. Kuleshov MV, Jones MR, Rouillard AD, et al. Enrichr: a comprehensive gene set enrichment analysis web server 2016 update. *Nucleic Acids Res.* 2016;44(W1):W90-W97.
 48. Fantin VR, Loboda A, Paweletz CP, et al. Constitutive activation of signal transducers and activators of transcription predicts vorinostat resistance in cutaneous T-cell lymphoma. *Cancer Res.* 2008;68(10): 3785-3794.
 49. Kopp KL, Ralfkiaer U, Gjerdrum LMR, et al. STAT5-mediated expression of oncogenic miR-155 in cutaneous T-cell lymphoma. *Cell Cycle.* 2013;12(12):1939-1947.
 50. Sibbesen NA, Kopp KL, Litvinov IV, et al. Jak3, STAT3, and STAT5 inhibit expression of miR-22, a novel tumor suppressor microRNA, in cutaneous T-cell lymphoma. *Oncotarget.* 2015;6(24):20555-20569.
 51. Zhang Q, Wang HY, Wei F, et al. Cutaneous T cell lymphoma expresses immunosuppressive CD80 (B7-1) cell surface protein in a STAT5-dependent manner. *J Immunol.* 2014;192(6):2913-2919.
 52. Orlova A, Wingelhofer B, Neubauer HA, et al. Emerging therapeutic targets in myeloproliferative neoplasms and peripheral T-cell leukemia and lymphomas. *Expert Opin Ther Targets.* 2018;22(1):45-57.
 53. Wingelhofer B, Maurer B, Heyes EC, et al. Pharmacologic inhibition of STAT5 in acute myeloid leukemia. *Leukemia.* 2018;32(5): 1135-1146.
 54. Ng SY, Yoshida N, Christie AL, et al. Targetable vulnerabilities in T- and NK-cell lymphomas identified through preclinical models. *Nat Commun.* 2018;9(1):2024.
 55. Reddy NM, Evens AM. Chemotherapeutic advancements in peripheral T-cell lymphoma. *Semin Hematol.* 2014;51(1):17-24.
 56. Kelly JA, Spolski R, Kovanen PE, et al. Stat5 Synergizes with T cell receptor/antigen stimulation in the development of lymphoblastic lymphoma. *J Exp Med.* 2003;198(1):79-89.
 57. Chen B, Yi B, Mao R, et al. Enhanced T cell lymphoma in NOD.Stat5b transgenic mice is caused by hyperactivation of Stat5b in CD8(+) thymocytes. *PLoS One.* 2013;8(2): e56600.
 58. Burchill MA, Goetz CA, Prlc M, et al. Distinct effects of STAT5 activation on CD4⁺ and CD8⁺ T cell homeostasis: development of CD4⁺CD25⁺ regulatory T cells versus CD8⁺ memory T cells. *J Immunol.* 2003;171(11):5853-5864.
 59. Joliot V, Cormier F, Medyouf H, Alcalde H, Ghysdael J. Constitutive STAT5 activation specifically cooperates with the loss of p53 function in B-cell lymphomagenesis. *Oncogene.* 2006;25(33):4573-4584.
 60. Lin W-c, Schmidt JW, Creamer BA, Triplett AA, Wagner K-U. Gain-of-function of Stat5 leads to excessive granulopoiesis and lethal extravasation of granulocytes to the lung. *PLoS One.* 2013;8(4):e60902.
 61. Wingelhofer B, Neubauer HA, Valent P, et al. Implications of STAT3 and STAT5 signaling on gene regulation and chromatin remodeling in hematopoietic cancer. *Leukemia.* 2018;32(8):1713-1726.
 62. Piccaluga PP, Rossi M, Agostinelli C, et al. Platelet-derived growth factor alpha mediates the proliferation of peripheral T-cell lymphoma cells via an autocrine regulatory pathway. *Leukemia.* 2014;28(8):1687-1697.
 63. Lauenborg B, Christensen L, Ralfkiaer U, et al. Malignant T cells express lymphotoxin α and drive endothelial activation in cutaneous T cell lymphoma. *Oncotarget.* 2015;6(17):15235-15249.
 64. Litvinov IV, Netchiporouk E, Cordeiro B, et al. The use of transcriptional profiling to improve personalized diagnosis and management of cutaneous T-cell lymphoma (CTCL). *Clin Cancer Res.* 2015;21(12):2820-2829.
 65. Bergmann AK, Schneppenheim S, Seifert M, et al. Recurrent mutation of JAK3 in T-cell prolymphocytic leukemia. *Genes Chromosomes Cancer.* 2014;53(4):309-316.
 66. Beachy SH, Onozawa M, Chung YJ, et al. Enforced expression of Lin28b leads to impaired T-cell development, release of inflammatory cytokines, and peripheral T-cell lymphoma. *Blood.* 2012;120(5):1048-1059.
 67. Muto H, Sakata-Yanagimoto M, Nagae G, et al. Reduced TET2 function leads to T-cell lymphoma with follicular helper T-cell-like features in mice. *Blood Cancer J.* 2014;4:e264.
 68. Pechloff K, Holch J, Ferch U, et al. The fusion kinase ITK-SYK mimics a T cell receptor signal and drives oncogenesis in conditional mouse models of peripheral T cell lymphoma. *J Exp Med.* 2010;207(5): 1031-1044.
 69. Tezuka K, Xun R, Tei M, et al. An animal model of adult T-cell leukemia: humanized mice with HTLV-1-specific immunity. *Blood.* 2014;123(3):346-355.
 70. Andersson EI, Pützer S, Yadav B, et al. Discovery of novel drug sensitivities in T-PLL by high-throughput ex vivo drug testing and mutation profiling. *Leukemia.* 2017;32(3):774-787.
 71. Zhang M, Mathews Griner LA, Ju W, et al. Selective targeting of JAK/STAT signaling is potentiated by Bcl-xL blockade in IL-2-dependent adult T-cell leukemia. *Proc Natl Acad Sci U S A.* 2015;112(40):12480-12485.



Biological and clinical implications of *BIRC3* mutations in chronic lymphocytic leukemia

Fary Diop,^{1*} Riccardo Moia,^{1*} Chiara Favini,¹ Elisa Spaccarotella,¹ Lorenzo De Paoli,¹ Alessio Bruscazzin,² Valeria Spina,² Lodovico Terzi-di-Bergamo,² Francesca Arruga,³ Chiara Tarantelli,⁴ Clara Deambrogi,¹ Silvia Rasi,¹ Ramesh Adhinaveni,¹ Andrea Patriarca,¹ Simone Favini,¹ Sruthi Sagiraju,¹ Clive Jabangwe,¹ Ahad A. Kodipad,¹ Denise Peroni,¹ Francesca R. Mauro,⁵ Ilaria Del Giudice,⁵ Francesco Forconi,^{6,7} Agostino Cortelezzi,⁸ Francesco Zaja,⁹ Riccardo Bomben,¹⁰ Francesca Maria Rossi,¹⁰ Carlo Visco,¹¹ Annalisa Chiarenza,¹² Gian Matteo Rigolin,¹³ Roberto Marasca,¹⁴ Marta Coscia,¹⁵ Omar Perbellini,¹⁶ Alessandra Tedeschi,¹⁷ Luca Laurenti,¹⁸ Marina Motta,¹⁹ David Donaldson,²⁰ Phil Weir,²⁰ Ken Mills,²¹ Patrick Thornton,²² Sarah Lawless,²⁰ Francesco Bertoni,⁴ Giovanni Del Poeta,²³ Antonio Cuneo,¹³ Antonia Follenzi,²⁴ Valter Gattei,¹⁰ Renzo Luciano Boldorini,²⁵ Mark Catherwood,²⁰ Silvia Deaglio,³ Robin Foà,⁵ Gianluca Gaidano^{1,°} and Davide Rossi^{2,°}

¹Division of Hematology, Department of Translational Medicine, Amedeo Avogadro University of Eastern Piedmont, Novara, Italy; ²Institute of Oncology Research and Oncology Institute of Southern Switzerland, Bellinzona, Switzerland; ³Department of Medical Sciences, University of Turin & Italian Institute for Genomic Medicine, Turin, Italy; ⁴Università della Svizzera Italiana, Institute of Oncology Research, Bellinzona, Switzerland; ⁵Hematology, Department of Cellular Biotechnologies and Hematology, Sapienza University, Rome, Italy; ⁶Cancer Sciences Unit, Southampton Cancer Research UK and National Institute for Health Research Experimental Cancer Medicine Centre, University of Southampton, Southampton, UK; ⁷Division of Hematology, University of Siena, Siena, Italy; ⁸Department of Hematology Oncology, Fondazione IRCCS Ca' Granda Ospedale Maggiore Policlinico and University of Milan, Milan, Italy; ⁹Clinica Ematologica, DAME, University of Udine, Udine, Italy; ¹⁰Clinical and Experimental Onco-Hematology Unit, Centro di Riferimento Oncologico, Istituto di Ricovero e Cura a Carattere Scientifico (IRCCS), Aviano, Italy; ¹¹Department of Cell Therapy and Hematology, Ospedale San Bortolo, Vicenza, Italy; ¹²Division of Hematology, Azienda Ospedaliera Universitaria Policlinico-OVE, Catania, Italy; ¹³Hematology Section, Azienda Ospedaliera Universitaria Arcispedale S. Anna, University of Ferrara, Ferrara, Italy; ¹⁴Division of Hematology, Department of Oncology and Hematology, University of Modena and Reggio Emilia, Modena, Italy; ¹⁵Division of Hematology, Azienda Ospedaliera Universitaria Città della Salute e della Scienza and University of Turin, Turin, Italy; ¹⁶Section of Hematology, Department of Medicine, University of Verona, Verona, Italy; ¹⁷Department of Oncology/Haematology, Niguarda Cancer Center, Niguarda Ca Granda Hospital, Milan, Italy; ¹⁸Fondazione Policlinico Universitario A. Gemelli, Rome, Italy; ¹⁹Department of Hematology, Spedali Civili, Brescia, Italy; ²⁰Clinical Haematology, Belfast City Hospital, Belfast Health and Social Care Trust, Belfast, Northern Ireland, UK; ²¹Centre for Cancer Research and Cell Biology (CCRCB), Queen's University Belfast, Belfast, Northern Ireland, UK; ²²Department of Haematology, Beaumont Hospital, Dublin, Ireland; ²³Department of Hematology, Tor Vergata University, Rome, Italy; ²⁴Department of Health Sciences, University of Eastern Piedmont Amedeo Avogadro, Novara, Italy; ²⁵Department of Pathology, University of Eastern Piedmont Amedeo Avogadro, Novara, Italy.

**FD and RM contributed equally to this work

°GG and DR contributed equally to this work.

Haematologica 2020
Volume 105(2):448-456

Correspondence:

DAVIDE ROSSI
davide.rossi@eoc.ch

GIANLUCA GAIDANO
gianluca.gaidano@med.uniupo.it

Received: March 29, 2019.

Accepted: July 24, 2019.

Pre-published: August 1, 2019.

doi:10.3324/haematol.2019.219550

Check the online version for the most updated information on this article, online supplements, and information on authorship & disclosures: www.haematologica.org/content/105/2/448

©2020 Ferrata Storti Foundation

Material published in *Haematologica* is covered by copyright. All rights are reserved to the Ferrata Storti Foundation. Use of published material is allowed under the following terms and conditions:

<https://creativecommons.org/licenses/by-nc/4.0/legalcode>.

Copies of published material are allowed for personal or internal use. Sharing published material for non-commercial purposes is subject to the following conditions:

<https://creativecommons.org/licenses/by-nc/4.0/legalcode>,

sect. 3. Reproducing and sharing published material for commercial purposes is not allowed without permission in writing from the publisher.



ABSTRACT

BIRC3 is a recurrently mutated gene in chronic lymphocytic leukemia (CLL) but the functional implications of *BIRC3* mutations are largely unexplored. Furthermore, little is known about the prognostic impact of *BIRC3* mutations in CLL cohorts homogeneously treated with first-line fludarabine, cyclophosphamide, and rituximab (FCR). By immunoblotting analysis, we showed that the non-canonical nuclear factor- κ B pathway is active in *BIRC3*-mutated cell lines and in primary CLL samples, as documented by the stabilization of MAP3K14 and by the nuclear localization of p52. In addition, *BIRC3*-mutated primary CLL cells are less sensitive to fludarabine. In order to confirm in patients that *BIRC3* mutations confer resistance to fludarabine-based chemoimmunotherapy, a retrospective multicenter cohort of 287 untreated patients receiving first-line FCR was analyzed

by targeted next-generation sequencing of 24 recurrently mutated genes in CLL. By univariate analysis adjusted for multiple comparisons *BIRC3* mutations identify a poor prognostic subgroup of patients in whom FCR treatment fails (median progression-free survival: 2.2 years, $P < 0.001$) similar to cases harboring *TP53* mutations (median progression-free survival: 2.6 years, $P < 0.0001$). *BIRC3* mutations maintained an independent association with an increased risk of progression with a hazard ratio of 2.8 (95% confidence interval 1.4-5.6, $P = 0.004$) in multivariate analysis adjusted for *TP53* mutation, 17p deletion and *IGHV* mutation status. If validated, *BIRC3* mutations may be used as a new molecular predictor to select high-risk patients for novel frontline therapeutic approaches.

Introduction

Nuclear factor- κ B (NF- κ B) signaling is a key component of the development and evolution of chronic lymphocytic leukemia (CLL).¹ Two NF- κ B pathways exist, namely the canonical and non-canonical pathways.² The former is triggered by B-cell receptor signaling via Bruton tyrosine kinase (BTK), while the latter is activated by members of the tumor necrosis factor (TNF) cytokine family.³ Upon receptor binding, the TRAF3/MAP3K14-TRAF2/BIRC3 negative regulatory complex of non-canonical NF- κ B signaling is disrupted, MAP3K14 (also known as NIK), the central activating kinase of the pathway, is released and activated to induce the phosphorylation and proteasomal processing of p100, thereby leading to the formation of p52-containing NF- κ B dimers. The p52 protein dimerizes with RelB to translocate into the nucleus, where it regulates gene transcription. BIRC3 (Baculoviral IAP Repeat Containing 3) is a negative regulator of non-canonical NF- κ B. Physiologically, BIRC3 (also known as cIAP2) catalyzes MAP3K14 protein ubiquitination in a manner that is dependent on the E3 ubiquitin ligase activity of its C-terminal RING domain. MAP3K14 ubiquitination results in its proteasomal degradation.⁴

B-cell neoplasia often pirates signaling pathways by molecular lesions to promote survival and proliferation. Although according to bioinformatics criteria *BIRC3* is one of the candidate driver genes of CLL, the functional implications of *BIRC3* mutations are partially unexplored.⁵⁻⁷ Furthermore, little is known about the prognostic impact of *BIRC3* mutations in CLL cohorts homogeneously treated first-line with fludarabine, cyclophosphamide, and rituximab (FCR).⁷

FCR is the most effective chemoimmunotherapy regimen for the management of CLL in young and fit patients devoid of *TP53* disruption.⁸ Survival after FCR is, however, variable, and is affected by the molecular characteristics of the CLL clone.⁹ Deletion of 17p and *TP53* mutations are present in most, but not all patients who are refractory to chemo-immunotherapy, which prompts the identification of additional biomarkers associated with early failure of FCR.¹⁰⁻¹²

Methods

Functional studies

The human CLL cell line MEC1, the splenic marginal zone lymphoma cell lines SSK41 and VL51, the mantle cell lymphoma cell lines MAVER-1, Z-138 and JEKO-1, the human HEK-293T cell line, as well as primary CLL cells were used in functional experiments. The entire non-canonical NF- κ B pathway was assessed by western blot analysis. Quantitative real-time polymerase chain reaction

(qRT-PCR) was utilized to analyze the non-canonical NF- κ B signature. Primary CLL were exposed to fludarabine and venetoclax for 24-48 h and apoptosis was measured using the eBioscience Annexin V Apoptosis Detection Kit APC (ThermoFisher). Details are supplied in the *Online Supplementary Methods*.

Cancer personalized profiling by deep sequencing

A retrospective multicenter cohort of 287 untreated CLL patients receiving first-line therapy with FCR was analyzed for mutations, including 173 patients from a previously published multicenter clinical series and 114 new patients not included in our previous report.¹⁰ The study was approved by the Ethical Committee of the Ospedale Maggiore della Carità di Novara associated with the Amedeo Avogadro University of Eastern Piedmont (study number CE 67/14). Further information is provided in the *Online Supplementary Methods*. A targeted resequencing gene panel was designed to include: (i) coding exons plus splice site of 24 genes known to be implicated in CLL pathogenesis and/or prognosis; (ii) 3'UTR of *NOTCH1*; and (iii) enhancer and promoter region of *PAX5* (size of the target region: 66627bp) (Table S1).^{6,7} The next-generation sequencing libraries for genomic DNA (gDNA) were constructed using the KAPA Library Preparation Kit (Kapa Biosystems) and those for RNA were constructed using the RNA Hyper Kit (Roche). Multiplexed libraries (n=10 per run) were sequenced using 300-bp paired-end runs on a MiSeq sequencer (Illumina) to obtain a coverage of at least 2000x in >90% of the target region (66627 bp) in 80% of cases (*Online Supplementary Table S2*). A robust and previously validated bioinformatics pipeline was used for variant calling (*Online Supplementary Appendix*).

Statistical analysis

Progression-free survival (PFS) was the primary endpoint. Survival analysis was performed with the Kaplan-Meier method and compared between strata using the log-rank test. To account for multiple testing, adjusted *P* values were calculated using the Bonferroni correction. The adjusted association between exposure variables and PFS was estimated by Cox regression. Internal validation of the multivariate analysis was performed using a bootstrap approach. Statistical significance was defined as a *P* value <0.05 (*Online Supplementary Appendix*).

Results

BIRC3 mutations associate with activation of non-canonical nuclear factor- κ B signaling

In order to map unique *BIRC3* mutations in CLL comprehensively, we compiled somatically confirmed variants identified in the current CLL study cohort with those identified in previous studies¹⁵ or listed in public CLL mutation catalogues (Figure 1A). Virtually all *BIRC3* mutations were frameshift mutations or stop codons clustering in two hotspot regions comprised between amino acids

367-438 and amino acids 537-564. *BIRC3* variants were predicted to generate aberrant truncated transcripts causing the elimination or truncation of the C-terminal RING domain of the *BIRC3* protein. The RING domain of

BIRC3 harbors the E3 ubiquitin ligase activity that is essential for proteasomal degradation of MAP3K14, the central activating kinase of non-canonical NF- κ B signaling. This observation points to non-canonical NF- κ B activation

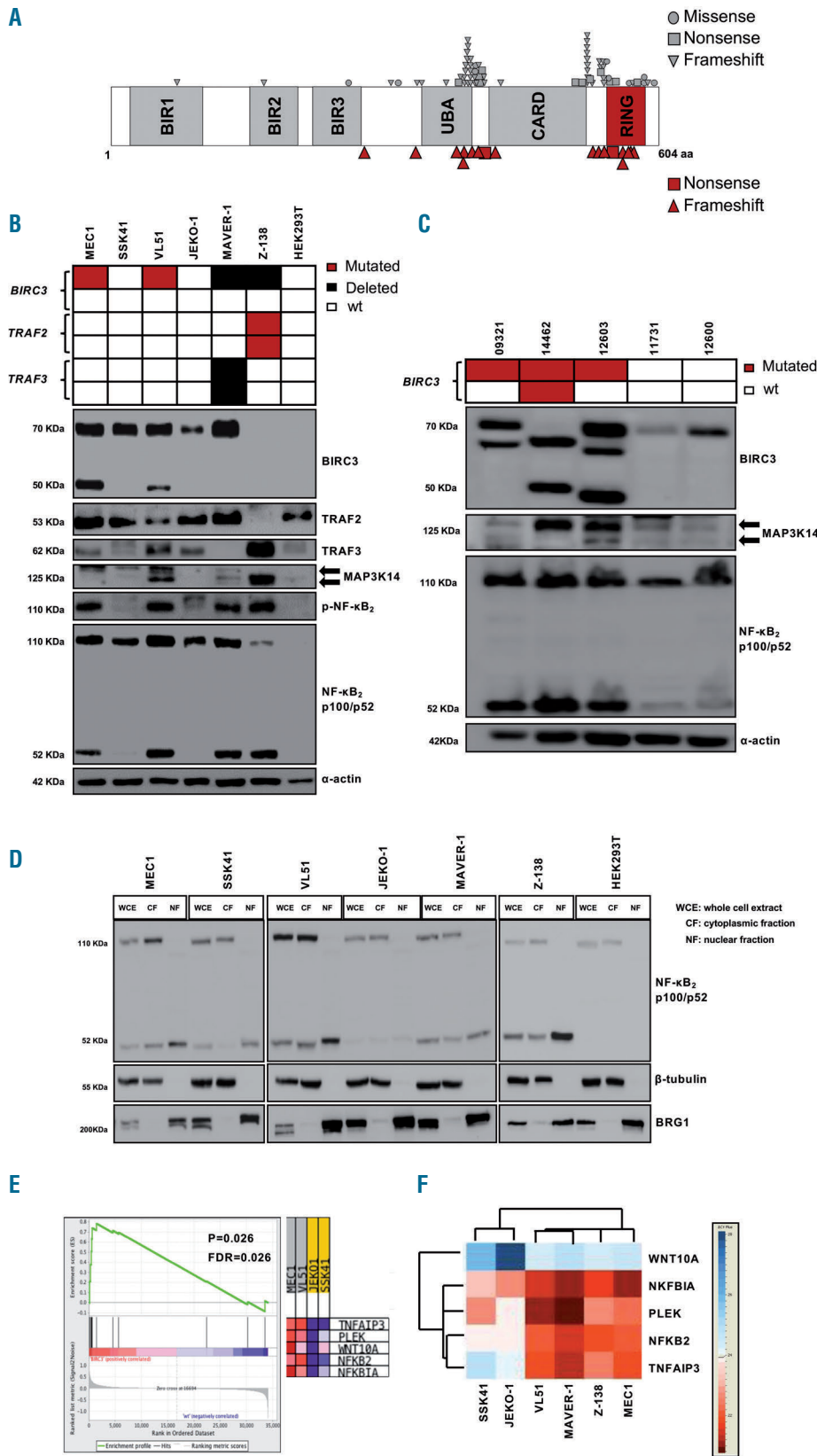


Figure 1. The non-canonical nuclear factor- κ B pathway is active in *BIRC3*-mutated chronic lymphocytic leukemia cell lines and primary samples. (A) Disposition of *BIRC3* mutations across the protein. The mutations identified by Landau *et al.*⁶, Puente *et al.*⁷ and from a public CLL mutation catalogue (COSMIC v85) are plotted in gray. Individual *BIRC3* mutations identified in the current studied cohort and in our previous study¹³ are plotted in red. (B) Western blot analysis of *BIRC3* protein expression and NF- κ B₂ activation and processing in the splenic marginal zone lymphoma (SMZL) cell lines SSK41, VL51 and in the chronic lymphocytic leukemia (CLL) cell line MEC1, carrying wildtype (wt) or disrupted *BIRC3*. The MAVER-1 and Z-138 cell lines were used as positive controls of non-canonical NF- κ B activation, harboring genetic activation of non-canonical NF- κ B signaling. The JEKO-1 and HEK 293T cell lines were used as negative controls for non-canonical NF- κ B signaling. α -actin was used as a loading control. Color codes indicate the gene status in each cell line. The aberrant *BIRC3* band expressed in MEC1 and VL51 cell lines corresponds in size to the predicted *BIRC3*-truncated protein, encoded by the mutant allele. (C) Western blot analysis showing *BIRC3* expression and NF- κ B₂ processing in purified primary tumor cells from five CLL and SMZL patients carrying wildtype or disrupted *BIRC3*. Color codes indicate the gene status in each cell line. The aberrant *BIRC3* bands in patients 09321, 14462 and 12603 correspond in size to the predicted *BIRC3*-truncated protein encoded by the mutant allele. α -actin was used as a loading control. (D) Western blot of whole cell extract, cytoplasmic or nuclear fractions of the SMZL and CLL cell lines probed for the NF- κ B₂ subunits p100 and p52. The MAVER-1 and Z-138 cell lines served as positive controls while the JEKO-1 and HEK 293T cell lines were used as negative controls. β -tubulin and BRG1 served as controls for the purity of the cytoplasmic and nuclear fractionations, respectively. (E) Gene set enrichment analysis score and distribution of non-canonical NF- κ B target genes along the rank of transcripts differentially expressed in the SMZL cell lines SSK41, VL51 and in the CLL cell line MEC1. The JEKO-1 cell line was used as a negative control. (F) Validation of expression of non-canonical NF- κ B target genes in the same SMZL and CLL cell lines as determined by quantitative real-time polymerase chain reaction analysis. Changes of gene expression were normalized to *GAPDH* expression; relative quantities were log₂ normalized to control samples (the mantle cell lymphoma cell line, JEKO-1).

through MAP3K14 stabilization as the predicted functional consequence of *BIRC3* mutations in CLL.

The non-canonical NF- κ B signaling was profiled by immunoblotting in B-cell tumor cell lines and primary CLL cells with different genetic make-up in the non-canonical NF- κ B pathway to verify whether *BIRC3* mutations lead to constitutive non-canonical NF- κ B activation. Additional genetic features of the above-mentioned cell lines and primary CLL cells are shown in *Online Supplementary Table S3*. In the VL51 splenic marginal zone lymphoma cell line and in the MEC1 CLL cell lines, both harboring endogenous truncating mutations of the *BIRC3* gene, non-canonical NF- κ B signaling was constitutively active, as documented by the stabilization of MAP3K14, phosphorylation of NF- κ B₂, its processing from p100 to p52, as well as the nuclear localization of p52 (Figure 1B-D). Consistent with the biochemical clues of non-canonical NF- κ B activation, the gene expression signature of the VL51 and MEC1 cell lines was significantly enriched in non-canonical NF- κ B target genes (Figure 1E, F). Non-canonical NF- κ B signaling in *BIRC3*-mutated cells was consistent with that in mantle cell lymphoma cell lines known to harbor a disrupted TRAF3/MAP3K14-TRAF2/*BIRC3* negative regulatory complex by loss of TRAF3 or TRAF2.¹⁴ Like *BIRC3*-mutated cell lines, primary CLL samples harboring inactivating mutations of *BIRC3* also showed stabilization of MAP3K14 and NF- κ B₂ processing from p100 to p52 (Figure 1C), thus confirming that non-canonical NF- κ B activation is also a feature of primary cells harboring *BIRC3* variants. MAP3K14 stabilization is largely associated with *BIRC3* mutations. Indeed all seven cases harboring non-canonical NF- κ B genetic lesions showed either a strong or a slight MAP3K14 band, while, conversely, only one out of five cases lacking a non-canonical NF- κ B lesion had MAP3K14 expression (Fisher exact test, $P=0.01$).

MAP3K14 was genetically targeted by shRNA to test whether *BIRC3*-mutated cells are addicted to its stabilization. Compared to non-targeting shRNA, the most efficient anti-MAP3K14 shRNA-D resulted in a partial silencing of MAP3K14 and in decreased NF- κ B₂ processing from p100 to p52. This translated into a reduced cell viability of

the *BIRC3*-mutated VL51 cell line transduced with shRNA-D. This observation indicates that MAP3K14 stabilization is a vulnerability of *BIRC3*-mutated cells (Figure 2). In order to test the contribution of BTK to non-canonical NF- κ B signaling when it is activated through *BIRC3* mutations, *BIRC3*-mutated cell lines, as well as cell lines harboring a disrupted or competent TRAF3/MAP3K14-TRAF2/*BIRC3* negative regulatory complex were treated with ibrutinib at different dosages and non-canonical NF- κ B signaling activation was probed by immunoblotting of the NF- κ B₂ processing from p100 to p52. Processing from p100 to p52 was unaffected by ibrutinib treatment in cell lines harboring *BIRC3* mutations (Figure 3) or a disrupted TRAF3/MAP3K14-TRAF2/*BIRC3* negative regulatory complex, consistent with the notion that *BIRC3* mutations activate non-canonical NF- κ B by bypassing BTK blockade by ibrutinib.¹⁴

***BIRC3* mutations confer resistance to fludarabine in primary chronic lymphocytic leukemia cells**

We performed *in vitro* pharmacological studies on primary CLL cells to verify the vulnerabilities of *BIRC3*-mutated cells. CLL cells purified from patients carrying *BIRC3* mutations were treated with increasing doses of fludarabine. Drug-induced apoptosis was compared to that of samples harboring *TP53* mutations, which represent a control for fludarabine resistance. CLL cells devoid of genetic lesions in either *BIRC3* or *TP53* were used as a control for fludarabine sensitivity. The molecular characteristic of the *ex-vivo* CLL cells are listed in *Online Supplementary Table S4*.

BIRC3-mutated cells showed delayed fludarabine-induced cell death, as no response was observed after 24 h of treatment, at variance with *TP53*- and *BIRC3*-wildtype samples. At this time point, cell viability curves of *BIRC3*-mutated samples overlapped almost completely with those of *TP53*-disrupted samples, which are known to be fludarabine resistant (Figure 4A). At 48 h, the viability of *BIRC3*-mutated cells was lower than that of *TP53*-mutated samples, but higher than that of *TP53*- and *BIRC3*-wildtype samples (Figure 4B).

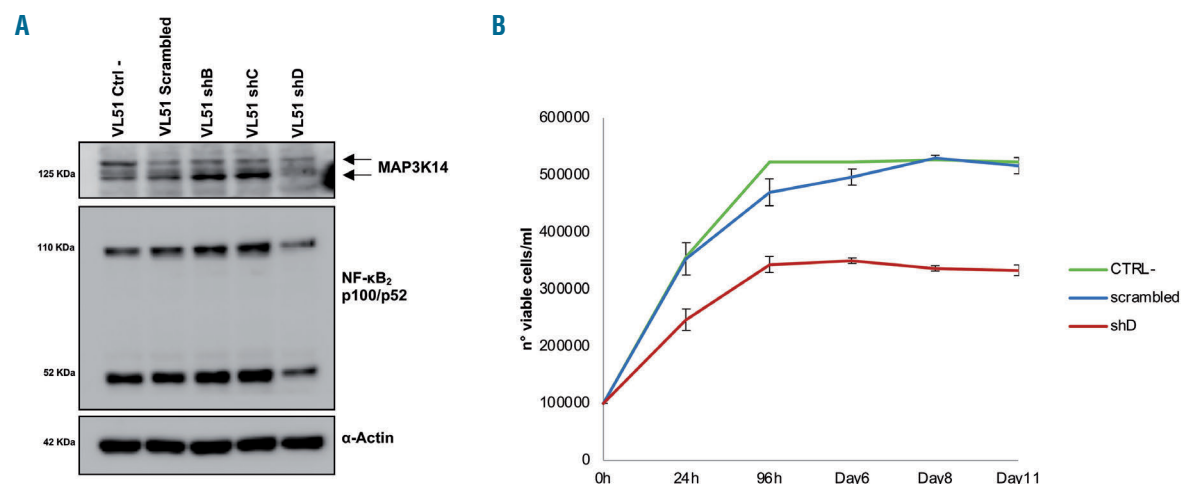


Figure 2. Knockdown of MAP3K14 by RNA interference in VL51 cells. (A) Western blot analysis for MAP3K14 expression and for NF- κ B₂ processing of p100 to p52. (B) VL51 cell viability assessed by trypan blue after transduction with lentiviral vectors expressing the shRNA-D_MAP3K14 (shD: in red), a scrambled shRNA (scrambled: in blue), and in non-transfected cells (CTRL: in green).

In order to assess whether *BIRC3* mutations interfere with apoptosis, primary CLL cells were treated with venetoclax. Venetoclax treatment resulted in a similar reduction of cell viability in *BIRC3*-mutated cells, *TP53*-mutated cells and *BIRC3/TP53*-wildtype cells (Figure 4C, D). Such divergent sensitivity to fludarabine and venetoclax of *BIRC3*-mutated CLL cells indirectly suggests that *BIRC3* mutations likely affect the upstream DNA damage response pathway rather than downstream apoptosis as a mechanism of inducing cell death.

Patients harboring *BIRC3* mutations are at risk of FCR failure

In order to confirm *in vivo* in patients that *BIRC3* mutations confer resistance to fludarabine-based chemioimmunotherapy, we correlated the *BIRC3* mutation status with PFS of CLL patients treated with FCR. Mutational profiling was performed in 287 patients who received first-line FCR. The baseline features of the study cohort were consistent with progressive, previously untreated CLL (Table 1). The median follow-up was 6.8 years, with

a median PFS and overall survival of 4.6 and 11.7 years, respectively (Table 1) consistent with observations in clinical trial cohorts.¹⁵ As expected, *SF3B1* and *NOTCH1* were the most frequently mutated genes identified in 13.9% and in 13.6% of patients, respectively, followed by *TP53* in 9.4% and *ATM* in 6.9% of patients. *BIRC3* was mutated in 3.1% of patients, reflecting the data reported in previous studies.^{6,7,13} Overall, 154/287 (53.6%) cases harbored at least one non-synonymous somatic mutation in one of the 24 CLL genes included in our panel (range, 1-5 mutation per patient), which is consistent with the typical mutational spectrum of CLL requiring first-line treatment (Figure 5, *Online Supplementary Table S5*).^{6,7,16}

By univariate analysis adjusted for multiple comparisons, among the genes analyzed in our panel, only *TP53* mutations (median PFS of 2.6 years; $P < 0.0001$) and *BIRC3* mutations (median PFS of 2.2 years; $P < 0.001$) (Figure 6A) were associated with significantly shorter PFS (Table 2). Following FCR treatment, the PFS of *BIRC3*-mutated patients was similar to that of cases har-

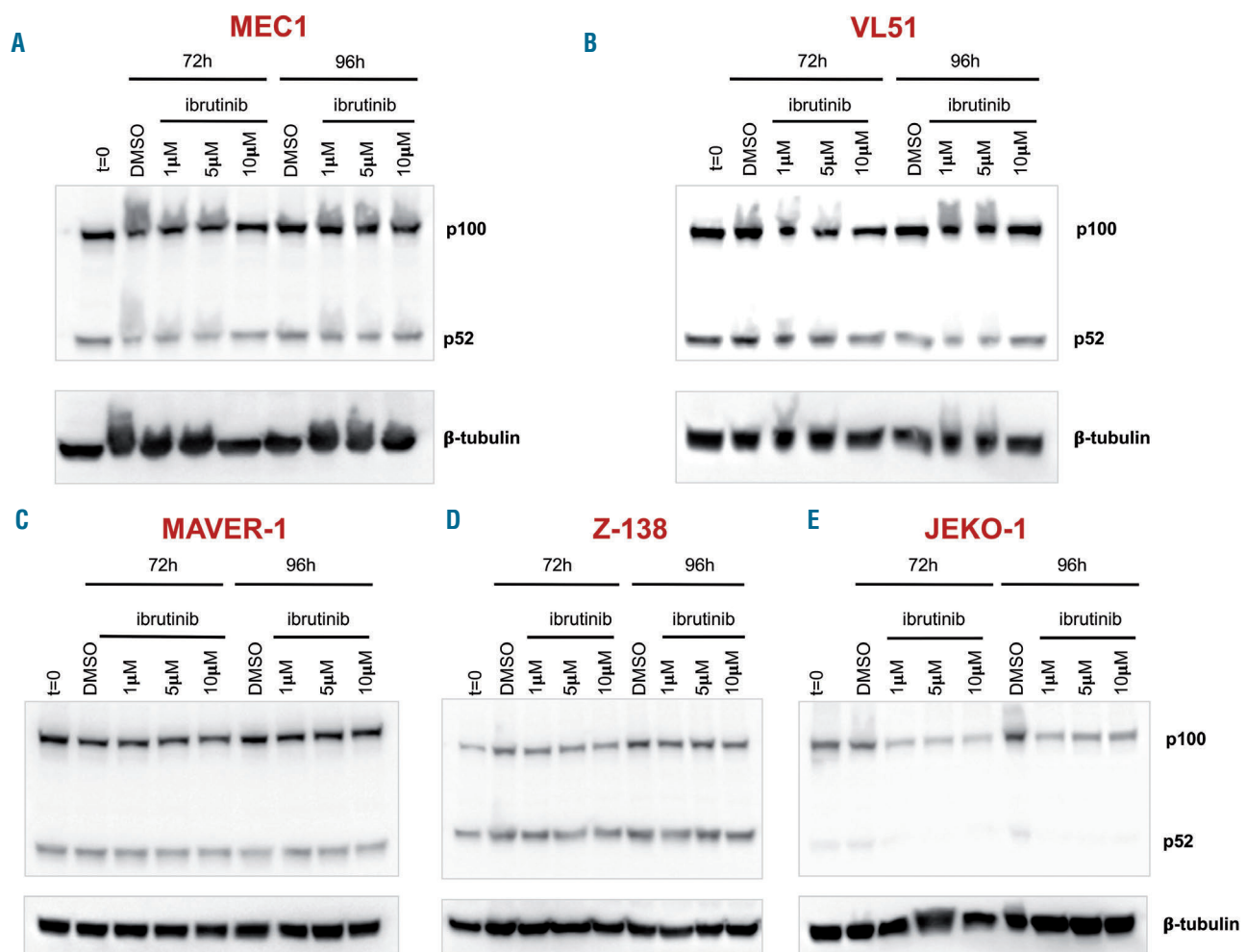


Figure 3. The non-canonical nuclear factor- κ B pathway is not switched off by ibrutinib in *BIRC3*-mutated cell lines. Western blot showing p100/p52 expression in (A) MEC1 and (B) VL51 cell lines that harbor *BIRC3* mutations. (C) MAVER-1 and (D) Z-138 cell lines, known to be affected by non-canonical NF- κ B pathway gene mutations and resistant to ibrutinib were used as positive controls. (E) The JEKO-1 cell line, known to be devoid of NF- κ B pathway gene mutations and sensitive to ibrutinib, was used as a negative control. All cell lines were treated with different concentrations of ibrutinib for 72 and 96 h. DMSO: dimethylsulfoxide.

boring *TP53* disruption (Figure 6B). Consistently, *BIRC3*-mutated patients had a lower likelihood of achieving complete response (22.2%) at the end of FCR compared to *BIRC3*-wildtype cases (76.7%; $P=0.001$). Well-known molecular prognostic biomarkers of CLL, such as unmutated *IGHV* gene status and 17p deletion also associated with a significantly shorter PFS, supporting the representativeness of the study cohort (Table 2). By multivariate analysis including variables showing a multiplicity-adjusted significant association with PFS, *BIRC3* mutations maintained an independent association with PFS, with a hazard ratio of 2.8 (95% confidence interval: 1.4-5.6; $P=0.004$) (Table 2).

Discussion

The results of this study provide evidence that: (i) *BIRC3* mutations are associated with activation of the non-canonical NF- κ B pathway and with resistance to fludarabine *in vitro*; and (ii) *BIRC3*-mutated patients, like cases harboring *TP53* disruption, are subject to failure of FCR chemoimmunotherapy.

The mere presence of somatic mutations is insufficient

to implicate a gene in cancer. Cancer geneticists and bioinformaticians differentiate “passenger” events, likely being randomly acquired, to distinguish them from mutations targeting candidate “cancer-driver” genes, likely implicated in the tumor biology, according to a statistical definition. Any given gene is labeled as a candidate “cancer driver” if it harbors somatic point mutations at a statistically significant rate or pattern in cancer samples. In CLL, more than 40 genes fulfill the statistical definition of a candidate “cancer driver”, including *BIRC3*, but few of them are biologically validated (i.e. *SF3B1*, *NOTCH1*, *TP53*, *ATM*, *FBXW7*).^{6,7,17-20} The *BIRC3* gene codes for a protein that ubiquitinates and negatively regulates the central activating kinase of the non-canonical NF- κ B pathway, namely MAP3K14 (also known as NIK).^{21,22} In lymphoid malignancies, the NF- κ B pathway is a pivotal and positive mediator of cell proliferation and survival.^{5,23,24} With regards to CLL, *BIRC3* mutations are absent in patients with monoclonal B-cell lymphocytosis, are rare at the time of diagnosis (3-4%), but are detectable in approximately 25% of fludarabine-refractory patients.¹³ In this study, we verified the biological consequences of *BIRC3* mutations, showing that they are associated with activation of the non-canonical NF- κ B pathway, that *BIRC3*-mutated lymphoid cells

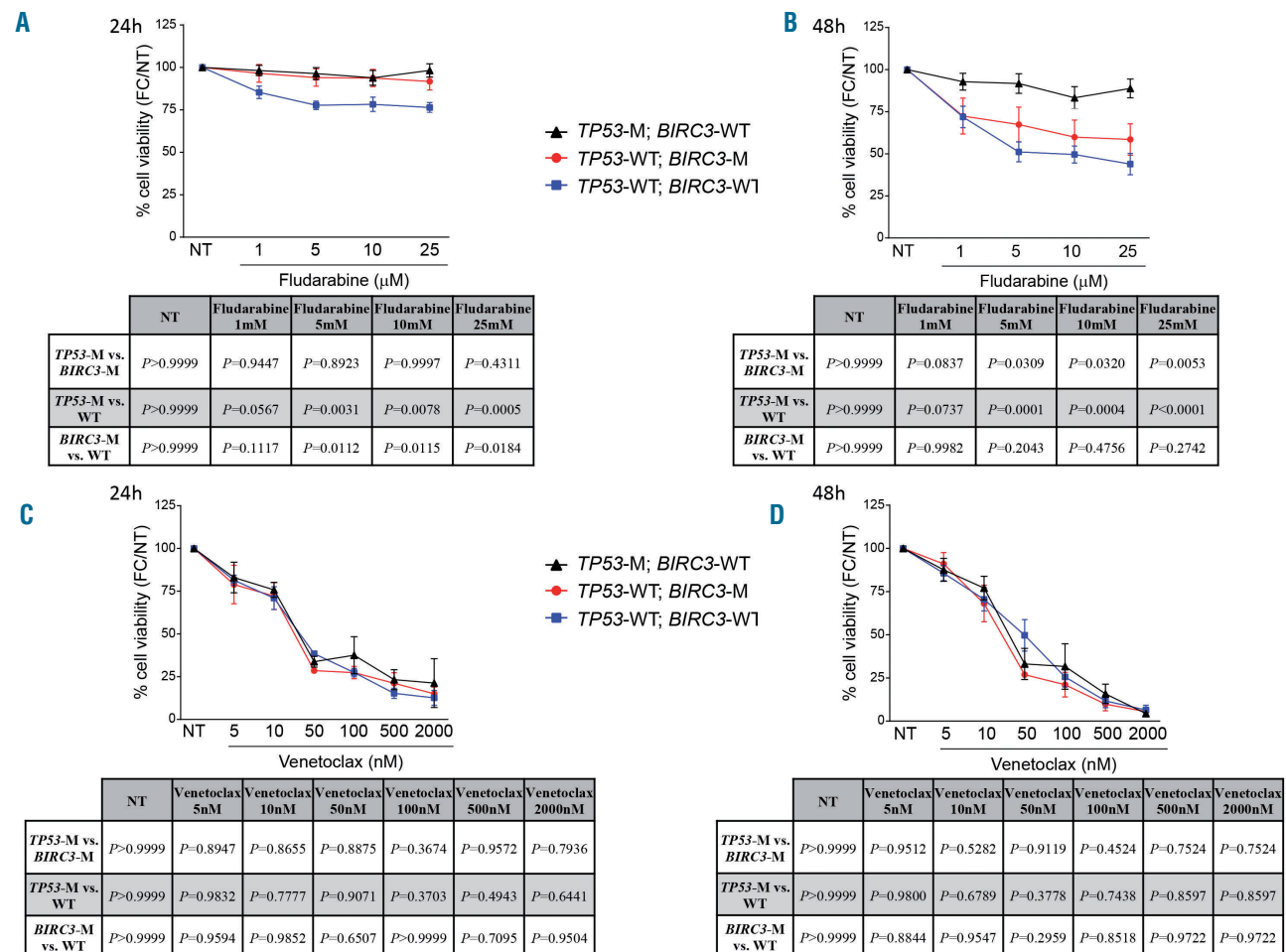


Figure 4. Responses of primary cells lines to fludarabine and venetoclax. (A-D) Viability of *BIRC3*-mutated (n=6 patients, red line), *TP53*-mutated (n=8 patients, black line) and wildtype (n=7 patients, blue line) primary CLL cells treated with different concentrations of fludarabine for 24 h (A) and 48 h (B) or venetoclax for 24 h (C) and 48 h (D). The pairwise *P* values are listed in the tables below the respective figures. M, mutated; WT, wildtype; NT, not treated.

are addicted to the non-canonical NF-κB pathway, and that *BIRC3*-mutated CLL are resistant to fludarabine both *in vitro* and in patients. It still remains to be clarified

whether NF-κB activation is the only molecular pathway that causes chemo-refractoriness in *BIRC3*-mutated CLL or whether other mechanisms are also involved.²⁴⁻²⁹

Table 1. Clinical data of FCR-treated chronic lymphocytic leukemia patients according to *BIRC3* mutational status.

Characteristics	Total	Number of patients (%)	<i>BIRC3</i> mutated patients (%)	<i>BIRC3</i> wildtype patients (%)
Male	N=287	198 (69.0%)	5 (55.6%)	193 (69.4%)
Female		89 (31.0%)	4 (44.4)	85 (30.6%)
Binet A	N=287	33 (11.5%)	1 (11.1%)	32 (11.5%)
Binet B-C		254 (88.5%)	8 (88.9%)	246 (88.5%)
<i>IGHV</i> mutated	N=280	100 (35.7%)	0 (0%)	100 (36.0%)
<i>IGHV</i> unmutated		180 (64.3%)	9 (100%)	171 (61.5%)
17p deletion	N=274	13 (4.7%)	0 (0%)	13 (4.7%)
No 17p deletion		261 (95.3%)	9 (100%)	252 (90.6%)
11q deletion	N=273	47 (17.2%)	5 (55.6%)	42 (15.1%)
No 11q deletion		226 (82.8%)	4 (44.4)	222 (79.9%)
13q deletion	N=273	111 (40.7%)	3 (33.3%)	108 (38.8%)
No 13q deletion		162 (59.3%)	6 (66.6%)	156 (56.1%)
Trisomy 12	N=272	50 (18.4%)	4 (44.4%)	46 (16.5%)
No trisomy 12		222 (81.6%)	5 (55.6%)	217 (78.1%)

Median follow-up (years)	6.8
Median PFS (years)	4.6
PFS % (7 years)	31.0%
Median OS (years)	11.7
OS % (7 years)	75.5%

PFS: progression-free survival; OS: overall survival; *IGHV*: immunoglobulin heavy variable gene.

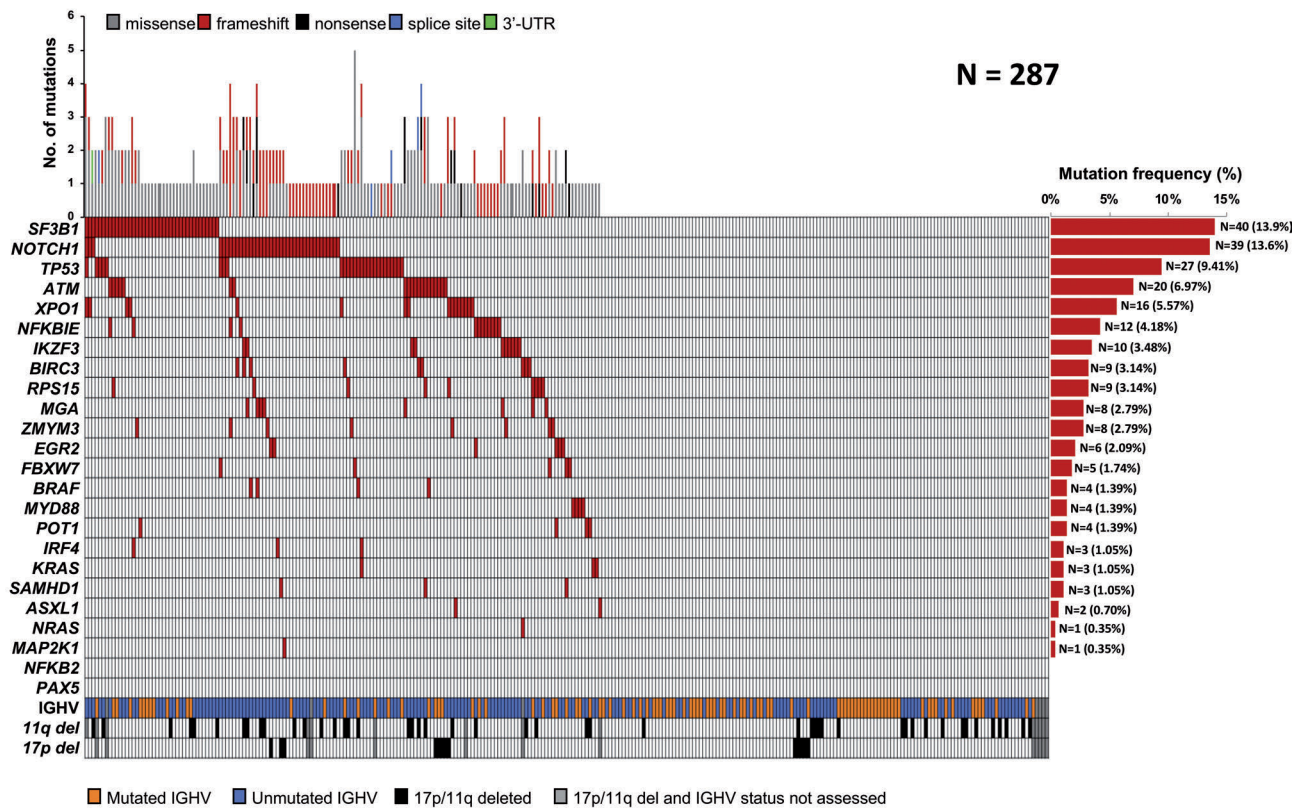


Figure 5. Mutational profile of the FCR-treated cohort. Case-level mutational profiles of 287 patients treated with FCR (fludarabine, cyclophosphamide, rituximab). Each column represents one tumor sample, each row represents one gene. The fraction of tumors with mutations in each gene is plotted on the right. The number and type of mutations in each patient are plotted above the heatmap. Mutations are highlighted in red. *IGHV* mutational status, 17p deletion and 11q deletion are plotted at the bottom of the heatmap.

The introduction of FCR was a breakthrough in the management of young, fit CLL patients, leading to improvements in both PFS and overall survival compared to those achieved with previous treatment regimens. In both clinical trials and real-life cohorts,¹⁰⁻¹² *IGHV* mutation status and *TP53* disruption emerged as strong predictors of poor response to FCR. However, these molecular biomarkers do

not fully capture all high-risk patients destined to relapse. We propose *BIRC3* mutations as a new biomarker for the identification of patients at high risk of FCR failure, similarly to cases harboring *TP53* disruption. If validated in independent series, *BIRC3* mutations may turn out as a new molecular predictor of FCR resistance that could be used to select patients to be treated with novel targeted agents.

Table 2. Univariate and multivariate analyses of progression-free survival.

Characteristics	7-y PFS (%)	Median PFS (y)	Univariate analysis			Multivariate analysis				Internal bootstrapping validation			
			95% CI	P	P*	HR	LCI	UCI	P	HR	LCI	UCI	Bootstrapping selection (%)
Binet A	40.3%	4.5	2.4-6.6	0.356	-	-	-	-	-	-	-	-	-
Binet B-C	30.0%	4.6	3.8-5.4										
<i>IGHV</i> mutated	49.3%	6.5	3.8-9.2	<0.001	0.003	-	-	-	0.001	-	-	-	98.8%
<i>IGHV</i> unmutated	23.0%	3.9	3.5-4.4			1.8	1.3	2.6		1.9	1.3	2.7	
No 11q deletion	33.4%	5.0	4.2-5.9	0.025	0.700	-	-	-	-	-	-	-	-
11q deletion	13.9%	3.6	2.4-4.9			-	-	-		-	-	-	
No 17p deletion	33.0%	4.8	4.1-5.6	<0.0001	<0.0001	-	-	-	<0.0001	-	-	-	99.5%
17p deletion	nr	1.1	0-2.6			4.0	2.2	7.5		4.9	2.5	9.8	
<i>TP53</i> wildtype	33.8%	5.4	4.3-5.8	<0.0001	<0.001	-	-	-	0.030	-	-	-	73.3%
<i>TP53</i> mutated	nr	2.8	2.0-3.5			1.7	1.1	2.8		1.8	1.1	3	
<i>BIRC3</i> wildtype	32.2%	4.8	4.1-5.6	<0.001	0.005	-	-	-	0.004	-	-	-	91.1%
<i>BIRC3</i> mutated	nr	2.2	0.9-3.5			2.8	1.4	5.6		3.4	1.6	7.3	
<i>EGR2</i> wildtype	31.5%	4.7	3.9-5.4	0.015	0.420	-	-	-	-	-	-	-	-
<i>EGR2</i> mutated	nr	1.5	0-3.8			-	-	-		-	-	-	
<i>ATM</i> wildtype	32.5%	4.8	4.1-5.6	0.029	0.812	-	-	-	-	-	-	-	-
<i>ATM</i> mutated	nr	3.2	2.4-4.1			-	-	-		-	-	-	

y: year; P: P-value; P*: Bonferroni correction; PFS: progression-free survival; CI: confidence interval; HR: hazard ratio; LCI: lower boundary of the confidence interval; UCI: upper boundary of the confidence interval; *IGHV*: immunoglobulin heavy variable gene; nr: not reached.

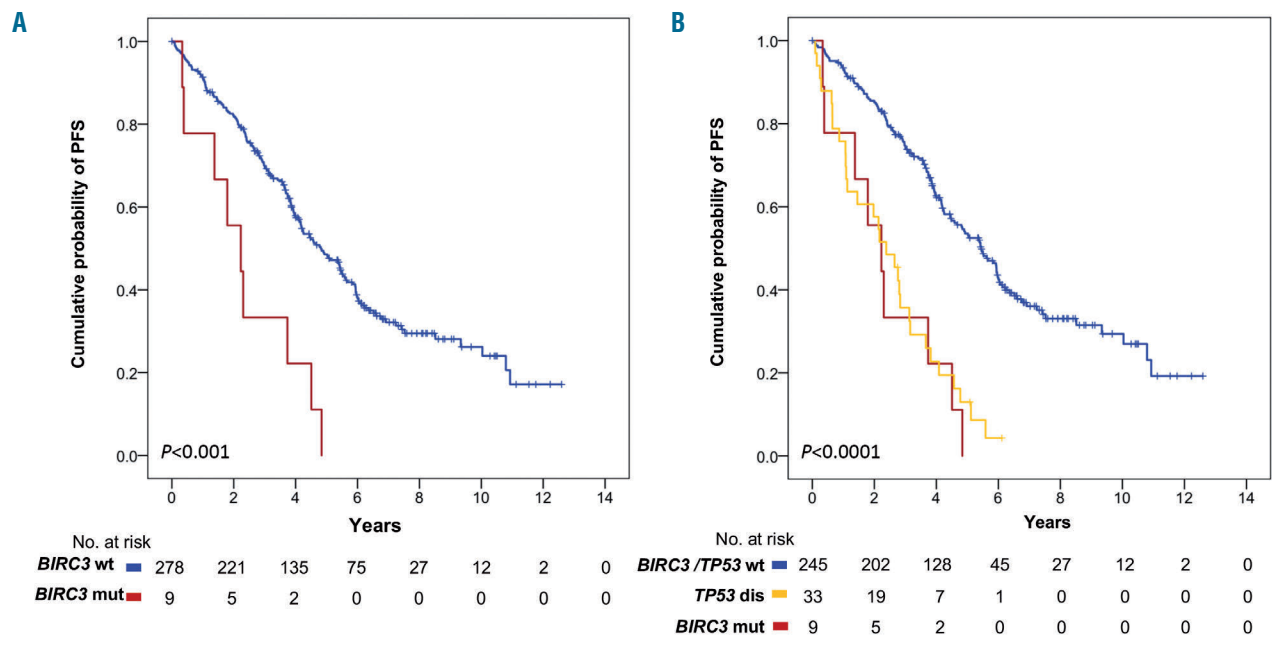


Figure 6. Kaplan-Meier estimates of progression-free survival in *BIRC3*-mutated patients. (A) Cases harboring *BIRC3* mutations are represented by the red line. *BIRC3*-wildtype cases are represented by the blue line. (B) Cases harboring *BIRC3* mutations are represented by the red line. Cases harboring *TP53* disruption (including *TP53* mutation and/or 17p deletion) are represented by the yellow line. Patients devoid of *BIRC3* mutation and *TP53* disruption are represented by the blue line.

Non-canonical NF- κ B activation by *BIRC3* mutations bypasses the block of BTK by ibrutinib. Consistently, NF- κ B activation and cell survival are unaffected by ibrutinib in both CLL cells (our study) and mantle cell lymphoma cells.¹⁴ If this preclinical evidence is validated in ibrutinib-treated patients, *BIRC3* mutations may also translate into a biomarker for informing selection of novel agents.

Acknowledgments

This work was supported by: *Molecular bases of disease dissemination in lymphoid malignancies to optimize curative therapeutic strategies, (5 x 1000 n. 21198), Associazione Italiana per la Ricerca sul Cancro Foundation, Milan, Italy (grants to GG and RF) and Progetti di Rilevante Interesse Nazionale (PRIN),*

(2015ZMRFEA), Rome, Italy; partially funded by the AGING Project – Department of Excellence – DIMET, Università del Piemonte Orientale, Novara, Italy; partially funded by Novara AIL ONLUS, Novara, Italy; Associazione Italiana per la Ricerca sul Cancro (AIRC IG-17314); Swiss Cancer League, ID HSR-4660-11-2018, Bern, Switzerland; Research Advisory Board of the Ente Ospedaliero Cantonale, Bellinzona, Switzerland; European Research Council (ERC) Consolidator grant CLL-CLONE ID: 772051; grant n. 320030_169670/1 Swiss National Science Foundation, Berne, Switzerland; Fondazione Fidinam, Lugano, Switzerland; Nelia & Amadeo Barletta Foundation, Lausanne, Switzerland; Fond'Action, Lausanne, Switzerland; Translational Research Program, grant n. 6594-20, The Leukemia & Lymphoma Society, New York, USA.

References

- Mansouri L, Papakonstantinou N, Ntoufa S, Stamatopoulos K, Rosenquist R. NF- κ B activation in chronic lymphocytic leukemia: a point of convergence of external triggers and intrinsic lesions. *Semin Cancer Biol.* 2016; 39:40-48.
- Bonizzi G, Karin M. The two NF- κ B activation pathways and their role in innate and adaptive immunity. *Trends Immunol.* 2004;25(6):280-288.
- Oeckinghaus A, Hayden MS, Ghosh S. Crosstalk in NF- κ B signaling pathways. *Nat Immunol.* 2011;12(8):695-708.
- Sun SC. The noncanonical NF- κ B pathway. *Immunol Rev.* 2012;246(1):125-140.
- Asslaber D, Wacht N, Leisch M, Qi Y, et al. *BIRC3* expression predicts CLL progression and defines treatment sensitivity via enhanced NF- κ B nuclear translocation. *Clin Cancer Res.* 2019;25(6):1901-1912.
- Puente XS, Beà S, Valdés-Mas R, et al. Non-coding recurrent mutations in chronic lymphocytic leukaemia. *Nature.* 2015;526(7574):519-524.
- Landau DA, Tausch E, Taylor-Weiner AN, et al. Mutations driving CLL and their evolution in progression and relapse. *Nature.* 2015;526(7574):525-530.
- Hallek M, Cheson BD, Catovsky D, et al. Guidelines for diagnosis, indications for treatment, response assessment and supportive management of chronic lymphocytic leukemia. *Blood.* 2018;131(25):2745-2760.
- Gaidano G, Rossi D. The mutational landscape of chronic lymphocytic leukemia and its impact on prognosis and treatment. *Hematology Am Soc Hematol Educ Program.* 2017;2017(1):329-337.
- Rossi D, Terzi-di-Bergamo L, De Paoli L, et al. Molecular prediction of durable remission after first-line fludarabine-cyclophosphamide-rituximab in chronic lymphocytic leukemia. *Blood.* 2015;126(16):1921-1924.
- Thompson PA, Tam CS, O'Brien SM, et al. Fludarabine, cyclophosphamide, and rituximab treatment achieves long-term disease-free survival in IGHV-mutated chronic lymphocytic leukemia. *Blood.* 2016;127(3):303-309.
- Fischer K, Bahlo J, Fink AM, et al. Long-term remissions after FCR chemoimmunotherapy in previously untreated patients with CLL: updated results of the CLL8 trial. *Blood.* 2016;127(2):208-215.
- Rossi D, Fangazio M, Rasi S, et al. Disruption of *BIRC3* associates with fludarabine chemorefractoriness in TP53 wild-type chronic lymphocytic leukemia. *Blood.* 2012;119(12):2854-2862.
- Rahal R, Frick M, Romero R, et al. Pharmacological and genomic profiling identifies NF- κ B-targeted treatment strategies for mantle cell lymphoma. *Nature Medicine.* 2014;20(1):87-92.
- Hallek M, Fischer K, Fingerle-Rowson G, et al. Addition of rituximab to fludarabine and cyclophosphamide in patients with chronic lymphocytic leukaemia: a randomised, open-label, phase 3 trial. *Lancet.* 2010;376(9747):1164-1174.
- Stilgenbauer S, Schnaiter A, Paschka P, et al. Gene mutations and treatment outcome in chronic lymphocytic leukemia: results from the CLL8 trial. *Blood.* 2014;123(21):3247-3254.
- Grossmann V, Kohlmann A, Schnittger A, et al. Recurrent ATM and *BIRC3* mutations in patients with chronic lymphocytic leukemia (CLL) and deletion 11q22-q23. *Blood.* 2012;120(21):1771.
- Rose-Zerilli MJ, Forster J, Parker H, et al. ATM mutation rather than *BIRC3* deletion and/or mutation predicts reduced survival in 11q-deleted chronic lymphocytic leukemia: data from the UK LRF CLL4 trial. *Haematologica.* 2014;99(4):736-742.
- Baliakas P, Hadzidimitriou A, Sutton LA, et al. Recurrent mutations refine prognosis in chronic lymphocytic leukemia. *Leukemia.* 2015;29(2):329-336.
- Nadeu F, Delgado J, Royo C, et al. Clinical impact of clonal and subclonal TP53, SF3B1, *BIRC3*, NOTCH1, and ATM mutations in chronic lymphocytic leukemia. *Blood.* 2016;127(17):2122-2130.
- Vince JE, Wong WW, Khan N, et al. IAP antagonists target cIAP1 to induce TNF α -dependent apoptosis. *Cell.* 2007;131(4):682-693.
- Jost PJ, Ruland J. Aberrant NF- κ B signaling in lymphoma: mechanisms, consequences, and therapeutic implications. *Blood.* 2007;109(7):2700-2707.
- Raponi S, Del Giudice I, Ilari C, et al. Biallelic *BIRC3* inactivation in chronic lymphocytic leukaemia patients with 11q deletion identifies a subgroup with very aggressive disease. *Br J Haematol.* 2019;185(1):156-159.
- Hewamana S, Lin TT, Jenkins C, et al. The novel nuclear factor- κ B inhibitor LC-1 is equipotent in poor prognostic subsets of chronic lymphocytic leukemia and shows strong synergy with fludarabine. *Clin Cancer Res.* 2008;14(24):8102-8111.
- Hewamana S, Alghazal S, Lin TT, et al. The NF- κ B subunit Rel A is associated with in vitro survival and clinical disease progression in chronic lymphocytic leukemia and represents a promising therapeutic target. *Blood.* 2008;111:4681-4689.
- Beg AA, Baltimore D. An essential role for NF- κ B in preventing TNF- α -induced cell death. *Science.* 1996;274:782-784.
- Wang CY, Mayo MW, Baldwin AS, Jr. TNF- and cancer therapy-induced apoptosis: potentiation by inhibition of NF- κ B. *Science.* 1996;274:784-787.
- Webster GA, Perkins ND. Transcriptional cross talk between NF- κ B and p53. *Mol Cell Biol.* 1999;19:3485-3495.
- Nakanishi C, Toi M. Nuclear factor- κ B inhibitors as sensitizers to anticancer drugs. *Nat Rev.* 2005;5:297-309.

Sialyltransferase inhibition leads to inhibition of tumor cell interactions with E-selectin, VCAM1, and MADCAM1, and improves survival in a human multiple myeloma mouse model

Alessandro Natoni,^{1*} Mariah L. Farrell,^{2,3,4*} Sophie Harris,^{2,3,4} Carolyne Falank,^{2,3,4} Lucy Kirkham-McCarthy,¹ Matthew S. Macauley,⁵ Michaela R. Reagan^{2,3,4**} and Michael O'Dwyer^{1**}

¹Apoptosis Research Center, National University of Ireland, Galway, Ireland; ²Maine Medical Center Research Institute, Scarborough, ME, USA; ³Tufts University School of Medicine, Boston, MA, USA; ⁴Graduate School of Biomedical Science and Engineering, University of Maine, Orono, ME, USA and ⁵Department of Chemistry and Department of Medical Microbiology and Immunology, University of Alberta, Alberta, Canada

*AN and MLF contributed equally to this work. **MRR and MOD are joint senior authors of this work.

ABSTRACT

A aberrant glycosylation resulting from altered expression of sialyltransferases, such as ST3 β -galactoside α 2-3-sialyltransferase 6, plays an important role in disease progression in multiple myeloma (MM). Hypersialylation can lead to increased immune evasion, drug resistance, tumor invasiveness, and disseminated disease. In this study, we explore the *in vitro* and *in vivo* effects of global sialyltransferase inhibition on myeloma cells using the pan-sialyltransferase inhibitor 3F_{ax}-Neu5Ac delivered as a per-acetylated methyl ester pro-drug. Specifically, we show *in vivo* that 3F_{ax}-Neu5Ac improves survival by enhancing bortezomib sensitivity in an aggressive mouse model of MM. However, 3F_{ax}-Neu5Ac treatment of MM cells *in vitro* did not reverse bortezomib resistance conferred by bone marrow (BM) stromal cells. Instead, 3F_{ax}-Neu5Ac significantly reduced interactions of myeloma cells with E-selectin, MADCAM1 and VCAM1, suggesting that reduced sialylation impairs extravasation and retention of myeloma cells in the BM. Finally, we showed that 3F_{ax}-Neu5Ac alters the post-translational modification of the α 4 integrin, which may explain the reduced affinity of α 4 β 1/ α 4 β 7 integrins for their counter-receptors. We propose that inhibiting sialylation may represent a valuable strategy to restrict myeloma cells from entering the protective BM microenvironment, a niche in which they are normally protected from chemotherapeutic agents such as bortezomib. Thus, our work demonstrates that targeting sialylation to increase the ratio of circulating to BM-resident MM cells represents a new avenue that could increase the efficacy of other anti-myeloma therapies and holds great promise for future clinical applications.

Introduction

Multiple myeloma (MM) is characterized by clonal expansion of malignant plasma cells in the bone marrow (BM). Despite significant advances in treatment, MM remains incurable, with drug resistance mediated by the BM microenvironment being an important contributory factor.^{1,2} A related remarkable feature of MM is the ability for MM cells to spread from one BM site to another, which implies a persistent trafficking of circulating MM cells into and out of the BM microenvironment.^{3,4}

Homing into the BM is physiologically governed by a diverse array of molecules such as Stromal cell-derived factor 1 α (SDF1 α), E-selectin, and various integrin co-receptors including Mucosal vascular addressin cell adhesion molecule 1 (MAD-CAM1).⁵ In the context of MM, SDF1 α plays a major role in migration, adhesion, homing, and possibly retention of MM cells in the BM.⁶⁻⁹ Mediators of SDF1 α activ-



Haematologica 2018
Volume 105(2):457-467

Correspondence:

MICHAEL O'DWYER
michael.odwyer@nuigalway.ie

Received: November 15, 2018.

Accepted: May 16, 2019.

Pre-published: May 17, 2019.

doi:10.3324/haematol.2018.212266

Check the online version for the most updated information on this article, online supplements, and information on authorship & disclosures: www.haematologica.org/content/105/2/457

©2020 Ferrata Storti Foundation

Material published in Haematologica is covered by copyright. All rights are reserved to the Ferrata Storti Foundation. Use of published material is allowed under the following terms and conditions:

<https://creativecommons.org/licenses/by-nc/4.0/legalcode>.

Copies of published material are allowed for personal or internal use. Sharing published material for non-commercial purposes is subject to the following conditions:

<https://creativecommons.org/licenses/by-nc/4.0/legalcode>, sect. 3. Reproducing and sharing published material for commercial purposes is not allowed without permission in writing from the publisher.



ity in MM include matrix metalloproteinase and integrin $\alpha 4\beta 1$ -dependent adhesion on fibronectin and Vascular cell adhesion molecule 1 (VCAM1).¹⁰⁻¹² Recently, E-selectin has also been shown to play a role in homing and retention of MM cells in the BM.^{13,14} In particular, we have shown that sialofucosylated structures recognized by E-selectin, such as Sialyl Lewis^x (SLe^x), enable MM cells to escape the cytotoxic effects of bortezomib *in vivo* most likely by hiding in the BM.¹⁴ Indeed, MM cells enriched for E-selectin ligands recognized by the monoclonal antibody Heca452, were resistant to bortezomib treatment *in vivo* and this resistance was reversed by a small glycomimetic molecule GMI-1271, which inhibits the interaction between E-selectin and E-selectin ligands.¹⁴ Thus, SDF1 α and E-selectin may act co-operatively to allow extravasation of MM cells into the BM niche where they can proliferate and evade drug treatments.

Post-translational glycosylation of proteins and lipids plays many physiological and pathophysiological roles. There is a growing appreciation that aberrant glycosylation is considered a hallmark of cancer,^{15,16} with one of the most prominent changes being a role for hypersialylation as a driver of tumor progression, metastasis and invasion.^{17,18} Hypersialylation is largely the result of overexpression of sialyltransferases (STs), which catalyze the attachment of sialic acids *via* different glycosidic linkages ($\alpha 2-3$, $\alpha 2-6$, or $\alpha 2-8$) to the underlying glycan chain.^{17,19} We have previously established an important role for aberrant sialylation in homing and survival in MM.²⁰ Specifically, high expression of the ST3 β -galactoside $\alpha 2-3$ -sialyltransferase 6 (ST3GAL6) in MM cell lines and patient samples is associated with inferior outcomes. Knocking down ST3GAL6 reduces sialic acid expression on MM cells, decreasing their ability to home to the BM. Since ST3GAL6 participates in the generation of SLe^x structures, which forms the minimal E-selectin ligand, and may also be involved in sialylation of other structures important in MM homing and adhesion,²¹⁻²³ we sought to investigate if we could therapeutically target sialylation on MM cells, and whether this would affect BM homing and survival in mice.

Here we show that pre-treatment of MM cells enriched for E-selectin ligands with 3F_{ax}-Neu5Ac, a global inhibitor of the ST family,²⁴ significantly reduces cell surface sialylation of these cells, prolongs survival in xenograft mice and enhances their *in vivo* sensitivity to bortezomib. *In vitro*, 3F_{ax}-Neu5Ac impairs the interaction between MM cells and E-selectin under shear stress and, surprisingly, also greatly reduces their interaction with VCAM1 and MAD-CAM1 under similar conditions. In this respect, we show that 3F_{ax}-Neu5Ac alters the post-translational modification of integrin $\alpha 4$ on MM cells. This implies a dual effect on homing, whereby blockade of selectin ligands and integrin-mediated interactions with BM endothelial cells prevents extravasation of MM cells in the BM. Our results suggest great potential for improved patient outcomes by targeting sialylation on MM cells, especially when used in combination with other active MM agents.

Methods

Selection of E-selectin ligand-enriched cells

The E-selectin ligand-enriched MM1S cell line (MM1S^{Heca452}) was generated from GFP⁺/Luc⁺ MM1S and

parental MM1S cell lines by two rounds of fluorescently-activated cell sorting (FACS) using the fluorescent Heca452 antibody (Biolegend; San Diego, CA, USA). Cells were maintained in RPMI-1640 (VWR; Radnor, PA, USA) containing L-glutamine, 10% heat inactivated fetal bovine serum (HI-FBS, VWR), and 1X antibiotic-antimycotic (Corning; Kennebunk, ME, USA).

Animal experiments

All experimental studies and procedures involving mice were performed in accordance with protocols approved by the governing Institutional Animal Care and Use Committee (IACUC) and all state and federal laws. In the toxicity study, 8-week old male and female C57BL/6J mice (n=8) received 0, 6.25, 12.5 or 25 mg/kg body weight doses of 3F_{ax}-Neu5Ac (EMD Millipore; Burlington, USA) delivered intraperitoneally (i.p.) once daily for seven days. The drug was dissolved in dimethyl sulfoxide (DMSO) (VWR) and subsequently diluted 2-fold in PEG-300 (Sigma Aldrich; St. Louis, MO, USA). Mice were monitored daily for signs of discomfort, especially at the site of injection. In the homing study, 6-week old female Fox Chase SCID-Beige mice (Charles River Laboratory; Wilmington, MA, USA) (n=9 or 10) were inoculated *via* tail vein injections with 5x10⁶ Heca452-enriched GFP⁺/Luc⁺ MM1S cells, which had been pre-treated with either vehicle or 300 μ M 3F_{ax}-Neu5Ac for seven days in culture before inoculation. Starting one day post inoculation, mice received either vehicle (PBS) or bortezomib (Selleck; Houston, TX, USA) injections intraperitoneally twice weekly. To monitor toxicity, mice were weighed twice weekly. Mice were frequently monitored for clinical signs of treatment-related side effects. Survival end points were mouse death or euthanasia as required by the IACUC (a single observation of >30% body weight loss, 3 consecutive measurements of >25% body weight loss, or impaired hind limb use). Survival differences were analyzed by the Kaplan-Meier method.

Bioluminescent imaging

Starting on day 7, and biweekly until day 30, tumor burden was assessed with bioluminescence imaging (BLI) in an IVIS[®] Lumina LT (Perkin Elmer Inc.; Waltham, MA, USA) equipped with a CCD camera (cooled at -90°C), mounted on a light-tight specimen chamber. Mice were injected with 150 mg/kg i.p. filter-sterilized D-luciferin substrate (VivoGlo, Promega; Madison, WI, USA) and imaged after 10 minutes. Data were acquired and analyzed using LivingImage software 4.5.1. (PerkinElmer). BLI flux equaling the radiance (photons/s) in each pixel integrated over the region of interest (ROI) area (cm²), where the ROI was the whole mouse, was used to quantify tumor burden. BLI and mouse weight data were graphed and analyzed only for days in which all mice remained in the study to avoid artifacts due to mouse death.

Statistical analysis

All data are expressed as mean \pm standard error of the mean (SEM), unless otherwise noted. Student's *t*-test, ordinary one-way or two-way ANOVA tests were used to determine significance, using $P < 0.05$ as the cut-off, with Tukey's multiple comparison *post-hoc* testing unless otherwise noted. **** $P < 0.0001$; *** $P < 0.001$; ** $P < 0.01$; * $P < 0.05$. GraphPad Prism 6.02 software (La Jolla, CA, USA) was used to compute all statistical calculations unless otherwise noted.

Additional information concerning materials and methods can be found in the *Online Supplementary Appendix*.

Results

Treatment of mice with 3F_{ax}-Neu5Ac causes a dose dependent decrease in sialoside expression on multiple organs systemically

Building upon the previous 3F_{ax}-Neu5Ac *in vivo* experience,^{25,26} we first studied the effects of global desialylation *in vivo* after systemic administration of 3F_{ax}-Neu5Ac. Mice were treated with 6.25, 12.5, and 25 mg/kg of 3F_{ax}-Neu5Ac daily for seven consecutive days. Sialylation was monitored using two different lectins after seven days of treatment: the *Sambucus nigra* lectin (SNA), which binds α 2-6 linked sialic acids, and the *Peanut agglutinin* lectin (PNA), which binds to desialylated T antigen. In mice treated with 25 mg/kg 3F_{ax}-Neu5Ac, there was a clear decrease in SNA staining in the kidney, spleen and liver (*Online Supplementary Figure S1A-C*), consistent with a reduction in α 2-6 linked sialic acid expression. Moreover, at the same dose, there was a contemporary increase in PNA staining (*Online Supplementary Figure S2A-C*) consistent with decreased sialic acid expression leading to exposure of terminal galactose residues, such as the T antigen (Gal β 1-3GalNAc α Ser/Thr). To determine the effects of 3F_{ax}-Neu5Ac treatment on sialylation of cells of the immune system, peripheral blood B cells were used as representative immune cells. The median fluorescent intensity (MFI) values for SNA and PNA positive staining were determined on the seventh day of treatment and the seventh day after the final treatment. Similar to what was observed in histology sections, 3F_{ax}-Neu5Ac treatment induced a decrease in the SNA MFI with the highest dose (25 mg/kg) having a significant fold change compared to the control at the seventh day of dosing (Figure 1A). As expected, the PNA lectin MFI significantly increased with 3F_{ax}-Neu5Ac treatment by the final day of treatment as well (Figure 1C). Sialic acid expression remained low after seven days of recovery after the 25 mg/kg dose, as particularly evident in cells stained with PNA, although a trend was also observed in the SNA-stained cells (Figure 1B and D), suggesting that recovery takes longer than seven days. Because sialylation is crucial to kidney filtration, we also determined the effects of the dose regimen in the kidneys. H&E staining showed no obvious histological changes in the kidney after seven days of recovery (Figure 1E). However, mice that received the highest dose, 25 mg/kg, did experience edema in the peritoneal cavity, as previously reported.²⁷ These data demonstrate that 3F_{ax}-Neu5Ac can successfully inhibit the expression of sialic acid systemically, but that local BM- or myeloma-specific delivery may be necessary to overcome effects on other organs in future studies.

Treatment of MM1S^{Heca452} with 3F_{ax}-Neu5Ac decreases sialylation *in vitro*

We next examined whether 3F_{ax}-Neu5Ac could significantly reduce the expression of sialic acid on MM1S^{Heca452} cells. These cells are enriched for E-selectin ligand expression compared to the MM1S parental line and *in vivo* generate a very aggressive disease which displays resistance to bortezomib.¹⁴ The MM1S^{Heca452} cell line has been extensively characterized; their sensitivity to bortezomib,

clonogenic potential, and proliferation *in vitro* are identical to the parental line and their aggressive phenotype becomes evident only *in vivo*.¹⁴ Sialylation was monitored using the Heca452 and CD15s antibodies, which recognize the sialofucosylated structure SLe^{ax}, the Maackia Amurensis Lectin II (MAL II), which preferentially binds to α 2-3 linked sialic acid, and SNA. Over a seven day span in culture, 300 μ M of 3F_{ax}-Neu5Ac significantly decreased the Heca452 staining in a time-dependent manner (*Online Supplementary Figure S3*). After seven days of treatment, 3F_{ax}-Neu5Ac decreased the MFI and the total number of the Heca452, CD15s, MALII and SNA positive cells (Figure 2). Importantly, 3F_{ax}-Neu5Ac treatment did not induce a significant change in the sensitivity to bortezomib *in vitro* (Figure 4). Based on these data, we chose to pre-treat the MM1S^{Heca452} cells with 300 μ M of 3F_{ax}-Neu5Ac for seven days to significantly reduce sialylation on the cell surface.

In vivo, pre-treatment of MM1S^{Heca452} cells with 3F_{ax}-Neu5Ac reduces tumor burden and increases survival, and co-treatment with bortezomib further enhances these outcomes

To study the impact of global sialylation inhibition specifically on MM cells and to avoid kidney toxicity related to 3F_{ax}-Neu5Ac treatment, we pre-treated the MM1S^{Heca452} cells with 300 μ M of 3F_{ax}-Neu5Ac or vehicle for seven days, inoculated these cells into immunocompromised mice, and followed tumor burden using bioluminescence imaging. Mice inoculated with 3F_{ax}-Neu5Ac-pre-treated MM1S^{Heca452} (3F_{ax}-Neu5Ac MM1S^{Heca452} mice) showed reduced tumor burden compared to mice inoculated with vehicle-pre-treated MM1S^{Heca452} (vehicle MM1S^{Heca452} mice) (Figure 3A and B). Two cohorts in this study in addition received bortezomib treatment, which decreased the tumor burden in the vehicle and 3F_{ax}-Neu5Ac MM1S^{Heca452} mice (Figure 3A and B). The 3F_{ax}-Neu5Ac MM1S^{Heca452} mice that received bortezomib treatment had the least tumor burden throughout the study compared to the other groups (Figure 3B). Importantly, even in the absence of bortezomib, pre-treatment of MM1S^{Heca452} cells with 3F_{ax}-Neu5Ac reduced tumor burden compared to vehicle MM1S^{Heca452} mice, suggesting that 3F_{ax}-Neu5Ac pre-treatment is beneficial even without the addition of chemotherapy. We also observed that the 3F_{ax}-Neu5Ac MM1S^{Heca452} mice survived significantly longer than the vehicle MM1S^{Heca452} mice (Figure 3C). Notably, bortezomib treatment did not prolong survival of the vehicle MM1S^{Heca452} mice, confirming our previous observation that in this *in vivo* model, these MM cells are more refractory to bortezomib treatment (Figure 3C).¹⁴ Above all, pre-treatment of MM1S^{Heca452} cells with 3F_{ax}-Neu5Ac in combination with bortezomib led to longer survival compared to the other groups, suggesting a synergistic therapeutic effect. No significant difference was observed in change in body weight between the treatment groups (Figure 3D). Overall, we demonstrate that 3F_{ax}-Neu5Ac reduces tumor burden and increases survival, and that additional treatment with bortezomib has a synergistic effect with 3F_{ax}-Neu5Ac.

3F_{ax}-Neu5Ac treatment partially reverts stroma but not endothelial-induced bortezomib resistance *in vitro*

To gain insight into the mechanism(s) of increased bortezomib sensitivity in response to 3F_{ax}-Neu5Ac treat-

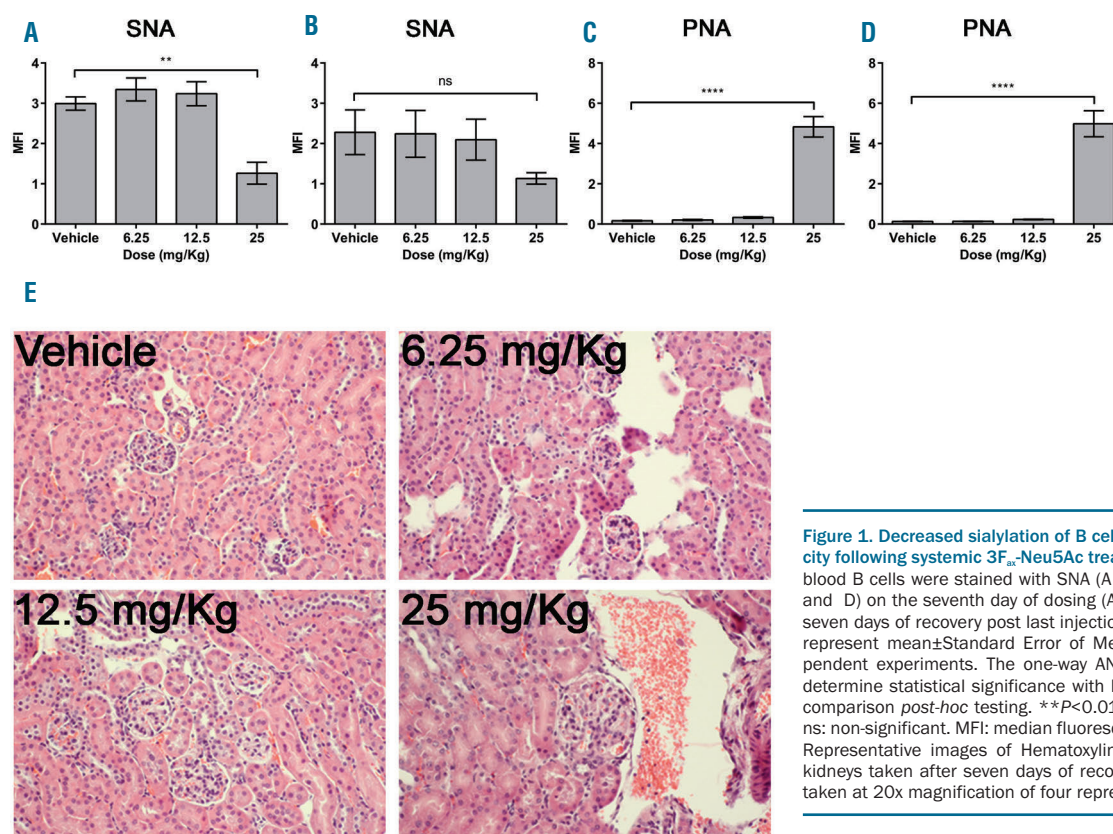


Figure 1. Decreased sialylation of B cells and kidney toxicity following systemic 3F_{ax}-Neu5Ac treatment. Peripheral blood B cells were stained with SNA (A and B) or PNA (C and D) on the seventh day of dosing (A and C) and after seven days of recovery post last injection (B and D). Bars represent mean±Standard Error of Mean of three independent experiments. The one-way ANOVA was used to determine statistical significance with Dunnett's multiple comparison *post-hoc* testing. ***P*<0.01; *****P*<0.0001; ns: non-significant. MFI: median fluorescence intensity. (E) Representative images of Hematoxylin & Eosin stained kidneys taken after seven days of recovery. Images were taken at 20x magnification of four representative mice.

ment, we sought to investigate *in vitro* the effects of 3F_{ax}-Neu5Ac pre-treatment on the sensitivity to bortezomib in MM1S^{Heca452} cells in co-culture conditions that partially recapitulate the BM environment. To this end, we used the well-established HS5 stromal cell line,²⁸ primary BM stromal cells (BMSC) derived from MM patients, and the BM endothelial cell line BMEC-60. The latter was also treated with 10 ng/mL TNF α for four hours before co-culture to induce activation. BMEC-60, BMSC and, to an even greater extent, HS5 induced resistance to bortezomib (5 nM) in MM1S^{Heca452} cells (Figure 4A-C). 3F_{ax}-Neu5Ac pre-treatment caused only minor, although significant re-sensitization to bortezomib in the presence of HS5 and BMSC (Figure 4A and B) and did not reverse BMEC-60-induced bortezomib resistance (Figure 4C). Importantly, in the absence of BM-derived cells, the 3F_{ax}-Neu5Ac pre-treatment had only a minor effect on the MM1S^{Heca452} response to bortezomib. Together these data indicate that, in MM cells, bortezomib resistance that is BM stromal cell-driven, although maybe not endothelial cell-driven, can be partially reversed by inhibition of sialylation.

3F_{ax}-Neu5Ac treatment does not affect migration in response to SDF1 α

Since 3F_{ax}-Neu5Ac did not completely reverse bortezomib resistance induced by BM cell lines and patient-derived-BMSC *in vitro*, we reasoned that the mechanism(s) of bortezomib re-sensitization *in vivo* induced by 3F_{ax}-Neu5Ac may also involve a defect in the ability of the MM1S^{Heca452} cells to home into the protective BM microenvironment. To explore this possibility, we first examined the effects of 3F_{ax}-Neu5Ac pre-treatment on migration in

response to SDF1 α in a transwell assay. DMSO and 3F_{ax}-Neu5Ac pre-treated MM1S^{Heca452} cells showed enhanced migration in response to SDF1 α (Figure 5A). However, spontaneous as well as SDF1 α -induced migration were similarly inhibited by 3F_{ax}-Neu5Ac pre-treatment (Figure 5A). Indeed, when we specifically examined migration in response to SDF1 α by subtracting spontaneous migration (no SDF1 α) to SDF1 α -containing samples, we observed that 3F_{ax}-Neu5Ac pre-treatment did not affect SDF1 α -driven migration (Figure 5B). These data suggest that 3F_{ax}-Neu5Ac pre-treatment has an impact on the motility of the cells but not specifically on SDF1 α -induced migration.

3F_{ax}-Neu5Ac treatment impairs adhesion and rolling of MM1S^{Heca452} cells on E-selectin, MADCAM1 and VCAM1

We next examined whether 3F_{ax}-Neu5Ac could influence adhesion and rolling on selectins and integrin co-receptors important in BM homing.³⁻⁵ To this end, we performed adhesion and rolling assays under shear stress on E-selectin, MADCAM1 and VCAM1-coated substrates. MM1S^{Heca452} cells showed robust interactions with E-selectin which could be subcategorized into firm adhesion and rolling (Figure 6A-C). 3F_{ax}-Neu5Ac pre-treatment dramatically impaired this interaction by decreasing the number of adherent cells (Figure 6A and C). The number of rolling cells was not affected (Figure 6B). However, when we looked at the rolling velocity, we observed an increase in the velocity of the MM1S^{Heca452} cells pre-treated with 3F_{ax}-Neu5Ac versus DMSO controls, indicating a decrease in the affinity of the E-selectin ligands for E-selectin (Online Supplementary Figure S4A-C). These data

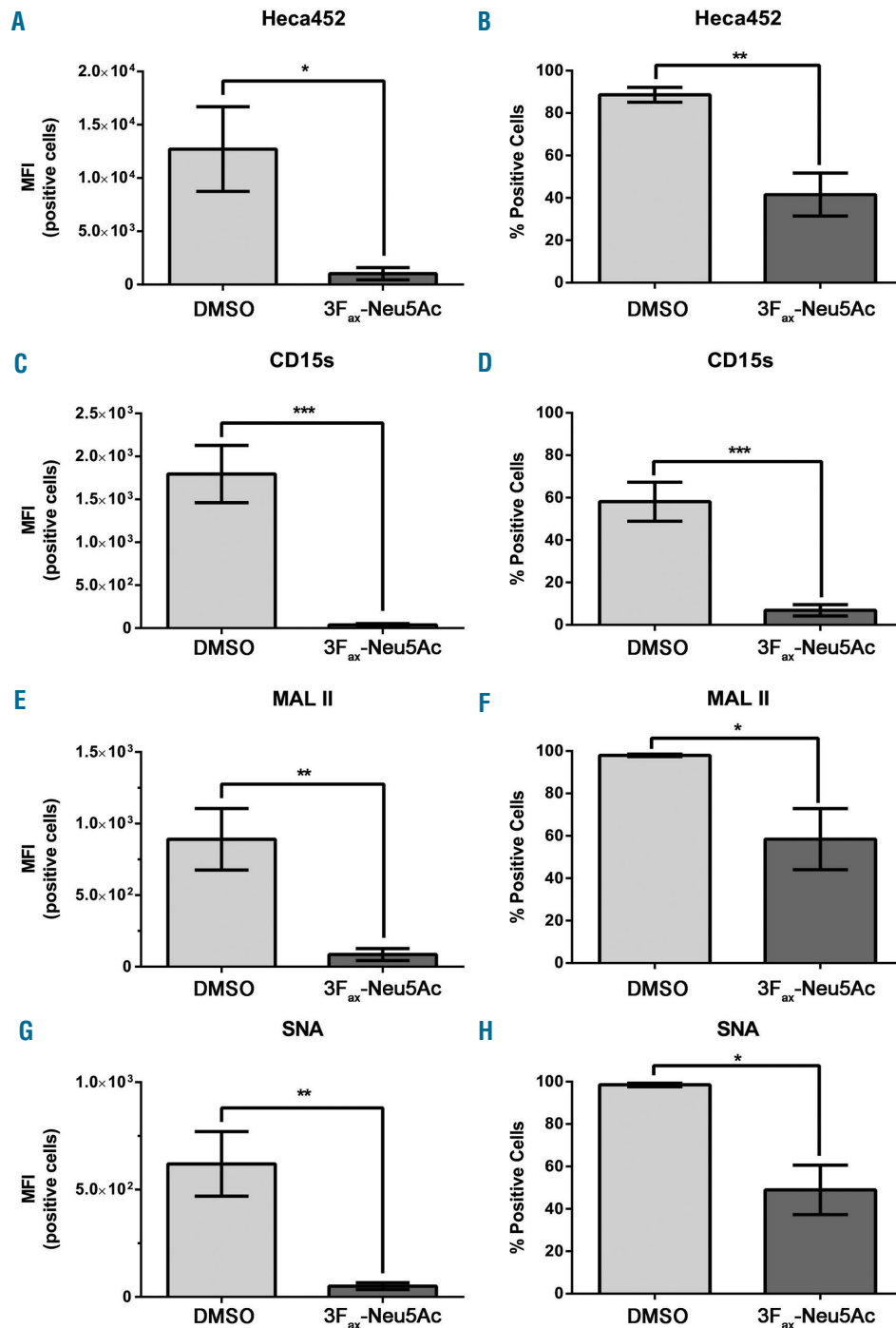


Figure 2. 3F_{ax}-Neu5Ac treatment decreases sialylation in the MM1S^{Heca452} cell line. MM1S^{Heca452} cells were treated with 300 μM 3F_{ax}-Neu5Ac or dimethyl sulfoxide (DMSO) (vehicle control) for seven days. After treatment, cells were collected and stained with the Heca452 (A and B), CD15s (C and D), MALII (F and G), or SNA (G and H) antibodies or lectins. Bars represent mean ± Standard Error of Mean of three independent experiments. Unpaired Student's *t*-test was used to determine statistical significance. **P*<0.05; ***P*<0.01; ****P*<0.001. MFI: median fluorescence intensity.

are consistent with a requirement of sialic acid for E-selectin binding. The MM1S^{Heca452} also showed robust adhesion and rolling on MADCAM1 under shear stress (Figure 6D-F). 3F_{ax}-Neu5Ac pre-treatment induced a decrease in the total number of cells interacting with MADCAM1 and, in particular, decreased the number of adherent cells while increasing the number of rolling cells, suggesting a decrease in the affinity of integrin α4β7 for MADCAM1. Again, the velocity of the rolling cells was increased by 3F_{ax}-Neu5Ac, indicating a weaker attachment (Online Supplementary Figure S4D-F). Finally, the 3F_{ax}-Neu5Ac pre-treatment induced a reduction in the number of MM1S^{Heca452} cells interacting with VCAM1,

which was exclusively adhesion (Figure 6G). Indeed, rolling on VCAM1 was not observed indicating strong interactions between integrin α4β1 and VCAM1. Altogether, these data indicate that desialylation of the MM1S^{Heca452} cells impairs interaction (a summation of adhesion and rolling) with E-selectin, MADCAM1 and VCAM1.

3F_{ax}-Neu5Ac treatment alters the post-translational modifications on integrin α4

Next, we examined whether 3F_{ax}-Neu5Ac treatment decreased protein expression of integrins α4β7 or α4β1, which bind VCAM1 and MADCAM1 respectively, on

MM1S^{Heca452} cells.²⁹⁻³¹ Flow cytometry analysis revealed that 3F_{ax}-Neu5Ac did not decrease α4, β1 or β7 expression (*Online Supplementary Figure S5D-F*). We then investigated whether 3F_{ax}-Neu5Ac affected post-translational modifications on these integrins, which in turn would result in an altered mobility on SDS-PAGE. Indeed, Western blot analysis of integrin α4 revealed a marked shift of the mature as well as the C-terminal cleavage form in response to 3F_{ax}-Neu5Ac, suggesting an alteration of α4 post-translational modifications probably due to its desialylation (Figure 7A). To our knowledge, this is the first evidence that integrin α4 is post-translationally sialylated. The integrins β1 and β7 were not heavily affected by

3F_{ax}-Neu5Ac pre-treatment (Figure 7B and C). Similar results were obtained in the parental MM1S cell line (*Online Supplementary Figure S6A-C*). Altogether, these data indicate that 3F_{ax}-Neu5Ac primarily alters integrin α4 post-translationally, which most likely results in the observed weaker interaction of the MM cells with MAD-CAM1 and VCAM1.

Discussion

In this study, we examined whether global inhibition of sialylation could increase bortezomib sensitivity in an

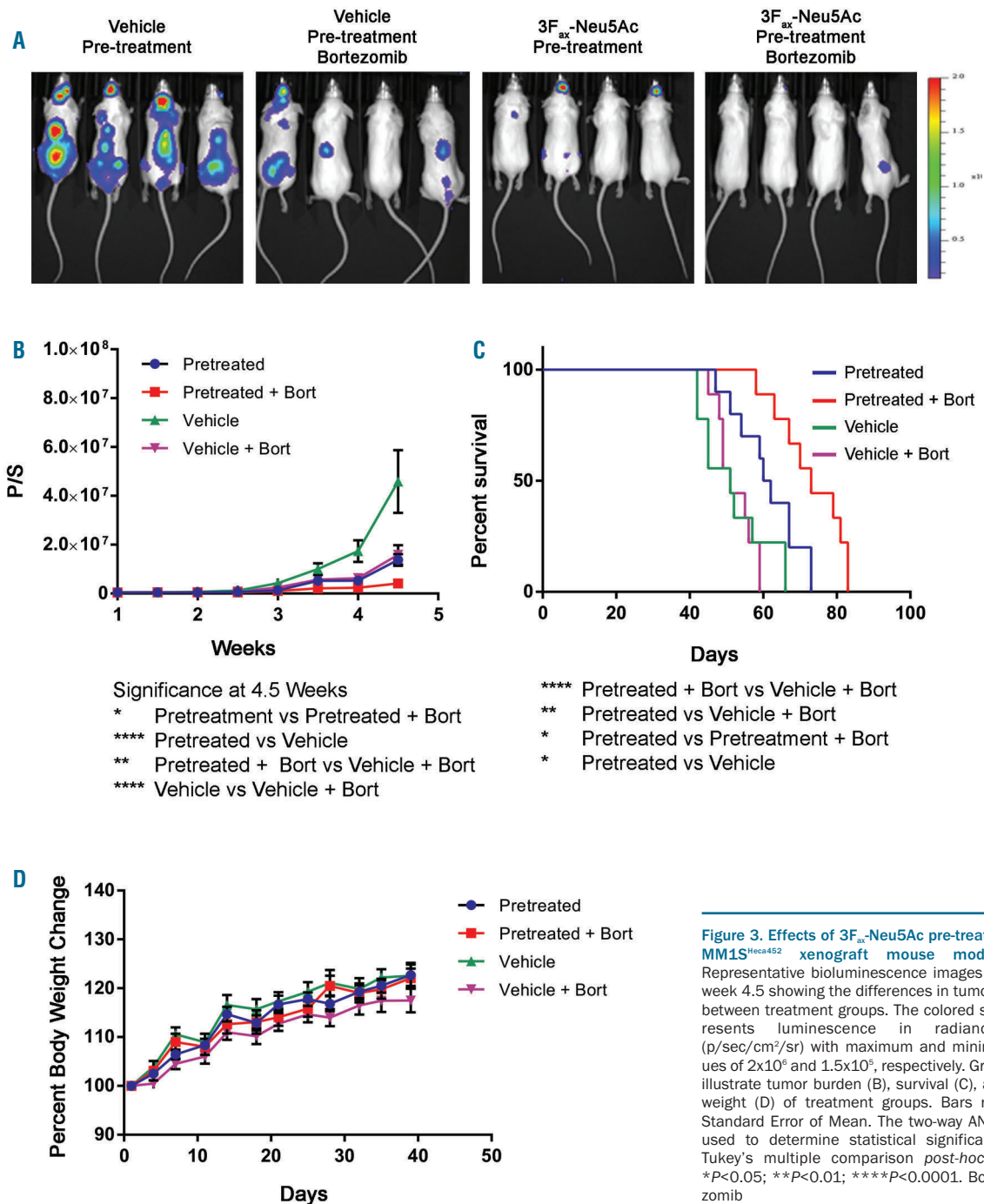


Figure 3. Effects of 3F_{ax}-Neu5Ac pre-treatment on MM1S^{Heca452} xenograft mouse models. (A) Representative bioluminescence images taken at week 4.5 showing the differences in tumor burden between treatment groups. The colored scale represents luminescence in radiance unit (p/sec/cm²/sr) with maximum and minimum values of 2x10⁶ and 1.5x10⁵, respectively. Graph lines illustrate tumor burden (B), survival (C), and body weight (D) of treatment groups. Bars represent Standard Error of Mean. The two-way ANOVA was used to determine statistical significance with Tukey's multiple comparison *post-hoc* testing. *P<0.05; **P<0.01; ****P<0.0001. Bort: bortezomib

aggressive MM mouse model, which employs xenotransplantation of MM cells that have been enriched for E-selectin ligands.¹⁴ To this end, we used the pan-sialyltransferase inhibitor 3F_{ax}-Neu5Ac, which had been previously shown to efficiently block sialylation in leukemic cells.²⁴

In a preliminary dose-finding *in vivo* study, we observed that 3F_{ax}-Neu5Ac decreased sialylation in various tissues, including cells of the immune system. At its effective

dose, 25 mg/kg, 3F_{ax}-Neu5Ac induced edema in the peritoneal cavity of mice suggesting that desialylation of the glomerulus could lead to dose-limiting toxicity, as previously reported.²⁷ To overcome 3F_{ax}-Neu5Ac-induced kidney toxicity and to examine the role of sialylation specifically in MM, we treated the E-selectin enriched MM1S cell line, MM1S^{Heca452}, with 3F_{ax}-Neu5Ac before inoculation, an approach that has been successfully used to uncover a crit-

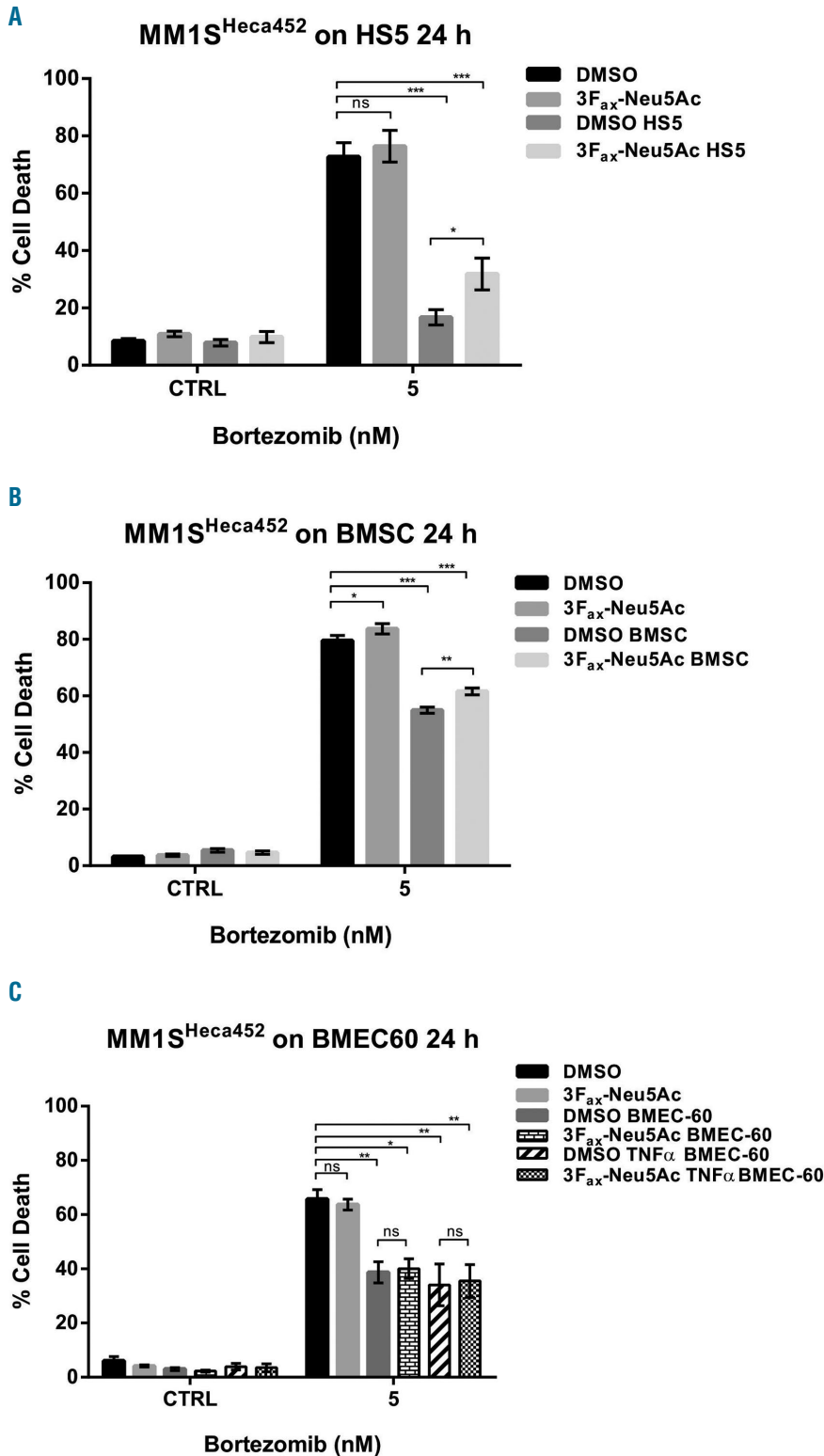
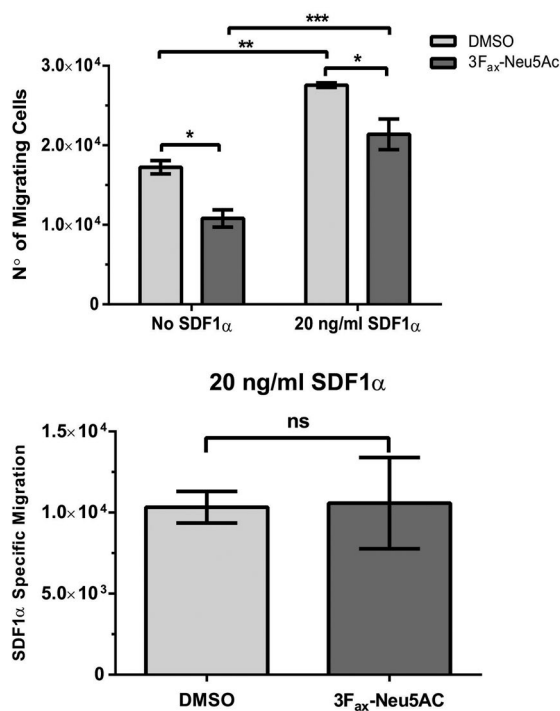


Figure 4. 3F_{ax}-Neu5Ac treatment has a minimal impact on stroma-mediated bortezomib resistance in MM1S^{Heca452} cell line. MM1S^{Heca452} cells were treated with 300 μ M 3F_{ax}-Neu5Ac or dimethyl sulfoxide (DMSO) [vehicle control (CTRL)] for seven days. After treatment, cells were seeded onto 80% confluent layer of HS5 expressing GFP (A), patient-derived bone marrow stromal cells (BMSC) (B) and BMEC-60 stained with Tag-it Violet™ (C) or plastic. BMEC-60 were also stimulated with 10 ng/mL TNF α for 4 hours (h) to induce activation. Cells were co-cultured for 24 h and then treated with 5 nM bortezomib for a further 24 h. After incubation, cells were collected and cell death was examined by Annexin V-APC and PI staining. One-way ANOVA was used to determine statistical significance with Dunnett's multiple comparison *post-hoc* testing. * P <0.05; ** P <0.01; *** P <0.001; ns: non-significant.



ical role of sialylation in melanoma metastasis and growth *in vivo*.³²

The vehicle-pre-treated MM1S^{Heca452} cells showed an initial response to bortezomib *in vivo*. Indeed, bortezomib was able to reduce tumor burden, however, despite this initial response, bortezomib alone was not able to improve survival. These data would suggest that the surviving MM1S^{Heca452} cells were so aggressive that they still induced death in mice at a similar rate to the non-bortezomib-treated mice. 3F_{ax}-Neu5Ac pre-treatment of MM1S^{Heca452} cells effectively blocked α 2-3 and α 2-6 sialylation as well as expression of SLe^{a/x}. More importantly, pre-treatment of MM1S^{Heca452} cells with 3F_{ax}-Neu5Ac blunted

Figure 5. 3F_{ax}-Neu5Ac treatment reduces motility of MM1S^{Heca452} independently of SDF1 α . MM1S^{Heca452} cells were treated with 300 μ M 3F_{ax}-Neu5Ac or dimethyl sulfoxide (DMSO) (vehicle control) for seven days. After treatment, cells were starved for 1 hour (h) and then seeded on the upper chamber of transwells. Lower chamber was filled with either serum-free media (No SDF1 α) or serum-free media supplemented with SDF1 α (20 ng/mL). Cells were allowed to migrate for 4 h at 37 °C. After incubation, cells in the lower chambers were collected and counted using a BD Accuri flow cytometer. Data are presented as (A) raw data or (B) as the difference between migrating cells in SDF1 α -containing media and control media. Bars represent mean \pm Standard Error of Mean of three independent experiments. One-way ANOVA test was used to determine statistical significance with Sidak's multiple comparison *post-hoc* testing. **P*<0.05; ***P*<0.01; ****P*<0.001; ns: non-significant.

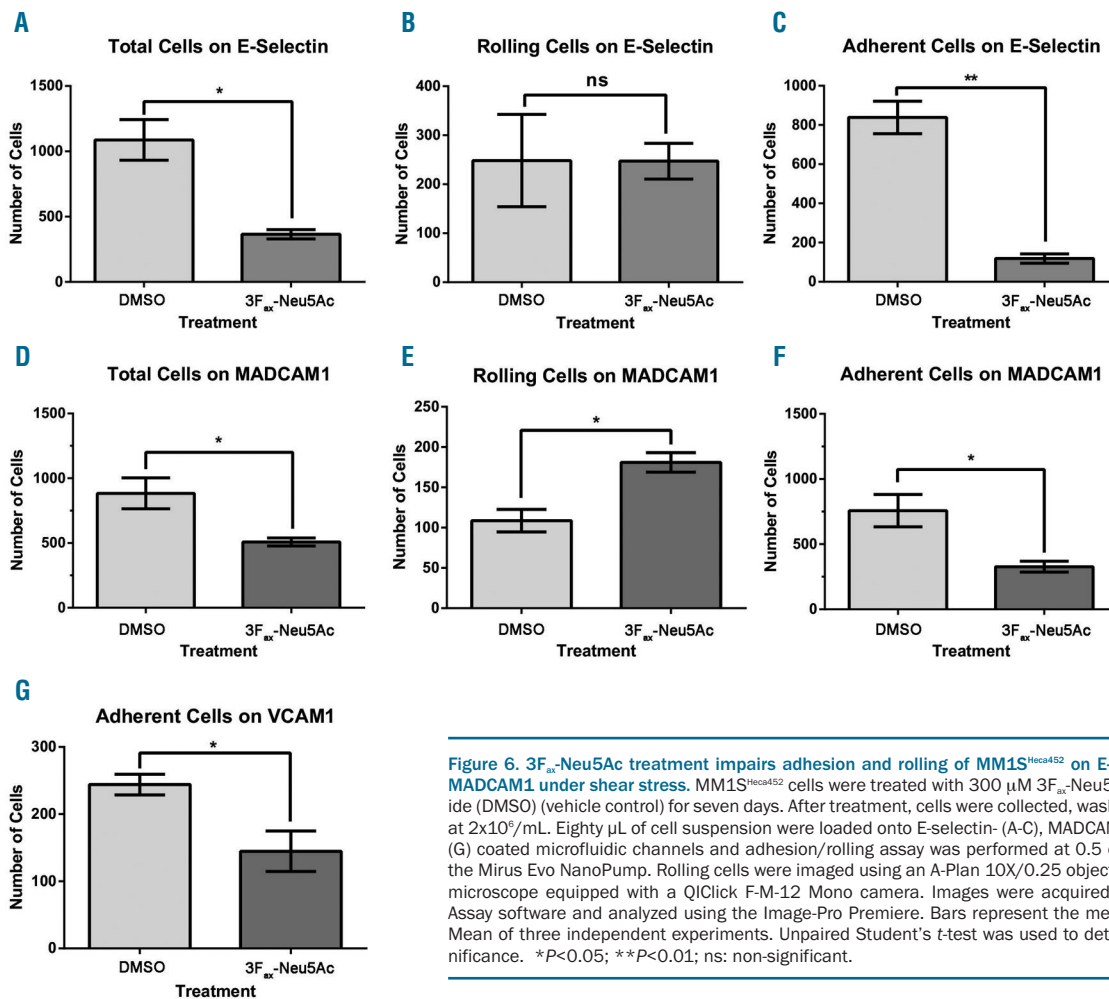


Figure 6. 3F_{ax}-Neu5Ac treatment impairs adhesion and rolling of MM1S^{Heca452} on E-selectin, VCAM1 and MADCAM1 under shear stress. MM1S^{Heca452} cells were treated with 300 μ M 3F_{ax}-Neu5Ac or dimethyl sulfoxide (DMSO) (vehicle control) for seven days. After treatment, cells were collected, washed and resuspended at 2 × 10⁶ /mL. Eighty μ L of cell suspension were loaded onto E-selectin- (A-C), MADCAM1- (D-F) and VCAM1- (G) coated microfluidic channels and adhesion/rolling assay was performed at 0.5 dyne/cm² at RT using the Mirus Evo NanoPump. Rolling cells were imaged using an A-Plan 10X/0.25 objective of an A10 Vert.A1 microscope equipped with a QIClick F-M-12 Mono camera. Images were acquired using the Vena Flux Assay software and analyzed using the Image-Pro Premiere. Bars represent the mean \pm Standard Error of Mean of three independent experiments. Unpaired Student's *t*-test was used to determine statistical significance. **P*<0.05; ***P*<0.01; ns: non-significant.

the aggressive nature of these cells. Indeed, 3F_{ax}-Neu5Ac treatment reduced tumor burden, increased bortezomib sensitivity and, most importantly, improved survival, suggesting that sialylation contributes to the aggressive phenotype of the MM1S^{Heca452} cells and inhibiting it could represent a valuable treatment in MM. Currently, systemic administration of 3F_{ax}-Neu5Ac is not feasible due to irreversible nephrotoxicity. While it is possible that a different dose and schedule could reveal a therapeutic window, clearly the potential for off-target toxicity is a major obstacle to clinical development. This is particularly relevant in MM where the kidney is one of the organs whose function is greatly impaired by the disease. However, alternative approaches could be explored to address this issue, including the development of more selective sialyltransferase inhibitors or the use of a targeted delivery system, which would release 3F_{ax}-Neu5Ac selectively into the BM microenvironment or the MM cells. Indeed, Bull *et al.* have previously reported that targeted delivery of antibody-labeled nanoparticles containing 3F_{ax}-Neu5Ac into melanoma cells facilitates long-term sialic acid blockade and, importantly, reduces lung metastasis *in vivo*.³³ A similar strategy could be employed using antibodies specific to MM antigens (such as CD38 and BCMA) or by incorporating bisphosphonates into the nanoparticles to target the BM.³⁴ Achievement of sufficiently high local BM concentrations of 3F_{ax}-Neu5Ac should result in sialylation inhibition on MM cells, without off target toxicity. Inhibiting sialylation using these approaches could also target the tumor microenvironment including the immune environment. For instance, it has been recently reported that sialic acid blockade *via* intratumoral injection of 3F_{ax}-Neu5Ac could suppress tumor growth by enhancing T-cell-mediated tumor immunity.³⁵ In addition to a reduction in sialic acid expression by tumor cells, sialyltransferase inhibition converted the immune suppressive tumor microenvironment to an immune promoting one with significantly higher numbers of activated effector immune cells, including CD8⁺ T cells and natural killer (NK) cells, along with a reduction in regulatory T cells (Tregs).³⁵ Sialyltransferase inhibition also

led to anti-tumor effects, which were mediated by CD8⁺ effector cells as well as potential activation of stimulated dendritic cells (DC).³⁵

A number of different mechanisms could account for the 3F_{ax}-Neu5Ac-mediated increased-sensitization of the MM1S^{Heca452} cells to bortezomib *in vivo*. First, we explored the possibility that 3F_{ax}-Neu5Ac could directly inhibit BM-mediated bortezomib resistance *in vitro*. HS5, patient-derived BMSC and the BM endothelial cell line BMEC-60 showed significant inhibition of bortezomib-induced cell death in MM1S^{Heca452}. However, we observed that 3F_{ax}-Neu5Ac induced only a partial re-sensitization to bortezomib on HS5 and patient-derived BMSC, suggesting that desialylation plays a minor role in blocking BM-mediated drug resistance. The BM microenvironment can induce drug resistance through cell adhesion-mediated drug resistance (CAM-DR) and soluble factors.^{1,36-39} It is possible that in our *in vitro* model system, inhibition of sialylation is not enough to inactivate all the pathways responsible for the BM-mediated bortezomib resistance.^{1,39,40} Therefore, it is conceivable that the increased-sensitization to bortezomib observed *in vivo* may be predominantly due to mechanisms other than blockade of BM-mediated drug resistance. Nonetheless, an important future direction will be to test 3F_{ax}-Neu5Ac in *in vitro* models that more faithfully reproduce the tumor microenvironment to better understand the effects of 3F_{ax}-Neu5Ac on the microenvironment-mediated drug resistance.

Previously, we showed that in the same model system, the small molecule glycomimetic GMI-1271, which inhibits interactions between E-selectin and E-selectin ligands, could increase the number of MM cell in circulation, where they are more susceptible to bortezomib.¹⁴ In a similar way, we hypothesized that inhibition of sialylation by 3F_{ax}-Neu5Ac could also inhibit homing and retention of MM cells in the BM. To this end, we examined the interaction of vehicle or 3F_{ax}-Neu5A-treated MM1S^{Heca452} with E-selectin under shear stress. We found that 3F_{ax}-Neu5Ac treatment, by reducing SLe^{a/x}, effectively inhibited the interaction between the MM1S^{Heca452} cells and E-selectin, confirming previous observations.²⁴ However, we re-

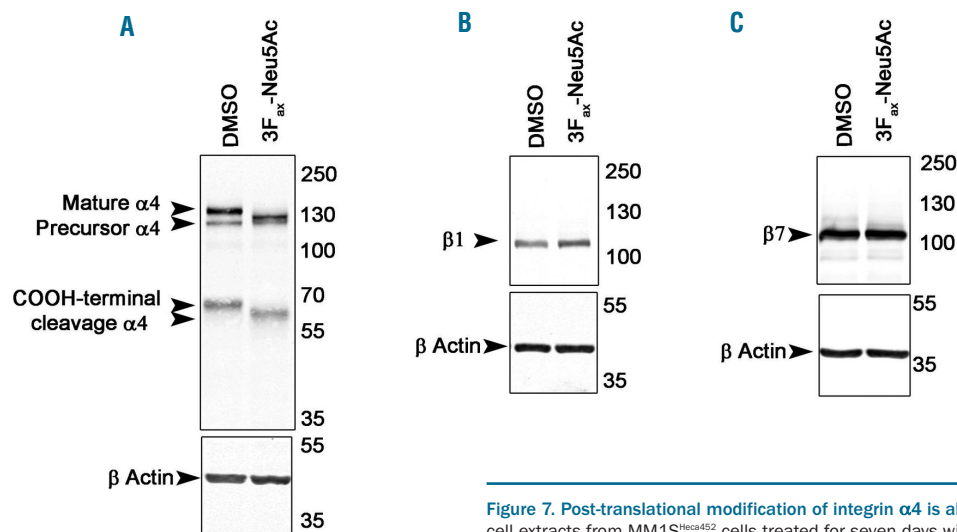


Figure 7. Post-translational modification of integrin $\alpha 4$ is altered by 3F_{ax}-Neu5Ac treatment. Whole cell extracts from MM1S^{Heca452} cells treated for seven days with 300 μ M 3F_{ax}-Neu5Ac or dimethyl sulfoxide (DMSO) (vehicle control) were subjected to SDS PAGE, transferred to nitrocellulose membrane and blotted for integrin $\alpha 4$ (A), $\beta 1$ (B), and $\beta 7$ (C).

soned that global suppression of sialylation could have effects beyond E-selectin. Indeed, 3F_{ax}-Neu5Ac induced a general reduction in the motility of treated cells. This prompted us to investigate whether desialylation would alter adhesion and rolling mediated by $\alpha4\beta7$ and $\alpha4\beta1$ integrins, which are highly expressed on MM cells.⁴¹⁻⁴⁴ In a shear stress adhesion assay, we observed that 3F_{ax}-Neu5Ac reduced the number of adherent cells on VCAM1 and, surprisingly, adhesion on MADCAM1. MADCAM1 is an immunoglobulin superfamily adhesion molecule expressed by mucosal venules that helps direct lymphocyte trafficking into Peyer's patches and the intestinal lamina propria.^{29,45} There is also evidence that interaction between HSC and endothelial MADCAM1 in the BM promotes the homing and engraftment of HSC in mice.⁴⁶⁻⁴⁸ In a similar way, MADCAM1 could co-operate with SDF1 α and E-selectin to facilitate homing of MM cell in the BM. Indeed, MADCAM1 ligand $\alpha4/\beta7$ has been shown to play a critical role in MM-cell adhesion, migration, invasion, BM homing, and adhesion-mediated drug resistance.^{43,49} Moreover, it was shown that the expression levels of $\beta7$ integrin on MM cells correlates with poor survival in MM patients.⁴³ Our results suggest the possibility of reduced interactions between endothelial MADCAM1 and $\alpha4/\beta7$ on MM cells as a result of desialylation. Indeed, we showed that 3F_{ax}-Neu5Ac altered the SDS-PAGE mobility of the $\alpha4$ chain and in particular of its mature forms, suggesting that desialylation interferes with $\alpha4$ maturation. The interaction between MM cells and MADCAM1 becomes apparent only under shear stress as we failed to

detect adhesion on MADCAM1 under static conditions (*data not shown*). This is highly reminiscent of L-selectin on leukocytes that requires a threshold shear stress to establish rolling and adhesion, below which no interactions are observed.⁵⁰ Thus, it is possible that MADCAM1 mediates or facilitates homing but not retention of the MM cells in the BM.

In conclusion, targeting sialylation in MM cells has the potential to block the ability of MM cells to home to the BM, which, in turn, could reduce the severity of the disease, because most existing therapies against MM, like bortezomib, are maximally effective on circulating MM cells.

Funding

The authors would like to acknowledge the Health Research Board (CSA 2012/10) and NIH's National Institute of General Medical Sciences (NIH P30 GM106391, P30GM103392, P20GM121301, and U54GM115516) for funding this work.

The authors' work is also supported by start-up funds from the Maine Medical Center Research Institute, a pilot awarded to Dr. Reagan and core facilities from the Massachusetts General Hospital Center for Skeletal Research (NIH/NIAMS P30AR066261), and a pilot grant from the American Cancer Society (Research Grant #IRG-16-191-33; Reagan PI).

Acknowledgments

The authors would also like to acknowledge the Flow Cytometry Core Facility at NUI Galway. The content is solely the responsibility of the authors and does not necessarily represent the official views of the National Institutes of Health.

References

- Di Marzo L, Desantis V, Solimando AG, et al. Microenvironment drug resistance in multiple myeloma: emerging new players. *Oncotarget*. 2016;7(37):60698-60711.
- Kawano Y, Moschetta M, Manier S, et al. Targeting the bone marrow microenvironment in multiple myeloma. *Immunol Rev*. 2015;263(1):160-172.
- Moschetta M, Kawano Y, Sacco A, et al. Bone Marrow Stroma and Vascular Contributions to Myeloma Bone Homing. *Curr Osteoporos Rep*. 2017;15(5):499-506.
- Ntoni A, Macauley MS, O'Dwyer ME. Targeting Selectins and Their Ligands in Cancer. *Front Oncol*. 2016;6:93.
- Sahin AO, Buitenhuis M. Molecular mechanisms underlying adhesion and migration of hematopoietic stem cells. *Cell Adh Migr*. 2012;6(1):39-48.
- Alsayed Y, Ngo H, Runnels J, et al. Mechanisms of regulation of CXCR4/SDF-1 (CXCL12)-dependent migration and homing in multiple myeloma. *Blood*. 2007;109(7):2708-2717.
- Azab AK, Runnels JM, Pitsillides C, et al. CXCR4 inhibitor AMD3100 disrupts the interaction of multiple myeloma cells with the bone marrow microenvironment and enhances their sensitivity to therapy. *Blood*. 2009;113(18):4341-4351.
- Bouyssou JM, Ghobrial IM, Roccaro AM. Targeting SDF-1 in multiple myeloma tumor microenvironment. *Cancer Lett*. 2016;380(1):315-318.
- Waldschmidt JM, Simon A, Wider D, et al. CXCL12 and CXCR7 are relevant targets to reverse cell adhesion-mediated drug resistance in multiple myeloma. *Br J Haematol*. 2017;179(1):36-49.
- Gazit Y, Akay C. Mobilization of myeloma cells involves SDF-1/CXCR4 signaling and downregulation of VLA-4. *Stem Cells*. 2004;22(1):65-73.
- Menu E, Asosingh K, Indraccolo S, et al. The involvement of stromal derived factor 1alpha in homing and progression of multiple myeloma in the 5TMM model. *Haematologica*. 2006;91(5):605-612.
- Parmo-Cabanas M, Bartolome RA, Wright N, Hidalgo A, Drager AM, Teixido J. Integrin alpha4beta1 involvement in stromal cell-derived factor-1alpha-promoted myeloma cell transendothelial migration and adhesion: role of cAMP and the actin cytoskeleton in adhesion. *Exp Cell Res*. 2004;294(2):571-580.
- Martinez-Moreno M, Leiva M, Aguilera-Montilla N, et al. In vivo adhesion of malignant B cells to bone marrow microvasculature is regulated by alpha4beta1 cytoplasmic-binding proteins. *Leukemia*. 2016;30(4):861-872.
- Ntoni A, Smith TAG, Keane N, et al. E-selectin ligands recognised by HECA452 induce drug resistance in myeloma, which is overcome by the E-selectin antagonist, GMI-1271. *Leukemia*. 2017;31(12):2642-2651.
- Glavey SV, Huynh D, Reagan MR, et al. The cancer glycome: carbohydrates as mediators of metastasis. *Blood Rev*. 2015;29(4):269-279.
- Vajaria BN, Patel PS. Glycosylation: a hallmark of cancer? *Glycoconj J*. 2017;34(2):147-156.
- Bull C, Stoel MA, den Brok MH, Adema GJ. Sialic acids sweeten a tumor's life. *Cancer Res*. 2014;74(12):3199-3204.
- Pearce OM, Laubli H. Sialic acids in cancer biology and immunity. *Glycobiology*. 2016;26(2):111-128.
- Rodrigues E, Macauley MS. Hypersialylation in cancer: modulation of inflammation and therapeutic opportunities. *Cancers (Basel)*. 2018;10(6):1-19.
- Glavey SV, Manier S, Ntoni A, et al. The sialyltransferase ST3GAL6 influences homing and survival in multiple myeloma. *Blood*. 2014;124(11):1765-1776.
- Kannagi R. Molecular mechanism for cancer-associated induction of sialyl Lewis X and sialyl Lewis A expression-The Warburg effect revisited. *Glycoconj J*. 2004;20(5):353-364.
- Magnani JL. The discovery, biology, and drug development of sialyl Le^x and sialyl Le^x. *Arch Biochem Biophys*. 2004;426(2):122-131.
- Varki A. Selectin ligands: will the real ones please stand up? *J Clin Invest*. 1997;100(11 Suppl):S31-35.
- Rillahan CD, Antonopoulos A, Lefort CT, et al. Global metabolic inhibitors of sialyl- and fucosyltransferases remodel the glycome. *Nat Chem Biol*. 2012;8(7):661-668.
- Varki A. Sialic acids in human health and disease. *Trends Mol Med*. 2008;14(8):351-360.
- Varki A, Gagneux P. Multifarious roles of sialic acids in immunity. *Ann N Y Acad Sci*.

- 2012;1253:16-36.
27. Macauley MS, Arlian BM, Rillahan CD, et al. Systemic blockade of sialylation in mice with a global inhibitor of sialyltransferases. *J Biol Chem.* 2014;289(51):35149-35158.
 28. Schmidmaier R, Baumann F, Meinhardt G. Cell-cell contact mediated signalling - no fear of contact. *Exp Oncol.* 2006;28(1):12-15.
 29. Berlin C, Berg EL, Brisikin MJ, et al. Alpha 4 beta 7 integrin mediates lymphocyte binding to the mucosal vascular addressin MAdCAM-1. *Cell.* 1993;74(1):185-195.
 30. Elices MJ, Osborn L, Takada Y, et al. VCAM-1 on activated endothelium interacts with the leukocyte integrin VLA-4 at a site distinct from the VLA-4/fibronectin binding site. *Cell.* 1990;60(4):577-584.
 31. Osborn L, Hession C, Tizard R, et al. Direct expression cloning of vascular cell adhesion molecule 1, a cytokine-induced endothelial protein that binds to lymphocytes. *Cell.* 1989;59(6):1203-1211.
 32. Bull C, Boltje TJ, Wassink M, et al. Targeting aberrant sialylation in cancer cells using a fluorinated sialic acid analog impairs adhesion, migration, and *in vivo* tumor growth. *Mol Cancer Ther.* 2013; 12(10):1935-1946.
 33. Bull C, Boltje TJ, van Dinther EA, et al. Targeted delivery of a sialic acid-blocking glycomimetic to cancer cells inhibits metastatic spread. *ACS Nano.* 2015; 9(1):733-745.
 34. Swami A, Reagan MR, Basto P, et al. Engineered nanomedicine for myeloma and bone microenvironment targeting. *Proc Natl Acad Sci U S A.* 2014;111(28):10287-10292.
 35. Bull C, Boltje TJ, Balneger N, et al. Sialic acid blockade suppresses tumor growth by enhancing T-cell-mediated tumor immunity. *Cancer Res.* 2018;78(13):3574-3588.
 36. Roecklein BA, Torok-Storb B. Functionally distinct human marrow stromal cell lines immortalized by transduction with the human papilloma virus E6/E7 genes. *Blood.* 1995;85(4):997-1005.
 37. Zhu D, Wang Z, Zhao JJ, et al. The Cyclophilin A-CD147 complex promotes the proliferation and homing of multiple myeloma cells. *Nat Med.* 2015;21(6):572-580.
 38. Yanamandra N, Colaco NM, Parquet NA, et al. Tipifarnib and bortezomib are synergistic and overcome cell adhesion-mediated drug resistance in multiple myeloma and acute myeloid leukemia. *Clin Cancer Res.* 2006;12(2):591-599.
 39. Farrell ML, Reagan MR. Soluble and cell-cell-mediated drivers of proteasome inhibitor resistance in multiple myeloma. *Front Endocrinol (Lausanne).* 2018;9(218):1-7.
 40. Abdi J, Chen G, Chang H. Drug resistance in multiple myeloma: latest findings and new concepts on molecular mechanisms. *Oncotarget.* 2013;4(12):2186-2207.
 41. Kim I, Uchiyama H, Chauhan D, Anderson KC. Cell surface expression and functional significance of adhesion molecules on human myeloma-derived cell lines. *Br J Haematol.* 1994;87(3):483-493.
 42. Luque R, Brieva JA, Moreno A, et al. Normal and clonal B lineage cells can be distinguished by their differential expression of B cell antigens and adhesion molecules in peripheral blood from multiple myeloma (MM) patients--diagnostic and clinical implications. *Clin Exp Immunol.* 1998;112(3):410-418.
 43. Neri P, Ren L, Azab AK, et al. Integrin beta7-mediated regulation of multiple myeloma cell adhesion, migration, and invasion. *Blood.* 2011;117(23):6202-6213.
 44. Tatsumi T, Shimazaki C, Goto H, et al. Expression of adhesion molecules on myeloma cells. *Jpn J Cancer Res.* 1996; 87(8):837-842.
 45. Streeter PR, Berg EL, Rouse BT, Bargatze RF, Butcher EC. A tissue-specific endothelial cell molecule involved in lymphocyte homing. *Nature.* 1988;331(6151):41-46.
 46. Murakami JL, Xu B, Franco CB, et al. Evidence that beta7 integrin regulates hematopoietic stem cell homing and engraftment through interaction with MAdCAM-1. *Stem Cells Dev.* 2016; 25(1):18-26.
 47. Katayama Y, Hidalgo A, Peired A, Frenette PS. Integrin alpha4beta7 and its counter-receptor MAdCAM-1 contribute to hematopoietic progenitor recruitment into bone marrow following transplantation. *Blood.* 2004;104(7):2020-2026.
 48. Tada T, Inoue N, Widadayati DT, Fukuta K. Role of MAdCAM-1 and its ligand on the homing of transplanted hematopoietic cells in irradiated mice. *Exp Anim.* 2008; 57(4):347-356.
 49. Masellis-Smith A, Belch AR, Mant MJ, Pilarski LM. Adhesion of multiple myeloma peripheral blood B cells to bone marrow fibroblasts: a requirement for CD44 and alpha4beta7. *Cancer Res.* 1997;57(5):930-936.
 50. Finger EB, Puri KD, Alon R, Lawrence MB, von Andrian UH, Springer TA. Adhesion through L-selectin requires a threshold hydrodynamic shear. *Nature.* 1996; 379(6562):266-269.



Ferrata Storti Foundation

Daratumumab-based regimens are highly effective and well tolerated in relapsed or refractory multiple myeloma regardless of patient age: subgroup analysis of the phase 3 CASTOR and POLLUX studies

Maria-Victoria Mateos,¹ Andrew Spencer,² Ajay K. Nooka,³ Ludek Pour,⁴ Katja Weisel,⁵ Michele Cavo,⁶ Jacob P. Laubach,⁷ Gordon Cook,⁸ Shinsuke Iida,⁹ Lotfi Benboubker,¹⁰ Saad Z. Usmani,¹¹ Sung-Soo Yoon,¹² Nizar J. Bahlis,¹³ Christopher Chiu,¹⁴ Jon Ukropec,¹⁵ Jordan M. Schechter,¹⁶ Xiang Qin,¹⁴ Lisa O'Rourke,¹⁴ and Meletios A. Dimopoulos¹⁷

Haematologica 2020
Volume 105(2):468-477

¹University Hospital of Salamanca/IBSAL, Salamanca, Spain; ²Malignant Haematology and Stem Cell Transplantation Service, Alfred Health-Monash University, Melbourne, Australia; ³Winship Cancer Institute, Emory University, Atlanta, GA, USA; ⁴University Hospital Brno, Brno, Czech Republic; ⁵University Medical Center of Hamburg-Eppendorf, Hamburg, Germany; ⁶Institute of Hematology Department of Experimental, Diagnostic and Specialty Medicine, University of Bologna, Bologna, Italy; ⁷Dana-Farber Cancer Institute, Harvard Medical School, Boston, MA, USA; ⁸St James's Institute of Oncology, Leeds Teaching Hospitals NHS Trust and University of Leeds, Leeds, United Kingdom; ⁹Nagoya City University Graduate School of Medical Sciences, Nagoya, Japan; ¹⁰Service d'Hématologie et Thérapie Cellulaire, Hôpital Bretonneau, Centre Hospitalier Régional Universitaire (CHRU), Tours, France; ¹¹Levine Cancer Institute/Atrium Health, Charlotte, NC, USA; ¹²Department of Internal Medicine, Seoul National University College of Medicine, Seoul, South Korea; ¹³Tom Baker Cancer Center, University of Calgary, Calgary, Alberta, Canada; ¹⁴Janssen Research and Development, LLC, Spring House, PA, USA; ¹⁵Janssen Global Medical Affairs, Horsham, PA, USA; ¹⁶Janssen Research & Development, LLC, Raritan, NJ, USA and ¹⁷National and Kapodistrian University of Athens, Athens, Greece

ABSTRACT

The phase 3 POLLUX and CASTOR studies demonstrated superior benefit of daratumumab plus lenalidomide/dexamethasone or bortezomib/dexamethasone in relapsed/refractory multiple myeloma. Efficacy and safety of daratumumab was analyzed according to age groups of 65 to 74 years and ≥ 75 years. Patients received ≥ 1 prior line of therapy. In POLLUX, patients received lenalidomide/dexamethasone \pm daratumumab (16 mg/kg weekly, cycles 1-2; every two weeks, cycles 3-6; monthly until progression). In CASTOR, patients received eight cycles of bortezomib/dexamethasone \pm daratumumab (16 mg/kg weekly, cycles 1-3; every three weeks, cycles 4-8; monthly until progression). Patients aged >75 years received dexamethasone 20 mg weekly. For patients aged ≥ 75 years in POLLUX (median follow-up: 25.4 months), daratumumab/lenalidomide/dexamethasone prolonged progression-free survival *versus* lenalidomide/dexamethasone (median: 28.9 *versus* 11.4 months; hazard ratio, 0.27; 95% confidence interval, 0.10-0.69; $P=0.0042$) and increased overall response rate (93.1% *versus* 76.5%; $P=0.0740$). Neutropenia was the most common grade 3/4 treatment-emergent adverse event (daratumumab: 44.8%; control: 31.4%). Infusion-related reactions occurred in 12 (41.4%) patients. For patients aged ≥ 75 years in CASTOR (median follow-up: 19.4 months), daratumumab/bortezomib/dexamethasone prolonged progression-free survival *versus* bortezomib/dexamethasone (median: 17.9 *versus* 8.1 months; hazard ratio, 0.26; 95% confidence interval, 0.10-0.65; $P=0.0022$) and increased overall response rate (95.0% *versus* 78.8%; $P=0.1134$). Thrombocytopenia was the most common grade 3/4 treatment-emergent adverse event (daratumumab: 45.0%; control: 37.1%). Infusion-related reactions occurred in 13 (65.0%) patients. Similar findings were reported for patients aged 65 to 74 years in both studies. Taken together, this subgroup analysis of efficacy and safety of daratumumab was largely consistent with the overall populations.

Correspondence:

MARIA-VICTORIA MATEOS
mvmateos@usal.es

Received: January 23, 2019.

Accepted: June 20, 2019.

Pre-published: June 20, 2019.

doi:10.3324/haematol.2019.217448

Check the online version for the most updated information on this article, online supplements, and information on authorship & disclosures: www.haematologica.org/content/105/2/468

©2020 Ferrata Storti Foundation

Material published in Haematologica is covered by copyright. All rights are reserved to the Ferrata Storti Foundation. Use of published material is allowed under the following terms and conditions:

<https://creativecommons.org/licenses/by-nc/4.0/legalcode>.

Copies of published material are allowed for personal or internal use. Sharing published material for non-commercial purposes is subject to the following conditions:

<https://creativecommons.org/licenses/by-nc/4.0/legalcode>, sect. 3. Reproducing and sharing published material for commercial purposes is not allowed without permission in writing from the publisher.



Introduction

Multiple myeloma (MM) is a disease of the elderly, which is evidenced by an increasing incidence with advancing age and a median onset age of 69 years.^{1,2} Treatment regimens including proteasome inhibitors and immunomodulatory drugs have significantly improved survival for patients with MM;³ however, survival benefits are less pronounced in patients aged >60 years.⁴ Among patients with MM, median survival times were shown to decrease steadily over each decade from age <50 years (5.2 years) to age ≥80 years (2.6 years).⁵ Aging is associated with organ dysfunction, reduced functional status, poor resilience to physiologic stressors, an increased burden of comorbidities, and an increased risk of frailty, which affects the ability of elderly patients to tolerate MM treatment regimens.⁶ Furthermore, higher age correlates with more advanced International Staging System (ISS) stage.⁵ Based on the challenges of treating MM in elderly patients, a need exists for effective treatment regimens that exhibit a favorable benefit/risk profile in this age group.

Daratumumab is a human immunoglobulin G1 (IgG1κ) monoclonal antibody targeting CD38 with a direct on-tumor⁷⁻¹⁰ and immunomodulatory¹¹⁻¹⁵ mechanism of action. Tumor cell death is induced by daratumumab via several CD38 immune-mediated actions, including complement-dependent cytotoxicity, antibody-dependent cellular cytotoxicity, antibody-dependent cellular phagocytosis, apoptosis, and modulation of CD38 enzymatic activity.⁷⁻¹⁰ Daratumumab exhibits immunomodulatory effects through reduction of CD38⁺ immunosuppressive cellular populations, including myeloid-derived suppressor cells, regulatory B cells and regulatory T cells; induction of helper and cytotoxic T-cell expansion; increased T-cell clonality, and production of interferon in response to viral peptides.¹¹

In two randomized, open-label, active-controlled, phase 3 studies (POLLUX and CASTOR), daratumumab in combination with standard-of-care regimens (lenalidomide and dexamethasone [RD] or bortezomib and dexamethasone [VD]) demonstrated superior clinical benefit compared with Rd or Vd alone in patients with MM who had received ≥1 prior line of therapy. In POLLUX, daratumumab in combination with Rd (D-Rd) reduced the risk of disease progression or death by 63% compared with Rd after a median follow-up of 13.5 months.¹⁴ Similarly, in CASTOR, the risk of the progression or death was reduced by 61% with daratumumab in combination with Vd (D-Vd) *versus* Vd after a median follow-up of 7.4 months.¹⁵ Findings from these pivotal studies led to the approval of daratumumab in combination with Rd or Vd in many countries for the treatment of patients with MM who received ≥1 prior line of therapy.¹⁶ This analysis reports the efficacy and safety of daratumumab in patients aged 65 to 74 years or ≥75 years from POLLUX and CASTOR after further median follow-up of 25.4 and 19.4 months, respectively.

Methods

Study design and patients

POLLUX and CASTOR were multicenter, randomized, open-label, active-controlled, phase 3 studies of patients with relapsed

or refractory MM (RRMM). Trials were approved by an institutional review board or independent ethics committee at each site. Study protocols were conducted in accordance with the principles of the Declaration of Helsinki and the International Conference on Harmonisation Good Clinical Practice guidelines. Detailed study designs were published previously.^{14,15} Briefly, patients received ≥1 prior line of therapy, had at least a partial response to ≥1 prior therapy, and had documented progressive disease, according to the International Myeloma Working Group (IMWG) criteria.^{14,15,17,18} Patients refractory or intolerant to lenalidomide were excluded from POLLUX. Patients refractory or intolerant to bortezomib, or refractory to another proteasome inhibitor were excluded from CASTOR.

Procedures

Patients were randomized 1:1 to D-Rd or Rd in POLLUX and D-Vd or Vd in CASTOR.^{14,15} Stratification was described previously and did not include age.^{14,15} In POLLUX, all patients received 28-day cycles of lenalidomide (25 mg orally [PO] on days 1-21 of each cycle) and dexamethasone (40 mg PO weekly in patients aged ≤75 years; 20 mg PO weekly in patients aged >75 years) with or without daratumumab (16 mg/kg intravenously [IV] weekly during cycles 1 and 2, every 2 weeks during cycles 3-6, and every 4 weeks thereafter until disease progression, unacceptable toxicity, or withdrawal of consent). Patients in the D-Rd group received a split dose of dexamethasone during daratumumab dosing weeks (20 mg before infusion; 20 mg the following day). Patients aged >75 years received the entire 20-mg dose prior to infusion.

In CASTOR, patients received eight, 21-day cycles of bortezomib (1.3 mg/m² subcutaneously [SC] on days 1, 4, 8, and 11) and dexamethasone (20 mg PO or IV on days 1, 2, 4, 5, 8, 9, 11, and 12; for a total dose of 160 mg/cycle during cycles 1-8) with or without daratumumab (16 mg/kg IV weekly in cycles 1-3, every three weeks during cycles 4-8, and every four weeks thereafter until withdrawal of consent, disease progression, or unacceptable toxicity). In patients aged >75 years, dexamethasone could be reduced to 20 mg weekly. In both studies, daratumumab-treated patients received pre- and post-infusion medications to prevent the onset of infusion-related reactions (IRR).^{14,15}

Outcomes and statistical analyses

Frailty score was not assessed as these studies were initiated before this metric was adopted.¹⁹ The safety analysis set included all patients who received ≥1 administration of study treatment. Efficacy was assessed by progression-free survival (PFS) and response rates,^{14,15} which were based on the intent-to-treat (ITT) and response-evaluable populations, respectively. A stratified log-rank test compared PFS between groups. Hazard ratios (HR) and 95% confidence intervals (CI) were estimated using a stratified Cox regression model, with treatment as the sole explanatory variable. Distributions were estimated using the Kaplan-Meier method. A stratified Cochran-Mantel-Haenszel chi-square test measured treatment differences in overall response rate (ORR) and rates of very good partial response (VGPR) or better and complete response (CR) or better.

Results

At the clinical cut-off date of March 7, 2017, the median (range) duration of follow-up was 25.4 (0-32.7) months for POLLUX. Of the 569 patients enrolled, 29/286 (D-Rd) and 35/283 (Rd) were aged ≥75 years, and 124/286 (D-Rd) and 108/283 (Rd) were aged 65 to 74 years. The clinical cut-off date for CASTOR was January 11, 2017, conferring a

Table 1. Baseline and demographic characteristics.

Characteristic: POLLUX	65-74 years		≥75 years	
	D-Rd (n=124)	Rd (n=108)	D-Rd (n=29)	Rd (n=35)
Age (years)				
Median (range)	69.0 (65-74)	69.0 (65-74)	77.0 (75-89)	78.0 (75-87)
Sex, n (%)				
Male	83 (66.9)	62 (57.4)	14 (48.3)	21 (60.0)
Female	41 (33.1)	46 (42.6)	15 (51.7)	14 (40.0)
Race, n (%) ^a				
White	95 (76.6)	72 (66.7)	19 (65.5)	21 (60.0)
Asian	18 (14.5)	19 (17.6)	6 (20.7)	4 (11.4)
Black or African American	2 (1.6)	3 (2.8)	1 (3.4)	2 (5.7)
Unknown	0	1 (0.9)	1 (3.4)	0
Not reported	9 (7.3)	13 (12.0)	2 (6.9)	8 (22.9)
Baseline ECOG score, n (%)				
0	60 (48.4)	54 (50.0)	10 (34.5)	11 (31.4)
1	60 (48.4)	46 (42.6)	15 (51.7)	21 (60.0)
2	4 (3.2)	8 (7.4)	4 (13.8)	3 (8.6)
ISS staging, n (%) ^b				
I	51 (41.1)	57 (52.8)	10 (34.5)	12 (34.3)
II	42 (33.9)	31 (28.7)	13 (44.8)	11 (31.4)
III	31 (25.0)	20 (18.5)	6 (20.7)	12 (34.3)
Time from diagnosis, years				
Median (range)	3.8 (0.4-22.5)	3.6 (0.4-18.3)	2.6 (0.8-27.0)	4.0 (0.8-14.6)
Prior lines of therapy, n (%)				
1	62 (50.0)	59 (54.6)	17 (58.6)	16 (45.7)
2	36 (29.0)	31 (28.7)	7 (24.1)	8 (22.9)
3	19 (15.3)	11 (10.2)	3 (10.3)	10 (28.6)
>3	7 (5.6)	7 (6.5)	2 (6.9)	1 (2.9)
Cytogenetic profile, n (%) ^c				
N	67	57	13	16
Standard	56 (83.6)	44 (77.2)	10 (76.9)	12 (75.0)
High	11 (16.4)	13 (22.8)	3 (23.1)	4 (25.0)
Characteristic: CASTOR	D-Vd (n=96)	Vd (n=87)	D-Vd (n=23)	Vd (n=35)
Age (years)				
Median (range)	69.0 (65-74)	69.0 (65-74)	78.0 (75-88)	78.0 (75-85)
Gender, n (%)				
Male	53 (55.2)	53 (60.9)	13 (56.5)	20 (57.1)
Female	43 (44.8)	34 (39.1)	10 (43.5)	15 (42.9)
Race, n (%) ^a				
White	83 (86.5)	81 (93.1)	22 (95.7)	29 (82.9)
Black or African American	6 (6.3)	1 (1.1)	0	1 (2.9)
Asian	4 (4.2)	2 (2.3)	0	2 (5.7)
American Indian or Alaska Native	1 (1.0)	0	0	0
Other	2 (2.1)	0	1 (4.3)	0
Unknown	0	0	0	1 (2.9)
Not reported	0	3 (3.4)	0	2 (5.7)
Baseline ECOG score, n (%)				
0	39 (40.6)	38 (43.7)	6 (26.1)	16 (45.7)
1	51 (53.1)	39 (44.8)	17 (73.9)	17 (48.6)
2	6 (6.3)	10 (11.5)	0	2 (5.7)

continued on the next page

continued from the previous page

ISS staging, n (%) ^b				
I	34 (35.4)	33 (37.9)	6 (26.1)	13 (37.1)
II	37 (38.5)	32 (36.8)	7 (30.4)	13 (37.1)
III	25 (26.0)	22 (25.3)	10 (43.5)	9 (25.7)
Time from diagnosis, years				
Median (range)	4.0 (0.7-20.7)	3.9 (0.9-17.2)	4.6 (1.0-14.7)	3.6 (1.2-18.6)
Prior lines of therapy, n (%)				
1	47 (49.0)	38 (43.7)	8 (34.8)	17 (48.6)
2	29 (30.2)	23 (26.4)	8 (34.8)	13 (37.1)
3	15 (15.6)	15 (17.2)	3 (13.0)	2 (5.7)
>3	5 (5.2)	11 (12.6)	4 (17.4)	3 (8.6)
Cytogenetic profile ^c , n (%)				
N	72	71	11	28
Standard	60 (83.3)	53 (74.6)	9 (81.8)	22 (78.6)
High	12 (16.7)	18 (25.4)	2 (18.2)	6 (21.4)

D-Rd: daratumumab/lenalidomide/dexamethasone; Rd: lenalidomide/dexamethasone; ECOG: Eastern Cooperative Oncology Group; daratumumab/bortezomib/dexamethasone; Vd: bortezomib/dexamethasone. ^aPercentages may not add up to 100% due to rounding. ^bISS staging is derived based on the combination of serum β 2-microglobulin and albumin. ^cCytogenetic risk determined by next-generation sequencing.

median (range) duration of follow-up of 19.4 (0-27.7) months. Of the 498 patients enrolled in CASTOR, 23/251 (D-Vd) and 35/247 (Vd) were aged \geq 75 years, and 96/251 (D-Vd) and 87/247 (Vd) were aged 65 to 74 years. In both studies, demographic and baseline clinical characteristics were well balanced between treatment groups (Table 1). In POLLUX, among patients aged \geq 75 years, 3/13 (23.1%) patients in the D-Rd group and 4/16 (25.0%) patients in the Rd group had high-risk cytogenetic abnormalities. Similarly, among patients aged \geq 75 years in CASTOR, 2/11 (18.2%) patients in the D-Vd group and 6/28 (21.4%) patients in the Vd group had high cytogenetic risk. Among patients aged 65 to 74 years in POLLUX, 11 (16.4%) patients in the D-Rd group and 13 (22.8%) of patients in the Rd group had high cytogenetic risk abnormalities. Similarly, among patients aged 65 to 74 years in CASTOR, 12 (16.7%) patients in the D-Vd group and 18 (25.4%) patients in the Vd group had high cytogenetic risk.

The dispositions of patients according to age from POLLUX and CASTOR are summarized in Figure 1. In POLLUX, nine (31.0%) patients aged \geq 75 years who were treated with D-Rd and 24 (68.6%) patients who were treated with Rd discontinued treatment. In CASTOR, 11 (55.0%) patients aged \geq 75 years who received D-Vd and 15 (42.9%) patients who were treated with Vd discontinued treatment. Among patients aged \geq 75 years who were randomized to D-Vd, 3 (13.0%) did not receive treatment. Similar findings were observed in the patients aged 65 to 74 years: in POLLUX, 51 (41.5%) patients who were treated with D-Rd and 76 (70.4%) patients who received Rd discontinued treatment, and in CASTOR, 56 (59.6%) patients who were treated with D-Vd and 44 (51.2%) patients who received Vd discontinued treatment.

In POLLUX, the median dose intensity of lenalidomide was generally lower in both treatment arms for patients aged \geq 75 years (D-Rd, 210.00 mg/cycle; Rd, 305.00 mg/cycle) compared with patients aged 65 to 74 years (D-Rd, 333.93 mg/cycle; Rd, 420.00 mg/cycle). In CASTOR, the median dose intensity of bortezomib was similar among patients aged \geq 75 years (D-Vd, 4.06

mg/m²/cycle; Vd, 4.37 mg/m²/cycle) and 65 to 74 years (D-Vd, 4.56 mg/m²/cycle; Vd, 4.70 mg/m²/cycle).

In POLLUX, in the ITT population, the clinical benefit of D-Rd over Rd was maintained after a median follow-up of 25.4 months (Figure 2). PFS was significantly prolonged with D-Rd *versus* Rd in the ITT population (median: not reached *versus* 17.5 months; HR, 0.41; 95% CI, 0.31-0.53; $P<0.0001$; Figure 2A),²⁰ with 18-month PFS rates of 75.3% and 48.5%, respectively. Similarly, PFS was significantly prolonged with D-Rd compared with Rd in patients aged \geq 75 years (median: 28.9 *versus* 11.4 months; HR, 0.27; 95% CI, 0.10-0.69; $P=0.0042$; Figure 2A), with 18-month PFS rates of 86.2% *versus* 36.9%, respectively. PFS was also significantly prolonged with D-Rd *versus* Rd in patients aged 65 to 74 years (median: not reached *versus* 17.1 months; HR, 0.40; 95% CI, 0.27-0.60; $P<0.0001$; Figure 2B), with 18-month PFS rates of 72.0% and 48.7%, respectively. At the time of the clinical cut-off, overall survival (OS) data were immature. Survival follow-up for POLLUX will continue until 330 deaths are observed in the ITT population.

In CASTOR, in the ITT population, the clinical benefit of D-Vd over Vd was maintained after a median follow-up of 19.4 months (Figure 2). PFS was significantly prolonged with D-Vd *versus* Vd in the ITT population (median: 16.7 *versus* 7.1 months; HR, 0.31; 95% CI, 0.24-0.39; $P<0.0001$; Figure 2C), with 18-month PFS rates of 48.0% *versus* 7.9%, respectively.²¹ Similarly, PFS was significantly prolonged with D-Vd compared with Vd in patients aged \geq 75 years (median: 17.9 *versus* 8.1 months; HR, 0.26; 95% CI, 0.10-0.65; $P=0.0022$; Figure 2C), with 18-month PFS rates of 45.8% *versus* 0%, respectively. PFS was also significantly prolonged for D-Vd *versus* Vd in patients aged 65 to 74 years (median: 18.9 *versus* 6.1 months; HR, 0.25; 95% CI, 0.16-0.40; $P<0.0001$; Figure 2D). Follow-up for OS in CASTOR will continue until 320 deaths are reported in the ITT population, per protocol.

In POLLUX, among patients aged \geq 75 years, higher ORR were observed with D-Rd *versus* Rd (93.1% *versus* 76.5%; $P=0.0740$), with significantly higher rates of VGPR

POLLUX			
Aged 65-74 years		Aged ≥75 years	
D-Rd n=124	Rd n=108	D-Rd n=29	Rd n=35
51 discontinued treatment 27 Progressive disease 18 Adverse event 2 Physician decision 0 Non-compliance ^a 1 Withdrawal by patient 2 Death 1 Other	76 discontinued treatment 50 Progressive disease 19 Adverse event 3 Physician decision 3 Non-compliance ^a 1 Withdrawal by patient 0 Death 0 Other	9 discontinued treatment 1 Progressive disease 5 Adverse event 0 Withdrawal by patient 2 Non-compliance ^a 1 Physician decision	24 discontinued treatment 14 Progressive disease 6 Adverse event 3 Withdrawal by patient 1 Non-compliance ^a 0 Physician decision
CASTOR ^b			
Aged 65-74 years		Aged ≥75 years	
D-Vd n=96	Vd n=87	D-Vd n=23	Vd n=35
56 discontinued treatment 36 Progressive disease 13 Adverse event 4 Non-compliance ^a 2 Death 1 Withdrawal by patient	44 discontinued treatment 28 Progressive disease 9 Adverse event 4 Non-compliance ^a 1 Death 2 Withdrawal by patient	11 discontinued treatment 4 Adverse event 7 Progressive disease 0 Non-compliance ^a 0 Death	15 discontinued treatment 7 Adverse event 3 Progressive disease 3 Non-compliance ^a 2 Death

Figure 1. Disposition of patients aged 65 to 74 years and ≥75 years based on the intent-to-treat population of (A) POLLUX and (B) CASTOR. D-Rd: daratumumab/lenalidomide/dexamethasone; Rd: lenalidomide/dexamethasone; D-Vd: daratumumab/bortezomib/dexamethasone; Vd, bortezomib/dexamethasone. ^aBased on reason 'patient refused to further study treatment'. ^bAll patients were to receive eight cycles of bortezomib and dexamethasone. After cycle 8, patients receiving only bortezomib and dexamethasone were entered into an observation phase, while patients in the daratumumab group continued to receive daratumumab monotherapy every 4 weeks. All patients had discontinued or completed eight cycles of bortezomib and dexamethasone by the interim analysis.¹⁵

or better (75.9% *versus* 41.2%; $P=0.0059$) and CR or better (55.2% *versus* 8.8%; $P<0.0001$), respectively (Table 2). Similar findings were observed in patients aged 65 to 74 years (ORR: 92.6% *versus* 80.2%; $P=0.0057$; VGPR or better: 76.2% *versus* 49.1%; $P<0.0001$; CR or better: 50.0% *versus* 22.6%; $P<0.0001$). In both age groups, deeper responses with D-Rd *versus* Rd translated to a significantly higher proportion of patients with minimal residual disease (MRD)-negative status at a sensitivity threshold of 10^{-5} (Table 2). Among patients aged ≥75 years, the rates of MRD negativity were 27.6% *versus* 5.7% ($P=0.014464$), and in patients aged 65 to 74, the rates were 23.4% *versus* 8.3% ($P=0.001520$).

In patients who received one prior line of therapy, a higher proportion of patients who received D-Rd achieved MRD negativity at a sensitivity threshold of 10^{-5} (Online Supplementary Table S1). Among patients aged ≥75 years, the rates of MRD negativity were 23.5% *versus* 12.5% ($P=0.407414$), and in patients aged 65 to 74 years, the rates were 24.2% *versus* 8.5% ($P=0.017519$).

In CASTOR, among patients aged ≥75 years, higher ORR were observed with D-Vd *versus* Vd (95.0% *versus* 78.8%; $P=0.1134$), including higher rates of VGPR or better (70.0% *versus* 18.2%; $P=0.0002$) and CR or better (25.0% *versus* 3.0%; $P=0.0154$), respectively (Table 2). Similar findings were observed for patients aged 65 to 74 years (ORR: 82.8% *versus* 62.4%; $P=0.0022$; VGPR or better: 64.5% *versus* 27.1%; $P<0.0001$; CR or better: 33.3%

versus 10.6%; $P=0.0003$). The rates of MRD-negative status (10^{-5} sensitivity) were significantly higher with D-Vd *versus* Vd among patients aged 65 to 74 years (15.6% *versus* 2.3%; $P=0.000959$; Table 2). One (4.3%) patient treated with D-Vd in the subgroup of patients aged ≥75 years achieved MRD-negative status (10^{-5} sensitivity) compared with no patients in the Vd treatment group. Rates of MRD negativity at sensitivity thresholds of 10^{-4} and 10^{-6} are presented for both POLLUX and CASTOR in the Online Supplementary Table S2.

In patients who received one prior line of therapy, a higher proportion of patients who received D-Vd achieved MRD negativity at a sensitivity threshold of 10^{-5} (Online Supplementary Table S1). Among patients aged ≥75 years, the rates of MRD negativity were 12.5% *versus* 0% ($P=0.123775$), and in patients aged 65 to 74, the rates were 19.1% *versus* 2.6% ($P=0.011285$).

In POLLUX and CASTOR, all patients aged ≥75 years reported at least 1 treatment-emergent adverse event (TEAE; Table 3). In POLLUX, among patients aged ≥75 years, grade 3/4 TEAE occurred in 25 (86.2%) and 27 (77.1%) patients in the D-Rd and Rd treatment groups, respectively (Table 3). Neutropenia was the most common grade 3/4 TEAE among patients aged ≥75 years (D-Rd: 44.8%; Rd: 31.4%) and among patients aged 65 to 74 years (D-Rd: 55.3%; Rd: 39.8%). Higher rates of pneumonia were observed with daratumumab in both age groups. In CASTOR, among patients aged ≥75 years, grade 3/4

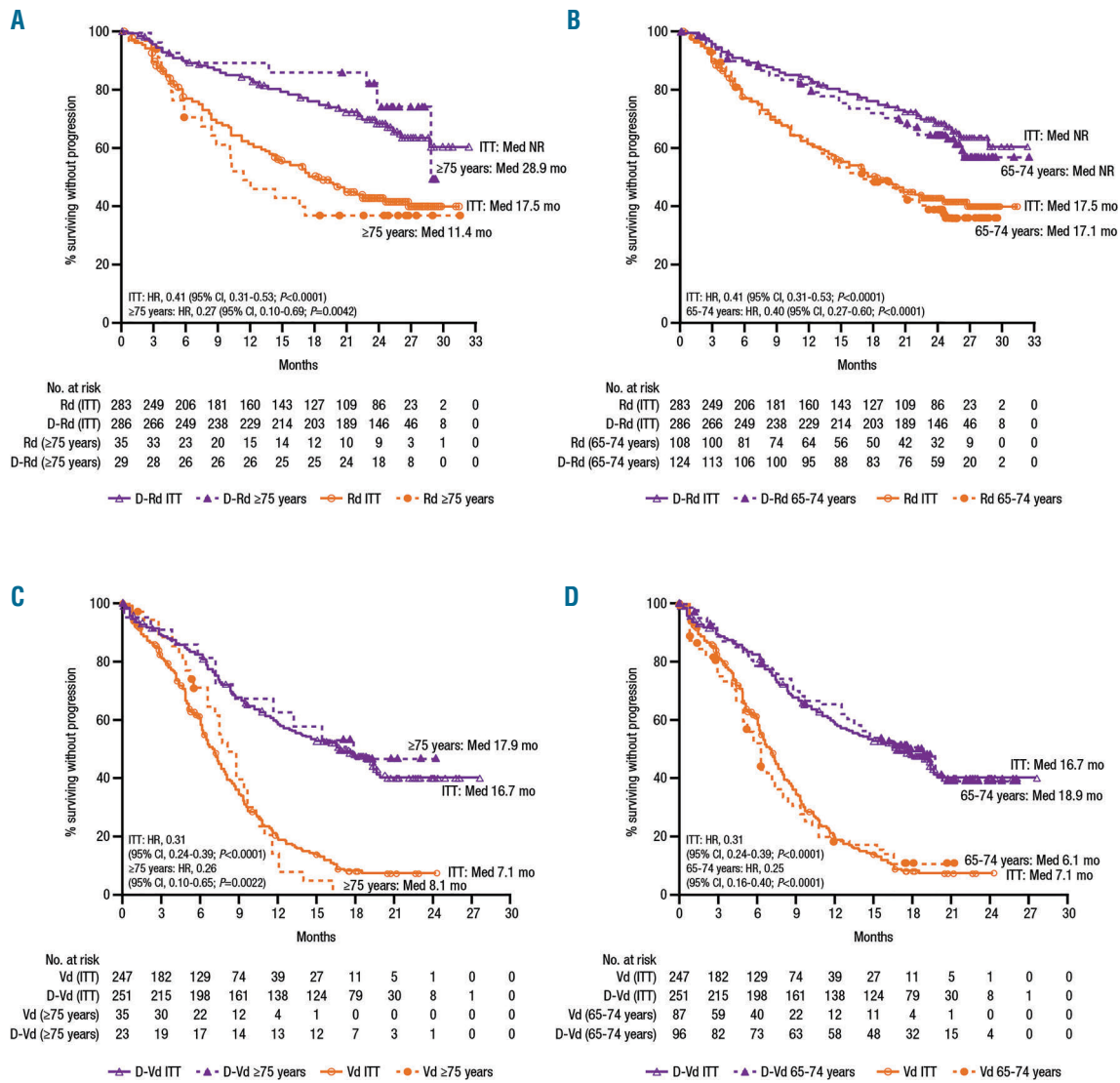


Figure 2. PFS of patients aged 65 to 74 years and ≥75 years in POLLUX and CASTOR. PFS in the ITT populations compared with patients aged ≥75 years (A) and 65 to 74 years (B) in POLLUX and with patients aged ≥75 years (C) and 65 to 74 years (D) in CASTOR. PFS is based on Kaplan-Meier estimates. PFS: progression-free survival; ITT: intent-to-treat; Med: median; NR: not reached; HR: hazard ratio; CI: confidence interval; Rd: lenalidomide/dexamethasone; D-Rd: daratumumab/lenalidomide/dexamethasone; Vd: bortezomib/dexamethasone; D-Vd: daratumumab/bortezomib/dexamethasone.

TEAE were reported in 18 (90.0%) and 26 (74.3%) patients in the D-Vd and Vd treatment groups, respectively (Table 3). Thrombocytopenia was the most common grade 3/4 TEAE in both treatment groups among patients aged ≥75 years (D-Vd: 45.0%; Vd: 37.1%) and in patients aged 65 to 74 years (D-Vd: 52.1%; Vd: 32.6%).

In POLLUX, IRR of any grade were reported in 12 (41.4%) patients aged ≥75 years and 57 (46.3%) patients aged 65 to 74 years (Table 4). The most common IRR in both age groups was dyspnea (≥75 years: 13.8%; 65-74 years: 10.6%). The majority of IRR were mild, with grade 3/4 IRR occurring in four (13.8%) patients aged ≥75 years and six (4.9%) patients aged 65 to 74 years. Among patients aged ≥75 years, all IRR occurred with the first infusion, with the exception of one IRR that occurred in a subsequent infusion. Among patients aged 65 to 74 years, two (1.6%) patients reported an IRR in the second infusion, and seven (5.9%) patients reported an IRR in subse-

quent infusions. In CASTOR, 13 (65.0%) patients aged ≥75 years and 43 (45.7%) patients aged 65 to 74 years reported an IRR of any grade (Table 4). IRR were generally mild, with grade 3/4 IRR occurring in 2 (10.0%) and 8 (8.5%) patients aged ≥75 and 65 to 74 years, respectively. Among patients aged ≥75 years, no IRR in the second or subsequent infusions were reported; only one patient (aged 65-74 years) had an IRR in the second infusion. In both studies, IRR were manageable and did not result in treatment discontinuations in these populations.

Discussion

MM is a disease of the elderly, and patients are a heterogeneous population with the potential for various comorbidities, reduced functional status, and increased risk of frailty.⁶ Approximately 35% to 40% of patients with MM

are aged >75 years, but conversely this age group is under-represented in clinical studies.²² To determine if treatment strategies are safe and effective for elderly patients with MM, subgroup analyses of clinical trial data are needed. In the current sub-analysis of POLLUX and CASTOR, the efficacy and safety of daratumumab in combination with standard-of-care regimens were evaluated in patients aged ≥ 75 years and 65 to 74 years.

Efficacy results were consistent with those observed in the overall study populations, showing significantly prolonged PFS for patients aged ≥ 75 years and 65 to 74 years. In both studies, ORR were significantly higher with daratumumab versus standard-of-care treatment in patients aged 65 to 74 years and numerically higher in patients aged ≥ 75 years, with significantly higher rates of CR or better and VGPR or better in both age categories. While responses were considerably deeper among patients treated with daratumumab, the lack of statistical significance

observed with ORR between groups may be due in part to the small number of patients aged ≥ 75 years in POLLUX (D-Rd, n=29; Rd, n=35) and CASTOR (D-Vd, n=23; Vd, n=35). Consistent with the overall study populations, deeper responses with daratumumab translated to a higher proportion of patients who achieved MRD-negative status. In both studies, safety analyses identified that the rates of common grade 3/4 hematologic TEAE were similar to those of the overall study populations.^{14,15} Importantly, IRR were manageable and did not result in treatment discontinuations. While the incidence of grade 3/4 IRR was numerically higher for patients aged ≥ 75 years versus patients aged 65-74 years (13.8% versus 4.9%) and what was reported for the primary analysis of POLLUX (grade 3 IRR; 5.3%),¹⁴ a larger sample size is needed to appropriately determine if this age group is more susceptible to experiencing an IRR.

There are limited clinical trial data focused on elderly

Table 2. Summary of response rates and MRD (10^{-5} sensitivity threshold) among patients aged 65 to 74 years and ≥ 75 years in POLLUX and CASTOR.

Response rate ^a , n (%) ^a	POLLUX								
	ITT			65-74 years			≥ 75 years		
	D-Rd (n=281)	Rd (n=276)	P	D-Rd (n=122)	Rd (n=106)	P	D-Rd (n=29)	Rd (n=34)	P
ORR	261 (92.9)	211 (76.4)	<0.0001	113 (92.6)	85 (80.2)	0.0057	27 (93.1)	26 (76.5)	0.0740
\geq CR	144 (51.2)	58 (21.0)	<0.0001	61 (50.0)	24 (22.6)	<0.0001	16 (55.2)	3 (8.8)	<0.0001
sCR	73 (26.0)	24 (8.7)		31 (25.4)	10 (9.4)		10 (34.5)	1 (2.9)	
CR	71 (25.3)	34 (12.3)		30 (24.6)	14 (13.2)		6 (20.7)	2 (5.9)	
\geq VGPR	221 (78.6)	132 (47.8)	<0.0001	93 (76.2)	52 (49.1)	<0.0001	22 (75.9)	14 (41.2)	0.0059
VGPR	77 (27.4)	74 (26.8)		32 (26.2)	28 (26.4)		6 (20.7)	11 (32.4)	
PR	40 (14.2)	79 (28.6)		20 (16.4)	33 (31.1)		5 (17.2)	12 (35.3)	
MR	5 (1.8)	26 (9.4)		1 (0.8)	9 (8.5)		0	5 (14.7)	
SD	13 (4.6)	33 (12.0)		7 (5.7)	11 (10.4)		2 (6.9)	3 (8.8)	
PD	0	4 (1.4)		0	1 (0.9)		0	0	
NE	2 (0.7)	2 (0.7)		1 (0.8)	0		0	0	
MRD ^b (10^{-5} sensitivity threshold)									
Patients evaluated, n	286	283		124	108		29	35	
MRD negative, n (%)	75 (26.2)	18 (6.4)	<0.000001	29 (23.4)	9 (8.3)	0.001520	8 (27.6)	2 (5.7)	0.014464
Response rate ^a , n (%) ^a	CASTOR								
	ITT			65-74 years			≥ 75 years		
	D-Vd (n=240)	Vd (n=234)	P	D-Vd (n=93)	Vd (n=85)	P	D-Vd (n=20)	Vd (n=33)	P
ORR	201 (83.8)	148 (63.2)	<0.0001	77 (82.8)	53 (62.4)	0.0022	19 (95.0)	26 (78.8)	0.1134
\geq CR	69 (28.8)	23 (9.8)	<0.0001	31 (33.3)	9 (10.6)	0.0003	5 (25.0)	1 (3.0)	0.0154
sCR	21 (8.8)	6 (2.6)		12 (12.9)	2 (2.4)		2 (10.0)	0	
CR	48 (20.0)	17 (7.3)		19 (20.4)	7 (8.2)		3 (15.0)	1 (3.0)	
\geq VGPR	149 (62.1)	68 (29.1)	<0.0001	60 (64.5)	23 (27.1)	<0.0001	14 (70.0)	6 (18.2)	0.0002
VGPR	80 (33.3)	45 (19.2)		29 (31.2)	14 (16.5)		9 (45.0)	5 (15.2)	
PR	52 (21.7)	80 (34.2)		17 (18.3)	30 (35.3)		5 (25.0)	20 (60.6)	
MR	9 (3.8)	20 (8.5)		2 (2.2)	4 (4.7)		0	4 (12.1)	
SD	23 (9.6)	47 (20.1)		13 (14.0)	18 (21.2)		1 (5.0)	3 (9.1)	
PD	5 (2.1)	16 (6.8)		0	10 (11.8)		0	0	
NE	2 (0.8)	3 (1.3)		1 (1.1)	0		0	0	
MRD ^b (10^{-5} sensitivity threshold)									
Patients evaluated, n	251	247		96	87		23	35	
MRD negative, n (%)	29 (11.6)	6 (2.4)	0.000034	15 (15.6)	2 (2.3)	0.000959	1 (4.3)	0	0.170712

MRD: minimal residual disease; ITT: intent-to-treat; D-Rd: daratumumab/lenalidomide/dexamethasone; Rd: lenalidomide/dexamethasone; ORR: overall response rate; CR: complete response; sCR: stringent complete response; VGPR: very good partial response; PR: partial response; MR: minimal response; SD: stable disease; PD: progressive disease; NE: not evaluated; D-Vd: daratumumab/bortezomib/dexamethasone; Vd: bortezomib/dexamethasone. ^aResponse-evaluable population. ^bBased on the ITT analysis set.

patients with RRMM, a population that is likely to exhibit tolerability and safety concerns with treatment.^{6,23} A retrospective, observational study was conducted to assess the efficacy and toxicity of bortezomib-based regimens used in combination with dexamethasone as salvage therapy for elderly patients with RRMM.²³ Patients (n=81) who

were aged 65 to 89 years (median, 73 years) and received a median of two prior lines of therapy (range 1-3) were included. A median of six cycles (range 1-11) of Vd were administered, and after a median follow-up of 24 months, the median PFS and OS were 8.7 and 22 months, respectively. Partial response or better was achieved in 65.4% of

Table 3. Most common TEAE among patients aged 65 to 74 years and ≥75 years in POLLUX and CASTOR.

TEAE: POLLUX ^a	65-74 years				≥75 years			
	Any grade (>25%)		Grade 3/4 (>10%)		Any grade (>25%)		Grade 3/4 (>10%)	
	D-Rd (n=123)	Rd (n=108)	D-Rd (n=123)	Rd (n=108)	D-Rd (n=29)	Rd (n=35)	D-Rd (n=29)	Rd (n=35)
Patients with TEAE, n (%)	122 (99.2)	104 (96.3)	113 (91.9)	89 (82.4)	29 (100.0)	35 (100.0)	25 (86.2)	27 (77.1)
Hematologic TEAE, n (%)								
Neutropenia	77 (62.6)	49 (45.4)	68 (55.3)	43 (39.8)	14 (48.3)	14 (40.0)	13 (44.8)	11 (31.4)
Anemia	52 (42.3)	47 (43.5)	23 (18.7)	24 (22.2)	12 (41.4)	13 (37.1)	3 (10.3)	7 (20.0)
Thrombocytopenia	37 (30.1)	37 (34.3)	19 (15.4)	16 (14.8)	10 (34.5)	9 (25.7)	3 (10.3)	5 (14.3)
Nonhematologic TEAE, n (%)								
Diarrhea	61 (49.6)	37 (34.3)	8 (6.5)	1 (0.9)	11 (37.9)	12 (34.3)	0	2 (5.7)
Fatigue	43 (35.0)	38 (35.2)	5 (4.1)	6 (5.6)	10 (34.5)	13 (37.1)	1 (3.4)	1 (2.9)
Nasopharyngitis	41 (33.3)	25 (23.1)	0	0	4 (13.8)	5 (14.3)	0	0
Upper respiratory tract infection	40 (32.5)	26 (24.1)	2 (1.6)	2 (1.9)	11 (37.9)	9 (25.7)	1 (3.4)	0
Constipation	39 (31.7)	30 (27.8)	2 (1.6)	0	7 (24.1)	12 (34.3)	0	1 (2.9)
Nausea	34 (27.6)	17 (15.7)	1 (0.8)	1 (0.9)	7 (24.1)	9 (25.7)	0	0
Muscle spasms	33 (26.8)	19 (17.6)	1 (0.8)	2 (1.9)	8 (27.6)	6 (17.1)	0	0
Cough	32 (26.0)	16 (14.8)	0	0	6 (20.7)	6 (17.1)	1 (3.4)	0
Dyspnea	31 (25.2)	11 (10.2)	7 (5.7)	0	7 (24.1)	11 (31.4)	3 (10.3)	0
Pneumonia	29 (23.6)	14 (13.0)	19 (15.4)	7 (6.5)	9 (31.0)	6 (17.1)	5 (17.2)	4 (11.4)
Peripheral edema	29 (23.6)	17 (15.7)	1 (0.8)	0	8 (27.6)	15 (42.9)	0	2 (5.7)
Asthenia	22 (17.9)	19 (17.6)	5 (4.1)	3 (2.8)	4 (13.8)	10 (28.6)	1 (3.4)	2 (5.7)
Back pain	21 (17.1)	20 (18.5)	1 (0.8)	3 (2.8)	8 (27.6)	7 (20.0)	2 (6.9)	1 (2.9)
Hypokalaemia	16 (13.0)	12 (11.1)	5 (4.1)	5 (4.6)	7 (24.1)	4 (11.4)	4 (13.8)	1 (2.9)
Pulmonary embolism	5 (4.1)	3 (2.8)	4 (3.3)	2 (1.9)	1 (3.4)	4 (11.4)	1 (3.4)	4 (11.4)
TEAE: CASTOR ^a	65-74 years				≥75 years			
	Any grade (>25%)		Grade 3/4 (>10%)		Any grade (>25%)		Grade 3/4 (>10%)	
	D-Vd (n=94)	Vd (n=86)	D-Vd (n=94)	Vd (n=86)	D-Vd (n=20)	Vd (n=35)	D-Vd (n=20)	Vd (n=35)
Patients with TEAE, n (%)	93 (98.9)	82 (95.3)	77 (81.9)	60 (69.8)	20 (100.0)	35 (100.0)	18 (90.0)	26 (74.3)
Hematologic TEAE, n (%)								
Thrombocytopenia	60 (63.8)	36 (41.9)	49 (52.1)	28 (32.6)	14 (70.0)	22 (62.9)	9 (45.0)	13 (37.1)
Anemia	29 (30.9)	31 (36.0)	14 (14.9)	15 (17.4)	5 (25.0)	15 (42.9)	2 (10.0)	4 (11.4)
Neutropenia	19 (20.2)	6 (7.0)	15 (16.0)	3 (3.5)	1 (5.0)	2 (5.7)	0	1 (2.9)
Lymphopenia	14 (14.9)	5 (5.8)	12 (12.8)	5 (5.8)	1 (5.0)	0	1 (5.0)	0
Nonhematologic TEAE, n (%)								
Peripheral sensory neuropathy	49 (52.1)	30 (34.9)	3 (3.2)	9 (10.5)	13 (65.0)	17 (48.6)	2 (10.0)	2 (5.7)
Diarrhea	38 (40.4)	13 (15.1)	2 (2.1)	1 (1.2)	11 (55.0)	13 (37.1)	2 (10.0)	0
Upper respiratory tract infection	30 (31.9)	13 (15.1)	2 (2.1)	0	5 (25.0)	7 (20.0)	0	0
Cough	29 (30.9)	13 (15.1)	0	0	10 (50.0)	5 (14.3)	0	0
Fatigue	23 (24.5)	15 (17.4)	6 (6.4)	1 (1.2)	7 (35.0)	14 (40.0)	3 (15.0)	4 (11.4)
Peripheral edema	23 (24.5)	11 (12.8)	1 (1.1)	0	8 (40.0)	4 (11.4)	0	0
Constipation	22 (23.4)	14 (16.3)	0	2 (2.3)	4 (20.0)	12 (34.3)	0	0
Pneumonia	16 (17.0)	9 (10.5)	12 (12.8)	6 (7.0)	5 (25.0)	6 (17.1)	3 (15.0)	6 (17.1)
Bronchitis	14 (14.9)	8 (9.3)	3 (3.2)	3 (3.5)	6 (30.0)	2 (5.7)	2 (10.0)	0
Dizziness	9 (9.6)	9 (10.5)	0	0	5 (25.0)	11 (31.4)	0	0
Bone pain	7 (7.4)	8 (9.3)	2 (2.1)	2 (2.3)	7 (35.0)	2 (5.7)	1 (5.0)	1 (2.9)

TEAE: treatment-emergent adverse event; D-Rd: daratumumab/lenalidomide/dexamethasone; Rd: lenalidomide/dexamethasone; D-Vd: daratumumab/bortezomib/dexamethasone; Vd: bortezomib/dexamethasone. ^aThe safety analysis set included all patients who received ≥1 administration of study treatment.

Table 4. Most common IRR among patients aged 65-74 years and ≥75 years in POLLUX and CASTOR.

TEAE (>5%): POLLUX ^a	65-74 years D-Rd (n=123)		≥75 years D-Rd (n=29)	
	Any grade	Grade 3/4	Any grade	Grade 3/4
Patients with IRR, n (%)	57 (46.3)	6 (4.9)	12 (41.4)	4 (13.8)
Dyspnea	13 (10.6)	1 (0.8)	4 (13.8)	1 (3.4)
Chills	8 (6.5)	0	3 (10.3)	1 (3.4)
Feeling cold	2 (1.6)	0	2 (6.9)	1 (3.4)
Wheezing	3 (2.4)	1 (0.8)	2 (6.9)	1 (3.4)
Vomiting	8 (6.5)	1 (0.8)	2 (6.9)	0
Bronchospasm	7 (5.7)	0	0	0
Cough	7 (5.7)	0	0	0
Nausea	7 (5.7)	0	0	0

TEAE (>5%): CASTOR ^a	65-74 years D-Vd (n=94)		≥75 years D-Vd (n=20)	
	Any grade	Grade 3/4	Any grade	Grade 3/4
Patients with IRR, n (%)	43 (45.7)	8 (8.5)	13 (65.0)	2 (10.0)
Bronchospasm	11 (11.7)	1 (1.1)	4 (20.0)	1 (5.0)
Throat irritation	2 (2.1)	0	4 (20.0)	0
Dyspnea	10 (10.6)	4 (4.3)	3 (15.0)	0
Cough	8 (8.5)	0	3 (15.0)	0
Nausea	6 (6.4)	0	0	0
Hypertension	6 (6.4)	5 (5.3)	0	0
Chills	3 (3.2)	0	2 (10.0)	0

IRR: infusion-related reaction; D-Rd: daratumumab/lenalidomide/dexamethasone; Rd: lenalidomide/dexamethasone; D-Vd: daratumumab/bortezomib/dexamethasone; Vd: bortezomib/dexamethasone. ^aThe safety analysis set included all patients who received ≥1 administration of study treatment.

patients, including 11% CR and 12.5% VGPR. The most common adverse events included peripheral neuropathy (47% of patients), gastrointestinal symptoms (22.2%), thrombocytopenia (11.1%), and anemia (7.4%). Overall, these results are comparable with studies of Vd in younger patients.²³

Sub-analyses of the phase 3 ASPIRE and ENDEAVOR studies demonstrated a benefit for carfilzomib in elderly patients with MM. The ASPIRE study of carfilzomib, lenalidomide, and dexamethasone (KRd) *versus* Rd demonstrated prolonged PFS with KRd in patients with relapsed multiple myeloma aged ≥70 years (median: 23.8 *versus* 16.0 months; HR, 0.75, 95% CI, 0.53-1.08) and an improved ORR (90.3% *versus* 66.1%, respectively).²⁴ While cardiovascular events occurred more frequently in the elderly population compared with patients aged <70 years, KRd demonstrated a favorable benefit-risk profile in elderly patients.²⁵ The ENDEAVOR study of carfilzomib and dexamethasone (Kd) *versus* Vd demonstrated prolonged PFS with Kd in patients with RRMM who received 1 to 3 prior lines of therapy and were aged 65 to 74 years (median: 15.6 *versus* 9.5 months; HR, 0.528, 95% CI, 0.382-0.728) or ≥75 years (median: 18.7 *versus* 8.9 months; HR, 0.383; 95% CI, 0.227-0.647).²⁶ While hypertension was the most common grade ≥3 TEAE in patients aged 65 to 74 years and ≥75 years who received Kd, the safety results were similar to the overall population in ENDEAVOR.

Due to the nature of drug development, clinical trials and regulatory approvals usually proceed with patients with more advanced disease. Ideally, moving these regimens into front-line treatment may provide the best

opportunity for patients to mount prolonged responses and delay relapse. Newly diagnosed elderly patients are usually excluded from receiving stem cell transplants due to their age. The VISTA phase 3 study of bortezomib, melphalan, and prednisone (VMP) established this regimen as a standard of care in transplant-ineligible newly diagnosed MM patients.²⁷ Of interest is whether the benefit of daratumumab-based regimens in RRMM could be extended to these patients. In the phase 3 ALCYONE study, daratumumab in combination with VMP reduced the risk of disease progression or death by 50% compared with VMP alone (HR, 0.50; 95% CI, 0.38-0.65).²⁸ Over 90% of patients were aged ≥65 years, and 30% were aged ≥75 years. In a prespecified subgroup analysis, the HR for the primary endpoint of PFS were similar for patients aged ≥75 years (0.53) and <75 years (0.49). The addition of daratumumab to VMP produced no new safety signals except for a higher rate of infections that resolved with few discontinuations.²⁸ Furthermore, Rd is also a standard treatment regimen for patients with transplant-ineligible newly diagnosed MM. Recently, in the phase 3 MAIA study, D-Rd significantly reduced the risk of disease progression or death and nearly doubled the rate of CR or better.²⁹ MAIA enrolled patients aged ≥65 years, 44% of whom were aged ≥75 years.²⁹

MM is a disease of the elderly with 35 to 40% of patients aged ≥75 years at diagnosis.²² One of the limitations of the current analysis is that the subgroup of patients aged ≥75 years in POLLUX and CASTOR was relatively small (<15% of the overall study population was ≥75 years of age). Comorbidities and other ailments, including frailty, that are often associated with elderly patients may have compro-

mised eligibility for the study, and it is recognized that this is a limitation of many MM studies.³⁰ However, differences in efficacy were still observed between the treatment groups. An additional limitation is that the study did not assess frailty. The IMWG frailty score system which is based on age, comorbidities, and functional status, can be used to predict survival and toxicity, making it a useful metric for determining feasibility of a treatment regimen and for clinical trial design.¹⁹ This metric was adopted after these studies were initiated.

In conclusion, the safety and efficacy of daratumumab in combination with Rd or Vd does not appear to be negatively impacted by age in patients studied in POLLUX and CASTOR, and is consistent with the overall study populations. This subgroup analysis supports the addition of daratumumab to standard-of-care regimens in patients with RRMM, regardless of age.

Acknowledgments

The authors thank the patients who participated in this study, the staff members at the study sites, the data and safety monitoring committee, and staff members who were involved in data collection and analyses.

Funding

These studies (ClinicalTrials.gov Identifiers: NCT02076009 and NCT02136134) were sponsored by Janssen Research & Development, LLC. The data sharing policy of Janssen Pharmaceutical Companies of Johnson & Johnson is available at <https://www.janssen.com/clinical-trials/transparency>. As noted on this site, requests for access to the study data can be submitted through Yale Open Data Access (YODA) Project site at <http://yoda.yale.edu>. Editorial and medical writing support were provided by Kristin Runkle, PhD, of MedErgy, and were funded by Janssen Global Services, LLC.

References

- Madan S, Kumar S. Current treatment options for elderly patients with multiple myeloma: clinical impact of novel agents. *Therapy*. 2011;3(4):415-429.
- Howlader N, Noone AM, Krapcho M, et al. SEER Cancer Statistics Review, 1975-2014. National Cancer Institute. 2017.
- Kumar SK, Rajkumar SV, Dispenzieri A, et al. Improved survival in multiple myeloma and the impact of novel therapies. *Blood*. 2008;111(5):2516-2520.
- Palumbo A, Bringhen S, Ludwig H, et al. Personalized therapy in multiple myeloma according to patient age and vulnerability: a report of the European Myeloma Network (EMN). *Blood*. 2011;118(17):4519-4529.
- Ludwig H, Bolejack V, Crowley J, et al. Survival and years of life lost in different age cohorts of patients with multiple myeloma. *J Clin Oncol*. 2010;28(9):1599-1605.
- Willan J, Eyre TA, Sharpley F, Watson C, King AJ, Ramasamy K. Multiple myeloma in the very elderly patient: challenges and solutions. *Clin Interv Aging*. 2016;11:423-435.
- de Weers M, Tai YT, van der Veer MS, et al. Daratumumab, a novel therapeutic human CD38 monoclonal antibody, induces killing of multiple myeloma and other hematological tumors. *J Immunol*. 2011;186(3):1840-1848.
- Lammerts van Bueren J, Jakobs D, Kaldenhoven N, et al. Direct in vitro comparison of daratumumab with surrogate analogs of CD38 antibodies MOR03087, SAR650984 and Ab79. *Blood*. 2014;124(21):3474.
- Overdijk MB, Verploegen S, Bogels M, et al. Antibody-mediated phagocytosis contributes to the anti-tumor activity of the therapeutic antibody daratumumab in lymphoma and multiple myeloma. *MAbs*. 2015;7(2):311-321.
- Overdijk MB, Jansen JH, Nederend M, et al. The therapeutic CD38 monoclonal antibody daratumumab induces programmed cell death via Fcγ receptor-mediated cross-linking. *J Immunol*. 2016;197(3):807-813.
- Krejci J, Casneuf T, Nijhof IS, et al. Daratumumab depletes CD38+ immune-regulatory cells, promotes T-cell expansion, and skews T-cell repertoire in multiple myeloma. *Blood*. 2016;128(3):384-394.
- Chiu C, Casneuf T, Axel A, et al. Daratumumab in combination with lenalidomide plus dexamethasone induces clonality increase and T-cell expansion: results from a phase 3 randomized study (POLLUX). *Blood*. 2016;128(22):4531.
- Adams HC, III, Stevenaert F, Krejci J, et al. High-parameter mass cytometry evaluation of relapsed/refractory multiple myeloma patients treated with daratumumab demonstrates immune modulation as a novel mechanism of action. *Cytometry A*. 2019;95(3):279-289.
- Dimopoulos MA, Oriol A, Nahi H, et al. Daratumumab, lenalidomide, and dexamethasone for multiple myeloma. *N Engl J Med*. 2016;375(14):1319-1331.
- Palumbo A, Chanan-Khan A, Weisel K, et al. Daratumumab, bortezomib, and dexamethasone for multiple myeloma. *N Engl J Med*. 2016;375(8):754-766.
- Blair HA. Daratumumab: a review in relapsed and/or refractory multiple myeloma. *Drugs*. 2017;77(18):2013-2024.
- Durie BGM, Harousseau JL, Miguel JS, et al. International uniform response criteria for multiple myeloma. *Leukemia*. 2006;20(9):1467-1473.
- Rajkumar SV, Harousseau JL, Durie B, et al. Consensus recommendations for the uniform reporting of clinical trials: report of the International Myeloma Workshop Consensus Panel 1. *Blood*. 2011;117(18):4691-4695.
- Palumbo A, Bringhen S, Mateos MV, et al. Geriatric assessment predicts survival and toxicities in elderly myeloma patients: an International Myeloma Working Group report. *Blood*. 2015;125(13):2068-2074.
- Dimopoulos M, San Miguel J, Belch A, et al. Daratumumab plus lenalidomide and dexamethasone versus lenalidomide and dexamethasone in relapsed/refractory multiple myeloma: updated analysis of POLLUX. *Haematologica*. 2018; 103(12):2088-2096.
- Spencer A, Lentzsch S, Weisel K, et al. Daratumumab plus bortezomib and dexamethasone versus bortezomib and dexamethasone in relapsed or refractory multiple myeloma: updated analysis of CASTOR. *Haematologica*. 2018;103(12):2079-2087.
- Zweegman S, Palumbo A, Bringhen S, Sonneveld P. Age and aging in blood disorders: multiple myeloma. *Haematologica*. 2014;99(7):1133-1137.
- Castelli R, Pantaleo G, Gallipoli P, et al. Salvage therapy with bortezomib and dexamethasone in elderly patients with relapsed/refractory multiple myeloma. *Anticancer Drugs*. 2015;26(10):1078-1082.
- Dimopoulos MA, Stewart AK, Masszi T, et al. Carfilzomib, lenalidomide, and dexamethasone in patients with relapsed multiple myeloma categorised by age: secondary analysis from the phase 3 ASPIRE study. *Br J Haematol*. 2017;177(3):404-413.
- Dimopoulos MA, Stewart AK, Masszi T, et al. Carfilzomib-lenalidomide-dexamethasone vs lenalidomide-dexamethasone in relapsed multiple myeloma by previous treatment. *Blood Cancer J*. 2017;7(4):e554.
- Nievesvizky R, Ludwig H, Spencer A, et al. Overall survival of relapsed/refractory multiple myeloma patients treated with carfilzomib and dexamethasone vs bortezomib and dexamethasone: results from the phase 3 endeavor study according to age subgroup. Presented at the 59th Annual Meeting & Exposition; December 9-12, 2017; Atlanta, GA.: 1885.
- San Miguel JF, Schlag R, Khuageva NK, et al. Bortezomib plus melphalan and prednisone for initial treatment of multiple myeloma. *N Engl J Med*. 2008;359(9):906-917.
- Mateos MV, Dimopoulos MA, Cavo M, et al. Daratumumab plus bortezomib, melphalan, and prednisone for untreated myeloma. *N Engl J Med*. 2018;378(6):518-528.
- Facon T, Kumar S, Plesner T, et al. Daratumumab plus lenalidomide and dexamethasone for untreated myeloma. *N Engl J Med*. 2019;380(22):2104-2115.
- Richardson PG, San Miguel JF, Moreau P, et al. Interpreting clinical trial data in multiple myeloma: translating findings to the real-world setting. *Blood Cancer J*. 2018;8(11):109.



Ferrata Storti Foundation

Ibrutinib induces multiple functional defects in the neutrophil response against *Aspergillus fumigatus*

Damien Blez,^{1,*} Marion Blaize,^{1,*} Carole Soussain,² Alexandre Boissonnas,¹ Aïda Meghraoui-Kheddar,¹ Natacha Menezes,³ Anaïs Portalier,⁴ Christophe Combadière,¹ Véronique Leblond,^{1,4} David Ghez^{5,b} and Arnaud Fekkar^{1,3,b}

¹Sorbonne Université, INSERM, CNRS, Centre d'Immunologie et des Maladies Infectieuses, Cimi-Paris, Paris; ²Hématologie, Institut Curie - Site de Saint-Cloud, Saint-Cloud; ³Service de Parasitologie Mycologie, Assistance Publique – Hôpitaux de Paris (AP-HP), Groupe Hospitalier Pitié-Salpêtrière, Paris; ⁴Service d'Hématologie, AP-HP, Groupe Hospitalier Pitié-Salpêtrière, Paris and ⁵Département d'Hématologie, Gustave Roussy, Villejuif, France

*DB and MB contributed equally to the work.

^bDG and AF share senior co-authorship.

Haematologica 2020
Volume 105(2):478-489

ABSTRACT

The Bruton tyrosine kinase inhibitor ibrutinib has become a leading therapy against chronic lymphoid leukemia. Recently, ibrutinib has been associated with the occurrence of invasive fungal infections, in particular invasive aspergillosis. The mechanisms underlying the increased susceptibility to fungal infections associated with exposure to ibrutinib are currently unknown. Innate immunity, in particular polymorphonuclear neutrophils, represents the cornerstone of anti-*Aspergillus* immunity; however, the potential impact of ibrutinib on neutrophils has been little studied. Our study investigated the response to *Aspergillus fumigatus* and neutrophil function in patients with chronic lymphoid leukemia or lymphoma, who were undergoing ibrutinib therapy. We studied the consequences of ibrutinib exposure on the functions and anti-*Aspergillus* responses of neutrophils obtained from healthy donors and 63 blood samples collected at different time points from 32 patients receiving ibrutinib for lymphoid malignancies. We used both flow cytometry and video-microscopy approaches to analyze neutrophils' cell surface molecule expression, cytokine production, oxidative burst, chemotaxis and killing activity against *Aspergillus*. Ibrutinib is associated, both *in vitro* and in patients under treatment, with multiple functional defects in neutrophils, including decreased production of reactive oxygen species, impairment of their capacity to engulf *Aspergillus* and inability to efficiently kill germinating conidia. Our results demonstrate that ibrutinib-exposed neutrophils develop significant functional defects that impair their response against *Aspergillus fumigatus*, providing a plausible explanation for the emergence of invasive aspergillosis in ibrutinib-treated patients.

Correspondence:

ARNAUD FEKKAR
arnaud.fekkar@aphp.fr

Received: February 15, 2019.

Accepted: June 6, 2019.

Pre-published: June 6, 2019.

doi:10.3324/haematol.2019.219220

Check the online version for the most updated information on this article, online supplements, and information on authorship & disclosures: www.haematologica.org/content/105/2/478

©2020 Ferrata Storti Foundation

Material published in *Haematologica* is covered by copyright. All rights are reserved to the Ferrata Storti Foundation. Use of published material is allowed under the following terms and conditions:

<https://creativecommons.org/licenses/by-nc/4.0/legalcode>. Copies of published material are allowed for personal or internal use. Sharing published material for non-commercial purposes is subject to the following conditions: <https://creativecommons.org/licenses/by-nc/4.0/legalcode>, sect. 3. Reproducing and sharing published material for commercial purposes is not allowed without permission in writing from the publisher.



Introduction

Bruton tyrosine kinase (BTK), a member of the TEC kinase family, plays a key role in the signaling pathway of the B-cell receptor, which controls B-cell development, activation and proliferation. In humans, inactivating BTK mutations are responsible for a maturation block in early B-cell development at the pro-B-cell stage which results in a nearly complete absence of B cells and agammaglobulinemia, a disease known as X-linked agammaglobulinemia (XLA).¹ Ibrutinib, a small covalent BTK inhibitor, has ushered a new era in the therapeutic strategy for chronic lymphocytic leukemia and displays interesting clinical efficacy in other types of lymphoid malignancies.² Recently, ibrutinib has been linked to the occur-

rence of invasive fungal infections, in particular invasive aspergillosis with an unusually high number of cases with central nervous system involvement.³⁻⁵ This association was somewhat unexpected since invasive fungal infections do not belong to the spectrum of infections observed in patients with XLA and patients with chronic lymphocytic leukemia are considered to be at low-risk of invasive aspergillosis.⁶

It has been known for decades that neutrophils represent the major effectors in the host's defense mechanisms against *Aspergillus*.^{7,8} Quantitative and qualitative (e.g. NADPH oxidase component deficiency in chronic granulomatous disease) defects affecting neutrophils are among the most important risk factors for developing invasive aspergillosis.^{7,9} BTK has been extensively studied in B cells but data on its role in neutrophils are limited. Although previous work indicates that BTK is expressed by neutrophils and plays a role in neutrophil development and function,¹⁰ very little is known about the potential effect of BTK or its inhibition on antifungal immunity.¹¹

This prompted us to test the hypothesis that ibrutinib administration might impair neutrophil responses against *Aspergillus*. We performed *in vitro* experiments on neutrophils from healthy donors and analyzed neutrophil functions in patients receiving ibrutinib at different time points during the course of treatment. Here we show that ibrutinib treatment is associated with multiple defects in neutrophil functions, in particular decreased CD11b surface expression, reduction of reactive oxygen species (ROS) production and impairment of the cells' capacity to kill *Aspergillus fumigatus*.

Methods

Patients

Thirty-three patients from three centers treated with ibrutinib for a lymphoid malignancy were enrolled in the study (Table 1). The main indications for ibrutinib treatment were chronic lymphocytic leukemia (n=23; 72% of patients) and mantle-cell lymphoma (n=4; 12.5% of patients). Patients receiving corticoid therapy or granulocyte colony-stimulating factors were not considered. Neutrophils were collected from patients just before ibrutinib treatment was initiated (M0; n=23) then approximately 1 month (M1; n=22) and 3 months later (M3; n=18). No patient was neutropenic. Because a complete longitudinal (M0, M1 and M3) follow up could not be obtained in all patients, the sample size varies between experiments and time points. No available data have been subtracted. No cases of invasive aspergillosis were diagnosed throughout the study.

Neutrophil isolation

Neutrophils were isolated using the dextran-Ficoll method, as detailed in the *Online Supplement*.

Stimulation conditions

Whole-blood samples (500 µL) were stimulated for 2 h at 37°C with either 10⁶ germinating conidia from an *Aspergillus fumigatus sensu stricto* clinical isolate or 5 ng/mL bacterial lipopolysaccharide (LPS) (Sigma Aldrich) or phosphate-buffered saline (PBS) as a control. Details are provided in the *Online Supplement*.

Surface molecule expression of neutrophils

For cytometry analysis anti-human antibodies directed against the following human antigens were used: CD11b, CD14, CD15,

Table 1. Characteristics of patients and blood samples included in the study.

Characteristics		Before ibrutinib therapy	Month 1	Month 3
Numbers of patients		23	22	18
Mean age in years [range]		69.9 [54-85]	66.9 [41-86]	66.1 [41-84]
Male/female sex		13/10	14/8	11/7
Disease: n (%)	Chronic lymphocytic leukemia	19	18	14
	Mantle-cell lymphoma	2	3	2
	Other lymphoid malignancies ^a	2	1	2
	280		1	2
Dosage of ibrutinib (mg/day)	420	not applicable	17	13
	560		4	3
Number of therapeutic lines before ibrutinib: mean [range]		1.8 [1-6]	1.8 [1-6]	1.8 [1-6]
	RFC ^b	7	6	5
Last therapeutic line before ibrutinib administration	R BENDA ^c	8	6	3
	R CHOP ^d	1	3	1
	R MTX ARA-C ^e	2	1	1
	Others	5	6	8
	< 6 months	4	5	4
Delay between the last therapeutic line and the start of ibrutinib therapy	6 months - 12 months	0	1	1
	12 months - 60 months	12	9	5
	> 60 months	7	7	8
Time to ibrutinib initiation: mean / median [range] (days)		not applicable	34.2 / 34 [18-62]	105 / 97 [76-161]
Neutrophil count: mean (cells/µL) [range]		5 388 [1 180-15 200]	4 945 [120-13 800]	3 145 [390-6 470]
Lymphocytes count: mean (cells/µL) [range]		22 890 [590-57 700]	45 426 [400-148 226]	37 195 [1 200-122 930]

^aOther lymphoid malignancies included primary central nervous system lymphoma (n=2), diffuse large B-cell lymphoma (n=1), intraocular lymphoma (n=1) and Waldenström macroglobulinemia; ^bRFC: rituximab-fludarabine-cyclophosphamide; ^cR BENDA: rituximab plus bendamustine; ^dR CHOP: rituximab plus cyclophosphamide, doxorubicin, vincristine, and prednisone or prednisolone; ^eR MTX ARA-C: rituximab plus methotrexate and cytarabine.

CD16, CD62L, Dectin 1, TLR2 and TLR4 (BD Biosciences) and CD66b (Biolegend).

Measurement of neutrophil oxidative burst

Neutrophils contained in 500 μ L heparinized whole-blood samples were incubated with 123-dihydro-rhodamine (Life Technologies) for 5 min at 37°C, then stimulated with the aforementioned stimuli for 2 h at 37°C.

Intracellular cytokine analysis

Whole-blood samples (500 μ L) were stimulated with the above-mentioned stimuli for 4 h at 37°C. Brefeldin A (Sigma-Aldrich) was added after 30 min of stimulation. Cells were stained with membrane antibodies, permeabilized using the Intracellular Fixation & Permeabilisation Buffer Set (eBioscience) and stained with the following anti-human antibodies: interleukin (IL)-8, IL-6, tumor necrosis factor alpha (TNF α) (BD Biosciences) and IL-1 β (R&D Systems). The concentration of IL-8 was determined using a Duo-Set enzyme-linked immunosorbent assay kit from R&D Systems (Minneapolis, MN, USA).

Video-microscopy experiments

Three thousand *Aspergillus fumigatus* conidia were seeded in black, 96-well clear-bottom plates (Greiner) and allowed to germinate. After two washes, 48,000 isolated neutrophils in RPMI medium and Sytox green (final concentration 2 μ M) were added. Interactions were visualized during 16 h of co-culture at 37°C using a Zeiss Axio Z1 fluorescent microscope (Carl Zeiss, Germany). Images were processed and analyzed using Imaris[®] software. The chemotaxis assay was performed using IncuCyte[®] ClearView 96-Well Chemotaxis Plates. Purified neutrophils stained by Hoechst (final concentration 10 μ M) were placed in the membrane insert and formyl-methionine-leucyl-phenylalanine (fMLP), as a chemo-attractant (final concentration 10 μ M), was put in the reservoir plate. More details are given in the *Online Supplement*.

Statistical analysis

GraphPad Prism 6 was used for statistical analyses (GraphPad software, La Jolla, CA, USA).

Ethics

This non-interventional study was performed in accordance with national regulations regarding the use of human material from healthy volunteers and patients. The local medical ethics committee (CPP Ile de France IV) approved the study, which was conducted in accordance with the principles of the Declaration of Helsinki. Signed informed consent to participation in the study was obtained from all patients.

Results

Effect of ibrutinib on CD11b, CD62L and Dectin-1 expression on neutrophils

Neutrophils were gated according to size and granularity by forward *versus* side scatter (FSC *vs.* SSC) and identified as CD66b⁺, CD15⁺, CD16^{+/low}, CD14⁻ cells (Figure 1A). Surface expression of CD11b and CD62L (L-selectin) was evaluated at baseline then following stimulation by germinating conidia or LPS. In association with CD18 (β 2 integrin), CD11b forms the heterodimeric integrin complement receptor 3 (CR3), also called macrophage-1 antigen, which is not only involved in the adhesion and migration of leukocytes but has also been

recognized as a major receptor for β -glucan.¹² CD11b is overexpressed at the surface of neutrophils after degranulation as it is contained in secondary and tertiary neutrophil granules.¹³ CD62L is involved in transient tethering of the neutrophils to the endothelial surface. Shedding of CD62L marks activation of neutrophils. As previously reported,¹⁴ germinating conidia and LPS induced significant activation of neutrophils, as evidenced by an increase in CD11b and a decrease in CD62L expression (Figure 1B and *data not shown*). Expressed as mean fluorescence intensity (MFI), mean CD11b surface expression of the M0 group increased 2-fold after stimulation with germinating conidia (9,053 *vs.* 4,414) and by 3-fold after LPS stimulation (13,392 *vs.* 4,414). CD11b surface expression on unstimulated neutrophils decreased after starting ibrutinib treatment (n=17 patients) in comparison with the expression prior to treatment initiation (n=17 patients) (Figure 1B). However, no statistically significant difference was observed when a paired analysis of eight patients sampled at M0, M1 and M3 was done (Figure 1C). After stimulating whole blood with germinating conidia, the increase of CD11b surface expression in M1 patients was statistically not different from that of the M0 group. Expressed as MFI, mean CD11b surface expression of the M1 group increased 3.3-fold after germinating conidia stimulation (6,857 *vs.* 2,070) and by 6-fold after LPS stimulation (12,394 *vs.* 2,070). Basal CD62L expression tended to increase over time with a statistically significant difference between M0 and M3 (Figure 1D) but CD62L shedding following stimulation by germinating conidia did not change over time (Figure 1E). Paired analysis of six patients sampled at M0, M1 and then M3 indicated no difference over time (Figure 1F). We also analyzed basal expression of Dectin-1, TLR2 and TLR4, which play important roles in antifungal defenses.^{15,16} Dectin-1 expression decreased over time but the difference was not statistically significant. No difference was observed for TLR2 and TLR4 (Figure 1G and *data not shown*). Collectively, these results suggest that neutrophils from patients receiving ibrutinib slightly altered CD11b surface expression but no other important immune receptors. In addition, ibrutinib-exposed neutrophils seemed to maintain their ability to trigger a marked response to *Aspergillus* and LPS stimuli.

Reactive oxygen species production after *Aspergillus* challenge is decreased in patients receiving ibrutinib

As previously reported,¹⁴ ROS production increased after 2 h of stimulation by germinating conidia or LPS plus fMLP (Figure 2A). ROS production by neutrophils sampled at M1 was statistically lower for all conditions, i.e. PBS control, *Aspergillus* stimulation and LPS stimulation (Figure 2A, B). Expressed as MFI, mean ROS production decreased at M1 by 51.5% for the basal PBS condition (2,333 *vs.* 1,131; $P < 0.05$), 51% after stimulation with germinating conidia (9,330 *vs.* 4,569; $P < 0.05$) and 31.6% after LPS stimulation (4,008 *vs.* 2,742; $P < 0.05$) in comparison with M0. The defect in ROS production persisted in neutrophils at M3. Paired analysis of samples collected at M0 and M1 after stimulation with germinating conidia or LPS was achievable in 12 and 9 patients, respectively. As shown in Figure 2C, ROS production decreased markedly after 1 month of ibrutinib treatment both before and after stimulation by *Aspergillus* conidia or LPS.

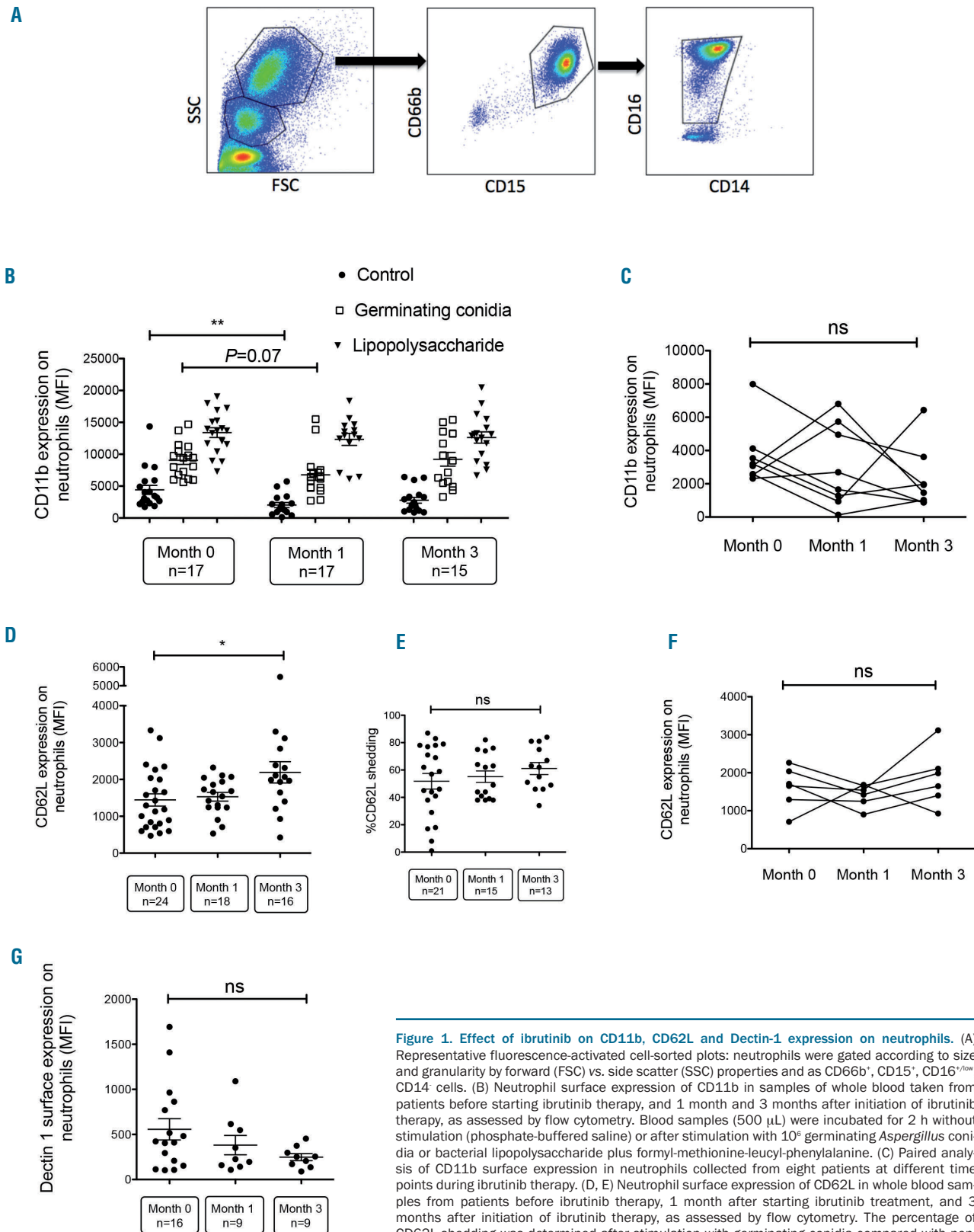


Figure 1. Effect of ibrutinib on CD11b, CD62L and Dectin-1 expression on neutrophils. (A) Representative fluorescence-activated cell-sorted plots: neutrophils were gated according to size and granularity by forward (FSC) vs. side scatter (SSC) properties and as CD66b⁺, CD15⁺, CD16^{+/low}, CD14⁺ cells. (B) Neutrophil surface expression of CD11b in samples of whole blood taken from patients before starting ibrutinib therapy, and 1 month and 3 months after initiation of ibrutinib therapy, as assessed by flow cytometry. Blood samples (500 μ L) were incubated for 2 h without stimulation (phosphate-buffered saline) or after stimulation with 10^8 germinating *Aspergillus* conidia or bacterial lipopolysaccharide plus formyl-methionine-leucyl-phenylalanine. (C) Paired analysis of CD11b surface expression in neutrophils collected from eight patients at different time points during ibrutinib therapy. (D, E) Neutrophil surface expression of CD62L in whole blood samples from patients before ibrutinib therapy, 1 month after starting ibrutinib treatment, and 3 months after initiation of ibrutinib therapy, as assessed by flow cytometry. The percentage of CD62L shedding was determined after stimulation with germinating conidia compared with non-stimulated cells. (F) Paired analysis of CD62L surface expression in neutrophils collected from six patients at different time points during ibrutinib therapy. (G) Neutrophil surface expression of Dectin-1 in whole blood taken from patients before ibrutinib therapy, 1 month after treatment initiation and 3 months after initiation of ibrutinib therapy, as assessed by flow cytometry. Long bars represent the mean fluorescence intensity (MFI), and short bars represent the standard error of the mean. Multiple groups were analyzed using the Kruskal-Wallis test with the Dunn multiple comparison post-test. Paired data were analyzed using the Friedman test. * $P < 0.05$; ** $P < 0.01$; ns: non-significant.

Neutrophils from ibrutinib-treated patients fail to produce interleukin-8 upon *Aspergillus* stimulation

We evaluated intracellular production of IL-1 β , IL-6, TNF α and IL-8 by neutrophils in whole blood by flow cytometry. In our experimental conditions, we did not detect changes in IL-1 β , IL-6 or TNF α either before or after *Aspergillus* or LPS challenge over time (*data not*

shown). We next focused on IL-8, a major chemoattractant for neutrophils. As shown in Figure 3A, the mean percentage of IL-8-positive cells increased 4.7-fold (20.1% vs. 4.3%) and 9.7-fold (41.7% vs. 4.3%) after stimulation for 4 h with LPS or germinating conidia, respectively (Figure 3A). The percentage of IL-8-positive cells decreased in the M1 group in comparison with the M0 group for all condi-

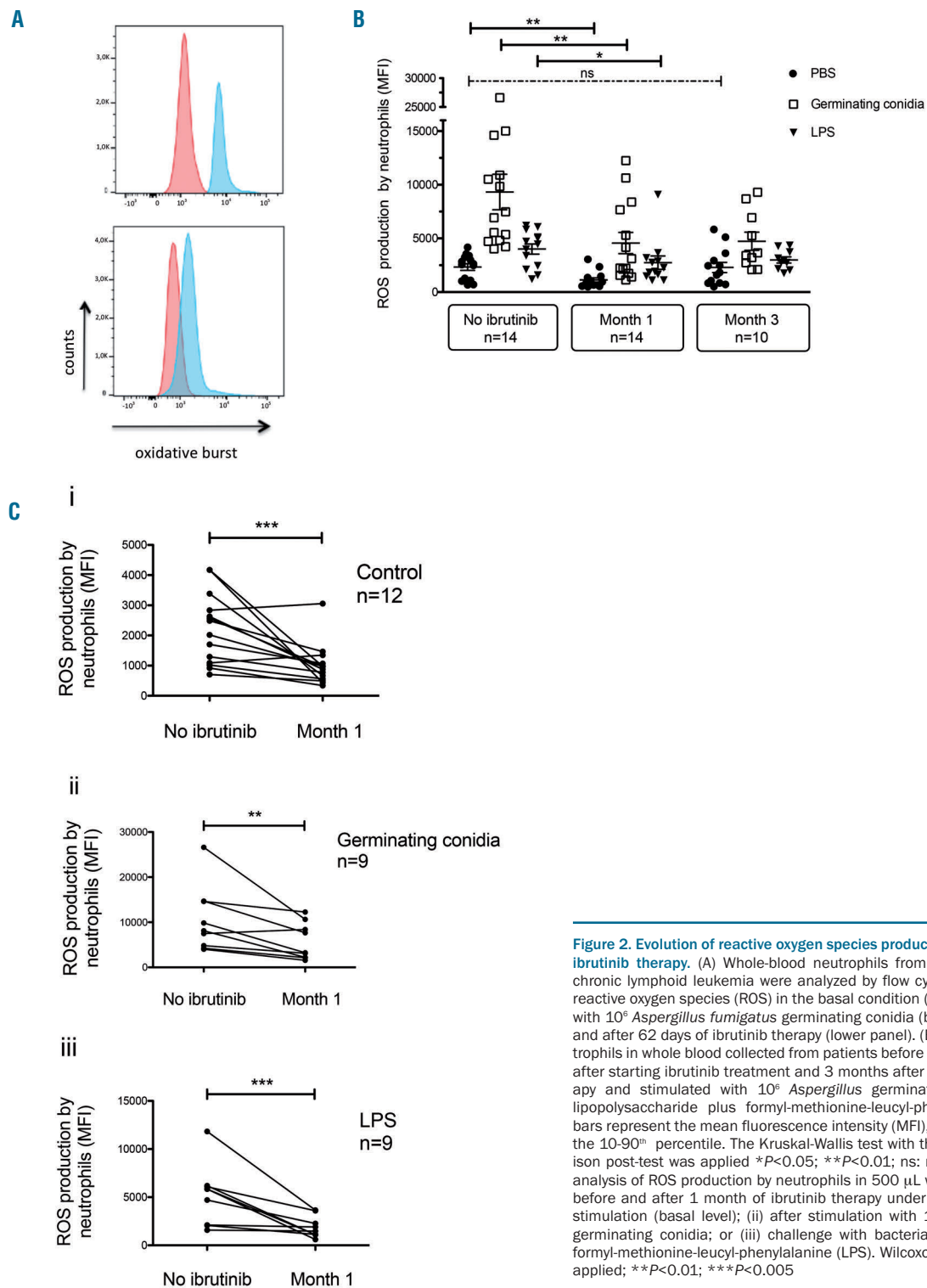


Figure 2. Evolution of reactive oxygen species production by neutrophils during ibrutinib therapy. (A) Whole-blood neutrophils from a 61-year old man with chronic lymphoid leukemia were analyzed by flow cytometry for production of reactive oxygen species (ROS) in the basal condition (red) and after stimulation with 10^6 *Aspergillus fumigatus* germinating conidia (blue) before (upper panel) and after 62 days of ibrutinib therapy (lower panel). (B) ROS production by neutrophils in whole blood collected from patients before ibrutinib therapy, 1 month after starting ibrutinib treatment and 3 months after initiation of ibrutinib therapy and stimulated with 10^6 *Aspergillus* germinating conidia or bacterial lipopolysaccharide plus formyl-methionine-leucyl-phenylalanine (LPS). Long bars represent the mean fluorescence intensity (MFI), and short bars represent the 10-90th percentile. The Kruskal-Wallis test with the Dunn multiple comparison post-test was applied * P <0.05; ** P <0.01; ns: non-significant. (C) Paired analysis of ROS production by neutrophils in 500 μ L whole blood from patients before and after 1 month of ibrutinib therapy under various conditions: (i) no stimulation (basal level); (ii) after stimulation with 10^6 *Aspergillus fumigatus* germinating conidia; or (iii) challenge with bacterial lipopolysaccharide plus formyl-methionine-leucyl-phenylalanine (LPS). Wilcoxon matched pairs test was applied; ** P <0.01; *** P <0.005

tions (control, germinating conidia and LPS). and was not modified when comparing the M1 to M3 group. We next measured the concentration of IL-8 in whole blood collected from at M0, M1 and M3 and infected for 2 h by *A. fumigatus* germinating conidia. These results confirmed that ibrutinib therapy was related to a decrease of IL-8 production after *Aspergillus* challenge in the M1 group (Figure 3B).

Ibrutinib has no effect on neutrophil mobility and chemotaxis

Because migration to infected sites is a prerequisite to mounting an efficient anti-fungal response, we tested the ability of neutrophils to react to the chemoattractant fMLP (Figure 4A). Percentage of chemotaxis was defined as the number of neutrophils that reached the pore against the total number of neutrophils in the surrounding area. As shown in Figure 4B, neutrophils derived from

treated and untreated patients displayed similar capacity to reach the reservoir containing fMLP, demonstrating that ibrutinib treatment did not alter the ability of neutrophils to migrate and respond to the fMLP signal.

Engulfment and killing of *Aspergillus fumigatus* by neutrophils are impaired in patients receiving ibrutinib

Video-microscopy was used to investigate the behavior of neutrophils and fungi (at the germinating conidia stage) as well as their interactions. Preliminary experiments using *Aspergillus* exposed to voriconazole, an antifungal drug with fungicidal activity against *Aspergillus*, indicated that dying *Aspergillus* stained transiently with Sytox green dye. As opposed to human cells, the fluorescence of the dead fungi was lost after approximately 15-20 min (*data not shown*). We therefore determined *Aspergillus* killing as the Sytox staining of the fungus and its inability to grow

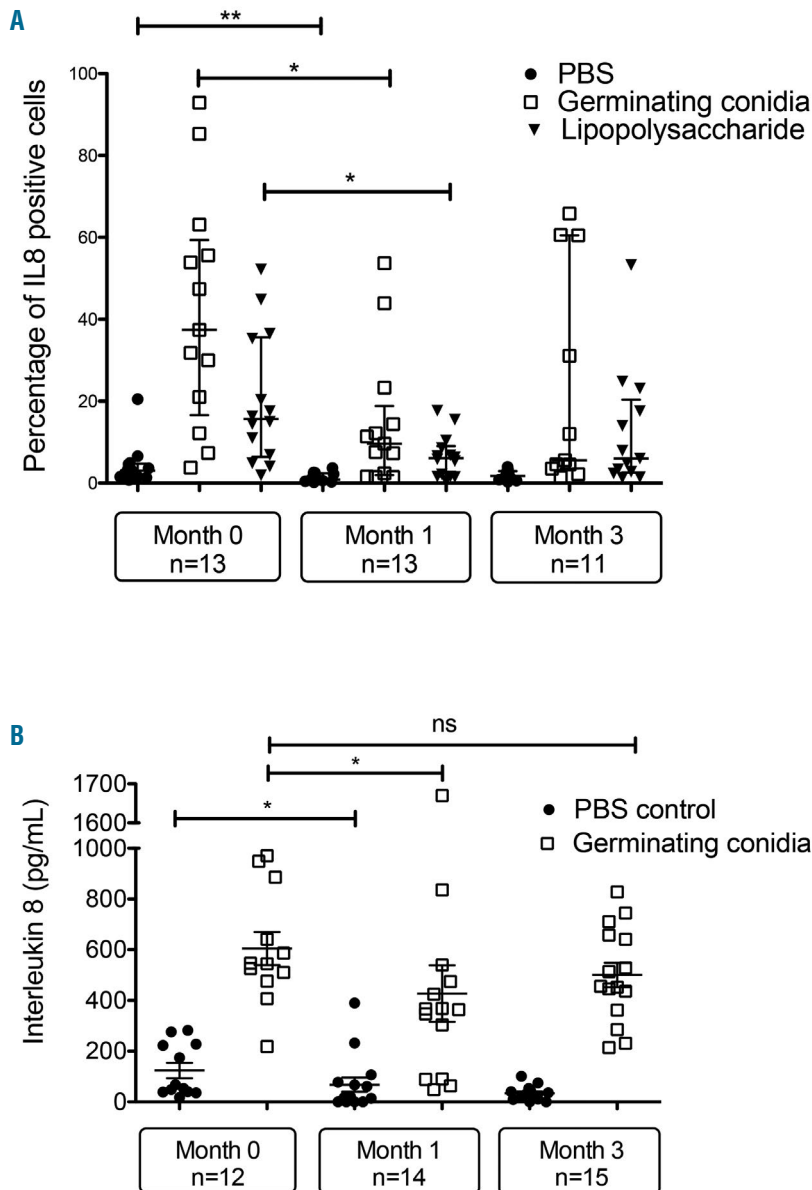


Figure 3. Production of interleukin 8 by neutrophils is impaired during ibrutinib therapy. (A) Neutrophils from whole blood taken from patients before ibrutinib treatment, and 1 and 3 months after starting ibrutinib therapy were untreated (exposed to phosphate-buffered saline, PBS), or stimulated with *Aspergillus* germinating conidia or lipopolysaccharide for 4 h at 37 °C. Brefeldin A was added after 30 min of stimulation. Cells were stained with membrane antibodies, permeabilized, stained with interleukin 8 (IL-8) antibody and then analyzed by flow cytometry. The results are expressed as the percentage of positive cells. (B) Whole blood samples were stimulated with *Aspergillus* germinating conidia for 2 h. The supernatants were collected and tested for IL8 concentration.

further. Because killing germinating conidia requires close contact, we focused on germinating conidia engulfed by neutrophils and calculated the percentage of killing as the number of dying *Aspergillus* as a proportion of the whole number of germinating conidia engulfed by neutrophils.

Aspergillus killing proceeds in two steps. First, neutrophils engulf i.e. deform and bind firmly to *Aspergillus*, next they prevent its growth and ultimately they kill the fungus 60 to 120 min later (Figure 5A). First, we found that the proportion of neutrophils that could engulf *Aspergillus* decreased after 1 and 3 months of treatment with ibrutinib (Figure 5B). This defect was restored when *Aspergillus* conidia were opsonized by addition of human autologous serum (Figure 5B). Strikingly, exposure to

ibrutinib was associated with a major impairment of the ability of neutrophils to kill *Aspergillus*. The percentage of germinating conidia killed by neutrophils fell from 50% at M0 to 1% at M1 and 0.8% at M3 (Figure 5C, D). Opsonization by autologous serum had no effect on the killing defect (Figure 5D).

Neutrophils exposed to ibrutinib *in vitro* have altered responses to *Aspergillus*

Similar experiments were conducted on neutrophils obtained from healthy donors. Addition of ibrutinib was associated with decreased cell surface expression of CD11b both at baseline (8,143 vs. 4,396; 46% decrease; $P < 0.05$) and after challenge with germinating conidia (13,298 vs. 9,811;

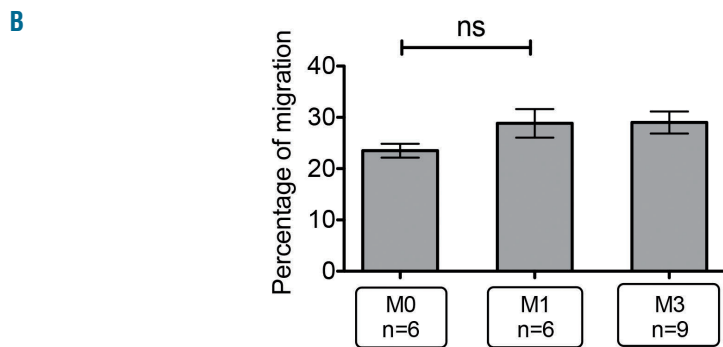
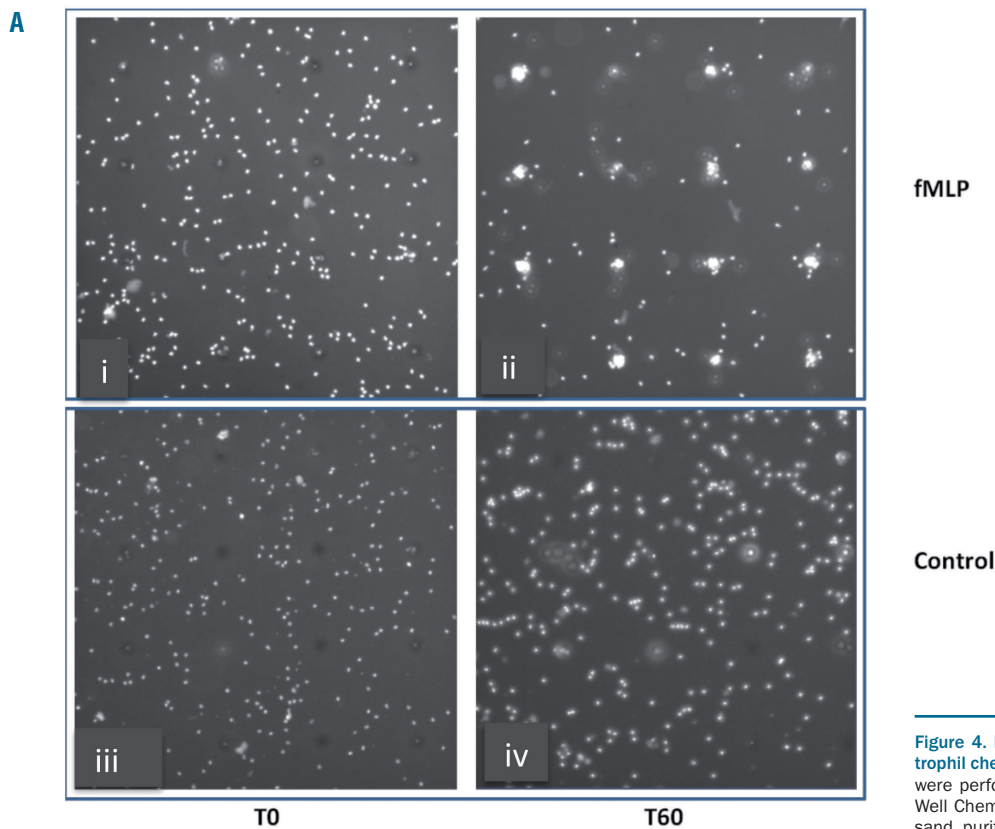


Figure 4. Ibrutinib therapy does not alter neutrophil chemotaxis. Neutrophil migration assays were performed using IncuCyte® ClearView 96-Well Chemotaxis Plates (BioScience). Ten thousand purified neutrophils were aliquoted into the membrane insert, while formyl-methionine-leucyl-phenylalanine (fMLP) was added to the reservoir plate. Migration of neutrophils towards the reservoir from the insert was observed in real time over the course of 60 min. The migration index was defined as the proportion of neutrophils migrating into the pore compared with all neutrophils crossing a square zone of 260 x 260 μm centered by the pore of interest. (A) At the beginning of the experiment (T0), the presence of fMLP (i) led to migration of neutrophils towards the pore after 60 minutes (T60) (ii), whereas the vehicle control has no effect (iii, iv). (B) Neutrophils collected from patients before (M0) or after 1 month (M1) and 3 months (M3) of ibrutinib therapy were submitted to the chemotaxis assay. Statistical analysis was performed by applying the Kruskal Wallis test with the Dunn multiple comparison post-test. ns: non-significant.

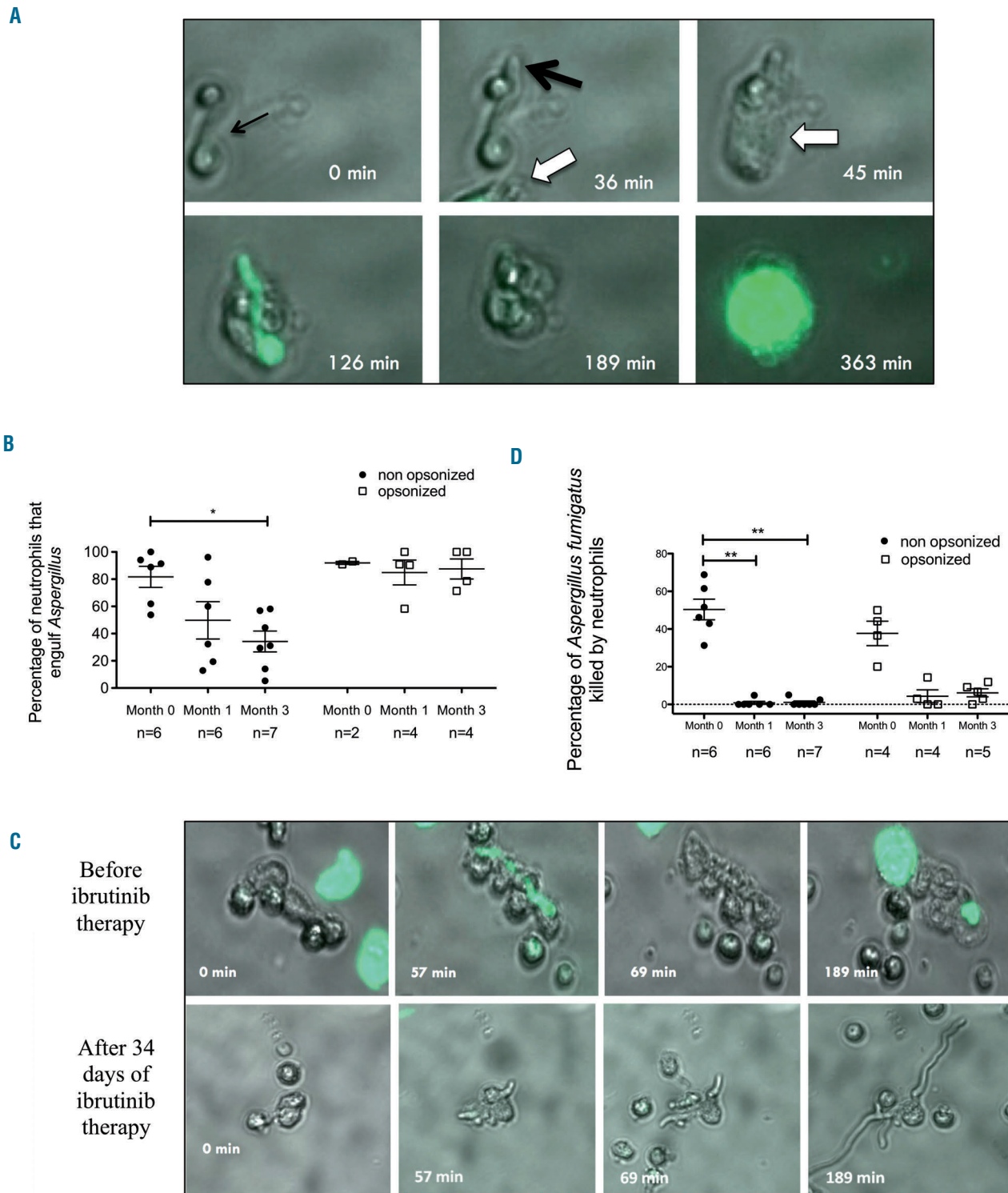


Figure 5. Engulfment and killing of *Aspergillus fumigatus* by neutrophils is impaired in patients receiving ibrutinib. Neutrophil-*Aspergillus fumigatus* interactions were tracked in real-time by video-microscopy during co-culture for 16 h. Three thousand *Aspergillus fumigatus* conidia were first allowed to germinate in a 96-well plate before 48,000 purified neutrophils were added. For opsonized conditions, autologous serum was added for 15 min and then removed before neutrophils were added. (A) The time sequence shows elongation of one germinating conidium (black arrows; time: 0 to 36 min after the start of experiment) before engulfment by a neutrophil from a patient with lymphoid malignancy prior to ibrutinib therapy (white arrow; time: 45 min). The neutrophil kills the *Aspergillus* conidium (as indicated by the fungus stained with Sytox green) after approximately 80 min of close non-discontinuous interactions. Approximately 4 h after killing the fungus, the neutrophil dies (time: 363 min). (B) Percentage of *Aspergillus fumigatus* engulfed by neutrophils in patient samples before ibrutinib therapy and 1 or 3 months after the start of ibrutinib therapy, with or without previous opsonization with autologous serum. The Kruskal-Wallis test with the Dunn multiple comparison post-test were applied; $*P < 0.05$. (C) Comparison of two different time sequences of a sample from a single patient with chronic lymphoid leukemia before ibrutinib therapy (upper) and after 34 days of ibrutinib therapy (lower). In the sample taken after ibrutinib treatment, the inability of the neutrophil to kill the germinating conidia led to uncontrolled fungal growth. (D) Rate of killing of *Aspergillus fumigatus* germinating conidia by neutrophils from patients before ibrutinib therapy and 1 or 3 months after the start of ibrutinib therapy, with or without previous opsonization with autologous serum. The Kruskal-Wallis test with the Dunn multiple comparison post-test were applied; $**P < 0.005$.

26.2% decrease; $P < 0.05$) (Figure 6A). Interestingly, CD11b expression was unmodified after LPS stimulation (17,789 vs. 15,674; decrease: 11.9%; $P = \text{NS}$), suggesting that the effect of ibrutinib was specific to the antifungal response pathway. Ibrutinib also impaired ROS production in all conditions, as evidenced by decreases of 68.2% from basal level (1,205 vs. 383; $P < 0.005$), 58.3% after challenge with germinating conidia (5,298 vs. 2,209; $P < 0.005$) and 69% after LPS stimulation (4,834 vs. 1,500; $P < 0.005$) (Figure 6B).

Finally, we confirmed the video-microscopy observations, using blood from healthy donors exposed to 5 μM ibrutinib for 10 min. Ibrutinib led to a decrease of engulfment ability and a dramatic impairment of *Aspergillus* killing by neutrophils (Figure 6C, D). Because we found that ibrutinib markedly impaired ROS production, we examined whether the inhibition of ROS production by diphenyleioidonium (DPI), a NADPH oxidase inhibitor, could lead to similar results. DPI caused not only a pre-

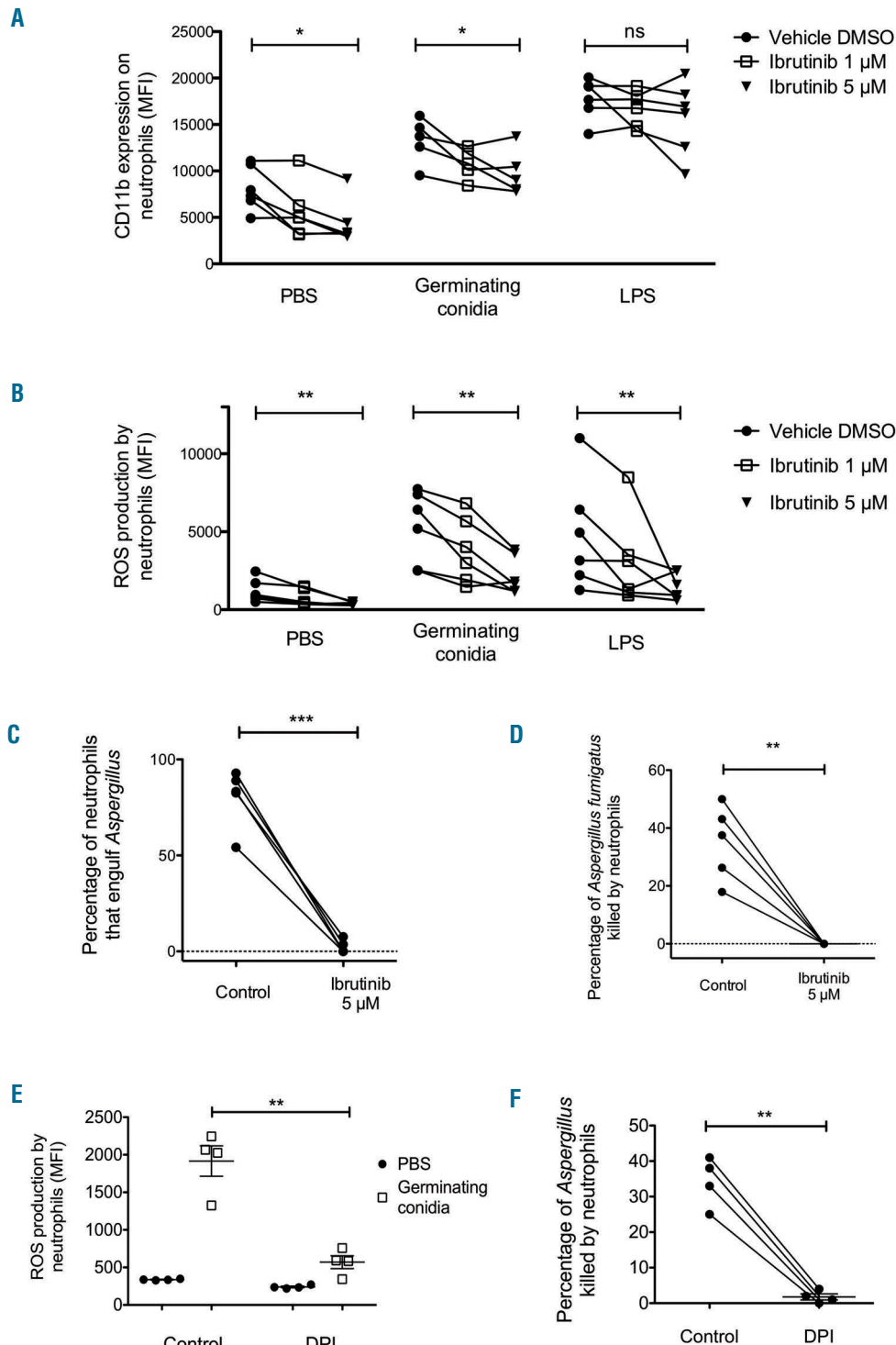


Figure 6. In vitro effect of ibrutinib on neutrophil reactive oxygen species production, CD11b surface expression and killing of *Aspergillus fumigatus*. Blood collected from six healthy donors was incubated for 10 min at 37 °C with ibrutinib (final concentration of 1 μM or 5 μM) or dimethylsulfoxide (DMSO) vehicle as a control and then stimulated for 2 h before flow cytometry analysis. The long horizontal bars indicate the mean, and the short bars indicate the standard error of the mean. (A) Expression of surface CD11b on neutrophils without stimulation (phosphate-buffered saline, PBS) or after stimulation with germinating *Aspergillus* conidia or bacterial lipopolysaccharide (LPS) plus formyl-methionine-leucyl-phenylalanine (fMLP). (B) Reactive oxygen species (ROS) production by neutrophils without stimulation (PBS) or stimulated by germinating *Aspergillus* conidia or LPS plus fMLP. Neutrophils were purified from blood collected from five healthy donors and then incubated for 10 min with ibrutinib (final concentration: 5 μM) or DMSO. (C) Engulfment of *Aspergillus* germinating conidia by neutrophils was observed in real-time by video-microscopy during co-culture for 16 h. (D) The rate of killing of *Aspergillus* germinating conidia by neutrophils was determined in real-time by video-microscopy during co-culture for 16 h. Blood collected from four healthy donors was incubated for 10 min with the NADPH oxidase inhibitor diphenyleioidonium (DPI; final concentration 5 μM) or DMSO before stimulation or neutrophil purification. (E) ROS production by neutrophils in blood with or without DPI and stimulated for 2 h with germinating conidia, assessed by flow cytometry analysis. (F) Rate of killing of *Aspergillus* germinating conidia by neutrophils isolated from blood incubated with or without DPI determined in real-time by video-microscopy during a 16 h co-culture. Multiple group analysis was assessed by the Friedman test for paired data with the Dunn multiple comparison post-test; two-group analysis was assessed by a paired t-test; * $P < 0.05$; ** $P < 0.005$; *** $P < 0.0005$; ns: non-significant.

dictable decrease in ROS in response to germinating conidia, but also decreased killing activity against growing *Aspergillus*, in a manner similar to that observed with ibrutinib (Figure 6E, F and *data not shown*). Interestingly, DPI had no effect on the engulfment process, which suggests that the inhibitory effect of ibrutinib is not caused by the sole inhibition of ROS production.

Discussion

Ibrutinib, an irreversible BTK inhibitor, displays significant clinical efficacy in some lymphoid malignancies.² Ibrutinib has, however, recently been associated with the occurrence of invasive fungal infections, in particular invasive aspergillosis.^{3,5} Intriguingly, patients with XLA do not experience aspergillosis and patients with lymphoid malignancies are usually considered to be at low risk of invasive aspergillosis. Consequently, the mechanism behind the emergence of invasive aspergillosis among patients receiving ibrutinib has remained unclear. The association of ibrutinib and fungal infections, in particular invasive aspergillosis,^{3,5} suggested that the drug could have a detrimental effect on antifungal immune responses.¹⁷

Because neutrophils are the cornerstone in the fight against fungi, the impact of ibrutinib on neutrophil functions had to be evaluated. Neutrophils act against *Aspergillus* through different mechanisms, depending on the stage of life of the fungus. Inhibition of the growth of resting conidia involves non-oxidative pathways and CD11b/CD18 recognition while hyphae are destroyed by oxidative derivatives after recognition by Fc-gamma receptor or CLR.^{18,19}

Analysis of CD11b, which like Dectin-1 is a very important receptor for β -glucan,²⁰ showed conflicting results. An unpaired comparison between 17 samples obtained before treatment and 17 samples after approximately 1 month of ibrutinib indicated that basal levels were reduced after initiating ibrutinib therapy. This result was further confirmed *in vitro*. However, paired analysis on eight longitudinally followed patients was inconclusive. The reason for this discrepancy is unclear. It might be due to an inadequate cohort size or to the patients' heterogeneity in terms of disease stage and treatment response. Interestingly, both *in vivo* and *in vitro* analyses showed that ibrutinib had no effect on CD11b surface expression in response to LPS, which suggests that the defect may be specific to the antifungal response. The C-type lectin receptor of β -glucan Dectin-1 is considered to be an essential component of the antifungal immune response. In human neutrophils Dectin-1 neutralization by monoclonal antibodies leads to an impairment of binding and phagocytosis of zymosan and diminished ROS production²¹ although contradictory results have been published.²⁰ We found a not statistically significant defect in Dectin-1 surface expression during ibrutinib therapy. Collectively, our results suggest that ibrutinib may alter CD11b surface expression on neutrophils from treated patients but has no effect on other important immune receptors and has little effect on their upregulation after *Aspergillus* and LPS stimuli.

ROS production is a major mechanism to kill fungi^{7,8} as exemplified by the phenotype of patients with chronic granulomatous disease. Neutrophils of these patients display a profound defect in ROS production caused by

mutations in components of the NADPH oxidase²² and therefore are unable to kill *Aspergillus* hyphae.¹⁹ Mangla *et al.* showed that neutrophils from X-linked immunodeficient mice lacking functional Btk had defective production of both ROS and nitric oxide after LPS challenge.²³ In agreement with these observations, a recent study also found that superoxide production in neutrophils stimulated with fMLP was reduced in Btk^{-/-} mice.²⁴ After 1 month of ibrutinib treatment, we found that neutrophil ROS decreased by approximately 50% in the presence of *Aspergillus* germinating conidia. A similar alteration in ROS production was also observed when ibrutinib was added to blood from healthy donors, which indicates that the impact of ibrutinib is prompt and seems to rule out an effect occurring during granulopoiesis. In contradiction with our results, Stadler *et al.* found no difference in ROS production by neutrophils challenged with zymosan or LPS in patients treated with ibrutinib.¹¹ It should however be noted that these results were obtained from a cohort of only six patients, for whom the duration and posology of ibrutinib therapy were not reported. Moreover, zymosan is a yeast extract containing β -glucan, the structure of which differs from that of *Aspergillus*. Since CD11b is important for neutrophil ROS production,²⁵ one may hypothesize that reduced CD11b expression after ibrutinib exposure may affect ROS, although this requires further investigation.

In human neutrophils, it has been shown that fMLP-induced IL-8 release is dependent on ROS production.²⁶ IL-8 is a major neutrophil chemoattractant and its levels have been found to be elevated in the serum and bronchoalveolar lavage of patients with invasive aspergillosis.²⁷ IL-8 production by neutrophils was reduced in samples from ibrutinib-treated patients upon *Aspergillus* stimulation. By contrast, the production of other cytokines did not change upon stimulation or during the course of ibrutinib therapy. Whether or not defective IL-8 production may result in insufficient neutrophil recruitment to the sites of *Aspergillus* infection deserves further investigation, including the use of animal models.

While ibrutinib did not seem to impair neutrophil chemotaxis, video-microscopy revealed that it reduced the cells' ability to interact closely with and engulf *Aspergillus*. The molecular mechanism by which ibrutinib hinders these interactions remains to be determined. More striking was the dramatic decrease in the ability of neutrophils to kill *Aspergillus* when exposed to ibrutinib. Altogether, given that the oxidative burst is the major mechanism of killing hyphae,¹⁸ it is very likely that ibrutinib impairs neutrophil killing at least in part through inhibition of ROS. We observed that *in vitro* exposure of neutrophils to the NADPH oxidase inhibitor DPI recapitulated the effect of ibrutinib except it did not impair *Aspergillus* engulfment by neutrophils, which suggests that the effect of ibrutinib on neutrophils extends beyond that of ROS inhibition and involves different pathways.

Collectively, our results show that ibrutinib induces multiple functional defects in neutrophils, which result in their inability to kill *Aspergillus*, and provide a first clue to explain clinical cases. One caveat of our study is that it was not designed to determine whether the effect of ibrutinib is caused by the inhibition of BTK itself. Essentially known for its key role in B cells, experimental evidence suggests that BTK is functional in neutrophils. In a Btk-

deficient mouse model, Fiedler *et al.* showed that Btk was important during granulopoiesis and that neutrophils from Btk^{-/-} mice lacked granule components important for their antimicrobial activity, such as elastase, lactoferrin and myeloperoxidase.¹⁰ Btk is involved in the activation of the PLC γ 2, AKT and p38MAPK pathways in neutrophils after stimulation.²⁴ Btk is also involved in phosphorylation of Myd88 and NF κ B activation after TLR2 or TLR4 engagement.^{28,29} Lionakis *et al.* reported that Btk^{-/-} mice died after *Aspergillus* challenge whereas wildtype animals did not.⁴ However, not all experimental evidence agrees with such a role for Btk. Indeed, Btk was found by Honda *et al.* to be a critical gatekeeper of neutrophil responses, preventing excessive inflammation through inhibition of ROS.³⁰ More recently Cavaliere *et al.* concluded that monocyte and neutrophil maturation and function were unaffected in XLA patients.³¹ Another limitation of our *in vitro* experiments is that we, as others,¹⁷ used higher concentrations of ibrutinib than those observed in patients³² to compensate for the very short time of exposure. However, several neutrophil functions, such as an increase in CD11b expression after LPS challenge, were unchanged, suggesting that the concentrations used did not lead to a global impairment of the neutrophils' cellular processes.

XLA patients are not particularly susceptible to fungal infections, unless one considers that alternative mechanisms may develop over time to compensate for BTK deficiency in humans. At present, whether neutrophil defects are caused by the sole inhibition of BTK by ibrutinib thus remains an open question. Like most kinase inhibitors, ibrutinib is not highly specific, which raises the hypothesis that impairment of antifungal activity may be caused by inhibition of other targets. Further work is required to unravel the precise molecular mechanisms responsible for the observed neutrophil defects. The development of a murine model would provide inter-

esting information on the antifungal response dynamics *in vivo*, e.g., whether the impact on CD11b alters the neutrophils' ability to reach infected tissues. A comparison with other BTK inhibitors, in particular acalabrutinib, which is more selective than ibrutinib, might help to explore the hypothesis of an off-target effect. Finally, it should be highlighted that despite these experimental results, invasive aspergillosis remains a relatively rare complication. This suggests that ibrutinib exposure is probably not sufficient by itself in most cases and that additional environmental and host factors, e.g., TLR or Dectin polymorphisms, the amount of conidia exposure, acquired immune defects related to the underlying disease or previous therapies, are required to enable the development of a clinical infection.

In conclusion, our study, which demonstrates that exposure to ibrutinib impairs the anti-*Aspergillus* responses of neutrophils both *in vitro* and *in vivo*, provides the first step in the road to understanding the relationship between invasive fungal infections and treatment with ibrutinib. The emergence of invasive aspergillosis in this population may be due to neutrophil defects in ROS production in response to fungi, inability of neutrophils to attach firmly to hyphae, and marked impairment in the neutrophils' capacity to kill fungi. Further work is required to unravel the exact mechanisms underlying this effect, in particular whether it is caused by the inhibition of BTK itself in neutrophils or by an off-target inhibition of other kinases in neutrophils and/or other cell types in the microenvironment.

Acknowledgments

We thank all patients and express our gratitude to healthcare providers for their assistance in the inclusion of patients.

This work was supported by a grant from The Janssen Company and grants from "Fondation pour la Recherche Médicale - Equipe Labelisée" and from "Agence Nationale de la Recherche", project CMOS 2015 (ANR-EMMA-050).

References

- Block H, Zarbock A. The role of the tyrosine kinase Bruton's tyrosine kinase (Btk) in leukocyte recruitment. *Int Rev Immunol.* 2012;31(2):104-118.
- Itchaki G, Brown JR. Experience with ibrutinib for first-line use in patients with chronic lymphocytic leukemia. *Ther Adv Hematol.* 2018;9(1):3-19.
- Ghez D, Calleja A, Protin C, et al. Early-onset invasive aspergillosis and other fungal infections in patients treated with ibrutinib. *Blood.* 2018;131(17):1955-1959.
- Lionakis MS, Dunleavy K, Roschewski M, et al. Inhibition of B cell receptor signaling by ibrutinib in primary CNS lymphoma. *Cancer Cell.* 2017;31(6):833-843.e5.
- Grommes C, Younes A. Ibrutinib in PCNSL: The curious cases of clinical responses and aspergillosis. *Cancer Cell.* 2017;31(6): 731-733.
- Tisi MC, Hohaus S, Cuccaro A, et al. Invasive fungal infections in chronic lymphoproliferative disorders: a monocentric retrospective study. *Haematologica.* 2017;102(3):e108-e111.
- Diamond RD, Clark RA. Damage to *Aspergillus fumigatus* and *Rhizopus oryzae* hyphae by oxidative and nonoxidative microbicidal products of human neutrophils *in vitro*. *Infect Immun.* 1982;38(2):487-495.
- Schaffner A, Douglas H, Braude A. Selective protection against conidia by mononuclear and against mycelia by polymorphonuclear phagocytes in resistance to *Aspergillus*. Observations on these two lines of defense *in vivo* and *in vitro* with human and mouse phagocytes. *J Clin Invest.* 1982;69(3):617-631.
- Baker RD. Leukopenia and therapy in leukemia as factors predisposing to fatal mycoses. *Mucormycosis, aspergillosis, and cryptococcosis.* *Am J Clin Pathol.* 1962;37: 358-373.
- Fiedler K, Sindrilaru A, Terszowski G, et al. Neutrophil development and function critically depend on Bruton tyrosine kinase in a mouse model of X-linked agammaglobulinemia. *Blood.* 2011;117(4):1329-1339.
- Stadler N, Hasibeder A, Lopez PA, et al. The Bruton tyrosine kinase inhibitor ibrutinib abrogates triggering receptor on myeloid cells 1-mediated neutrophil activation. *Haematologica.* 2017;102(5):e191-e194.
- Thornton BP, Vetrivcka V, Pitman M, Goldman RC, Ross GD. Analysis of the sugar specificity and molecular location of the beta-glucan-binding lectin site of complement receptor type 3 (CD11b/CD18). *J Immunol.* 1996;156(3):1235-1246.
- Cowland JB, Borregaard N. Granulopoiesis and granules of human neutrophils. *Immunol Rev.* 2016;273(1):11-28.
- Imbert S, Bresler P, Boissonnas A, et al. Calcineurin inhibitors impair neutrophil activity against *Aspergillus fumigatus* in allogeneic hematopoietic stem cell transplant recipients. *J Allergy Clin Immunol.* 2016;138(3):860-868.
- Hohl TM, Van Epps HL, Rivera A, et al. *Aspergillus fumigatus* triggers inflammatory responses by stage-specific beta-glucan display. *PLoS Pathog.* 2005;1(3):e30.
- Dubourdeau M, Athman R, Balloy V, et al. *Aspergillus fumigatus* induces innate immune responses in alveolar macrophages through the MAPK pathway independently of TLR2 and TLR4. *J Immunol.* 2006;177(6): 3994-4001.
- Bercusson A, Colley T, Shah A, Warris A,

- Armstrong-James D. Ibrutinib blocks Btk-dependent NF- κ B and NFAT responses in human macrophages during *Aspergillus fumigatus* phagocytosis. *Blood*. 2018;132(18):1985-1988.
18. Gazendam RP, van Hamme JL, Tool AT, et al. Human neutrophils use different mechanisms to kill *Aspergillus fumigatus* conidia and hyphae: evidence from phagocyte defects. *J Immunol*. 2016;196(3): 1272-1283.
 19. Zarembek KA, Sugui JA, Chang YC, Kwon-Chung KJ, Gallin JI. Human polymorphonuclear leukocytes inhibit *Aspergillus fumigatus* conidial growth by lactoferrin-mediated iron depletion. *J Immunol*. 2007;178(10): 6367-6373.
 20. van Bruggen R, Drewniak A, Jansen M, et al. Complement receptor 3, not Dectin-1, is the major receptor on human neutrophils for beta-glucan-bearing particles. *Mol Immunol*. 2009;47(2-3):575-581.
 21. Kennedy AD, Willment JA, Dorward DW, Williams DL, Brown GD, DeLeo FR. Dectin-1 promotes fungicidal activity of human neutrophils. *Eur J Immunol*. 2007;37(2):467-478.
 22. Lekstrom-Himes JA, Gallin JI. Immunodeficiency diseases caused by defects in phagocytes. *N Engl J Med*. 2000;343(23):1703-1714.
 23. Mangla A, Khare A, Vineeth V, et al. Pleiotropic consequences of Bruton tyrosine kinase deficiency in myeloid lineages lead to poor inflammatory responses. *Blood*. 2004;104(4):1191-1197.
 24. Volmering S, Block H, Boras M, Lowell CA, Zarbock A. The neutrophil Btk signalosome regulates integrin activation during sterile inflammation. *Immunity*. 2016;44(1):73-87.
 25. Clark HL, Abbondante S, Minns MS, Greenberg EN, Sun Y, Pearlman E. Protein deiminase 4 and CR3 regulate *aspergillus fumigatus* and beta-glucan-induced neutrophil extracellular trap formation, but hyphal killing is dependent only on CR3. *Front Immunol*. 2018;9:1182.
 26. Hidalgo MA, Carretta MD, Teuber SE, et al. fMLP-induced IL-8 release is dependent on NADPH oxidase in human neutrophils. *J Immunol Res*. 2015;2015:120348.
 27. Heldt S, Eigl S, Prattes J, et al. Levels of interleukin (IL)-6 and IL-8 are elevated in serum and bronchoalveolar lavage fluid of haematological patients with invasive pulmonary aspergillosis. *Mycoses*. 2017;60(12):818-825.
 28. Gray P, Dunne A, Brikos C, Jefferies CA, Doyle SL, O'Neill LA. MyD88 adapter-like (Mal) is phosphorylated by Bruton's tyrosine kinase during TLR2 and TLR4 signal transduction. *J Biol Chem*. 2006;281(15): 10489-10495.
 29. Doyle SL, Jefferies CA, O'Neill LA. Bruton's tyrosine kinase is involved in p65-mediated transactivation and phosphorylation of p65 on serine 536 during NF κ B activation by lipopolysaccharide. *J Biol Chem*. 2005;280(25):23496-23501.
 30. Honda F, Kano H, Kanegane H, et al. The kinase Btk negatively regulates the production of reactive oxygen species and stimulation-induced apoptosis in human neutrophils. *Nat Immunol*. 2012;13(4):369-378.
 31. Cavaliere FM, Prezzo A, Bilotta C, Iacobini M, Quinti I. The lack of BTK does not impair monocytes and polymorphonuclear cells functions in X-linked agammaglobulinemia under treatment with intravenous immunoglobulin replacement. *PLoS One*. 2017;12(4):e0175961.
 32. Byrd JC, Furman RR, Coutre SE, et al. Targeting BTK with ibrutinib in relapsed chronic lymphocytic leukemia. *N Engl J Med*. 2013;369(1):32-42.



Ferrata Storti Foundation

Increased incidence of cancer in the follow-up of obstetric antiphospholipid syndrome within the NOH-APS cohort

Jean-Christophe Gris,^{1,2,3,4} Ève Mousty,⁵ Sylvie Bouvier,^{1,2,3} Sylvie Ripart,⁵ Éva Cochery-Nouvellon,^{1,3} Pascale Fabbro-Peray,⁶ Jonathan Broner,⁷ Vincent Letouzey⁵ and Antonia Pérez-Martin^{3,8}

¹Department of Hematology, University Hospital of Nîmes, Nîmes, France; ²Faculty of Pharmaceutical and Biological Sciences, University of Montpellier, Montpellier, France; ³UPRES EA2992 "Caractéristiques Féminines des Dysfonctions des Interfaces Vasculaires", University of Montpellier, Montpellier, France; ⁴I.M. Sechenov First Moscow State Medical University, Moscow, Russian Federation; ⁵Department of Gynecology and Obstetrics, University Hospital of Nîmes, Nîmes, France; ⁶Department of Biostatistics, Epidemiology, Public Health, Innovation and Methodology, University Hospital of Nîmes, Nîmes, France; ⁷Department of Internal Medicine, University Hospital of Nîmes, Nîmes, France and ⁸Department of Vascular Medicine, University Hospital of Nîmes, Nîmes, France

Haematologica 2020
Volume 105(2):490-497

ABSTRACT

Malignancies can be associated with positive antiphospholipid antibodies but the incidence of cancer among women with the purely obstetric form of antiphospholipid syndrome (APS) is currently unknown. Our aim was to investigate the comparative incidence of cancers in women with a history of obstetric APS within a referral university hospital-based cohort (NOH-APS cohort). We performed a 17-year observational study of 1,592 non-thrombotic women with three consecutive spontaneous abortions before the 10th week of gestation or one fetal death at or beyond the 10th week of gestation. We compared the incidence of cancer diagnosis during follow-up among the cohort of women positive for antiphospholipid antibodies (n=517), the cohort of women carrying the *F5* rs6025 or *F2* rs1799963 polymorphism (n=279) and a cohort of women with negative thrombophilia screening results (n=796). The annualized rate of cancer was 0.300% (0.20%-0.44%) for women with obstetric APS and their cancer risk was substantially higher than that of women with negative thrombophilia screening [adjusted hazard ratio (aHR) 2.483; 95% confidence interval (CI) 1.27-4.85]. The computed standardized incidence ratio for women with obstetric APS was 2.89; 95% CI: 1.89-4.23. Among antiphospholipid antibodies, lupus anticoagulant was associated with incident cancers (aHR 2.608; 95% CI: 1.091-6.236). Our cohort study shows that the risk of cancer is substantially higher in women with a history of obstetric APS than in the general population, and in women with a similar initial clinical history but negative for antiphospholipid antibodies.

Correspondence:

JEAN-CHRISTOPHE GRIS
jean.christophe.gris@chu-nimes.fr

Received: December 10, 2018.

Accepted: May 16, 2019.

Pre-published: May 17, 2019.

doi:10.3324/haematol.2018.213991

Check the online version for the most updated information on this article, online supplements, and information on authorship & disclosures: www.haematologica.org/content/105/2/490

©2020 Ferrata Storti Foundation

Material published in *Haematologica* is covered by copyright. All rights are reserved to the Ferrata Storti Foundation. Use of published material is allowed under the following terms and conditions:

<https://creativecommons.org/licenses/by-nc/4.0/legalcode>. Copies of published material are allowed for personal or internal use. Sharing published material for non-commercial purposes is subject to the following conditions: <https://creativecommons.org/licenses/by-nc/4.0/legalcode>, sect. 3. Reproducing and sharing published material for commercial purposes is not allowed without permission in writing from the publisher.



Introduction

A number of case reports describe the association of antiphospholipid (aPL) antibodies with hematologic and solid organ malignancies.¹ Especially in elderly patients, thrombotic events associated with aPL antibodies can be the first manifestation of malignancy.¹ Cancer-associated monoclonal gammopathy of the IgM type can be accompanied by positive lupus anticoagulant (LA) or an anticardiolipin (aCL) IgM.² Cancer and antiphospholipid antibody syndrome (APS) can coexist in sporadic cases, while some cancer patients with or without thrombosis may show transient positivity for aPL antibodies;³ the most striking symptomatic clinical feature, catastrophic APS, has been described in cancer patients.⁴

Some reports suggest a significant incidence of malignancies in APS patients. Cancer was the second cause of death (13.9%), after bacterial infection, during the 10-year follow-up of 1,000 APS patients studied by the Euro-Phospholipid Project

Group.⁵ However, since no control group was simultaneously evaluated, the risk of cancer in patients with APS is still uncertain.

The Nîmes Obstetricians and Hematologists APS (NOH-APS) study⁶ was based on the recruitment of a cohort of women with no history of thrombosis, who had experienced pregnancy loss fulfilling the clinical criteria of obstetric APS, who were either positive for aPL antibodies (APS group), or positive for the *F5* rs6025 or *F2* rs1799963 polymorphism (Thrombophilia group), or negative for thrombophilia screening (Control group). This provided us with the opportunity to prospectively assess the comparative incidence of cancer in women who had been diagnosed with obstetric APS. This evaluation was carried out during the 2017 medical follow-up step, corresponding to a median follow-up of 17 years. We used an external, local population-derived control group, the registry of tumors in Montpellier area (*Registre des Tumeurs de l'Hérault*), to compute standardized incidence ratios.

Methods

Study design and patients

The NOH-APS study is a referral university hospital-based, longitudinal cohort study which was initiated in 1995, with an inclusion period lasting 10 years. The recruitment is presented in Figure 1 and has been described in detail elsewhere.^{6,7-10} Patients were classified as having had primary pregnancy loss (no previous successful pregnancy) or secondary pregnancy loss. The results of thrombophilia screening generated (i) an APS group of 517 women with only canonical aPL antibodies: LA, aCL IgM antibodies (aCL-M), aCL IgG antibodies (aCL-G), anti- β 2GPI (a β 2GPI) IgM antibodies (a β 2GPI-M) or a β 2GPI IgG antibodies (a β 2GPI-G); (ii) a Thrombophilia group of 279 women with isolated *F5* rs6025 or *F2* rs1799963 polymorphism; and (iii) a Control group of 796 women.

The patients have undergone clinical re-evaluation annually in our outpatient department. The loss of patients to follow-up ($n=23$: 1.44%) was minimized by directly contacting the general practitioners and the patients themselves. Symptoms were evaluated and the treatments taken during the year were recorded.

The management of the women included has already been detailed.^{6,10} APS patients received chronic primary thromboprophylaxis, i.e. low-dose aspirin (100 mg/day).

The study protocol and consent forms were approved by the Institutional Review Board of the University Hospital of Nîmes and the appropriate ethics committee (the local *Comité de Protection des Personnes Participant à la Recherche Biomédicale*). This clinical investigation was performed in accordance with the Helsinki Declaration, as formulated in 1975 and revised in 1996. All the women gave informed consent to participation. The study was declared to the *Commission Nationale de l'Informatique et des Libertés* (CNIL) under the number 2150873 v 0.

Outcome data

The incidence of a cancer diagnosis was the primary outcome. After questioning the patients and having performed their clinical examination, clinical details were obtained from the women's medical charts and details were verified with the medical, surgical and oncological teams involved in the diagnosis and treatment of the various incident cancers, both in our University Hospital and, for a minority, in the external relevant medical institutions that had assumed care.

Details of the statistical analysis can be found in the *Online Supplementary Material*.

Results

The analyses included 1,592 women with no initial history of thrombosis but a history of unexplained pregnancy loss (recurrent abortions or fetal death), categorized according to the results of thrombophilia screening, who collectively contributed data for a total of 26,588 person-years.

The characteristics of the patients at baseline and at follow-up evaluation are presented in Table 1. Women in the Control group initially had an obstetric history including more recurrent abortions, women in the APS group more often had an inflammatory disease and women in the Thrombophilia group more often had a family history of venous thromboembolism (VTE) or of atherothrombosis. The mortality rate was higher among women in the APS group: this was true for both global mortality, and also death from non-cancer-related causes (catastrophic APS in 1, pulmonary embolism in 2, stroke in 3, myocardial infarction in 3, viral infection in 4, bacterial infection in 8). Women in the APS group also more often developed an inflammatory non-cancerous disease (systemic lupus erythematosus in 47, rheumatoid arthritis in 7, systemic sclerosis in 4, inflammatory bowel disease in 3, ANCA-associated vasculitis in 2, sarcoidosis in 1). Focusing on the obstetric histories after inclusion into the cohort, fewer women in the APS group delivered at least one living neonate, and a higher percentage of them had a stillbirth, experienced a neonatal death, developed a placenta-mediated complication during one of their pregnancies, had to be admitted into an intensive care unit due to pregnancy complications, or delivered a neonate who had to be admitted into a specific intensive care unit. Focusing on vascular events that were diagnosed after inclusion into the cohort, a higher percentage of women in the APS group had VTE (distal or proximal deep vein thrombosis, pulmonary embolism) despite primary thromboprophylaxis using low-dose aspirin. The rate of superficial vein thrombosis was also higher in this group. Furthermore, these women more often developed arterial thrombotic events (transient ischemic attacks/strokes and myocardial infarction).

A diagnosis of cancer was made in 52 women, the annualized rate of cancer being computed as 0.20% [95% confidence interval (95% CI): 0.15%-0.26%] in the whole cohort. We observed 29 breast cancers, seven colon cancers, four pancreatic cancers, three non-Hodgkin lymphomas, three thyroid cancers, three endometrial cancers, two primary brain tumors and one lung cancer. Table 2A presents the incidence of cancer in the three groups of women: the risk of a cancer diagnosis was higher in the APS group than in the Control group, whereas it was not statistically different between the Thrombophilia group and the Control group. The incidence of cancer diagnosis remained significantly higher in the APS group than in the merged Control and Thrombophilia groups: hazard ratio (HR) 2.07 (95% CI: 1.30-3.57). The comparison between the APS and Thrombophilia groups did not reveal a statistically significant difference (HR 1.73; 95% CI: 0.78-3.81). The analysis adjusted (aHR) for characteristics of the women at inclusion and during follow-up (Table 2B) showed results similar to those of the unadjusted analysis (APS group: aHR 2.26; 95% CI: 1.20-4.24; $P=0.0115$). The Kaplan-Meier estimates of cancer-free survival among women are shown in Figure 2: the log-rank test revealed a statistically significantly increased incidence of cancers in women in the APS group.

Among women in the APS group, 64 (12.4%) developed

Table 1. Characteristics of the patients at baseline and at follow-up.

	Control group	Thrombophilia group	APS group
Number	796	279	517
BASELINE			
Age, years	30 (5) [17-44]	29 (4) [18-44]	29 (4) [16-41]
Age >35 years	43 (5.4%)	12 (4.3%)	15 (2.9%)
Body mass index, kg/m ²	25.6 (4.5) [15.3-36.1]	25.9 (4.2) [13.5-34.1]	26.0 (4.6) [15.3-37.0]
>30	78 (9.8%)	29 (10.4%)	60 (11.6%)
<18.5	12 (1.5%)	3 (1.1%)	5 (1%)
Ethnicity			
Caucasian-European	647 (81.3%)	227 (81.4%)	420 (81.2%)
Caucasian-North African	106 (13.3%)	37 (13.2%)	69 (13.4%)
Black African	36 (4.5%)	12 (4.3%)	22 (4.2%)
Asian	7 (0.9%)	3 (1.1%)	6 (1.2%)
PL subtype			
Embryonic PL at <10 WG	483 (60.7%)	93 (33.3%)	206 (39.8%)
Fetal PL at ≤10 WG	313 (39.3%)	186 (66.6%)	311 (60.2%)
Primary PL	549 (68.9%)	185 (66.3%)	342 (66.1%)
Secondary PL	247 (31.1%)	94 (33.7%)	175 (33.9%)
Inflammatory disease	7 (0.9%)	4 (1.4%)	32 (6.2%)
Risk factors for vascular diseases			
Varicose veins	187 (23.5%)	58 (20.8%)	117 (22.6%)
Current smoker	83 (10.4%)	30 (10.8%)	50 (9.7%)
Hypertension	19 (2.4%)	8 (2.9%)	17 (3.3%)
Hypercholesterolemia	42 (5.3%)	13 (4.7%)	31 (6.0%)
Hypertriglyceridemia	34 (4.3%)	11 (3.9%)	27 (5.2%)
Diabetes mellitus	11 (1.4%)	2 (0.7%)	6 (1.2%)
Positive history in a first-degree relative			
Venous thromboembolism	15 (1.9%)	29 (10.4%)	12 (2.3%)
Atherothrombosis	96 (12.1%)	46 (16.5%)	53 (10.3%)
Prevalence of thrombophilia laboratory markers			
Positive for LA	0	0	319 (61.7%)
Positive for aCL-G	0	0	244 (47.2%)
Positive for aCL-M	0	0	372 (71.9%)
Positive for aβ2GPI-G	0	0	114 (22.1%)
Positive for aβ2GPI-M	0	0	210 (40.6%)
Positive for LA+aCL+ aβ2GPI	0	0	149 (28.8%)
Positive for F5 rs6025	0	176 (63.1%)	11 (2.1%)
Positive for F2 rs179963	0	103 (36.9%)	6 (1.2%)
FOLLOW-UP (data obtained during the last evaluation)			
Follow-up duration, days	6209 (1758) [371-8029]	6166 (1770) [1294-8011]	6251 (1768) [1085-8030]
Lost to follow-up	23 (2.9%)	8 (2.9%)	6 (1.2%)
Deceased	13 (1.6%)	5 (1.8%)	29 (5.6%)
Deceased, <i>non-cancer-related</i>	8 (1.0%)	4 (1.4%)	21 (4.1%)
Age, years	46 (7) [27-64]	46 (6) [32-63]	46 (7) [30-61]
Body mass index, kg/m ²	27.8 (4.7) [17.4-41.1]	27.6 (4.5) [17.9-40.5]	28.0 (4.9) [18.1-40.8]
>30	121 (15.2%)	44 (15.8%)	82 (15.9%)
<18.5	31 (3.9%)	12 (4.3%)	20 (3.9%)
Cancer history, first-degree relatives	164 (20.6%)	52 (18.6%)	114 (22.1%)
Current smokers	237 (29.8%)	89 (31.9%)	163 (31.5%)
Inflammatory disease	23 (2.9%)	10 (3.6%)	64 (12.4%)
Diabetes mellitus	27 (3.4%)	10 (3.6%)	21 (4.1%)
Number of new pregnancies	2 [1-3]	2 [1-3]	2 [1-4]
Outcomes of new pregnancies			
At least one living neonate	695 (87.3%)	233 (83.5%)	417 (80.7%)
Embryonic PL <10 WG	297 (37.3%)	96 (34.4%)	198 (38.3%)
Fetal death ≥10 WG	101 (12.7%)	37 (13.3%)	85 (16.4%)
Stillbirth	36 (4.5%)	15 (5.4%)	46 (8.9%)
Neonatal death	12 (1.5%)	6 (2.2%)	27 (5.2%)

continued on the next page

continued from the previous page

	Control group	Thrombophilia group	APS group
Placenta-mediated complications	139 (17.5%)	62 (22.2%)	149 (28.8%)
ICU admission, patient	48 (6.0%)	23 (8.2%)	67 (12.9%)
ICU admission, neonate	67 (8.4%)	37 (13.3%)	89 (17.2%)
Venous thrombosis			
All deep events	59 (7.4%)	27 (9.7%)	129 (24.9%)
Deep vein thrombosis, all	59 (7.4%)	27 (9.7%)	129 (24.9%)
Deep vein thrombosis, distal	23 (2.9%)	6 (2.2%)	47 (9.1%)
Deep vein thrombosis, proximal	36 (4.5%)	21 (7.5%)	82 (15.9%)
Pulmonary embolism	17 (2.1%)	6 (2.2%)	38 (7.4%)
Superficial vein thrombosis	20 (2.5%)	18 (6.5%)	40 (7.7%)
Arterial thrombosis			
All events	21 (2.6%)	15 (5.4%)	49 (9.5%)
Transient ischemic attack / stroke	14 (1.8%)	10 (3.6%)	30 (5.8%)
Myocardial infarction	5 (0.6%)	3 (1.1%)	11 (2.1%)
Antithrombotic treatments, last evaluation			
Low-dose aspirin	9 (1.1%)	6 (2.2%)	362 (70%)
Thienopyridine	21 (2.6%)	15 (5.4%)	84 (16.2%)
Vitamin K antagonists	0	0	120 (23.2%)
Direct oral anticoagulants	35 (4.4%)	20 (7.2%)	0
Low-molecular weight heparin	1 (0.1%)	1 (0.4%)	5 (1%)

Quantitative data are given as median (interquartile range) [range] and qualitative data as number (percentage) values. APS: antiphospholipid syndrome; PL: pregnancy loss; WG: weeks of gestation; LA: lupus anticoagulant; aCL: anticardiolipin; ICU: intensive care unit

was the only aPL antibody found to be significantly associated with incident cancers (Table 3).

As the aPL antibodies did not always remain positive during follow-up, we studied the association with individual exposures to positive aPL antibodies during the follow-up, that is, the “E” parameter, which, for each of the five aPL antibodies, is the sum of all the annual positivities throughout the duration of the follow-up (Table 4). Only exposure to LA was associated with incident cancers.

We also explored the association between the strength of the antibody titers and the risk of cancer, studying intensities of exposure to aPL antibodies during the follow-up, that is, the “IE” parameter, which, for each of the five aPL antibodies, is the sum of the corresponding positive antibody titers throughout the duration of the follow-up (Table 5). Only intensity of exposure to LA was associated with incident cancers.

A total of 14 women developed symptomatic VTE before a diagnosis of cancer: nine in the APS group, two in the Thrombophilia group and three in the Control group. These cases accounted for a minority of all cases of VTE (n=215) observed during the follow-up of the cohort [14/215: 6.5% (3.9%-10.6%)]. In six cases, VTE occurred in the 100 days preceding the diagnosis of cancer, and was thus considered to be related to the malignancy (4 pancreatic cancers and the 2 primary brain tumors). In our population, incident VTE was a limited global indicator of an underlying cancer [6/52: 11.5% (5.4%-22.9%)], but was associated with types of cancer known to activate the hemostatic system strongly.

Discussion

In this exploratory analysis of long-term follow-up data from a cohort of women with a personal history of pregnancy loss categorized according to the results of thrombophilia screening, a diagnosis of obstetric APS was asso-

ciated with a higher rate of incident cancers than the rate in women with negative thrombophilia screening. The risk of a diagnosis of cancer was influenced by age, body mass index, development of diabetes mellitus during follow-up and evidence of atherothrombosis in a first-degree relative. The risk of cancer was associated with positivity for LA, not with anti-β2GP1 antibodies, both in terms of initial positivity at inclusion and in terms of cumulative exposure to this aPL antibody during follow-up. The risk was not associated with positivity for anti-β2GP1 antibodies.

We did not observe a significantly increased cancer risk in the APS group compared to that in the Thrombophilia group. However, this latter group was the smallest, thus limiting the capacity to detect significant differences, since there was a clear lack of statistical power for detecting moderate differences. For the same reason, we cannot definitely exclude that the risk of incident cancer in women positive for the *F5* rs6025 or *F2* rs1799963 polymorphism is slightly higher than that in women with negative thrombophilia screening, intermediate between the risk in the Control group and the risk in the APS group. Finally, the mean standardized incidence ratio of cancer was close to 1.5 in the Control group, but was not significant. Here also, we paid the price of a lack of statistical power. A huge retrospective population-based study in the southern district of Israel, which included 106,265 patients with a history of two or more consecutive pregnancy losses and a mean follow-up of 12 years, evidenced an aHR of 1.4 for the future risk of female malignancies.¹² Part of the association between aPL antibodies and the increased risk of incident cancers may thus be related to the unfavorable obstetric outcomes. However, in women sharing the same initial clinical history, aPL antibodies were associated with an increased risk.

A recent systematic review and meta-analysis of data from individual patients showed that occult cancer is detected in around one in 20 patients within a year of

receiving a diagnosis of unprovoked VTE.¹⁵ The data from our cohort are of the same order of magnitude [6/178: 3.4% (1.6%-7.2%)]. Of interest, most of the VTE events observed in our cohort were unprovoked [178/215: 82.8% (77.2%-87.3%)], probably because systematic thromboprophylaxis with low molecular weight heparin was proposed to the women in the Thrombophilia and APS groups, known to be more prone to VTE in the case of an intercurrent risk factor for thrombosis. Another point is that women in the APS group received primary thromboprophylaxis with low-dose aspirin, which may have affected the rate of unprovoked events in that group. We cannot, therefore, consider that the thrombotic events observed within our cohort reflect a natural pattern of evolution.

There is now clear evidence that chronic low-dose aspirin treatment can prevent one-third of colorectal, gastric, and esophageal cancers,¹⁴ and possibly some other types of cancer.¹⁵ Preclinical and clinical studies show that tumorigenesis and metastasis can be promoted by platelets through a wide variety of crosstalk between platelets and cancer cells.¹⁶ It is thus likely that the incidence of cancer in our APS group does not correspond to the natural evolution of that group, and that the panel of cancer types developed by the women with APS is not the natural panel. The potentially protective effect of chronic low-dose aspirin treatment does, however, reinforce the finding of a higher incidence of cancers in the follow-up of APS women, and adds support to a wider use of this non-consensual care.

The β 2GP1/anti- β 2GP1 autoantibody progressively becomes the dominant one in thrombotic APS,¹⁷ albeit with some remaining uncertainty in purely obstetric APS. The main finding of this observational study is the association between LA and incident cancers; a putative association with anti- β 2GP1 autoantibody did not reach statistical significance. This could of course be the consequence of a lack of statistical power, positive anti- β 2GP1 autoantibodies being less prevalent in our women with obstetric APS. It is also possible that the type and strength of aPL antibodies influence the appearance of incident cancer in positive women, in terms of both the types of cancer and in the differential levels of risk. Our study cannot resolve this issue. A more complex model may be needed to explain why some aPL antibodies did not appear to have an effect in this limited first analysis. A further possibility is that another aPL antibody cofactor, not β 2GP1, may better explain the increased incidence of cancer in our women with APS. The most likely candidate for further investigation is coagulation factor II (prothrombin), because of the impact of LA.¹⁸

The association between aPL antibodies and the increased incidence of cancers is difficult to interpret. There is currently no definitive demonstration of an association between chronic hypercoagulability and the risk of cancer, although one prospective study showed that men with higher levels of prothrombin fragments 1+2 had an increased risk of digestive tract cancers during a 10-year follow-up.¹⁹ At the phenotypic level, circumstantial evidence suggests a role for coagulation factors, particularly tissue factor and thrombin, in the signaling pathways of tumorigenesis (e.g., angiogenesis, apoptosis, evasion, invasion, and metastasis).²⁰⁻²³ Some polymorphisms in the *F5*, *F7*, *F10*, *F13A*, and *PROCR* genes, whose effects on the coagulation phenotype are not fully characterized,

are associated with the risk of solid tumors;²⁴ for instance, breast cancer is associated with polymorphisms in the *F5*, *F10* and *PROCR* genes.²⁵ However, the aPL antibody most significantly associated with incident cancers (i.e., LA)

Table 2A. Incidence of cancer in the three groups of women constituting the NOH-APS cohort. Crude data and unadjusted analysis with the Control group as the reference.

Group	Control	Thrombophilia	APS
Patient-years of follow-up	13 260.35	4 662.77	8 664.98
Cancer diagnosis: number of cases.	18*	8**	26***
Annualized rates of cancer, % (95% CI)	0.14 (0.10-0.21)	0.17 (0.09-0.34)	0.30 (0.20-0.44)
Hazard ratio 95% CI	1	1.28 (0.56-2.95)	2.22 (1.22-4.06)
P		0.56	0.0092

*APS: antiphospholipid syndrome; 95% CI: 95% confidence interval; HR: hazard ratio. *Breast cancer (n=10), colon cancer (n=3), endometrial cancer (n=2), pancreatic cancer (n=1), thyroid cancer (n=1), lung cancer (n=1). **Breast cancer (n=7), colon cancer (n=1). ***Breast cancer (n=12), non-Hodgkin lymphoma (n=3), colon cancer (n=3), pancreatic cancer (n=3), endometrial cancer (n=1), thyroid cancer (n=2), primary brain tumor (n=2).

Table 2B. Associations of clinical parameters and biological parameters in women with an incident cancer during follow-up as compared with women with no cancer.

	Univariate analysis HR (95% CI) P		Multivariate analysis** aHR (95% CI) P	
Clinical associations				
<i>Inclusion:</i>				
Age, years *	1.14 (1.06-1.22)	0.0003	1.15 (1.07-1.24)	0.0002
Body mass index, kg/m ² *	1.10 (1.01-1.19)	0.0284	1.10 (1.01-1.20)	0.0217
Fetal death	1.08 (0.63-1.86)	0.79		
Secondary pregnancy loss	0.70 (0.40-1.21)	0.203		
<i>Follow-up:</i>				
Family history of cancer	0.72 (0.34-1.55)	0.41		
Family history of VTE	0.92 (0.22-3.79)	0.91		
Family history of atherothrombosis*	2.04 (1.07-3.89)	0.0300	2.47 (1.28-4.76)	0.0071
Active smoking	1.15 (0.49-2.68)	0.75		
Non-cancerous inflammatory disease	0.76 (0.11-5.52)	0.79		
Immunosuppressive treatment	0.74 (0.10-5.54)	0.76		
Diabetes mellitus*	5.46 (1.32-22.5)	0.0186	5.13 (1.16-22.7)	0.0311
Pregnancy loss	0.87 (0.49-1.55)	0.63		
Fetal death	0.82 (0.32-2.10)	0.68		
Stillbirth	0.77 (0.18-3.19)	0.71		
Neonatal death	1.35 (0.33-5.57)	0.67		
Placenta-mediated complication	1.08 (0.51-2.30)	0.84		
Venous thromboembolism	1.37 (0.67-2.80)	0.40		
Pulmonary embolism	1.58 (0.49-5.06)	0.44		
Deep vein thrombosis				
Proximal*	1.82 (0.86-3.88)	0.119		
Distal	0.45 (0.06-3.30)	0.44		
Superficial vein thrombosis*	2.13 (0.85-5.38)	0.108		
Arterial thrombosis*	2.89 (1.04-8.05)	0.0419		
Biological associations (comparator: Control group)				
APS*	2.23 (1.22-4.06)	0.0092	2.26 (1.20-4.24)	0.0115
Thrombophilia	1.28 (0.56-2.95)	0.56		

HR: hazard ratio; 95% CI: 95% confidence interval; aHR: adjusted hazard ratio; VTE: venous thromboembolism; APS: antiphospholipid syndrome. *Variables included in the multivariate analysis. **Likelihood ratio of the model: χ^2 41.15, 10 degrees of freedom, P<0.0001.

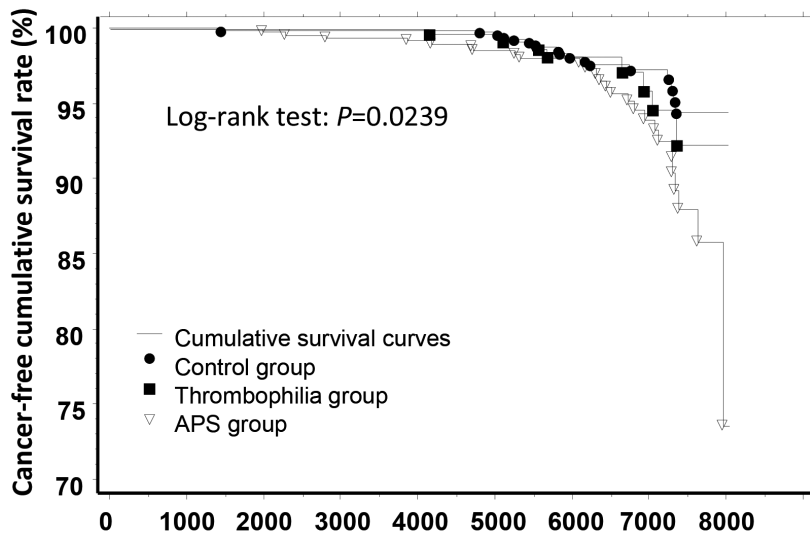


Figure 2. Cancer-free survival in the three groups of women in the NOH-APS study. APS: antiphospholipid syndrome.

Groups	N with follow-up									
Control	796	794	785	775	773	646	444	207	7	
Thrombophilia	279	279	276	272	271	228	155	73	1	
APS	517	517	517	512	511	425	304	212	4	

Follow-up (days)

was not the one currently perceived as being the most thrombogenic (i.e., aβ2GP1-G). Chronic cell activation, engagement of cell signaling pathways, modulation of cell autophagy and apoptosis, and induction of an uncontrolled inflammatory cascade are new hypotheses regarding aPL antibody-related pathogenesis, which may play a role in this association.^{17,26} There is increasing evidence to suggest that patients with systemic lupus erythematosus have a slightly higher overall risk of malignancy but the underlying mechanisms remain speculative.²⁷ Finally, currently unidentified factors, more frequently present in patients with autoimmune diseases, may be the real culprits, for example DNA-damaging autoantibodies,²⁸ as well as key inflammatory chemokines and cytokines.²⁹

Our study has various limitations. The first drawback of this study is that it was performed in a single center. Multicenter replication studies should be carried out to confirm its results. Second, the investigators were not

Table 3. Hazard ratios for an incident cancer according to the type of antiphospholipid antibody present at inclusion.

	aHR*	95% CI	P
Age at inclusion, per year	1.29	1.15-1.45	<0.0001
Positive aPL antibody:			
LA	2.61	1.09-6.24	0.0312
aCL-G	0.99	0.44-2.19	0.97
aCL-M	1.17	0.46-2.95	0.75
aβ2GP1-G	0.67	0.26-1.75	0.41
aβ2GP1-M	0.85	0.38-1.94	0.70

aHR: adjusted hazard ratio; 95% CI: 95% confidence interval; aPL antiphospholipid; LA: lupus anticoagulant; aCL-G: anticardiolipin IgG isotype; aCL-M: anticardiolipin IgM isotype; aβ2GP1-G: anti-β2GP1 IgG isotype; aβ2GP1-M: anti-β2GP1 IgM isotype. *For each of the five aPL antibodies, adjustment on the four others, and for age at inclusion.

Table 4. Analysis of incident cancers according to exposure to antiphospholipid antibodies during the follow-up.

	aOR*	95% CI	P
Age at inclusion, per year	1.28	1.14-1.43	<0.0001
E ^{LA}	1.08	1.02-1.13	0.0061
E ^{aCL-G}	1.01	0.96-1.06	0.79
E ^{aCL-M}	1.04	0.98-1.10	0.22
E ^{aβ2GP1-G}	0.99	0.93-1.04	0.59
E ^{aβ2GP1-M}	1.00	0.95-1.05	0.94

For a given antiphospholipid antibody, exposure (E) is defined as the sum of all the annual positivities throughout the duration of the follow-up. aOR: adjusted odds ratio; 95% CI: 95% confidence interval; aβ2GP1-G: anti-β2GP1 IgG isotype; aβ2GP1-M: anti-β2GP1 IgM isotype; E^{LA}: exposure to lupus anticoagulant; E^{aCL-G}: anticardiolipin IgG isotype; E^{aCL-M}: anticardiolipin IgM isotype; E^{aβ2GP1-G}: anti-β2GP1 IgG isotype; E^{aβ2GP1-M}: anti-β2GP1 IgM isotype. *For each of the five E parameters: adjustment on the four others, and on age at inclusion.

Table 5. Analysis of incident cancers according to intensity of exposure to antiphospholipid antibodies during the follow-up.

	aOR*	95% CI	P
Age at inclusion, per year	1.28	1.14-1.43	<0.0001
IE ^{LA}	1.04	1.01-1.07	0.0059
IE ^{aCL-G}	0.99	0.98-1.01	0.57
IE ^{aCL-M}	1.03	1.01-1.07	0.0288
IE ^{aβ2GP1-G}	0.99	0.96-1.01	0.23
IE ^{aβ2GP1-M}	1.01	0.97-1.06	0.59

For a given antiphospholipid antibody, the intensity of exposure (IE) is defined as the sum of all the antibody titers of annual positivities throughout the duration of the follow-up. aOR: adjusted odds ratio; 95% CI: 95% confidence interval; IE^{LA}: intensity of exposure to lupus anticoagulant; IE^{aCL-G}: intensity of exposure to anticardiolipin IgG isotype; IE^{aCL-M}: intensity of exposure to anticardiolipin IgM isotype; IE^{aβ2GP1-G}: intensity of exposure to anti-β2GP1 IgG isotype; IE^{aβ2GP1-M}: intensity of exposure to anti-β2GP1 IgM isotype. *For each of the five IE: adjustment on the four others, and on age at inclusion.

blinded to the group to which the patient was assigned. However, symptomatic cancer diagnosis leaves little room for individual interpretation. Third, incident cancers remained rare during the follow-up, occurring in only 3.3% of the women, thus limiting the potential for a more precise description of their full association with biological parameters which are not independent of each other. The very low number of symptomatic cancers that were diagnosed in our patients is a strong limitation of the study. A multicenter evaluation including a huge number of cases is necessary. Fourth, aPL antibodies may be a non-causal artifact rather than a direct risk factor.

Our study also has several strengths. It received substantial support from the NOHA administrative region-hospital medical network through which we were able to recruit a substantial number of patients. Only a very small

number of patients were lost to follow-up. The primary outcome was not ambiguous and only objectively-proven clinical events and parameters were analyzed.

In summary, we found an increased incidence of cancers during the follow-up of women with pure obstetric APS, with a significant association with LA. A very large prospective, multicenter replication study is now needed. If such a study confirms our data, it would legitimate more fundamental studies to elucidate the underlying pathophysiology.

Funding

Financial support was provided by Nîmes University Hospital via an internal funding scheme. The funder had no role in study design, data collection and analysis, decision to publish, or preparation of the manuscript.

References

- Gómez-Puerta JA, Cervera R, Espinosa G, et al. Antiphospholipid antibodies associated with malignancies: clinical and pathological characteristics of 120 patients. *Semin Arthritis Rheum.* 2006;35(5):322-332.
- Asherson RA. Antiphospholipid antibodies, malignancies and paraproteinemias. *J Autoimmun.* 2000;15(2):117-122.
- Font C, Vidal L, Espinosa G, et al. Solid cancer, antiphospholipid antibodies, and venous thromboembolism. *Autoimmun Rev.* 2011;10(4):222-227.
- De Meis E, Brandão BC, Capella FC, Garcia JA, Gregory SC. Catastrophic antiphospholipid syndrome in cancer patients: an interaction of clotting, autoimmunity and tumor growth? *Isr Med Assoc J.* 2014;16 (9):544-547.
- Cervera R, Serrano R, Pons-Estel GJ, et al. Morbidity and mortality in the antiphospholipid syndrome during a 10-year period: a multicentre prospective study of 1000 patients. *Ann Rheum Dis.* 2015;74(6):1011-1018.
- Gris JC, Bouvier S, Molinari N, et al. Comparative incidence of a first thrombotic event in purely obstetric antiphospholipid syndrome with pregnancy loss: the NOH-APS observational study. *Blood.* 2012;119(11):2624-2632.
- http://invs.santepubliquefrance.fr/surveillance/cancers/estimations_cancers/temp/registre_tumeurs_herault.htm.
- Bouvier S, Cochery-Nouvellon E, Lavigne-Lissalde G, et al. Comparative incidence of pregnancy outcomes in treated obstetric antiphospholipid syndrome: the NOH-APS observational study. *Blood.* 2014;123(3):404-413.
- Bouvier S, Cochery-Nouvellon E, Lavigne-Lissalde G, et al. Comparative incidence of pregnancy outcomes in thrombophilia-positive women from the NOH-APS observational study. *Blood.* 2014;123(3):414-421.
- Gris JC, Cyprien F, Bouvier S, et al. Antiphospholipid antibodies are associated with positive screening for common mental disorders in women with previous pregnancy loss. The NOHA-PSY observational study. *World J Biol Psychiatry.* 2019;20(1):51-63.
- Breslow NE, Day NE. Statistical methods in cancer research. Volume II-The design and analysis of cohort studies. *IARC Sci Publ.* 1987;(82):1-406.
- Charach R, Sheiner E, Beharier O, Sergienko R, Kessous R. Recurrent pregnancy loss and future risk of female malignancies. *Arch Gynecol Obst.* 2018;298(4):781-787.
- van Es N, Le Gal G, Otten HM, et al. Screening for occult cancer in patients with unprovoked venous thromboembolism: a systematic review and meta-analysis of individual patient data. *Ann Intern Med.* 2017;167(6):410-417.
- Cuzick J. Progress in preventive therapy for cancer: a reminiscence and personal viewpoint. *Br J Cancer.* 2018;118(9):1155-1161.
- Cuzick J. Preventive therapy for cancer. *Lancet Oncol.* 2017;18(8):e472-e482.
- Xu XR, Yousef GM, Ni H. Cancer and platelet crosstalk: opportunities and challenges for aspirin and other antiplatelet agents. *Blood.* 2018;131(16):1777-1789.
- Schreiber K, Sciascia S, de Groot PG, et al. Antiphospholipid syndrome. *Nat Rev Dis Primers.* 2018;4:17103.
- Permpikul P, Rao LV, Rapaport SI. Functional and binding studies of the roles of prothrombin and beta 2-glycoprotein I in the expression of lupus anticoagulant activity. *Blood.* 1994;83(10):2878-2892.
- Miller GJ, Bauer KA, Howarth DJ, Cooper JA, Humphries SE, Rosenberg RD. Increased incidence of neoplasia of the digestive tract in men with persistent activation of the coagulant pathway. *J Thromb Haemost.* 2004;2(12):2107-2114.
- Hjortoe GM, Petersen LC, Albrektsen T, et al. Tissue factor-factor VIIa-specific up-regulation of IL-8 expression in MDA-MB-231 cells is mediated by PAR-2 and results in increased cell migration. *Blood.* 2004;103(8):3029-3037.
- Versteeg HH, Schaffner F, Kerver M, et al. Inhibition of tissue factor signaling suppresses tumor growth. *Blood.* 2008;111(1):190-199.
- Hembrough TA, Swartz GM, Papathanassiou A, et al. Tissue factor/factor VIIa inhibitors block angiogenesis and tumor growth through a nonhemostatic mechanism. *Cancer Res.* 2003;63(11):2997-3000.
- Jiang X, Guo YL, Bromberg ME. Formation of tissue factor-factor VIIa-factor Xa complex prevents apoptosis in human breast cancer cells. *Thromb Haemost.* 2006;96(2):196-201.
- Tinholt M, Sandset PM, Iversen N. Polymorphisms of the coagulation system and risk of cancer. *Thromb Res.* 2016;140 (Suppl 1):S49-S54.
- Tinholt M, Viken MK, Dahm AE, et al. Increased coagulation activity and genetic polymorphisms in the F5, F10 and EPCR genes are associated with breast cancer: a case-control study. *BMC Cancer.* 2014;14:845.
- Cavazzana I, Andreoli L, Limper M, Franceschini F, Tincani A. Update on antiphospholipid syndrome: ten topics in 2017. *Curr Rheumatol Rep.* 2018;20(3):15.
- Choi MY, Flood K, Bernatsky S, Ramsey-Goldman R, Clarke AE. A review on SLE and malignancy. *Best Pract Res Clin Rheumatol.* 2017;31(3):373-396.
- Noble PW, Bernatsky S, Clarke AE, Isenberg DA, Ramsey-Goldman R, Hansen JE. DNA-damaging autoantibodies and cancer: the lupus butterfly theory. *Nat Rev Rheumatol.* 2016;12(7):429-434.
- Pylayeva-Gupta Y. Molecular pathways: interleukin-35 in autoimmunity and cancer. *Clin Cancer Res.* 2016;22(20):4973-4978.



Structural analysis of ischemic stroke thrombi: histological indications for therapy resistance

Senna Staessens,¹ Frederik Denorme,¹ Olivier François,² Linda Desender,¹ Tom Dewaele,² Peter Vanacker,^{3,4,5} Hans Deckmyn,¹ Karen Vanhoorelbeke,¹ Tommy Andersson^{2,6} and Simon F. De Meyer¹

¹Laboratory for Thrombosis Research, KU Leuven Campus Kulak Kortrijk, Kortrijk, Belgium; ²Department of Medical Imaging, AZ Groeninge, Kortrijk, Belgium; ³Department of Neurology, AZ Groeninge, Kortrijk, Belgium; ⁴Department of Neurology, University Hospitals Antwerp, Antwerp, Belgium; ⁵Department of Translational Neuroscience, University of Antwerp, Antwerp, Belgium and ⁶Department of Neuroradiology, Karolinska University Hospital and Clinical Neuroscience, Karolinska Institute, Stockholm, Sweden

Haematologica 2020
Volume 105(2):498-507

ABSTRACT

Ischemic stroke is caused by a thromboembolic occlusion of cerebral arteries. Treatment is focused on fast and efficient removal of the occluding thrombus, either *via* intravenous thrombolysis or *via* endovascular thrombectomy. Recanalization, however, is not always successful and factors contributing to failure are not completely understood. Although the occluding thrombus is the primary target of acute treatment, little is known about its internal organization and composition. The aim of this study, therefore, was to better understand the internal organization of ischemic stroke thrombi on a molecular and cellular level. A total of 188 thrombi were collected from endovascularly treated ischemic stroke patients and analyzed histologically for fibrin, red blood cells (RBC), von Willebrand factor (vWF), platelets, leukocytes and DNA, using bright field and fluorescence microscopy. Our results show that stroke thrombi are composed of two main types of areas: RBC-rich areas and platelet-rich areas. RBC-rich areas have limited complexity as they consist of RBC that are entangled in a meshwork of thin fibrin. In contrast, platelet-rich areas are characterized by dense fibrin structures aligned with vWF and abundant amounts of leukocytes and DNA that accumulate around and in these platelet-rich areas. These findings are important to better understand why platelet-rich thrombi are resistant to thrombolysis and difficult to retrieve *via* thrombectomy, and can guide further improvements of acute ischemic stroke therapy.

Correspondence:

SIMON F. DE MEYER
simon.demeyer@kuleuven.be

Received: February 22, 2019.

Accepted: April 24, 2019.

Pre-published: May 12, 2019.

doi:10.3324/haematol.2019.219881

Check the online version for the most updated information on this article, online supplements, and information on authorship & disclosures: www.haematologica.org/content/105/2/498

©2020 Ferrata Storti Foundation

Material published in *Haematologica* is covered by copyright. All rights are reserved to the Ferrata Storti Foundation. Use of published material is allowed under the following terms and conditions:

<https://creativecommons.org/licenses/by-nc/4.0/legalcode>.

Copies of published material are allowed for personal or internal use. Sharing published material for non-commercial purposes is subject to the following conditions:

<https://creativecommons.org/licenses/by-nc/4.0/legalcode>,

sect. 3. Reproducing and sharing published material for commercial purposes is not allowed without permission in writing from the publisher.



Introduction

Ischemic stroke is mainly caused by a thrombus that is occluding one or multiple arteries in the brain. As a consequence of the impaired cerebral blood flow, irreversible damage occurs in the associated brain tissue. Currently, only two US Food and Drug Administration (FDA)-approved treatment regimens are available to remove the thrombus and thus recanalize the occluded blood vessel in stroke patients: (i) pharmacological thrombolysis using recombinant tissue plasminogen activator (rt-PA), which promotes degradation of fibrin in the thrombus; and (ii) mechanical removal of the thrombus *via* endovascular thrombectomy.

Despite recent advances, efficient recanalization in ischemic stroke patients remains a challenge. rt-PA can only be administered within the first 4.5 hours after the onset of stroke symptoms due to the risk of cerebral bleeding when treatment is delayed. As a consequence, rt-PA treatment is available to less than 15% of patients in most European countries.¹ Strikingly, even in patients who receive rt-PA, more than half fail to respond to the drug.^{2,3} Factors contributing to this so-called rt-PA resistance are not well understood, but size and characteristics of the thrombus itself are thought to play an important role. As of 2015, several positive trials

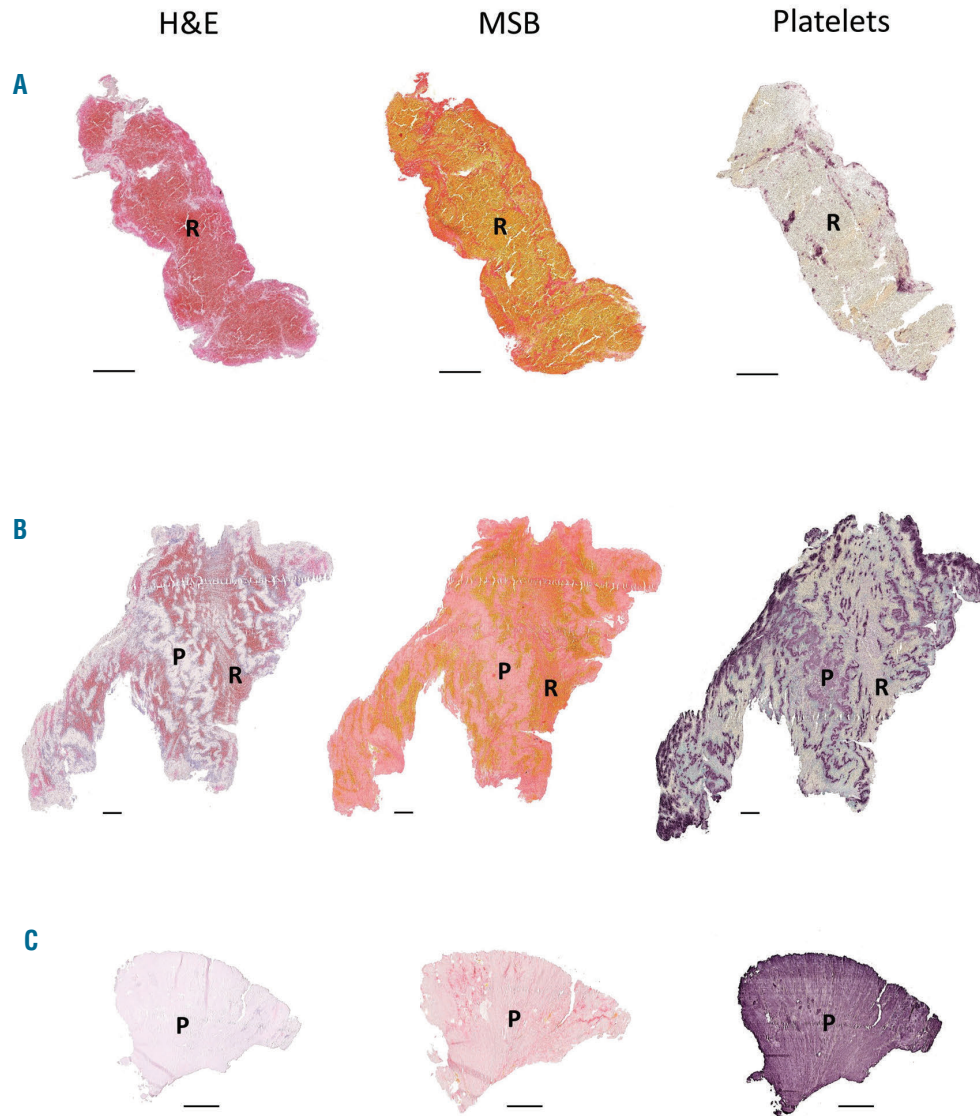


Figure 1. Stroke thrombi typically consist of distinct red blood cell (RBC)-rich and platelet-rich areas. Consecutive thrombus sections were stained with Hematoxylin & Eosin (H&E), Martius Scarlet Blue (MSB) and an anti-platelet GPIb α antibody. Classical H&E staining (left) was used to visualize overall thrombus composition and organization. On H&E staining, RBC-rich areas appear red whereas RBC-poor areas appear light pink. On MSB staining (middle), red areas show the presence of fibrin, whereas RBC appear yellow. Platelets were stained purple using an anti-GPIb α antibody (right). Overall, stroke thrombi consist of two distinct areas: RBC-rich areas (R), and platelet-rich areas (P). Examples of representative thrombi are shown, which are RBC-rich/platelet-poor (A), mixed (B), and RBC-poor/platelet-rich (C). Scale = 500 μ m.

have instigated large scale implementation of endovascular treatment, based on mechanical removal of the occluding thrombus.^{4,9} These positive trials have shown the benefits of this approach, but also revealed procedural challenges that can hamper efficient treatment. One of the most important obstacles in endovascular therapy is that thrombi tend to differ in consistency and removability. Indeed, mechanical thrombectomy is not successful in removing the thrombus in up to 20% of the patients.¹⁰ Beside vascular access, thrombus composition is considered an important factor responsible for thrombectomy failure.^{10,11}

In spite of the fact that the occluding thrombus is the primary target in both pharmacological and mechanical recanalization therapy, very little is known about the gen-

eral composition and structural organization of stroke thrombi or about the interplay between their cellular and molecular components. The main reason for this lack of knowledge was the unavailability of stroke thrombi in the past. However, endovascular thrombectomy procedures now provide patient thrombus material for detailed analysis.¹¹

Good understanding of thrombus structure and composition will be crucial to meet the pressing demand for improved pharmacological or endovascular recanalization efficiency in acute stroke treatment. An increasing number of studies have now started to report first insights into stroke thrombus composition, mostly based on Hematoxylin & Eosin (H&E) staining and looking at fibrin and red blood cells (RBC) only. However, more specific

staining can reveal novel molecular and cellular markers that could be extremely important for stroke pathophysiology. The aim of this study was to assess and define the internal organization and common structural features of stroke thrombi, using specific immunohistochemical and immunofluorescence histology procedures.

Methods

Patient thrombi

Thrombi (n=188) were collected from acute ischemic stroke patients after a thrombectomy procedure was performed at the AZ Groeninge Hospital in Kortrijk, Belgium, regardless of prior treatment with rt-PA. All patients or their legal representative gave written consent under the approval of the AZ Groeninge Hospital ethical committee (AZGS2015065). Thrombi were retrieved using a stent retriever and/or aspiration device according to the judgment of the treating neuro-interventionalist. Thrombus material collected from multiple passes of one patient was pooled and further considered as one thrombus. Of the 188 collected thrombi, eleven thrombi were excluded because insufficient material was available to perform all analyses.

Thrombus histology

After retrieval, thrombi were gently removed from the device, washed in saline and immediately incubated in 4% paraformaldehyde for 24 hours at room temperature. Next, samples were embedded in paraffin and cut into 5 µm sections. To check for differences in content throughout the thrombus, sections were analyzed for fibrin, RBC, platelets, and von Willebrand Factor (vWF) every 75 µm in randomly selected thrombi. No substantial differences in the quantity and general organization of these components were found between different sections of a single thrombus.¹² Thus, one section per thrombus, exposing a large thrombus surface, was deemed representative and was used to quantify the Martius Scarlet Blue (MSB) staining.

Thrombus sections were stained with H&E (HT110216, Sigma-Aldrich, St. Louis, MO, USA), Martius Scarlet Blue [fibrin (dark pink/red) and RBC (yellow) staining] or Feulgen's reaction [DNA staining (pink), 1079070001, Merck Chemicals, MA, USA]. Alternatively, thrombus sections were examined *via* immunohistochemistry and immunofluorescence for the presence of vWF (A008202-2, Dako, Glostrup, Denmark, and ab11713, Abcam, Cambridge, UK, respectively), platelets (GPIb α , MA5-11642, Invitrogen, Waltham, MA, USA), fibrin(ogen) (A0080, Dako), and leukocytes (CD45, 304002, Biolegend, San Diego, CA, USA). For

immunohistochemical stainings, nucleated cells were stained green using a Methyl Green solution (H-3402, Vector Laboratories). Images were acquired using a single slide scanner (Nanozoomer SQ, Hamamatsu Photonics, Japan). For immunofluorescent stainings, DNA was stained using 4,6-diamidino-2-phenylindole (DAPI, P36935, Invitrogen). RBC were visualized *via* their inherent autofluorescence at a wavelength of 555 nm. Images from immunofluorescent stainings were acquired using an Axio Observer Z1 inverted fluorescent microscope (Zeiss, Carl Zeiss AG, Oberkochen, Germany) or a laser scanning confocal microscope (LSM710, Zeiss). Images were processed by Zen 2012 (blue edition, version 2.3, Zeiss) software. Negative controls of the immunohistochemical (Online Supplementary Figure S1A-D) and immunofluorescent (Online Supplementary Figure S1E and F) staining were achieved by omission of the primary antibody or by using isotype primary antibodies. A more detailed description of all histology procedures is provided in the Online Supplementary Methods.

Results

Red blood cell-rich and platelet-rich areas form distinct structural components of stroke thrombi

To better understand the structural features of acute ischemic stroke thrombi, we collected and histologically analyzed 177 thrombi retrieved by thrombectomy from patients with ischemic stroke. As shown in Online Supplementary Figure S2, the macroscopic appearance of retrieved thrombi was heterogeneous in size, shape and color. All thrombi were sectioned and stained with H&E and MSB to visualize their general internal organization. H&E allows identification of fibrin/platelet aggregates (pink), RBC (red), and nucleated cells (dark blue) (Figure 1, left), whereas MSB staining selectively demonstrates the presence of fibrin (dark pink/red), RBC (yellow), and collagen (blue) (Figure 1, middle). H&E and MSB stainings revealed a typical common pattern in all thrombi, which is the presence of two distinct types of thrombus material: (i) RBC-rich/fibrin-poor material that appears red on H&E stainings and yellow on MSB stainings; and (ii) RBC-poor/fibrin-rich areas that appear as light pink areas on H&E staining and pink to red areas on MSB stainings. Interestingly, large amounts of blood platelets are only present in the RBC-poor/fibrin-rich areas and not in the RBC-rich areas, as shown *via* platelet-specific immunostaining (Figure 1, right). Consequently, thrombi can be RBC-rich/platelet-poor (Figure 1A), mixed (Figure 1B), or

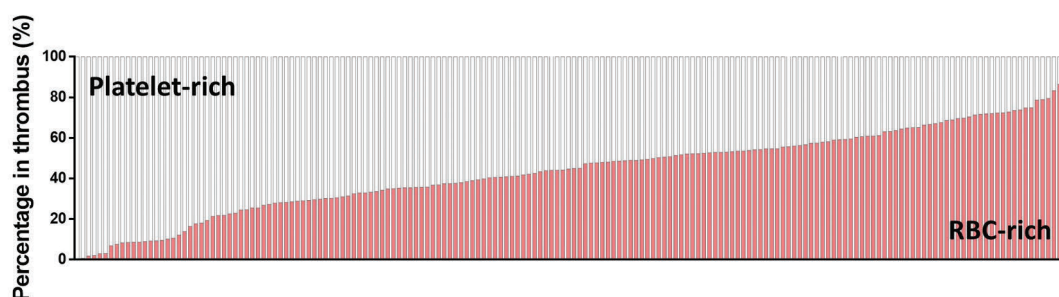


Figure 2. General stroke thrombus composition. Stroke thrombi (n=177, vertical bars) were quantitatively analyzed and the percentage of red blood cell (RBC)-rich areas (red) and platelet-rich areas (white) were determined. Thrombus composition ranges from very platelet-rich to very RBC-rich areas, with almost all thrombi containing significant amounts of both areas.

RBC-poor/platelet-rich (Figure 1C). Based on these clear and distinct differences, RBC-rich/fibrin-poor areas will be referred to as RBC-rich (R), whereas the term platelet-rich (P) will be used to indicate the RBC-poor/fibrin-rich/platelet-rich areas. Blue MSB staining, indicative for collagen, was not observed.

Relative contribution of red blood cell-rich and platelet-rich regions

To assess the relative contribution of each type of thrombus material, we quantified the total amount of RBC-rich and platelet-rich areas for all thrombi (Figure 2). The amount of RBC-rich and platelet-rich areas varied

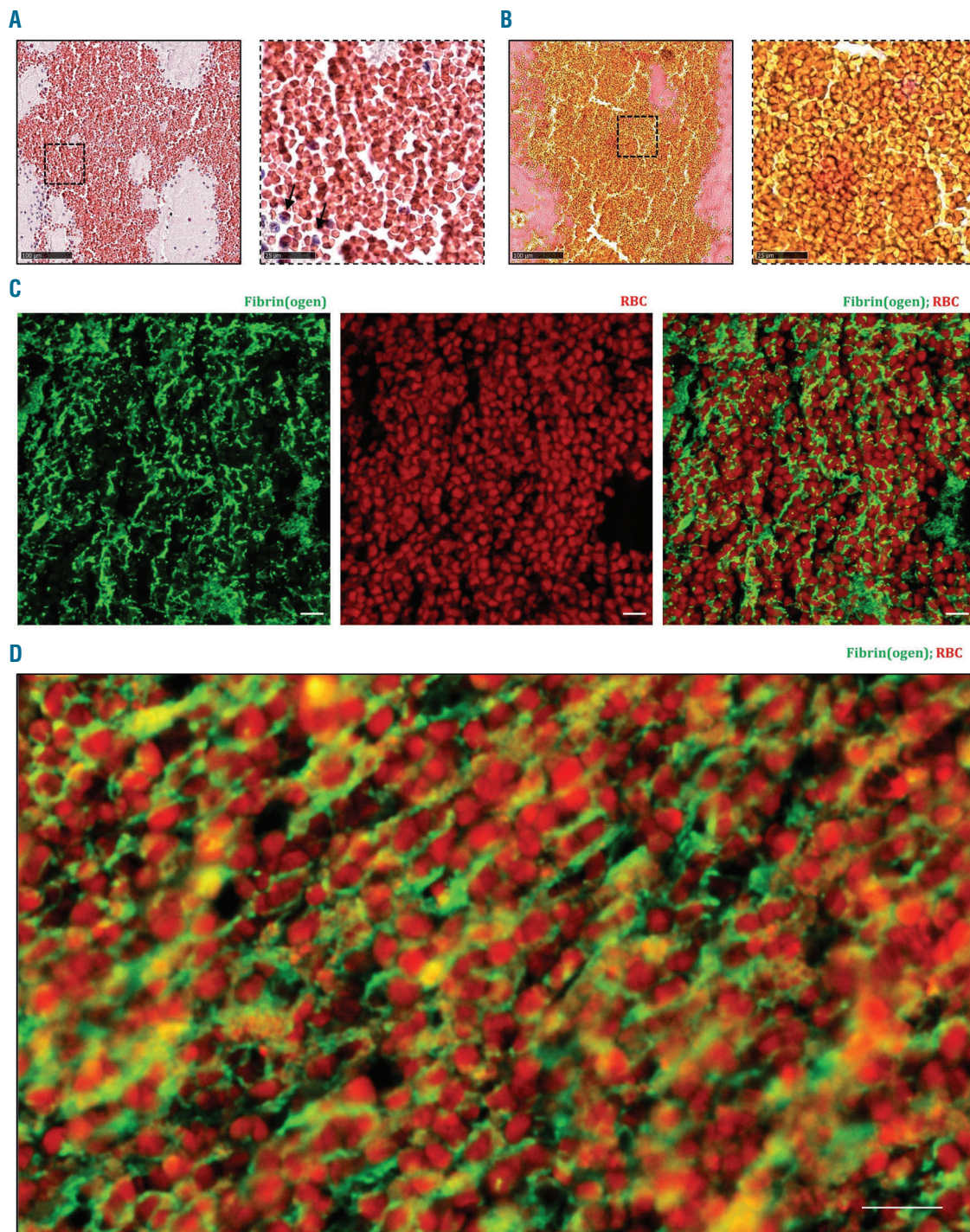


Figure 3. Red blood cell (RBC)-rich areas are composed of densely packed RBC in a fibrin network. Hematoxylin & Eosin (H&E) staining (A) and Martius Scarlet Blue (MSB) staining (B) show the abundance of RBC with little or no nucleated cells (black arrows), appearing red in H&E staining and yellow in MSB staining. Fibrin is stained red in MSB staining. (A and B, right panels) Magnification of the area indicated in the left panel. Occasional presence of nucleated cells in RBC-rich areas (blue on H&E) is observed. (C and D) Immunofluorescent staining was performed to specifically visualize fibrin(ogen) (green) and RBC (autofluorescence, red). RBC are found within a network of fibrin(ogen). Scale bars are: (A and B, left panels) 100 μ m; (A and B, right panels) 25 μ m; (C and D) 10 μ m.

between thrombi. Whereas some thrombi were platelet-dominant, others were RBC-dominant (Figure 2). Overall, the amount of RBC-rich material ranged from 0.4% to 89.0% (mean $43.9 \pm 20.4\%$), which corresponds to a range from 11% to 99.6% (mean $56.1 \pm 20.4\%$) for platelet-rich material. Typically, both regions are interspersed through each other within a thrombus. However, some thrombi typically consisted of an RBC-rich core that was surrounded by platelet-rich material (*Online Supplementary Figure S3*).

The relative amount of RBC-rich or platelet-rich material most likely affects the way stroke thrombi react to pharmacological or endovascular intervention. To better understand the specific characteristics of both regions, we performed a more detailed microscopic analysis.

Red blood cell-rich areas are composed of packed red blood cells within a meshwork of fibrin

Higher magnifications of RBC-rich areas stained by H&E and MSB showed the presence of RBC that were packed together with little or no nucleated cells (Figure 3A and B). To further characterize these RBC-rich zones, immunofluorescent stainings were performed for fibrin(ogen), platelets and vWF. RBC were identified based on their inherent autofluorescence. Interestingly, fluorescent co-stainings showed densely-packed RBC within a meshwork of thin fibrin strands (Figure 3C and D). vWF (sometimes together with platelets) was only rarely detected and did not form a main constituent of these RBC-rich areas (*Online Supplementary Figure S4*). Taken together, the RBC-rich portion of ischemic stroke thrombi

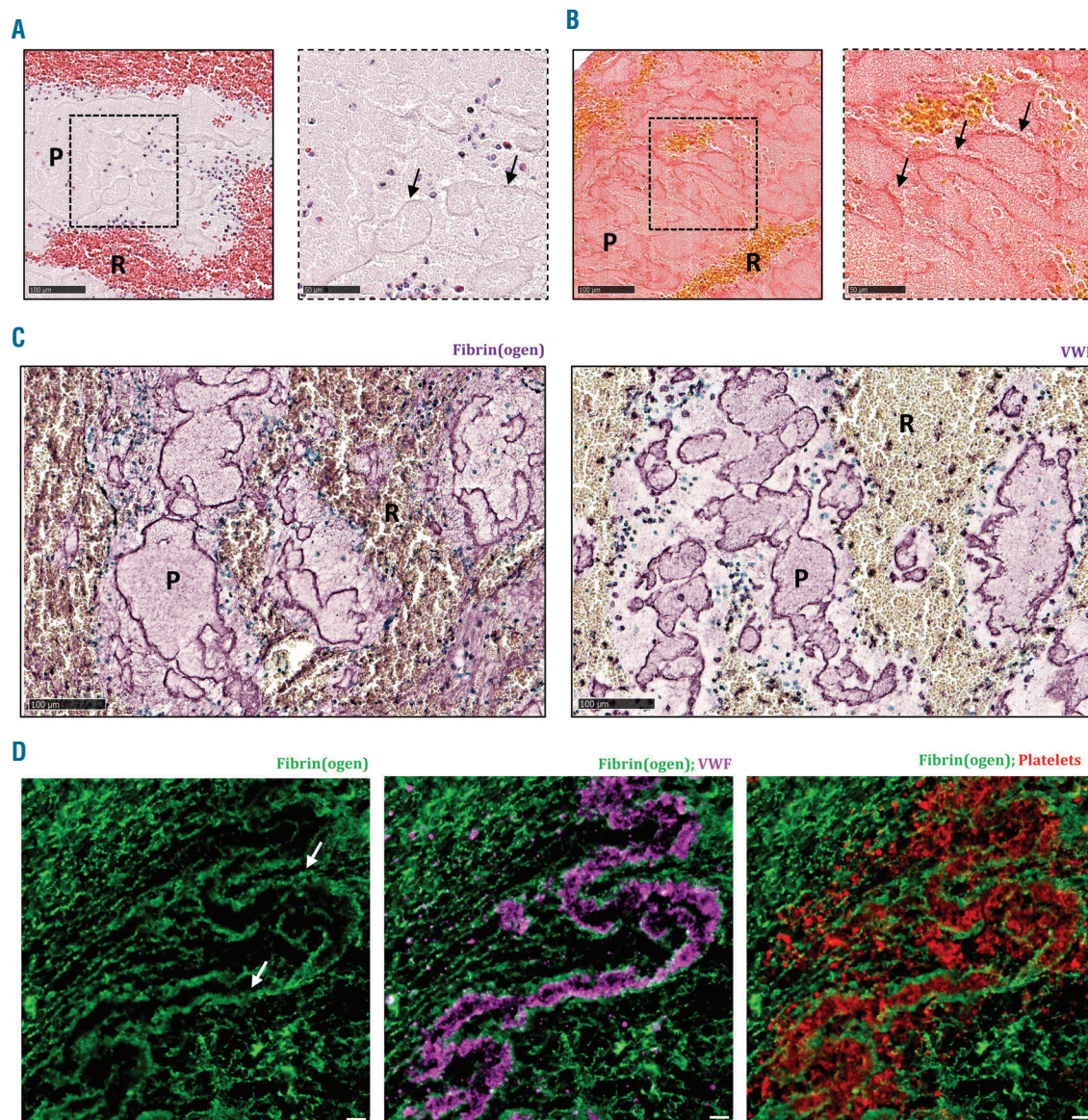


Figure 4. Platelet-rich areas consist of dense fibrin structures lined with von Willebrand Factor (vWF) and filled with platelets. Hematoxylin & Eosin (H&E) staining (A) and Martius Scarlet Blue (MSB) staining (B) show the presence of dense fibrin structures, indicated by the black arrows, within platelet-rich areas. (C) Immunohistochemical staining was used to specifically visualize fibrin(ogen) (left panel, purple) and vWF (right panel, purple). (D) Immunofluorescence analysis allowed to visualize fibrin (green), vWF (purple), and platelets (red). Dense fibrin structures (white arrows) are lined with vWF and filled with platelets. Scale bars are: (A and B, left panels, and C) 100 μm ; (A and B, right panels) 25 μm ; (D) 10 μm . P: platelet-rich area; R: RBC-rich area.

is composed of rather homogeneously distributed RBC that are densely packed and embedded in thin fibrin strands, with no other main structural components.

Platelet-rich areas consist of dense structures of fibrin, von Willebrand Factor and platelets

Platelet-rich thrombus material appeared light pink on H&E staining, without clear cellular elements (Figure 4A). MSB staining showed pink, dense fibrin structures that were clearly visible throughout the platelet-rich regions (Figure 4B). To gain more detailed insight into the microstructural organization of these platelet-rich areas, both immunohistochemical and immunofluorescent co-stainings were performed combining fibrin(ogen) with vWF and/or platelets. In accordance with the MSB staining, fluorescence microscopy for fibrin(ogen) confirmed the dense fibrin structures that demarcate platelet-rich zones (Figure 4C and D). Remarkably, co-staining with vWF showed that these dense fibrin structures are also positive for vWF (Figure 4C and D), suggesting an interaction between vWF and fibrin. Together, fibrin and vWF delineate substructures that are filled with platelets. Indeed, co-staining of platelets and fibrin(ogen) or vWF shows the presence of such platelet islands within these structures of fibrin and vWF. Hence, in contrast to the

RBC-rich zones, the platelet-rich zones contain no RBC, but are mainly composed of dense formations of fibrin and vWF, packed with platelets. Figure 5 shows a typical overview picture of both zones in one thrombus, illustrating on the one hand platelet-rich areas surrounded by dense fibrin with little fibrin between platelets and on the other hand RBC-rich areas with densely packed RBC (not stained) entangled in a thin fibrin network.

Leukocytes and DNA are mainly present on the interface between red blood cell-rich and platelet-rich areas

We and others have previously shown the abundant presence of leukocytes in stroke thrombi, but apart from their presence, not much is known about their specific cellular or molecular distribution.^{11,18} Remarkably, when staining for RBC-rich and platelet-rich areas, we observed that leukocytes are primarily found at the interface between RBC-rich and platelet-rich areas (Figure 6A-D and *Online Supplementary Figure S5*). Besides their specific presence in these boundary zones, leukocytes are also abundantly present within the platelet-rich zones. In contrast, leukocytes are not commonly found in RBC-rich areas, where, if present, they are homogeneously distributed throughout the RBC (Figure 6E).

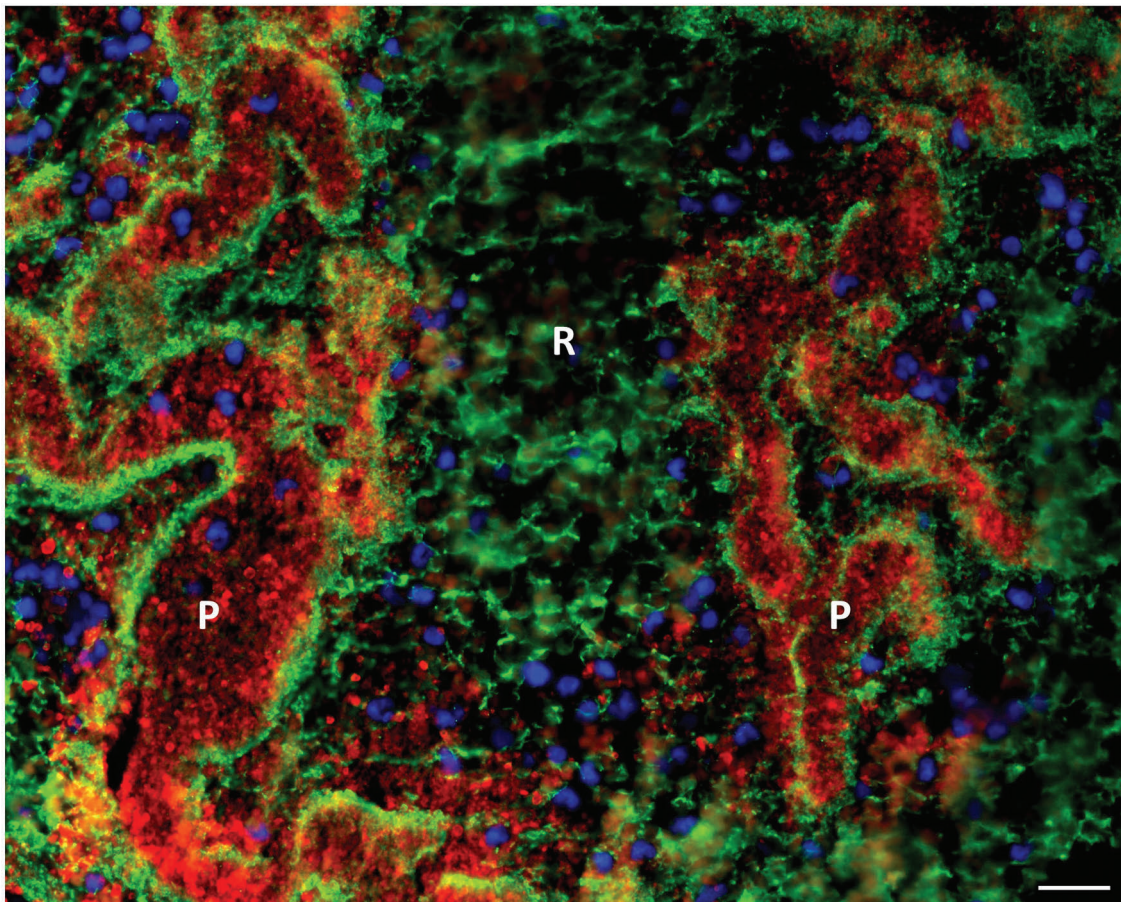


Figure 5. Immunofluorescent overview picture of red blood cell (RBC)-rich and platelet-rich areas. Immunofluorescent analysis was used to visualize fibrin(ogen) (green), platelets (red), and nuclei (blue). RBC-rich areas consist of thin fibrin strands and RBC (not stained), whereas platelet-rich areas consist of dense fibrin structures packed with platelets. Nucleated cells were mainly found near platelet-rich areas. Scale bar = 20 μm . P: platelet-rich area; R: RBC-rich area.

Interestingly, leukocytes have been shown to promote thrombus formation by the formation of extracellular DNA traps. We and others recently described the presence of neutrophil extracellular DNA traps (NET) in acute ischemic stroke thrombi.^{14,15} To further examine the presence and internal organization of DNA networks in stroke thrombi, we performed a highly sensitive Feulgen's DNA staining on a subset of 100 stroke thrombi. Strikingly, large extracellular DNA networks, appearing as extracellular smears, were seen throughout the majority of thrombi. Again, abundant amounts of extracellular DNA were observed particularly in the platelet-rich areas and in the boundary areas between platelet-rich and RBC-rich regions (Figure 7). No extracellular DNA was found within the RBC-rich regions (Figure 7E). In conclusion, leukocytes and networks of extracellular DNA were found specifically on the interface of the platelet-rich and RBC-rich regions, and in the platelet-rich regions.

Discussion

This study provides a detailed description of compositional features of ischemic stroke thrombi. We found that

stroke thrombi consist of RBC-rich and platelet-rich areas. RBC-rich areas have a limited complexity and are composed of densely packed RBC that are contained in a meshwork of thin fibrin, with a small number of leukocytes that are spread homogeneously throughout the RBC. In contrast, platelet-rich areas are more complex and contain various scaffolds that include fibrin, vWF and DNA. Dense fibrin structures are aligned with vWF and are packed with platelets. In addition, leukocytes and DNA tend to accumulate within the platelet-rich areas and on the interface between platelet- and RBC-rich areas. Why different parts of the same thrombus have such distinct underlying architecture is an intriguing point. Local hemodynamic forces are known to regulate the thrombotic pathways and thus the biochemical make-up of thrombi. Interestingly, also thrombus contraction, which is mediated by contractile forces of platelets on fibrin, has been suggested to mediate spatial separation of RBC and platelet aggregates.¹⁶ Thrombus contraction leads to the compression of RBC to so-called polyhydrocytes, forming large clusters of densely packed RBC, and to redistribution of platelets to the exterior.¹⁶ Although our histology does not allow us to unequivocally identify the typical convex, irregular polyhedral structure of compressed RBC, some confocal images (e.g. Figure 3C) are

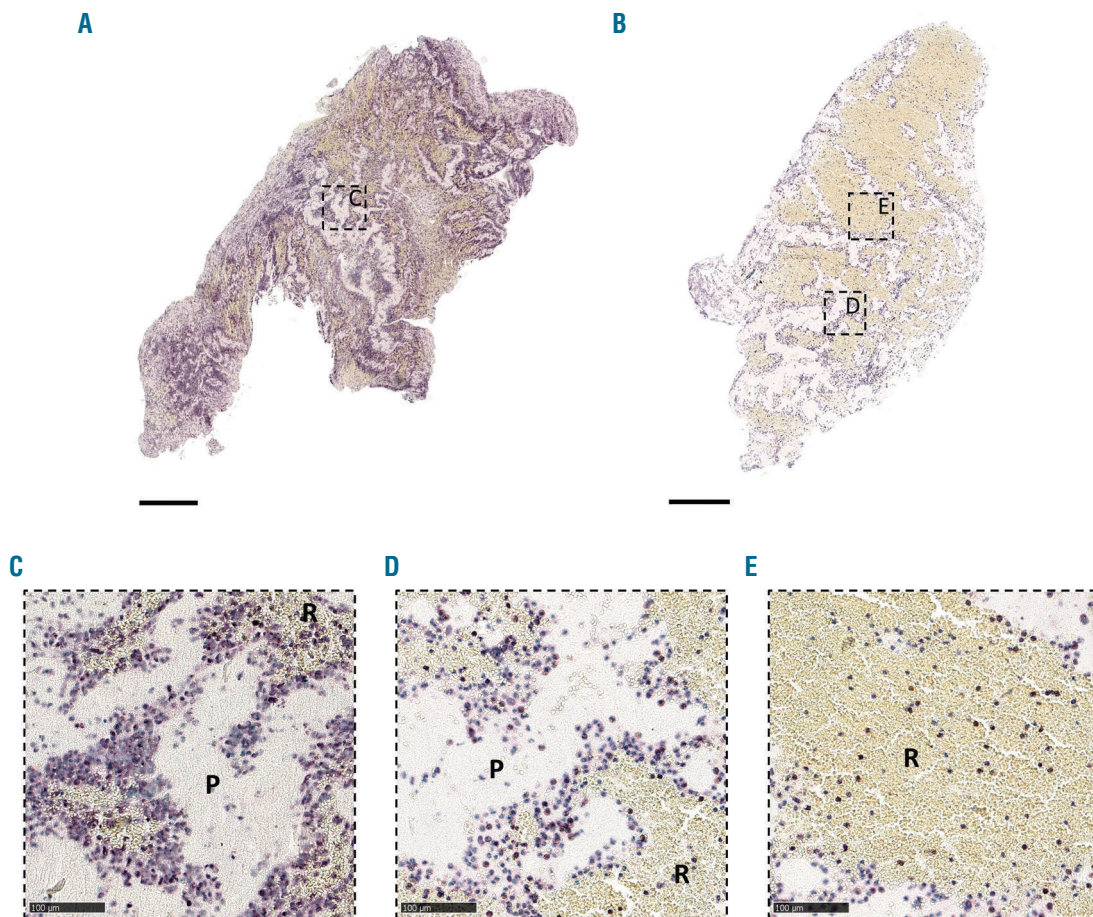


Figure 6. Leukocytes accumulate in platelet-rich areas and at the interface between platelet-rich and red blood cell (RBC)-rich areas. Stroke thrombi were immunohistochemically analyzed for leukocytes (purple). (A and B) Two representative images of stroke thrombi stained for leukocytes. (C-E) Magnifications show that leukocytes tend to accumulate in platelet-rich areas (C) or at the boundary between platelet-rich and RBC-rich areas (D), whereas leukocytes are homogeneously spread within RBC-rich areas (E). Scale bars are: (A and B) 500 µm; (C-E) 100 µm. P: platelet-rich area; R: RBC-rich area.

reminiscent of polyhedrocytes observed in contracted thrombi.^{16,17} Thrombus contraction was reported to be reduced in patients with ischemic stroke, but could have profound effects on thrombus organization, thrombus volume (and thus blood flow past thrombo-embolic occlusions), and thrombus density.¹⁸ More studies are needed to fully understand the potential effect of thrombus contraction in ischemic stroke patients.

In general, our findings are important to advance our understanding of ischemic stroke pathophysiology and, more importantly, to guide the development of better recanalization strategies in stroke patients *via* thrombolysis or thrombectomy.

As far as thrombolysis is concerned, recombinant tissue plasminogen activator is currently the only FDA-approved drug for pharmacological thrombolysis of ischemic stroke thrombi. However, it is only effective in less than half of the patients that receive rt-PA.^{2,3} The mechanisms underlying this so-called "rt-PA-resistance" are not completely understood, but previous reports indicated that RBC-dominant thrombi respond better to rt-PA than platelet-dominant thrombi.¹⁹⁻²⁷ Our histological findings provide new molecular insights on the composition of RBC-rich and platelet-rich thrombus material. It seems plausible that rt-

PA, which promotes the degradation of fibrin, can have a direct and efficient thrombolytic effect on the RBC-rich areas in which thin fibrin is the main extracellular scaffold. In contrast, however, our histological analyses reveal that platelet-rich thrombus material contains denser fibrin structures that also include vWF. In addition, we show that platelet-rich areas comprise substantial amounts of extracellular DNA. Therefore it is tempting to speculate that vWF and DNA, together with fibrin, form the structural basis of platelet-rich thrombi, and that vWF and DNA, at least partially, could be responsible for the observed rt-PA-resistance of platelet-rich thrombi in patients.

Extracellular DNA and histones have indeed been shown to modify the structure of fibrin, making it more resistant to enzymatic degradation *via* rt-PA.²⁸ The exact source of DNA observed in our study remains to be investigated, but neutrophils support thrombosis *via* the formation of neutrophil extracellular DNA structures that can act as a thrombogenic scaffold.²⁹⁻³¹ Importantly, *ex vivo* thrombolysis experiments have shown that rt-PA in combination with DNase-1 is more effective than rt-PA alone, further underlining the potential importance of extracellular DNA for rt-PA-resistance.^{14,15}

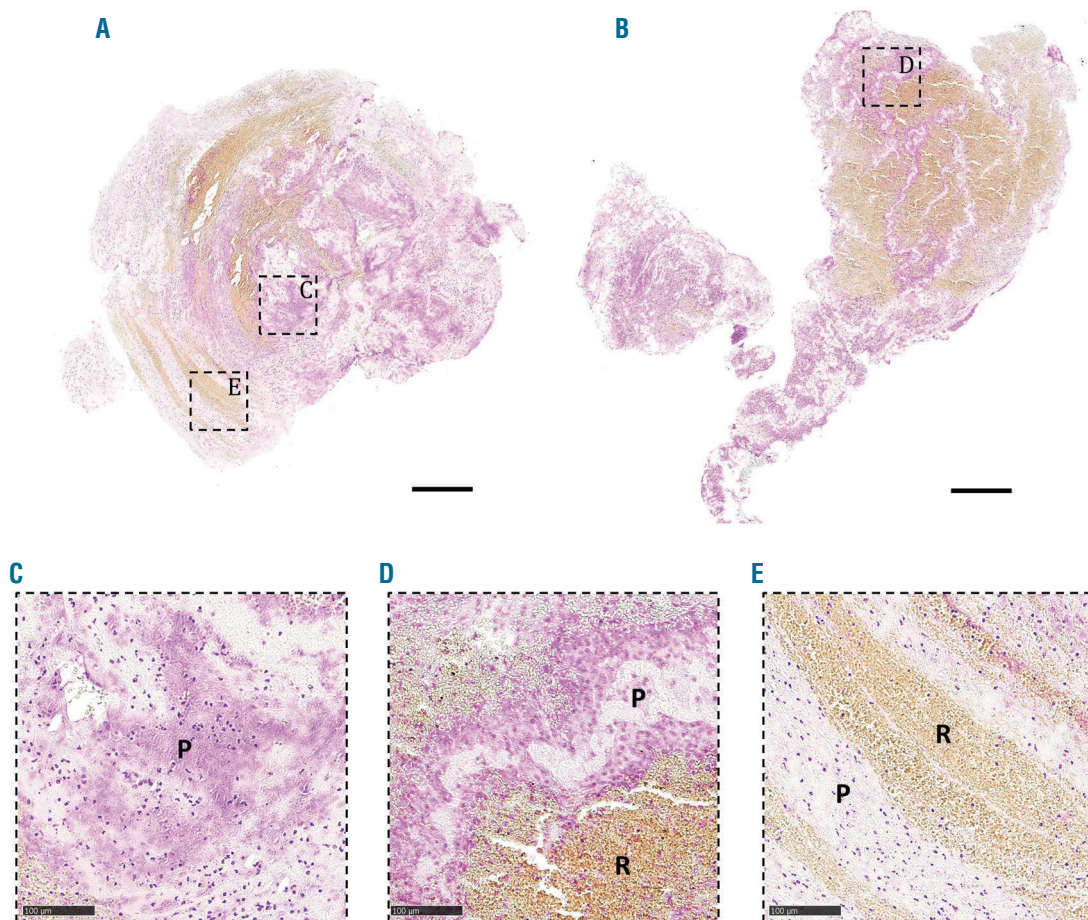


Figure 7. Extracellular DNA accumulates in platelet-rich areas and on the interface between platelet-rich and red blood cell (RBC)-rich areas. Stroke thrombi were stained using a Feulgen's reaction to visualize intra (nuclei) and extracellular (smears) DNA (pink). (A and B) Two representative images of stroke thrombi stained for DNA. (C-E) Magnifications show that extracellular DNA tends to accumulate within platelet-rich areas (C) or at the boundary between platelet-rich and RBC-rich areas (D). No extracellular DNA is observed in RBC-rich areas (E). Scale bar: (A and B) 500 μm ; (C-E) 100 μm . P: platelet-rich area; R: RBC-rich area.

Our observation that vWF is closely associated with fibrin in platelet-rich regions further supports a potentially novel link between vWF and fibrin in thrombus formation. It has been shown *in vitro* that fibrin and vWF can interact with each other *via* covalent crosslinking by FXIII or *via* thrombin-dependent incorporation, enhancing thrombus formation.^{32,34} Our histological data on vWF and fibrin indicate that fibrin degradation *via* plasmin alone might not be sufficient to achieve effective thrombolysis of platelet-rich thrombus material. Indeed, we and others have recently shown that targeting vWF, for example using the vWF-cleaving enzyme ADAMTS13, improves thrombolysis of rt-PA-resistant thrombi, reducing ischemic stroke brain injury in mice.^{19,35} Of note, plasmin can also cleave vWF, and plasmin activity was shown to regulate ADAMTS13 activity.³⁶⁻³⁸ It will be interesting to further elucidate the interplay between plasmin and ADAMTS13 in the degradation of fibrin/vWF structures that are present in ischemic stroke thrombi.

Taken together, our detailed histological analysis reveals different structural features in ischemic stroke thrombi that could be highly relevant for developing efficient pharmacological thrombolysis strategies. The presence of fibrin, vWF and DNA could explain why the current 'one size fits all' therapy aiming only at fibrinolysis *via* rt-PA is not effective in all patients. Furthermore, we found that some thrombi consist of an RBC-rich core surrounded by a dense platelet-rich shell, which could further hamper rt-PA-mediated thrombolysis.

As far as thrombectomy is concerned, emerging evidence indicates that RBC-rich stroke thrombi are more easily retrieved *via* endovascular procedures in comparison to more complex fibrin/platelet-rich thrombi.^{15,39} Even though it may seem intuitive that the retriever devices and techniques available today favor softer thrombi, the mechanisms that render platelet-rich thrombi more resistant to thrombectomy are not completely understood. Weafer *et al.* have recently shown that the degree of clot integration into the thrombectomy device is decreased in fibrin-rich thrombi, making these thrombi more resistant to mechanical removal.⁴⁰ Our study reveals that platelet-rich thrombus material from ischemic stroke patients has particular features that include dense fibrin/vWF structures, leukocytes and DNA. Thick fibrin strands have been shown to increase clot rigidity and fibrin was shown to influence the thrombus coefficient of friction and level of physical compression.^{10,41,42} Interestingly, whether or not the association of vWF with fibrin influences the mechanical properties of thrombi needs to be further investigated. Of note, DNA is able to modify the structure of fibrin, rendering it more resistant to mechanical forces.^{28,42} In fact, Ducroux *et al.* found a positive correlation between the amount of neutrophil extracellular DNA traps and the number of device passes needed to achieve successful

recanalization.¹⁵ Further studies are now needed to better understand how fibrin, DNA, vWF and platelets influence not only the mechanical properties of the occluding thrombus, but also its interaction with the thrombectomy device and the vessel wall.

This study has several limitations that are worth considering. First, only thrombi from those patients in whom the thrombus did not dissolve spontaneously or during prior rt-PA treatment, and in whom the thrombus could be successfully retrieved, were available for study. This impedes the assessment of thrombi that were rt-PA susceptible or thrombectomy resistant. Second, the scope of this study was focused on the description of common structural features of patient stroke thrombi, and did not include clinical and procedural parameters. Ongoing research on larger sets of stroke thrombi are needed to further elucidate the clinical impact of the described structural features. Our hypothesis is that the relative contribution of platelet-rich and RBC-rich areas will most likely determine the success rate of any given pharmacological and endovascular recanalization strategy. Interestingly, non-contrast computed tomography (NCCT) and magnetic resonance imaging are able to identify the presence of RBC-dominant thrombi *via* the presence of a hyperdense artery sign or a blooming artefact.^{43,44} Such information could guide treatment selection in the future. Better understanding of thrombus composition and its link with stroke etiology could also help to assess the likely thrombus origin in patients with embolic stroke of undetermined source, and to guide the development of targeted strategies for secondary stroke prevention.

As a final note, we emphasize that we describe typical features that are generally found in the majority of ischemic stroke thrombi, and that the heterogeneity between thrombi (Figure 2) does not allow for a single typical thrombus model.

In conclusion, we show that stroke thrombi consist of RBC-rich areas and platelet-rich areas. We found that RBC-rich areas have a limited complexity, while platelet-rich areas are characterized by dense fibrin structures aligned with vWF and abundant amounts of leukocytes and extracellular DNA. These findings are important to further improve acute ischemic stroke therapy, especially concerning platelet-rich thrombi that are rt-PA resistant and difficult to retrieve *via* thrombectomy.

Funding

This work was supported by research grants to SFDM from the Fonds voor Wetenschappelijk Onderzoek – Vlaanderen (FWO) (research grants G.0A86.13, G.0785.17 and 1509216N), the KU Leuven (OT/14/099 and ISP/14/02L2), the Queen Elisabeth Medical Foundation and by the European Union's Horizon 2020 Research and Innovation Program INSIST under grant agreement No 777072. FD is a postdoctoral fellow of the FWO (12U7818N).

References

1. Aguiar de Sousa D, von Martial R, Abilleira S, et al. Access to and delivery of acute ischaemic stroke treatments: A survey of national scientific societies and stroke experts in 44 European countries. *Eur Stroke J.* 2019;4(1):13-28.
2. Prabhakaran S, Ruff I, Bernstein RA. Acute Stroke Intervention: A Systematic Review. *JAMA.* 2015;313(14):1451-1462.
3. Vanacker P, Lambrou D, Eskandari A, et al. Improving the Prediction of Spontaneous and Post-thrombotic Recanalization in Ischemic Stroke Patients. *J Stroke Cerebrovasc Dis.* 2015;24(8):1781-1786.
4. Berkhemer OA, Fransen PSS, Beumer D, et al. A randomized trial of intraarterial treatment for acute ischemic stroke. *N Engl J Med.* 2015;372(1):11-20.
5. Riedel CH, Zimmermann P, Ulf J-K, Stingele R, Deuschl G, Jansen O. The importance of size: successful recanalization by intravenous thrombolysis in acute anterior stroke depends on thrombus length. *Stroke.* 2011;42(6):1775-1777.
6. Saver JL, Goyal M, Bonafé A, et al. Stent-

- retriever thrombectomy after intravenous t-PA vs. t-PA alone in stroke. *N Engl J Med.* 2015;372(24):2285-2295.
7. Campbell BC, Mitchell PJ, Kleinig TJ, et al. Endovascular therapy for ischemic stroke with perfusion-imaging selection. *N Engl J Med.* 2015;372(11):1009-1018.
 8. Jovin TG, Chamorro A, Cobo E, et al. Thrombectomy within 8 Hours after Symptom Onset in Ischemic Stroke. *N Engl J Med.* 2015;372(24):2296-2306.
 9. Goyal M, Demchuk AM, Menon BK, et al. Randomized assessment of rapid endovascular treatment of ischemic stroke. *N Engl J Med.* 2015;372(11):1019-1030.
 10. Yoo AJ, Andersson T. Thrombectomy in Acute Ischemic Stroke: Challenges to Procedural Success. *J Stroke.* 2017; 19(2):121-130.
 11. De Meyer SF, Andersson T, Baxter B, et al. Analyses of thrombi in acute ischemic stroke: A consensus statement on current knowledge and future directions. *Int J Stroke.* 2017;12(6):606-614.
 12. Staessens S, Fitzgerald S, Andersson T, et al. Histological stroke clot analysis after thrombectomy: technical aspects and recommendations. *Int J Stroke.* 2019. doi 10.1177/1747493019884527
 13. Brinjikji W, Duffy S, Burrows A, et al. Correlation of imaging and histopathology of thrombi in acute ischemic stroke with etiology and outcome: a systematic review. *J Neurointerv Surg.* 2017;9(6):529-534.
 14. Laridan E, Denorme F, Desender L, et al. Neutrophil extracellular traps in ischemic stroke thrombi. *Ann Neurol.* 2017;82(2):223-232.
 15. Ducroux C, Di Meglio L, Loyau S, et al. Thrombus Neutrophil Extracellular Traps Content Impair tPA-Induced Thrombolysis in Acute Ischemic Stroke. *Stroke.* 2018;49(3):754-757.
 16. Cines DB, Lebedeva T, Nagaswami C, et al. Clot contraction: compression of erythrocytes into tightly packed polyhedra and redistribution of platelets and fibrin. *Blood.* 2014;123(10):1596-1603.
 17. Tutwiler V, Mukhitov AR, Peshkova AD, et al. Shape changes of erythrocytes during blood clot contraction and the structure of polyhedrocytes. *Sci Rep.* 2018;8(1):17907.
 18. Tutwiler V, Peshkova AD, Andrianova IA, Khasanova DR, Weisel JW, Litvinov RI. Contraction of Blood Clots Is Impaired in Acute Ischemic Stroke. *Arter Thromb Vasc Biol.* 2017;37(2):271-279.
 19. Denorme F, Langhauser F, Desender L, et al. ADAMTS13-mediated thrombolysis of t-PA-resistant occlusions in ischemic stroke in mice. *Blood.* 2016;127(19):2337-2345.
 20. Niesten JM, van der Schaaf IC, van der Graaf Y, et al. Predictive value of thrombus attenuation on thin-slice non-contrast CT for persistent occlusion after intravenous thrombolysis. *Cerebrovasc Dis.* 2014; 37(2):116-122.
 21. Moftakhar P, English JD, Cooke DL, et al. Density of thrombus on admission CT predicts revascularization efficacy in large vessel occlusion acute ischemic stroke. *Stroke.* 2013;44(1):243-245.
 22. Nam HS, Kim EY, Kim SH, et al. Prediction of thrombus resolution after intravenous thrombolysis assessed by CT-based thrombus imaging. *Thromb Haemost.* 2012; 107(04):786-794.
 23. Puig J, Pedraza S, Demchuk A, et al. Quantification of thrombus Hounsfield units on noncontrast CT predicts stroke subtype and early recanalization after intravenous recombinant tissue plasminogen activator. *Am J Neuroradiol.* 2012;33(1):90-96.
 24. Shin JW, Jeong HS, Kwon H-JJ, Song KS, Kim J. High red blood cell composition in clots is associated with successful recanalization during intra-arterial thrombectomy. *PLoS One.* 2018;13(5):e0197492.
 25. Choi M, Park G, Lee J, et al. Erythrocyte Fraction Within Retrieved Thrombi Contributes to Thrombolytic Response in Acute Ischemic Stroke. *Stroke.* 2018; 49(3):652-659.
 26. Jang IK, Gold HK, Ziskind AA, et al. Differential sensitivity of erythrocyte-rich and platelet-rich arterial thrombi to lysis with recombinant tissue-type plasminogen activator. A possible explanation for resistance to coronary thrombolysis. *Circulation.* 1989;79(4):920-928.
 27. Tomkins AJ, Schleicher N, Murtha L, et al. Platelet rich clots are resistant to lysis by thrombolytic therapy in a rat model of embolic stroke. *Exp Transl Stroke Med.* 2015;7(1):2.
 28. Longstaff C, Varjú I, Sótónyi P, et al. Mechanical stability and fibrinolytic resistance of clots containing fibrin, DNA, and histones. *J Biol Chem.* 2013;288(10):6946-6956.
 29. Fuchs TA, Brill A, Duerschmied D, et al. Extracellular DNA traps promote thrombosis. *Proc Natl Acad Sci U S A.* 2010; 107(36):15880-15885.
 30. Fuchs TA, Brill A, Wagner DD. Neutrophil extracellular trap (NET) impact on deep vein thrombosis. *Arter Thromb Vasc Biol.* 2012;32(8):1777-1783.
 31. Grässle S, Huck V, Pappelbaum KI, et al. von Willebrand factor directly interacts with DNA from neutrophil extracellular traps. *Arter Thromb Vasc Biol.* 2014; 34(7):1382-1389.
 32. Miszta A, Pelkmans L, Lindhout T, et al. Thrombin-dependent Incorporation of von Willebrand Factor into a Fibrin Network. *J Biol Chem.* 2014;289(52):35979-35986.
 33. Hada M, Kaminski M, Bockenstedt P, et al. Covalent crosslinking of von Willebrand factor to fibrin. *Blood.* 1986;68(1):95-101.
 34. Keuren JFW, Baruch D, Legendre P, et al. Von Willebrand factor C1C2 domain is involved in platelet adhesion to polymerized fibrin at high shear rate. *Blood.* 2004;103(5):1741-1746.
 35. de Lizarrondo S, Gakuba C, Herbig BA, et al. Potent Thrombolytic Effect of N-Acetylcysteine on Arterial Thrombi. *Circulation.* 2017;136(7):646-660.
 36. Tersteeg C, de Maat S, De Meyer SF, et al. Plasmin cleavage of von Willebrand Factor as an emergency bypass for ADAMTS13 deficiency in thrombotic microangiopathy. *Circulation.* 2014; 129(12):1320-1331.
 37. Clark CC, Mebius MM, de Maat S, et al. Truncation of ADAMTS13 by Plasmin Enhances Its Activity in Plasma. *Thromb Haemost.* 2018;118(3):471-479.
 38. Crawley JTB, Lam JK, Rance JB, Mollica LR, O'Donnell JS, Lane DA. Proteolytic inactivation of ADAMTS13 by thrombin and plasmin. *Blood.* 2005;105(3):1085-93.
 39. Maekawa K, Shibata M, Nakajima H, et al. Erythrocyte-rich thrombus is associated with reduced number of maneuvers and procedure time in patients with acute ischemic stroke undergoing mechanical thrombectomy. *Cerebrovasc Dis Extra.* 2018;8(1):39-49.
 40. Weafer FM, Duffy S, Machado I, et al. Characterization of strut indentation during mechanical thrombectomy in acute ischemic stroke clot analogs. *J Neurointerv Surg.* 2019 Jan 19. [Epub ahead of print]
 41. Gunning GM, Kevin M, Mirza M, Duffy S, Gilvarry M, Brouwer PA. Clot friction variation with fibrin content; implications for resistance to thrombectomy. *J Neurointerv Surg.* 2018;10(1):34-38.
 42. Ryan EA, Mockros LF, Weisel JW, Lorand L. Structural origins of fibrin clot rheology. *Biophys J.* 1999;77(5):2813-2826.
 43. Liebeskind DS, Sanossian N, Yong WH, et al. CT and MRI early vessel signs reflect clot composition in acute stroke. *Stroke.* 2011;42(5):1237-1243.
 44. Kim SK, Yoon W, Kim TS, Kim HS, Heo TW, Park MS. Histologic analysis of retrieved clots in acute ischemic stroke: correlation with stroke etiology and gradient-echo MRI. *Am J Neuroradiol.* 2015; 36(9):1756-1762.



Variable readthrough responsiveness of nonsense mutations in hemophilia A

Lluís Martorell,^{1,2} Vicente Cortina,³ Rafael Parra,⁴ Jordi Barquineró^{1,*} and Francisco Vidal^{2,5,6*}

¹Gene and Cell Therapy Laboratory, Vall d'Hebron Institut de Recerca (VHIR), Universitat Autònoma de Barcelona (UAB); ²Congenital Coagulopathies Laboratory, Banc de Sang i Teixits (BST); ³Vall d'Hebron Core Laboratory (Section of Thrombosis and Haemostasis), Hospital Vall d'Hebron; ⁴Banc de Sang i Teixits-Hospital Vall d'Hebron; ⁵Molecular Diagnosis and Therapy Unit, VHIR-UAB and ⁶CIBER de Enfermedades Cardiovasculares (CIBERCV), Barcelona, Spain

*JB and FV contributed equally to this work as co-senior authors

Haematologica 2020
Volume 105(2):508-518

ABSTRACT

Readthrough therapy relies on the use of small molecules that enable premature termination codons in mRNA open reading frames to be misinterpreted by the translation machinery, thus allowing the generation of full-length, potentially functional proteins from mRNA carrying nonsense mutations. In patients with hemophilia A, nonsense mutations potentially sensitive to readthrough agents represent approximately 16% of the point mutations. The aim of this study was to measure the readthrough effect of different compounds and to analyze the influence of premature termination codon context in selected nonsense mutations causing hemophilia A. To this end, primary fibroblasts from three patients with hemophilia A caused by nonsense mutations (p.W1586X, p.Q1636X and p.R1960X) and Chinese hamster ovary (CHO) cells transfected with 12 different plasmids encoding mutated *F8* (p.Q462X, p.Q1705X, p.Q1764X, p.W274X, p.W1726X, p.W2015X, p.W2131X, p.R1715X, p.R1822X, p.R1960X, p.R2071X and p.R2228X) were treated with gentamicin, geneticin, PTC124, RTC13 or RTC14. Responses were assessed by analyzing not only *F8* mRNA expression and FVIII biosynthesis (FVIII antigen by ELISA, western blot and immunofluorescence) but also the FVIII activity (by chromogenic assay). In the patients' fibroblasts, readthrough agents neither stabilized *F8* mRNA nor increased FVIII protein or activity to detectable levels. In CHO cells, only in five of the 12 *F8* variants, readthrough treatment increased both FVIII antigen and activity levels, which was associated with a reduction in intracellular accumulation of truncated forms and an increase in full-length proteins. These results provide experimental evidence of genetic context dependence of nonsense suppression by readthrough agents and of factors predicting responsiveness.

Correspondence:

JORDI BARQUINERO/FRANCISCO VIDAL PEREZ
jordi.barquiner@vhir.org/fvidal@bst.cat

Received: November 23, 2018.

Accepted: June 11, 2019.

Pre-published: June 13, 2019.

doi:10.3324/haematol.2018.212118

Check the online version for the most updated information on this article, online supplements, and information on authorship & disclosures: www.haematologica.org/content/105/2/508

©2020 Ferrata Storti Foundation

Material published in *Haematologica* is covered by copyright. All rights are reserved to the Ferrata Storti Foundation. Use of published material is allowed under the following terms and conditions:

<https://creativecommons.org/licenses/by-nc/4.0/legalcode>.

Copies of published material are allowed for personal or internal use. Sharing published material for non-commercial purposes is subject to the following conditions:

<https://creativecommons.org/licenses/by-nc/4.0/legalcode>,

sect. 3. Reproducing and sharing published material for commercial purposes is not allowed without permission in writing from the publisher.



Introduction

Hemophilia A (HA) is an X-linked disorder caused by molecular defects in the coagulation factor VIII gene (*F8*). Nonsense mutations represent approximately 16% of point mutations leading HA (<http://www.factorviii-db.org>). These patients usually have severe HA and a high risk of FVIII inhibitor development.¹ HA predisposes patients to recurrent bleeds, primarily into the joints and soft tissues, with the severity of the disease inversely correlated to FVIII:C activity. Therapy is based on the prevention of bleeding using FVIII replacement (either recombinant or plasma-derived), with an annual estimated cost of >150,000 euros in severely affected patients.²

Although major advances have been reported with gene therapy in both HA³ and hemophilia B (HB),⁴ it has yet to be approved for clinical use and will not, therefore, be commercially available for the majority of patients in the immediate future. Recently, readthrough therapy has emerged as a potential strategy for the treat-

Table 1. Molecular and clinical data of patients with hemophilia A included in the study.

Patient	Gene region	Nucleotide change	Amino acid change [HGVS]	Nucleotide context (-1Stop+4)	Phenotype	FVIII:C %	Inhibitors	FVIII:Ag %
#1	Exon 14	c.4757G>A	p.W1586X	TTAGG	Severe	<1	Yes	nd
#2	Exon 14	c.4906C>T	p.Q1636X	ATAAA	Severe	<1	nd	nd
#3	Exon 18	c.5878C>T	p.R1960X	TTGAT	Moderate	4	No	nd
#4	Exon 18	c.5879G>A	p.R1960Q	(missense)	Mild	10-15	No	nd

FVIII:Ag: FVIII antigen levels; FVIII:C: Factor VIII coagulant activity; HGVS: Human Genome Variation Society nomenclature; nd: not determined.

ment of hereditary diseases caused by nonsense mutations. It is based on the use of small molecules that cause ribosomes to ignore premature termination codons (PTC) during translation, thus allowing the generation of full-length, potentially functional, proteins from the mutant mRNA. PTC are estimated to occur in approximately 10-15% of the patients with monogenic disease (homo or heterozygotes), who may potentially benefit from readthrough agents (RTA). However, this approach has important limitations, including the toxicities of some of these compounds (which require long-term administration), the usually very low levels of readthrough that can be obtained, and the fact that an amino acid different from that originally encoded may be introduced at the PTC site, with potentially detrimental consequences in terms of protein function. Nonetheless, clinical trials or pilot studies of RTA have already been carried out in patients with cystic fibrosis,^{5,6} Duchenne muscular dystrophy^{7,8} or hemophilia,⁹ although often with inconclusive results.

The aminoglycosides gentamicin and geneticin, as well as non-aminoglycoside compounds, such as PTC124 (Ataluren),¹⁰ RTC13 and RTC14,¹¹ have been used as RTA based on their ability to suppress PTC and to allow the generation of full-length proteins with at least partial functionality. However, the efficiency of RTA therapy varies according to not only the PTC type and sequence context,¹²⁻¹⁴ but also to the specific agent that is used, which can influence the binding of specific aminoacyl-tRNA to the PTC and thus the amino acid added to the nascent peptide, with consequences for the functionality of the recoded protein.¹⁵ Here, we present an analysis of the effect of five RTA (gentamicin, geneticin, PTC124, RTC13 and RTC14) on *F8* mRNA expressed in primary skin fibroblasts from three patients with HA as well as in a Chinese hamster ovary (CHO)-cell-based model of HA. Our aim was to assess the readthrough effect of these RTA on the FVIII activity, in addition to FVIII:Ag levels, and the influence of the molecular context, including type of stop codon, adjacent sequences, and the amino acid originally encoded by the wild-type (WT) protein at the mutated site.

Methods

Patients and isolation of skin fibroblasts

Four patients with HA caused by either nonsense mutations (p.W1568X, p.Q1636X and p.R1960X) or a missense mutation (p.R1960Q), diagnosed at the Hemophilia Unit of the Vall d'Hebron University Hospital and genetically characterized at the Congenital Coagulopathies Laboratory of the Blood and Tissue Bank of Catalonia (BST)¹⁶ were selected for this study. All partici-

pating patients and controls provided informed consent in accordance with the Declaration of Helsinki. The study was approved by our institutional Research Ethics Committee.

The genetic characteristics of each patient and their plasma FVIII:C activities at the time of diagnosis are summarized in Table 1.

Generation of *F8* variants harboring premature termination codon mutations

All *F8* B-domain deleted (*F8BDD*) cDNA variants were designed according to our hypotheses and purchased from GeneArt (Thermo Fisher Scientific, Waltham, MA, USA). All the mutations studied are shown in Figure 1A.

Cell lines and Chinese hamster ovary-cellular model

Human hepatocarcinoma cell line Huh-7 was kindly provided by Dr. J. Quer (VHIR, Barcelona) while CHO-S cells were purchased from Thermo Fisher Scientific. Both cell lines were cultured in Dulbecco's Modified Eagle's Medium supplemented with 10% fetal bovine serum, penicillin and streptomycin (all from Biowest, Nuaille, France). For CHO transfection, cells were passed three times and seeded at 4.5×10^4 cells in 12-well plates to achieve a confluence of 50-80%. The day after, the cells were transfected with 1.5 μ g of the WT or mutated *F8BDD* plasmids using 1.5 μ L lipofectamine-LTX (Thermo Fisher Scientific) per well, following the manufacturer's recommendations.

Readthrough agent treatment

Patient-derived skin fibroblasts (3.5×10^3 cells/cm²) were seeded in 6-well plates and grown to 70-80% confluence before RTA treatment, while CHO cells were treated after 8 hours of transfection. The cells were treated with gentamicin, geneticin (Thermo Fisher Scientific), PTC124 (Selleckchem Co., Houston, TX, USA), RTC13 or RTC14 (ID: 5735019 and ID: 5311257) (ChemBridge, San Diego, CA, USA) using a range of concentrations reported to induce PTC readthrough *in vitro* (50-100 μ g/mL for gentamicin and geneticin, 10 μ M for PTC124, RTC13 and RTC14).^{17,18}

F8 mRNA analysis

Total RNA was extracted using the RNeasy mini kit followed by on-column DNase I treatment (Qiagen, Hilden, Germany). Single-stranded cDNA was generated with the high capacity cDNA reverse transcription kit (Thermo Fisher Scientific) using 500 ng of total RNA and random primers in a final volume of 25 μ L, as previously described.¹⁹ The cDNA obtained was used to quantify *F8* mRNA expression.

FVIII Ag levels of *F8BDD* variants

Human FVIII antigen levels (FVIII:Ag) were determined in culture supernatants using the IMUBIND[®] factor VIII ELISA kit (Sekisui Diagnostics, Lexington, MA, USA).

Table 2. Summary of the *in silico* analysis of the predicted readthrough effect at the protein level using the SIFT and Polyphen-2 softwares.

F8 variant	Mutation HGVS*	Mutation Legacy ¹ domain	Affected FVIII	Predicted MW (kDa)/ (%) [‡]	Predicted AA change	SIFT prediction		Polyphen-2 prediction		Sequence context/RT efficiency [¶]	Expected effect on protein increase)	FVIII:C (fold increase)	FVIII:Ag (% before/after RT)
						Score [0-1]	Predicted	Score [1-0]	Predicted				
0	WT	WT	N.A	166.19	N.A	N.A	N.A	N.A	N.A	A TGA C	N.A	N.A	N.A
1	W274X	W255X	A1	30.92	W/W(98)	1	SAME AA	0	SAME AA	T TGA C/ Highest	Mainly WT variant	3.7	1.55 / 24.6 (15.87)
					W/R(1.2)	0	DAMAGING	1	DAMAGING				
					W/C(0.4)	0	DAMAGING	1	DAMAGING				
2	Q462X	Q443X	A2	52.8	Q/Q(64)	1	SAME AA	0	SAME AA	T TAG C/ High	Mainly WT variant	2.6	3.65 / 18.7 (5.12)
					Q/K(34)	0.26	TOLERATED	0.99	DAMAGING				
					Q/L(0.5)	0.02	DAMAGING	0.99	DAMAGING				
3	Q1705X	Q1686X	A3	91.66	Q/Q(64)	1	SAME AA	0	SAME AA	T TAG A/ Low	Mainly WT variant	1	1.25 / 4.5 (3.6)
					Q/K(34)	0.37	TOLERATED	0.99	DAMAGING				
					Q/L(0.5)	0.37	TOLERATED	0.397	BENIGN				
4	R1715X	R1696X	A3	92.85	R/W(98)	0.05	DAMAGING	1	DAMAGING	A TGA C/ High	Mainly non functional variant	1.2	0.6 / 6.7 (11.17)
					R/R(1.2)	1	SAME AA	0	SAME AA				
					R/C(0.4)	0	DAMAGING	1	DAMAGING				
5	W1726X	W1707X	A3	94.21	W/W(98)	1	SAME AA	0	SAME AA	C TGA G/ Low	WT variant	1	0.75 / 5.0 (6.67)
					W/R(1.2)	0	DAMAGING	1	DAMAGING				
					W/C(0.4)	0	DAMAGING	1	DAMAGING				
6	Q1764X	Q1745X	A3	98.51	Q/Q(64)	1	SAME AA	0	SAME AA	T TAG C/ High	Mainly WT variant	3.3	1.6 / 13.4 (8.37)
					Q/K(34)	0.67	TOLERATED	0.062	BENIGN				
					Q/L(0.5)	0.13	TOLERATED	0.012	BENIGN				
7	R1822X	R1803X	A3	105.24	R/W(98)	0.04	DAMAGING	0.887	DAMAGING	T TGA A/ Medium	Mainly non functional variant	1.3	0.4 / 5.3 (13.25)
					R/R(1.2)	1	SAME AA	0	SAME AA				
					R/C(0.4)	0.01	DAMAGING	0.84	DAMAGING				
8	R1960X	R1941X	A3	121.5	R/W(98)	0	DAMAGING	1	DAMAGING	T TGA T/ Medium	Mainly non functional variant	1	1.1 / 9.55 (8.68)
					R/R(1.2)	1	SAME AA	0	SAME AA				
					R/C(0.4)	0	DAMAGING	1	DAMAGING				
9	W2015X	W1996X	A3	127.9	W/W(98)	1	SAME AA	0	SAME AA	T TGA C/ Highest	WT variant	2.9	0.5 / 15.65 (31.3)
					W/R(1.2)	0.01	DAMAGING	1	DAMAGING				
					W/C(0.4)	0	DAMAGING	1	DAMAGING				
10	R2071X	R2052X	C1	134.11	R/W(98)	0	DAMAGING	1	DAMAGING	C TGA C/ High	Mainly non functional variant	1.2	0.35 / 7 (20)
					R/R(1.2)	1	SAME AA	0	SAME AA				
					R/C(0.4)	0	DAMAGING	1	DAMAGING				
11	W2131X	W2112X	C1	140.99	W/W(98)	1	SAME AA	0	SAME AA	G TGA C/ High	WT variant	2.7	2.85 / 13 (4.56)
					W/R(1.2)	0	DAMAGING	1	DAMAGING				
					W/C(0.4)	0	DAMAGING	1	DAMAGING				
12	R2228X	R2209X	C2	151.85	R/W(98)	0	DAMAGING	1	DAMAGING	T TGA C/ Highest	Mainly non functional variant	1.1	0.6 / 3 (5)
					R/R(1.2)	1	SAME AA	0	SAME AA				
					R/C(0.4)	0	DAMAGING	1	DAMAGING				

*HGVS: Human Genome Variation Society numbering, where codons are numbered with codon +1 coding for the first residue (Met) of the 19-residue signal peptide (this is -19 in Legacy numbering). ¹Legacy numbering, where codon +1 refers to that encoding the first AA of the mature FVIII protein (in HGVS numbering, it is codon +20). [‡]According to Roy *et al.*¹⁵. [¶]According to nucleotide context rule (-1-Stop+4). AA: amino acid. N.A: not applicable. RT: readthrough. WT: wild type.

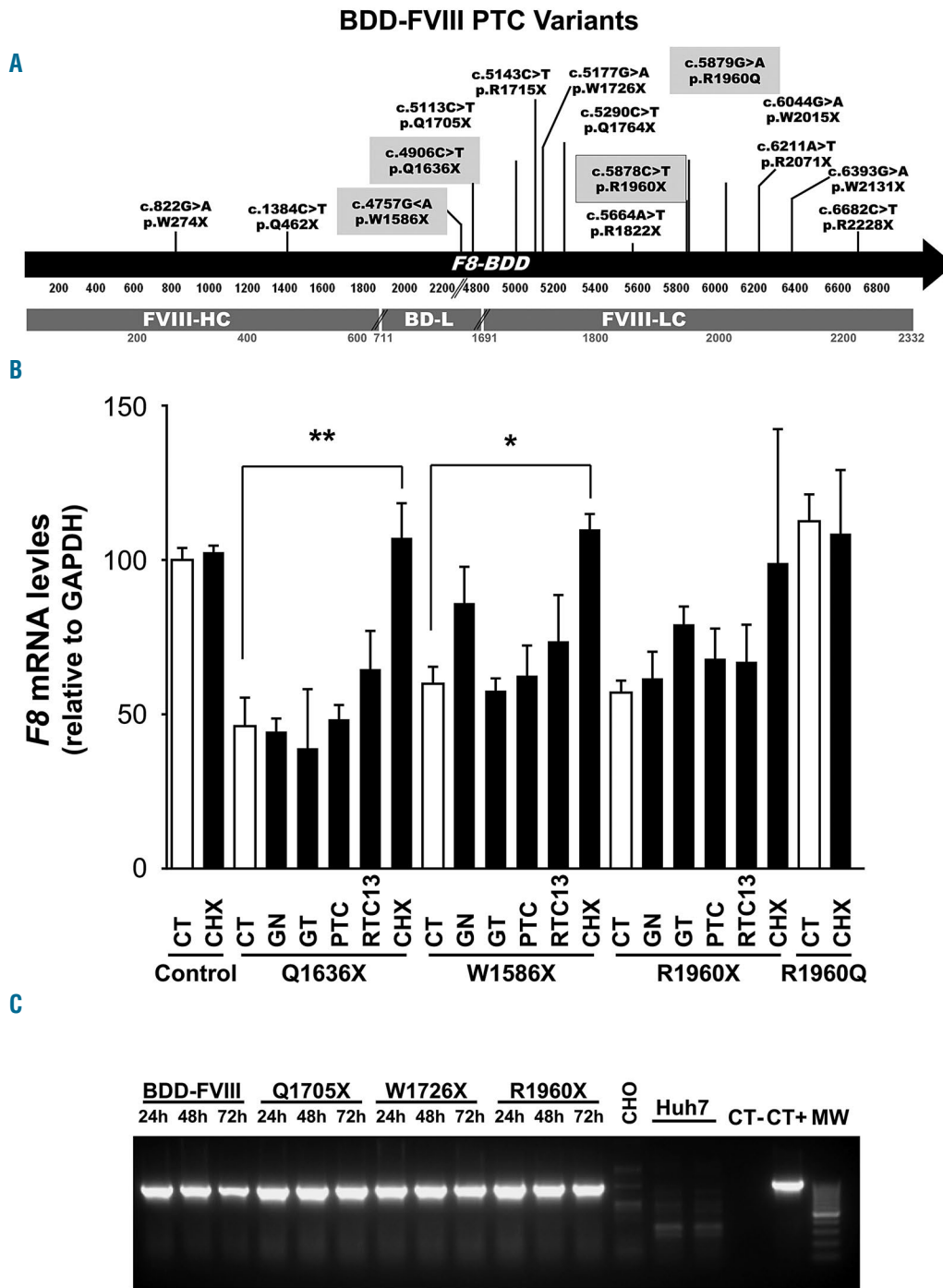


Figure 1. F8 mutations studied and detection of F8 mRNA levels. (A) Schematic representation of the distribution of premature termination codons (PTC) across the F8BDD cDNA generated by site-directed mutagenesis for the Chinese hamster ovary (CHO) model or naturally occurring in the hemophilia A (HA) patients. The black arrow represents the F8 cDNA (5' to 3'), numbers below the arrow correspond to the nucleotide position, while the gray bar represents the BDD-FVIII protein, and numbers below correspond to the amino acid position according to the Human Genome Variation Society (HGVS) nomenclature. The distribution of mutations in F8 mRNA analyzed in CHO model, patients' fibroblasts (in gray boxes) or both cellular models (black lined gray box) are also shown. BD-L: BDD-linker; FVIII-HC: heavy chain; FVIII-LC: light chain. (B) F8 mRNA levels detected by quantitative real-time polymerase chain reaction in the fibroblasts of HA-patients or a normal control. GAPDH: glyceraldehyde 3-phosphate dehydrogenase; Control: fibroblasts of a HB patient; Q1636X, W1586X and R1960X HA patients fibroblasts harboring these nonsense mutations; and R1960Q: HA patient fibroblasts harboring this missense mutation. CT: untreated cells; GN: gentamicin 100 µg/mL; GT: gentamicin 100 µg/mL; PTC: PTC124 10 µM; RTC13: RTC13 10 µM; CHX: cycloheximide 1 µg/mL (n=3). (C) Time course of F8BDD mRNA levels detected by BDD-specific semi-quantitative polymerase chain reaction in the CHO-based HA-model. F8BDD: WT variant; p.Q1705X, p.W1726X and p.R1960X: F8BDD variants harboring PTC; CHO: non transfected CHO cells; Huh-7: human hepatocellular carcinoma cell line (a cell line that expresses high levels of endogenous F8 but used here as a negative control of the F8BDD-specific amplification); MW: 100-bp DNA ladder. P values: *P<0.05, **P<0.01 and *** P<0.001. (n=3).

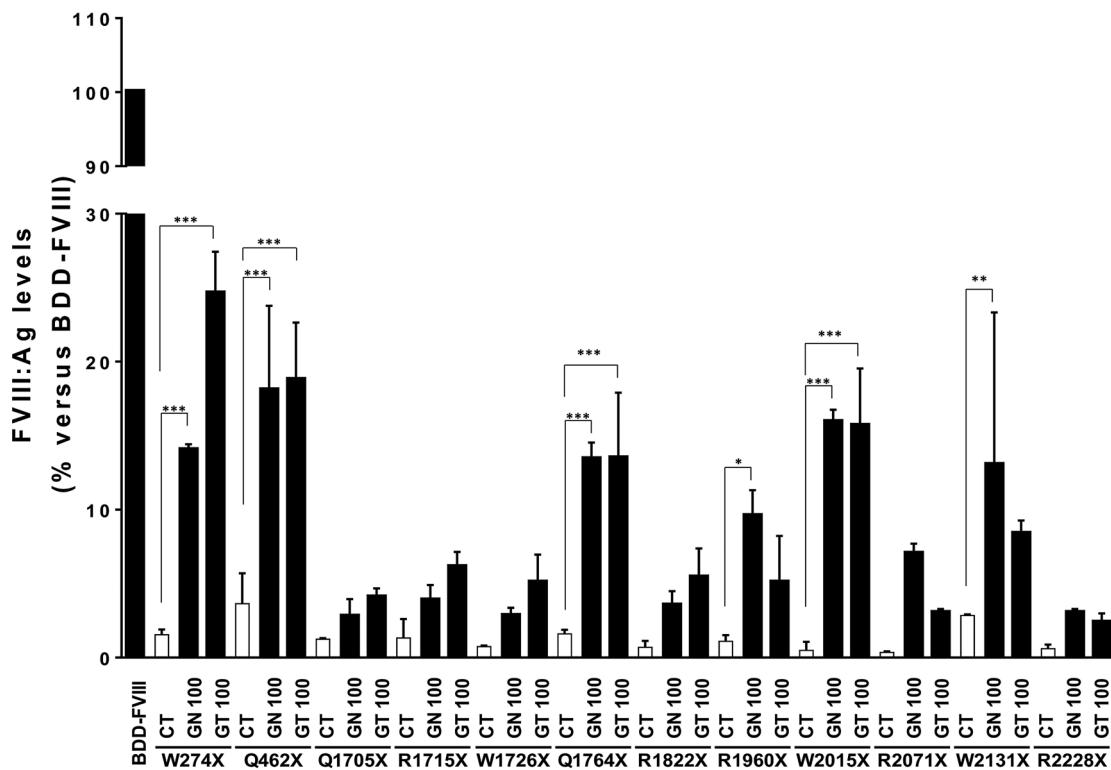


Figure 2. Readthrough agents (RTA) can increase FVIII antigen levels in the supernatants of some transfected Chinese hamster ovary (CHO) cells. Human FVIII:Ag levels analyzed by ELISA in the supernatants of CHO cells transiently transfected with the F8 variants, showing the increase in FVIII:Ag levels before and after RTA-treatment versus the F8 wild-type (WT) variant. BDD-FVIII: WT; CT: untreated controls; GN100: 100 µg geneticin/mL and GT100: 100 µg gentamicin/mL. * $P < 0.05$; ** $P < 0.01$; *** $P < 0.001$. (N=3).

FVIII immunodetection of F8BDD variants

Chinese hamster ovary lines transfected with the F8BDD variants were stained with several anti-FVIII antibodies for the immunodetection of FVIII in cell homogenates (*Online Supplementary Table S4*).

FVIII activity of F8BDD variants

The FVIII activity (FVIII:C) of the supernatants of cultured fibroblasts or CHO cells transfected with F8BDD variants, treated or not with RTA, was assessed by the chromogenic method using the COAMATIC FVIII kit (Chromogenix, Werfen, Barcelona, Spain). The protocol was modified from Yatuv *et al.*²⁰

Results

F8 mRNA levels after readthrough agent treatment

In the fibroblasts of HA-patients harboring nonsense mutations, F8 mRNA levels measured by quantitative real-time-polymerase chain reaction (qRT-PCR) were <60% (p.Q1636X: 46.23%±9.19; p.W1586X: 59.89%±5.55; p.R1960X: 57.09%±3.81) of those detected in control fibroblasts from healthy individuals or from the HA patients caused by the missense mutation. Treatment with the protein synthesis inhibitor cycloheximide, which also inhibits nonsense-mediated decay (NMD), restored the levels of PTC-containing transcripts to normal values, which suggested a role for NMD in our HA patients harboring nonsense mutations (Figure 1B). We then analyzed the ability of RTA to suppress PTC and stabilize PTC-con-

taining mRNA, as reported in previous studies.^{21,22} Although some of the RTA increased F8 mRNA levels in the fibroblasts of HA patients, the differences were not statistically significant: p.W1586X: 59.89%±5.55 (CT) versus 86.01%±11.82 (100 µg geneticin/mL); p.Q1636X: 46.23%±9.19 (CT) versus 64.68%±12.41 (10 µM RTC13), and p.R1960X: 57.09%±3.82 (CT) versus 79.21%±5.66 (100 µg gentamicin/mL) (Figure 1B). A possible explanation for this could be that none of the nonsense mutations analyzed in patients' fibroblasts met the PTC rule.

In addition, we used CHO cells, which is the most commonly used cell line for commercial production of FVIII,²³ to analyze F8 mRNA levels to measure the effects of RTA. Time course qRT-PCR analysis using F8BDD-specific primers showed that the CHO cell model expressed high levels of F8 mRNA without any presence of NMD over time (Figure 1C).

Analysis of the human FVIII:Ag levels in the culture media

Although fibroblasts ectopically express F8 mRNA, they do not synthesize FVIII protein.²⁴ For this reason, and because none of the nonsense mutations analyzed in patients' fibroblasts met the PTC rule, all protein studies were performed in the CHO cellular model. To determine the ability of the already established RTAs geneticin and gentamicin to increase FVIII production, FVIII:Ag levels in the culture supernatants of the treated CHO cells were analyzed by ELISA (Table 2 and Figure 2). Compared to

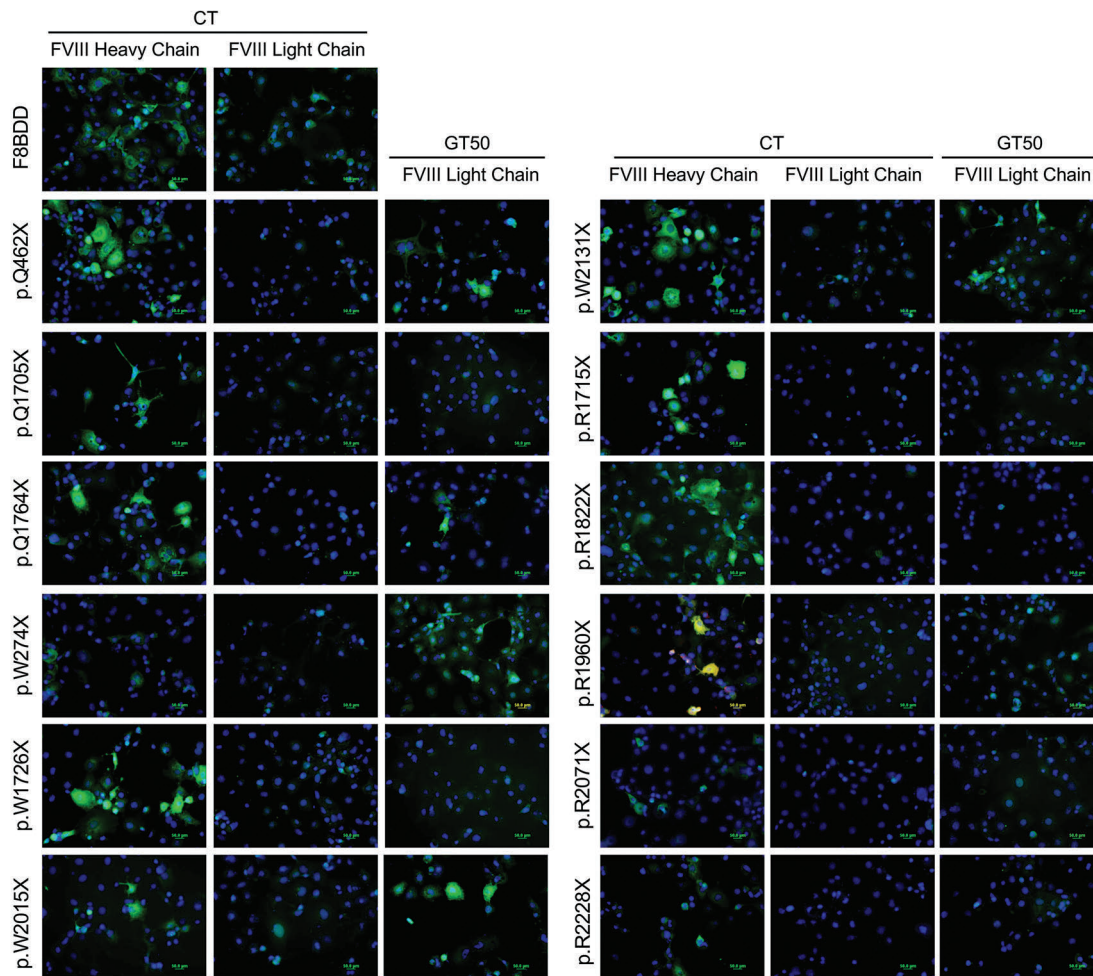


Figure 3. Gentamicin increased FVIII biosynthesis in some transfected Chinese hamster ovary (CHO) cells. Representative images of the immunofluorescence detection of FVIII in transiently transfected CHO cells stained with antibodies against either FVIII heavy chain or FVIII light chain (both in green). Gentamicin treatment (GT50: 50 µg/mL) increased FVIII labeling using the anti-FVIII light chain antibody in CHO cells transiently transfected with variants harboring the p.W274X, p.Q462X, p.Q1764X, p.W2015X and p.W2131X premature termination codons.

the controls (CT), these two drugs, each at 100 µg/mL, significantly increased the human FVIII:Ag levels of the variants p.W274X (CT=1.55 vs. 24.6% with gentamicin), p.Q462X (CT=3.65 vs. 18.75% with gentamicin), p.Q1764X (CT=1.6 vs. 13.45% with geneticin), p.W2015X (CT=0.5 vs. 15.9% with geneticin) and p.W2131X (CT=2.85 vs. 13% with geneticin). In the p.R1960X variants, FVIII:Ag levels increased significantly only in cells treated with 100 µg geneticin/mL (CT=1.1 vs. 9.55%). Smaller, non-significant, increases were observed for the p.Q1715X, p.R1715X, p.W1726X, p.R18822x, p.R2071X and p.R2228X variants.

Immunodetection of FVIII after readthrough agent treatment

To establish the mechanism by which the previously used RTA increased FVIII production, protein levels were analyzed in transfected CHO cells by immunofluorescence using antibodies generated against either heavy (N-terminal) or light (C-terminal) chains (*Online Supplementary Table S1*). Before RTA treatment, light chain staining was detected only in cells transfected with the

WT F8BDD variant (Figure 3). However, after treatment of the transfectants with 50 µg gentamicin/mL, staining for light chain was visible in cells transfected with variants p.W274X, p.Q462X, p.Q1764X, p.R1960X, p.W2015X, and p.W2131X (Figure 3). FVIII production in cell lysates was also analyzed, using an anti-FVIII antibody raised against FVIII heavy chain (Nt). Before RTA treatment, truncated FVIII accumulated intracellularly in cells transfected with the different constructs harboring PTC, which is, in addition to a faulty degradation, one of the possible consequences of the inability of FVIII to fold properly.²³ In contrast, treatment with some of the RTA reduced the amount of intracellular accumulation (Figure 4 and *Online Supplementary Figure S1*). In the p.Q462X, the highest reduction in FVIII accumulation was observed with geneticin, at the two tested concentrations. The p.Q1764X and p.W2015X variants were also responsive to geneticin, but the highest reduction in intracellular accumulation of FVIII was achieved with RTC13. The p.R1822X showed a reduction in intracellular accumulation only with the higher concentration of gentamicin tested. Other variants also showed a qualitative reduction (p.Q1705X for geneticin

and gentamicin; R1960X for geneticin, gentamicin but also PTC124, and p.W2131X for geneticin, and RTC13) or only a minimal qualitative reduction (p.W1726X and p.R2228X) in the intracellular accumulation of truncated FVIII (Online Supplementary Figure S1).

Rescue of FVIII:C activity after readthrough agent treatment

Finally, we focused in the RTA-mediated effect on the protein functionality rather than on the protein levels. To this end, we analyzed the FVIII:C activity by means of a

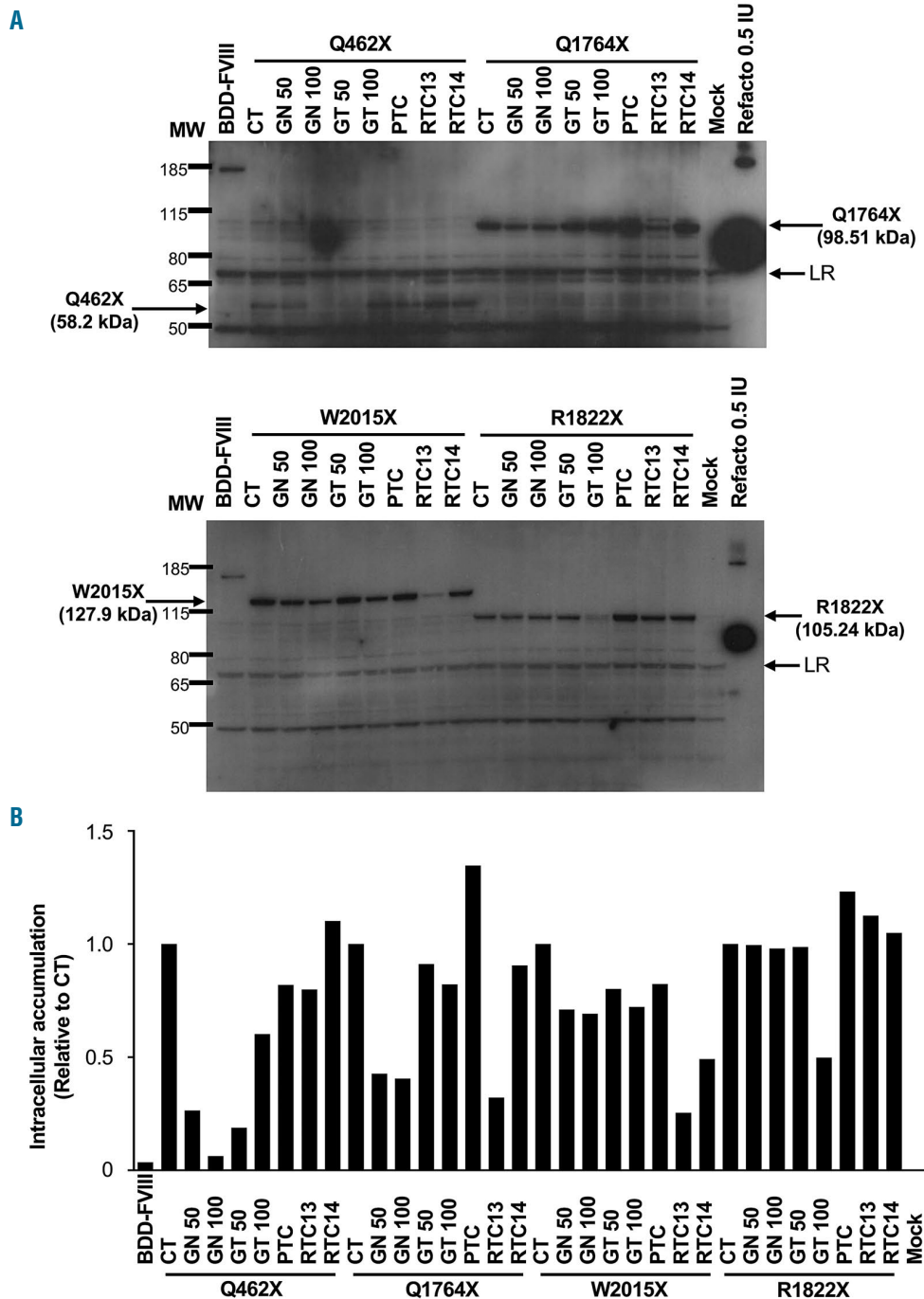


Figure 4. Readthrough agents (RTA) reduced intracellular accumulation of FVIII in transfected Chinese hamster ovary (CHO) cells. Representative images of the immunodetection of FVIII heavy chain in cell homogenates of transiently transfected CHO cells. (A) Western blot of CHO cells transfected with either wild-type (WT) BDD-FVIII (166.19 kDa), the p.Q462X (52.8 kDa), p.Q1764X (98.51 kDa) (top panel), p.W2015X (127.9 kDa), or the p.R1822X (105.24 kDa) variants (bottom panel). The intracellular accumulation of BDD-FVIII or the truncated proteins before and after RTA-treatment is shown. (B) Densitometry of the bands in (A). CT: Untreated cells; GN50: 50 µg geneticin/mL; GN100: 100 µg geneticin/mL; GT50: 50 µg gentamicin/mL; GT100: 100 µg gentamicin/mL; PTC: PTC124 10 µM; RTC13 and RTC14: 10 µM; Mock: untransfected cells; MW: Pageruler Plus prestained protein ladder; Refacto®: recombinant human BDD-FVIII (Pfizer); LR: loading reference used for densitometry normalization.

chromogenic assay using not only the well established RTA geneticin and gentamicin, but also other RTA such as PTC, RTC13 and RTC14. RTA treatment resulted in a significant dose-dependent increase in FVIII:C in only five of the 12 variants (Table 2 and Figure 5). The strongest

readthrough response was that of p.W274X, in which a 3.7-fold increase in activity was obtained after treatment with 100 μg gentamicin/mL. Smaller increases in FVIII:C activity were measured at a lower dose of gentamicin (50 $\mu\text{g}/\text{mL}$) or geneticin (50 and 100 $\mu\text{g}/\text{mL}$). Increases in

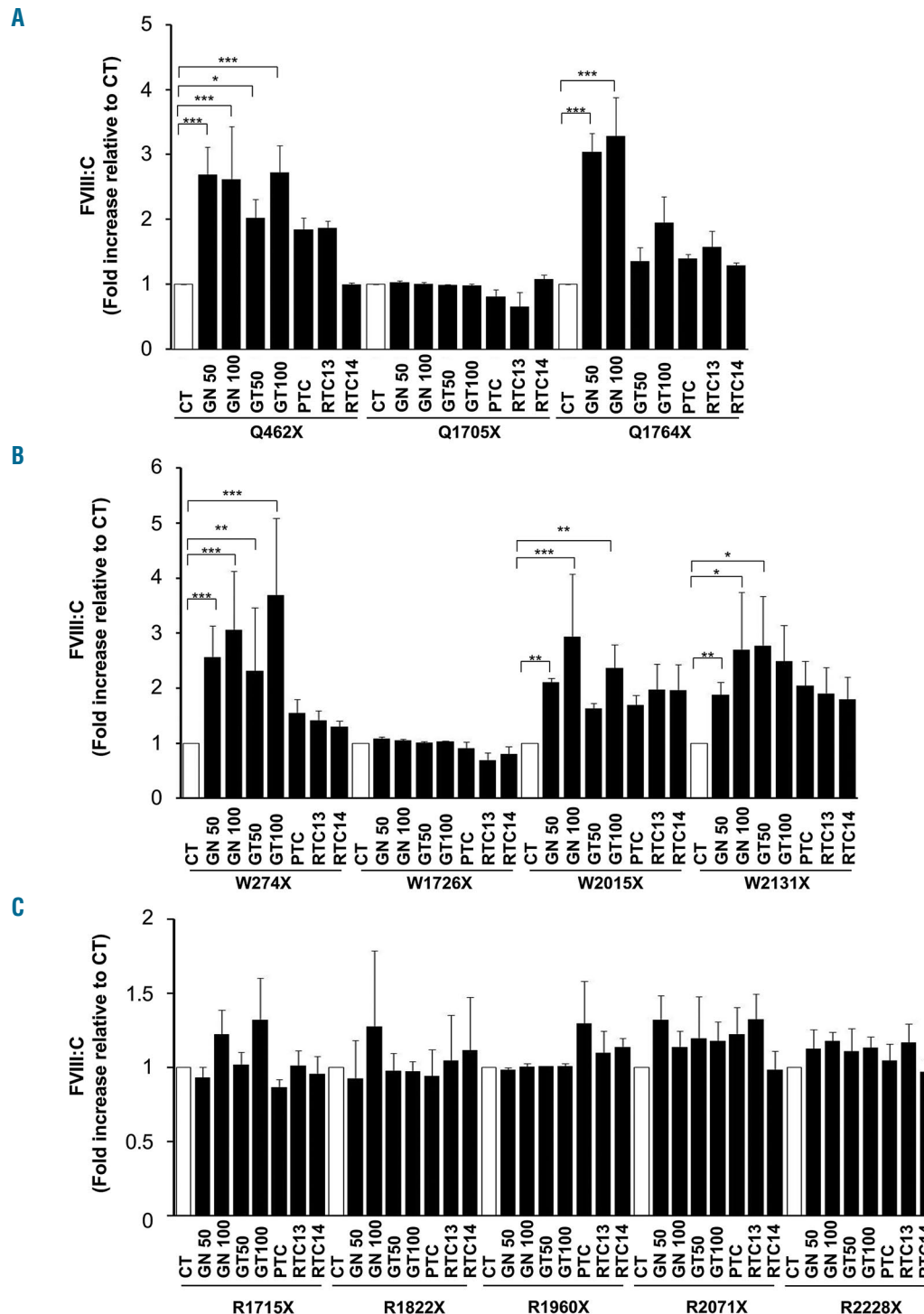


Figure 5. Readthrough agents (RTA) increase FVIII coagulant activity in the supernatants of transfected Chinese hamster ovary (CHO) cells. (A) Fold increase of FVIII:C (relative to untreated controls) in the supernatants of cultured CHO cells transiently transfected with variants harboring a QX premature termination codons (PTC) (see legend to Figure 1). (B) Fold increase of FVIII:C in the supernatants of cultured CHO cells transiently transfected with variants harboring a WX PTC (see legend to Figure 1). (C) Fold increase of FVIII:C in the supernatants of cultured CHO cells transiently transfected with variants harboring a RX PTC (see legend to Figure 1). CT: untreated controls; GN50: 50 μg geneticin/mL; GN100: 100 μg geneticin/mL; GT50: 50 μg gentamicin/mL; GT100: 100 μg gentamicin/mL; PTC: PTC124 10 μM ; RTC13 and RTC14: 10 μM . * $P<0.05$; ** $P<0.01$; *** $P<0.001$. (N=3).

FVIII:C after exposure to 100 µg geneticin/mL were also observed in the p.W2015X and p.W2131X variants (2.9- and 2.7-fold, respectively) and in the p.Q462X and p.Q1764X variants (up to 2.6- and 3.3-fold, respectively). These variants were also responsive, although to a lesser extent, to treatment with 100 µg gentamicin/mL but the increases in FVIII:C were smaller. Variants responsive to either gentamicin or geneticin showed a slight response to other RTA, particularly to PTC124 and RTC13, but these increases were not statistically significant.

In silico analysis of the premature termination codons

Variable responses to RTA-induced nonsense suppression related to the sequences adjacent to the PTC have been reported. We therefore analyzed the PTC type and the context effect in both the patients' fibroblasts and the 12 *F8*BDD variants (Tables 1 and 2, and *Online Supplementary Table S2*). In patients' fibroblasts responsive to RTA, we would expect at least a partial restoration of the *F8* mRNA levels; however, none of the PTC sequence context filled the PTC rule, so we cannot expect any mRNA stabilization. In contrast, in the CHO model, we could evaluate the readthrough effect on the production of full-length protein and on the restoration of FVIII:C activity. The results suggested a TGA≥TAG hierarchy of PTC suppression sensitivity and a positive RTA readthrough effect on both FVIII:Ag levels and FVIII:C activity for sequences in which a C was located at position +4 and a T at position -1 as present in variants pW274X, pQ462X, pQ1764X and pW2015X. Furthermore, the pW2131X variant also showed responsiveness even when a G is present at position -1 instead of a T. In contrast, variants pR1715X, pR2071X and pR2228X, even containing a TGA and a T at position -1 and a C at position +4 were unable to significantly increase FVIII:C activity. Similarly, the pR1822X variant was also unresponsive to RTA, despite the fact that it contains a TGA and a T at position -1.

Although positions -5 (A, C>G) and +8 (G>C) were also reported to influence readthrough, our data show that T, G and A at position -5 as well as T or C at position +8 promoted PTC suppression, as measured by FVIII:C levels; other tested combinations may have positive effects measured by FVIII:Ag levels. Whether positive effects are associated with yet other nucleotide combinations could not be determined due to the limited number of *F8* variants tested (*Online Supplementary Table S2*).

Discussion

The present study represents a comprehensive analysis of factors influencing the responsiveness to RTA of a series of nonsense mutations that are representative of those causing HA. Readthrough therapy is not expected to restore the synthesis and activity of the recoded proteins to curative levels in most patients harboring nonsense mutations. However, in the case of hemophilia, even a relatively small percentage of restoration may be very valuable. Thus, in patients with severe HA (<1% of FVIII:C), a slight increase in activity to 2-5% could significantly improve the bleeding phenotype as reported for FIX production in severe HB patients treated with gentamicin.⁹

Our study uses a CHO-based HA model in which

NMD is absent, as cells were transfected with plasmid containing the *F8* cDNA, but lacking the exon-exon junction complexes (EJC) which are necessary for PTC-containing mRNA to be targeted by NMD, thus providing a clean tool to amplify and detect eventual readthrough activity of RTA. While cDNA models do not mimic the *in vivo* situation (in which NMD is present), they can be used for assessing potential readthrough effects and to identify new RTA.^{10,11,17,25} In practice, to show a readthrough effect *in vivo* or in primary cells, RTA will probably have to be combined with NMD inhibition. Nonetheless, the CHO-based HA model allowed us to demonstrate that the effectiveness of readthrough therapy is mutation-specific and that *in vitro* assays may be useful for classifying patients that can likely benefit from RTA.

It has recently become clear that different types of endothelial cells, including liver sinusoidal endothelial cells (LSEC), constitute the main source of FVIII production in humans,^{24,26-29} perhaps to a greater extent than hepatocytes. This may explain why, although ectopically expressed at the mRNA level, none of the fibroblasts from HA patients analyzed showed a significant stabilization of *F8* mRNA levels. However, as the PTC sequence context does not fill the PTC rule, we cannot draw any conclusions as to the effectiveness of the RTA used. Furthermore, since fibroblasts do not produce FVIII,²⁴ we could not expect to detect FVIII protein.

Despite the limitations of this study, which include the relatively low number of mutations analyzed, the intrinsic variability in the transfection efficiencies, and the low levels of FVIII:C achieved (in the low range of detection by FVIII:C assays, i.e. 0.5-3%), the observed increases in the FVIII:C activity in some mutations suggest a potential phenotypic improvement, from severe to moderate/mild HA. Thus, RTA treatment significantly rescued FVIII production in some of the *F8*BDD variants, as measured by FVIII:Ag levels. This increase was associated with a qualitative reduction in intracellular accumulation of FVIII observed in the western blots, and a concomitant increase in light-chain FVIII detection by immunofluorescence. Moreover, data obtained in the FVIII:C analyses highlighted the importance of the amino acid incorporated upon RTA treatment in the partial restoration of FVIII:C activity. In our study, after drug treatment, only variants that natively encoded tryptophan (Trp=W) or glutamine (Gln=Q) and had a cytosine at position +4, regardless of the PTC type, were able to significantly increase FVIII:C in the culture supernatants, while this activity was not increased in variants natively encoding arginine (Arg=R), even when a cytosine at position +4 was present, likely because the RTA may promote the incorporation of amino acids that do not necessarily restore FVIII functionality.

Nonsense suppression was observed in only five of the 12 transfected *F8*BDD variants (p.Q462X, p.Q1764X, p.W274X, p.W2015X and p.W2131X). This apparent discrepancy between protein levels and restored activity can be explained by the context-dependent ability of RTA to restore the full-length recoded protein¹⁵ and by the preferred aminoacyl tRNA that will recognize each PTC in RTA-treated cells.¹⁵ Accordingly, upon secretion, only full-length protein that has incorporated the native amino acid (or another one with similar chemical properties) is expected to have a greater chance of restoring maximum or partial levels of FVIII:C activity. Additionally, the phy-

logenetic conservation of this amino acid, or whether deleterious missense mutations have been described in this codon, are additional important factors to be considered.

Under our experimental conditions, the ability of RTA to increase C-terminal (light chain) positive staining or FVIII:Ag levels did not always correlate with the ability of RTA to restore FVIII:C activity. This suggests that the amino acid incorporated at the PTC and its structural similarity with the natively encoded amino acid can be critical for the restoration of FVIII:C, but not necessarily for that of FVIII:Ag. According to the PTC context rule,¹³ the hierarchy of RTA responsiveness is T-TGA-C>T-TAG-C>T-TAA-C; thus, a stronger RTA effect at TGA (opal) is expected in PTC originally encoding tryptophan and arginine. However, we found that PTC generated at triplets natively encoding arginine and fulfilling the PTC context rule led to production of a non-functional protein, although this situation can also result in a gain of function, as reported in a cellular model of readthrough in hemophilia B.³⁰ Conversely, according to the PTC context rule, a PTC generated at triplets encoding glutamine is predicted to be less responsive to RTA treatment. However, in our study, RTA allowed partial restoration of FVIII:C levels in 2 of 3 recoded FVIII mutants originally encoding glutamine (pQ462X and pQ1764X). A similar result was reported in a study of cystic fibrosis in which patients harboring the Y122X mutation had a better than expected response to RTA, even though the PTC was caused by a TAA codon, followed by a C nucleotide at position +4, which was previously reported to have the lowest RTA sensitiveness.¹⁵ However, both the readthrough effect due to the presence of cytosine at position +4, and the incorporation of the natively encoded tyrosine might have been facilitated by the RTA treatment,¹⁵ which would account for the clinical benefit observed.

Our work points out the importance of not only evaluating RTA-mediated protein biosynthesis, but also the functional activity of the recoded protein generated. This is particularly important in studies of the potential clinical benefit of RTA therapy and the search for safer and more

effective RTA. By taking into account the functionality of the restored protein generated by RTA, our cellular model, or other similar models, provide a method for testing the effectiveness of new RTA.³¹

Although we evaluated only a small number of F8BDD variants, and these results cannot be generalized, our analysis of the molecular environment of these PTC provides valuable information on additional factors involved in eventual responses to RTA treatment. From these results we can conclude that: 1) responsiveness is greater in PTC with the consensus sequence T-Stop-C; 2) in TGA (opal) than in TAG (amber) PTC; and 3) it will be higher when the mutated original amino acid is tryptophan or glutamine as opposed to arginine, in which, despite the efficient intracellular reduction of truncated protein and extracellular increase of FVIII:Ag levels, the increase observed in FVIII:C activity was minimal.

In conclusion, the results obtained with our model represent a proof-of-concept that RTA are capable of suppressing PTC in some nonsense mutations causing HA, albeit with different efficiencies and different functional consequences depending on the sequence context. This model, linked to a functional assay based on the determination of FVIII:C activity, and the application of the PTC rule described here, allowed for the first time the identification of five RTA-responsive nonsense mutations in HA and may facilitate the classification of nonsense mutations reported in the HA database into categories based on the predicted levels of responsiveness to RTA, thus promoting patient selection in readthrough therapy clinical trials.³²

Acknowledgments

The authors thank the participating patients and their families. We also thank Yvonne Richaud-Patin and Dr. Angel Raya (CMRB, Spain) for their help with the fibroblast isolation.

Funding

This project was supported by two grants from the Instituto de Salud Carlos III (PI11/03024 and PI11/03029) / e-Rare-2 (HEMO-iPS) that were cofinanced by the European Regional Development Fund (FEDER), and the Europe Aspire 2013 Award in Hemophilia Research.

References

- Gouw SC, van den Berg HM, Oldenburg J, et al. F8 gene mutation type and inhibitor development in patients with severe hemophilia A: systematic review and meta-analysis. *Blood*. 2012;119(12):2922-2934.
- Escobar MA. Health economics in haemophilia: a review from the clinician's perspective. *Haemophilia*. 2010;16:29-34.
- Rangarajan S, Walsh L, Lester W, et al. AAV5-Factor VIII Gene Transfer in Severe Hemophilia A. *N Engl J Med*. 2017;377(26):2519-2530.
- George LA, Sullivan SK, Giermasz A, et al. Hemophilia B Gene Therapy with a High-Specific-Activity Factor IX Variant. *N Engl J Med*. 2017;377(23):2215-2227.
- Linde L, Boelz S, Nissim-Rafinia M, et al. Nonsense-mediated mRNA decay affects nonsense transcript levels and governs response of cystic fibrosis patients to gentamicin. *J Clin Invest*. 2007;117(3):683-692.
- Sermet-Gaudelus I, Renouil M, Fajac A, et al. In vitro prediction of stop-codon suppression by intravenous gentamicin in patients with cystic fibrosis: a pilot study. *BMC Med*. 2007;5:5.
- Finkel RS, Flanigan KM, Wong B, et al. Phase 2a study of ataluren-mediated dystrophin production in patients with nonsense mutation Duchenne muscular dystrophy. *PLoS One*. 2013;8(12):e81302.
- Bushby K, Finkel R, Wong B, et al. Ataluren treatment of patients with nonsense mutation dystrophinopathy. *Muscle Nerve*. 2014;50(4):477-487.
- James PD, Raut S, Rivard GE, et al. Aminoglycoside suppression of nonsense mutations in severe hemophilia. *Blood*. 2005;106(9):3043-3048.
- Welch EM, Barton ER, Zhuo J, et al. PTC124 targets genetic disorders caused by nonsense mutations. *Nature*. 2007;447(7140):87-91.
- Du L, Damoiseaux R, Nahas S, et al. Nonaminoglycoside compounds induce readthrough of nonsense mutations. *J Exp Med*. 2009;206(10):2285-2297.
- Manuvakhova M, Keeling K, Bedwell DM. Aminoglycoside antibiotics mediate context-dependent suppression of termination codons in a mammalian translation system. *RNA*. 2000;6(7):1044-1055.
- Floquet C, Hatin I, Rousset J-P, Bidou L. Statistical analysis of readthrough levels for nonsense mutations in mammalian cells reveals a major determinant of response to gentamicin. *PLoS Genet*. 2012;8(3):e1002608.
- Dabrowski M, Bukowy-Bieryllo Z, Zietkiewicz E. Translational readthrough potential of natural termination codons in eucaryotes--The impact of RNA sequence. *RNA Biol*. 2015;12(9):950-958.
- Roy B, Leszyk JD, Mangus DA, Jacobson A.

- Nonsense suppression by near-cognate tRNAs employs alternative base pairing at codon positions 1 and 3. *Proc Natl Acad Sci U S A*. 2015;112(10):3038-3043.
16. Vidal F, Farssac E, Altisent C, Puig L, Gallardo D. Rapid hemophilia A molecular diagnosis by a simple DNA sequencing procedure: identification of 14 novel mutations. *Thromb Haemost*. 2001;85(4):580-583.
 17. Jung ME, Ku J-M, Du L, Hu H, Gatti RA. Synthesis and evaluation of compounds that induce readthrough of premature termination codons. *Bioorg Med Chem Lett*. 2011;21(19):5842-5848.
 18. Yu H, Liu X, Huang J, et al. Comparison of readthrough effects of aminoglycosides and PTC124 on rescuing nonsense mutations of HERG gene associated with long QT syndrome. *Int J Mol Med*. 2014;33(3):729-735.
 19. Martorell L, Corrales I, Ramirez L, et al. Molecular characterization of ten *F8* splicing mutations in RNA isolated from patient's leucocytes: assessment of in silico prediction tools accuracy. *Haemophilia*. 2015;21(2):249-257.
 20. Yatuv R, Dayan I, Baru M. A modified chromogenic assay for the measurement of very low levels of factor VIII activity (FVIII:C). *Haemophilia*. 2006;12(3):253-257.
 21. Bedwell DM, Kaenjak A, Benos DJ, et al. Suppression of a CFTR premature stop mutation in a bronchial epithelial cell line. *Nat Med*. 1997;3(11):1280-1284.
 22. Keeling KM, Brooks DA, Hopwood JJ, et al. Gentamicin-mediated suppression of Hurler syndrome stop mutations restores a low level of alpha-L-iduronidase activity and reduces lysosomal glycosaminoglycan accumulation. *Hum Mol Genet*. 2001;10(3):291-299.
 23. Kumar SR. Industrial production of clotting factors: Challenges of expression, and choice of host cells. *Biotechnol J*. 2015;10(7):995-1004.
 24. Turner NA, Moake JL. Factor VIII Is Synthesized in Human Endothelial Cells, Packaged in Weibel-Palade Bodies and Secreted Bound to ULVWF Strings. *PLoS One*. 2015;10(10):e0140740.
 25. Benhabiles H, Gonzalez-Hilarion S, Amand S, et al. Optimized approach for the identification of highly efficient correctors of nonsense mutations in human diseases. *PLoS One*. 2017;12(11):e0187930.
 26. Hollestelle MJ, Thinnes T, Crain K, et al. Tissue distribution of factor VIII gene expression in vivo—a closer look. *Thromb Haemost*. 2001;86(3):855-861.
 27. Wion KL, Kelly D, Summerfield JA, Tuddenham EG, Lawn RM. Distribution of factor VIII mRNA and antigen in human liver and other tissues. *Nature*. 1985;317(6039):726-729.
 28. Olgasi C, Talmon M, Merlin S, et al. Patient-Specific iPSC-Derived Endothelial Cells Provide Long-Term Phenotypic Correction of Hemophilia A. *Stem Cell Rep*. 2018;11(6):1391-1406.
 29. Suzuki Y, Kakisaka K, Matsumoto T, et al. Orthotopic liver transplantation for haemophilia A may not always lead to a phenotypic cure of haemophilia A: A case report. *Haemophilia*. 2018;24(6):e420-e422.
 30. Branchini A, Ferrarese M, Campioni M, et al. Specific factor IX mRNA and protein features favor drug-induced readthrough over recurrent nonsense mutations. *Blood*. 2017;129(16):2303-2307.
 31. Baradaran-Heravi A, Balgi AD, Zimmerman C, et al. Novel small molecules potentiate premature termination codon readthrough by aminoglycosides. *Nucleic Acids Res*. 2016;44(14):6583-6598.
 32. Schmittgen TD, Zakrajsek BA, Mills AG, et al. Quantitative reverse transcription-polymerase chain reaction to study mRNA decay: comparison of endpoint and real-time methods. *Anal Biochem*. 2000;285(2):194-204.

Validation of Minnesota acute graft-versus-host disease Risk Score

Margaret L. MacMillan,^{1,2} Todd E. DeFor,^{1,3} Shernan G. Holtan,^{1,4}
Armin Rashidi,^{1,4} Bruce R. Blazar^{1,2} and Daniel J. Weisdorf^{1,4}

¹Blood and Marrow Transplant Program, University of Minnesota Medical School, Minneapolis, MN; ²Department of Pediatrics, University of Minnesota Medical School, Minneapolis, MN; ³Biostatistics and Informatics Core, Masonic Cancer Center, University of Minnesota Medical School, Minneapolis, MN and ⁴Department of Medicine, University of Minnesota Medical School, Minneapolis, MN, USA



Haematologica 2020
Volume 105(2):519-524

ABSTRACT

Using multicenter data, we developed a novel acute graft-versus-host disease Risk Score which more accurately predicts response to steroid treatment, survival and transplant related mortality than other published risk scores based upon clinical grading criteria.¹ To validate this Risk Score in a contemporary cohort, we examined 355 recent University of Minnesota patients (2007-2016) diagnosed with acute graft-versus-host disease and treated with prednisone 60 mg/m²/day for 14 days, followed by an 8-week taper. Overall response [complete response + partial response] was higher in the 276 standard risk versus 79 high risk graft-versus-host disease patients at day 14 (71% versus 56%, $P < 0.01$), day 28 (74% versus 59%, $P = 0.02$) and day 56 (68% versus 49%, $P < 0.01$) after steroid initiation. Day 28 response did not differ by the initial graft-versus-host disease grade. In multiple regression analysis, patients with high risk graft-versus-host disease were less likely to respond at day 28 (odds ratio 0.5, 95% CI 0.3-0.9, $P < 0.01$) and had higher risks of 2 year transplant related mortality (Hazard Ratio 1.8, 95% CI, 1.0-2.1, $P = 0.03$) and overall mortality (Hazard Ratio 1.7, 95% CI, 1.2-2.4, $P < 0.01$) than patients with a standard risk graft-versus-host disease. This analysis confirms the Minnesota graft-versus-host disease Risk Score as a valuable bedside tool to define risk in patients with acute graft-versus-host disease. A tailored approach to upfront acute graft-versus-host disease therapy based upon the Minnesota Risk Score may improve outcomes and facilitate testing of novel treatments in these patients.

Introduction

Acute graft-versus-host disease (GvHD) remains a major cause of morbidity and mortality after allogeneic hematopoietic cell transplantation (HCT).² Immediate, real time risk determination at diagnosis may facilitate initiation of more appropriate and potentially effective upfront therapy. In 2015, we developed a novel GvHD Risk Score based on the number of organs involved and severity of GvHD at the onset of systemic steroid treatment in 1723 patients from four centers and the Blood and Marrow Transplant Clinical Trials Network (BMT CTN) treated from 1990-2007.¹ Using clinical groupings, descriptive statistics and recursive partitioning, we identified poorly responsive, high-risk (HR) acute GvHD defined by the number of involved organs and organ stage, thus determining the severity of GvHD at onset. HR-GvHD is defined as either skin stage 4; lower gastrointestinal (GI) stage 3-4 or liver stage 3-4; or skin stage 3+ and either lower GI 2-4 or liver stage 2-4 GvHD. Standard risk (SR)-GvHD includes single organ involvement (either stage 1-3 skin or stage 1-2 GI) or 2 organ involvement (either stage 1-3 skin plus stage 1 GI; or stage 1-3 skin plus stage 1-4 liver). We designed a free web-based program to easily determine the GvHD risk group for a given patient using our refined Risk Score, available at: <https://z.umn.edu/MNACuteGVHDRiskScore>. Patients with HR-GvHD were three times less likely to respond to steroid therapy and had a >2 fold increased risk of overall mortality and transplant-related mortality (TRM) than patients in the SR-GvHD group.¹

Correspondence:

MARGARET L. MACMILLAN
macmi002@umn.edu

Received: March 29, 2019.

Accepted: July 12, 2019.

Pre-published: July 18, 2019.

doi:10.3324/haematol.2019.220970

Check the online version for the most updated information on this article, online supplements, and information on authorship & disclosures: www.haematologica.org/content/105/2/519

©2020 Ferrata Storti Foundation

Material published in *Haematologica* is covered by copyright. All rights are reserved to the Ferrata Storti Foundation. Use of published material is allowed under the following terms and conditions:

<https://creativecommons.org/licenses/by-nc/4.0/legalcode>. Copies of published material are allowed for personal or internal use. Sharing published material for non-commercial purposes is subject to the following conditions: <https://creativecommons.org/licenses/by-nc/4.0/legalcode>, sect. 3. Reproducing and sharing published material for commercial purposes is not allowed without permission in writing from the publisher.



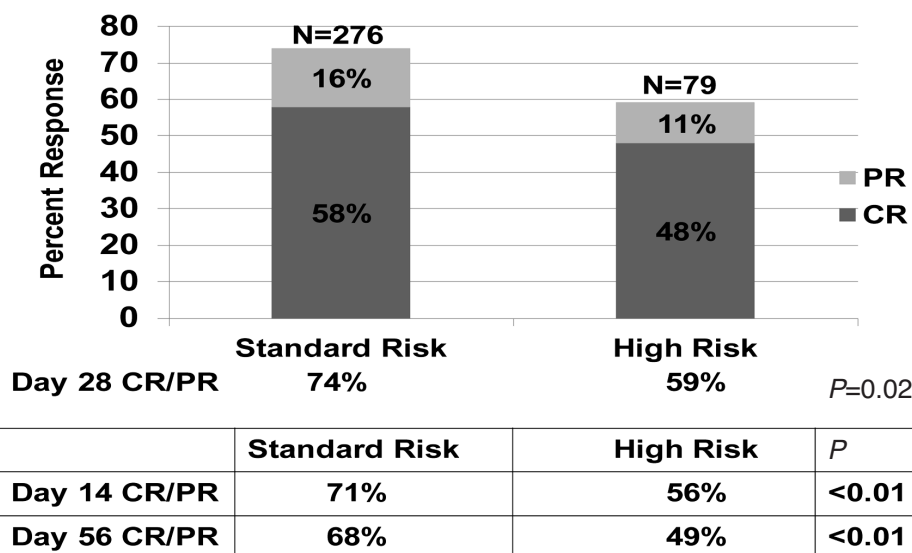


Figure 1. Response by Minnesota GvHD Risk Score.

As measured by the net reclassification index, the Minnesota GvHD Risk Score improves both the true-positive and false-positive rates and is a better predictor of response to upfront steroid therapy, survival and TRM than other published GvHD Risk Scores based upon clinical grading criteria.¹ Our previous analysis revealed that this GvHD Risk Score would reclassify 83% patients graded by the Center for International Blood and Marrow Transplant Research (CIBMTR) grading system³ and 27% if the Minnesota GvHD grading system^{4,5} were used allowing for more appropriate, risk stratified therapy at initial GvHD diagnosis.³⁻⁶

To validate this Minnesota GvHD Risk Score in a contemporary cohort with greater variety of conditioning regimens and donor grafts, we examined an independent cohort of 355 patients diagnosed with acute GvHD who were treated with systemic steroids as initial therapy at the University of Minnesota.

Methods

Between December 2007 and December 2016, 355 first allogeneic HCT patients developed grade I-IV acute GvHD and were treated with prednisone 60 mg/m²/day per os (PO) (or methylprednisolone 48 mg/m²/day intravenously (IV)) as initial therapy and are included in this analysis. Patients with grade I GvHD not treated with systemic therapy were excluded from this analysis. All HCT protocols were reviewed and approved by the Masonic Cancer Center Protocol Review Committee and the Institutional Review Board at the University of Minnesota.

Patient and transplant characteristics

Patient and transplant characteristics are shown in Table 1 for our new cohort of 355 patients as well as our old cohort of 1723 patients for comparison. The date of transplant did not overlap between the two groups. The median patient age was similar being 49 years (range, 0.2-75) and 40 years (range 0.2-76). In each cohort, 62% were males and the majority had a malignant disease.

In both groups approximately 1/3 of patients received a human leukocyte antigen (HLA)-matched sibling bone marrow (BM) or peripheral blood stem cell (PBSC) donor graft. In our new cohort, there were fewer HLA matched or mismatched unrelated donor (URD) grafts used. A much greater proportion of patients received an umbilical cord blood (UCB) graft; now 55% compared to only 15% previously. Details of the preparative therapy, GvHD prophylaxis and supportive therapies have been previously reported.⁷⁻¹⁰ In the new cohort, 50% patients received reduced intensity conditioning (RIC) compared to only 26% patients previously. In our new cohort, GvHD prophylaxis consisted of cyclosporine A (CSA) or tacrolimus based therapy in 92% of patients, *ex vivo* T-cell depletion in 1% of patients, and sirolimus plus mycophenolate mofetil (MMF) in 7% of patients.

GvHD therapy and measurement of response to prednisone

All patients were to receive daily, thrice divided doses of prednisone 60 mg/m²/day orally (or methylprednisolone IV equivalent, 48 mg/m²) for seven consecutive days, followed by daily prednisone for seven days as initial therapy for acute GvHD. Patients were maintained on therapeutic levels of CSA, tacrolimus or sirolimus. Additionally, patients with skin acute GvHD were treated with topical 0.1% triamcinolone cream or 1% hydrocortisone cream (for facial rash) three times daily. If a response to prednisone was observed, patients continued therapy with oral prednisone 60 mg/m²/day through day 14 and then commenced a taper of steroids over eight weeks.^{11,12} Response to therapy was evaluated by the attending physician and prospectively recorded weekly in the University of Minnesota BMT Database by determining the GvHD clinical stage score for each time point (± 3 days).¹³ Additional detail of GvHD data collection and scoring, supportive care and statistical analyses are detailed in the *Online Supplementary Methods* section.

Results

For the entire cohort, the median time from HCT to initiation of steroid therapy was 37 days (range 10-170,

interquartile range 26-57). All patients had ≥ 6 months follow-up after steroid initiation (median 3.2 years, range 0.5-9 years).

The initial organ stage of GvHD at onset of steroid treatment is shown in Table 2. Initial GvHD organ involvement was skin only (45%), upper gastrointestinal (GI) only (5%), upper and/or lower GI only (33%), liver only (1%) or multi-organ (21%). At onset of steroid therapy, 11% had grade I GvHD, 53% patients had grade II GvHD, 30% had grade III GvHD and 6% had grade IV GvHD. Of the 355 patients, 79 (22%) had Minnesota HR GvHD and 276 (78%) had Minnesota SR GvHD. The median onset of GvHD treatment in SR patients was 37 days [range, 10-170, interquartile range (IQR), 26.5-57] and 39 days (range, 13-156, IQR, 23-57) in HR patients.

Overall response (CR + PR) at day 28 was observed in 250 of 355 patients [70%: 95% confidence interval (CI), 65-75%]. CR was observed in 199 patients [56%: 95% CI, 51-61%] and PR in 51 patients [14%: 95% CI, 11-18%]. CR/PR was significantly higher in the 276 SR versus 79 HR GvHD patients at day 14 (71% versus 56%, $P < 0.01$), day 28 (74% versus 59%, $P = 0.02$; Figure 1) and day 56 (68% versus 49%, $P < 0.01$) after steroid initiation. Day 28 CR/PR did not differ by initial GvHD grade being 64%, 77%, 65% and 50% for grade I, II, III and IV ($P = 0.07$), noting that Grade I, II and III had similar day 28 CR/PR. Evaluating high risk for each index as classified by Minnesota HR GvHD, grades III/IV for the Minnesota GvHD grading system, and grades C/D for the CIBMTR grading system, the positive predictive value for no response was 41% (95% CI, 30-52%), 38% (95% CI, 29-47%) and 33% (95% CI, 27-40%), respectively.

TRM at six months was significantly higher in the HR (34%: 95% CI, 23-45%) versus SR patients [21%: 95% CI, 16-25%; $P < 0.01$] as shown in Figure 2. TRM at six months was also higher in patients with no response to steroids at day 28 (44%: 95% CI, 32-55%) versus those who achieved a PR (16%: 95% CI, 6-27%) or CR (13%: 95% CI, 9-18%; $P < 0.01$) as shown in Figure 3.

In multiple regression analysis, adjusting for clinically significant variables, the odds of day 28 CR/PR were lower in HR versus SR GvHD patients [odds ratio (OR) 0.5, 95% CI, 0.3-0.9, $P = 0.01$]. Donor type was the only other factor significantly associated with response. HLA matched URD BM/PBSC recipients were less likely to achieve a CR/PR at day 28 (OR 0.3, 95% CI, 0.2-0.7, $P < 0.01$) versus HLA sibling donor BM/PBSC recipients, whereas single UCB graft recipients were 3.6 times as likely to respond (OR 3.6, 95% CI, 1.4-9.2, $P = 0.01$) and double UCB recipients 1.9 times as likely to respond (OR 1.9, 95% CI, 1.0-3.5, $P = 0.04$) as shown in Table 3. There were no statistically significant interactions in donor, graft or other variables with response.

We also performed a logistic regression analysis of day 28 CR/PR only in the 159 BM/PBSC (non-UCB recipients). Compared to Minnesota SR GvHD patients, the HR group had OR of 0.2 of achieving a day 28 CR and 0.2 of achieving CR/PR (both $P < 0.01$). The Minnesota GvHD Risk Score also predicted CR/PR in the small number of patients with non-malignant disease as well (*data not shown*).

In multiple regression analysis, factors statistically significantly associated with greater TRM through 2 years included HR GvHD (Hazard Ratio (HzR) 1.8, 95% CI, 1.1-2.7, $P = 0.01$), and matched URD BM/PBSC recipients (HzR

2.0, 95% CI, 1.1-3.5, $P = 0.02$). Lower TRM was associated with patients 18-35 years of age (HzR 0.6, 95% CI, 0.3-1.1, $P = 0.02$), single UCB (HzR 0.4, 95% CI, 0.2-1.0, $p = 0.04$) and early onset (< 28 days from HCT) GvHD (HzR 0.92, 95% CI, 0.87-0.97, $P = 0.05$). Similarly, mortality through 2 years was higher in HR GvHD (HzR 1.7, 95% CI, 1.2-2.4, $P < 0.01$), matched URD BM/PBSC recipients (HzR 1.8, 95% CI, 1.1-3.0, $P = 0.01$) and HCT-comorbidity

Table 1. Patient and transplant characteristics.

Characteristic	New cohort	Old cohort
Number of patients	355	1723
Year of transplant		
1990-2000		581 (33%)
2001-2007		1142 (67%)
2007-2010	112 (32%)	
2011-2016	243 (68%)	
Age, years		
Median (range)	49 (<1-75)	40 (<1-76)
Gender: male	221 (62%)	1067 (62%)
Disease		
Acute leukemia	196 (55%)	741 (43%)
CML	13 (4%)	217 (13%)
CLL/other leukemia	20 (6%)	73 (4%)
MDS/MPN	57 (16%)	194 (11%)
HL/NHL	20 (6%)	236 (14%)
Other malignancies	10 (3%)	69 (4%)
Non-malignant	39 (11%)	193 (11%)
Donor type		
HLA identical sibling	101 (28%)	598 (35%)
1 antigen mismatched sibling	2 (1%)	73 (4%)
HLA matched unrelated	49 (14%)	626 (36%)
1 antigen mismatched unrelated	8 (2%)	164 (10%)
Umbilical cord blood	195 (55%)	262 (15%)
Conditioning		
Myeloablative	178 (50%)	37 (47%)
Reduced Intensity	177 (50%)	42 (53%)
Initial GvHD Grade		
I	39 (11%)	426 (25%)
II	188 (53%)	953 (55%)
III	108 (30%)	311 (18%)
IV	20 (6%)	33 (2%)
Organ involvement		
Multi-organ	76 (21%)	556 (32%)
Skin only	158 (45%)	910 (53%)
Liver Only	2 (1%)	23 (1%)
Lower GI +/- upper GI	118 (33%)	346 (20%)
Upper GI only	19 (5%)	111 (6%)
Days from transplant to initial steroids		
Median (range)	37 (10-170)	30 (2-178)
Follow-up (years)		
Median (range)	3.2 years (0.5-9)	4.9 years (0.3-17.7)

CML: chronic myelogenous leukemia; CLL: chronic lymphocytic leukemia; MDS: myelodysplastic syndrome; MPN: myeloproliferative neoplasm; HL: Hodgkin lymphoma; NHL: Non-Hodgkin lymphoma.

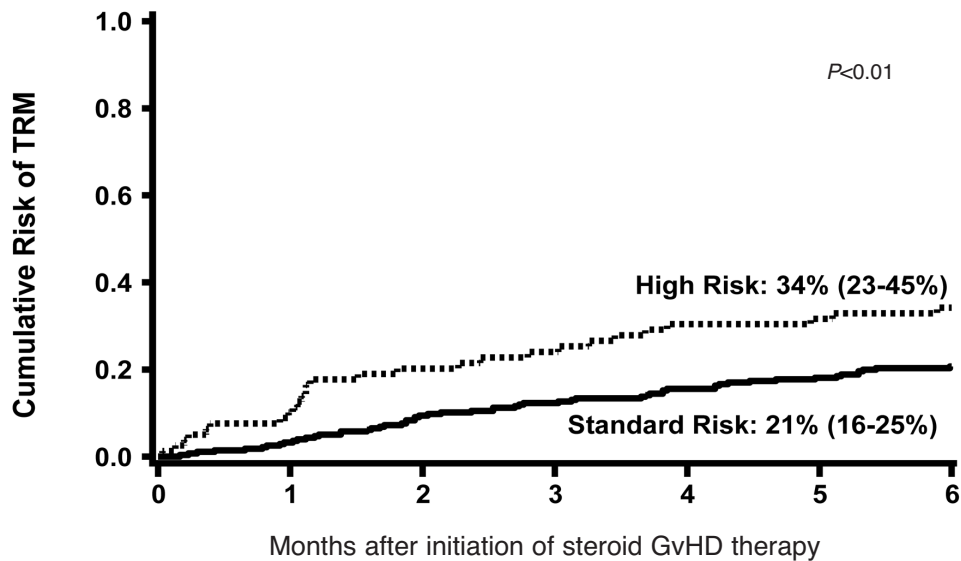


Figure 2. Cumulative incidence of TRM at 6 months after onset of steroid therapy by Minnesota GvHD Risk Score.

Table 2. GvHD organ stage at onset of steroid treatment.

Organ Stage	0	1	2	3	4
Skin	121 (34%)	26 (7%)	52 (15%)	150 (42%)	6 (2%)
Liver	343 (97%)	7 (2%)	2 (1%)	2 (1%)	1 (<1%)
Lower GI	200 (56%)	37 (10%)	56 (16%)	48 (14%)	14 (4%)
Upper GI	232 (65%)	123 (35%)			

index (CI) score ≥ 3 (HzR 1.7, 95% CI, 1.2-2.5, $P < 0.01$). There was a trend toward lower mortality in early onset GvHD (HzR 0.71, 95% CI, 0.50-1.01, $P = 0.06$). There were no statistically significant interactions with other covariates.

Two years after the initiation of the steroid therapy, 92 patients had developed chronic GvHD for a cumulative incidence of 26% (95% CI 21-31%). No differences in the incidence of chronic GvHD were observed in those with SR or HR acute GvHD (28% versus 20%, $P = 0.54$). Risks of chronic GvHD, however, were significantly lower in UCB recipients (HzR 0.6, 95% CI, 0.5-0.9, $P = 0.01$) and in early onset GvHD (HzR 0.95, 95% CI, 0.92-0.98, $P < 0.01$), but were higher in patients greater than 18 years of age ((HzR > 2.8), $P \leq 0.01$).

Discussion

We previously demonstrated that our refined multicenter Minnesota GvHD Risk Score, based upon the initial GvHD stage, serves as a better predictor of response and survival than either our previously published GvHD Risk Score based upon the initial GvHD grade, or the reported Minnesota or CIBMTR GvHD grading systems.¹⁴ To validate this refined Minnesota GvHD Risk Score, we examined a new, contemporary cohort of patients with acute GvHD treated at the University of Minnesota. This new cohort had a greater proportion of patients receiving RIC

and more UCB recipients. Our results confirm that the Minnesota GvHD Risk Score, based upon the initial GvHD stage, is a valuable and immediately available bedside tool to define the risk in patients with acute GvHD. It also predicts the outcomes of response, survival and TRM better than other published GvHD Risk Scores determined by clinical grading criteria. These data suggest that a tailored approach to upfront GvHD therapy based upon this Minnesota acute GvHD Risk Score and other risk factors should be considered in order to improve outcomes and to plan novel treatment studies in patients with acute GvHD.

In 1974, the Glucksberg grading system was developed by examining the clinical severity of acute GvHD in 43 adult patients who received matched sibling donor (MSD) transplants after myeloablative conditioning from 1969-1973.¹⁵ This grading system was later modified, but in all iterations, grade III-IV acute GvHD was considered high risk. 4,12,16 In 1997, the CIBMTR grading system was developed from 2129 adult who received MSD transplants after myeloablative conditioning from 1986-1992, and patients with grades C and D are deemed high risk based upon subsequent survival, yet GvHD treatment response was not examined.³ However, clinical observations suggest there are some patients with grade III GvHD who do well while some patients with grade II GvHD fare poorly.

We first attempted to better identify HR acute GvHD at diagnosis by examining the outcomes of 864 patients at

Table 3. Factors associated with day 28 CR/PR, mortality and TRM: multiple regression analyses.

Factors	N	Odds Ratio of Day 28 CR/PR (95% CI)	P	Hazard Ratio of 2 year Mortality (95% CI)	P	Hazard Ratio of 2 year TRM (95% CI)	P
Age			NS		NS		
<18*	65	1.0		1.0		1.0	
18-35**	50	2.2 (0.8-6.0)		0.7 (0.4-1.3)		0.6 (0.3-1.1)	0.09
36-59	151	1.2 (0.5-2.5)		0.8 (0.5-1.3)		0.5 (0.3-0.9)	0.02
60+	89	1.1 (0.5-2.5)		1.1 (0.6-2.0)		0.9 (0.5-1.5)	0.59
HCT-CI			NS				NS
0*	172	1.0		1.0		1.0	
1-2	88	1.0 (0.5-1.8)		0.9 (0.6-1.4)	0.66	0.9 (0.5-1.5)	
3+	95	1.2 (0.6-2.1)		1.7 (1.2-2.5)	<0.01	1.5 (1.0-2.3)	
Donor Type							
Sibling*	103	1.0		1.0		1.0	
Matched URD	49	0.3 (0.2-0.7)	<0.01	1.8 (1.1-3.0)	0.02	2.0 (1.1-3.5)	0.02
Mismatched URD	8	1.9 (0.3-10.4)	0.48	1.0 (0.4-3.0)	0.95	1.0 (0.3-3.4)	0.98
Single UCB	54	3.6 (1.4-9.2)	0.01	0.8 (0.4-1.4)	0.41	0.4 (0.2-1.0)	0.04
Double UCB	141	1.9 (1.0-3.5)	0.04	1.2 (0.8-1.8)	0.38	1.2 (0.7-1.9)	0.57
Weeks from HCT to Initial Steroid Rx Continuous (/week)		1.02 (0.96-1.08)	NS	0.71 (0.50-1.01)	0.06	0.92 (0.87-0.97)	0.05
GVHD Risk [†]							
Standard Risk*	276	1.0		1.0		1.0	
High Risk	79	0.5 (0.3-0.9)		1.7 (1.2-2.4)	<0.01	1.8 (1.1-2.7)	0.01

Bold indicates statistical significance. *Reference group †Standard Risk: single organ involvement (stage 1-3 skin or stage 1-2 GI) or two organ involvement (stage 1-3 skin plus stage 1 GI; or stage 1-3 skin plus stage 1-4 liver). All other patients are High Risk.

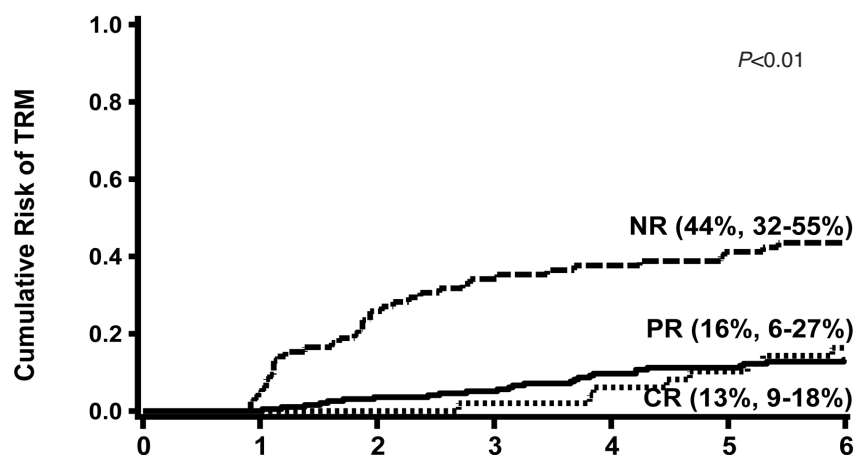


Figure 3. Cumulative incidence of TRM at 6 months after onset of steroid therapy by response to steroids at day 28.

the University of Minnesota using a combined Minnesota-CIBMTR grading system devised by combining the initial GvHD grade as determined by the Minnesota and the CIBMTR grade.¹⁴ Patients with this HR GvHD were less likely to respond to steroid therapy and had a twofold increased risk of TRM compared to patients with SR GvHD. Thirty-three percent of the HR group in the Minnesota GvHD scoring system and 79% of the HR in the CIBMTR system were reclassified as being SR.¹⁴

We tested this reported GvHD Risk Score, in a larger, multicenter and heterogeneous group of 1723 patients who received steroids as initial systemic therapy for acute GvHD.¹ However, recognizing the variability in GvHD

grading across sites, we then examined the details of initial GvHD organ stage combinations to determine whether stage groupings would better identify the patients at the highest risk than GvHD grading. We divided the 1723 patients into 67 categories by organ stage and, thus by the extent of GvHD involvement at onset. We collapsed these categories into 17 larger categories clustered as clinically similar cohorts with comparable CR+PR at day 28 and evaluated these new GvHD staging categories for CR+PR, survival, and TRM. We found a clear demarcation between categories according to the CR+ PR rate at day 28 which also predicted the risks of 6-month mortality and TRM. This allowed the division of the entire cohort

into SR-GvHD and HR-GvHD groups to define our refined acute Minnesota GvHD Risk Score.¹ As measured by the net reclassification index, our refined definition of GvHD improved both the true-positive and false-positive rates among our study population.¹

In the current report including an independent contemporary cohort, even though with some differences in clinical characteristics, we now validate this Minnesota GvHD Risk Score, demonstrating prognostic utility that remains reliable in the new cohort. While biomarkers can associate with later outcomes, their assay takes time and requires measurement accuracy of a variety of reported indicators. Our clinical risk score should be the immediate and initial step in tailoring GvHD therapy, as it can be performed in real time.

The approach of stratification by this Minnesota GvHD Risk Score and later adjustment by biomarkers was used prospectively for the first time to establish eligibility criteria in the BMT CTN Protocol 1501, a randomized, phase II trial evaluating sirolimus *versus* prednisone in patients with SR GvHD.¹⁷ Of 122 patients classified by the Minnesota Risk Score at enrollment as having SR acute GvHD, only 4 patients (3%) were deemed high risk by the biomarkers. Thus, we confirmed the accuracy of

the Minnesota Risk Score using bedside GvHD risk assessment.

Further prospective trials using the Minnesota GvHD Risk Score along with informative and reliable biomarker results if available quickly are needed to better explore the GvHD risk. Additional studies using clinical classifiers supplemented with biomarkers may be of interest. A tailored approach to upfront acute GvHD therapy based upon the Minnesota GvHD Risk Score should be considered in order to improve outcomes in patients with acute GvHD. It may also improve risk stratification for future trials of initial GvHD therapy.

Acknowledgments

The authors thank the nurses, nurse coordinators, pharmacists and physicians who cared for these patients and their families. In addition, we gratefully acknowledge the nurses and research staff whose dedicated efforts facilitated the prospective collection of the GvHD data. The authors also thank the patients and the families for participating in the clinical research trials.

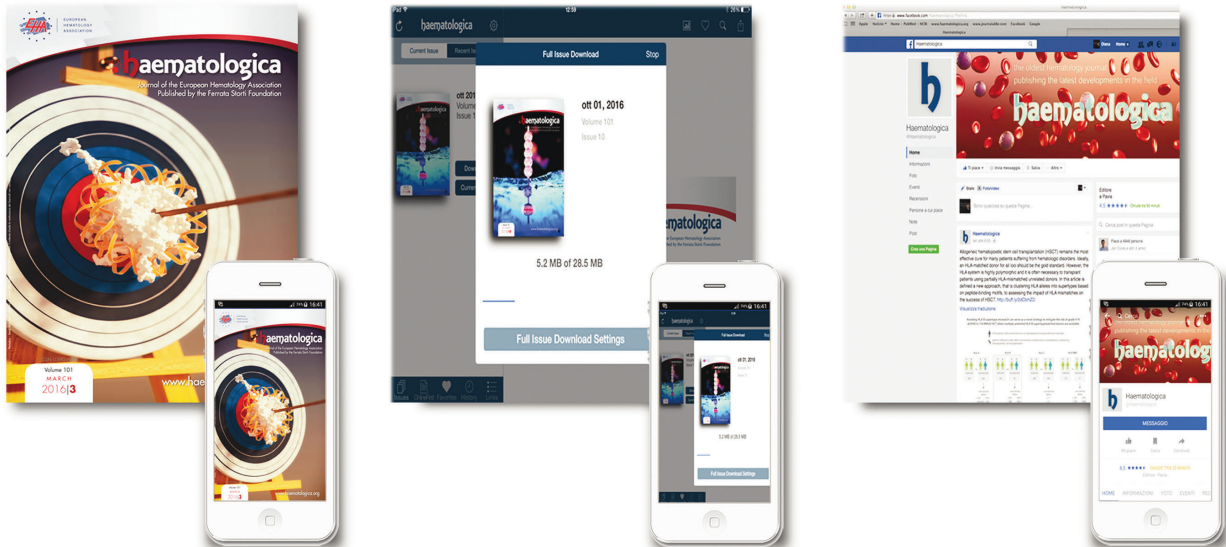
Funding

This study was supported in part by the National Institutes of Health, National Cancer Institute grant P01 CA065493-20.

References

- MacMillan ML, Robin M, Harris AC, et al. A refined risk score for acute graft-versus-host disease that predicts response to initial therapy, survival, and transplant-related mortality. *Biol Blood Marrow Transplant.* 2015;21(4):761-767.
- Zeiser R, Blazar BR. Acute graft-versus-host disease - biologic process, prevention, and therapy. *N Engl J Med.* 2017; 377(22):2167-2179.
- Rowlings PA, Przepiorka D, Klein JP, et al. IBMTR Severity Index for grading acute graft-versus-host disease: retrospective comparison with Glucksberg grade. *Br J Haematol.* 1997;97(4):855-864.
- Przepiorka D, Weisdorf D, Martin P, et al. 1994 Consensus Conference on acute GvHD grading. *Bone Marrow Transplant.* 1995;15(6):825-828.
- Weisdorf DJ, Snover DC, Haake R, et al. Acute upper gastrointestinal graft-versus-host disease: clinical significance and response to immunosuppressive therapy. *Blood.* 1990;76(3):624-629.
- Weisdorf D, Haake R, Blazar B, et al. Treatment of moderate/severe acute graft-versus-host disease after allogeneic bone marrow transplantation: an analysis of clinical risk features and outcome. *Blood.* 1990;75(4):1024-1030.
- MacMillan ML, DeFor TE, Weisdorf DJ. The best endpoint for acute GVHD treatment trials. *Blood.* 2010;115(26):5412-5417.
- Miller WP, Rothman SM, Nascene D, et al. Outcomes after allogeneic hematopoietic cell transplantation for childhood cerebral adrenoleukodystrophy: the largest single-institution cohort report. *Blood.* 2011; 118(7):1971-1978.
- Mallhi KK, Smith AR, DeFor TE, Lund TC, Orchard PJ, Miller WP. Allele-Level HLA Matching impacts key outcomes following umbilical cord blood transplantation for inherited metabolic disorders. *Biol Blood Marrow Transplant.* 2017;23(1):119-125.
- MacMillan ML, DeFor TE, Young JA, et al. Alternative donor hematopoietic cell transplantation for Fanconi anemia. *Blood.* 2015; 125(24):3798-3804.
- Hings IM, Filipovich AH, Miller WJ, et al. Prednisone therapy for acute graft-versus-host disease: short- versus long-term treatment. A prospective randomized trial. *Transplantation.* 1993;56(3):577-580.
- MacMillan ML, Weisdorf DJ, Wagner JE, et al. Response of 443 patients to steroids as primary therapy for acute graft-versus-host disease: comparison of grading systems. *Biol Blood Marrow Transplant.* 2002; 8(7):387-394.
- Hings IM, Severson R, Filipovich AH, et al. Treatment of moderate and severe acute GVHD after allogeneic bone marrow transplantation. *Transplantation.* 1994; 58(4):437-442.
- MacMillan ML, DeFor TE, Weisdorf DJ. What predicts high risk acute graft-versus-host disease (GVHD) at onset?: identification of those at highest risk by a novel acute GVHD risk score. *Br J Haematol.* 2012;157(6):732-741.
- Glucksberg H, Storb R, Fefer A, et al. Clinical manifestations of graft-versus-host disease in human recipients of marrow from HL-A-matched sibling donors. *Transplantation.* 1974;18(4):295-304.
- Thomas ED, Storb R, Clift RA, et al. Bone-marrow transplantation (second of two parts). *N Engl J Med.* 1975;292(17):895-902.
- Pidala JA, Hamadani M, Dawson P, et al. Sirolimus Vs. prednisone as initial systemic therapy for Minnesota standard risk (MNSR), Ann Arbor 1/2 acute graft-vs.-host disease (GVHD): primary results of the multicenter randomized phase II BMT CTN 1501 Trial. Vol. 25 (3), Supplement. *Biol Blood Marrow Transplant.* 2019:S50-S51.

RESEARCH, READ & CONNECT



We reach more than
6 hundred thousand readers each year

The first Hematology Journal in Europe

Impressions YTD

9,621,645

Digital Readers

4,431

Total Audience

554,484

Worldwide rank

7th

Impact factor

7.570

Total citations

16,255

The logo for haematologica, featuring a stylized red and white 'h' icon followed by the word 'haematologica' in a lowercase, sans-serif font.

Journal of the Ferrata Storti Foundation

